

DESIGN OF STRUCTURES AND FOUNDATIONS FOR VIBRATING MACHINES

VR ULASSI

VOLUME 1 OF 4

IN PARTIAL FULFILLMENT OF THE DEGREE OF MASTER OF SCIENCE IN
ENGINEERING (COURSEWORK) COMPRISING 72 CREDITS OF 144 FOR THE
DEGREE

DATE SUBMITTED: 13 DECEMBER 2002

SUPERVISOR: PROFESSOR H D SCHREINER

As the Supervisor I have/have not approved this dissertation for submission

Signed: _____

Date : _____

ACKNOWLEDGEMENTS

I wish to thank the following people for their contribution and support in making this study possible:

Professor H D Schreiner

Dr D L Webb

Colleagues

My Family

ABSTRACT

The lack of methods for rigorous dynamic analysis of foundations and structures for vibrating machines has resulted in below optimum performance and in some cases reduction of life of machines, structures and foundations. The costs and complexities of these machines make it necessary to conduct proper geotechnical site investigations and dynamic analyses to obtain the response of the soil, foundation and structure as a system to excitation. In order to highlight the use of dynamic analyses, the response of the foundations and structures were compared to the “rule of thumb” which is based on mass ratio. Furthermore sensitivity analyses were carried out comprising the following variables:

- Shear modulus of soil, G
- Poisson’s ratio of soil, ν
- Type of structure (ie raft, table top and multi-storey)
- Stiffness of structure
- Stiffness of foundation

The fundamentals of structural dynamics have not been dealt with in this dissertation. The dynamic analyses were carried out using a finite element analysis program called Strand 7. The results were typical of a finite element analysis, giving stresses, strains, deflections, amplitudes, frequencies and velocities of vibration.

The traditional “elastic halfspace model” is deficient as it does not account for soil comprising various layers. The theory has been based on an isolated circular footing. Most foundations are located in soils with layered mediums, are rectangular and in some cases are affected by the interaction of foundations in close proximity. Furthermore there is a need to account for the non-linear effects and properties of soil. It is therefore becoming more attractive to adopt mathematical models of soils using finite elements, where the visco-elastoplastic properties of soils can be realized and modeled. Furthermore the finite element method overcomes limitations such as layering and shapes or foot-prints of foundations.

The “rule of thumb” or mass ratio method of design procedure is as follows:-

- firstly the requirements of stresses and serviceability must be satisfied. This is usual in a statically loaded system.

- the ratio of the machine mass to that of the foundation together with the structure should be greater than 3 in the case of a revolving machine and 5 in the case of a reciprocating machine.
- in order to obtain uniform settlement of the foundation the distance of the combined centre of gravity of the machine and foundation from the centre of area in contact with the soil is limited to 5% of the corresponding dimension of the foundation.

It is evident that the mass ratio lacks accuracy in that there are several parameters that are required to describe the satisfactory performance of a system such as amplitude, frequency and velocity of vibration. The finite element method allows for calibration of the model to account for the real behaviour of the system. Calibration is generally conducted using sensitive transducers called accelerometers. The accelerometers produce power spectral density (PSD) graphs from which deflections and stresses can be back calculated. The deflections and stresses are compared with calculated deflections and stresses. Descriptions of the methods of analysis followed by presentation of results, discussions and interpretations have been included. To motivate the use of dynamic analyses case histories have been presented and discussed. Finally the dissertation concludes with findings of the study together with recommendations for the way forward in terms of research.

TABLE OF CONTENTS

CHAPTER	DESCRIPTION	PAGE NUMBERS
<u>1.0</u>	<u>INTRODUCTION</u>	1
<u>2.0</u>	<u>GEOTECHNICAL CONSIDERATIONS</u>	3
2.1.	Introduction	3
2.2.	Elastic Half Space model (EHSM)	4
2.2.1	Evaluation of Soil Parameters	5
2.2.2	Shear Modulus	6
2.2.3	Published Correlation: Sands and Gravel	6
2.2.4	Published Correlation: Saturated Clays	7
2.2.5	Calculation of Shear Modulus for Structure-Soil Interaction Analysis	7
2.2.6	Selection of Shear Strain Magnitude for Computing Approximate Shear Modulus Beneath Footings	8
2.2.7	Damping Ratio	9
2.2.8	Selection of Poisson's Ratio and Soil Density	9
2.2.9	Effect of Foundation Embedment	10
2.2.10	Effect of Stiff Underlying Stratum	10
2.3	Elasto-viscoplastic Halfspace Model	11
2.3.1	Vertically Oscillating Rigid Foundation	11
2.3.2	Lateral Rocking and Torsional Vibration of Rigid Foundation	16
<u>3.0</u>	<u>ANALYSIS OF STRUCTURES AND FOUNDATIONS</u>	19
3.1	Introduction	19
3.2	Machine parameters	19
3.3	Analysis of Structures	20
3.4	Load Combinations	21
3.4.1	Static Analysis	21
3.4.2	Dynamic Analysis	21
3.5	Soil Parameters	21
3.6	Dynamic Forcing Function	22
3.7	Time Periods	22
3.8	Types of Structures	22
3.8.1	Raft	22
3.8.2	Table Top	22
3.8.3	Multi-storey Structure	24
<u>4.0</u>	<u>RESULTS</u>	25
4.1	Introduction	25
4.2	Use of Results in Design	25
4.2.1	Static Member Forces	25
4.2.2	Displacements Under Static Loads	25
4.2.3	Natural Frequencies	26
4.2.4	Mode Shapes	26
4.2.5	Dynamic Displacements	26
4.2.6	Dynamic Velocities	26

CHAPTER	DESCRIPTION	PAGE NUMBERS
<u>5.0</u>	<u>DISCUSSIONS AND INTERPRETATIONS</u>	27
5.1	Introduction	27
5.2	Effect of Soil Properties	28
5.2.1	Raft	28
5.2.2	Table Top	30
5.2.3	Multi-storey	32
5.3	Effect of Foundation Thickness	33
5.3.1	Raft	33
5.3.2	Table Top	35
5.3.3	Multi-storey	37
5.4	Effect of Beam vs Plate Model	38
5.4.1	Raft	39
5.5	Effect of Foundation Thickness on the Plate Model	41
5.5.1	Raft	41
5.6	Effect of Modeling Machine as Multi-Mass System	43
5.6.1	Raft	43
5.6.2	Table Top	46
5.6.3	Multi-storey	49
5.7	Effect of Transverse Beam Section Properties	52
5.7.1	Table Top	52
5.7.2	Multi-storey	54
5.8	Effect of Column Section Properties	56
5.8.1	Table Top	56
5.8.2	Multi-storey	58
5.9	Natural Frequencies	60
5.9.1	Effect of Soil Properties	60
5.10	Effect of Type of Structures	62
5.10.1	Raft, table top and multi-storey	62
<u>6.0</u>	<u>CASE HISTORIES</u>	65
6.1	Introduction	65
6.2	Case Histories	66
6.2.1	Case History 1: SP 78, Karabinis and Fowler (1982)	66
6.2.2	Case History 2: SP 78, Srinivasulu and Lakshmanan (1982)	66
6.2.3	Case History 3: du Preez et al (1999)	67
6.2.4	Case History 4: Daming et al (1983)	70
6.2.4	Conclusion	71
<u>7.0</u>	<u>CONCLUSION</u>	73
7.1	Introduction	73
7.2	Geotechnical Considerations	74
7.3	Dynamic Analysis using Finite Element Analysis	75

DESCRIPTION	PAGE NUMBERS
<u>FIGURES</u>	
Figure 1	Distribution of displacements waves from a circular footing homogeneous, isotropic, elastic half-space 78
Figure 2	Definition of material damping 78
Figure 3	Hypothetical Shear Stress-Strain Curve for soil 79
Figure 4	Relationship of K_o to Plasticity Index and OCR 79
Figure 5	Determination of σ_{vmin} 80
Figure 6	Relationship of K_2 to shear strain amplitude and relative density 80
Figure 7	In situ shear modulus for saturated clay 81
Figure 8	Effect of embedment on damping 81
Figure 9	Effect of embedment of resonant frequency 82
Figure 10	Geometric Interpretation of Constitutive Model Parameter: a) Hardening, Perfect Plasticity, and Softening; b) Viscous and Inviscid Plasticity; c) Isotropic, Kinematic, and Combined Hardening and d) Viscous Translation and Expansion of Yield Surface on π Plane 82
Figure 11	Finite Element Mesh for Analysis of Vertically Oscillating Circular Foundation 83
Figure 12	Mesh Convergence Study 83
Figure 13	Establishing Steady-State Waves and Yield Zones for Circular Foundation Problem: Arrows Denote Instantaneous Direction of Force; E = Extensional Yielding; C= Compressional Yielding 84
Figure 14	Vertically Oscillating Circular Foundation on Kinematically Hardening Viscoplastic Half Space 84
Figure 15	Vertically Oscillating Circular Foundation on Elastoplastic Half-Space Influence of H' on a) Amplitude versus Frequency Plot; b Time History Plot 85
Figure 16	Symmetry and Antisymmetry for Vertical, Lateral, Rocking and Torsional Vibration Modes [Arrows Denote Free Degrees of Freedom (DOFs); Circles Denotes Fixed DOFs] 85
Figure 17	Amplitude-Frequency Plot for Horizontally Vibrating Square Foundation showing Effects of Viscosity 86
Figure 18	Amplitude-Frequency Plot for Harmonically Rocking Square Foundation showing Effects of Soil Plastic Modulus 86
Figure 19	Amplitude-Frequency Plot for Torsionally Vibrating Square Foundation Showing Effects of Initial Yield Stress 87
Figure 20	Raft Model 88

<u>DESCRIPTION</u>	PAGE NUMBERS
Figure 21 Table Top Model	90
Figure 22 Multi-storey Model	93
Figure 23 Vibration performance of rotating machines	95
Figure 24 Model Mode shapes	95

DESCRIPTION**PAGE
NUMBERS****TABLES**

Table 1	Equivalent Spring Constants for Rigid Circular and Rectangular Footings	96
Table 2	Equivalent Damping Ratio for Rigid Circular and Rectangular Footings	96
Table 3	Values of K	96
Table 4	Summary of Derived Expressions for a Single-Degree of Freedom System	97
Table 5	Embedment Coefficient for Spring Constants	97
Table 6	Effect of Depth of Embedment on Damping Ratio	97
Table 7	Approximate k_z Variation with Stratum Thickness	98
Table 8	Resonant Vertical Displacement for Stratum Overlying Rigid Base: $\nu = 0.25$	98
Table 9	Frequency in Vertical Mode for Stratum Overlying Rigid Base: $\nu = 0.25$	98
Table 10.1	Nonlinear Transient Response: Raft	99
Table 10.2	Nonlinear Transient Response: Table Top	100
Table 10.3	Nonlinear Transient Response: Multi-storey	101
Table 11.1	Natural Frequencies: Raft	102
Table 11.2	Natural Frequencies: Table Top	103
Table 11.3	Natural Frequencies: Multi-storey	104
Table 12.1	Structure Dimensions: Raft	105
Table 12.2	Structure Dimensions: Table Top	106
Table 12.3	Structure Dimensions: Multi-storey	107
Table 12.4	Equivalent Stiffness of Rectangular Footings	108

REFERENCE LIST

109

APPENDICES

A1.1	Background to Solvers used in Strand 7 Finite Element Analysis	A1.1-A1.8
A2.1	Computer printout of calculations	A2.1-A2.31
B	Non Linear Transient Response: Raft	
C	(Volume 2 of 4)	B1.1-B5.24
D	Non Linear Transient Response: Table Top	
	(Volume 3 of 4)	C1.1-C5.18
	Non Linear Transient Response: Multi-storey	
	(Volume 4 of 4)	D1.1-D5.18

CHAPTER 1: INTRODUCTION

The analysis and design of foundations and structures for vibrating loads is complex and requires a good understanding of the theory of vibration and interaction with geotechnical engineering. Generally theoretical investigations, economy and design tradition result in approximate, non-dynamic design with "fudge" factors incorporated to qualitatively account for vibration.

The lack of rigorous dynamic analysis of structures and foundations for vibrating machines has resulted in below optimum performance and in some cases reduction of life of machines, structures and foundations. The capital costs of these machines generally range between R50 to R100 million. Breakdowns have serious economic impact especially when replacements parts are to be imported. It therefore becomes imperative to conduct detailed site investigations to establish the soil properties. The soil properties that define the dynamic characteristics should be determined with adequate confidence so that the resulting models reflect the true behaviour of the soil. Furthermore the foundation and structures should be designed using models and analysis methods that predict the real behaviour as close as possible. In order to achieve this finite element analysis was used to derive dynamic parameters such as natural frequencies, amplitudes and velocities that characterize the performance of foundations and structures.

The dynamic design of the machine foundation and structure must consider possible fatigue failure of the machine components and supporting structure. There are environmental demands placed on the overall structure and these may include physiological effects on persons and possible undesirable effects on adjacent sensitive equipment

The performance shall then be compared with the traditional "rule of thumb" which is based on mass ratio. The intention of this dissertation is to highlight the benefit of conducting dynamic analyses and in doing so test the sensitivities of certain parameters such as shear modulus, thickness of foundation and other geometric properties.

The dissertation has been set out as follows:

- Chapter 2 deals with the literature survey carried out on the geotechnical models. The first geotechnical model is the elastic half space model followed by the viscoplastic halfspace model of a vertically oscillating rigid foundation. The model of a nonlinear lateral rocking and torsional vibration of the rigid foundation is also discussed and is based on an elasto-viscoplastic halfspace.
- Chapter 3 describes the machine parameters, analysis method, load combinations, soil parameters, dynamic forcing function, time periods and the types of structures used in the study.
- Results have been presented in Chapter 4
- Chapter 5 deals with the discussion and interpretation of the results.
- Certain published and unpublished case histories have been discussed in Chapter 6.
- Chapter 7 concludes the dissertation with recommendations made based on the studies carried out.

CHAPTER 2: GEOTECHNICAL CONSIDERATIONS

2.1 Introduction

Chapter 2 comprises a literature survey that was carried out on the geotechnical models. It was noted that during the period 1960 to 1976 many researchers published papers on soil parameters and mathematical models pertaining to dynamically loaded foundations. Further distinctions were made between earthquake excitation and vibrations arising from machines. The research of these two types of excitations were dealt with separately owing to their differences in frequencies and periods of vibration. The above research resulted in the publishing of constants such as shear moduli, damping ratio and Poisson's ratio for various soil types. During this period research was predominantly based on the elastic behaviour of soil. The elastic half space model was accepted by many researchers when modeling the response of foundations. Kausel, et al (1976) published a paper on nonlinear behaviour in soil structure interaction. However, the material properties were assumed to be linearly visco-elastic. It was in the early 1990's that researchers such as Borja, et al (1992) considered elasto-viscoplastic soil models. Finite element analyses were used to research the nonlinear soil behaviour in response to vibration.

When a foundation is excited by a periodic force, the foundation becomes the source of periodic impulses. These impulses travel radially into the underlying soil similar to sound waves (refer Figure 1). The soil particles also undergo periodic motion. Soil located directly below the foundation moves in phase with the foundation motion. A zone is reached at some distance away from the foundation where the soil moves opposite to the foundation motion and is said to be 180° out of phase. The location of this zone is dependent on the type of soil. Richart (1960) has stated that "in an infinite, elastic, isotropic and homogeneous body disturbances may be propagated by waves of volume change, designated as the compressive wave or P-wave and by waves of distortion of constant volume designated as shear waves or S-wave." A third wave called the Rayleigh or R-wave results from the free surface as a surface wave. The velocity of propagation of the shear wave is given by $V_s = (G/\rho)^{0.5}$, where G = shear modulus of soil and ρ = mass density of soil. The velocities of the P- and R-waves are dependent on the Poisson's ratio as shown in Figure 1. The elastic half space model has been based on the above principle. Section 2.2 below deals with the elastic half space model. The property of the soil is assumed to be linear elastic.

Although researchers such as Kausel et al (1976) recognized that the behaviour of soil is nonlinear, they adopted an iterative method using a linear solution for a nonlinear problem. The authors of the paper concluded that the cost of the iterations and the refinement of the finite element analysis was not worth the expense. Borja et al (1993, 1994) investigated the nonlinear soil behaviour on harmonically excited foundations. The first paper deals with vertically oscillating foundations whilst the second deals with rocking and torsional vibrations of foundations. In both cases the research was based on an elasto-viscoplastic half space model. Finite element analyses were used to model soil structure interaction. The above papers are discussed in sections 2.3 and 2.4.

2.2 Elastic Half Space Model (EHSM)

Dynamically loaded foundations induce strains in the underlying soils, requiring the foundation to displace in a compatible manner. Therefore there is a need to adopt models to predict the response of soil to dynamic loading. Several models are available, the most common being the Elastic Half Space Model (EHSM) which is used for shallow foundations and presumes the following:

- circular footings rest on the surface of an elastic halfspace which extends to an infinite depth
- the soil is homogeneous
- the soil is isotropic and stress-strain properties are defined using 2 elastic constants (ie shear modulus, G and Poisson ratio, ν).

EHSM is used to predict deformation versus time, the soil's response to harmonic vertical forces, rocking and twisting moments, horizontal shears and their combinations together with the dissipation of energy through geometric damping. Mathematical expressions are derived from EHSM from which the stiffness of soil and amount of damping are defined. The soil stiffness and damping are functions of elastic properties of the soil and the frequency of loading. The soil is represented by linear springs resisting vertical and horizontal, twisting and rocking modes. Dashpots represent viscous damping. It is possible to assign spring constants and damping ratios to soil and determine the deformation – time relationships using lumped parameter relationships where the mass taken is that of the footing and load vibrating in phase with footings. Soil mass is excluded.

EHSM is valid only for isolated foundations. No theory has been developed for 2 or more foundations situated near each other. The use of finite element modeling of the soil itself should be considered in cases where multiple foundations are located in close proximity to each other.

For design purposes, frequency independence of stiffness and damping is valid for low frequencies.

$$\text{ie } f < (1/\pi r_o)(Gg/\gamma)^{0.5} \quad \{1\} \quad (\text{Arya et al 1984})$$

where

r_o = radius of circular footing or $(BL/\pi)^{0.5}$ translatory motion

or $r_o = (BL^3/3\pi)^{0.25}$ rocking motion for rectangular footing.

The supporting soil is modeled as a series of elastic springs having translational and rotational stiffnesses. Expressions for these spring stiffnesses are given in Table 1. Furthermore these springs are damped and hence damping ratios need to be calculated. Damping ratios are computed from mass or inertia ratios (refer to Table 2). Masses in the mass ratio expressions include the footing and machine weights, vibrating in phase. The primary objective is to maximize geometric damping. Damping ratios for halfspace increase with foundation size. This implies that foundations should be as wide and shallow as possible.

2.2.1 Evaluation of Soil Parameters

To evaluate spring constants and corresponding damping ratios for structure and soil interaction it is necessary to determine shear modulus, G ; Poisson's ratio, ν ; mass density, ρ and internal material damping ratio, D_m .

Soil dynamics is a relatively new discipline, hence problems are not addressed rigorously and the theory is considered for ideal conditions eg assessment of permanent settlements for near surface vibratory loads, response of soil beneath flexible mats loaded by vibrating machinery and response of pile groups. However rational analysis should be carried out. Arya et al (1984) present procedures for the evaluation of parameters and prediction of foundation behaviour based on rigorous dynamic solutions verified by observations. The procedures are based on static and dynamic models, modified empirically based on experience.

2.2.2 Shear Modulus

Unbalanced loads on vibrating machinery produce shear strains in soil smaller than those produced under static loading. Mechanism controlling stress-strain at small strains involves stress deformation behaviour and characteristics of soil particles in contact, which is not controlled by relative slippage of particles, associated with larger strain levels. Shear modulus cannot be obtained from triaxial compression test or field plate bearing test unless strains can be measured accurately for very small magnitudes of strains.

At small values of strain, the stress-strain relationship is nonlinear. Therefore it is desired to define shear modulus as an equivalent linear modulus, the slope of which is derived from line joining extremities of the closed loop stress - strain curve (refer to Figure 3). Shear modulus, G decreases with number of cycles until a stable condition is reached. When this stable condition is reached a line joining the extremities is drawn. The gradient of this line defines the shear modulus.

Richart (1975) has listed 8 factors affecting shear modulus, which are as follows:

1. amplitude of dynamic strain (only dynamic compression is considered)
2. mean effective stress and length of time since stress applied
3. void ratio
4. structure of soil
5. stress history
6. frequency vibrations
7. degree of saturation
8. temperature

2.2.3 Published Correlation: Sands and Gravels

Hardin and Richart (1963) published expressions for shear modulus of sand from resonant column test. Two expressions were obtained:

$$\begin{aligned}
 \text{a)} \quad G &= \frac{2630 (2.17 - e)^2 (\bar{\sigma}_0)^{0.5}}{1 + e} & \{2\} & \quad (\text{Hardin and Richart (1963)}) \\
 \text{b)} \quad G &= \frac{1230 (2.97 - e)^2 (\bar{\sigma}_0)^{0.5}}{1 + e} & \{3\} & \quad (\text{Hardin and Richart (1963)})
 \end{aligned}$$

where e = void ratio

$\bar{\sigma}_o$ = mean normal effective stress

2.2.4 Published Correlation: Saturated Clays

Hardin and Drnevich (1972) published expressions for shear modulus for clays from resonant column tests as follows:

$$G_{\max} = 1230 \frac{(2.937-e)^2}{1+e} (\text{OCR})^k (\bar{\sigma}_o)^{0.5} \quad \{4\} \quad (\text{Hardin and Drnevich (1972)})$$

where k = plasticity constant determined from Table 3

$$G = G_{\max} / (1+\gamma/\gamma_r) \quad \{5\} \quad (\text{Hardin and Drnevich (1972)})$$

where G_{\max} = shear modulus at shear strain amplitude of 0.25×10^{-4} . According to Hardin and Drnevich (1972) the shear strain amplitude is higher for foundation analysis for vibrating machines.

γ = desired shear strain expressed as a percentage

γ_r = reference strain = $(\tau_{\max} / G_{\max})100$

τ_{\max} is obtained from Mohr-Coulomb failure theory.

2.2.5 Calculation of Shear Modulus for Structure–Soil Interaction Analysis

Shear modulus is a function of effective confining pressure, geostatic and net bearing stresses produced by the structure. Static machine and foundation weights can be neglected when considering the expression for τ_{\max} as their effects on shear modulus reduction is small. The expression for τ_{\max} is as follows:

$$\tau_{\max} = [(1+k_o)/2 \bar{\sigma}_v \sin \bar{\phi} + \bar{c} \cdot \cos \bar{\phi}]^2 - [(1-k_o)/2 \cdot \bar{\sigma}_v]^2]^{0.5} \quad \{6\}$$

(Hardin and Drnevich (1972))

where $\bar{\sigma}_v = \sigma_v - u$

k_o = coefficient of earth pressure at rest and obtained from Figure 4

$\bar{\phi}$ = effective stress angle of internal friction

\bar{c} = effective stress cohesion

For reasonably uniform soils it is sufficient to evaluate shear modulus at one depth d_c below ground (refer to Figure 5).

If the soil is an over consolidated clay and remains over consolidated after loading, the imposed stresses have little effect on G . When soil consists of normally consolidated clay (which is rare) or clay that will become normally consolidated after application of load and excess pore pressure has dissipated, the shear modulus will increase with time. Two values for shear modulus and two spring constant values result: The first case results from the unconsolidated undrained condition, after the static load has been applied. The second case results from the fully consolidated condition that occurs at some time in the future. The shear modulus for the first condition should be evaluated using geostatic stress conditions and soil properties prior to the placement of the foundation and the structure. In the second condition the undrained shear strength at depth d_c should be assessed at the end of the consolidation.

2.2.6 Selection of Shear Strain Magnitude for Computing Approximate Shear Modulus Beneath Footings

When a particle of soil is subjected to a stress, it is accompanied by corresponding strain. As the stress increases so does the strain increase. This is true for the elastic behaviour of the soil. The ratio of stress to strain is termed the Young's modulus, E of the soil. The shear modulus, G can be defined in the similar way as the ratio of the shear stress to the shear strain (τ/γ). However at small magnitudes of shear strains the function defining the relationship of shear stress to shear strain is nonlinear. (refer Figure 3)

It is necessary to estimate shear strain magnitude to use in calculation of soil spring constants. Arya et al (1984) recommended the following approximate procedure for vertical loading:

1. Select shear strain in range of crosshatched area shown in Figures 6 and 7. According to Seed and Idriss (1970) the typical range for shear strain applicable to machine foundations is between 10^{-3} to 10^{-2} percent. G may be computed as follows:
 - from Figure 6 a chosen shear strain will result in a value for k_2 . Therefore $G = 83.3 k_2 (\bar{\sigma}_0)^{0.5}$ Seed and Idriss (1970)
 - from Figure 7 a chosen shear strain will result in a value for G/S_u where S_u = undrained shear strength of the soil.
2. Conduct structure – soil interaction analysis and determine transmissibility factor, T_r (Table 4) for forcing frequency.

3. Multiply unbalanced vertical force by T_r and divide contact area of footing resulting in the dynamic bearing stress q_d
4. Approximate average shear strain, γ (%) = $12 q_d / G$.
 - presumes q_d induces same strains as static stress
 - yields order of magnitude strain levels
 - Used to refine values of G . If shear strains differ significantly, steps 1 to 4 are repeated until the strains converge to an acceptable difference.

2.2.7 Damping Ratio

Damping comprises a geometric component and a material component. Geometric damping is a measure of energy radiated away from the immediate region of the foundation. Geometric damping ratios are related to mass or inertia ratios. Material damping is a measure of energy lost from hysteresis effects. Hardin and Drnevich (1972) have defined material damping using Figure 2, where

$$D_m = A_L / (4 \pi A_T) \quad \{7\} \quad (\text{Hardin and Drnevich (1972)})$$

where A_L = area of soil hysteresis loop (energy lost)

A_T = area under the hysteresis loop (energy input)

Table 2 gives the expressions for the damping ratios D for the various modes of vibration

2.2.8 Selection of Poisson's Ratio and Soil Density.

Soil foundation interaction is not that sensitive to Poisson's ratio, ν and soil mass density, ρ . Poisson's ratio is generally selected on the predominant soil type. Arya et al (1984) have published typical values for Poisson's ratio and they are as follows:

Soil type	ν
saturated clay	0.45 – 0.50
dense sand or gravel	0.4 – 0.5
medium dense sand or gravel	0.3 – 0.4

2.2.9 Effect of Foundation Embedment.

When foundations are embedded the resulting equivalent spring constants and geometric damping ratios increase. The equivalent spring constants calculated from Table 1 is multiplied by the respective coefficients obtained from Table 5 (eg $k_x \eta_x$). The damping ratio, D obtained from Table 2 is multiplied by the embedment factor obtained from Table 6. Foundations are considered embedded if they are cast against undisturbed soil or compacted so that the soil can offer lateral support. Stokoe and Richart (1974) have researched the response of model circular footings embedded in dense, dry, poorly graded sand to vertical and horizontal rocking excitation. The 2 sets of tests tabled were based on:

- a. footings cast against soil and
- b. with air gap between sides of footings and soil.

It can be seen from Figure 8 that there is negligible change in the $D_t/D_{t, \text{surface}}$ for the foundation that has no lateral support from the soil. However the $D_t/D_{t, \text{surface}}$ ratio increases exponentially. D_t = total damping ratio and $D_{t, \text{surface}}$ = total damping ratio when the foundation is located at the surface. Figure 9 indicates that the ratio of embedment/radius is proportional to the ratio of $f_{mr}/f_{mr, \text{surface}}$, where f_{mr} = resonant frequency with damping included and $f_{mr, \text{surface}}$ = resonant frequency with damping included for a foundation located at the surface.

2.2.10 Effect of Stiff Underlying Stratum

According to Arya et al (1984) , if the subgrade consists of softer soil overlying stiffer soil or bedrock approximately 2 to 3 footing diameters of the base of the footing, the response is altered significantly. A stiff stratum interface reflects considerable proportion of the energy, producing lower geometric damping ratio than homogeneous subgrade. However the above effect is offset to a certain extent as the spring constant is increased due to stiff stratum.

Quantitative research has shown that the vertical response of a foundation on layered media described by Warburton (1957) indicates that there is little information available for rocking and sliding modes and has suggested the use of the finite element method for the rocking and sliding modes. Richart, Hall and Woods (1970) researched torsional response of a layered system.

Table 7 gives the relationships to calculate k_z for values of H/r_o , where H = distance from the base of the foundation to the stiff soil. Stiff soil is assumed to be fully rigid hence the displacement is zero.

The establishment of a damping ratio is difficult. Geometric damping ratio in the vertical motion is given by $D \approx 0.06 / \sqrt{B_z}$ (Whitman and Richart (1967)). Material damping in underlying soil is important since B_z is a mass ratio. The damping ratio is inversely proportional to the mass ratio. The response of a single degree of freedom (SDOF) system undergoing vertical oscillations comprising layered soils was studied approximately using Tables 8 and 9, giving theoretical values for displacement at resonance and resonant frequency. Geometric damping was considered. Richart, Hall and Woods (1970) observed that at frequencies below 60% of resonance and 140% above resonance, dynamic displacements would not exceed the static displacements by more than 50%.

2.3 Elasto-viscoplastic Halfspace Model

2.3.1 Vertically Oscillating Rigid Foundation

It is recognized by researchers in the geotechnical engineering fraternity that the dynamic response of soil is non linear, hysteretic and irreversible. At high strain levels deformation of soil is rate dependent. There has been little work to incorporate these effects in soil-structure interaction (SSI) models. This has been due to lack of efficient mathematical tools that can transform hyperbolic structural dynamics problem to elliptic problem as in linear analysis. Analysts neglect non linear effects due to lack of effective SSI models. The paper by Borja et al (1993) presents generalized finite element (FE) methodology, modeling non linear SSI effects and applies the model to machine foundations.

Hysteresis, rate dependence and irreversible deformation are typical features of cyclic soil behaviour. Elasto-plastic and elasto-viscoplastic models can be appropriate for modeling soil behaviour. The presence of hysteretic damping requires the soil model to be of kinematically hardening type (Prager 1956). The paper Borja et al (1993) demonstrates the effect of soil stiffness degradation, rate of loading and hysteresis on dynamic response of machine foundation. It is for this reason that the elasto-viscoplastic theory of Duvaut and Lions (1976) is used to model soil behaviour.

Repeated loading on machine foundations creates a zone of intense yielding and inelastic deformation beneath the foundation, resulting in dynamic non-homogeneity. The paper by Borja et al (1993) shows that plastic deformation and soil stiffness degradation for vertically oscillating circular and square foundations result in the overall increase in the vibrational displacement amplitudes and the creation of resonance frequencies.

2.3.1.1 Soil-Structure Model

The soil-structure model (refer Figure 10) comprises a massless rigid foundation of arbitrary shape, excited by a forcing function, $F_{EXT}(t)$. The finite element dynamic equation of motion may be written as follows:

$$\mathbf{M}\ddot{\mathbf{x}} + \mathbf{F}_{INT} = \mathbf{F}_{EXT} \quad \{8\} \quad (\text{Borja et al (1993)})$$

where \mathbf{M} = mass matrix

$\ddot{\mathbf{x}}$ = nodal acceleration vector

\mathbf{F}_{INT} = internal nodal force vector

$$\mathbf{F}_{INT} = \int_{\Omega} \mathbf{B}^T \boldsymbol{\sigma} d\Omega \quad \{9\} \quad (\text{Borja et al (1993)})$$

where: \mathbf{B}^T = strain displacement transform matrix

$\boldsymbol{\sigma}$ = Cauchy stress vector

Ω = problem domain (eg time)

For a given time domain equation {9} may be integrated as follows:

$$\mathbf{M}\mathbf{a}_{n+1} + (1+\alpha)(\mathbf{F}_{INT})_{n+1} - \alpha(\mathbf{F}_{INT})_n = \mathbf{F}_{EXT}(t_{n+1+\alpha}) \quad \{10\} \quad (\text{Borja et al (1993)})$$

where: $\mathbf{a}_{n+1} \approx \ddot{\mathbf{x}}(t_{n+1})$

α = parameter for linear structural dynamics that defines the predictor values for displacements and velocities. α is introduced to achieve an optimal balance between effective numerical dissipation and loss of accuracy.

The residual form of equation {10} is as follows:

$$r(\mathbf{a}_{n+1}) = \mathbf{F}_{EXT}(t_{n+1+\alpha}) - \mathbf{M} \cdot \mathbf{a}_{n+1} - (1+\alpha)(\mathbf{F}_{INT})_{n+1} + \alpha(\mathbf{F}_{INT})_n = 0 \quad \{11\}$$

(Borja et al (1993))

A fully implicit solution of equation {11} requires solving simultaneous equations for each iteration.

The constitutive model used presently is the deviatoric elasto-viscoplastic model of Duvaut and Lions (1976). The counterpart of this model is the Von Mises elastoplastic model with a linear combination of isotropic and kinematic hardening. The model can account for the following typical characteristics of soils under dynamic loads:

- path dependence
- plasticity
- hardening and softening
- Bauschinger effect
- viscous damping

This simple model provides a basis upon which more robust models may be calibrated.

The general rate dependent constitutive model for the viscoplastic case is of the form:

$$\dot{\sigma} = \dot{\sigma}^{tr} - g(\eta)(\sigma - \bar{\sigma}), \quad g(\eta) = 1/\eta \quad \{12\} \quad (\text{Borja et al (1993)})$$

where: $\bar{\sigma}$ = solution of the rate constitutive equation

$\dot{\sigma}^{tr}$ = trial rate of stress

η = viscosity coefficient

The material and damping stiffness matrices are as follows:

$$\mathbf{C}^T = 0 \quad \{13\} \quad (\text{Borja et al (1993)})$$

$$\mathbf{K}^T = 1/(1+\tau) \mathbf{K}^e + \tau/(1+\tau) \int \mathbf{B}^T \sigma'_{n+1}(\epsilon_{n+1}) \mathbf{B} d\Omega \quad \{14\} \quad (\text{Borja et al (1993)})$$

where \mathbf{C}^T = algorithmic damping matrix

\mathbf{K}^T = algorithmic stiffness matrix

\mathbf{K}^e = elastic stiffness matrix

τ = step size to damping ratio

$\sigma'_{n+1}(\epsilon_{n+1})$ = consistent algorithmic moduli (refer Simo and Taylor (1985)).

The visco-plastic model allows the modeling of material stiffness degradation using a plastic modulus parameter H' . The Bauschinger effect is modeled using a kinematic hardening parameter, θ . The nonproportional damping is accounted for using the viscosity coefficient η . The model parameters are shown in Figure 10. There is no limit placed on H' . As H' tends to ∞ , the elasto-plastic solution approaches the elastic solution. To account for softening plasticity H' is set as less than 0, the limitation being that $H' > -3 \times$ elastic shear modulus, μ . The kinematic hardening parameter, θ allows the yield surface to translate in the deviatoric stress space. The following may be noted:

- for pure kinematic translation $\theta=0$
- for pure isotropic hardening and softening $\theta=1$
- for linear combination of isotropic and kinematic hardening $0<\theta<1$.

The above theory is best illustrated by an example presented by (Borja et al (1993)) comprising a vertically oscillating circular foundation.

A 3 dimensional FE mesh is shown in Figure 11. The mesh comprises 936 nodes and 875 bilinear axisymmetric elements resulting in a total of 1751 unknown degrees of freedom. The rigid foundation is subjected to a sinusoidal vertical forcing function $f(t)$ applied at the center of the foundation. Figure 12 is used to determine whether the spatial pattern adequately simulated the dynamic behaviour of the soil-structure interaction (SSI) model. For each value of a_0 the foundation was subjected to a harmonic forcing function $f(t)$. The dynamic displacement amplitude, Δ^* for each frequency parameter, a_0 was calculated. $a_0 = \omega r/v_s$ Borja et al (1993). The static displacement, Δ was also calculated for each a_0 . In each case the dynamic displacement is normalized with respect to the corresponding static displacement ie Δ^*/Δ . The graph of Δ^*/Δ versus a_0 was drawn. The finite element analysis is carried out in time steps, $\Delta t = T/16$, where T = period of the exciting force. Hence the analysis is based on a time domain. The amplitude versus frequency curve is obtained from the following equation:

$$\Delta^*/\Delta = 1/(\alpha^2 + a_0^2 \beta^2)^{0.5} \quad \{15\} \quad (\text{Borja et al (1993)})$$

where α = real coefficient of k_d , dynamic impedance function

β = imaginary coefficient of k_d , dynamic impedance function

The above equation contains the frequency parameter, a_0 , resulting in a frequency domain. According to Borja et al (1993) there is good agreement between time domain finite element solution and frequency domain amplitude- frequency curve, indicating that the mesh is adequate for study. A numerical tool commonly used in digital signal processing is the exponential window method. This method permits analyses to be carried out on undamped structures in the frequency domain. According to Kausel and Roesset (1992) the solution involves the following:

- find the transfer function and forward Fourier transform of the excitation for the complex frequencies
- perform a standard inverse Fourier transform into the time domain
- remove the effect of complex frequencies by means of an exponential factor or window

A typical example of the above would be output from an accelerometer processed via an electronic signal processing unit were the signal is in the form of an acceleration power spectral density (PSD). The graph that is generated is in the form of acceleration versus frequency. The raw data produces complex curves. Fast Fourier Transform (FFT) is used to produce smooth sine curves for analysis purposes.

No artificial boundary conditions for the halfspace were used in the above analysis. When the foundation is excited compression or P-waves and shear or S- waves are emitted. The velocity of the P-waves are dependent on the soil properties. The time of arrival of the reflected waves will also be dependent on the soil properties. Therefore there will be some time lapse after the excitation. The phase distance is denoted by ϕ (refer Figure 12).

The half space is now assumed to be elasto-viscoplastic where the yield surface can be assumed to translate but not expand in the stress space. The yield surface is assumed to translate to force kinematic hardening to model the soil response. Isotropic hardening is simulated by not allowing expansion in the zones of stress. The zones of stress are indicated as the shaded elements in Figure 13. The results of the non linear analyses are shown in Figures 14 and 15.

The following observations by Borja et al (1993) may be tabled:

- a) plasticity increases vibrational amplitudes (displacements). Plasticity in this context is the stage at which the element sustains irrecoverable strain. The strain continues to increase without an increase in stress.

- b) resonance frequencies are created at low values of η and a_0 (dimensionless frequency factor)
- c) increasing material damping coefficient η decreases vibrational displacement amplitudes.
- d) resonant peaks disappear at sufficiently large η
- e) elasto-viscoplastic static displacements for different values of material damping coefficient η are the same.
- f) elasto-viscoplastic response approaches the elastic response as a_0 becomes large.

According to Borja et al (1993) radiation damping is smaller in the case of a half space problem containing a yield zone than for the same half space without a yield zone. Further explanation is given in section 2.3.2. Therefore local yielding creates resonant peaks on the amplitude – frequency curves and increases as the ratio between elastic to elastoplastic modeling increases. This phenomenon is consistent with known results for problem of finite size foundations on uniform layer over bedrock.

A contribution of the paper by Borja et al (1993) is the advance in non linear soil-structure interaction analysis. A non linear model provides a means of understanding influence of factors that dominate SSI response viz hysteretic soil behaviour and soil stiffness degradation. Nonlinear models allow extrapolation of numerical results beyond limits of traditional linear models. The increasing use of computers makes it feasible to analyse large scale nonlinear SSI using finite elements.

2.3.2 Lateral Rocking and Torsional Vibration of Rigid Foundation

The objective of the study conducted by Borja et al (1994) was to investigate the influence of nonlinear soil behaviour on dynamic response of vibrating rigid foundations with respect to lateral, rocking and torsional modes. Nonlinear finite element (FE) analyses were used to construct time history responses and steady state amplitude frequency curves for various modes of oscillation. Amplitude-frequency curves were used to assess the impact of soil nonlinearities on the foundation behaviour and to determine the range of excitation frequencies over which nonlinear effects dominate. Studies by Borja et al (1994) indicate that the localized soil yielding beneath vertically oscillating foundations amplifies foundation motion and enhances the creation of

resonance frequencies. An explanation for this could be attributed to the fact that localized yielding has the effect of creating softer zones surrounded by stiffer medium thereby reducing effective radiation damping. Studies by Borja et al (1994) indicate that as excitation frequency increases, nonlinear effects decrease (ie elastic behaviour dominates foundation in high frequency range).

The same methodology for the vertically oscillating foundations in section 2.3.1 has been adopted by Borja et al (1994) to study the non linear response of foundations in the lateral, rocking and torsional modes. The soil response was modeled using elasto-viscoplastic kinematically hardening theory of Duvaut and Lions (1976). It allows for soil hysteretic behaviour, stiffness degradation and non proportional damping. A hysteretic model with a closed loop steady – state cyclic stress-strain feature results in hysteretic material damping and reduced secant moduli, typical of soil undergoing plastic cyclic deformation.

2.3.2.1 Soil-Structure Model

The soil-structure model is similar to that used for the vertical vibration case, based on a finite element dynamic equation of motion discussed in the section 2.3.1.1. The forcing functions used in the study are shown in Figure 16 for the respective modes of vibration. The vertical and lateral forcing functions are concentrated forces whilst for the rocking mode the forcing function is a couple applied as a pair of eccentric and opposite vertical nodal forces. The torsional forcing functions are of the form of a pair of orthogonal oscillating forces acting in phase on the sides of the foundation.

Mesh convergence studies are important when conducting finite element analysis as the predicted dynamic responses vary according to the quality of the FE mesh, especially for nonlinear analysis. Classical theory of elasticity predicts that the static displacements under vertical, lateral, rocking and torsional loads are finite. Therefore these displacements can be used to normalize the corresponding amplitudes – frequency response curves. For the horizontal, rocking and torsional modes the normalized responses are written as horizontal displacements Δ^*/Δ^e , angular rotation θ^*/θ^e and angular twist ϕ^*/ϕ^e respectively. The predicted amplitude-frequency plots are shown in Figures 17, 18 and 19 for a square foundation.

The study conducted by Borja et al (1994) has indicated the following:

- a) localized soil yielding beneath the foundation results in increased vibrational amplitudes. The soil behaves plastically. The strain creeps without any stress increase. This increased strain amplifies the vibrational amplitudes.
- b) resonance peaks occur at low-frequency excitation.
- c) compared to the rocking mode, nonlinear soil effects are more dominant over a wider range of excitation frequencies for the lateral and torsional modes.

The dynamic response of a harmonically excited foundations has been investigated in the context of 2 and 3 dimensional nonlinear FE analyses. Localized soil yielding under foundation results in increased vibrational amplitudes of response and creation of resonance at low frequency excitations. At high frequency excitations amplification of the harmonic response due to nonlinear soil effects is possible when the motion is dominated by shearing modes, contrary to common understanding that nonlinear soil effects are unimportant in high frequency range.

Mesh convergence studies are important in assessing adequacy of FE grid. The time domain solution methodology is an effective analysis of nonlinear machine foundation response in all modes of vibration. The use of computer especially in time stepping schemes is making the FE method more attractive and feasible.

The studies by Borja et al (1993, 1994) have been a significant contribution to the understanding of nonlinear soil behaviour. However in both the above studies the models are assumed to have an abrupt transition from an elastic soil response to a plastic soil response. In real soils the behaviour is elasto-plastic in this transition zone.

CHAPTER 3: ANALYSIS OF STRUCTURES AND FOUNDATIONS

3.1 Introduction

The primary objective of this dissertation is to compare the rule of thumb with dynamic analyses when assessing the response of foundations and structures supporting vibrating machines. It was therefore imperative to carry out analyses using both the methods and compare the results. The machine parameters were selected on the basis of discussions with experienced colleagues in the industry. It was evident from the discussions that foundations and structures supporting centrifugal compressors operating at speeds between 6000 to 8000 rpm coupled with wear on the bearings were subjected to excessive vibrations. In order to protect claims against the client and suppliers further details can not be divulged. However it is important to note that the machine analysed in this study falls within the above category. The machine parameters remained unchanged throughout the study. The best known method to conduct dynamic analyses is the finite element method. Therefore this method has been adopted using a finite element program called Strand 7. The analyses comprise static and dynamic calculations. The structures and foundations must satisfy the requirements of statics before any dynamic analyses are carried out. Sensitivity analyses were carried out on the following variables:

- a) structure types (raft, table top and multi storey)
- b) soil parameters (shear modulus, G and Poisson's ratio, ν)
- c) stiffness of structure
- d) stiffness of foundations

3.2 Machine Parameters:

The machine comprises a compressor powered by a turbine having the parameters listed below. These parameters have been adopted in the design of the structures and foundations that follow. For the purposes of the study these parameters remain unchanged for the raft, table top and multi-storey cases to facilitate the sensitivity analyses of other variables such as structure types, soil parameters, stiffnesses of structures and foundations.

Total machine weight	= 667.23kN
Turbine speed	= 6949 rpm, $\omega = 727.7$ rad/sec
Compressor speed	= 6949 rpm
Turbine rotor weight	= 0.707kN
Amplitude of turbine force	= $(W/g) e \omega^2$ = 1.27 kN
Compressor rotor weight	= 19.25 kN
Amplitude of compressor force	= $(W/g) e \omega^2$ = 34.67kN

3.3 Analysis of Structures

Analysis of a dynamically loaded structure was carried out using the Finite Element program, Strand 7 to obtain the following:

1. Forces and deflections in members and joints for static loading to check if structure was statically safe.
2. Owing to the boundary conditions the non linear transient dynamic analysis has been used to determine natural frequencies of the structure, mode shapes, displacements and member forces at various time intervals (refer pA1.6). The main aim of the dynamic analysis was to ascertain possible resonance conditions, checking whether the natural frequencies coincide with the machine acting frequency. The technique used in the dynamic analysis is the full method not allowing for mode participation, resulting in the calculation of frequencies and mode shapes (refer pA1.5). Mode participation is generally used in linear, elastic modeling where the principle of superposition is valid with respect to mode shapes. In the full method the influence of other mode shapes are excluded with each mode being a separate entity. The masses of the structure and the machine have been lumped at the joints in the X, Y, Z directions. Rotational inertia has been neglected as noted by Arya et al (1984).

The axes are orientated as follows:

X – Longitudinal axis

Y – Vertical axis

Z – Transverse axis

Appendix A comprises a description of the analytical steps used in Strand 7 program. Whilst the output of the analyses contain stresses and reactions, emphasis is placed on dynamic parameters such as amplitude, frequency and velocity of vibration.

3.4 Load Combinations

3.4.1 Static Analysis

An equivalent static strength analysis of a structure supporting a centrifugal machine is usually made for the following loading conditions:

1. Total vertical load + 0.5 full load acting in the vertical direction.
2. Total vertical load + 0.3 full load acting in the vertical direction.
3. Total vertical load + 0.1 full load acting in the longitudinal direction.

According to Arya et al (1984) the above factors viz 0.5, 0.3 and 0.1 are considered appropriate for a machine with acting frequency of 1800 rpm and considered very stiff in the longitudinal direction, resulting in a safe structure

3.4.2 Dynamic Analysis

In the dynamic analysis the full dynamic loads are applied to the structure.

3.5 Soil Parameters

Soil parameters are known only within certain limits. It therefore becomes necessary to study the effects of variations of soil parameters viz. Poisson's ratio, ν and the shear modulus, G . The springs represent the resistance of soil to displacement in the vertical and horizontal directions. The spring stiffness is a function of the supporting soil properties and bearing area. The Poisson's ratio and shear modulus are used to calculate the spring constants (refer Table 12.4). The analysis numbers have been referenced in terms of the shear modulus, G (in psi) eg. G4000 refers to a model having $G=4000$ psi. The range over which the soil parameter have been varied are applicable to conditions accounted in practice.

3.6 Dynamic Forcing Function

The forcing functions in the vertical (Y) and transverse (Z) directions were applied at the nodes at which they occurred as node loads and include a force amplitude equal to the unbalanced machine force, a frequency ie acting machine frequency and a phase angle for the transverse function to simulate rotating loads. The dynamic forcing functions were applied at the centerline of the machine shaft and were the same for all the analyses.

3.7 Time Periods

As a minimum requirement the integration time period is 12 steps per single complete operating frequency cycle to achieve approximately 5% accuracy in the results. The structure was initially excited for 50 complete cycles. The number of cycles were increased due to higher amplitudes occurring beyond the 50th cycle. The structure has been modeled for 291 complete cycles with 12 steps in each cycle. According to Arya et al (1984) 3 complete cycles may be sufficient to study the response of the structure.

3.8 Types of Structures

In practice the raft, table top and multi-storey structures are commonly used to support vibrating machines. These structures have been analysed using the same machine parameters as follows:

3.8.1 Raft

The raft structure comprises mesh modeled as a plate at foundation level. The plinth has been modeled as beams, columns and plates. Both the structure and the machine masses are lumped at the joints of the structure in 3 linear directions. Rotational inertia has negligible effect on the results and therefore omitted. Sensitivity analyses have been conducted to examine the impact of thickness of foundation and section properties of the transverse plates. The analysis numbers in Table 10.1 have been referenced as follows:

G15 000-F1: the file extension "F1" denotes the first increment of increase with respect to foundation thickness. Each increment is approximately 305 mm. The purpose of

varying the foundation thickness was to ascertain the contribution of the foundation to the stiffness of structure with respect to vibration.

G15 000-p: the file extension "p" denotes the first increment of increase in the thickness of plate. Each increment is approximately 305 mm.

G15 000p-F1: the file extension "p-F1" denotes the first increment of increase in thickness of foundation in the plate model. Each increment of foundation thickness is approximately 305 mm. Figure 20 represents the typical model used in the finite element analysis.

3.8.2 Table Top

The table top structure comprises a foundation (mat) modeled as a plate in the same manner as the raft foundation. The mat supports the superstructure consisting of columns and beams. Sensitivity analyses have been conducted to examine the impact of the section properties of the transverse beams and the columns. Figure 21 represents the typical model used in the finite element analysis. The analysis numbers in Table 10.2 have been referenced as follows:-

G15 000-F1: the file extension "F1" denotes the first increment of increase with respect to foundation thickness. Each increment is approximately 305 mm.

G15000-B1: the file extension "B1" denotes the first increment of increase with respect to beam depth. Each increment is approximately 305 mm. The purpose of varying the beam and column depths was to ascertain the contribution of the beams and columns to the stiffness of structure with respect to vibration. The beam depth varied independently of the column depth so that the benefit of each parameter contributing to the increased stiffness could be established. In carrying out the variations it was also important to compare the change in amplitudes and velocities of vibration. Sensitivity analyses are also carried out in practice to produce efficient structures and foundations.

G15000-C1: the file extension "C1" denotes the first increment of increase with respect to column depth (in the transverse direction). Each increment is approximately 305 mm. In addition to the above the following needs to be noted:

G15000-mdof: the file extension "mdof" denotes a multi mass system, G15000-stf: the file extension "stf" denotes an infinitely stiff structure. The resulting response is a measure of the amplitude of vibration sustained by the soil. G15000-ps and G15000-fs: the extension "ps" denotes pinned support whilst "fs" denotes fixed support and are measures of the structure's contribution to the amplitude of vibration. The above comments also apply to the multi-storey structures.

3.8.3 Multi-storey Structure

The multi-storey structure is an extension of the table top structure comprising 2 storeys of equal height. The structure is modeled in a similar manner as the table top, for ease of comparison between the table top and multi-storey structure the section properties of the respective beams and columns have been kept the same. Figure 22 represents the typical model used in the finite element analysis.

CHAPTER 4: RESULTS

4.1 Introduction

The results produced by Strand 7 have been presented using both tables and graphs. The nodal displacements and velocities with respect to time was best shown as graphs due to the volume of data (refer Appendices B, C and D). The maximum amplitudes and velocities were obtained from the graphs. In all cases the maximum amplitudes and velocities occur at Node 20 which is in the super-structure. The maximum amplitudes and velocities in the foundations occur at Node 8. The results for both these nodes have been included. Tables 10.1, 10.2 and 10.3 present the natural frequencies, maximum amplitudes, maximum velocities, masses, mass ratios and centres of gravity of the structures and foundations. The mass ratio was based on the mass of the structure and foundation to the mass of the machine. These tables are comprehensive in that the amplitudes are classified in terms of vibration performance and the velocities are classified in terms of machine operation. Tables 11.1, 11.2 and 11.3 comprise the first 10 modes of natural frequencies for the various types of structures and foundations.

4.2 Use of Results in Design

The results may be tabled as follows:

4.2.1 Static Member Forces:

Axial forces, shear and moments at each member are given for each loading condition. Members and deflections are checked for maximum applied loads. At this stage longitudinal reinforcement is selected based on force and moment and transverse reinforcement is selected based on shear.

4.2.2 Displacements Under Static Loads

Displacements of joints (at supports and nodes) are compared to acceptable limits, based on piping and equipment.

4.2.3 Natural Frequencies

The first 10 natural frequencies are tabulated. Each frequency corresponds to a mode shape. The acting machine frequency = $727.7 \text{ rads/sec} = 6949 \text{ rpm}$ or 115.8 cycles/sec , the 10 natural frequencies for the structure are well below the acting frequency. The structure is therefore said to be under tuned. To avoid resonance during machine operation the natural frequencies should be less than 80% (92.64 cycles/sec) or greater than 120% ($138.96 \text{ cycles/sec}$) the compressor frequency. At preliminary design stage the natural frequencies of columns and beams should be checked for any resonant condition. During start up the machine passes through resonant conditions where the machine frequencies coincide with that of the structure. However, this study deals with the instantaneous operating frequency.

4.2.4 Mode Shapes

Mode shapes are characterized by Eigenvalues and vectors during the calculation of natural frequencies.

4.2.5 Dynamic Displacements

Maximum displacements of the structure have been tabulated (refer Table 10). In all 3 types of structures joint 20 has the maximum displacements, occurring at varying times. The maximum amplitude of displacement is compared with the vibration performance plotted on Figure 23 at the given machine frequency of 6949 rpm .

A complete set of input information together with output results have been attached in Appendix A2.

4.2.6 Dynamic Velocities

Maximum velocities of the structure have been tabulated (refer Table 10). In all 3 types of structures joint 20 has the maximum velocities, occurring at varying times.

For the intents and purposes of this dissertation only the dynamic response of the foundations and structures shall be examined. The dynamic responses include natural frequencies, dynamic displacements or amplitude and dynamic velocities. It should be noted that the static response is an integral component of the design.

CHAPTER 5: DISCUSSIONS AND INTERPRETATIONS

5.1 Introduction

The results referred to in chapter 4 need to be processed in line with the objectives of the study. This chapter comprises comparative studies of the following:

- 5.2: effect of soil properties
- 5.3: effect of foundation thickness
- 5.4: effect of beam versus plate model
- 5.5: effect of foundation thickness on the plate model
- 5.6: effect of modeling machine as a multi-mass system
- 5.7: effect of transverse beam section properties
- 5.8: effect of column section properties
- 5.9: natural frequencies based on variation of soil properties
- 5.10: type of structures

The above studies have been carried out separately for each type of structure. The amplitudes and velocities of vibration have been separated into their vertical and transverse components. The natural frequencies do not vary significantly with respect to items 5.2 to 5.8 above. (refer Tables 10.1, 10.2 and 10.3). Therefore the effect of natural frequencies has been based on soil properties.

The unit of amplitudes is inches (in) and velocity is inches per second (in/s). These units have been based on those appearing in Figure 23 and the classification of machine operation (Baxter and Bernhard, 1967). The performance descriptions that follow for the amplitudes and velocities of vibrations are based on the above.

5.2 Effect of Soil Properties

5.2.1 Raft

5.2.1.1 Vertical Amplitude of Vibration (D_y)

The vertical amplitude from Table 10.1 varies as follows:

Analysis No	Reference Figures (Appendix B)	Amplitude (in)	Performance	Amplitude – infinitely Stiff Structure (in)
G4 000	B1.1	0.000308	B	0.000405
G10 000	B2.1	0.000697	C	0.000301
G15 000	B3.1	0.000834	C	0.000222
G20 000	B4.1	0.001646	E	0.000250
G30 000	B5.1	0.000680	C	0.000246

There is a general increase in the vertical amplitude as the supporting soil conditions improve, with the exception of G30 000 where there is 42% decrease. In all cases the waveforms are complex, indicating the presence of vibrations of several frequencies acting simultaneously. A vibration beat is apparent in the case of G20 000, having a period of approximately 1.44 seconds. With the exception of G20 000 the performance of the structure together with the supporting soil is within the "minor faults" to "faulty" range. The contribution of the soil properties to the total vibration in each case can be seen when comparing the responses of the infinitely stiff structure to the structure modeled (having finite stiffness). Since the response is based on non-linear analyses a direct difference between the respective amplitudes will not result in the contribution of the structure itself to the amplitude of vibration. It can be seen that in the cases of weaker soil, the soil properties contribute significantly (G4 000 and G10 000) to the amplitude of vibration.

5.2.1.2 Transverse Amplitude of Vibration (D_z)

The transverse amplitude from Table 10.1 varies as follows:

Analysis No	Reference Figures (Appendix B)	Amplitude (in)	Performance	Amplitude – infinitely Stiff Structure (in)
G4 000	B1.2	0.000204	B	0.000186
G10 000	B2.2	0.000148	A	0.000095
G15 000	B3.2	0.000156	A	0.000115
G20 000	B4.2	0.000175	A	0.000142
G30 000	B5.2	0.000191	A	0.000153

There is 38% decrease in the amplitude of vibration when comparing G4 000 and G10 000 after which it gradually increases as the supporting soil conditions improve. The amplitudes resulting from infinitely stiff structure does not differ drastically from the actual model having finite stiffness. The variation in the soil properties therefore does not affect the response of the structure in the transverse direction. The performance of the structure together with the supporting soil is within “minor faults” range. In all cases the waveforms are complex, indicating the presence of vibrations of several frequencies acting simultaneously.

5.2.1.3 Vertical and Transverse Velocities of Vibration (V_y and V_z)

The vertical and transverse velocities from Table 10.1 varies as follows:

Analysis No	Reference Figures (Appendix B)	V_y (in/s)	V_z (in/s)
G4 000	B1.3 & B1.4	0.113	0.146
G10 000	B2.3 & B2.4	0.200	0.094
G15 000	B3.3 & B3.4	0.249	0.065
G20 000	B4.3 & B4.4	0.526	0.061
G30 000	B5.3 & B5.4	0.210	0.068

The vertical velocity increases with the stiffer soil conditions, with the exception of G30 000. However the velocity in the transverse direction generally decreases with stiffer soil conditions, again with the exception of G30 000. In terms of machine operation the performance lies in the “slightly rough” to “rough” range (in the vertical

direction) and in the "fair" range (in the transverse direction). The waveforms are complex and being the first derivative of displacement exhibits similar waveforms and trends as the displacement response.

5.2.2 Table Top

5.2.2.1 Vertical Amplitude of Vibration (D_v)

The vertical amplitude from Table 10.2 varies as follows:

Analysis No	Reference Figures (Appendix C)	Amplitude (in)	Performance	Amplitude – infinitely Stiff Structure (in)
G4 000	C1.1	0.001954	E	0.000314
G10 000	C2.1	0.001654	E	0.000228
G15 000	C3.1	0.002204	E	0.000192
G20 000	C4.1	0.011939	E	0.000192
G30 000	C5.1	0.019521	E	0.000160

The amplitude of vibration initially decreases (G4 000 to G10 000) before increasing progressively as the supporting soil conditions improve. The contribution of the soil properties to the amplitude of vibration is minimal when comparing the response of the infinitely stiff structure to the model. This implies that the stiffness of the structure plays a significant role in the response to vibration. In all cases the waveforms are complex, indicating the presence of vibrations of several frequencies acting simultaneously. A vibration beat is apparent in the case of G20 000 and G30 000 each having a period of 3.72 and 3.26 seconds respectively.

5.2.2.2 Transverse Amplitude of Vibration (D_z)

The transverse amplitude from Table 10.2 varies as follows:

Analysis No	Reference Figures (Appendix C)	Amplitude (in)	Performance	Amplitude – infinitely Stiff Structure (in)
G4 000	C1.2	0.000438	B	0.000262
G10 000	C2.2	0.020210	E	0.000223
G15 000	C3.2	0.015434	E	0.000206
G20 000	C4.2	0.007266	E	0.000201
G30 000	C5.2	0.002313	E	0.000168

Except for G4 000 the amplitude of vibration decreases as the soil conditions improve. In the case of G4 000 the soil properties contribute approximately 60% to the total amplitude of vibration but thereafter the stiffness of the structure becomes significant. In all cases the waveforms are complex, indicating the presence of vibrations of several frequencies acting simultaneously. A vibration beat is apparent in the case of G15 000 and G20 000, each having a period of 8.05 and 3.22 seconds respectively.

5.2.2.3 Vertical and Transverse Velocities of Vibration (V_y and V_z)

The vertical and transverse velocities from Table 10.2 vary as follows:

Analysis No	Reference Figures (Appendix C)	V_y (in/s)	V_z (in/s)
G4 000	C1.3 & C1.4	0.571	0.079
G10 000	C2.3 & C2.4	0.188	2.590
G15 000	C3.3 & C3.4	0.291	1.897
G20 000	C4.3 & C4.4	1.523	0.894
G30 000	C5.3 & C5.4	2.680	0.248

There are no consistent trends with respect to velocities in the vertical direction. However except for G4 000 the velocity decreases as the soil properties improve. In terms of the machine operation the performance generally lies in the “rough” to “very rough” range (with the exception of four cases that lie in the “fair” to “slightly rough” range).

5.2.3 Multi-storey

5.2.3.1 Vertical Amplitude of Vibration (D_y)

The vertical amplitude from Table 10.3 varies as follows:

Analysis No	Reference Figures (Appendix D)	Amplitude (in)	Performance	Amplitude – infinitely Stiff Structure (in)
G4 000	D1.1	0.001757	E	0.000251
G10 000	D2.1	0.001285	C	0.000181
G15 000	D3.1	0.001169	C	0.000143
G20 000	D4.1	0.001344	C	0.000139
G30 000	D5.1	0.001747	E	0.000128

The amplitude decreases up to G15 000 before increasing again. The stiffness of the structure plays a significant role in response to vibration. In all cases the waveforms are complex, indicating the presence of vibrations of several frequencies acting simultaneously. In terms of machine operation the performance generally lies in the “faulty” range except for G4 000 and G30 000 which is in the “dangerous” range.

5.2.3.2 Transverse Amplitude of Vibration (D_z)

The transverse amplitude from Table 10.3 varies as follows:

Analysis No	Reference Figures (Appendix D)	Amplitude (in)	Performance	Amplitude – infinitely Stiff Structure (in)
G4 000	D1.2	0.000049	A	0.000061
G10 000	D2.1	0.000464	B	0.000258
G15 000	D3.2	0.000438	B	0.000236
G20 000	D4.2	0.000045	A	0.000048
G30 000	D5.2	0.000423	B	0.000223

The amplitudes of vibration vary randomly, the highest occurring in G10 000. The stiffness of the structure contributes to more than 50% of the amplitude of vibration. In all cases the waveforms are complex, indicating the presence of vibrations of several frequencies acting simultaneously.

5.2.3.3 Vertical and Transverse Velocities of Vibration (V_y and V_z)

The vertical and transverse velocities from Table 10.3 vary as follows:

Analysis No	Reference Figures (Appendix D)	V_y (in/s)	V_z (in/s)
G4 000	D1.3 & D1.4	0.499	0.072
G10 000	D2.3 & D2.4	0.373	0.079
G15 000	D3.3 & D3.4	0.325	0.071
G20 000	D4.3 & D4.4	0.373	0.070
G30 000	D5.3 & D5.4	0.500	0.068

There are no apparent trends with regards to velocities in the vertical and transverse directions. The vertical velocities are much higher than the transverse direction. The transverse velocities are similar in magnitude. The machine performance in terms of velocity is "rough" in the vertical direction but "fair" in the transverse direction.

5.3 Effect of Foundation Thickness

5.3.1 Raft

5.3.1.1 Vertical Amplitude of Vibration (D_y)

The vertical amplitude varies from Table 10.1 as follows:

Analysis No	Reference Figures (Appendix B)	Amplitude (in)	Performance
G15 000	B3.1	0.000834	C
G15 000 – F1	B3.7	0.000834	C
G15 000 – F2	B3.13	0.001113	C
G15 000 – F3	B3.19	0.000241	A
G15 000 – F4	B3.25	0.000733	C

There are no apparent trends in the amplitude of vibration. G15 000 – F2 has the highest amplitude. In all cases the waveforms are complex, indicating the presence of vibrations of several frequencies acting simultaneously. In terms of the machine

performance, the amplitudes lie within the zone of “no faults” to “failure is near”. The most suitable foundation thickness appears to be in the region of G15 000 – F3 where the performance is acceptable.

5.3.1.2 Transverse Amplitude of Vibration (D_z)

The transverse amplitude from Table 10.1 varies as follows:

Analysis No	Reference Figures (Appendix B)	Amplitude (in)	Performance
G15 000	B3.2	0.000156	A
G15 000 – F1	B3.8	0.000156	A
G15 000 – F2	B3.14	0.000160	A
G15 000 – F3	B3.20	0.004610	E
G15 000 – F4	B3.26	0.000226	B

The amplitude of vibration increases as the thickness of the foundation increases but reduces sharply at G15 000 – F4. In all cases the waveforms are complex, indicating the presence of vibrations of several frequencies acting simultaneously. In terms of the machine performance, the amplitudes lay within the zone of “minor faults”, with the exception of G15 000 – F3 which lies in the “dangerous ” zone. G15 000 – F3 appears to be the point at which increase in the foundation thickness also increases the vertical lever -arm between the centre line of the rotating shaft and the bottom of the foundation.

5.3.1.3 Vertical and Transverse Velocities of Vibration (V_y and V_z)

The vertical and transverse amplitude from Table 10.1 varies as follows:

Analysis No	Reference Figures (Appendix B)	$V_y(\text{in/s})$	$V_z(\text{in/s})$
G15 000	B3.3 & B 3.4	0.249	0.065
G15 000 – F1	B3.9 & B3.10	0.249	0.065
G15 000 – F2	B3.15 & B3.16	0.360	0.066
G15 000 – F3	B3.21 & B 3.22	0.035	0.153
G15 000 – F4	B3.27 & B3.28	0.253	0.094

The velocities in the vertical and transverse directions vary randomly and are generally within the “slightly rough “ range. The vertical velocities are much higher than the transverse velocities and will therefore govern critical performance.

5.3.2 Table Top

5.3.2.1 Vertical Amplitude of Vibration (D_y)

The vertical amplitude from Table 10.2 varies as follows:

Analysis No	Reference Figures (Appendix C)	Amplitude (in)	Performance
G15 000	C3.1	0.002204	E
G15 000 – F1	C3.75	0.011138	E
G15 000 – F2	C3.81	0.001471	D
G15 000 – F3	C3.87	0.000760	C
G15 000 – F4	C3.93	0.000530	B

There is a sharp increase between G15 000 and G15 000 – F1 after which amplitude decreases. The increase in the foundation thickness tends to reduce the amplitude, changing the machine performance from a “dangerous” to “minor fault” zone. In all cases the waveforms are complex, indicating the presence of vibrations of several frequencies acting simultaneously. A vibration beat is evident in the case of G15 000 – F1, having a period of approximately 4.74 seconds. The waveforms are repetitive in the case of G15 000 – F2.

5.3.2.2 Transverse Amplitude of Vibration (D_z)

The transverse amplitude from Table 10.2 varies as follows:

Analysis No	Reference Figures (Appendix C)	Amplitude (in)	Performance	Vibration Beat (seconds)
G15 000	C3.2	0.015434	E	8.05
G15 000 – F1	C3.76	0.006078	E	2.62
G15 000 – F2	C3.82	0.004587	E	2.07
G15 000 – F3	C3.88	0.004284	E	1.84
G15 000 – F4	C3.94	0.003792	E	1.15

The amplitude of vibration decreases as the foundation thickness increases. However the reduction in amplitude is not sufficient to make safe the performance of the structure. As noted previously increasing the thickness of the foundation also increases the excitation force by virtue of the additional vertical lever arm. This implies that a threshold will be reached beyond which no significant benefit will be derived from foundation thickness. In all cases vibration beats are evident (refer table above) and decreases with increasing thickness of foundation. The waveforms are complex indicating the presence of vibrations of several frequencies acting simultaneously.

5.3.2.3 Vertical and Transverse Velocities of Vibration (V_y and V_z)

The vertical and transverse velocities from Table 10.2 vary as follows:

Analysis No	Reference Figures (Appendix C)	V_y (in/s)	V_z (in/s)
G15 000	C3.3 & C3.4	0.291	1.897
G15 000 – F1	C3.77 & C3.78	1.412	0.754
G15 000 – F2	C3.83 & C3.84	0.208	0.572
G15 000 – F3	C3.89 & C3.90	0.104	0.530
G15 000 – F4	C3.95 & C3.96	0.071	0.467

With the exception of the vertical velocity in the case of G15 000, the vertical and transverse velocities generally decrease as the foundation thickness increases. The waveforms are complex and being the first derivative of displacement have similar waveforms (including beats). In terms of the machine performance, the velocities vary

erratically from “slightly rough” to “very rough”. The transverse velocities govern the performance of the structure.

5.3.3 Multi-storey

5.3.3.1 Vertical Amplitude of Vibration (D_y)

The vertical amplitude from Table 10.3 varies as follows:

Analysis No	Reference Figures (Appendix D)	Amplitude (in)	Performance
G15 000	D3.1	0.001169	C
G15 000 – F1	D3.61	0.001568	E
G15 000 – F2	D3.67	0.001088	C
G15 000 – F3	D3.73	0.001088	C
G15 000 – F4	D3.79	0.000885	C

Generally the amplitude decreases as the foundation thickness increases (except for G15 000). The vibration performance is generally within the “faulty” range. In all cases the waveforms are complex, indicating the presence of vibrations of several frequencies acting simultaneously.

5.3.3.2 Transverse Amplitude of Vibration (D_z)

The transverse amplitude from Table 10.3 varies as follows:

Analysis No	Reference Figures (Appendix D)	Amplitude (in)	Performance
G15 000	D3.2	0.000438	B
G15 000 – F1	D3.62	0.000434	B
G15 000 – F2	D3.68	0.000458	B
G15 000 – F3	D3.74	0.000458	B
G15 000 – F4	D3.80	0.000436	B

There are no significant changes in the amplitude and hence no benefit in increasing the thickness of the foundation with respect to the transverse vibration.

5.3.3.3 Vertical and Transverse Velocities of Vibration (V_y and V_z)

The vertical and transverse velocities from Table 10.3 vary as follows:

Analysis No	Reference Figures (Appendix D)	V_y (in/s)	V_z (in/s)
G15 000	D3.3 & D3.4	0.325	0.071
G15 000 – F1	D3.63 & D3.64	0.447	0.070
G15 000 – F2	D3.69 & D3.70	0.315	0.067
G15 000 – F3	D3.75 & D3.76	0.315	0.068
G15 000 – F4	D3.81 & D3.82	0.268	0.072

The vertical velocity generally decreases as the foundation thickness increases (except for G15 000), whilst the transverse velocity is fairly constant and insensitive to foundation thickness. This implies that the vertical velocity governs the performance of the structure. All the transverse velocities lie in the “fair ” zone whilst the vertical velocities range from “slightly rough” to “rough”.

5.4 Effect of Beam vs Plate Model

These studies were carried out on the raft model only. The plinth is usually a solid mass of concrete cast with the foundation. Modeling the plinth as beams and columns will be conservative as the beam will deflect more than the real case. The plate model is a stiffer model and is closer to the real behaviour than the beam model. The study that follows will be used to verify the above.

5.4.1 Raft

5.4.1.1 Vertical Amplitude of Vibration (D_y)

The vertical amplitude from Table 10.1 varies as follows:

Analysis No	Reference Figures (Appendix B)	Amplitude (in)	Performance
G15 000	B3.1	0.000834	C
G 15 000 - p	B3.43	0.000525	B
G15 000 – p1	B3.49	0.000541	B
G15 000 – p2	B3.55	0.000500	B
G15 000 – p3	B3.61	0.000360	B

The amplitude of vibration decreases when comparing the beam to the plate model and is indicative of stiffer response from the plates. Furthermore when the thickness of plates is increased the amplitude of vibration reduces. The plate model is a more accurate representation of the structure. The vibration performance improves from being in the “faulty” to the “minor faults” zone. The waveforms are repetitive and are complex, indicating the presence of vibrations of several frequencies acting simultaneously.

5.4.1.2 Transverse Amplitude of Vibration (D_z)

The transverse amplitude from Table 10.1 varies as follows:

Analysis No	Reference Figures (Appendix B)	Amplitude (in)	Performance
G15 000	B3.2	0.000156	A
G 15 000 - p	B3.44	0.000137	A
G15 000 – p1	B3.50	0.000165	A
G15 000 – p2	B3.56	0.000209	A
G15 000 – p3	B3.62	0.000344	B

The amplitude of vibration initially decreases before increasing. The machine performance remains predominantly in the “no faults” zone, with the exception of

G15 000 – p3. The waveforms are complex, indicating the presence of vibrations of several frequencies acting simultaneously. The waveform for G15 000 – p3 repeats itself approximately every 0.36 seconds.

5.4.1.3 Vertical and Transverse Velocities of Vibration (V_y and V_z)

The vertical and transverse velocities from Table 10.1 vary as follows:

Analysis No	Reference Figures (Appendix B)	V_y (in/s)	V_z (in/s)
G15 000	B3.3 & B3.4	0.249	0.065
G 15 000 - p	B3.45 & B3.46	0.122	0.051
G15 000 – p1	B3.51 & B3.52	0.148	0.047
G15 000 – p2	B3.57 & B3.58	0.125	0.062
G15 000 – p3	B3.63 & B 3.64	0.077	0.107

The vertical velocities generally decrease as the plate thickness increases (except for G15 000 p). The transverse velocities initially decrease but increases for the stiffer plate models, suggesting that the benefit of stiffer plates has a threshold. The vertical velocities lie in the “fair” to “slightly rough” zone whilst the transverse velocities lie in the “fair” zone. The waveforms are repetitive in some cases and in all cases complex, indicating the presence of vibrations of several frequencies acting simultaneously.

5.5 Effect of Foundation Thickness on the Plate Model

5.5.1 Raft

5.5.1.1 Vertical amplitude of Vibration (D_y)

The vertical amplitude from Table 10.1 varies as follows:

Analysis No	Reference Figure	Amplitude (in)	Performance
G15 000 p	B3.43	0.000525	C
G15 000 p-F1	B3.67	0.000311	B
G15 000 p-F2	B3.73	0.000211	A
G15 000 p-F3	B3.79	0.000241	A
G15 000 p-F4	B3.85	0.000144	A

The amplitude of the vibration decreases as the foundation thickness increases. This trend exists up to G15 000 p-F2. Thereafter there are no significant changes. The most suitable foundation thickness is at G15 000 p-F4. The performance changes from “faulty” to “no faults”. The waveforms are repetitive in some cases and in all cases complex, indicating the presence of vibrations of several frequencies acting simultaneously.

5.5.1.2 Transverse Amplitude of Vibration(D_z)

The transverse amplitude from Table 10.1 varies as follows:

Analysis No	Reference Figure	Amplitude (in)	Performance
G15 000 p	B3.44	0.000137	A
G15 000 p-F1	B3.68	0.000119	A
G15 000 p-F2	B3.74	0.000143	A
G15 000 p-F3	B3.80	0.000461	B
G15 000 p-F4	B3.86	0.000090	A

The amplitude vary randomly and remains predominantly in the “no faults” zone, except for G15 000 p-F3. Hence there is no significant benefit in increasing the foundation thickness. The waveforms are repetitive in some cases and in all cases complex, indicating the presence of vibrations of several frequencies acting simultaneously.

5.5.1.3 Vertical and Transverse Velocities of Vibration (V_y and V_z)

The vertical and transverse velocities from Table 10.1 vary as follows:

Analysis No	Reference Figure	V_y (in/s)	V_z (in/s)
G15 000 p	B3.45 & B3.46	0.122	0.051
G15 000 p-F1	B3.69 & B3.70	0.070	0.054
G15 000 p-F2	B3.75 & B3.78	0.053	0.075
G15 000 p-F3	B3.81 & B3.82	0.035	0.153
G15 000 p-F4	B3.87 & B3.88	0.036	0.051

The vertical velocities decrease as the foundation thickness increases. However the velocities vary randomly in the transverse direction. All the velocities lie in the “fair” zone of performance and therefore indicate that there is no significant benefit in increasing the foundation thickness. The waveforms are repetitive in some cases and in all cases complex, indicating the presence of vibrations of several frequencies acting simultaneously.

5.6 Effect of Modeling Machine as Multi Mass System

5.6.1 Raft

5.6.1.1 Vertical Amplitude of Vibration (D_y)

The vertical amplitude from Table 10.1 varies as follows:

Analysis No	Reference Figures (Appendix B)	Amplitude (in)	Performance
G4 000	B1.1	0.000308	B
G4 000 mdof	B1.37	0.000262	B
G10 000	B2.1	0.000697	C
G10 000 mdof	B2.7	0.000606	C
G15 000	B3.1	0.000834	C
G15 000 mdof	B3.31	0.000605	C
G20 000	B4.1	0.001646	E
G20 000 mdof	B4.7	0.000705	C
G30 000	B5.1	0.000680	C
G30 000 mdof	B5.7	0.000519	B

In general the multi-mass system results in lower amplitudes of vibration. The vibration performance ranges from "minor faults" to "faulty". It is only in the case of G20 000 where the multi-mass system improves the performance from "dangerous" to "faulty". The waveforms are repetitive in some cases and in all cases complex, indicating the presence of vibrations of several frequencies acting simultaneously.

5.5.1.2 Transverse Amplitude of Vibration (D_z)

The transverse amplitude from Table 10.1 varies as follows:

Analysis No	Reference Figures (Appendix B)	Amplitude (in)	Performance
G4 000	B1.2	0.000204	B
G4 000 mdof	B1.38	0.000360	B
G10 000	B2.2	0.000148	A
G10 000 mdof	B2.8	0.000142	A
G15 000	B3.2	0.000156	A
G15 000 mdof	B3.32	0.000138	A
G20 000	B4.2	0.000175	A
G20 000 mdof	B4.8	0.000518	B
G30 000	B5.2	0.000191	A
G30 000 mdof	B5.8	0.000157	A

The amplitudes vary randomly whilst the vibration performance ranges between the “no faults” and “minor faults” zone. The waveforms are repetitive in most cases and are complex in all cases, indicating the presence of vibrations of several frequencies acting simultaneously.

5.5.1.3 Vertical and Transverse Velocities of Vibration (V_y and V_z)

The vertical and transverse velocities from Table 10.1 vary as follows:

Analysis No	Reference Figures (Appendix B)	$V_y(\text{in/s})$	$V_z(\text{in/s})$
G4000	B1.3 & B1.4	0.113	0.146
G4000 mdof	B1.39 & B1.40	0.063	0.271
G10 000	B2.3 & B 2.4	0.200	0.094
G10 000 mdof	B2.9 & B2.10	0.197	0.079
G15 000	B3.3 & B3.4	0.249	0.065
G15 000 mdof	B3.33 & B3.34	0.229	0.064
G20 000	B4.3 & B4.4	0.526	0.061
G20 000 mdof	B4.9 & 4.10	0.150	0.173
G30 000	B5.3 & B5.4	0.210	0.068
G30 000 mdof	B5.9 & B5.10	0.174	0.068

Generally the velocities decrease when comparing the single to the multi mass system. (except for the transverse velocity for G20 000 and G20 000 mdof). In terms of the machine operation the velocities lie between the “fair” and “slightly rough” zone, again with the exception of G20 000. The waveforms are repetitive in most cases and are complex in all cases, indicating the presence of vibrations of several frequencies acting simultaneously.

5.6.2 Table Top

5.6.2.1 Vertical Amplitude of Vibration (D_y)

The vertical amplitude of vibration from Table 10.2 varies as follows:

Analysis No	Reference Figures (Appendix C)	Amplitude (in)	Performance
G4 000	C1.1	0.001954	E
G4 000 mdof	C1.5	0.003884	E
G10 000	C2.1	0.001654	E
G10 000 mdof	C2.7	0.002463	E
G15 000	C3.1	0.002204	E
G15 000 mdof	C3.105	0.002669	E
G20 000	C4.1	0.011939	D
G20 000 mdof	C4.7	0.011929	D
G30 000	C5.1	0.019521	E
G30 000 mdof	C5.7	0.001580	E

There is generally an increase in the amplitude, with the exception of G20 000 and G30 000, However the vibration performance remains in the respective zones. The waveforms are repetitive in most cases and are complex in all cases, indicating the presence of vibrations of several frequencies acting simultaneously.

5.6.2.2 Transverse Amplitude of Vibration (D_z)

The transverse amplitude of vibration from Table 10.2 varies as follows:

Analysis No	Reference Figures (Appendix C)	Amplitude (in)	Performance
G4000	C1.2	0.000438	B
G4000 mdof	C1.6	0.000421	B
G10 000	C2.2	0.020210	E
G10 000 mdof	C2.8	0.000437	B
G15 000	C3.2	0.015434	E
G15 000 mdof	C3.106	0.000277	B
G20 000	C4.2	0.007266	E
G20 000 mdof	C4.8	0.009668	E
G30 000	C5.2	0.002313	E
G30 000 mdof	C5.8	0.000461	B

Generally the amplitude decreases when comparing the respective models (except for G20 000). The reduction in amplitude is significant for G10 000, G15 000 and G30 000. G20 000 is the only case where both the single and multi-mass models have vibration beats of 3.44 and 5.29 seconds respectively. The waveforms are complex in all cases, indicating the presence of vibrations of several frequencies acting simultaneously.

5.6.2.3 Vertical and Transverse Velocities of Vibration (V_y and V_z)

The vertical and transverse velocities from Table 10.2 vary as follows:

Analysis No	Reference Figures (Appendix C)	V_y (in/s)	V_z (in/s)
G4 000	C1.3 & C1.4	0.571	0.079
G4 000 mdof	C1.7 & C1.8	1.253	0.083
G10 000	C2.3 & C2.4	0.188	2.590
G10 000 mdof	C2.9 & C2.10	0.795	0.086
G15 000	C3.3& C3.4	0.291	1.897
G15 000 mdof	C3.107 & C3.108	0.836	0.070
G20 000	C4.3 & C4.4	1.523	0.894
G20 000 mdof	C4.9 & C4.10	1.487	1.170
G30 000	C5.3 & C5.4	2.680	0.248
G30 000 mdof	C5.9 & C5.10	0.525	0.088

The velocities vary randomly when comparing the respective soil conditions. The waveforms are repetitive in most cases and complex in all cases, indicating the presence of vibrations of several frequencies acting simultaneously.

5.6.3 Multi-storey

5.6.3.1 Vertical Amplitude of Vibration (D_y)

The vertical amplitude of vibration from Table 10.3 varies as follows:

Analysis No	Reference Figures (Appendix D)	Amplitude (in)	Performance
G4 000	D1.1	0.001757	E
G4 000 mdof	D1.7	0.001028	C
G10 000	D2.1	0.001285	C
G10 000 mdof	D2.7	0.000983	C
G15 000	D3.1	0.001169	D
G15 000 mdof	D3.85	0.001751	E
G20 000	D4.1	0.001344	C
G20 000 mdof	D4.7	0.001957	E
G30 000	D5.1	0.001747	E
G30 000 mdof	D5.7	0.001782	E

The amplitude decreases in the weaker soil conditions (G4 000 and G10 000) but increases thereafter. The vibration performance lies between the “faulty” to “dangerous” zones. The waveforms in some cases are repetitive and in all cases complex, indicating the presence of vibrations of several frequencies acting simultaneously.

5.6.3.2 Transverse Amplitude of Vibration (D_z)

The transverse amplitude of vibration from Table 10.3 varies as follows:

Analysis No	Reference Figures (Appendix D)	Amplitude (in)	Performance
G4 000	D1.2	0.000049	A
G4 000 mdof	D1.8	0.000050	A
G10 000	D2.2	0.000464	B
G10 000 mdof	D2.8	0.000429	B
G15 000	D3.2	0.000438	B
G15 000 mdof	D3.86	0.000432	B
G20 000	D4.2	0.000045	A
G20 000 mdof	D4.8	0.000038	A
G30 000	D5.2	0.000423	B
G30 000 mdof	D5.8	0.000426	B

The amplitude decreases when comparing the single with multi-mass model, however the reduction is not significant. In terms of the machine vibration performance, the amplitude lies within the “no faults” and “minor faults” zone. The waveforms are complex, indicating the presence of vibrations of several frequencies acting simultaneously.

5.6.3.3 Vertical and Transverse Velocities of Vibration (V_y and V_z)

The vertical and transverse velocities from Table 10.3 vary as follows:

Analysis No	Reference Figures (Appendix D)	$V_y(\text{in/s})$	$V_z(\text{in/s})$
G4 000	D1.3 & D1.4	0.499	0.072
G4 000 mdof	D1.9 & D1.10	0.260	0.081
G10 000	D2.3 & D2.4	0.373	0.079
G10 000 mdof	D2.9 & D2.10	0.290	0.079
G15 000	D3.3 & 3.4	0.325	0.071
G15 000 mdof	D3.87 & D3.88	0.562	0.080
G20 000	D4.3 & D4.4	0.373	0.070
G20 000 mdof	D4.9 & D4.10	0.603	0.080
G30 000	D5.3 & D5.4	0.500	0.068
G30 000 mdof	D5.9 & D5.10	0.504	0.079

The vertical velocities initially decrease for the weaker soil conditions (G4 000 and G10 000) but increase thereafter. The transverse velocities do not change significantly and may be considered constant. The vibration performance in the vertical direction lies between "fair" and "rough" whilst the transverse velocities are all "fair". The waveforms in some cases are repetitive and in all cases complex, indicating the presence of vibrations of several frequencies acting simultaneously.

5.7 Effect of Transverse Beam Section Properties

The above effect is only applicable to the table top and multi-storey structures as the plinths in the raft structures have been modeled as plates in the transverse direction.

5.7.1 Table Top

5.7.1.1 Vertical Amplitude of Vibration (D_y)

The vertical amplitude of vibration from Table 10.2 varies as follows:

Analysis No	Reference Figures (Appendix C)	Amplitude (in)	Performance
G15 000	C3.1	0.002204	E
G 15 000 – B1	C3.21	0.002754	E
G15 000 – B2	C3.27	0.001907	E
G15 000 – B3	C3.33	0.000693	C
G15 000 – B4	C3.39	0.002294	E

The amplitude of vibration varies randomly. It is only at G15 000 – B3 where the benefit of stiffer transverse beam properties can be realized. At this point the vibration performance changes from “dangerous” to “faulty”. It appears that this point (G15 000-B3) is the turning point after which the amplitude continues to increase. The only case where the vibration beat emerges is G15 000-B2, having a period of approximately 1.89 seconds. In some cases the waveforms are repetitive whilst in all cases are complex, indicating the presence of vibrations of several frequencies acting simultaneously.

5.7.1.2 Transverse Amplitude of Vibration (D_z)

The transverse amplitude of vibration from Table 10.2 varies as follows:

Analysis No	Reference Figures (Appendix C)	Amplitude (in)	Performance
G15 000	C3.2	0.015434	E
G 15 000 – B1	C3.22	0.000743	C
G15 000 – B2	C3.28	0.000801	C
G15 000 – B3	C3.34	0.000378	B
G15 000 – B4	C3.40	0.003242	E

The amplitude of vibration varies randomly. As noted in the vertical direction it is only at G15 000-B3 where the benefit of stiffer transverse beam properties can be realized. The vibration performance changes from “faulty” to “minor faults”. There is a sharp increase beyond this point, indicating that there is a narrow band within which the benefit can be achieved. A vibration beat emerges only in the case of G15 000, having a period of 8.05 seconds. In all cases the waveforms are complex, indicating the presence of vibrations of several frequencies acting simultaneously.

5.7.1.3 Vertical and Transverse Velocities of Vibration (V_y and V_z)

The vertical and transverse velocities from Table 10.2 vary as follows:

Analysis No	Reference Figures (Appendix C)	V_y (in/s)	V_z (in/s)
G15 000	C3.3 & C3.4	0.291	1.897
G 15 000 – B1	C3.23 & C3.24	0.690	0.098
G15 000 – B2	C3.29 & C3.330	0.446	0.117
G15 000 – B3	C3.35 & C3.36	0.197	0.054
G15 000 – B4	C3.41 & C3.42	0.306	0.541

The vertical velocity decreases between G15 000-B1 to G15 000-B3. Whilst the transverse velocities vary randomly. Once again the cut off point appears to be G15 000-B3. The velocities vary between “fair” to “very rough”. In some cases the waveforms are repetitive and all cases the waveforms are complex, indicating the presence of vibrations of several frequencies acting simultaneously

5.7.2 Multi-storey

5.7.2.1 Vertical Amplitude of Vibration (D_y)

The vertical amplitude of vibration from Table 10.3 varies as follows:

Analysis No	Reference Figures (Appendix D)	Amplitude (in)	Performance
G15 000	D3.1	0.001169	D
G 15 000 – B1	D3.7	0.003046	E
G15 000 – B2	D3.13	0.001774	E
G15 000 – B3	D3.19	0.001087	C
G15 000 – B4	D3.24	0.001772	E

The vertical amplitude decreases between G15 000-B1 and G15 000-B3 and thereafter increases. As in the case of the tabletop structure, G15 000-B3 appears to be the cut off point where the benefit of stiff transverse beam emerges. At this point the vibration performance changes from “dangerous” to “faulty” before returning to “dangerous” again. Vibration beats emerge in G15 000-B1, G15 000-B2 and G15 000-B3 having periods of approximately 2.76, 1.49 and 1.95 seconds respectively. In some cases the waveforms are repetitive and all cases the waveforms are complex, indicating the presence of vibrations of several frequencies acting simultaneously.

5.7.2.2 Transverse Amplitude of Vibration (D_z)

The transverse amplitude of vibration from Table 10.3 varies as follows:

Analysis No	Reference Figures (Appendix D)	Amplitude (in)	Performance
G15 000	D3.2	0.000438	B
G 15 000 – B1	D3.8	0.000854	C
G15 000 – B2	D3.14	0.001503	E
G15 000 – B3	D3.20	0.000468	B
G15 000 – B4	D3.25	0.001742	E

There are no benefits in varying the section properties of the transverse beam when considering transverse amplitude. The waveforms are complex, indicating the presence of vibrations of several frequencies acting simultaneously.

5.7.2.3 Vertical and Transverse Velocities of Vibration (V_y and V_z)

The vertical and transverse velocities from Table 10.3 vary as follows:

Analysis No	Reference Figures (Appendix D)	$V_y(\text{in/s})$	$V_z(\text{in/s})$
G15 000	D3.3 & D3.4	0.325	0.071
G 15 000 – B1	D3.9 & D3.10	0.713	0.110
G15 000 – B2	D3.15 & D3.16	0.387	0.243
G15 000 – B3	D3.21 & D3.22	0.285	0.055
G15 000 – B4	D3.26 & D3.27	0.206	0.179

The vertical and transverse velocities vary randomly, the vertical velocities being greater in each case. The velocities range from “slightly rough” to “very rough” in the vertical direction and “fair” to “slightly rough” in the transverse direction. The waveforms are complex, indicating the presence of vibrations of several frequencies acting simultaneously.

5.8 Effect of Column Section Properties

5.8.1 Table Top

5.8.1.1 Vertical Amplitude of Vibration (D_y)

The vertical amplitude of vibration from Table 10.2 varies as follows:

Analysis No	Reference Figures (Appendix C)	Amplitude (in)	Performance
G15 000	C3.1	0.002204	E
G 15 000 – C1	C3.45	0.004493	E
G15 000 – C2	C3.51	0.002065	E
G15 000 – C3	C3.57	0.000899	C
G15 000 – C4	C3.63	0.002294	E
G15 000 – C5	C3.69	0.000665	C

The amplitude of vibration varies randomly, the only significant decreases emerging are for G15 000 - C3 and G15 000 – C5. At these two points the vibration performance changes from “dangerous” to “faulty”. Hence to examine the sensitivity of vibration with respect to column section properties these two points should be used as references. In some cases the waveforms are repetitive and in all cases the waveforms are complex, indicating the presence of vibrations of several frequencies acting simultaneously.

5.8.1.2 Transverse Amplitude of Vibration (D_z)

The transverse amplitude of vibration from Table 10.2 varies as follows:

Analysis No	Reference Figures (Appendix C)	Amplitude (in)	Performance
G15 000	C3.2	0.015434	E
G 15 000 – C1	C3.46	0.007008	E
G15 000 – C2	C3.52	0.000412	B
G15 000 – C3	C3.58	0.000401	B
G15 000 – C4	C3.64	0.003242	E
G15 000 – C5	C3.70	0.000299	B

The amplitude of vibration varies randomly. The only cases of significance are G15 000-C2, G15 000-C3 and G15 000-C5, where the vibration performance changes from "dangerous" to "minor faults". Vibration beats emerge in G15 000, G15 000-C1 and G15 000-C2 having periods of 8.05, 4.14 and 0.29 seconds respectively. In some cases the waveforms are repetitive and in all cases the waveforms are complex, indicating the presence of vibrations of several frequencies acting simultaneously.

5.8.1.3 Vertical and Transverse Velocities of Vibration (V_y and V_z)

The vertical and transverse velocities from Table 10.2 vary as follows:

Analysis No	Reference Figures (Appendix C)	V_y (in/s)	V_z (in/s)
G15 000	C3.3 & C3.4	0.291	1.897
G 15 000 – C1	C3.47 & C3.48	0.574	0.900
G15 000 – C2	C3.53 & C3.54	0.676	0.068
G15 000 – C3	C3.59 & C3.60	0.300	0.081
G15 000 – C4	C3.65 & C3.66	0.306	0.541
G15 000 – C5	C3.71 & C3.72	0.228	0.061

The velocities vary randomly, however there is a significant decrease in the transverse direction, which is expected as the stiffness in the transverse direction, increases, changing the vibration performance from "very rough" to "fair". In some cases the waveforms are repetitive and in all cases the waveforms are complex, indicating the presence of vibrations of several frequencies acting simultaneously.

5.8.2 Multi-storey

5.8.2.1 Vertical Amplitude of Vibration (D_y)

The vertical amplitude of vibration from Table 10.3 varies as follows:

Analysis No	Reference Figures (Appendix D)	Amplitude (in)	Performance
G15 000	D3.1	0.001169	C
G 15 000 – C1	D3.31	0.000892	C
G15 000 – C2	D3.37	0.001141	C
G15 000 – C3	D3.43	0.002778	E
G15 000 – C4	D3.49	0.000952	C
G15 000 – C5	D3.55	0.004322	E

The amplitude of vibration varies randomly, the only relatively significant decrease emerging are for G15 000-C1 and G15 000 – C4. At G15 000-C1 the vibration performance decreases but remains in the same performance range of “faulty” whilst in the case of G15 000-C4 the performance changes from “dangerous” to “faulty”. Hence the sensitivity of vibration with respect to column section properties pivots about these two points. Vibration beats emerge in the cases of G15 000-C1 and G15 000-C3, having periods of 3.33 and 3.75 seconds respectively. In some cases the waveforms are repetitive and in all cases the waveforms are complex, indicating the presence of vibrations of several frequencies acting simultaneously.

5.8.2.2 Transverse Amplitude of Vibration (D_z)

The transverse amplitude of vibration from Table 10.3 varies as follows:

Analysis No	Reference Figures (Appendix D)	Amplitude (in)	Performance
G15 000	D3.2	0.000438	B
G 15 000 – C1	D3.32	0.006623	E
G15 000 – C2	D3.38	0.000407	B
G15 000 – C3	D3.44	0.000719	C
G15 000 – C4	D3.50	0.000366	B
G15 000 – C5	D3.56	0.001982	E

There are only two points at which decreases in amplitudes results viz G15 000-C2 and G15 000-C4. These two cases could be used as references to test the sensitivity of varying column section properties. The waveforms are complex, indicating the presence of vibrations of several frequencies acting simultaneously.

5.8.2.3 Vertical and Transverse Velocities of Vibration (V_y and V_z)

The vertical and transverse velocities from Table 10.3 vary as follows:

Analysis No	Reference Figures (Appendix D)	V_y (in/s)	V_z (in/s)
G15 000	D3.3 & D3.4	0.325	0.071
G 15 000 – C1	D3.33. & D3.34	1.458	0.109
G15 000 – C2	D3.39 & D3.40	0.348	0.066
G15 000 – C3	D3.45 & D3.46	0.832	0.121
G15 000 – C4	D3.51 & D3.52	0.305	0.060
G15 000 – C5	D3.57 & D3.58	0.676	0.240

The velocities vary randomly, with vertical velocities exceeding the transverse velocities. The only case showing any benefit from the varying column section properties is G15 000-C4. In terms of the machine operation the vertical velocity lies in the “slightly rough” zone whilst the transverse velocity lies in the “fair” zone. The waveforms in all cases are complex, indicating the presence of vibrations of several frequencies acting simultaneously.

5.9 Natural Frequencies (f_n)

5.9.1 Effect of Soil Properties:

5.9.1.1 Raft

The natural frequencies (in Hz) from Table 11.1 vary as follows:

Analysis No	Mode 1	Mode 2	Mode 3	Mode 4	Mode 5	Mode 6	Mode 7	Mode 8	Mode 9	Mode 10
G4 000	7.48	7.52	8.52	8.71	9.47	10.35	26.19	34.77	46.95	56.21
G10 000	11.85	11.85	13.47	13.78	15.00	16.34	28.89	35.10	36.57	46.70
G15 000	13.90	13.91	15.70	16.45	17.89	19.18	35.48	36.81	43.01	46.59
G20 000	16.51	16.63	18.85	19.41	21.07	23.05	33.05	35.70	39.05	47.47
G30 000	20.64	21.01	24.44	24.66	27.54	30.25	35.65	38.27	42.58	47.65

The natural frequency increases as the soil conditions improve. The first 6 modes appear to be within the same range (except for G30 000). Frequency is a measure of stiffness and therefore it is expected that the stiffer soil conditions result in stiffer responses with respect to frequency. The magnitudes are well below the forcing frequency and are therefore low tuned.

5.9.1.2 Table Top

The natural frequencies (in Hz) from Table 11.2 vary as follows:

Analysis No	Mode 1	Mode 2	Mode 3	Mode 4	Mode 5	Mode 6	Mode 7	Mode 8	Mode 9	Mode 10
G4 000	7.19	8.55	9.90	21.20	28.70	33.82	43.01	47.48	48.82	55.74
G10 000	5.24	5.39	7.78	12.47	14.73	15.15	16.65	18.45	20.38	23.96
G15 000	5.78	6.21	8.06	16.27	18.89	19.32	20.41	20.59	21.84	27.33
G20 000	5.90	6.39	8.20	17.18	20.56	20.60	21.37	22.68	23.24	28.31
G30 000	5.61	6.26	7.74	18.20	20.59	24.79	26.08	27.11	27.95	28.44

The natural frequency initially decreases from G4 000 to G10 000 but could be considered constant over the remaining cases. This implies that the stiffness of the structure dominates the vibration performance in terms of frequency. The first 3 modes appear to be in the same range. The magnitudes are well below the forcing frequency and are therefore low tuned.

5.9.1.3 Multi-storey

The natural frequencies (in Hz) from Table 11.3 vary as follows:

Analysis No	Mode 1	Mode 2	Mode 3	Mode 4	Mode 5	Mode 6	Mode 7	Mode 8	Mode 9	Mode 10
G4 000	2.08	2.29	4.63	7.06	8.68	8.90	10.56	14.27	15.07	17.25
G10 000	2.85	2.97	4.98	10.87	12.19	13.21	14.94	16.23	17.87	18.42
G15 000	3.29	3.31	5.08	13.06	14.01	15.00	16.54	19.11	20.25	20.94
G20 000	3.38	3.38	5.11	13.24	14.74	15.46	16.84	20.06	20.26	22.65
G30 000	3.62	3.73	5.17	13.47	16.00	17.15	18.48	20.29	23.85	27.82

Whilst the natural frequency increases as the soil conditions improve, the increase is marginal and may be considered constant. This implies that the stiffness of the structure dominates the vibration performance in terms of frequency. The first 2 modes appear to be in the same range. The magnitudes are well below the forcing frequency and is said to be low tuned.

When comparing the natural frequencies of the various types of structure, it is no surprise that the raft has the stiffest response followed by the table top and thereafter the multi-storey. It can be concluded that the raft is the most efficient structure to limit frequency response.

There is very little change in the respective natural frequencies when comparing the effect of foundation thickness, beam versus plate model, effect of modeling machines as a multi-mass system, effects of transverse beam and column section properties. This is evident and self explanatory when referring to Table 11. Therefore no further discussion will be presented.

The extremely high magnitudes for the higher modes of vibration viz modes 7 to 10 inclusive for each soil condition and each type of structure are associated with the pitching mode (refer Tables 11.1, 11.2 and 11.3). These modes represent the vibration about the longitudinal axis of the shaft of the turbine and compressor assembly. The axis is extremely stiff compared to the other axes. This results in the much higher natural frequencies.

5.10 Effect of Type of Structures

5.10.1 Raft, Table Top and Multi-storey

5.10.1.1 Vertical Amplitude of Vibration (D_y)

The vertical amplitudes of vibration from Table 10.1, 10.2 and 10.3 vary as follows:

Analysis No	Raft		Table Top		Multi-storey	
	Amplitude	Performance	Amplitude	Performance	Amplitude	Performance
G4 000	0.000308	B	0.001954	E	0.001757	E
G10 000	0.000697	C	0.001654	E	0.001285	D
G15 000	0.000834	C	0.002204	E	0.001169	C
G20 000	0.001646	E	0.011939	E	0.001344	D
G30 000	0.000680	C	0.019521	E	0.001747	E

The discussion with respect to waveforms have been addressed in Section 5.2. Except for G20 000, the raft structure has the stiffest response followed by the multi-storey. The stiff response of the raft is expected. The table top structure is stiffer than the multi-storey and therefore tends to attract a greater proportion of the vibration than the multi-storey. This implies that the soil conditions play an important role in the case of multi-storey structure. There appears to be an optimum condition between G10 000 and G15 000 for all three structures. In practice finer sensitivity analyses are necessary to further optimize the design.

5.10.1.2 Transverse Amplitude of Vibration (D_z)

The transverse amplitudes of vibration from Tables 10.1, 10.2 and 10.3 vary as follows:

Analysis No	Raft		Table Top		Multi-storey	
	Amplitude	Performance	Amplitude	Performance	Amplitude	Performance
G4 000	0.000204	B	0.000438	B	0.000049	A
G10 000	0.000148	A	0.020210	E	0.000464	B
G15 000	0.000156	A	0.015434	E	0.000438	B
G20 000	0.000175	A	0.007266	E	0.000045	A
G30 000	0.000191	A	0.002313	E	0.000423	B

Again the raft structure has the stiffest response followed by the multi-storey. The stiff response of the raft is expected. The table top structure is stiffer than the multi-storey and therefore tends to attract a greater proportion of the vibration than the multi-storey. This implies that the soil conditions play an important role in the case of multi-storey structure. The response of the raft, table top and multi-storey structures are fairly consistent. However finer sensitivity analyses are necessary between G4 000 and G10 000 for the table top structure to ascertain the optimum conditions for the supporting soil and structure stiffness.

5.10.1.3 Vertical and Transverse Velocities of Vibration (V_y and V_z)

The vertical and transverse velocities of vibration from Tables 10.1, 10.2 and 10.3 vary as follows:

Analysis No	Raft		Table Top		Multi-storey	
	V_y (in/s)	V_z (in/s)	V_y (in/s)	V_z (in/s)	V_y (in/s)	V_z (in/s)
G4 000	0.113	0.146	0.571	0.079	0.499	0.072
G10 000	0.200	0.094	0.188	2.590	0.373	0.079
G15 000	0.249	0.065	0.291	1.897	0.325	0.071
G20 000	0.526	0.061	1.523	0.894	0.373	0.070
G30 000	0.210	0.068	2.680	0.248	0.500	0.068

Velocity is the first derivative of displacement. The displacement trends are therefore similar to the velocity trends. In terms of performance the raft has the best response

followed by the multi-storey. The optimum conditions appear to be around the G15 000 case for all the structures.

CHAPTER 6: CASE HISTORIES

6.1 Introduction

The design of foundations and structures to support large vibrating equipment is becoming increasingly important. In the industrial environment the consequences of excessive vibration are severe. Sensitive processes may become inoperable, resulting in the damage of process and mechanical equipment. Work conditions could become physiologically intolerable to operators.

The responses of the soil, foundations and structures to vibration are complex. Hence traditional structural mechanics and theory of elasticity are not adequate to solve all the problems. The analytical modeling technique presented in this dissertation viz. finite element analysis has certain limitations as it is based on a mathematical model. As an example of the limitations of this model, the mass of the structure is lumped at nodes to limit the degrees of freedom for calculation purposes. However the mass in the real structure is distributed along the length of each element in the structure resulting in almost infinite degrees of freedom. This approximation is used to facilitate calculation time and costs. The real behaviour of the soil, foundations and structures need to be compared with the analytical model to check the accuracy of the technique. Ideally displacements with respect to time could be measured under operating conditions of the equipment at various points in the structure. However for the intents and purposes of this dissertation it was more economical to examine case histories in which the modeling techniques used were similar to those presented in this dissertation instead of constructing a model of the equipment, foundation and structure. Correlation to failures provides an opportunity to identify deficiencies in the analytical model.

Generally case histories documenting failures are seldom published. Case histories 1 to 2 have been recorded in the American Concrete Institute Publication SP – 78 entitled "Foundations for Equipment and Machinery " (1982). Case history 3 is an unpublished report prepared by a colleague for a compressor. Case history 4 is a study carried out by Daming et al (1983).

6.2 Case Histories

6.2.1 Case History No 1: SP 78, Karabinis and Fowler: (1982)

This horizontal compressor was founded on a spread foundation. No dynamic analysis was carried out. Severe vibrations were encountered during start up. A dynamic analysis of the foundation indicated that the frequency of the first rocking mode of vibration was close to the operating speed of the compressor. Sand bags were stacked on each end of the foundation to reduce the level of vibration. Pipe connections were changed to flexible types. Whilst these measures reduced the vibrations they were still beyond the recommend limits. This case history illustrates two important points:

- i) it is difficult to correct a poorly designed foundation
- ii) mass ratio did not give adequate indication as to the cause of the problem as the mass of the foundation was 41 730 kg whilst the mass of the compressor was 2 722 kg, a ratio of 15:1.

In summary the authors have recommended the following:

- a) the main aim of any foundation design is to avoid resonance. This is achieved by keeping the ratio of fundamental natural frequency to operating speed either less than 0.5 or greater than 1.5.
- b) when operational dynamic loads are known, an effort should be made to limit the amplitudes of vibration to acceptable levels.
- c) simple finite element models often suffice for dynamic analysis
- d) damped response should be considered at near resonant conditions but may be ignored for highly tuned foundations
- e) mass distribution and foundation geometry are important aspects in the dynamic design of foundations.

6.2.2 Case History No. 2: SP 78 Srinivasulu and Lakshmanan: (1982)

Turbo – generator set: – Problem relates to an existing table top turbo-generator support. The structure was the last of a series of five turbo-generator sets built in a row. The first three units were 50 mega watts each while the last two were each 100

mega watts. The foundations were stiff and overtuned. However the tops of the columns of the last unit had cracked 6 months after the machinery was commissioned and the damage increased with time. The soil was not suspected to be cause of the cracks as an existing 100 mega watt unit was founded on similar soil conditions and performed acceptably. The amplitudes of vibrations were very low due to the increased damping arising from the cracked structure. In addition to vibration measurements, ultrasonic tests were conducted to check crack propagation and strength of concrete. It was established that concreting stopped for some period while casting the foundation and there was honeycombing at certain beam-column intersections and the construction joint. Wave travel velocities measured across the foundation confirmed presence of loose pockets. Epoxy grout was injected through holes drilled into the columns that were affected. The vibration was monitored periodically before continuous operation of the machine resumed. This case history also indicates that if joints are carefully planned and designed they could be used to increase damping in the structure. The case study emphasizes the need for good specifications and the importance of details at construction joints and that not all operational problems should be ascribed to design faults.

6.2.3 Case History No 3: du Preez et al (1999)

Table top Compressor Structure: Vibrations on a table top structure was excited by the drive motor. The objective of the exercise was to assess the integrity of the structure. A finite element model was composed. Amplitudes of vibration were measured by site personnel and were input into the finite element model. A comprehensive correlation between the calculated and measured response was carried out. Six accelerometers were used during the measurements of which 2 remained in the same position as reference. Each set was recorded at a frequency of 800 Hz and a duration of approximately 2 seconds. The following tables indicate the positions and directions of the vibration and the maximum amplitudes measured at the respective points.

Measurement positions and directions of Accelerometers

Set	Channel 3		Channel 4		Channel 5		Channel 6	
A	SW motor bolt	Vert	SW motor bolt	Lat	NE motor bolt	Vert	NW motor bolt	Vert
B	Old conc cross member under motor	Vert	S steel beam HD bolt 3	Vert	Steel cross member NDE motor	Vert	S steel beam HD bolt 1	Vert
C	S steel beam HD bolt 3	Vert	S steel beam HD bolt 4	Vert	S steel beam HD bolt 5	Vert	S steel beam HD bolt 6	Vert
D	Motor end of N steel beam	Axial	Motor end of S steel beam	Axial	S steel beam HD bolt 2	Lat	S steel beam HD bolt 3	Lat
E	S steel beam HD bolt 3	Lat	S steel beam HD bolt 4	Lat	S steel beam HD bolt 5	Lat	S steel beam HD bolt 6	Lat
F	Center of new conc wall N	Lat	S steel beam HD bolt 4	Lat	N steel beam HD bolt 4	Lat	Centre of new conc wall S	Lat
G	Center of new conc column SW	Lat	Centre of new conc column SW	Lat	Centre of old conc column SE	Lat	Centre of new conc wall	Lat
H	N steel beam HD bolt 1	Lat	N steel beam HD bolt 2	Lat	N steel beam HD bolt 6	Lat	N steel beam HD bolt 5	Lat
I	N steel beam HD bolt 1	Vert	N steel beam HD bolt 2	Vert	N steel beam HD bolt 6	Vert	N steel beam HD bolt 5	Vert

Abbreviations:

N – north

S – south

E – east

W – west

HD – hold down bolts,

Bolt 1 – motor end

Bolt 6 – compressor end

Conc - concrete

Maximum displacement amplitudes at measuring points [μm]						
Set	Channel 1	Channel 2	Channel 3	Channel 4	Channel 5	Channel 6
A	13.4	12.7	22.9	19.9	14.1	13.8
B			6.1	7.8	13.9	11.5
C			6.4	7.2	5.9	7.7
D			12.4	10.9	23.3	18.9
E			9.5	9.1	13.1	14.8
F			19.2	9.4	8.4	17.5
G			9.8	12.8	14.6	16.9
H			24.7	19.4	14.5	10.5
I			7.5	8.9	6.1	6.4

The finite element model comprised beam elements (viz. columns and cross beams) and shell elements (longitudinal beams). The model was excited by applying the prescribed displacements in terms of harmonic functions using Fourier Transforms. A Finite Element dynamic analysis was carried out using modal superposition. The correlation between the measured and calculated displacements was based on the vertical and lateral displacements of the southern beam. The measured and calculated displacements were available at the positions of six hold-down bolts. Bolt 1 was at the motor end and bolt 6 was at the compressor end. The table below compares the maximum measured displacements to the maximum calculated displacements for 6 hold-down bolts.

Maximum measured and calculated displacement amplitudes for southern steel beam				
Location	Vertical (μm)		Lateral (μm)	
	Measured	Calculated	Measured	Calculated
Bolt 1	11.5	11.4	18.9	14.0
Bolt 2	7.8	7.2	23.3	9.5
Bolt 3	6.4	2.0	9.5	9.2
Bolt 4	7.2	3.4	9.1	8.0
Bolt 5	5.9	1.8	13.1	6.5
Bolt 6	7.7	2.8	14.8	6.0

The natural frequencies for the first 10 modes have been tabled below. According to the authors there were no natural frequencies at the primary excitation frequencies of 25 Hz and 50 Hz.

Natural frequencies of first 10 modes	
Mode	Frequency (Hz)
1	12.9
2	21.0
3	44.0
4	60.8
5	63.2
6	67.5
7	74.6
8	79.9
9	85.8
10	90.3

The 25 Hz frequency corresponded to the rotating frequency of the motor and was therefore always present. The 50 Hz frequency which was double the rotating frequency may have been caused by some level of imbalance in the motor. Whilst there were some discrepancies the general correlation is good. The final assessment of the case study was that the state of the compressor, motor and structure was acceptable in terms of safety but the motor required continuous monitoring in terms of levels of vibration.

6.2.4 Case History 4: Daming et al (1983)

The paper by Daming et al (1983) comprises studies of a table top structure modeled using finite element analyses. A model experiment to measure its vibration behaviour was constructed. The results of the analyses and the experiment for natural frequencies and mode shapes were compared. The following assumptions were made for the analysis:

- 1) the transverse beam, longitudinal beam and column intersected orthogonally at a point;
- 2) the masses of the foundation were concentrated at nodes
- 3) the footings of the columns were totally clamped at the foundation. Therefore the mechanical model of the foundation was a system of multi-degrees of

freedom. The model experiment comprised a 1/5 size table top structure constructed in reinforced concrete. Details of the structure and machine were not published in the paper. However it was noted that the turbine was of high rotational speed. The frequencies and modal shapes of the structure were determined from low to high frequencies. In the study by Daming et al (1983) only vertical vibration was studied. The table below comprises comparisons of measured and calculated values. The discrepancies vary up to a maximum of 13%. Five modal shapes are horizontal, one is torsional and 12 are vertical. The modal shapes are shown in Figure 24. It can be seen that the influence of shear deformation on frequency is predominant. The close correlation of the frequencies confirms that the finite element analysis method is the best analytical tool available for the study of dynamic behaviour.

Direction of Vibration	Measured Values	Calculated Values	Direction of Vibration	Measured Values	Calculated Values
Horizontal	15.0	16.4	Vertical	338.0	293.2
Horizontal	15.9	16.2	Vertical	398.0	386.3
Torsional	18.0	18.1	Vertical	460.0	459.2
Horizontal	170.0	163.5	Horizontal	465.0	438.7
Horizontal	174.0	177.8	Vertical	543.0	600.9
Vertical	218.0	202.8	Vertical	688.0	638.3
Vertical	225.0	226.9	Vertical	960.0	839.8
Vertical	280.0	257.2	Vertical	876.0	855.1
Vertical	285.0	270.1	Vertical	1140.0	1113.2

Natural Frequencies of Model (Hz)

6.2.5 Conclusion

Case history number 1 demonstrates the importance of conducting dynamic analyses. Furthermore it emphasizes that it is difficult to correct a poorly designed foundation and structure. The mass of the foundation did not play a dominant role in the dynamic response. Case history number 2 highlights the benefit of comparing the performances of similar systems subjected to vibrations so that the cause of the problem could be identified. It can also be seen that whilst good design procedures are essential, these

procedures need to be complemented by explicit specifications for construction. Case history numbers 3 and 4 confirm the accuracy of the finite element analyses. These case histories also highlight the importance of the use of field measurements, using appropriate instruments to test and verify the analytical model. This provides a good basis for further research and the development of more accurate finite element models and analyses.

CHAPTER 7: CONCLUSION

7.1 Introduction

The rule of thumb method of design is based on mass ratio. Often the mass ratio was determined as follows:

- for a revolving machine this ratio was a minimum of 3
- for a reciprocating machine this ratio was a minimum of 5.

The mass ratio is defined as the total mass of foundation divided by the total mass of the machine. The prerequisite for this method is that machine is perfectly balanced. Often machine manufacturers insist that their machines are balanced. This is only true when the machine is new and the bearings have no wear. This condition is only one instant in time. It is well understood that with constant or repeated use of the machine the moving components of the machine experience wear due to friction. This causes wobble of the shaft within the journal. The other source of vibration results from the imbalanced masses either rotating or reciprocating. The rule of thumb will not guarantee that amplitudes of vibration will be acceptable as it does not have any means of assessing the amplitudes of vibration. It can be seen from Tables 10.1, 10.2 and 10.3 that whilst the requirements of mass ratio are satisfied displacement and velocity requirements are not satisfied.

It is clear that the rule of thumb method is not an adequate means to assess the response of structures and foundations to vibration, as it does not quantify the necessary parameters such as natural frequency, amplitude of vibration and velocity of vibration that characterize the performance of structures and foundations. Researchers such as Blake (1964), Reiher and Meister (1931), Raush (1943), Crandale (1949), Kruglov (1959) and Baxter and Bernhard (1967) have published thresholds for displacements and velocities of vibrations with respect to frequencies of machines based on the following:

- various physiological requirements of persons
- machines and machine foundations

The results of a typical dynamic analysis are the following:

- natural frequencies of the system (ie foundation, structure and supporting soil)
- amplitudes of vibration
- velocities of vibration

These calculated parameters can be compared to published thresholds mentioned above. Hence the performance of the system can be assessed. The rule of thumb method does not allow for assessment of vibration. Efforts should rather be concentrated on dynamic analyses and one such tool is the finite element method. The case histories by du Preez, et al (1999) and Daming et al (1983) indicate good correlations to the real behaviour of machine, structure and foundation. The correlations mean that the results of the dynamic analyses are the appropriate indicators or parameters to assess the response of the system to vibration. The emphasis then shifts to devising models that simulate the real behaviour of the soil, foundation and structure. This chapter is not intended to conclusively arrive at solutions but rather provide directions to which further research should be adopted so that the theory on dynamics of soil – structure - machine interaction is dealt with holistically, changing the approach to a science rather than an art. The soil models researched by Borja et al (1993, 1994) have been based on elasto-viscoplastic soil behaviour. Research is needed on the elasto-plastic soil behaviour and mathematical models. Furthermore correlation studies should be carried out on various soil types to verify the theory. The nonlinear model and response of piled foundations is a subject where more research is required. Often poor soil conditions are encountered and the use of piles becomes necessary. Information on damping with reference to vibrating machinery is rare and is often based on experience. Research should be carried out so that damping models can be produced to understand and quantify damping. It is for this reason that the sub headings that follow have been drawn to steer the line of thought based on the responses of the various models that have been studied.

7.2 Geotechnical Considerations

The traditional “elastic halfspace model” is based on an infinite depth of soil that is homogeneous and isotropic. This soil is defined by two elastic properties viz. shear modulus, G and Poisson’s ratio, ν . The elastic halfspace model is only valid for isolated foundations.

The “elastic halfspace model” is deficient in that it does not model accurately real soils that invariably comprise various layers. Furthermore the theory is based on a circular footing located at the surface of the elastic halfspace and is not valid for footings situated near each other. Further complexities arise in the case of piled footings as the stiffness of the piles can only be approximated.

In view of the complex behaviour and the configuration of equipment it is becoming necessary to adopt models that alleviate the guess work and accommodate the real situations. It is apparent that the trend is to adopt more rigorous finite element models where ideally the soil, foundation and superstructure is modeled as an integral system. The mathematical model should account for the elastoplastic and the elasto-viscoplastic characteristics of soil with special reference to hysteresis, irreversible deformation and cyclic soil behaviour. The advance in the nonlinear soil structure interaction analysis presented by Borja et al (1993, 1994) for vertically oscillating foundations, rocking and torsional vibration of foundation goes beyond the limits and capabilities of the linear models and incorporates hysteretic soil behaviour and soil stiffness degradation. The increasing capabilities of computers, coupled with the efficiencies of computing time is making the finite element approach more viable and attractive to model the complex response of soils to dynamic excitation.

7.3 Dynamic Analysis using Finite Element Analysis

The finite element analysis is the best analytical tool that we have to model the dynamic behaviour of the vibrating structure, foundations and soil interaction with good correlations to the actual response of the structure to forced excitation. However the accuracy of the analysis relies heavily on the assumptions made with respect to boundary (soil) conditions, restraints, loading conditions, load combinations and frequency. In setting up the mathematical model for analysis the following has been noted:

- when dealing with large cross sections of members (such as beams columns and foundations) and the centre to centre dimensions in the model, there is a tendency to omit the actual stiffness that exists at the joint. This leads to a more conservative analysis.
- deep sections are best modeled using plates rather than beams initially an error was incurred in that the exciting force was modeled for a duration shorter than the requested response. This was analogous to exciting the structure for a

given duration and thereafter removing the exciting forces. The response of both the displacement and velocity with respect to time vibrated about the zero axes for the given time. Thereafter the response shifted to a datum below the time axis. The program used the maximum force amplitude to generate this response.

It therefore becomes imperative to conduct verifications on the real system (machine, superstructure, foundation and supporting soil) so that the model can be calibrated. In order to calibrate the models three quantities are of interest viz. displacement, velocity and acceleration over a given time period. These quantities are inter-related by either differentiating or integration. It therefore does not matter which quantity is measured. It is preferred to measure acceleration using sensitive transducers such as accelerometers for two reasons:

- a) they are small in size and therefore do not load the member significantly.
- b) they can measure vibration at a point (not spread over an area)
- c) they produce repeatable results.

The accelerometer produces a power spectral density (PSD) graph from which deflections and stresses can be back calculated and hence the model may be calibrated. This procedure can also be used to monitor the performance of the machine and structure.

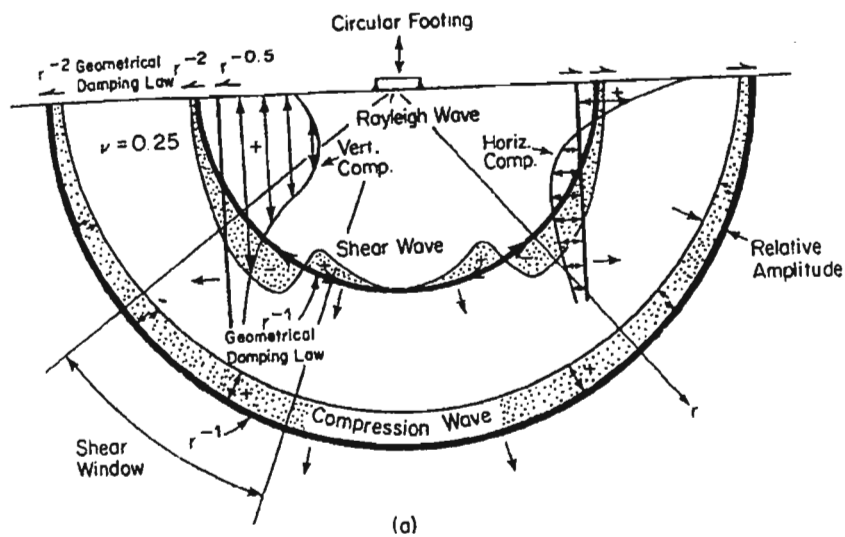
The responses of the raft, table top and multi storey structures are typical of random vibrations where motion cycles are irregular, never repeating themselves exactly. To obtain a complete description of the vibration an infinitely long time record is necessary and this is impossible. Statistical mechanics and communication theory involving amplitude probability distributions in terms of probability densities and continuous vibration frequency spectra in terms of mean square spectral densities or power spectral density (PSD) is adopted.

One of the basic requirements is to attain natural frequency higher than excitation frequency by approximately 50%. It is most practical to effect a change in dynamic response by modifying the natural frequencies of the system than the damping characteristics. If fundamental frequency is less than disturbing frequency, resonance will occur during start up and shut down. It is recommended that the natural frequency be outside the range of 0.5 to 1.5 times the operating speeds of the equipment.

The calibration of Finite Element models with actual behaviour is key to the success of dynamic analysis and to assess performance of systems so that catastrophic failure is prevented, thus enhancing the running life of machines, structures and foundations.

This dissertation has shown that the rule of thumb can not adequately describe the dynamic behaviour of vibrating structures and foundations. Consideration should therefore be given to dynamic analyses using finite elements. The good correlations between behaviour of the real system and model with the two case histories justify the use of the dynamic analysis method.

FIGURES



Wave Type	Per Cent of Total Energy
Rayleigh	67
Shear	26
Compression	7

Figure 1 - Distribution of displacement waves from a circular footing on a homogeneous, isotropic, elastic half-space
Richart et al (1970)

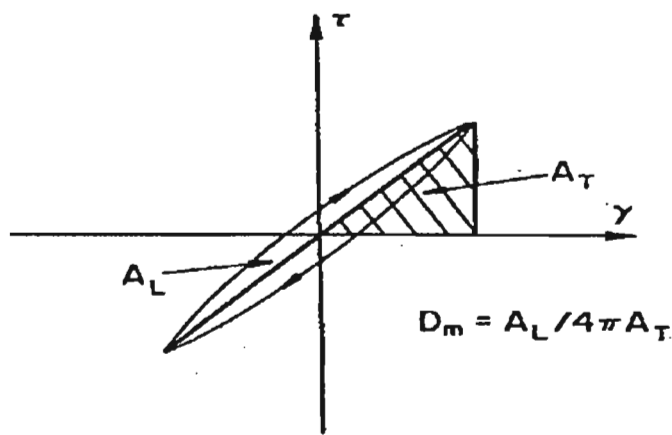


Figure 2 – Definition of material damping
Hardin and Drnevich, (1972)

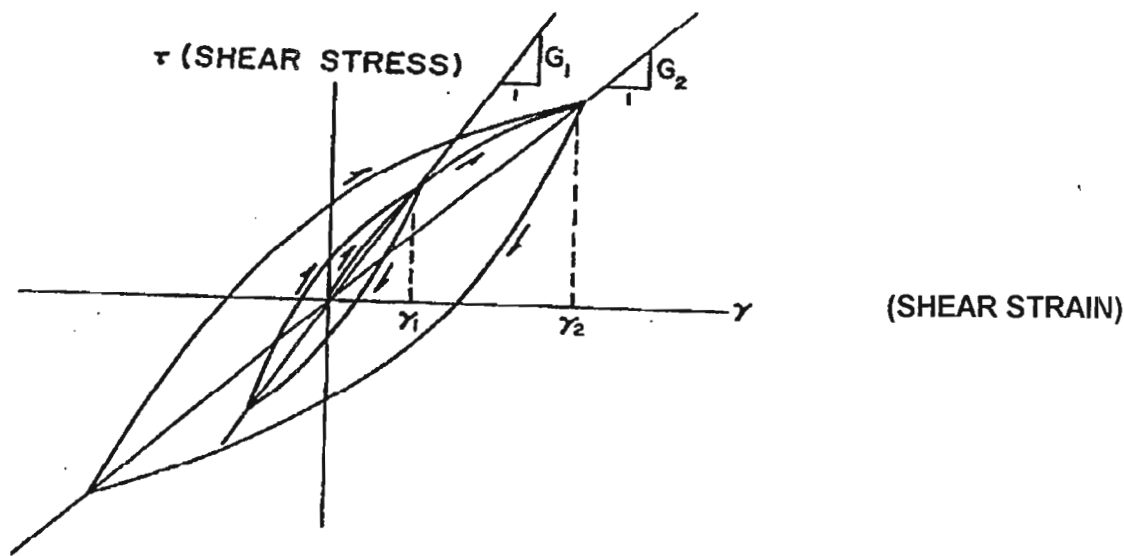


Figure 3 – Hypothetical Shear Stress-Strain Curve for soil Arya et al (1984)

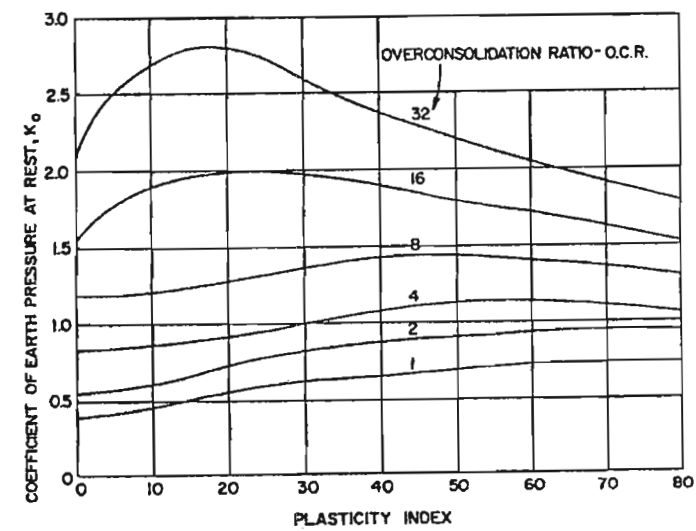


Figure 4 - Relationship of K_0 to Plasticity Index and OCR Arya et al (1984)

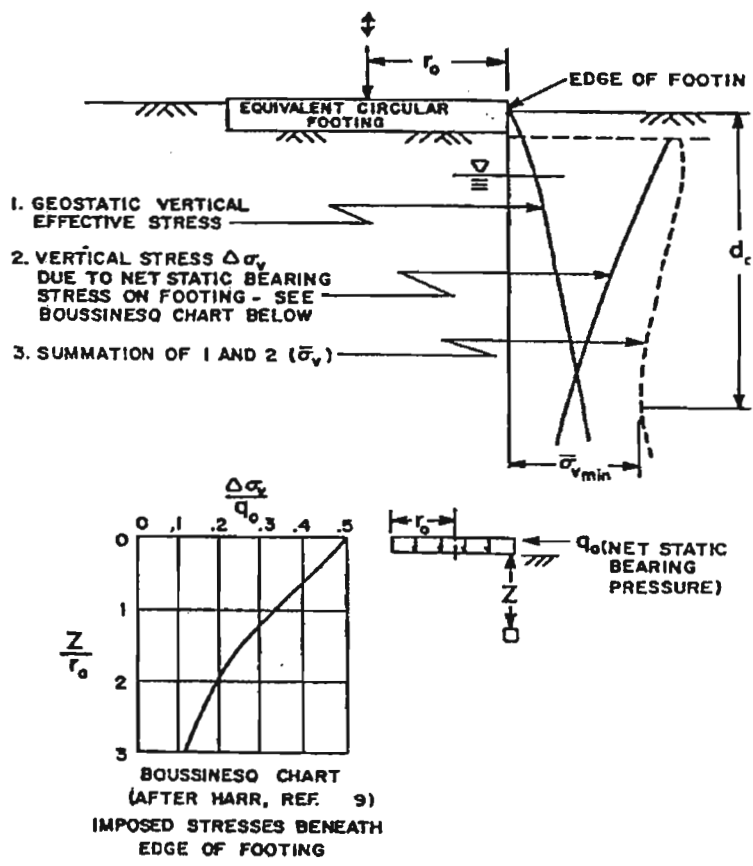


Figure 5 – Determination of σ_{vmin}
Arya et al (1984)

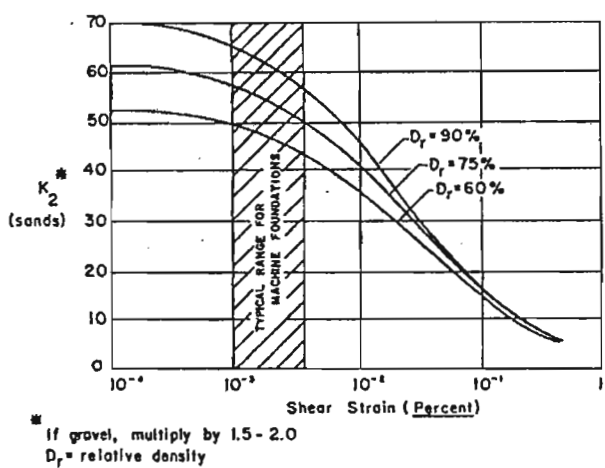


Figure 6 – Relationship of K_2 to shear strain amplitude and relative density
Seed and Idriss, (1970)

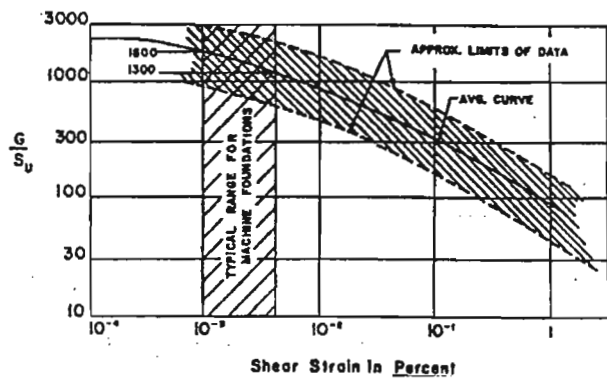


Figure 7 – In situ shear modulus for saturated clay
Seed and Idriss, (1970)

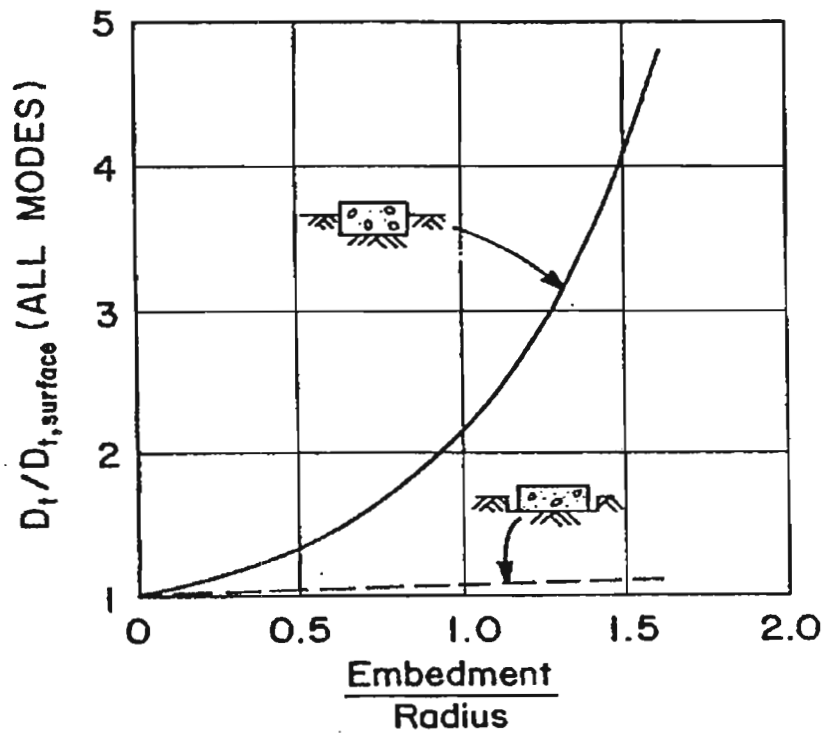


Figure 8 – Effect of embedment on damping
Stokoe and Richart (1974)

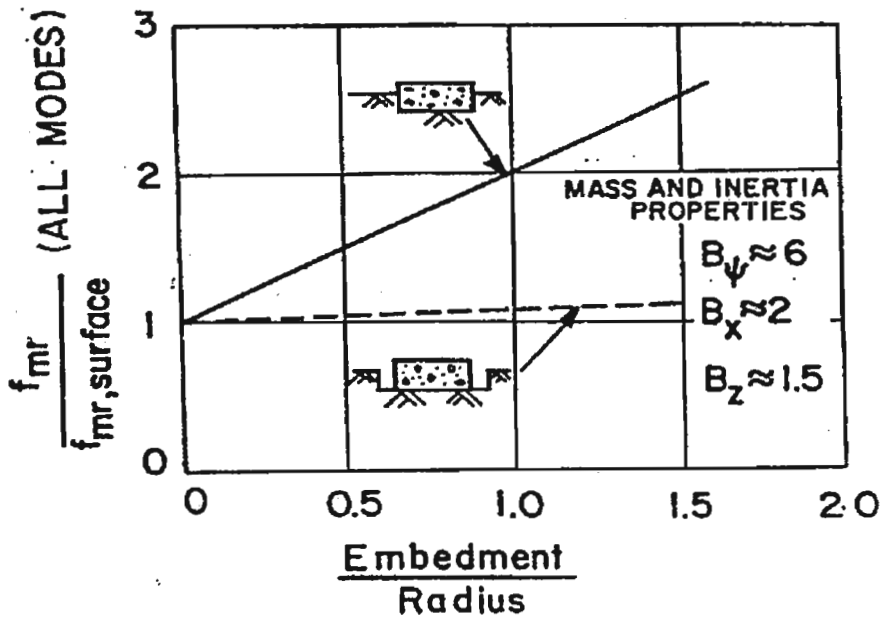


Figure 9 – Effect of embedment of resonant frequency
Stokoe and Richart (1974)

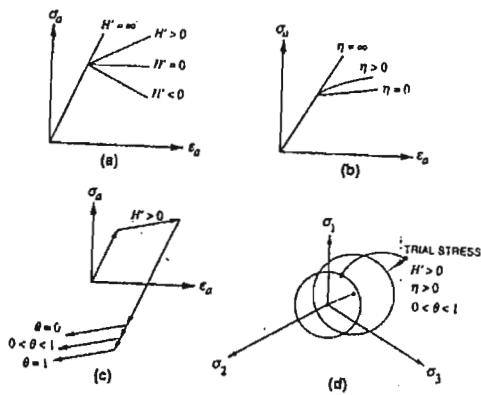


Figure 10 - Geometric Interpretation of Constitutive Model Parameter: (a) Hardening, Perfect Plasticity, and Softening; (b) Viscous and Inviscid Plasticity; (c) Isotropic, Kinematic, and Combined Hardening; and (d) Viscous Translation and Expansion of Yield Surface on π Plane
Borja et al (1993)

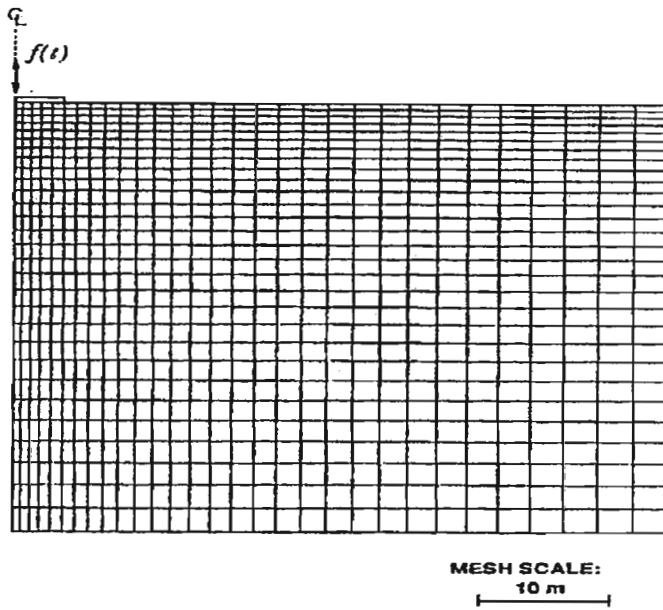


Figure 11 Finite Element Mesh for Analysis of Vertically Oscillating Circular Foundation
Borja et al (1993)

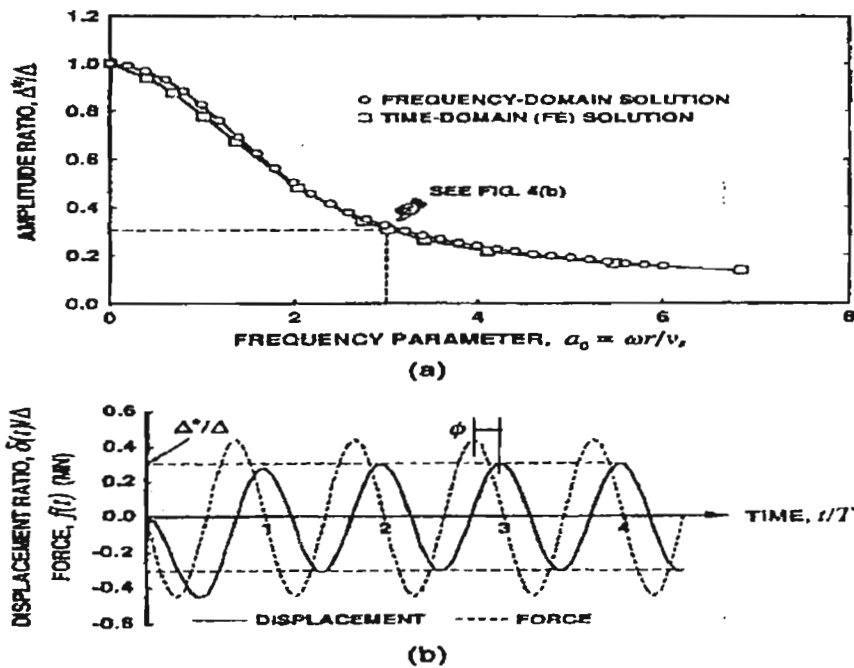


Figure 12 - Mesh Convergence Study. Vertically Oscillating Circular Foundation on Elastic Half-Space: (a) Amplitude versus Frequency Plot; and (b) Time History Plot
Borja et al (1993)

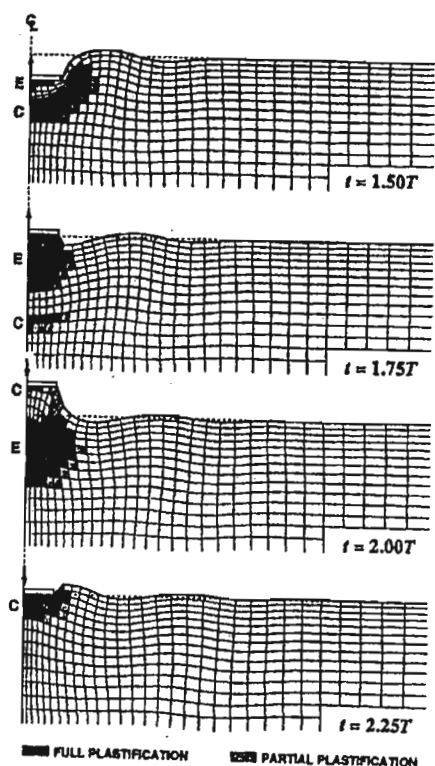


Figure 13 – Establishing Steady-State Waves and Yield Zones for Circular Foundation Problem: Arrows Denote Instantaneous Direction of Force; E = Extensional Yielding; C= Compressional Yielding
Borja et al (1993)

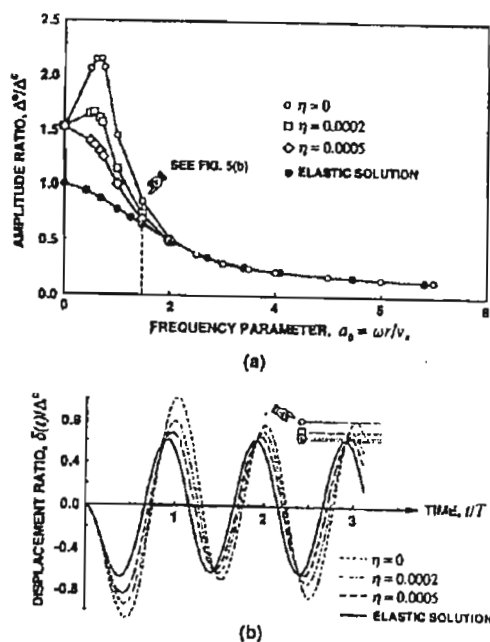


Figure 14 – Vertically Oscillating Circular Foundation on Kinetically Hardening Viscoplastic Half Space:
a) Amplitude versus Frequency Plot, and b) Time History Plot
Borja et al (1993)

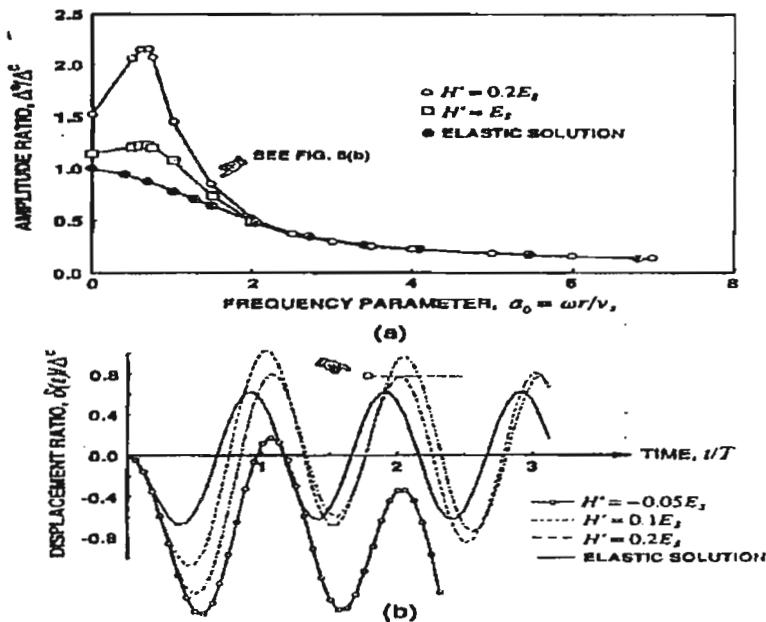


Figure 15 – Vertically Oscillating Circular Foundation on Elastoplastic Half-Space Influence of H on a) Amplitude versus Frequency Plot; b) Time History Plot
Borja et al (1993)

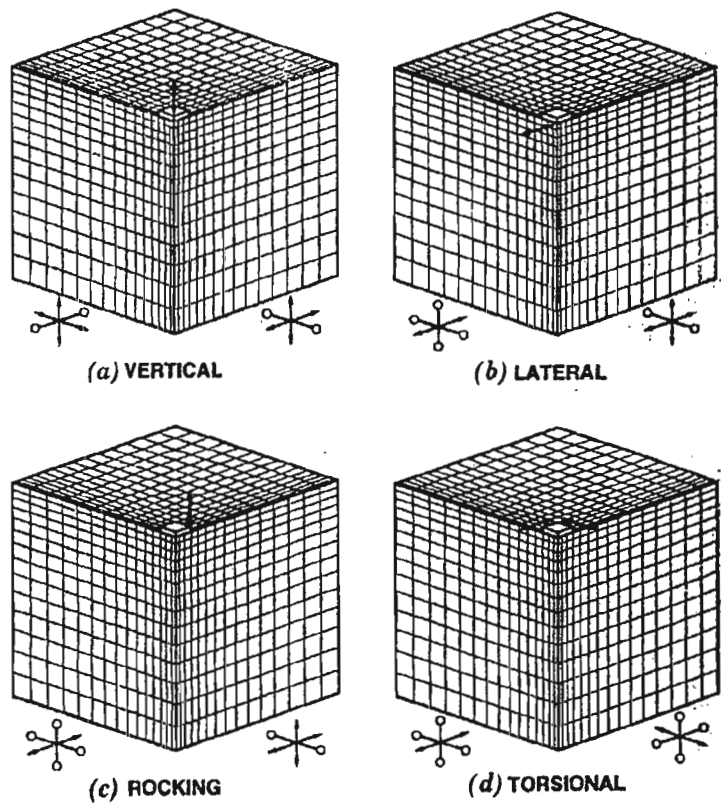


Figure 16 – Symmetry and Antisymmetry for Vertical, Lateral, Rocking and Torsional Vibration Modes [Arrows Denote Free Degrees of Freedom (DOFs); Circles Denotes Fixed DOFs]
Borja et al (1994)

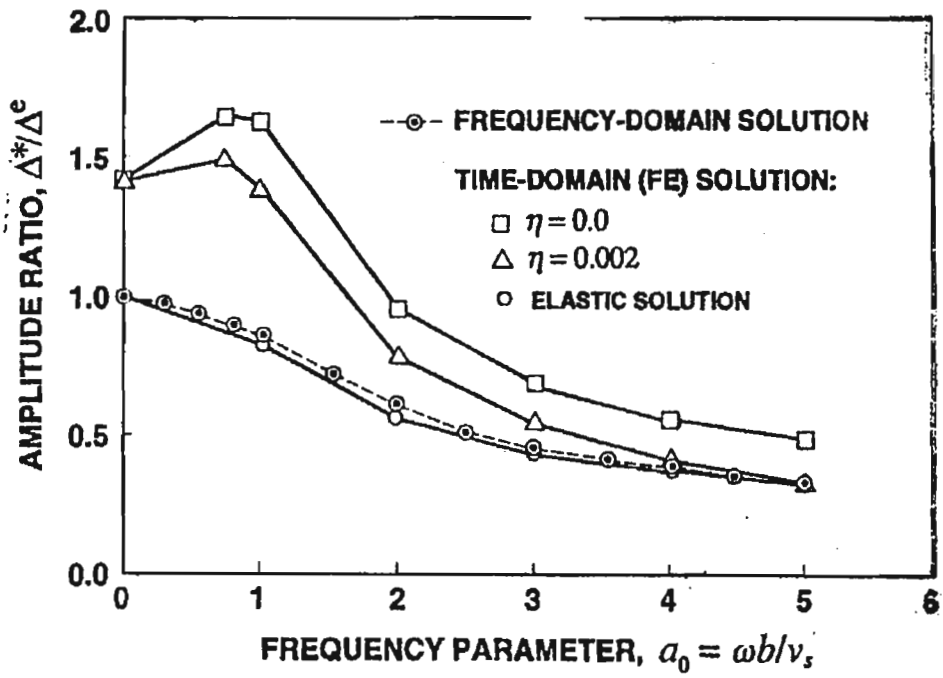


Figure 17 - Amplitude-Frequency Plot for Horizontally Vibrating Square Foundation showing Effects of Viscosity
Borja et al (1994)

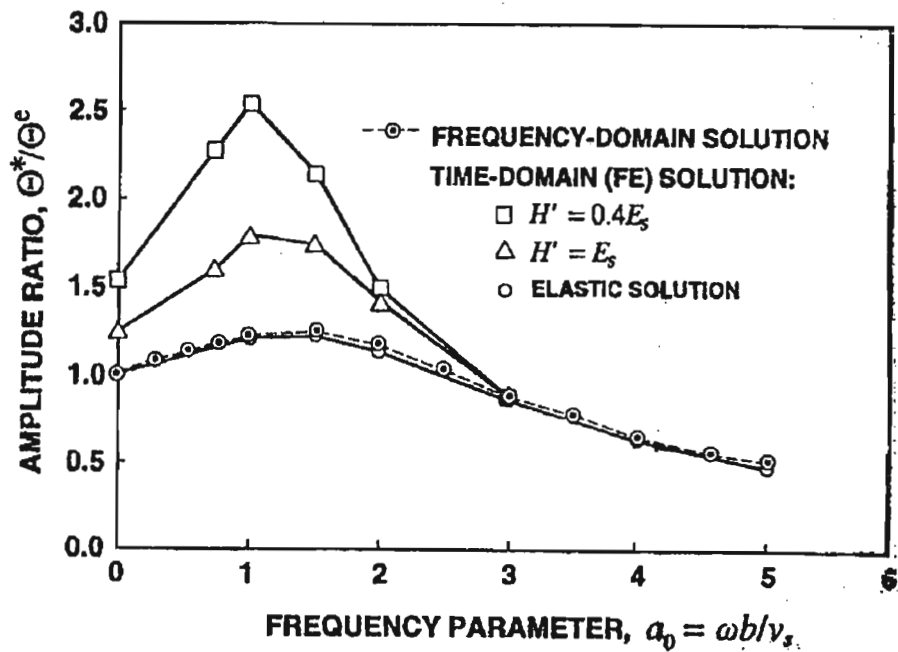


Figure 18 - Amplitude-Frequency Plot for Harmonically Rocking Square Foundation showing Effects of Soil Plastic Modulus
Borja et al (1994)

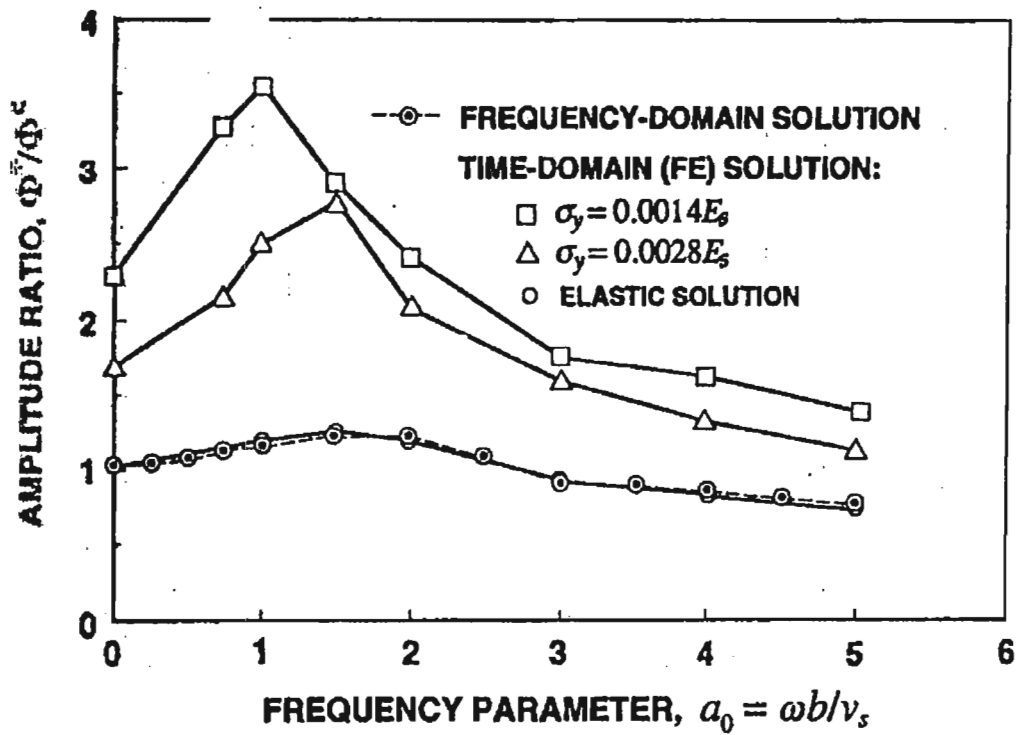


Figure 19- Amplitude-Frequency Plot for Torsionally Vibrating Square Foundation Showing Effects of Initial Yield Stress
Borja et al (1994)

FIGURE 20: RAFT MODEL

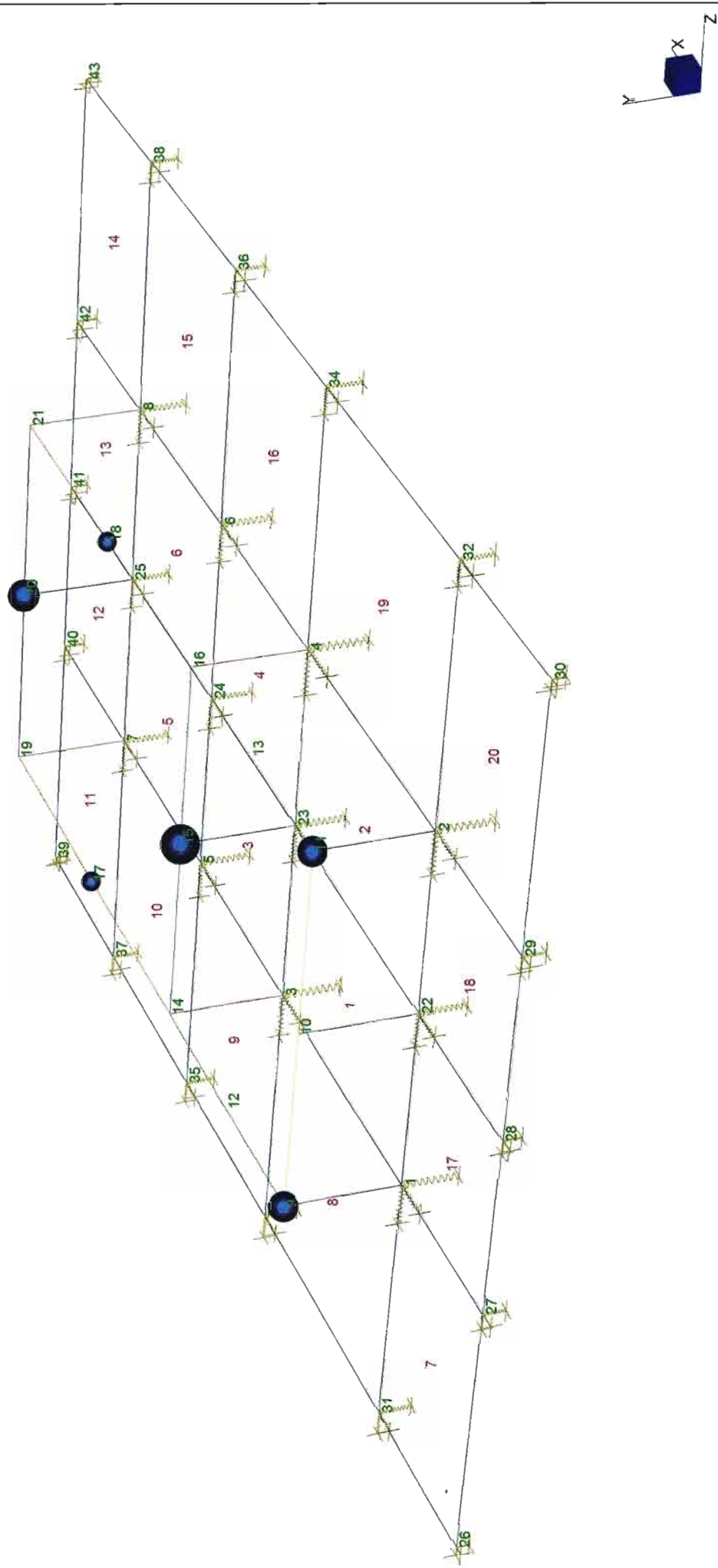


FIGURE 20a: RAFT MODEL

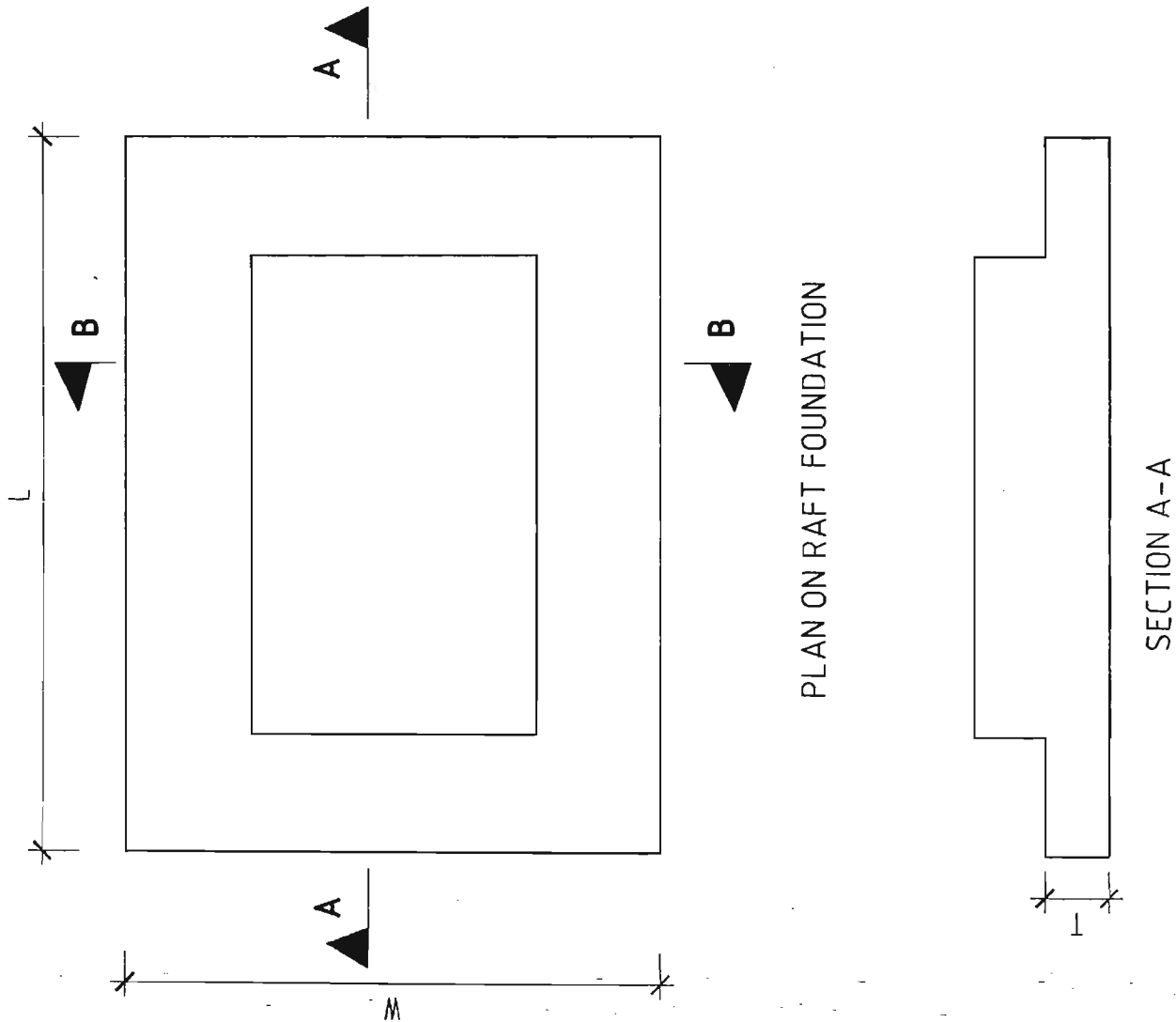


FIGURE 21: TABLE TOP MODEL

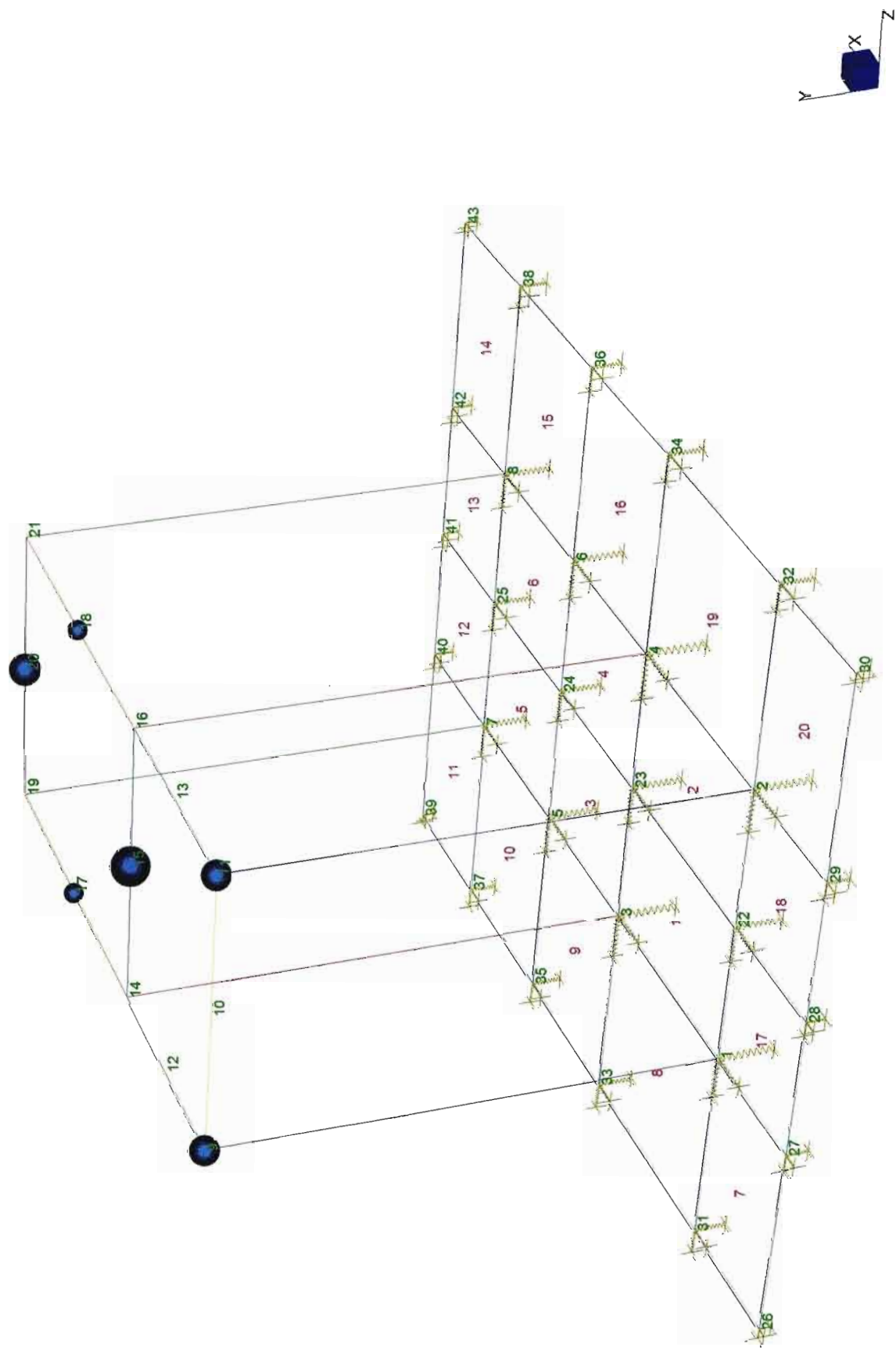
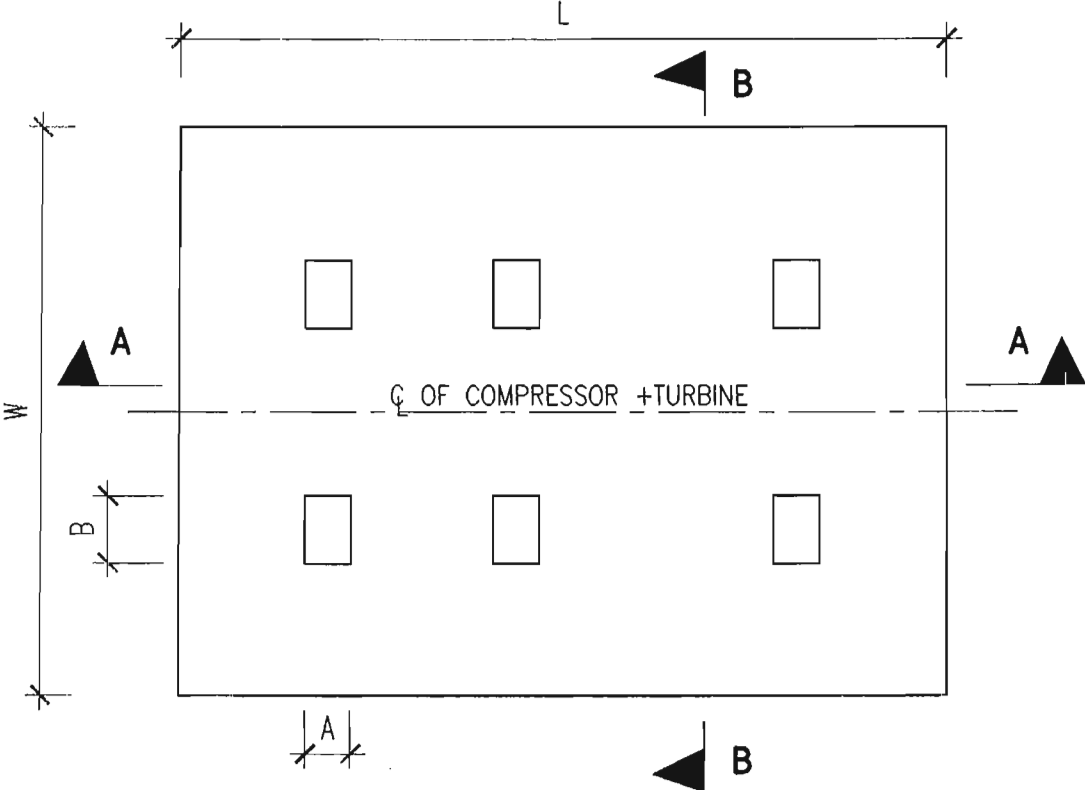


FIGURE 21a: TABLE TOP MODEL



PLAN ON FOUNDATION FOR
TABLE TOP & MULTISTOREY STRUCTURES

FIGURE 21b: TABLE TOP MODEL

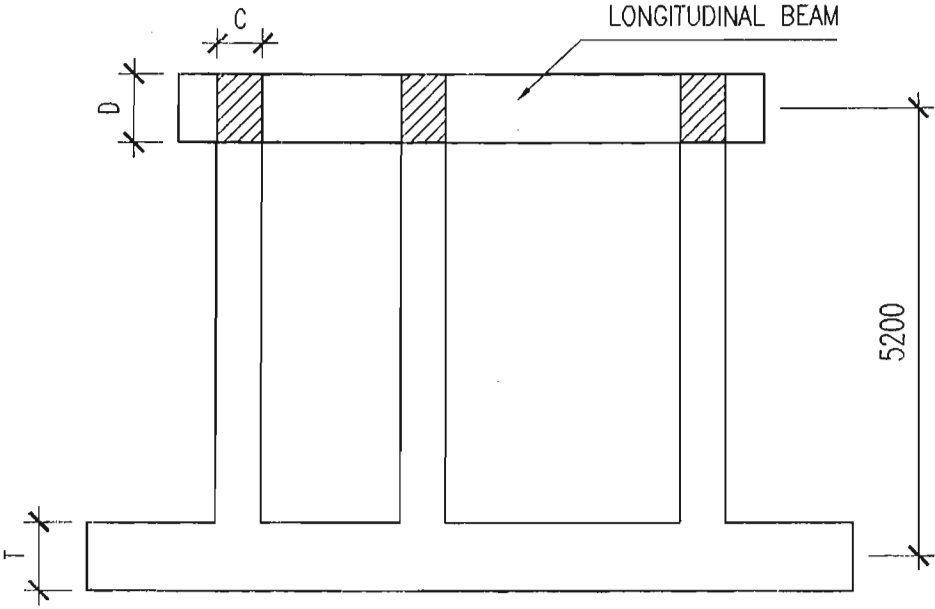


TABLE TOP: SECTION A-A

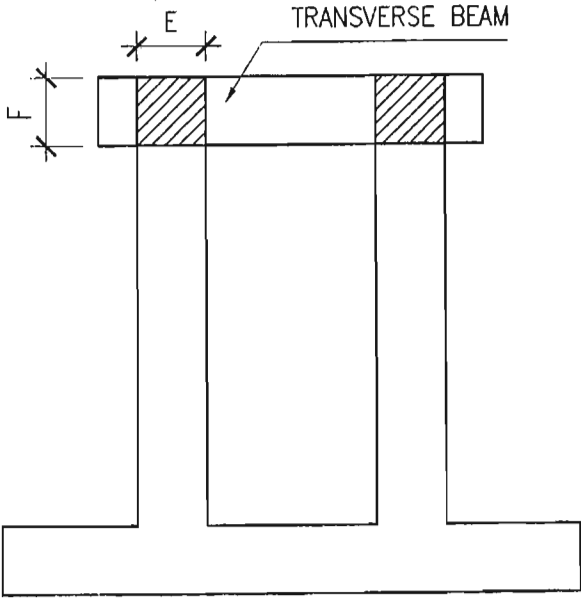


TABLE TOP: SECTION B-B

FIGURE 22: MULTI-STOREY MODEL

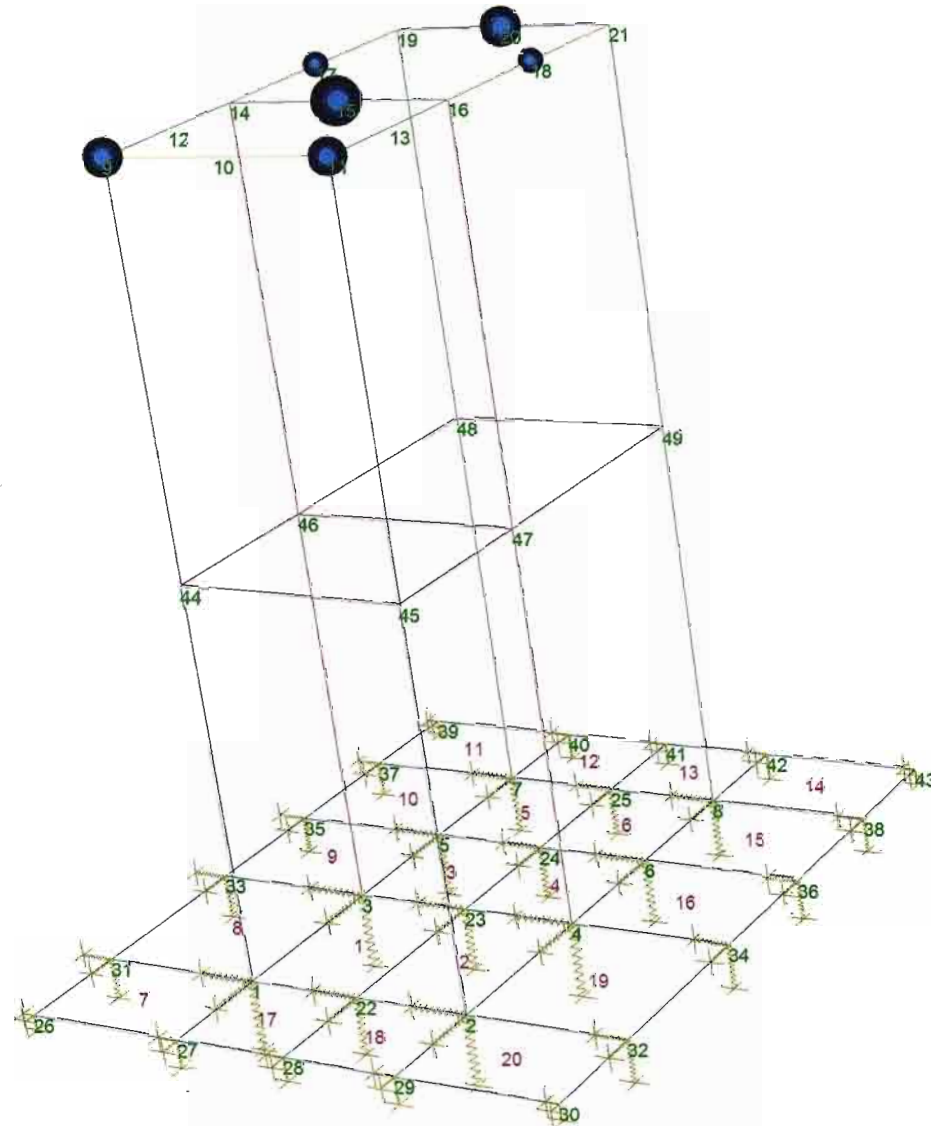
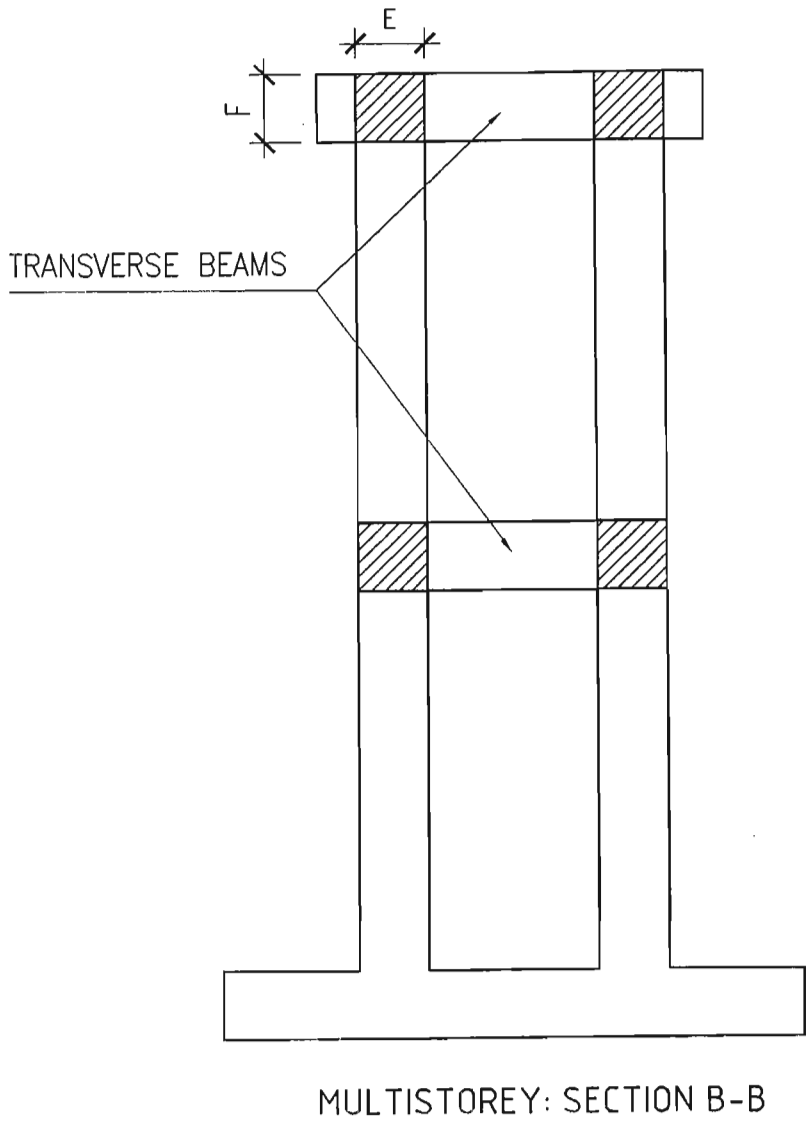
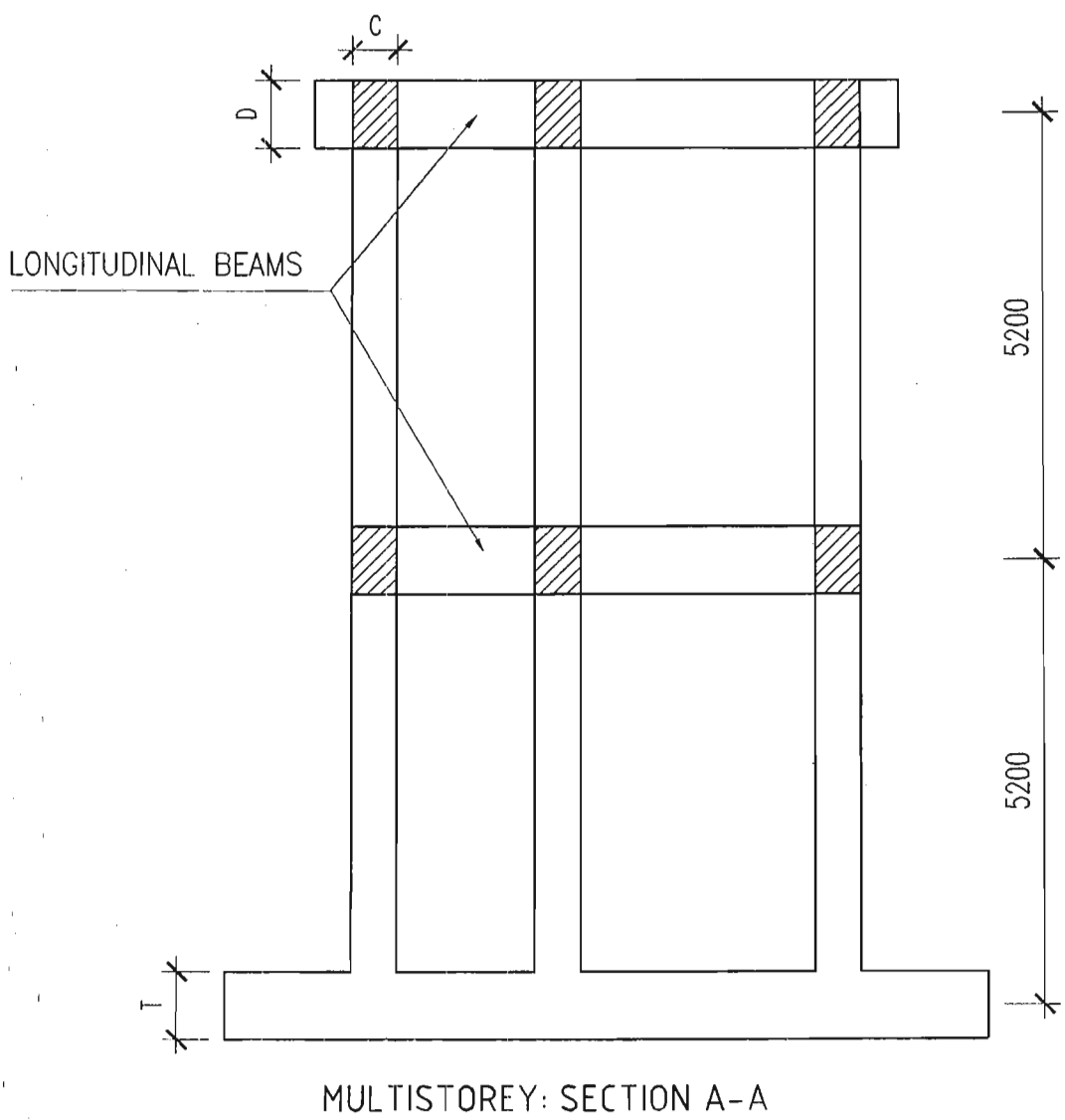
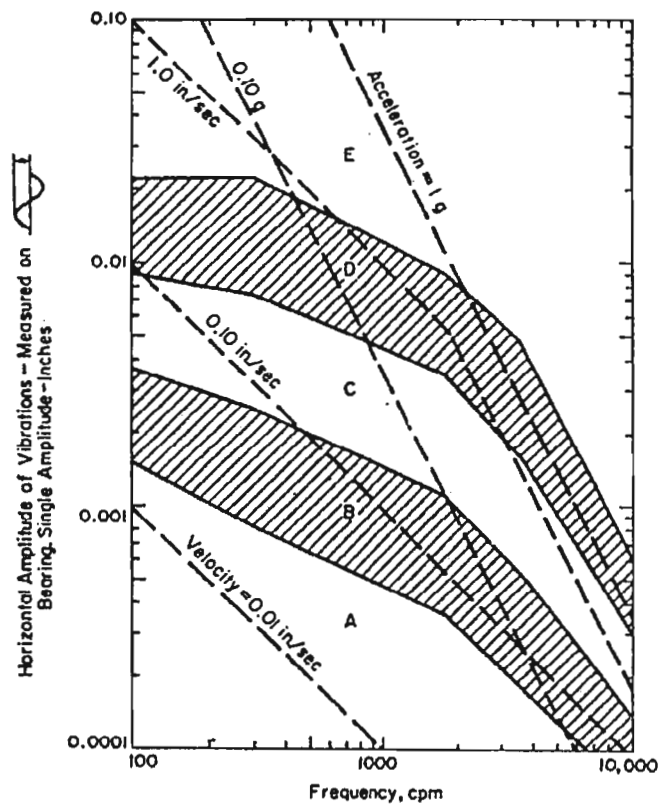


FIGURE 22a: MULTISTOREY MODEL





EXPLANATION OF CASES

E DANGEROUS. SHUT IT DOWN NOW TO A

D FAILURE IS NEAR. CORRECT WITHIN 1

TO AVOID BREAKDOWN.

C FAULTY. CORRECT WITHIN 10 DAYS TO

MAINTENANCE DOLLARS.

B MINOR FAULTS. CORRECTION WASTES D

A NO FAULTS. TYPICAL NEW EQUIPMENT

Figure 23 – Vibration performance of rotating machines
Arya et al (1984)

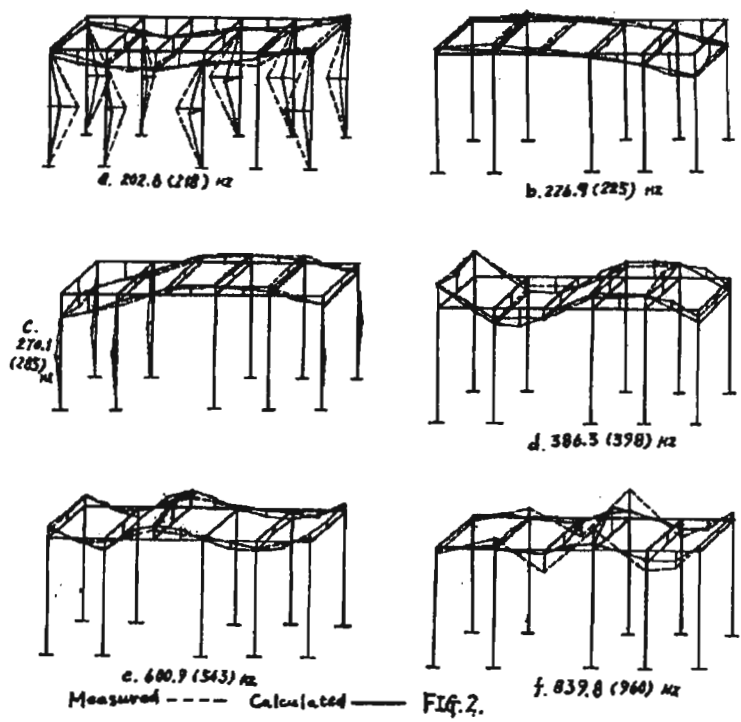


Figure 24: Model Mode shapes
Daming et al (1983)

Mode of Vibration	Circular Footing	Rectangular Footing
Vertical	$k_z = \frac{4Gr_0}{1-\nu} \eta_z$	$k_z = \frac{G}{1-\nu} \beta_z \sqrt{BL} \eta_z$
Horizontal	$k_x = \frac{32(1-\nu)Gr_0}{7-8\nu} \eta_x$	$k_x = 2(1+\nu)G\beta_x \sqrt{BL} \eta_x$
Rocking	$k_\psi = \frac{8Gr_0^3}{3(1-\nu)} \eta_\psi$	$k_\psi = \frac{G}{1-\nu} \beta_\psi BL^2 \eta_\psi$
Torsional	$k_\theta = \frac{16Gr_0^3}{3}$	No solution available; Use r_0 from Table 4-2

Table 1 – Equivalent Spring Constants for Rigid Circular and Rectangular Footings
Whitman and Richart (1967)

Mode of Vibration	Mass (or Inertia) Ratio	Damping Ratio D
Vertical	$B_z = \frac{(1-\nu)}{4} \frac{W}{\gamma r_0^2}$	$D_z = \frac{0.425}{\sqrt{B_z}} \alpha_z$
Horizontal	$B_x = \frac{7-8\nu}{32(1-\nu)} \frac{W}{\gamma r_0^2}$	$D_x = \frac{0.288}{\sqrt{B_x}} \alpha_x$
Rocking	$B_\psi = \frac{3(1-\nu)}{8} \frac{I_\psi}{\rho r_0^5}$	$D_\psi = \frac{0.15 \alpha_\psi}{(1+n_\psi B_\psi) \sqrt{n_\psi B_\psi}}$
Torsional	$B_\theta = \frac{I_\theta}{\rho r_0^5}$	$D_\theta = \frac{0.50}{1+2B_\theta}$

Table 2: Equivalent Damping Ratio for Rigid Circular and Rectangular Footings
Richart, Hall and Woods (1970)

Plasticity Index	k
0	0
20	0.18
40	0.30
60	0.41
80	0.48
≥ 100	0.50

Table 3: Values of K
Arya et al (1984)

Expression	Constant Force Excitation F_0 Constant	Rotating Mass-type Excitation, $F_0 = m_1 e \omega^2$
Magnification factor	$M = \frac{1}{\sqrt{(1-r^2)^2 + (2Dr)^2}}$	$M_r = \frac{r^2}{\sqrt{(1-r^2)^2 + (2Dr)^2}}$
Amplitude at frequency f	$Y = M (F_0/k)$	$Y = M_r (m_1 e/m)$
Resonant frequency	$f_{mr} = f_0 \sqrt{1-2D^2}$	$f_{mr} = \frac{f_0}{\sqrt{1-2D^2}}$
Amplitude at resonant frequency f_r	$Y_{max} = \frac{(F_0/k)}{2D\sqrt{1-D^2}}$	$Y_{max} = \frac{(m_1 e/m)}{2D\sqrt{1-D^2}}$
Transmissibility factor	$T_r = \frac{\sqrt{1+(2Dr)^2}}{\sqrt{(1-r^2)^2 + (2Dr)^2}}$	$\bar{T}_r = \frac{r^2 \sqrt{1+(2Dr)^2}}{\sqrt{(1-r^2)^2 + (2Dr)^2}}$

where $r = \omega/\omega_n$
 ω_n (Undamped natural circular frequency) = $\sqrt{k/m}$
 D (Damping ratio) = C/C_0
 C_0 (Critical Damping) = $2\sqrt{km}$
 T_r = Force transmitted/ F_0
 \bar{T}_r = Force transmitted/ $m_1 e \omega^2$

Table 4 – Summary of Derived Expressions for a Single-Degree of Freedom System
Arya et al (1984)

Mode of Vibration	r_0 for Rectangular Foundation	Coefficient
Vertical	$\sqrt{BL/\pi}$	$\eta_v = 1 + 0.6(1-\nu)(h/r_0)$
Horizontal	$\sqrt{BL/\pi}$	$\eta_h = 1 + 0.55(2-\nu)(h/r_0)$
Rocking	$\sqrt[3]{BL^3/3\pi}$	$\eta_\psi = 1 + 1.2(1-\nu)(h/r_0) + 0.2(2-\nu)(h/r_0)^3$
Torsional	$\sqrt[3]{BL(B^2 + L^2)/6\pi}$	None available

Notes: h is the depth of foundation embedment below grade;
 L is horizontal dimension perpendicular to axis of rocking;
 B is remaining horizontal dimension.

Table 5 – Embedment Coefficient for Spring Constants
Arya et al (1984)

Mode of Vibration	Damping Ratio Embedment Factor
Vertical	$\alpha_v = \frac{1 + 1.9(1-\nu) \frac{h}{r_0}}{\sqrt{\eta_v}}$
Horizontal	$\alpha_h = \frac{1 + 1.9(2-\nu) \frac{h}{r_0}}{\sqrt{\eta_h}}$
Rocking	$\alpha_\psi = \frac{1 + 0.7(1-\nu)(h/r_0) + 0.6(2-\nu)(h/r_0)^3}{\sqrt{\eta_\psi}}$

Table 6 - Effect of Depth of Embedment on Damping Ratio
Arya et al (1984)

H/r_0	$k_z/[4Gr_0/(1-\nu)]$
1	2.1
2	1.8
∞	1.0

Table 7 – Approximate k_z Variation with Stratum Thickness
Richart, Hall and Woods (1970)

H/r_0	$W/\gamma_s r_0^3 =$	$A_z, \text{ resonance}$			
		$[(3/16)/(Q_0/Gr_0)]$			
		5	10	20	30
1		5.8	11	21	29
2		8.0	16	31	41
∞		1.2	1.6	2.2	2.7

W = weight of footing plus machinery vibrating in phase.
 Q_0 = unbalanced vertical force.
 G = shear modulus of soft soil.
 γ_s = total unit weight of soft soil.
 ν = Poisson's ratio of soft soil.

Table 8 – Resonant Vertical Displacement for Stratum Overlying Rigid Base: $\nu = 0.25$
Richart, Hall and Woods (1970)

$W/\gamma_s r_0^3$	$f_0/\sqrt{G_g/\gamma_s r_0^2}$			
	$H/r_0 =$	1	2	∞
5		0.21	0.15	—
10		0.16	0.12	0.10
20		0.12	0.094	0.080
30		0.097	0.080	0.064

f_0 = fundamental resonant frequency (in cps if g is in linear units/sec²).

Table 9 – Frequency in Vertical Mode for Stratum Overlying Rigid Base: $\nu = 0.25$
Richart, Hall and Woods (1970)

TABLE 10.1: NON LINEAR TRANSIENT RESPONSE: RAFT

ANALYSIS No	NATURAL FREQUENCY (Hz)	MAXIMUM AMPLITUDE STRUCTURE				MAXIMUM VELOCITY STRUCTURE		MASS (lb)	MASS RATIO	CENTRE OF GRAVITY OF STRUCTURE					
		VERT (Y) in	mm	TRANS (Z) in	mm	Vy in/s	Vz in/s			Cm (X)	mm	Cm (Y)	mm	Cm (Z)	mm
RAFT															
G4000	7.48	0.000308	0.0078232	0.000204	0.0051816	0.113	0.146	465,720	3.1	8.91	2716	1.30	396	5.00	1524
G4000-mdof	7.48	0.000262	0.0066548	0.000360	0.0091440	0.063	0.271	420,276	2.8	9.37	2856	1.23	375	5.00	1524
G4000-stf	7.49	0.000405	0.0102870	0.000186	0.0047244	0.042	0.026	420,273	2.8	9.38	2859	1.23	375	5.00	1524
G10000	11.85	0.000697	0.0177038	0.000148	0.0037592	0.200	0.094	412,174	2.7	9.37	2856	1.22	372	5.00	1524
G10000-mdof	11.86	0.000606	0.0153924	0.000142	0.0036068	0.197	0.079	412,177	2.7	9.37	2856	1.22	372	5.00	1524
G10000p	12.00	0.000443	0.0112522	0.000124	0.0031496	0.084	0.045	412,174	2.7	9.37	2856	1.22	372	5.00	1524
G10000-stf	11.93	0.000301	0.0076454	0.000095	0.0024130	0.044	0.028	520,167	3.5	9.00	2743	1.00	305	5.00	1524
G15000	13.90	0.000834	0.0211836	0.000156	0.0039624	0.249	0.065	520,167	3.5	9.00	2743	1.00	305	5.00	1524
G15000-F1	13.90	0.000834	0.0211836	0.000156	0.0039624	0.249	0.065	520,167	3.5	9.00	2743	1.00	305	5.00	1524
G15000-F2	12.99	0.001113	0.0282702	0.000160	0.0040640	0.360	0.066	628,160	4.2	10.00	3048	1.00	305	5.00	1524
G15000-F3	12.22	0.000241	0.0061214	0.004610	0.1170940	0.035	0.153	736,153	4.9	10.00	3048	1.00	305	5.00	1524
G15000-F4	11.57	0.000733	0.0186182	0.000226	0.0057404	0.253	0.094	844,146	5.6	10.00	3048	1.00	305	5.00	1524
G15000-mdof	13.92	0.000605	0.0153670	0.000138	0.0035052	0.229	0.064	520,170	3.5	9.00	2743	1.00	305	5.00	1524
G15000-stf	14.01	0.000222	0.0056388	0.000115	0.0029210	0.038	0.024	520,167	3.5	9.00	2743	1.00	305	5.00	1524
G15000p	15.24	0.000525	0.0133350	0.000137	0.0034798	0.122	0.051	520,167	3.5	9.00	2743	1.00	305	5.00	1524
G15000p-1	14.80	0.000541	0.0137414	0.000165	0.0041910	0.148	0.047	419,373	2.8	10.00	3048	1.00	305	5.00	1524
G15000p-2	14.31	0.000500	0.0127000	0.000209	0.0053086	0.125	0.062	432,872	2.9	10.00	3048	1.00	305	5.00	1524
G15000p-3	13.78	0.000360	0.0091440	0.000344	0.0087376	0.077	0.107	446,371	3.0	10.00	3048	1.00	305	5.00	1524
G15000p-F1	14.06	0.000311	0.0078994	0.000119	0.0030226	0.070	0.054	520,167	3.5	9.00	2743	1.00	305	5.00	1524
G15000p-F2	13.11	0.000211	0.0053594	0.000143	0.0036322	0.053	0.075	628,160	4.2	10.00	3048	1.00	305	5.00	1524
G15000p-F3	12.31	0.000241	0.0061214	0.000461	0.0117094	0.035	0.153	736,153	4.9	10.00	3048	1.00	305	5.00	1524
G15000p-F4	11.65	0.000144	0.0036576	0.000090	0.0022860	0.036	0.051	844,146	5.6	10.00	3048	1.00	305	5.00	1524
G20000	16.51	0.001646	0.0418084	0.000175	0.0044450	0.526	0.061	412,174	2.7	9.00	2743	1.00	305	5.00	1524
G20000-mdof	16.59	0.000705	0.0179070	0.000518	0.0131572	0.150	0.173	412,177	2.7	9.00	2743	1.00	305	5.00	1524
G20000p	16.88	0.000611	0.0155194	0.000145	0.0036830	0.143	0.045	412,174	2.7	9.00	2743	1.00	305	5.00	1524
G20000-stf	16.87	0.000250	0.0063500	0.000142	0.0036068	0.048	0.031	412,174	2.7	9.00	2743	1.00	305	5.00	1524
G30000	20.64	0.000680	0.0172720	0.000191	0.0048514	0.210	0.068	672,257	4.5	9.00	2743	1.50	457	5.00	1524
G30000-mdof	20.85	0.000519	0.0131826	0.000157	0.0039878	0.174	0.068	412,177	2.7	9.00	2743	1.00	305	5.00	1524
G30000p	21.37	0.000535	0.0135890	0.000158	0.0040132	0.148	0.061	672,257	4.5	9.00	2743	1.50	457	5.00	1524
G30000-stf	21.51	0.000246	0.0062484	0.000153	0.0038862	0.058	0.037	412,174	2.7	9.00	2743	1.00	305	5.00	1524

Classification of Machine Operation (Baxter and Bernhard (1967))

Green Fair (.08-.16) in/s
 Blue Slightly rough (.16-.315) in/s
 Red Rough (.315-.63) in/s
 Pink Very Rough (>.63) in/s

A
B
C
D
E

Vibration Performance of Rotating Machines (Fig 23)

No faults 0.0001 in
 Minor faults 0.00025 in
 Faulty 0.0006 in
 Failure is near 0.0015 in
 Dangerous > .0015 in

General Limits of Vibration Amplitude (ref. 1)

Machine foundation 0.0004 in

TABLE10.2: NON LINEAR TRANSIENT RESPONSE: TABLE TOP

ANALYSIS NO.	NATURAL FREQUENCY (Hz)	MAXIMUM AMPLITUDE STRUCTURE				MAXIMUM VELOCITY STRUCTURE		MASS (lb)	MASS RATIO	CENTRE OF GRAVITY OF STRUCTURE					
		VERT (Y) in	mm	TRANS (Z) in	mm	Vy (in/s)	Vz (in/s)			Cm (X)	mm	Cm (Y)	mm	Cm (Z)	mm
G4000	7.2	0.001954	0.0496316	0.000438	0.0111252	0.571	0.079	494,068	3.3	9.24	2816	7.14	2176	5.00	1524
G4000-mdof	3.92	0.003884	0.0986536	0.000421	0.0106934	1.253	0.083	494,071	3.3	9.24	2816	7.14	2176	5.00	1524
G4000-stf	4.38	0.000314	0.0079756	0.000262	0.0066548	0.029	0.034	494,068	3.3	9.24	2816	7.14	2176	5.00	1524
G10000	5.24	0.001654	0.0420116	0.020210	0.5133340	0.188	2.590	494,068	3.3	9.24	2816	7.14	2176	5.00	1524
G10000-mdof	5.25	0.002463	0.0625602	0.000437	0.0110998	0.795	0.086	494,071	3.3	9.24	2816	7.14	2176	5.00	1524
G10000-stf	6.93	0.000228	0.0057912	0.000223	0.0056642	0.031	0.036	494,068	3.3	9.24	2816	7.14	2176	5.00	1524
G15000	5.78	0.002204	0.0559816	0.015434	0.3920236	0.291	1.897	494,068	3.3	9.00	2743	7.00	2134	5.00	1524
G15000 beam	20.03	0.001788	0.0454152	0.000138	0.0035052	0.598	0.098	494,068	3.3	9.24	2816	7.14	2176	5.00	1524
G15000fs	9.88	0.000171	0.0043434	0.000290	0.0073660	0.092	0.074	594,862	4.0	9.48	2890	6.99	2131	5.00	1524
G15000ps	9.31	0.000182	0.0046228	0.000274	0.0069596	0.099	0.075	594,862	4.0	9.48	2890	6.99	2131	5.00	1524
G15000-B1	4.27	0.002754	0.069952	0.000743	0.0188722	0.690	0.098	480,569	3.2	10.00	3048	7.00	2134	5.00	1524
G15000-B2	4.19	0.001907	0.0484378	0.000801	0.0203454	0.446	0.117	494,068	3.3	9.00	2743	8.00	2438	5.00	1524
G15000-B3	4.11	0.000693	0.0176022	0.000378	0.0096012	0.197	0.054	521,067	3.5	9.00	2743	8.00	2438	5.00	1524
G15000-B4	4.03	0.002294	0.0582676	0.003242	0.0823468	0.306	0.541	521,067	3.5	9.00	2743	8.00	2438	5.00	1524
G15000-C1	4.39	0.004493	0.1141222	0.007008	0.1780032	0.574	0.900	455,821	3.0	9.00	2743	7.00	2134	5.00	1524
G15000-C2	5.14	0.002065	0.052451	0.000412	0.0104648	0.676	0.068	486,419	3.2	9.00	2743	7.00	2134	5.00	1524
G15000-C3	5.49	0.000899	0.0228346	0.000401	0.0101854	0.300	0.081	517,017	3.4	9.00	2743	7.00	2134	5.00	1524
G15000-C4	5.72	0.002294	0.0582676	0.003242	0.0823468	0.306	0.541	547,615	3.7	9.00	2743	7.00	2134	5.00	1524
G15000-C5	5.86	0.000665	0.016891	0.000299	0.0075946	0.228	0.061	578,213	3.9	9.00	2743	7.00	2134	5.00	1524
G15000-F1	5.90	0.011138	0.2829052	0.006078	0.1543812	1.412	0.754	602,061	4.0	9.00	2743	6.00	1829	5.00	1524
G15000-F2	5.94	0.001471	0.0373634	0.004587	0.1165098	0.208	0.572	710,055	4.7	9.00	2743	5.00	1524	5.00	1524
G15000-F3	5.94	0.000760	0.019304	0.004284	0.1088136	0.104	0.530	818,048	5.5	9.00	2743	5.00	1524	5.00	1524
G15000-F4	5.94	0.000530	0.013462	0.003792	0.0963168	0.071	0.467	926,041	6.2	10.00	3048	4.00	1219	5.00	1524
G15000-stf	9.14	0.000192	0.0048768	0.000206	0.0052324	0.032	0.038	494,068	3.3	9.24	2816	7.14	2176	5.00	1524
G15000-mdof	5.21	0.002669	0.0677926	0.000277	0.0070358	0.836	0.070	558,070	3.7	9.57	2917	8.03	2448	5.00	1524
G15000-H	5.78	0.002228	0.0565912	0.002466	0.0626364	0.286	0.280	501,662	3.3	9.25	2819	7.25	2210	5.00	1524
G20000	5.90	0.011939	0.3032506	0.007266	0.1845564	1.523	0.894	494,068	3.3	9.00	2743	7.00	2134	5.00	1524
G20000-mdof	5.90	0.011929	0.3029966	0.009668	0.2455672	1.487	1.170	494,071	3.3	9.24	2816	7.14	2176	5.00	1524
G20000-stf	9.81	0.000192	0.0048768	0.000201	0.0051054	0.033	0.039	494,068	3.3	9.24	2816	7.14	2176	5.00	1524
G20000-H	5.82	0.013130	0.333502	0.013381	0.3398774	1.678	1.656	500,818	3.3	9.19	2801	7.24	2207	5.00	1524
G30000	5.61	0.019521	0.4958334	0.002313	0.0587502	2.680	0.248	494,068	3.3	9.00	2743	7.00	2134	5.00	1524
G30000-mdof	6.25	0.001580	0.040132	0.000461	0.0117094	0.525	0.088	494,071	3.3	9.24	2816	7.14	2176	5.00	1524
G30000-stf	11.84	0.000160	0.004064	0.000168	0.0042672	0.032	0.033	558,070	3.7	9.57	2917	8.03	2448	5.00	1524

Classification of Machine Operation (Baxter and Bernhard (1967))

Vibration Performance of Rotating Machines (Fig 23)

General Limits of Vibration Amplitude (ref. 1)

Green	Fair (.08-.16) in/s	A	No faults	0.0001 in
Blue	Slightly rough (.16-.315) in/s	B	Minor faults	0.00025 in
Red	Rough (.315-.63) in/s	C	Faulty	0.0006 in
Pink	Very Rough (>.63) in/s	D	Failure is near	0.0015 in
		E	Dangerous	> .0015 in

Machine foundation 0.0004 in

TABLE 10.3: NON LINEAR TRANSIENT RESPONSE: MULTI-STOREY

ANALYSIS NO.	NATURAL FREQUENCY (Hz)	MAXIMUM AMPLITUDE STRUCTURE				MAXIMUM VELOCITY OF STRUCTURE		MASS (lb) OF STRUCTURE	MASS RATIO	CENTRE OF GRAVITY OF STRUCTURE					
		VERT (Y) in	mm	TRANS (Z) in	mm	Vy (in/s)	Vz (in/s)			Cm (X)	mm	Cm (Y)	mm	Cm (Z)	mm
MULTI STOREY															
G4000	2.08	0.001757	0.0446278	0.000049	0.0012446	0.499	0.072	672,257	4.5	9.17	2795	14.86	4529	5.00	1524
G4000-mdof	2.08	0.001028	0.0261112	0.000050	0.0012700	0.260	0.081	672,257	4.5	9.17	2795	14.86	4529	5.00	1524
G4000-stf	2.35	0.000251	0.0063754	0.000061	0.0015494	0.020	0.033	672,257	4.5	9.17	2795	14.86	4529	5.00	1524
G10000	2.85	0.001285	0.0326390	0.000464	0.0117856	0.373	0.079	672,257	4.5	9.17	2795	14.86	4529	5.00	1524
G10000-mdof	2.85	0.000983	0.0249682	0.000429	0.0108966	0.290	0.079	672,257	4.5	9.17	2795	14.86	4529	5.00	1524
G10000-stf	3.72	0.000181	0.0045974	0.000258	0.0065532	0.021	0.034	672,257	4.5	9.17	2795	14.86	4529	5.00	1524
G15000	3.29	0.001169	0.0296926	0.000438	0.0111252	0.325	0.071	672,257	4.5	9.00	2743	15.00	4572	5.00	1524
G15000-B1	2.49	0.003046	0.0773684	0.000854	0.0216916	0.713	0.110	640,759	4.3	10.00	3048	15.00	4572	5.00	1524
G15000-B2	2.45	0.001774	0.0450596	0.001503	0.0381762	0.387	0.243	667,757	4.5	10.00	3048	16.00	4877	5.00	1524
G15000-B3	2.40	0.001087	0.0276098	0.000468	0.0118872	0.285	0.055	694,756	4.6	9.00	2743	16.00	4877	5.00	1524
G15000-B4	2.35	0.001772	0.0450088	0.001742	0.0442468	0.206	0.179	721,754	4.8	9.00	2743	16.00	4877	5.00	1524
G15000-C1	2.56	0.000892	0.0226568	0.006623	0.1682242	1.458	0.109	595,762	4.0	9.00	2743	15.00	4572	5.00	1524
G15000-C2	3.04	0.001141	0.0289814	0.000407	0.0103378	0.348	0.066	656,958	4.4	9.00	2743	15.00	4572	5.00	1524
G15000-C3	3.18	0.002778	0.0705612	0.000719	0.0182626	0.832	0.121	718,154	4.8	9.00	2743	15.00	4572	5.00	1524
G15000-C4	3.25	0.000952	0.0241808	0.000366	0.0092964	0.305	0.060	779,350	5.2	9.00	2743	15.00	4572	5.00	1524
G15000-C5	3.29	0.004322	0.1097788	0.001982	0.0503428	0.676	0.240	840,546	5.6	9.00	2743	15.00	4572	5.00	1524
G15000-F1	3.34	0.001568	0.0398272	0.000434	0.0110236	0.447	0.070	780,250	5.2	9.00	2743	13.00	3962	5.00	1524
G15000-F2	3.36	0.001088	0.0276352	0.000458	0.0116332	0.315	0.067	888,243	5.9	9.00	2743	12.00	3658	5.00	1524
G15000-F3	3.36	0.001088	0.0276352	0.000458	0.0116332	0.315	0.068	888,243	5.9	9.00	2743	12.00	3658	5.00	1524
G15000-F4	3.37	0.000885	0.0224790	0.000436	0.0110744	0.268	0.072	1,104,229	7.4	9.00	2743	10.00	3048	5.00	1524
G15000-mdof	3.29	0.001751	0.0444754	0.000432	0.0109728	0.562	0.080	672,257	4.5	9.00	2743	15.00	4572	5.00	1524
G15000-stf	4.93	0.000143	0.0036322	0.000236	0.0059944	0.021	0.034	672,257	4.5	9.00	2743	15.00	4572	5.00	1524
G20000	3.38	0.001344	0.0341376	0.000045	0.0011430	0.373	0.070	672,257	4.5	9.00	2743	15.00	4572	5.00	1524
G20000-mdof	3.38	0.001957	0.0497078	0.000038	0.0009652	0.603	0.080	672,257	4.5	9.00	2743	15.00	4572	5.00	1524
G20000-stf	5.26	0.000139	0.0035306	0.000048	0.0012192	0.022	0.035	672,257	4.5	9.17	2795	14.86	4529	5.00	1524
G30000	3.62	0.001747	0.0443738	0.000423	0.0107442	0.500	0.068	672,257	4.5	9.00	2743	15.00	4572	5.00	1524
G30000-mdof	3.62	0.001782	0.0452628	0.000426	0.0108204	0.504	0.079	672,257	4.5	9.00	2743	15.00	4572	5.00	1524
G30000-stf	6.97	0.000128	0.0032512	0.000223	0.0056642	0.024	0.037	672,257	4.5	9.00	2743	15.00	4572	5.00	1524

Classification of Machine Operation (Baxter and Bernhard (1967))

Green Fair (.08-.16) in/s
Blue Slightly rough (.16-.315) in/s
Red Rough (.315-.63) in/s
Pink Very Rough (>.63) in/s

A
B
C
D
E

Vibration Performance of Rotating Machines (Fig 23)

No faults 0.0001 in
Minor faults 0.00025 in
Faulty 0.0006 in
Failure is near 0.0015 in
Dangerous > .0015 in

General Limits of Vibration Amplitude (ref. 1)
Machine foundation 0.0004 in

TABLE 11.1: NATURAL FREQUENCIES

ANALYSIS NO. <u>RAFT</u>	Mode 1	Mode 2	Mode 3	Mode 4	Mode 5	Mode 6	Mode 7	Mode 8	Mode 9	Mode 10
G4000	7.48	7.52	8.52	8.71	9.47	10.35	26.19	34.77	46.95	56.21
G4000-mdof	7.48	7.53	8.52	8.74	9.47	10.46	26.65	34.90	47.24	56.34
G4000-stf	7.49	7.54	8.55	8.72	9.49	10.37	6292.74	6372.25	7207.81	8097.25
G10000	11.85	11.85	13.47	13.78	15.00	16.34	28.89	35.10	36.57	46.70
G10000-mdof	11.86	11.88	13.48	13.83	15.01	16.52	29.40	36.39	44.46	48.96
G10000p	12.00	12.07	13.62	13.83	14.99	16.41	29.66	39.63	45.48	59.19
G10000-stf	11.93	12.01	13.61	13.85	15.11	16.40	6062.45	6371.54	7097.72	7964.37
G15000	13.90	13.91	15.70	16.45	17.89	19.18	35.48	36.81	43.01	46.59
G15000-F1	13.90	13.91	15.70	16.45	17.89	19.18	35.48	36.81	43.01	46.59
G15000-F2	12.99	12.99	14.38	15.33	16.49	17.41	35.46	43.06	46.06	49.02
G15000-F3	12.22	12.23	13.34	14.41	15.30	16.06	35.42	45.87	50.00	54.43
G15000-F4	11.57	11.59	12.50	13.63	14.37	14.98	35.38	45.68	57.14	58.25
G15000-mdof	13.92	13.94	15.75	16.45	17.91	19.35	37.38	43.24	44.88	57.59
G15000-stf	14.01	14.11	15.77	16.60	18.03	19.24	8155.88	8497.38	9550.38	10630.40
G15000p	15.24	15.35	17.52	18.01	19.80	21.69	32.83	41.74	47.85	60.68
G15000p-1	14.80	14.90	17.32	17.79	19.58	21.43	32.36	43.25	49.15	59.04
G15000p-2	14.31	14.38	17.10	17.57	19.37	21.14	31.73	43.94	49.56	56.57
G15000p-3	13.78	13.79	16.86	17.36	19.17	20.83	30.96	43.91	49.43	53.69
G15000p-F1	6.13	6.16	6.66	6.92	7.30	7.68	48.68	58.63	64.97	68.05
G15000p-F2	13.11	13.17	14.41	15.49	16.47	17.48	43.63	52.79	63.87	68.08
G15000p-F3	12.31	12.37	13.37	14.54	15.31	16.11	50.57	59.97	65.08	68.15
G15000p-F4	11.65	11.69	12.52	13.73	14.37	15.02	57.80	64.39	68.26	68.94
G20000	16.51	16.63	18.85	19.41	21.07	23.05	33.05	35.70	39.05	47.47
G20000-mdof	16.59	16.66	18.86	19.46	21.08	23.29	33.54	33.20	44.59	51.91
G20000p	16.88	16.99	19.11	19.50	21.10	23.12	33.72	42.33	48.52	61.11
G20000-stf	16.87	16.99	19.25	19.59	21.36	23.20	6062.48	6371.57	7097.75	7964.39
G30000	20.64	21.01	24.44	24.66	27.54	30.25	35.65	38.27	42.58	47.65
G30000-mdof	20.85	21.05	24.54	24.69	27.64	30.73	38.97	42.80	44.97	56.15
G30000p	21.37	21.56	24.65	25.10	27.78	30.42	39.05	46.12	52.88	63.03
G30000-stf	21.51	21.68	24.87	25.60	28.33	30.76	6062.52	6371.61	7097.78	7964.42

All frequencies in Hertz

TABLE 11.2: NATURAL FREQUENCIES

ANALYSIS NO.	Mode 1	Mode 2	Mode 3	Mode 4	Mode 5	Mode 6	Mode 7	Mode 8	Mode 9	Mode 10
TABLE TOP										
G4000	7.19	8.55	9.90	21.20	28.70	33.82	43.01	47.48	48.82	55.74
G4000-mdof	3.92	4.06	6.77	8.02	9.37	9.62	12.16	15.07	20.21	21.02
G4000-stf	4.38	4.84	8.12	8.30	9.40	9.62	5958.97	6242.74	6706.64	6770.61
G10000	5.24	5.39	7.78	12.47	14.73	15.15	16.65	18.45	20.38	23.96
G10000-mdof	5.25	5.40	7.87	12.48	14.73	15.18	16.66	18.46	20.40	24.01
G10000-stf	6.93	7.65	12.84	13.12	14.86	15.21	5958.98	6242.76	6706.66	6770.62
G15000	5.78	6.21	8.06	16.27	18.89	19.32	20.41	20.59	21.84	27.33
G15000 beam	20.03	20.36	20.47	34.48	37.71	41.05	43.31	43.84	44.82	48.75
G15000fs	9.88	22.40	25.61	38.50	40.79	57.89	65.51	70.38	75.84	78.86
G15000ps	9.31	22.39	25.55	38.18	40.27	57.85	65.32	70.16	75.80	78.74
G15000-B1	4.27	4.36	5.28	16.25	18.71	19.78	20.26	20.47	23.16	27.89
G15000-B2	4.19	4.26	5.16	16.07	18.53	19.77	20.26	20.42	23.10	27.67
G15000-B3	4.11	4.17	5.05	15.88	18.33	19.76	20.26	20.38	23.02	27.32
G15000-B4	4.03	4.08	4.93	15.70	18.12	19.75	20.26	20.35	22.93	26.92
G15000-C1	4.39	4.57	5.53	16.53	19.04	19.79	20.25	20.51	20.58	23.23
G15000-C2	5.14	6.02	7.64	16.39	18.80	19.44	20.22	20.37	20.78	26.56
G15000-C3	5.49	6.75	8.86	16.15	18.48	19.08	19.91	20.46	20.94	28.27
G15000-C4	5.72	7.05	9.47	15.86	18.14	18.73	19.53	20.47	21.05	28.06
G15000-C5	5.86	7.15	9.73	15.58	17.81	18.40	19.09	20.42	21.12	27.68
G15000-F1	5.90	6.28	8.28	15.33	16.89	17.10	18.08	20.08	20.67	24.78
G15000-F2	5.94	6.28	8.36	14.46	15.38	15.49	16.37	18.68	20.79	22.79
G15000-F3	5.94	6.26	8.38	13.69	14.21	14.27	15.08	17.53	20.85	31.23
G15000-F4	5.94	6.23	8.37	12.99	13.29	13.30	14.08	16.58	19.96	20.89
G15000-stf	9.14	10.06	16.66	17.07	19.12	19.50	5959.00	6242.78	6706.67	6770.64
G15000-mdof	5.21	5.59	7.59	15.39	18.45	18.78	19.34	20.54	21.19	26.30
G15000-H	5.78	6.22	8.12	16.16	18.86	19.31	20.56	21.63	21.92	27.66
G20000	5.90	6.39	8.20	17.18	20.56	20.60	21.37	22.68	23.24	28.31
G20000-mdof	5.90	6.40	8.25	17.20	20.48	20.56	21.41	22.69	23.24	28.46
G20000-stf	9.81	10.82	18.16	18.59	21.02	21.52	5959.13	6243.14	6707.46	6771.13
G20000-H	5.82	6.32	8.13	17.05	20.09	20.54	21.35	22.68	23.22	27.99
G30000	5.61	6.26	7.74	18.20	20.59	24.79	26.08	27.11	27.95	28.44
G30000-mdof	6.25	7.02	8.40	20.57	22.05	26.12	27.25	28.31	28.40	28.60
G30000-stf	11.84	13.10	22.98	23.08	26.72	27.50	5915.89	6218.10	6659.97	6748.34

All frequencies in Hertz

TABLE 11.3: NATURAL FREQUENCIES

ANALYSIS NO.	Mode 1	Mode 2	Mode 3	Mode 4	Mode 5	Mode 6	Mode 7	Mode 8	Mode 9	Mode 10
MULTI STOREY										
G4000	2.08	2.29	4.63	7.06	8.68	8.90	10.56	14.27	15.07	17.25
G4000-mdof	2.08	2.49	4.67	7.06	8.69	8.90	10.57	14.28	15.07	17.25
G4000-stf	2.35	2.75	7.20	7.52	8.97	9.09	5846.86	5957.05	6494.87	6594.74
G10000	2.85	2.97	4.98	10.87	12.19	13.21	14.94	16.23	17.87	18.42
G10000-mdof	2.85	2.97	5.02	10.87	12.19	13.23	14.96	16.24	17.87	18.42
G10000-stf	3.72	4.35	11.38	11.89	14.18	14.38	5846.87	5957.06	6494.88	6594.76
G15000	3.29	3.31	5.08	13.06	14.01	15.00	16.54	19.11	20.25	20.94
G15000-B1	2.49	2.64	3.42	9.45	9.48	10.71	13.89	17.37	19.90	20.25
G15000-B2	2.45	2.57	3.34	9.12	9.13	10.33	13.63	17.02	19.88	20.24
G15000-B3	2.40	2.50	3.26	8.81	8.82	9.98	13.37	16.67	19.85	20.22
G15000-B4	2.35	2.45	3.18	8.53	8.55	9.66	13.12	16.33	19.81	20.21
G15000-C1	2.56	2.77	3.58	9.97	10.10	11.37	14.33	17.99	19.94	20.29
G15000-C2	3.04	3.23	4.74	11.07	14.16	14.45	15.57	18.14	20.14	20.28
G15000-C3	3.18	3.49	5.37	11.63	13.85	16.23	17.51	18.07	19.71	20.25
G15000-C4	3.25	3.59	5.68	11.95	13.50	16.51	17.92	18.00	19.20	20.21
G15000-C5	3.29	3.61	5.81	12.12	13.16	16.41	17.75	18.06	18.67	20.14
G15000-F1	3.34	3.37	5.19	13.01	13.50	14.55	16.02	17.64	19.10	19.29
G15000-F2	3.36	3.39	5.25	12.78	12.96	13.86	15.13	16.47	18.11	18.18
G15000-F3	3.36	3.39	5.25	12.78	12.96	13.86	15.13	16.47	18.11	18.18
G15000-F4	3.37	3.40	5.29	11.90	12.05	12.43	13.29	15.16	16.30	17.42
G15000-mdof	3.29	3.31	5.12	13.07	14.02	15.02	16.06	19.12	20.27	20.95
G15000-stf	4.93	5.77	15.09	15.14	18.10	18.31	5846.89	5957.08	6494.90	6594.78
G20000	3.38	3.38	5.11	13.24	14.74	15.46	16.84	20.06	20.26	22.65
G20000-mdof	3.38	3.38	5.16	13.25	14.75	15.48	16.86	20.08	20.27	22.65
G20000-stf	5.26	6.15	16.09	16.81	20.06	20.33	5846.90	5957.09	6494.91	6594.78
G30000	3.62	3.73	5.17	13.47	16.00	17.15	18.48	20.29	23.85	27.82
G30000-mdof	3.62	3.73	5.22	13.49	16.02	17.17	18.49	20.31	23.90	27.84
G30000-stf	6.97	8.15	21.34	21.42	25.59	25.90	5846.94	5957.13	6494.95	6594.82

All frequencies in Hertz

TABLE 12.1: STRUCTURE DIMENSIONS: RAFT

ANALYSIS No	Soil Properties		Foundation Dimensions		
			W	L	T
	Description	G (kPa)	Width (mm)	Length (mm)	Thickness (mm)

RAFT

G4000	soft clay	27579	7315	9144	914
G4000-mdof	soft clay	27579	7315	9144	914
G4000-stf	soft clay	27579	7315	9144	914
G10000	stiff clay	68948	7315	9144	914
G10000-mdof	stiff clay	68949	7315	9144	914
G10000p	stiff clay	68950	7315	9144	914
G10000-stf	stiff clay	68951	7315	9144	914
G15000	dense sand	103421	7315	9144	914
G15000-F1	dense sand	103422	7315	9144	1219
G15000-F2	dense sand	103423	7315	9144	1524
G15000-F3	dense sand	103424	7315	9144	1829
G15000-F4	dense sand	103425	7315	9144	2134
G15000-mdof	dense sand	103426	7315	9144	914
G15000-stf	dense sand	103427	7315	9144	914
G15000p	dense sand	103428	7315	9144	914
G15000p-1	dense sand	103429	7315	9144	914
G15000p-2	dense sand	103430	7315	9144	914
G15000p-3	dense sand	103431	7315	9144	914
G15000p-F1	dense sand	103432	7315	9144	1219
G15000p-F2	dense sand	103433	7315	9144	1524
G15000p-F3	dense sand	103434	7315	9144	1829
G15000p-F4	dense sand	103435	7315	9144	2134
G20000	medium dense gravel	137895	7315	9144	914
G20000-mdof	medium dense gravel	137896	7315	9144	914
G20000p	medium dense gravel	137897	7315	9144	914
G20000-stf	medium dense gravel	137898	7315	9144	914
G30000	dense gravel	206843	7315	9144	914
G30000-mdof	dense gravel	206844	7315	9144	914
G30000p	dense gravel	206845	7315	9144	914
G30000-stf	dense gravel	206846	7315	9144	914

TABLE 12.2: STRUCTURE DIMENSIONS: TABLE TOP

ANALYSIS No	Soil Properties		Foundation			DIMENSIONS					
			W	L	T	Columns		Transverse Beam		Longitudinal Beam	
	Description	G (kPa)	Width (mm)	Length (mm)	Thickness (mm)	A Width (mm)	B Depth (mm)	C Width (mm)	D Depth (mm)	E Width (mm)	F Depth (mm)

TABLE TOP

G4000	soft clay	27579	7315	9144	914	610	914	914	914	914	914
G4000-mdof	soft clay	27579	7315	9144	914	610	914	914	914	914	914
G4000-stf	soft clay	27579	7315	9144	914	610	914	914	914	914	914
G10000	stiff clay	68948	7315	9144	914	610	914	914	914	914	914
G10000-mdof	stiff clay	68948	7315	9144	914	610	914	914	914	914	914
G10000-stf	stiff clay	68948	7315	9144	914	610	914	914	914	914	914
G15000	dense sand	103421	7315	9144	914	610	914	914	914	914	914
G15000 beam	dense sand	103421	7315	9144	914	610	914	914	914	914	914
G15000fs	dense sand	103421	7315	9144	914	610	914	914	914	914	914
G15000ps	dense sand	103421	7315	9144	914	610	914	914	914	914	914
G15000-B1	dense sand	103421	7315	9144	914	610	914	914	1219	914	914
G15000-B2	dense sand	103421	7315	9144	914	610	914	914	1524	914	914
G15000-B3	dense sand	103421	7315	9144	914	610	914	914	1829	914	914
G15000-B4	dense sand	103421	7315	9144	914	610	914	914	2134	914	914
G15000-C1	dense sand	103421	7315	9144	914	610	610	914	914	914	914
G15000-C2	dense sand	103421	7315	9144	914	610	914	914	914	914	914
G15000-C3	dense sand	103421	7315	9144	914	610	1219	914	914	914	914
G15000-C4	dense sand	103421	7315	9144	914	610	1524	914	914	914	914
G15000-C5	dense sand	103421	7315	9144	914	610	1829	914	914	914	914
G15000-F1	dense sand	103421	7315	9144	1219	610	914	914	914	914	914
G15000-F2	dense sand	103421	7315	9144	1524	610	914	914	914	914	914
G15000-F3	dense sand	103421	7315	9144	1829	610	914	914	914	914	914
G15000-F4	dense sand	103421	7315	9144	2134	610	914	914	914	914	914
G15000-stf	dense sand	103421	7315	9144	914	610	914	914	914	914	914
G15000-mdof	dense sand	103421	7315	9144	914	610	914	914	914	914	914
G15000-H	dense sand	103421	7315	9144	914	610	914	914	914	914	914
G20000	medium dense s	137895	7315	9144	914	610	914	914	914	914	914
G20000-mdof	medium dense s	137895	7315	9144	914	610	914	914	914	914	914
G20000-stf	medium dense s	137895	7315	9144	914	610	914	914	914	914	914
G20000-H	medium dense s	137895	7315	9144	914	610	914	914	914	914	914
G30000	dense gravel	206843	7315	9144	914	610	914	914	914	914	914
G30000-mdof	dense gravel	206843	7315	9144	914	610	914	914	914	914	914
G30000-stf	dense gravel	206843	7315	9144	914	610	914	914	914	914	914

TABLE 12.3: STRUCTURE DIMENSIONS: MULTI-STOREY

ANALYSIS No		Soil Properties		DIMENSIONS								
				Foundation			Columns		Transverse Beam		Longitudinal Beam	
				W	L	T	A	B	C	D	E	F
Description		G (kPa)	Width (mm)	Length (mm)	Thickness (mm)	Width (mm)	Depth (mm)	Width (mm)	Depth (mm)	Width (mm)	Depth (mm)	

MULTI STOREY

G4000	soft clay	27579	7315	9144	914	610	914	914	914	914	914
G4000-mdof	soft clay	27579	7315	9144	914	610	914	914	914	914	914
G4000-stf	soft clay	27579	7315	9144	914	610	914	914	914	914	914
G10000	stiff clay	68948	7315	9144	914	610	914	914	914	914	914
G10000-mdof	stiff clay	68948	7315	9144	914	610	914	914	914	914	914
G10000-stf	stiff clay	68948	7315	9144	914	610	914	914	914	914	914
G15000	dense sand	103421	7315	9144	914	610	914	914	914	914	914
G15000-B1	dense sand	103421	7315	9144	914	610	914	914	1219	914	914
G15000-B2	dense sand	103421	7315	9144	914	610	914	914	1524	914	914
G15000-B3	dense sand	103421	7315	9144	914	610	914	914	1829	914	914
G15000-B4	dense sand	103421	7315	9144	914	610	914	914	2134	914	914
G15000-C1	dense sand	103421	7315	9144	914	610	610	914	914	914	914
G15000-C2	dense sand	103421	7315	9144	914	610	914	914	914	914	914
G15000-C3	dense sand	103421	7315	9144	914	610	1219	914	914	914	914
G15000-C4	dense sand	103421	7315	9144	914	610	1524	914	914	914	914
G15000-C5	dense sand	103421	7315	9144	914	610	1829	914	914	914	914
G15000-F1	dense sand	103421	7315	9144	1219	610	914	914	914	914	914
G15000-F2	dense sand	103421	7315	9144	1524	610	914	914	914	914	914
G15000-F3	dense sand	103421	7315	9144	1829	610	914	914	914	914	914
G15000-F4	dense sand	103421	7315	9144	2134	610	914	914	914	914	914
G15000-mdof	dense sand	103421	7315	9144	914	610	914	914	914	914	914
G15000-stf	dense sand	103421	7315	9144	914	610	914	914	914	914	914
G20000	medium dense gravel	137895	7315	9144	914	610	914	914	914	914	914
G20000-mdof	medium dense gravel	137895	7315	9144	914	610	914	914	914	914	914
G20000-stf	medium dense gravel	137895	7315	9144	914	610	914	914	914	914	914
G30000	dense gravel	206843	7315	9144	914	610	914	914	914	914	914
G30000-mdof	dense gravel	206843	7315	9144	914	610	914	914	914	914	914
G30000-stf	dense gravel	206843	7315	9144	914	610	914	914	914	914	914

TABLE 12.4: EQUIVALENT STIFFNESS OF RECTANGULAR FOOTINGS

Node	G=4 000 psi			G=10 000 psi			G=15 000 psi			G=20 000 psi			G=30 000 psi		
	Area (ft ²)	Kx=Kz	Ky	Area	Kx=Kz	Ky	Area	Kx=Kz	Ky	Area	Kx=Kz	Ky	Area	Kx=Kz	Ky
1	39	2,260,396	2,833,545	39	5,650,991	7,083,863	39	9104374	12557758	39	11301982	14167727	39	18208749	25115516
2	39	2,260,396	2,833,545	39	5,650,991	7,083,863	39	9104374	12557758	39	11301982	14167727	39	18208749	25115516
3	42	2,434,273	3,051,510	42	6,085,683	7,628,776	42	9804711	13523739	42	12171365	15257552	42	19609422	27047478
4	42	2,434,273	3,051,510	42	6,085,683	7,628,776	42	9804711	13523739	42	12171365	15257552	42	19609422	27047478
5	36	2,086,520	2,615,580	36	5,216,299	6,538,951	36	8404038	11591776	36	10432599	13077902	36	16808076	23183553
6	36	2,086,520	2,615,580	36	5,216,299	6,538,951	36	8404038	11591776	36	10432599	13077902	36	16808076	23183553
7	33	1,912,643	2,397,615	33	4,781,608	5,994,038	33	7703701	10625795	33	9563216	11988076	33	15407403	21251590
8	33	1,912,643	2,397,615	33	4,781,608	5,994,038	33	7703701	10625795	33	9563216	11988076	33	15407403	21251590
22	32.5	1,883,664	2,361,288	32.5	4,709,159	5,903,219	32.5	7586979	10464798	32.5	9418318	11806439	32.5	15173957	20929596
23	35	2,028,561	2,542,925	35	5,071,402	6,357,313	35	8170592	11269783	35	10142804	12714627	35	16341185	22539565
24	30	1,738,766	2,179,650	30	4,346,916	5,449,126	30	7003365	9659814	30	8693832	10898251	30	14006730	19319627
25	27.5	1,593,869	1,998,013	27.5	3,984,673	4,995,032	27.5	6419751	8854829	27.5	7969346	9990064	27.5	12839502	17709658
26	8.75	507,140	635,731	8.75	1,267,851	1,589,328	8.75	2042648	2817446	8.75	2535701	3178657	8.75	4085296	5634891
27	15	869,383	1,089,825	15	2,173,458	2,724,563	15	3501682	4829907	15	4346916	5449126	15	7003365	9659814
28	12.5	724,486	908,188	12.5	1,811,215	2,270,469	12.5	2918069	4024922	12.5	3622430	4540938	12.5	5836137	8049845
29	15	869,383	1,089,825	15	2,173,458	2,724,563	15	3501682	4829907	15	4346916	5449126	15	7003365	9659814
30	8.75	507,140	635,731	8.75	1,267,851	1,589,328	8.75	2042648	2817446	8.75	2535701	3178657	8.75	4085296	5634891
31	22.75	1,318,565	1,652,901	22.75	3,296,411	4,132,254	22.75	5310885	7325359	22.75	6592823	8264507	22.75	10621770	14650717
32	22.75	1,318,565	1,652,901	22.75	3,296,411	4,132,254	22.75	5310885	7325359	22.75	6592823	8264507	22.75	10621770	14650717
33	24.5	1,419,993	1,780,048	24.5	3,549,982	4,450,119	24.5	5719415	7888848	24.5	7099963	8900239	24.5	11438829	15777696
34	24.5	1,419,993	1,780,048	24.5	3,549,982	4,450,119	24.5	5719415	7888848	24.5	7099963	8900239	24.5	11438829	15777696
35	21	1,217,137	1,525,755	21	3,042,841	3,814,388	21	4902355	6761870	21	6085683	7628776	21	9804711	13523739
36	21	1,217,137	1,525,755	21	3,042,841	3,814,388	21	4902355	6761870	21	6085683	7628776	21	9804711	13523739
37	19.25	1,115,708	1,398,609	19.25	2,789,271	3,496,522	19.25	4493826	6198380	19.25	5578542	6993045	19.25	8987652	12396761
38	19.25	1,115,708	1,398,609	19.25	2,789,271	3,496,522	19.25	4493826	6198380	19.25	5578542	6993045	19.25	8987652	12396761
39	8.75	507,140	635,731	8.75	1,267,851	1,589,328	8.75	2042648	2817446	8.75	2535701	3178657	8.75	4085296	5634891
40	15	869,383	1,089,825	15	2,173,458	2,724,563	15	3501682	4829907	15	4346916	5449126	15	7003365	9659814
41	12.5	724,486	908,188	12.5	1,811,215	2,270,469	12.5	2918069	4024922	12.5	3622430	4540938	12.5	5836137	8049845
42	15	869,383	1,089,825	15	2,173,458	2,724,563	15	3501682	4829907	15	4346916	5449126	15	7003365	9659814
43	8.75	507,140	635,731	8.75	1,267,851	1,589,328	8.75	2042648	2817446	8.75	2535701	3178657	8.75	4085296	5634891
Total	720	41,730,395	52,311,606	720	104,325,988	130,779,016	720	1.68E+08	2.32E+08	720	2.09E+08	2.62E+08	720	3.36E+08	4.64E+08

REFERENCE LIST

- 1 Arya, S., O'Neil, M. and Pincus, G., (1984) **"Design of Structures and Foundations for Vibrating Machines"**, Gulf Publishing, Houston, Texas.
- 2 Anonymous, 2002
- 3 Assimaki, D., Kausel, E. and Whittle, A., (2000) **"Model for Dynamic Shear Modulus and Damping for Granular Soils"**, Journal of Geotechnical and Geoenvironmental Engineering, A.S.C.E., Vol 126, No. 10, October, pp 859 – 869.
- 4 Borja, R.I., Wu, Wen-Hwa and Allison Smith, H., (1994) **"Nonlinear Lateral, Rocking, and Torsional Vibration of Rigid Foundations"**, Journal of Geotechnical Engineering, A.S.C.E., Vol 120, No. 3, March, pp 491 – 513
- 5 Borja, R.I., Wu, Wen-Hwa and Allison Smith, H., (1993) **"Nonlinear Response of Vertically Oscillating Rigid Foundations"**, Journal of Geotechnical Engineering, A.S.C.E., Vol 119, No. 5, May, pp 893 – 911
- 6 Borja, R.I., Wu, Wen-Hwa, (1994) **"Vibration of Foundations on Incompressible Soils with No Elastic Region"**, Journal of the Geotechnical Engineering, A.S.C.E., Vol 120, No. 9, September, pp 1570 – 1592.
- 7 Bruel and Kjaer, unpublished, **"Application of B and K Equipment to Mechanical Vibration and Shock Measurements"**.
- 8 Christian, J.T. (1980) **"Probabilistic Soil Dynamics: State of-the-Art"**, Journal of the Geotechnical Engineering Division, A.S.C.E., Vol 106, No. GT4, April, pp 385 – 397
- 9 Clough, R.W., and Penzien, J., (1975) **"Dynamics of Structures"**, McGraw – Hill,.
- 10 Cuellar V., Bazant, Z.P., Krizek R.J. and Silver M.L., (1977) **"Densification and Hysteresis of Sand Under Cyclic Shear"**, Journal of the Geotechnical Engineering Division, A.S.C.E., Vol 103, No. GT5, May, pp 399 – 416.
- 11 D'Appolonia, F., (1970) **"Dynamic Loading"**, Journal of the Soil Mechanics and Foundations Division, A.S.C.E., Vol 96, No. SM1, January, pp 49 – 72.
- 12 Daming, Z., Zesheng, M., Weisong, L., Zhangzhu, W. and Yuan, W., (1983) **"Study on Vibration of Framed Machine Foundation"**, A.S.C.E. Conference Proceedings Recent Advances in Engineering Mechanics and their Impact on Civil Engineering Practice by WF Chen et al. pp 519 – 522
- 13 Desai, C.S. and Rigby, D.B., (1997) **"Cyclic Interface and Joint Shear Device Including Pore Pressure Effects"**, Journal of Geotechnical and Geoenvironmental Engineering, A.S.C.E., Vol 123, No. 6, June, pp 568 – 579.
- 14 Dobry, R. and Gazetas, G., (1986) **"Dynamic Response of Arbitrarily Shaped Foundations"**, Journal of Geotechnical Engineering, A.S.C.E., Vol 112, No. 2, February, pp 109 – 154.

REFERENCE LIST (continued)

- 15 Duvaut, G., and Lions, J.L. (1976) **"Inequalities in mechanics and physics."** Springer-Verlag, New York, N.Y.
- 16 Du Preez, R.J., Wannenburg, J. and Minnaar, R.J., (1999) **"Report on Finite Element Analysis on Compressor Frame"** unpublished.
- 17 Karabinis, A.H. and Fowler, T.J. (1982) **"Design Considerations for Dynamically Loaded Equipment Foundations"** American Concrete Institute, Publication SP-78: Foundation for Equipment and Machinery.
- 18 Gazetas, G. and Tassoulas J.L., (1987) **" Horizontal Damping of Arbitrarily Shaped Embedded Foundations"**, Journal of the Geotechnical Engineering, A.S.C.E., Vol 113, No. 5, May, pp 458 – 475.
- 19 Glaser, S., (1995) **System Identification and its Application to Estimating Soil Properties"**, Journal of Geotechnical Engineering, A.S.C.E., Vol 121, No. 7, July, pp 553 – 560.
- 20 Hardin, B.O. and Drnevich, V.P. (1972) **"Shear Modulus and Damping in Soils: Design Equations and Curves"** Journal of the Soil Mechanics and Foundations Division, A.S.C.E., Vol 98, No. SM7, July, pp 667 – 692.
- 21 Hardin, B.O. and Richart, F.E., (1963) **"Elastic Wave Velocities in Granular Soils"**, Journal of the Soil Mechanics and Foundations Division, A.S.C.E., Vol 89, No. SM1, February, pp 33 – 65.
- 22 Hryciw, R.D., (1990) **"Small Strain Shear Modulus of Soil by Dilatometer"** Journal of Geotechnical Engineering, A.S.C.E., Vol 116, No. 11, November, pp 1700 – 1716.
- 23 Kausel, E., and Roesset, J.M. (1992) **"Frequency Domain Analysis of Undamped Systems"**, Journal of Engineering Mechanics, A.S.C.E., Vol 118, No. 4, April, pp 721 – 734.
- 24 Kausel, E., Roesset, J.M. and Christian J.T., (1976) **"Nonlinear Behavior in Soil Structure Interaction"**, Journal of the Geotechnical Engineering, A.S.C.E., Vol 102, No. GT11, November, pp 1159 – 1170.
- 25 Kausel, E., Roesset, J.M. and Waas, G., (1975) **"Dynamic Analysis of Footing on Layered Media"**, Journal of the Geotechnical Engineering, A.S.C.E., Vol 101, No. EM5, October, pp 679 – 693.
- 26 Li, X.S., Cai, Z.Y., (1999) **"Effects of Low-Number Previbration Cycles on Dynamic Properties of Dry Sand"**, Journal of Geotechnical and Geoenvironmental Engineering, A.S.C.E., Vol 125, No. 11, November, pp 979 – 987.
- 27 Lin, J.S., (1994) **"Extraction of Dynamic Soil Properties Using Extended Kalman Filter"**, Journal of Geotechnical Engineering, A.S.C.E., Vol 120, No. 12, December, pp 2100 – 2117.

REFERENCE LIST (continued)

- 28 Moore, P.J., (1985) **"Analysis and Design of Foundations for Vibrations"**, A.A.Balkema, Rotterdam/Boston.
- 29 Nayfeh, A.H. and Serhan, S.J., (1989) **"Vertical Vibration of Machine Foundations"**, Journal of Geotechnical Engineering, A.S.C.E., Vol 115, No. 1, January, pp 56 – 74.
- 30 Norman-Gregory, G.M., and Selig, E.T., (1989) **"Analytical Model for Longitudinal Soil Vibration"**, Journal of Geotechnical Engineering, A.S.C.E., Vol 115, No. 3, March, pp 304 – 321.
- 31 Norman-Gregory, G.M., and Selig, E.T., (1989) **"Volume Change Behaviour of Vibrated Sand Columns"**, Journal of the Geotechnical Engineering, A.S.C.E., Vol 115, No. 3, March, pp 289 – 303.
- 32 Novak, M., and Beredugo, Y.O., (1972) **"Vertical Vibration of Embedded Footings"**, Journal of the Soil Mechanics and Foundations Division, A.S.C.E., Vol 98, No. SM12, December, pp 1291 – 1310.
- 33 Novak, M.M. and Howell, J.F., (1977) **"Torsional Vibration of Pile Foundations"**, Journal of the Geotechnical Engineering Division, A.S.C.E., Vol 103, No. GT4, April, pp 271 – 285.
- 34 Poulos, H.G., (1971) **"Behaviour of Laterally Loaded Piles: ii –Pile Groups"** Journal of the Soil Mechanics and Foundations Division, A.S.C.E., Vol 97, No. SM5, May, pp 733 – 751.
- 35 Poulos, H.G., (1972) **"Behaviour of Laterally Loaded Piles: iii – Socketed Piles"**, Journal of the Soil Mechanics and Foundations Division, A.S.C.E., Vol 98, No. SM4, April, pp 341 – 360.
- 36 Prager, W., (1956) **"A new method of analysing stresses and strains in work-hardening plastic solids."**, Journal of Applied Mechanics, Volume 23 No 4, pp 493 – 496.
- 37 Prakash, S. and Puri, V.K., (1981) **"Dynamic Properties of Soils from In-Situ Tests"**, Journal of the Geotechnical Engineering Division, A.S.C.E., Vol 107, No. GT7, July, pp 943 – 963
- 38 Prevost, J.H., Abdel-Ghaffar, A.M. and Elgamal A.W.M. (1985) **"Nonlinear Hysteretic Dynamic Response of Soil Systems"**, Journal of Engineering Mechanics, A.S.C.E., Vol 111, No. 5, May, pp 696 – 713.
- 39 Richart, F.E., (1975) **"Some Effects of Dynamic Soil Properties on Soil-Structure Interaction"**, A.S.C.E., Vol 101, No. GT12, December, pp 1197 – 1240.
- 40 Richart, F.E., Hall, J.R. and Woods, R.D. (1970) **"Vibrations of Soils and Foundations"**, Prentice – Hall,.
- 41 Richart, F.E., (1960) **"Foundation Vibrations"**, Journal of the Soil Mechanics and Foundation Division, August, pp 863, – 925.

REFERENCE LIST (continued)

- 42 Saul W.E., (1968) **Static and Dynamic Analysis of Pile Foundations**", Journal of the Structural Division, A.S.C.E., Vol 94, No. ST5, May, pp 1077 – 1100
- 43 Seed, H.B., and Idriss, I.M., (1970) **"Soil Moduli and Damping Factors for Dynamic Response Analysis."**, Report No 70-1, E.E.R.C., Berkeley, California, December
- 44 Sienkiewicz, Z. and Wilczynski, B., (1993) **"Minimum Weight Design of Machine Foundation under Vertical Load"**, Journal of Engineering Mechanics, A.S.C.E., Vol 119, No. 9, September, pp 1781 – 1797.
- 45 Simo, J.C., and Taylor, R.L., (1985) **"Consistent tangent operators for rate-independent elasto-plasticity."**, Comput. Methods Appl. Mech. Engineering, Volume 48, No 1, pp 101 – 118
- 46 Singh, J.P., Donovan, N.C. and Jobsis, A.C., (1977) **"Design of Machine Foundations on Piles"**, Journal of the Geotechnical Engineering Division, A.S.C.E., Vol 103, No. GT8, August, pp 863 – 877.
- 47 Sreekantiah H.R., (1982) **"Rocking Vibrations of Footings"**, Journal of the Geotechnical Engineering Division, A.S.C.E., Vol 108, No. GT7, July, pp 905 – 917.
- 48 Sridharan, A., Gandhi, N.S.V.V.S.J. and Suresh, S., (1990) **"Stiffness Coefficients of Layered Soil Systems"**, Journal of Geotechnical Engineering, A.S.C.E., Vol 116, No. 4, April, pp 604 – 624.
- 49 Stokoe, K.H., and Woods, R.D., (1972) **"In Situ Shear Wave Velocity by Cross-Hole Method"**, Journal of the Soil Mechanics and Foundations Division, A.S.C.E., Vol 98, No. SM5, May, pp 443 – 460.
- 50 Stokoe, K.H. and Richart, F.E., (1974) **"Dynamic Response of Embedded Machine Foundations"**, Journal of the Geotechnical Engineering Division, A.S.C.E., Vol 100, No. GT4, April, pp 427 – 447.
- 51 Structural Dynamics Course Notes prepared by Prof. Dougherty, B.K., University of Natal.
- 52 Thomson, W.T., (1993) **"Theory of Vibration with Application"**, Fourth Edition, Chapman and Hall, London.
- 53 **"Using Strand 7"**, G+D Computing, May 1999.
- 54 Veletsos, A.S. and Nair, D.V.V., (1974) **"Torsional Vibration of Viscoelastic Foundations"**, Journal of the Geotechnical Engineering Division, A.S.C.E., Vol 100, No. GT3, March, pp 225 – 246.
- 55 Walters, D.B. and Kirby, J.B., (1982) **"Design of Fan Foundations"**, Journal of the Energy Division, A.S.C.E., Vol 108, No. E.Y1, March, pp 23 – 27.
- 56 Warbuton, G.B., (1957) **"Forced Vibration of a Body upon an Elastic Stratum"**, Journal of Applied Mechanics, Transactions, A.S.M.E., Volume 24.

REFERENCE LIST (continued)

- 57 Whitman, R.V and Richart, F.E (1967) "**Design Procedures for Dynamically Loaded foundations**", Journal of the Soil Mechanics and Foundations Division, A.S.C.E., Vol 93, No. SM6, November, pp 169 – 193.

- A_L = area within hysteresis loop
 A_y = age of soil deposit
 A_T = crosshatched area under hysteresis loop
 A_s = amplitude of displacement
 B_s, B_z = mass ratios
 B_v, B_ψ = inertia ratios
 τ = effective stress cohesion
 D = geometric damping ratio
 D_m = material damping ratio
 D_r = relative density
 D_t = total damping ratio
 D_{10} = equivalent grain diameter for which 10% of sample is smaller
 d_c = characteristic depth
 E = Young's modulus
 e = void ratio
 f = frequency in cycles per second
 f_n = undamped natural frequency
 f_{mr} = resonant frequency with damping included
 f_o = fundamental resonant frequency
 G = shear modulus of soil
 G_{max} = shear modulus at very low-strain amplitude
 G_{1000} = shear modulus after 1000 min of consolidation
 g = gravitational constant
 H = thickness of soft stratum
 h = depth of embedment or borehole spacing
 I_x, I_ψ = mass moment of inertia
 K_0 = at rest earth pressure coefficient
 K_2 = shear modulus factor
 k = plasticity factor
 k_x = spring constant for horizontal excitation
 k_z = spring constant for vertical excitation
 k_θ = spring constant for torsional excitation
 k_ψ = spring constant for pure rocking excitation
 L_R = length of Rayleigh wave
 M = mass of footing plus load vibrating in phase
 m = relative density term
 N = number of stress cycles
 N_s = number of log cycles of time required for re-establishment of soil fabric
 n = relative density term
 n_ψ = correction factor for B_ψ
 OCR = overconsolidation ratio
 Q_o = unbalanced vertical force
 q_d = dynamic bearing stress
 q_o = static bearing stress
 r_o = effective radius of footing
 s_u = undrained shear strength
 t_s = time for shear wave to pass from penetrometer to geophone
 u = pore fluid pressure
 W = weight of foundation plus load vibrating in phase
 z = depth coordinate
 z_1, z_2 = displacement amplitudes for two successive cycles
 α = embedment factor for damping
 γ = shear strain amplitude
 γ_r = reference shear strain
 γ_s = unit weight of soil
 ΔG = increase in shear modulus
 $\Delta \sigma_v$ = vertical stress due to static load
 ϵ_p = permanent axial (vertical) strain
 η = embedment factor for stiffness
 $\lambda = \sigma_d / \sigma_c$
 ν = Poisson's ratio
 ρ = mass density
 σ_c = confining pressure
 σ_d = vertical dynamic stress
 $\bar{\sigma}_h$ = horizontal effective stress
 $\bar{\sigma}_o$ = octahedral normal effective stress
 σ_v = vertical total stress
 $\bar{\sigma}_v$ = vertical effective stress
 τ = shear stress
 τ_{max} = shear stress related to shear strain through G_{max}
 Φ = effective stress angle of internal friction

NOTATIONS TO CHAPTER 2

APPENDIX A

- A1: Background to Solvers used in Strand 7 Finite Element Analysis**
- A2: Computer Printout of Calculations**

A1: BACKGROUND TO SOLVERS USED IN STRAND 7 – FINITE ELEMENT ANALYSIS

A1.1 Linear static solver

For the response of a structure to be linear, the mechanical behaviour of all materials in the model must follow Hooke's law; i.e element forces are linearly proportional to element deformation and when the loading is removed, the material returns to its original shape. In addition, the deformation must be so small such that the deformed geometry cannot be distinguished from the undeformed one. Based on these two assumptions, solution can be arbitrarily combined to consider more complex loading conditions. A load is regarded as static if its magnitude and direction do not change with time. Structures under static loading conditions are analysed with the inertial and damping properties ignored.

The linear static solver performs the following steps:

- Calculates and assembles element stiffness matrices, equivalent element force vectors and external nodal force vectors. Constraints are also assembled in this process.

At the end of this assembly procedure, the following linear system of equilibrium equations is formed:

$$[K]\{d\} = \{P\}$$

where

$[K]$ Global stiffness matrix

$\{d\}$ Unknown nodal displacement vector(s)

$\{P\}$ Global nodal load vector(s)

- Solves the equations of equilibrium for the unknown nodal displacements.
- Calculates elements strains, stresses, stress resultants and strain energy densities as requested.

Notes

1. As the stiffness matrix is independent of the loading conditions, multiple load cases can be considered in one solution execution. At the end of the solution, displacements and other results for all loading cases are calculated.
2. If combined loading conditions from the basic load cases are of interest, the post-processor can be used to find the structure's response by simply combining the results for the basic load cases, without running the linear static solver again.

A1.2 Natural Frequency Solver

The natural frequency solver is used to calculate the natural frequencies (or free vibration frequencies) and corresponding vibration modes of an undamped structure. The natural frequency analysis problem, is formulated as the following eigenvalue problem:

$$[K]\{x\} = \omega^2[M]\{x\}$$

Where

$[K]$ Global stiffness matrix

$[M]$ Global mass matrix

$\{x\}$ Vibration mode vector

ω Natural (circular) frequency (radians/sec)

The natural frequency solver performs the following steps:

- Calculates and assembles the element stiffness and mass matrices to form the global stiffness and mass matrices. Either a consistent or lumped mass matrix can be used according to the solver option setting. The geometric stiffness matrix will be formed and assembled to the global stiffness matrix when an initial solution is applied. Constraints are assembled in this process.

If the initial file is from a nonlinear solution, the stiffness and mass matrices calculation will be based on the current material status and geometry. More

specifically, the current material modulus values will be used for nonlinear elastic material. The current geometry is used if geometric nonlinearity is considered in the initial solution.

- Modifies the stiffness matrix if a shift value is applied. A shift may be used to determine modes near to desired value.
- Solves the eigenvalue problem to get frequencies and the corresponding mode shapes using the Sub-Space Iteration Method.

A1.3 Linear and Nonlinear Transient Dynamic Solver

The transient dynamic solver is used to calculate the time history of the dynamic response of a structure subjected to any arbitrary forcing function and initial conditions.

Linear dynamic equilibrium equations are in the following form:

$$[M]\{\ddot{x}(t)\} + [C]\{\dot{x}(t)\} + [K]\{x(t)\} = \{R(t)\}$$

where

$[M]$ Mass matrix

$[C]$ Damping matrix

$[K]$ Stiffness matrix

$\{x(t)\}$ Nodal displacement vector

$\{\dot{x}(t)\}$ Nodal velocity vector

$\{\ddot{x}(t)\}$ Nodal acceleration vector

$\{R(t)\}$ Load vector

For the nonlinear transient dynamic solver, the above expression is modified to include the effects of nonlinearities on the equilibrium. As in the nonlinear transient dynamic solver the nonlinear equilibrium equations are always linearised in each time step, the following discussion, based on the above expression is still valid.

Forcing Function

Dynamic loads can be applied as follows:

1. Dynamic loads applied to the model are factored through the use of factor vs time tables, which can be any time history. Loads can be point forces and moments, elements loads. Multiple load cases may be combined to form a single loading condition. Each loads case may included, excluded or factored according to a factor vs time table.
2. Multiple freedom cases may also be included if the full system option is used. The constant terms in the freedom cases may be factored in the same way as the loads in the load cases. This provides support for time dependent displacements.

Initial Conditions

Three types of initial conditions can be specified:

1. A linear static solution which specifies the displacement of a structure initially under certain static loads.
2. A transient solution, which specifies the dynamic response of the structure at a time instance. The solution will start from any selected time step.
3. Initial velocity and acceleration of all free nodes in the structure.

Solution Techniques

Two approaches to transient dynamic solutions are available: mode superposition and full system.

Mode Superposition

Using the mode superposition method, responses of the individual modes of the structure are calculated separately and then combined to produce the total

response of the structure. This is only applicable to linear transient dynamic analysis.

In addition to the other advantages of the mode superposition technique, this method offers more in a transient dynamic analysis. One of the advantages is that modal damping can be used in addition to (or instead of) Rayleigh damping. When experimental data are available, modal damping gives a more accurate representation of the damping in the system.

The mode superposition method is best suited to structures where the lower frequencies dominate the response (i.e earthquakes). Typically, 10 modes will provide good accuracy for these problems. Modal superposition is not suitable for problems such as shock loads or impacts where the higher frequency modes are excited. In these cases, 50 or more modes may be required and the cost to calculate this many modes can significantly offset the saving in the transient solution. The most serious disadvantage of this approach is that it is not capable of handling any nonlinearity in the solution.

Full System

This approach does not have the limitations of mode superposition, but can be computationally very expensive, as all nodal displacements are numerically integrated at the specified time steps. This method is also referred to as direct integration.

The linear transient dynamic solver performs the following steps:

- Initialises the nodal displacement, velocity and acceleration vectors according to the specified initial conditions.
- For mode superposition calculates and assembles equivalent element force vectors and external nodal force vectors. If base acceleration is included, the global mass matrix is also formed for the calculation of the pseudo load vector.

A1.6

- For direct integration, calculates and assembles element stiffness, mass and damping matrices, equivalent element force vectors and external nodal force vectors. In the stiffness calculation, material temperature dependency is considered. The element geometric stiffness matrix is also included if initial conditions are used. *Rayleigh* damping and element material damping can be included. Either consistent or lumped element equivalent load vectors can be calculated according to the option setting. Constraints are also assembled in this process, and the constant terms in enforced displacement and shrink links are combined and applied. At the end of this assembly procedure, and three global matrices in the equation of dynamic equilibrium are formed:

$$[M]\{\ddot{x}(t)\} + [C]\{\dot{x}(t)\} + [K]\{x(t)\} = \{R(t)\}$$

- If the full system approach is used, decomposes the global stiffness matrix such that $[K] = [L][D][L]^T$
- Loops through the specified time steps and calculates displacement, velocity and acceleration using either the Wilson theta or Newmark beta method. When base acceleration is applied, either relative or absolute values of displacement, velocity and acceleration may be calculated.
- Calculates element results such as stress and strain.

The nonlinear transient dynamic solver perform the following steps:

- Initializes the nodal displacement, velocity and acceleration vectors according to the specified initial conditions. For a restart run, all quantities required for describing the current element deformation and/or stress status are recovered from both the initial and the temporary solution file.
- Starts a new time step and calculates the constants required for the time integration if the time stepping is different from the previous one.
- Calculates and assembles the element stiffness matrices, equivalent element force vectors and external nodal force vectors. Depending on whether material and/or geometric nonlinearity is considered, the current material modulus and geometry will be used. The element geometric stiffness matrix is also included if the

A1.7

- corresponding option is set. Either consistent or lumped element equivalent load vectors can be calculated according to the option setting. Constraints are also assembled in this process and the constant terms in enforced displacement and shrink links are combined and applied. At the end of this assembly procedure, the global stiffness, mass and damping matrices and nodal force vector are formed.
- Uses the Newmark beta method to calculate the displacement, velocity and acceleration vectors and then updates the current displacement vector.
- Checks for convergence

Displacement norm

$$\frac{\|\Delta d\|}{\|d\|} < \varepsilon_d$$

Residual force norm

$$\frac{\|R\|}{\|P_0\|} < \varepsilon_r$$

Where

ε_d and ε_r are convergence tolerance on displacement and residual force,

$\|\Delta d\|$ and $\|d\|$ are norms of incremental and total displacement vectors,

$\|P_0\|$ is the norm of residual force vector at the first iteration of each time step and

$\|R\|$ is the norm of residual force vector in the current iteration.

If both of the convergence criteria are satisfied and there are more time steps, the solution continues with the next step otherwise it stops. If either of the criteria is not satisfied, the solution continues the integration and iterates on the current step.

Notes

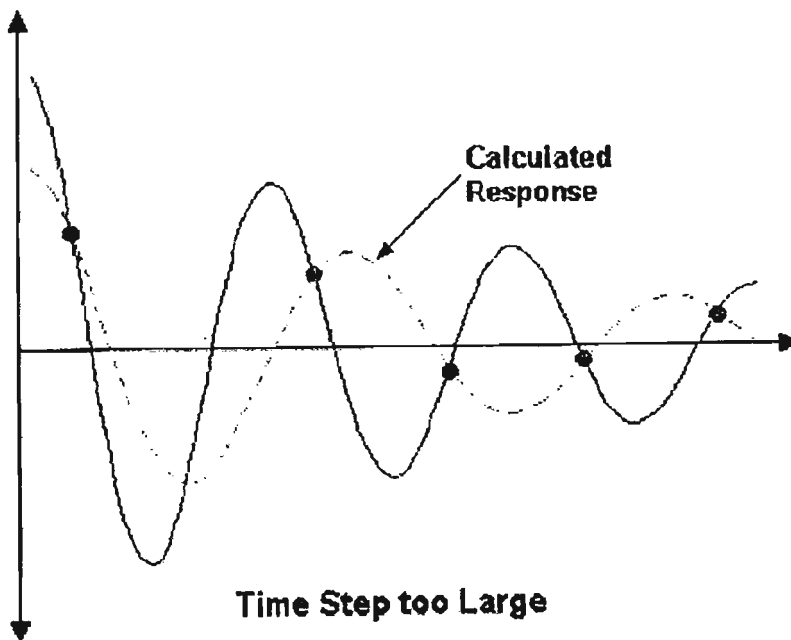
1. The results of a transient analysis are provided as series of solutions for discrete points in time throughout the time period of interest. The number and spacing of the results sets can be controlled using the time steps in the solver parameters.

The results include the nodal displacements, velocity and acceleration, as well as element stresses, strains and other quantities at the particular time instance.

2. The choice of the correct time step size is important to ensure that the complete response of the structure is captured by the solution and that the solution is stable and free from divergence. This is particularly important for nonlinear solutions.

In general the smaller the time step the more accurate the solution. However there are practical limits on how small the step can be, as more solution steps will be required for smaller time step and the running time will normally increase accordingly. Therefore, a limit may be set by the time required for the solution. The size of the time step is also limited by the number of sets of results that can be physically stored. However, the latter limit can be removed in Strand 7 by using a periodical saving option.

If the time step is too large then much of the higher frequency response of the structure will be missed and the solution may not adequately represent the real behaviour of the structure as shown below.



Model: table top G4000

Quantity: Node Degees of Freedom

Group: Model

Freedom Case: 1: Freedom Case 1: Static

	Coord Syste...	DX (in)	DY (in)	DZ (in)	RX (deg)	RY (deg)	RZ (deg)
Node 1	Global XYZ	DX	DY	DZ	RX	RY	RZ
Node 2	Global XYZ	DX	DY	DZ	RX	RY	RZ
Node 3	Global XYZ	DX	DY	DZ	RX	RY	RZ
Node 4	Global XYZ	DX	DY	DZ	RX	RY	RZ
Node 5	Global XYZ	DX	DY	DZ	RX	RY	RZ
Node 6	Global XYZ	DX	DY	DZ	RX	RY	RZ
Node 7	Global XYZ	DX	DY	DZ	RX	RY	RZ
Node 8	Global XYZ	DX	DY	DZ	RX	RY	RZ
Node 22	Global XYZ	DX	DY	DZ	RX	RY	RZ
Node 23	Global XYZ	DX	DY	DZ	RX	RY	RZ
Node 24	Global XYZ	DX	DY	DZ	RX	RY	RZ
Node 25	Global XYZ	DX	DY	DZ	RX	RY	RZ
Node 26	Global XYZ	DX	DY	DZ	RX	RY	RZ
Node 27	Global XYZ	DX	DY	DZ	RX	RY	RZ
Node 28	Global XYZ	DX	DY	DZ	RX	RY	RZ
Node 29	Global XYZ	DX	DY	DZ	RX	RY	RZ
Node 30	Global XYZ	DX	DY	DZ	RX	RY	RZ
Node 31	Global XYZ	DX	DY	DZ	RX	RY	RZ
Node 32	Global XYZ	DX	DY	DZ	RX	RY	RZ
Node 33	Global XYZ	DX	DY	DZ	RX	RY	RZ
Node 34	Global XYZ	DX	DY	DZ	RX	RY	RZ
Node 35	Global XYZ	DX	DY	DZ	RX	RY	RZ
Node 36	Global XYZ	DX	DY	DZ	RX	RY	RZ
Node 37	Global XYZ	DX	DY	DZ	RX	RY	RZ
Node 38	Global XYZ	DX	DY	DZ	RX	RY	RZ
Node 39	Global XYZ	DX	DY	DZ	RX	RY	RZ
Node 40	Global XYZ	DX	DY	DZ	RX	RY	RZ
Node 41	Global XYZ	DX	DY	DZ	RX	RY	RZ
Node 42	Global XYZ	DX	DY	DZ	RX	RY	RZ
Node 43	Global XYZ	DX	DY	DZ	RX	RY	RZ

Model: table top G4000
Quantity: Node coordinates
Group: Model

	X (in)	Y (in)	Z (in)
Node 1	0.000000x10 ⁰	0.000000x10 ⁰	0.000000x10 ⁰
Node 2	0.000000x10 ⁰	0.000000x10 ⁰	120.000000
Node 3	96.000000	0.000000x10 ⁰	0.000000x10 ⁰
Node 4	96.000000	0.000000x10 ⁰	120.000000
Node 5	168.000000	0.000000x10 ⁰	0.000000x10 ⁰
Node 6	168.000000	0.000000x10 ⁰	120.000000
Node 7	240.000000	0.000000x10 ⁰	0.000000x10 ⁰
Node 8	240.000000	0.000000x10 ⁰	120.000000
Node 9	0.000000x10 ⁰	204.000000	0.000000x10 ⁰
Node 10	0.000000x10 ⁰	204.000000	60.000000
Node 11	0.000000x10 ⁰	204.000000	120.000000
Node 12	48.000000	204.000000	0.000000x10 ⁰
Node 13	48.000000	204.000000	120.000000
Node 14	96.000000	204.000000	0.000000x10 ⁰
Node 15	96.000000	204.000000	60.000000
Node 16	96.000000	204.000000	120.000000
Node 17	168.000000	204.000000	0.000000x10 ⁰
Node 18	168.000000	204.000000	120.000000
Node 19	240.000000	204.000000	0.000000x10 ⁰
Node 20	240.000000	204.000000	60.000000
Node 21	240.000000	204.000000	120.000000
Node 22	0.000000x10 ⁰	0.000000x10 ⁰	60.000000
Node 23	96.000000	0.000000x10 ⁰	60.000000
Node 24	168.000000	0.000000x10 ⁰	60.000000
Node 25	240.000000	0.000000x10 ⁰	60.000000
Node 26	-60.000000	0.000000x10 ⁰	-84.000000
Node 27	-60.000000	0.000000x10 ⁰	0.000000x10 ⁰
Node 28	-60.000000	0.000000x10 ⁰	60.000000
Node 29	-60.000000	0.000000x10 ⁰	120.000000
Node 30	-60.000000	0.000000x10 ⁰	204.000000
Node 31	0.000000x10 ⁰	0.000000x10 ⁰	-84.000000
Node 32	0.000000x10 ⁰	0.000000x10 ⁰	204.000000
Node 33	96.000000	0.000000x10 ⁰	-84.000000
Node 34	96.000000	0.000000x10 ⁰	204.000000
Node 35	168.000000	0.000000x10 ⁰	-84.000000
Node 36	168.000000	0.000000x10 ⁰	204.000000
Node 37	240.000000	0.000000x10 ⁰	-84.000000
Node 38	240.000000	0.000000x10 ⁰	204.000000
Node 39	300.000000	0.000000x10 ⁰	-84.000000
Node 40	300.000000	0.000000x10 ⁰	0.000000x10 ⁰
Node 41	300.000000	0.000000x10 ⁰	60.000000
Node 42	300.000000	0.000000x10 ⁰	120.000000
Node 43	300.000000	0.000000x10 ⁰	204.000000

Model: table top G4000

Quantity: Node Force

Group: Model

Load Case: 1: FULL LOAD ACTING VERT DIRECTION

	FX (lbf)	FY (lbf)	FZ (lbf)
Node 1	0.000000x10 ⁰	-38.400000x10 ³	0.000000x10 ⁰
Node 2	0.000000x10 ⁰	-38.400000x10 ³	0.000000x10 ⁰
Node 3	0.000000x10 ⁰	-34.400000x10 ³	0.000000x10 ⁰
Node 4	0.000000x10 ⁰	-34.400000x10 ³	0.000000x10 ⁰
Node 5	0.000000x10 ⁰	-21.400000x10 ³	0.000000x10 ⁰
Node 6	0.000000x10 ⁰	-21.400000x10 ³	0.000000x10 ⁰
Node 7	0.000000x10 ⁰	-33.200000x10 ³	0.000000x10 ⁰
Node 8	0.000000x10 ⁰	-33.200000x10 ³	0.000000x10 ⁰
Node 9	0.000000x10 ⁰	-38.500000x10 ³	0.000000x10 ⁰
Node 10	0.000000x10 ⁰	-6.800000x10 ³	0.000000x10 ⁰
Node 11	0.000000x10 ⁰	-38.500000x10 ³	0.000000x10 ⁰
Node 12	0.000000x10 ⁰	-3.600000x10 ³	0.000000x10 ⁰
Node 13	0.000000x10 ⁰	-3.600000x10 ³	0.000000x10 ⁰
Node 14	0.000000x10 ⁰	-16.900000x10 ³	0.000000x10 ⁰
Node 15	0.000000x10 ⁰	-50.000000x10 ³	0.000000x10 ⁰
Node 16	0.000000x10 ⁰	-16.900000x10 ³	0.000000x10 ⁰
Node 17	0.000000x10 ⁰	-17.800000x10 ³	0.000000x10 ⁰
Node 18	0.000000x10 ⁰	-17.800000x10 ³	0.000000x10 ⁰
Node 19	0.000000x10 ⁰	-9.800000x10 ³	0.000000x10 ⁰
Node 20	0.000000x10 ⁰	-31.900000x10 ³	0.000000x10 ⁰
Node 21	0.000000x10 ⁰	-9.800000x10 ³	0.000000x10 ⁰
Node 22	0.000000x10 ⁰	-16.900000x10 ³	0.000000x10 ⁰
Node 23	0.000000x10 ⁰	-13.100000x10 ³	0.000000x10 ⁰
Node 24	0.000000x10 ⁰	-11.300000x10 ³	0.000000x10 ⁰
Node 25	0.000000x10 ⁰	-15.000000x10 ³	0.000000x10 ⁰

Strand7 Release 2.1.7

C:\MSc Eng\Table Top\Table Top 1\table top G4000.st7

27 October 2002 12:39 pm

Model: table top G4000

Quantity: Node Force

Group: Model

Load Case: 2: FULL LOAD ACTING LONGITUDINAL DIRECTION

	FX (lbf)	FY (lbf)	FZ (lbf)
Node 1	38.400000×10^3	0.000000×10^0	0.000000×10^0
Node 2	38.400000×10^3	0.000000×10^0	0.000000×10^0
Node 3	34.400000×10^3	0.000000×10^0	0.000000×10^0
Node 4	34.400000×10^3	0.000000×10^0	0.000000×10^0
Node 5	21.400000×10^3	0.000000×10^0	0.000000×10^0
Node 6	21.400000×10^3	0.000000×10^0	0.000000×10^0
Node 7	33.200000×10^3	0.000000×10^0	0.000000×10^0
Node 8	33.200000×10^3	0.000000×10^0	0.000000×10^0
Node 9	38.500000×10^3	0.000000×10^0	0.000000×10^0
Node 10	6.800000×10^3	0.000000×10^0	0.000000×10^0
Node 11	38.500000×10^3	0.000000×10^0	0.000000×10^0
Node 12	3.600000×10^3	0.000000×10^0	0.000000×10^0
Node 13	3.600000×10^3	0.000000×10^0	0.000000×10^0
Node 14	16.900000×10^3	0.000000×10^0	0.000000×10^0
Node 15	50.000000×10^3	0.000000×10^0	0.000000×10^0
Node 16	16.900000×10^3	0.000000×10^0	0.000000×10^0
Node 17	17.800000×10^3	0.000000×10^0	0.000000×10^0
Node 18	17.800000×10^3	0.000000×10^0	0.000000×10^0
Node 19	9.800000×10^3	0.000000×10^0	0.000000×10^0
Node 20	31.900000×10^3	0.000000×10^0	0.000000×10^0
Node 21	9.800000×10^3	0.000000×10^0	0.000000×10^0
Node 22	16.900000×10^3	0.000000×10^0	0.000000×10^0
Node 23	13.100000×10^3	0.000000×10^0	0.000000×10^0
Node 24	11.300000×10^3	0.000000×10^0	0.000000×10^0
Node 25	15.000000×10^3	0.000000×10^0	0.000000×10^0

Model: table top G4000
 Quantity: Node Force
 Group: Model
 Load Case: 3: FULL LOAD ACTING TRANSVERSE DIRECTION

	FX (lbf)	FY (lbf)	FZ (lbf)
Node 1	0.000000x10 ⁰	0.000000x10 ⁰	38.400000x10 ³
Node 2	0.000000x10 ⁰	0.000000x10 ⁰	38.400000x10 ³
Node 3	0.000000x10 ⁰	0.000000x10 ⁰	34.400000x10 ³
Node 4	0.000000x10 ⁰	0.000000x10 ⁰	34.400000x10 ³
Node 5	0.000000x10 ⁰	0.000000x10 ⁰	21.400000x10 ³
Node 6	0.000000x10 ⁰	0.000000x10 ⁰	21.400000x10 ³
Node 7	0.000000x10 ⁰	0.000000x10 ⁰	33.200000x10 ³
Node 8	0.000000x10 ⁰	0.000000x10 ⁰	33.200000x10 ³
Node 9	0.000000x10 ⁰	0.000000x10 ⁰	38.500000x10 ³
Node 10	0.000000x10 ⁰	0.000000x10 ⁰	6.800000x10 ³
Node 11	0.000000x10 ⁰	0.000000x10 ⁰	38.500000x10 ³
Node 12	0.000000x10 ⁰	0.000000x10 ⁰	3.600000x10 ³
Node 13	0.000000x10 ⁰	0.000000x10 ⁰	3.600000x10 ³
Node 14	0.000000x10 ⁰	0.000000x10 ⁰	16.900000x10 ³
Node 15	0.000000x10 ⁰	0.000000x10 ⁰	50.000000x10 ³
Node 16	0.000000x10 ⁰	0.000000x10 ⁰	16.900000x10 ³
Node 17	0.000000x10 ⁰	0.000000x10 ⁰	17.800000x10 ³
Node 18	0.000000x10 ⁰	0.000000x10 ⁰	17.800000x10 ³
Node 19	0.000000x10 ⁰	0.000000x10 ⁰	9.800000x10 ³
Node 20	0.000000x10 ⁰	0.000000x10 ⁰	31.900000x10 ³
Node 21	0.000000x10 ⁰	0.000000x10 ⁰	9.800000x10 ³
Node 22	0.000000x10 ⁰	0.000000x10 ⁰	16.900000x10 ³
Node 23	0.000000x10 ⁰	0.000000x10 ⁰	13.100000x10 ³
Node 24	0.000000x10 ⁰	0.000000x10 ⁰	11.300000x10 ³
Node 25	0.000000x10 ⁰	0.000000x10 ⁰	15.000000x10 ³

Model: table top G4000
Quantity: Node Force
Group: Model
Load Case: 4: CENTRIFUGAL FORCES Y

	FX (lbf)	FY (lbf)	FZ (lbf)
Node 10	0.000000×10^0	143.000000	0.000000×10^0
Node 15	0.000000×10^0	4.040000×10^3	0.000000×10^0
Node 20	0.000000×10^0	3.897000×10^3	0.000000×10^0

Model: table top G4000
Quantity: Node Force
Group: Model
Load Case: 5: CENTRFUGAL FORCES Z

	FX (lbf)	FY (lbf)	FZ (lbf)
Node 10	0.000000x10 ⁰	0.000000x10 ⁰	143.000000
Node 15	0.000000x10 ⁰	0.000000x10 ⁰	4.040000x10 ³
Node 20	0.000000x10 ⁰	0.000000x10 ⁰	3.897000x10 ³

Model: table top G4000
Quantity: Node Mass
Group: Model

	MX (lb)	MY (lb)	MZ (lb)
Node 9	27.000000x10 ³	27.000000x10 ³	27.000000x10 ³
Node 11	27.000000x10 ³	27.000000x10 ³	27.000000x10 ³
Node 15	45.500000x10 ³	45.500000x10 ³	45.500000x10 ³
Node 17	11.000000x10 ³	11.000000x10 ³	11.000000x10 ³
Node 18	11.000000x10 ³	11.000000x10 ³	11.000000x10 ³
Node 20	28.500000x10 ³	28.500000x10 ³	28.500000x10 ³

Model: table top G4000

Quantity: Node Stiffness (Translation)

Group: Model

	Coord Sys...	KX (lbf/in)	KY (lbf/in)	KZ (lbf/in)
Node 1	Global XYZ	188.366333×10^3	236.128750×10^3	188.366333×10^3
Node 2	Global XYZ	188.366333×10^3	236.128750×10^3	188.366333×10^3
Node 3	Global XYZ	202.856083×10^3	254.292500×10^3	202.856083×10^3
Node 4	Global XYZ	202.856083×10^3	254.292500×10^3	202.856083×10^3
Node 5	Global XYZ	173.876667×10^3	217.965000×10^3	173.876667×10^3
Node 6	Global XYZ	173.876667×10^3	217.965000×10^3	173.876667×10^3
Node 7	Global XYZ	159.386917×10^3	199.801250×10^3	159.386917×10^3
Node 8	Global XYZ	159.386917×10^3	199.801250×10^3	159.386917×10^3
Node 22	Global XYZ	156.972000×10^3	196.774000×10^3	156.972000×10^3
Node 23	Global XYZ	169.046750×10^3	211.910417×10^3	169.046750×10^3
Node 24	Global XYZ	144.897167×10^3	181.637500×10^3	144.897167×10^3
Node 25	Global XYZ	132.822417×10^3	166.501083×10^3	132.822417×10^3
Node 26	Global XYZ	42.261667×10^3	52.977583×10^3	42.261667×10^3
Node 27	Global XYZ	72.448583×10^3	90.818750×10^3	72.448583×10^3
Node 28	Global XYZ	60.373833×10^3	75.682333×10^3	60.373833×10^3
Node 29	Global XYZ	72.448583×10^3	90.818750×10^3	72.448583×10^3
Node 30	Global XYZ	42.261667×10^3	52.977583×10^3	42.261667×10^3
Node 31	Global XYZ	109.880417×10^3	137.741750×10^3	109.880417×10^3
Node 32	Global XYZ	109.880417×10^3	137.741750×10^3	109.880417×10^3
Node 33	Global XYZ	118.332750×10^3	148.337333×10^3	118.332750×10^3
Node 34	Global XYZ	118.332750×10^3	148.337333×10^3	118.332750×10^3
Node 35	Global XYZ	101.428083×10^3	127.146250×10^3	101.428083×10^3
Node 36	Global XYZ	101.428083×10^3	127.146250×10^3	101.428083×10^3
Node 37	Global XYZ	92.975667×10^3	116.550750×10^3	92.975667×10^3
Node 38	Global XYZ	92.975667×10^3	116.550750×10^3	92.975667×10^3
Node 39	Global XYZ	42.261667×10^3	52.977583×10^3	42.261667×10^3
Node 40	Global XYZ	72.448583×10^3	90.818750×10^3	72.448583×10^3
Node 41	Global XYZ	60.373833×10^3	75.682333×10^3	60.373833×10^3
Node 42	Global XYZ	72.448583×10^3	90.818750×10^3	72.448583×10^3
Node 43	Global XYZ	42.261667×10^3	52.977583×10^3	42.261667×10^3

Model: table top G4000

Quantity: Beam Elements

Group: Model

	Type	Property	Angle (deg)	Offset 1 (in)	Offset 2 (in)	Free Length (in)	N1	N2
Beam 1	Beam2	1: Beam Property 1	90.000000	0.000000x10 ⁰	0.000000x10 ⁰	0.000000x10 ⁰	1	9
Beam 2	Beam2	1: Beam Property 1	90.000000	0.000000x10 ⁰	0.000000x10 ⁰	0.000000x10 ⁰	2	11
Beam 3	Beam2	2: Beam Property 2	0.000000x10 ⁰	0.000000x10 ⁰	0.000000x10 ⁰	0.000000x10 ⁰	3	14
Beam 4	Beam2	2: Beam Property 2	0.000000x10 ⁰	0.000000x10 ⁰	0.000000x10 ⁰	0.000000x10 ⁰	4	16
Beam 5	Beam2	3: Beam Property 3	90.000000	0.000000x10 ⁰	0.000000x10 ⁰	0.000000x10 ⁰	7	19
Beam 6	Beam2	3: Beam Property 3	90.000000	0.000000x10 ⁰	0.000000x10 ⁰	0.000000x10 ⁰	8	21
Beam 7	Beam2	4: Beam Property 4	0.000000x10 ⁰	0.000000x10 ⁰	0.000000x10 ⁰	0.000000x10 ⁰	9	10
Beam 8	Beam2	4: Beam Property 4	0.000000x10 ⁰	0.000000x10 ⁰	0.000000x10 ⁰	0.000000x10 ⁰	10	11
Beam 9	Beam2	5: Beam Property 5	0.000000x10 ⁰	0.000000x10 ⁰	0.000000x10 ⁰	0.000000x10 ⁰	14	15
Beam 10	Beam2	5: Beam Property 5	0.000000x10 ⁰	0.000000x10 ⁰	0.000000x10 ⁰	0.000000x10 ⁰	15	16
Beam 11	Beam2	6: Beam Property 6	0.000000x10 ⁰	0.000000x10 ⁰	0.000000x10 ⁰	0.000000x10 ⁰	19	20
Beam 12	Beam2	6: Beam Property 6	0.000000x10 ⁰	0.000000x10 ⁰	0.000000x10 ⁰	0.000000x10 ⁰	20	21
Beam 13	Beam2	7: Beam Property 7	0.000000x10 ⁰	0.000000x10 ⁰	0.000000x10 ⁰	0.000000x10 ⁰	11	13
Beam 14	Beam2	7: Beam Property 7	0.000000x10 ⁰	0.000000x10 ⁰	0.000000x10 ⁰	0.000000x10 ⁰	13	16
Beam 15	Beam2	8: Beam Property 8	0.000000x10 ⁰	0.000000x10 ⁰	0.000000x10 ⁰	0.000000x10 ⁰	16	18
Beam 16	Beam2	8: Beam Property 8	0.000000x10 ⁰	0.000000x10 ⁰	0.000000x10 ⁰	0.000000x10 ⁰	18	21
Beam 17	Beam2	7: Beam Property 7	0.000000x10 ⁰	0.000000x10 ⁰	0.000000x10 ⁰	0.000000x10 ⁰	9	12
Beam 18	Beam2	7: Beam Property 7	0.000000x10 ⁰	0.000000x10 ⁰	0.000000x10 ⁰	0.000000x10 ⁰	12	14
Beam 19	Beam2	8: Beam Property 8	0.000000x10 ⁰	0.000000x10 ⁰	0.000000x10 ⁰	0.000000x10 ⁰	14	17
Beam 20	Beam2	8: Beam Property 8	0.000000x10 ⁰	0.000000x10 ⁰	0.000000x10 ⁰	0.000000x10 ⁰	17	19

Strand7 Release 2.1.7

C:\MSc Eng\Table Top\Table Top 1\table top G4000.s17

27 October 2002 12:44 pm

42.10

Model: table top G4000

Quantity: Plate Elements

Group: Model

	Type	Propert...	Angle (deg)	Offset (in)	N1	N2	N3	N4
Plate 1	Quad4	1: base	0.000000x10 ⁰	0.000000x10 ⁰	1	22	23	3
Plate 2	Quad4	1: base	0.000000x10 ⁰	0.000000x10 ⁰	22	2	4	23
Plate 3	Quad4	1: base	0.000000x10 ⁰	0.000000x10 ⁰	3	23	24	5
Plate 4	Quad4	1: base	0.000000x10 ⁰	0.000000x10 ⁰	23	4	6	24
Plate 5	Quad4	1: base	0.000000x10 ⁰	0.000000x10 ⁰	5	24	25	7
Plate 6	Quad4	1: base	0.000000x10 ⁰	0.000000x10 ⁰	24	6	8	25
Plate 7	Quad4	1: base	0.000000x10 ⁰	0.000000x10 ⁰	26	31	1	27
Plate 8	Quad4	1: base	0.000000x10 ⁰	0.000000x10 ⁰	31	33	3	1
Plate 9	Quad4	1: base	0.000000x10 ⁰	0.000000x10 ⁰	33	35	5	3
Plate 10	Quad4	1: base	0.000000x10 ⁰	0.000000x10 ⁰	35	37	7	5
Plate 11	Quad4	1: base	0.000000x10 ⁰	0.000000x10 ⁰	37	39	40	7
Plate 12	Quad4	1: base	0.000000x10 ⁰	0.000000x10 ⁰	40	41	25	7
Plate 13	Quad4	1: base	0.000000x10 ⁰	0.000000x10 ⁰	41	42	8	25
Plate 14	Quad4	1: base	0.000000x10 ⁰	0.000000x10 ⁰	42	43	38	8
Plate 15	Quad4	1: base	0.000000x10 ⁰	0.000000x10 ⁰	6	8	38	36
Plate 16	Quad4	1: base	0.000000x10 ⁰	0.000000x10 ⁰	4	6	36	34
Plate 17	Quad4	1: base	0.000000x10 ⁰	0.000000x10 ⁰	27	1	22	28
Plate 18	Quad4	1: base	0.000000x10 ⁰	0.000000x10 ⁰	28	22	2	29
Plate 19	Quad4	1: base	0.000000x10 ⁰	0.000000x10 ⁰	2	4	34	32
Plate 20	Quad4	1: base	0.000000x10 ⁰	0.000000x10 ⁰	29	2	32	30

Strand7 Release 2.1.7

C:\MSc Eng\Table Top\Table Top 1\table top G4000.sl7

27 October 2002 12:44 pm

42-11

Model: table top G4000

Result type: Node displacement

Coordinate system: Global XYZ

Freedom case: 1: Freedom Case 1: Static

Result cases: All

Group: Model

Properties: All

	DX (in)	DY (in)	DZ (in)	RX (deg)	RY (deg)	RZ (deg)
Node 1: 1: FULL LOAD ACTING VERT DIRECTION	0.000000	0.000000	0.000000	0.000000	0.000000	0.000000
Node 1: 2: FULL LOAD ACTING LONGITUDINAL DIRECTION	0.000000	0.000000	0.000000	0.000000	0.000000	0.000000
Node 1: 3: FULL LOAD ACTING TRANSVERSE DIRECTION	0.000000	0.000000	0.000000	0.000000	0.000000	0.000000
Node 1: 4: FLA VERT DIRN	0.000000	0.000000	0.000000	0.000000	0.000000	0.000000
Node 1: 5: FLA LONG DIRN	0.000000	0.000000	0.000000	0.000000	0.000000	0.000000
Node 1: 6: FLA TRANS DIRN	0.000000	0.000000	0.000000	0.000000	0.000000	0.000000
Node 1: 7: VERT+.3 TRANS	0.000000	0.000000	0.000000	0.000000	0.000000	0.000000
Node 1: 8: VERT+.1 LONG	0.000000	0.000000	0.000000	0.000000	0.000000	0.000000
Node 1: 9: VERT + 0.5 VERT	0.000000	0.000000	0.000000	0.000000	0.000000	0.000000
Node 2: 1: FULL LOAD ACTING VERT DIRECTION	0.000000	0.000000	0.000000	0.000000	0.000000	0.000000
Node 2: 2: FULL LOAD ACTING LONGITUDINAL DIRECTION	0.000000	0.000000	0.000000	0.000000	0.000000	0.000000
Node 2: 3: FULL LOAD ACTING TRANSVERSE DIRECTION	0.000000	0.000000	0.000000	0.000000	0.000000	0.000000
Node 2: 4: FLA VERT DIRN	0.000000	0.000000	0.000000	0.000000	0.000000	0.000000
Node 2: 5: FLA LONG DIRN	0.000000	0.000000	0.000000	0.000000	0.000000	0.000000
Node 2: 6: FLA TRANS DIRN	0.000000	0.000000	0.000000	0.000000	0.000000	0.000000
Node 2: 7: VERT+.3 TRANS	0.000000	0.000000	0.000000	0.000000	0.000000	0.000000
Node 2: 8: VERT+.1 LONG	0.000000	0.000000	0.000000	0.000000	0.000000	0.000000
Node 2: 9: VERT + 0.5 VERT	0.000000	0.000000	0.000000	0.000000	0.000000	0.000000
Node 3: 1: FULL LOAD ACTING VERT DIRECTION	0.000000	0.000000	0.000000	0.000000	0.000000	0.000000
Node 3: 2: FULL LOAD ACTING LONGITUDINAL DIRECTION	0.000000	0.000000	0.000000	0.000000	0.000000	0.000000
Node 3: 3: FULL LOAD ACTING TRANSVERSE DIRECTION	0.000000	0.000000	0.000000	0.000000	0.000000	0.000000
Node 3: 4: FLA VERT DIRN	0.000000	0.000000	0.000000	0.000000	0.000000	0.000000
Node 3: 5: FLA LONG DIRN	0.000000	0.000000	0.000000	0.000000	0.000000	0.000000
Node 3: 6: FLA TRANS DIRN	0.000000	0.000000	0.000000	0.000000	0.000000	0.000000
Node 3: 7: VERT+.3 TRANS	0.000000	0.000000	0.000000	0.000000	0.000000	0.000000
Node 3: 8: VERT+.1 LONG	0.000000	0.000000	0.000000	0.000000	0.000000	0.000000
Node 3: 9: VERT + 0.5 VERT	0.000000	0.000000	0.000000	0.000000	0.000000	0.000000
Node 4: 1: FULL LOAD ACTING VERT DIRECTION	0.000000	0.000000	0.000000	0.000000	0.000000	0.000000
Node 4: 2: FULL LOAD ACTING LONGITUDINAL DIRECTION	0.000000	0.000000	0.000000	0.000000	0.000000	0.000000
Node 4: 3: FULL LOAD ACTING TRANSVERSE DIRECTION	0.000000	0.000000	0.000000	0.000000	0.000000	0.000000
Node 4: 4: FLA VERT DIRN	0.000000	0.000000	0.000000	0.000000	0.000000	0.000000
Node 4: 5: FLA LONG DIRN	0.000000	0.000000	0.000000	0.000000	0.000000	0.000000

Node 4: 6: FLA TRANS DIRN	0.000000	0.000000	0.000000	0.000000	0.000000	0.000000
Node 4: 7: VERT+.3 TRANS	0.000000	0.000000	0.000000	0.000000	0.000000	0.000000
Node 4: 8: VERT+.1 LONG	0.000000	0.000000	0.000000	0.000000	0.000000	0.000000
Node 4: 9: VERT + 0.5 VERT	0.000000	0.000000	0.000000	0.000000	0.000000	0.000000
Node 5: 1: FULL LOAD ACTING VERT DIRECTION	0.000000	0.000000	0.000000	0.000000	0.000000	0.000000
Node 5: 2: FULL LOAD ACTING LONGITUDINAL DIRECTION	0.000000	0.000000	0.000000	0.000000	0.000000	0.000000
Node 5: 3: FULL LOAD ACTING TRANSVERSE DIRECTION	0.000000	0.000000	0.000000	0.000000	0.000000	0.000000
Node 5: 4: FLA VERT DIRN	0.000000	0.000000	0.000000	0.000000	0.000000	0.000000
Node 5: 5: FLA LONG DIRN	0.000000	0.000000	0.000000	0.000000	0.000000	0.000000
Node 5: 6: FLA TRANS DIRN	0.000000	0.000000	0.000000	0.000000	0.000000	0.000000
Node 5: 7: VERT+.3 TRANS	0.000000	0.000000	0.000000	0.000000	0.000000	0.000000
Node 5: 8: VERT+.1 LONG	0.000000	0.000000	0.000000	0.000000	0.000000	0.000000
Node 5: 9: VERT + 0.5 VERT	0.000000	0.000000	0.000000	0.000000	0.000000	0.000000
Node 6: 1: FULL LOAD ACTING VERT DIRECTION	0.000000	0.000000	0.000000	0.000000	0.000000	0.000000
Node 6: 2: FULL LOAD ACTING LONGITUDINAL DIRECTION	0.000000	0.000000	0.000000	0.000000	0.000000	0.000000
Node 6: 3: FULL LOAD ACTING TRANSVERSE DIRECTION	0.000000	0.000000	0.000000	0.000000	0.000000	0.000000
Node 6: 4: FLA VERT DIRN	0.000000	0.000000	0.000000	0.000000	0.000000	0.000000
Node 6: 5: FLA LONG DIRN	0.000000	0.000000	0.000000	0.000000	0.000000	0.000000
Node 6: 6: FLA TRANS DIRN	0.000000	0.000000	0.000000	0.000000	0.000000	0.000000
Node 6: 7: VERT+.3 TRANS	0.000000	0.000000	0.000000	0.000000	0.000000	0.000000
Node 6: 8: VERT+.1 LONG	0.000000	0.000000	0.000000	0.000000	0.000000	0.000000
Node 6: 9: VERT + 0.5 VERT	0.000000	0.000000	0.000000	0.000000	0.000000	0.000000
Node 7: 1: FULL LOAD ACTING VERT DIRECTION	0.000000	0.000000	0.000000	0.000000	0.000000	0.000000
Node 7: 2: FULL LOAD ACTING LONGITUDINAL DIRECTION	0.000000	0.000000	0.000000	0.000000	0.000000	0.000000
Node 7: 3: FULL LOAD ACTING TRANSVERSE DIRECTION	0.000000	0.000000	0.000000	0.000000	0.000000	0.000000
Node 7: 4: FLA VERT DIRN	0.000000	0.000000	0.000000	0.000000	0.000000	0.000000
Node 7: 5: FLA LONG DIRN	0.000000	0.000000	0.000000	0.000000	0.000000	0.000000
Node 7: 6: FLA TRANS DIRN	0.000000	0.000000	0.000000	0.000000	0.000000	0.000000
Node 7: 7: VERT+.3 TRANS	0.000000	0.000000	0.000000	0.000000	0.000000	0.000000
Node 7: 8: VERT+.1 LONG	0.000000	0.000000	0.000000	0.000000	0.000000	0.000000
Node 7: 9: VERT + 0.5 VERT	0.000000	0.000000	0.000000	0.000000	0.000000	0.000000
Node 8: 1: FULL LOAD ACTING VERT DIRECTION	0.000000	0.000000	0.000000	0.000000	0.000000	0.000000
Node 8: 2: FULL LOAD ACTING LONGITUDINAL DIRECTION	0.000000	0.000000	0.000000	0.000000	0.000000	0.000000
Node 8: 3: FULL LOAD ACTING TRANSVERSE DIRECTION	0.000000	0.000000	0.000000	0.000000	0.000000	0.000000
Node 8: 4: FLA VERT DIRN	0.000000	0.000000	0.000000	0.000000	0.000000	0.000000
Node 8: 5: FLA LONG DIRN	0.000000	0.000000	0.000000	0.000000	0.000000	0.000000
Node 8: 6: FLA TRANS DIRN	0.000000	0.000000	0.000000	0.000000	0.000000	0.000000
Node 8: 7: VERT+.3 TRANS	0.000000	0.000000	0.000000	0.000000	0.000000	0.000000
Node 8: 8: VERT+.1 LONG	0.000000	0.000000	0.000000	0.000000	0.000000	0.000000
Node 8: 9: VERT + 0.5 VERT	0.000000	0.000000	0.000000	0.000000	0.000000	0.000000
Node 9: 1: FULL LOAD ACTING VERT DIRECTION	0.000856	-0.003082	0.000008	0.000688	-0.000020	0.000308
Node 9: 2: FULL LOAD ACTING LONGITUDINAL DIRECTION	0.181466	0.005786	0.000047	0.000009	-0.000004	-0.009566
Node 9: 3: FULL LOAD ACTING TRANSVERSE DIRECTION	0.000273	0.004976	0.128825	0.015286	-0.000205	-0.000496

Node 9: 4: FLA VERT DIRN	0.000856	-0.003082	0.000008	0.000688	-0.000020	0.000308
Node 9: 5: FLA LONG DIRN	0.181466	0.005786	0.000047	0.000009	-0.000004	-0.009566
Node 9: 6: FLA TRANS DIRN	0.000273	0.004976	0.128825	0.015286	-0.000205	-0.000496
Node 9: 7: VERT+.3 TRANS	0.000938	-0.001589	0.038656	0.005274	-0.000081	0.000159
Node 9: 8: VERT+.1 LONG	0.019003	-0.002503	0.000013	0.000689	-0.000020	-0.000649
Node 9: 9: VERT + 0.5 VERT	0.001284	-0.004622	0.000012	0.001032	-0.000029	0.000462
Node 10: 1: FULL LOAD ACTING VERT DIRECTION	0.000846	-0.003581	0.000000	0.000000	0.000000	0.000308
Node 10: 2: FULL LOAD ACTING LONGITUDINAL DIRECTION	0.181603	0.005781	0.000000	0.000000	0.000000	-0.009566
Node 10: 3: FULL LOAD ACTING TRANSVERSE DIRECTION	0.000000	0.000000	0.128876	-0.000516	-0.000288	0.000000
Node 10: 4: FLA VERT DIRN	0.000846	-0.003581	0.000000	0.000000	0.000000	0.000308
Node 10: 5: FLA LONG DIRN	0.181603	0.005781	0.000000	0.000000	0.000000	-0.009566
Node 10: 6: FLA TRANS DIRN	0.000000	0.000000	0.128876	-0.000516	-0.000288	0.000000
Node 10: 7: VERT+.3 TRANS	0.000846	-0.003581	0.038663	-0.000155	-0.000086	0.000308
Node 10: 8: VERT+.1 LONG	0.019006	-0.003003	0.000000	0.000000	0.000000	-0.000649
Node 10: 9: VERT + 0.5 VERT	0.001268	-0.005371	0.000000	0.000000	0.000000	0.000462
Node 11: 1: FULL LOAD ACTING VERT DIRECTION	0.000856	-0.003082	-0.000008	-0.000688	0.000020	0.000308
Node 11: 2: FULL LOAD ACTING LONGITUDINAL DIRECTION	0.181466	0.005786	-0.000047	-0.000009	0.000004	-0.009566
Node 11: 3: FULL LOAD ACTING TRANSVERSE DIRECTION	-0.000273	-0.004976	0.128825	0.015286	-0.000205	0.000496
Node 11: 4: FLA VERT DIRN	0.000856	-0.003082	-0.000008	-0.000688	0.000020	0.000308
Node 11: 5: FLA LONG DIRN	0.181466	0.005786	-0.000047	-0.000009	0.000004	-0.009566
Node 11: 6: FLA TRANS DIRN	-0.000273	-0.004976	0.128825	0.015286	-0.000205	0.000496
Node 11: 7: VERT+.3 TRANS	0.000774	-0.004574	0.038639	0.003898	-0.000042	0.000457
Node 11: 8: VERT+.1 LONG	0.019003	-0.002503	-0.000013	-0.000689	0.000020	-0.000649
Node 11: 9: VERT + 0.5 VERT	0.001284	-0.004622	-0.000012	-0.001032	0.000029	0.000462
Node 12: 1: FULL LOAD ACTING VERT DIRECTION	0.000860	-0.002780	0.000041	0.001836	-0.000047	0.000326
Node 12: 2: FULL LOAD ACTING LONGITUDINAL DIRECTION	0.181256	0.004650	0.000507	0.000010	-0.000550	0.001079
Node 12: 3: FULL LOAD ACTING TRANSVERSE DIRECTION	0.000277	0.004423	0.128837	0.018671	0.000169	-0.000699
Node 12: 4: FLA VERT DIRN	0.000860	-0.002780	0.000041	0.001836	-0.000047	0.000326
Node 12: 5: FLA LONG DIRN	0.181256	0.004650	0.000507	0.000010	-0.000550	0.001079
Node 12: 6: FLA TRANS DIRN	0.000277	0.004423	0.128837	0.018671	0.000169	-0.000699
Node 12: 7: VERT+.3 TRANS	0.000944	-0.001453	0.038692	0.007437	0.000003	0.000116
Node 12: 8: VERT+.1 LONG	0.018986	-0.002314	0.000091	0.001837	-0.000102	0.000434
Node 12: 9: VERT + 0.5 VERT	0.001291	-0.004169	0.000061	0.002754	-0.000071	0.000489
Node 13: 1: FULL LOAD ACTING VERT DIRECTION	0.000860	-0.002780	-0.000041	-0.001836	0.000047	0.000326
Node 13: 2: FULL LOAD ACTING LONGITUDINAL DIRECTION	0.181256	0.004650	-0.000507	-0.000010	0.000550	0.001079
Node 13: 3: FULL LOAD ACTING TRANSVERSE DIRECTION	-0.000277	-0.004423	0.128837	0.018671	0.000169	0.000699
Node 13: 4: FLA VERT DIRN	0.000860	-0.002780	-0.000041	-0.001836	0.000047	0.000326
Node 13: 5: FLA LONG DIRN	0.181256	0.004650	-0.000507	-0.000010	0.000550	0.001079
Node 13: 6: FLA TRANS DIRN	-0.000277	-0.004423	0.128837	0.018671	0.000169	0.000699
Node 13: 7: VERT+.3 TRANS	0.000777	-0.004106	0.038610	0.003765	0.000098	0.000536
Node 13: 8: VERT+.1 LONG	0.018986	-0.002314	-0.000091	-0.001837	0.000102	0.000434
Node 13: 9: VERT + 0.5 VERT	0.001291	-0.004169	-0.000061	-0.002754	0.000071	0.000489
Node 14: 1: FULL LOAD ACTING VERT DIRECTION	0.000865	-0.002909	0.000071	0.002984	-0.000015	-0.000995

Node 14: 2: FULL LOAD ACTING LONGITUDINAL DIRECTION	0.180982	-0.002087	0.000057	0.000010	0.002170	-0.022941
Node 14: 3: FULL LOAD ACTING TRANSVERSE DIRECTION	0.000281	0.004014	0.129072	0.022055	-0.001352	-0.000152
Node 14: 4: FLA VERT DIRN	0.000865	-0.002909	0.000071	0.002984	-0.000015	-0.000995
Node 14: 5: FLA LONG DIRN	0.180982	-0.002087	0.000057	0.000010	0.002170	-0.022941
Node 14: 6: FLA TRANS DIRN	0.000281	0.004014	0.129072	0.022055	-0.001352	-0.000152
Node 14: 7: VERT+.3 TRANS	0.000949	-0.001705	0.038792	0.009601	-0.000420	-0.001040
Node 14: 8: VERT+.1 LONG	0.018963	-0.003118	0.000077	0.002985	0.000202	-0.003289
Node 14: 9: VERT + 0.5 VERT	0.001298	-0.004364	0.000106	0.004476	-0.000022	-0.001492
Node 15: 1: FULL LOAD ACTING VERT DIRECTION	0.000857	-0.006017	0.000000	0.000000	0.000000	-0.000995
Node 15: 2: FULL LOAD ACTING LONGITUDINAL DIRECTION	0.185594	-0.002093	0.000000	0.000000	0.000000	-0.022941
Node 15: 3: FULL LOAD ACTING TRANSVERSE DIRECTION	0.000000	0.000000	0.129628	-0.005277	0.000273	0.000000
Node 15: 4: FLA VERT DIRN	0.000857	-0.006017	0.000000	0.000000	0.000000	-0.000995
Node 15: 5: FLA LONG DIRN	0.185594	-0.002093	0.000000	0.000000	0.000000	-0.022941
Node 15: 6: FLA TRANS DIRN	0.000000	0.000000	0.129628	-0.005277	0.000273	0.000000
Node 15: 7: VERT+.3 TRANS	0.000857	-0.006017	0.038888	-0.001583	0.000082	-0.000995
Node 15: 8: VERT+.1 LONG	0.019417	-0.006226	0.000000	0.000000	0.000000	-0.003289
Node 15: 9: VERT + 0.5 VERT	0.001286	-0.009025	0.000000	0.000000	0.000000	-0.001492
Node 16: 1: FULL LOAD ACTING VERT DIRECTION	0.000865	-0.002909	-0.000071	-0.002984	0.000015	-0.000995
Node 16: 2: FULL LOAD ACTING LONGITUDINAL DIRECTION	0.180982	-0.002087	-0.000057	-0.000010	-0.002170	-0.022941
Node 16: 3: FULL LOAD ACTING TRANSVERSE DIRECTION	-0.000281	-0.004014	0.129072	0.022055	-0.001352	0.000152
Node 16: 4: FLA VERT DIRN	0.000865	-0.002909	-0.000071	-0.002984	0.000015	-0.000995
Node 16: 5: FLA LONG DIRN	0.180982	-0.002087	-0.000057	-0.000010	-0.002170	-0.022941
Node 16: 6: FLA TRANS DIRN	-0.000281	-0.004014	0.129072	0.022055	-0.001352	0.000152
Node 16: 7: VERT+.3 TRANS	0.000781	-0.004114	0.038651	0.003632	-0.000391	-0.000949
Node 16: 8: VERT+.1 LONG	0.018963	-0.003118	-0.000077	-0.002985	-0.000202	-0.003289
Node 16: 9: VERT + 0.5 VERT	0.001298	-0.004364	-0.000106	-0.004476	0.000022	-0.001492
Node 17: 1: FULL LOAD ACTING VERT DIRECTION	0.000859	-0.004759	0.000072	0.003027	0.000009	-0.000440
Node 17: 2: FULL LOAD ACTING LONGITUDINAL DIRECTION	0.181620	-0.010842	0.000055	-0.000011	-0.001039	0.004215
Node 17: 3: FULL LOAD ACTING TRANSVERSE DIRECTION	0.000243	0.004314	0.131492	0.020585	-0.000481	0.000525
Node 17: 4: FLA VERT DIRN	0.000859	-0.004759	0.000072	0.003027	0.000009	-0.000440
Node 17: 5: FLA LONG DIRN	0.181620	-0.010842	0.000055	-0.000011	-0.001039	0.004215
Node 17: 6: FLA TRANS DIRN	0.000243	0.004314	0.131492	0.020585	-0.000481	0.000525
Node 17: 7: VERT+.3 TRANS	0.000931	-0.003465	0.039520	0.009203	-0.000135	-0.000282
Node 17: 8: VERT+.1 LONG	0.019021	-0.005843	0.000078	0.003026	-0.000095	-0.000018
Node 17: 9: VERT + 0.5 VERT	0.001288	-0.007138	0.000109	0.004541	0.000013	-0.000660
Node 18: 1: FULL LOAD ACTING VERT DIRECTION	0.000859	-0.004759	-0.000072	-0.003027	-0.000009	-0.000440
Node 18: 2: FULL LOAD ACTING LONGITUDINAL DIRECTION	0.181620	-0.010842	-0.000055	0.000011	0.001039	0.004215
Node 18: 3: FULL LOAD ACTING TRANSVERSE DIRECTION	-0.000243	-0.004314	0.131492	0.020585	-0.000481	-0.000525
Node 18: 4: FLA VERT DIRN	0.000859	-0.004759	-0.000072	-0.003027	-0.000009	-0.000440
Node 18: 5: FLA LONG DIRN	0.181620	-0.010842	-0.000055	0.000011	0.001039	0.004215
Node 18: 6: FLA TRANS DIRN	-0.000243	-0.004314	0.131492	0.020585	-0.000481	-0.000525
Node 18: 7: VERT+.3 TRANS	0.000786	-0.006053	0.039375	0.003148	-0.000153	-0.000597
Node 18: 8: VERT+.1 LONG	0.019021	-0.005843	-0.000078	-0.003026	0.000095	-0.000018

Node 18: 9: VERT + 0.5 VERT	0.001288	-0.007138	-0.000109	-0.004541	-0.000013	-0.000660
Node 19: 1: FULL LOAD ACTING VERT DIRECTION	0.000852	-0.003277	0.000056	0.003071	0.000014	0.001875
Node 19: 2: FULL LOAD ACTING LONGITUDINAL DIRECTION	0.181879	-0.003539	-0.000170	-0.000032	0.002527	0.002614
Node 19: 3: FULL LOAD ACTING TRANSVERSE DIRECTION	0.000205	0.005072	0.129582	0.019115	0.002060	0.000579
Node 19: 4: FLA VERT DIRN	0.000852	-0.003277	0.000056	0.003071	0.000014	0.001875
Node 19: 5: FLA LONG DIRN	0.181879	-0.003539	-0.000170	-0.000032	0.002527	0.002614
Node 19: 6: FLA TRANS DIRN	0.000205	0.005072	0.129582	0.019115	0.002060	0.000579
Node 19: 7: VERT+.3 TRANS	0.000913	-0.001756	0.038931	0.008805	0.000632	0.002049
Node 19: 8: VERT+.1 LONG	0.019040	-0.003631	0.000039	0.003067	0.000266	0.002137
Node 19: 9: VERT + 0.5 VERT	0.001278	-0.004916	0.000084	0.004606	0.000021	0.002813
Node 20: 1: FULL LOAD ACTING VERT DIRECTION	0.000859	-0.006052	0.000000	0.000000	0.000000	0.001875
Node 20: 2: FULL LOAD ACTING LONGITUDINAL DIRECTION	0.188745	-0.003523	0.000000	0.000000	0.000000	0.002614
Node 20: 3: FULL LOAD ACTING TRANSVERSE DIRECTION	0.000000	0.000000	0.130055	-0.002292	-0.001324	0.000000
Node 20: 4: FLA VERT DIRN	0.000859	-0.006052	0.000000	0.000000	0.000000	0.001875
Node 20: 5: FLA LONG DIRN	0.188745	-0.003523	0.000000	0.000000	0.000000	0.002614
Node 20: 6: FLA TRANS DIRN	0.000000	0.000000	0.130055	-0.002292	-0.001324	0.000000
Node 20: 7: VERT+.3 TRANS	0.000859	-0.006052	0.039016	-0.000688	-0.000397	0.001875
Node 20: 8: VERT+.1 LONG	0.019734	-0.006404	0.000000	0.000000	0.000000	0.002137
Node 20: 9: VERT + 0.5 VERT	0.001289	-0.009078	0.000000	0.000000	0.000000	0.002813
Node 21: 1: FULL LOAD ACTING VERT DIRECTION	0.000852	-0.003277	-0.000056	-0.003071	-0.000014	0.001875
Node 21: 2: FULL LOAD ACTING LONGITUDINAL DIRECTION	0.181879	-0.003539	0.000170	0.000032	-0.002527	0.002614
Node 21: 3: FULL LOAD ACTING TRANSVERSE DIRECTION	-0.000205	-0.005072	0.129582	0.019115	0.002060	-0.000579
Node 21: 4: FLA VERT DIRN	0.000852	-0.003277	-0.000056	-0.003071	-0.000014	0.001875
Node 21: 5: FLA LONG DIRN	0.181879	-0.003539	0.000170	0.000032	-0.002527	0.002614
Node 21: 6: FLA TRANS DIRN	-0.000205	-0.005072	0.129582	0.019115	0.002060	-0.000579
Node 21: 7: VERT+.3 TRANS	0.000790	-0.004799	0.038818	0.002664	0.000604	0.001702
Node 21: 8: VERT+.1 LONG	0.019040	-0.003631	-0.000039	-0.003067	-0.000266	0.002137
Node 21: 9: VERT + 0.5 VERT	0.001278	-0.004916	-0.000084	-0.004606	-0.000021	0.002813
Node 22: 1: FULL LOAD ACTING VERT DIRECTION	0.000000	0.000000	0.000000	0.000000	0.000000	0.000000
Node 22: 2: FULL LOAD ACTING LONGITUDINAL DIRECTION	0.000000	0.000000	0.000000	0.000000	0.000000	0.000000
Node 22: 3: FULL LOAD ACTING TRANSVERSE DIRECTION	0.000000	0.000000	0.000000	0.000000	0.000000	0.000000
Node 22: 4: FLA VERT DIRN	0.000000	0.000000	0.000000	0.000000	0.000000	0.000000
Node 22: 5: FLA LONG DIRN	0.000000	0.000000	0.000000	0.000000	0.000000	0.000000
Node 22: 6: FLA TRANS DIRN	0.000000	0.000000	0.000000	0.000000	0.000000	0.000000
Node 22: 7: VERT+.3 TRANS	0.000000	0.000000	0.000000	0.000000	0.000000	0.000000
Node 22: 8: VERT+.1 LONG	0.000000	0.000000	0.000000	0.000000	0.000000	0.000000
Node 22: 9: VERT + 0.5 VERT	0.000000	0.000000	0.000000	0.000000	0.000000	0.000000
Node 23: 1: FULL LOAD ACTING VERT DIRECTION	0.000000	0.000000	0.000000	0.000000	0.000000	0.000000
Node 23: 2: FULL LOAD ACTING LONGITUDINAL DIRECTION	0.000000	0.000000	0.000000	0.000000	0.000000	0.000000
Node 23: 3: FULL LOAD ACTING TRANSVERSE DIRECTION	0.000000	0.000000	0.000000	0.000000	0.000000	0.000000
Node 23: 4: FLA VERT DIRN	0.000000	0.000000	0.000000	0.000000	0.000000	0.000000
Node 23: 5: FLA LONG DIRN	0.000000	0.000000	0.000000	0.000000	0.000000	0.000000
Node 23: 6: FLA TRANS DIRN	0.000000	0.000000	0.000000	0.000000	0.000000	0.000000

[illegible]

[illegible]

[illegible]

Node 42: 8: VERT+.1 LONG	0.000000	0.000000	0.000000	0.000000	0.000000	0.000000
Node 42: 9: VERT + 0.5 VERT	0.000000	0.000000	0.000000	0.000000	0.000000	0.000000
Node 43: 1: FULL LOAD ACTING VERT DIRECTION	0.000000	0.000000	0.000000	0.000000	0.000000	0.000000
Node 43: 2: FULL LOAD ACTING LONGITUDINAL DIRECTION	0.000000	0.000000	0.000000	0.000000	0.000000	0.000000
Node 43: 3: FULL LOAD ACTING TRANSVERSE DIRECTION	0.000000	0.000000	0.000000	0.000000	0.000000	0.000000
Node 43: 4: FLA VERT DIRN	0.000000	0.000000	0.000000	0.000000	0.000000	0.000000
Node 43: 5: FLA LONG DIRN	0.000000	0.000000	0.000000	0.000000	0.000000	0.000000
Node 43: 6: FLA TRANS DIRN	0.000000	0.000000	0.000000	0.000000	0.000000	0.000000
Node 43: 7: VERT+.3 TRANS	0.000000	0.000000	0.000000	0.000000	0.000000	0.000000
Node 43: 8: VERT+.1 LONG	0.000000	0.000000	0.000000	0.000000	0.000000	0.000000
Node 43: 9: VERT + 0.5 VERT	0.000000	0.000000	0.000000	0.000000	0.000000	0.000000

42.21

Model: table top G4000
Result type: Node reaction
Coordinate system: Global XYZ
Freedom case: 1: Freedom Case 1: Static
Result cases: All
Group: Model
Properties: All

	FX (lbf)	FY (lbf)	FZ (lbf)	MX (lbfin)	MY (lbfin)	MZ (lbfin)
Node 1: 1: FULL LOAD ACTING VERT DIRECTION	-256.941169	79145.593795	500.748068	33934.569979	218.574517	22797.807017
Node 1: 2: FULL LOAD ACTING LONGITUDINAL DIRECTION	-58493.693785	-76499.437562	-12.966276	-1544.031702	45.628121	3175525.571153
Node 1: 3: FULL LOAD ACTING TRANSVERSE DIRECTION	111.651288	-65794.126008	-80241.740233	-4648844.827450	2282.046721	-5894.601995
Node 1: 4: FLA VERT DIRN	-256.941169	79145.593795	500.748068	33934.569979	218.574517	22797.807017
Node 1: 5: FLA LONG DIRN	-68493.693785	-76499.437562	-12.966276	-1544.031702	45.628121	3175525.571153
Node 1: 6: FLA TRANS DIRN	111.651288	-65794.126008	-80241.740233	-4648844.827450	2282.046721	-5894.601995
Node 1: 7: VERT+.3 TRANS	-223.445783	59407.355993	-23571.774002	-1360718.878256	903.188533	21029.426419
Node 1: 8: VERT+.1 LONG	-7106.310548	71495.650039	499.451441	33780.166808	223.137329	340350.364133
Node 1: 9: VERT + 0.5 VERT	-385.411753	118718.390693	751.122102	50901.854968	327.861775	34196.710526
Node 2: 1: FULL LOAD ACTING VERT DIRECTION	-256.941169	79145.593795	-500.748068	-33934.569979	-218.574517	22797.807017
Node 2: 2: FULL LOAD ACTING LONGITUDINAL DIRECTION	-68493.693785	-76499.437562	12.966276	1544.031702	-45.628121	3175525.571153
Node 2: 3: FULL LOAD ACTING TRANSVERSE DIRECTION	-111.651288	65794.126008	-80241.740233	-4648844.827450	2282.046721	5894.601995
Node 2: 4: FLA VERT DIRN	-256.941169	79145.593795	-500.748068	-33934.569979	-218.574517	22797.807017
Node 2: 5: FLA LONG DIRN	-68493.693785	-76499.437562	12.966276	1544.031702	-45.628121	3175525.571153
Node 2: 6: FLA TRANS DIRN	-111.651288	65794.126008	-80241.740233	-4648844.827450	2282.046721	5894.601995
Node 2: 7: VERT+.3 TRANS	-290.436555	98883.831598	-24573.270138	-1428588.018213	466.039500	24566.187616
Node 2: 8: VERT+.1 LONG	-7106.310548	71495.650039	-499.451441	-33780.166808	-223.137329	340350.364133
Node 2: 9: VERT + 0.5 VERT	-385.411753	118718.390693	-751.122102	-50901.854968	-327.861775	34196.710526
Node 3: 1: FULL LOAD ACTING VERT DIRECTION	563.707236	92102.812351	3261.634467	220291.754836	395.126304	-20030.884896
Node 3: 2: FULL LOAD ACTING LONGITUDINAL DIRECTION	-121601.346446	41398.526486	-23.686867	-2809.330439	-58558.410300	9758571.748833
Node 3: 3: FULL LOAD ACTING TRANSVERSE DIRECTION	-6.648152	-79620.056204	-90282.344236	-6530659.301963	36478.952147	6407.233615
Node 3: 4: FLA VERT DIRN	563.707236	92102.812351	3261.634467	220291.754836	395.126304	-20030.884896
Node 3: 5: FLA LONG DIRN	-121601.346446	41398.526486	-23.686867	-2809.330439	-58558.410300	9758571.748833
Node 3: 6: FLA TRANS DIRN	-6.648152	-79620.056204	-90282.344236	-6530659.301963	36478.952147	6407.233615
Node 3: 7: VERT+.3 TRANS	561.712791	68216.795490	-23823.068804	-1738906.035753	11338.811949	-18108.714811
Node 3: 8: VERT+.1 LONG	-11596.427408	96242.665000	3259.265780	220010.821792	-5460.714726	955826.289988
Node 3: 9: VERT + 0.5 VERT	845.560855	138154.218527	4892.451700	330437.632254	592.689457	-30046.327344
Node 4: 1: FULL LOAD ACTING VERT DIRECTION	563.707236	92102.812351	-3261.634467	-220291.754836	-395.126304	-20030.884896
Node 4: 2: FULL LOAD ACTING LONGITUDINAL DIRECTION	-121601.346446	41398.526486	23.686867	2809.330439	58558.410300	9758571.748833
Node 4: 3: FULL LOAD ACTING TRANSVERSE DIRECTION	6.648152	79620.056204	-90282.344236	-6530659.301963	36478.952147	-6407.233615
Node 4: 4: FLA VERT DIRN	563.707236	92102.812351	-3261.634467	-220291.754836	-395.126304	-20030.884896
Node 4: 5: FLA LONG DIRN	-121601.346446	41398.526486	23.686867	2809.330439	58558.410300	9758571.748833

Node 4: 6: FLA TRANS DIRN	6.648152	79620.056204	-90282.344236	-6530659.301963	36478.952147	-6407.233615
Node 4: 7: VERT+.3 TRANS	565.701682	115988.829212	-30346.337738	-2179489.545425	10548.559340	-21953.054980
Node 4: 8: VERT+.1 LONG	-11596.427408	96242.665000	-3259.265780	-220010.821792	5460.714726	955826.289988
Node 4: 9: VERT + 0.5 VERT	845.560855	138154.218527	-4892.451700	-330437.632254	-592.689457	-30046.327344
Node 5: 1: FULL LOAD ACTING VERT DIRECTION	0.000000	21400.000000	0.000000	0.000000	0.000000	0.000000
Node 5: 2: FULL LOAD ACTING LONGITUDINAL DIRECTION	-21400.000000	0.000000	0.000000	0.000000	0.000000	0.000000
Node 5: 3: FULL LOAD ACTING TRANSVERSE DIRECTION	0.000000	0.000000	-21400.000000	0.000000	0.000000	0.000000
Node 5: 4: FLA VERT DIRN	0.000000	21400.000000	0.000000	0.000000	0.000000	0.000000
Node 5: 5: FLA LONG DIRN	-21400.000000	0.000000	0.000000	0.000000	0.000000	0.000000
Node 5: 6: FLA TRANS DIRN	0.000000	0.000000	-21400.000000	0.000000	0.000000	0.000000
Node 5: 7: VERT+.3 TRANS	0.000000	21400.000000	-6420.000000	0.000000	0.000000	0.000000
Node 5: 8: VERT+.1 LONG	-2140.000000	21400.000000	0.000000	0.000000	0.000000	0.000000
Node 5: 9: VERT + 0.5 VERT	0.000000	32100.000000	0.000000	0.000000	0.000000	0.000000
Node 6: 1: FULL LOAD ACTING VERT DIRECTION	0.000000	21400.000000	0.000000	0.000000	0.000000	0.000000
Node 6: 2: FULL LOAD ACTING LONGITUDINAL DIRECTION	-21400.000000	0.000000	0.000000	0.000000	0.000000	0.000000
Node 6: 3: FULL LOAD ACTING TRANSVERSE DIRECTION	0.000000	0.000000	-21400.000000	0.000000	0.000000	0.000000
Node 6: 4: FLA VERT DIRN	0.000000	21400.000000	0.000000	0.000000	0.000000	0.000000
Node 6: 5: FLA LONG DIRN	-21400.000000	0.000000	0.000000	0.000000	0.000000	0.000000
Node 6: 6: FLA TRANS DIRN	0.000000	0.000000	-21400.000000	0.000000	0.000000	0.000000
Node 6: 7: VERT+.3 TRANS	0.000000	21400.000000	-6420.000000	0.000000	0.000000	0.000000
Node 6: 8: VERT+.1 LONG	-2140.000000	21400.000000	0.000000	0.000000	0.000000	0.000000
Node 6: 9: VERT + 0.5 VERT	0.000000	32100.000000	0.000000	0.000000	0.000000	0.000000
Node 7: 1: FULL LOAD ACTING VERT DIRECTION	-306.766067	65701.593854	1881.216960	127257.520587	-74.808633	22980.567298
Node 7: 2: FULL LOAD ACTING LONGITUDINAL DIRECTION	-46854.959769	35100.911076	39.539397	4699.352118	-13757.326431	1381225.479183
Node 7: 3: FULL LOAD ACTING TRANSVERSE DIRECTION	-90.509679	-50301.649399	-66425.915531	-3791345.973935	-11216.165429	6665.000354
Node 7: 4: FLA VERT DIRN	-306.766067	65701.593854	1881.216960	127257.520587	-74.808633	22980.567298
Node 7: 5: FLA LONG DIRN	-46854.959769	35100.911076	39.539397	4699.352118	-13757.326431	1381225.479183
Node 7: 6: FLA TRANS DIRN	-90.509679	-50301.649399	-66425.915531	-3791345.973935	-11216.165429	6665.000354
Node 7: 7: VERT+.3 TRANS	-333.918971	50611.099034	-18046.557699	-1010146.271594	-3439.658262	24980.067404
Node 7: 8: VERT+.1 LONG	-4992.262044	69211.684961	1885.170900	127727.455798	-1450.541277	161103.115216
Node 7: 9: VERT + 0.5 VERT	-460.149101	98552.390781	2821.825440	190886.280880	-112.212950	34470.850946
Node 8: 1: FULL LOAD ACTING VERT DIRECTION	-306.766067	65701.593854	-1881.216960	-127257.520587	74.808633	22980.567298
Node 8: 2: FULL LOAD ACTING LONGITUDINAL DIRECTION	-46854.959769	35100.911076	-39.539397	-4699.352118	13757.326431	1381225.479183
Node 8: 3: FULL LOAD ACTING TRANSVERSE DIRECTION	90.509679	50301.649399	-66425.915531	-3791345.973935	-11216.165429	-6665.000354
Node 8: 4: FLA VERT DIRN	-306.766067	65701.593854	-1881.216960	-127257.520587	74.808633	22980.567298
Node 8: 5: FLA LONG DIRN	-46854.959769	35100.911076	-39.539397	-4699.352118	13757.326431	1381225.479183
Node 8: 6: FLA TRANS DIRN	90.509679	50301.649399	-66425.915531	-3791345.973935	-11216.165429	-6665.000354
Node 8: 7: VERT+.3 TRANS	-279.613164	80792.088674	-21808.991619	-1264661.312767	-3290.040995	20981.067191
Node 8: 8: VERT+.1 LONG	-4992.262044	69211.684961	-1885.170900	-127727.455798	1450.541277	161103.115216
Node 8: 9: VERT + 0.5 VERT	-460.149101	98552.390781	-2821.825440	-190886.280880	112.212950	34470.850946
Node 9: 1: FULL LOAD ACTING VERT DIRECTION	0.000000	0.000000	0.000000	0.000000	0.000000	0.000000
Node 9: 2: FULL LOAD ACTING LONGITUDINAL DIRECTION	0.000000	0.000000	0.000000	0.000000	0.000000	0.000000
Node 9: 3: FULL LOAD ACTING TRANSVERSE DIRECTION	0.000000	0.000000	0.000000	0.000000	0.000000	0.000000

[illegible]

42.28

Node 18: 9: VERT + 0.5 VERT	0.000000	0.000000	0.000000	0.000000	0.000000	0.000000
Node 19: 1: FULL LOAD ACTING VERT DIRECTION	0.000000	0.000000	0.000000	0.000000	0.000000	0.000000
Node 19: 2: FULL LOAD ACTING LONGITUDINAL DIRECTION	0.000000	0.000000	0.000000	0.000000	0.000000	0.000000
Node 19: 3: FULL LOAD ACTING TRANSVERSE DIRECTION	0.000000	0.000000	0.000000	0.000000	0.000000	0.000000
Node 19: 4: FLA VERT DIRN	0.000000	0.000000	0.000000	0.000000	0.000000	0.000000
Node 19: 5: FLA LONG DIRN	0.000000	0.000000	0.000000	0.000000	0.000000	0.000000
Node 19: 6: FLA TRANS DIRN	0.000000	0.000000	0.000000	0.000000	0.000000	0.000000
Node 19: 7: VERT+.3 TRANS	0.000000	0.000000	0.000000	0.000000	0.000000	0.000000
Node 19: 8: VERT+.1 LONG	0.000000	0.000000	0.000000	0.000000	0.000000	0.000000
Node 19: 9: VERT + 0.5 VERT	0.000000	0.000000	0.000000	0.000000	0.000000	0.000000
Node 20: 1: FULL LOAD ACTING VERT DIRECTION	0.000000	0.000000	0.000000	0.000000	0.000000	0.000000
Node 20: 2: FULL LOAD ACTING LONGITUDINAL DIRECTION	0.000000	0.000000	0.000000	0.000000	0.000000	0.000000
Node 20: 3: FULL LOAD ACTING TRANSVERSE DIRECTION	0.000000	0.000000	0.000000	0.000000	0.000000	0.000000
Node 20: 4: FLA VERT DIRN	0.000000	0.000000	0.000000	0.000000	0.000000	0.000000
Node 20: 5: FLA LONG DIRN	0.000000	0.000000	0.000000	0.000000	0.000000	0.000000
Node 20: 6: FLA TRANS DIRN	0.000000	0.000000	0.000000	0.000000	0.000000	0.000000
Node 20: 7: VERT+.3 TRANS	0.000000	0.000000	0.000000	0.000000	0.000000	0.000000
Node 20: 8: VERT+.1 LONG	0.000000	0.000000	0.000000	0.000000	0.000000	0.000000
Node 20: 9: VERT + 0.5 VERT	0.000000	0.000000	0.000000	0.000000	0.000000	0.000000
Node 21: 1: FULL LOAD ACTING VERT DIRECTION	0.000000	0.000000	0.000000	0.000000	0.000000	0.000000
Node 21: 2: FULL LOAD ACTING LONGITUDINAL DIRECTION	0.000000	0.000000	0.000000	0.000000	0.000000	0.000000
Node 21: 3: FULL LOAD ACTING TRANSVERSE DIRECTION	0.000000	0.000000	0.000000	0.000000	0.000000	0.000000
Node 21: 4: FLA VERT DIRN	0.000000	0.000000	0.000000	0.000000	0.000000	0.000000
Node 21: 5: FLA LONG DIRN	0.000000	0.000000	0.000000	0.000000	0.000000	0.000000
Node 21: 6: FLA TRANS DIRN	0.000000	0.000000	0.000000	0.000000	0.000000	0.000000
Node 21: 7: VERT+.3 TRANS	0.000000	0.000000	0.000000	0.000000	0.000000	0.000000
Node 21: 8: VERT+.1 LONG	0.000000	0.000000	0.000000	0.000000	0.000000	0.000000
Node 21: 9: VERT + 0.5 VERT	0.000000	0.000000	0.000000	0.000000	0.000000	0.000000
Node 22: 1: FULL LOAD ACTING VERT DIRECTION	0.000000	16900.000000	0.000000	0.000000	0.000000	0.000000
Node 22: 2: FULL LOAD ACTING LONGITUDINAL DIRECTION	-16900.000000	0.000000	0.000000	0.000000	0.000000	0.000000
Node 22: 3: FULL LOAD ACTING TRANSVERSE DIRECTION	0.000000	0.000000	-16900.000000	0.000000	0.000000	0.000000
Node 22: 4: FLA VERT DIRN	0.000000	16900.000000	0.000000	0.000000	0.000000	0.000000
Node 22: 5: FLA LONG DIRN	-16900.000000	0.000000	0.000000	0.000000	0.000000	0.000000
Node 22: 6: FLA TRANS DIRN	0.000000	0.000000	-16900.000000	0.000000	0.000000	0.000000
Node 22: 7: VERT+.3 TRANS	0.000000	16900.000000	-5070.000000	0.000000	0.000000	0.000000
Node 22: 8: VERT+.1 LONG	-1690.000000	16900.000000	0.000000	0.000000	0.000000	0.000000
Node 22: 9: VERT + 0.5 VERT	0.000000	25350.000000	0.000000	0.000000	0.000000	0.000000
Node 23: 1: FULL LOAD ACTING VERT DIRECTION	0.000000	13100.000000	0.000000	0.000000	0.000000	0.000000
Node 23: 2: FULL LOAD ACTING LONGITUDINAL DIRECTION	-13100.000000	0.000000	0.000000	0.000000	0.000000	0.000000
Node 23: 3: FULL LOAD ACTING TRANSVERSE DIRECTION	0.000000	0.000000	-13100.000000	0.000000	0.000000	0.000000
Node 23: 4: FLA VERT DIRN	0.000000	13100.000000	0.000000	0.000000	0.000000	0.000000
Node 23: 5: FLA LONG DIRN	-13100.000000	0.000000	0.000000	0.000000	0.000000	0.000000
Node 23: 6: FLA TRANS DIRN	0.000000	0.000000	-13100.000000	0.000000	0.000000	0.000000

Node 23: 7: VERT+.3 TRANS	0.000000	13100.000000	-3930.000000	0.000000	0.000000	0.000000
Node 23: 8: VERT+.1 LONG	-1310.000000	13100.000000	0.000000	0.000000	0.000000	0.000000
Node 23: 9: VERT + 0.5 VERT	0.000000	19650.000000	0.000000	0.000000	0.000000	0.000000
Node 24: 1: FULL LOAD ACTING VERT DIRECTION	0.000000	11300.000000	0.000000	0.000000	0.000000	0.000000
Node 24: 2: FULL LOAD ACTING LONGITUDINAL DIRECTION	-11300.000000	0.000000	0.000000	0.000000	0.000000	0.000000
Node 24: 3: FULL LOAD ACTING TRANSVERSE DIRECTION	0.000000	0.000000	-11300.000000	0.000000	0.000000	0.000000
Node 24: 4: FLA VERT DIRN	0.000000	11300.000000	0.000000	0.000000	0.000000	0.000000
Node 24: 5: FLA LONG DIRN	-11300.000000	0.000000	0.000000	0.000000	0.000000	0.000000
Node 24: 6: FLA TRANS DIRN	0.000000	0.000000	-11300.000000	0.000000	0.000000	0.000000
Node 24: 7: VERT+.3 TRANS	0.000000	11300.000000	-3390.000000	0.000000	0.000000	0.000000
Node 24: 8: VERT+.1 LONG	-1130.000000	11300.000000	0.000000	0.000000	0.000000	0.000000
Node 24: 9: VERT + 0.5 VERT	0.000000	16950.000000	0.000000	0.000000	0.000000	0.000000
Node 25: 1: FULL LOAD ACTING VERT DIRECTION	0.000000	15000.000000	0.000000	0.000000	0.000000	0.000000
Node 25: 2: FULL LOAD ACTING LONGITUDINAL DIRECTION	-15000.000000	0.000000	0.000000	0.000000	0.000000	0.000000
Node 25: 3: FULL LOAD ACTING TRANSVERSE DIRECTION	0.000000	0.000000	-15000.000000	0.000000	0.000000	0.000000
Node 25: 4: FLA VERT DIRN	0.000000	15000.000000	0.000000	0.000000	0.000000	0.000000
Node 25: 5: FLA LONG DIRN	-15000.000000	0.000000	0.000000	0.000000	0.000000	0.000000
Node 25: 6: FLA TRANS DIRN	0.000000	0.000000	-15000.000000	0.000000	0.000000	0.000000
Node 25: 7: VERT+.3 TRANS	0.000000	15000.000000	-4500.000000	0.000000	0.000000	0.000000
Node 25: 8: VERT+.1 LONG	-1500.000000	15000.000000	0.000000	0.000000	0.000000	0.000000
Node 25: 9: VERT + 0.5 VERT	0.000000	22500.000000	0.000000	0.000000	0.000000	0.000000
Node 26: 1: FULL LOAD ACTING VERT DIRECTION	0.000000	0.000000	0.000000	0.000000	0.000000	0.000000
Node 26: 2: FULL LOAD ACTING LONGITUDINAL DIRECTION	0.000000	0.000000	0.000000	0.000000	0.000000	0.000000
Node 26: 3: FULL LOAD ACTING TRANSVERSE DIRECTION	0.000000	0.000000	0.000000	0.000000	0.000000	0.000000
Node 26: 4: FLA VERT DIRN	0.000000	0.000000	0.000000	0.000000	0.000000	0.000000
Node 26: 5: FLA LONG DIRN	0.000000	0.000000	0.000000	0.000000	0.000000	0.000000
Node 26: 6: FLA TRANS DIRN	0.000000	0.000000	0.000000	0.000000	0.000000	0.000000
Node 26: 7: VERT+.3 TRANS	0.000000	0.000000	0.000000	0.000000	0.000000	0.000000
Node 26: 8: VERT+.1 LONG	0.000000	0.000000	0.000000	0.000000	0.000000	0.000000
Node 26: 9: VERT + 0.5 VERT	0.000000	0.000000	0.000000	0.000000	0.000000	0.000000
Node 27: 1: FULL LOAD ACTING VERT DIRECTION	0.000000	0.000000	0.000000	0.000000	0.000000	0.000000
Node 27: 2: FULL LOAD ACTING LONGITUDINAL DIRECTION	0.000000	0.000000	0.000000	0.000000	0.000000	0.000000
Node 27: 3: FULL LOAD ACTING TRANSVERSE DIRECTION	0.000000	0.000000	0.000000	0.000000	0.000000	0.000000
Node 27: 4: FLA VERT DIRN	0.000000	0.000000	0.000000	0.000000	0.000000	0.000000
Node 27: 5: FLA LONG DIRN	0.000000	0.000000	0.000000	0.000000	0.000000	0.000000
Node 27: 6: FLA TRANS DIRN	0.000000	0.000000	0.000000	0.000000	0.000000	0.000000
Node 27: 7: VERT+.3 TRANS	0.000000	0.000000	0.000000	0.000000	0.000000	0.000000
Node 27: 8: VERT+.1 LONG	0.000000	0.000000	0.000000	0.000000	0.000000	0.000000
Node 27: 9: VERT + 0.5 VERT	0.000000	0.000000	0.000000	0.000000	0.000000	0.000000
Node 28: 1: FULL LOAD ACTING VERT DIRECTION	0.000000	0.000000	0.000000	0.000000	0.000000	0.000000
Node 28: 2: FULL LOAD ACTING LONGITUDINAL DIRECTION	0.000000	0.000000	0.000000	0.000000	0.000000	0.000000
Node 28: 3: FULL LOAD ACTING TRANSVERSE DIRECTION	0.000000	0.000000	0.000000	0.000000	0.000000	0.000000
Node 28: 4: FLA VERT DIRN	0.000000	0.000000	0.000000	0.000000	0.000000	0.000000

[illegible]

[illegible]

[illegible]

Node 42: 8: VERT+.1 LONG	0.000000	0.000000	0.000000	0.000000	0.000000	0.000000
Node 42: 9: VERT + 0.5 VERT	0.000000	0.000000	0.000000	0.000000	0.000000	0.000000
Node 43: 1: FULL LOAD ACTING VERT DIRECTION	0.000000	0.000000	0.000000	0.000000	0.000000	0.000000
Node 43: 2: FULL LOAD ACTING LONGITUDINAL DIRECTION	0.000000	0.000000	0.000000	0.000000	0.000000	0.000000
Node 43: 3: FULL LOAD ACTING TRANSVERSE DIRECTION	0.000000	0.000000	0.000000	0.000000	0.000000	0.000000
Node 43: 4: FLA VERT DIRN	0.000000	0.000000	0.000000	0.000000	0.000000	0.000000
Node 43: 5: FLA LONG DIRN	0.000000	0.000000	0.000000	0.000000	0.000000	0.000000
Node 43: 6: FLA TRANS DIRN	0.000000	0.000000	0.000000	0.000000	0.000000	0.000000
Node 43: 7: VERT+.3 TRANS	0.000000	0.000000	0.000000	0.000000	0.000000	0.000000
Node 43: 8: VERT+.1 LONG	0.000000	0.000000	0.000000	0.000000	0.000000	0.000000
Node 43: 9: VERT + 0.5 VERT	0.000000	0.000000	0.000000	0.000000	0.000000	0.000000

DESIGN OF STRUCTURES AND FOUNDATIONS FOR VIBRATING MACHINES

VR ULASSI

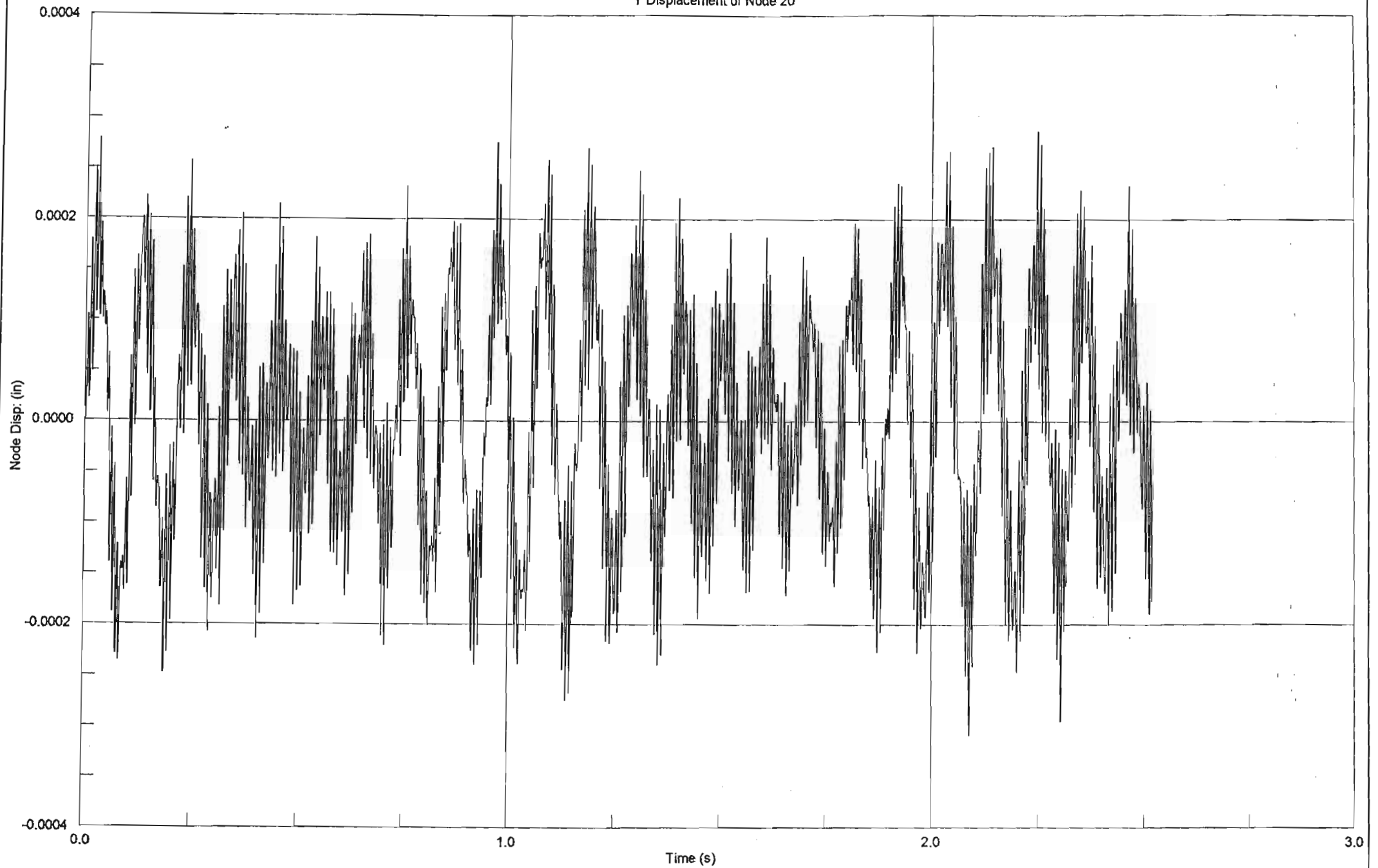
VOLUME 2 OF 4

IN PARTIAL FULFILLMENT OF THE DEGREE OF MASTER OF SCIENCE IN
ENGINEERING (COURSEWORK) COMPRISING 72 CREDITS OF 144 FOR THE
DEGREE

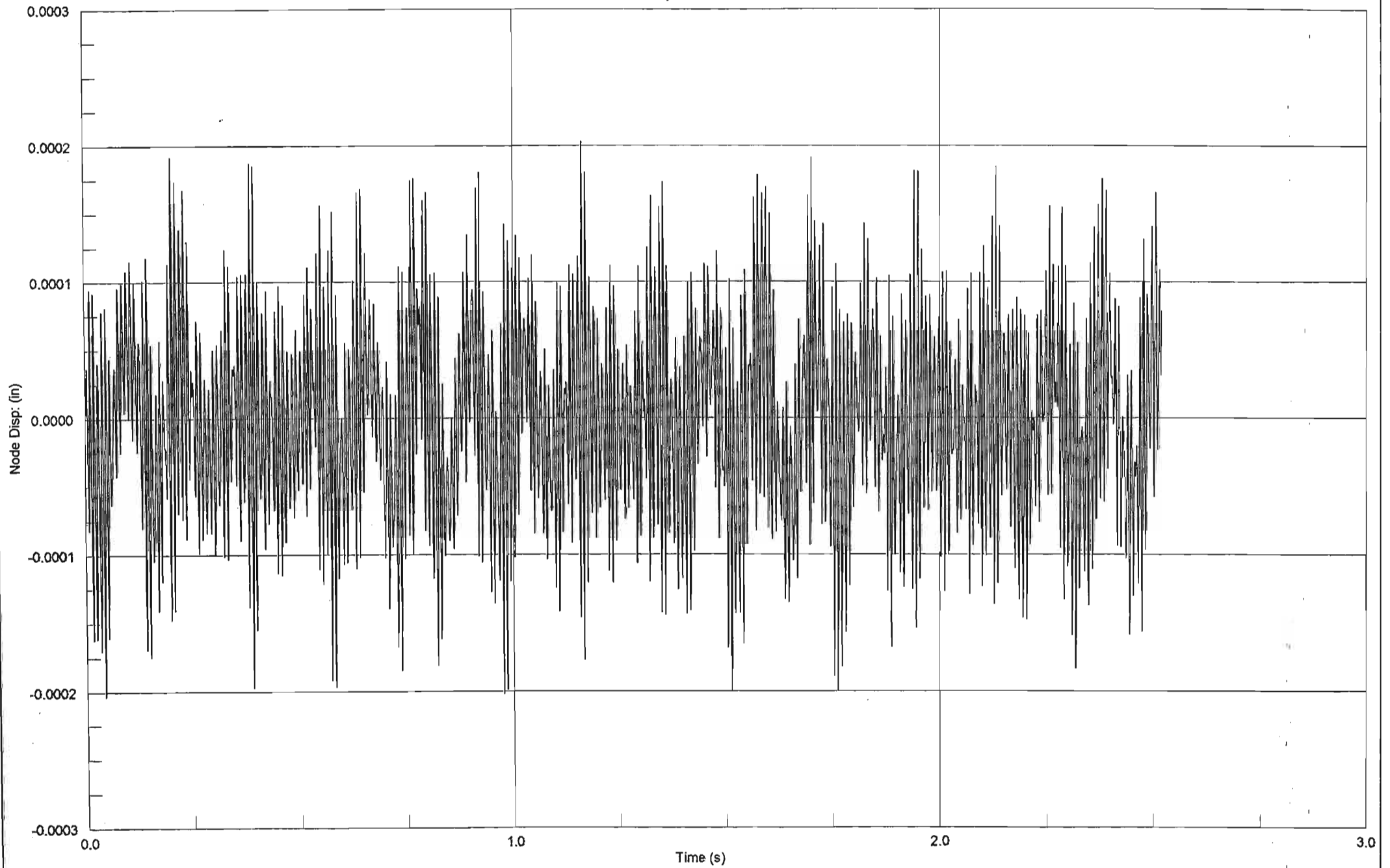
DATE SUBMITTED: 13 DECEMBER 2002

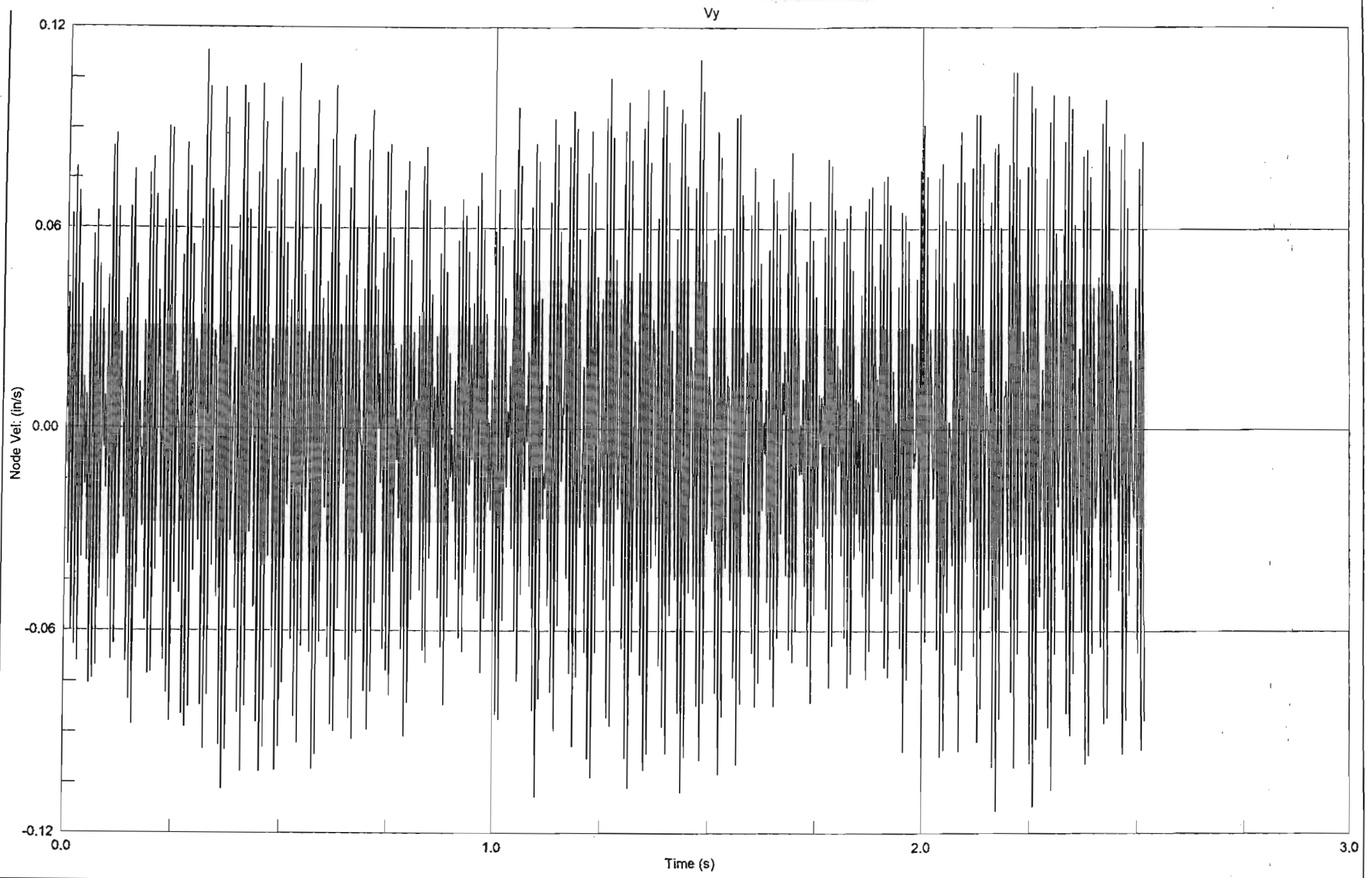
SUPERVISOR: PROFESSOR H D SCHREINER

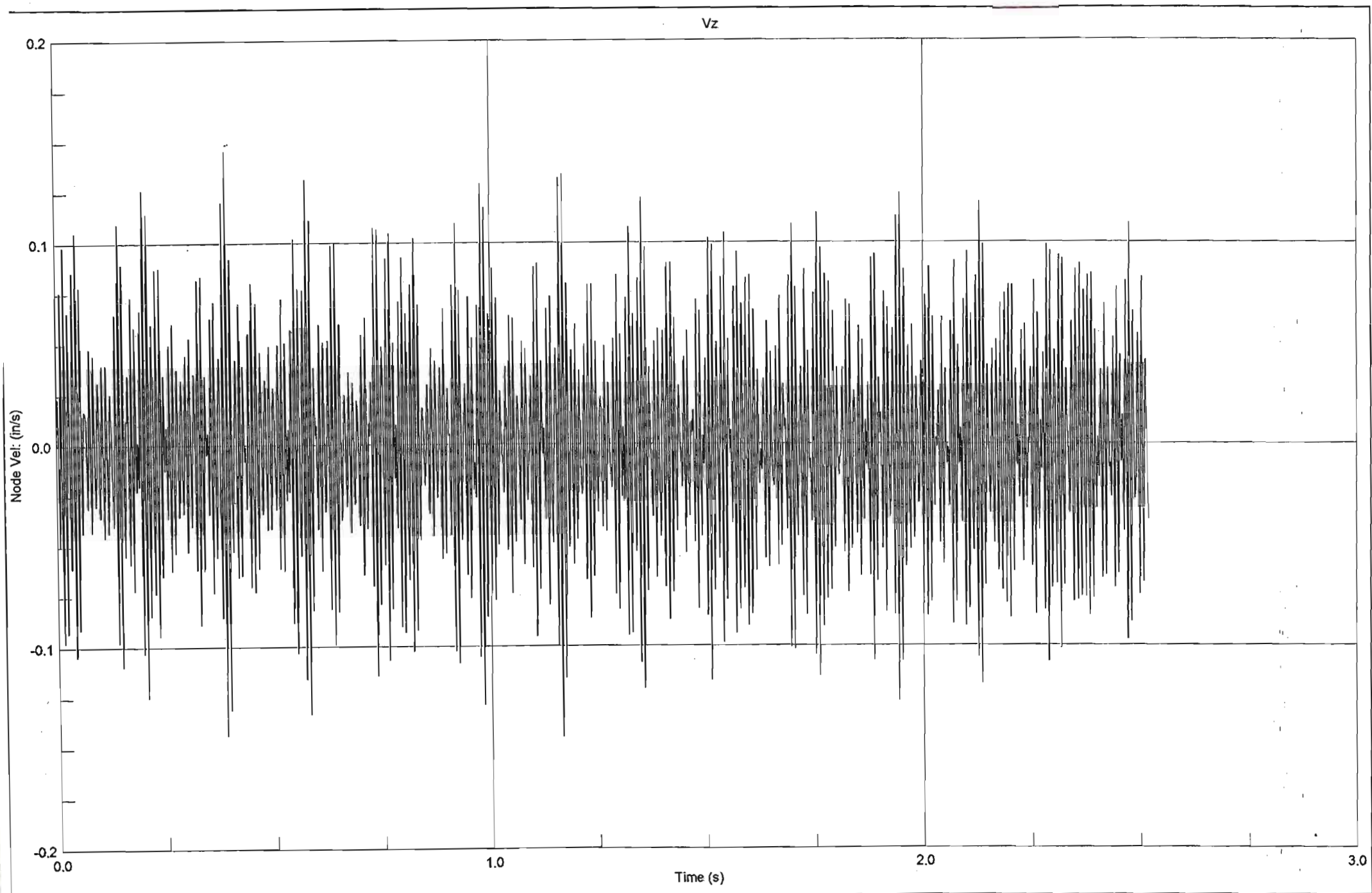
Y Displacement of Node 20

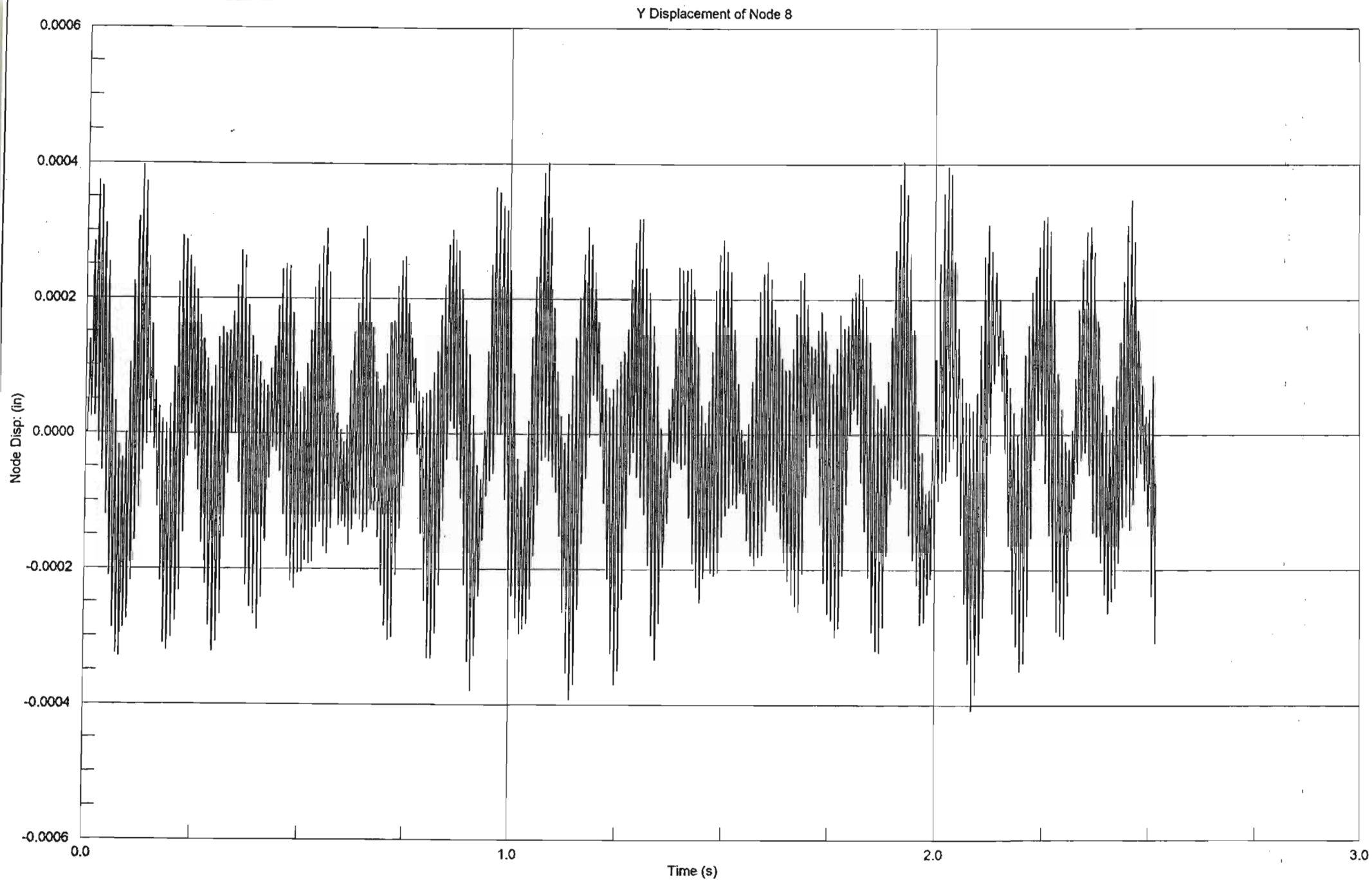


Z Displacement of Node 20

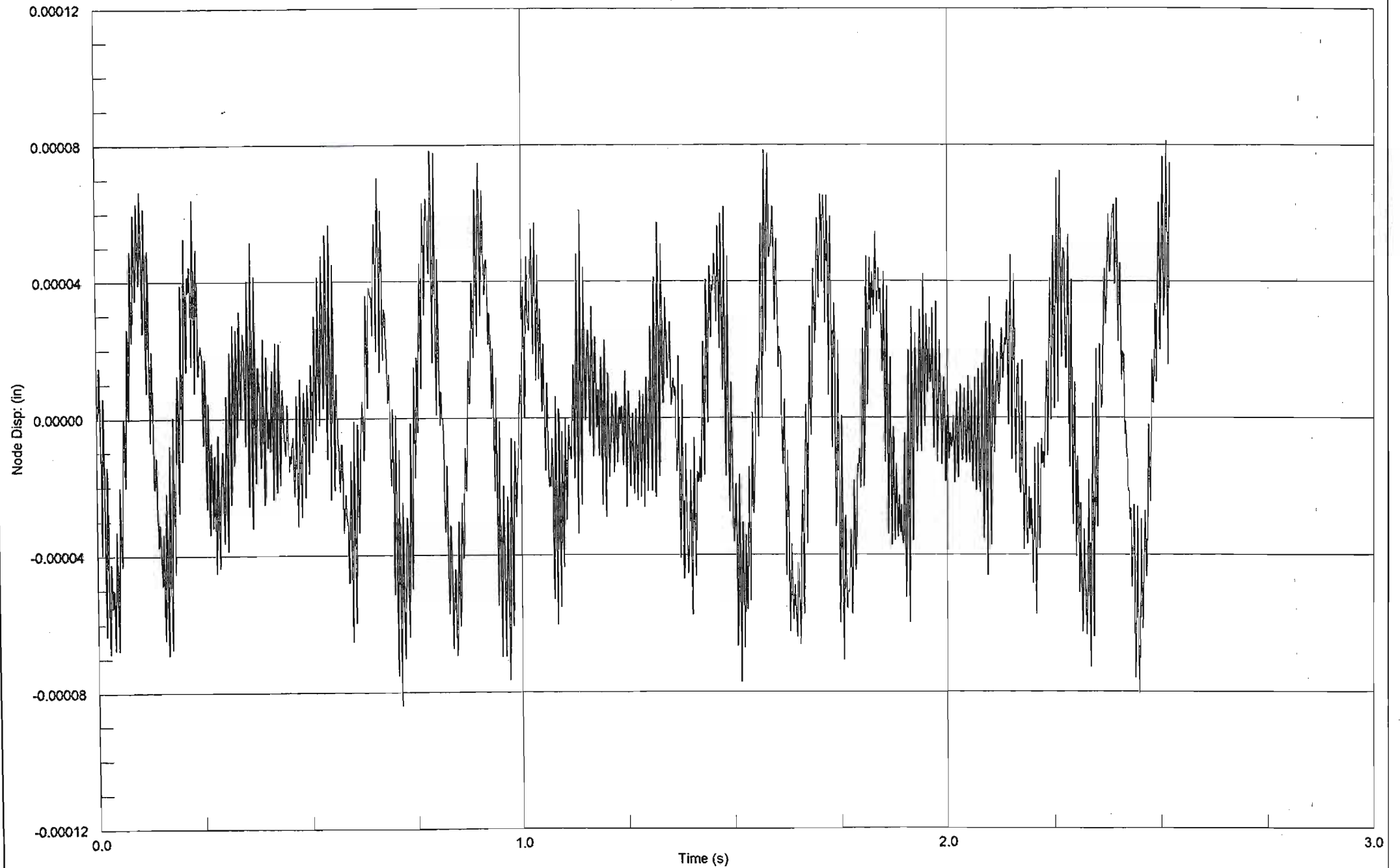




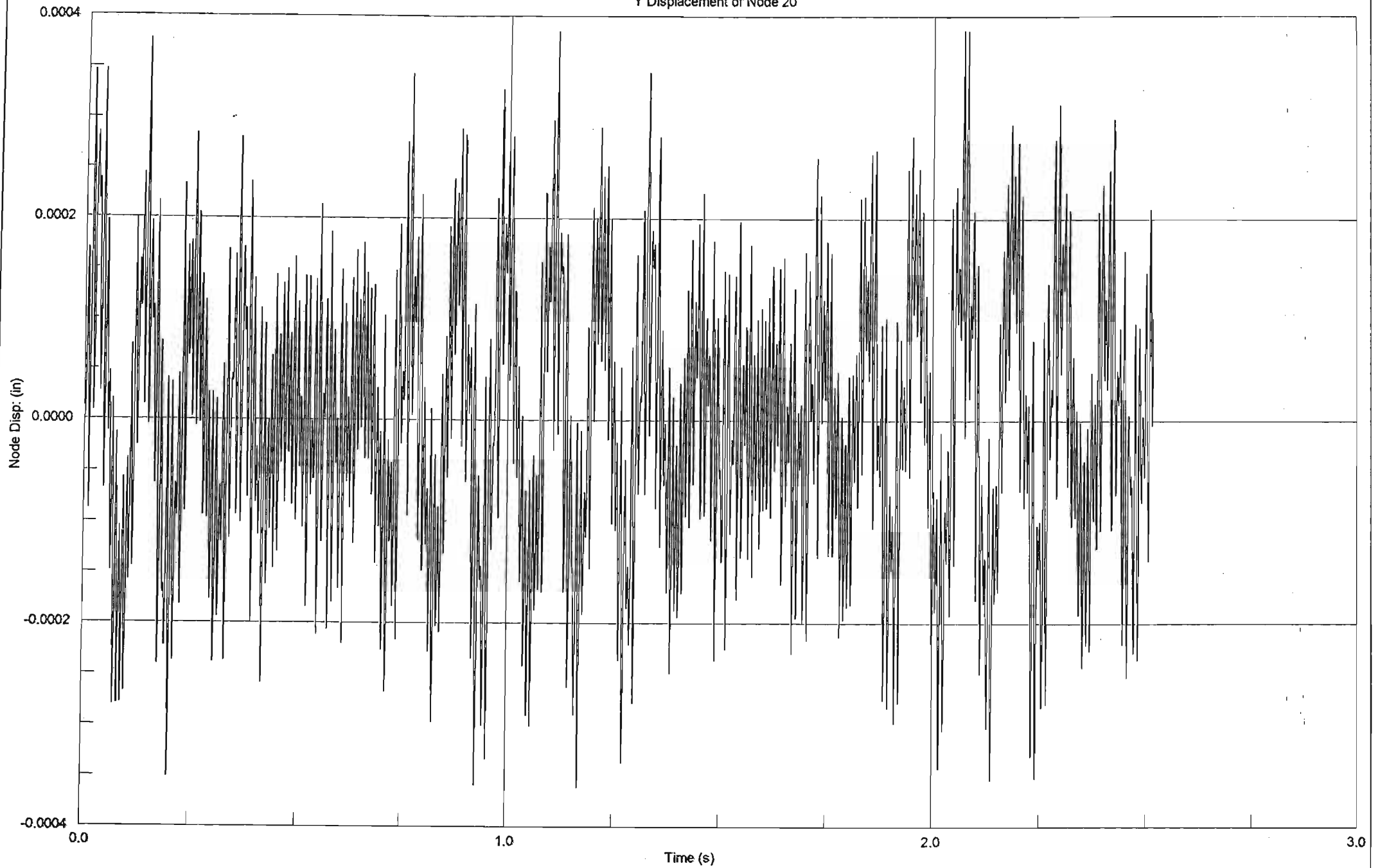


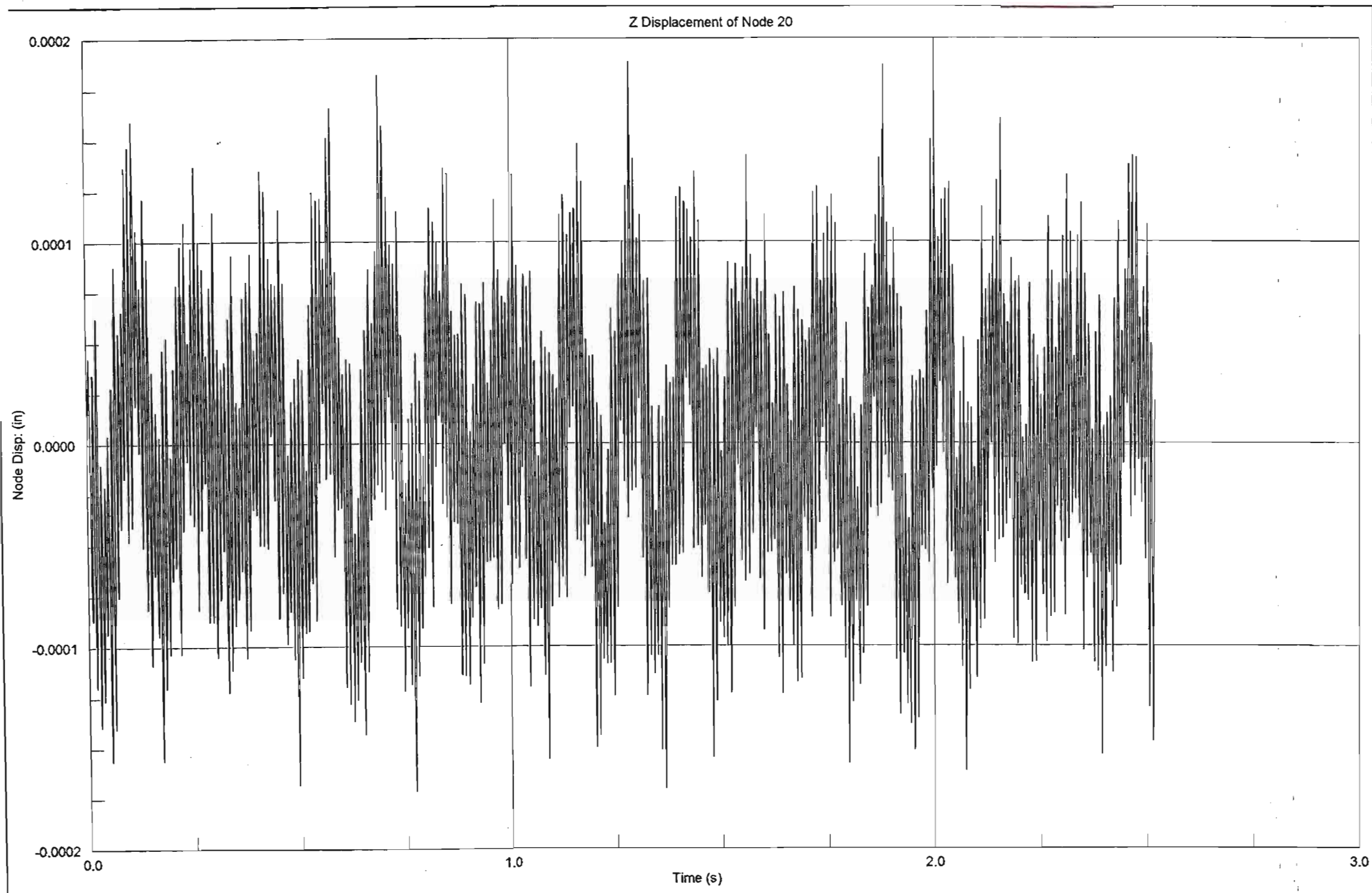


Z Displacement of Node 8

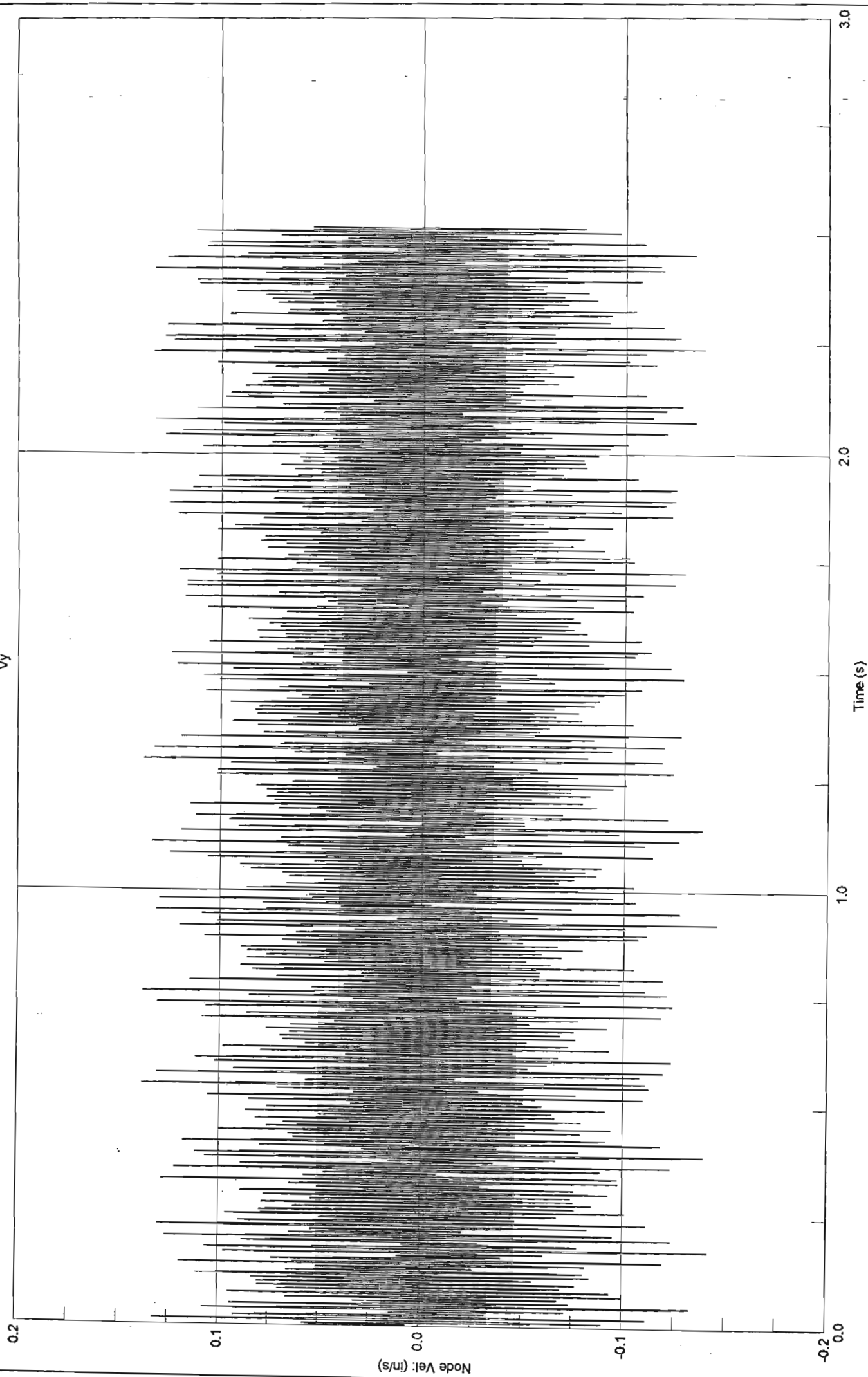


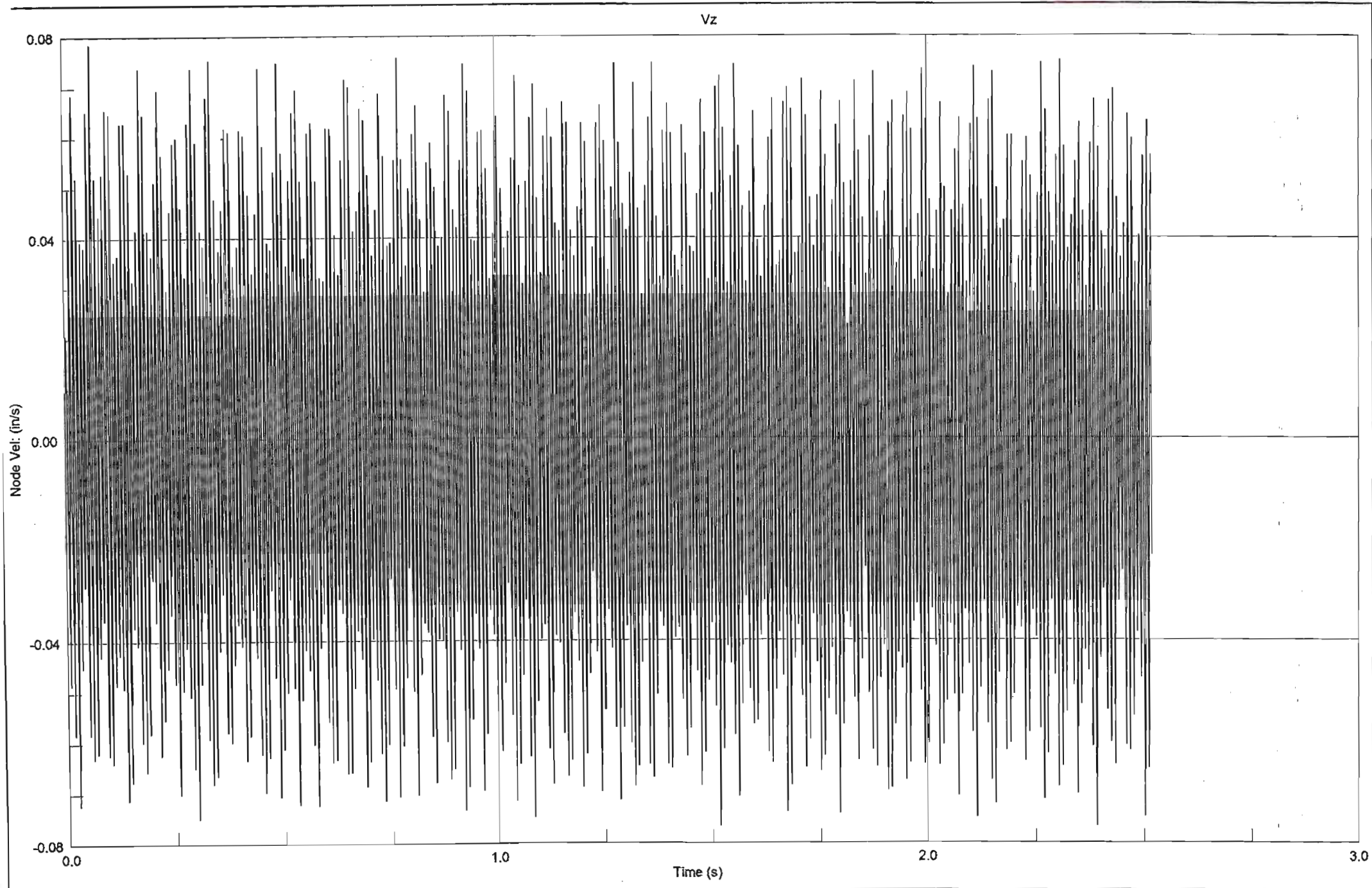
Y Displacement of Node 20

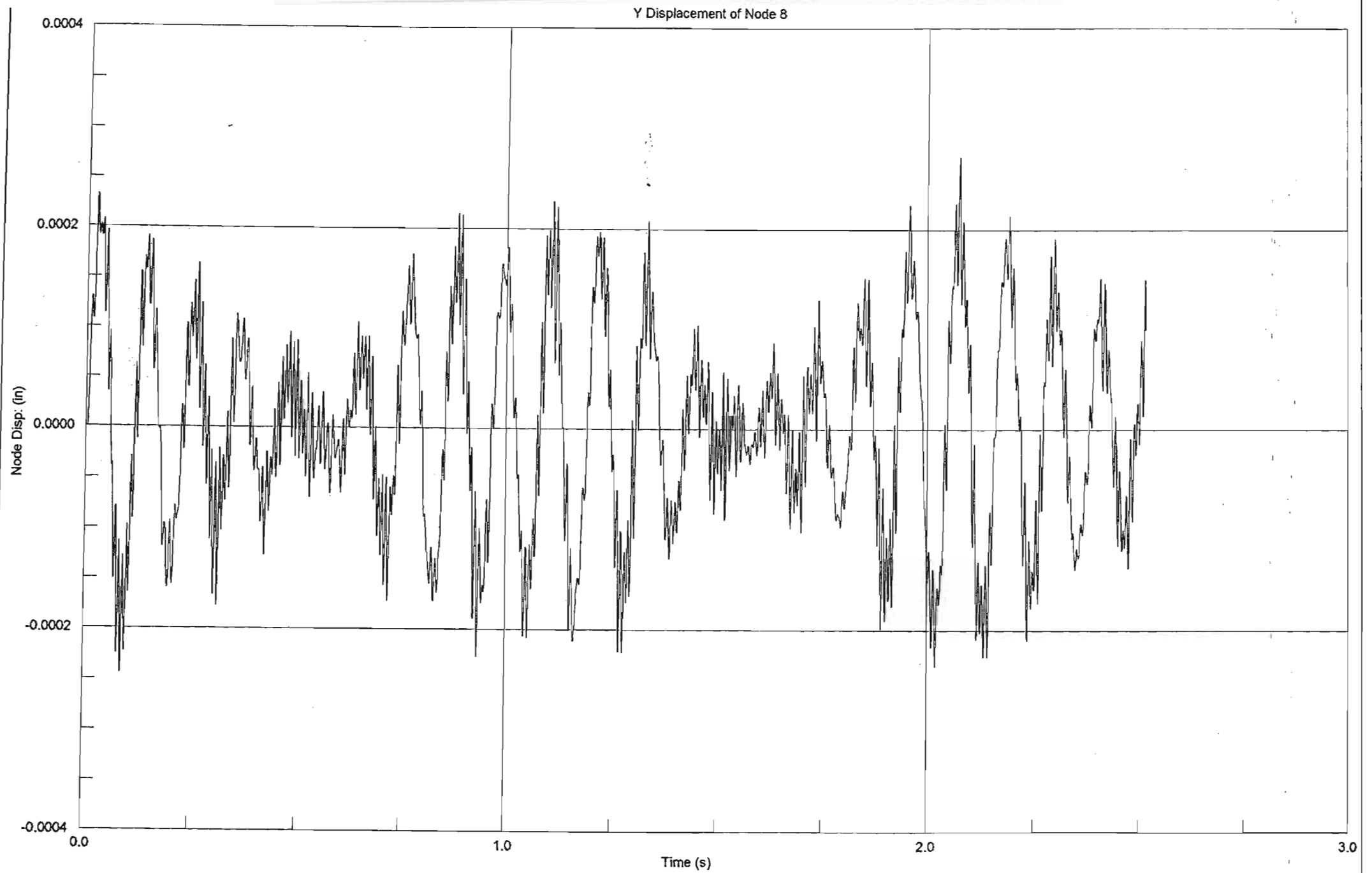




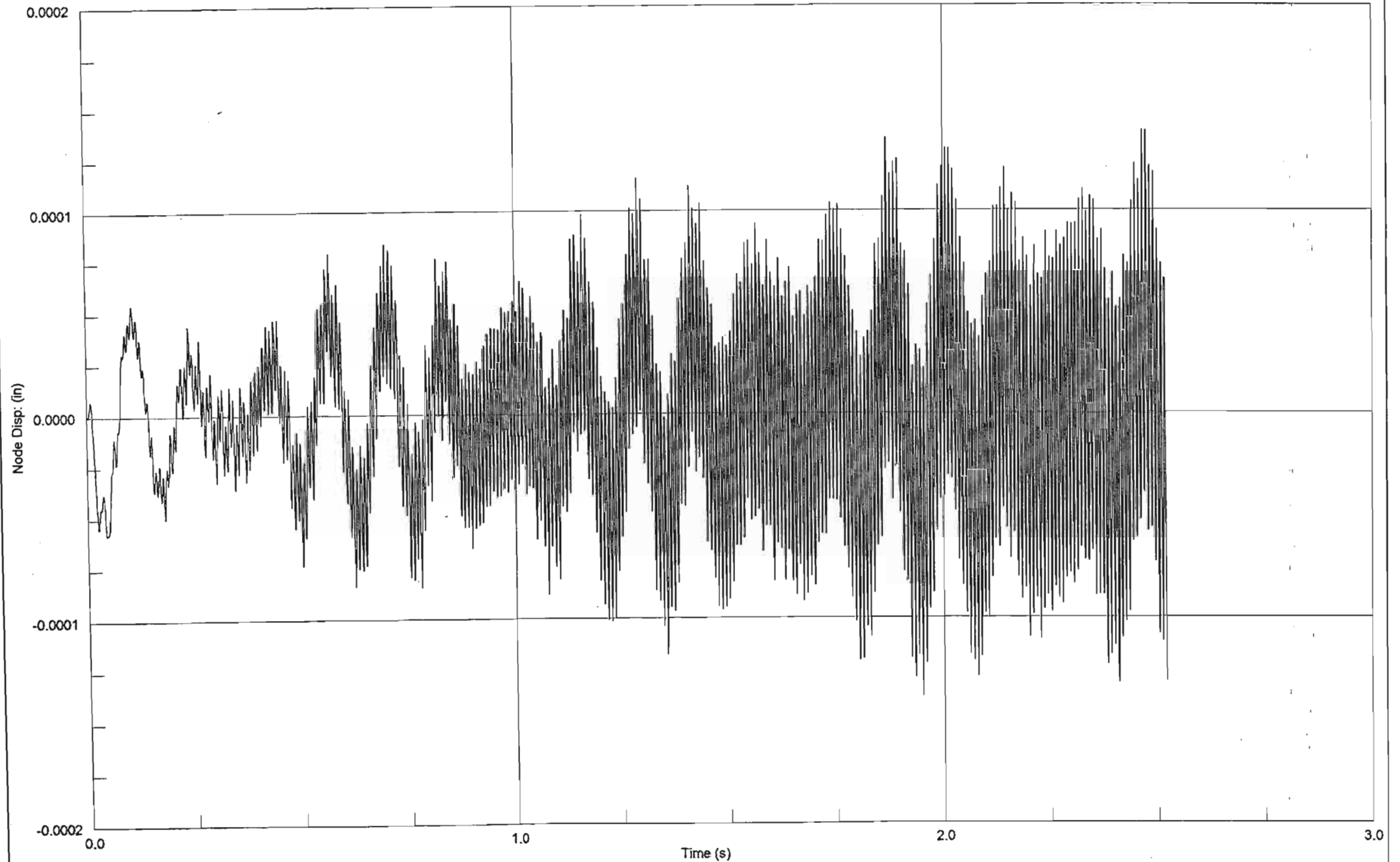
Vy

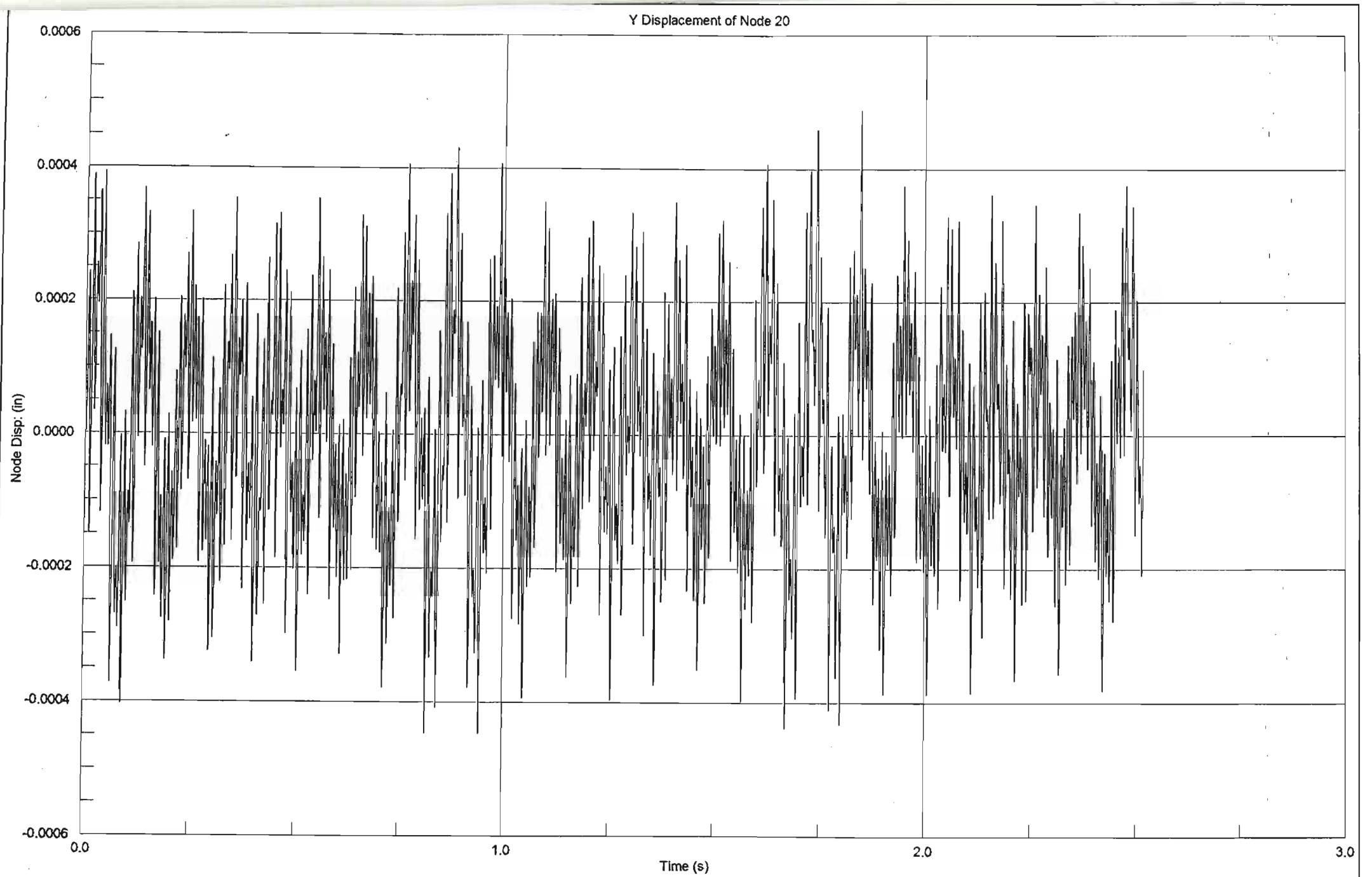




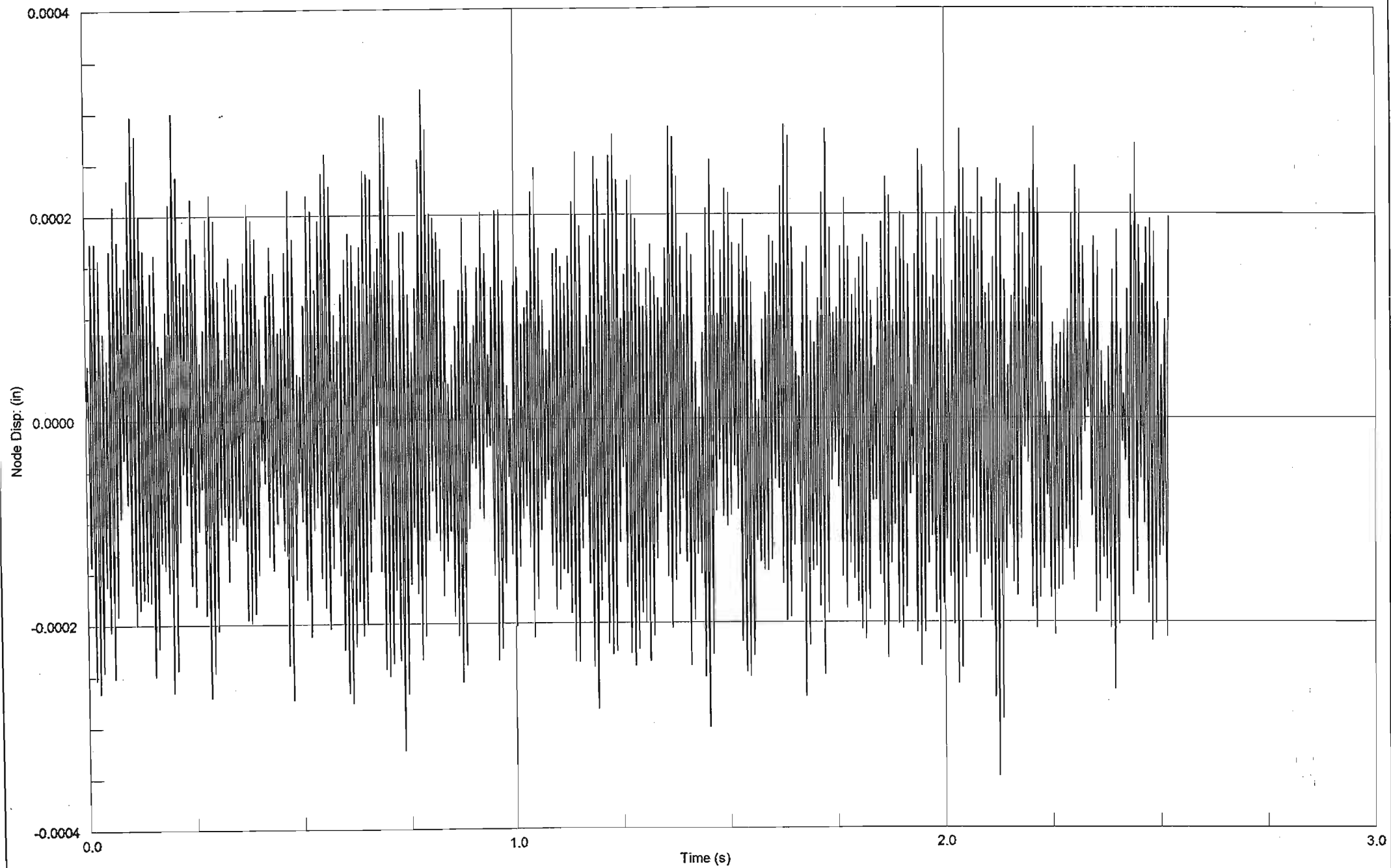


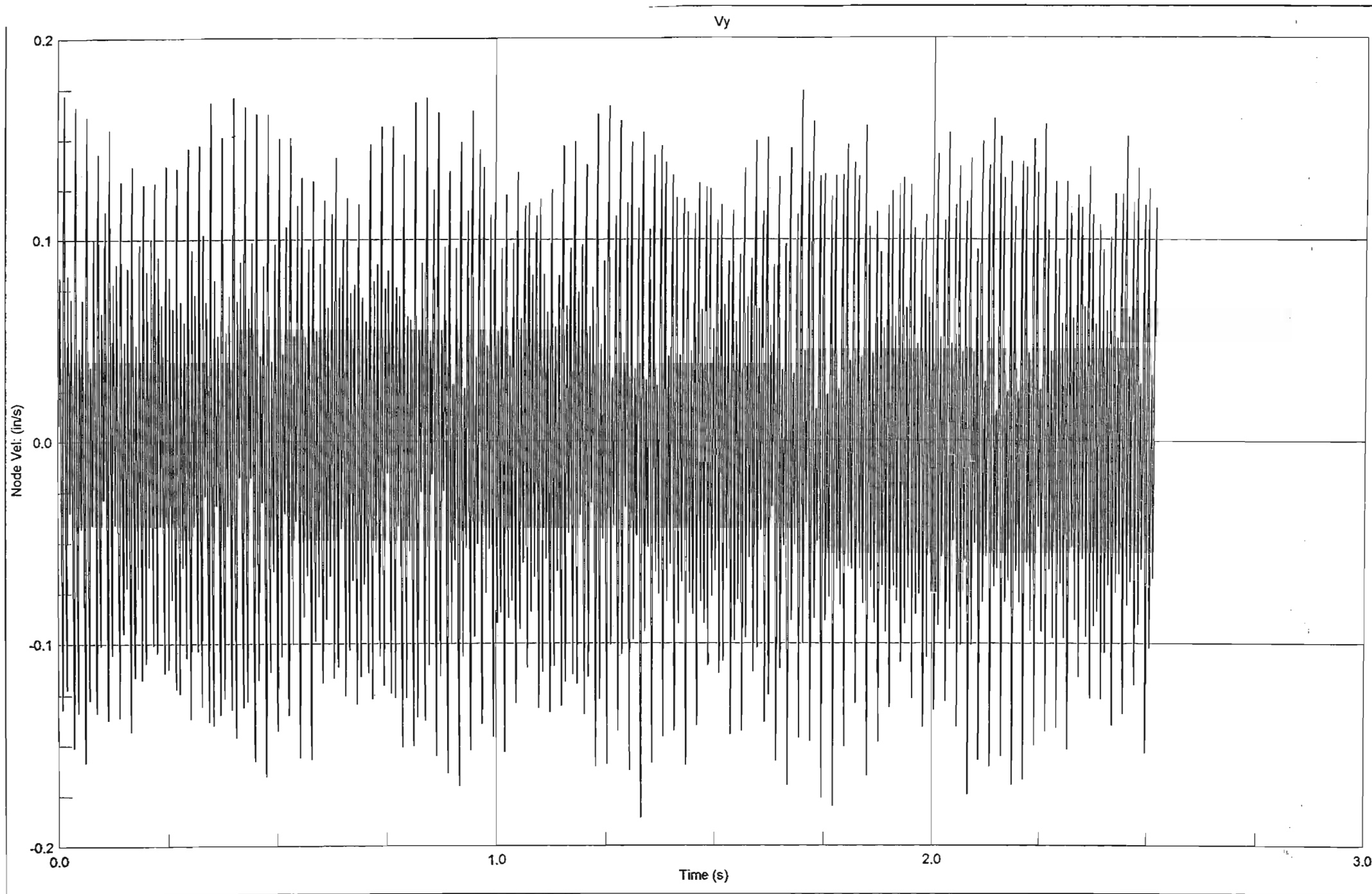
Z Displacement of Node 8

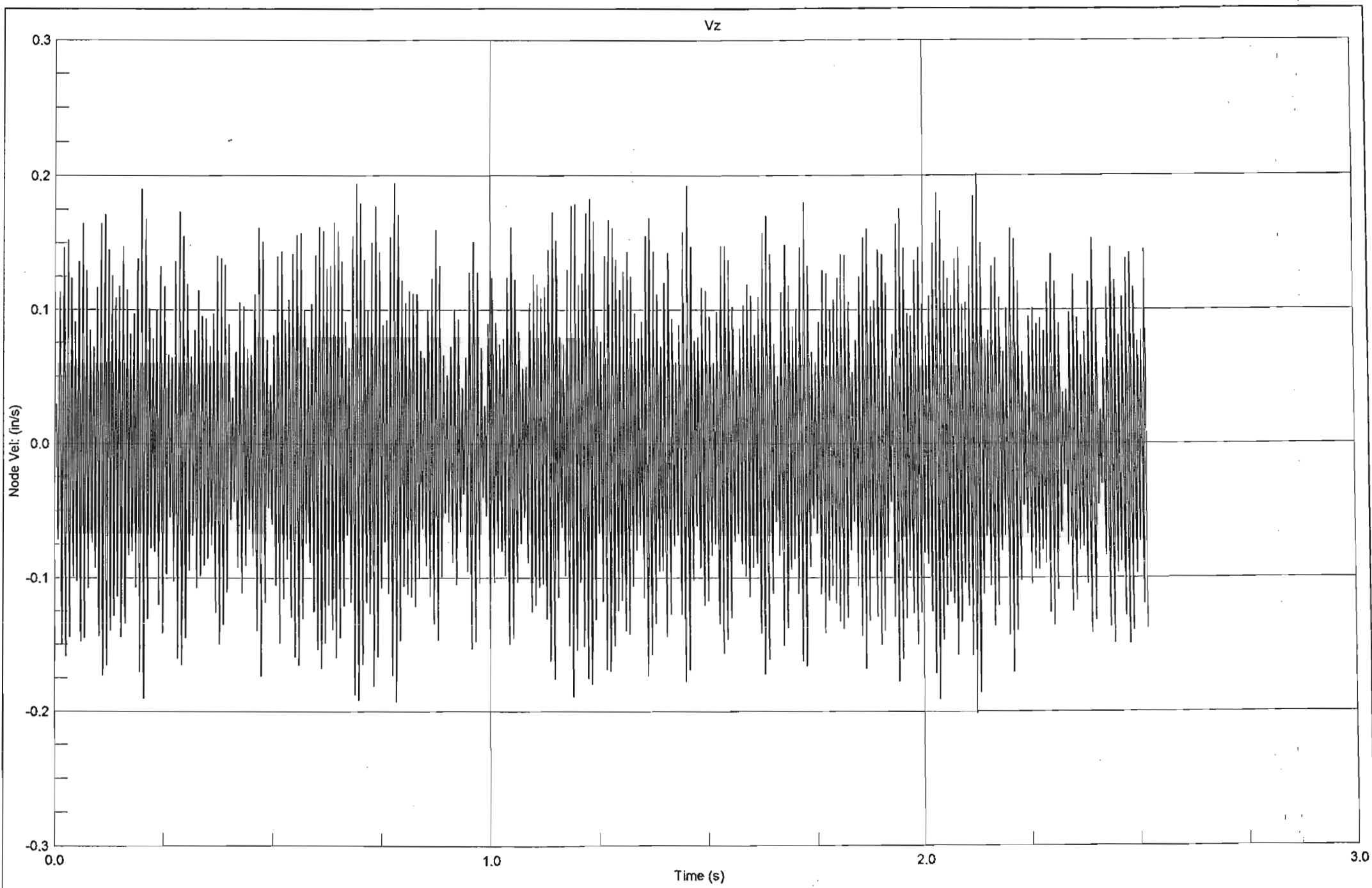




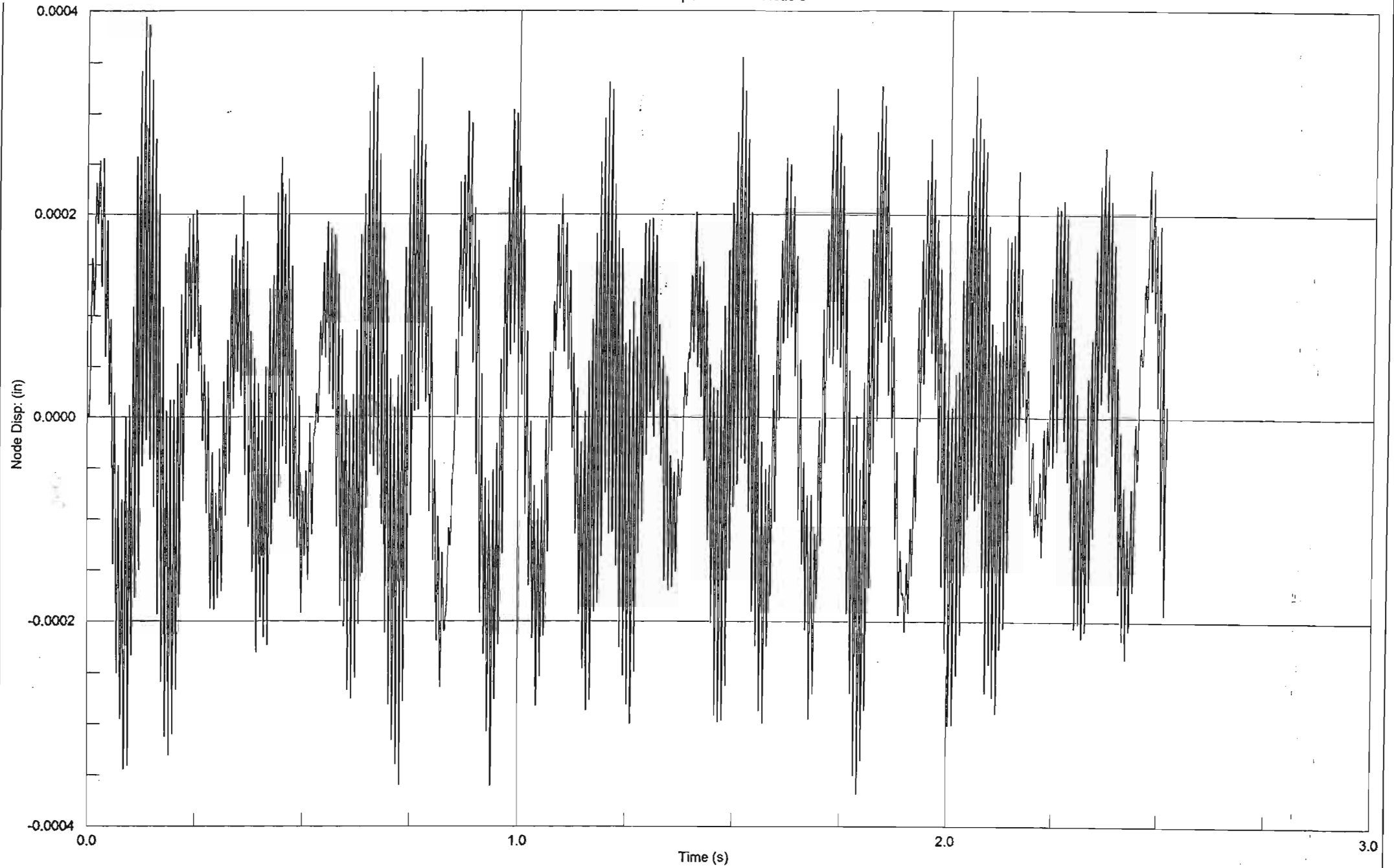
Z Displacement of Node 20

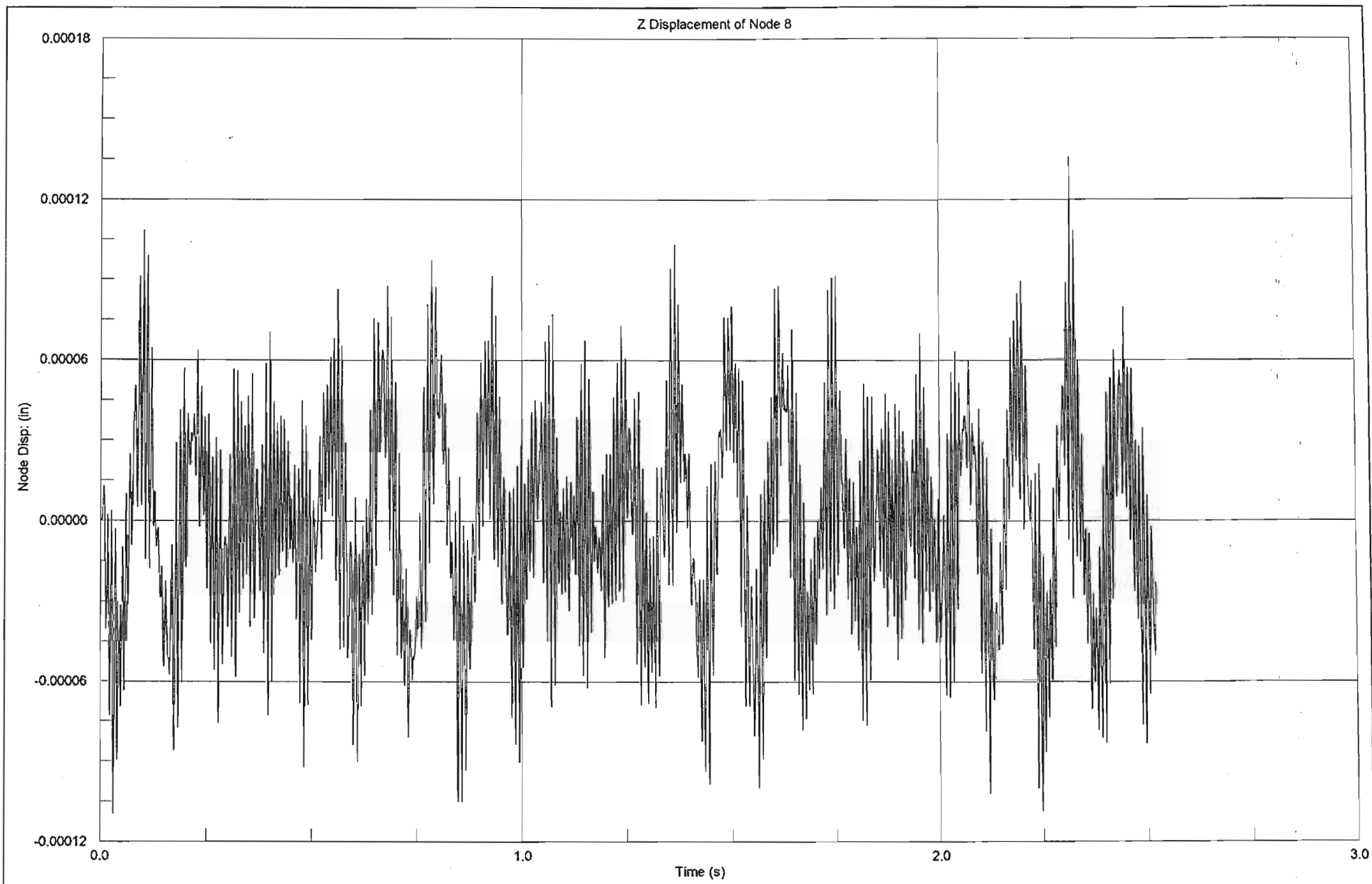




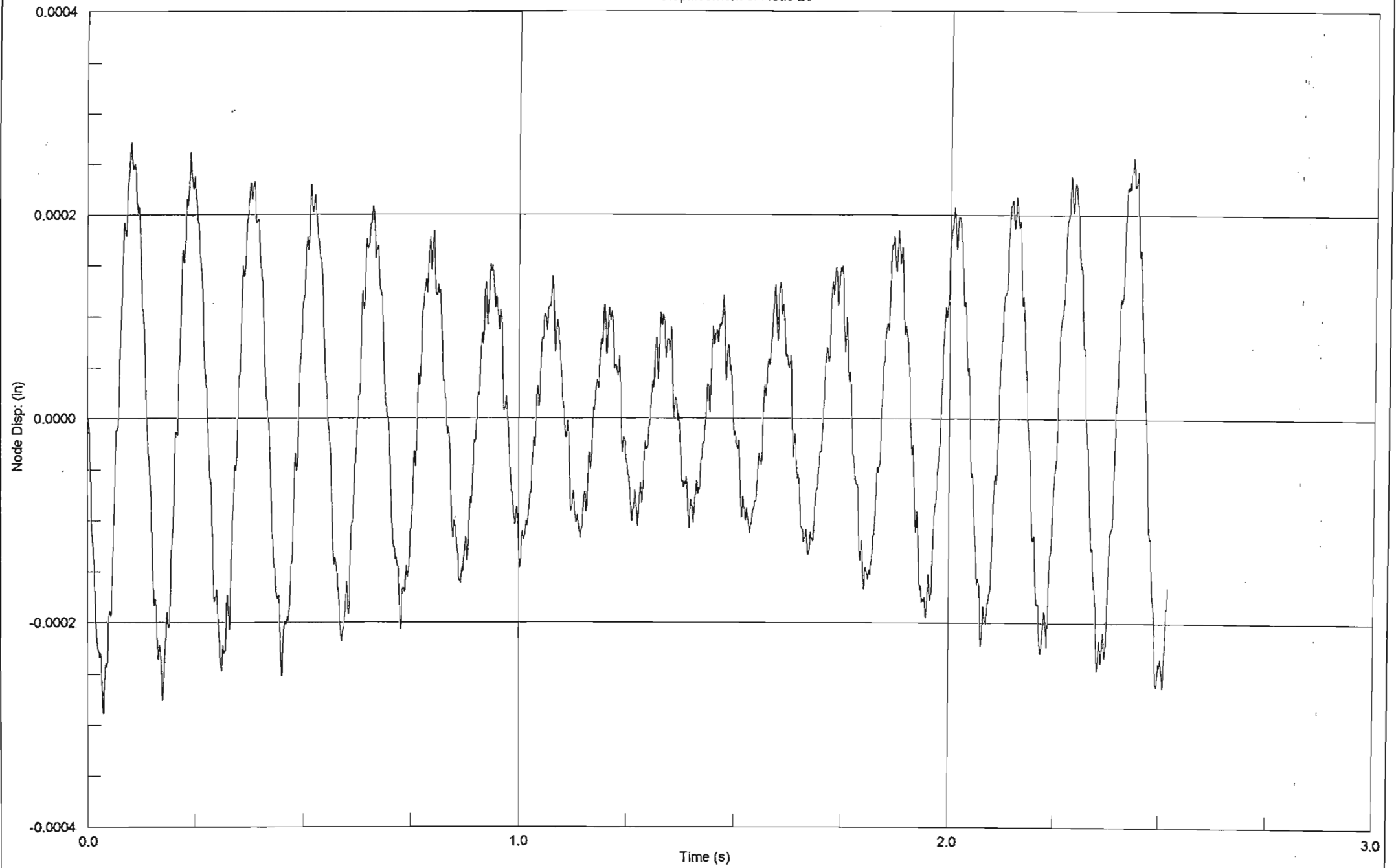


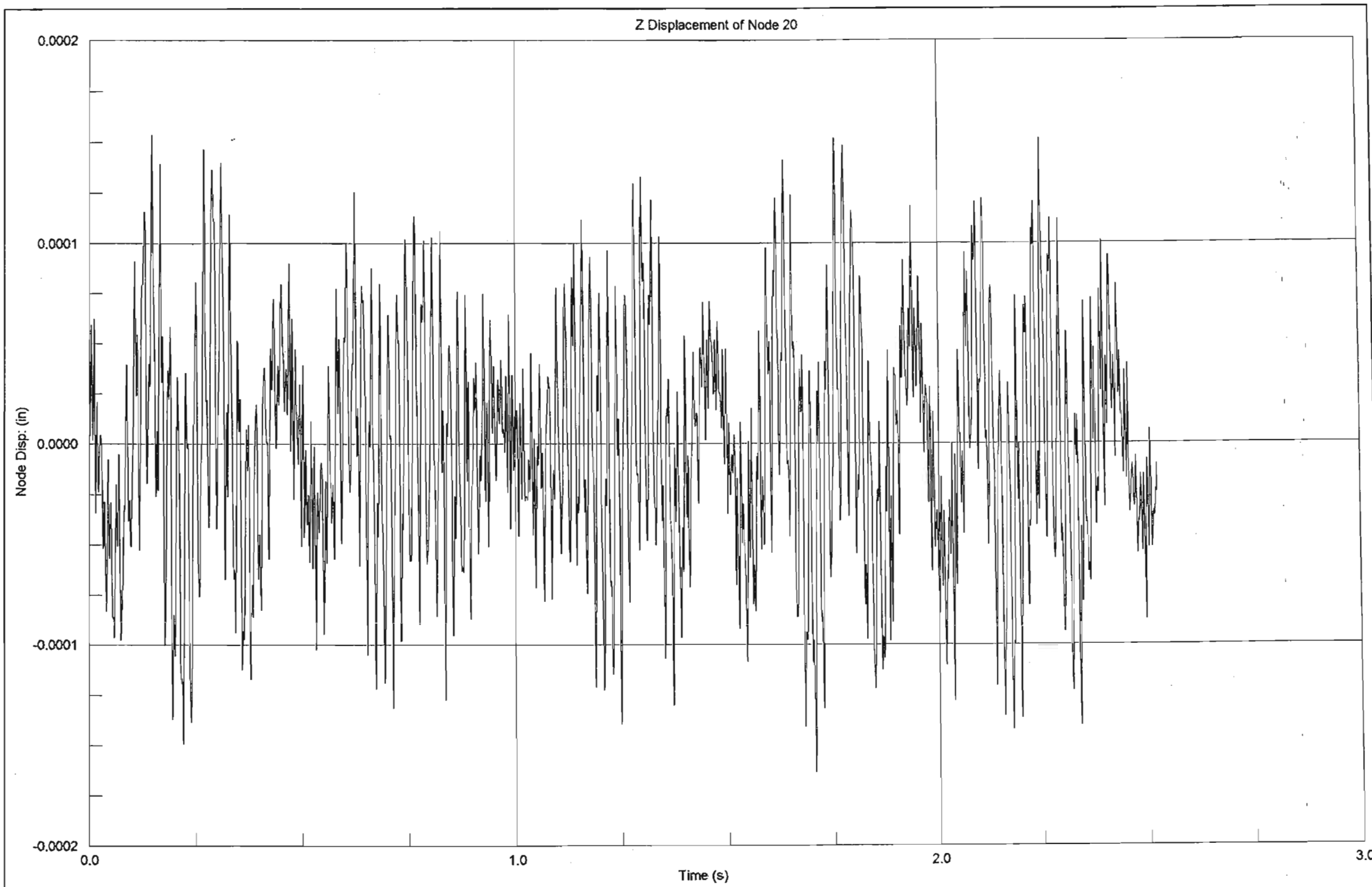
Y Displacement of Node 8

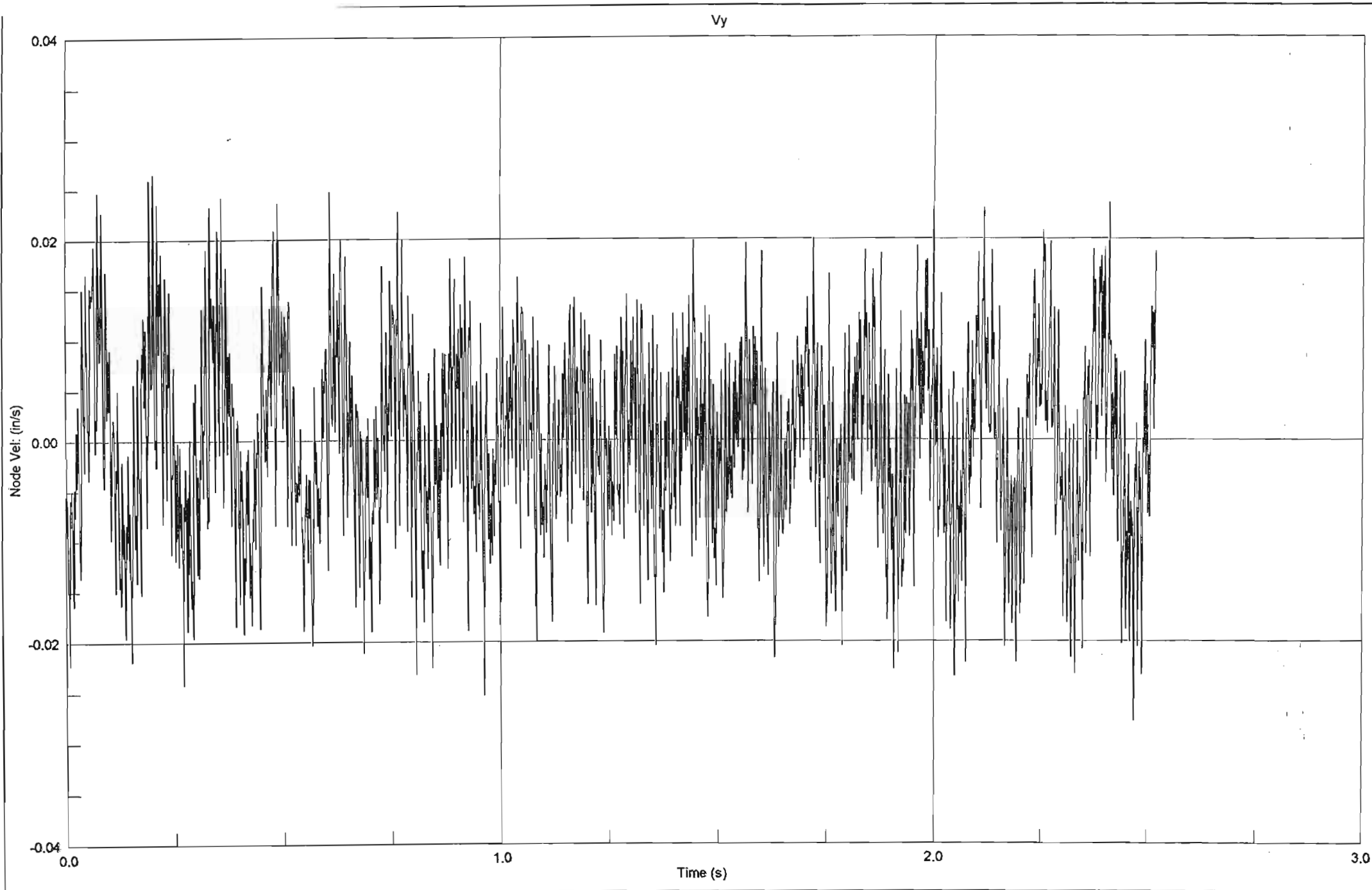


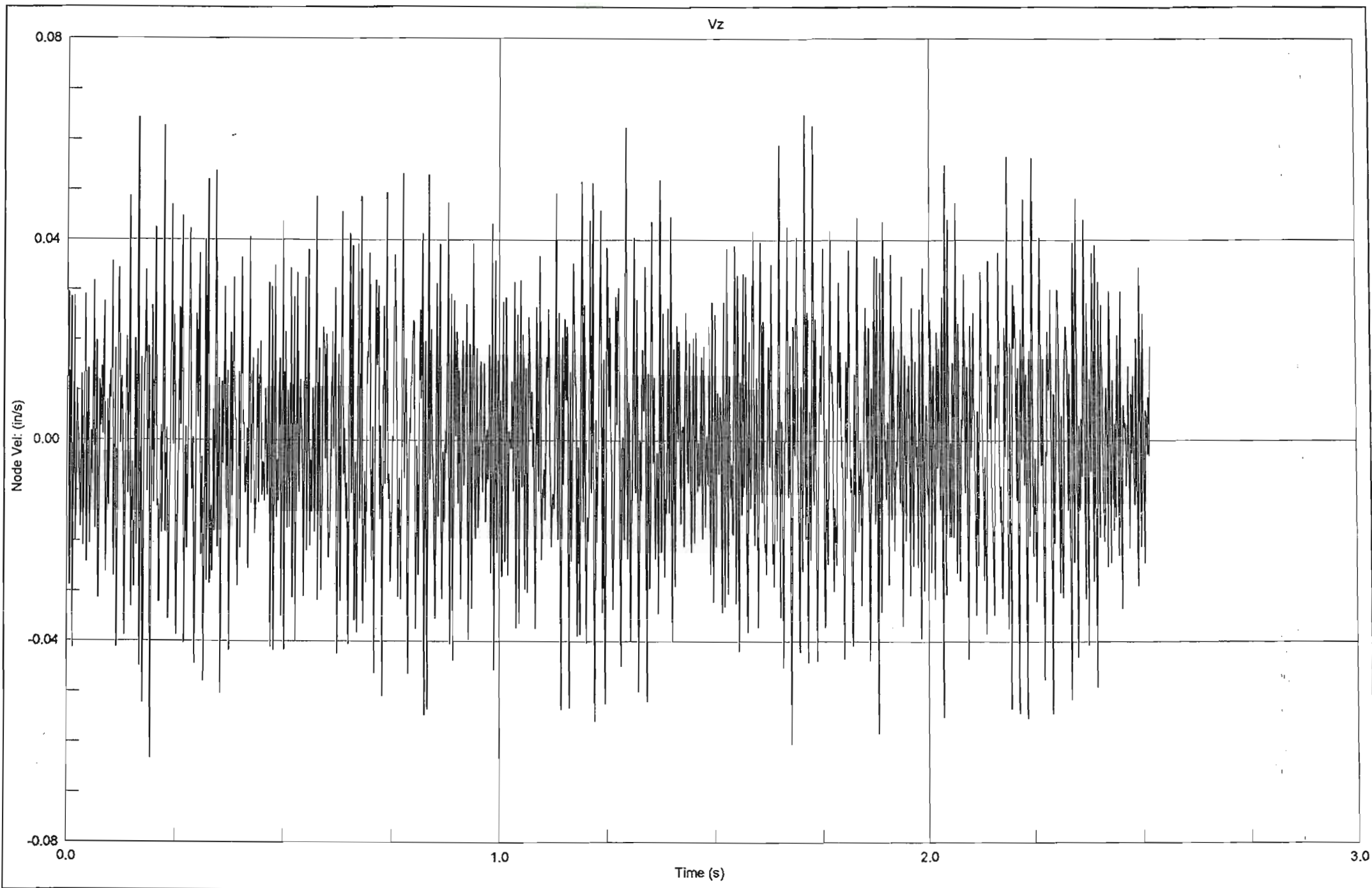


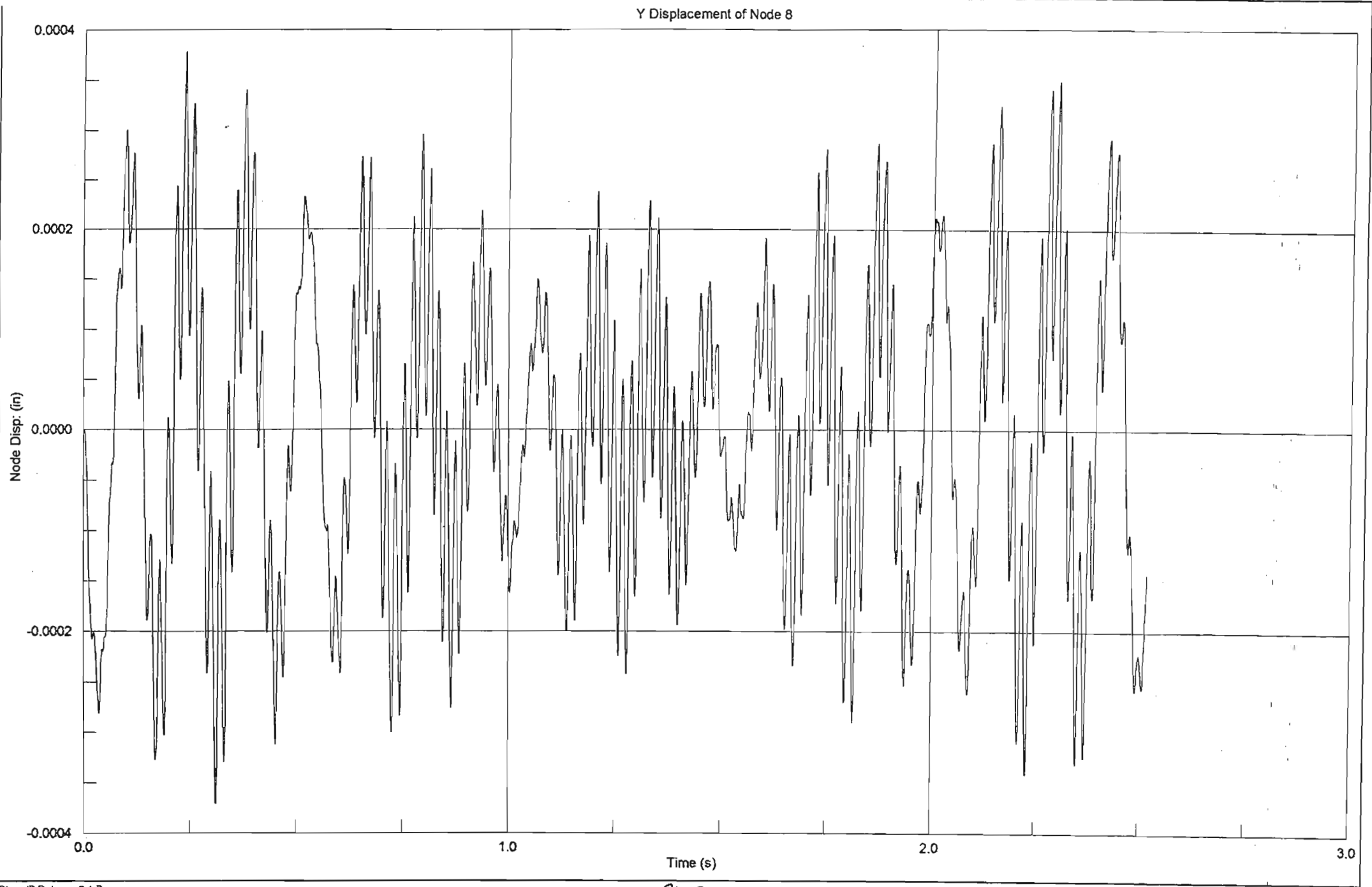
Y Displacement of Node 20

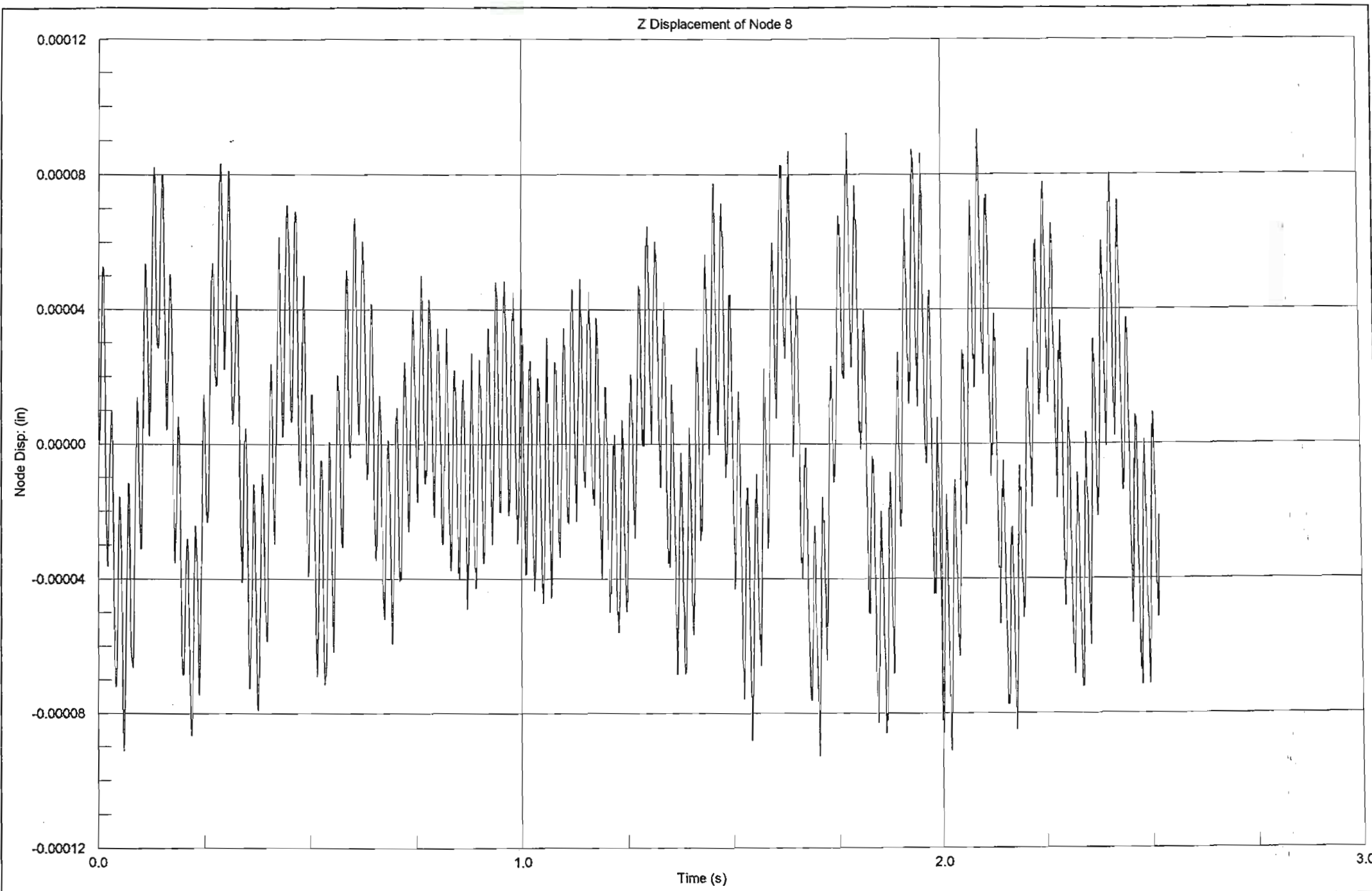




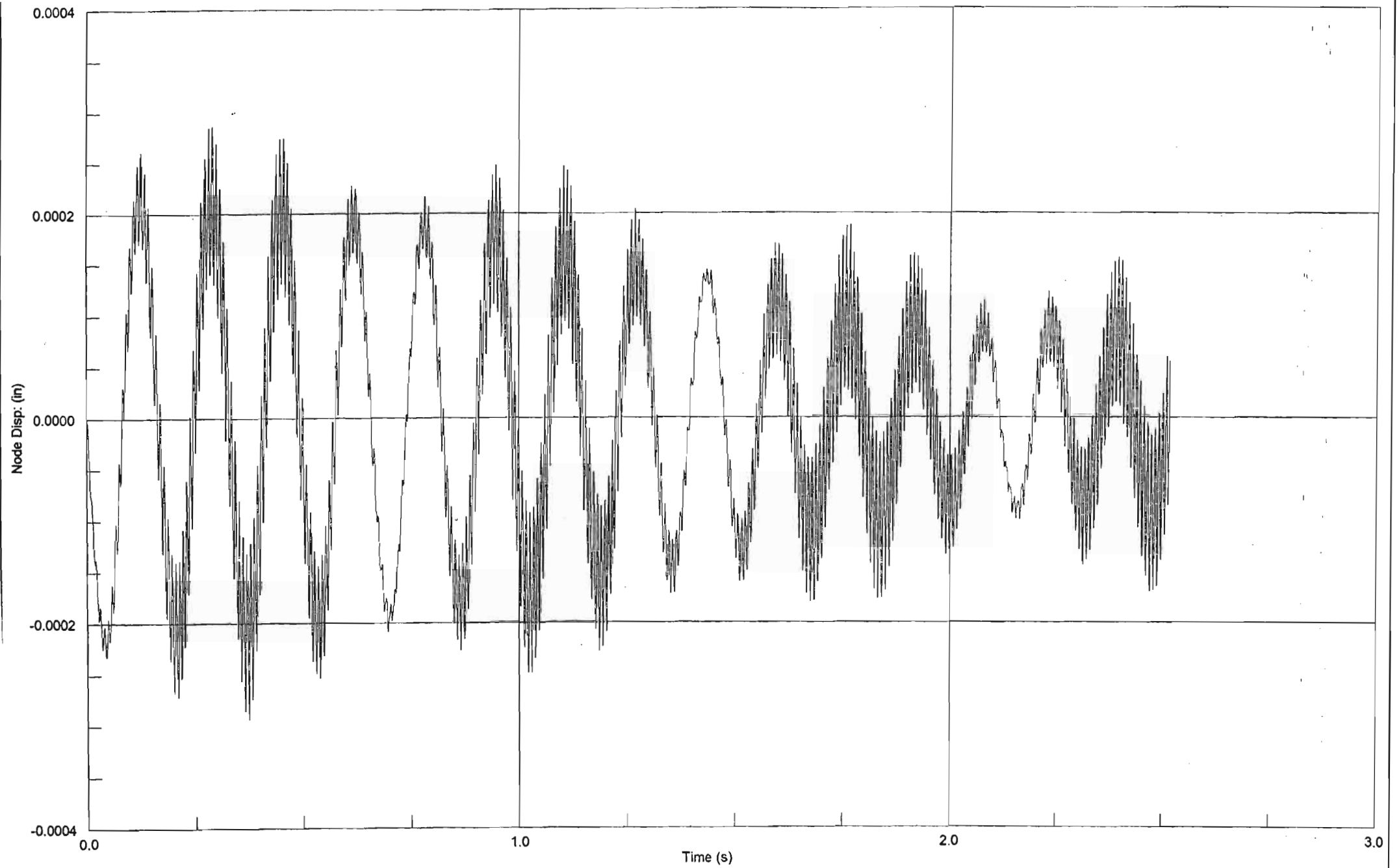


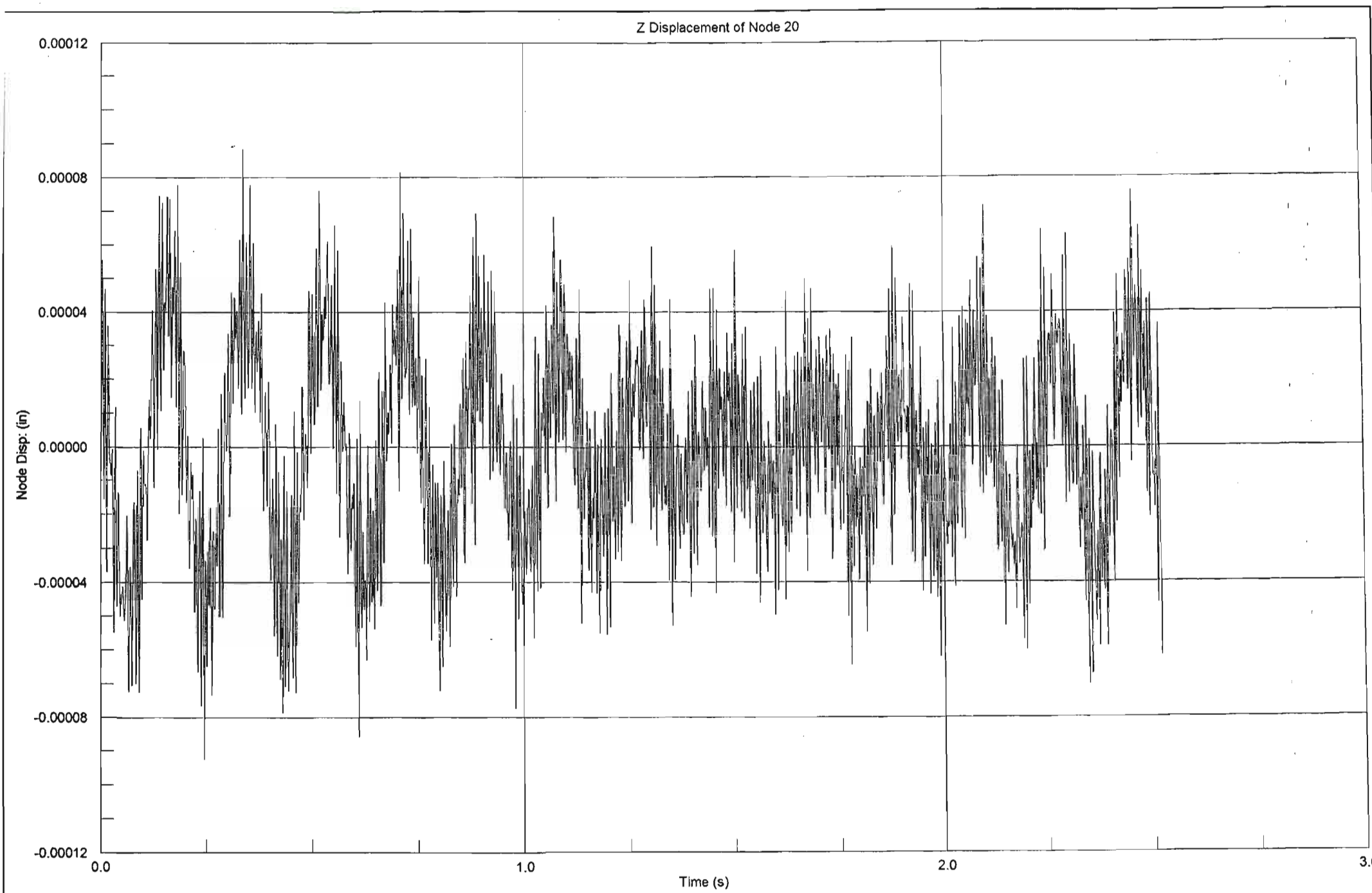


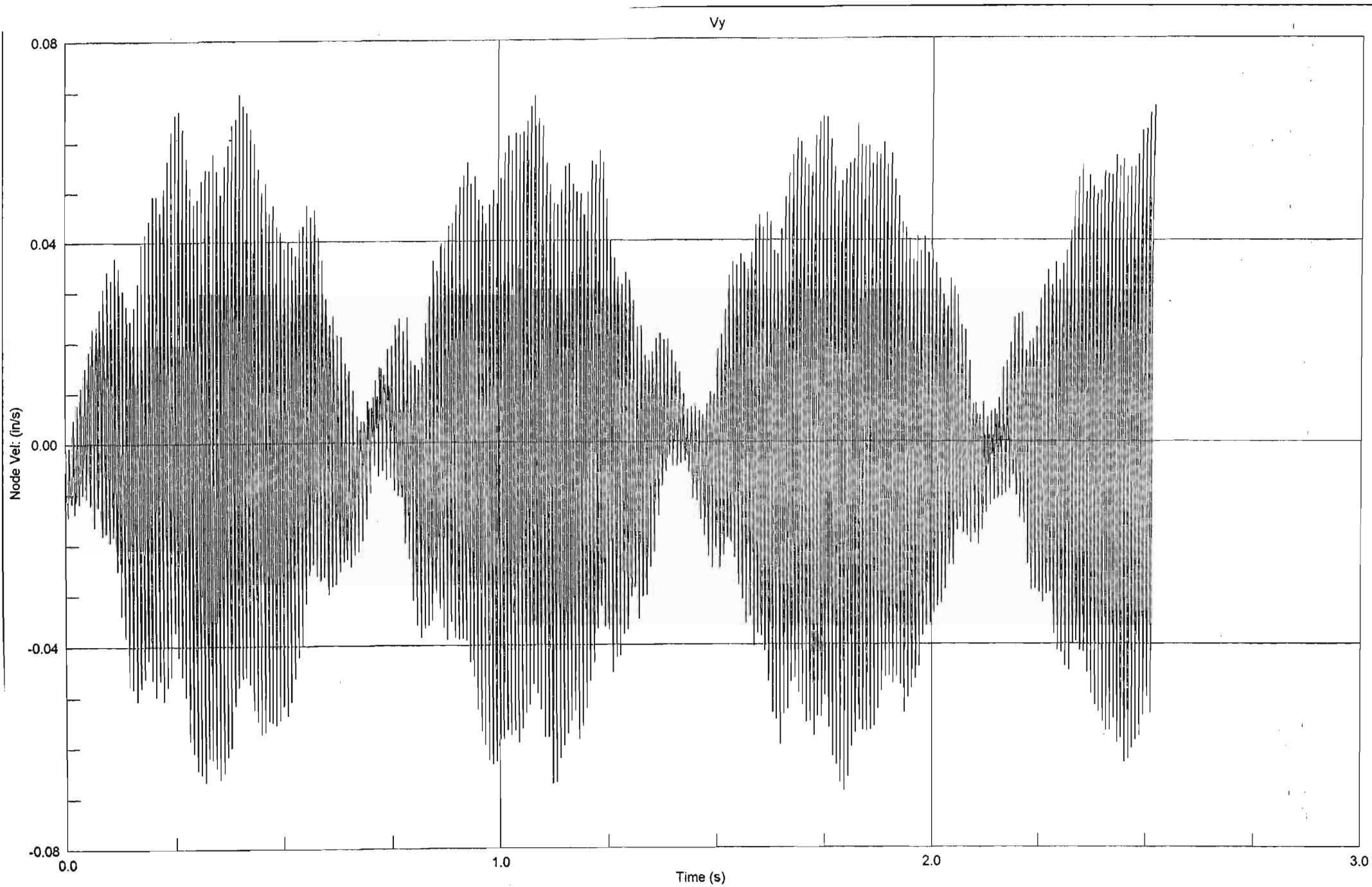




Y Displacement of Node 20





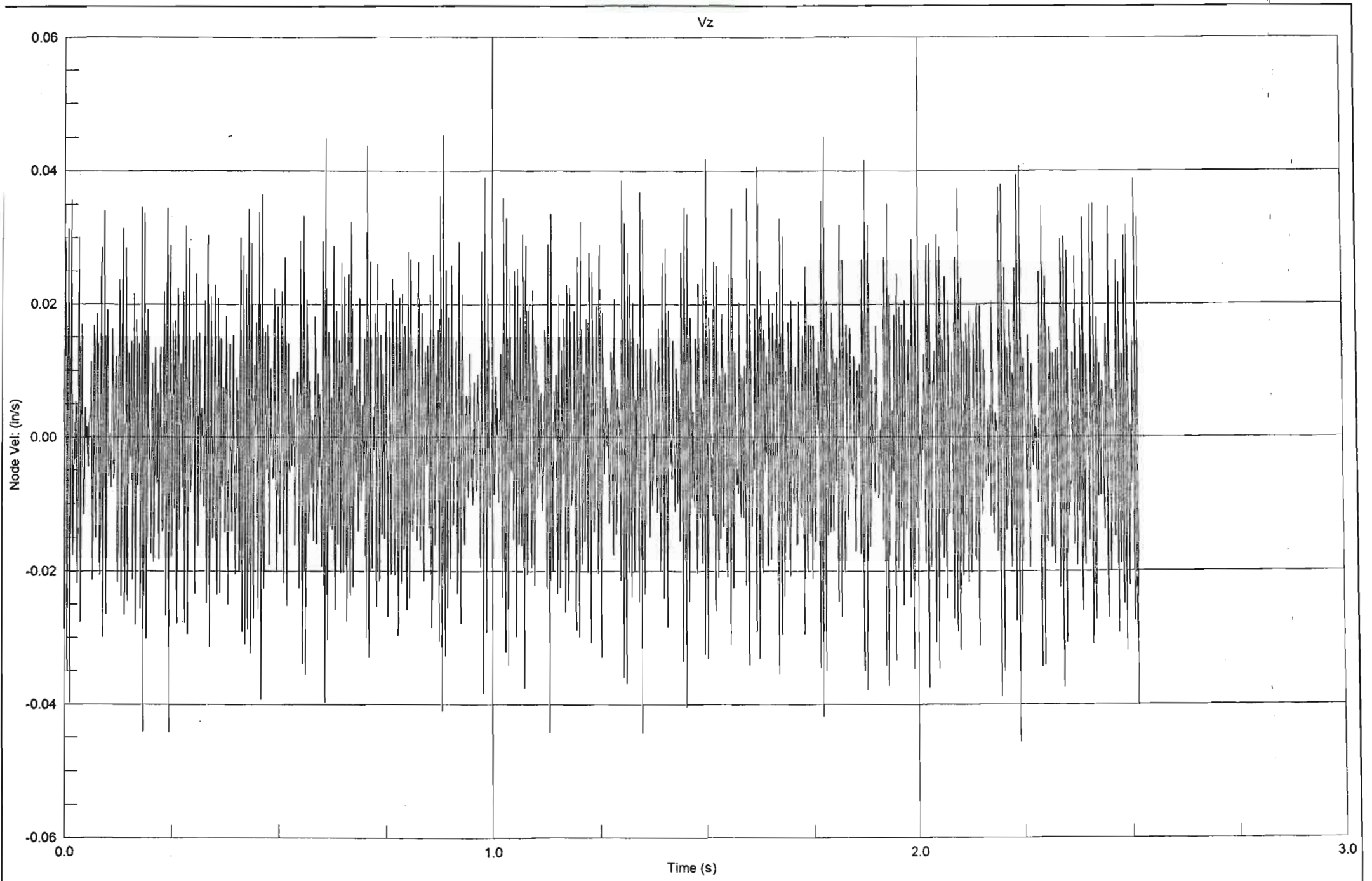


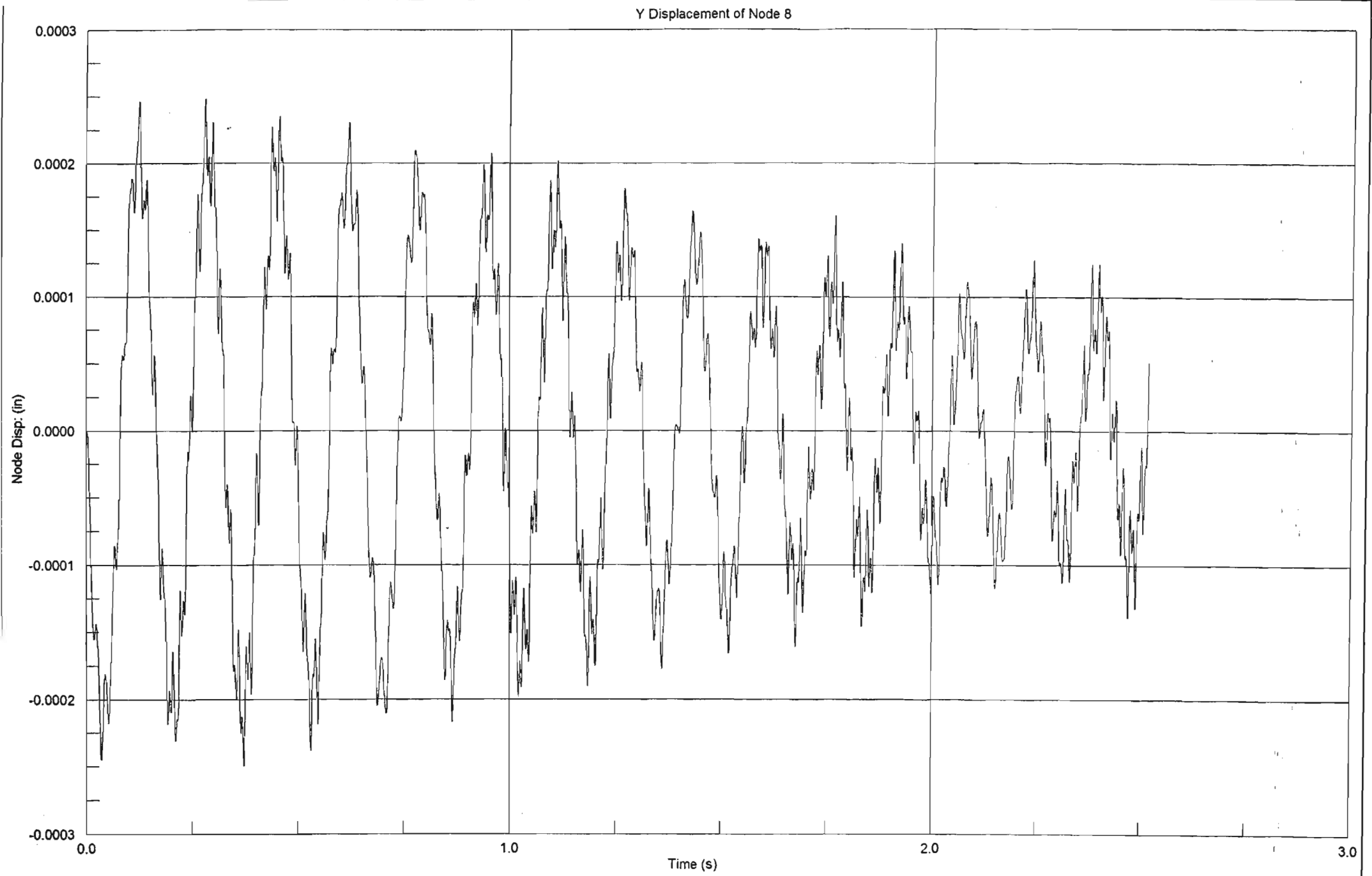
rand7 Release 2.1.7

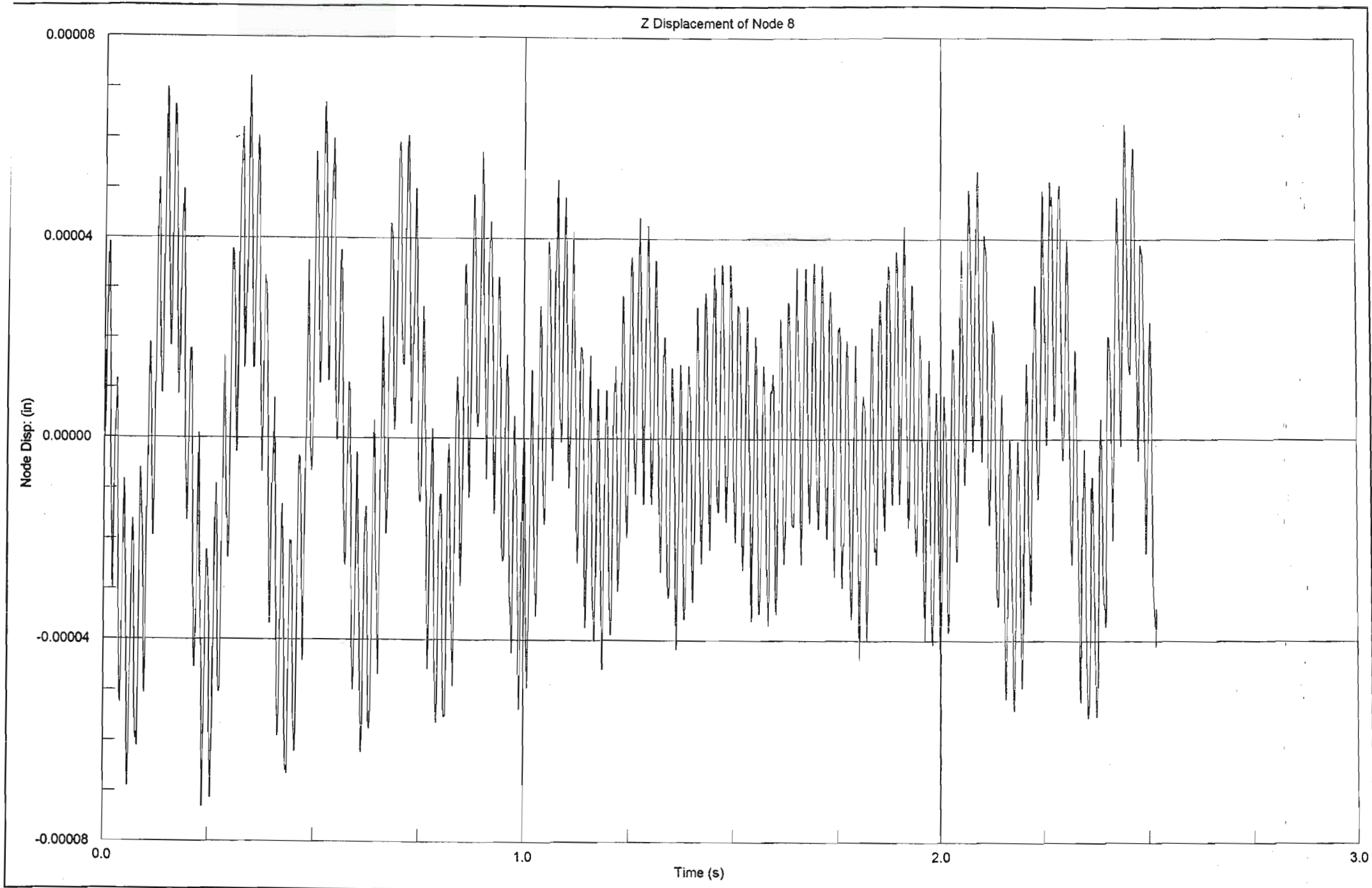
:\MSc Eng\Raft\Raft 3v\ra G4000p-F2.s17

October 2002 2:38 pm

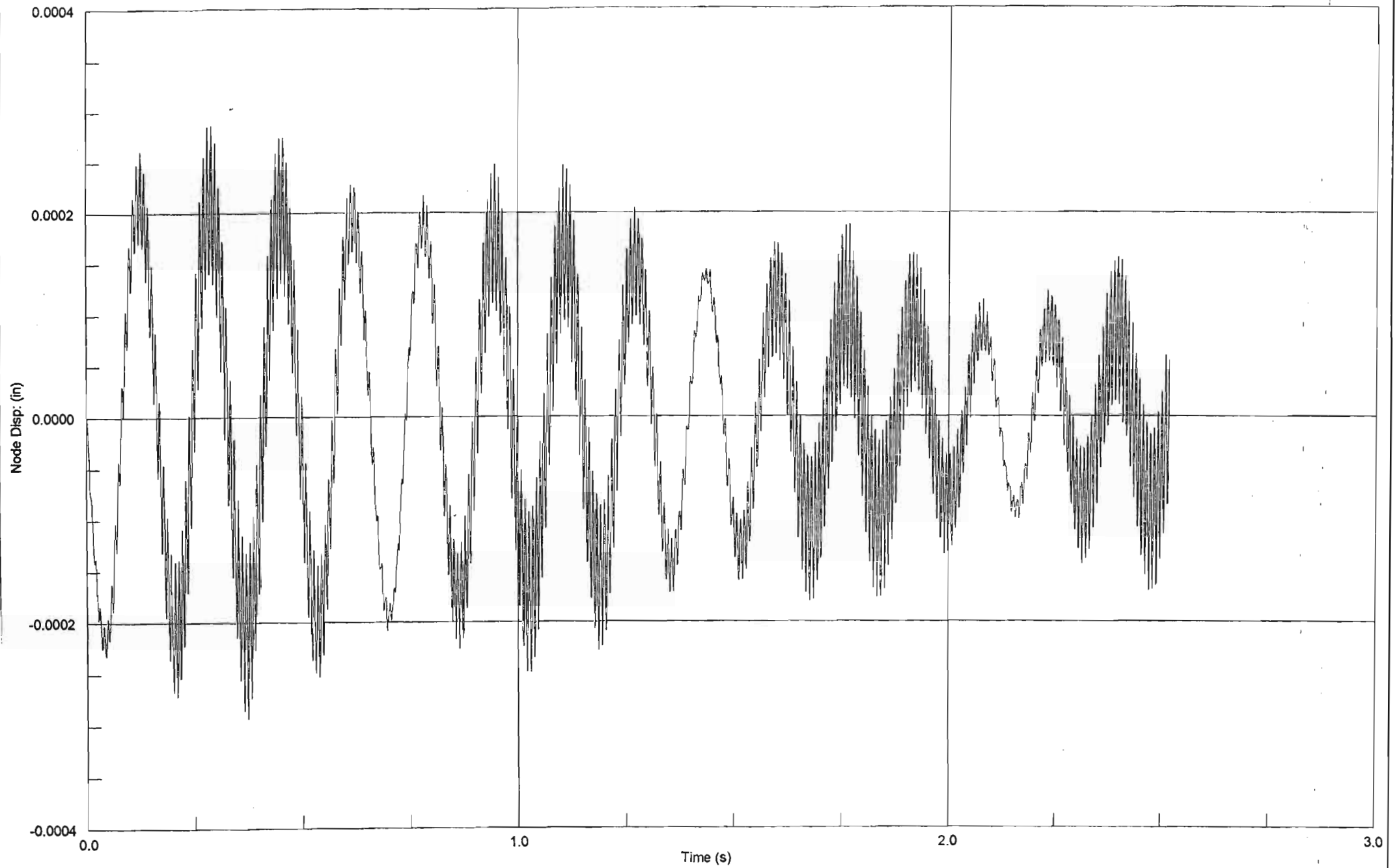
81.27.

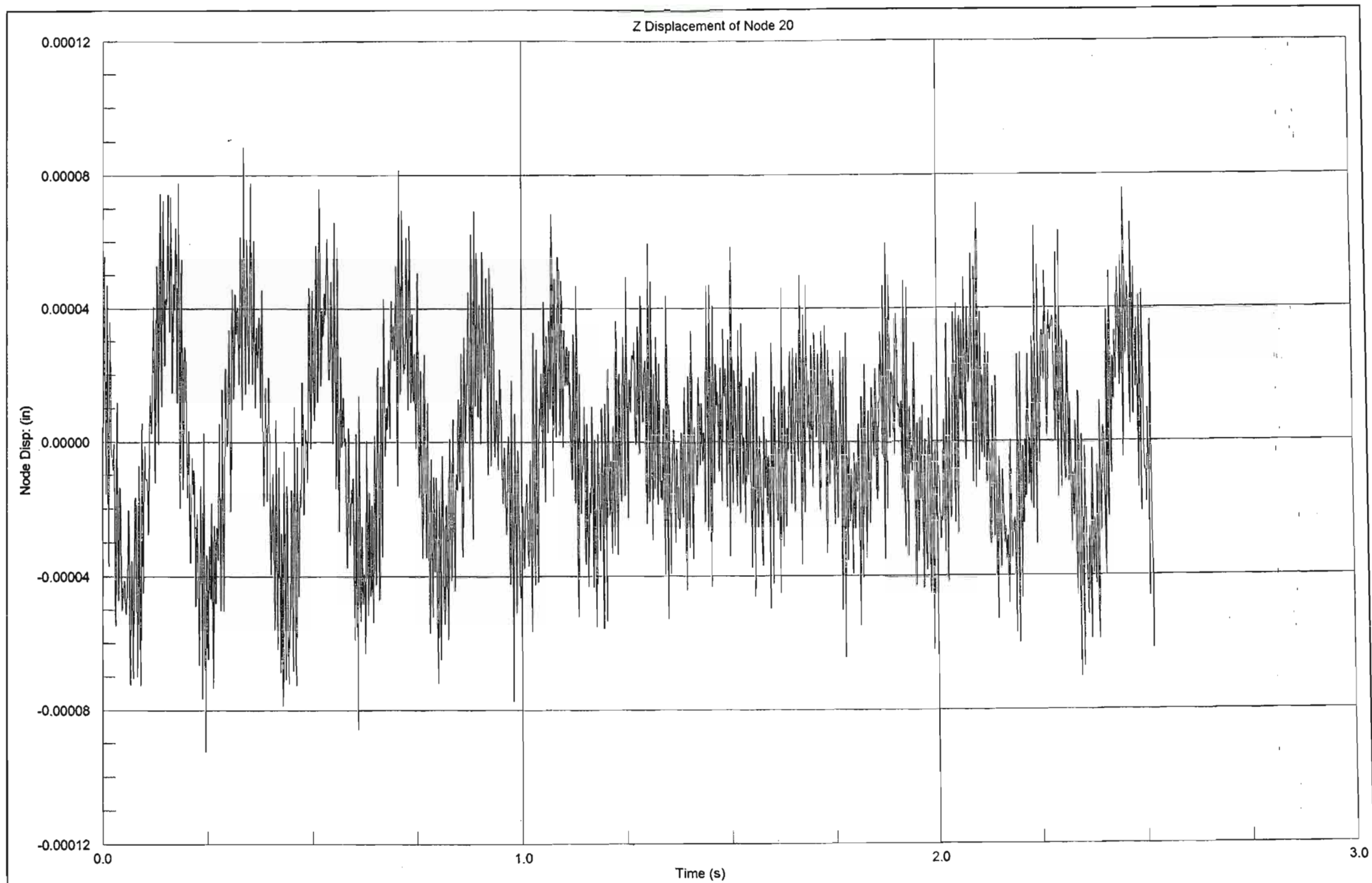


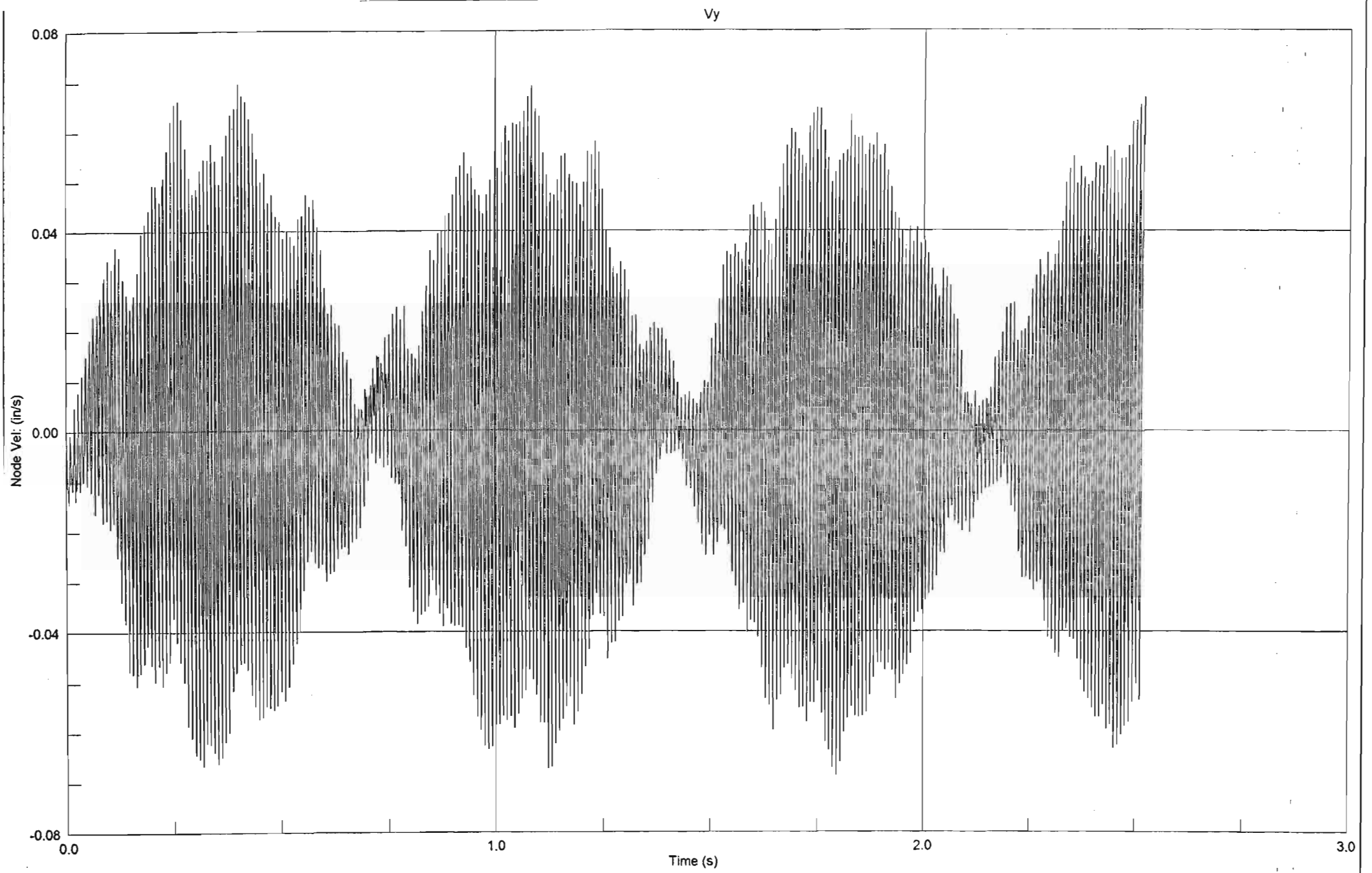


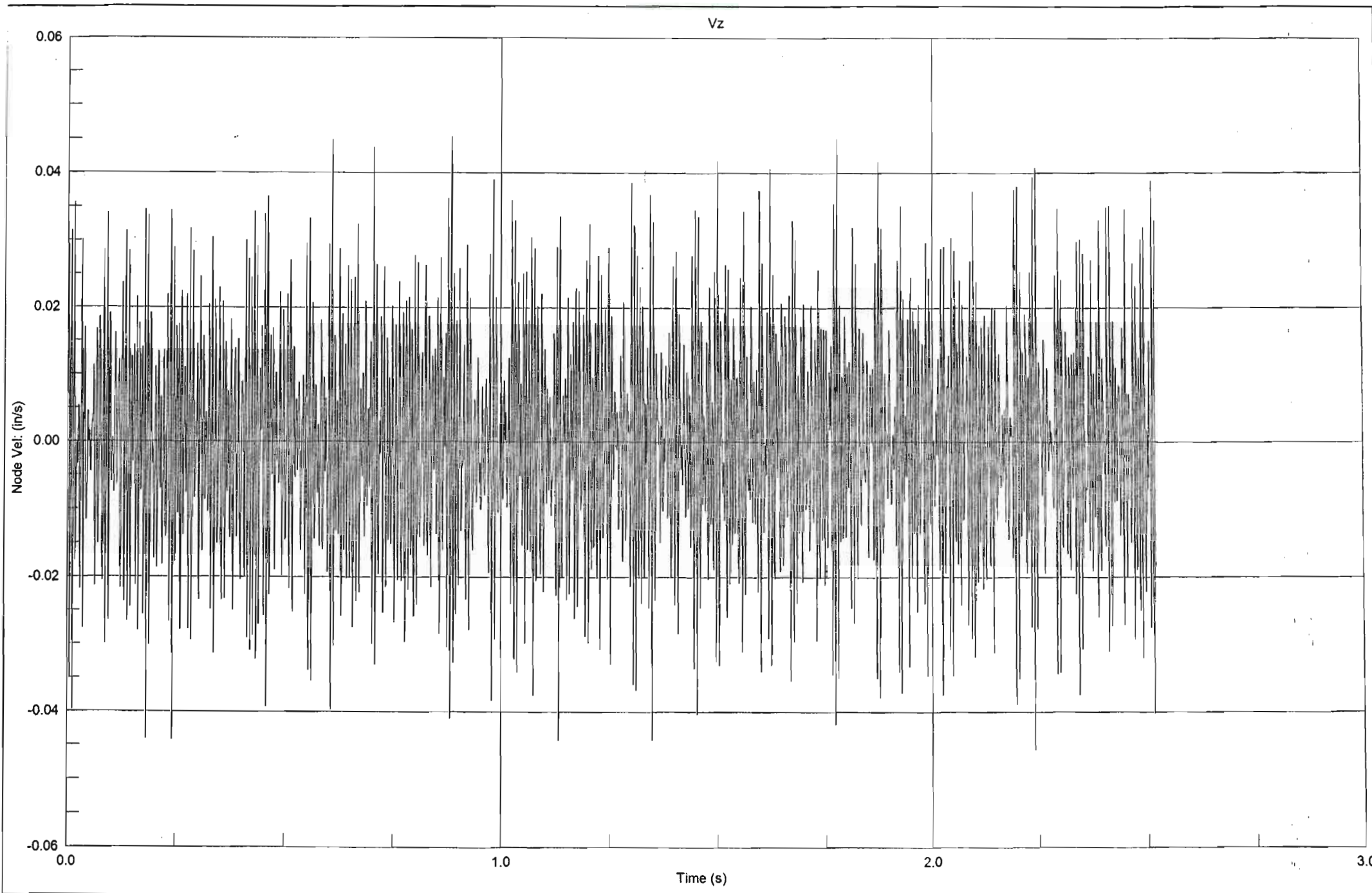


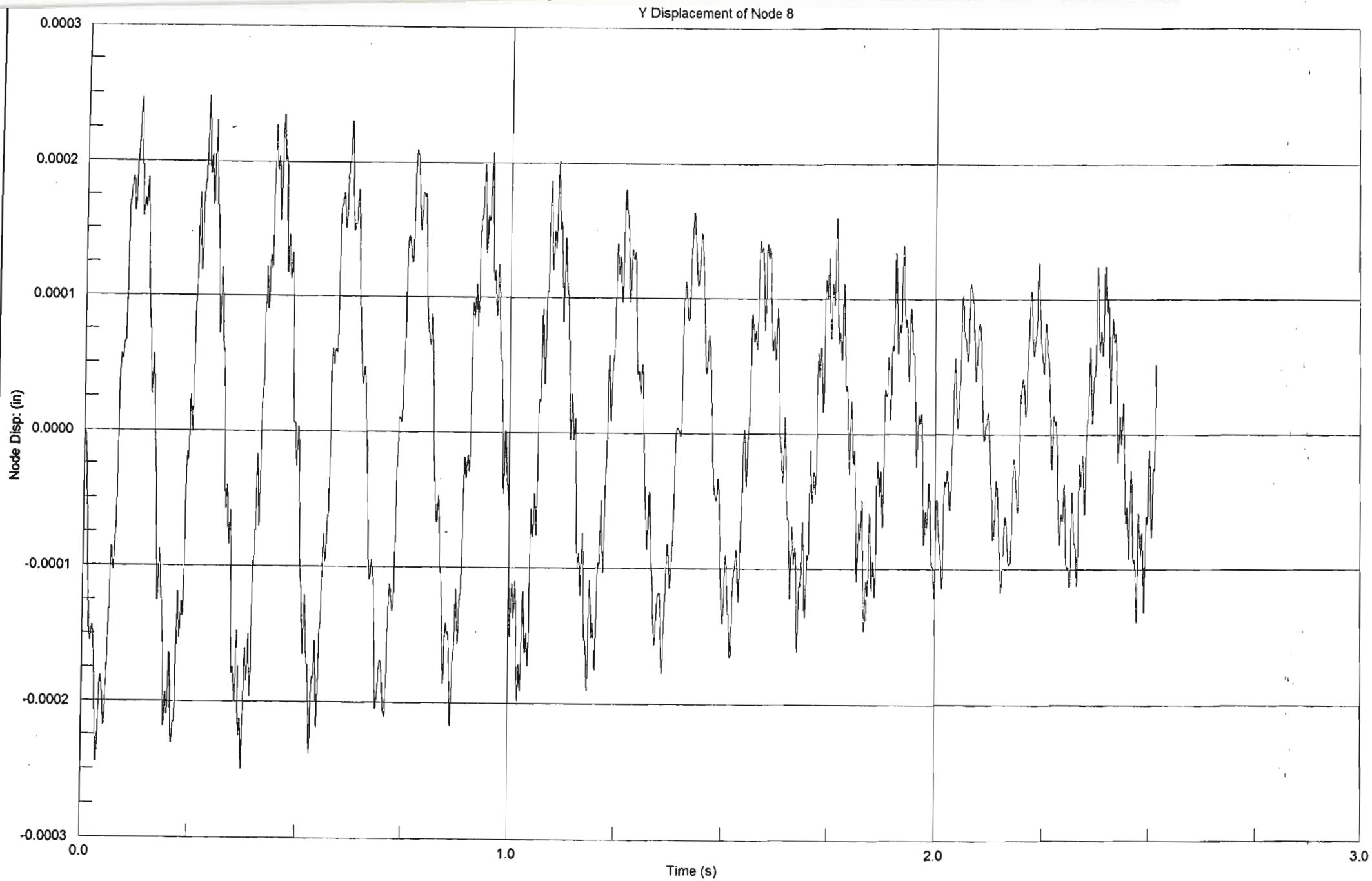
Y Displacement of Node 20

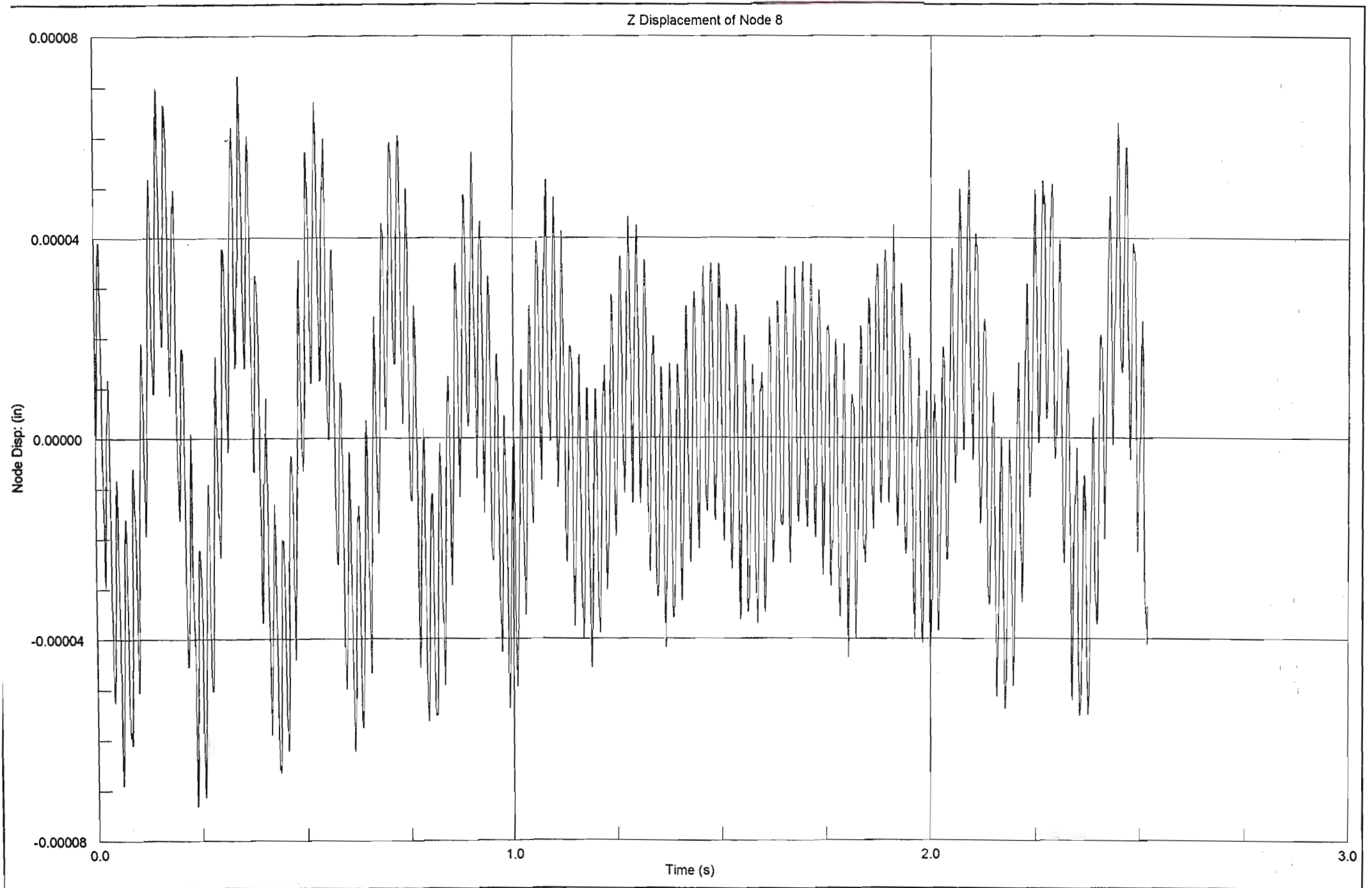


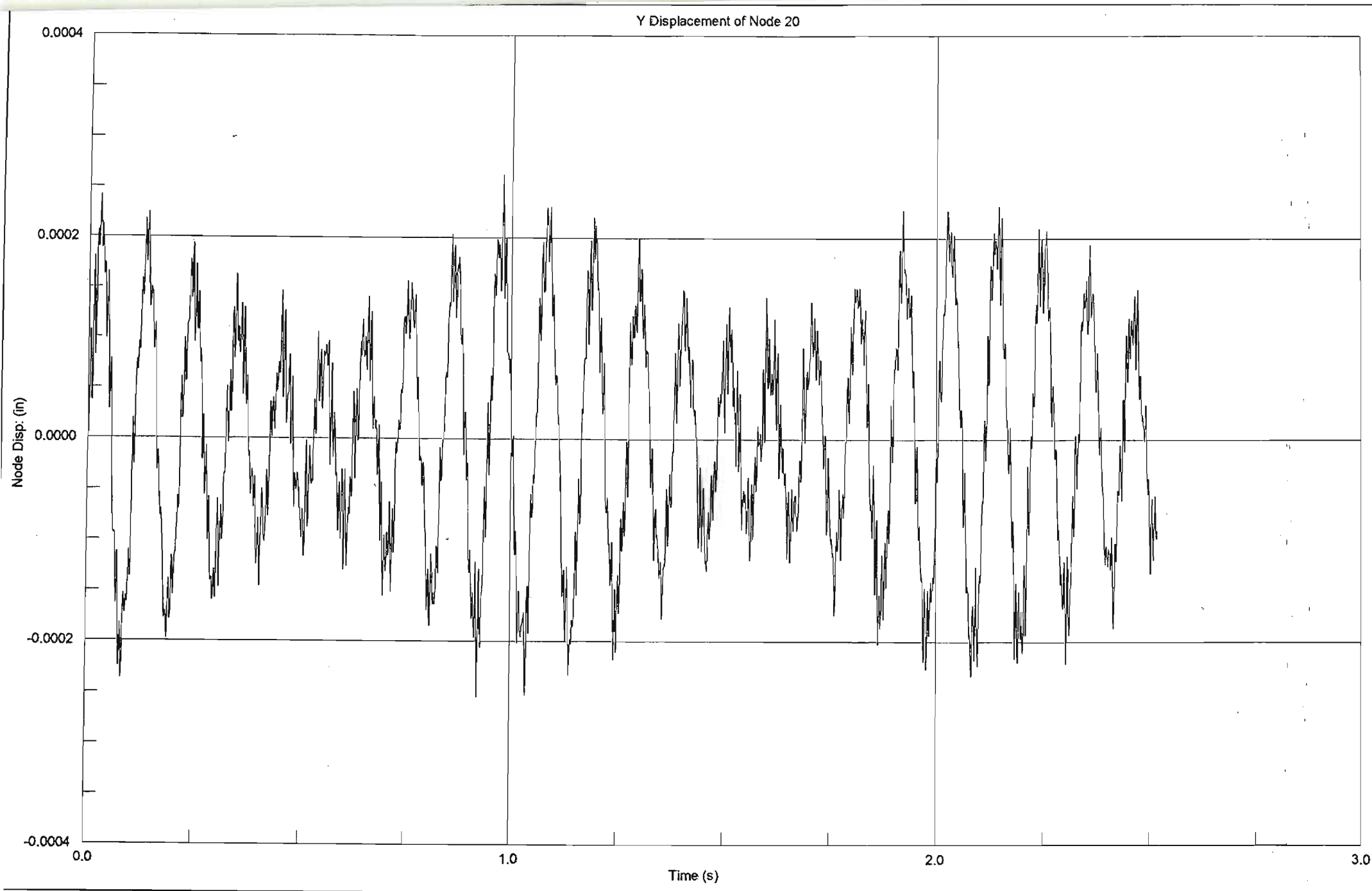


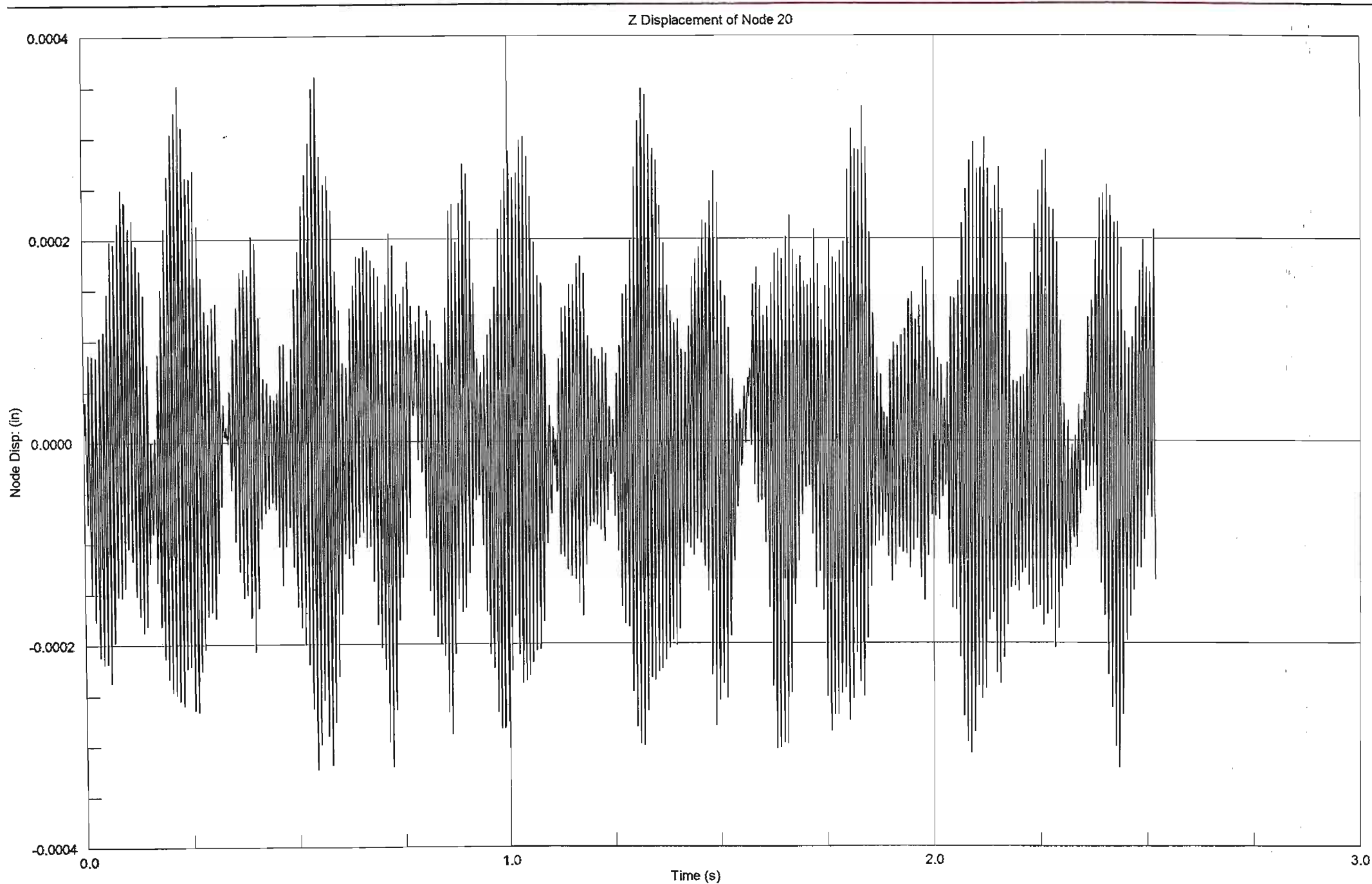




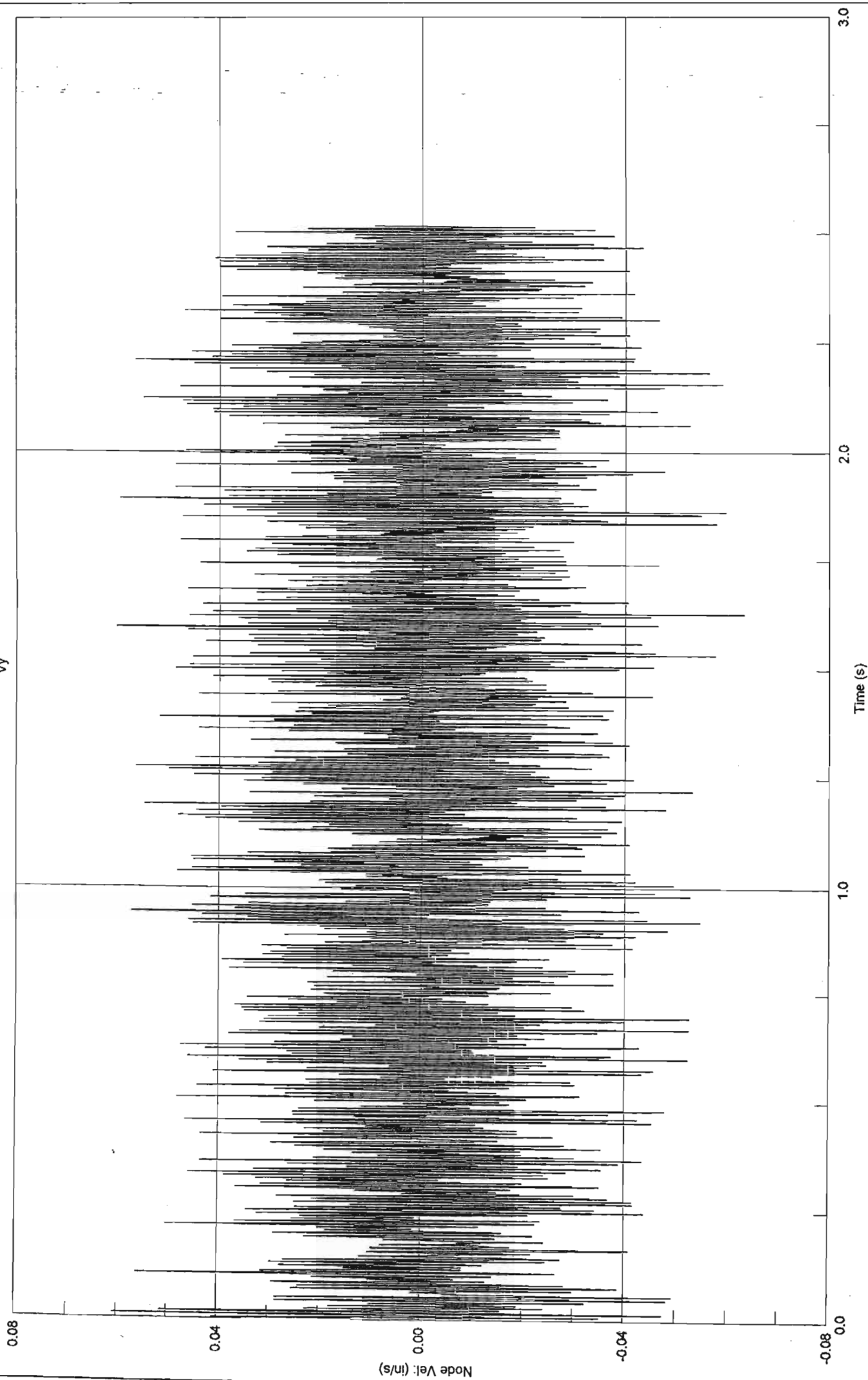




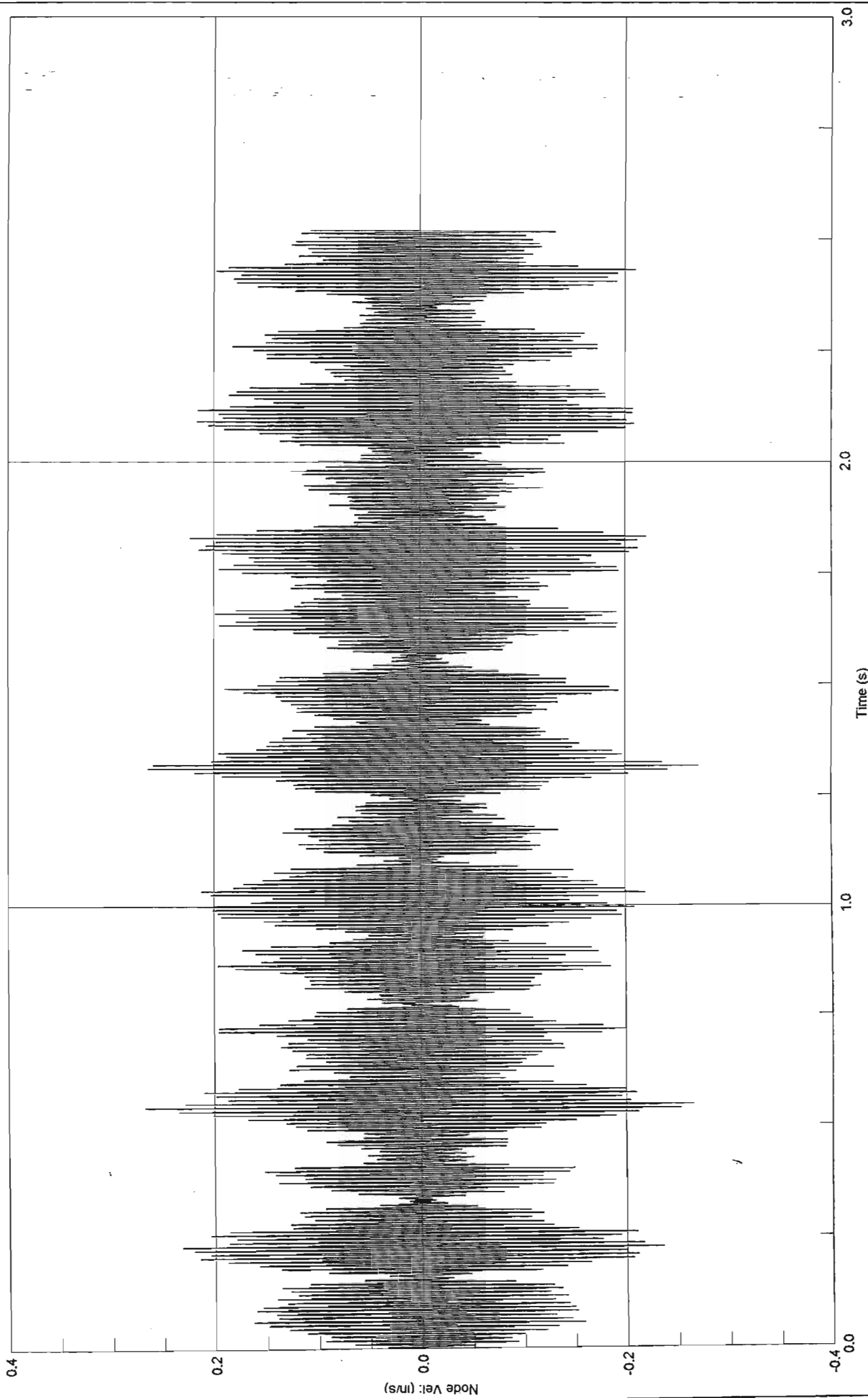


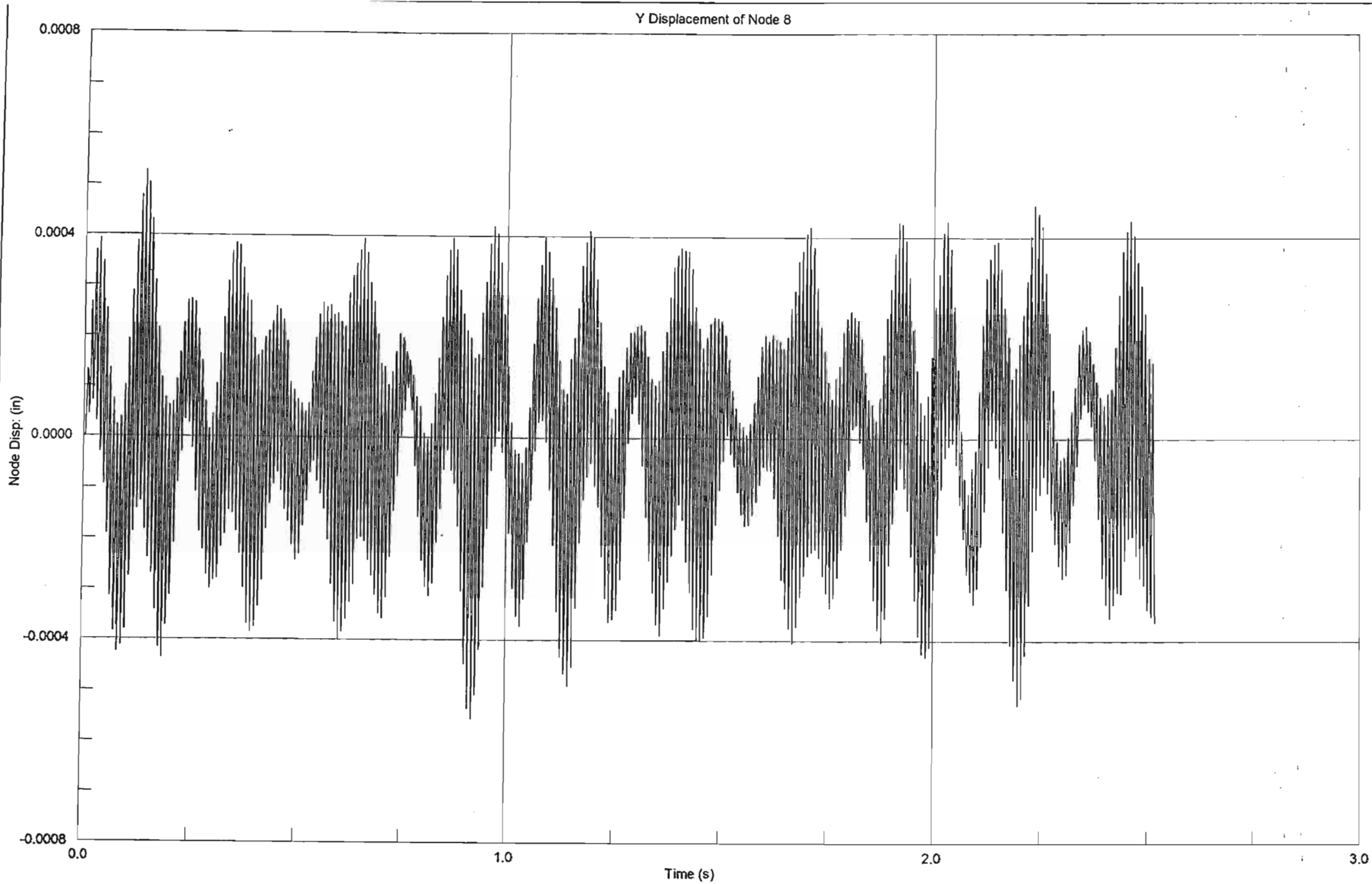


Vy

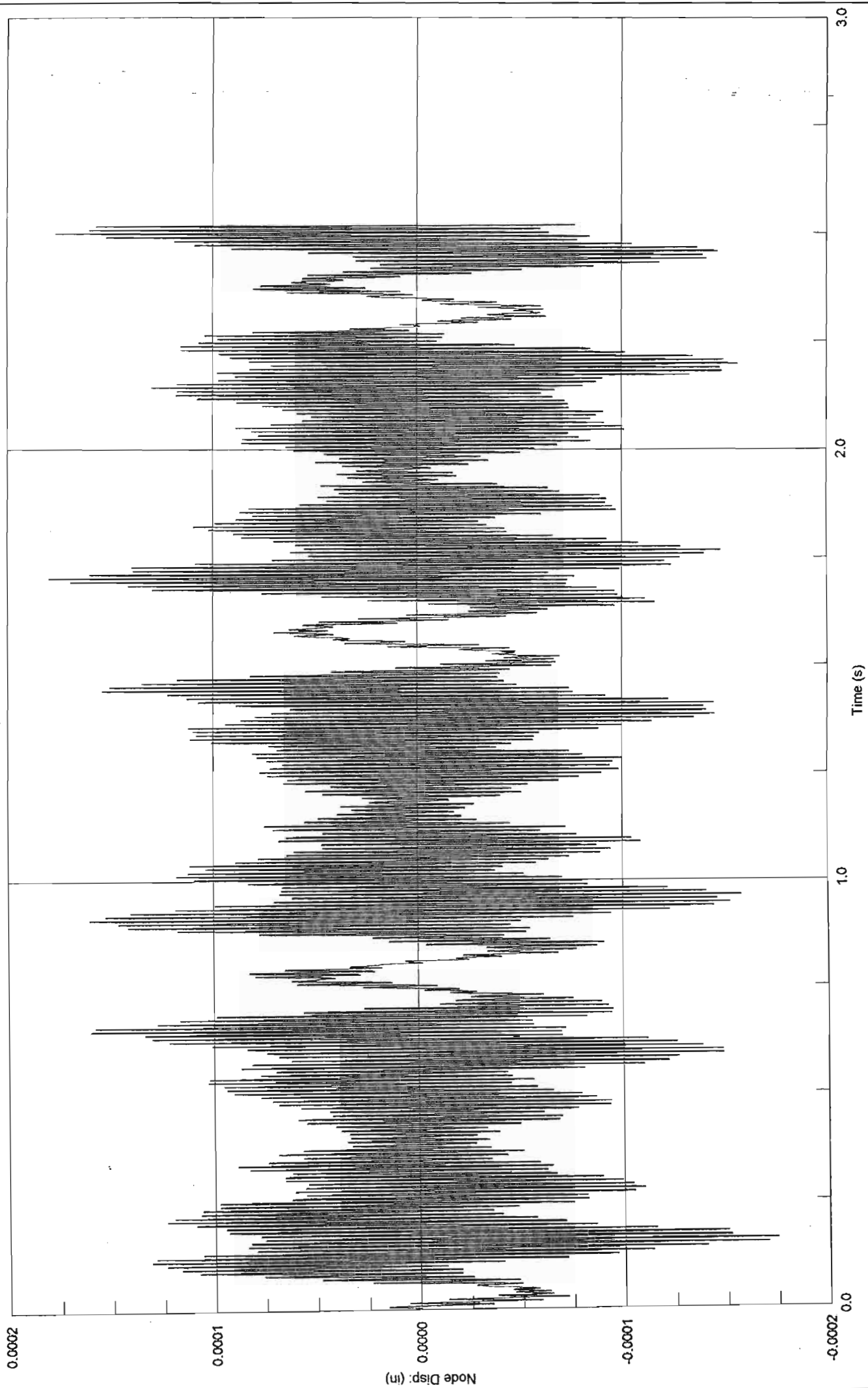


Vz

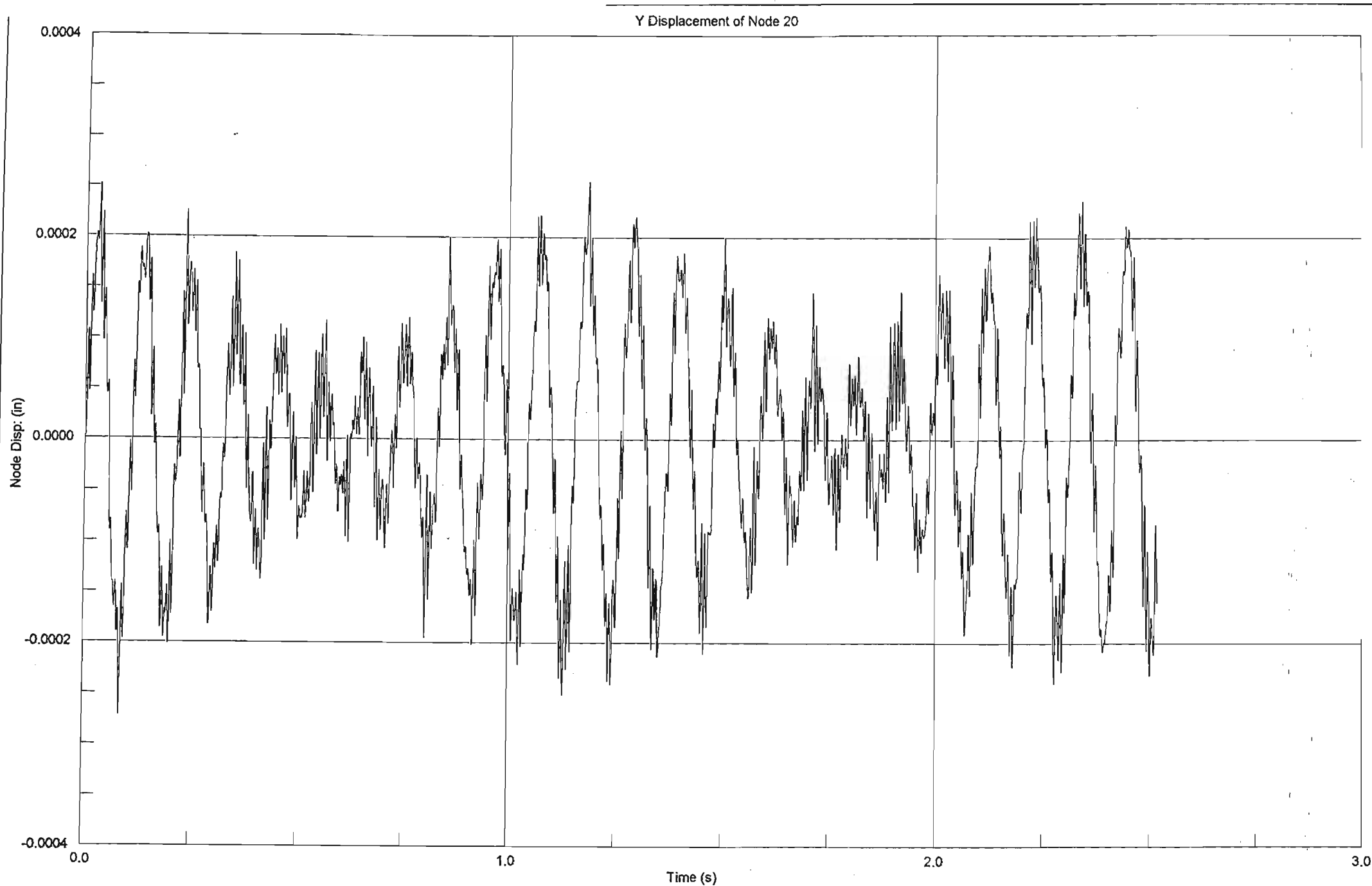


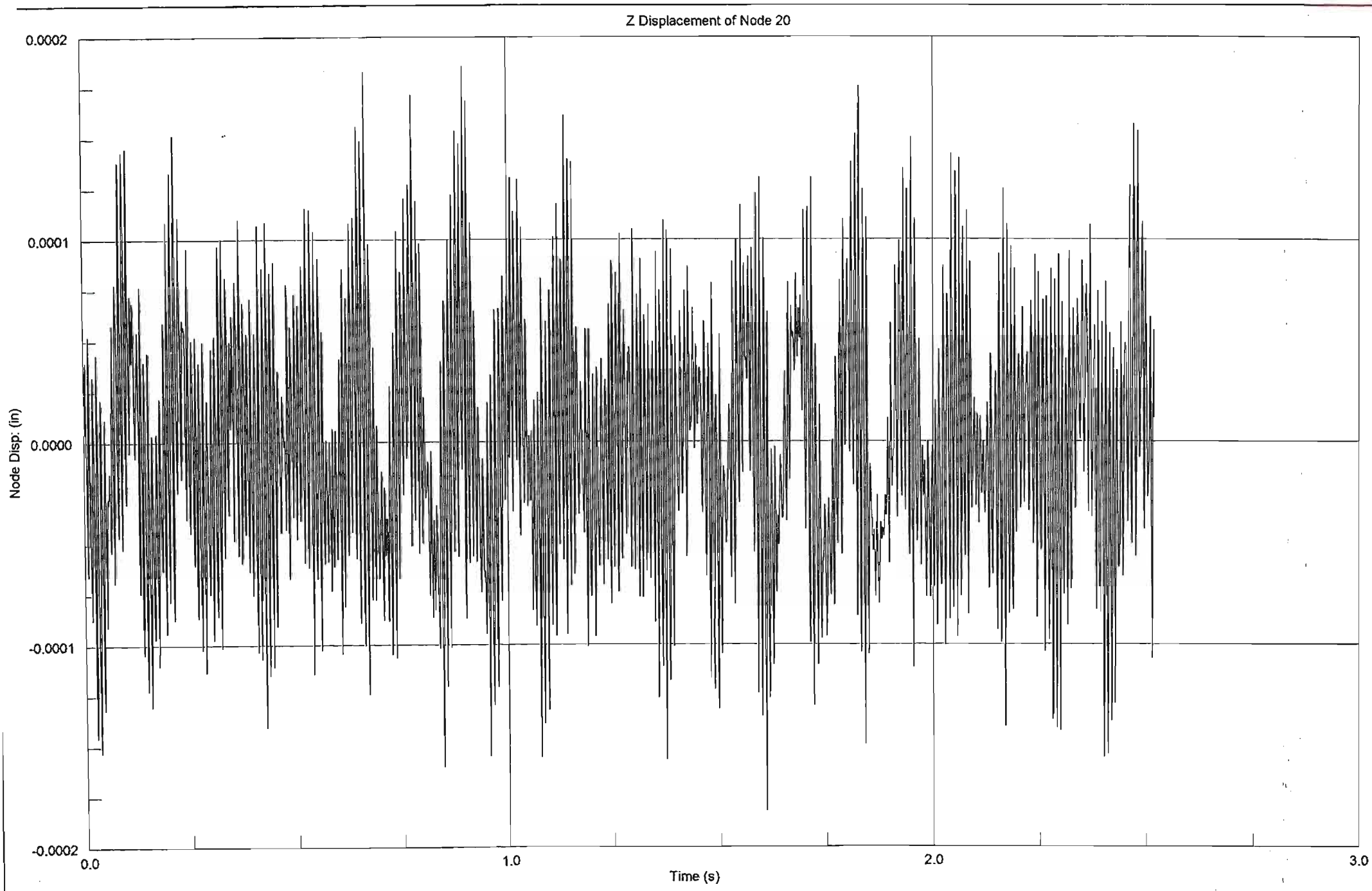


Z Displacement of Node 8

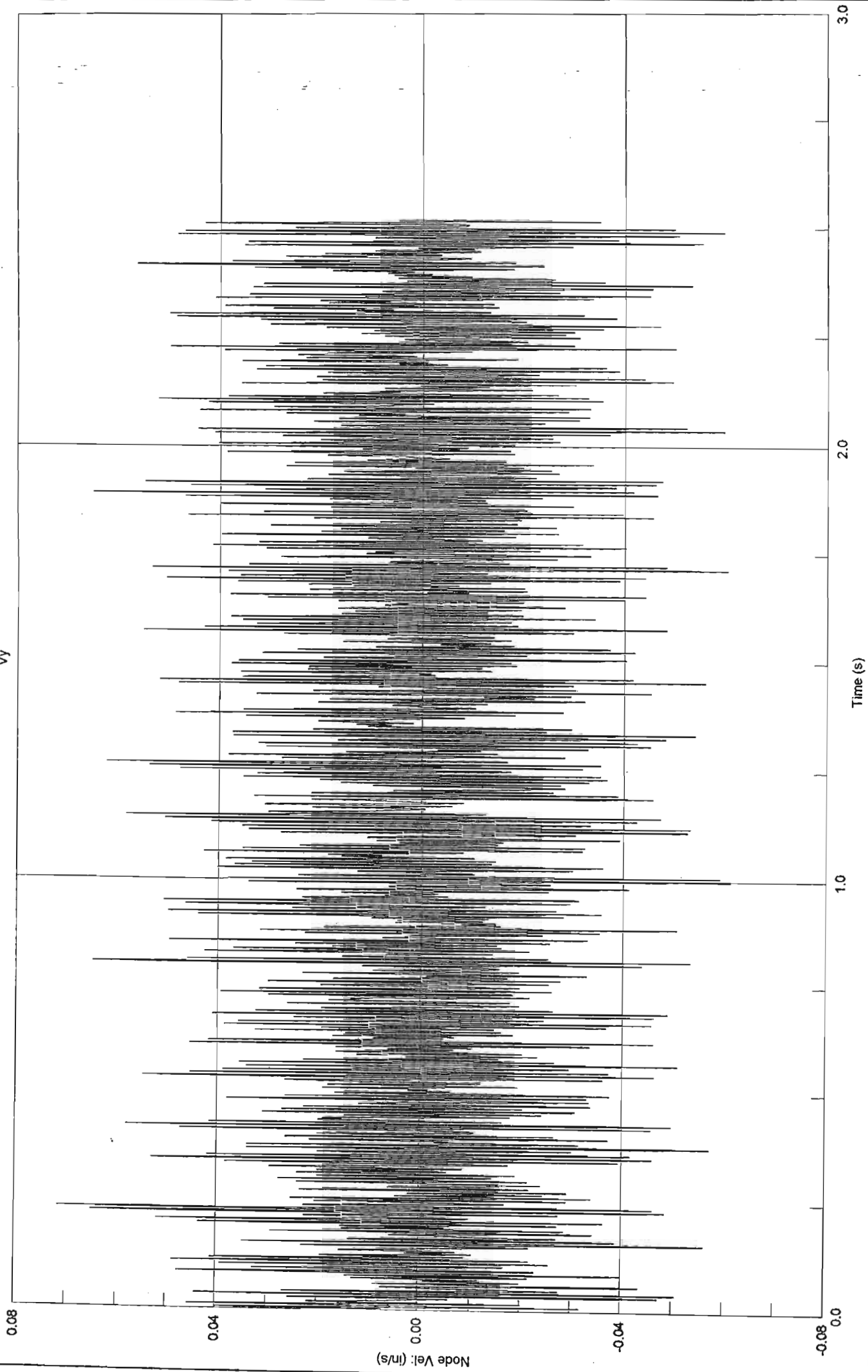


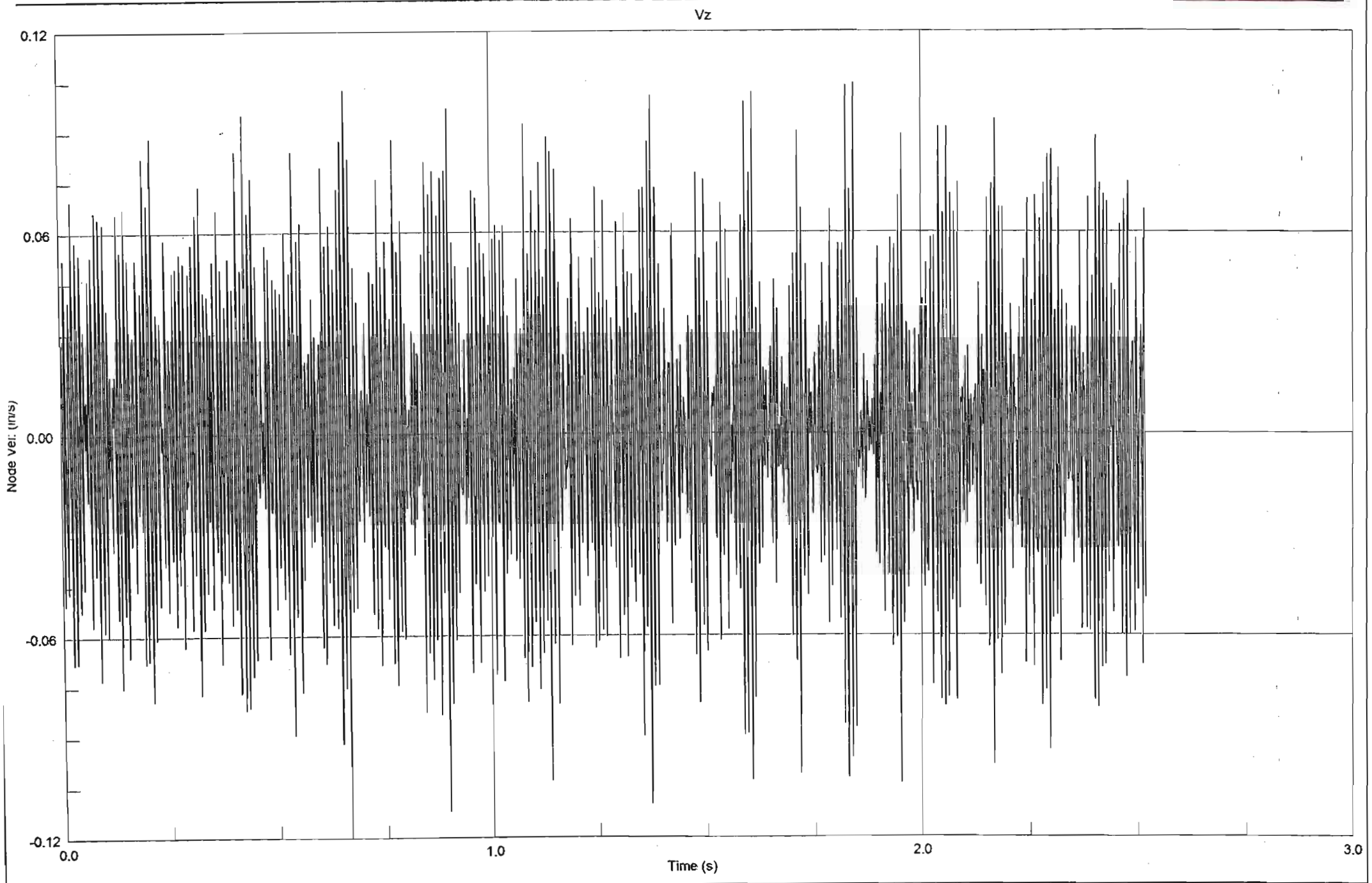
61.42.

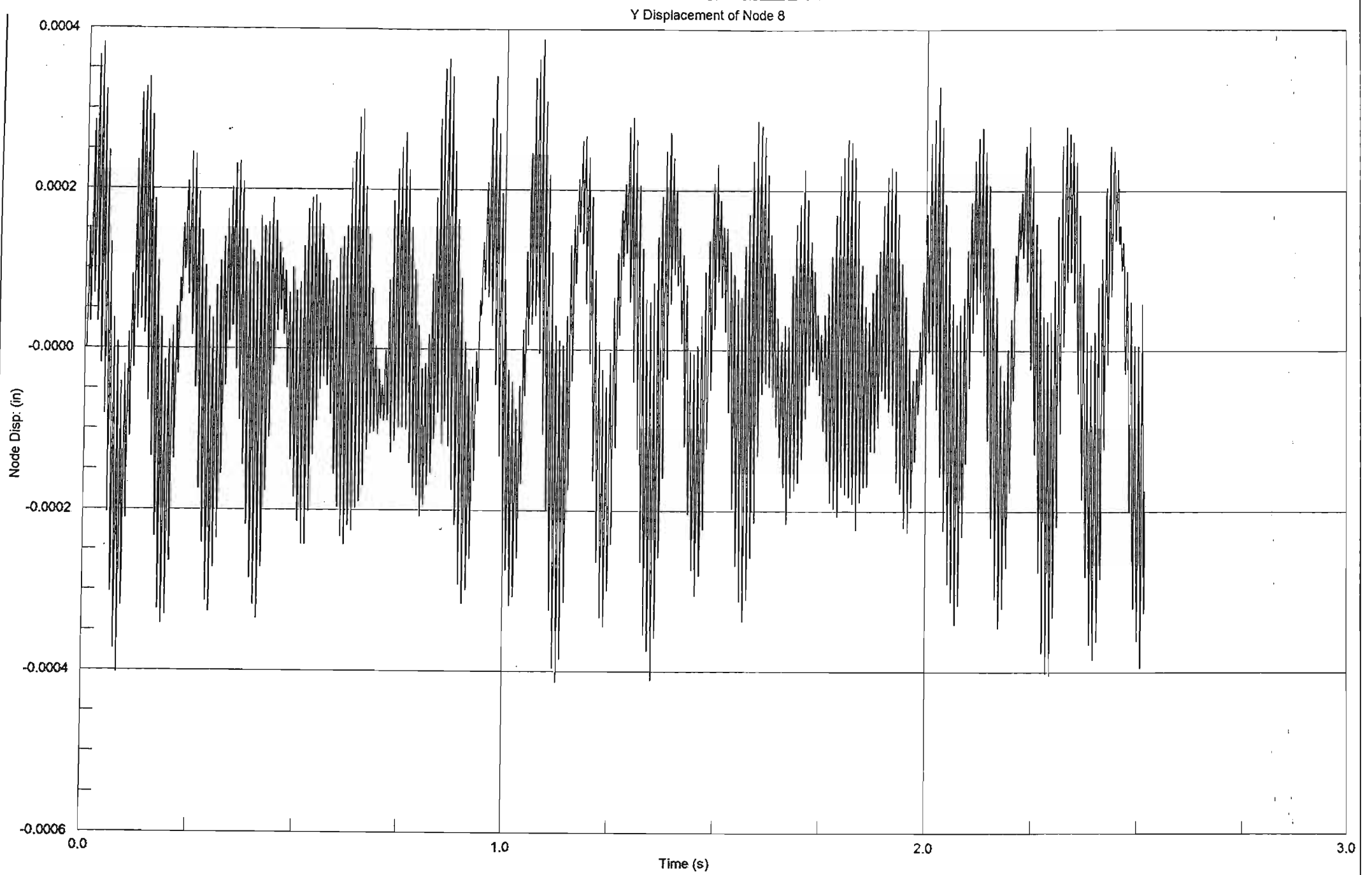




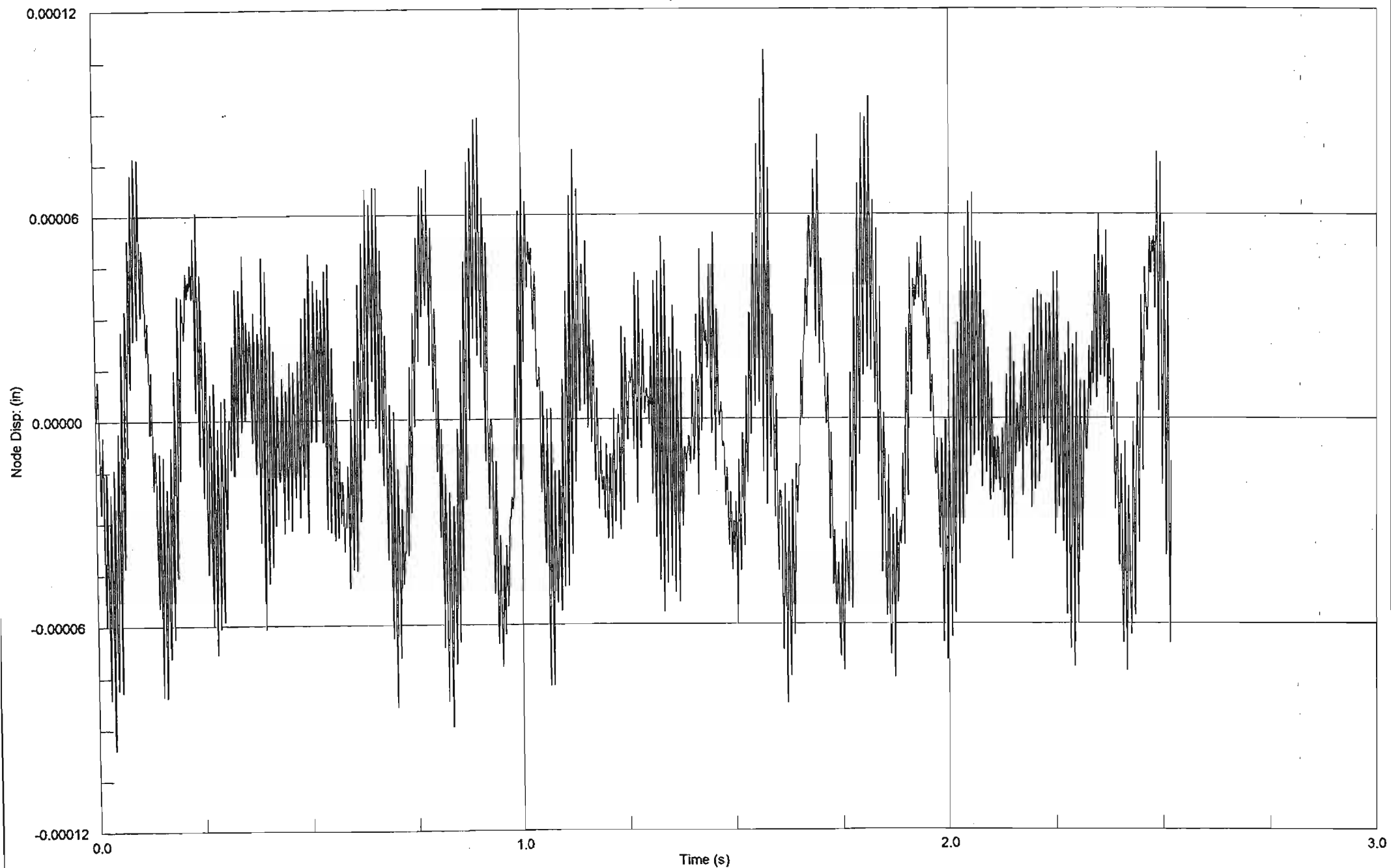
Vy

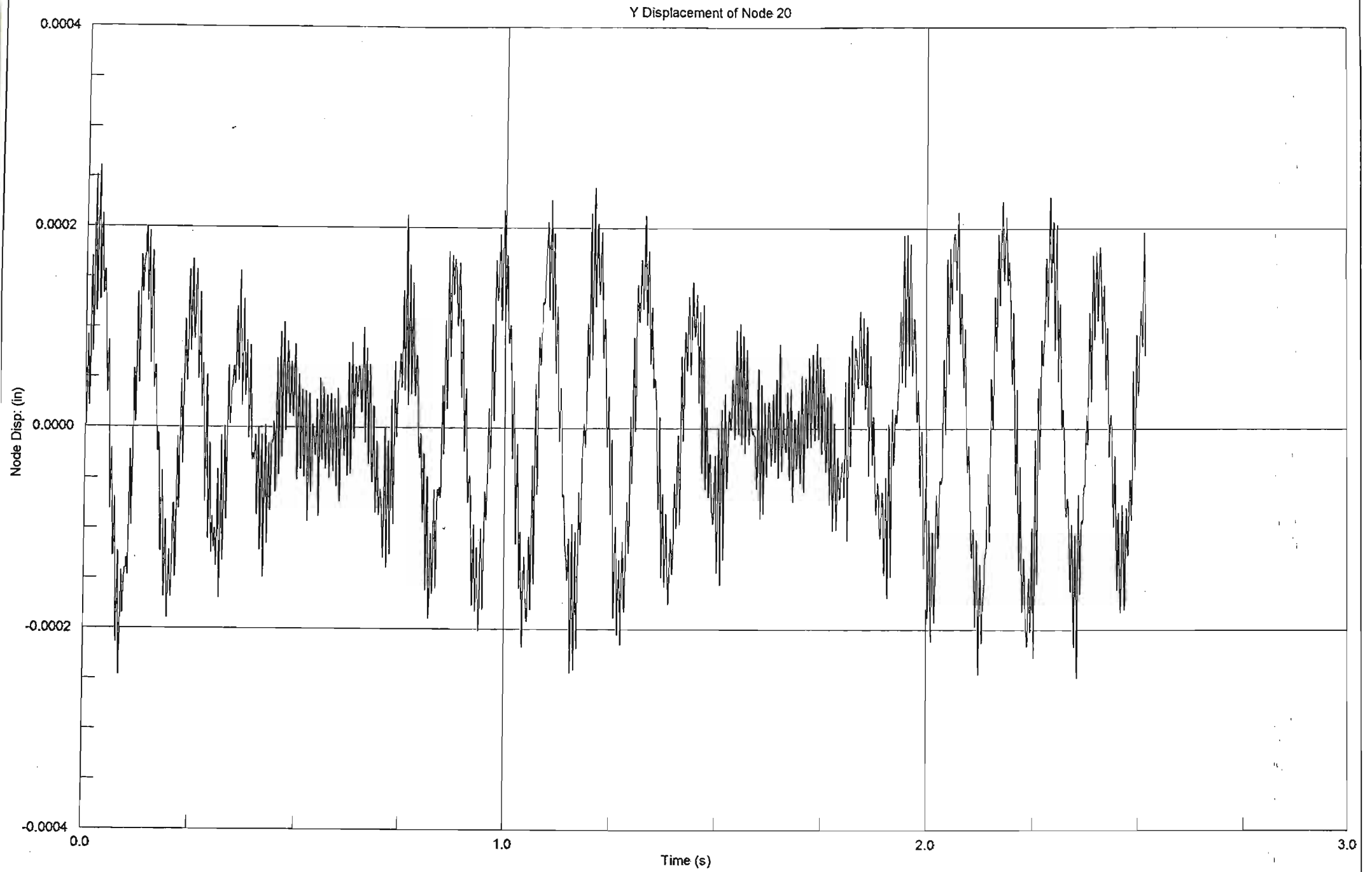




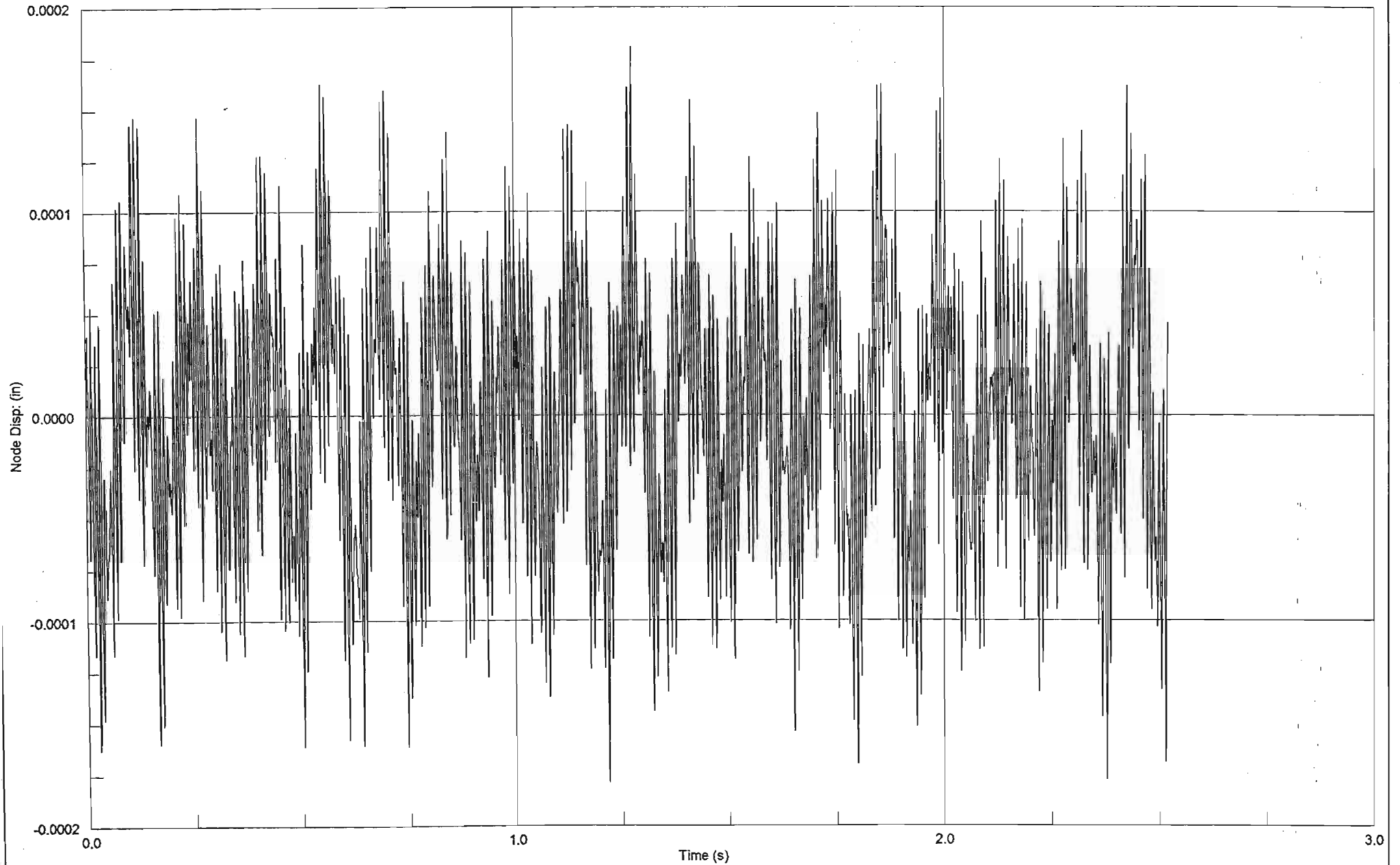


Z Displacement of Node 8

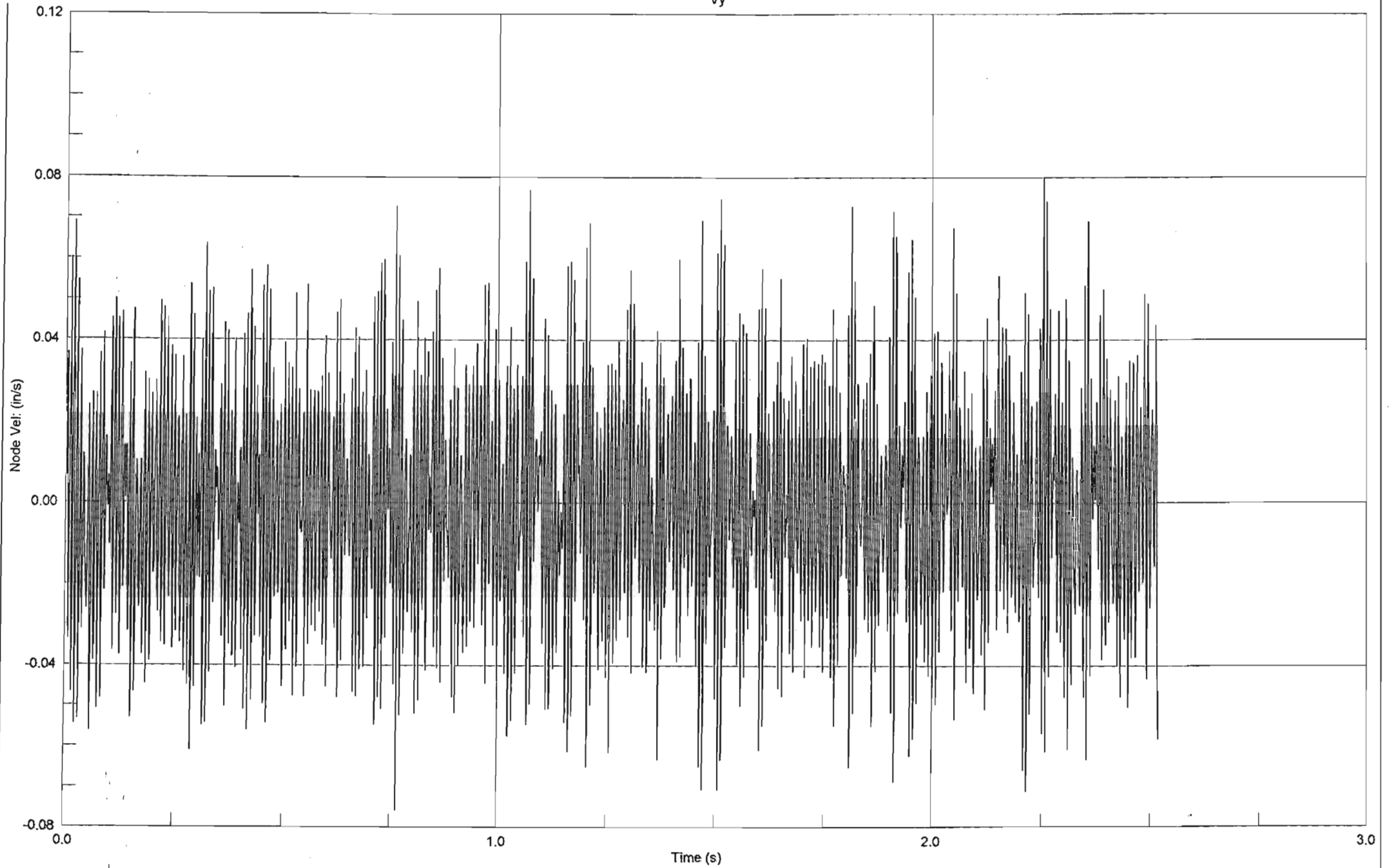




Z Displacement of Node 20



Vy

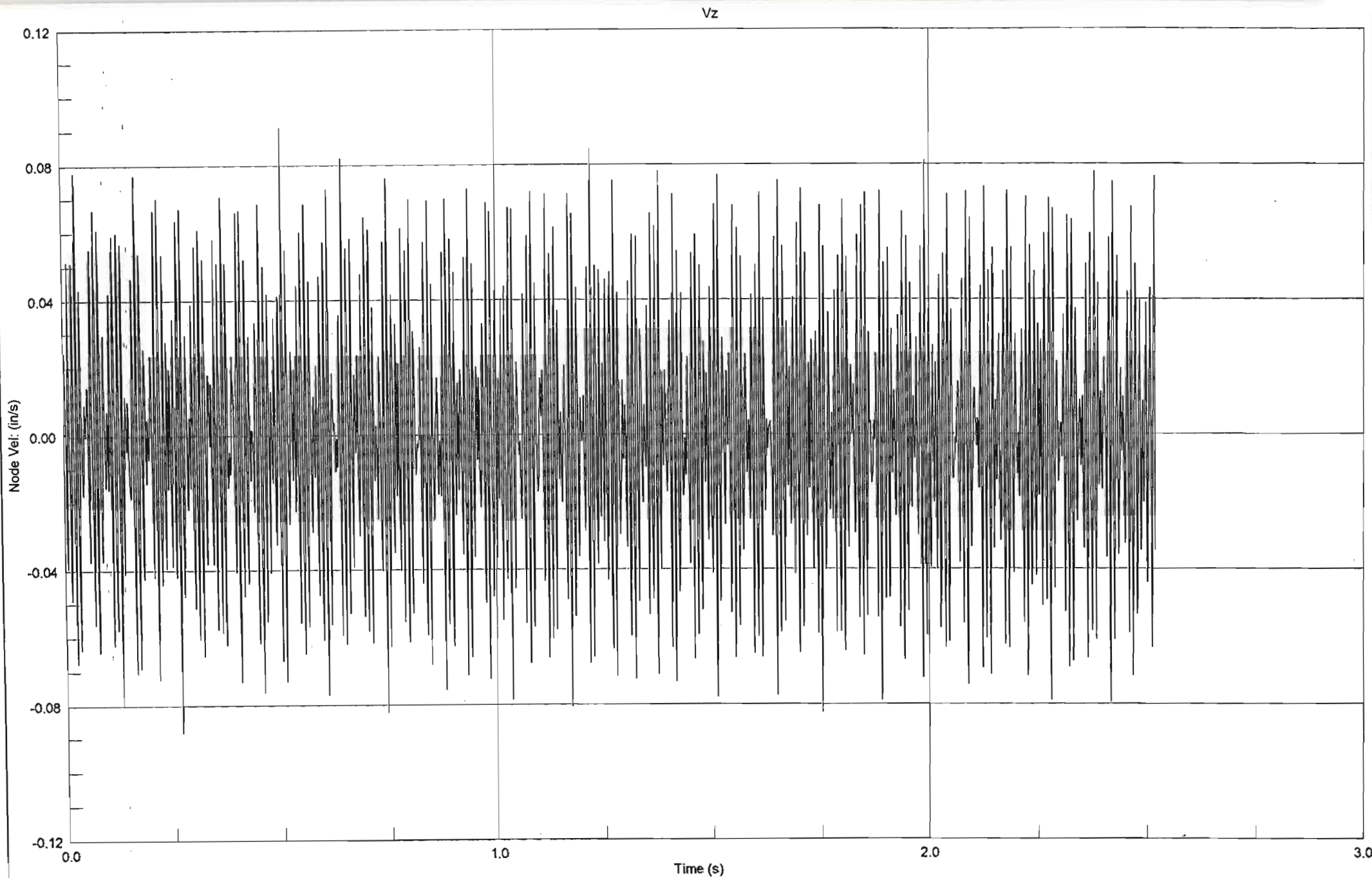


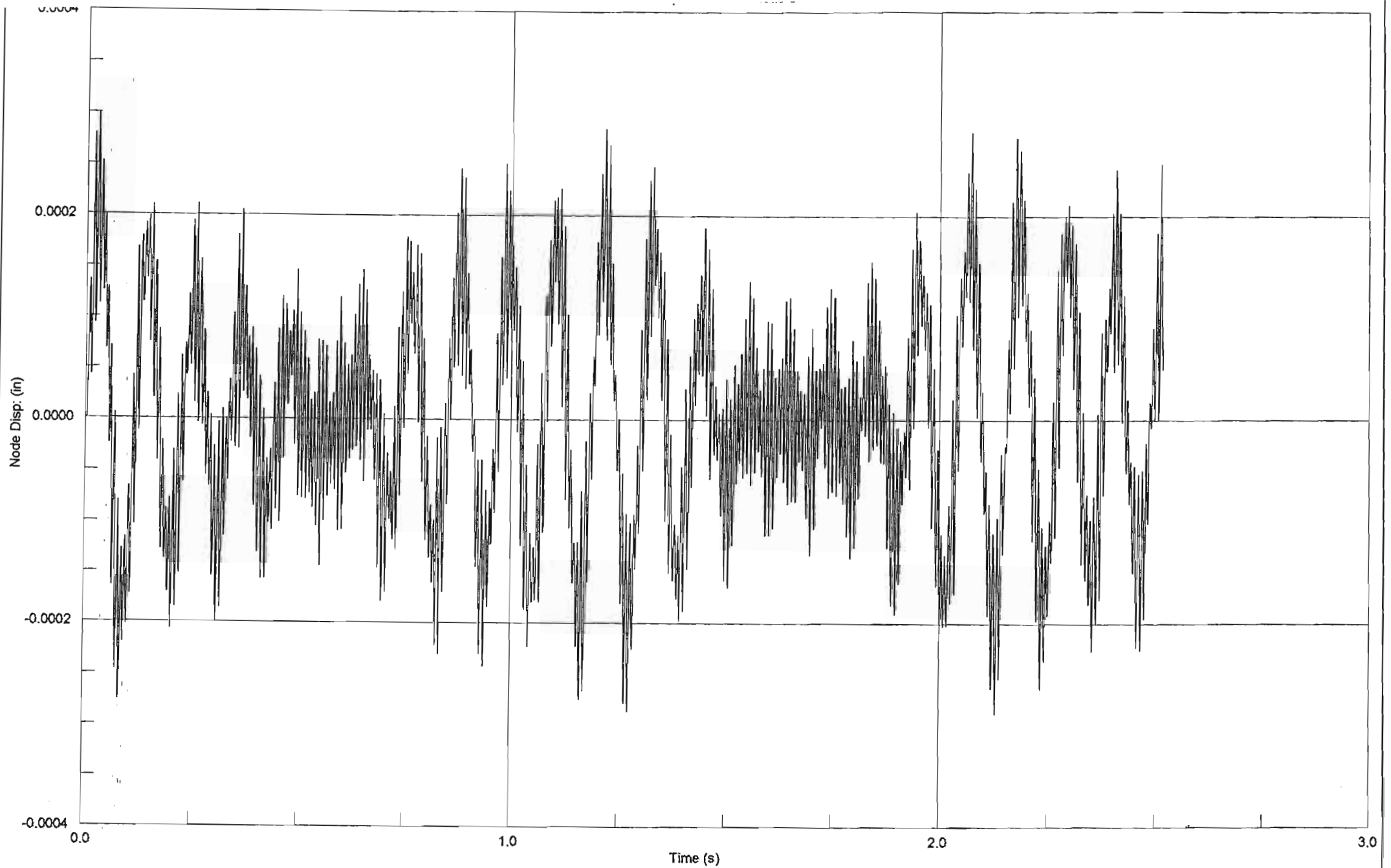
Strand7 Release 2.1.7

C:\MSc Eng\Raft\Raft 1\raft G4000p-1.st7

4 October 2002 11:03 pm

B 1.51





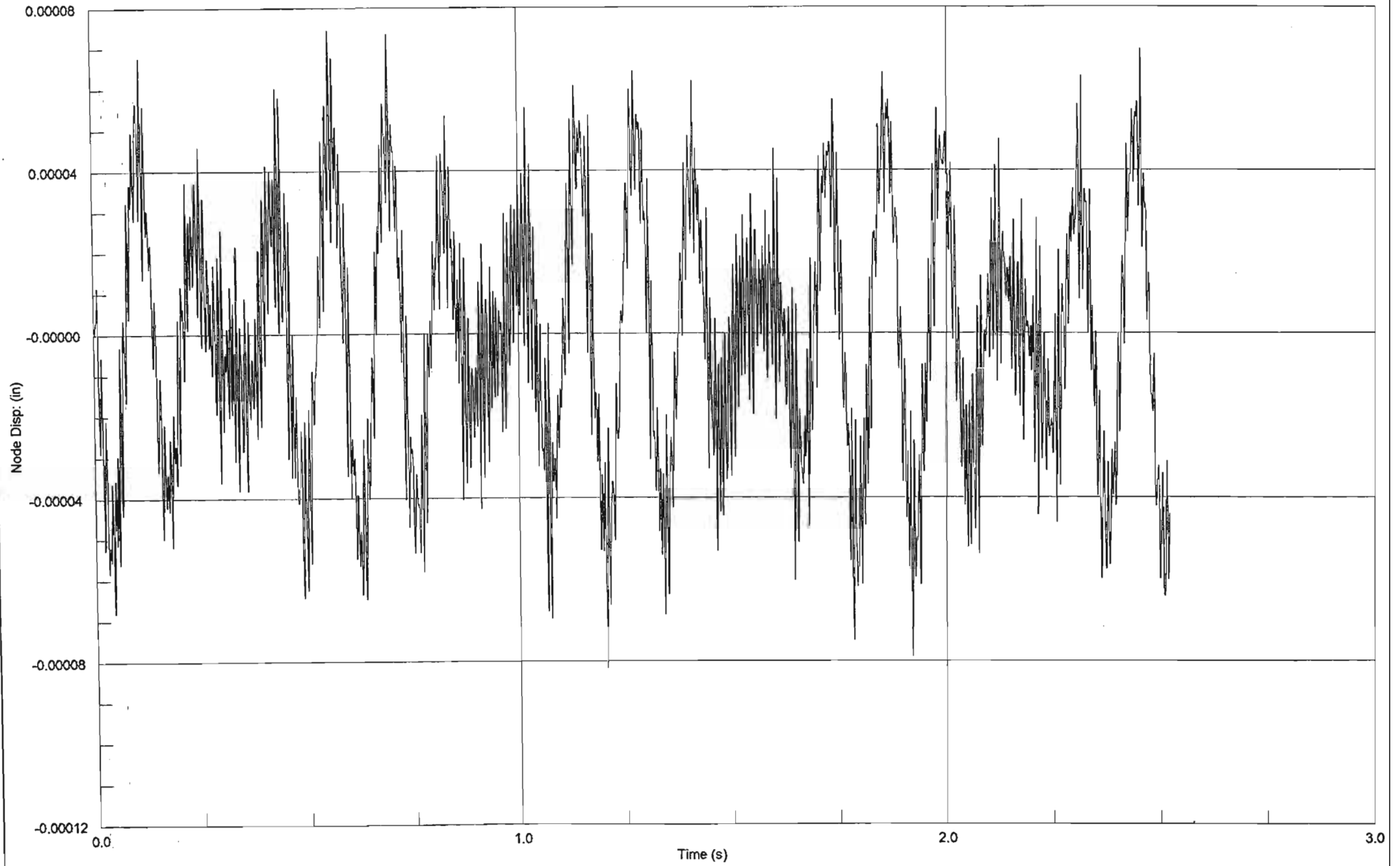
Strand7 Release 2.1.7

C:\MSc Eng\Raft\Raft 1\raft G4000p-1.s17

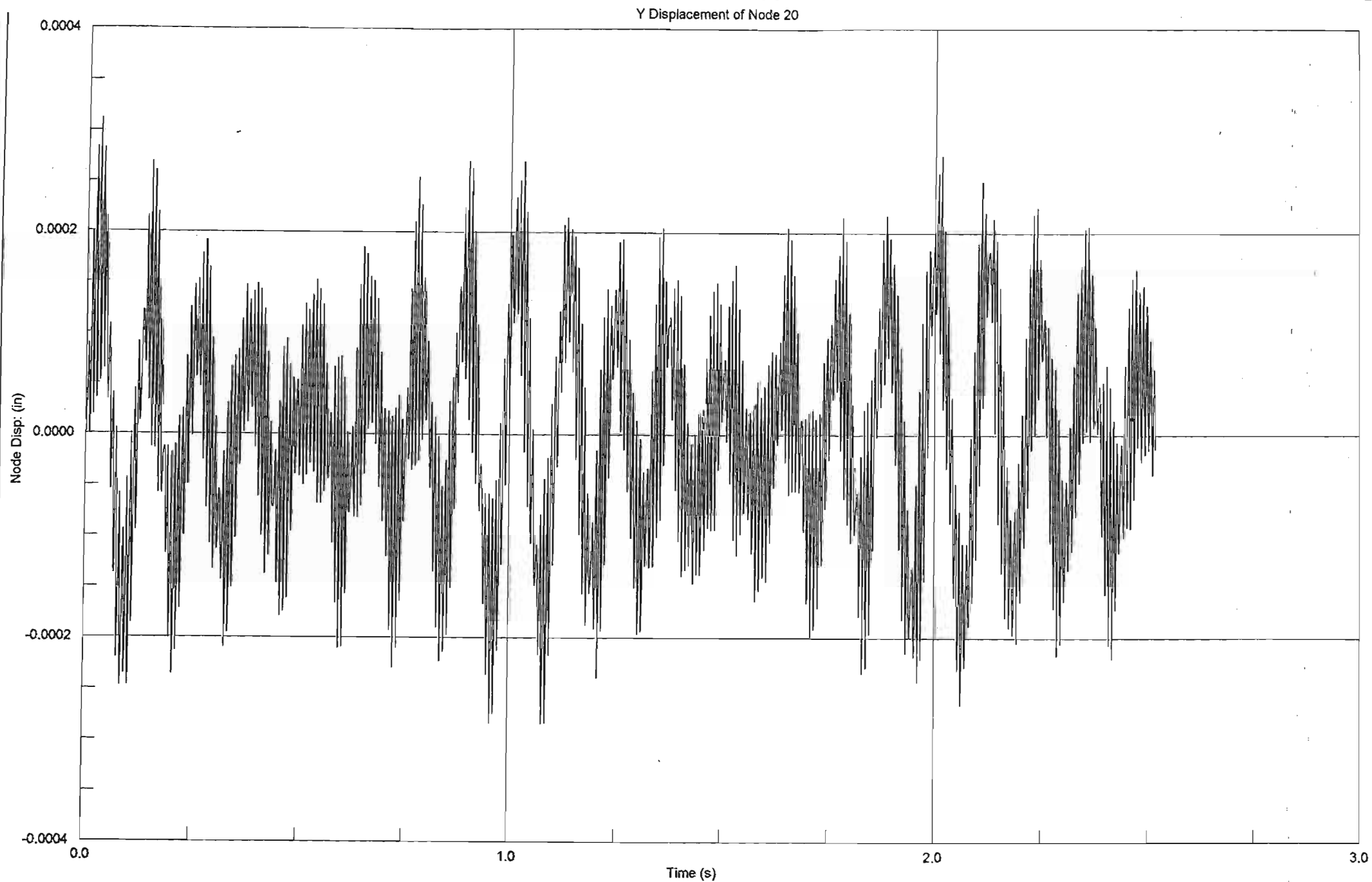
4 October 2002 11:01 pm

B1.53

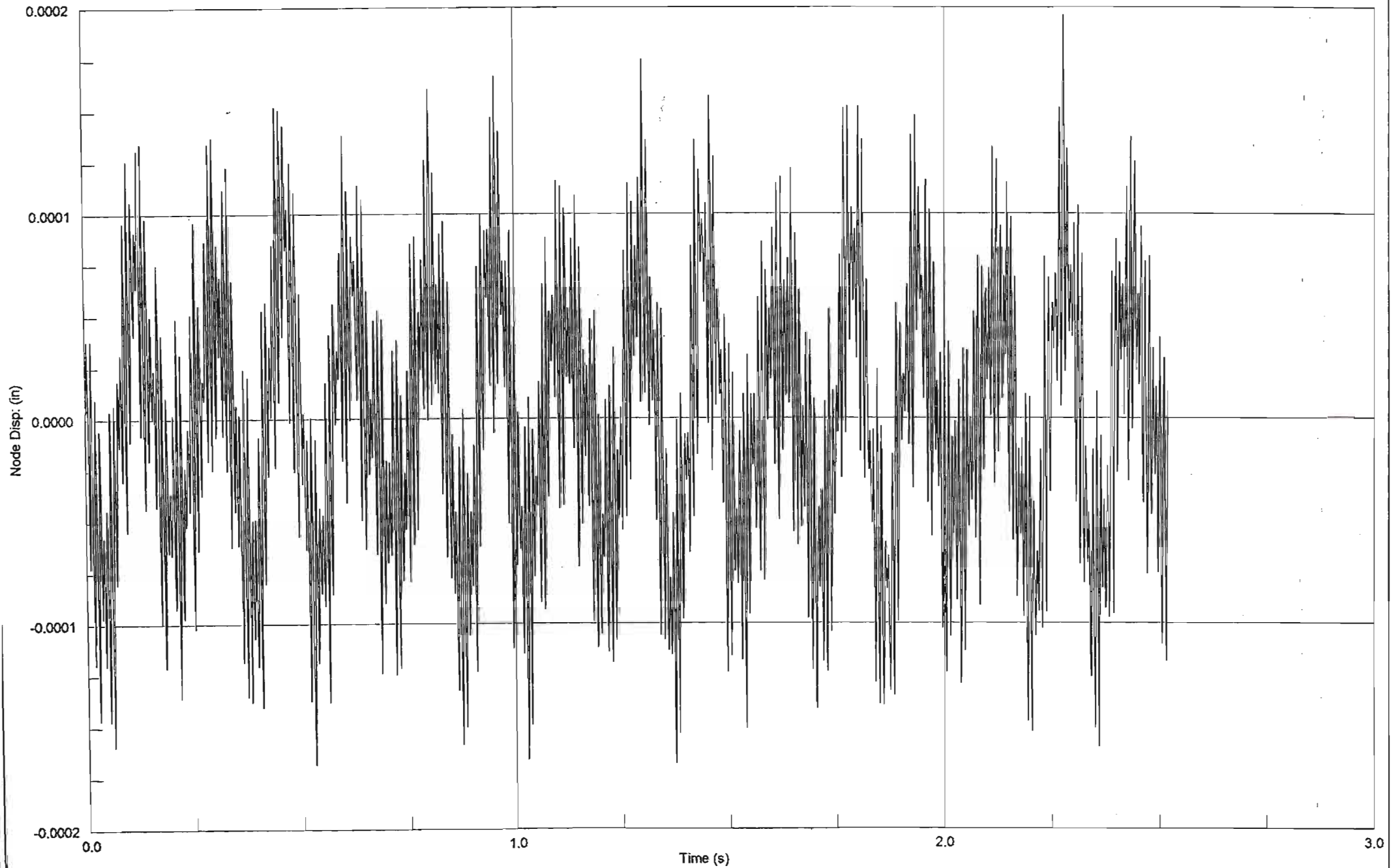
Z Displacement of Node 8



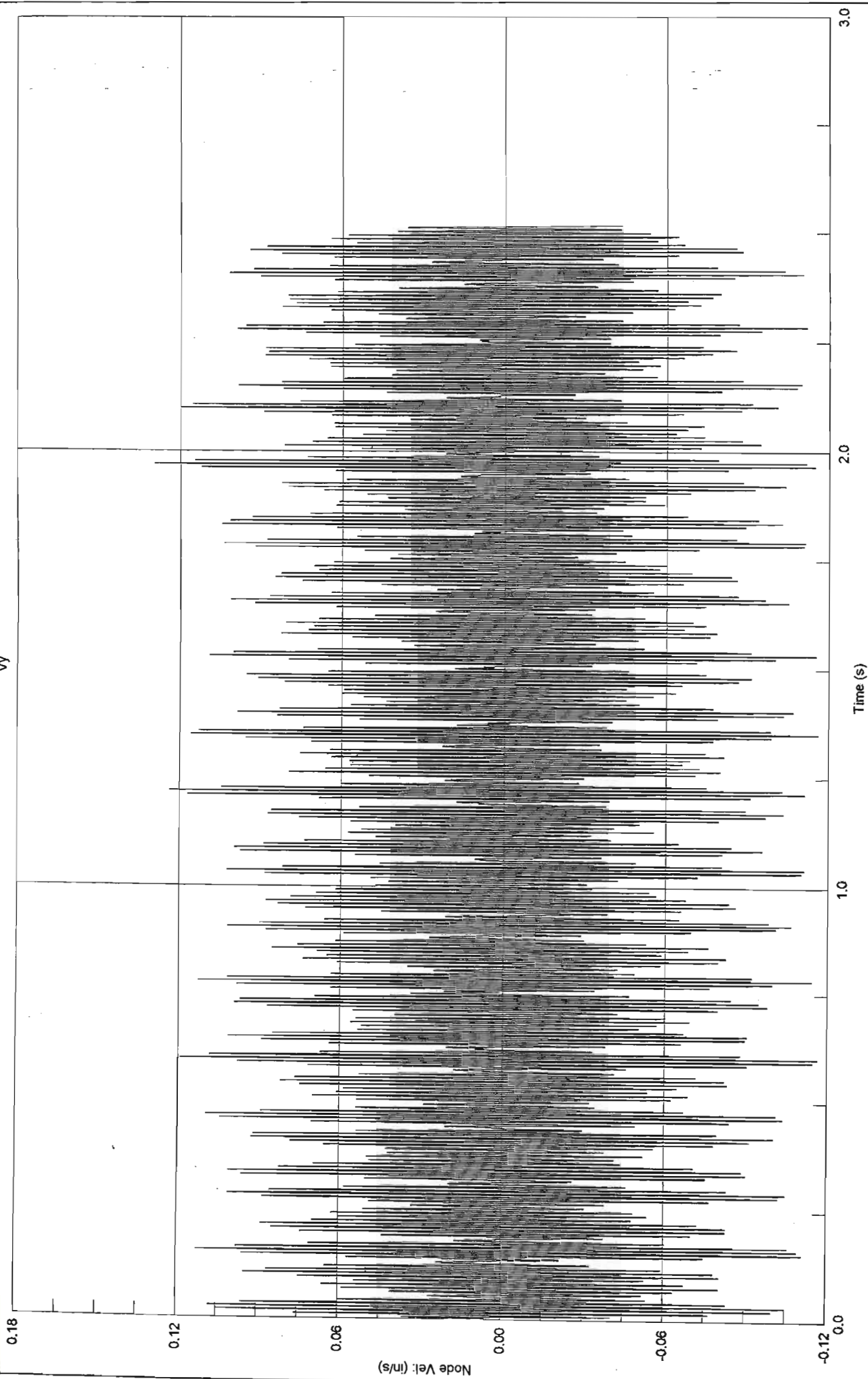
81.54

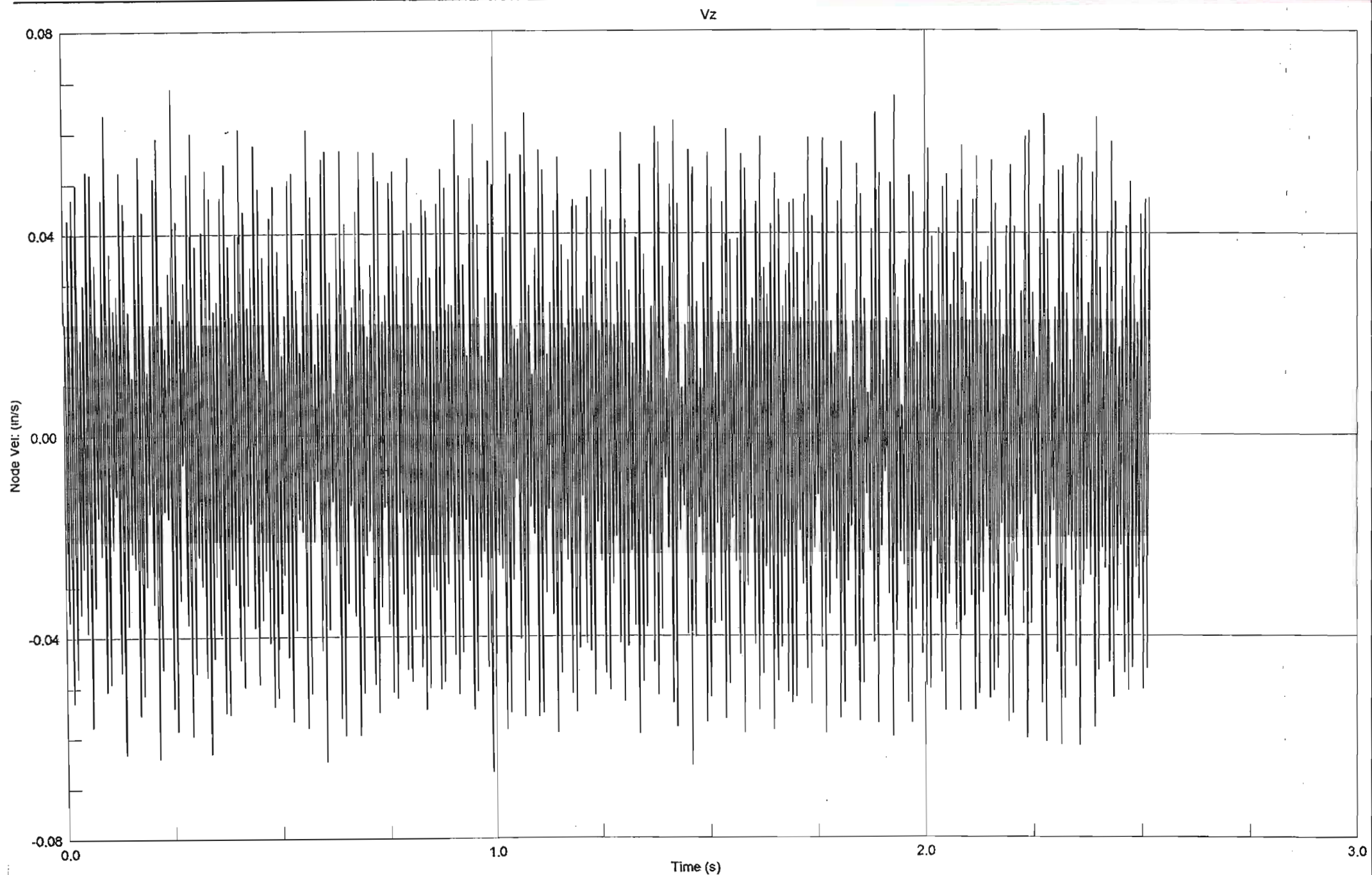


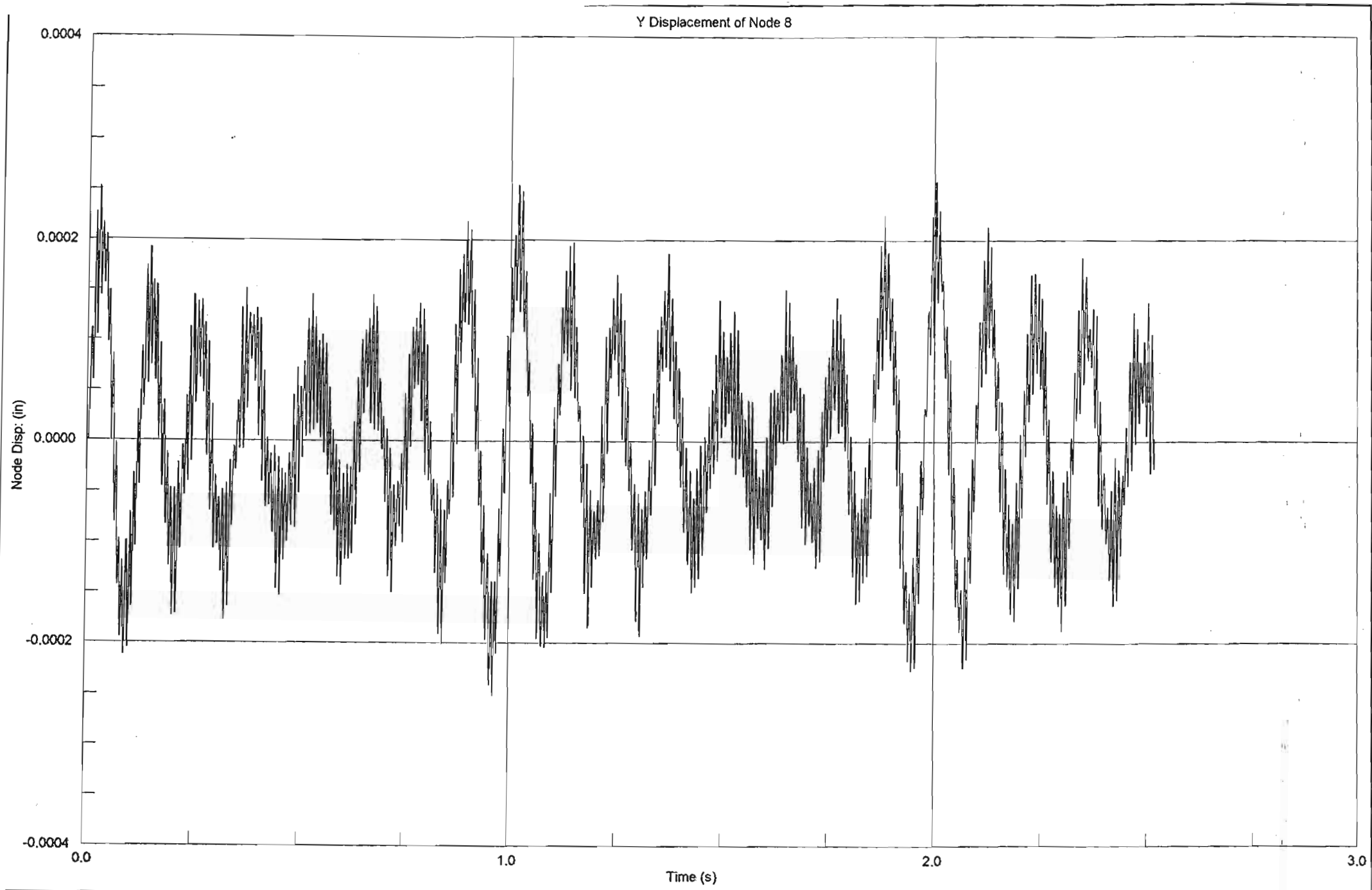
Z Displacement of Node 20



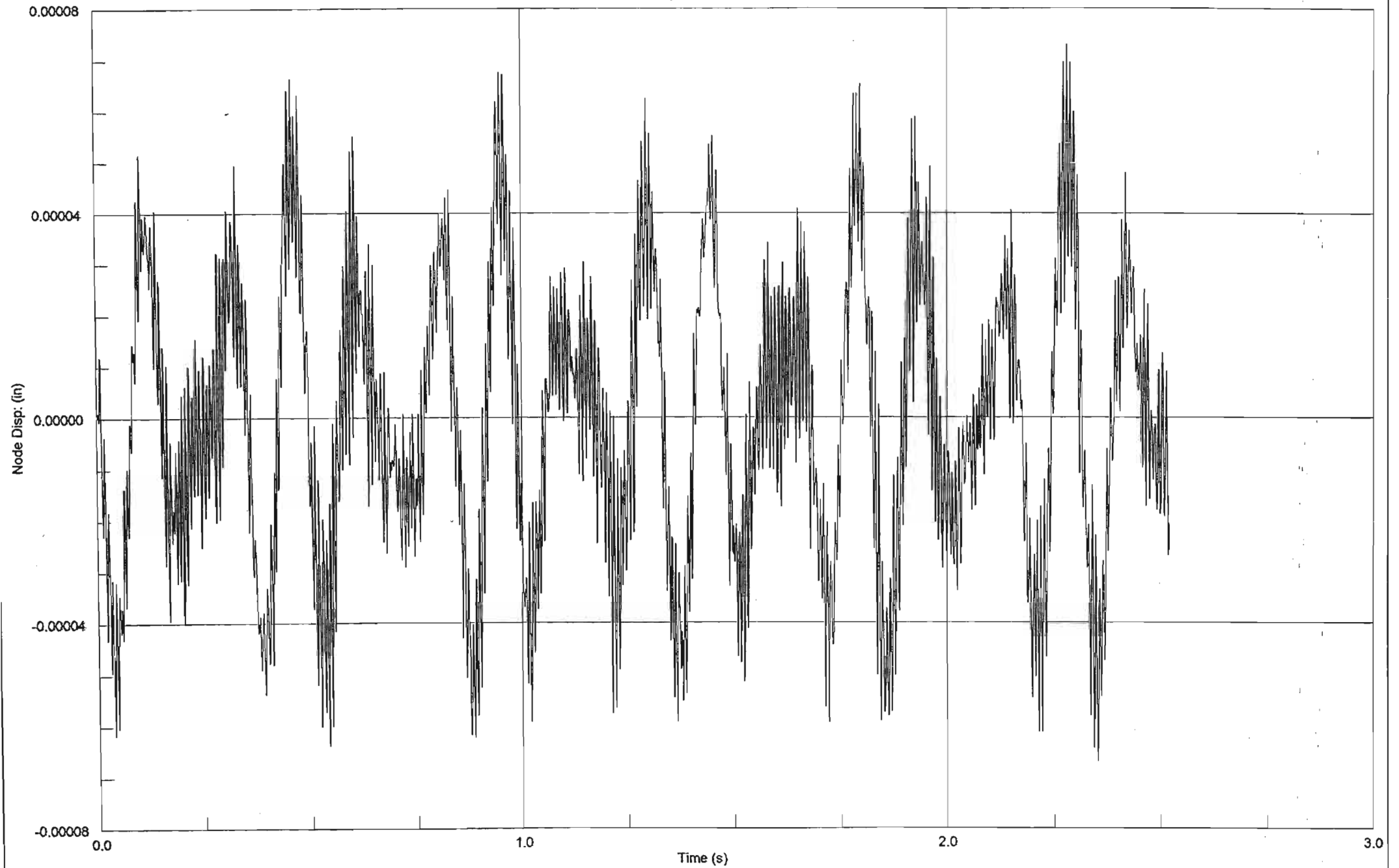
Vy

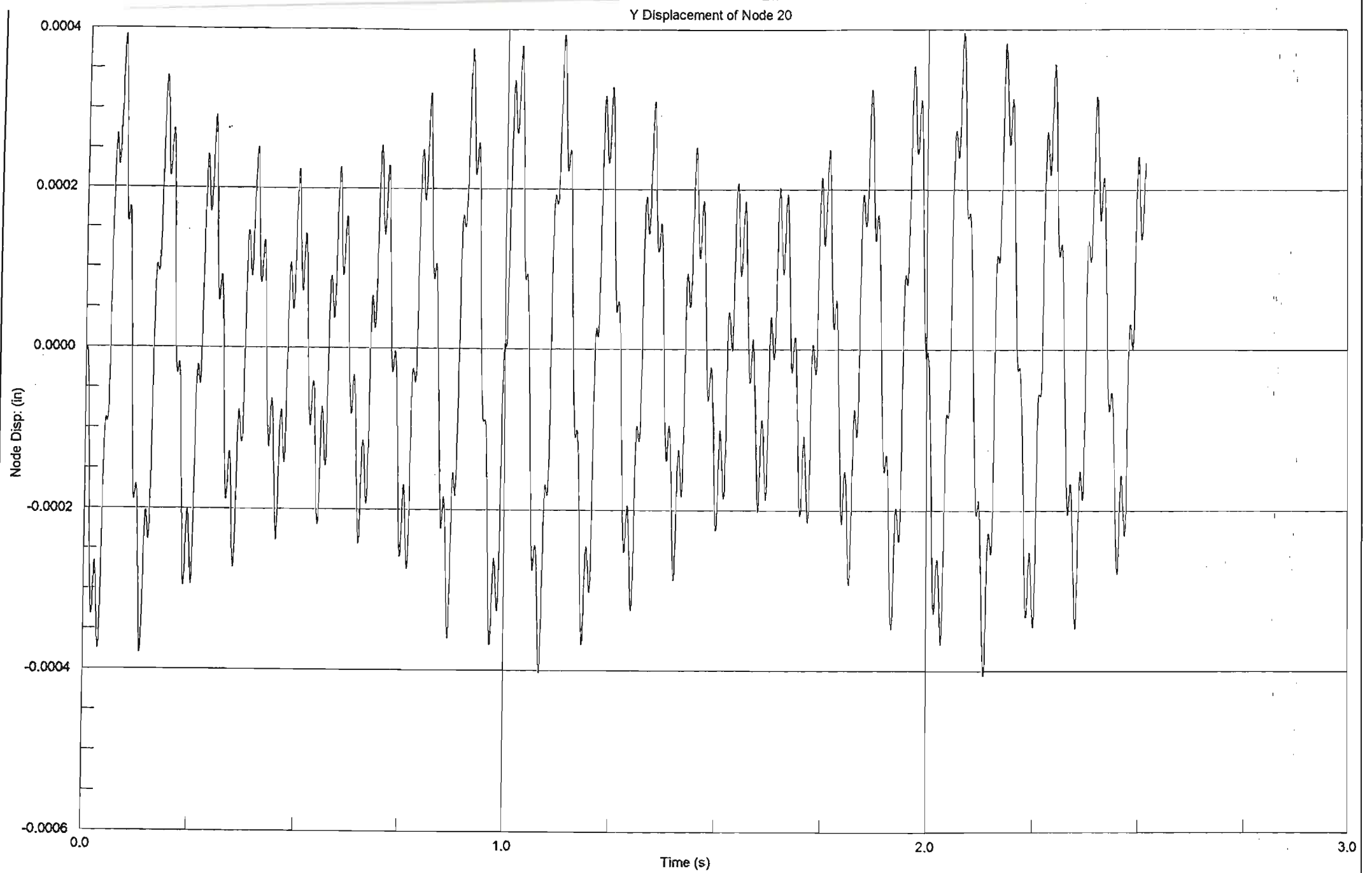


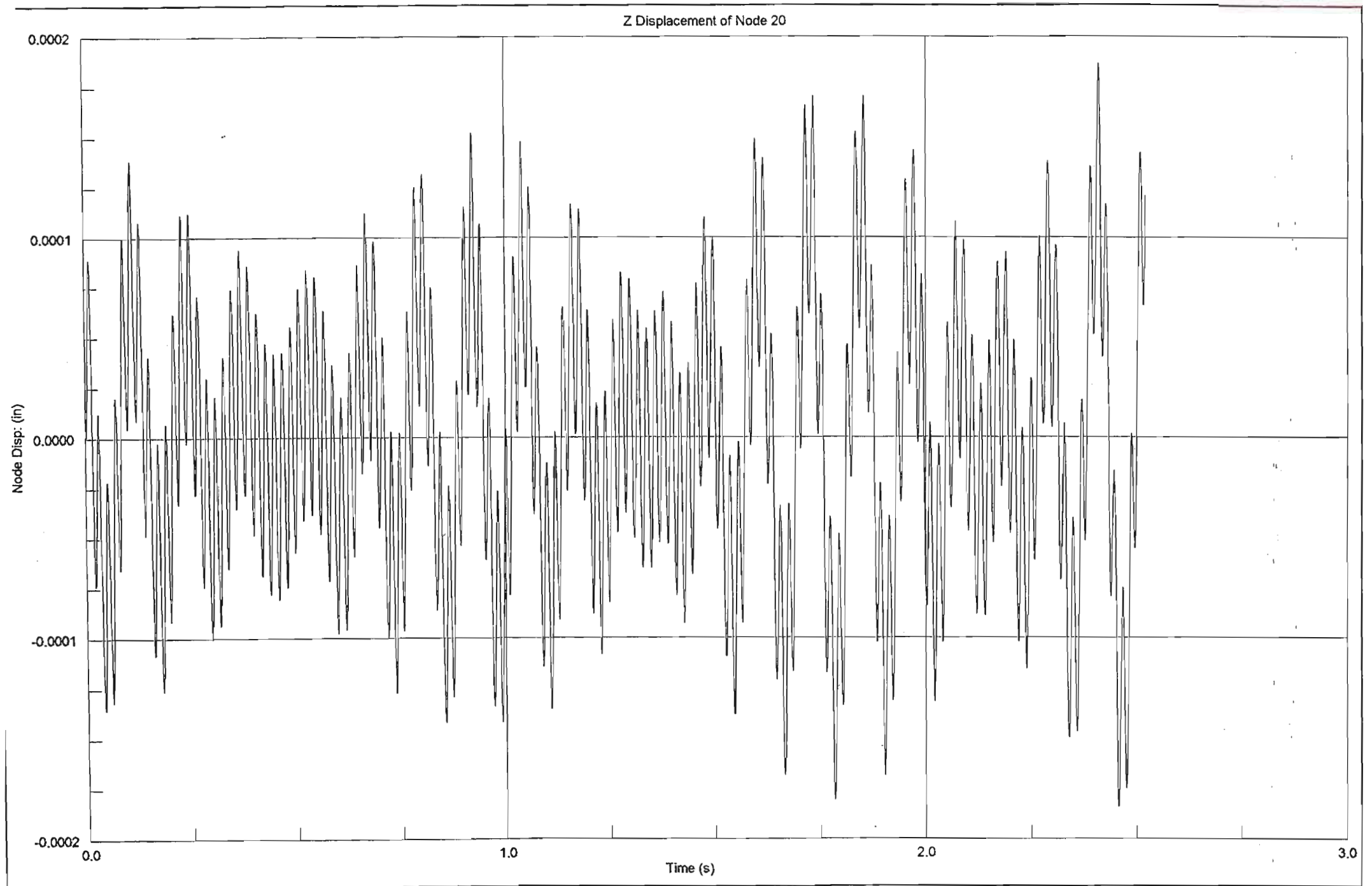


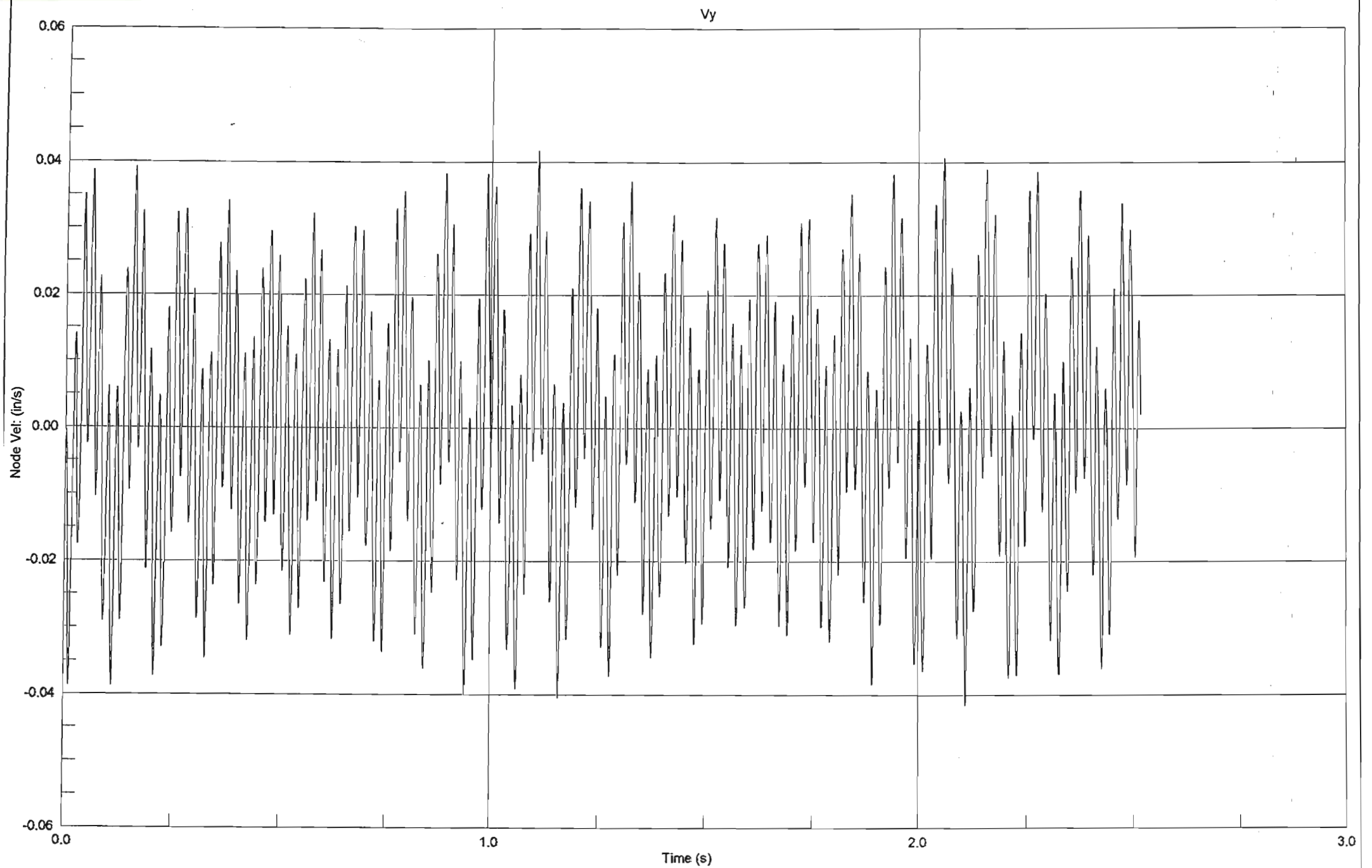


Z Displacement of Node 8

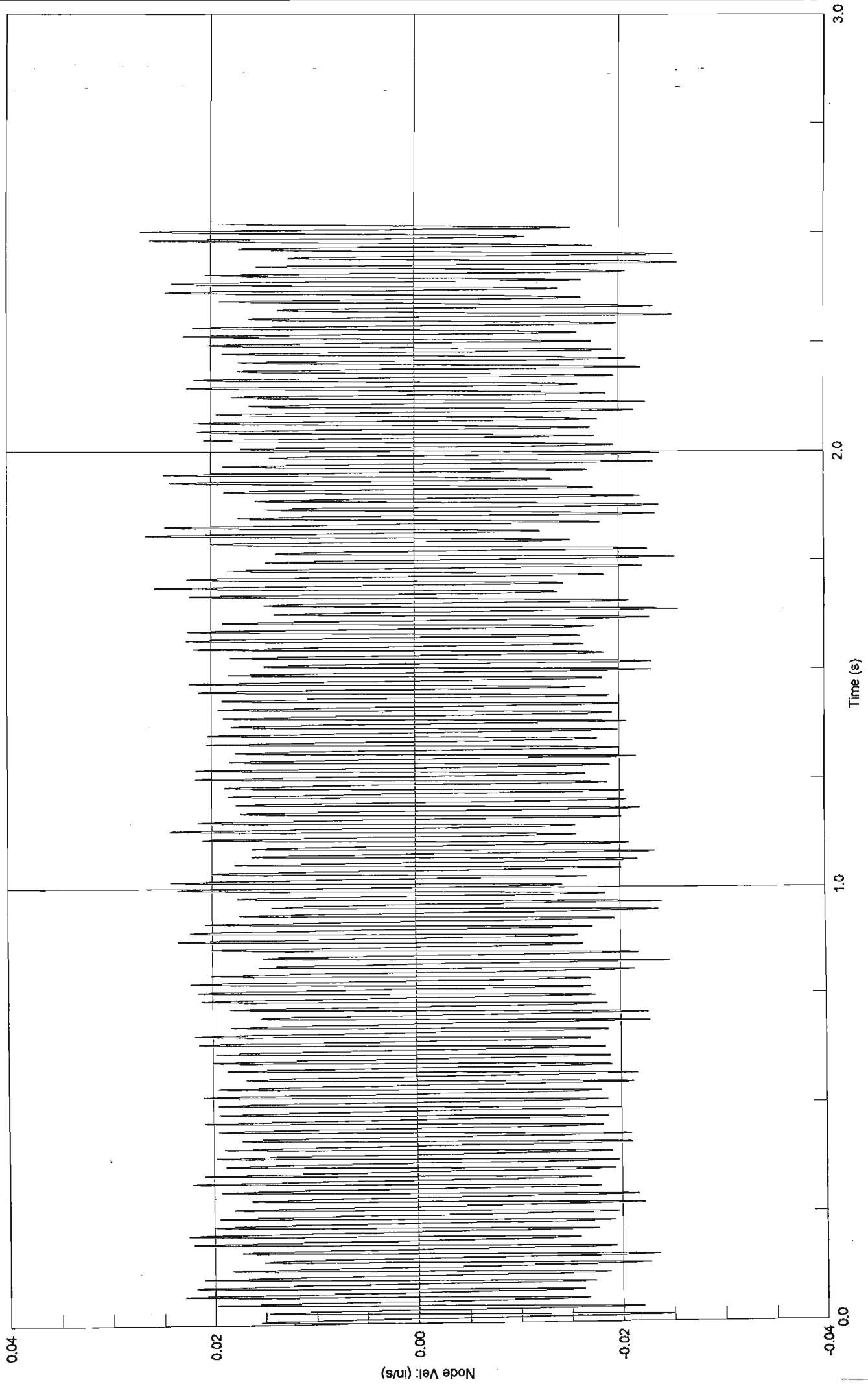


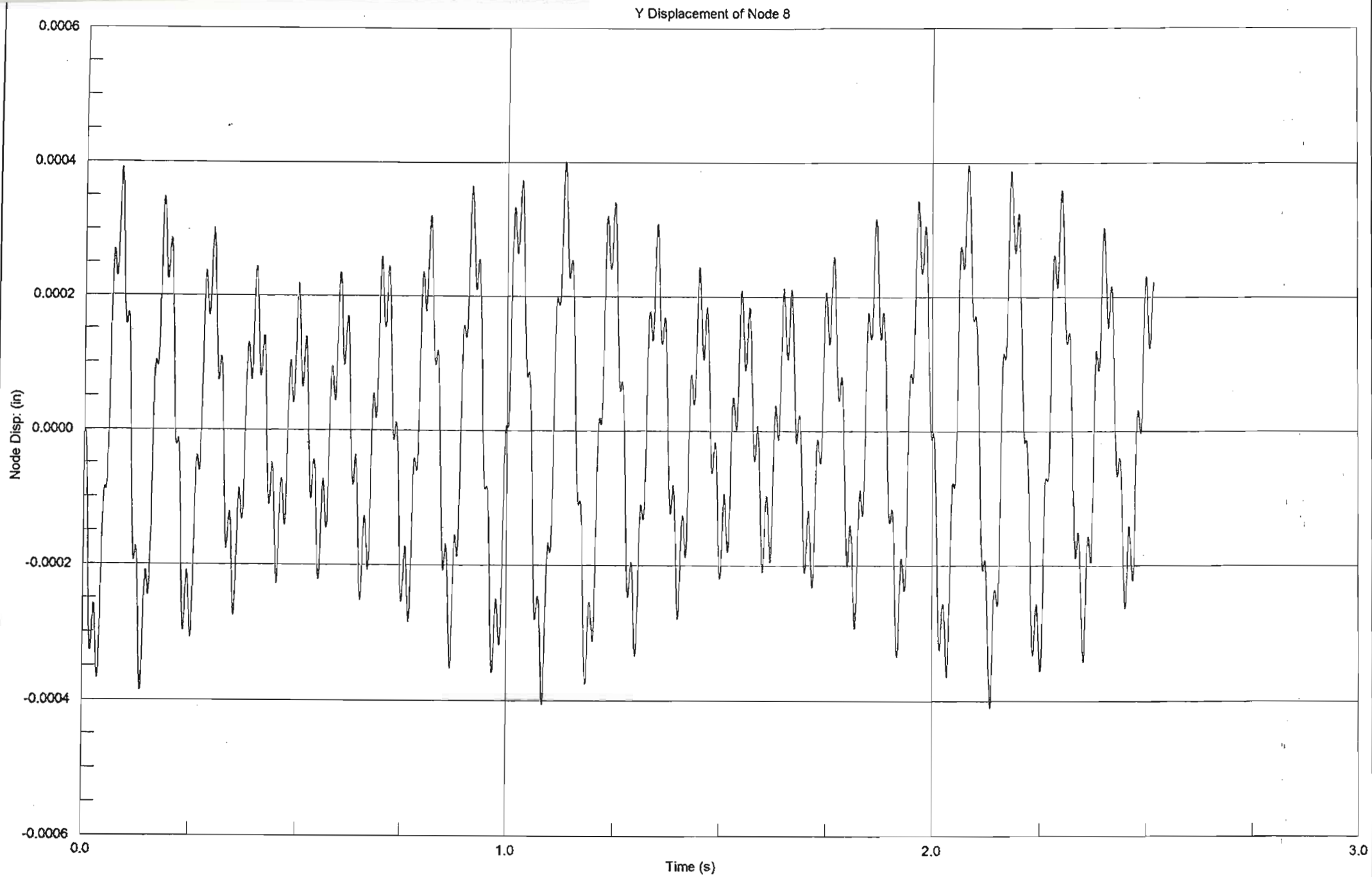


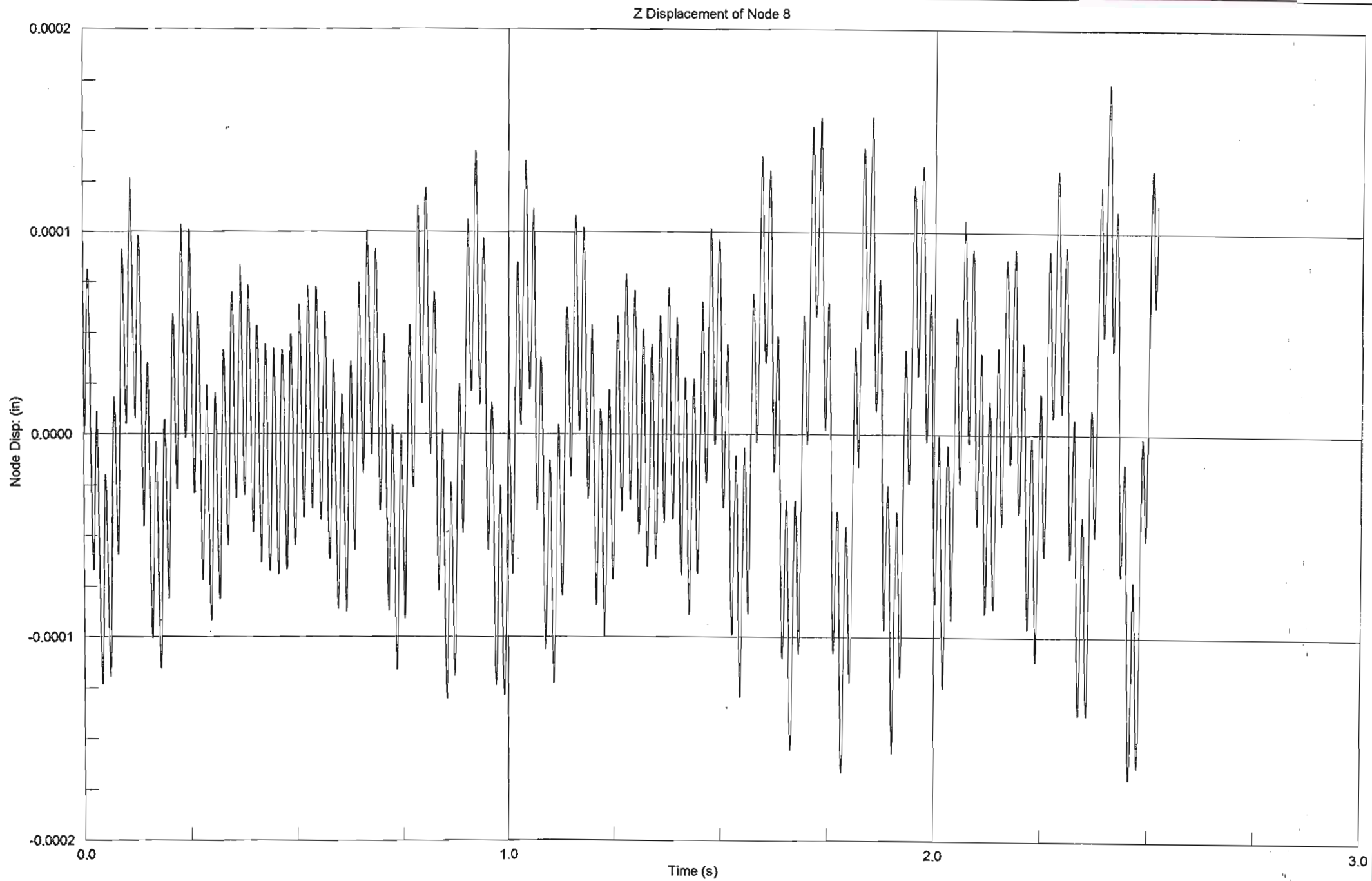




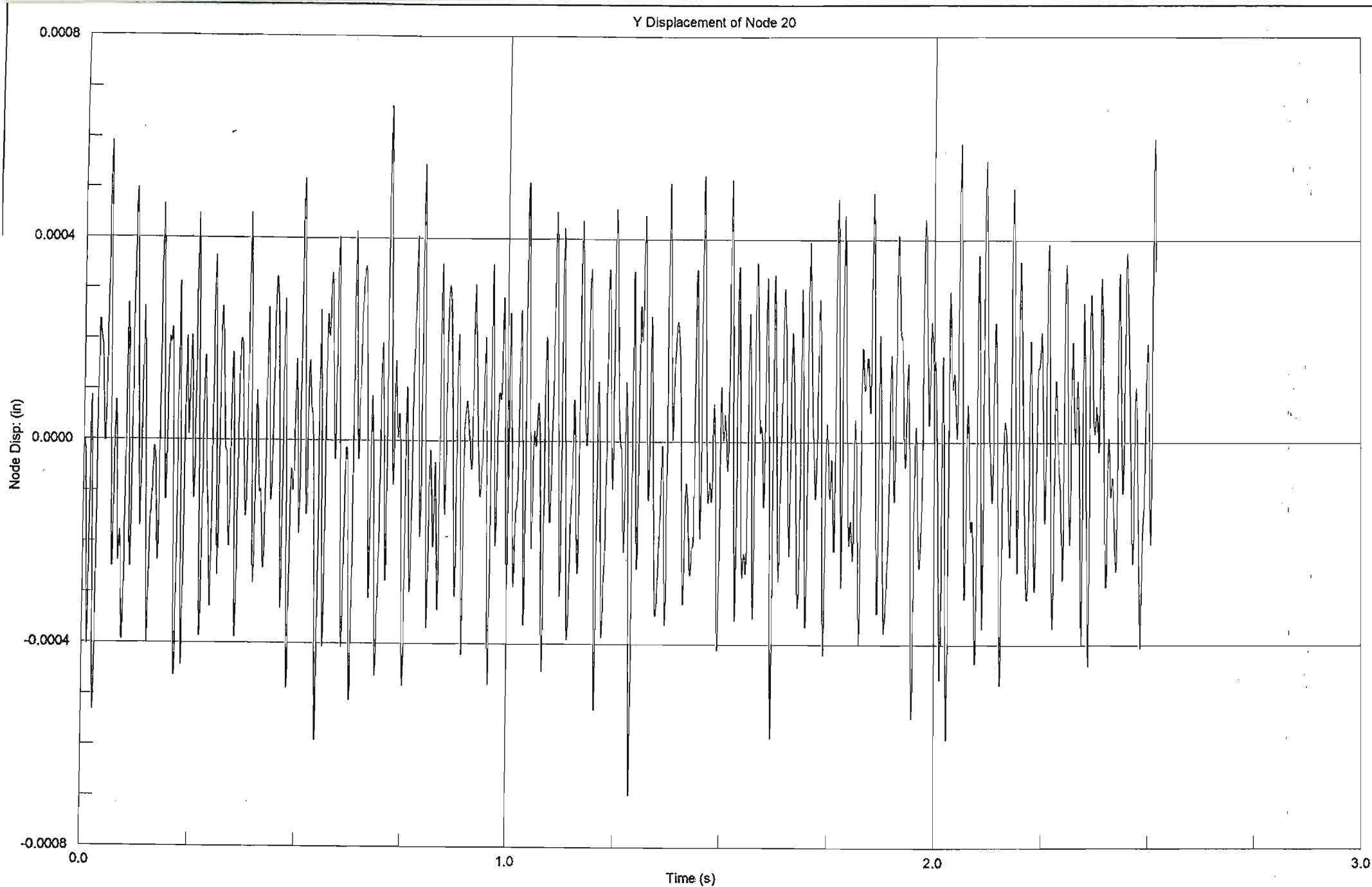
Vz

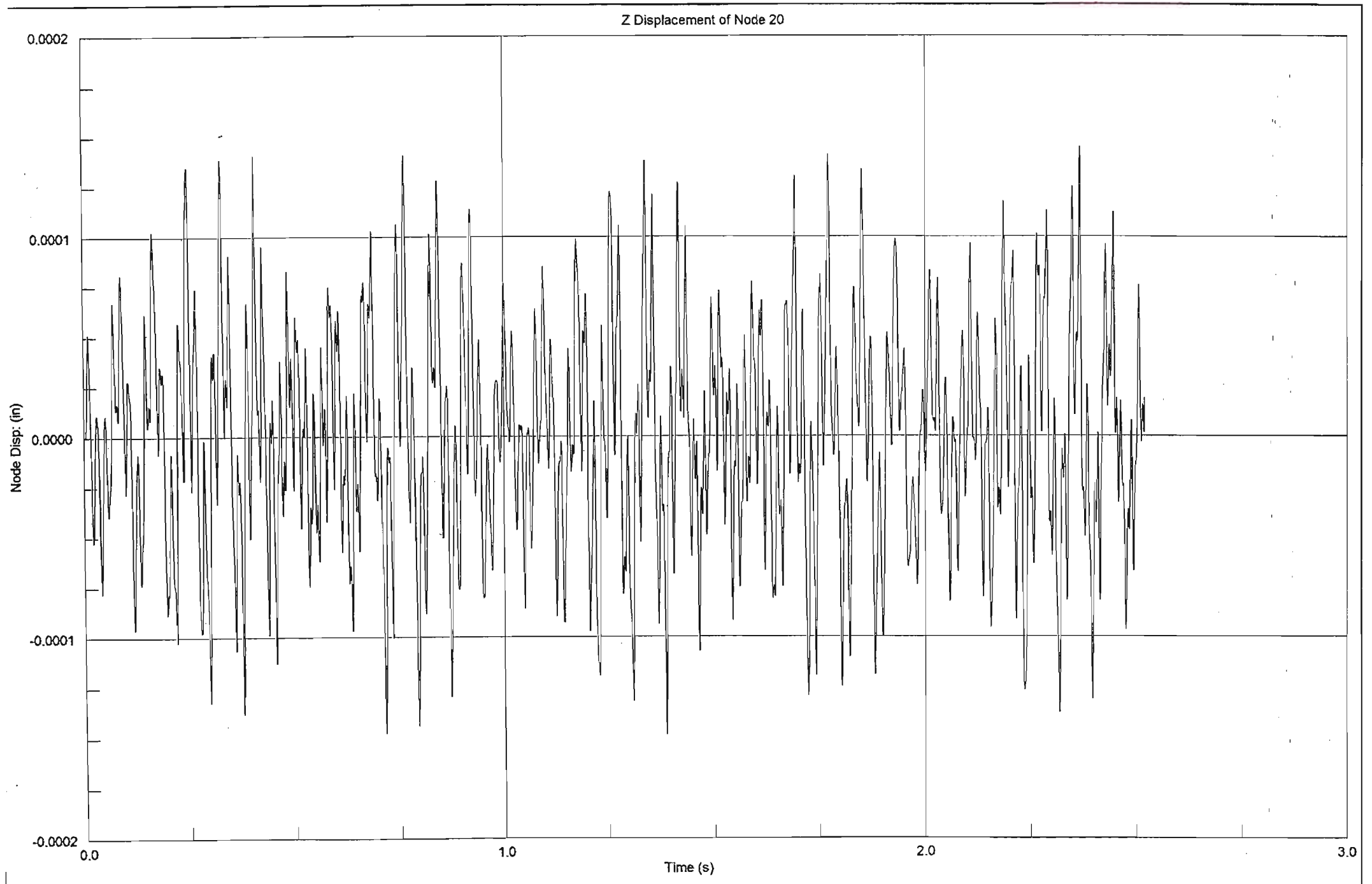


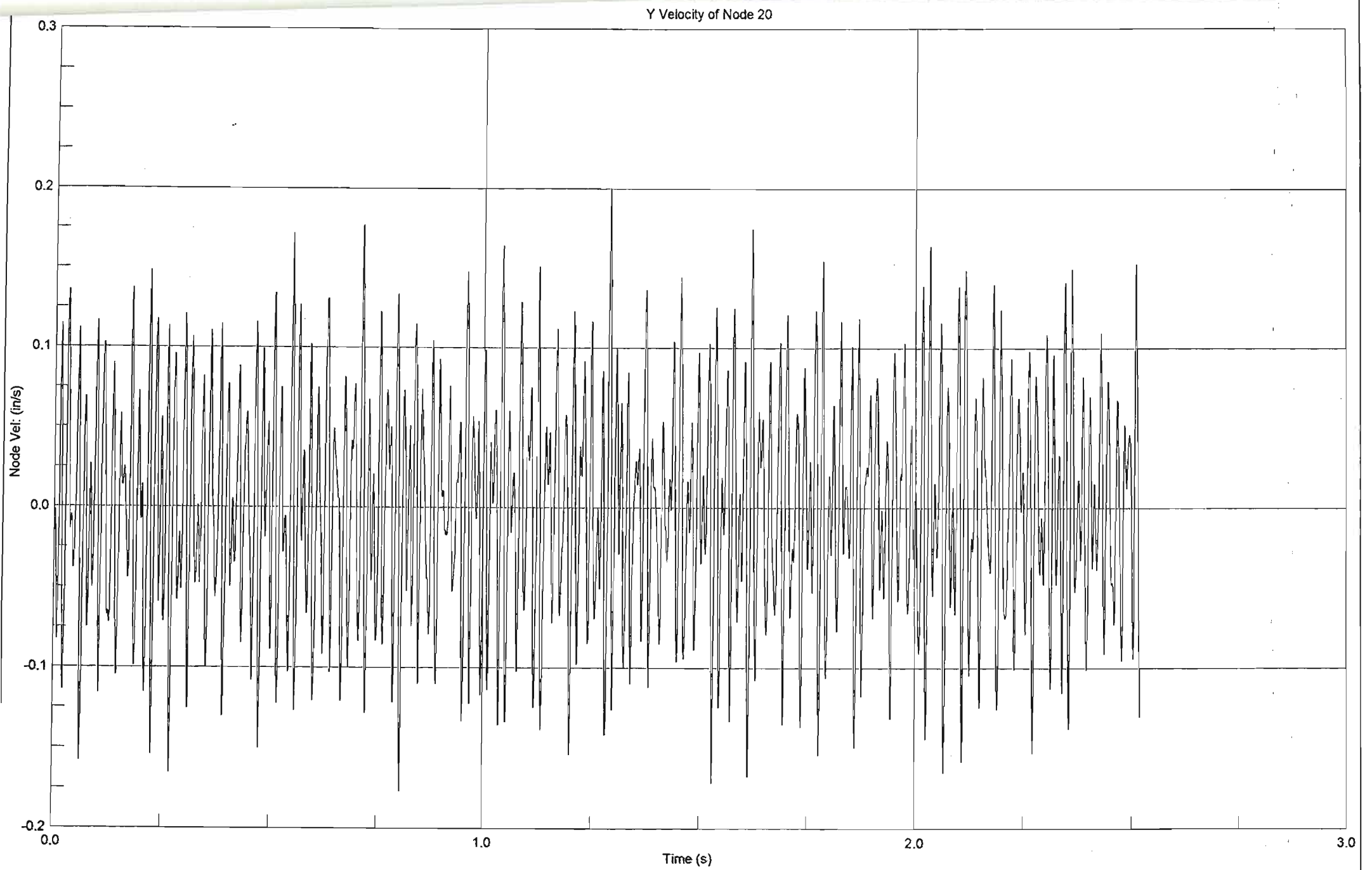




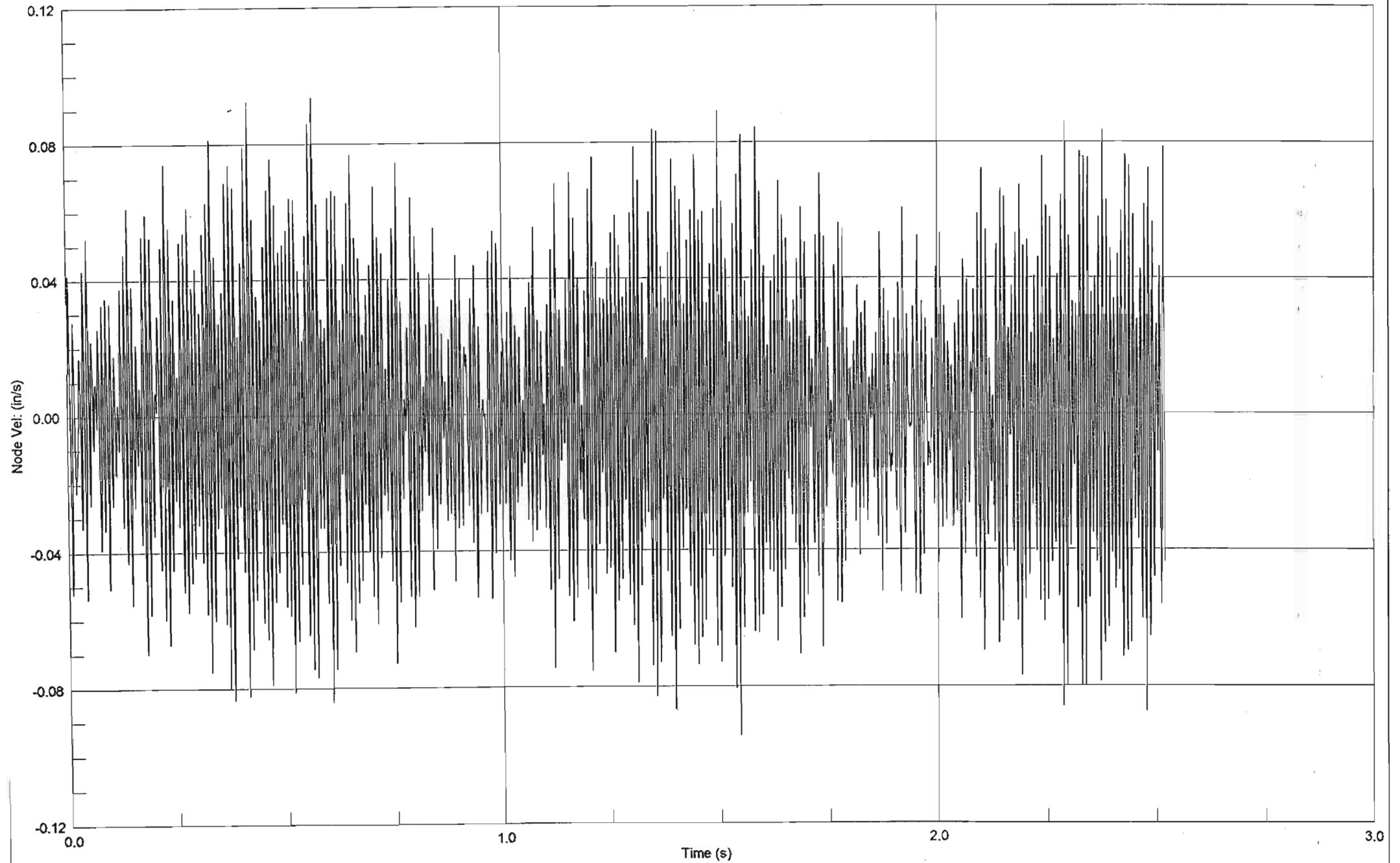
81.66

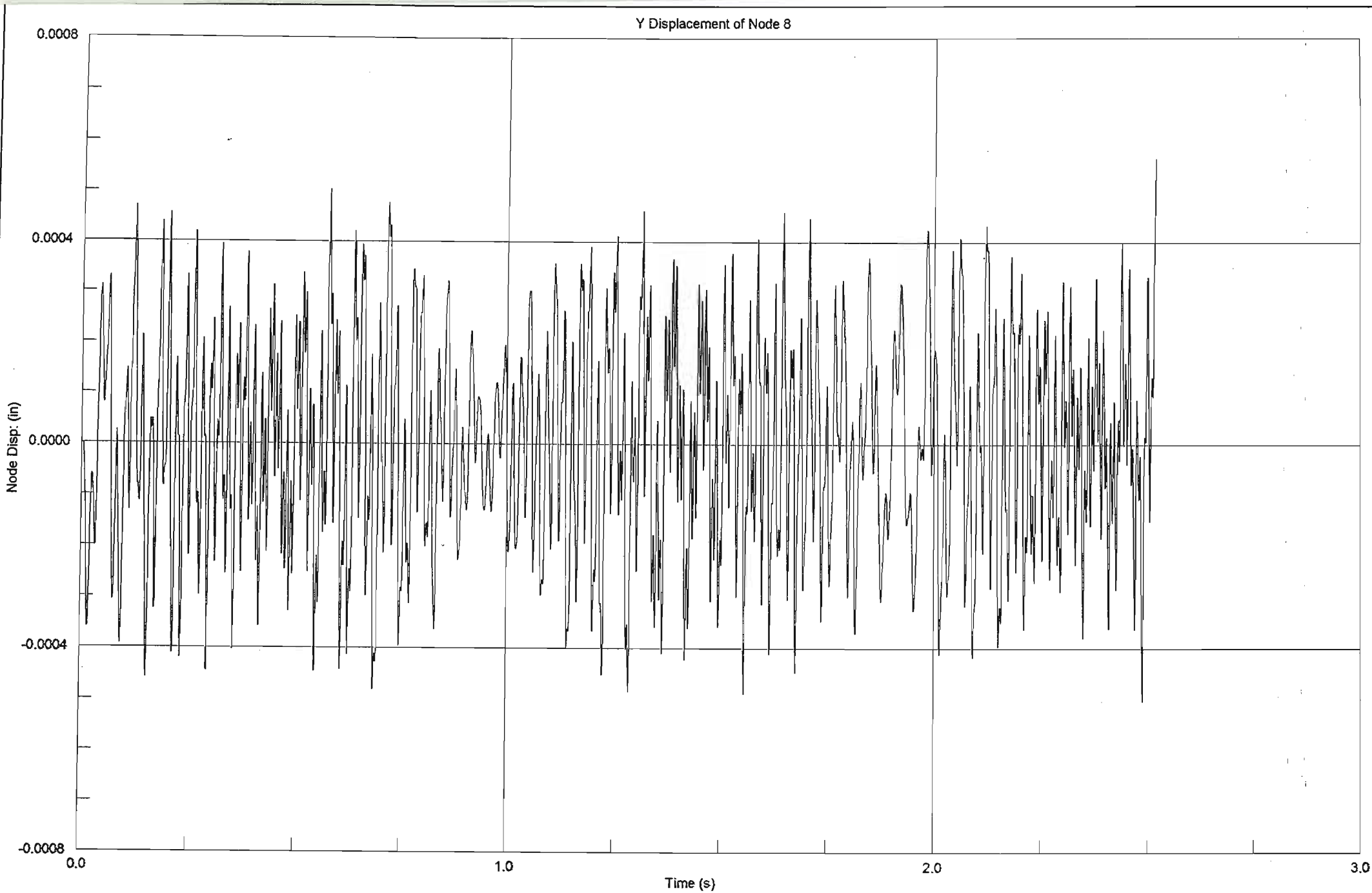


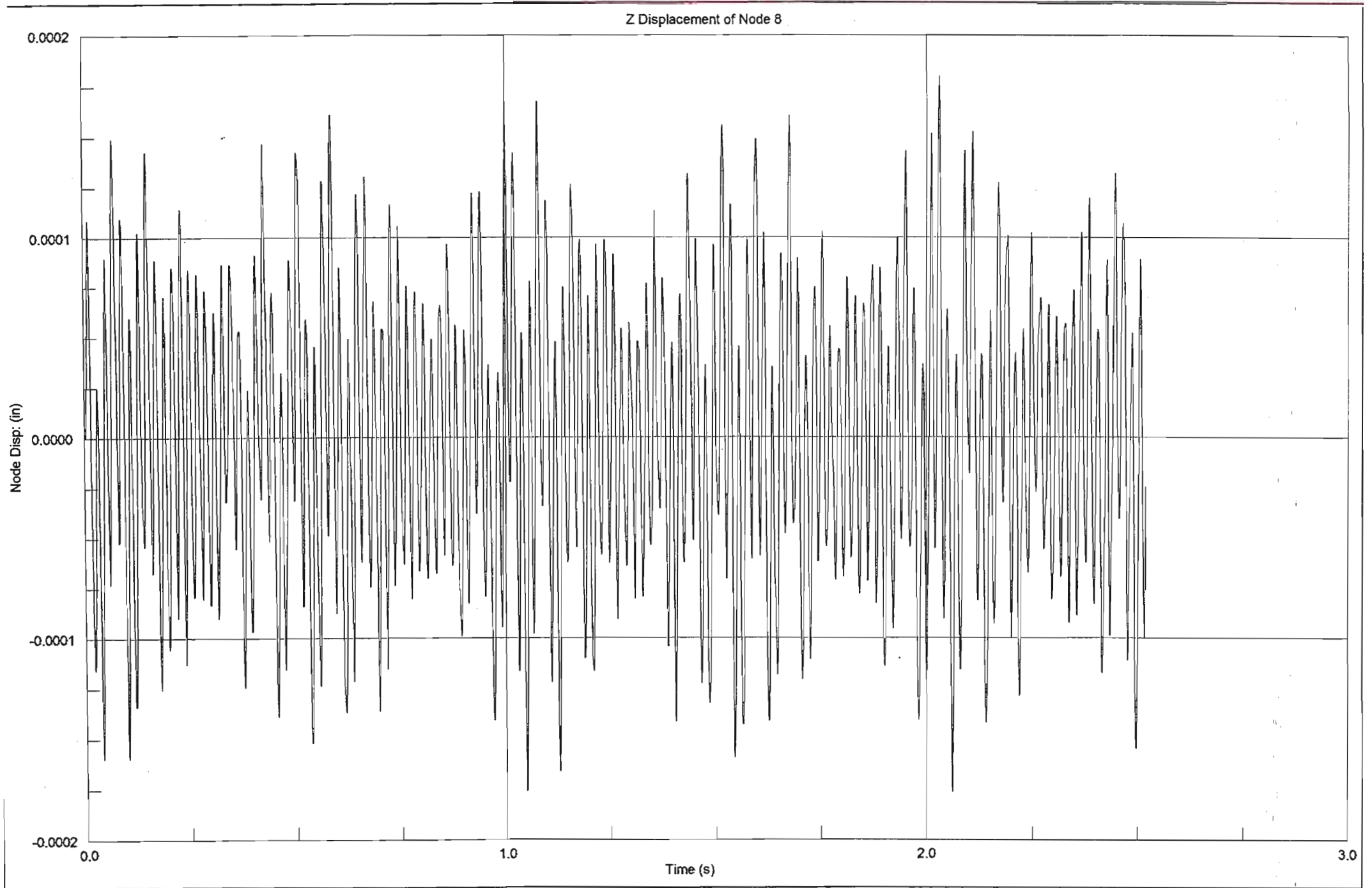


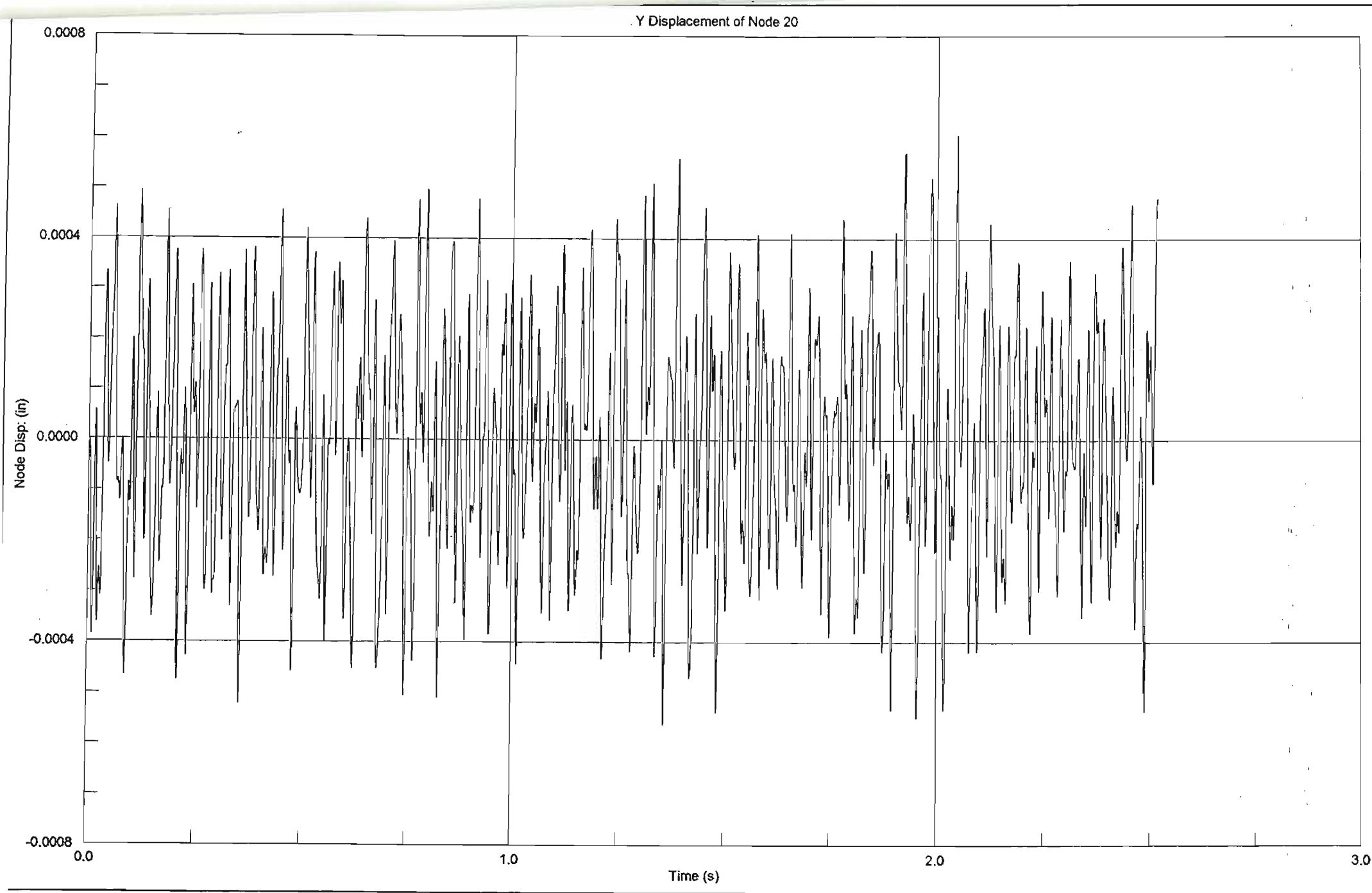


Z Velocity of Node 20

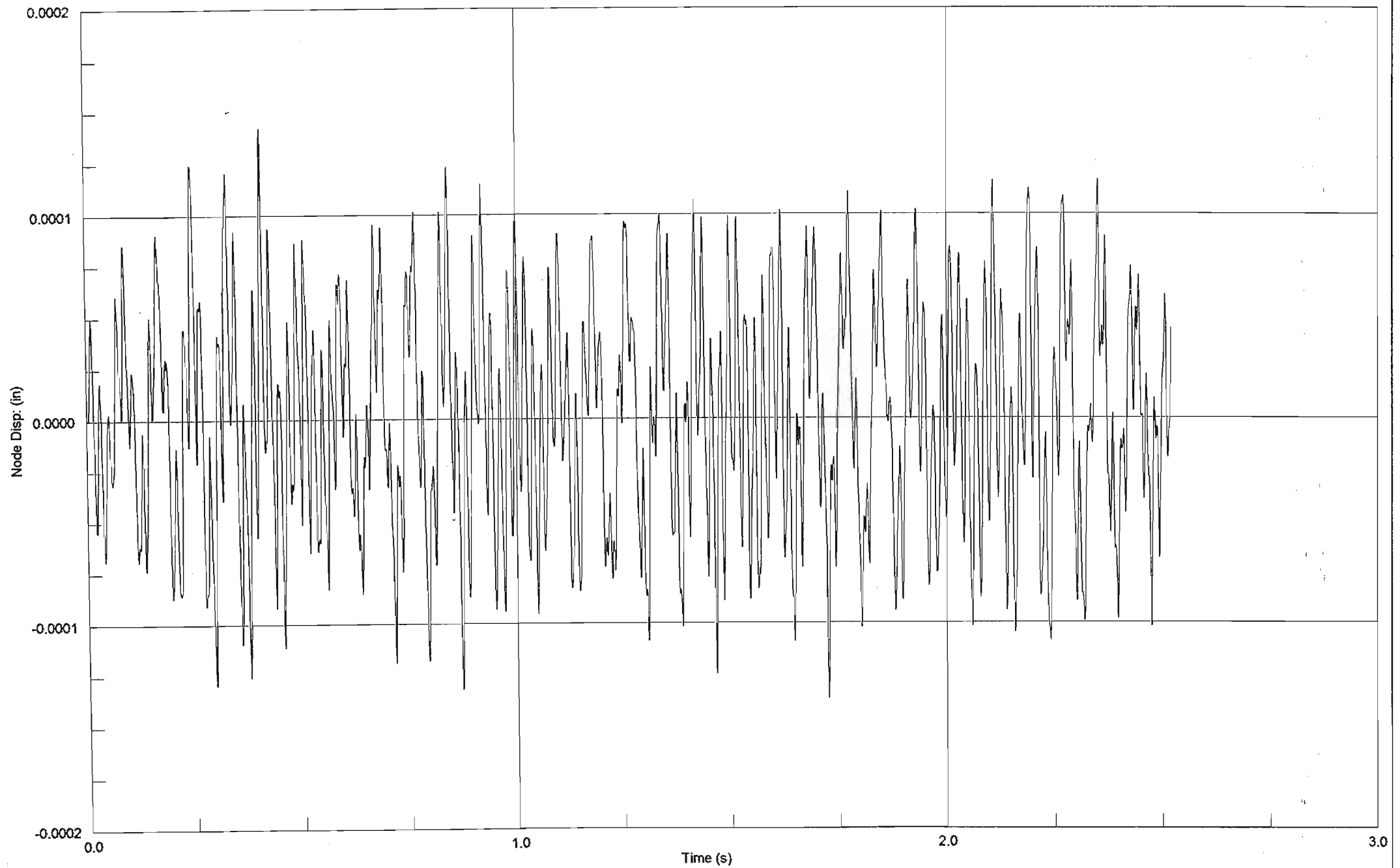


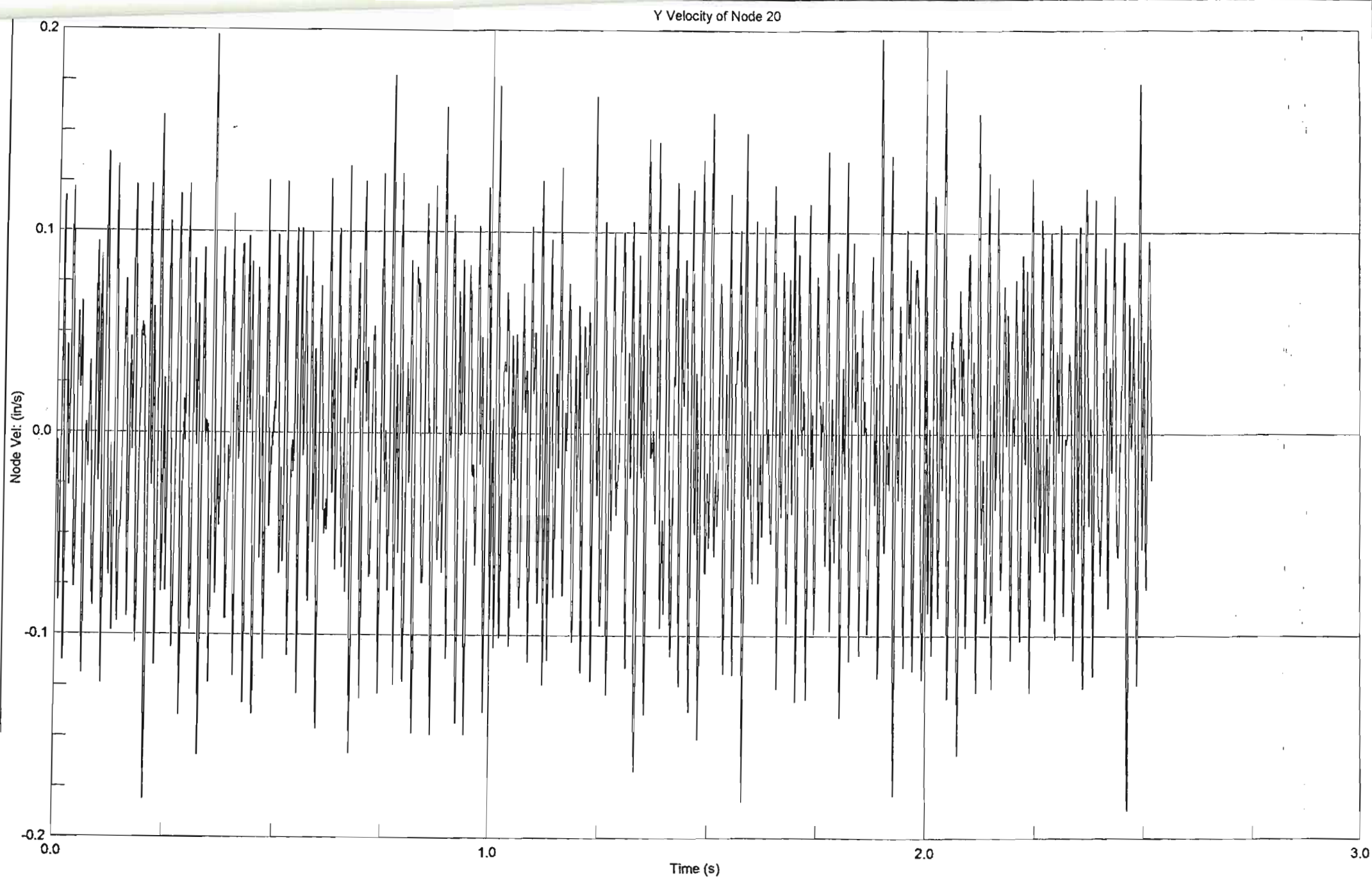


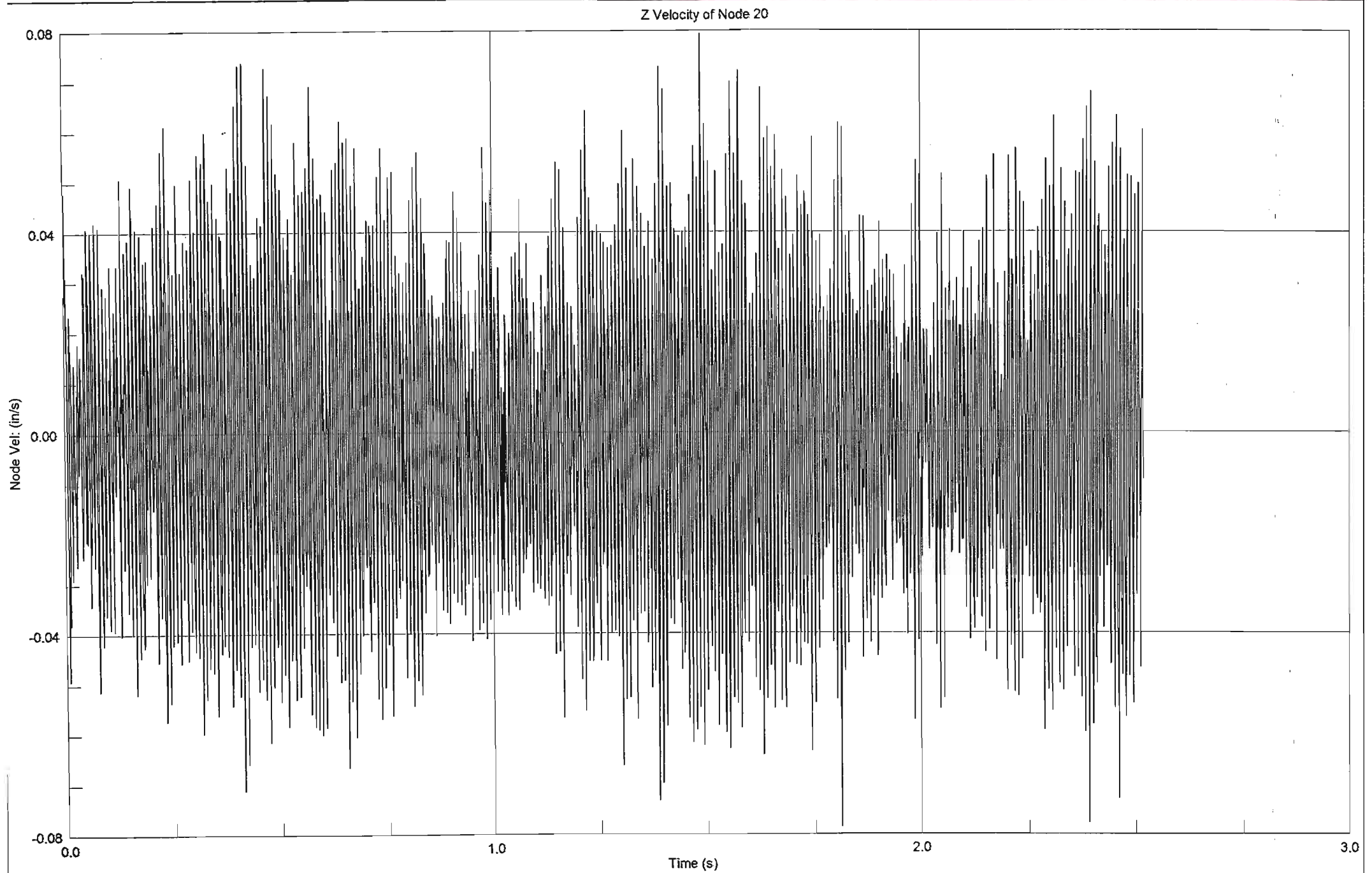


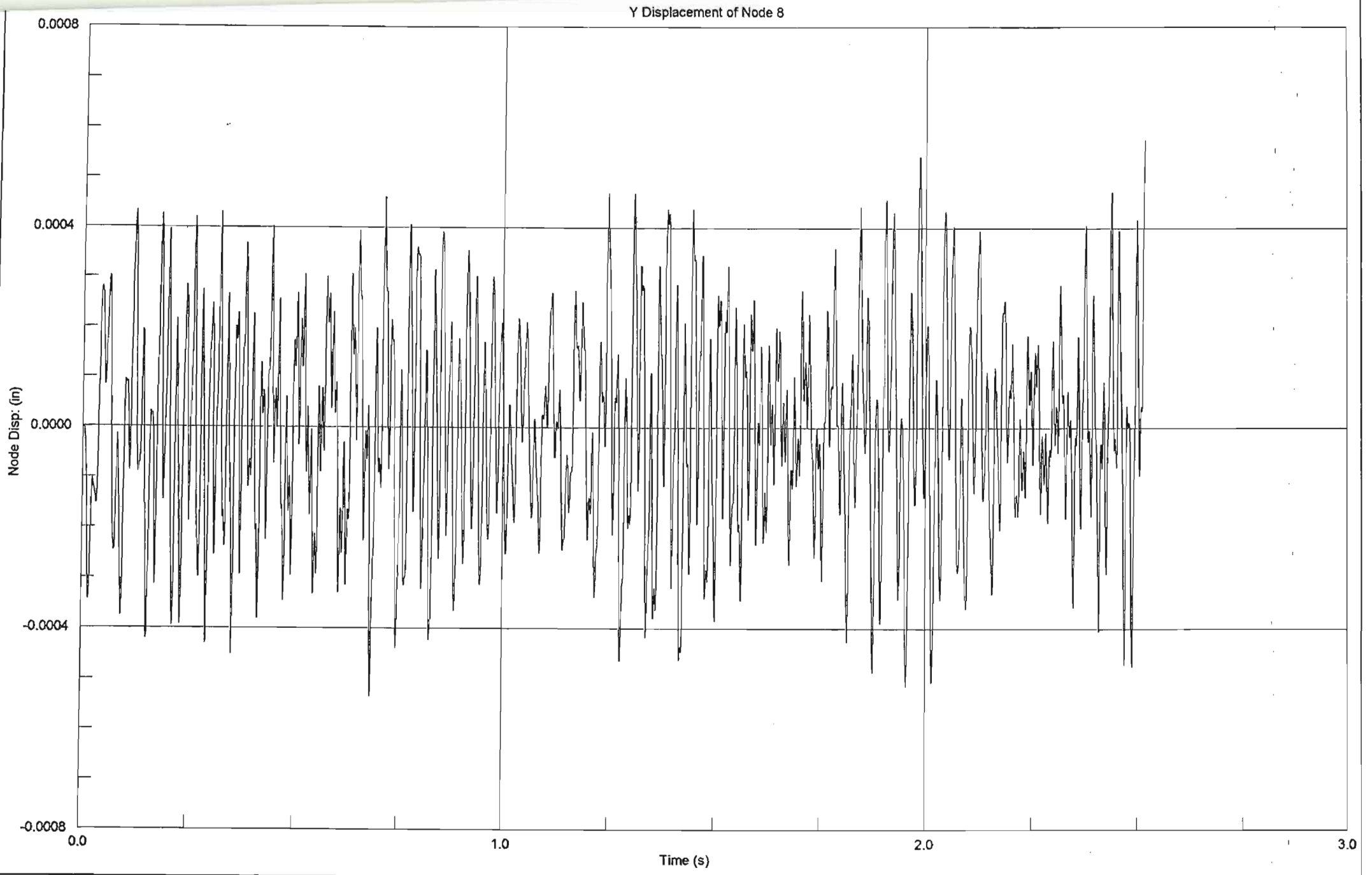


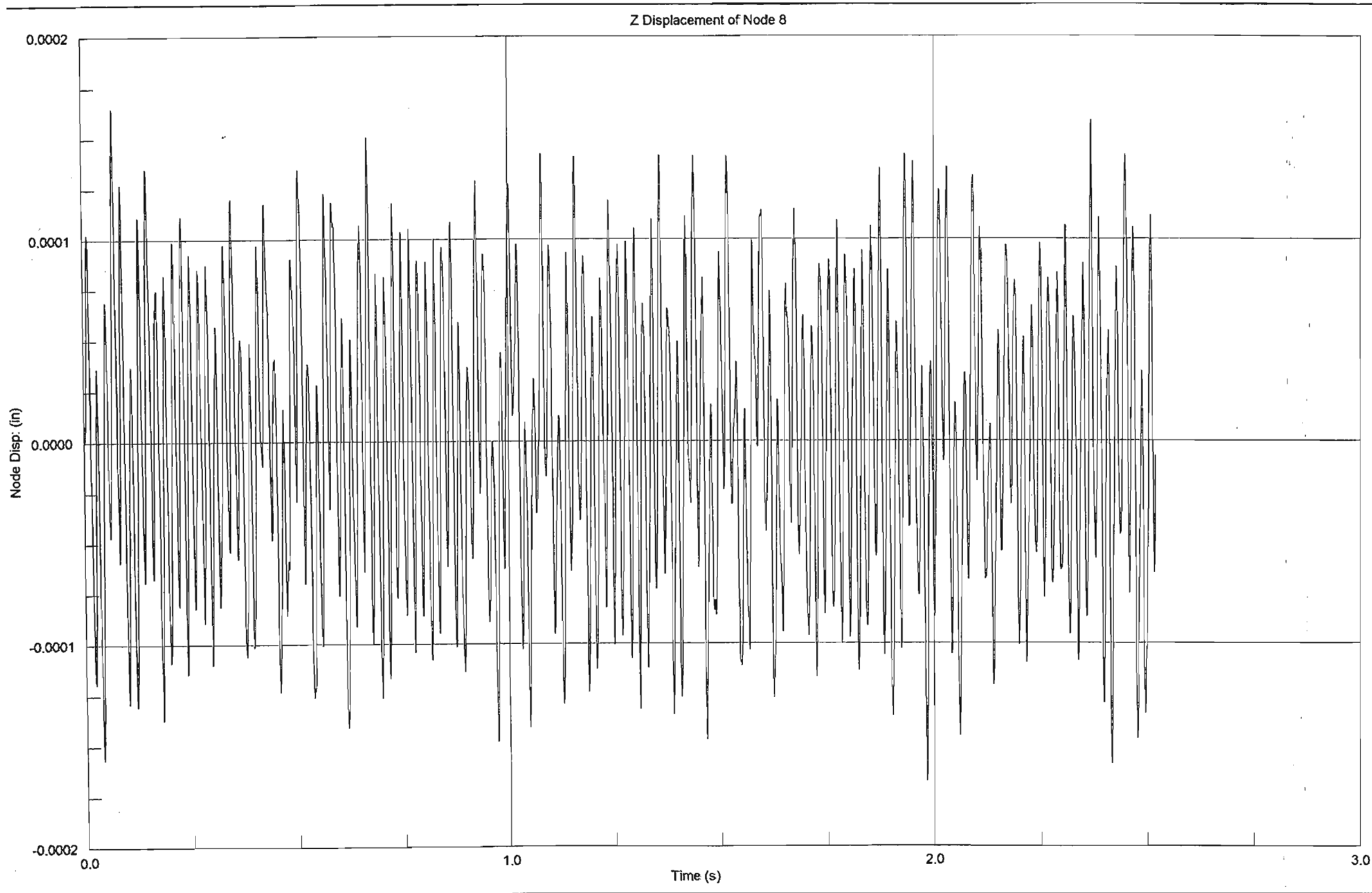
Z Displacement of Node 20

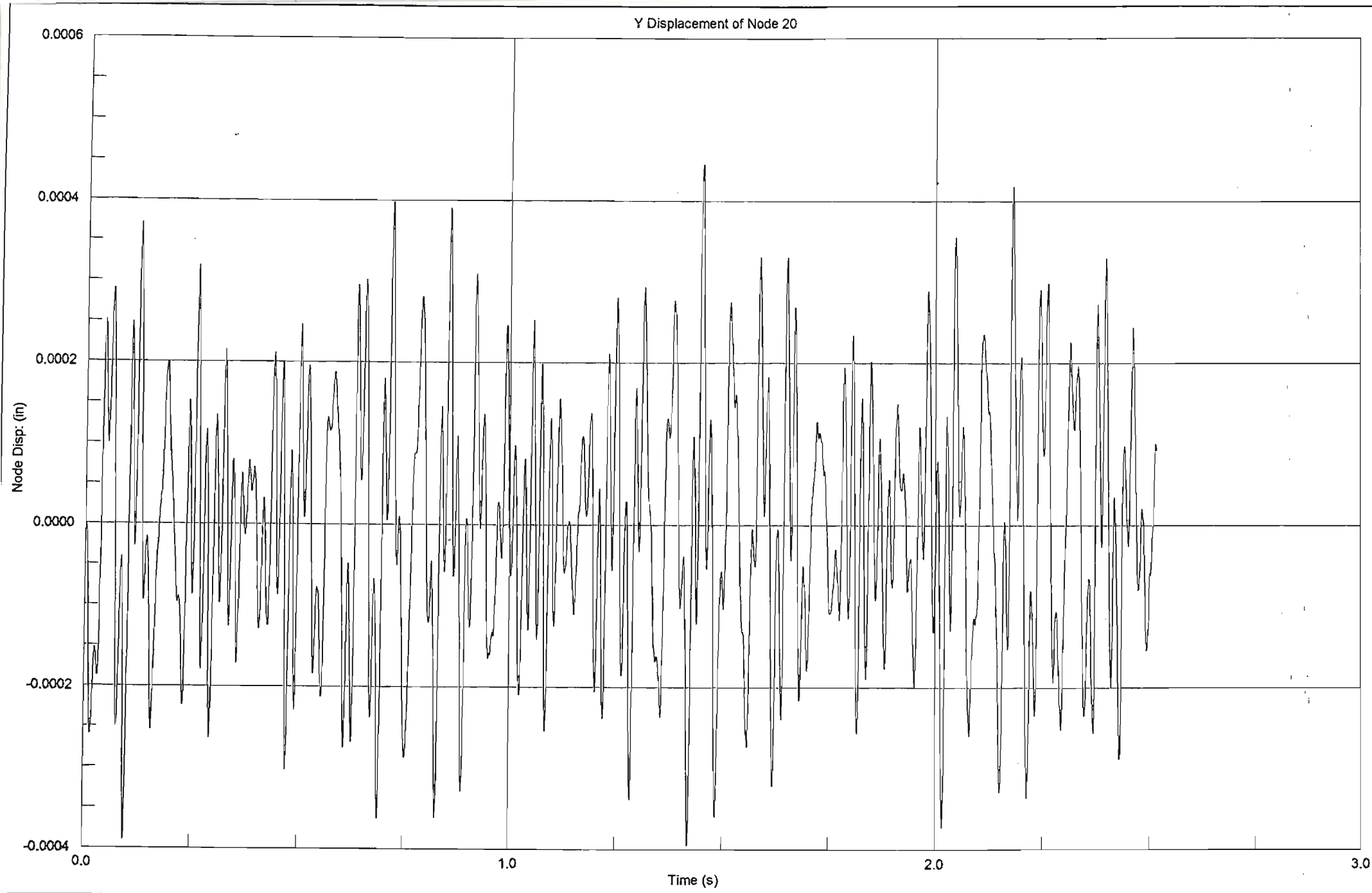




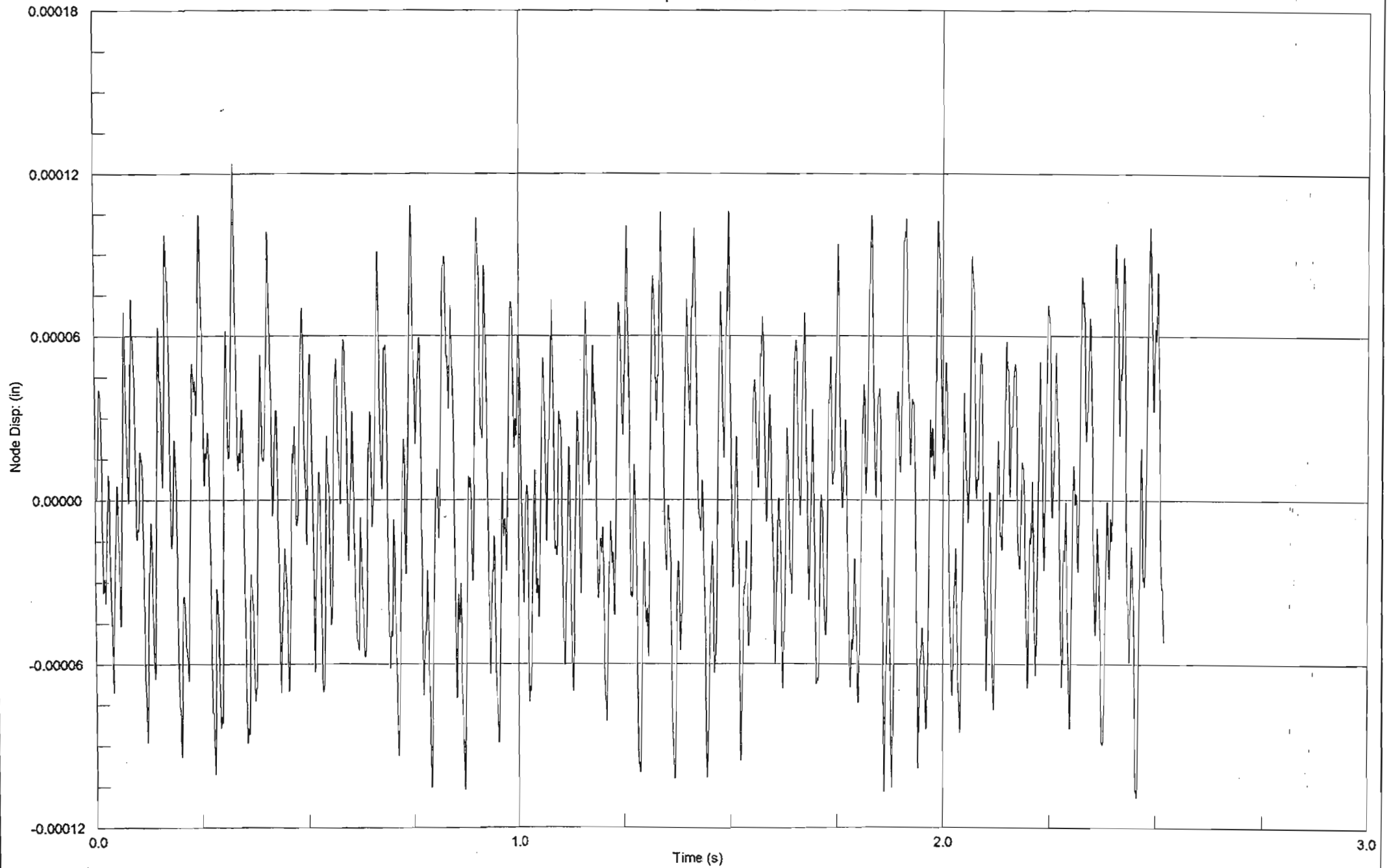


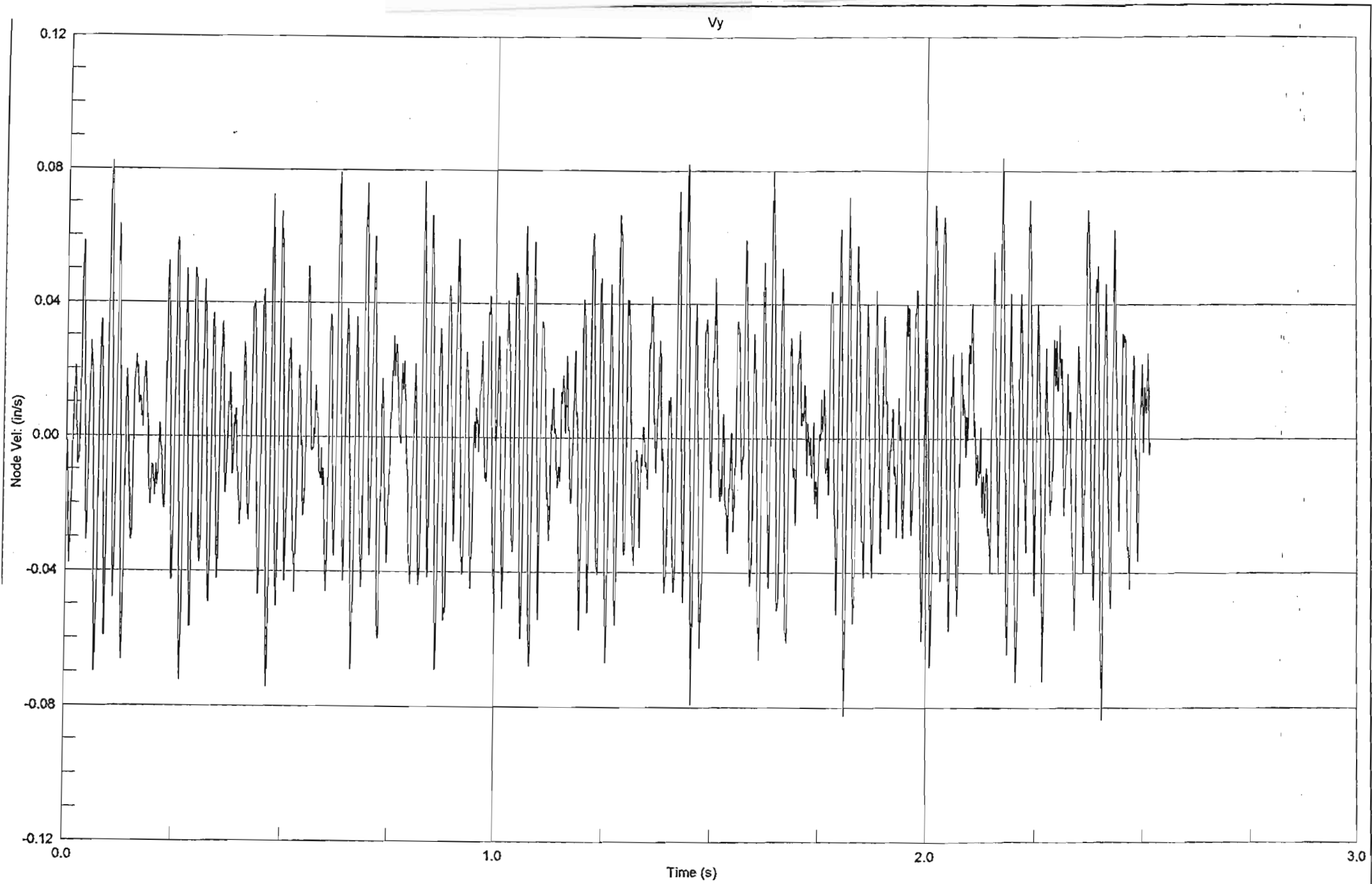


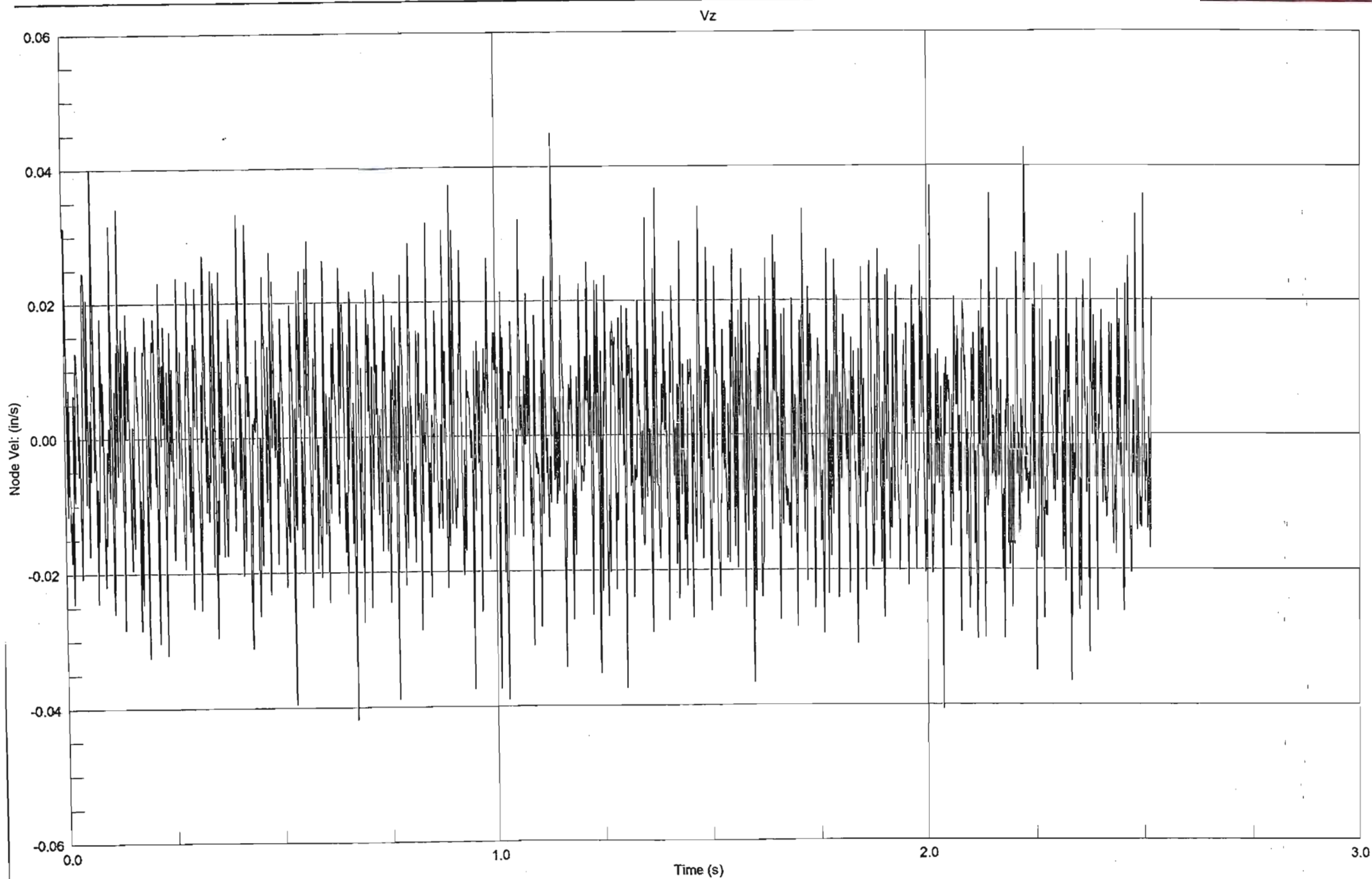


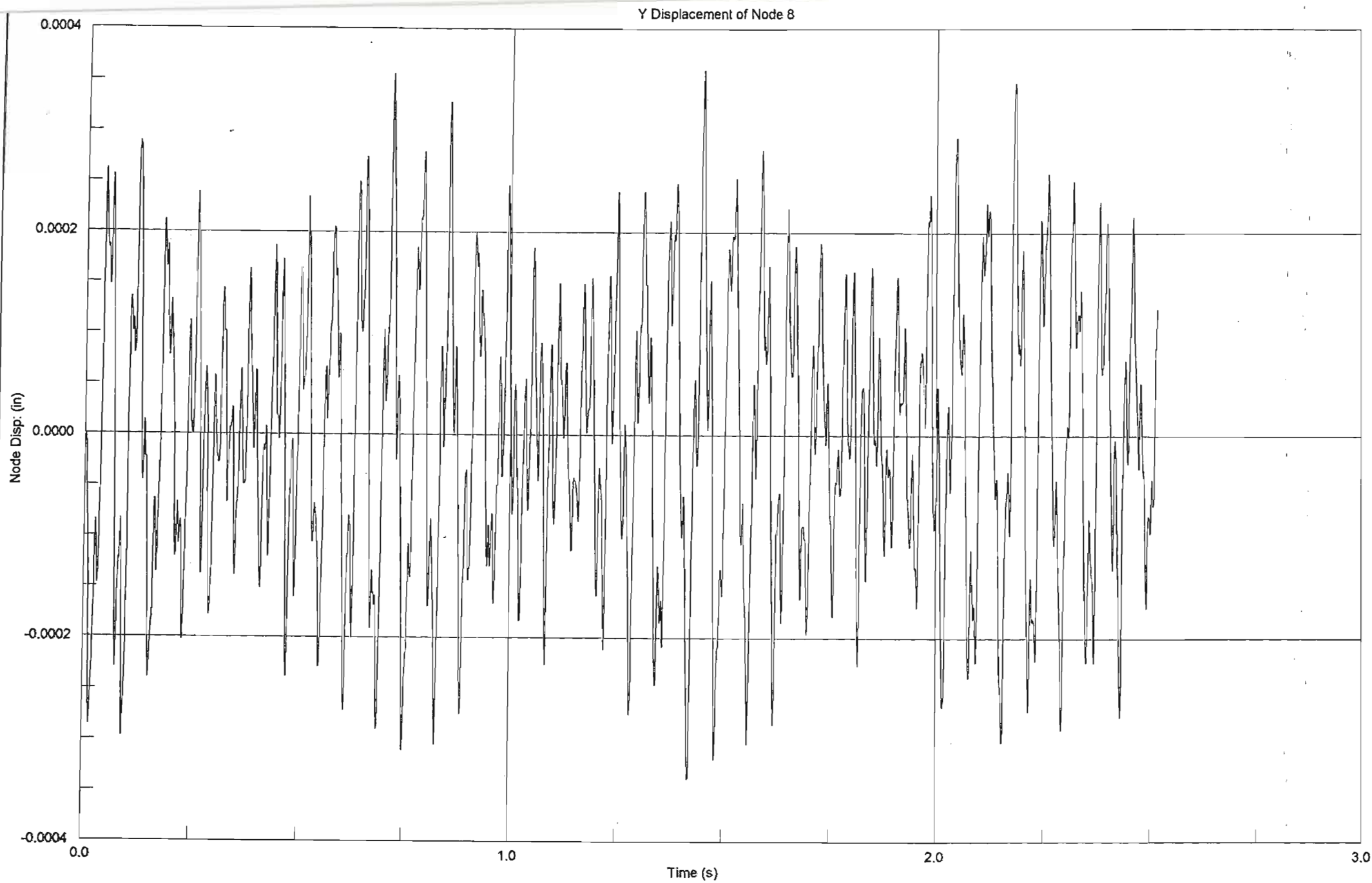


Z Displacement of Node 20

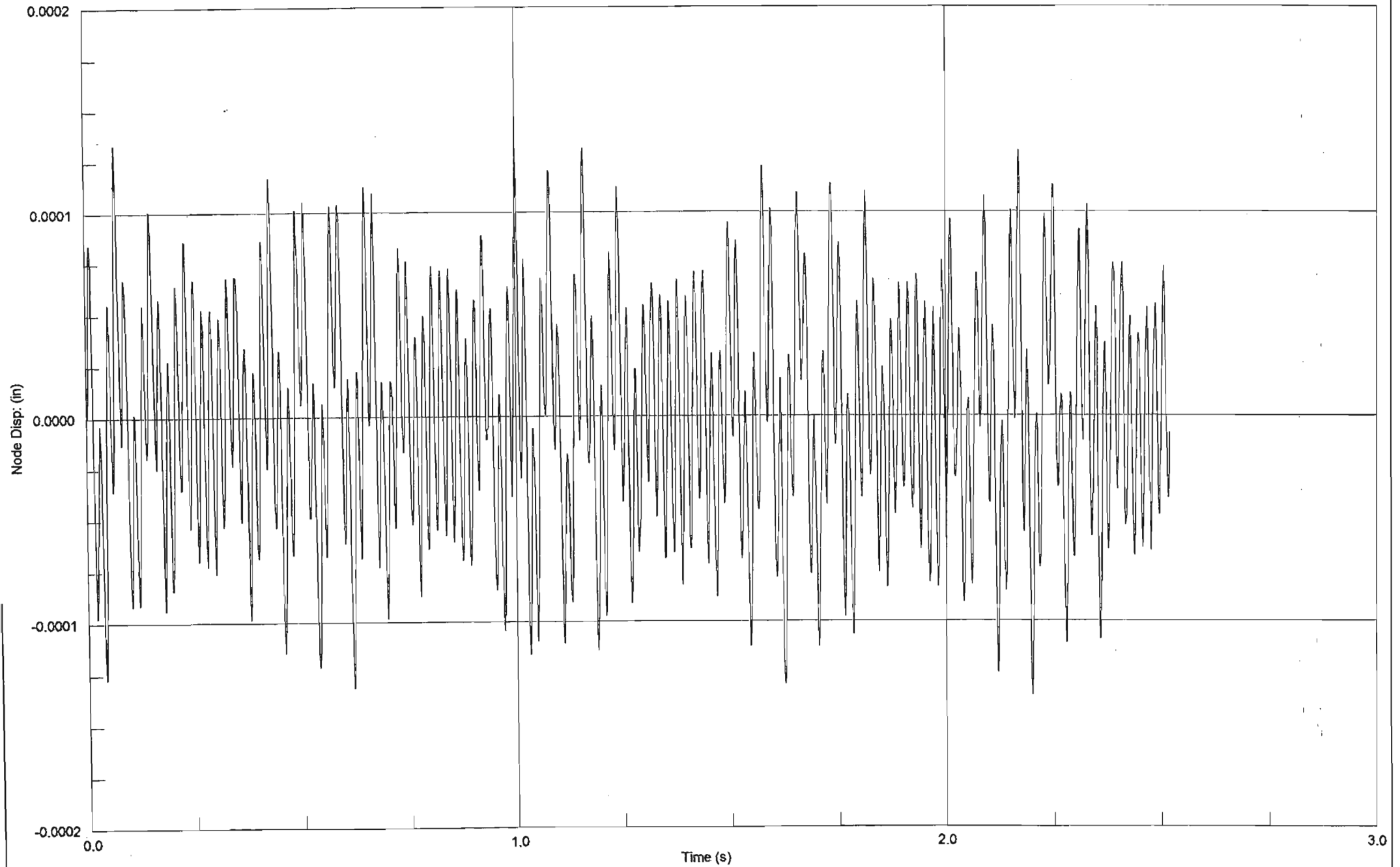


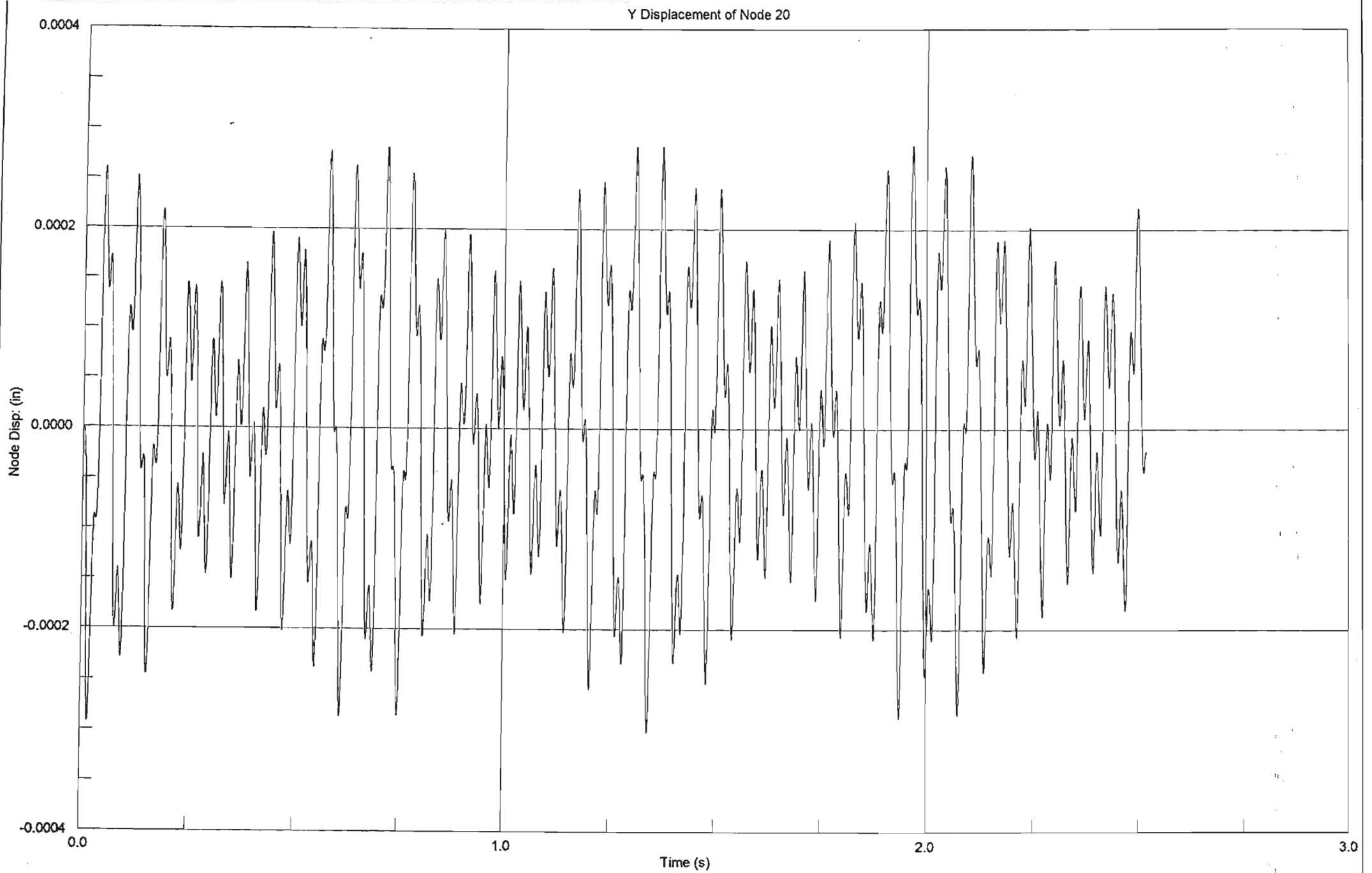




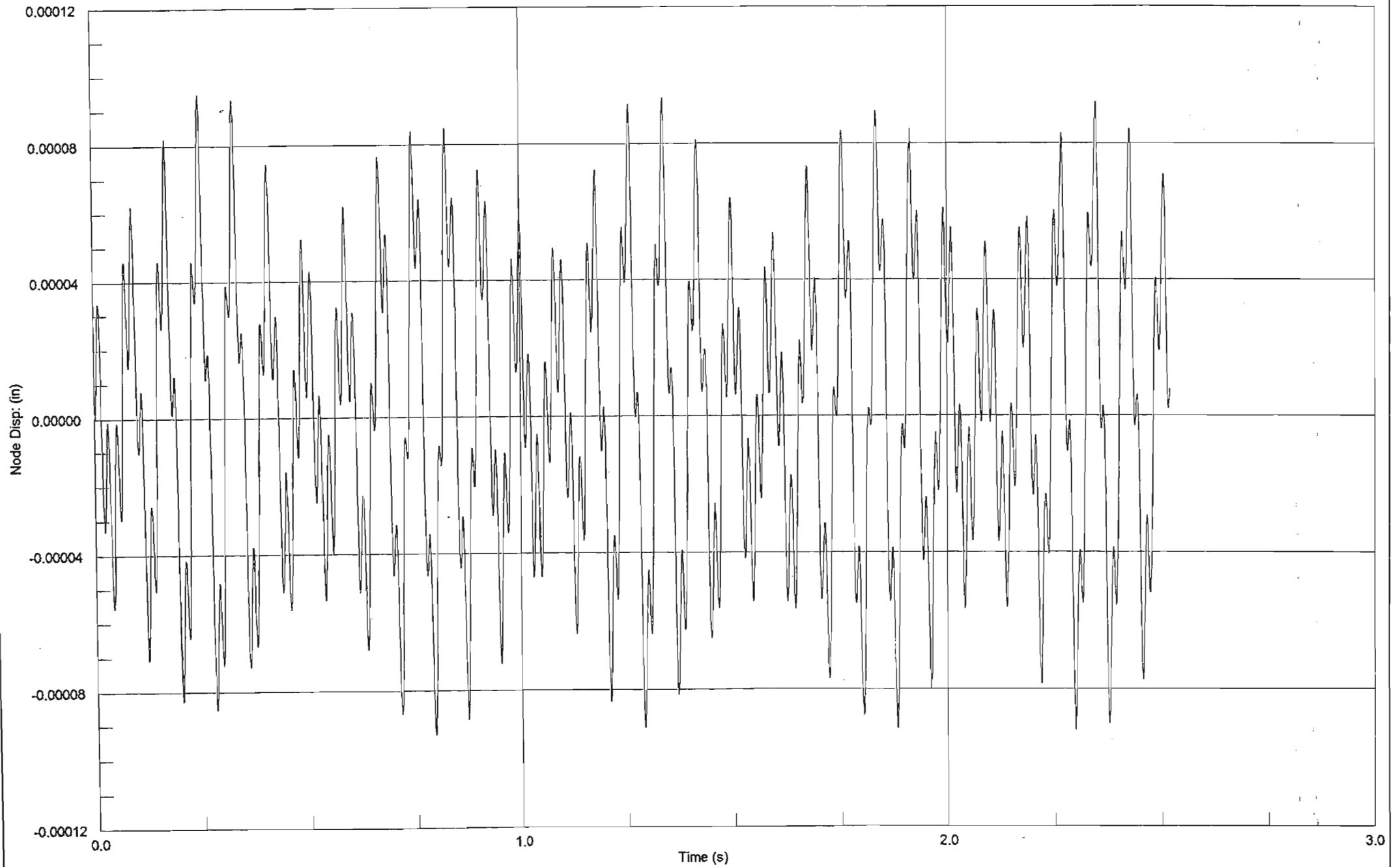


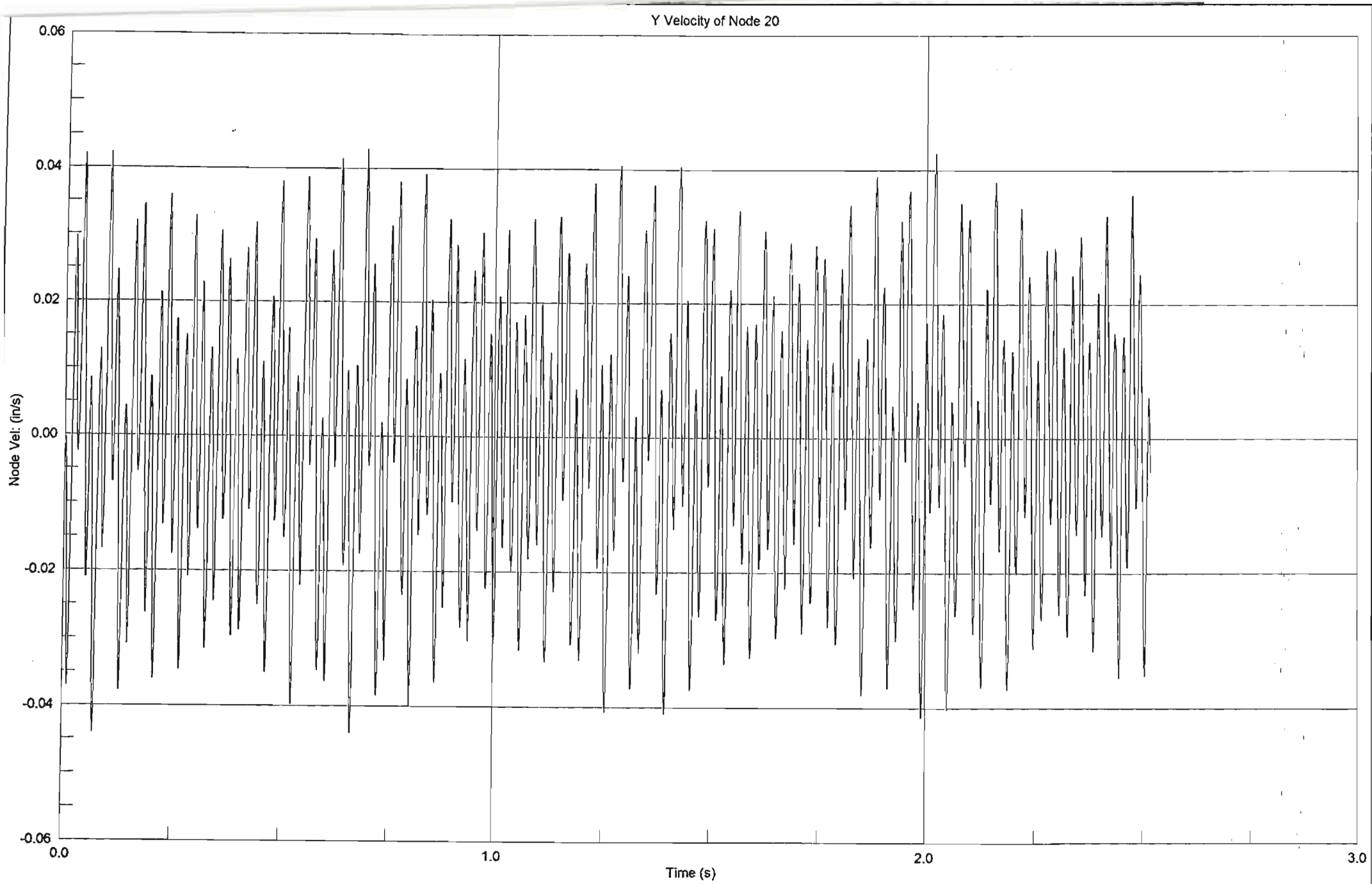
Z Displacement of Node 8



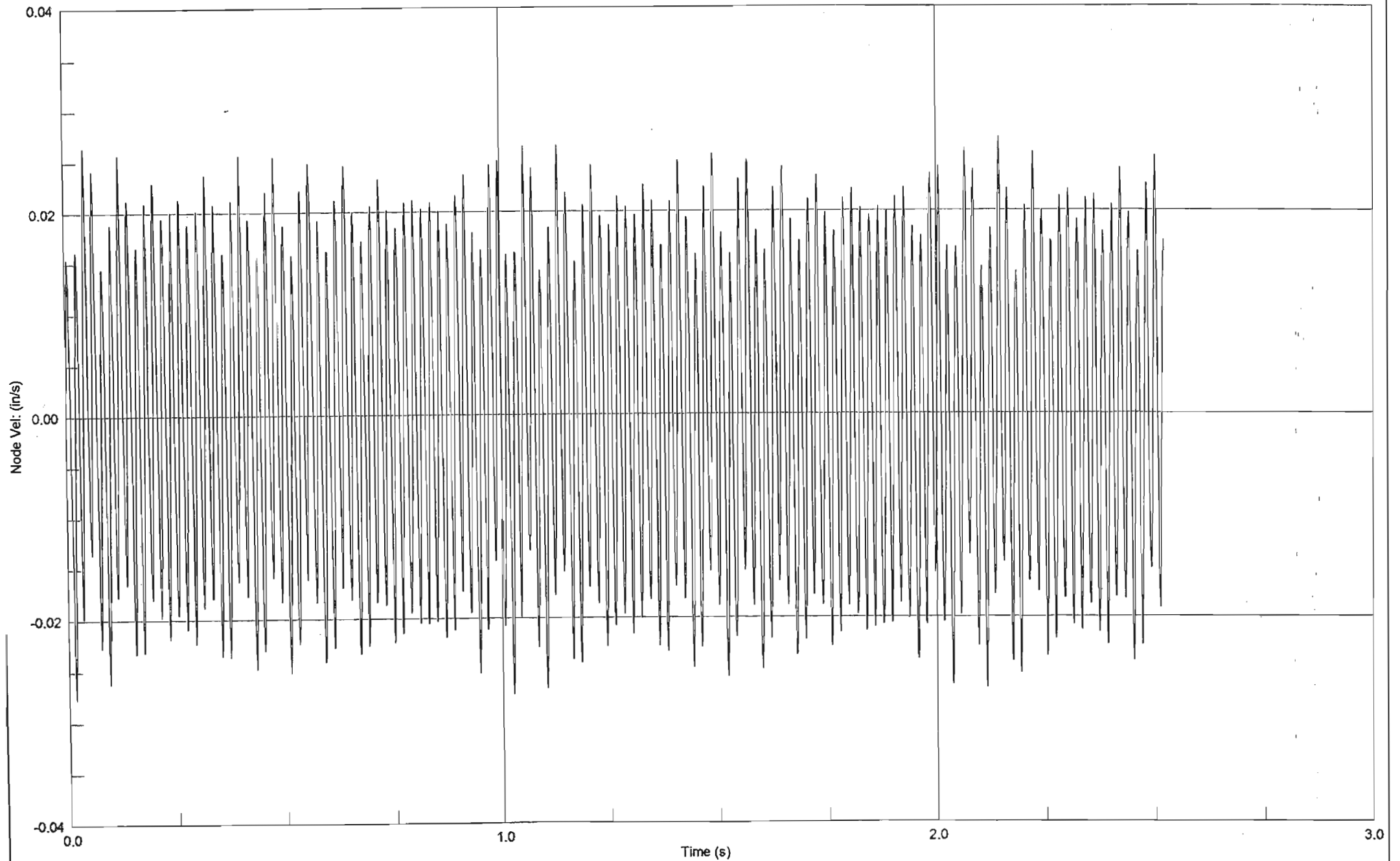


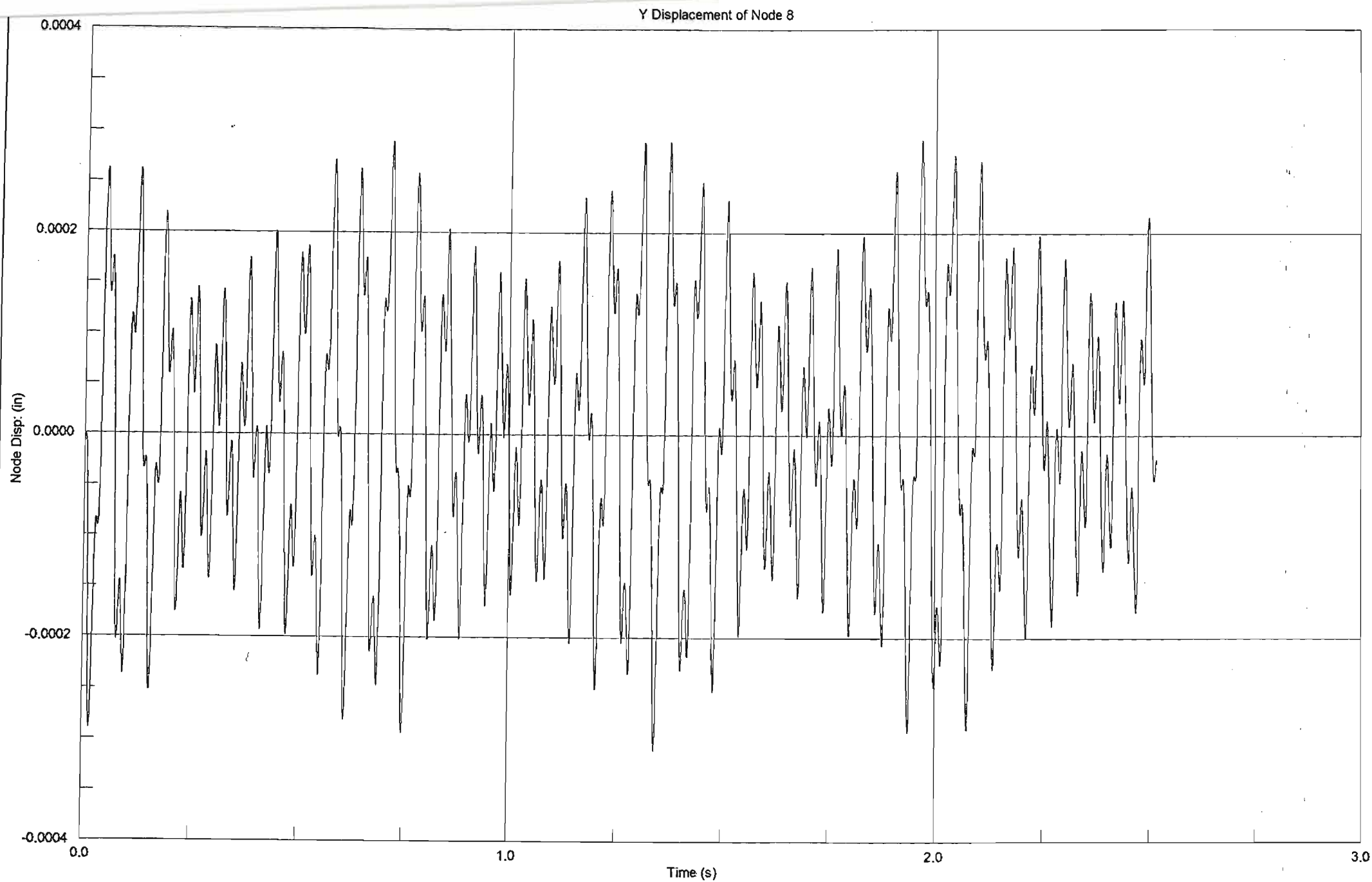
Z Displacement of Node 20



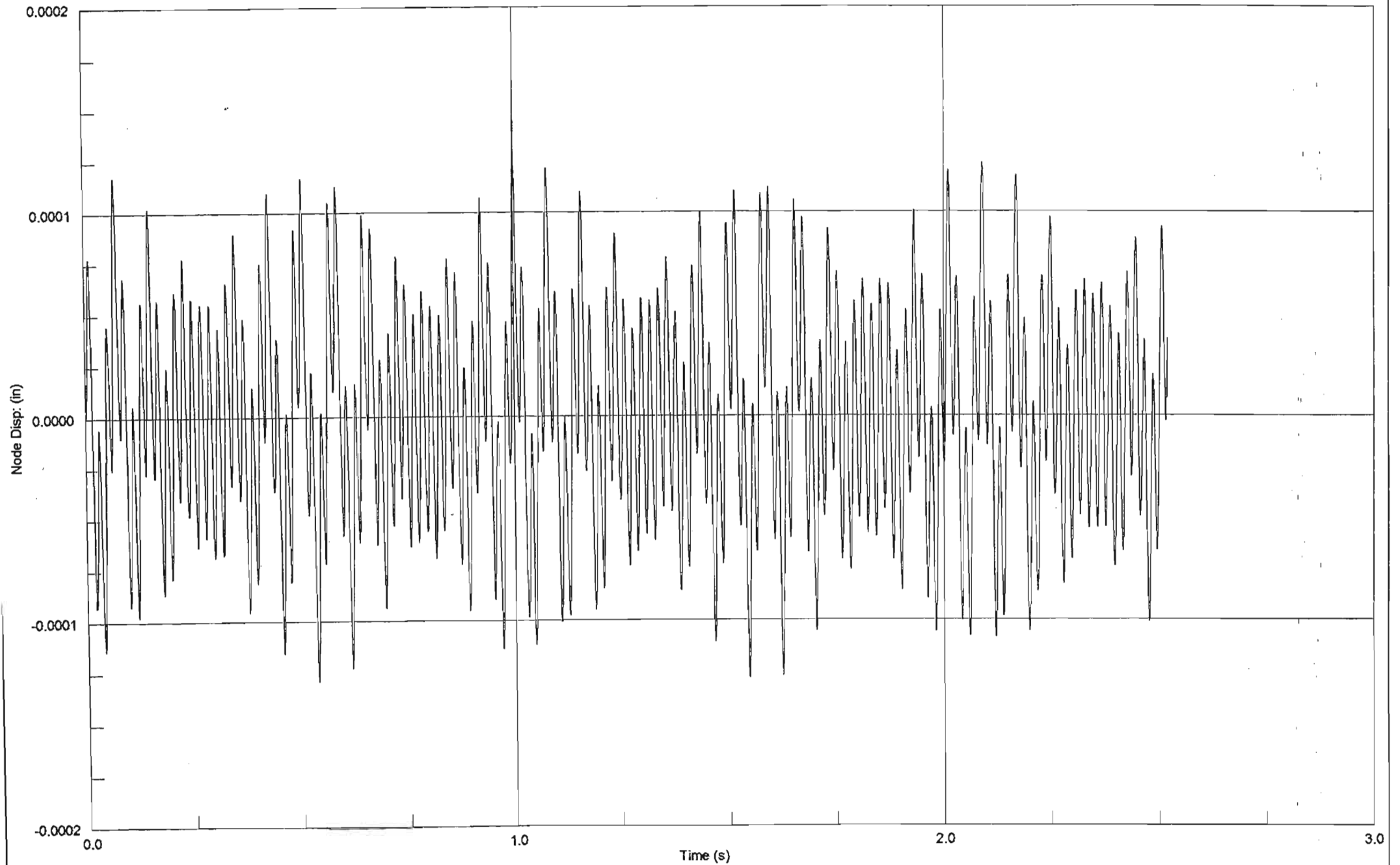


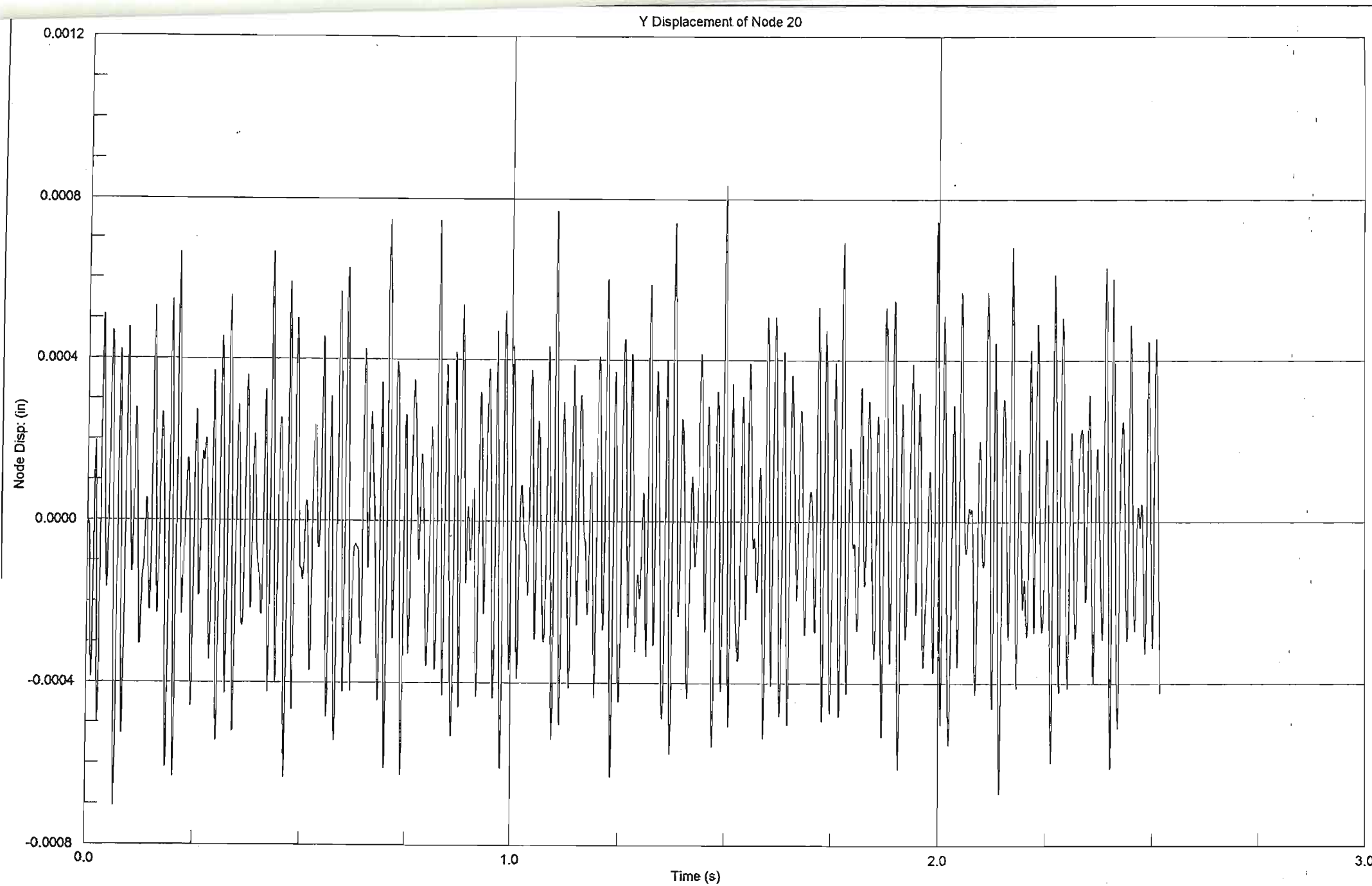
Z Velocity of Node 20

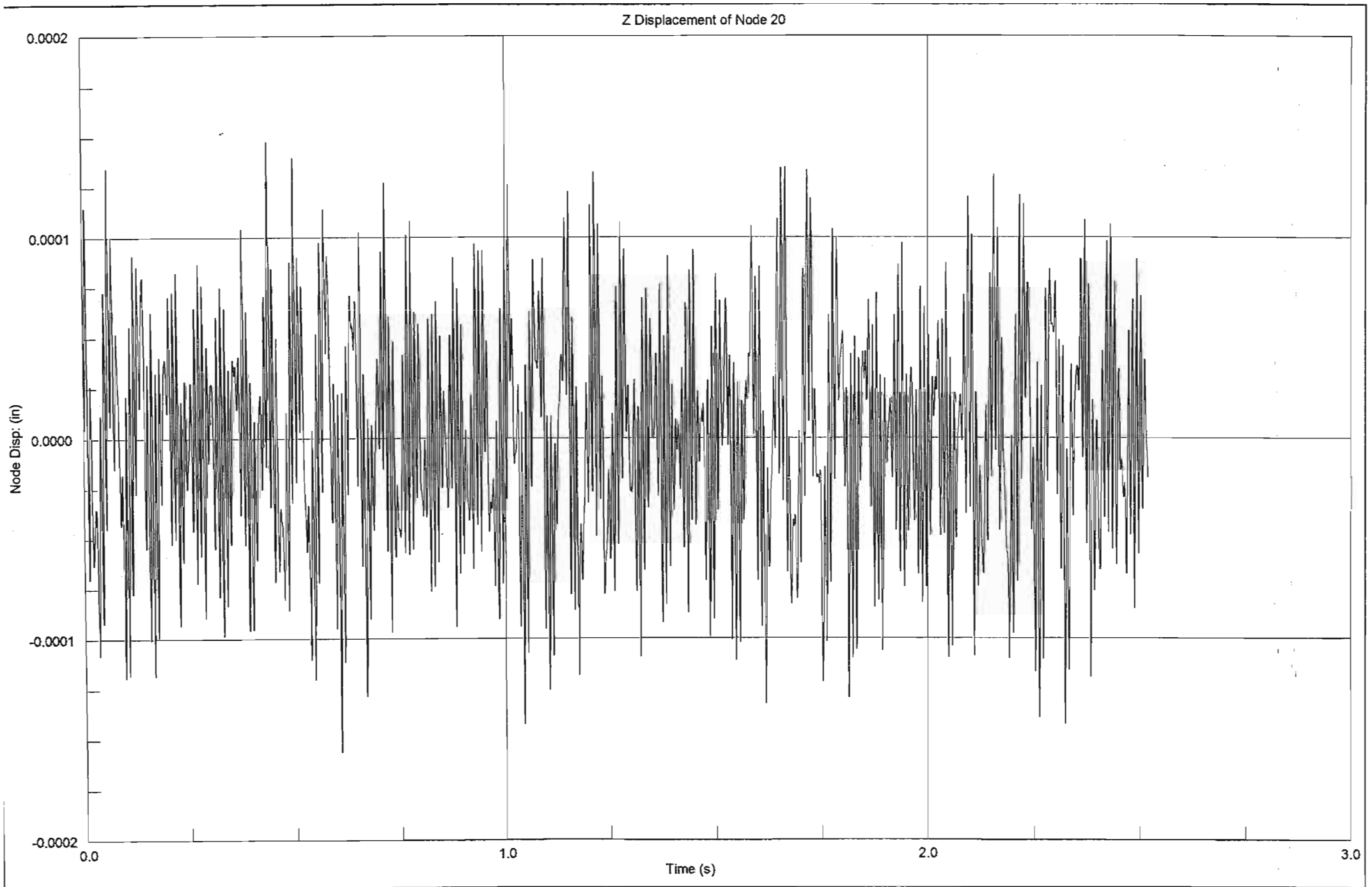


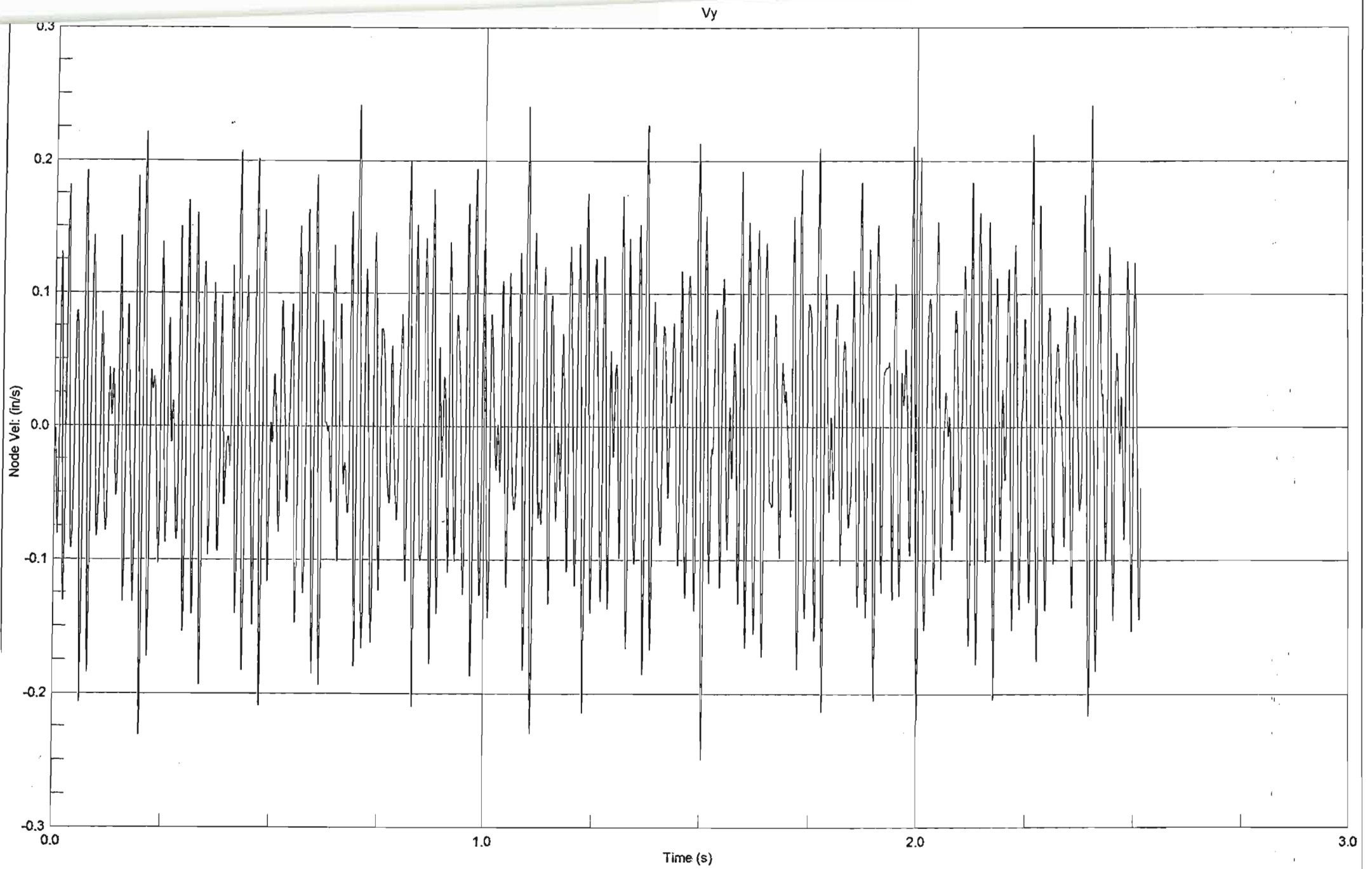


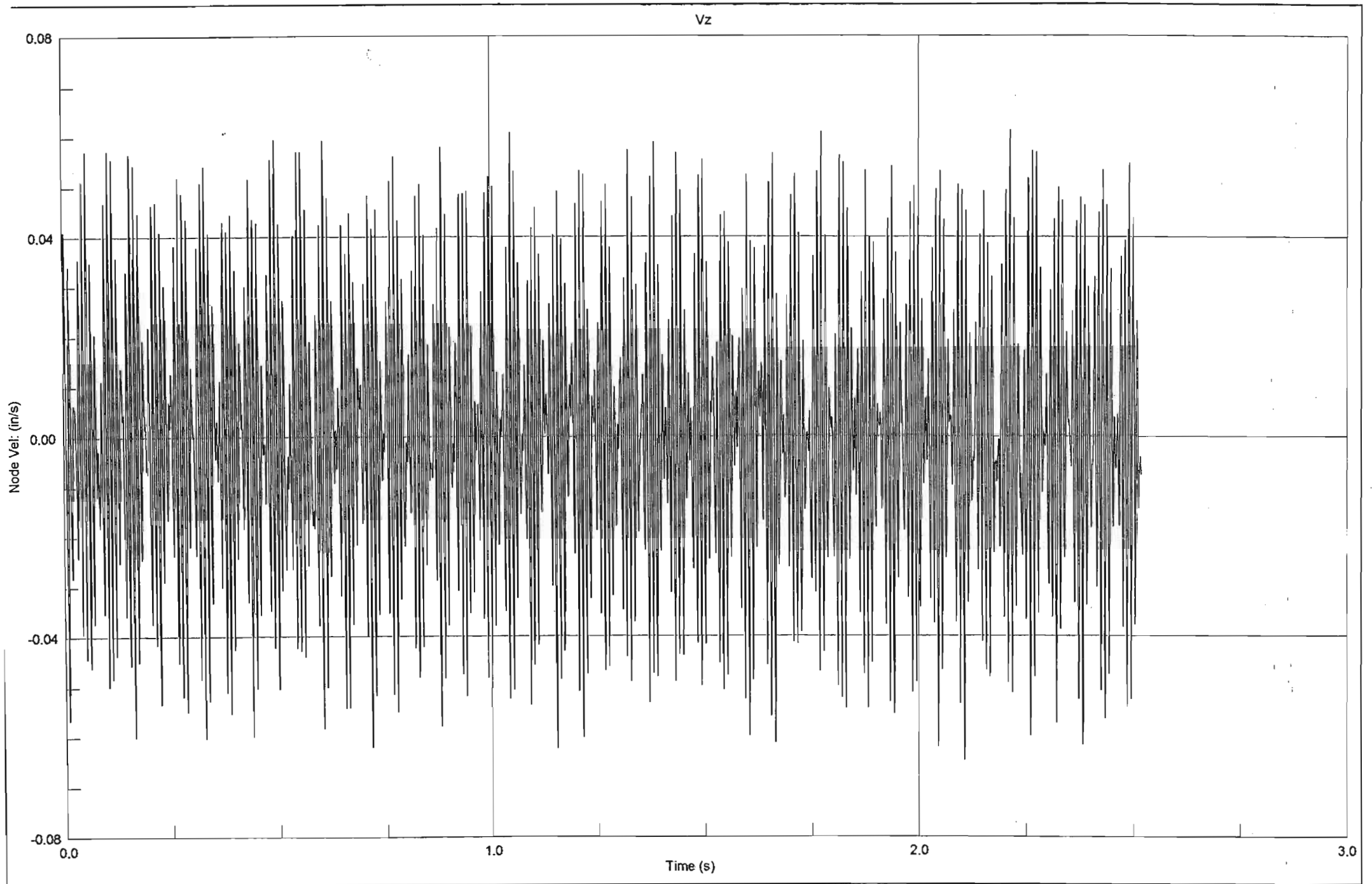
Z Displacement of Node 8

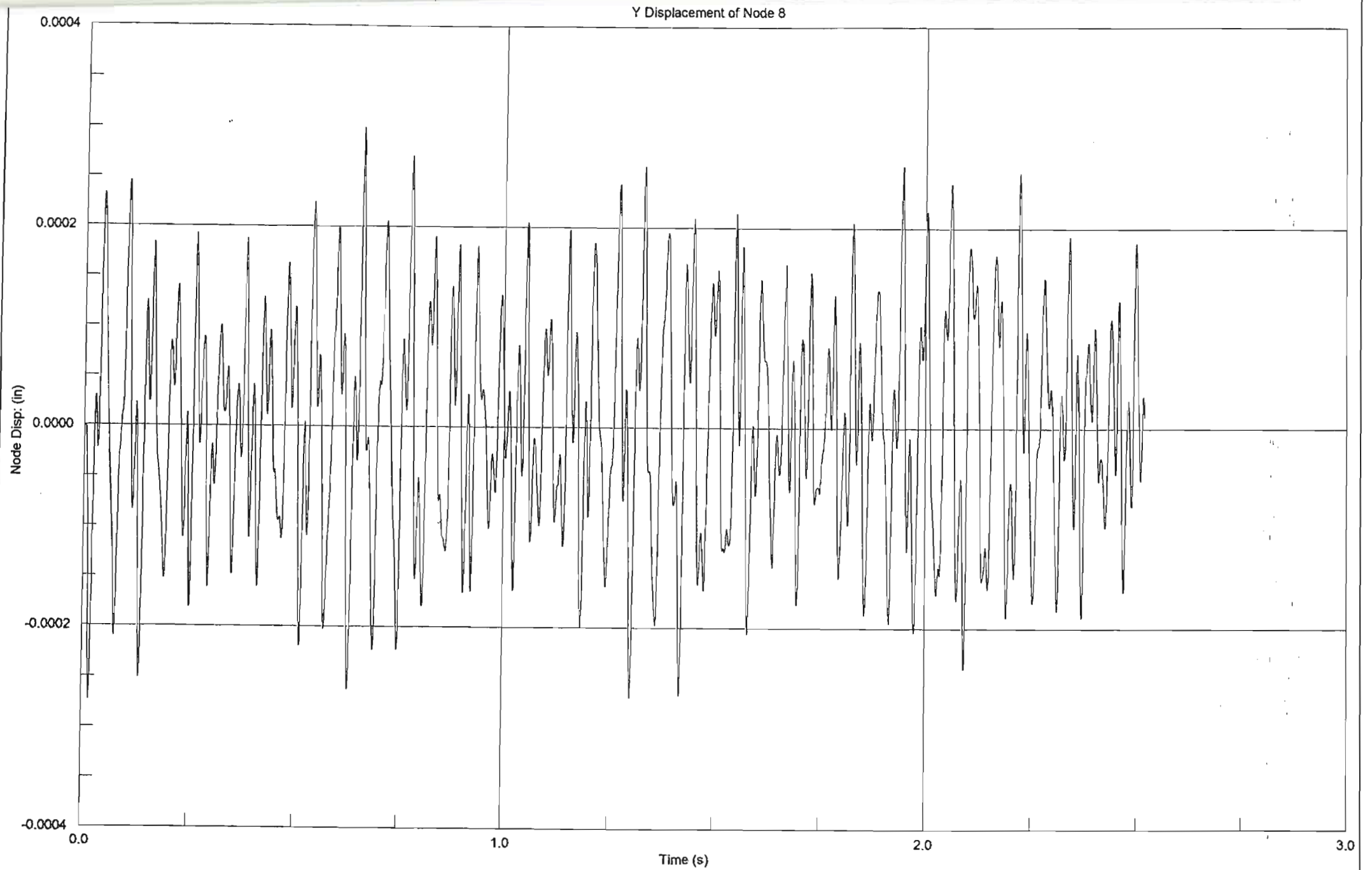




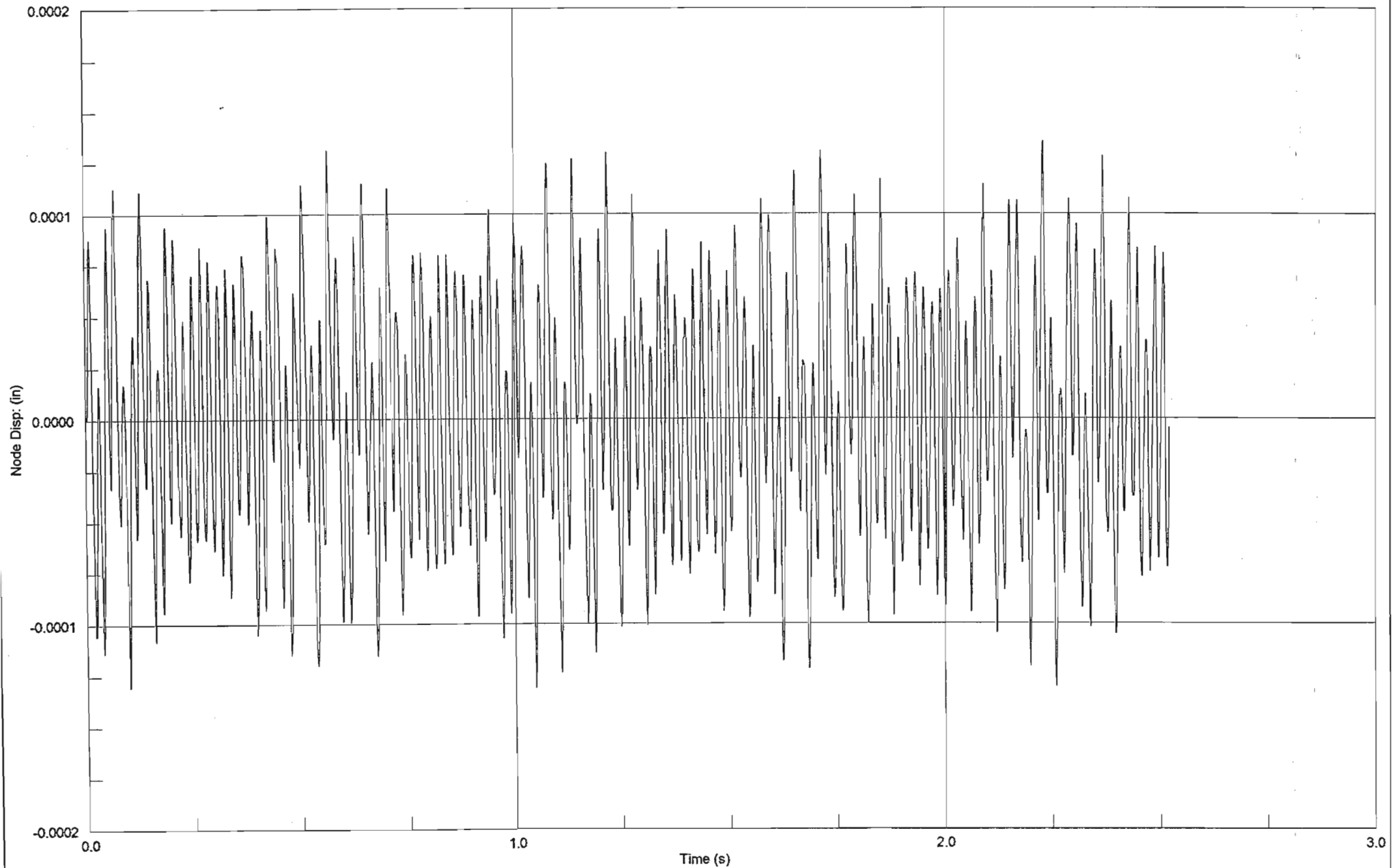




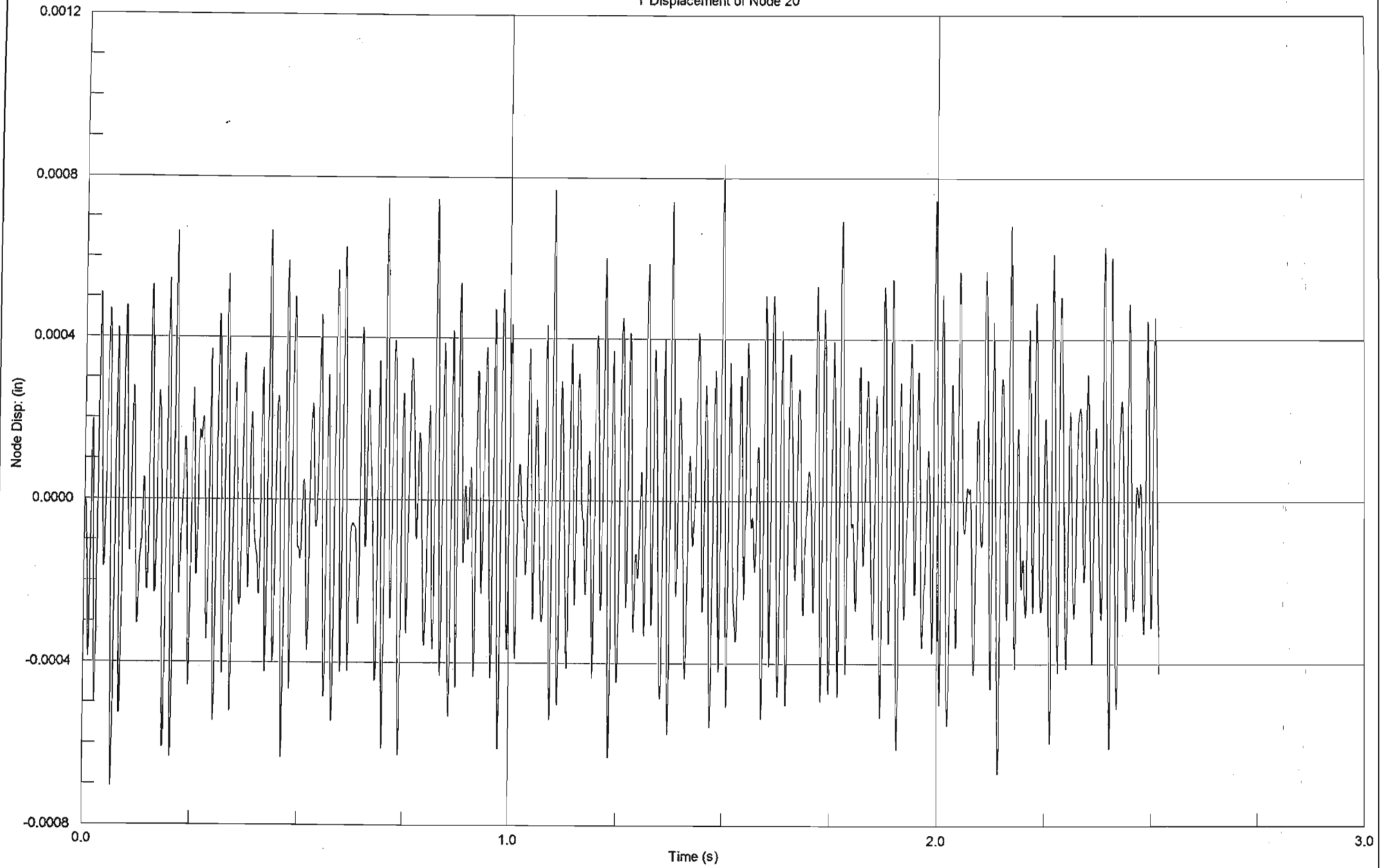




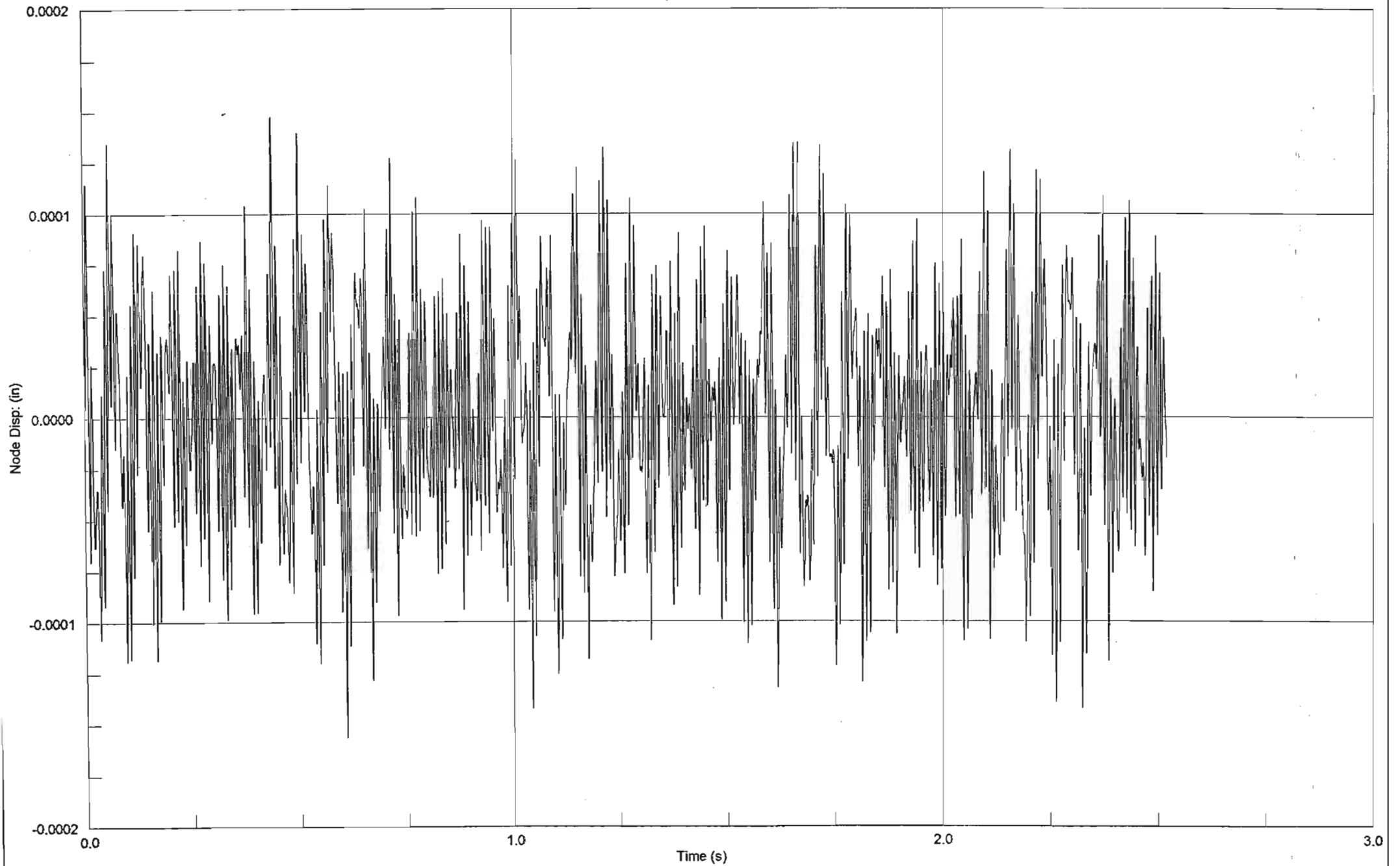
Z Displacement of Node 8

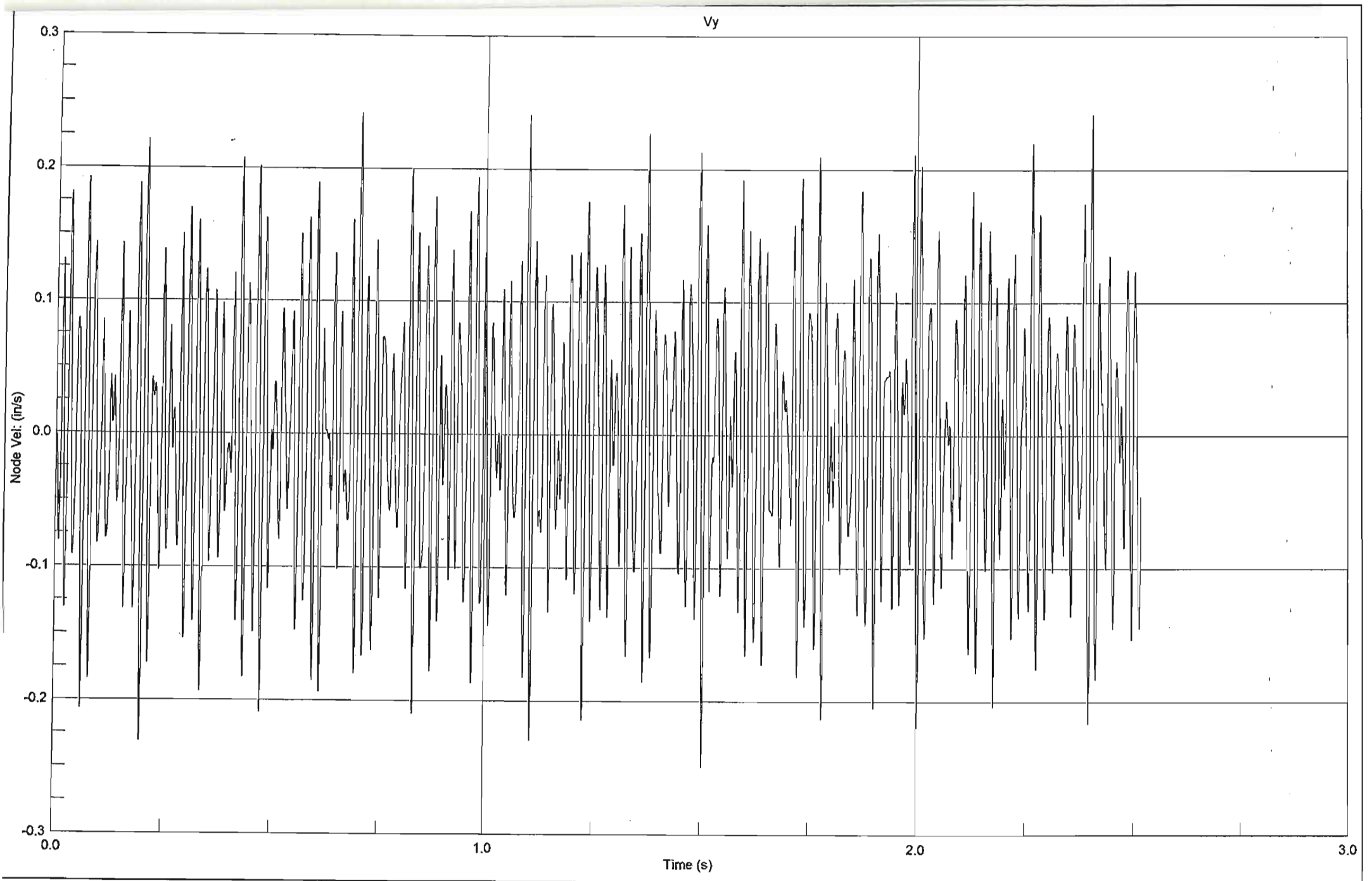


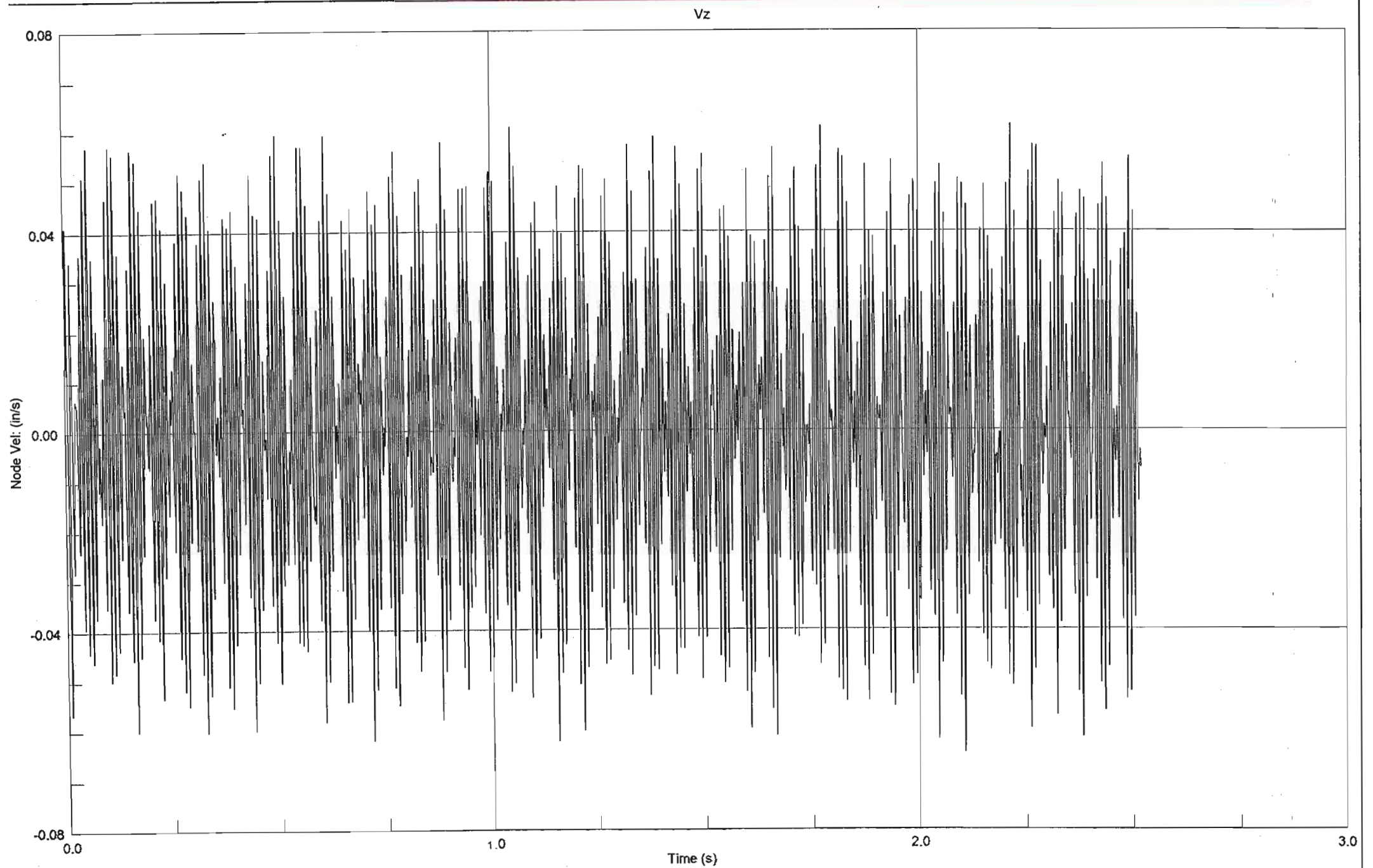
Y Displacement of Node 20

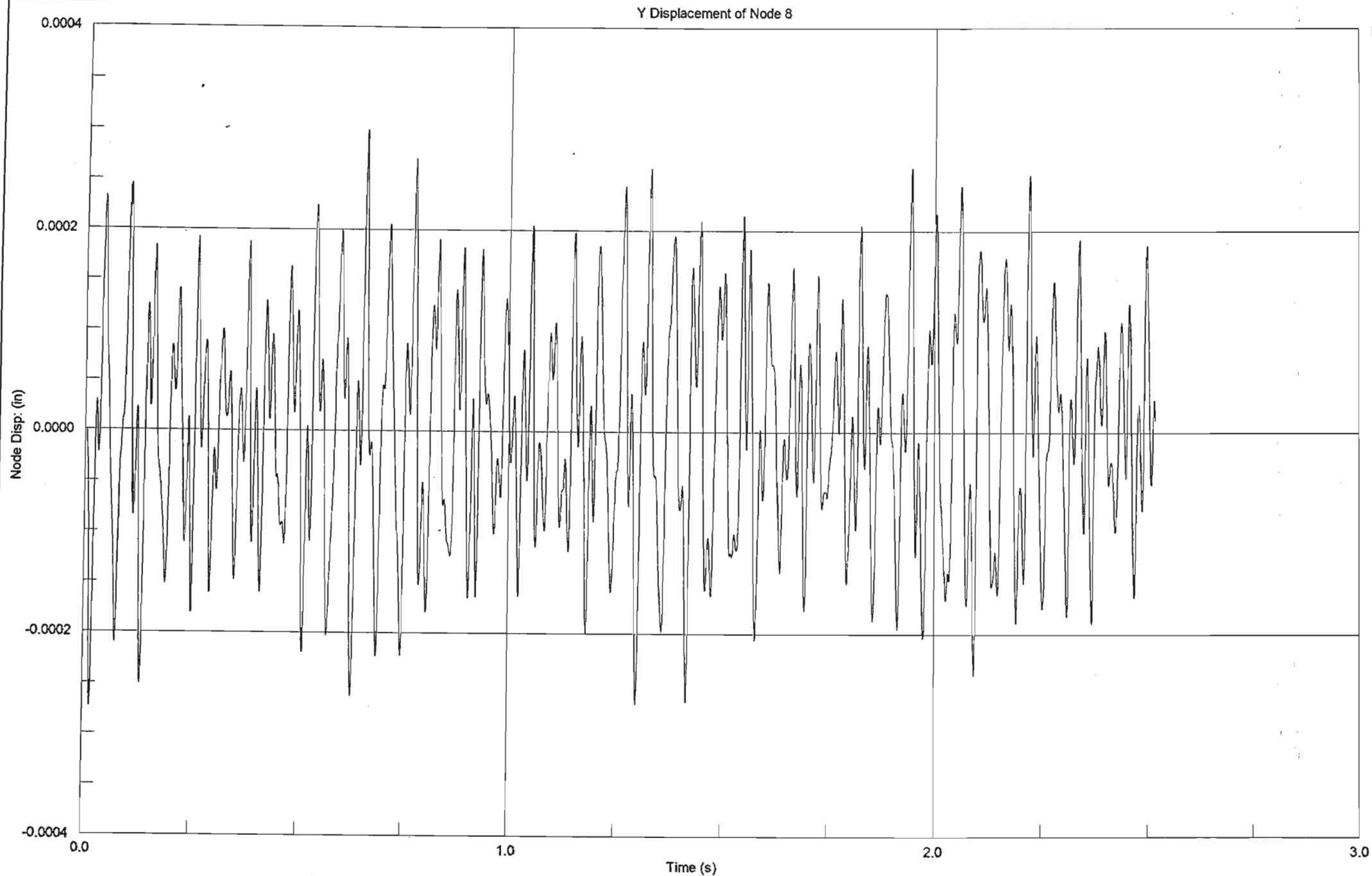


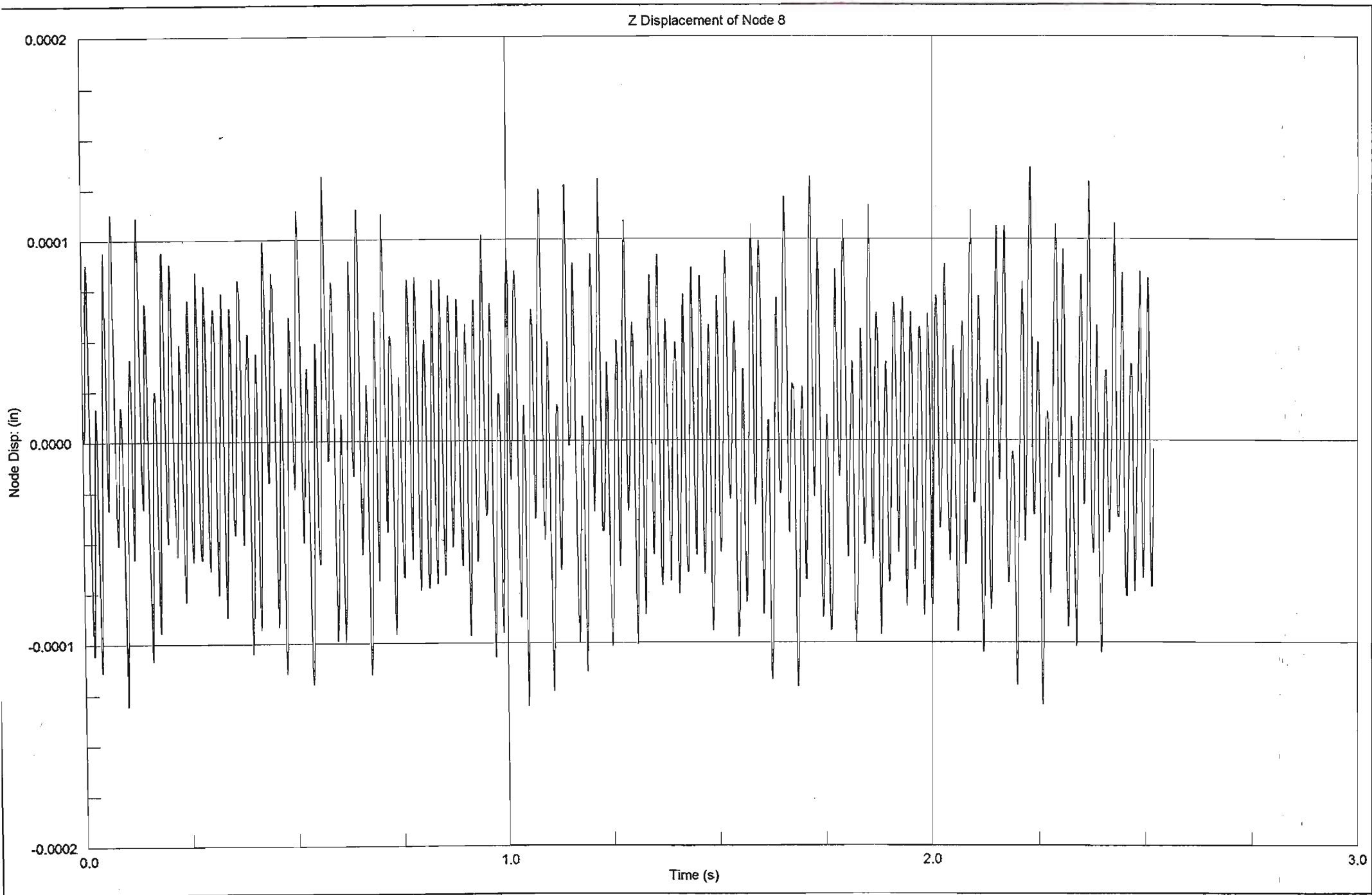
Z Displacement of Node 20

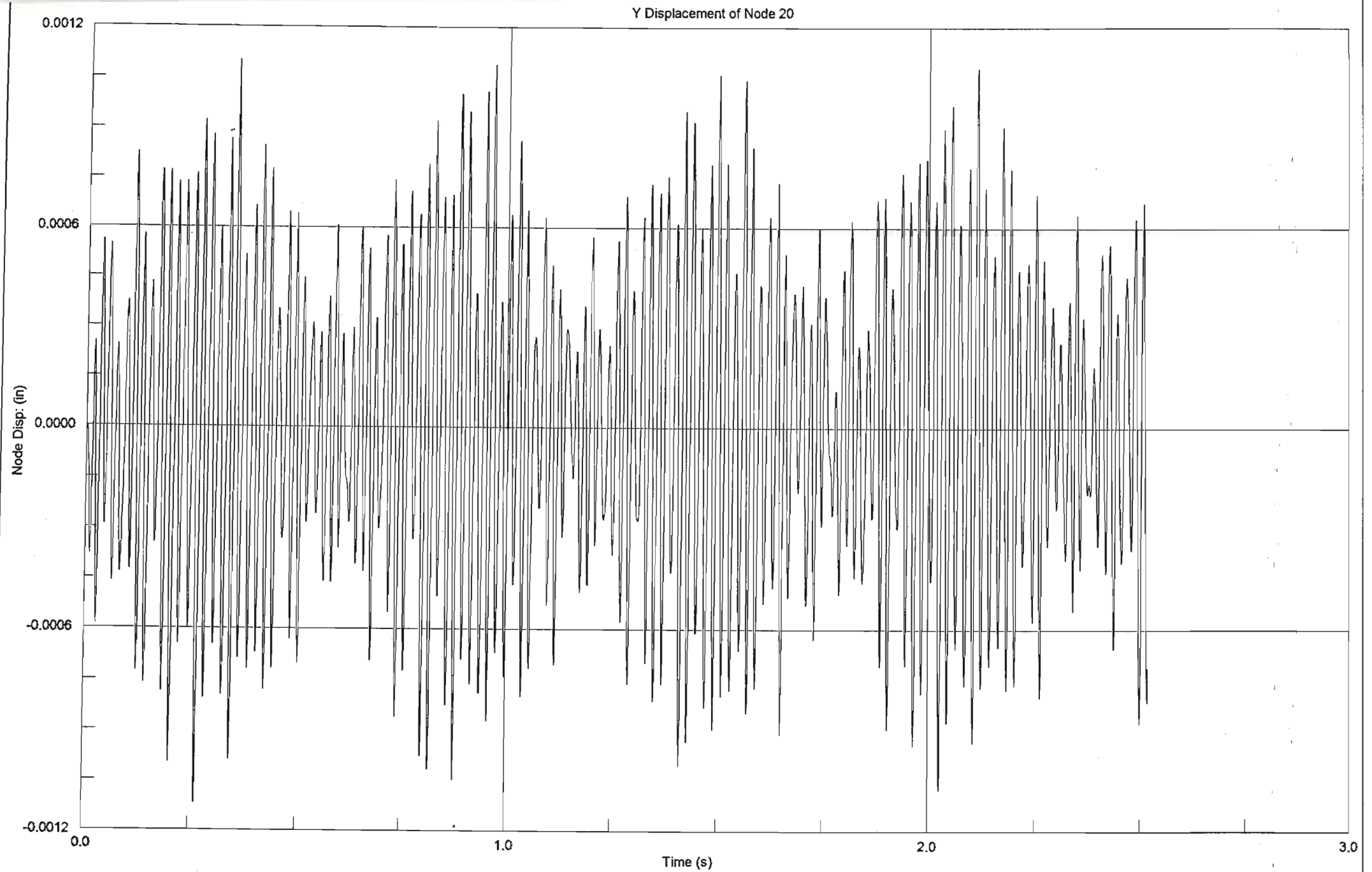




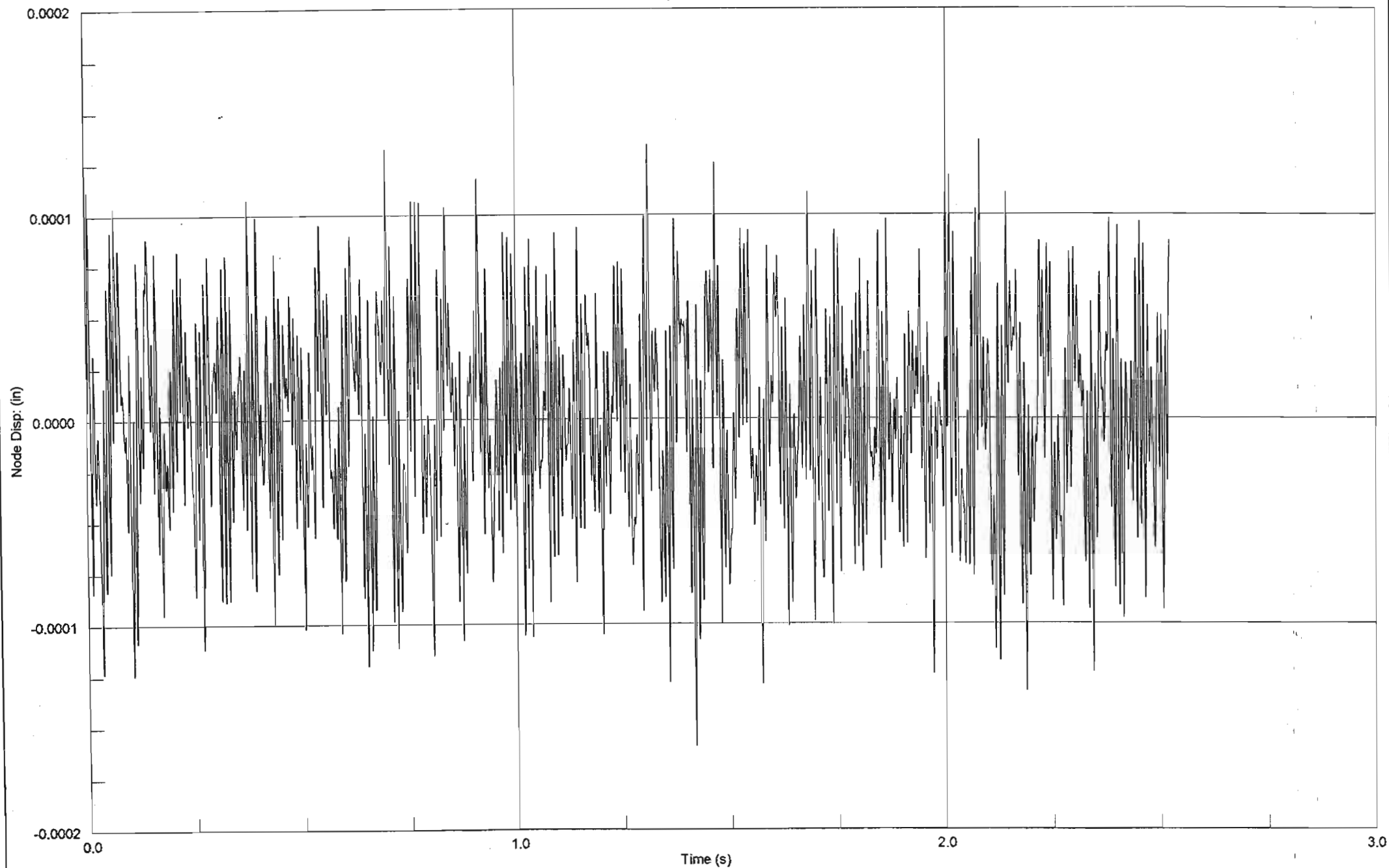


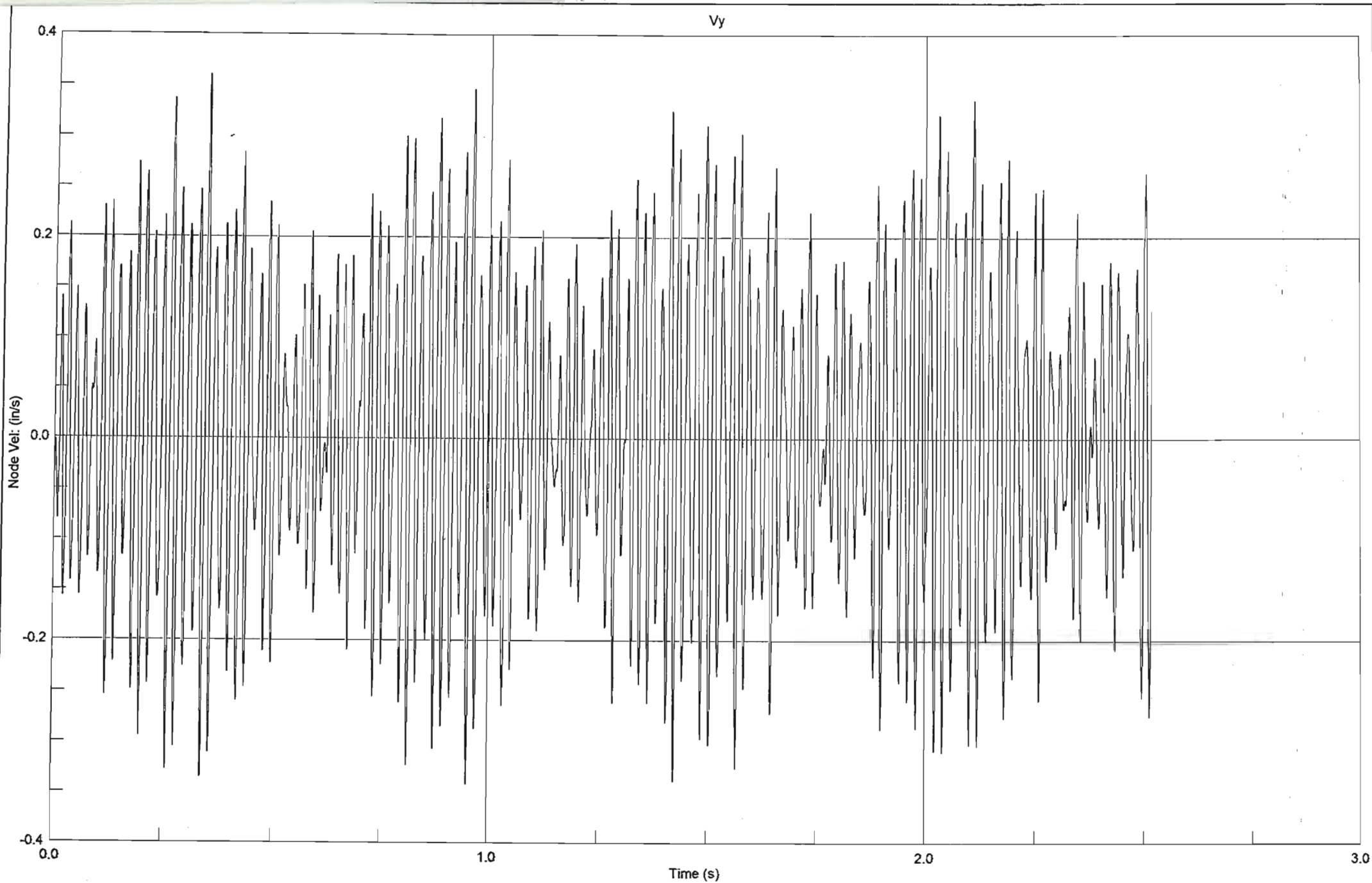


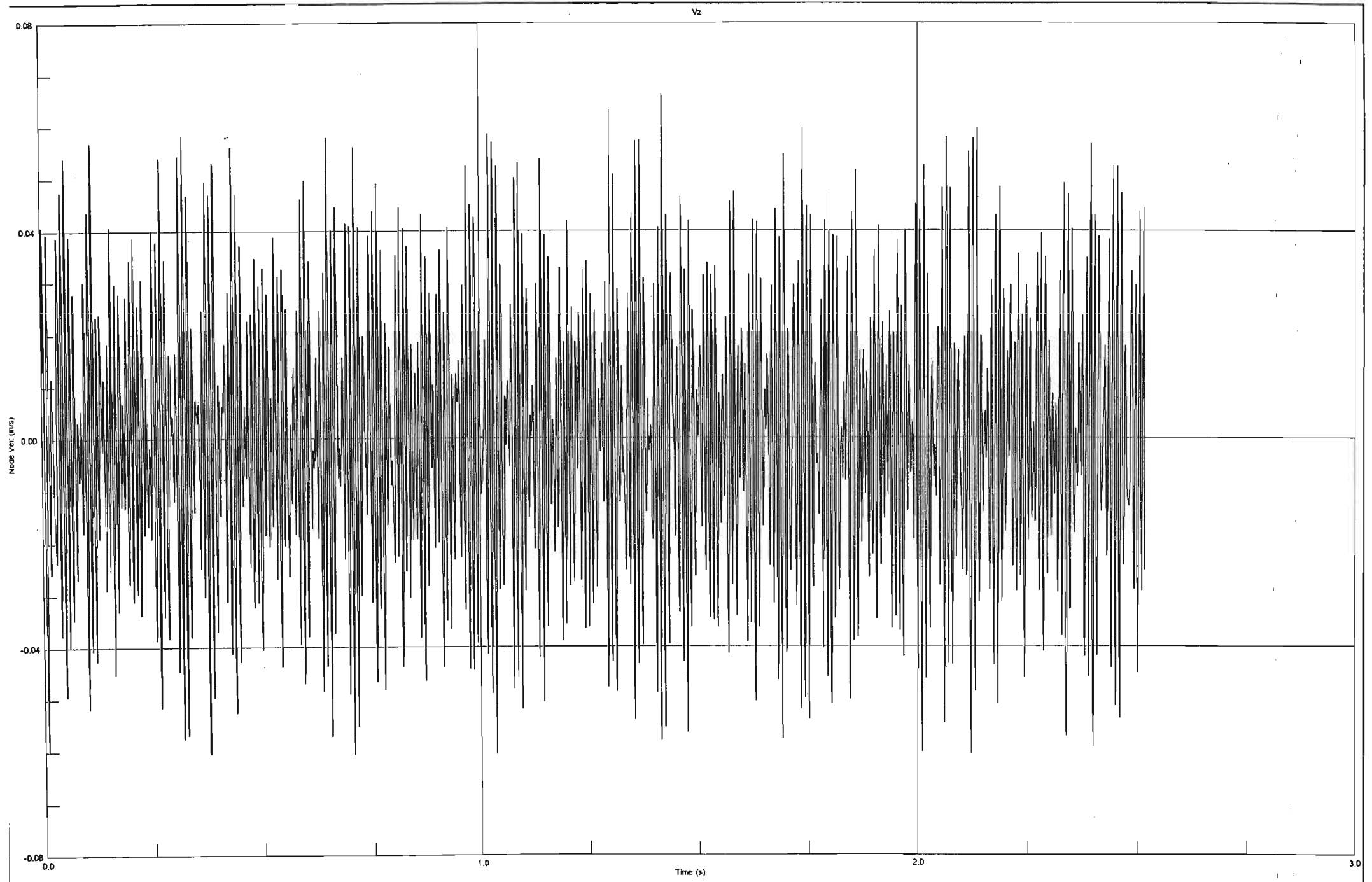


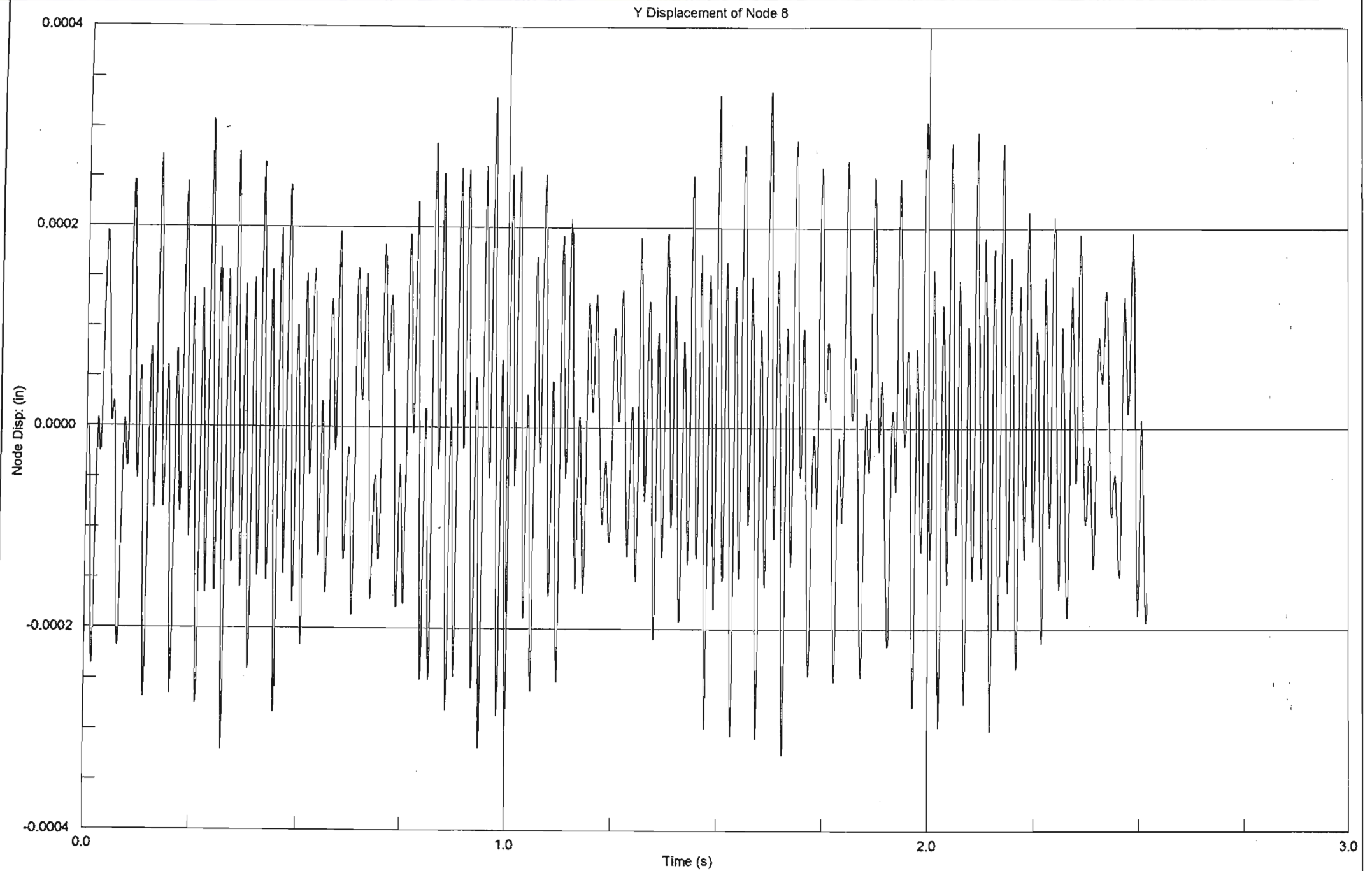


Z Displacement of Node 20

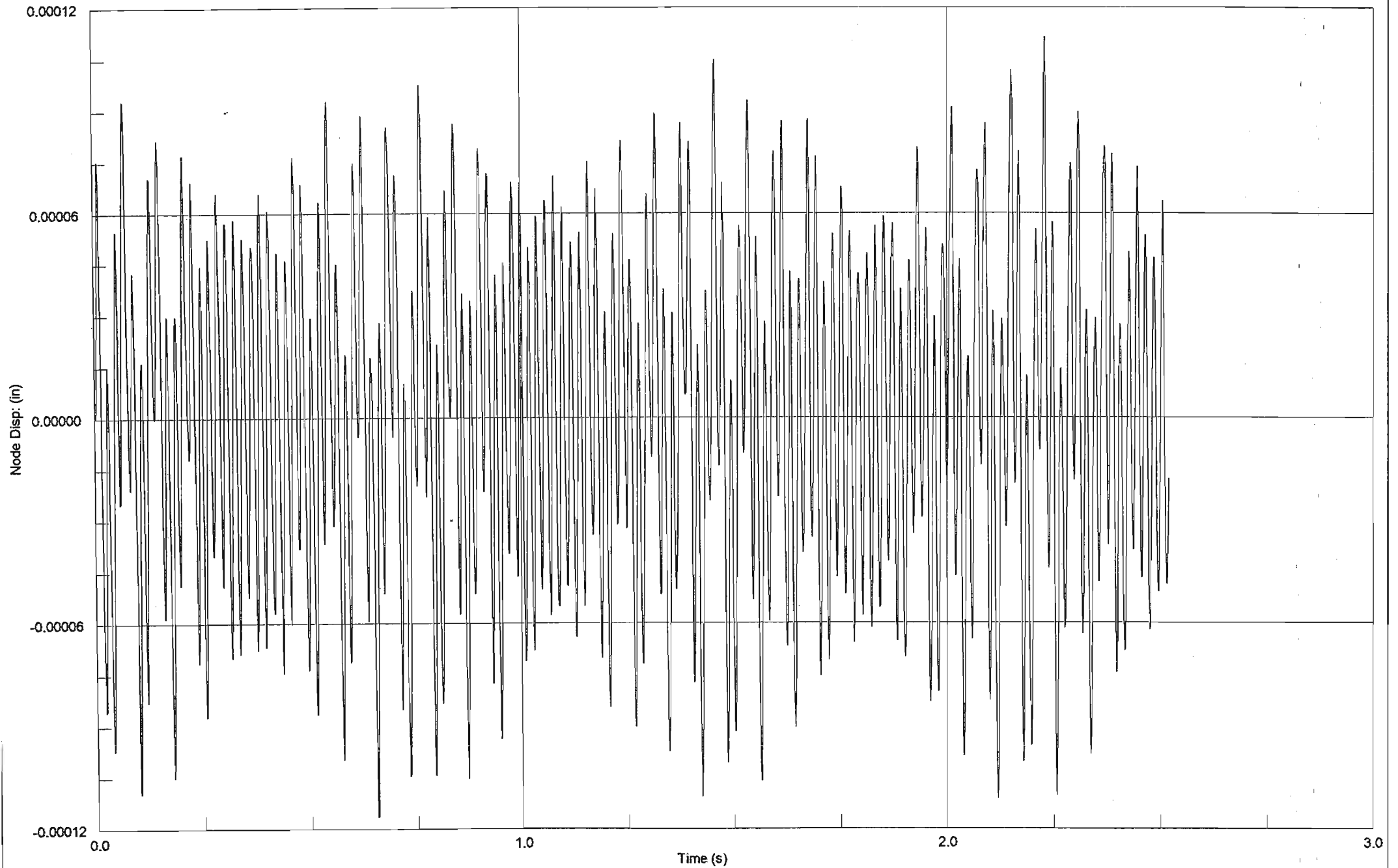


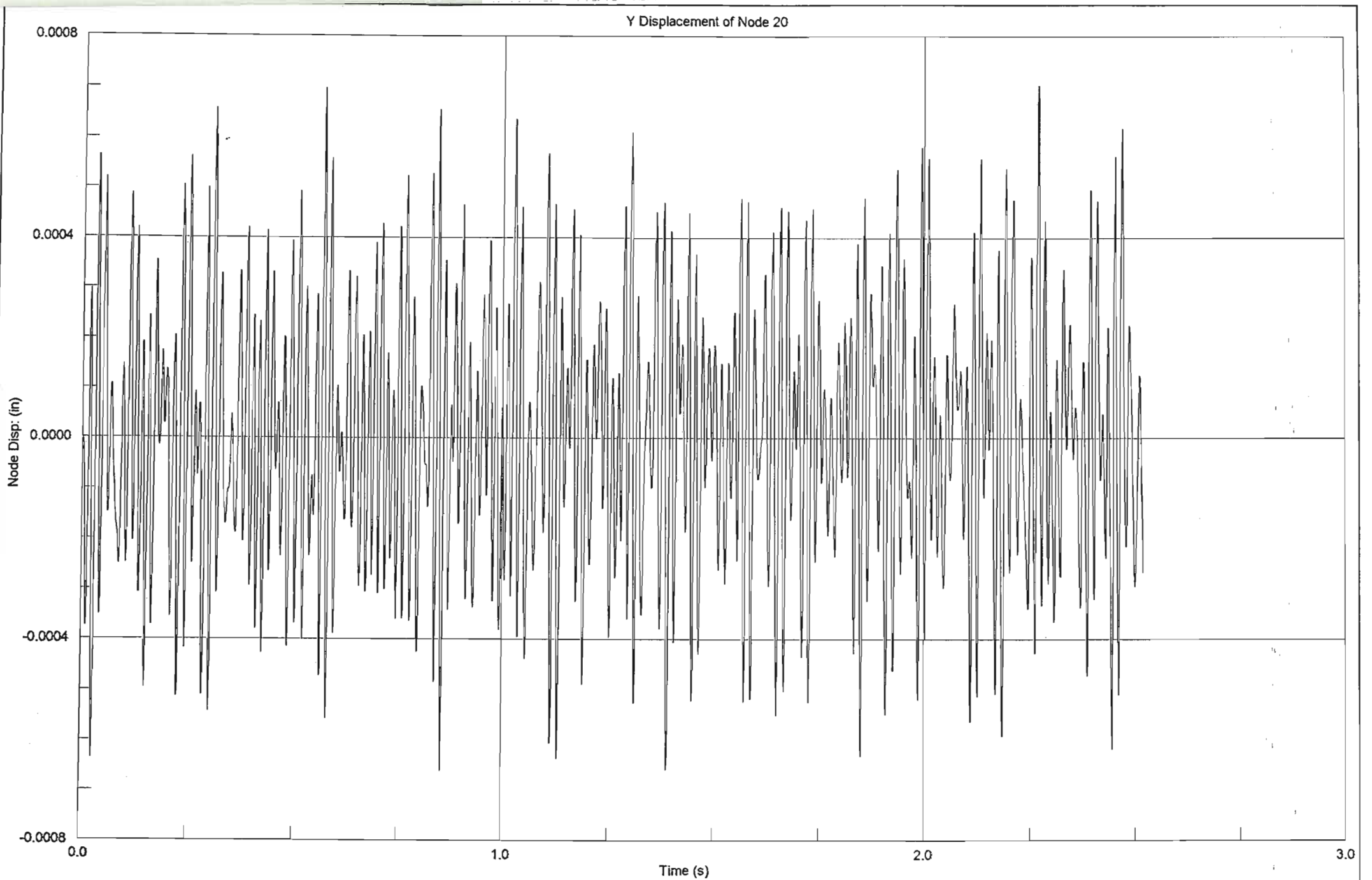




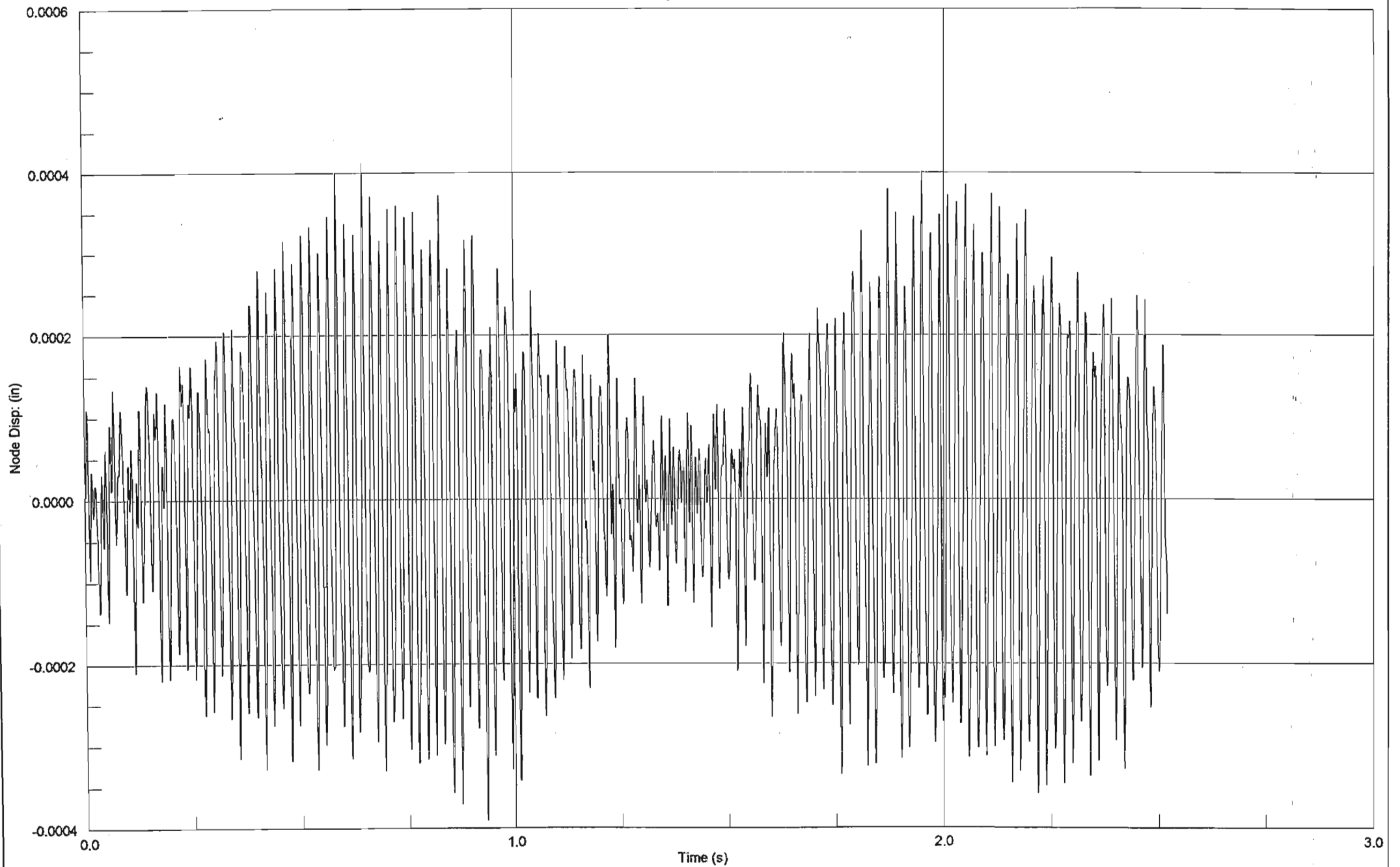


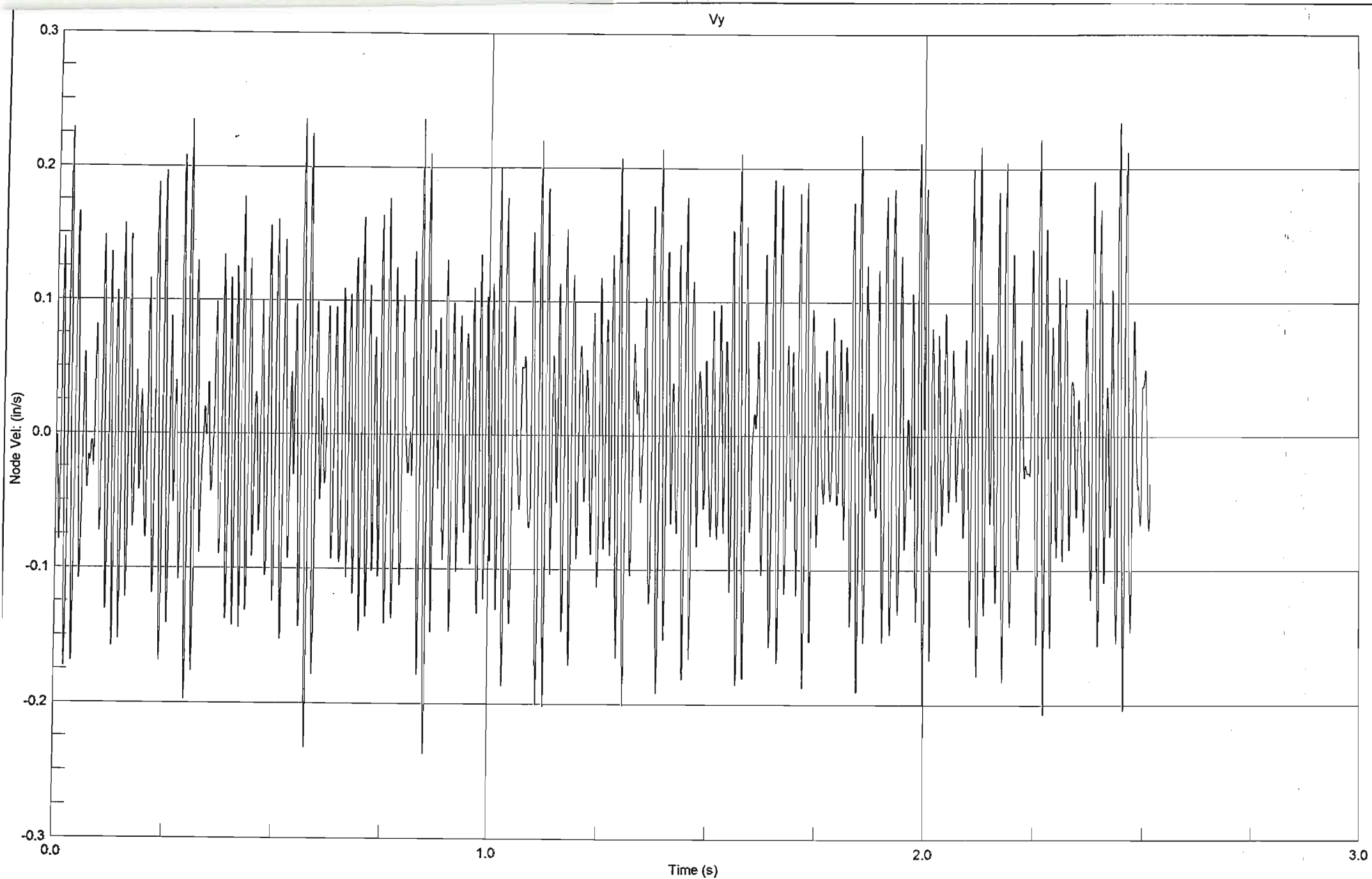
Z Displacement of Node 8

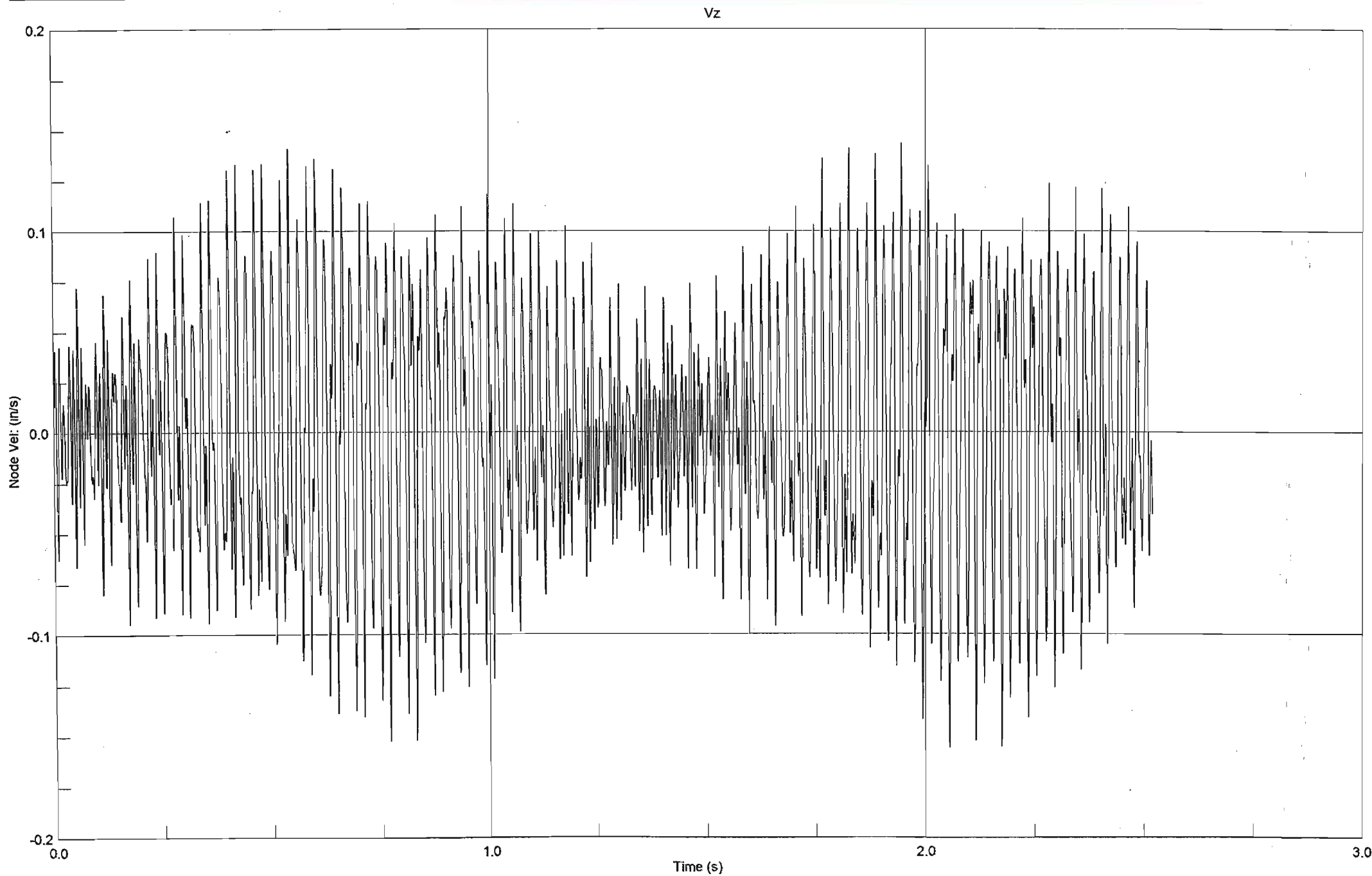


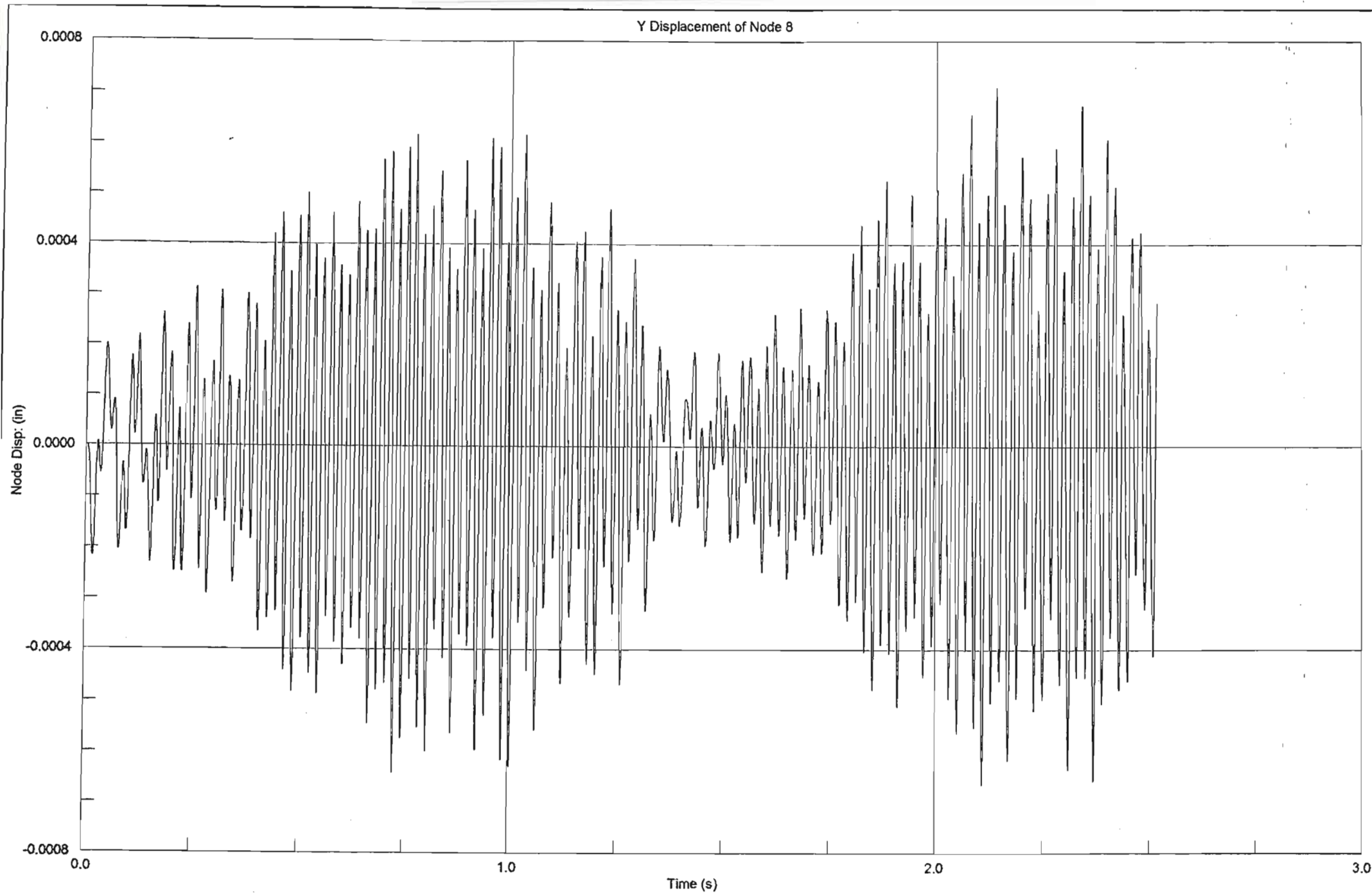


Z Displacement of Node 20

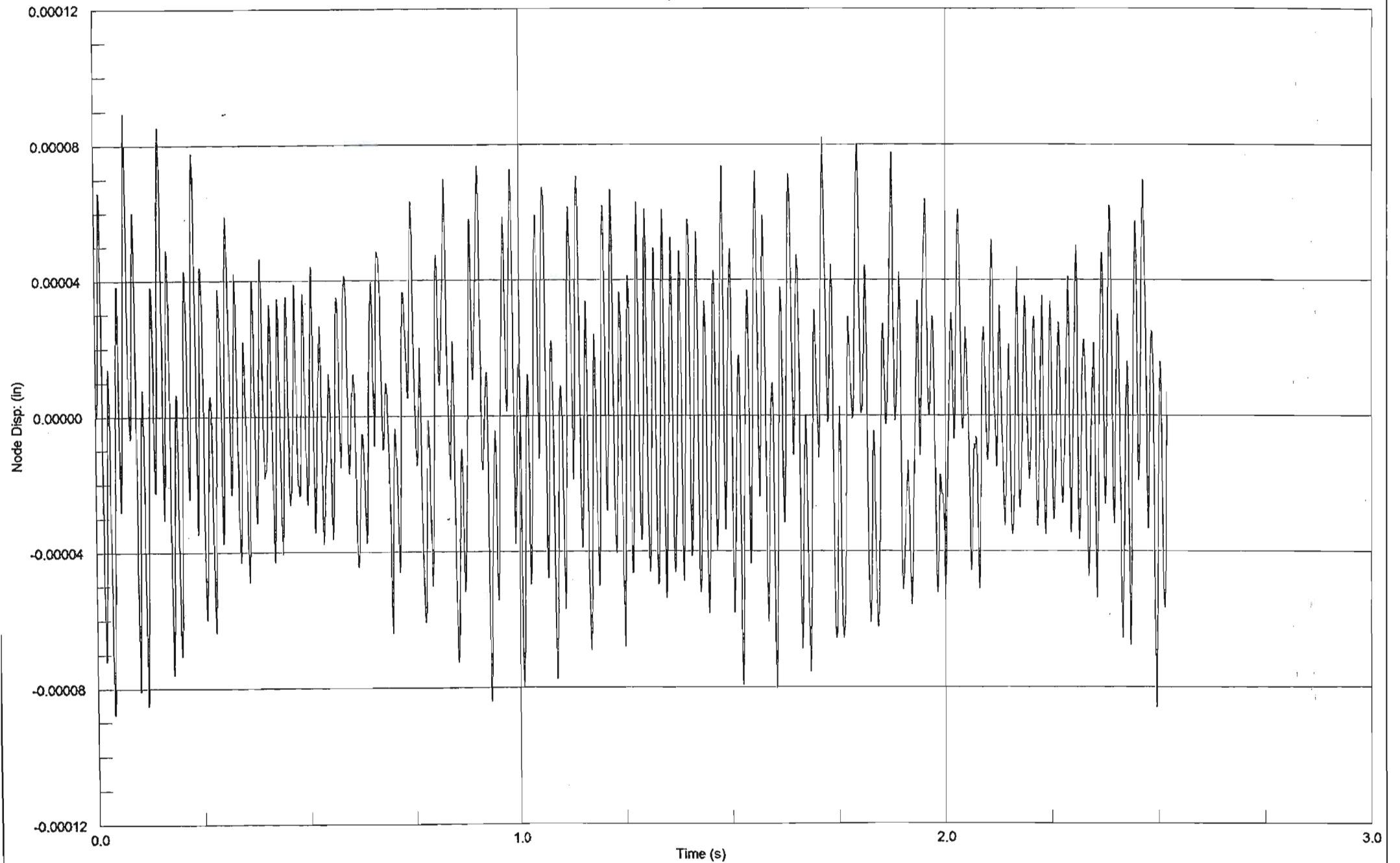


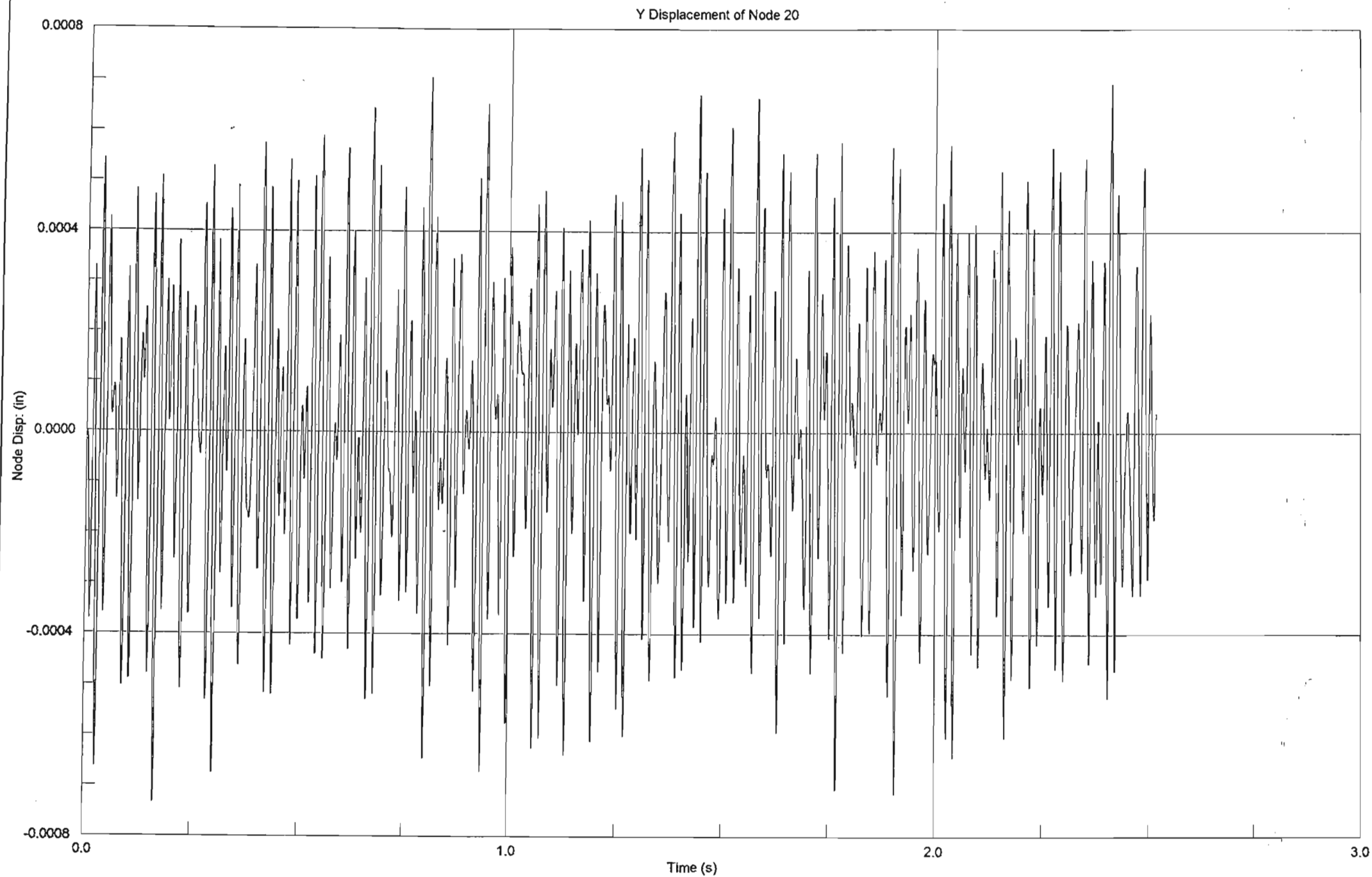




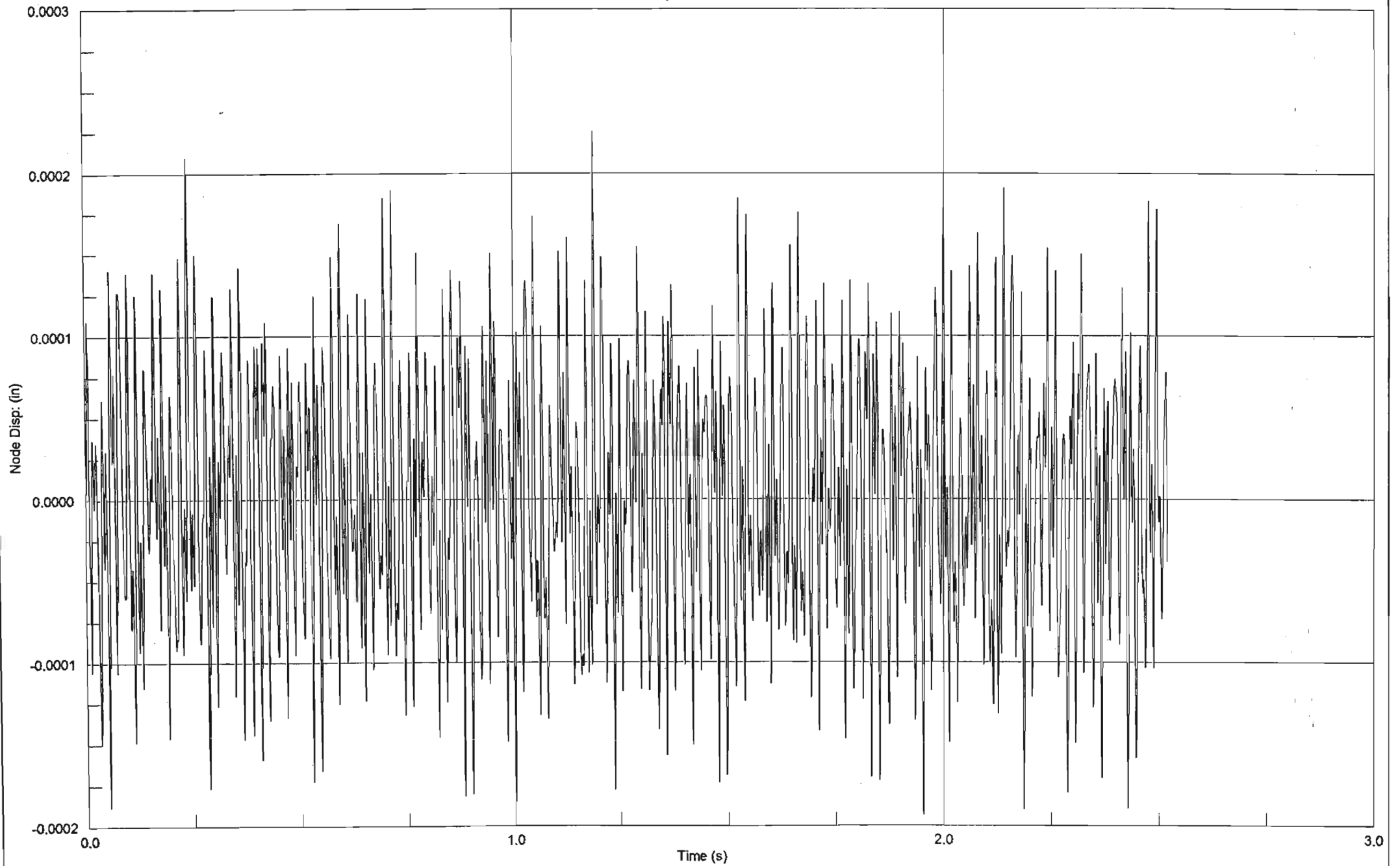


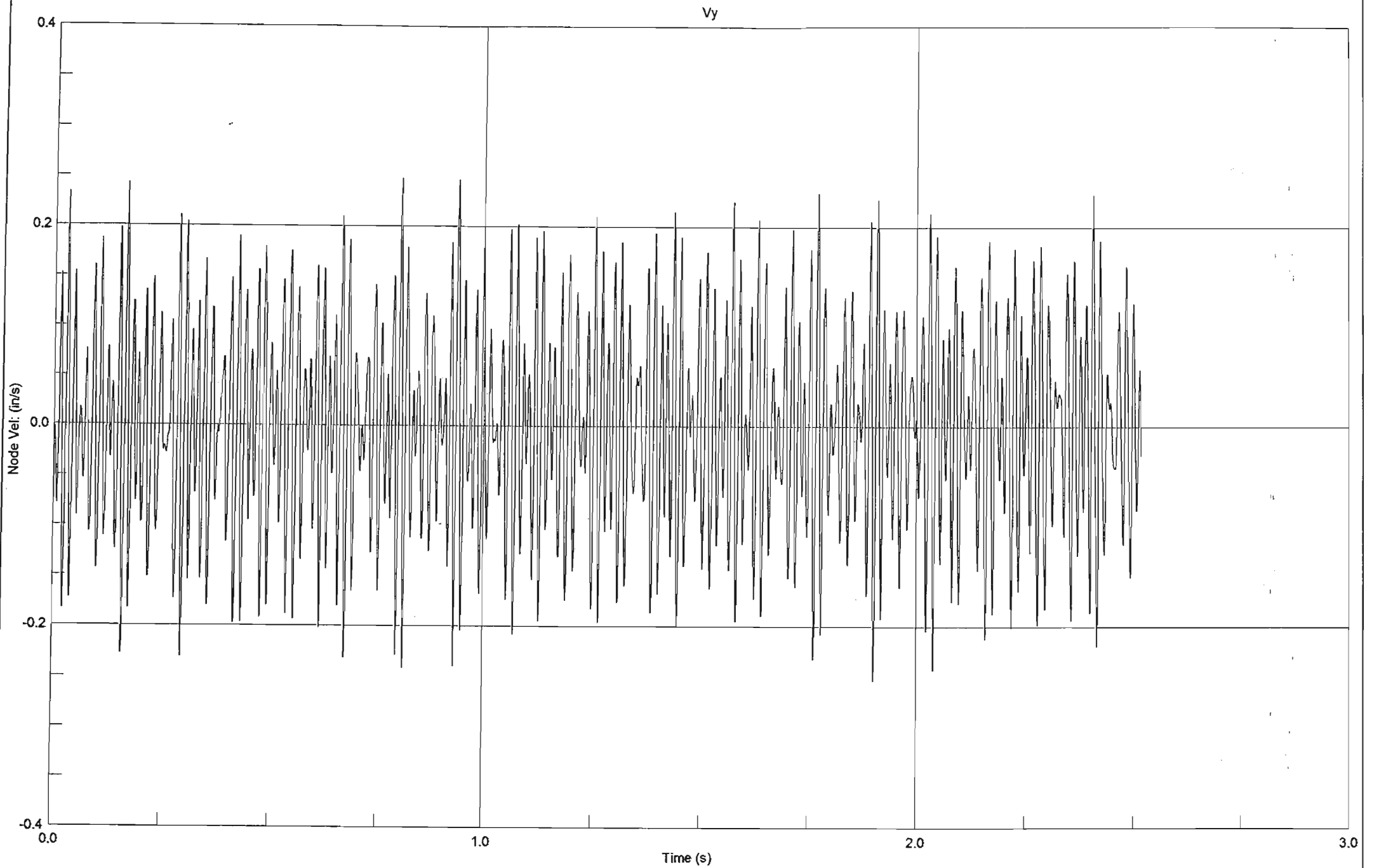
Z Displacement of Node 8

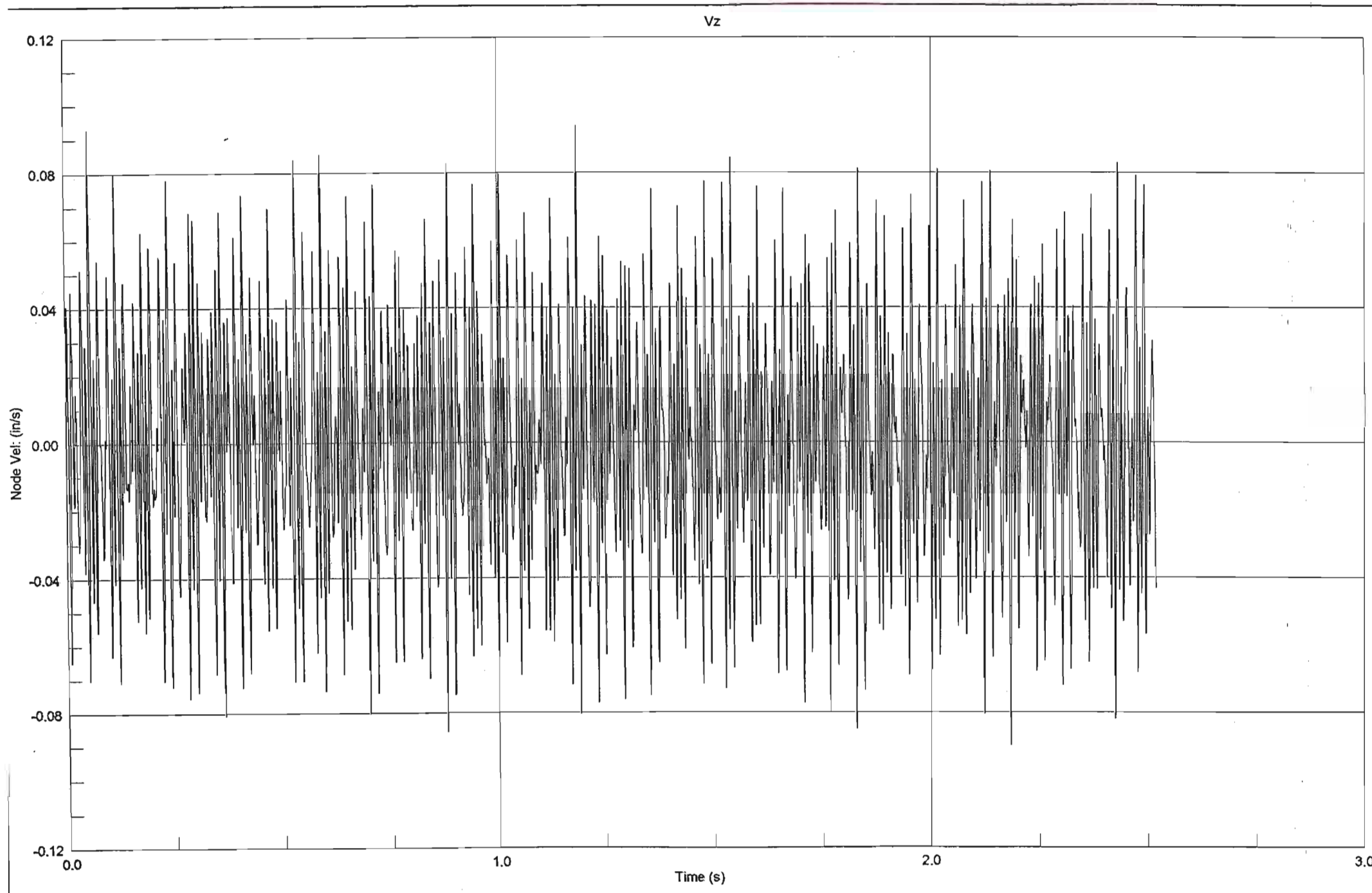


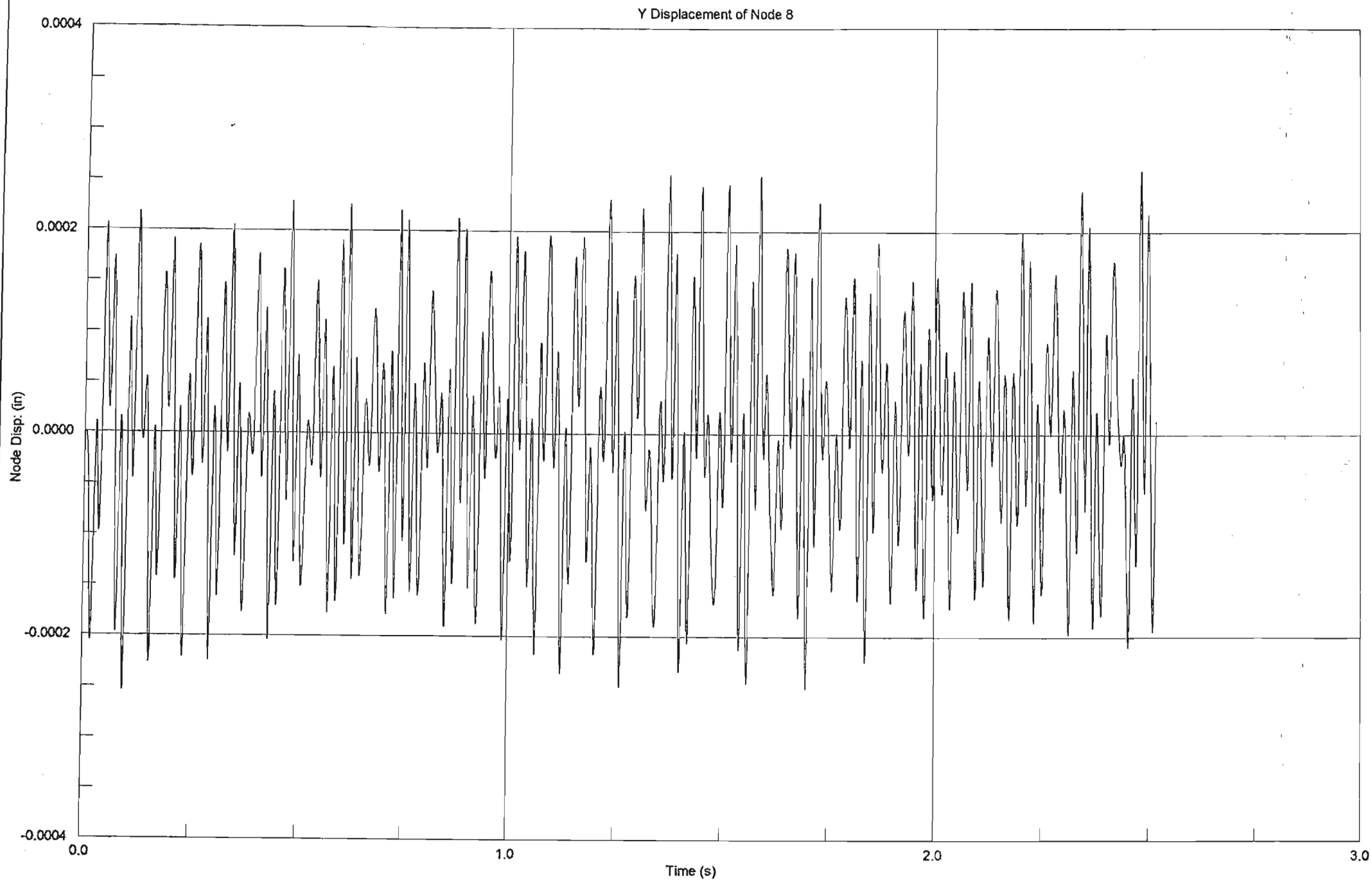


Z Displacement of Node 20

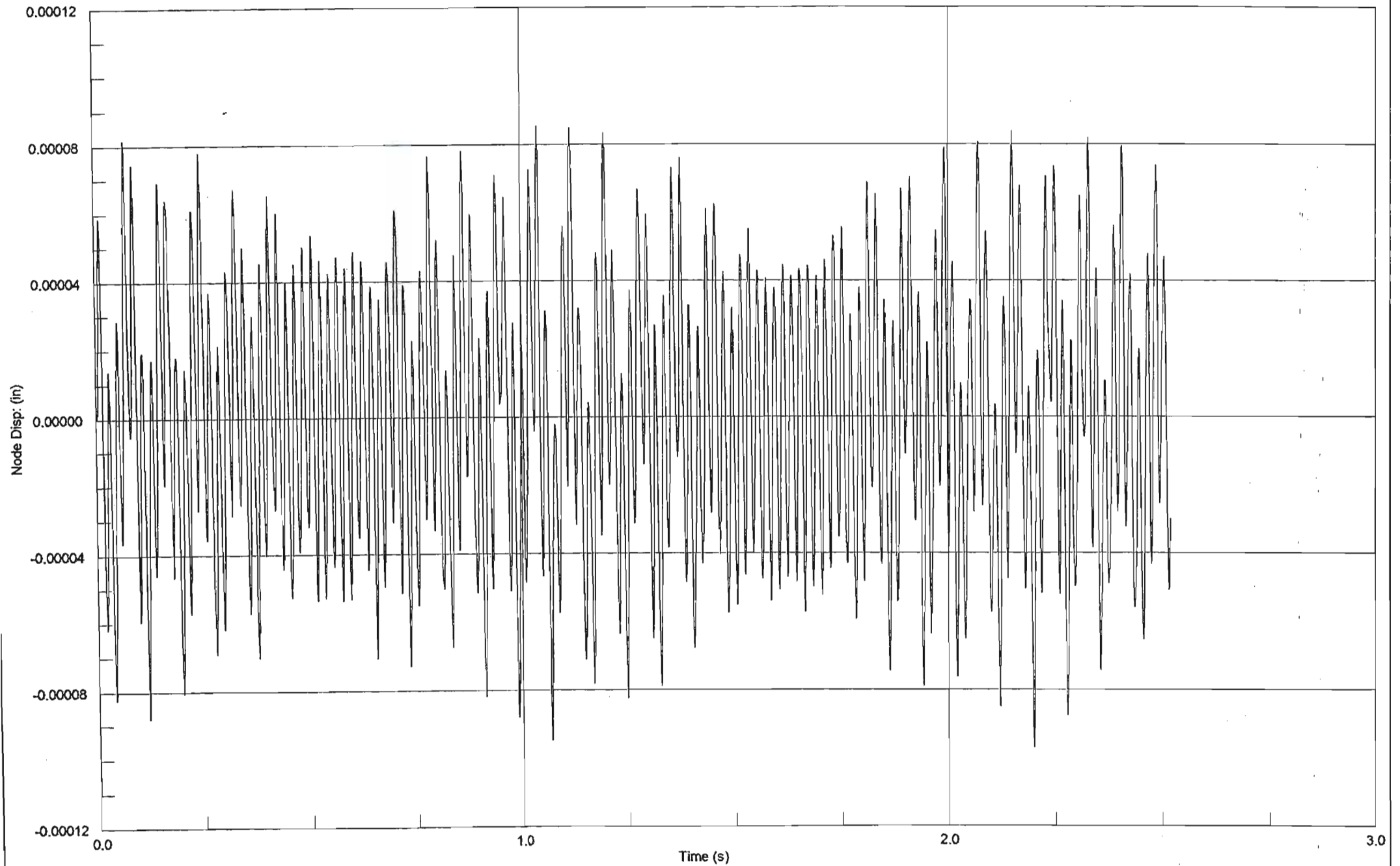


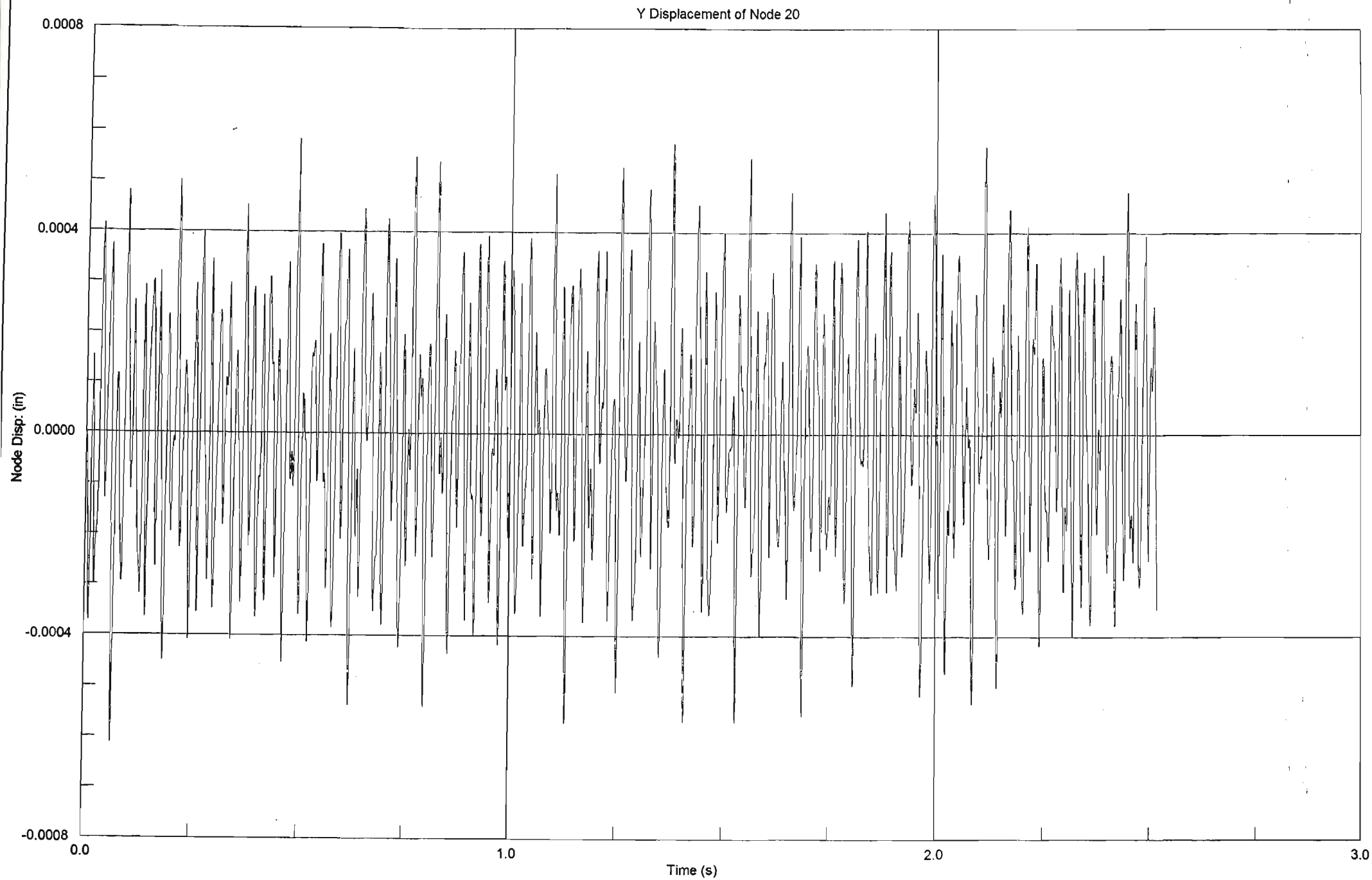




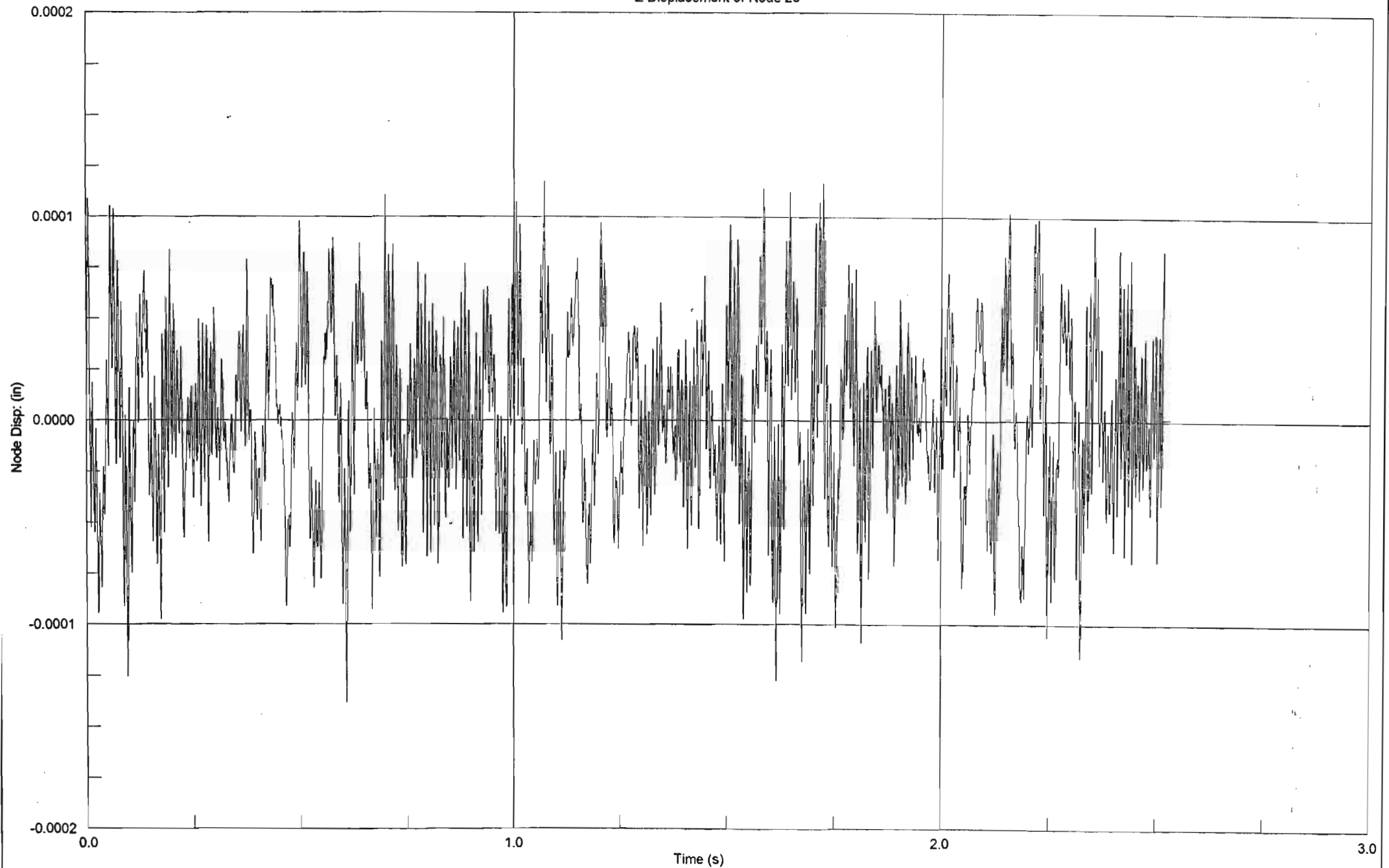


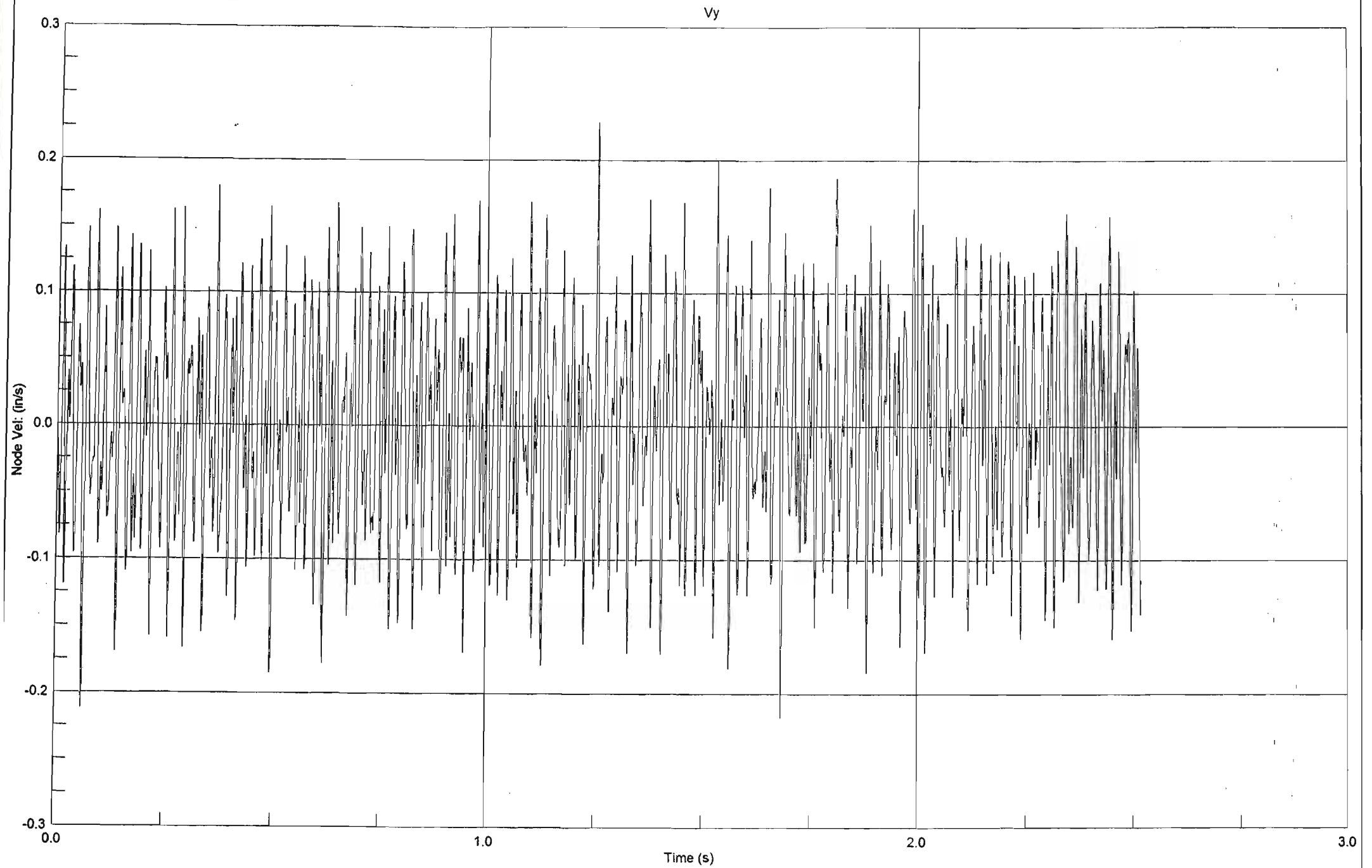
Z Displacement of Node 8

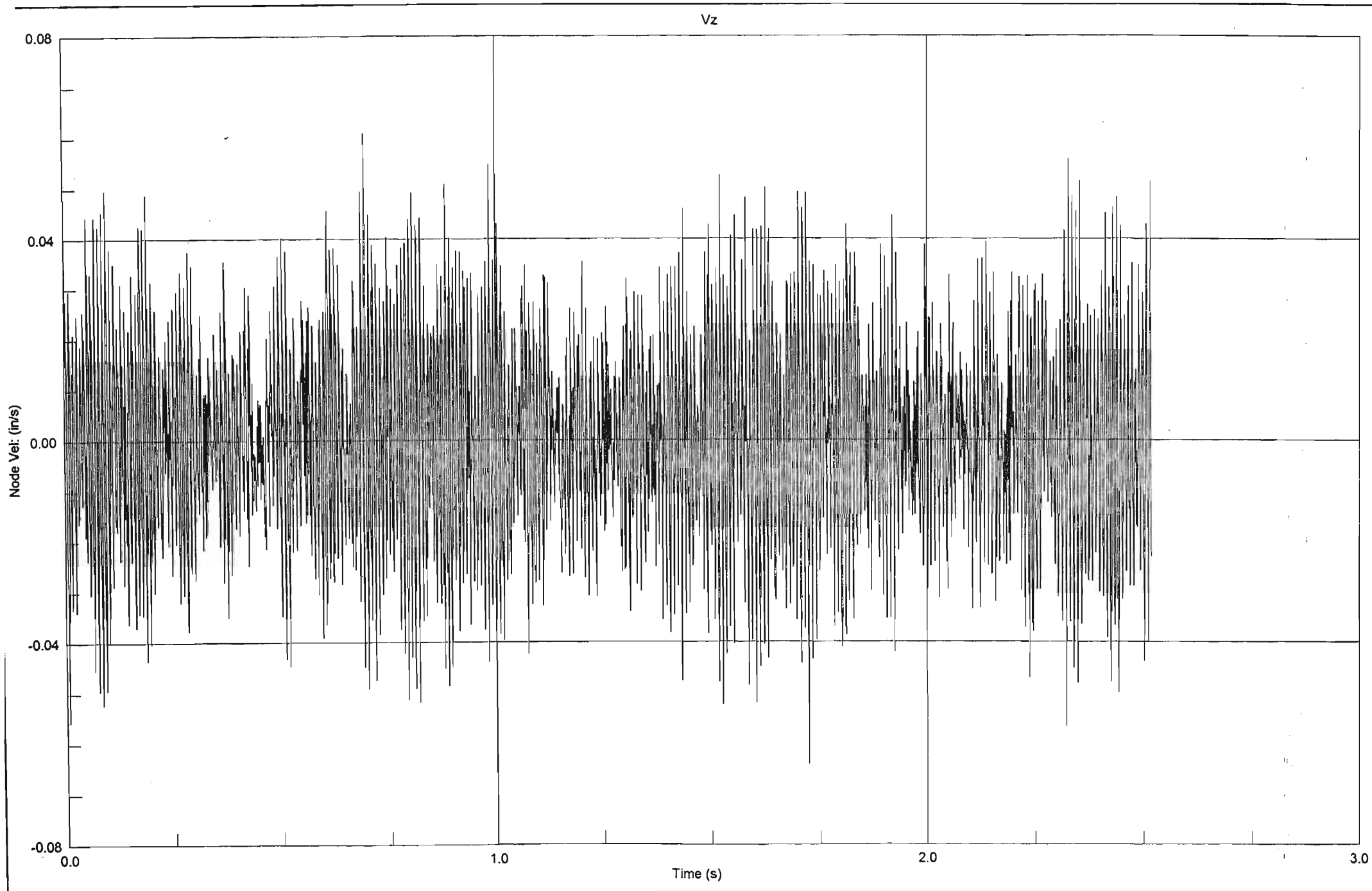


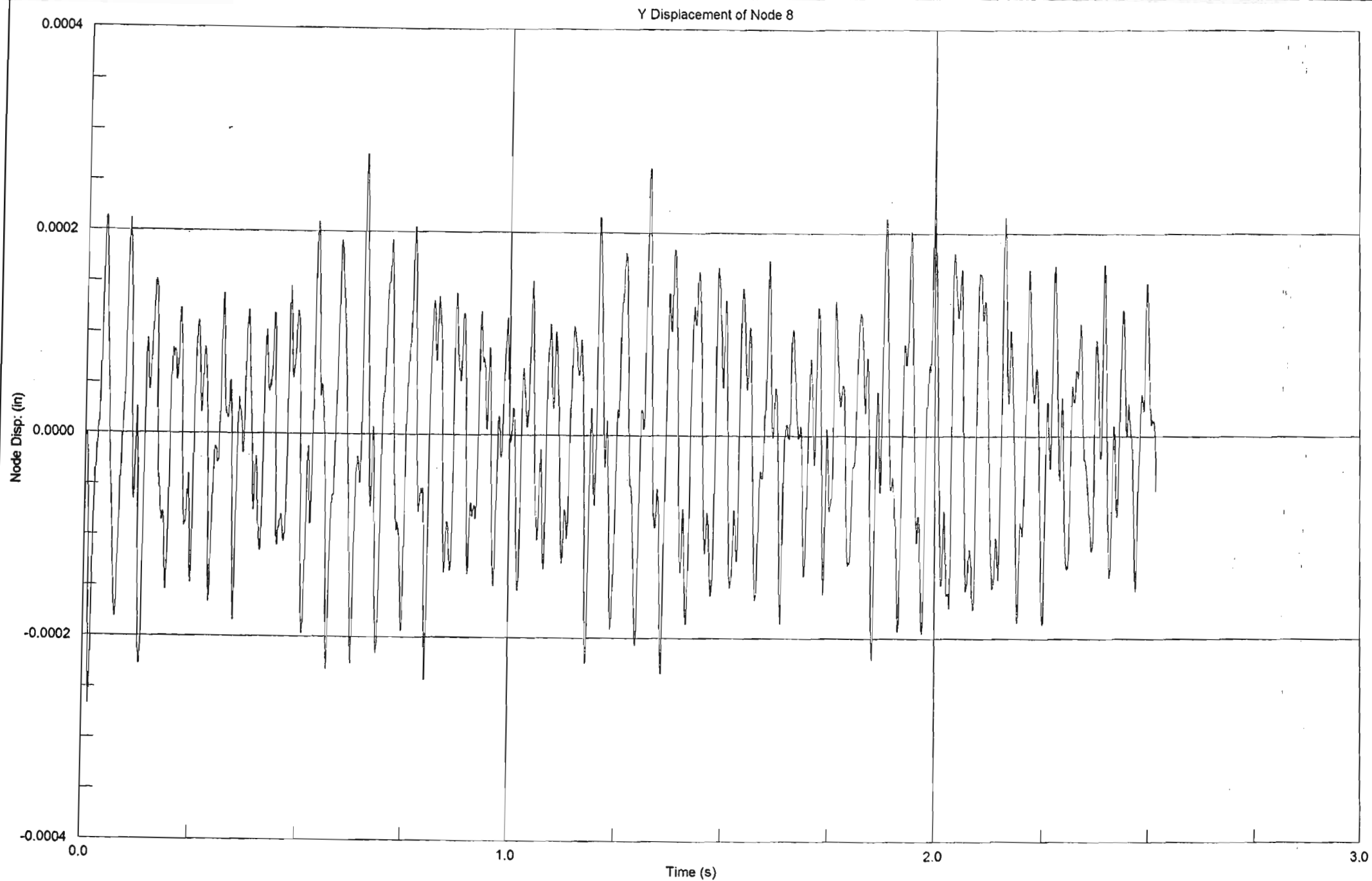


Z Displacement of Node 20

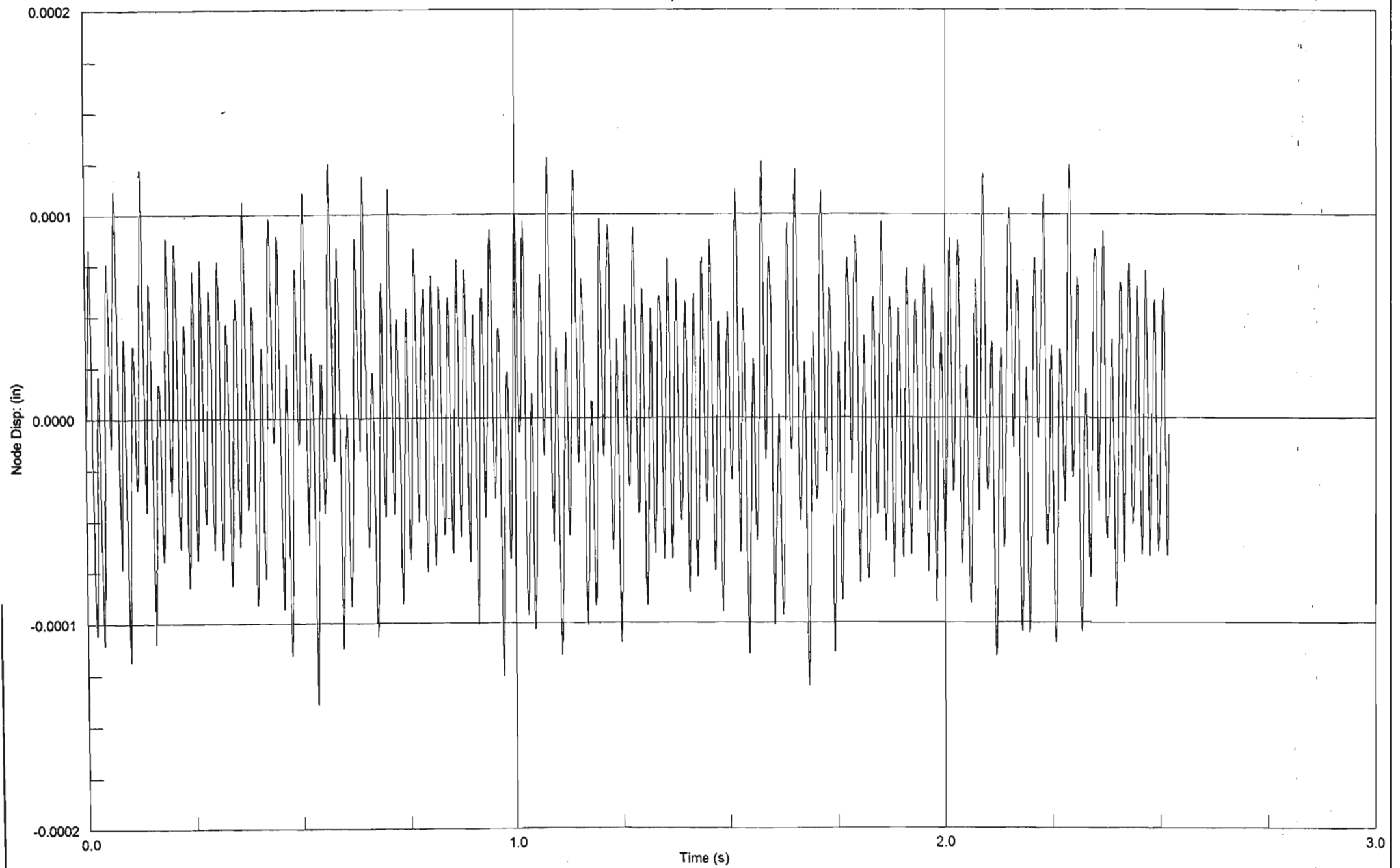


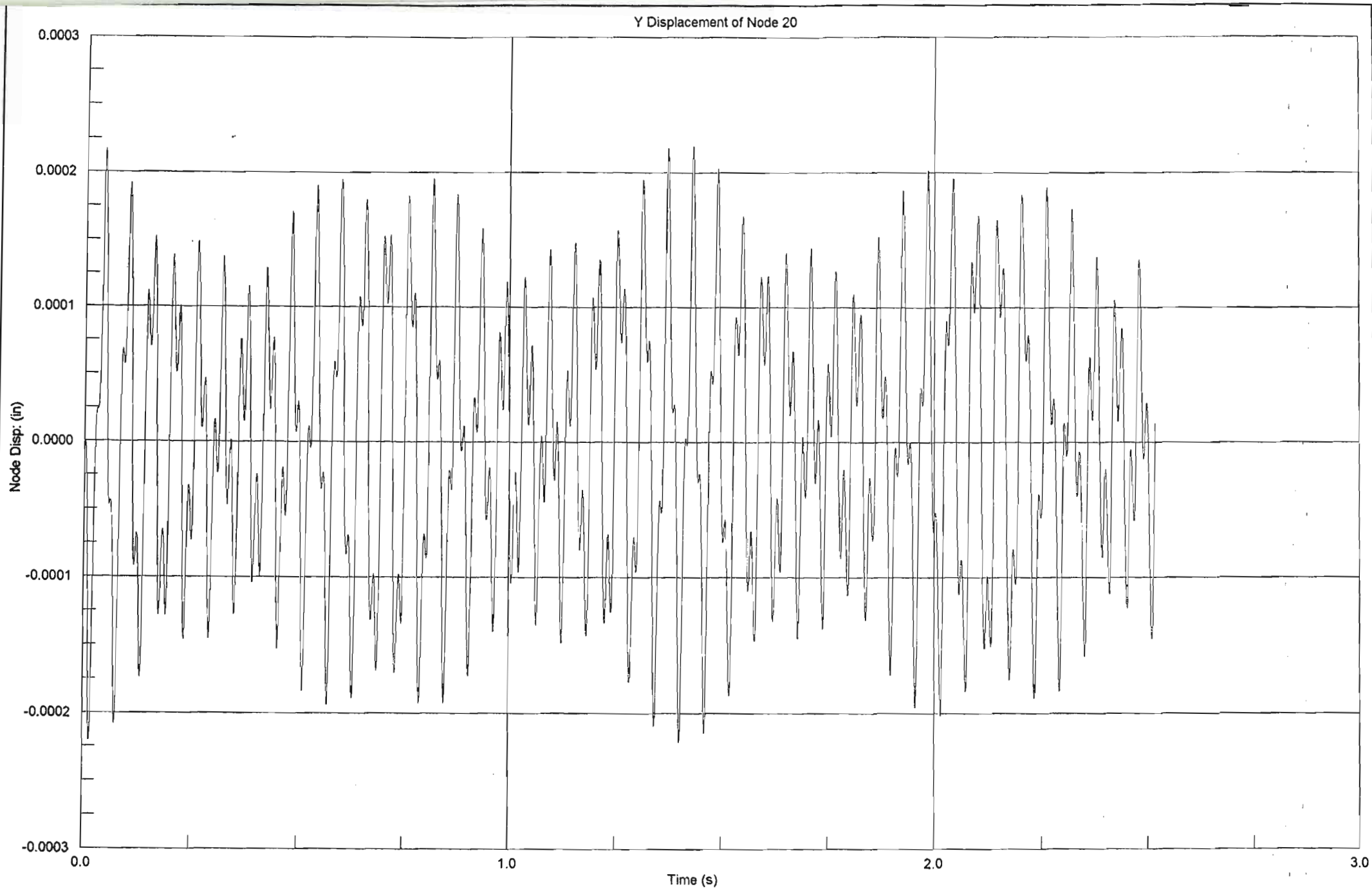




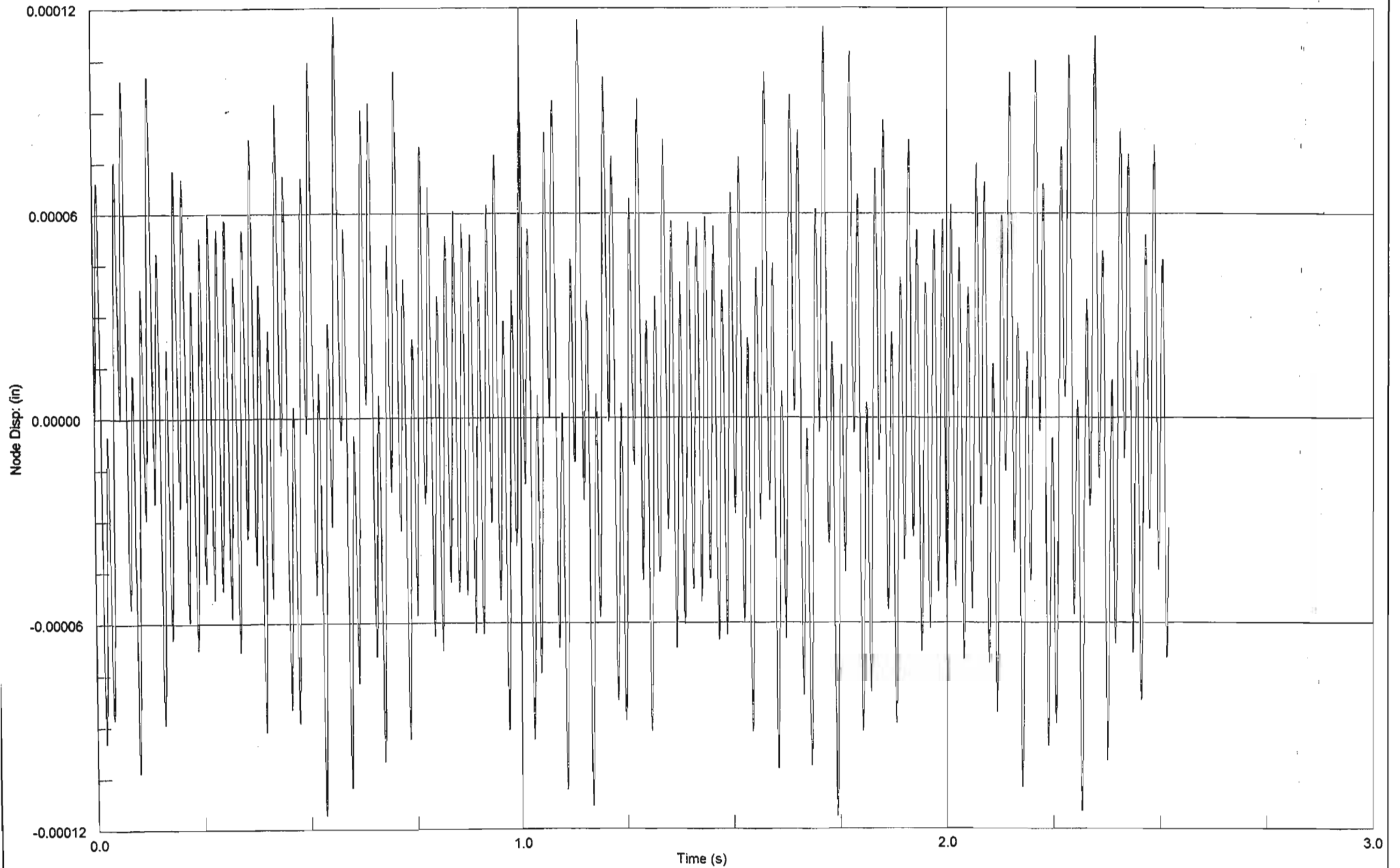


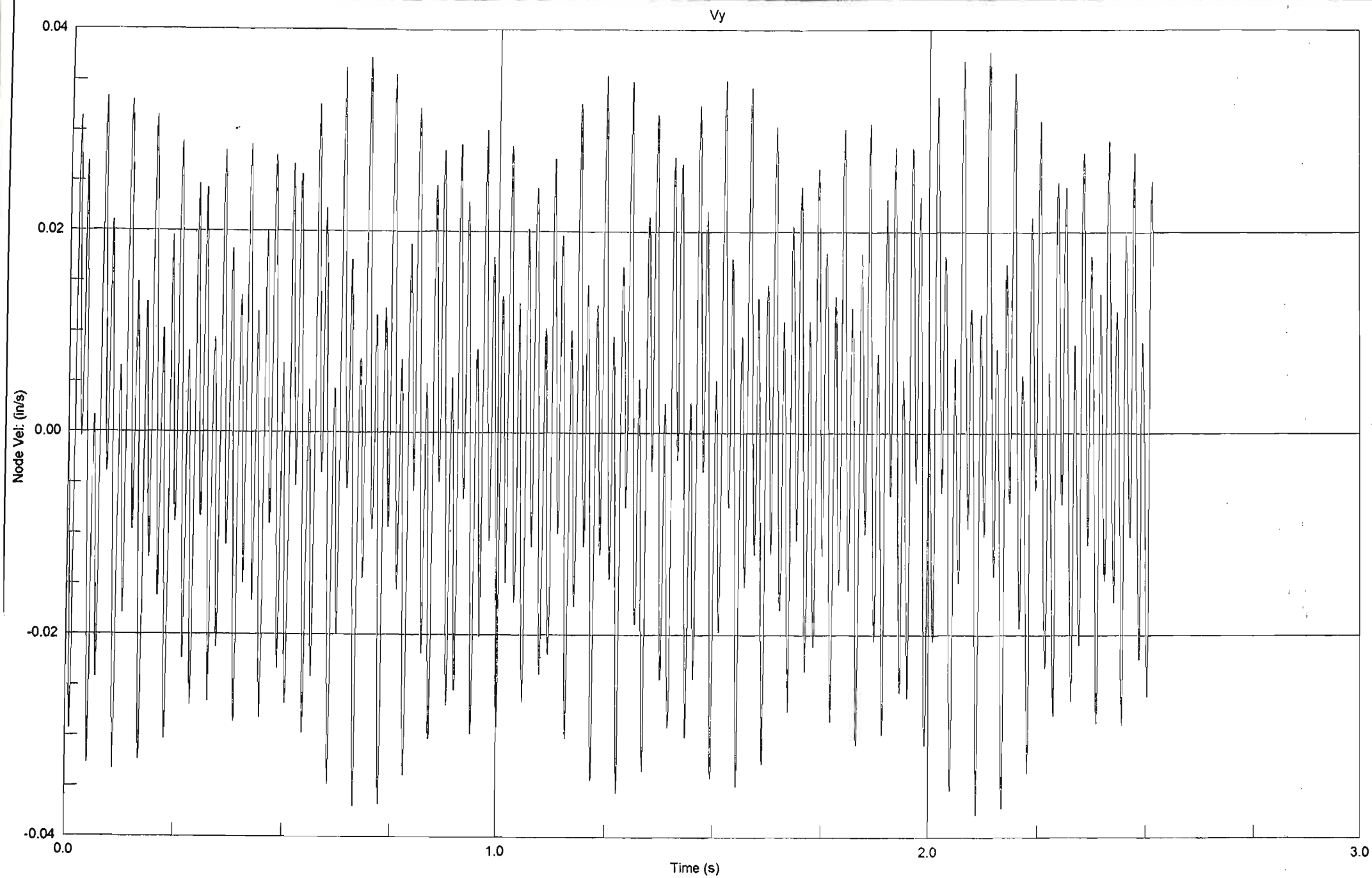
Z Displacement of Node 8

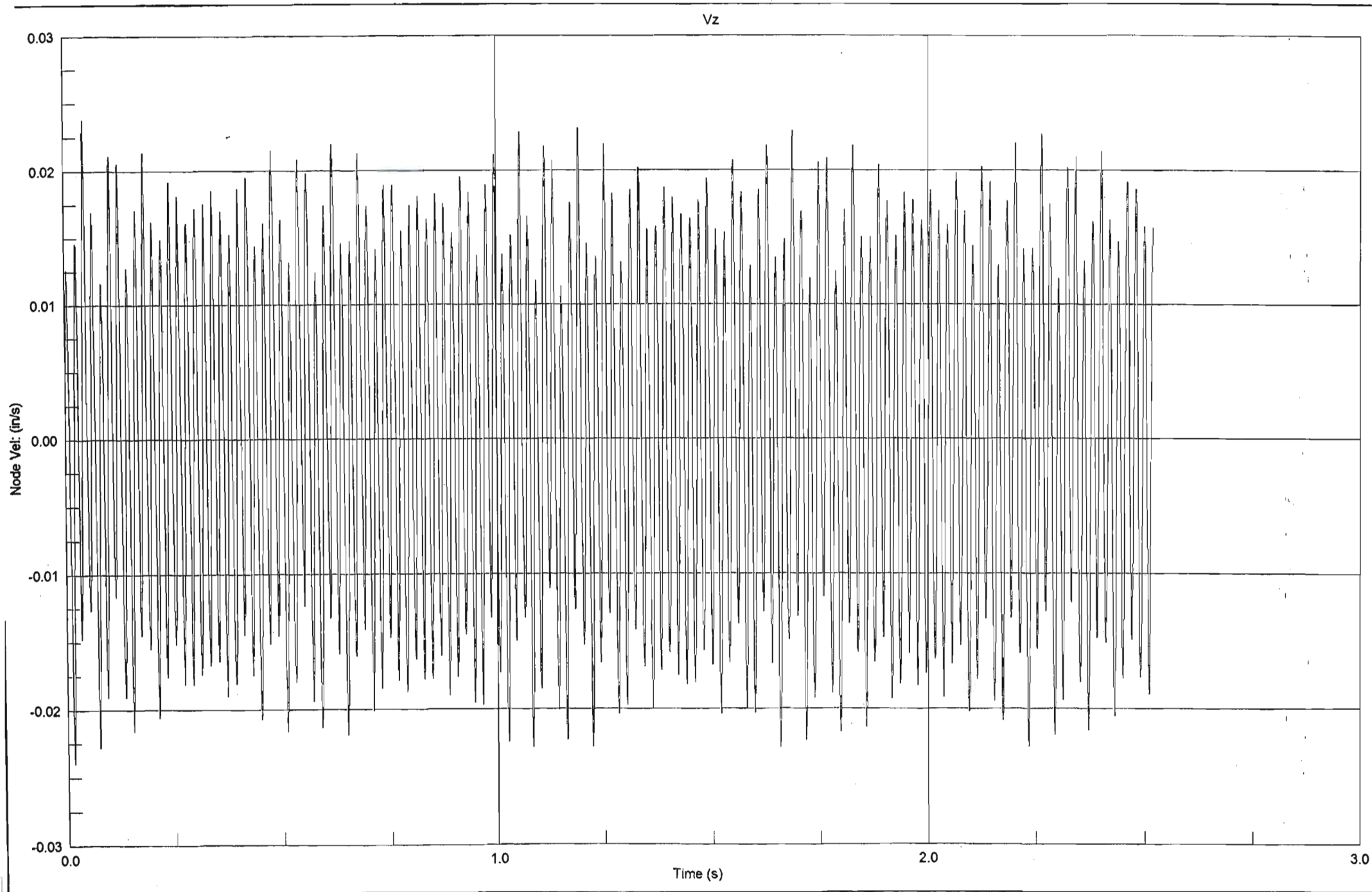


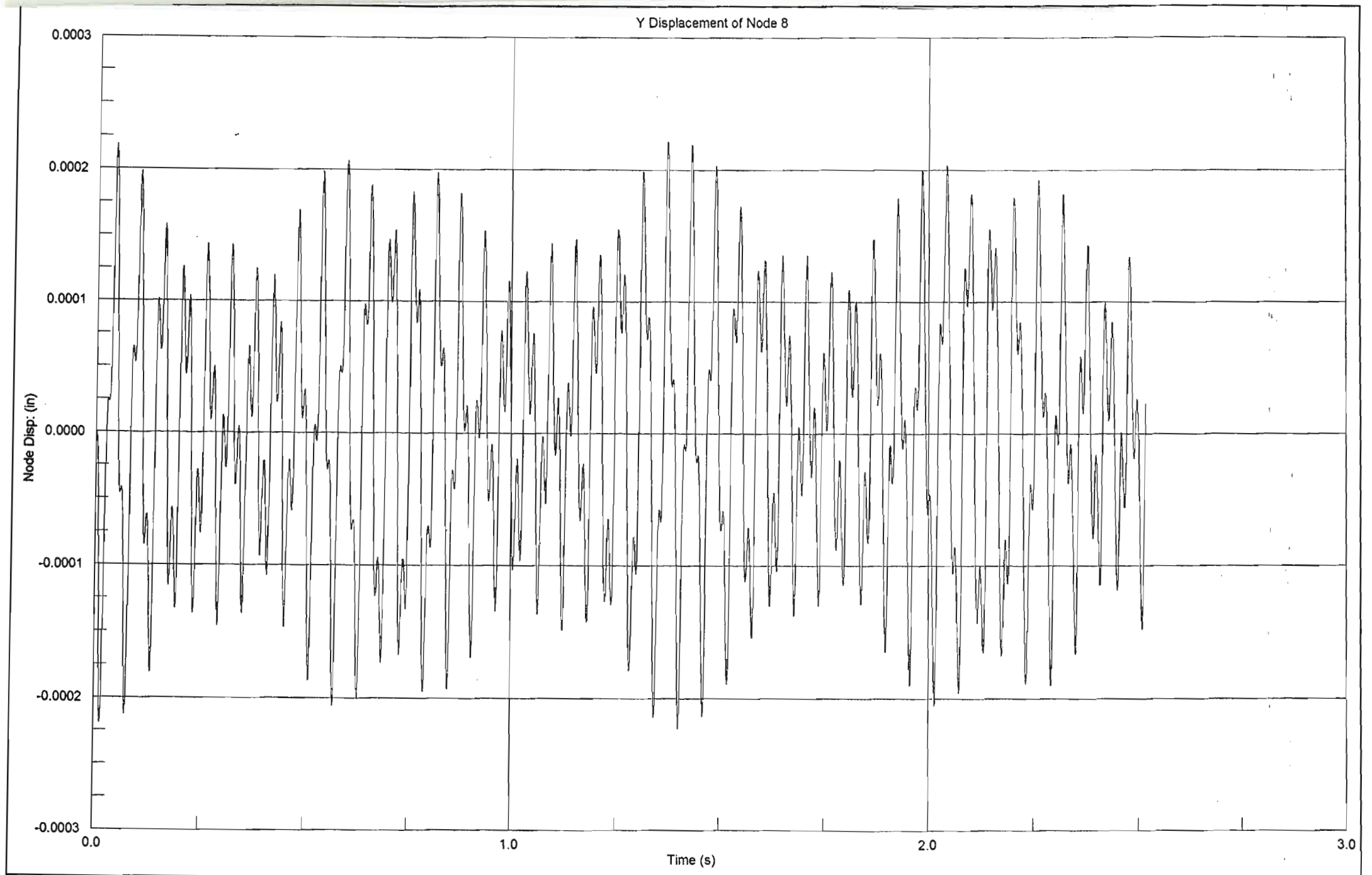


Z Displacement of Node 20

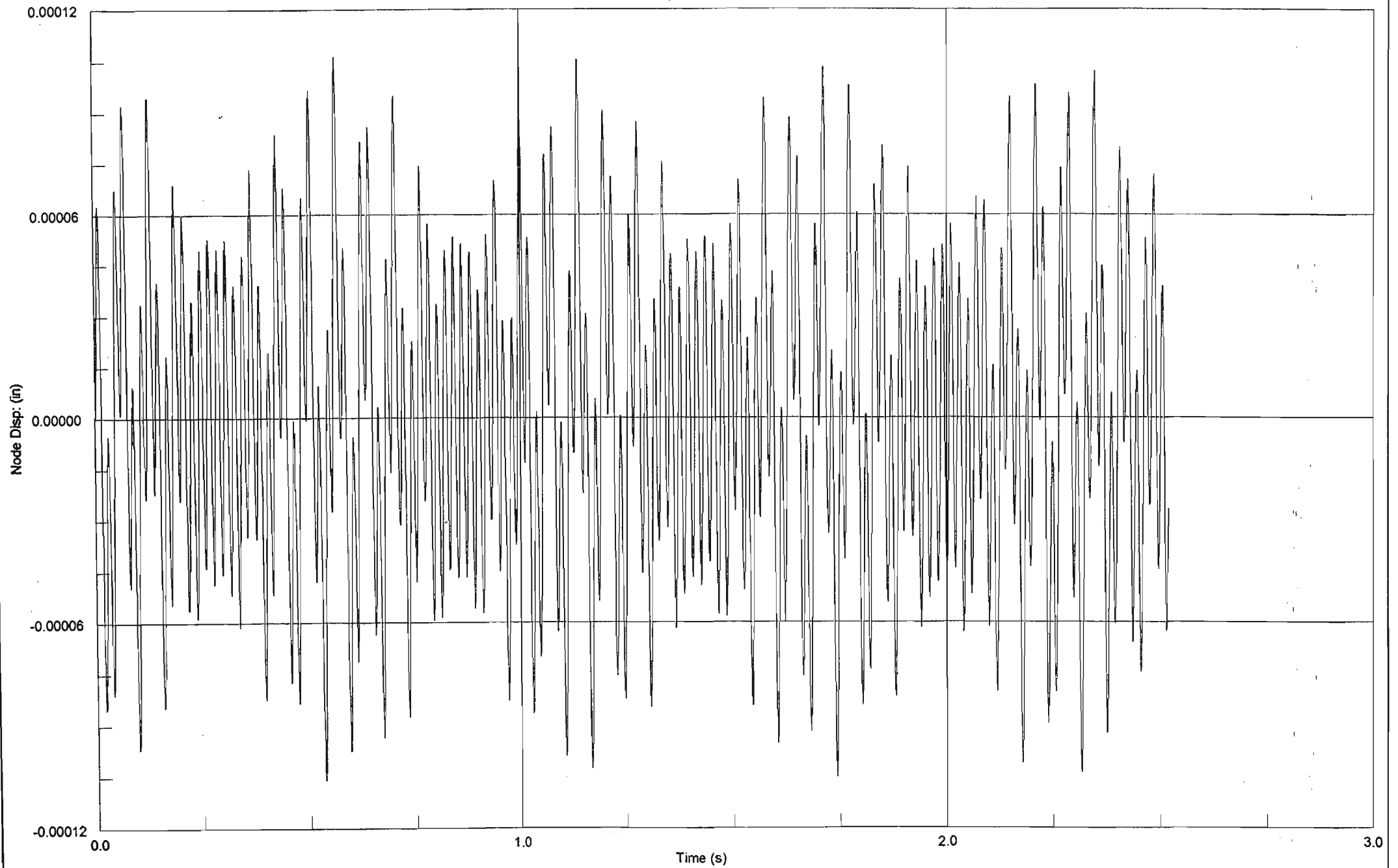


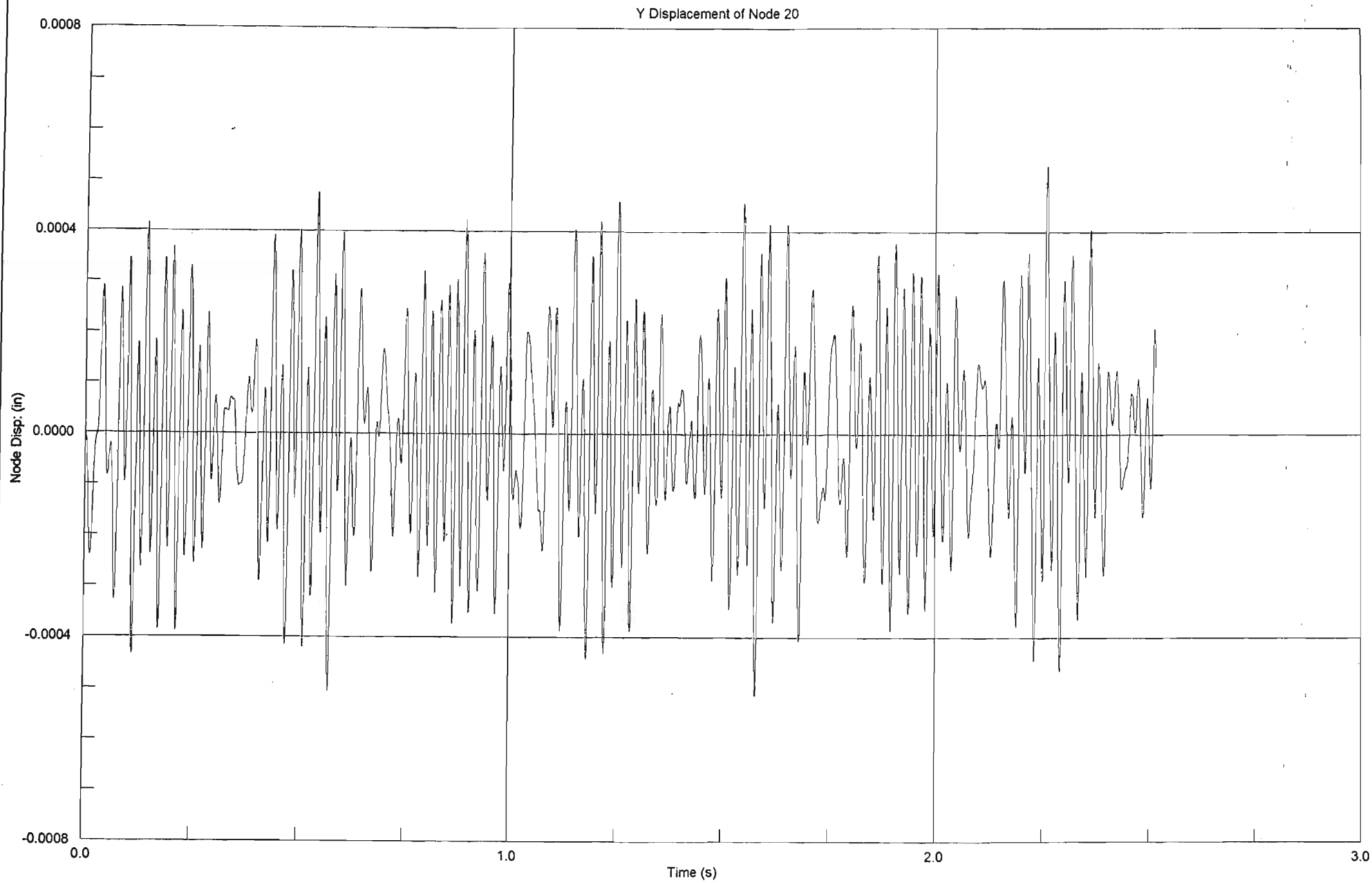




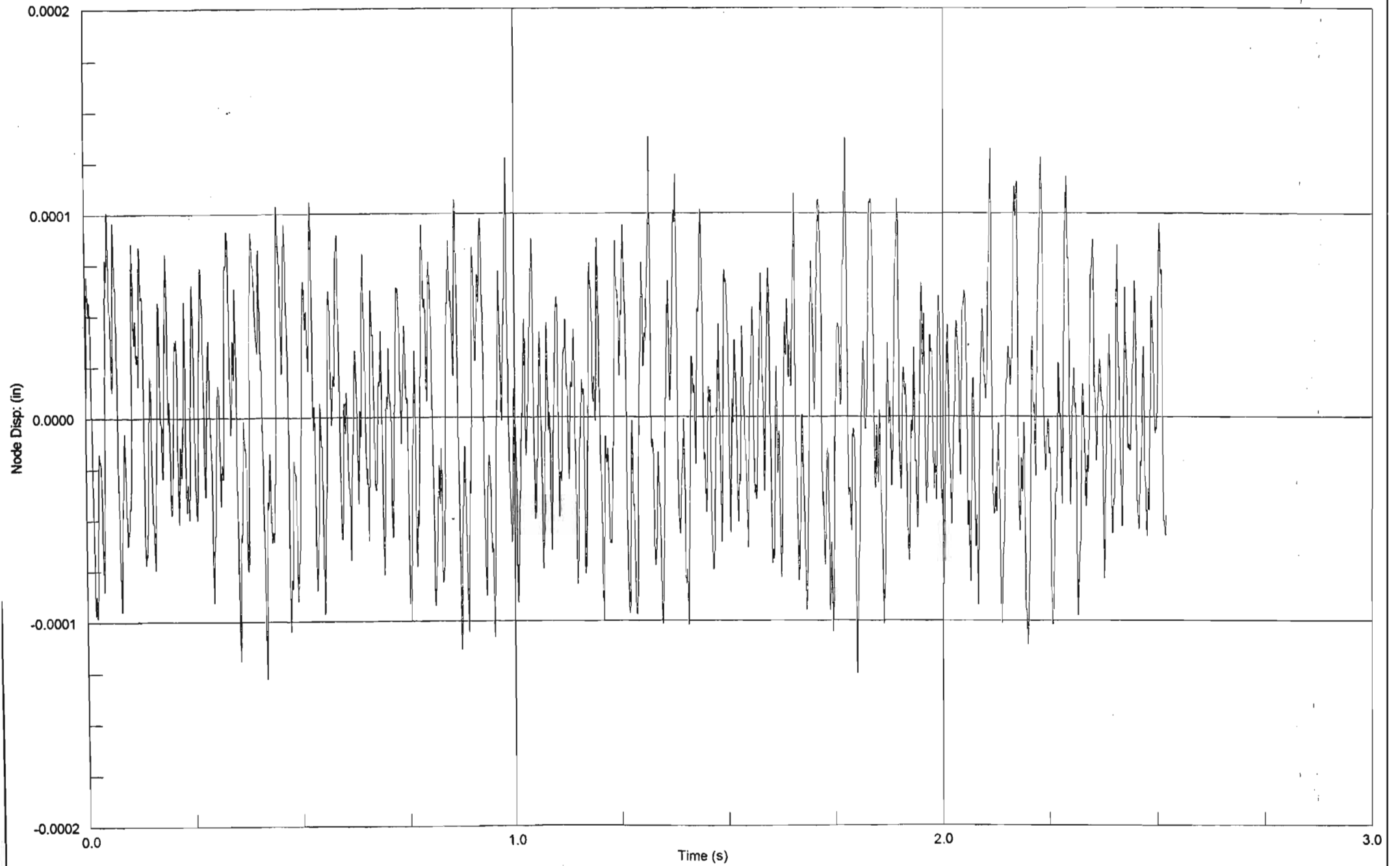


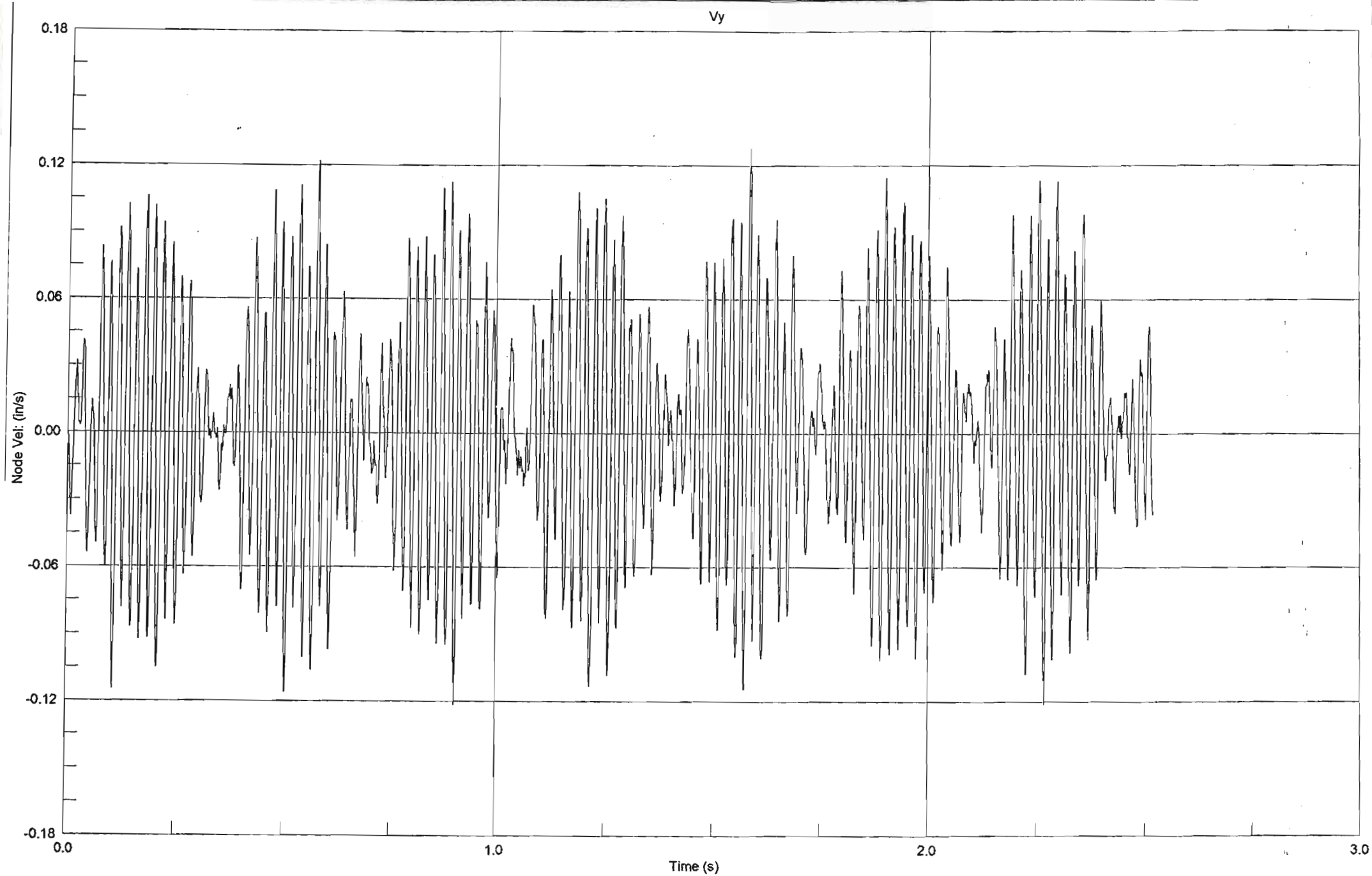
Z Displacement of Node 8

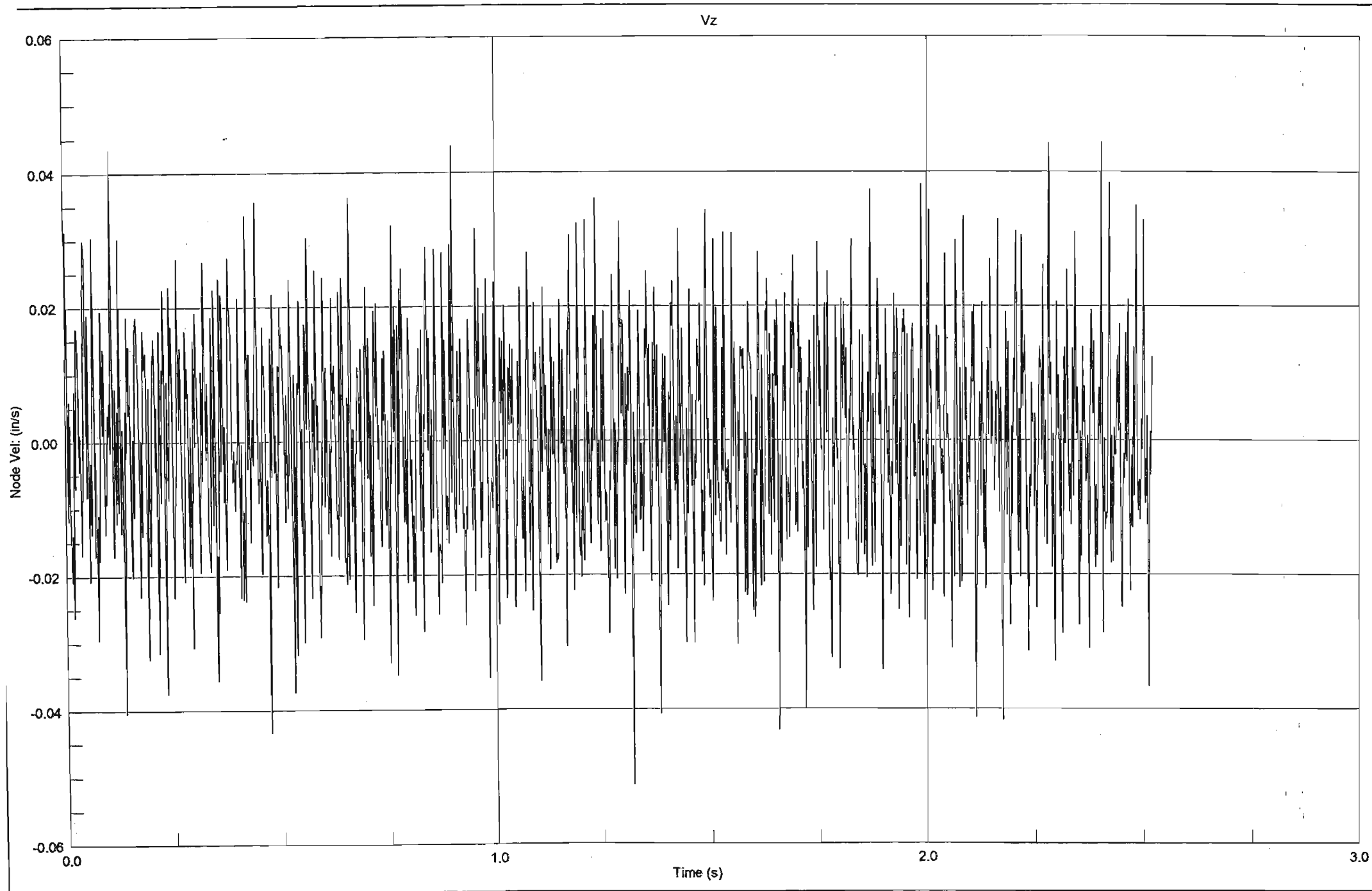


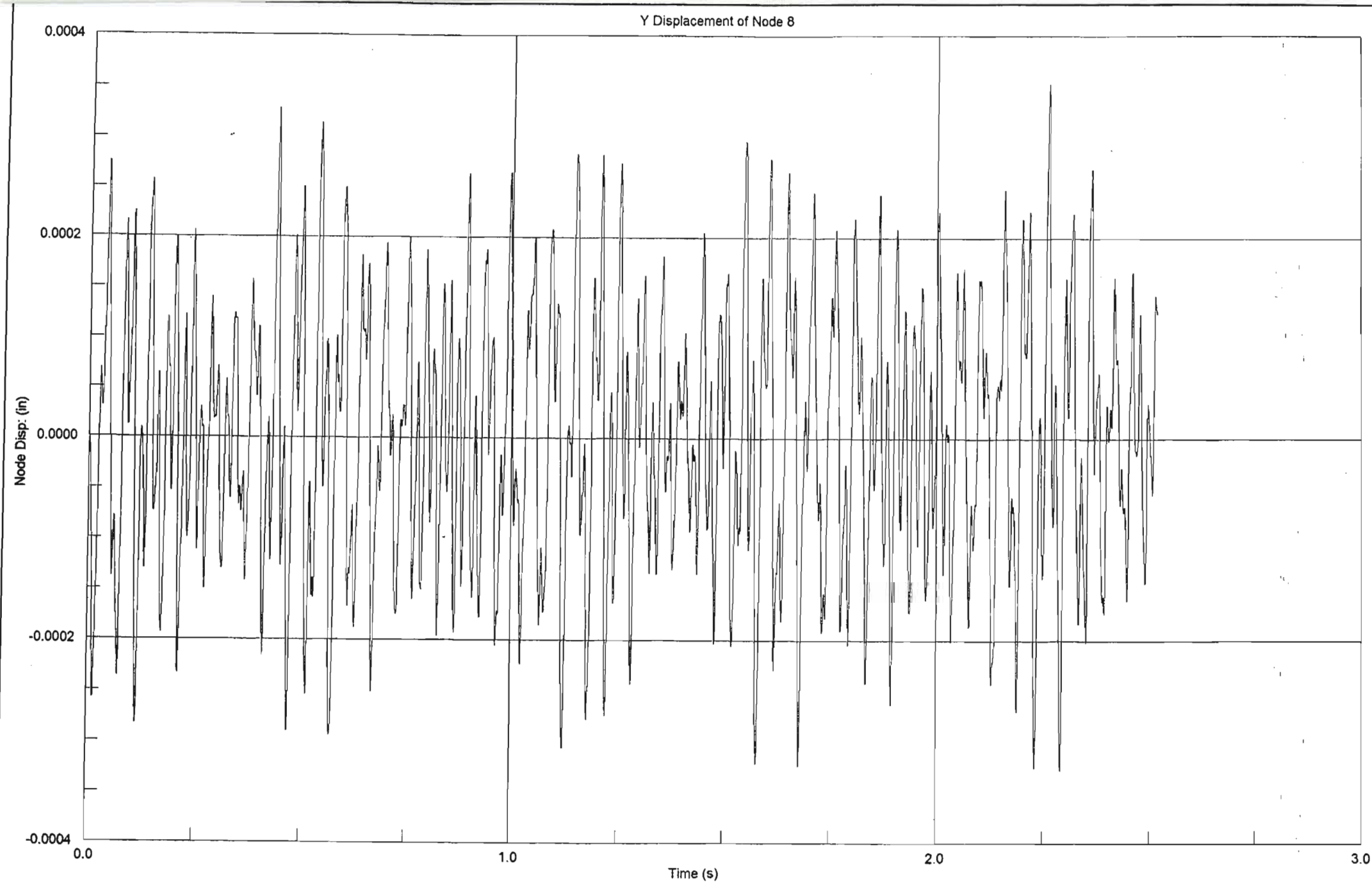


Z Displacement of Node 20

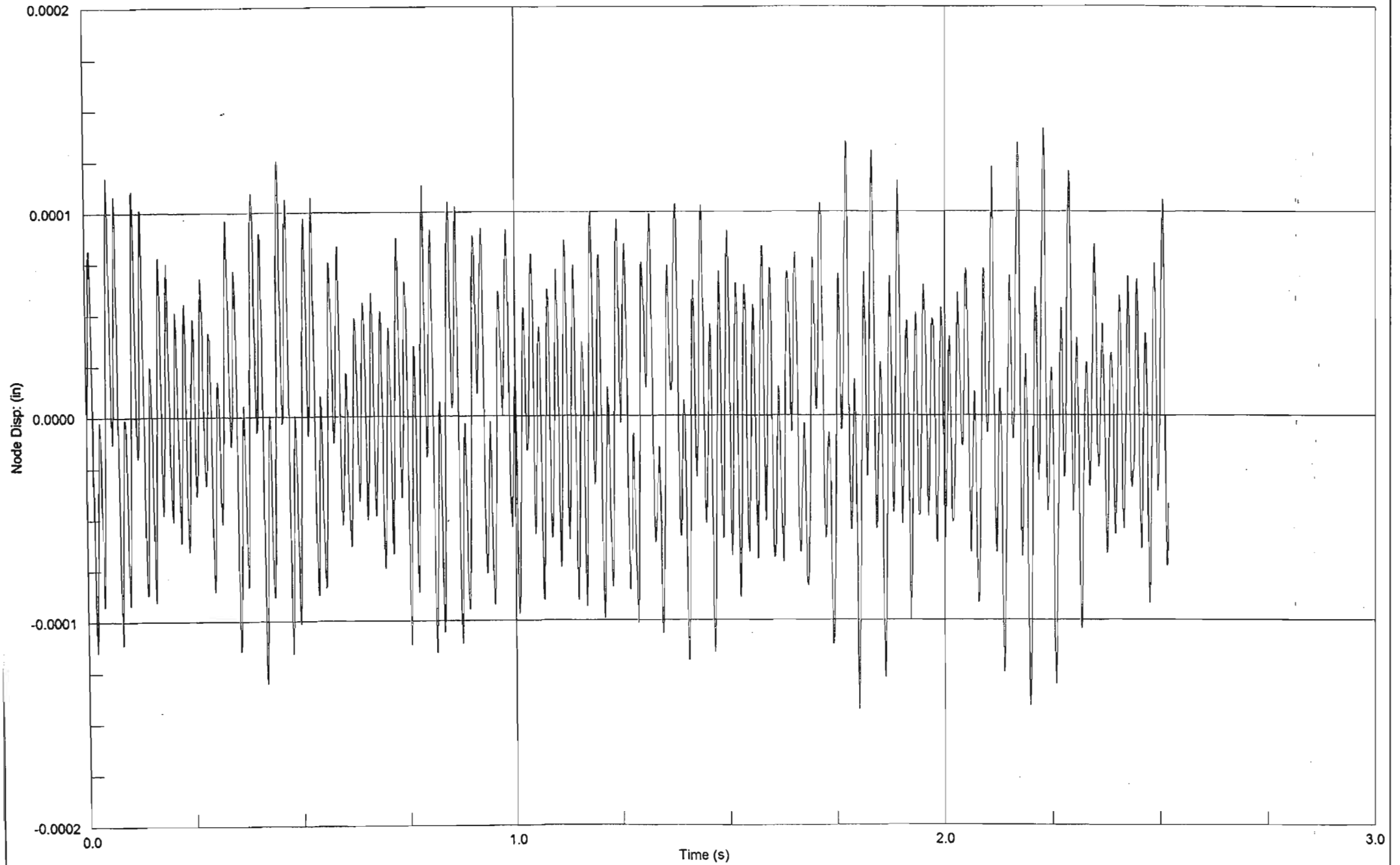


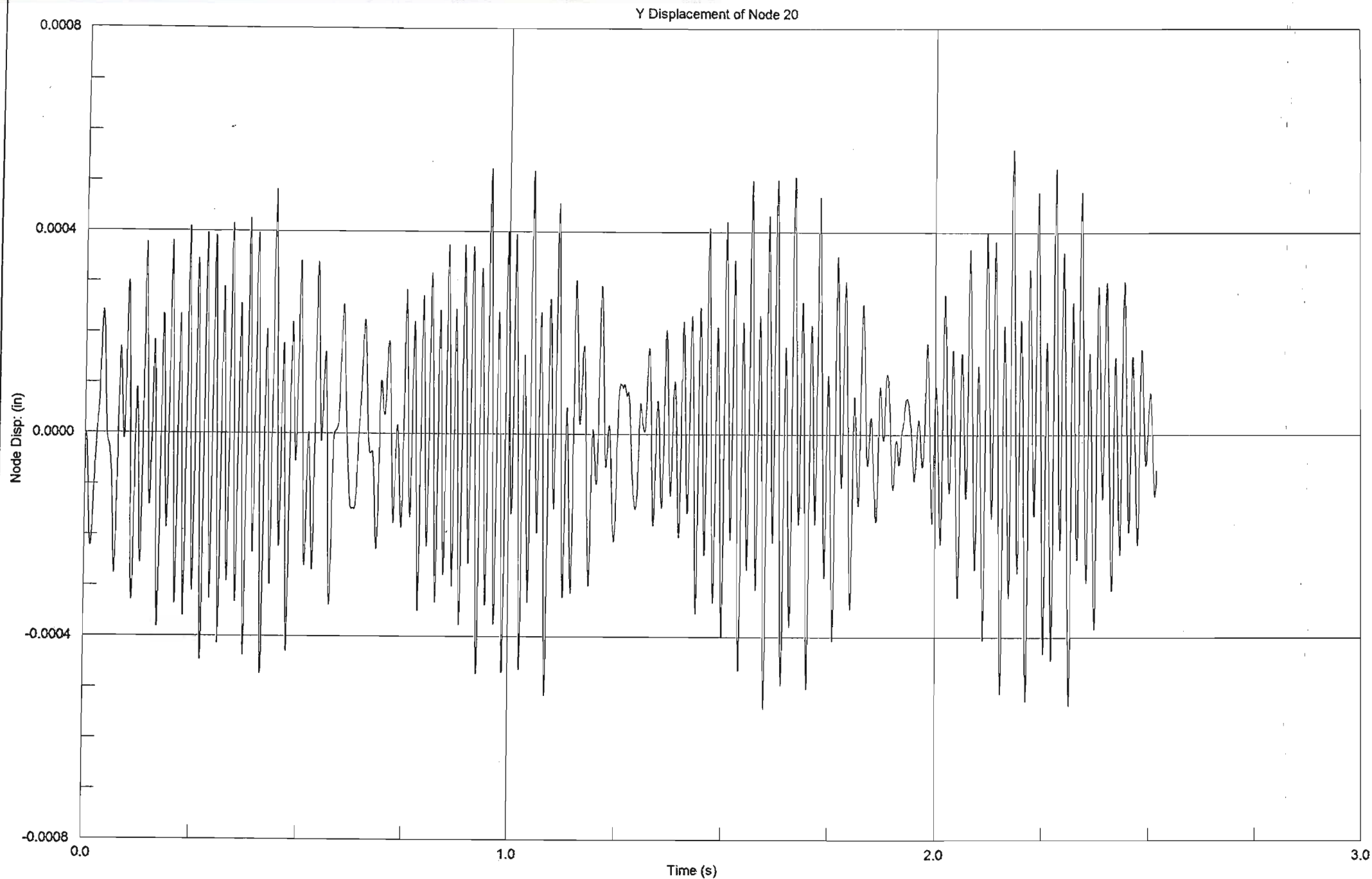


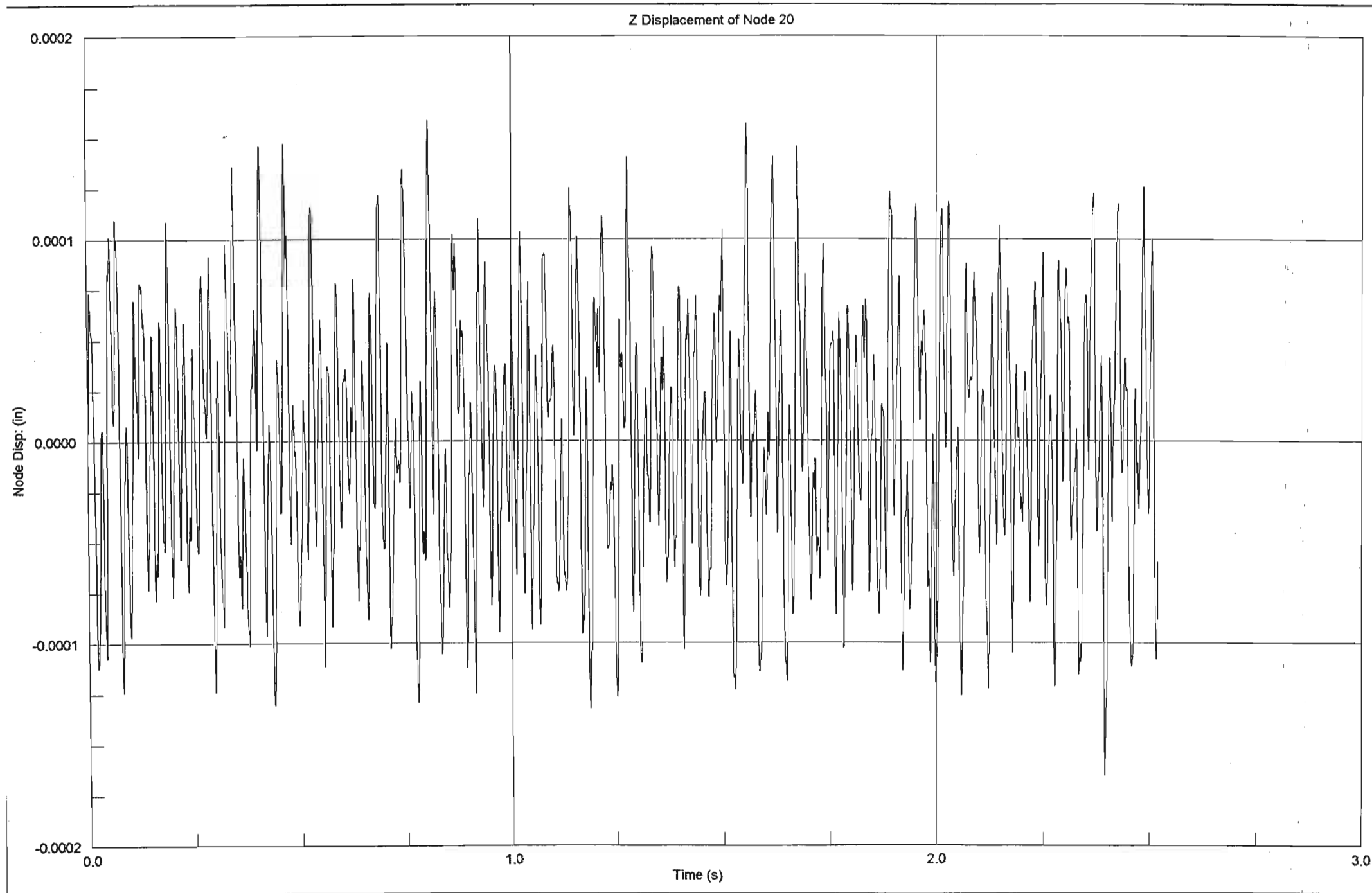


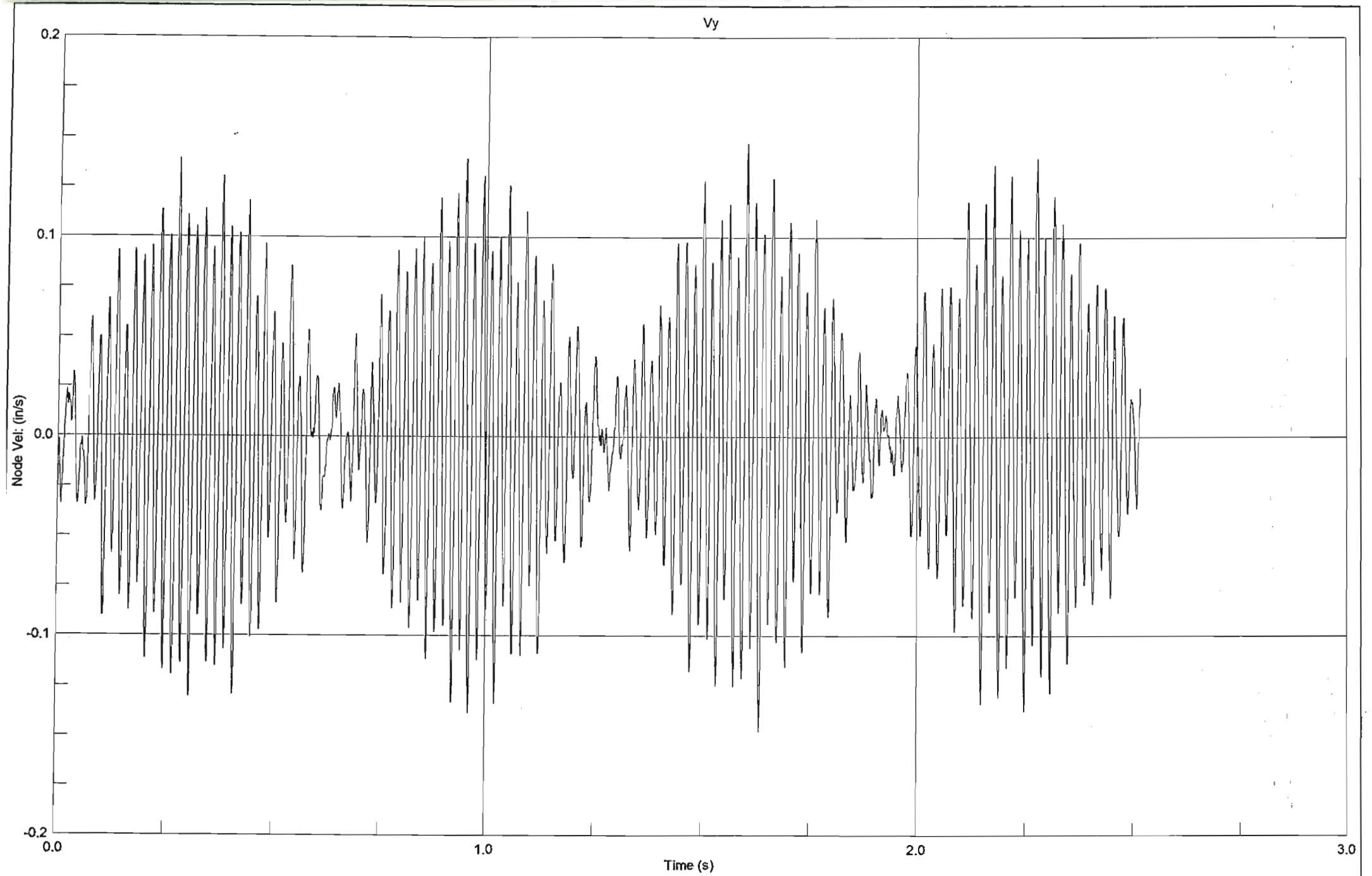


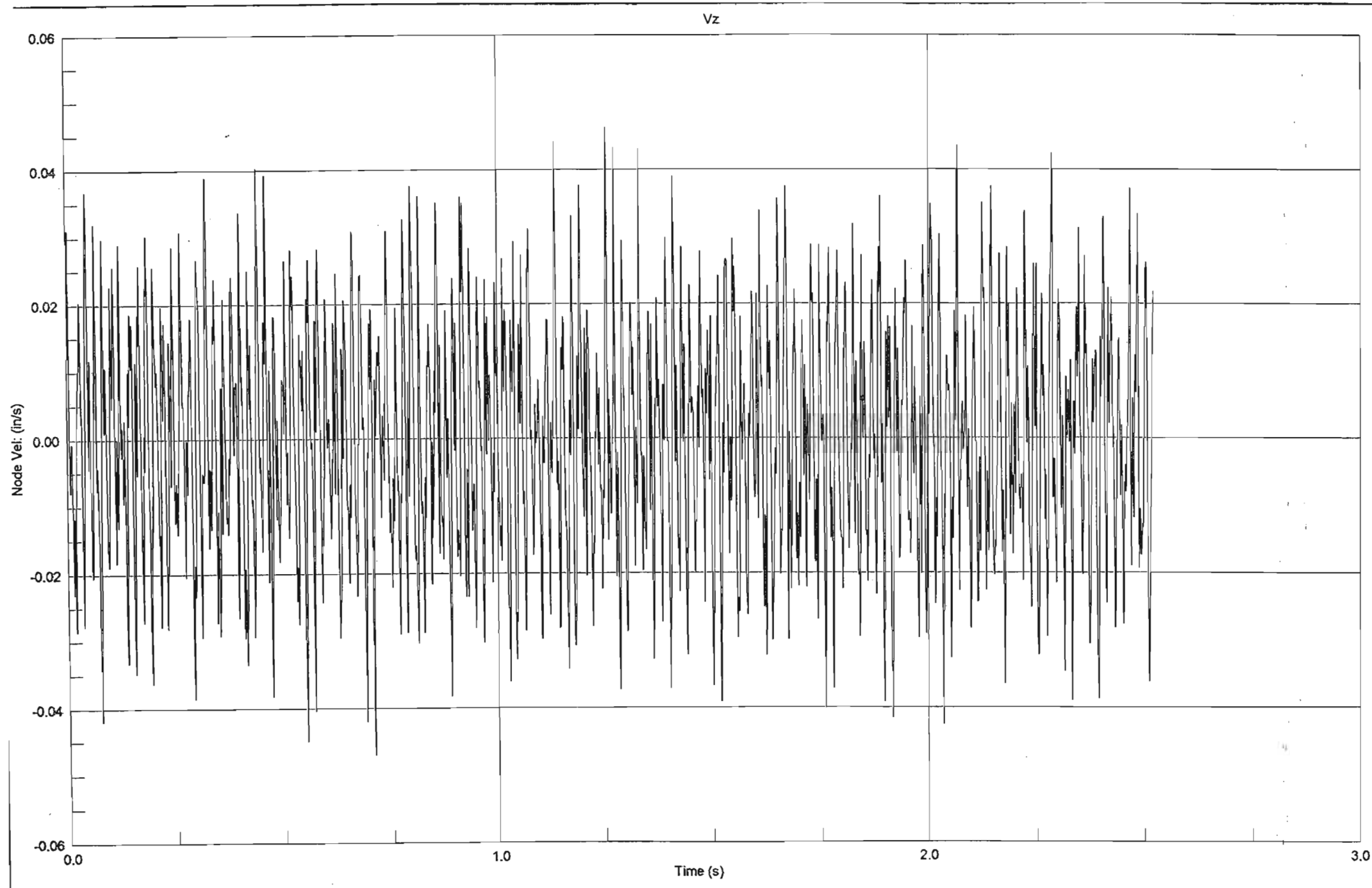
Z Displacement of Node 8

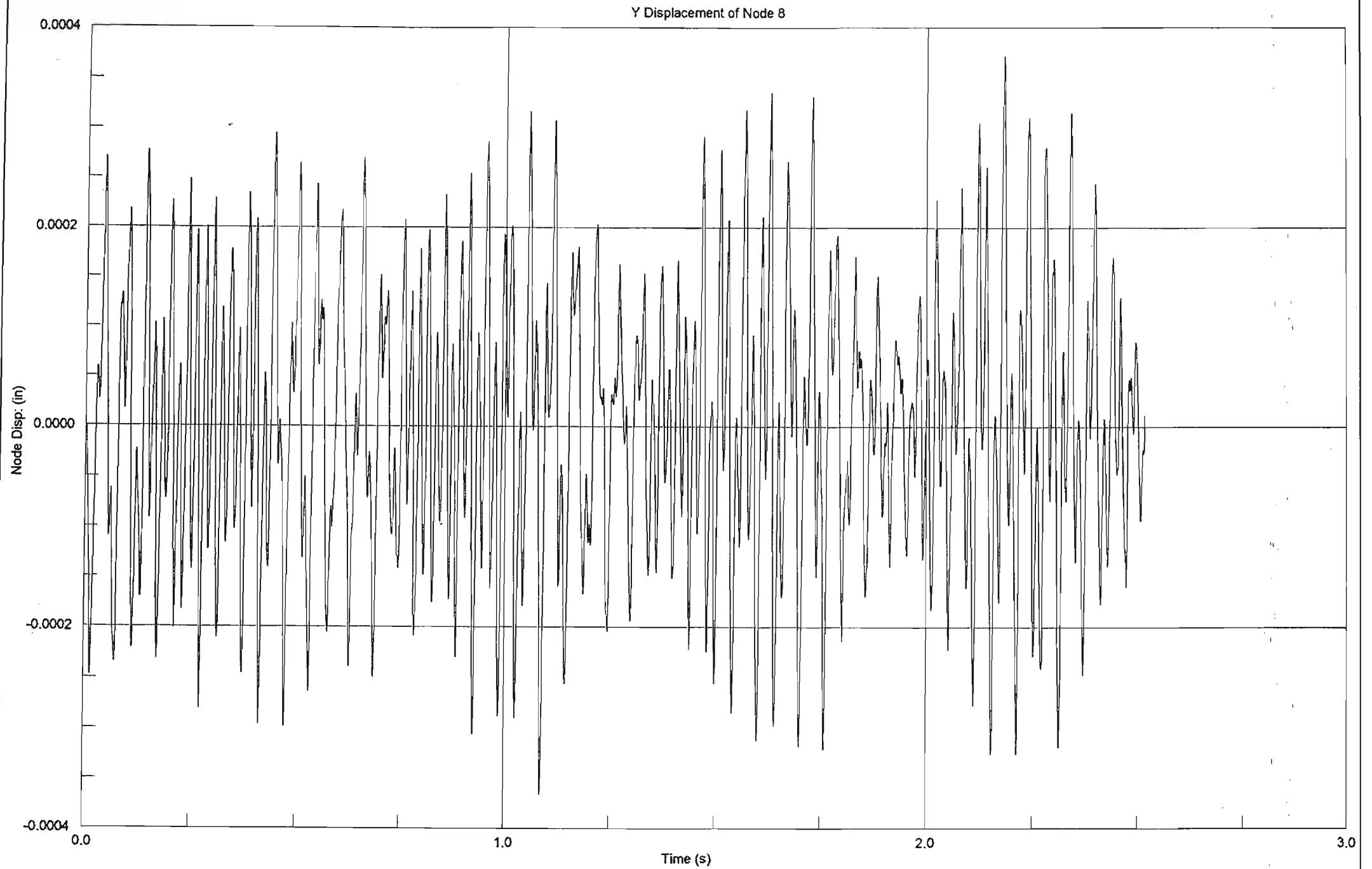




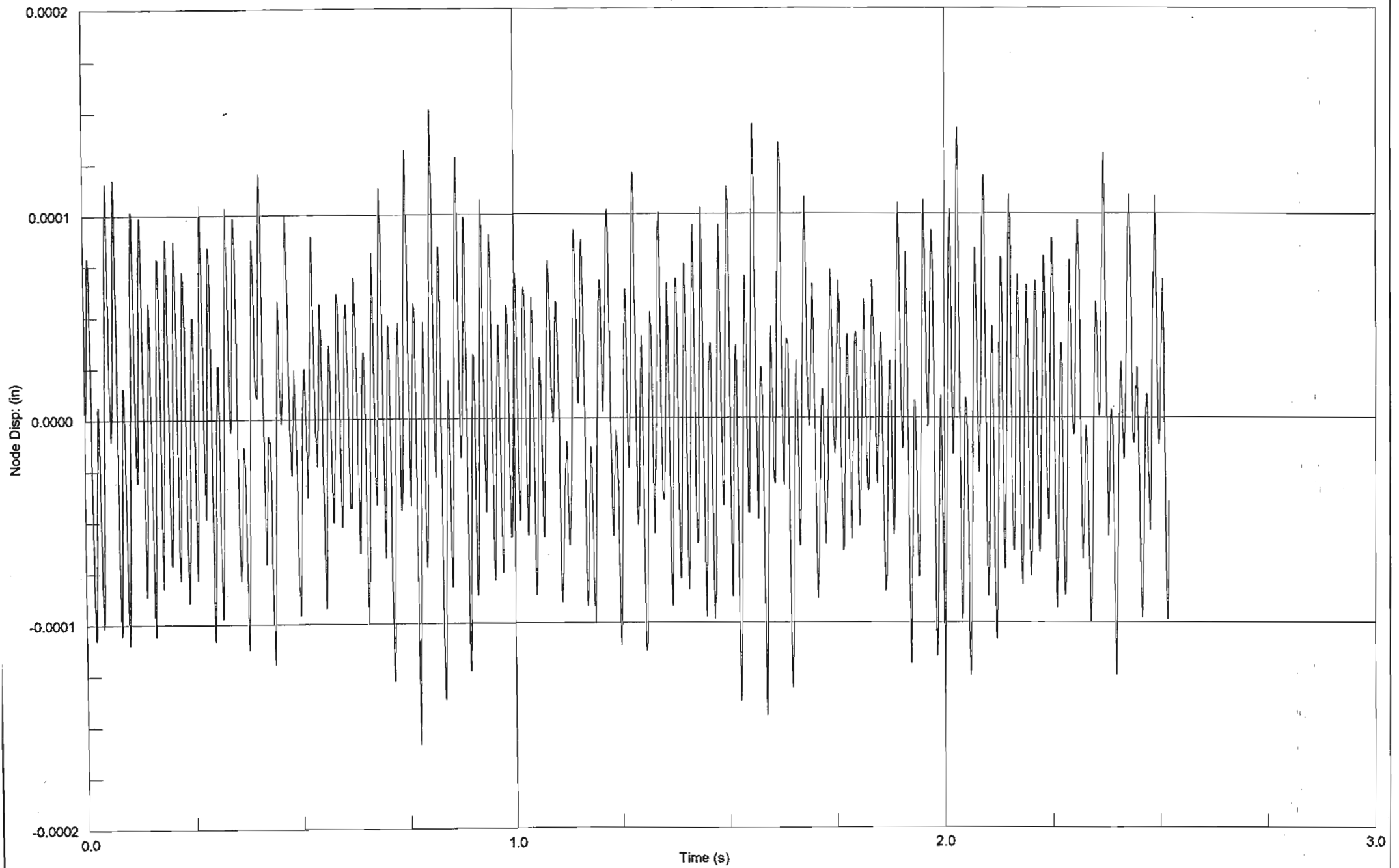


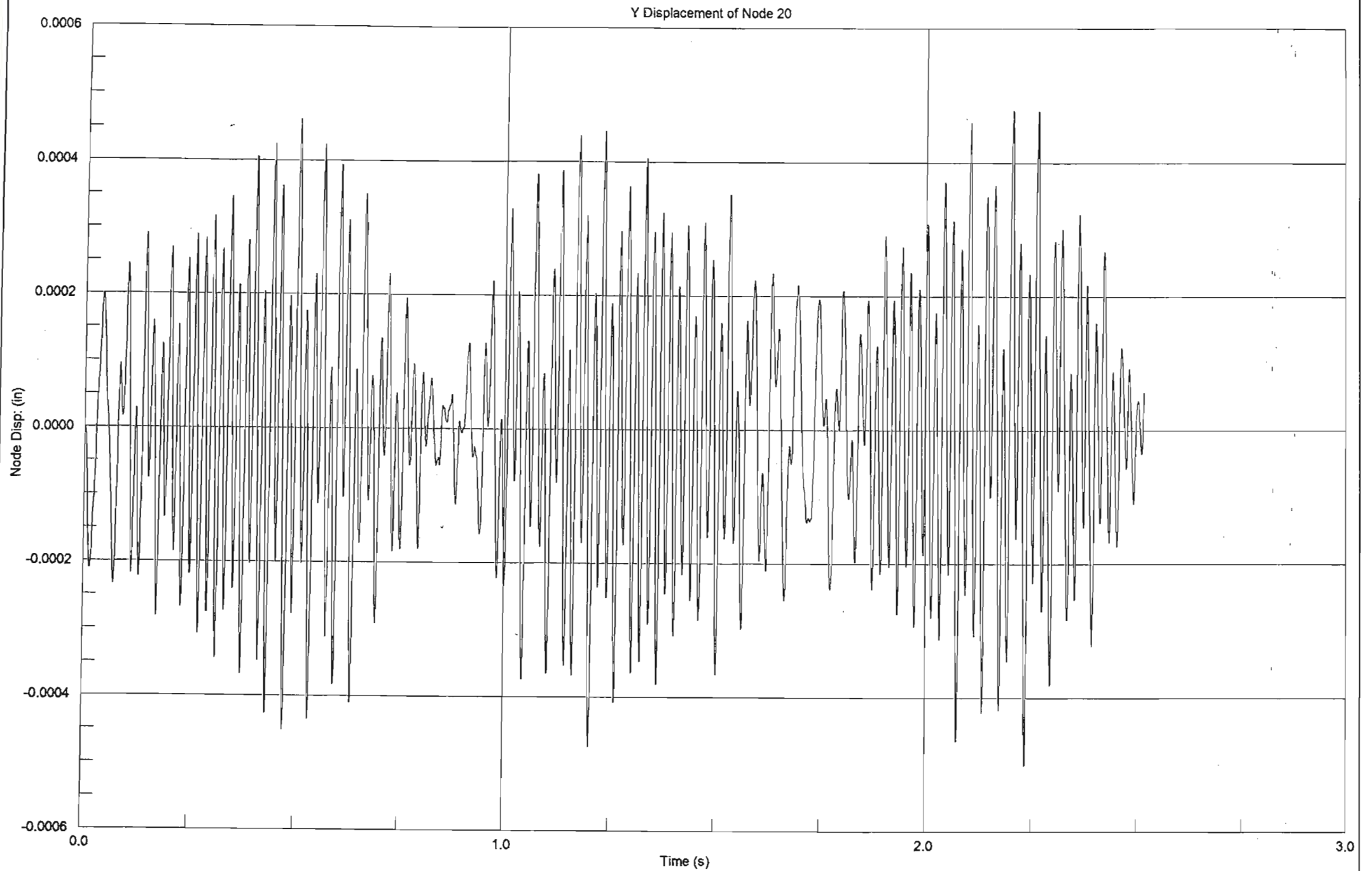


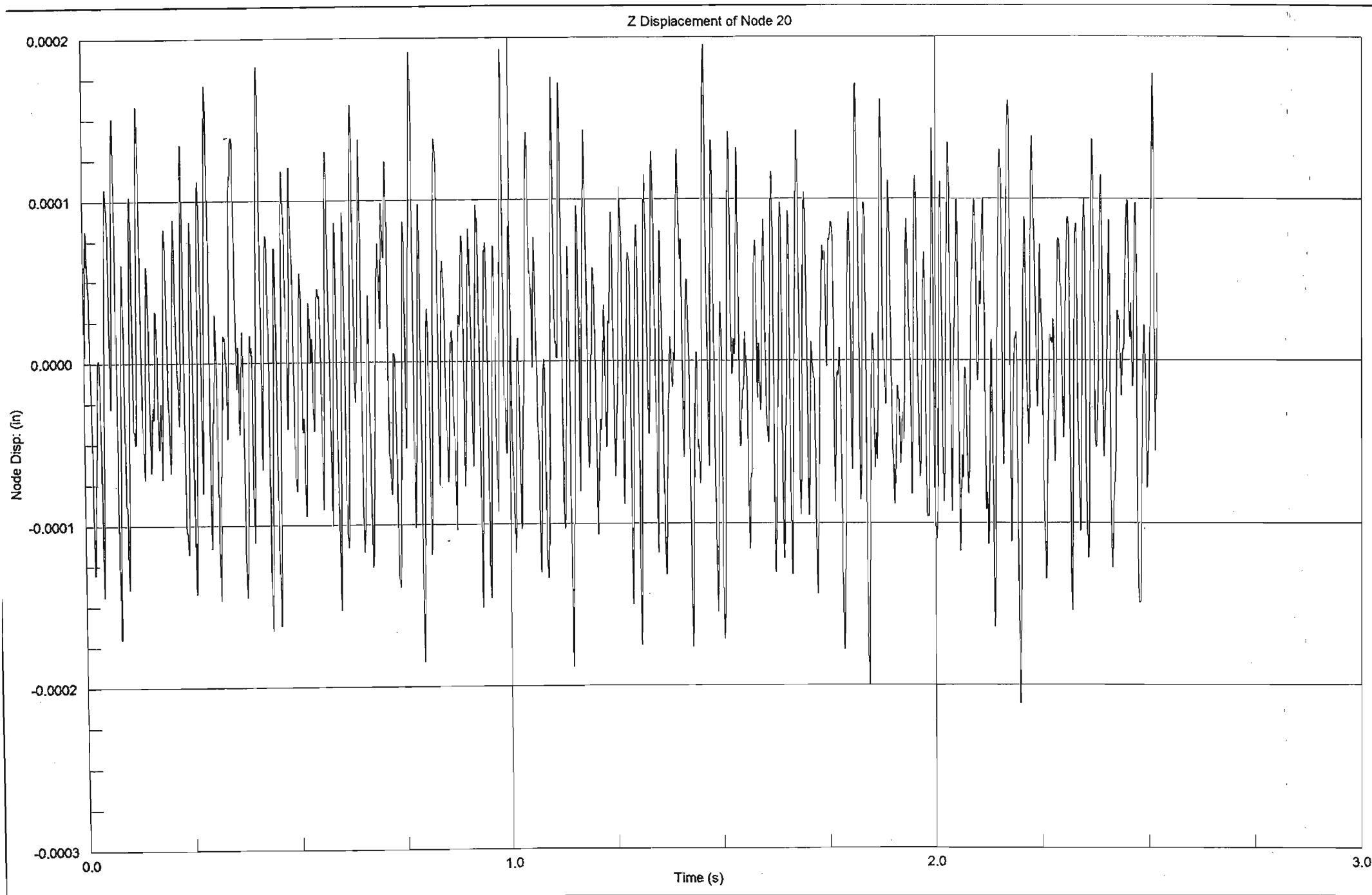


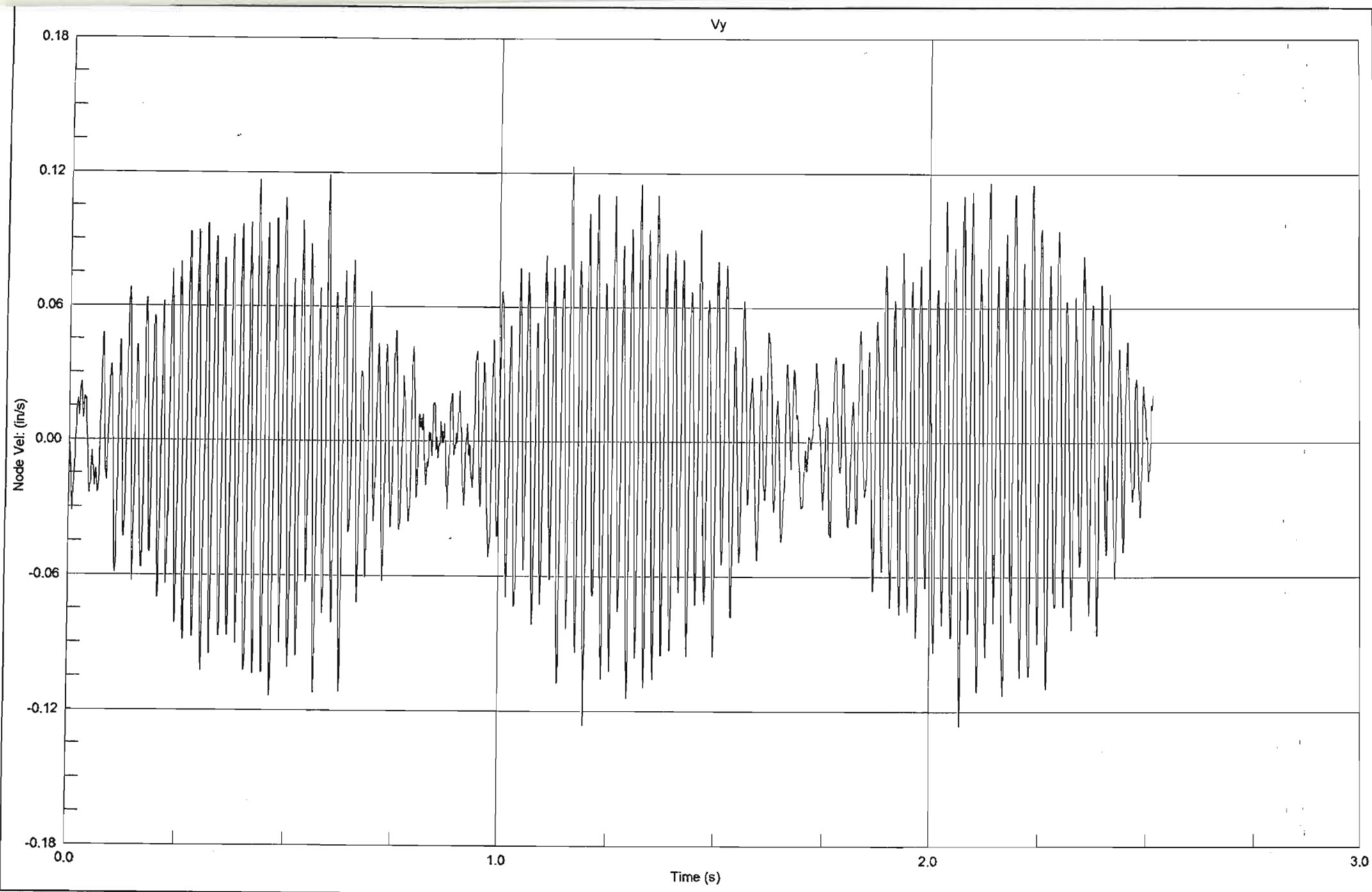


Z Displacement of Node 8

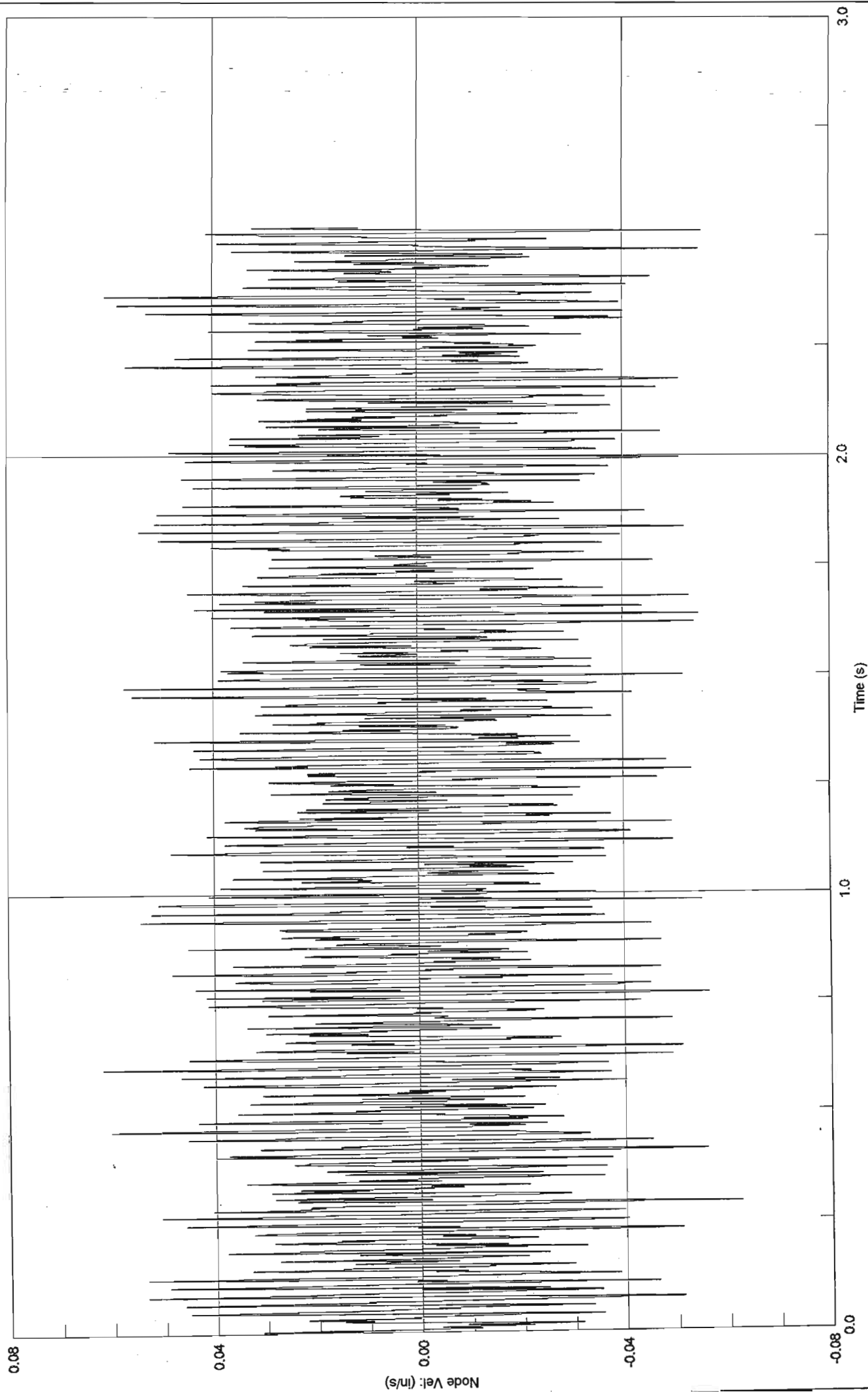




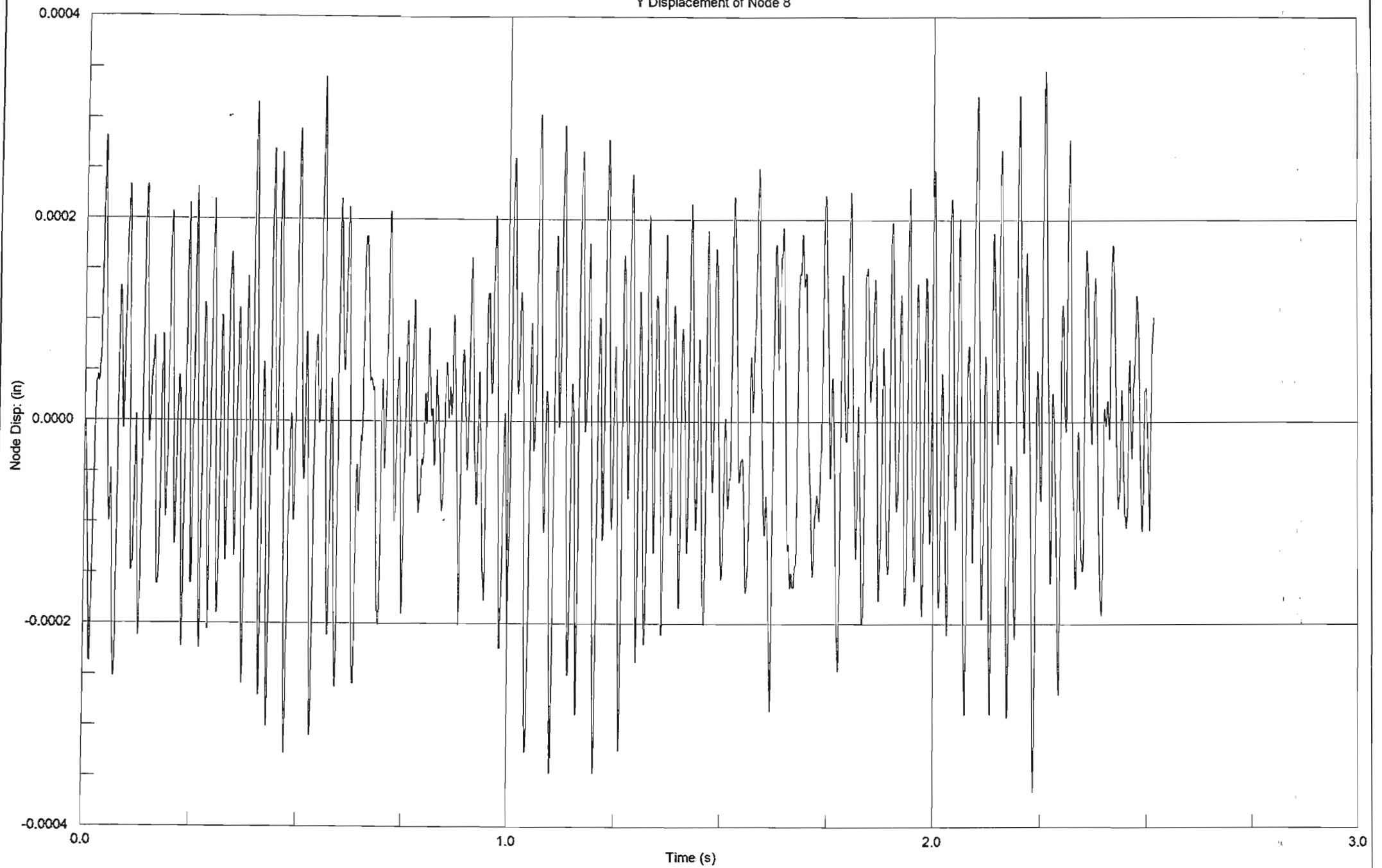


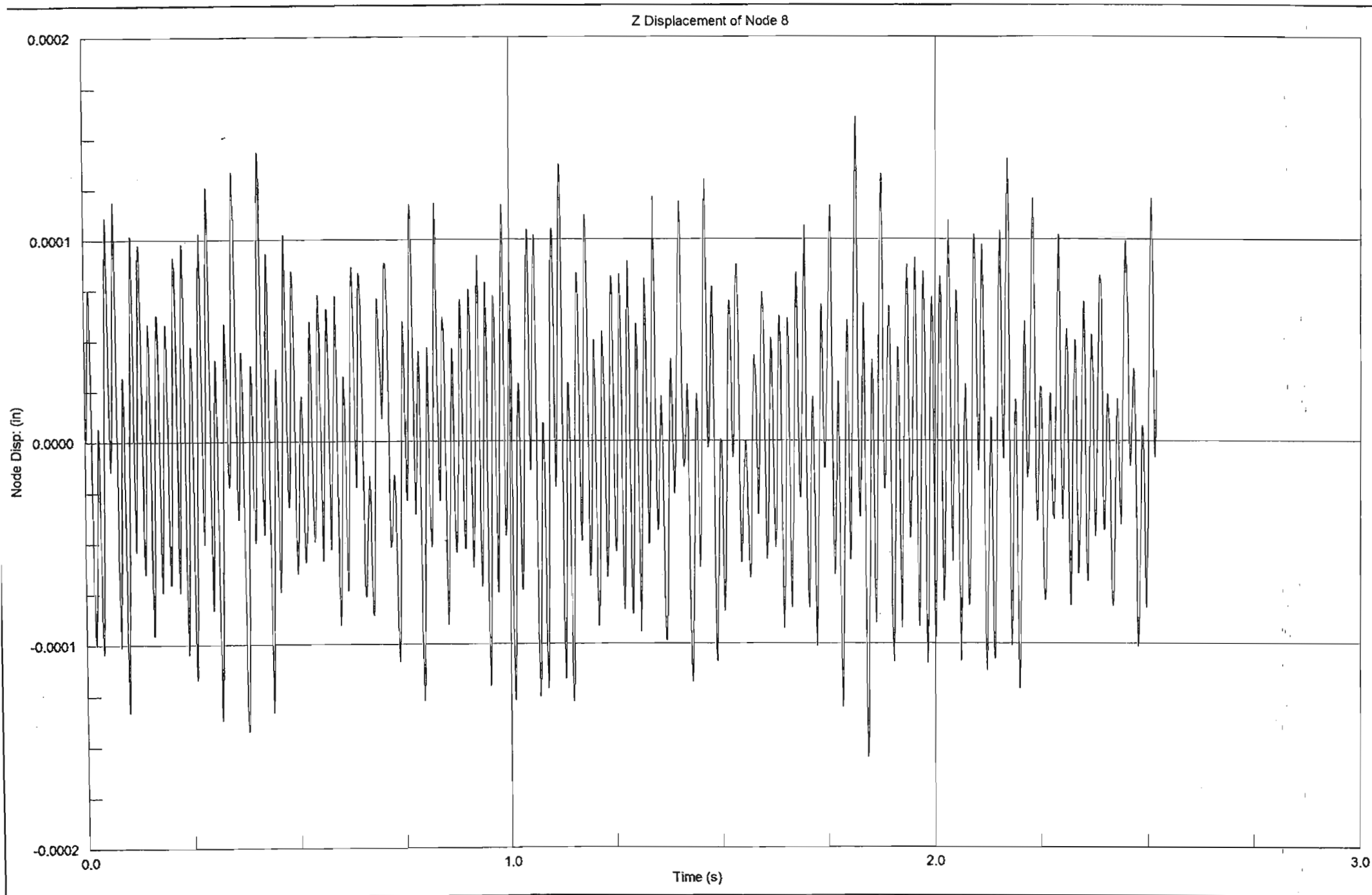


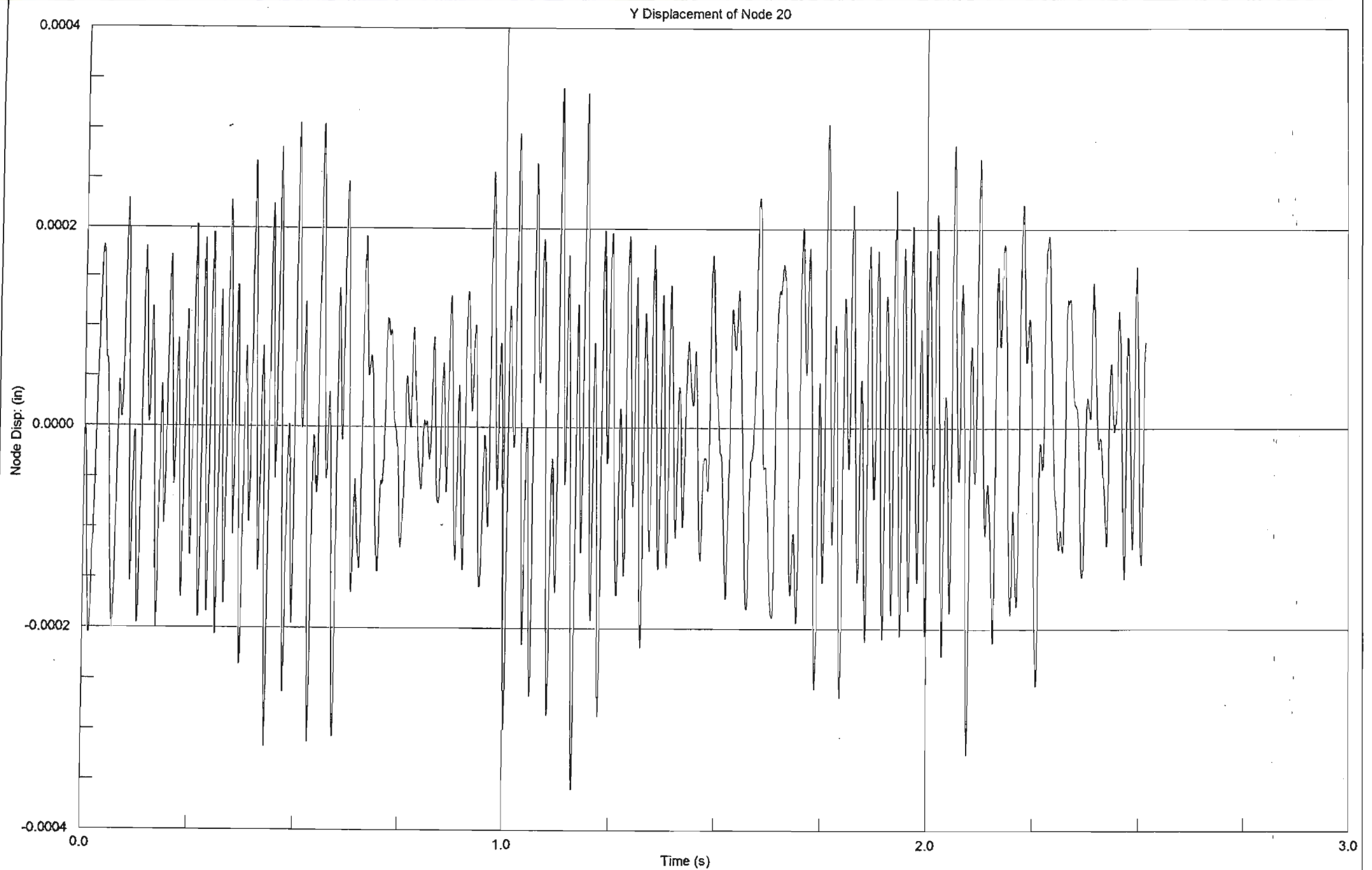
Vz



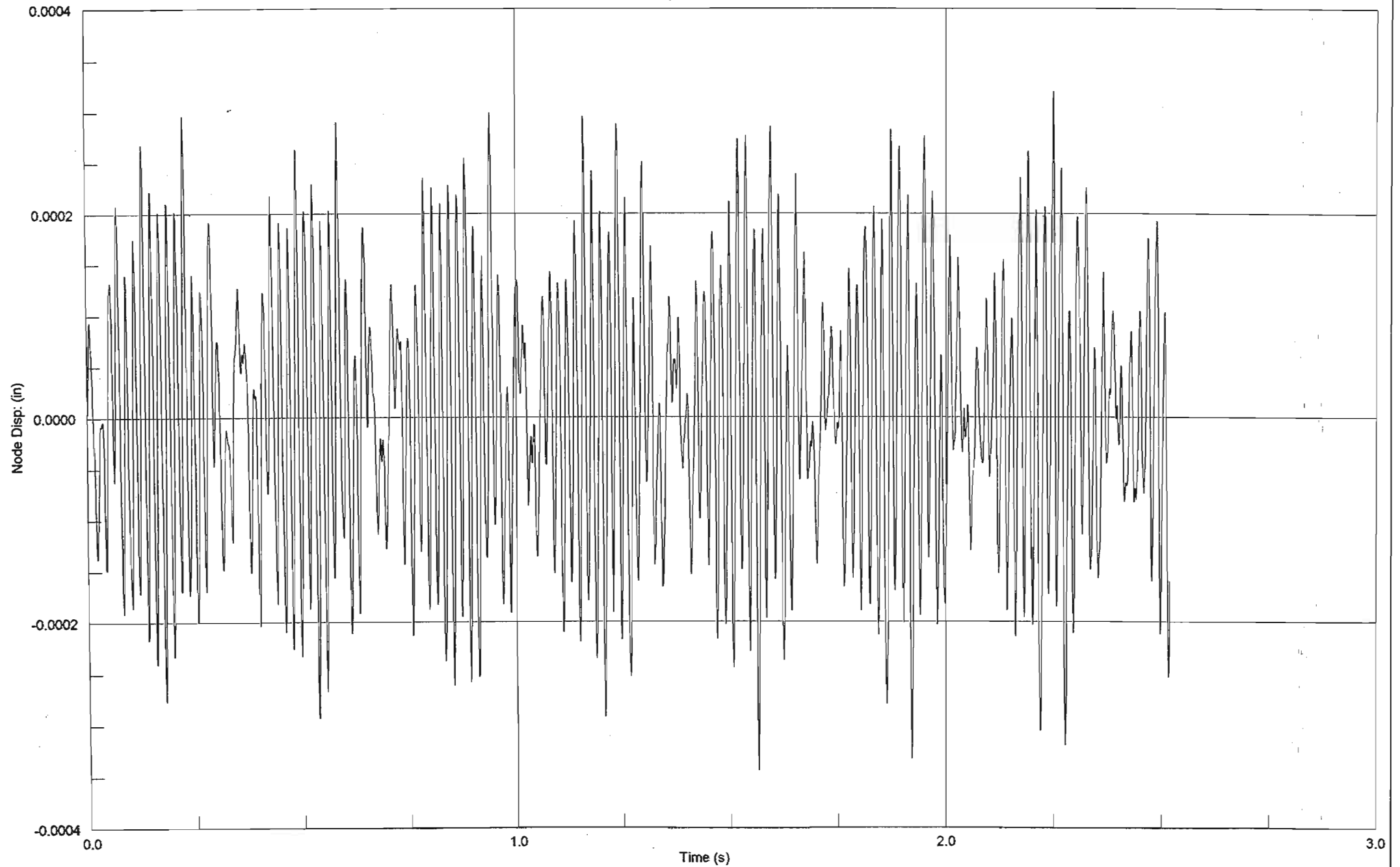
Y Displacement of Node 8

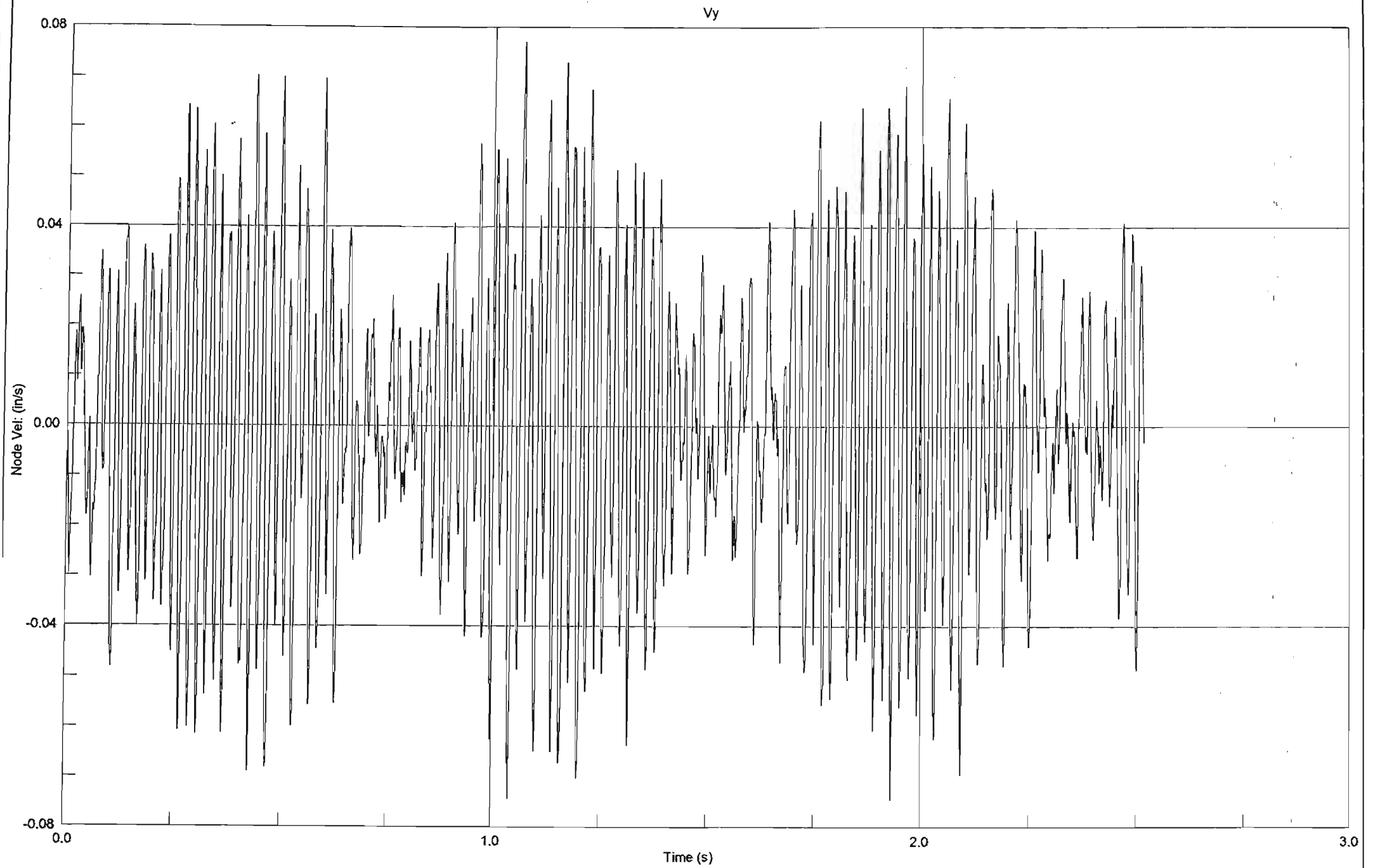




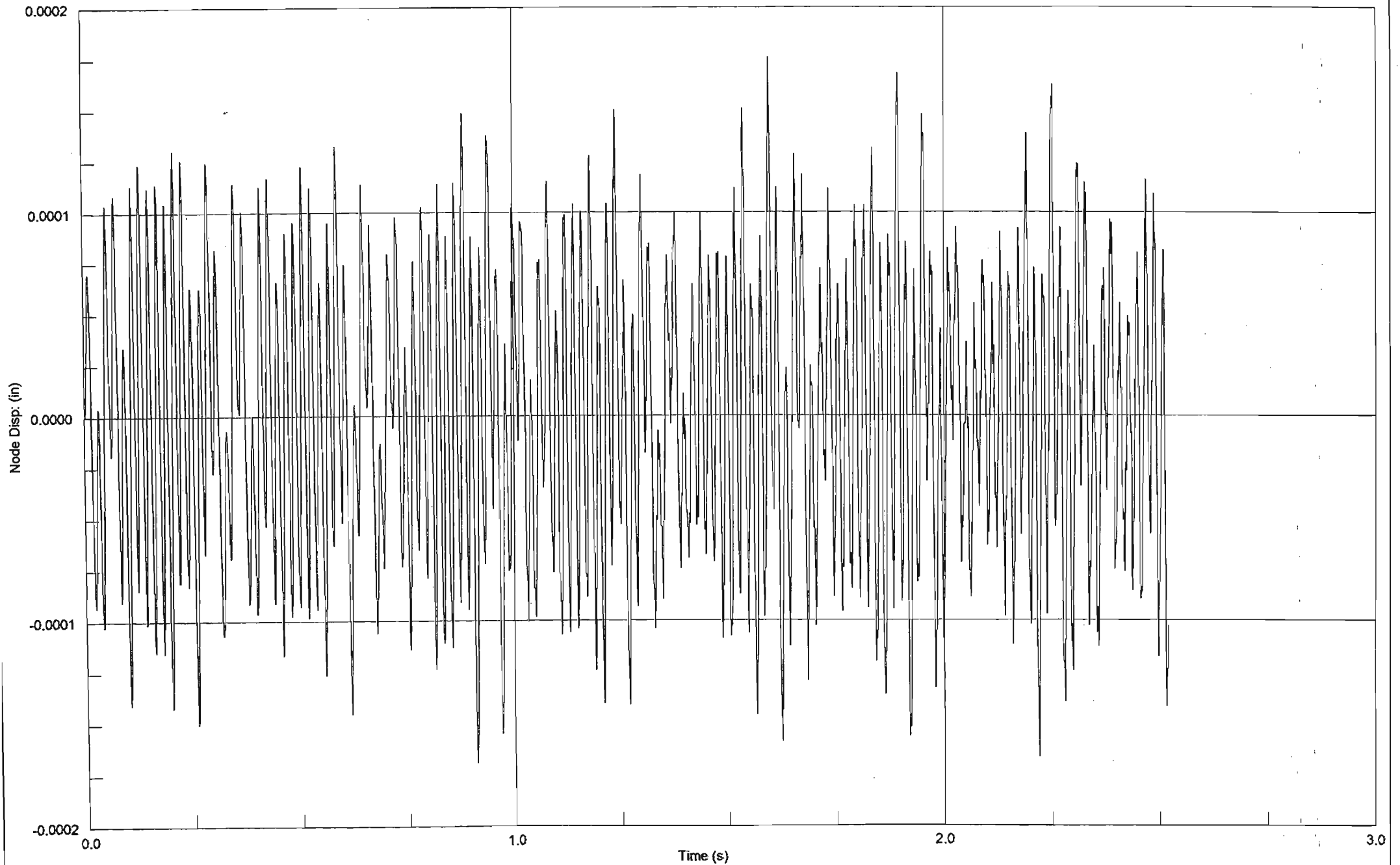


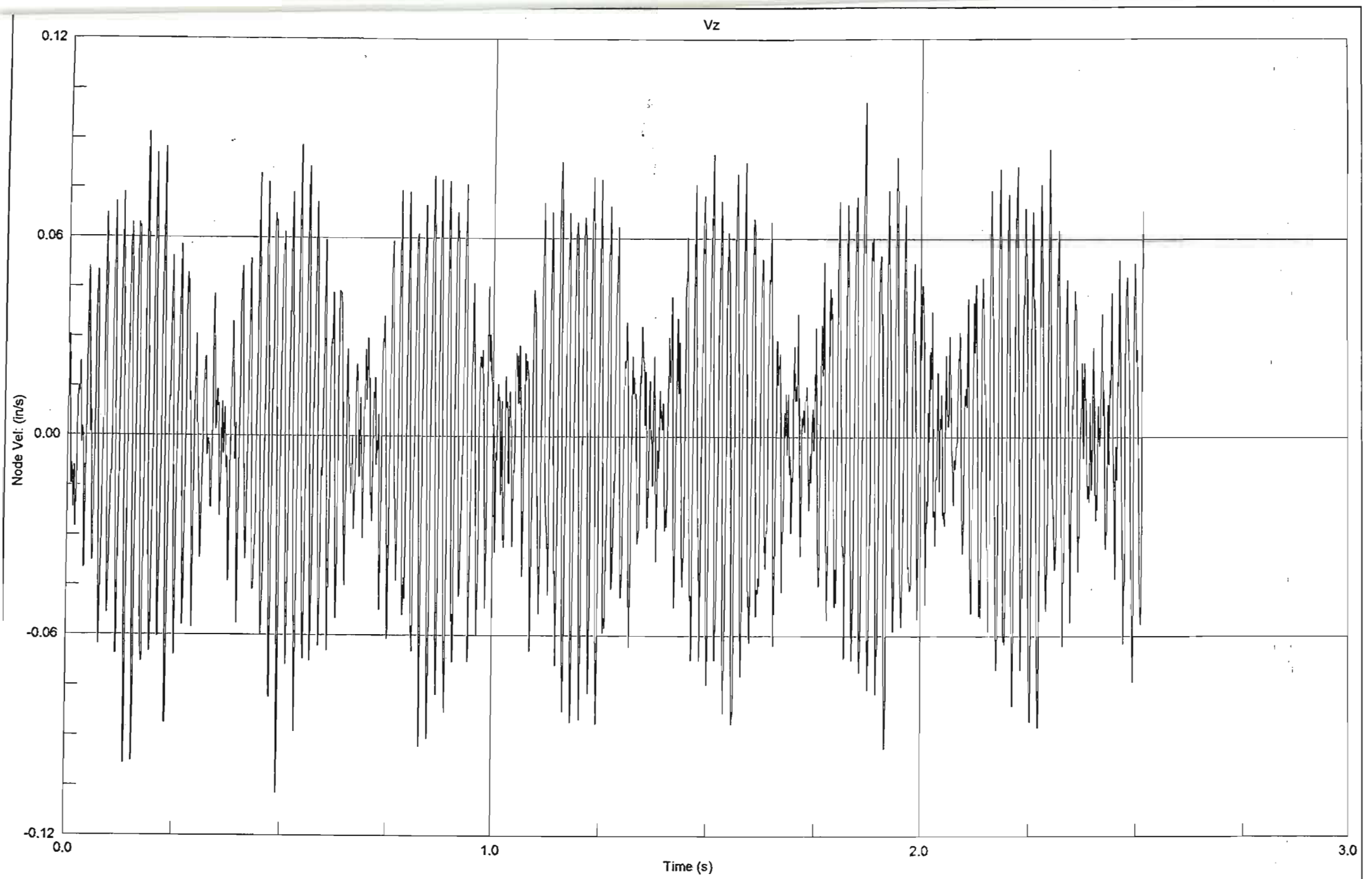
Z Displacement of Node 20



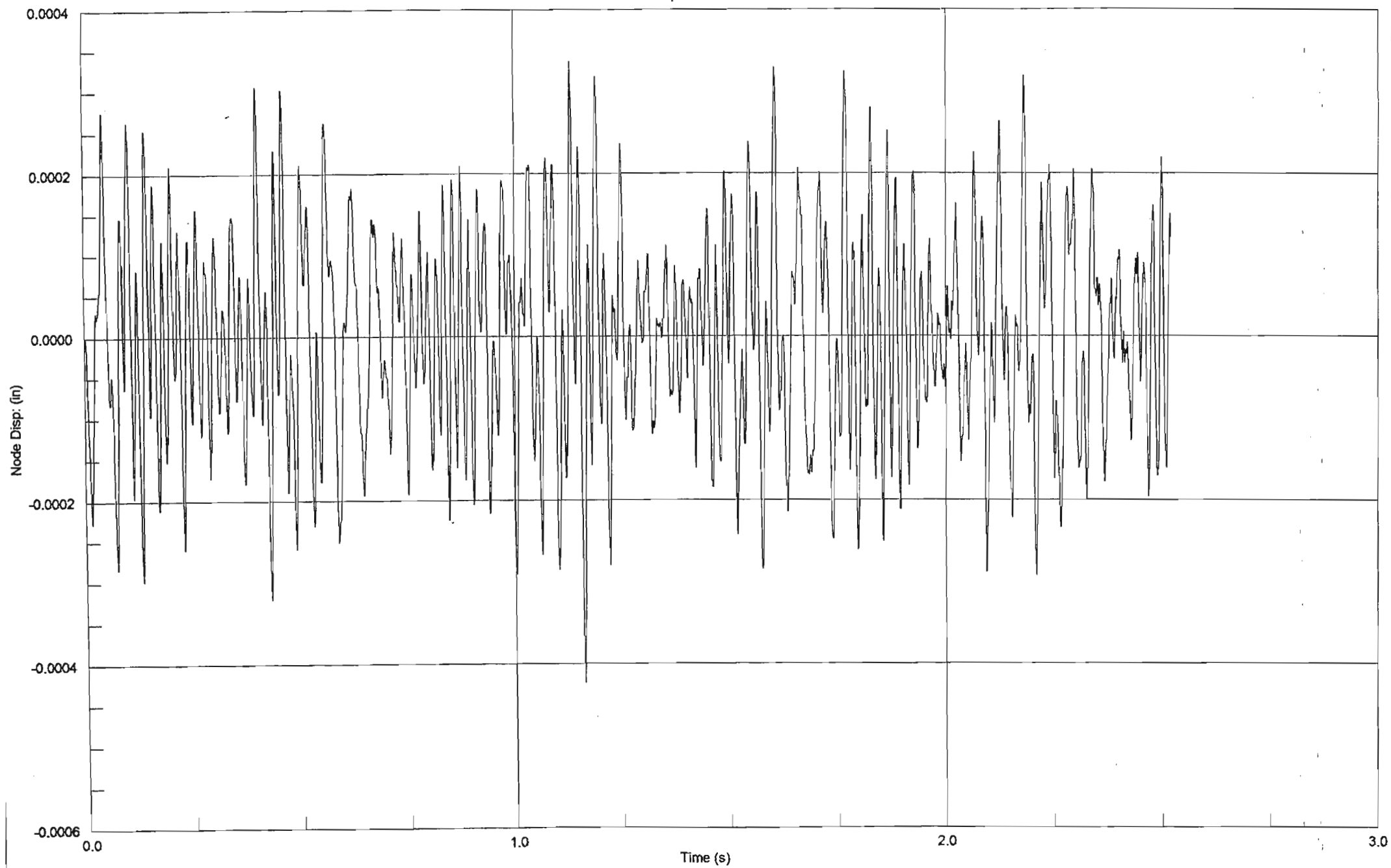


Z Displacement of Node 8

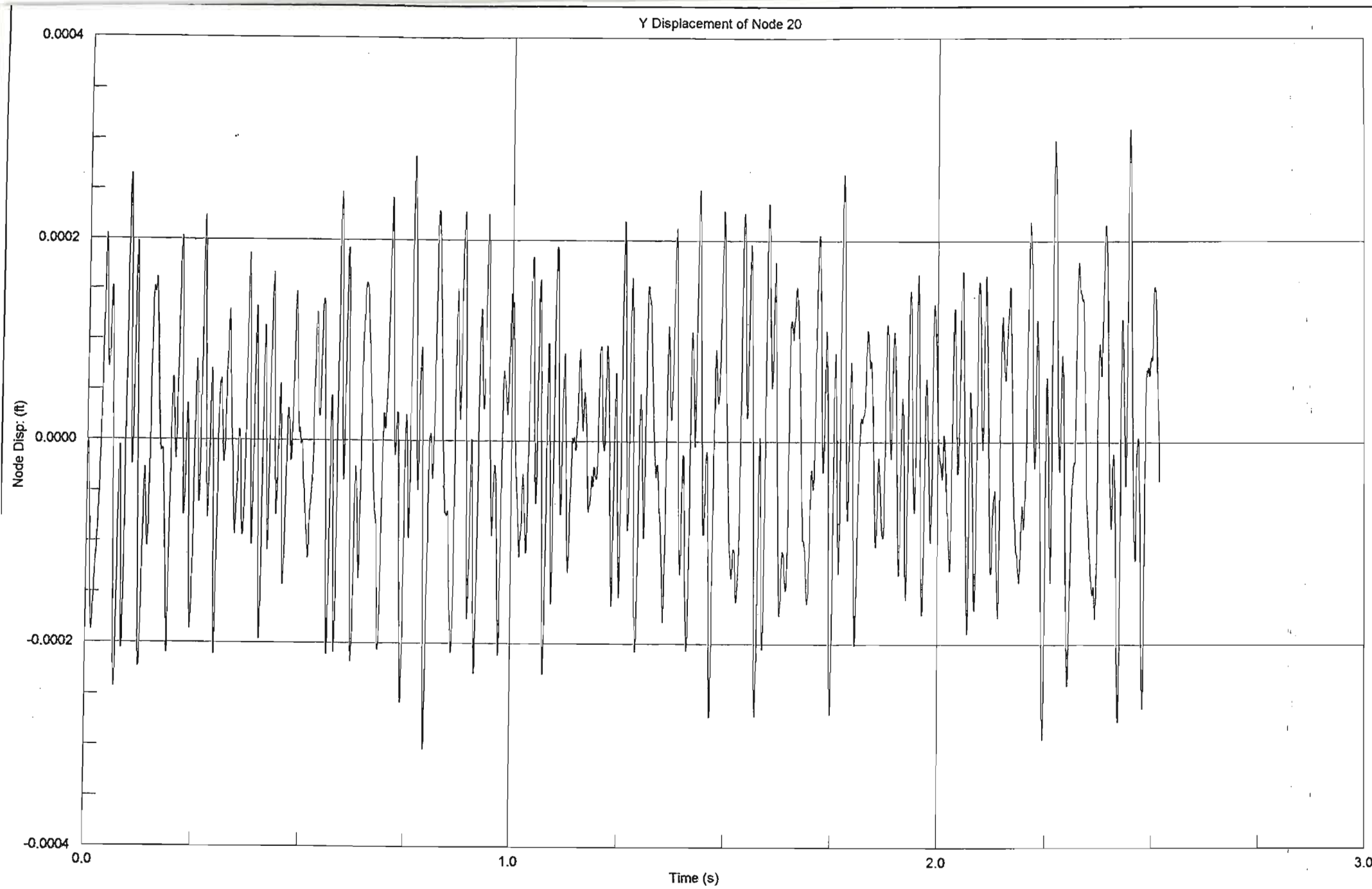




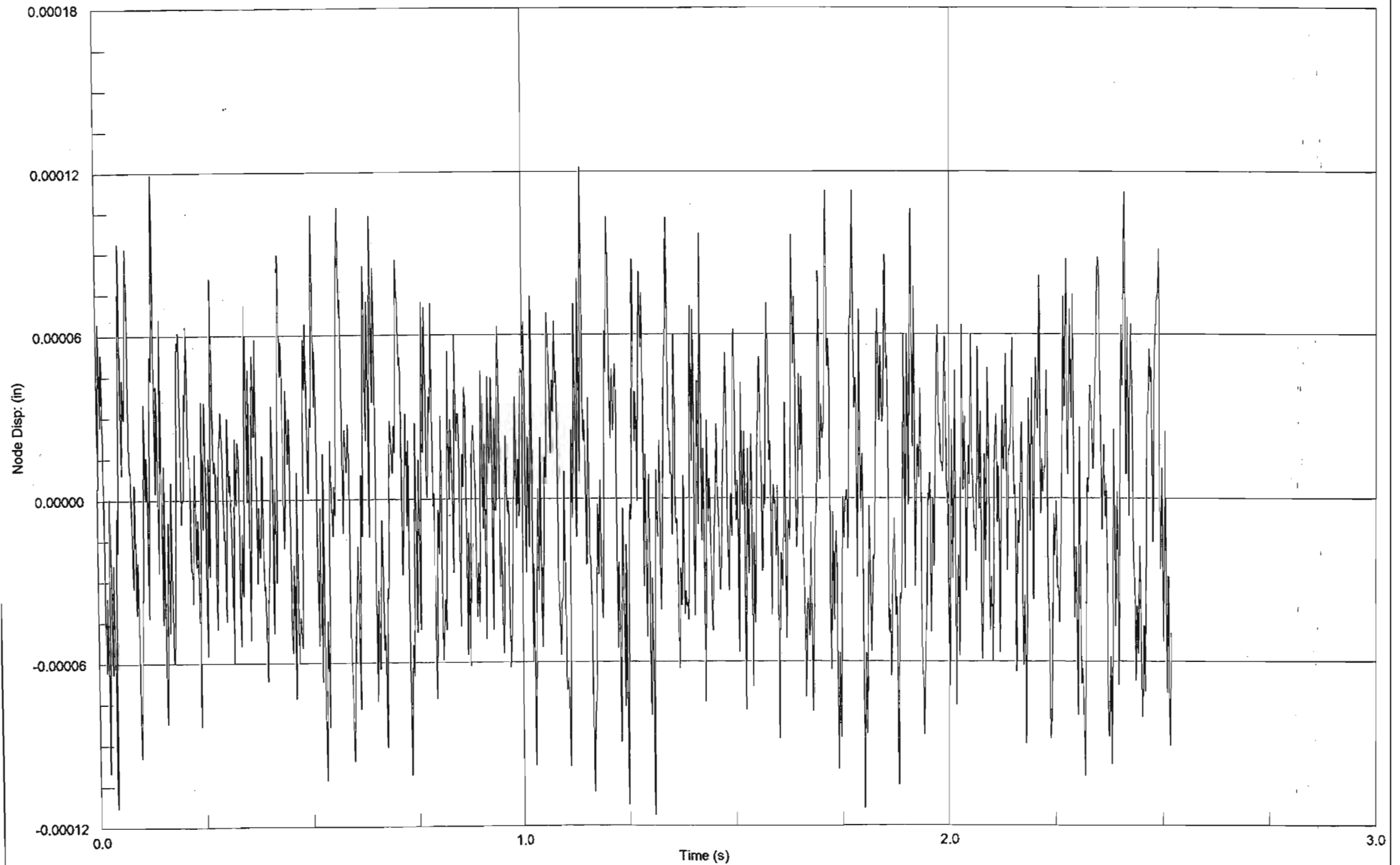
Y Displacement of Node 8

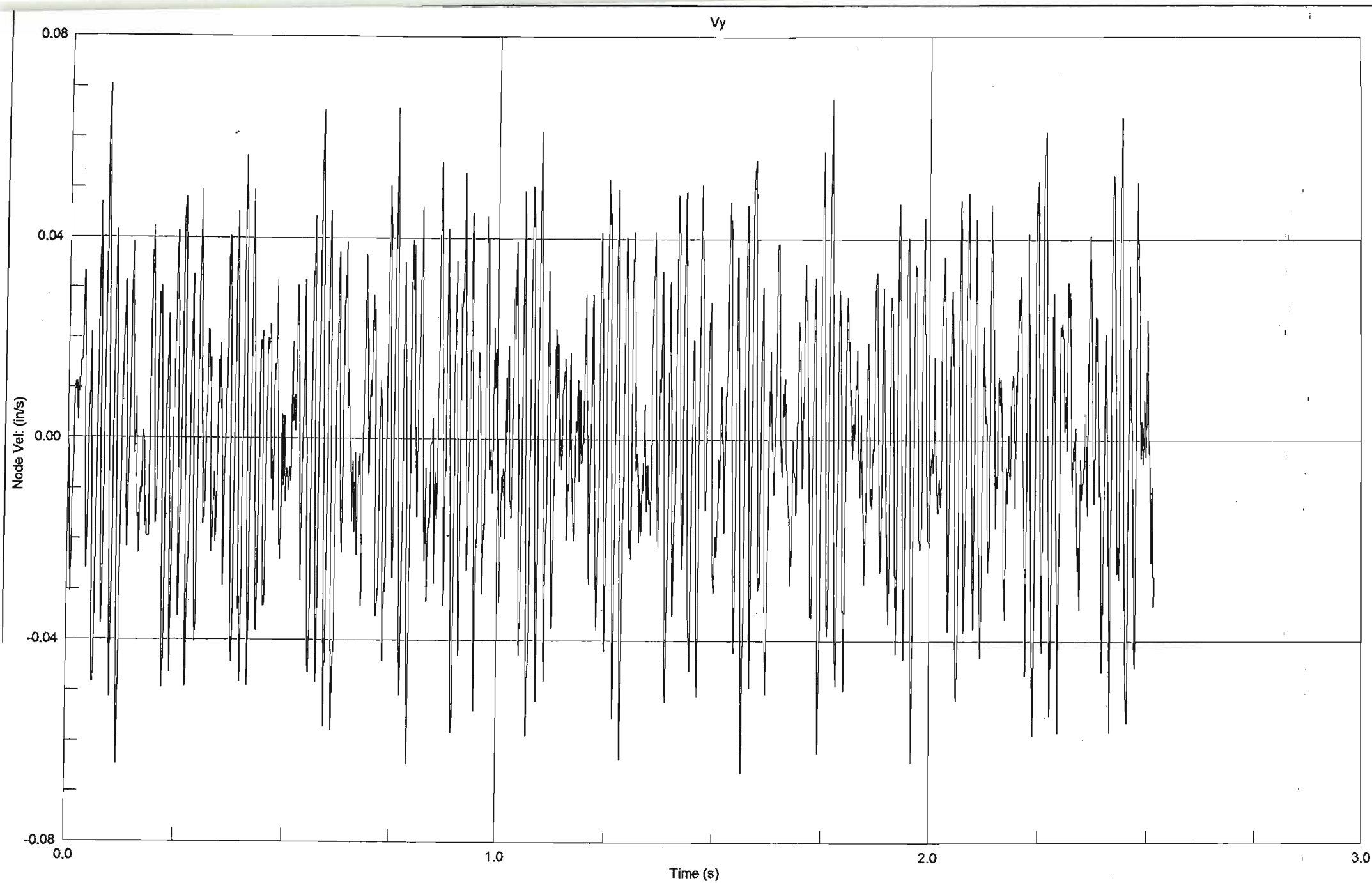


B 3.66

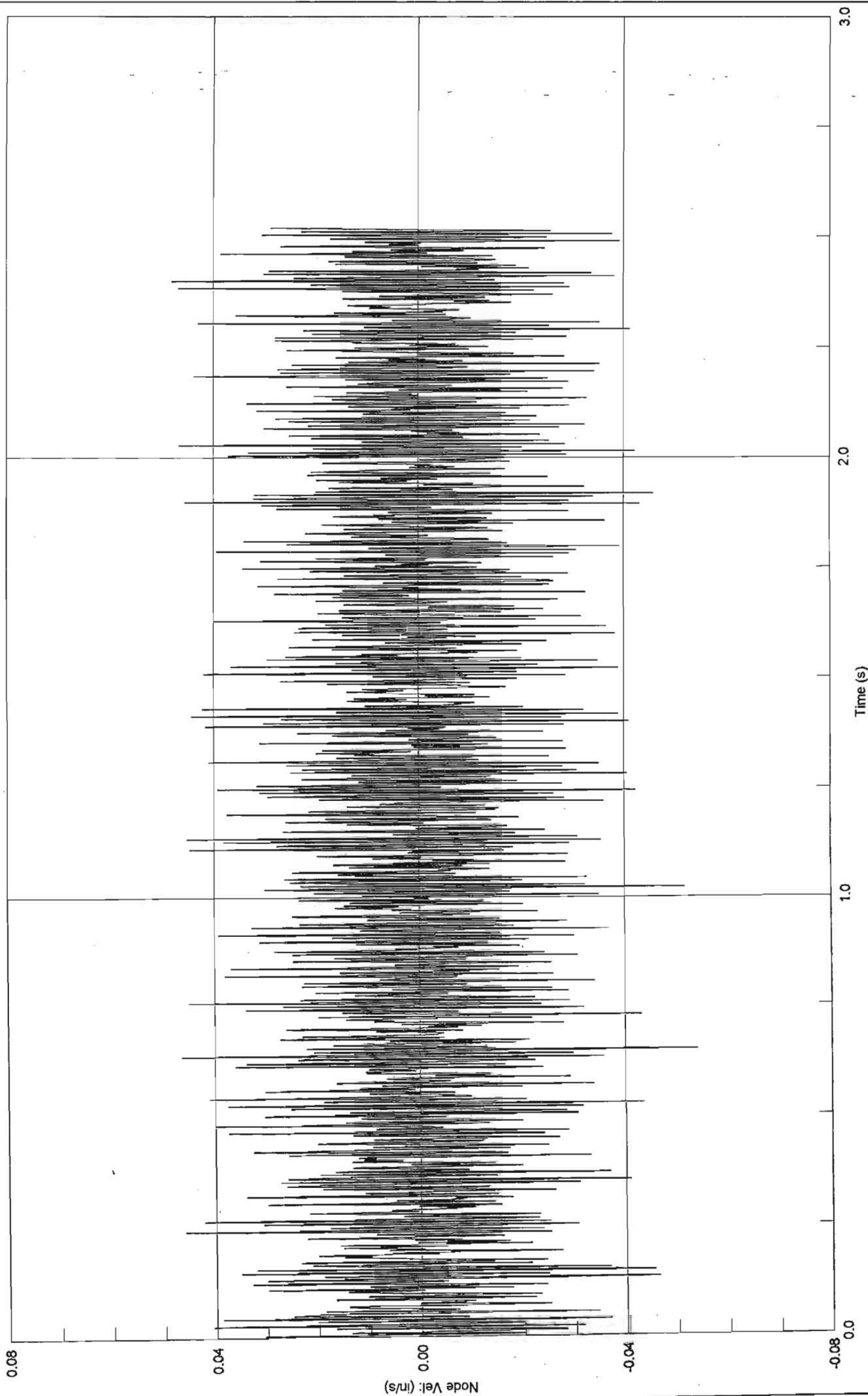


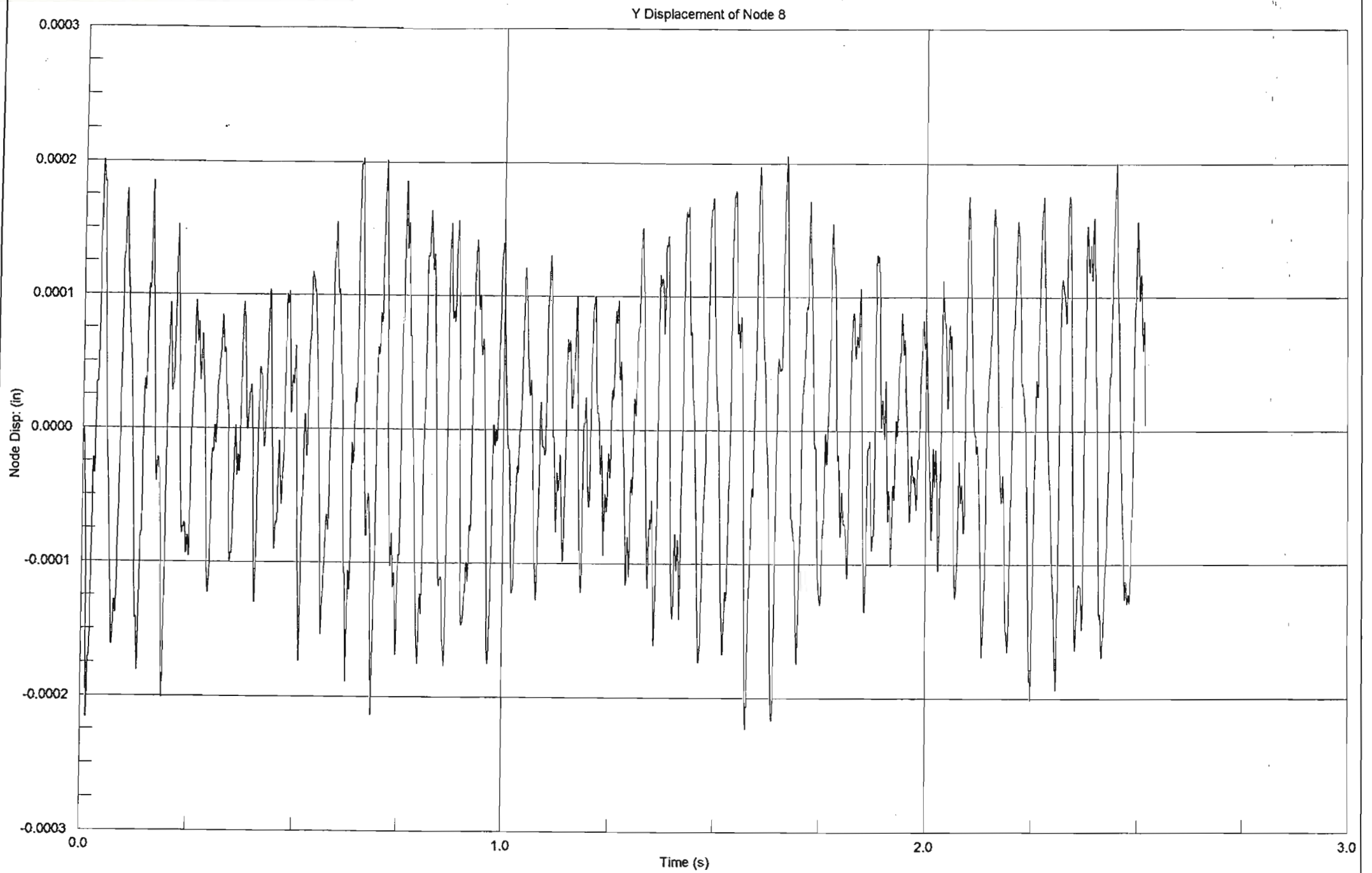
Z Displacement of Node 20



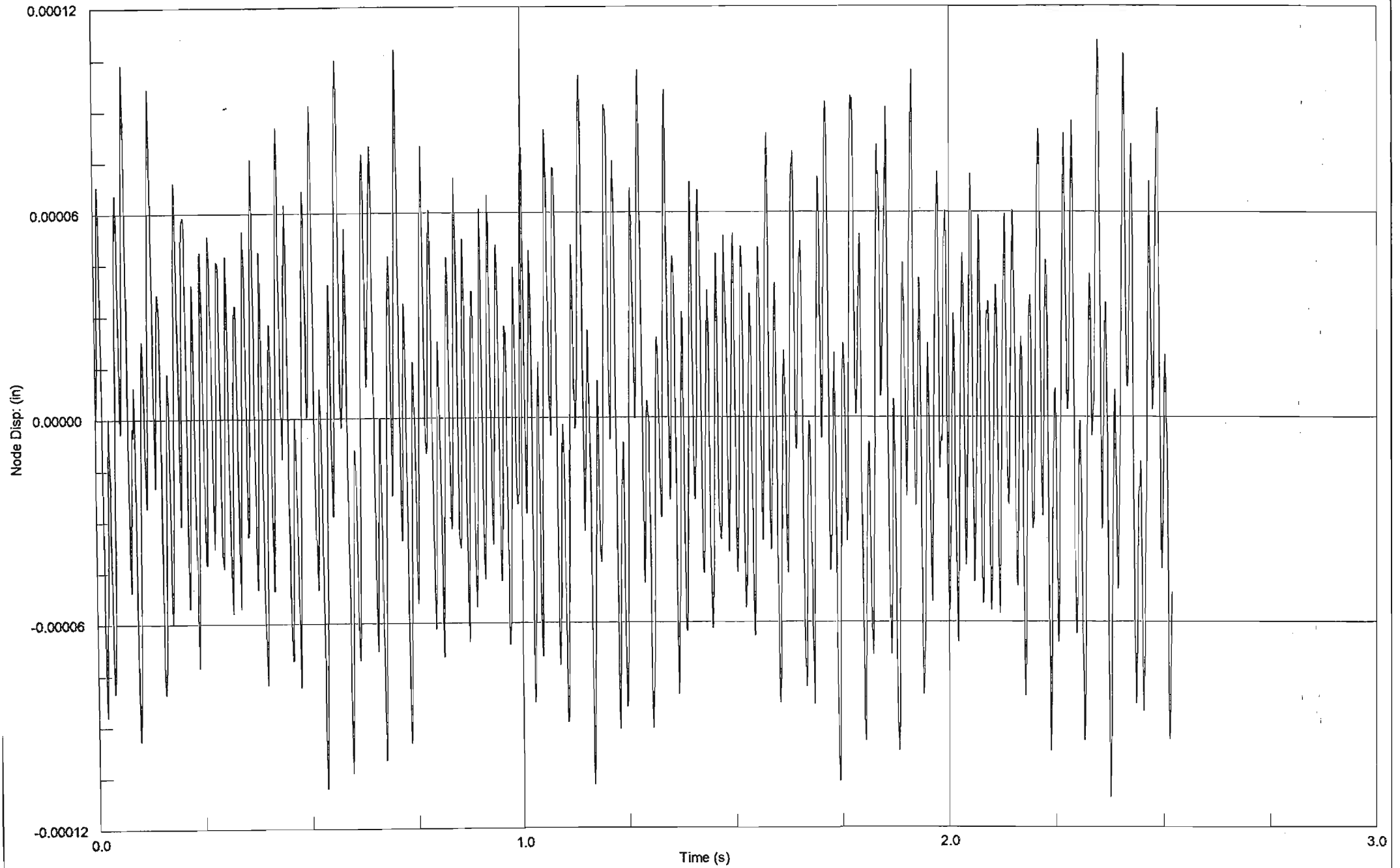


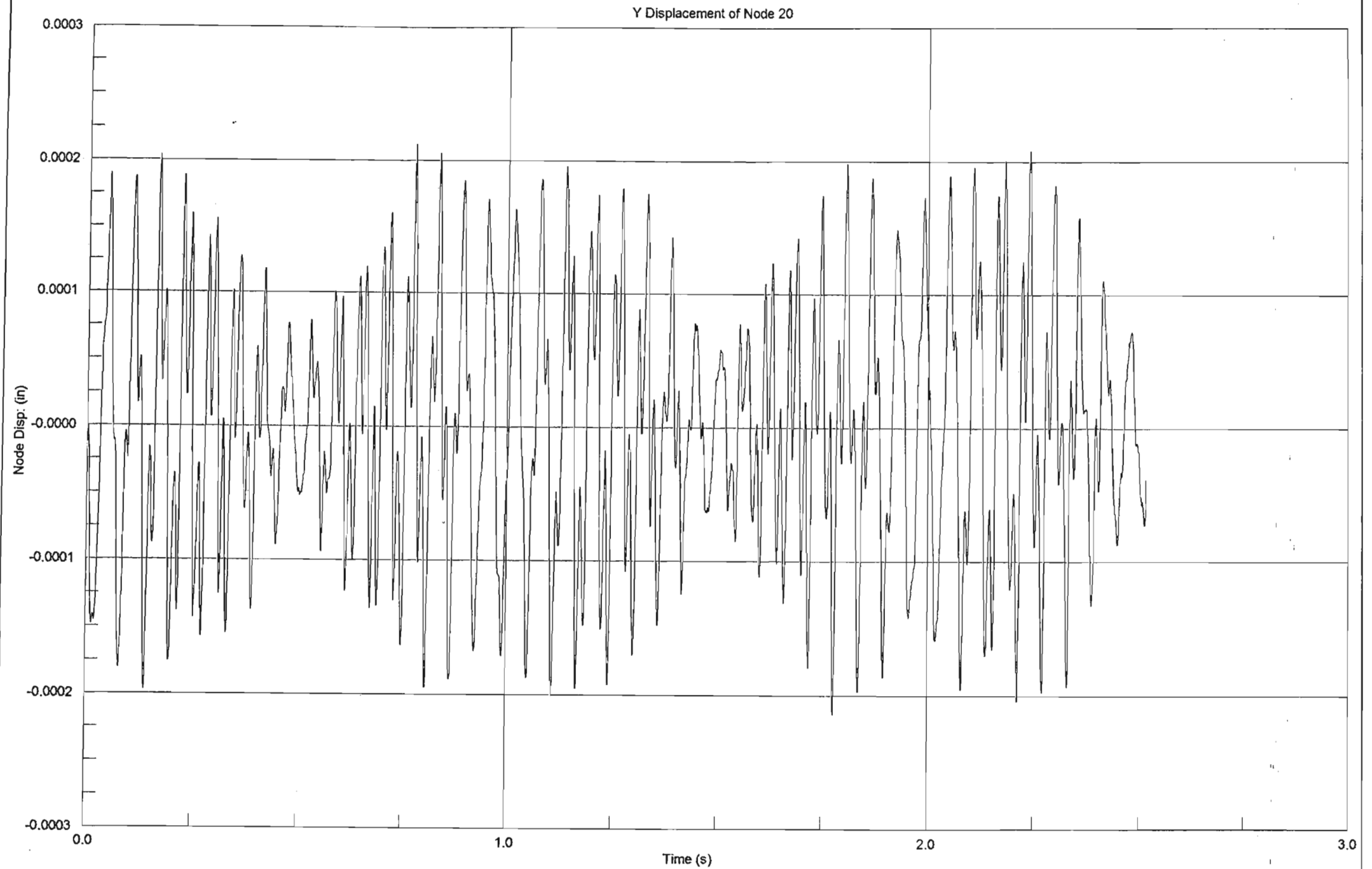
Vz



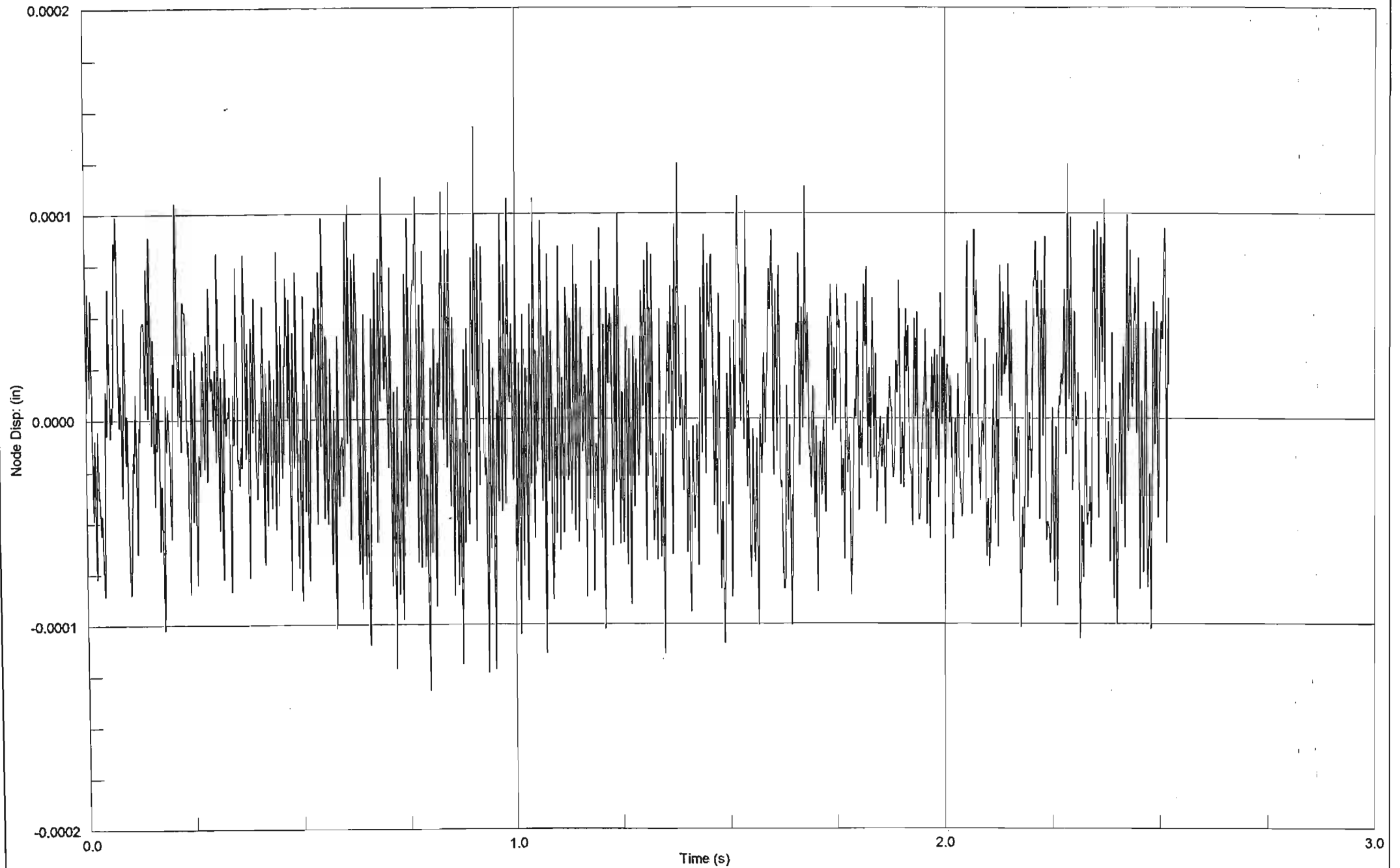


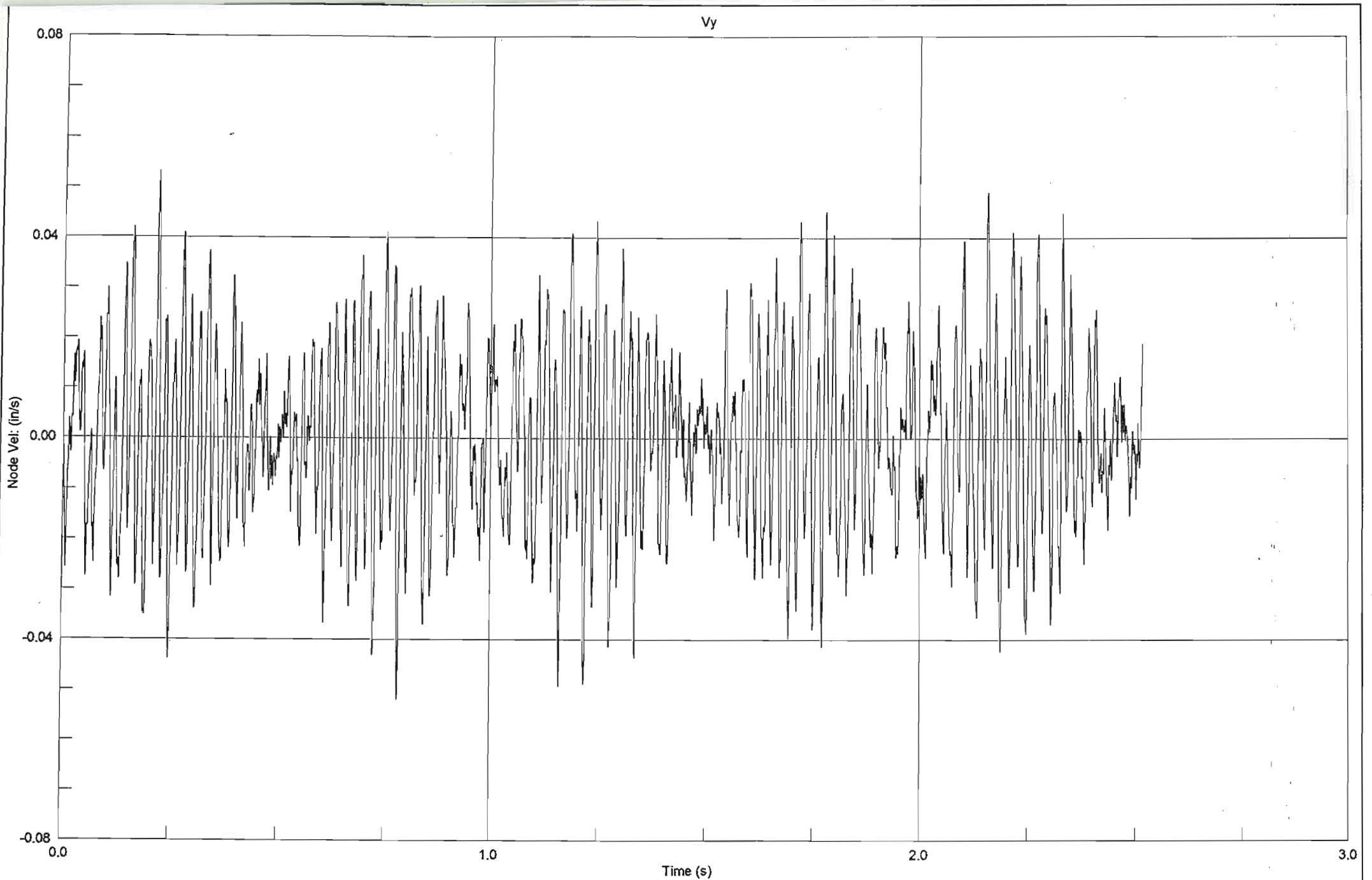
Z Displacement of Node 8

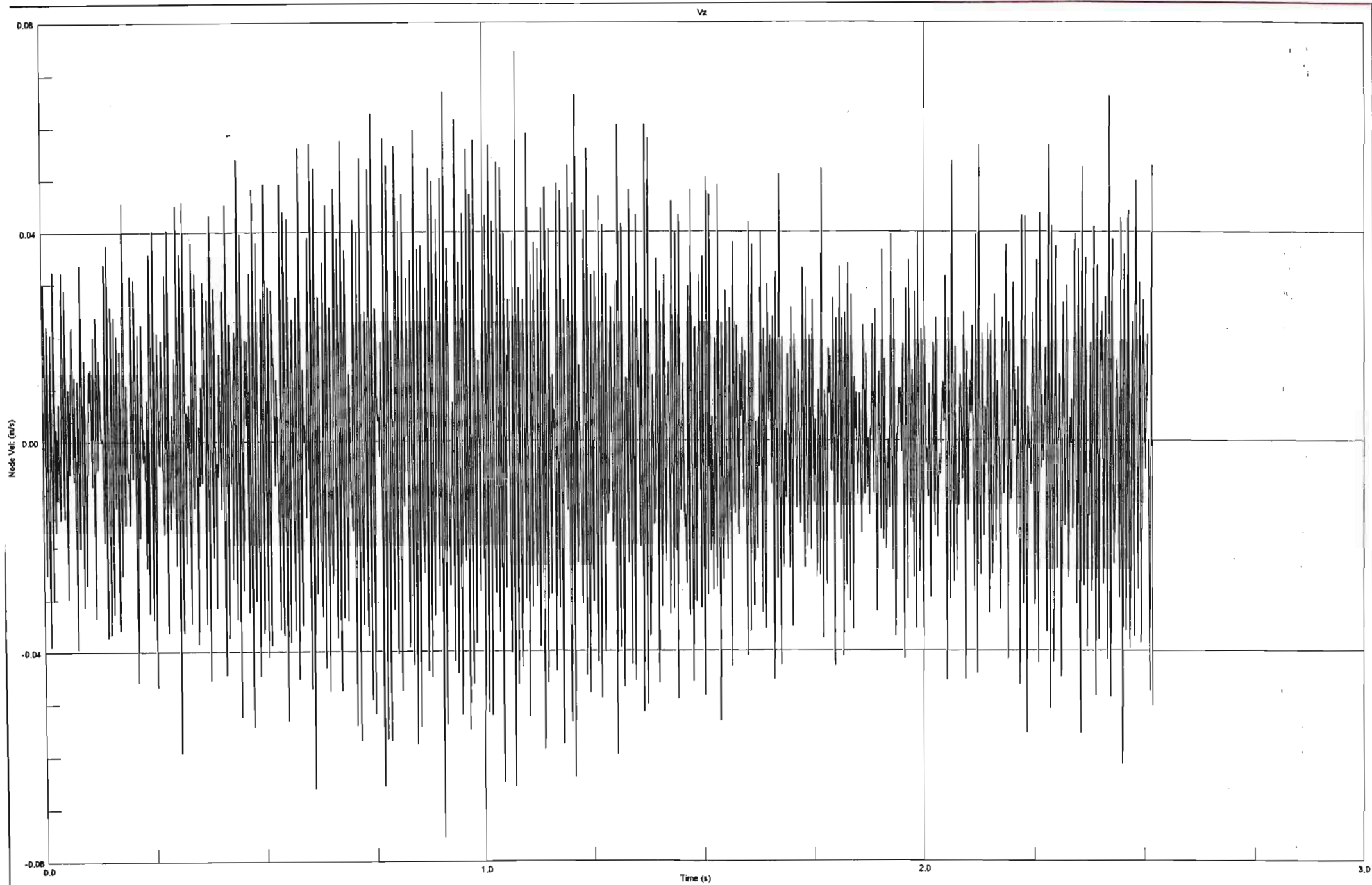


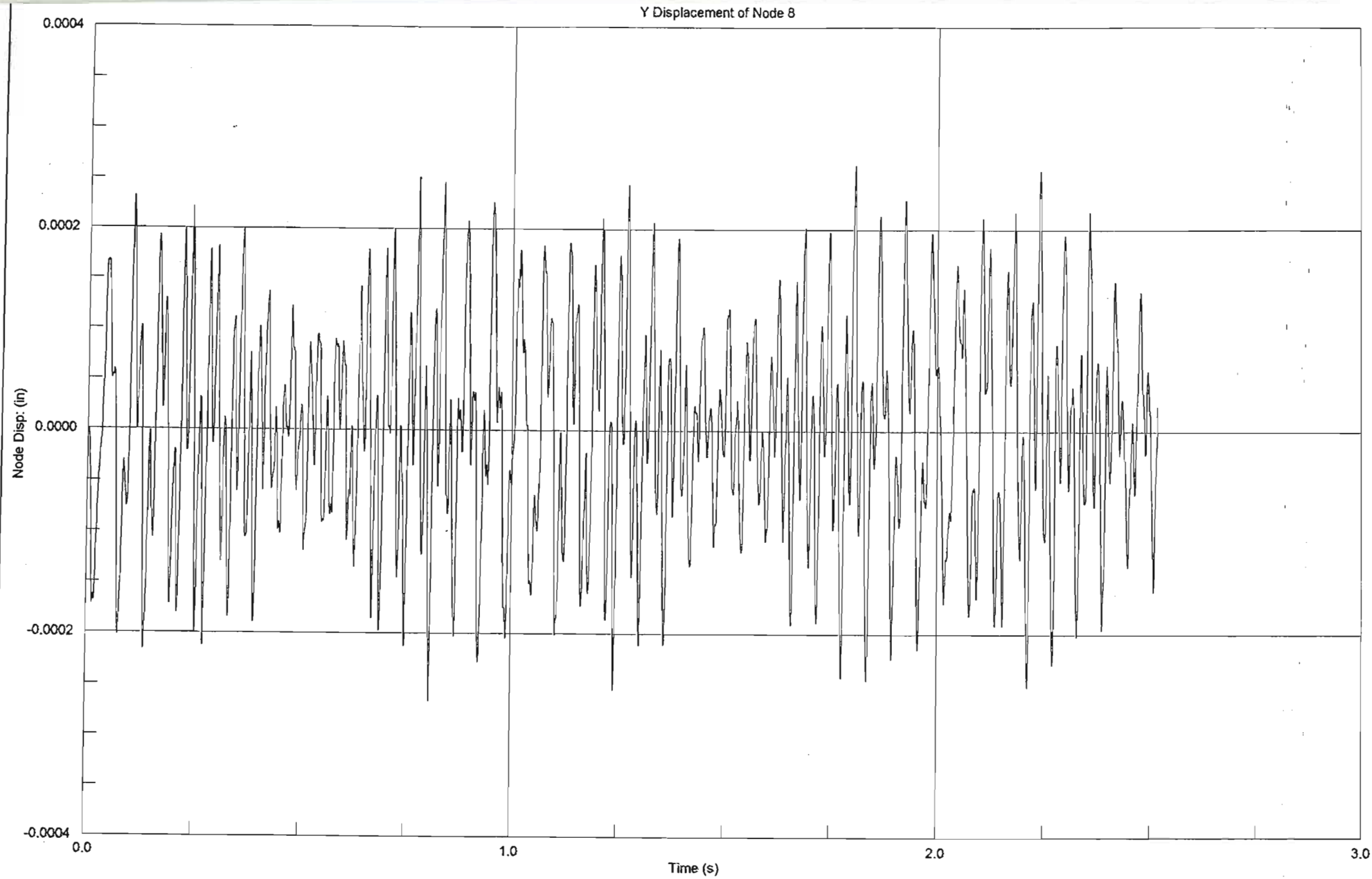


Z Displacement of Node 20

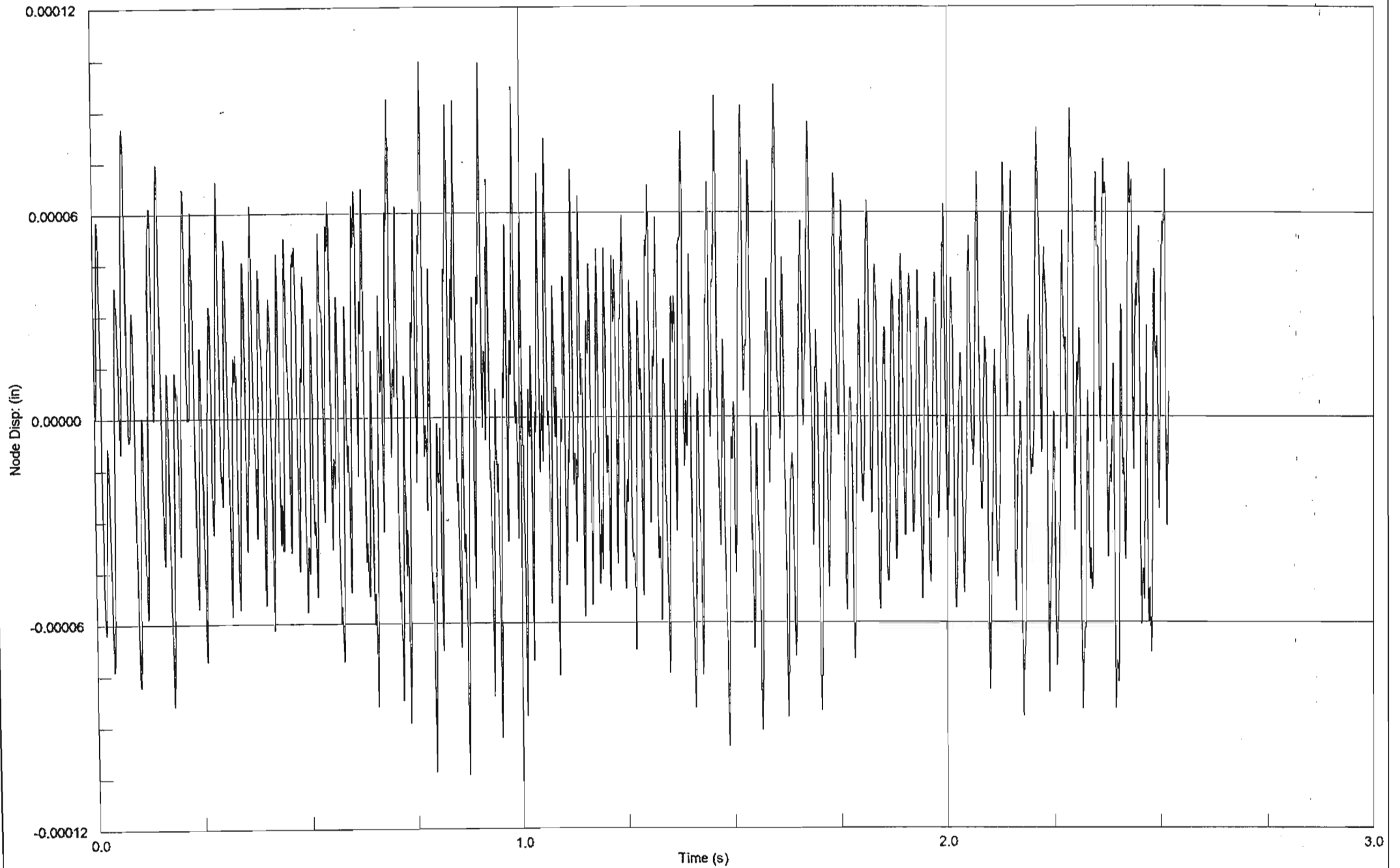


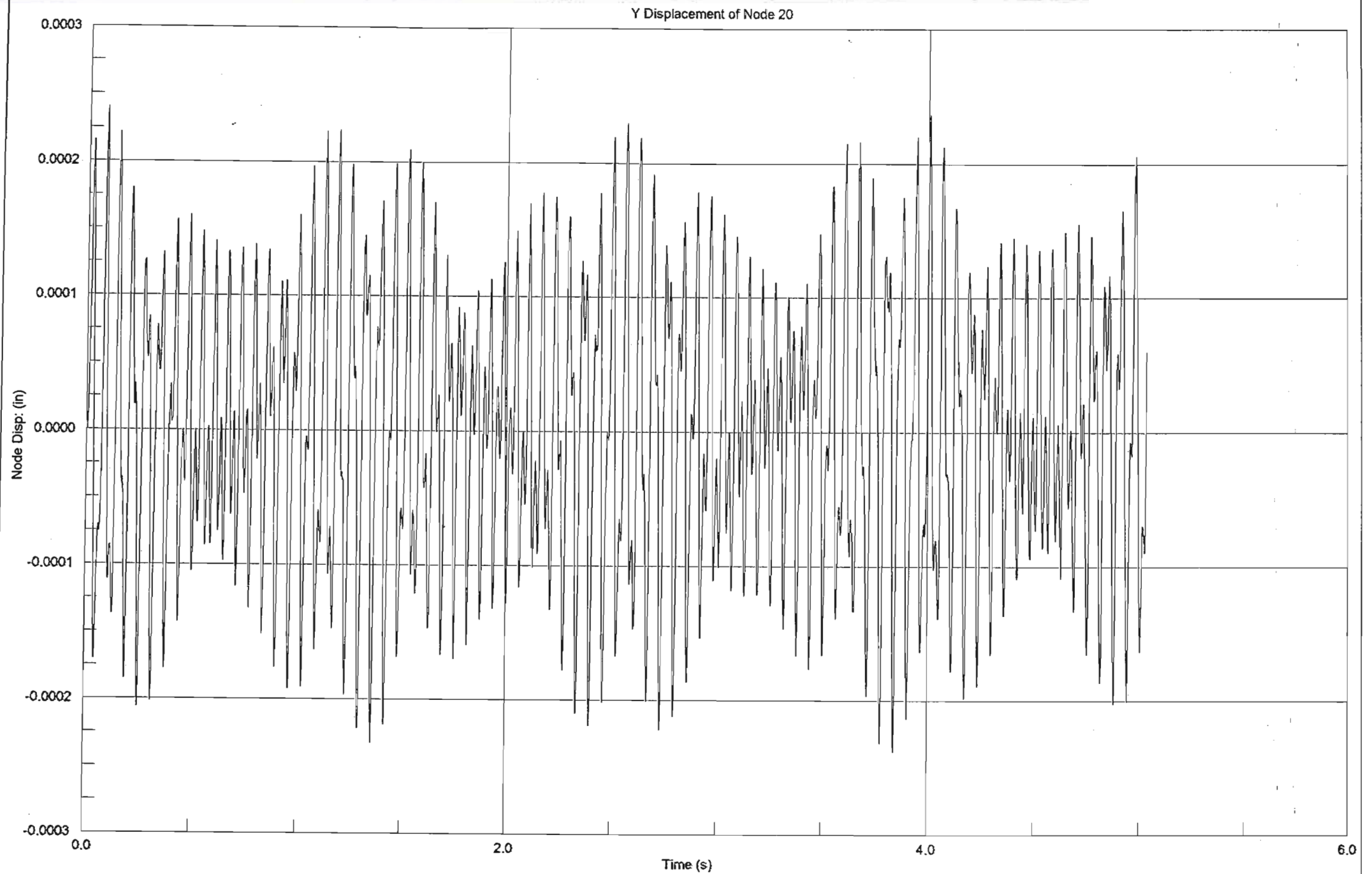


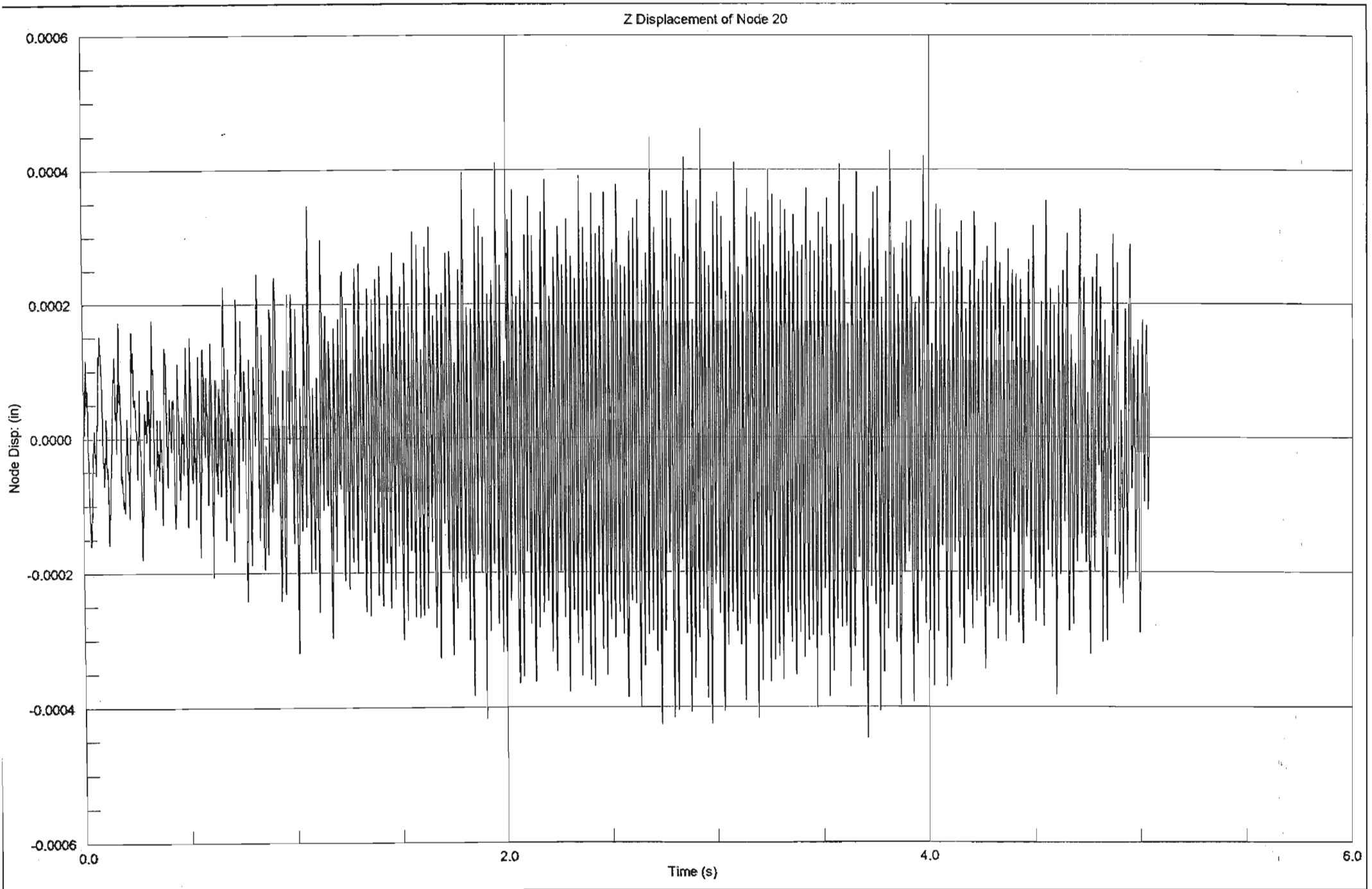


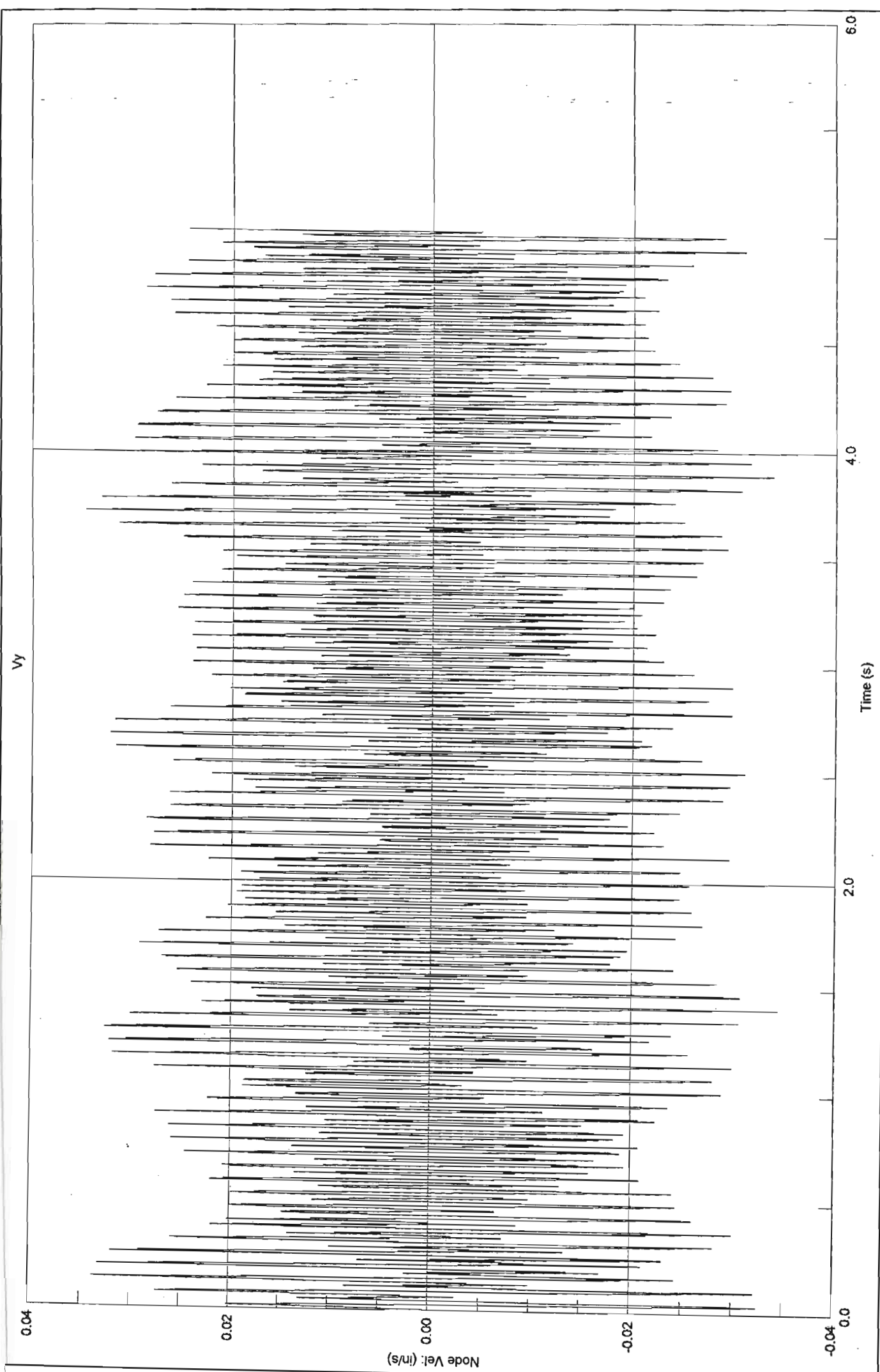


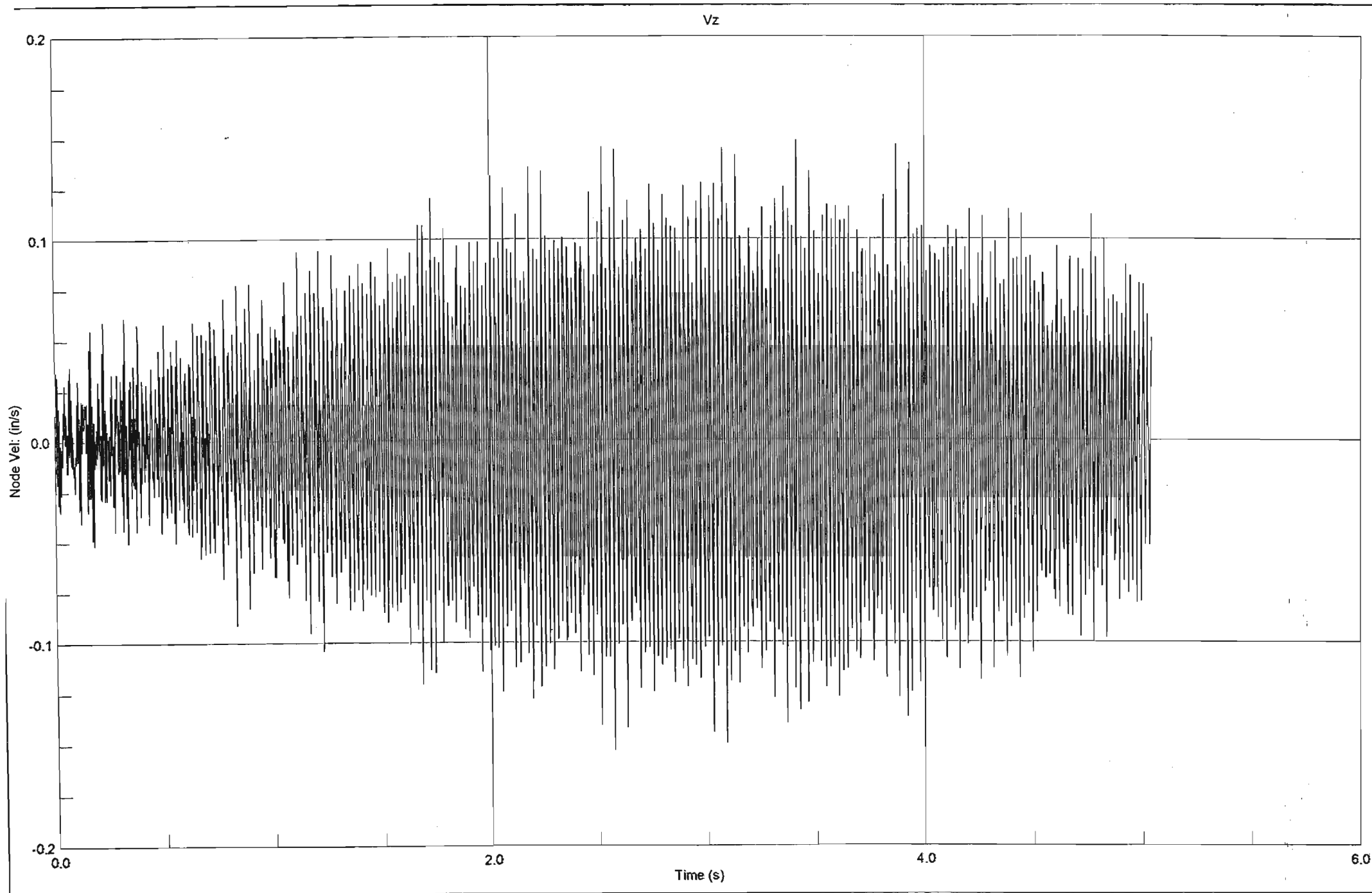
Z Displacement of Node 8









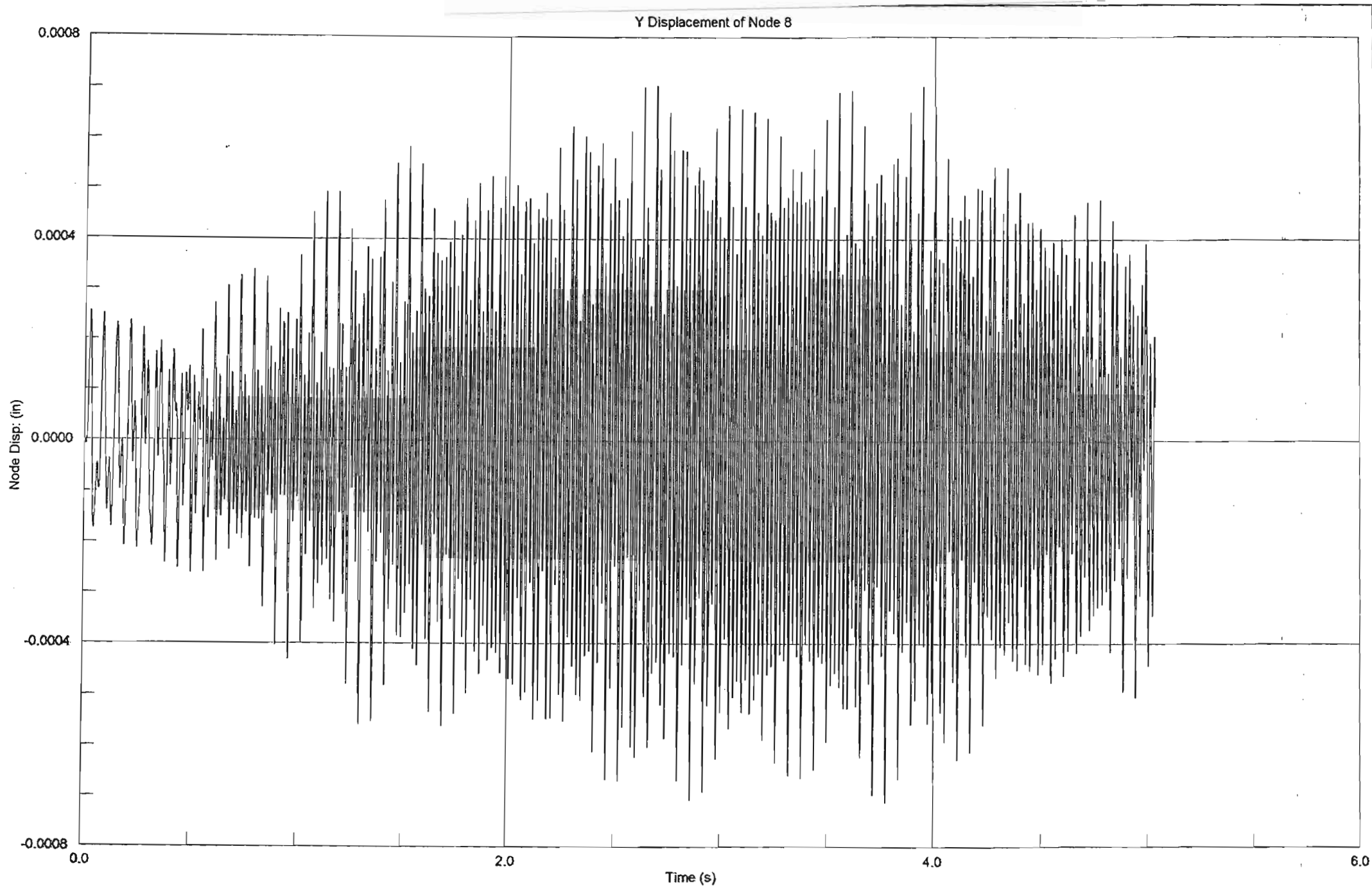


Strand7 Release 2.1.7

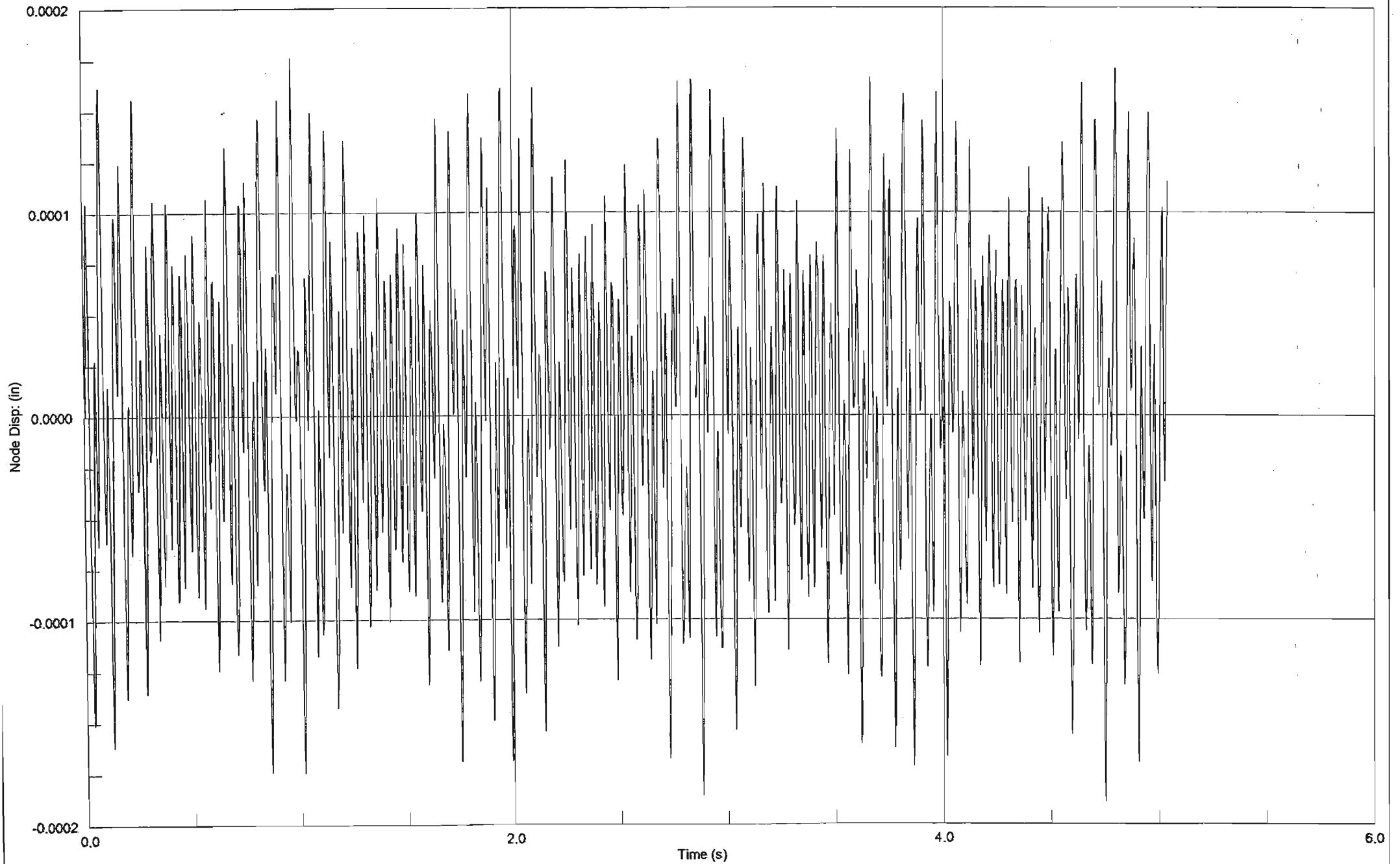
C:\MSc Eng\Ref\Ref 4\raft G15000p-F3.st7

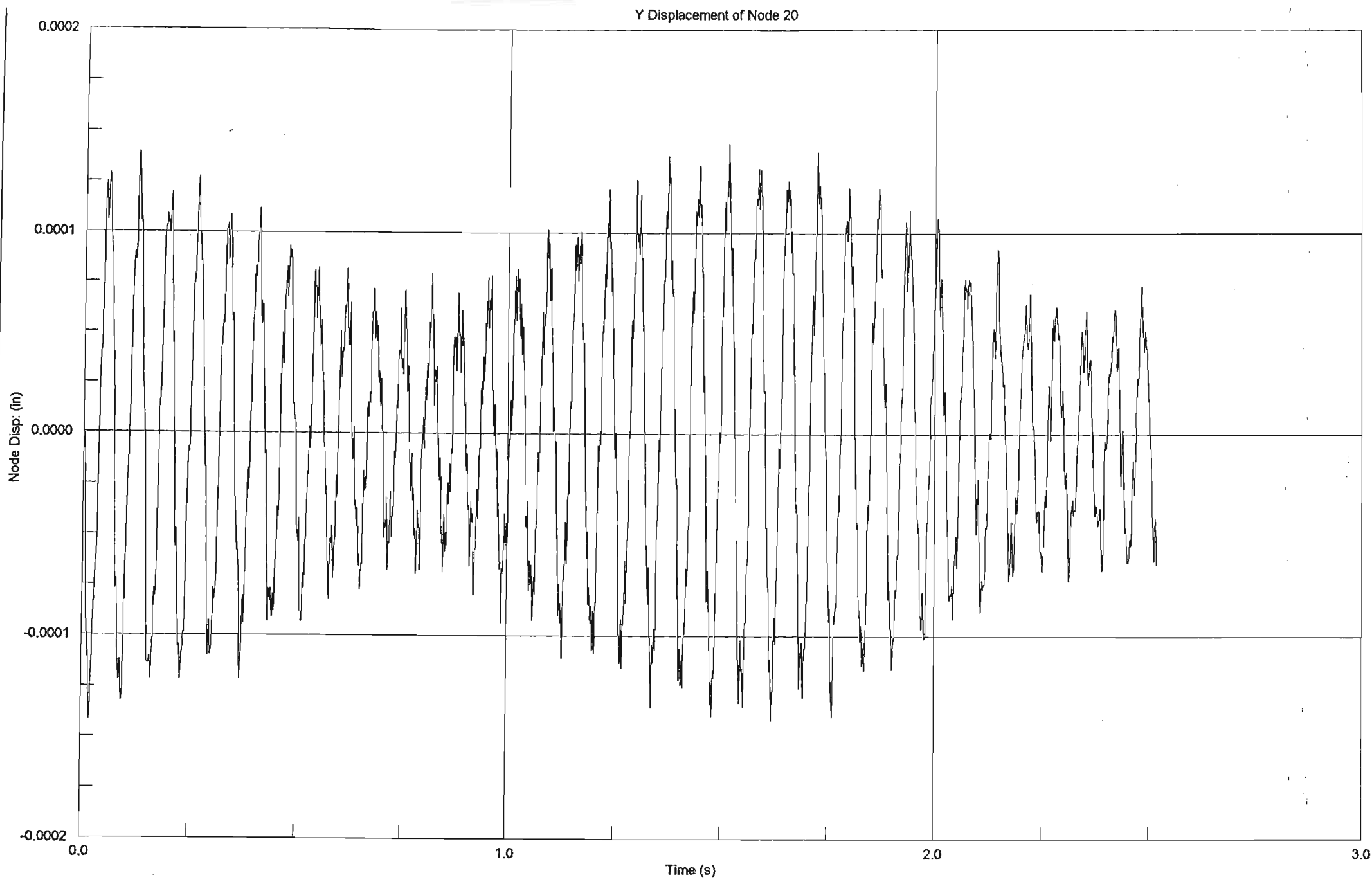
10 October 2002 11:39 am

83.82

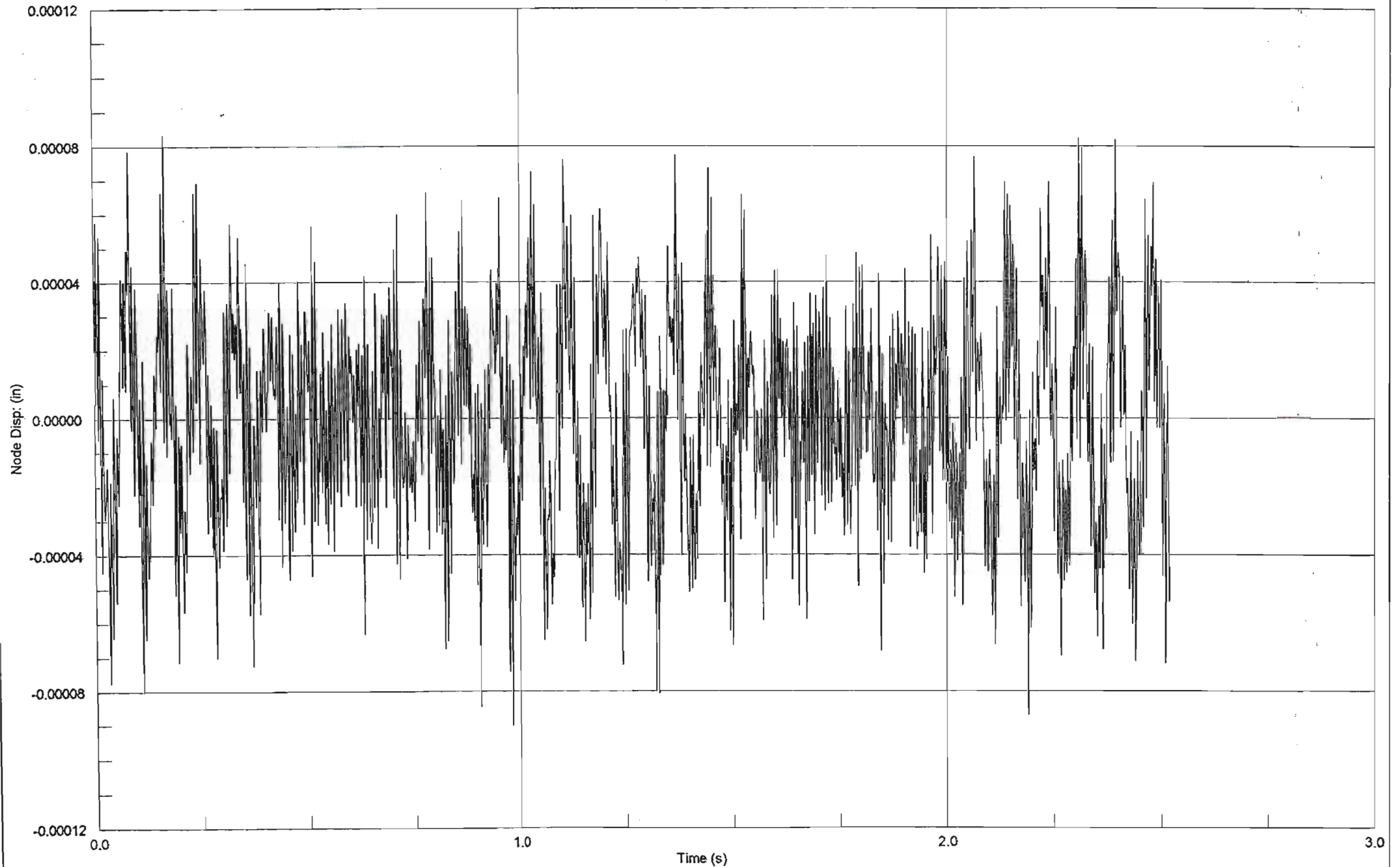


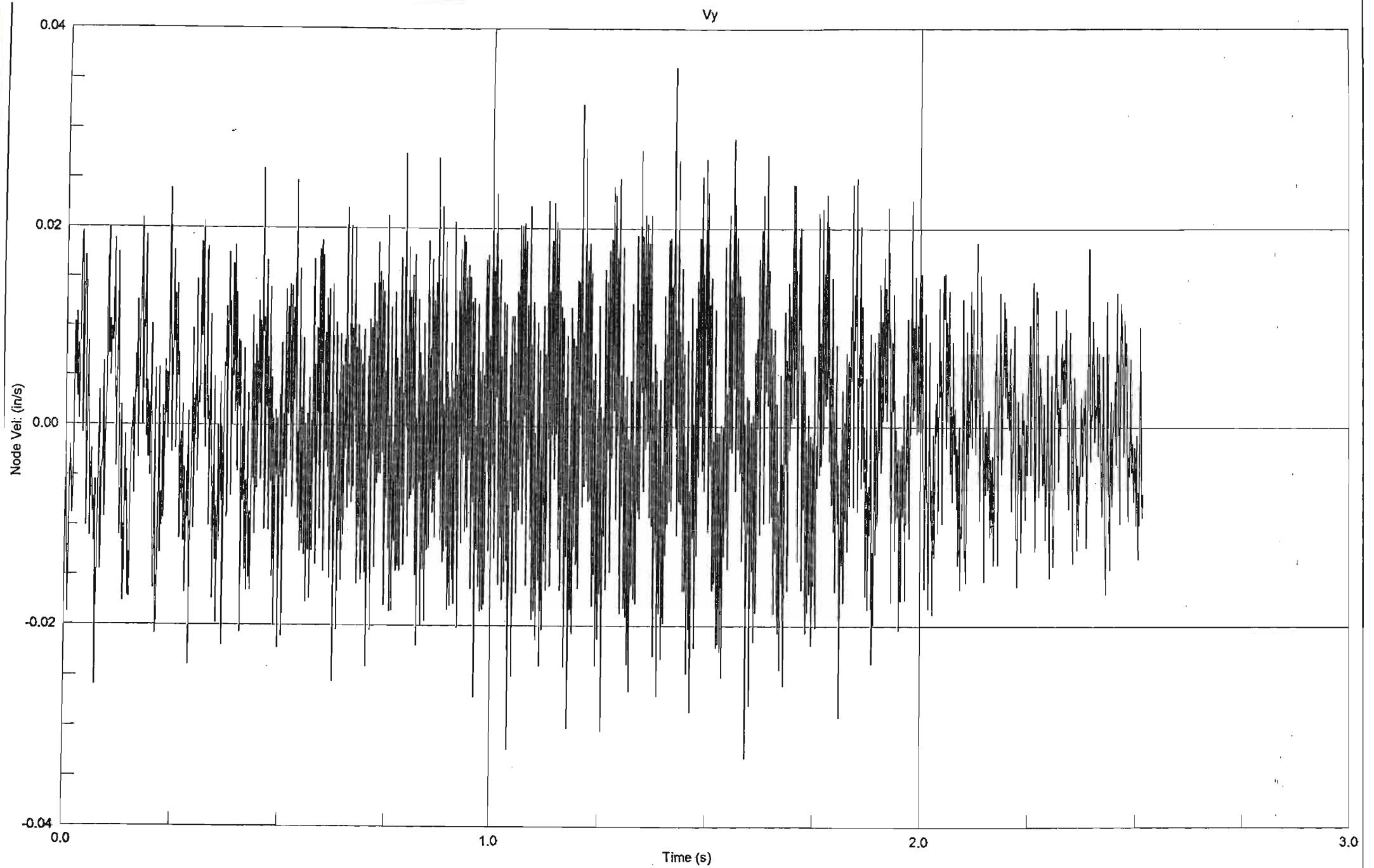
Z Displacement of Node 8

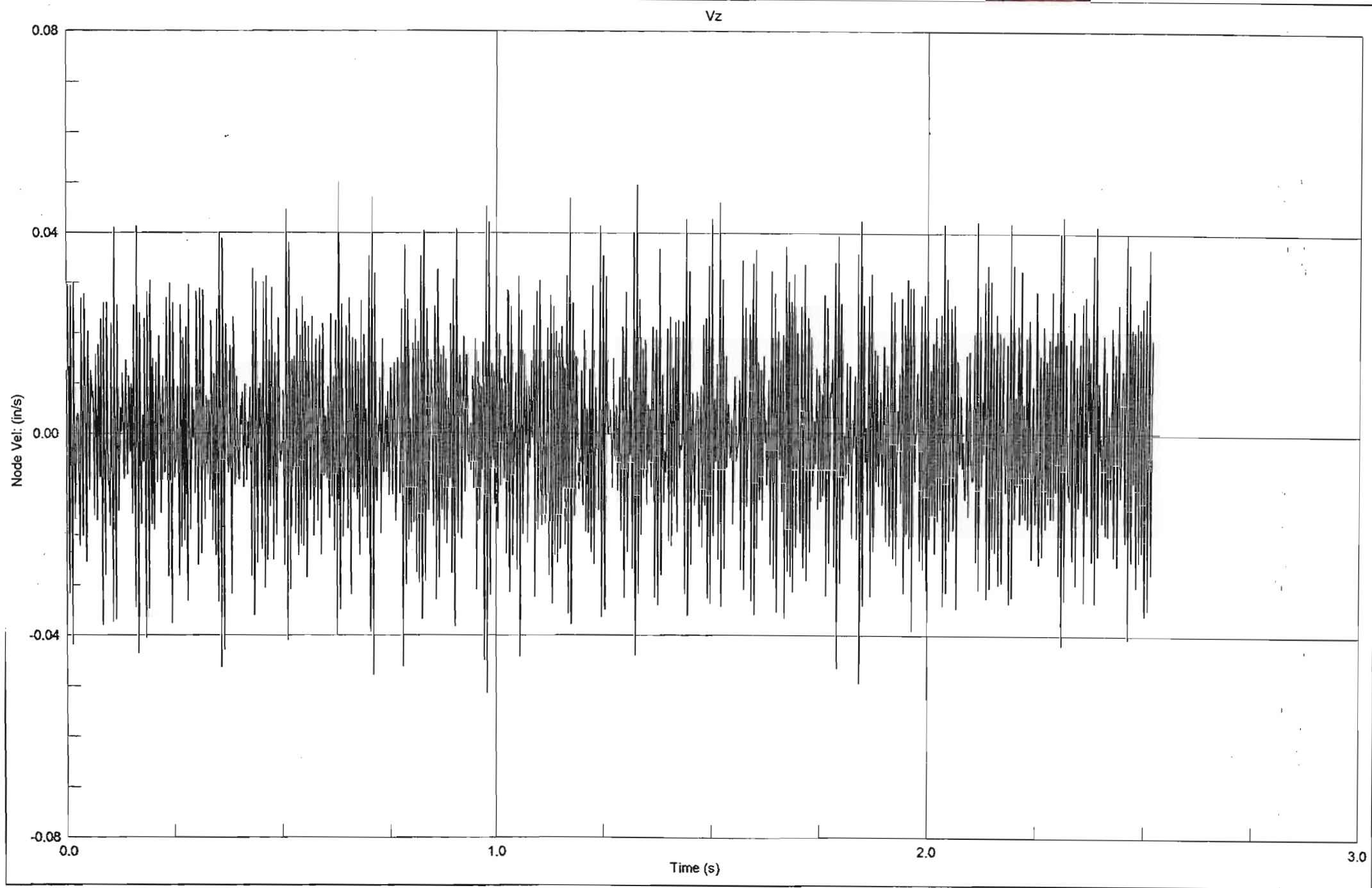


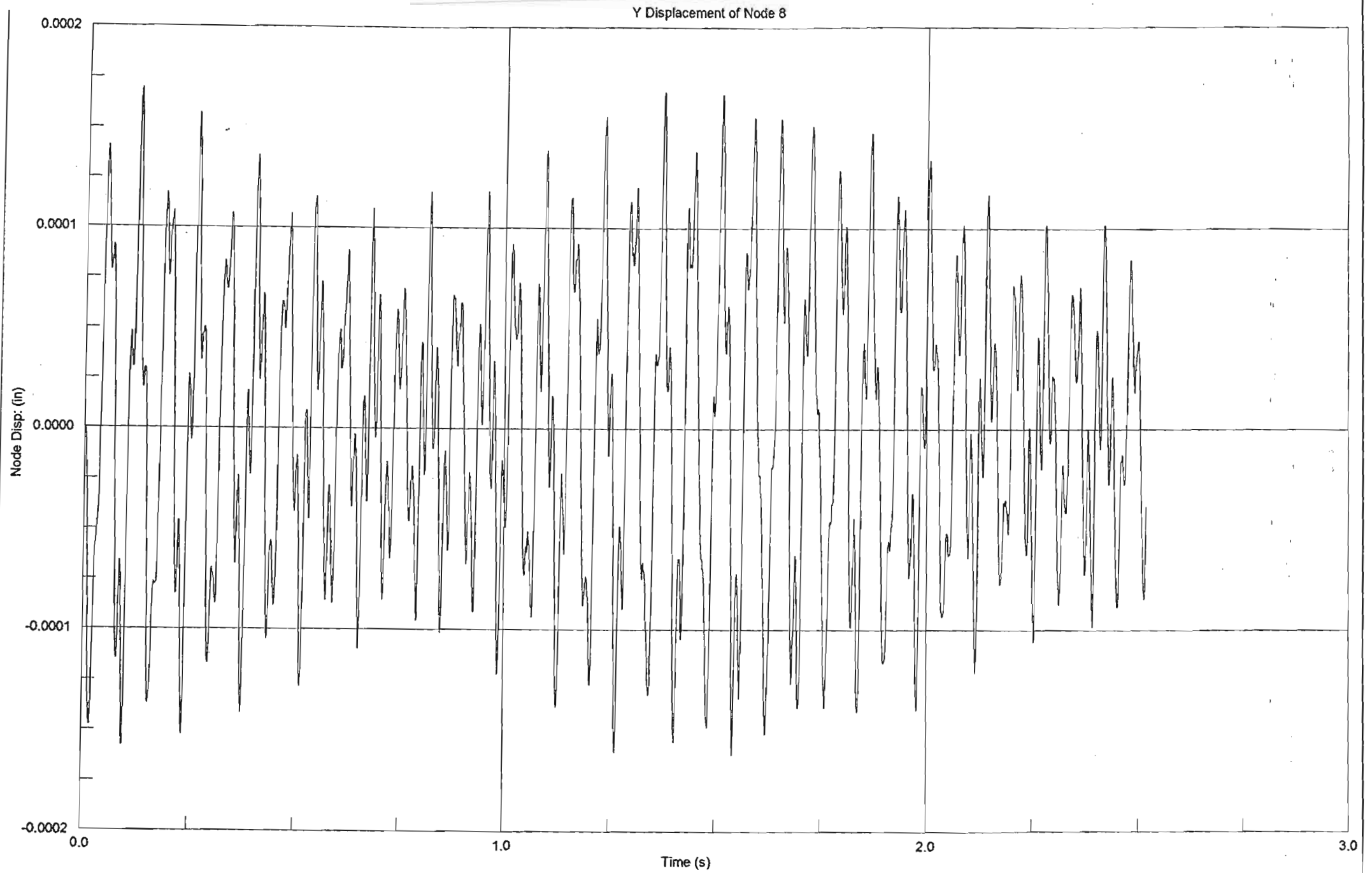


Z Displacement of Node 20

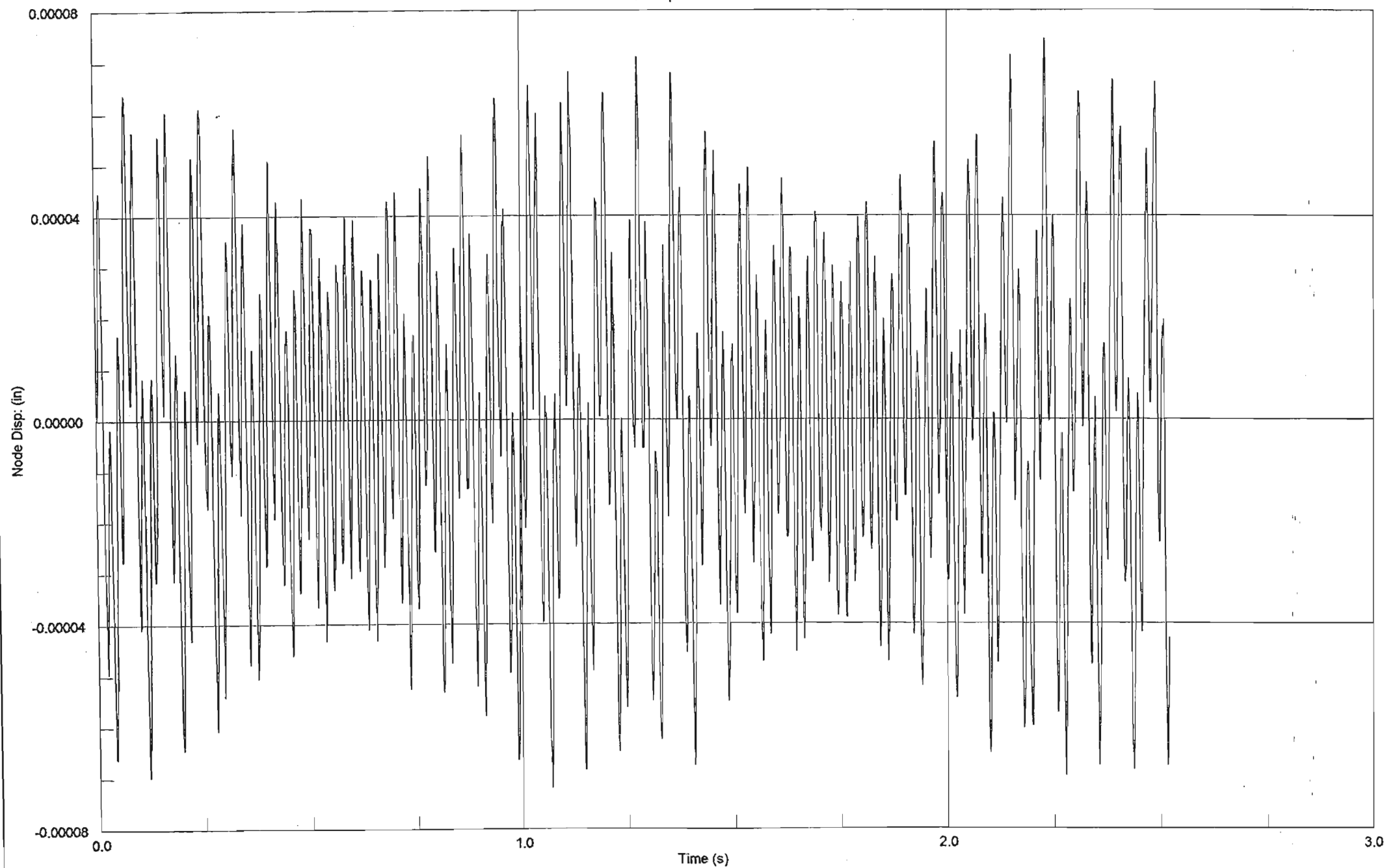


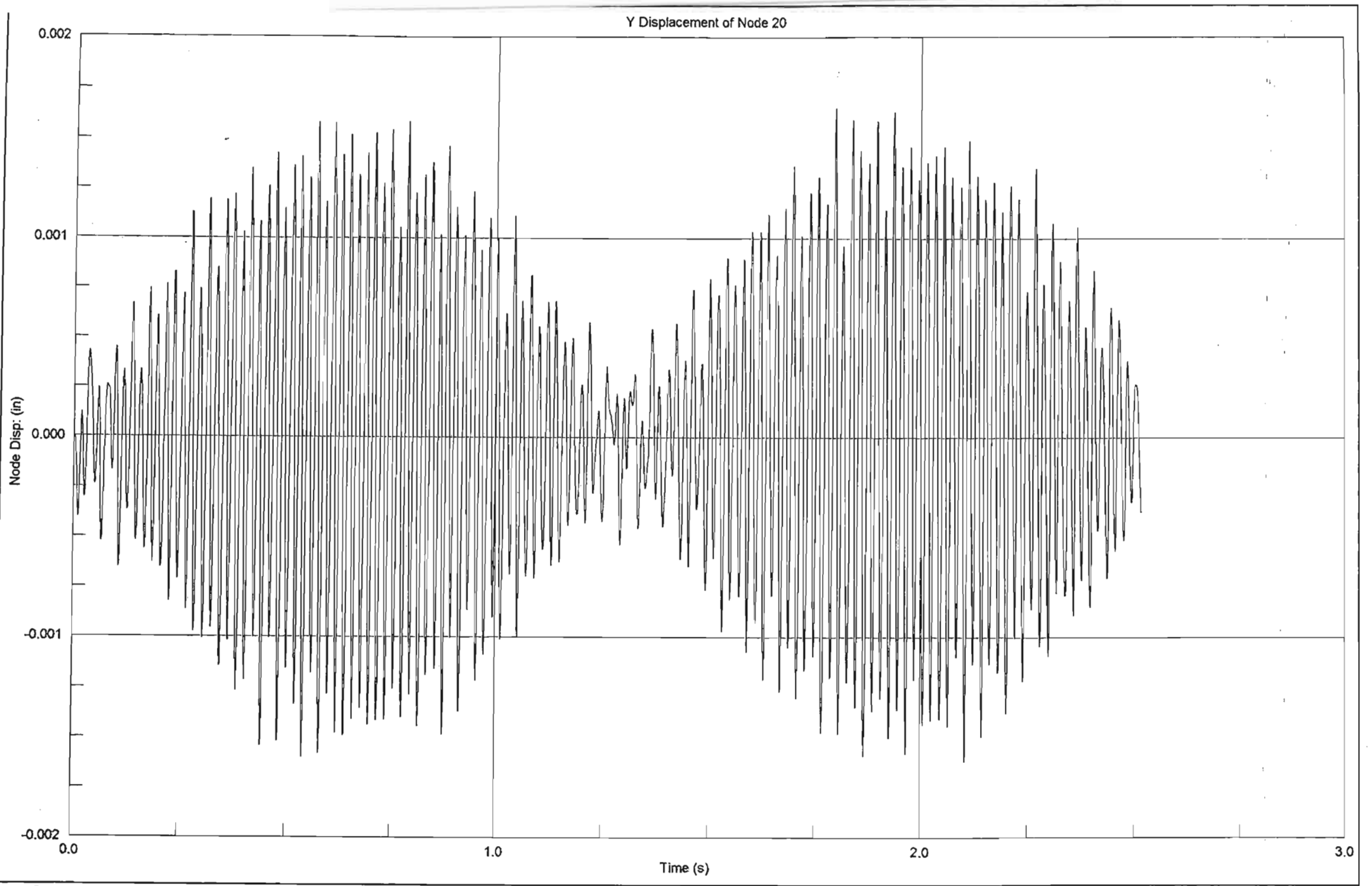




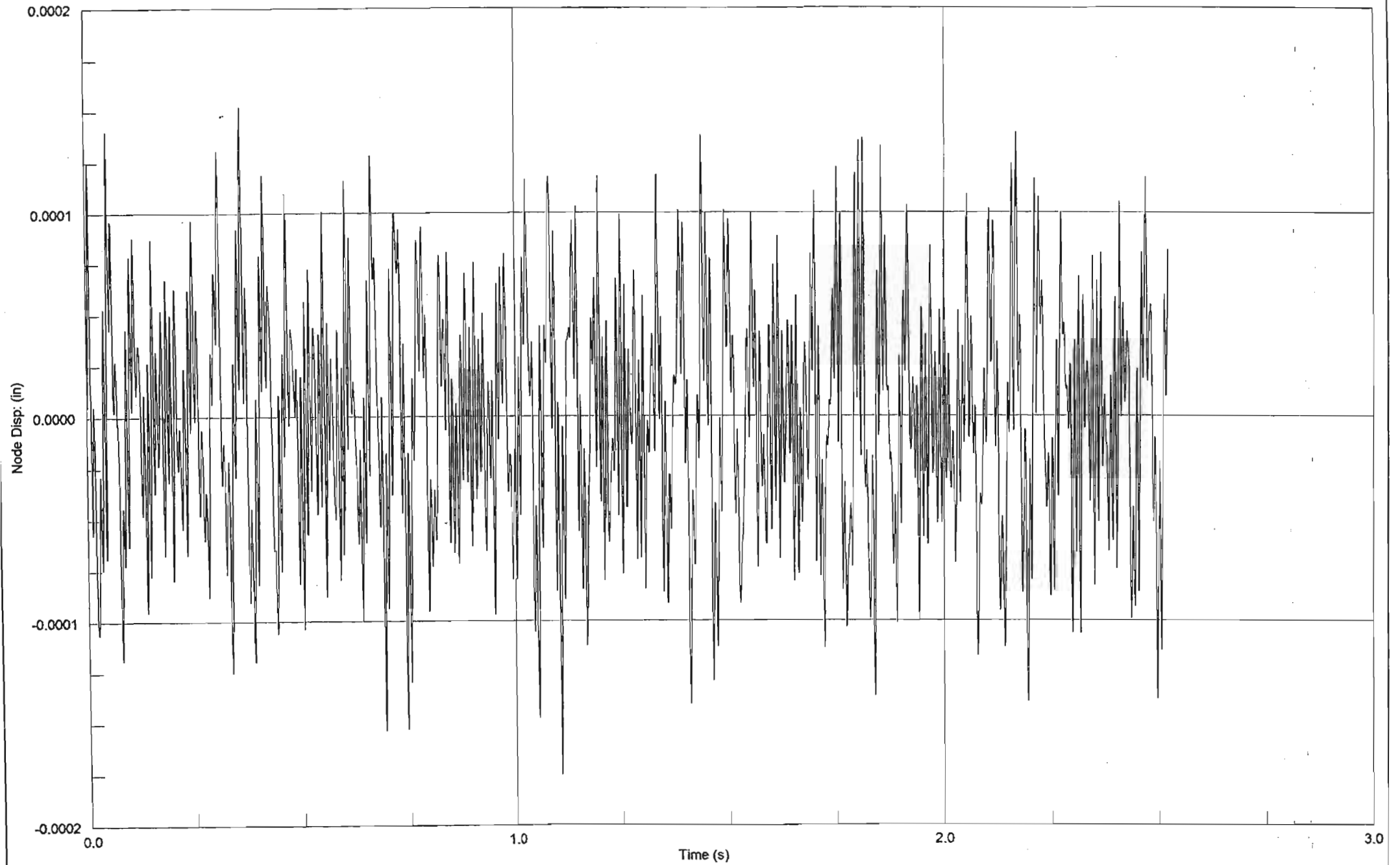


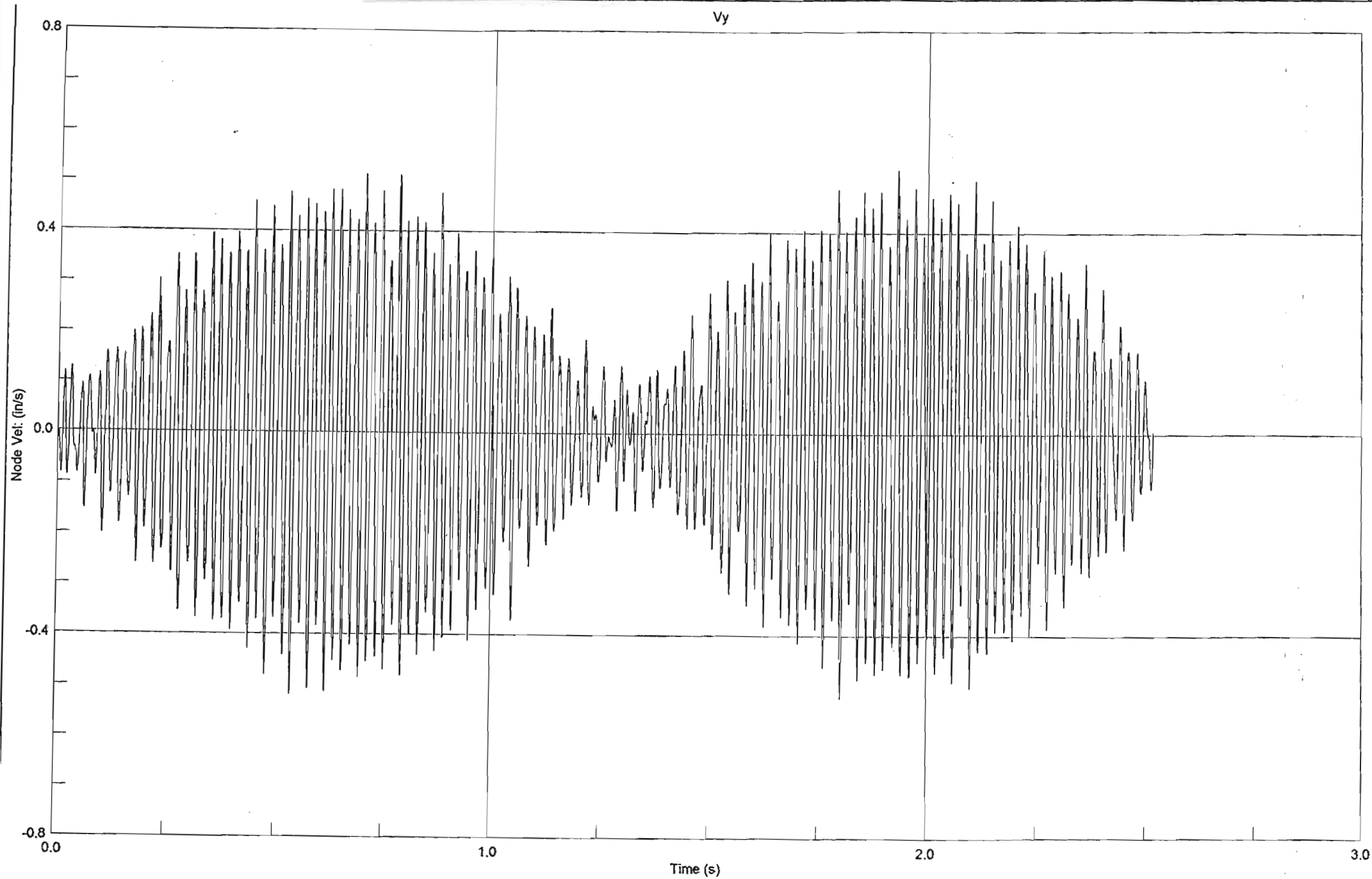
Z Displacement of Node 8

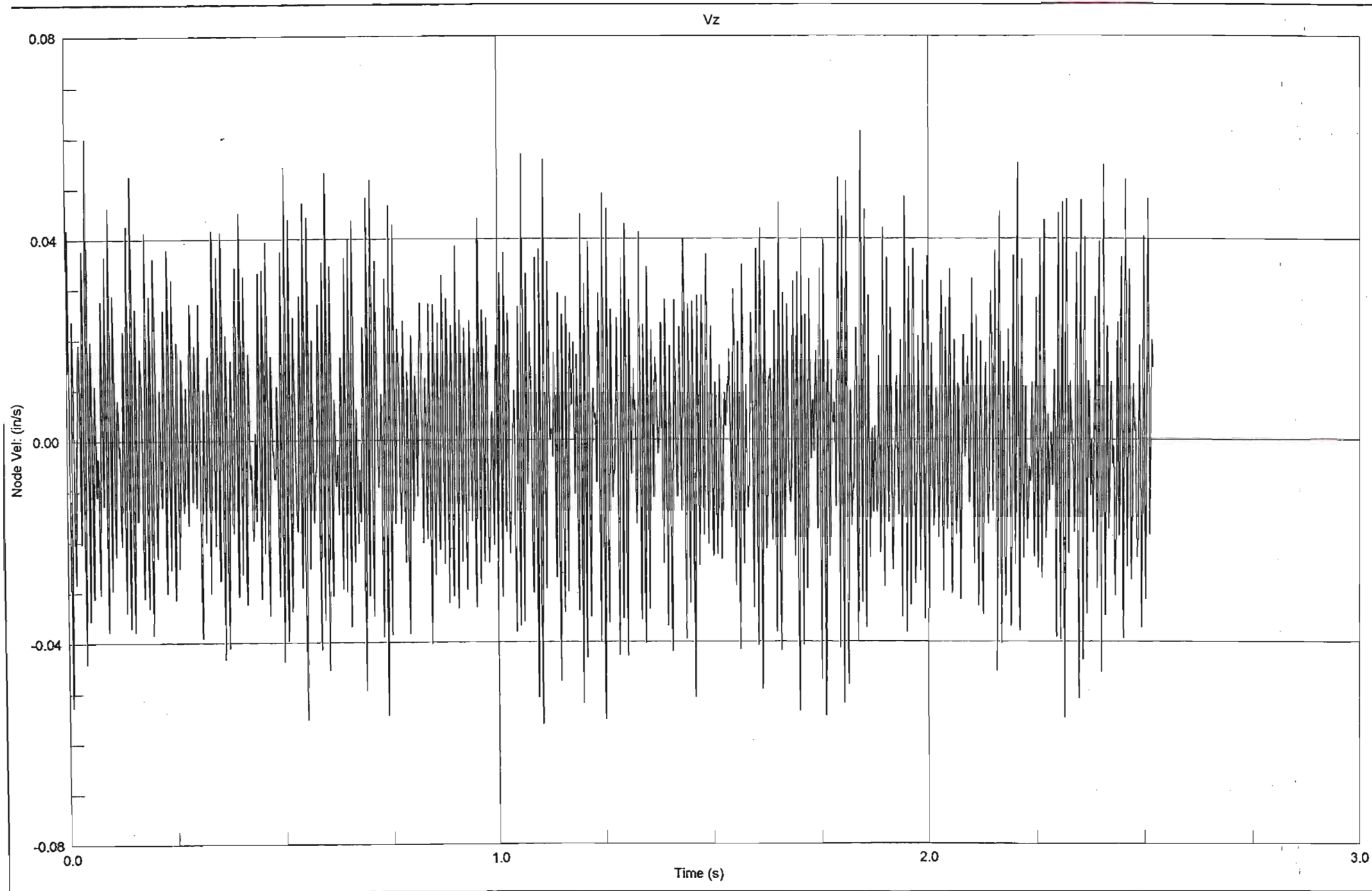


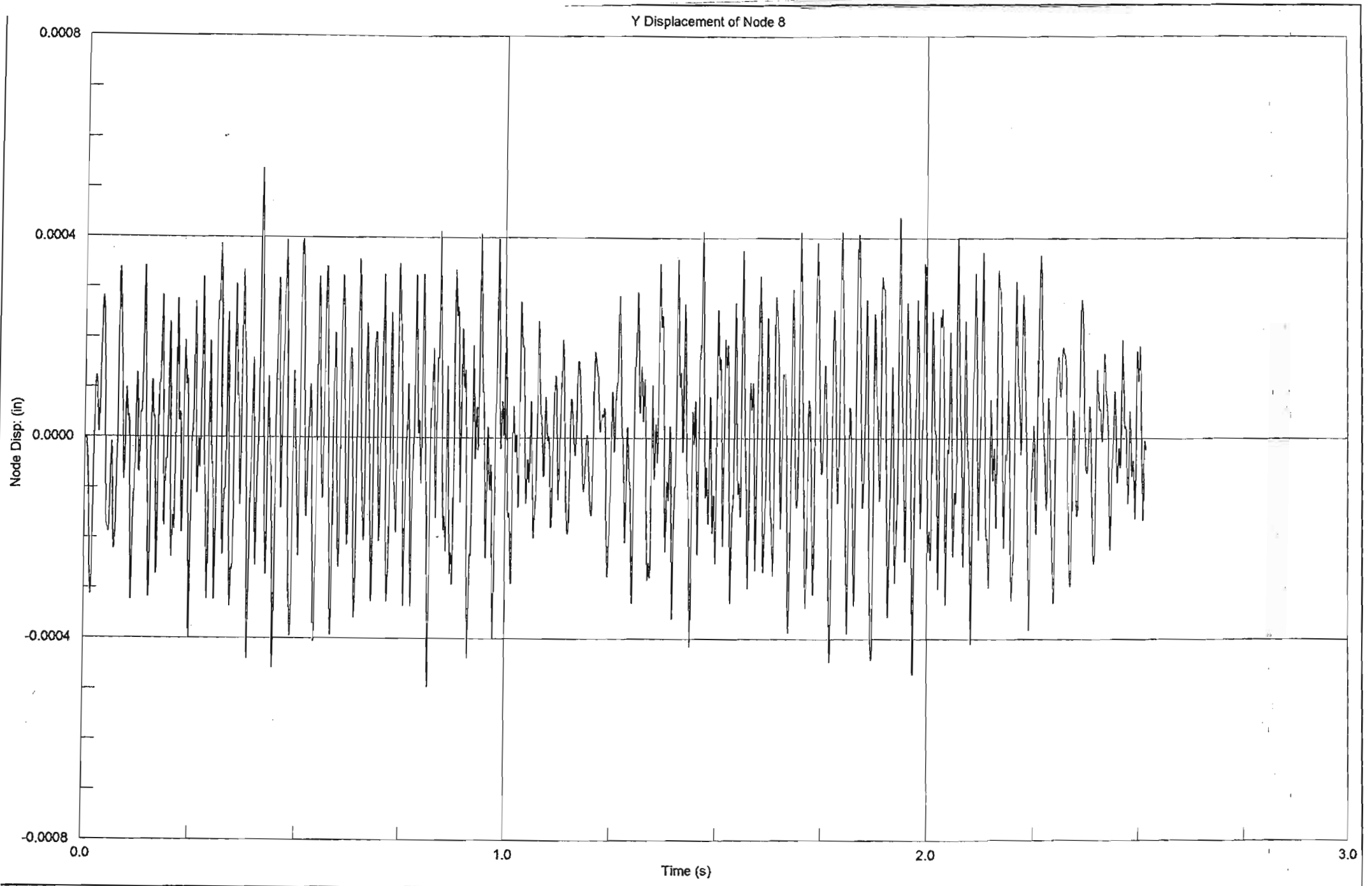


Z Displacement of Node 20

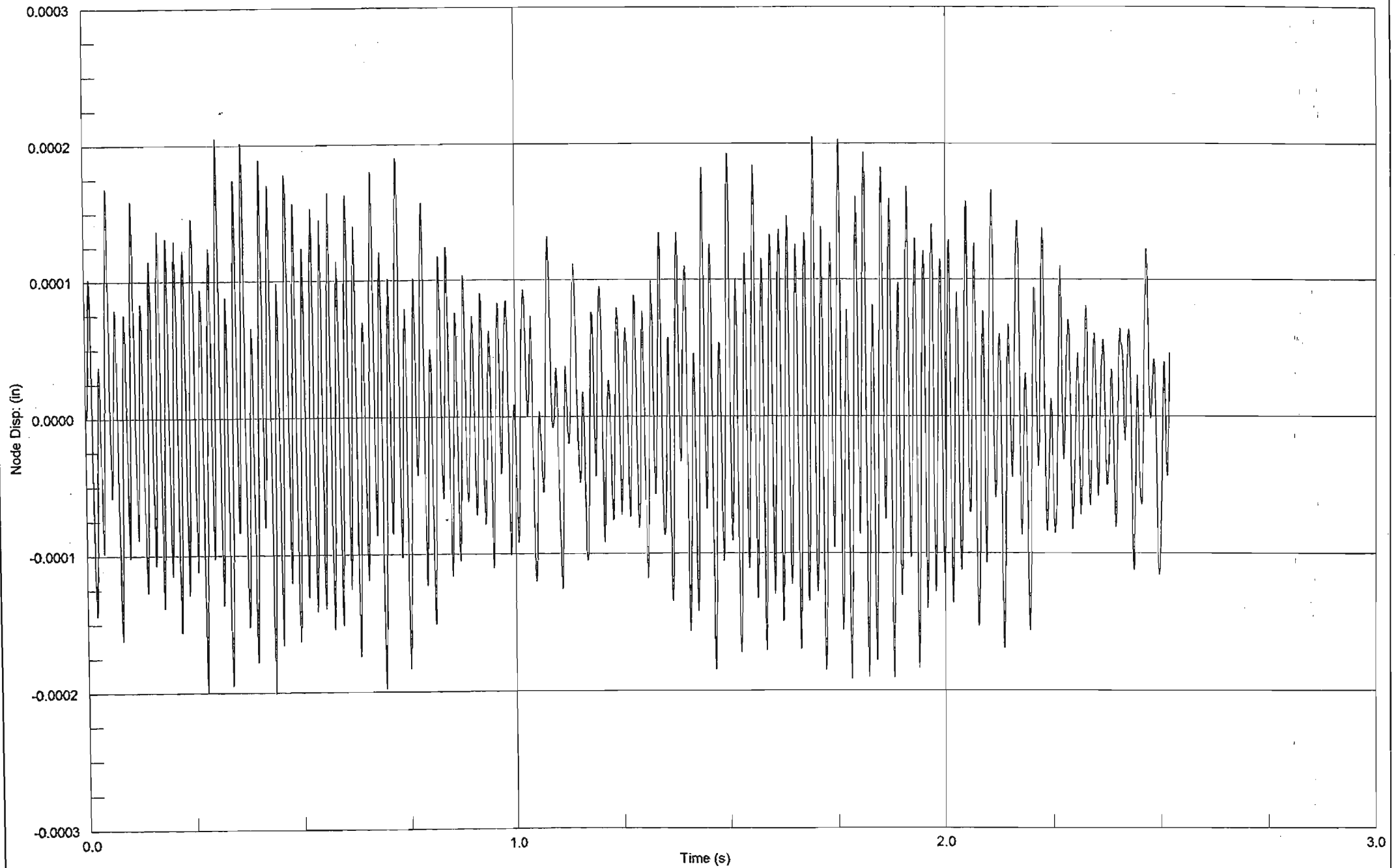


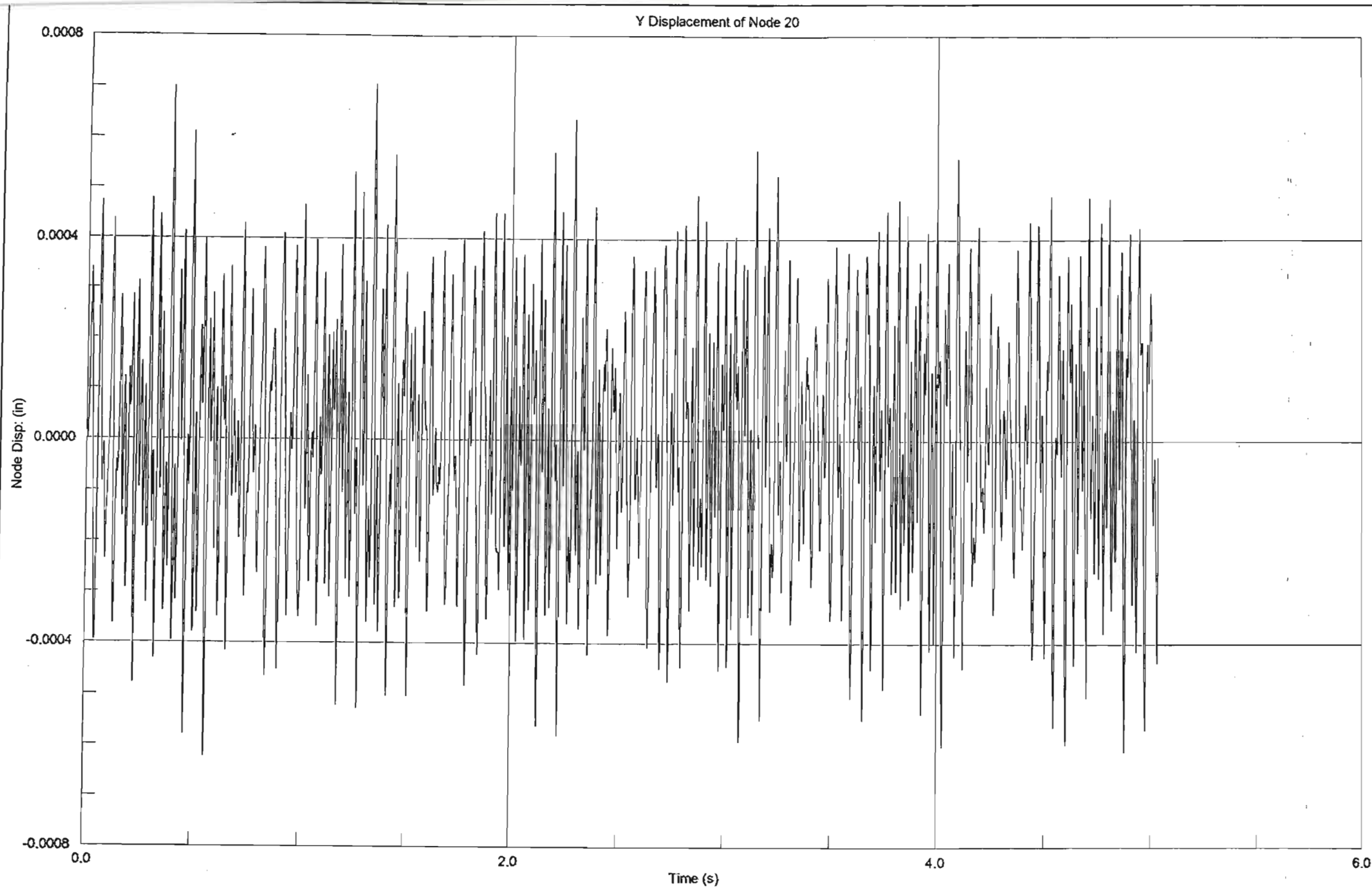


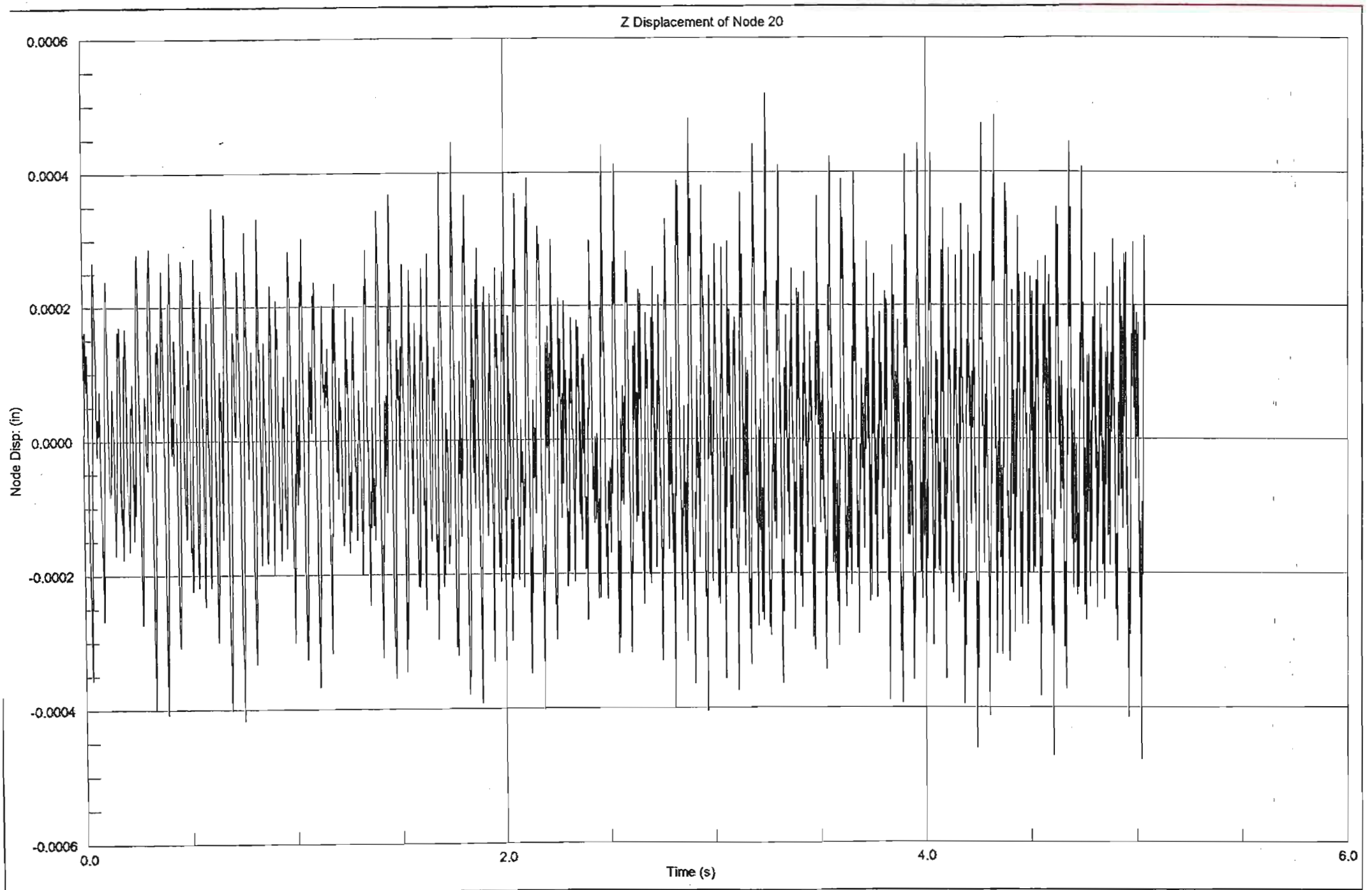


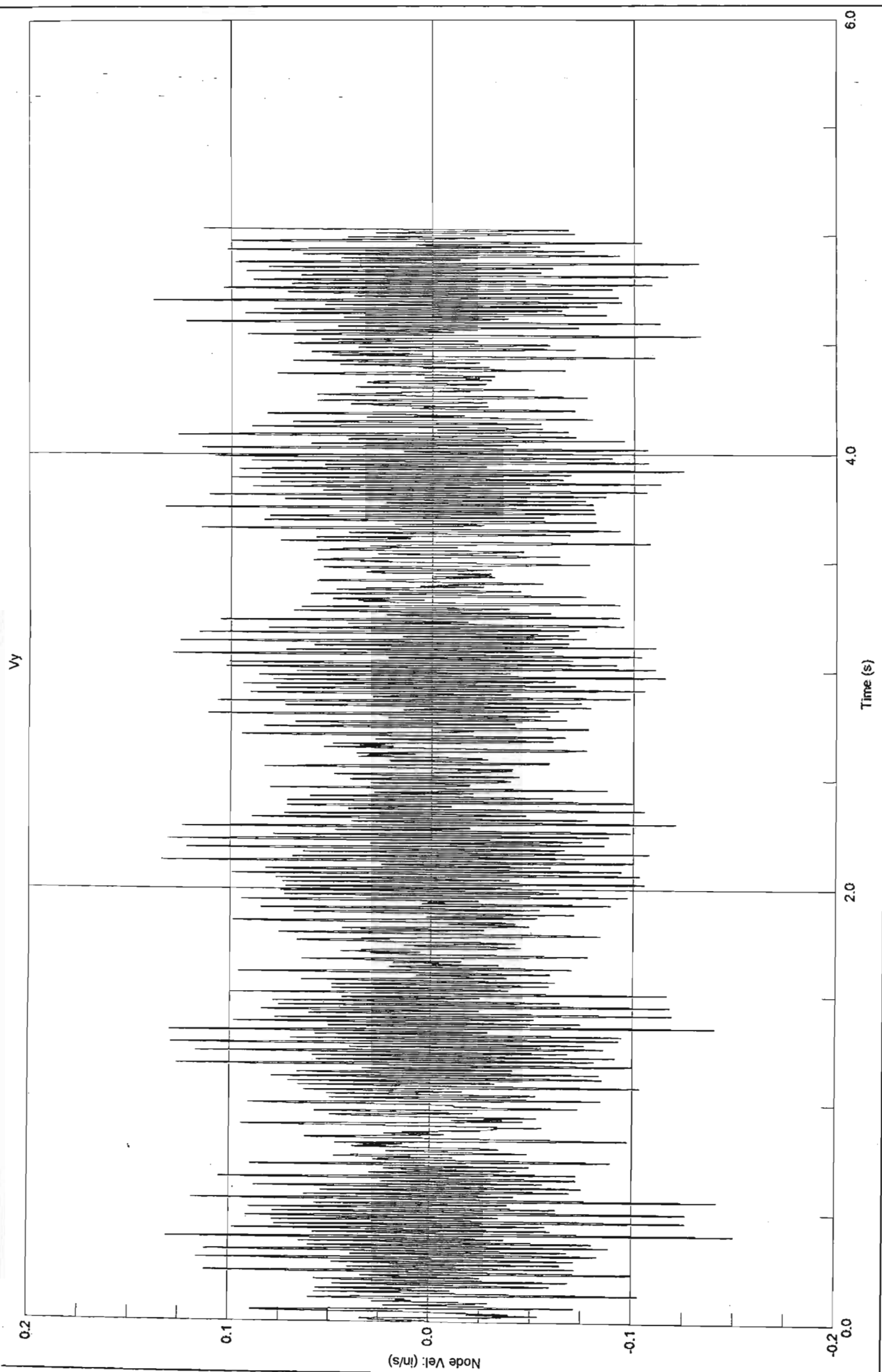


Z Displacement of Node 8

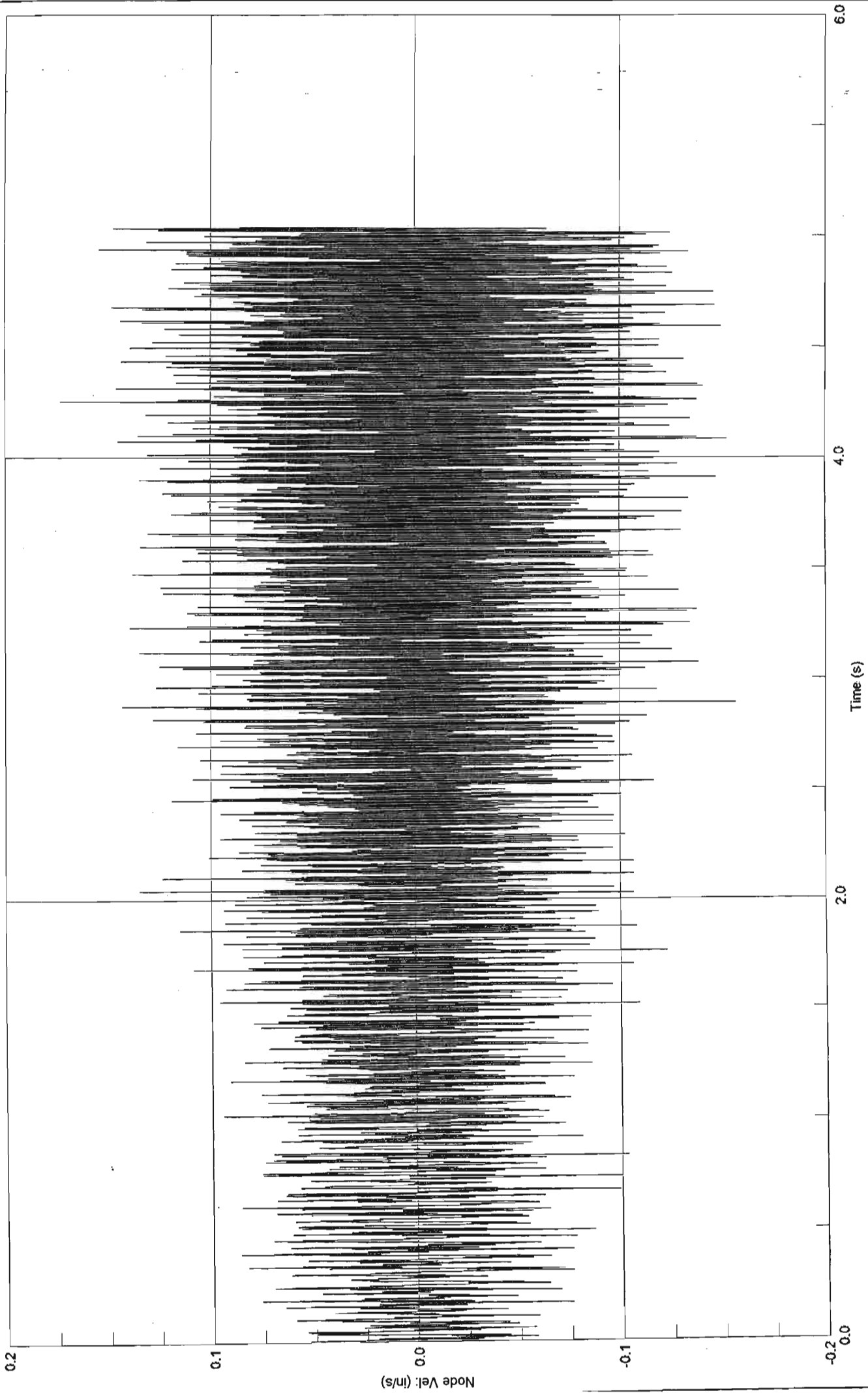


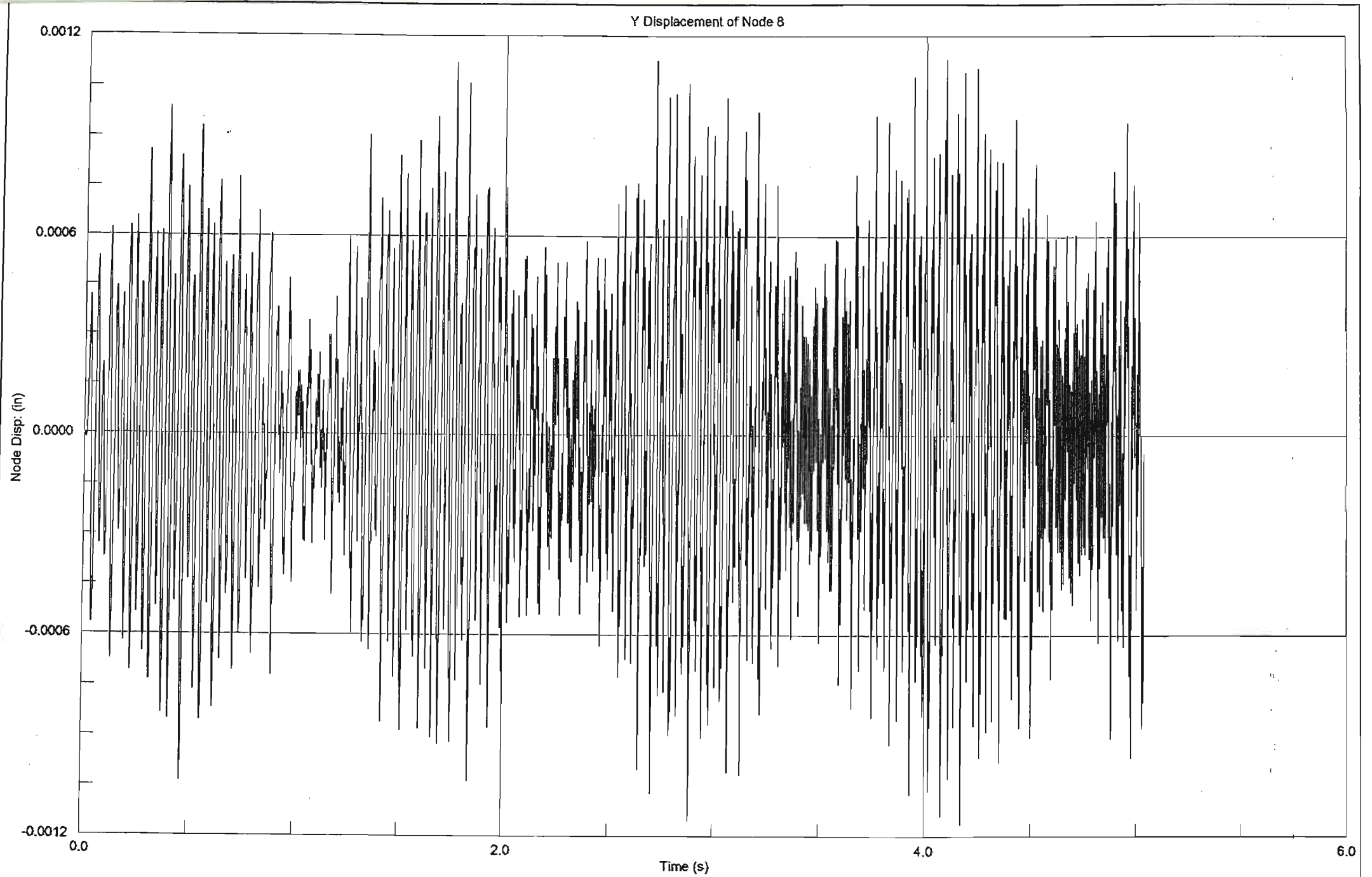


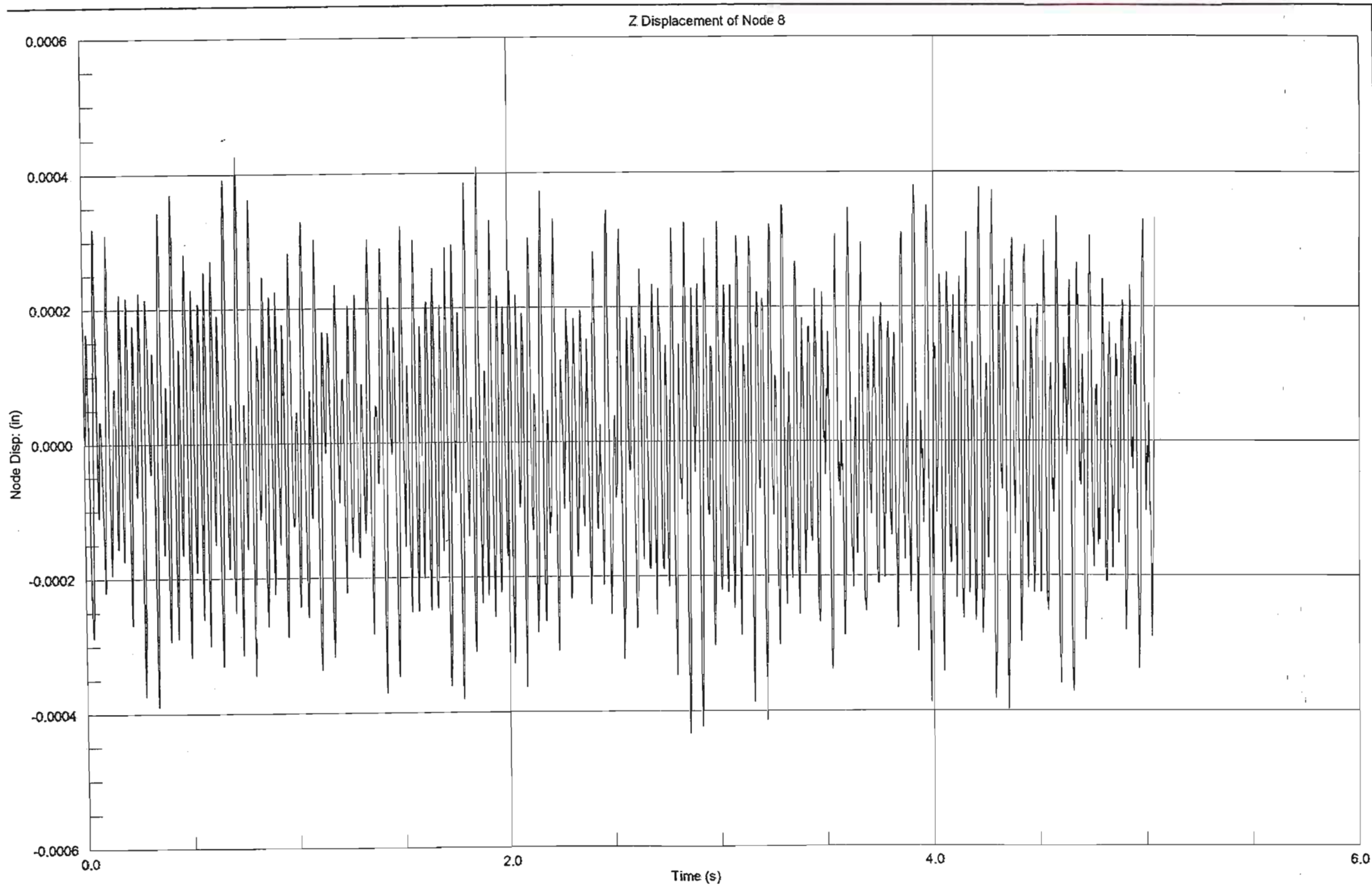




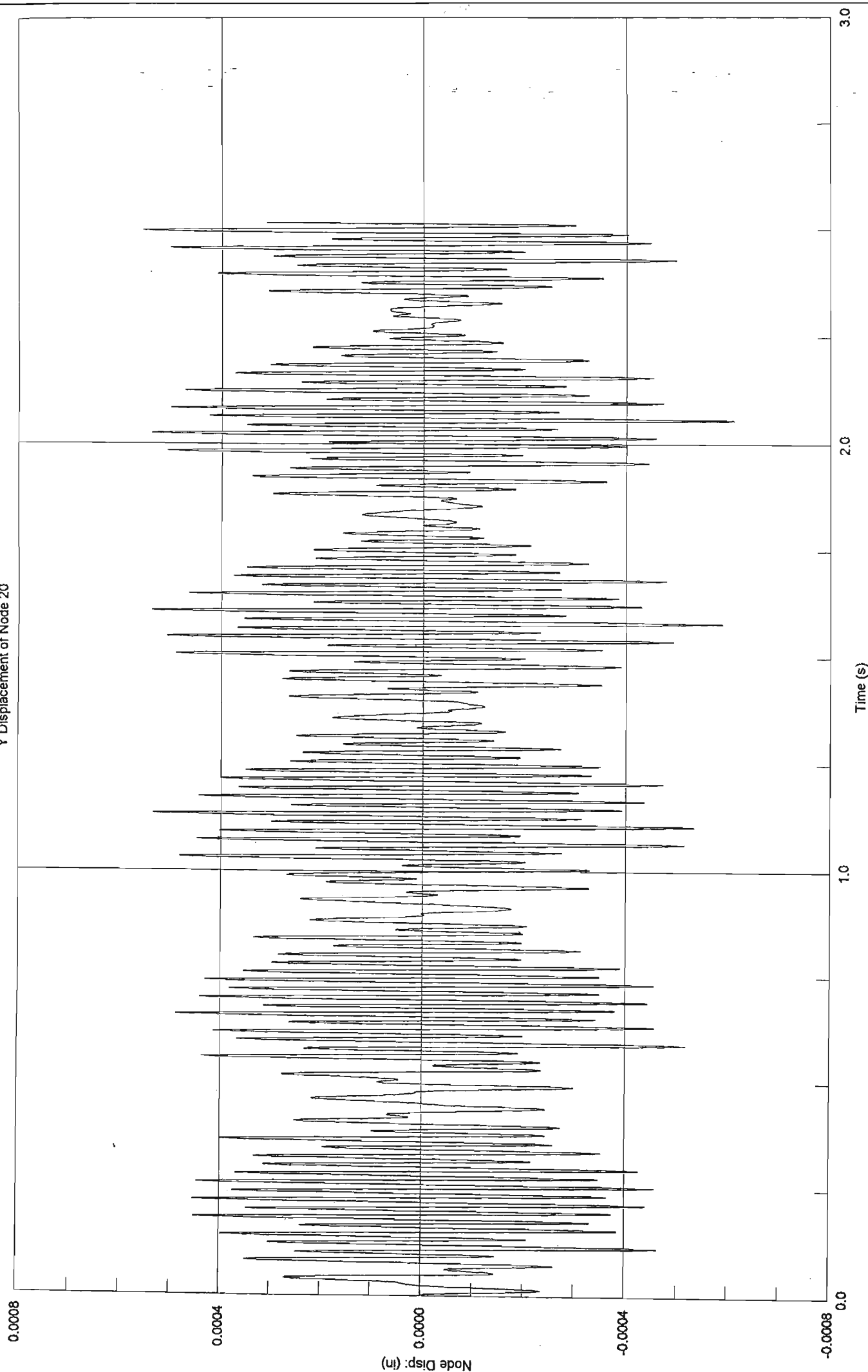
Vz

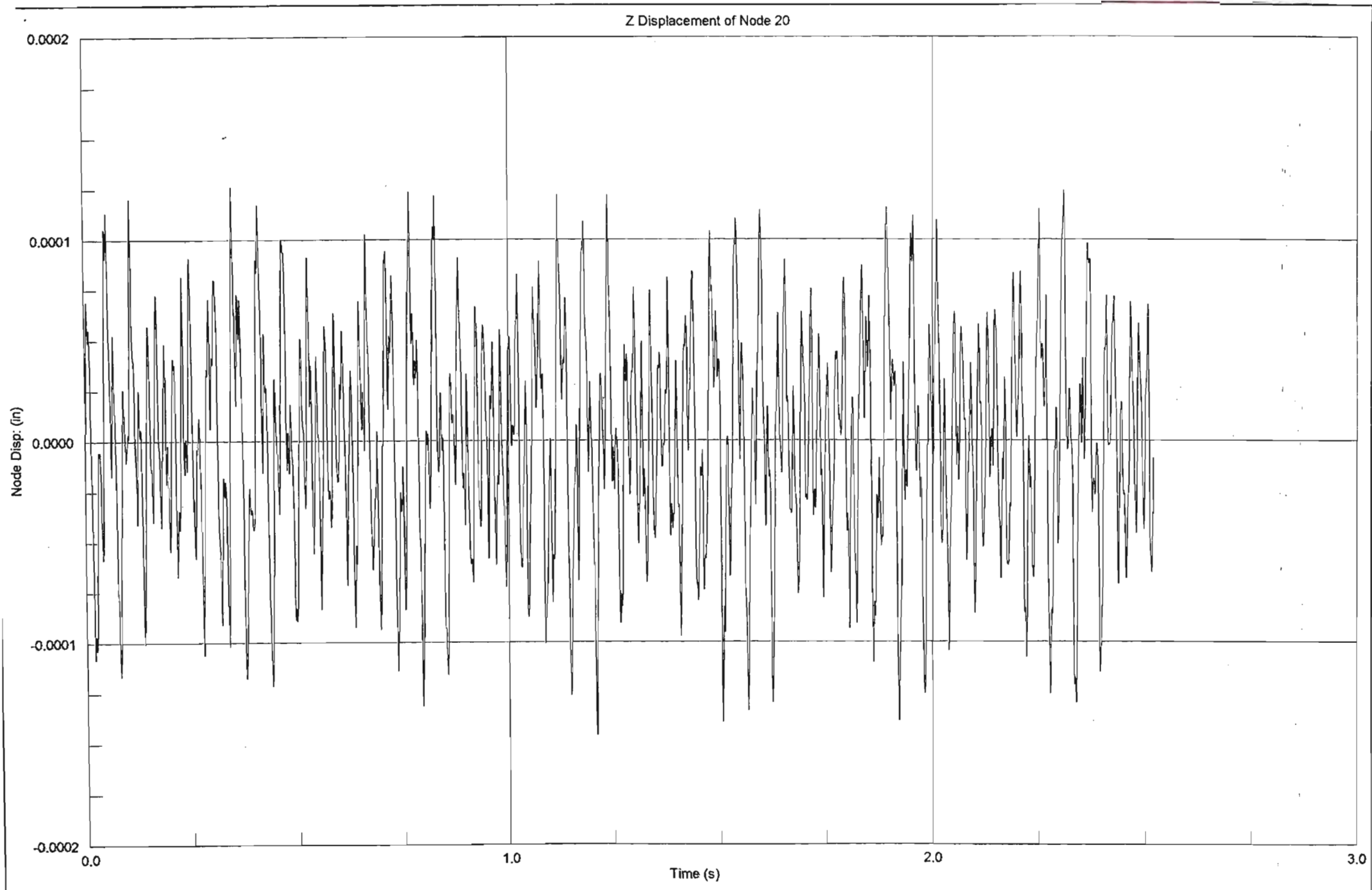


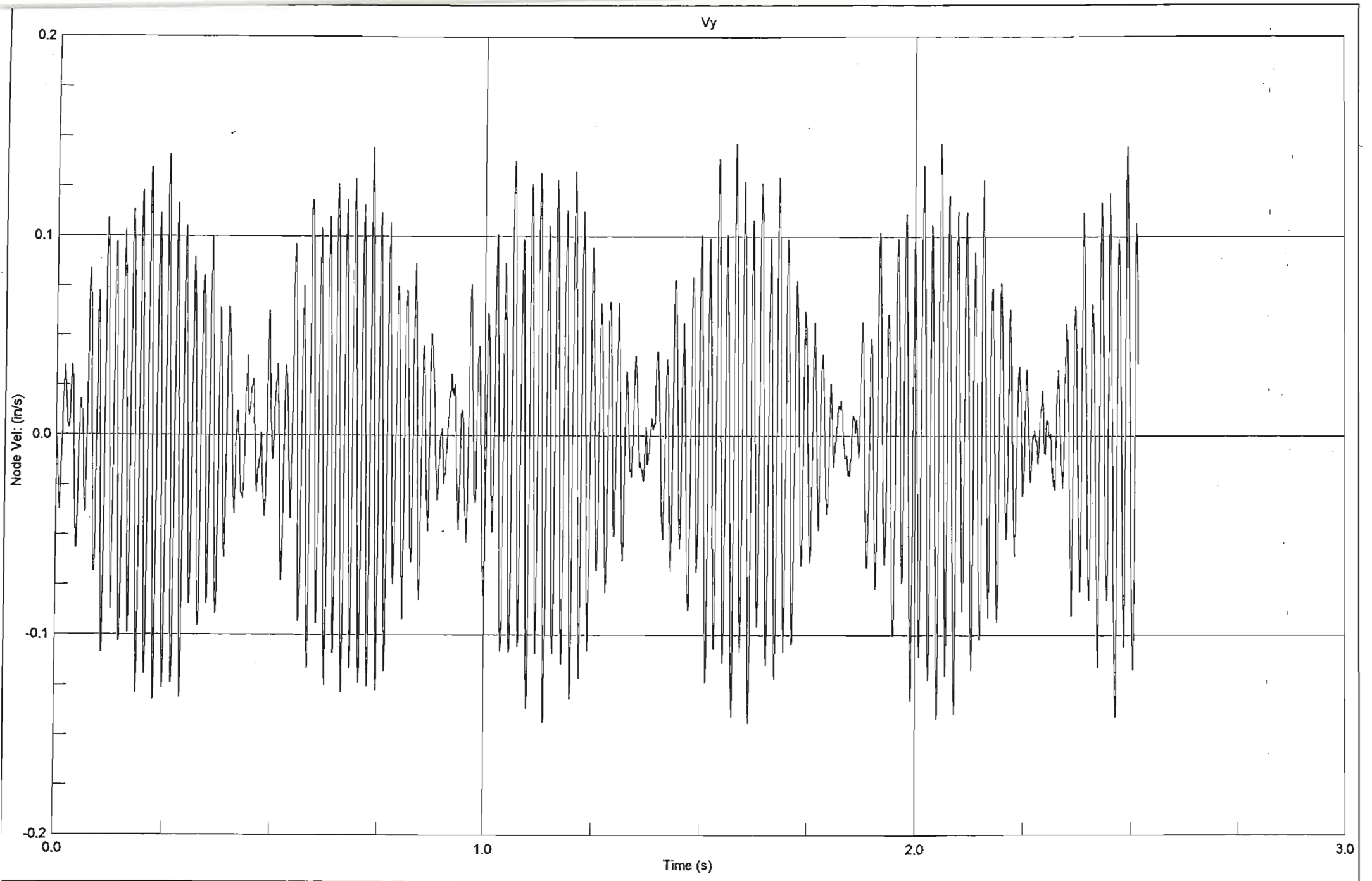




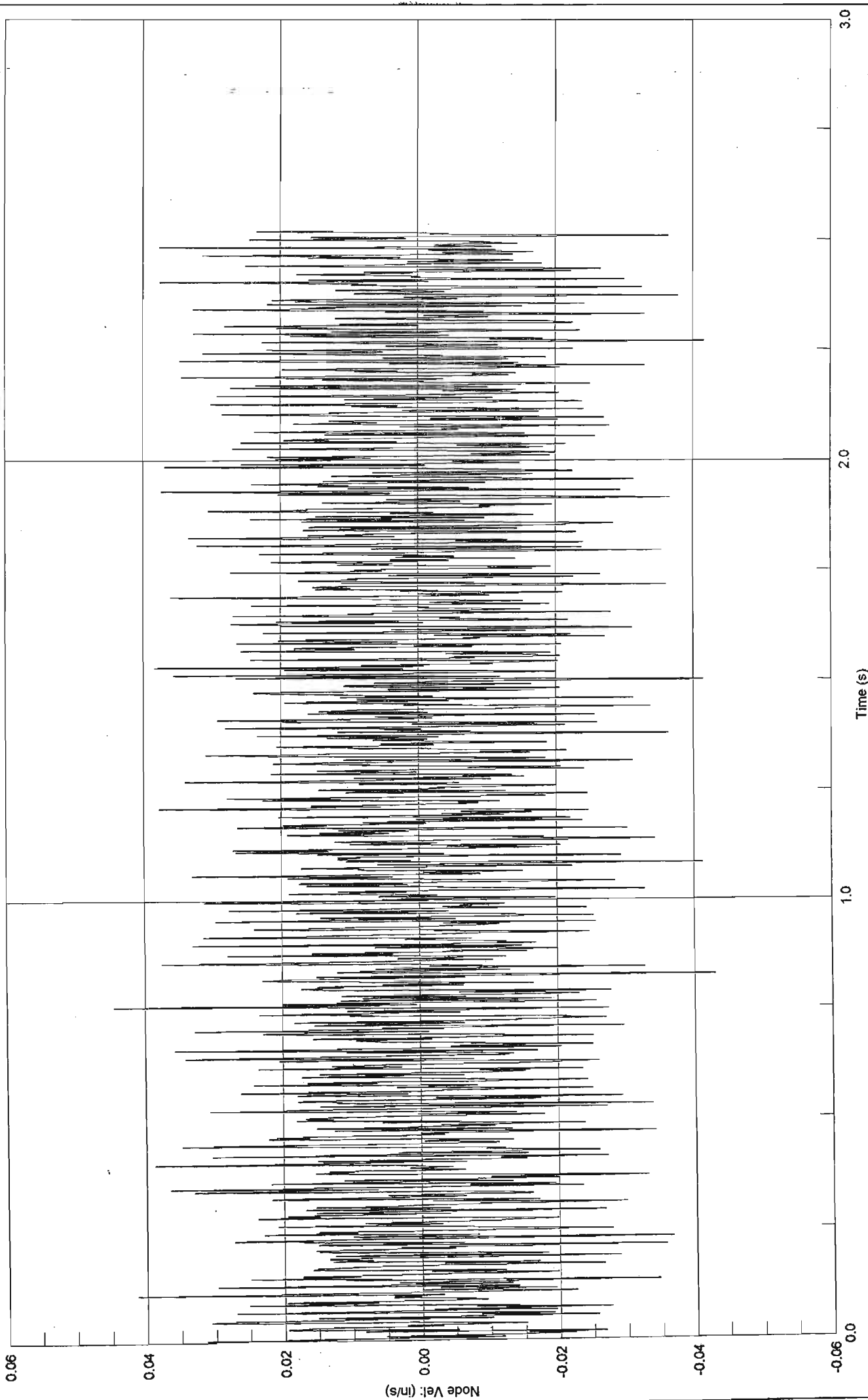
Y Displacement of Node 20

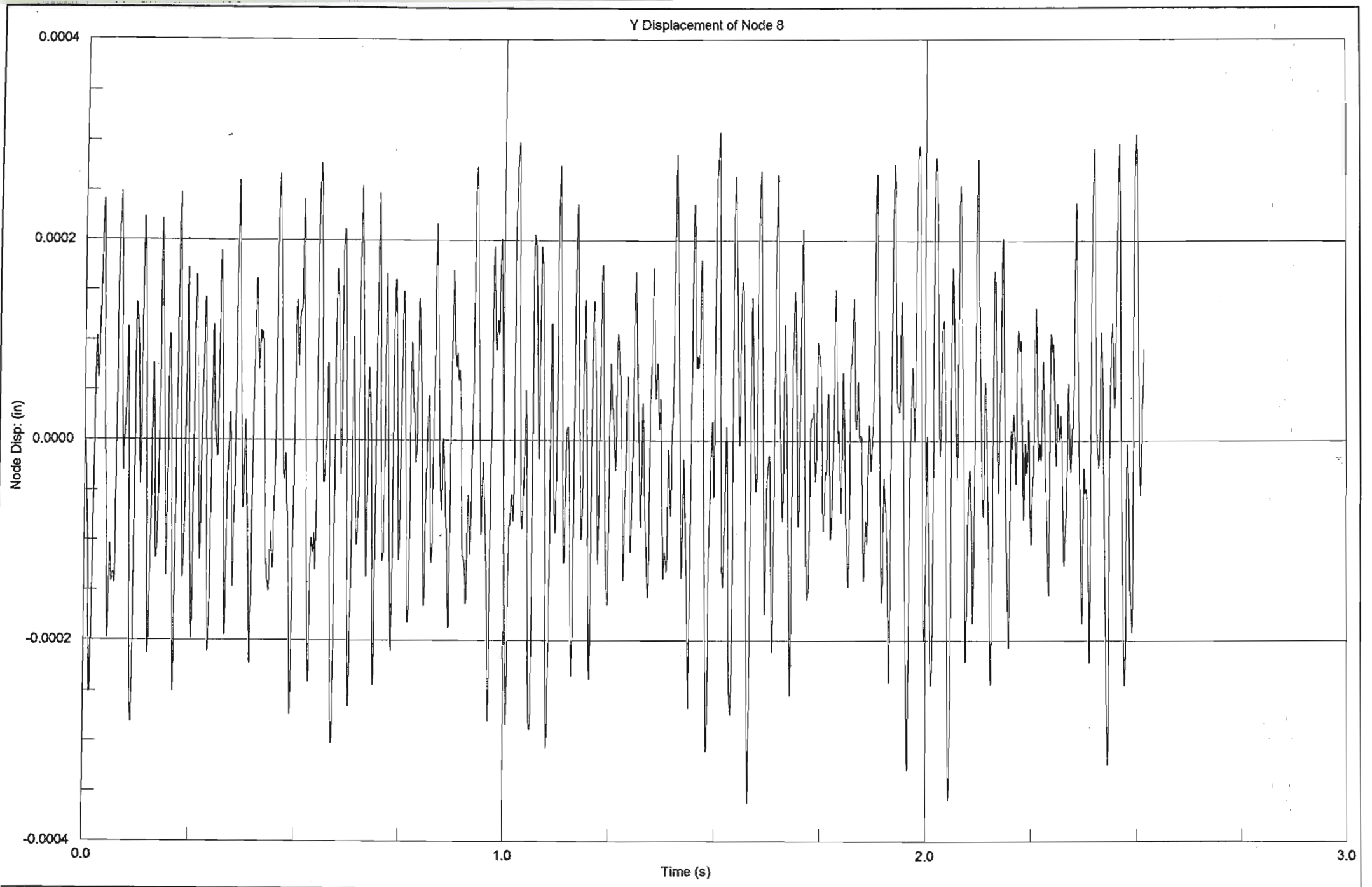


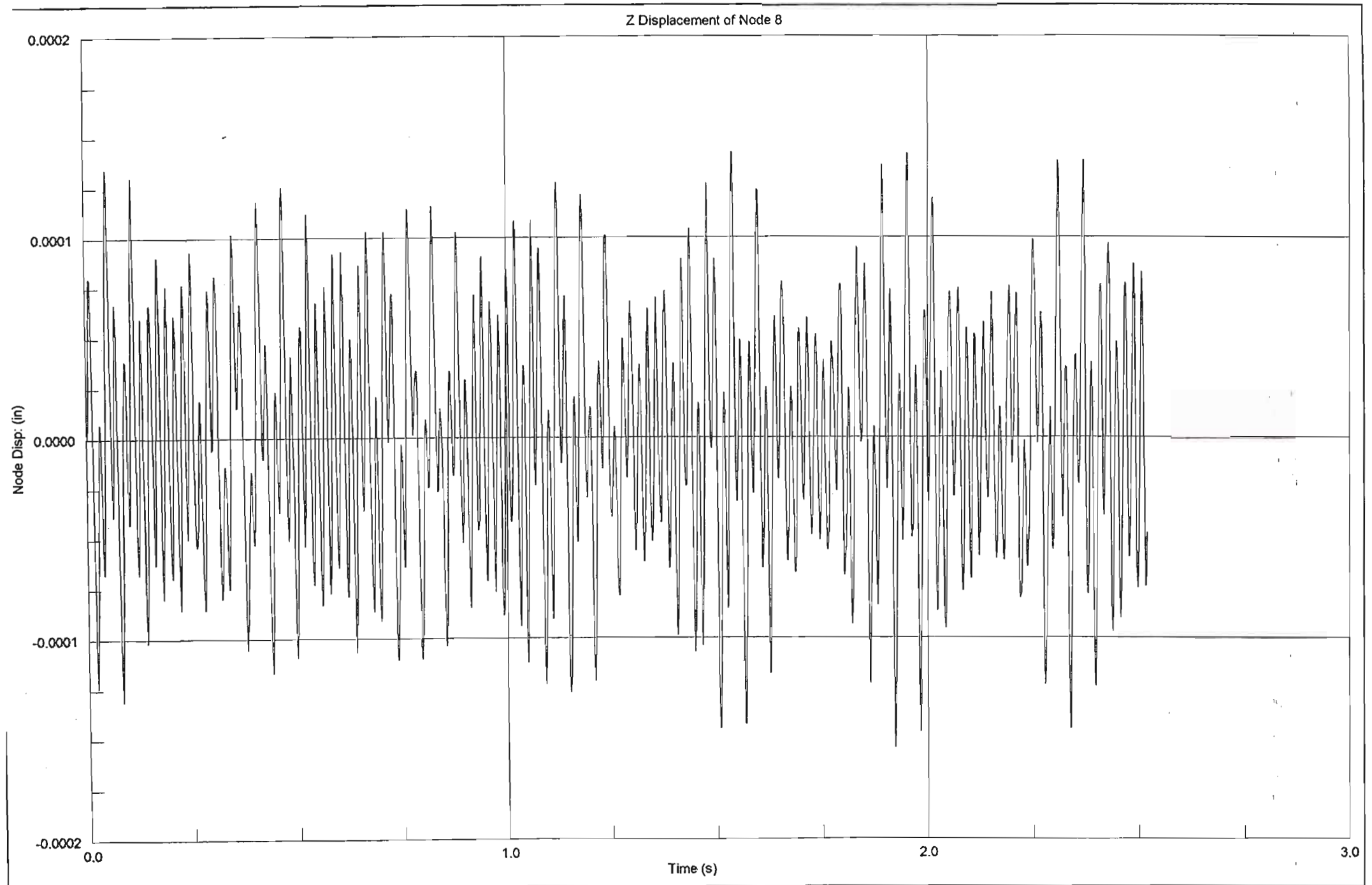


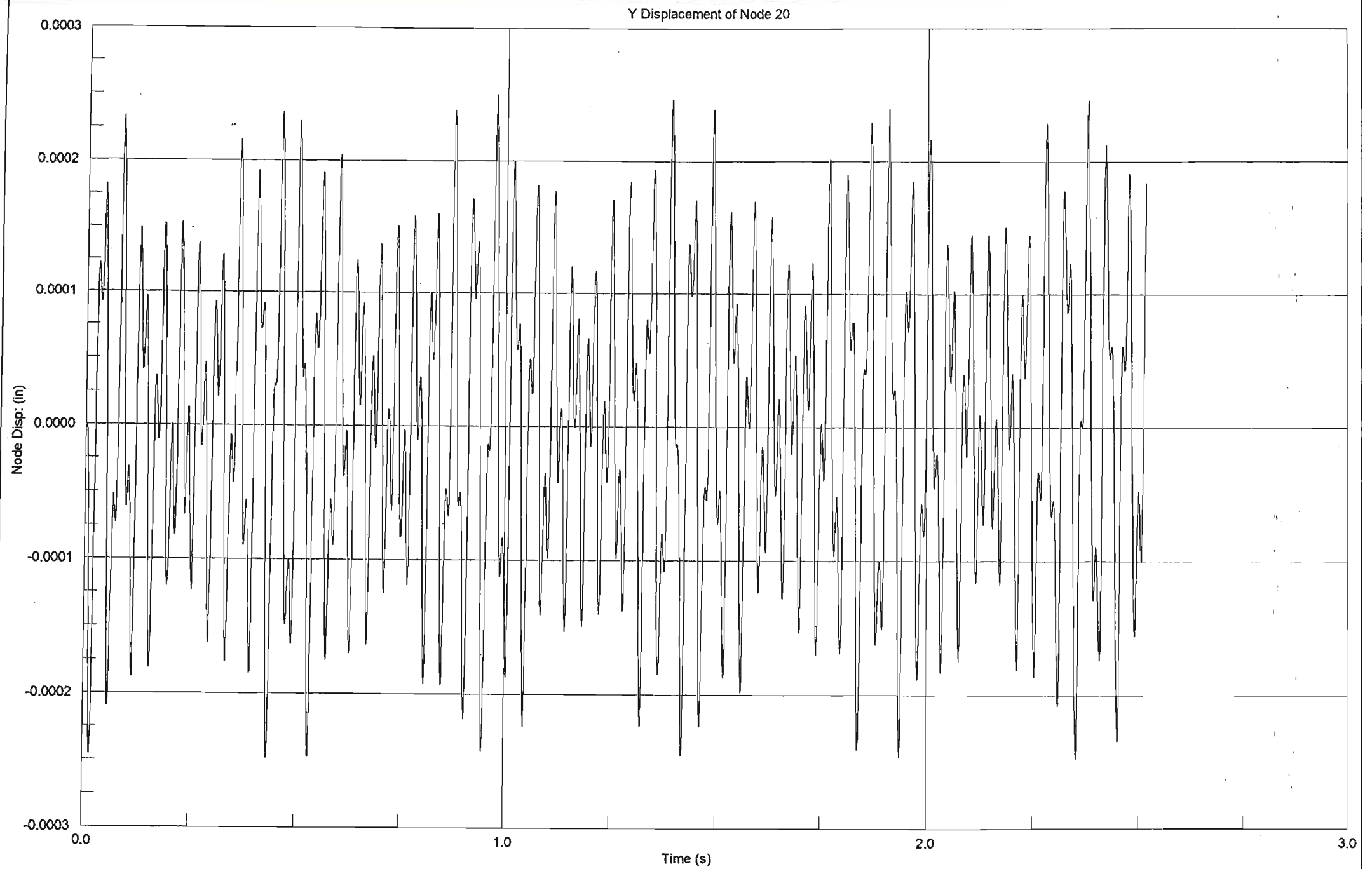


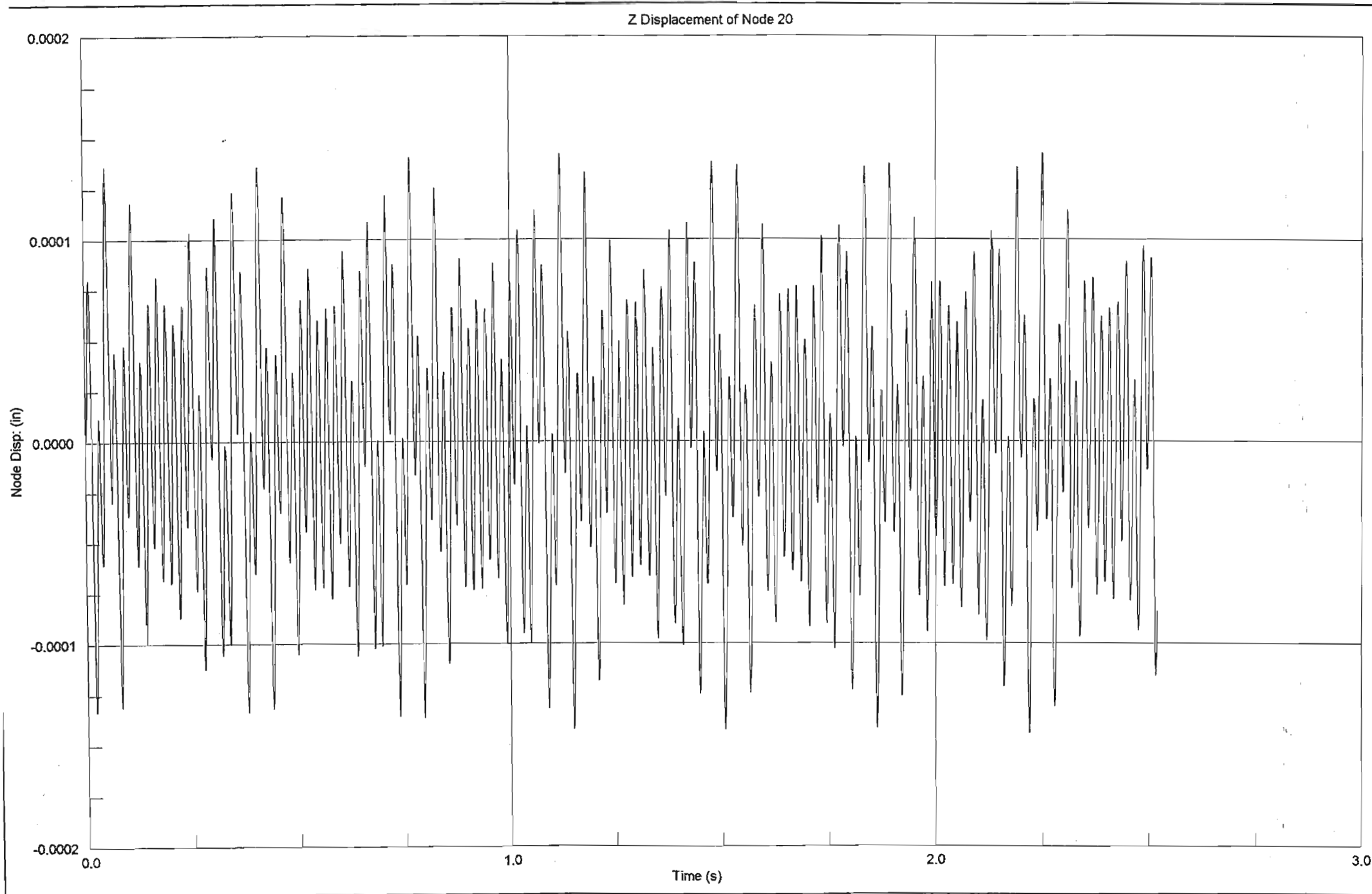
Vz

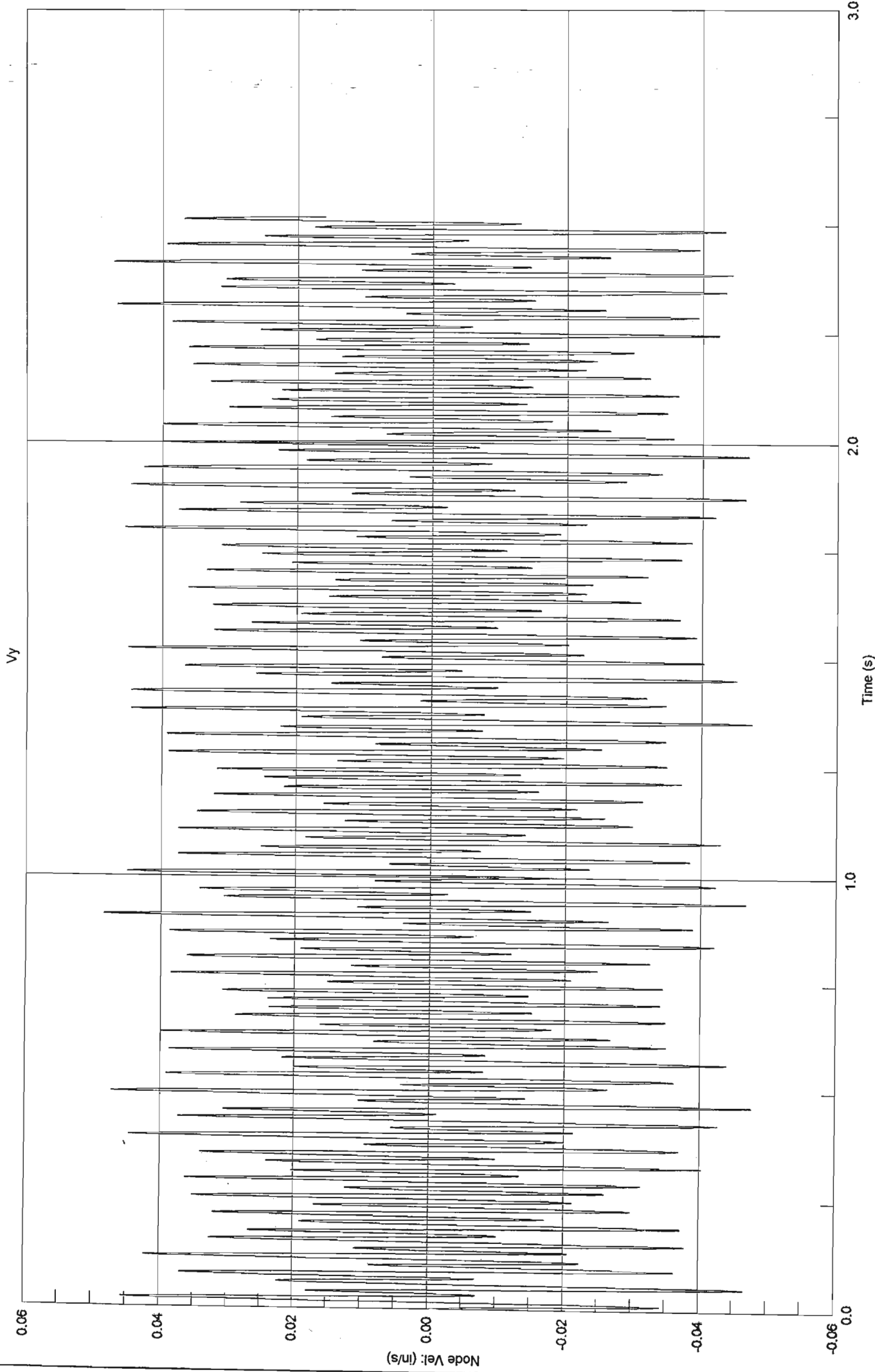


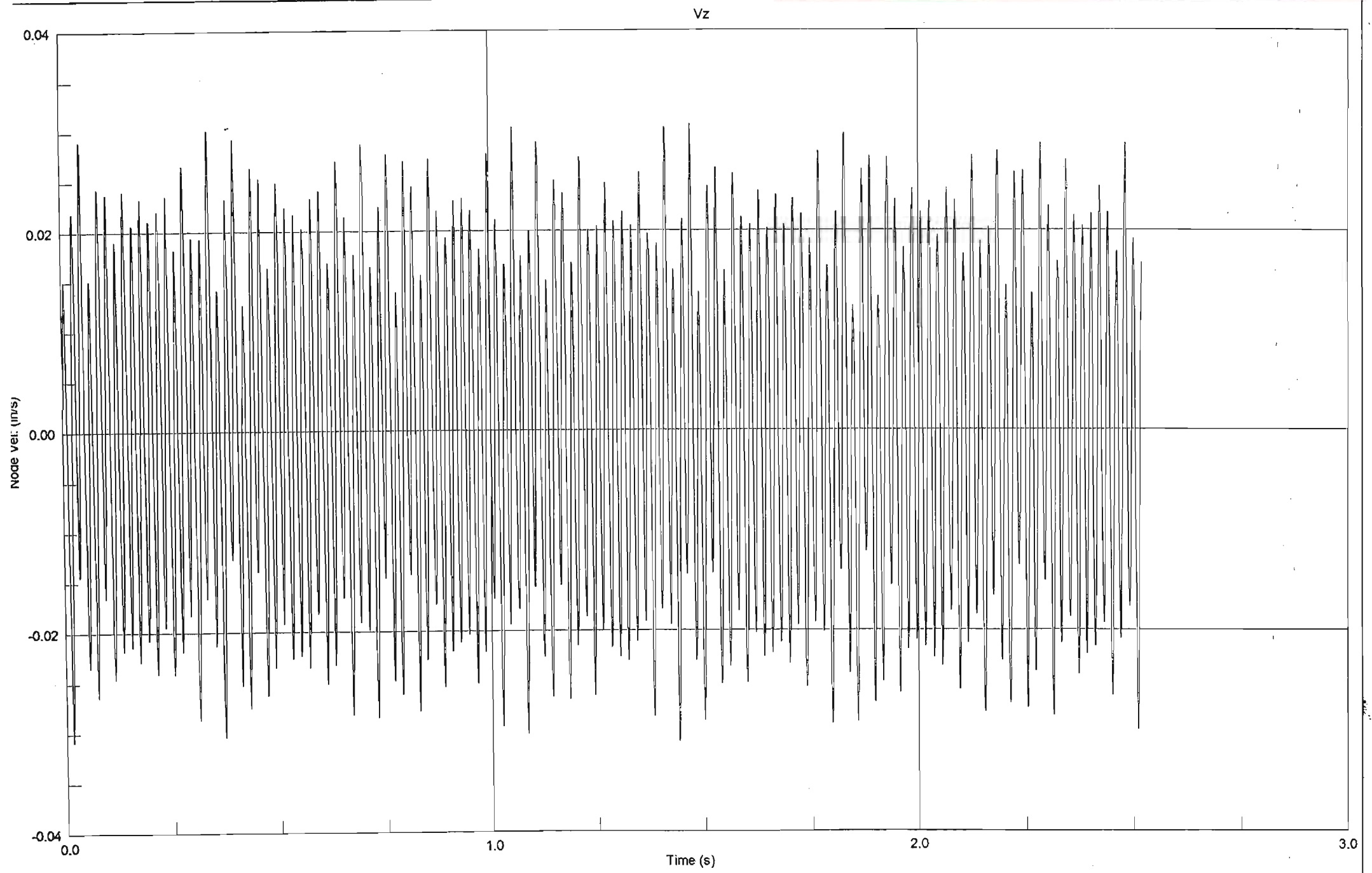




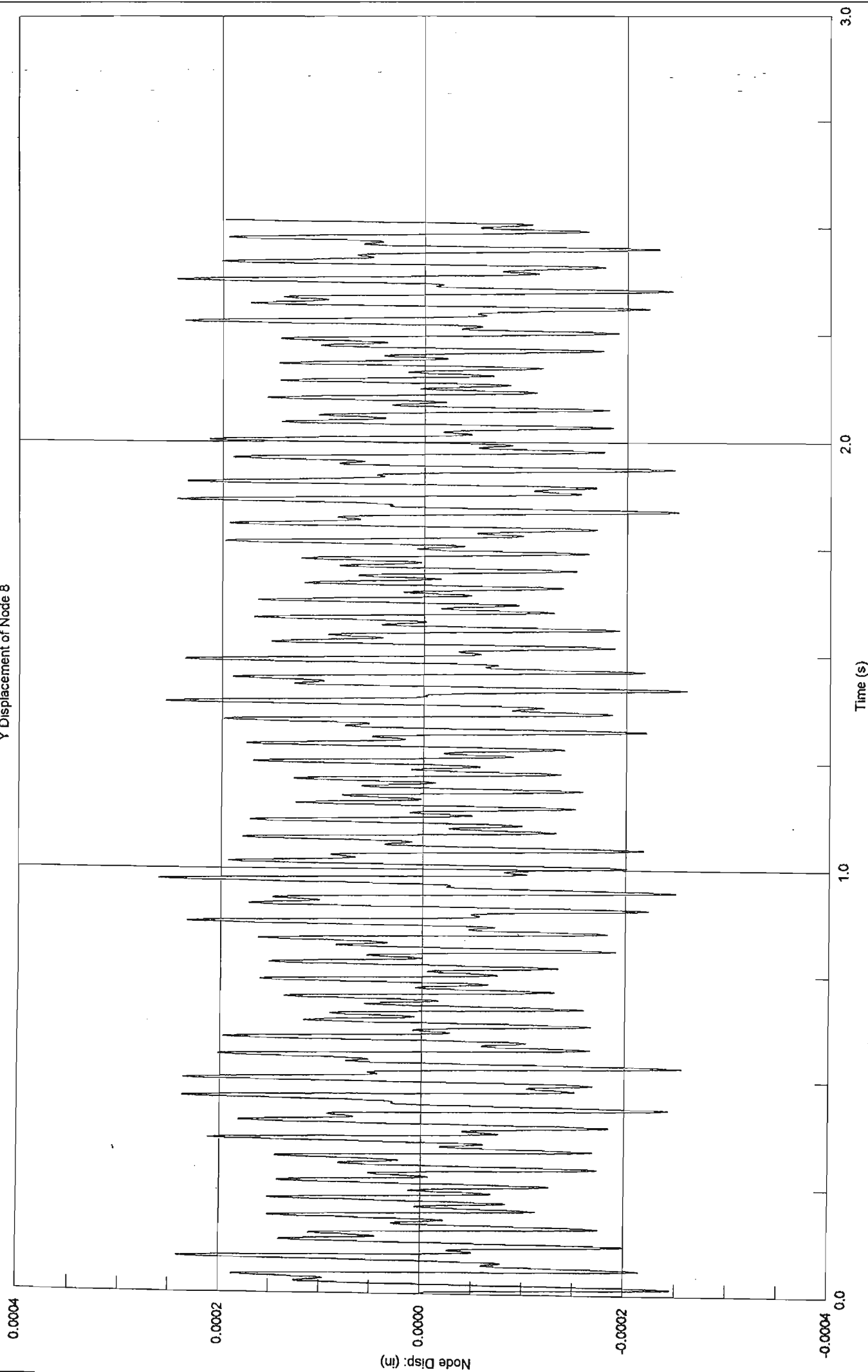




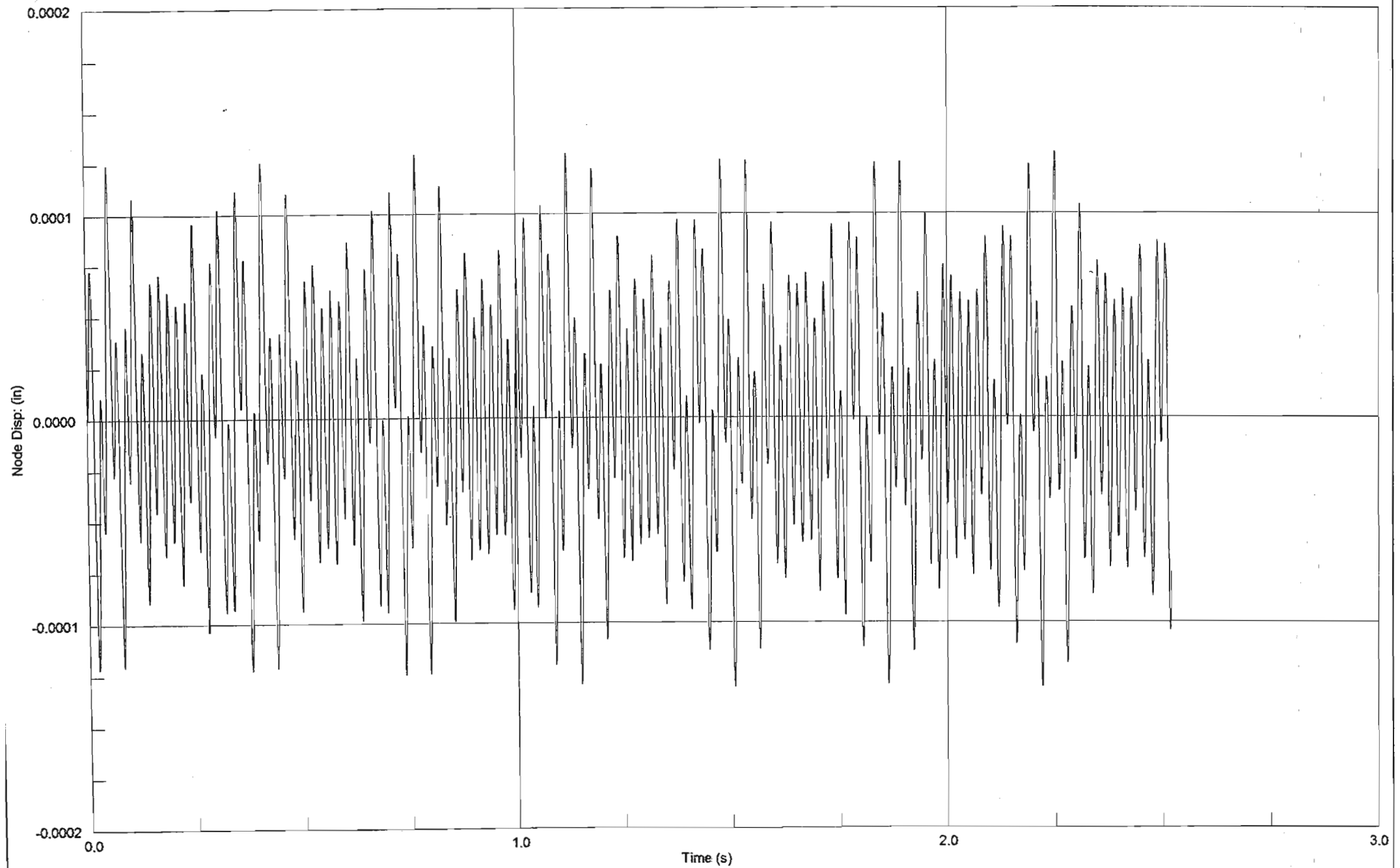


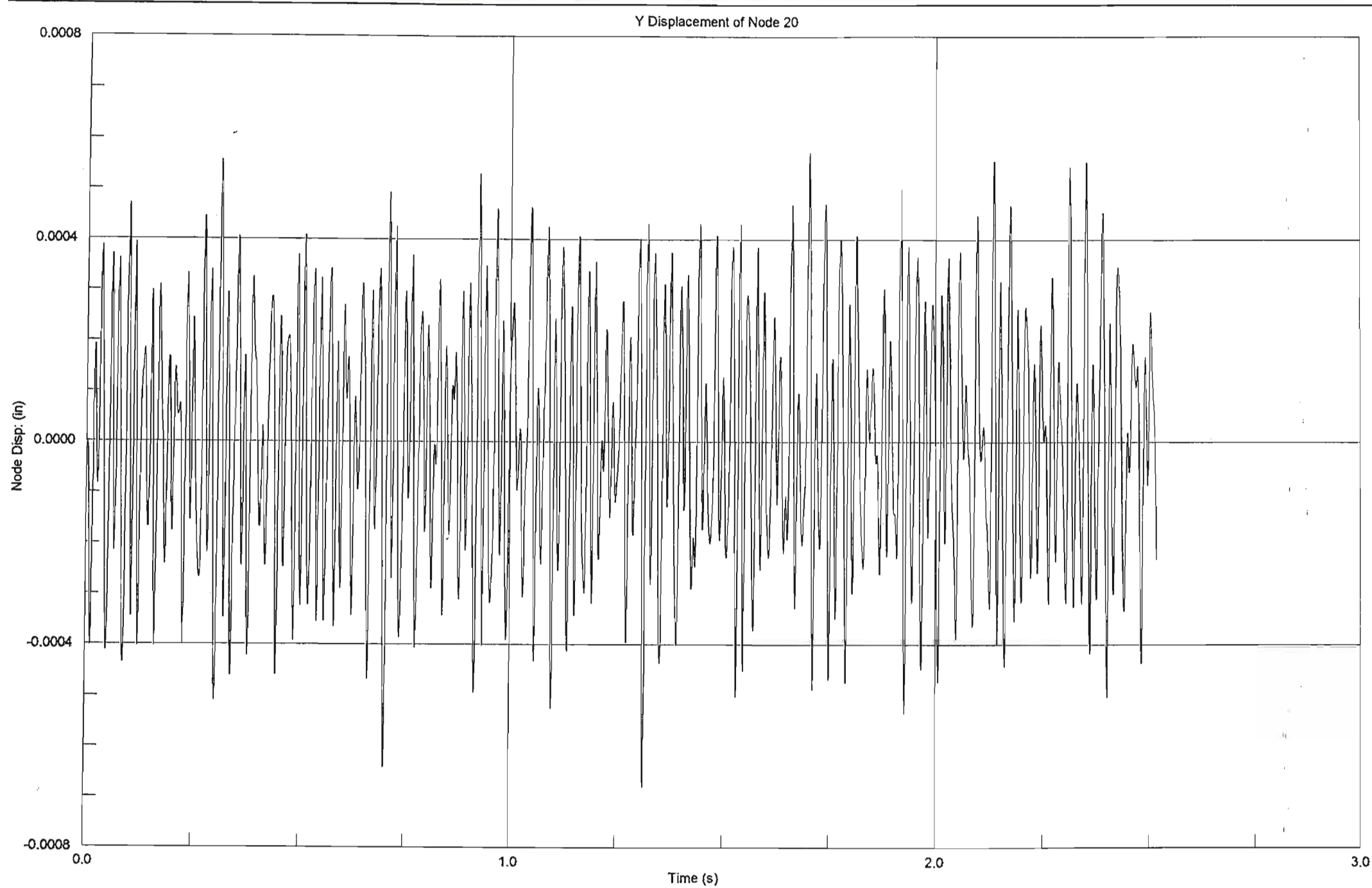


Y Displacement of Node 8

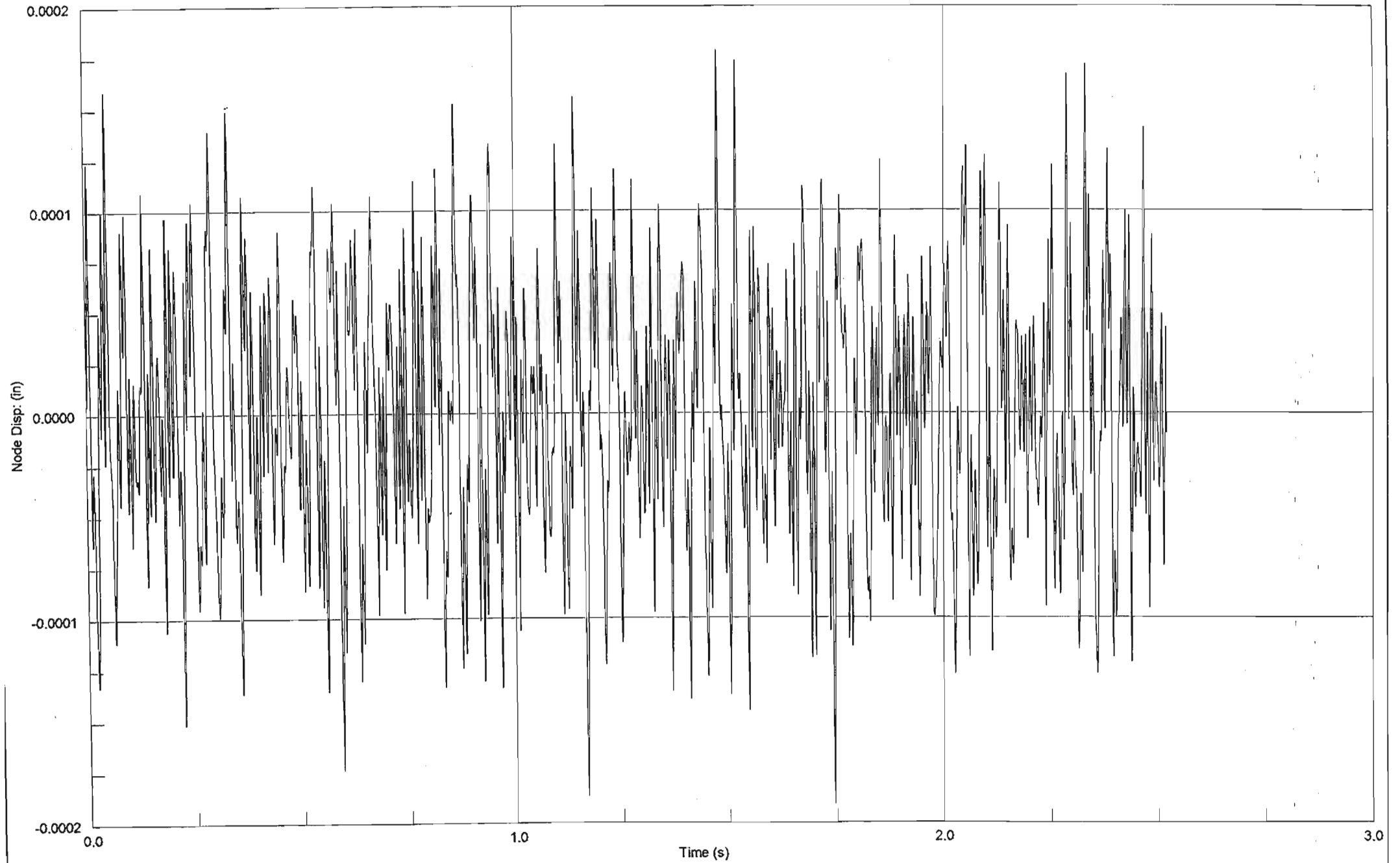


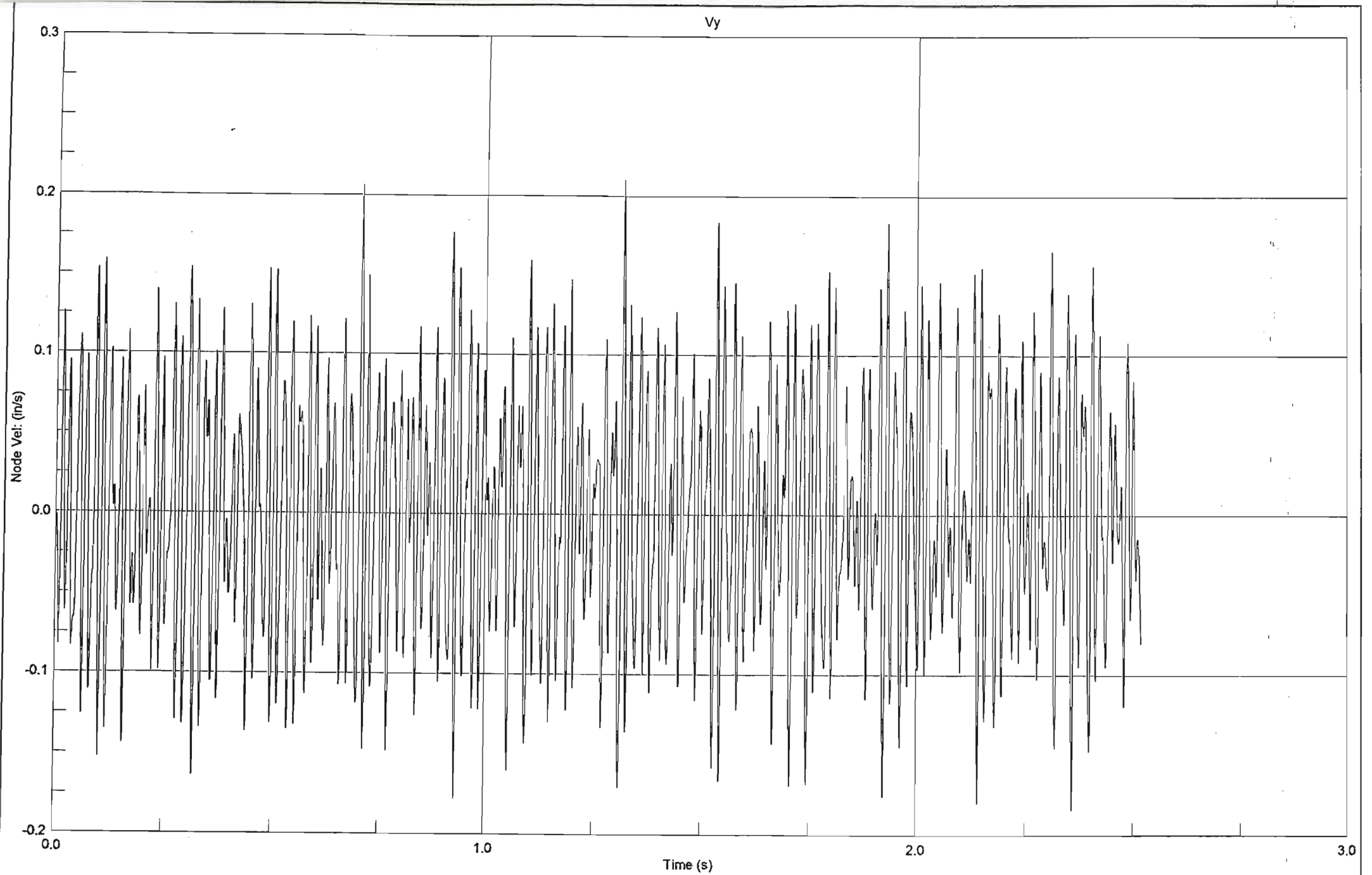
Z Displacement of Node 8



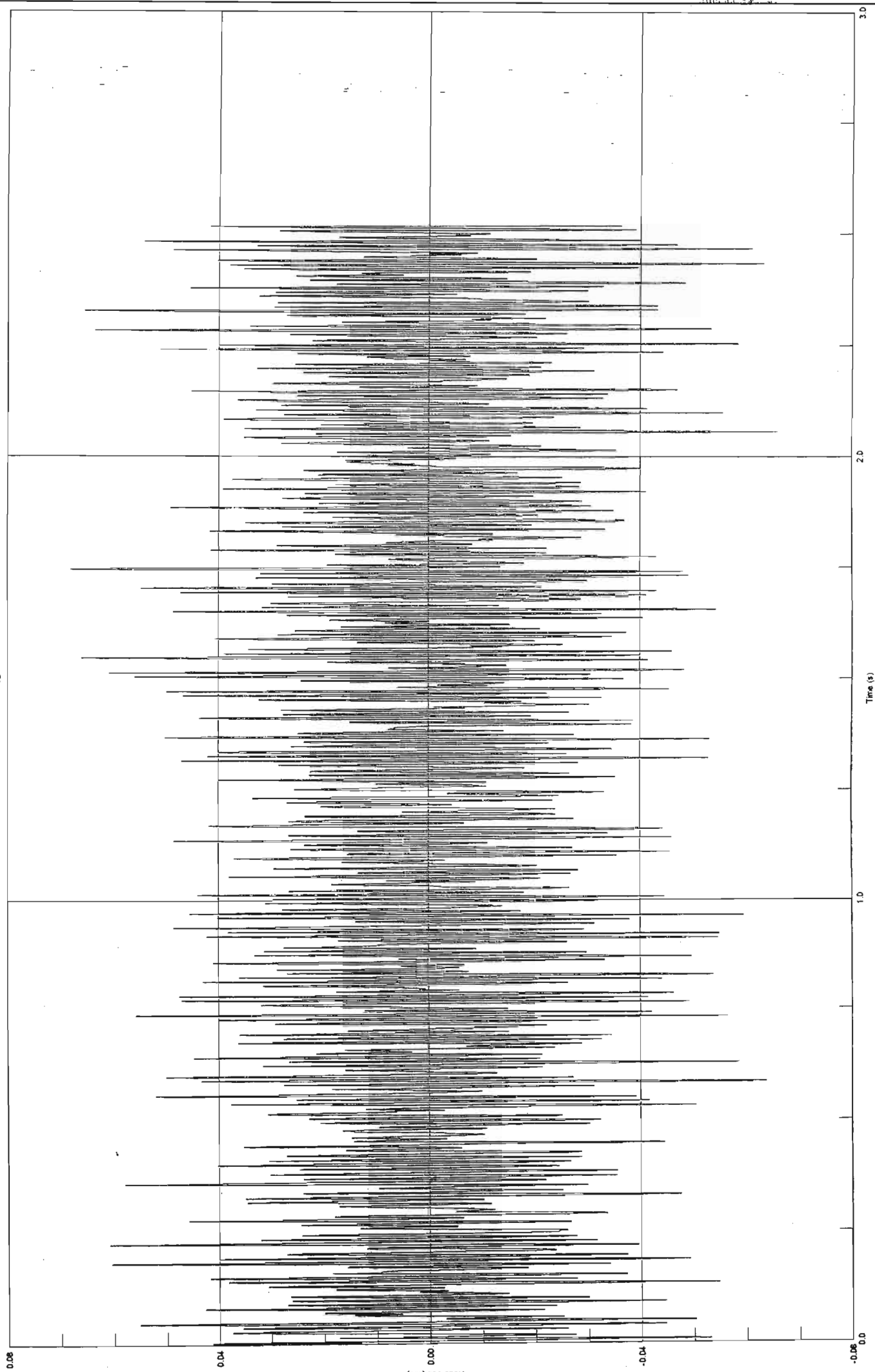


Z Displacement of Node 20

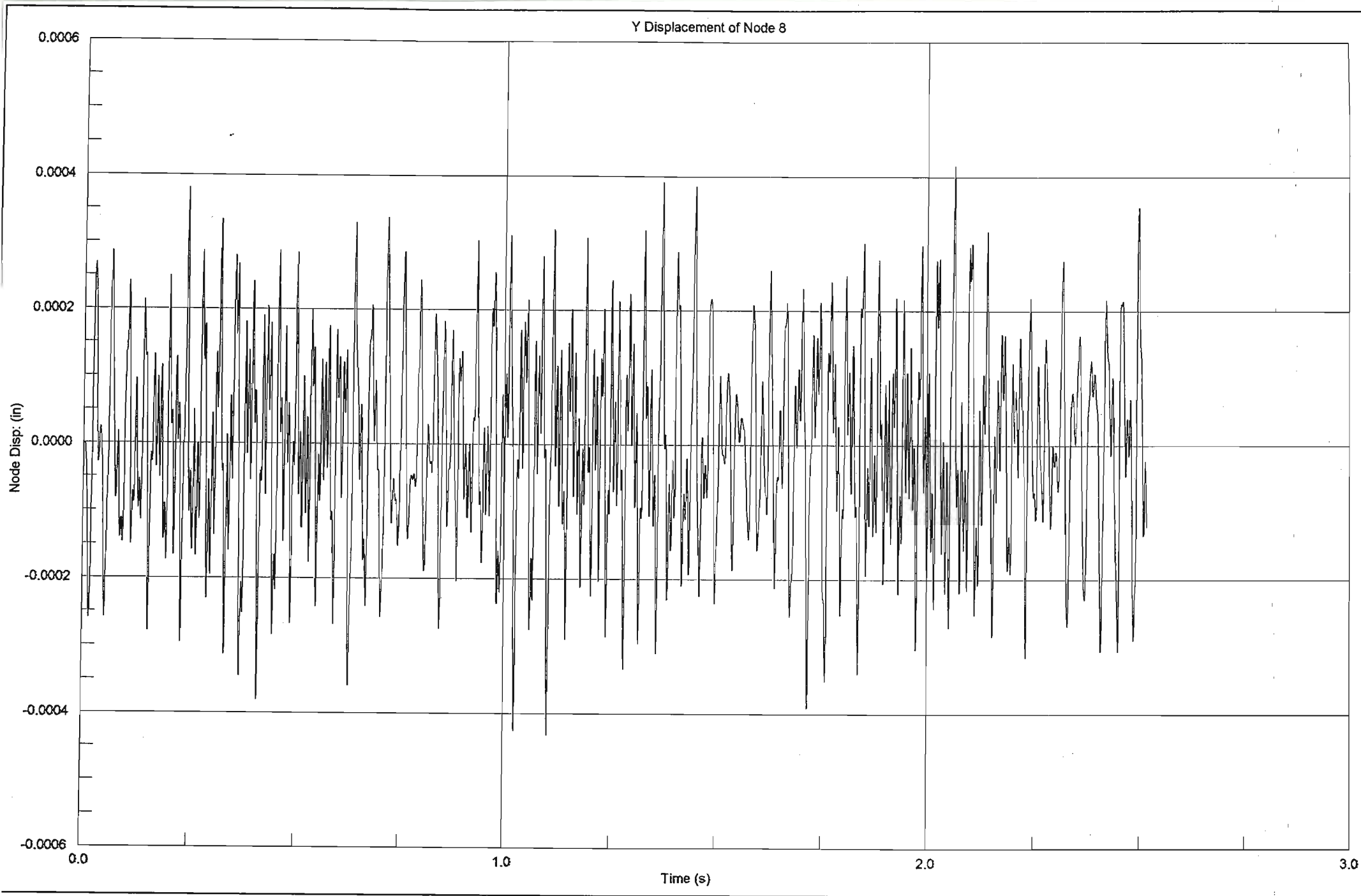


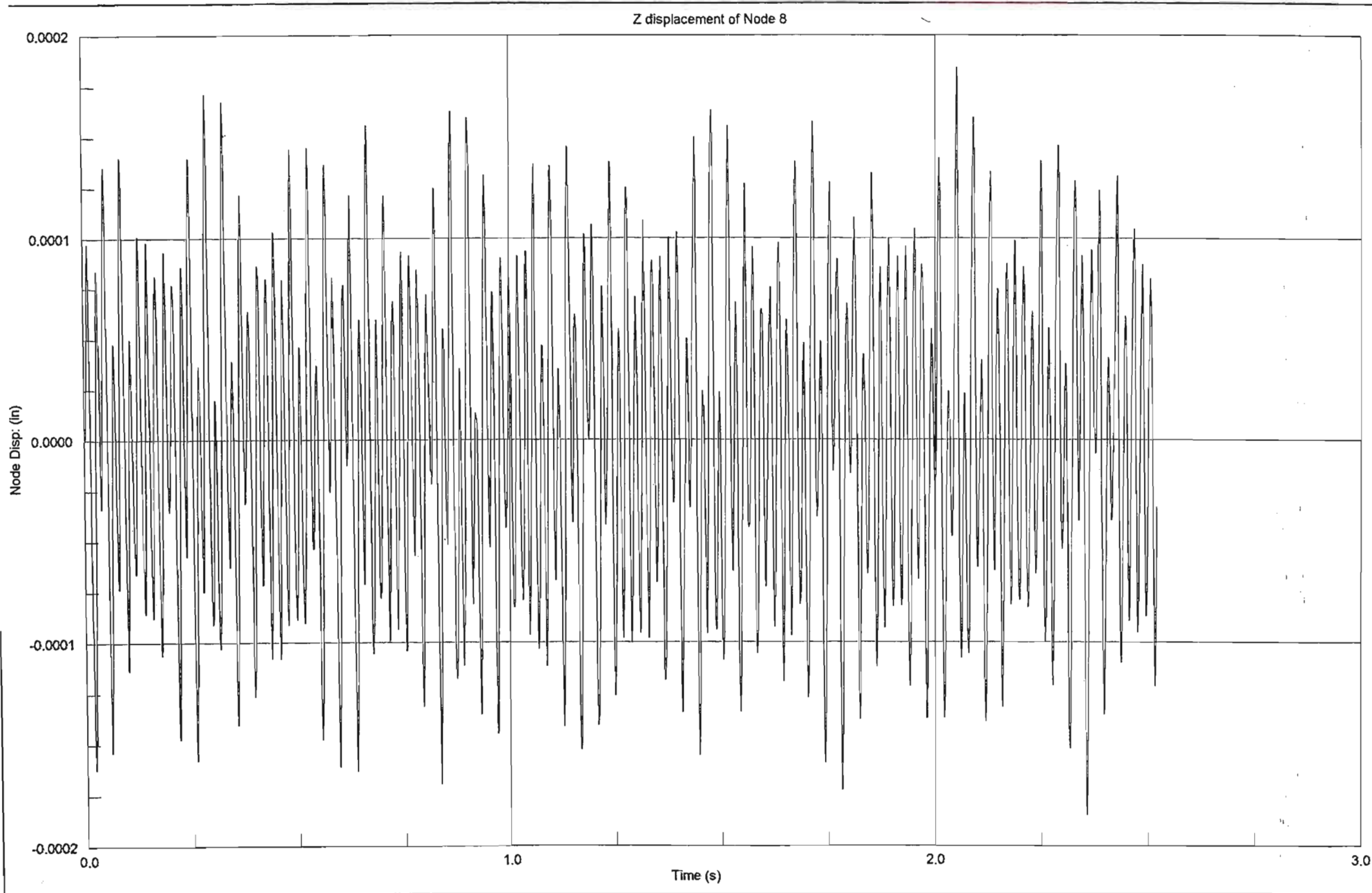


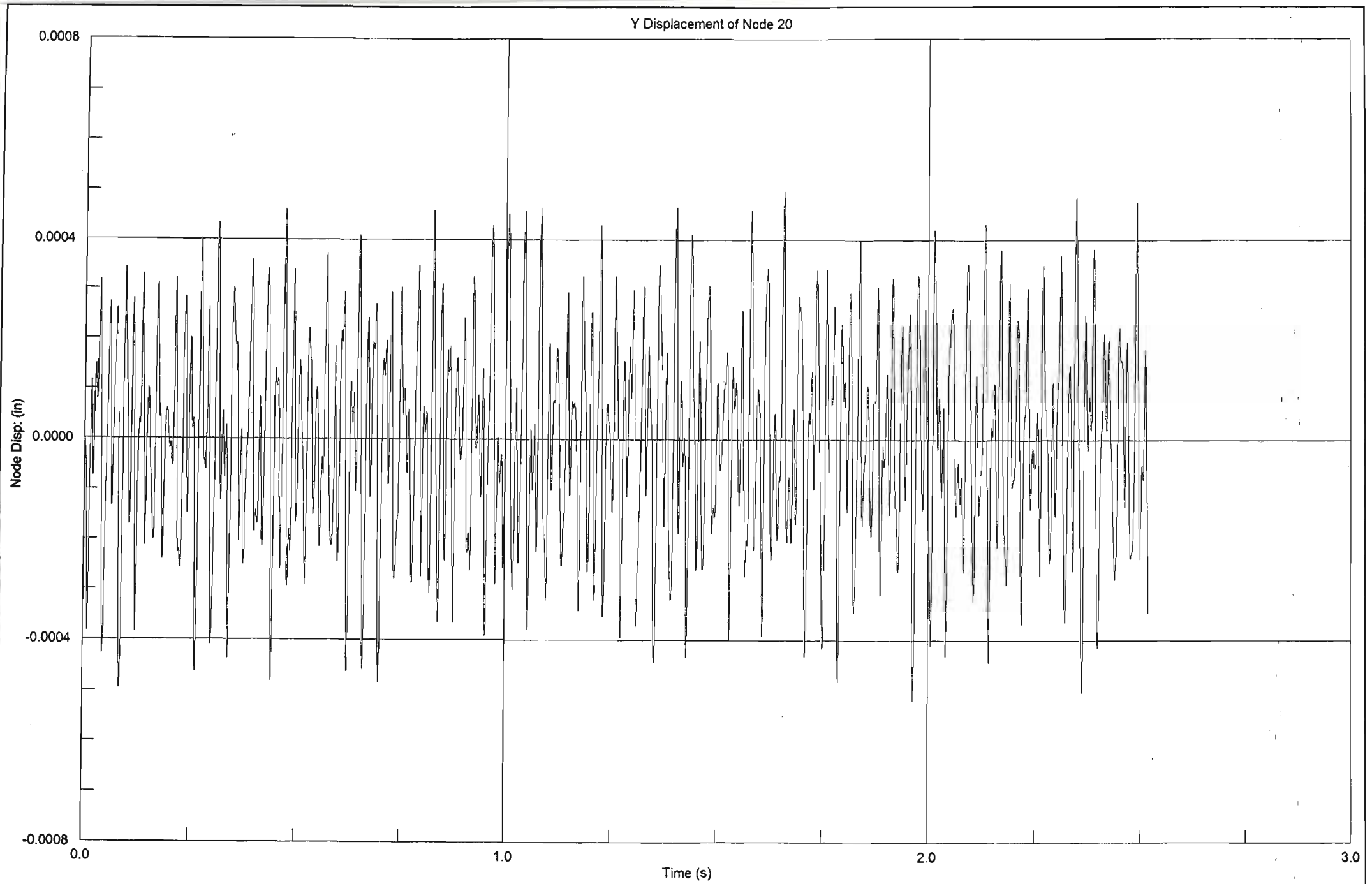
Vz



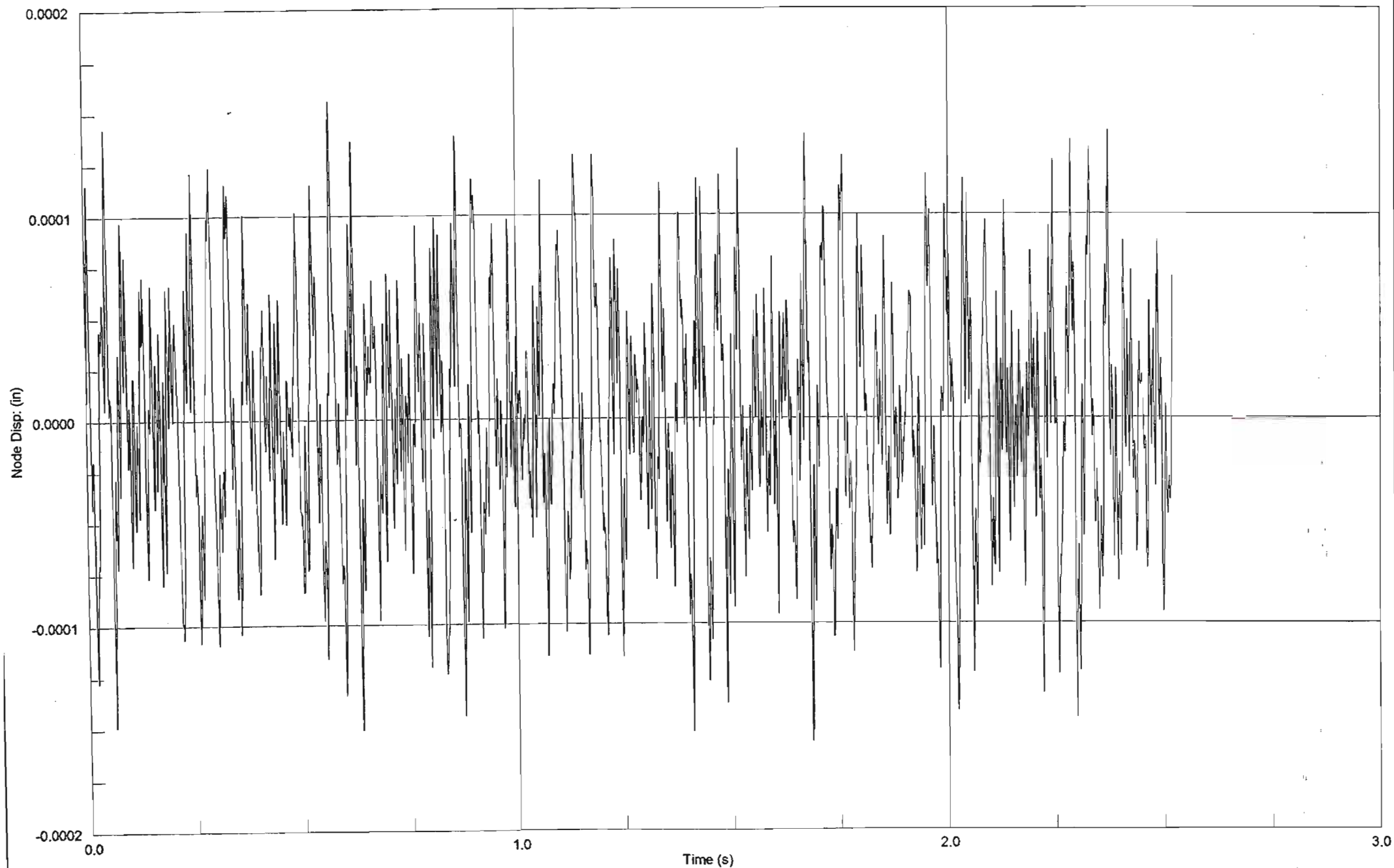
BS.4

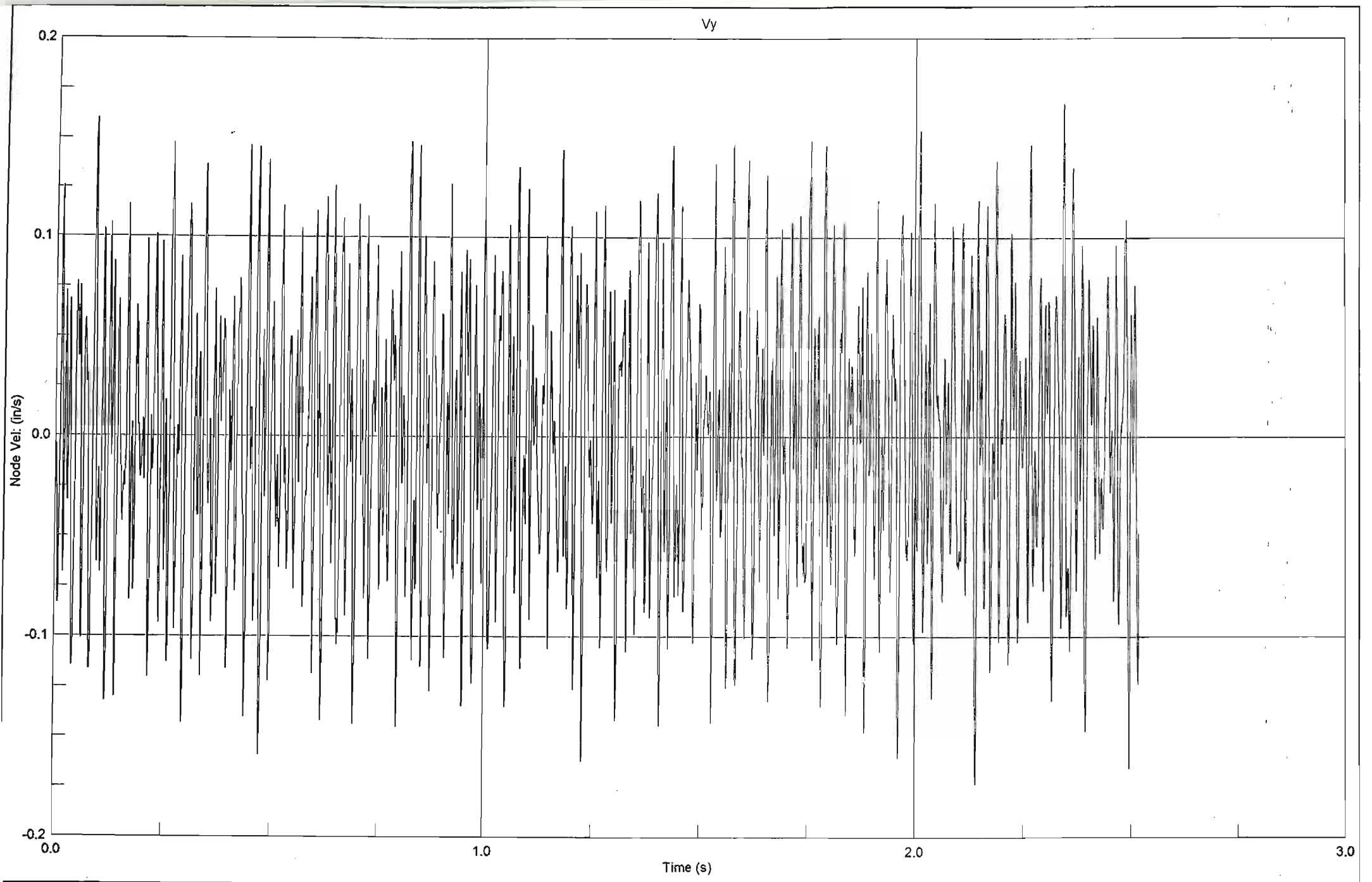


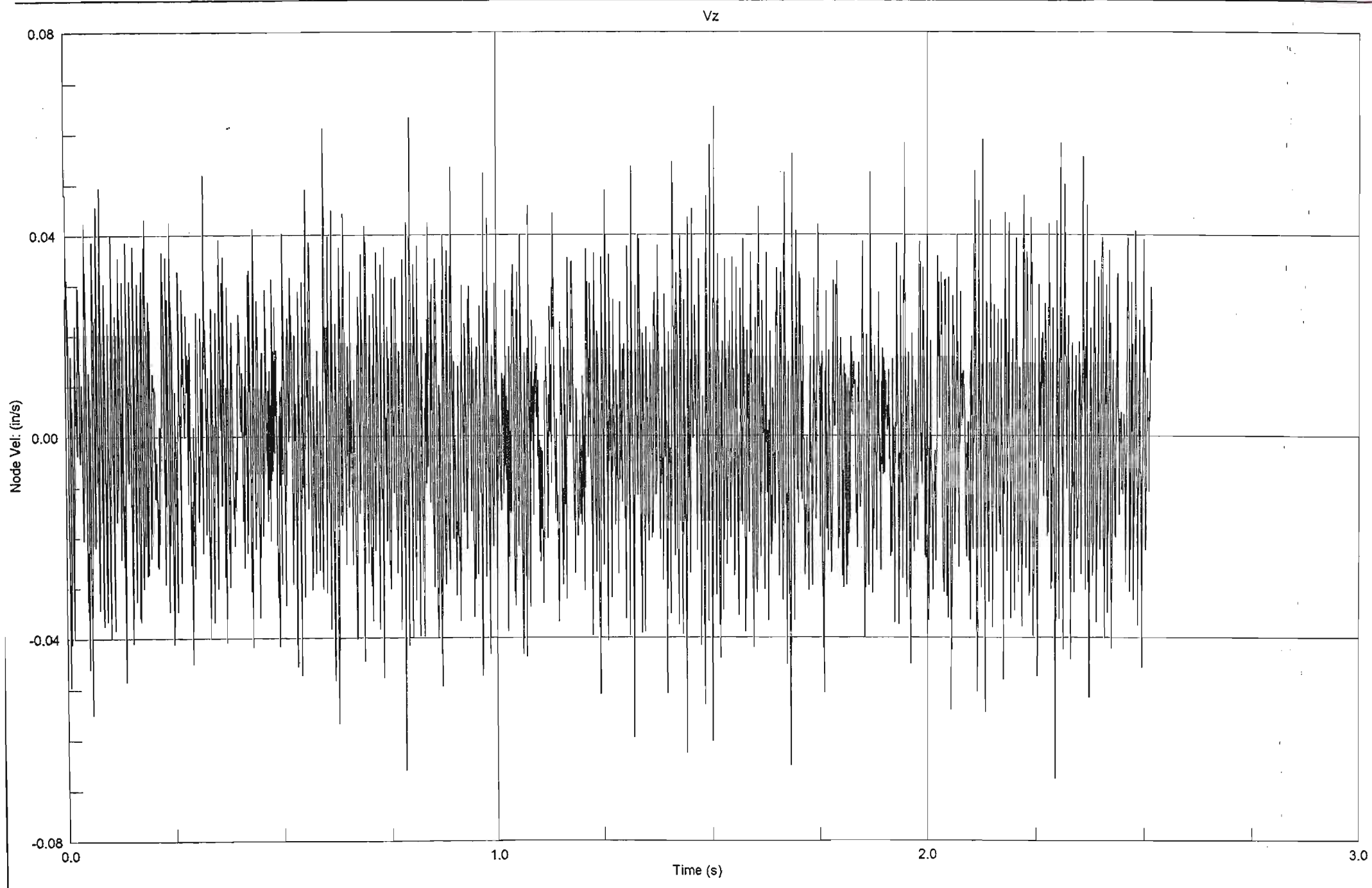


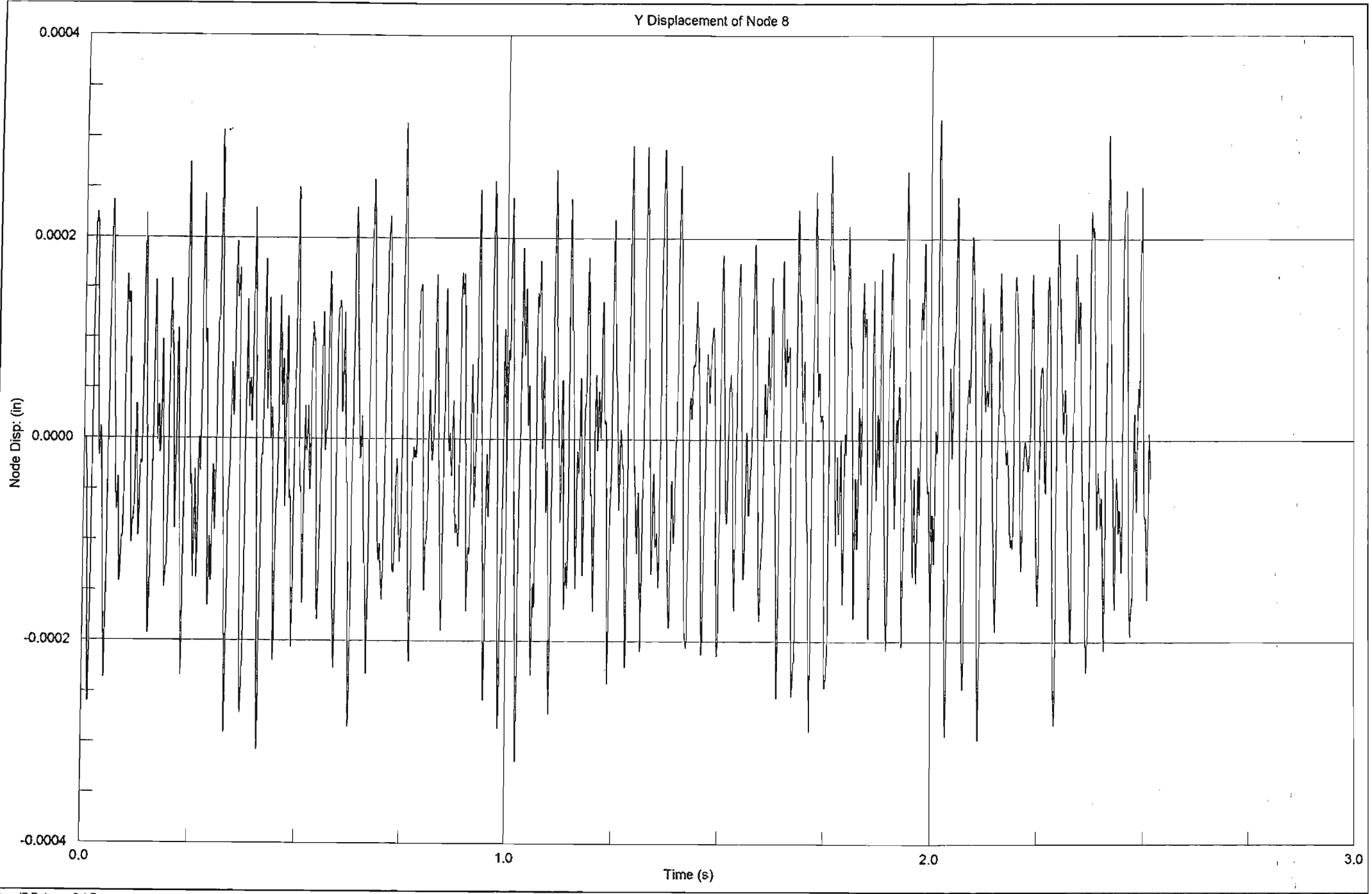


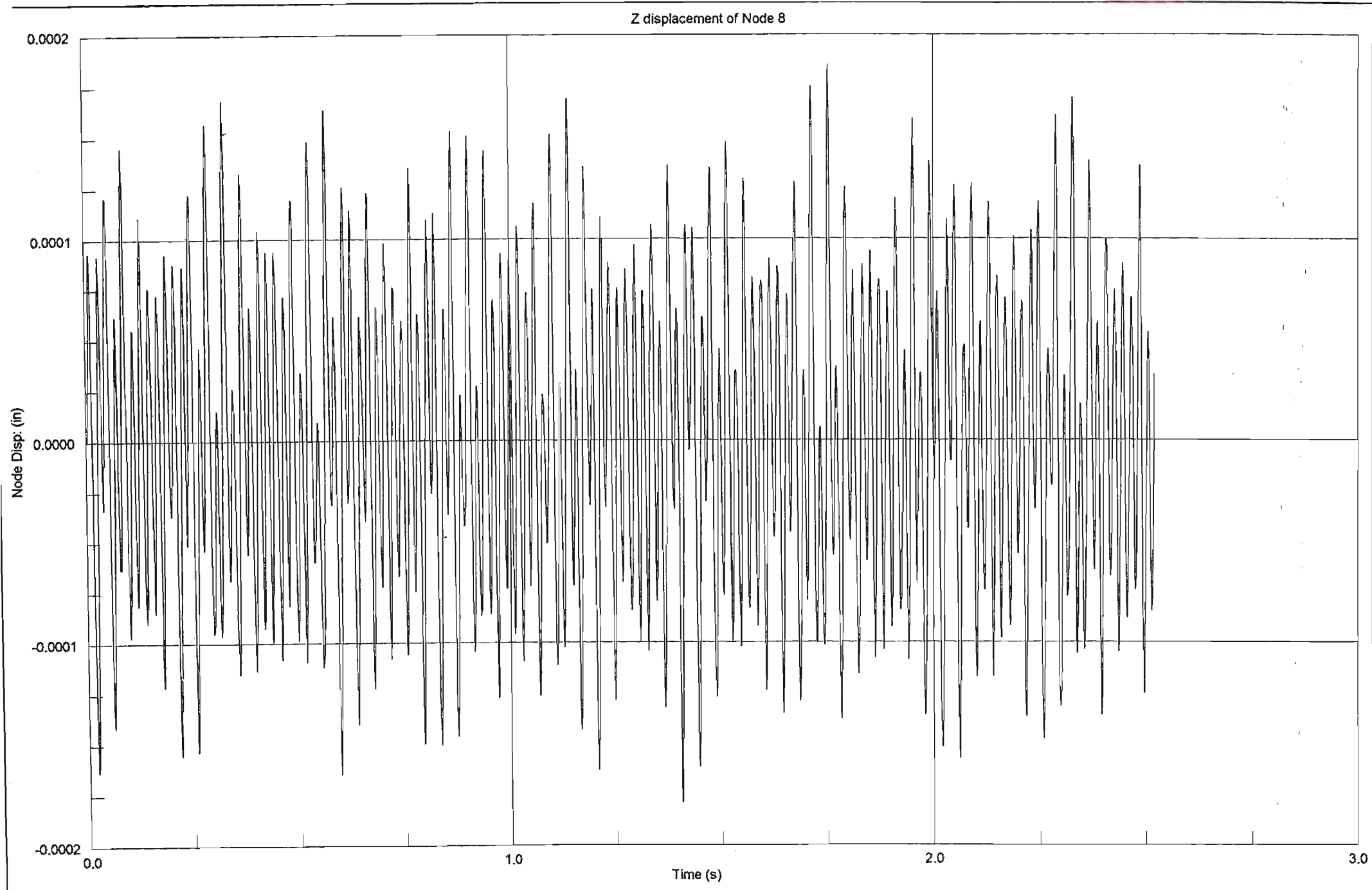
Z Displacement of Node 20

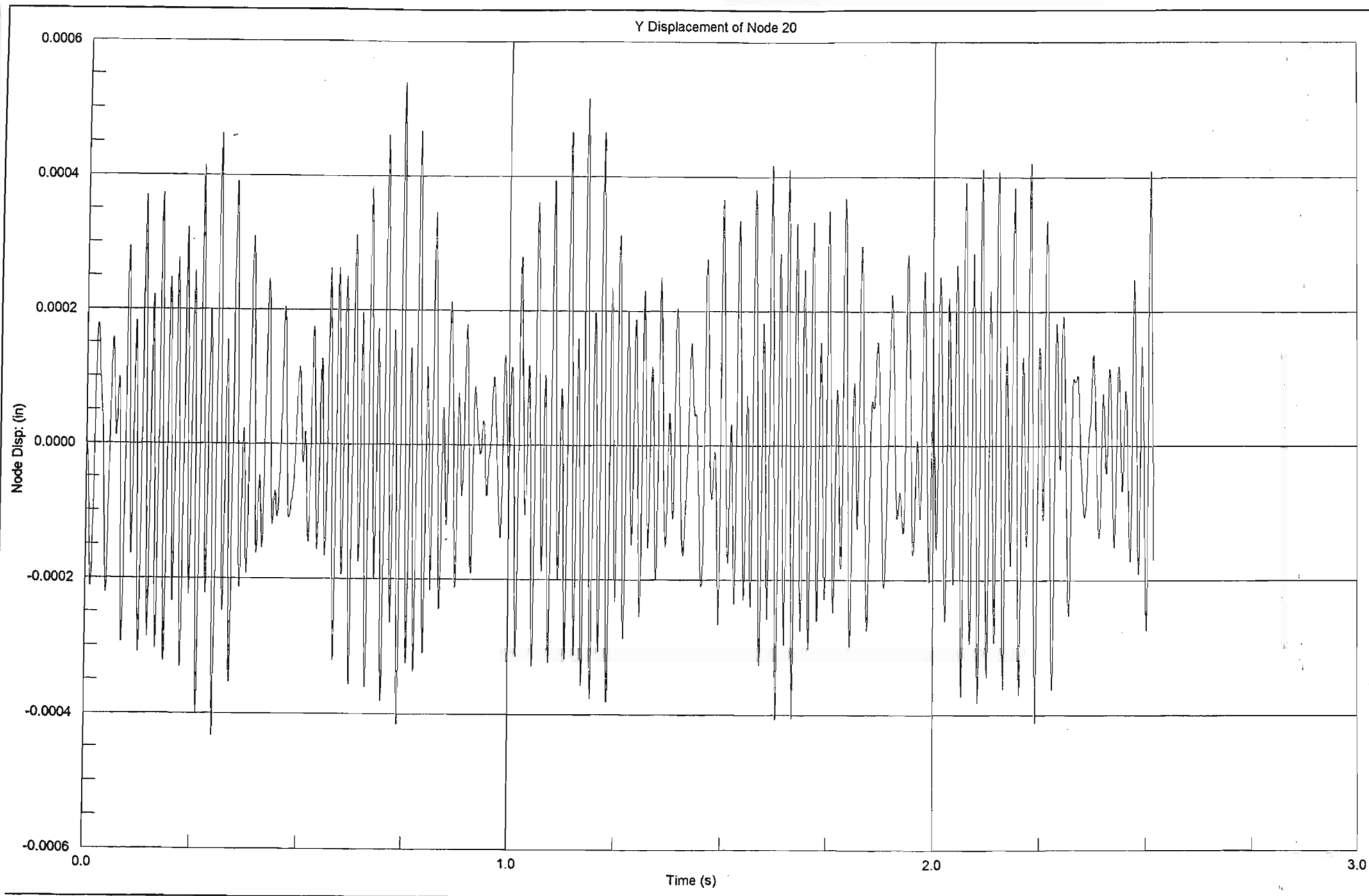




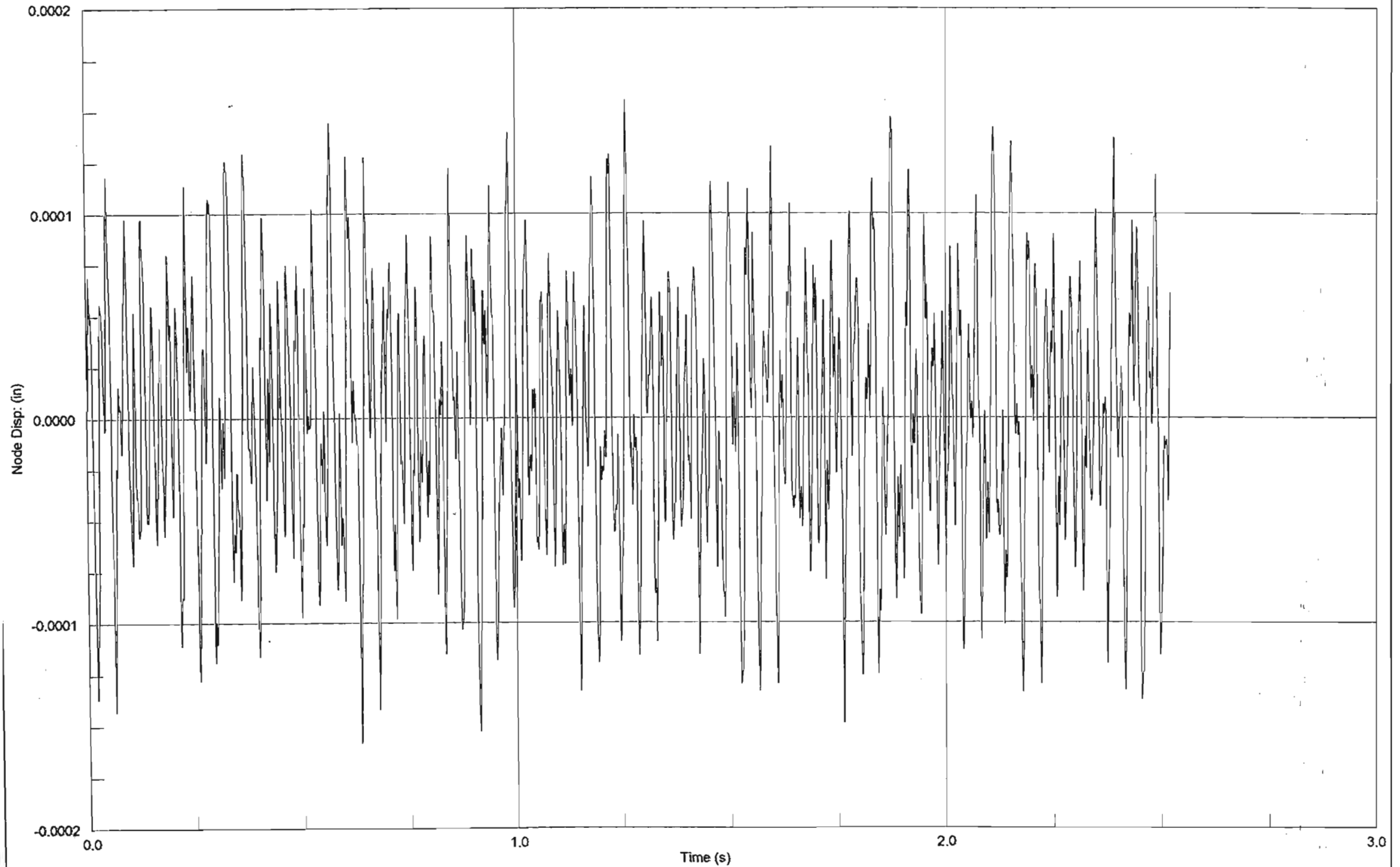


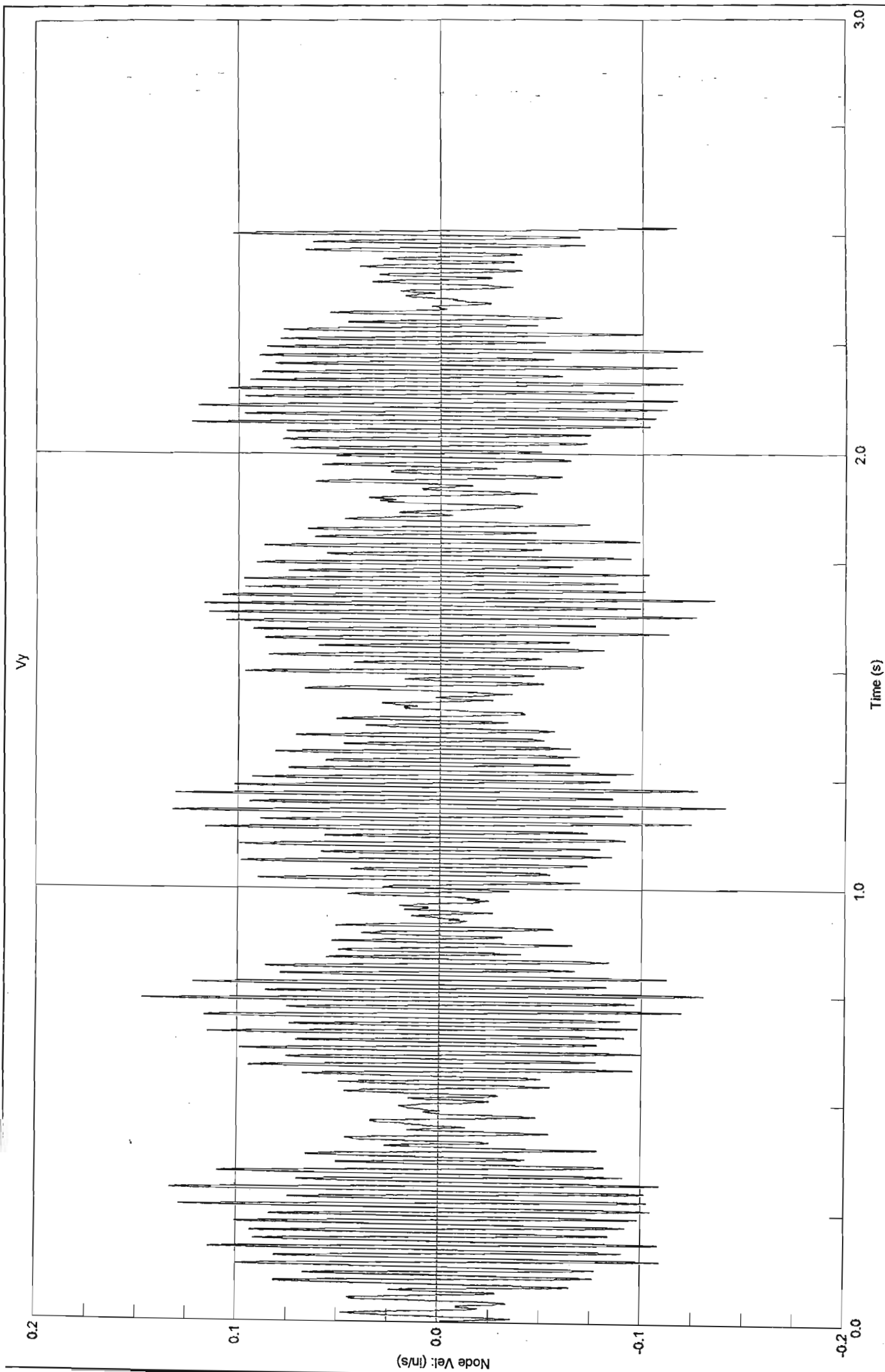




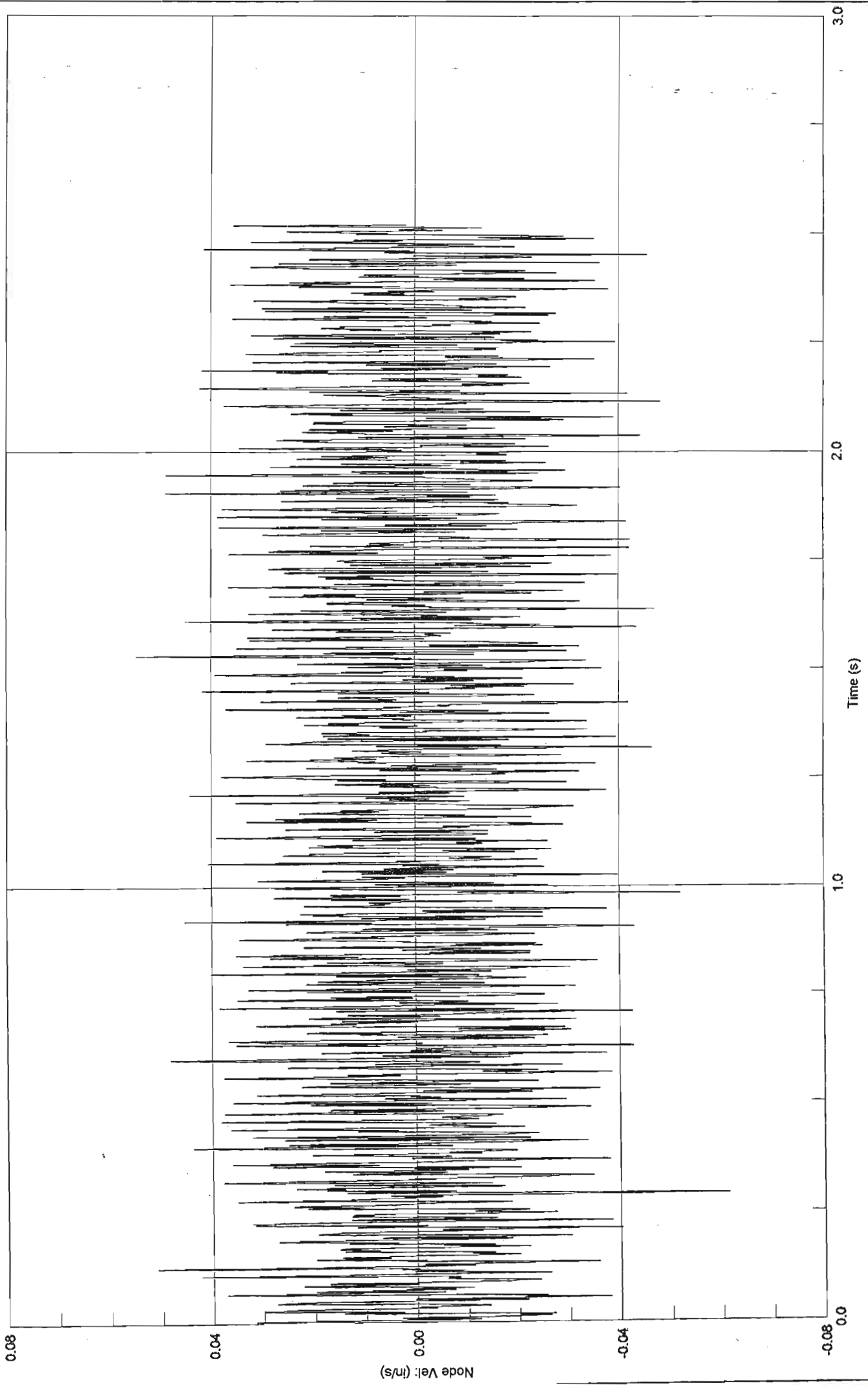


Z Displacement of Node 20

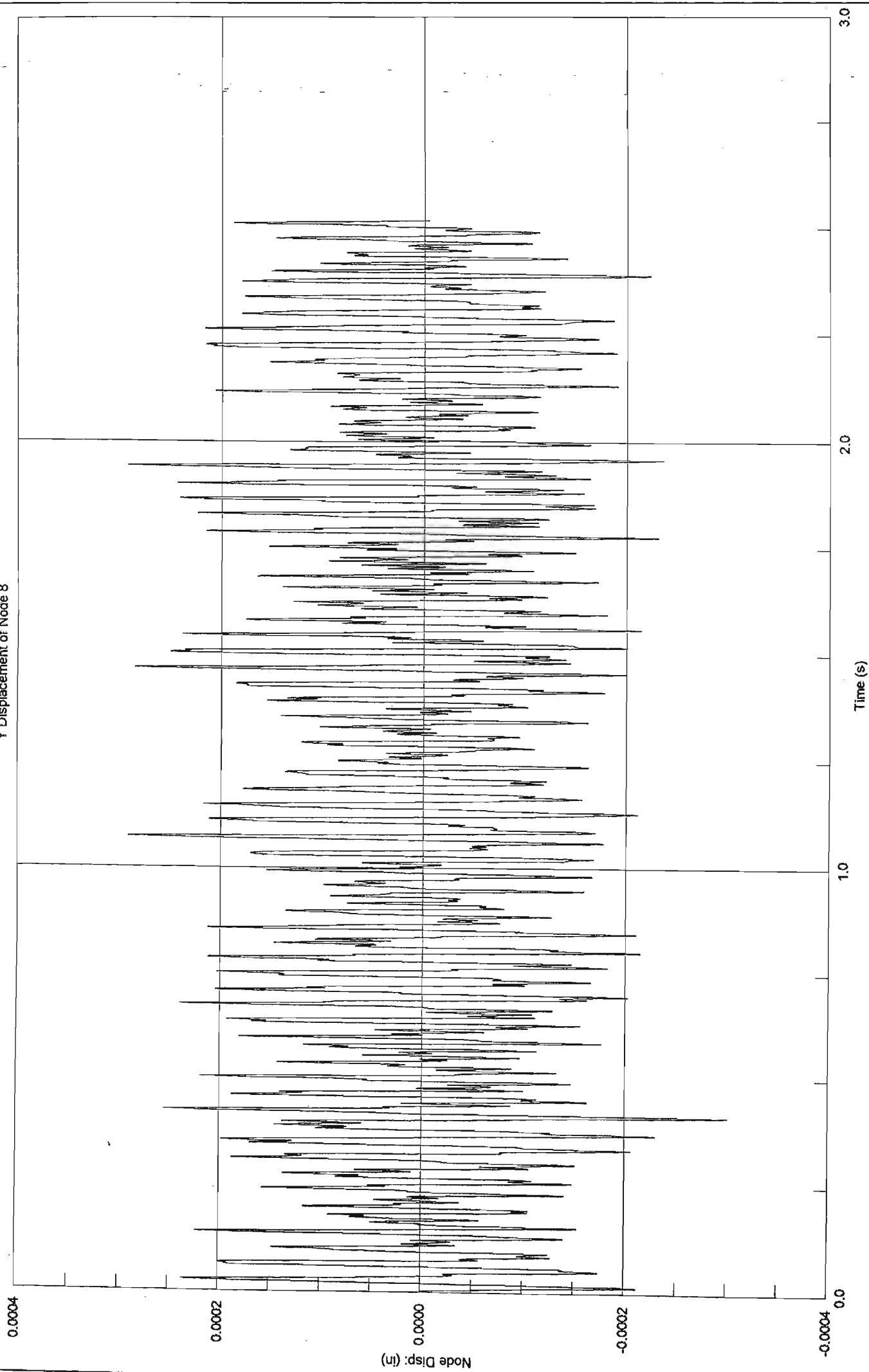


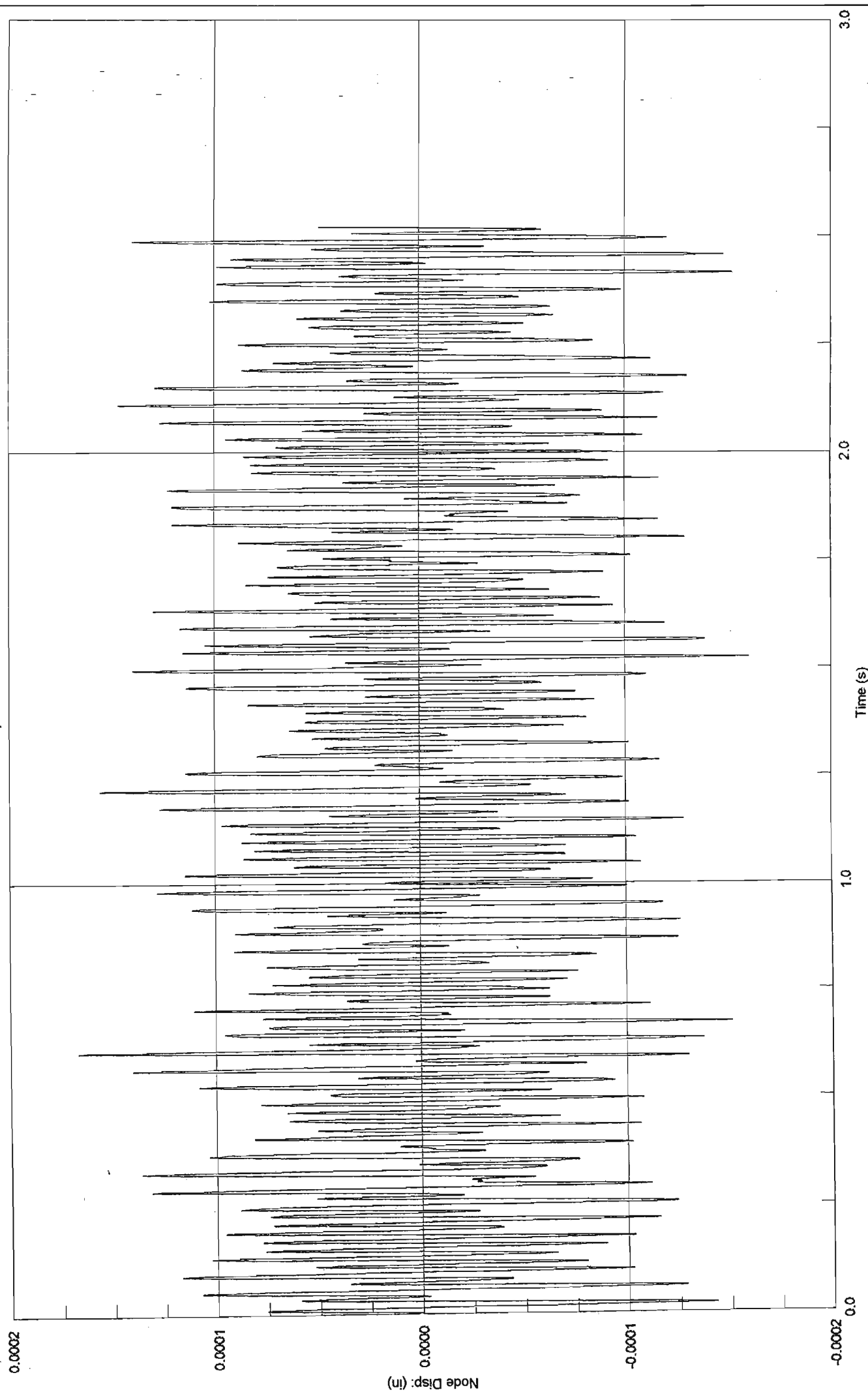


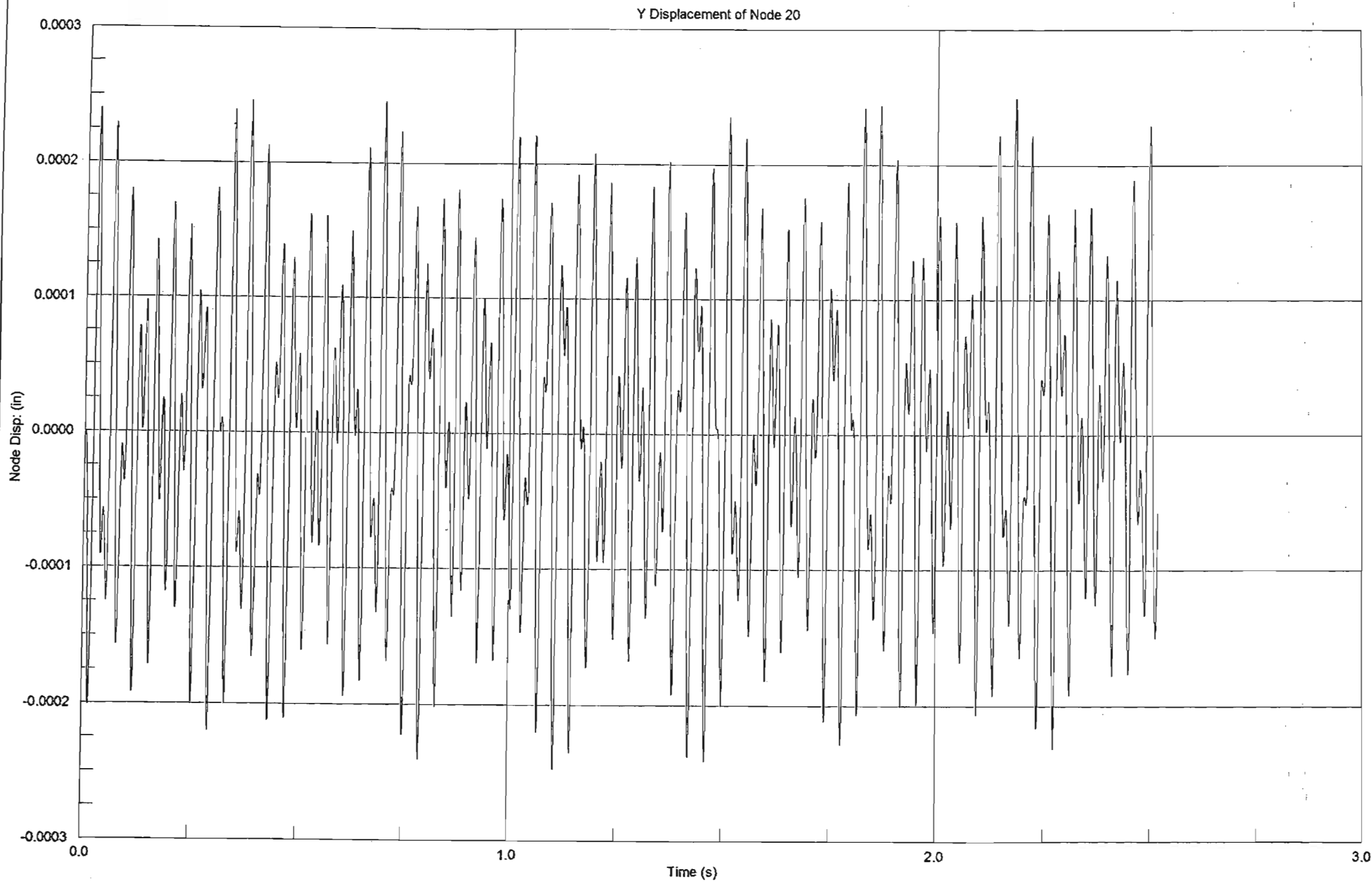
Vz

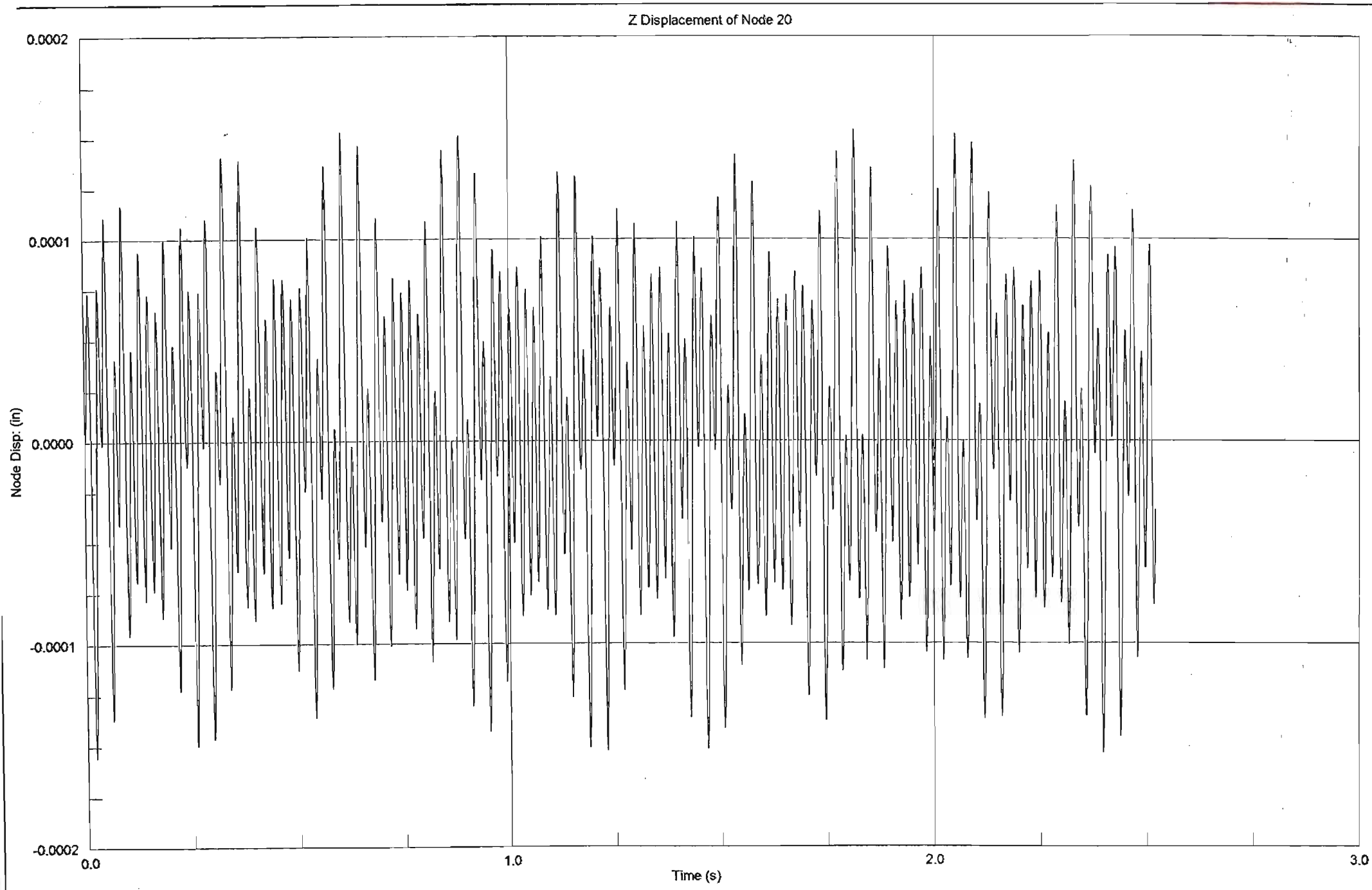


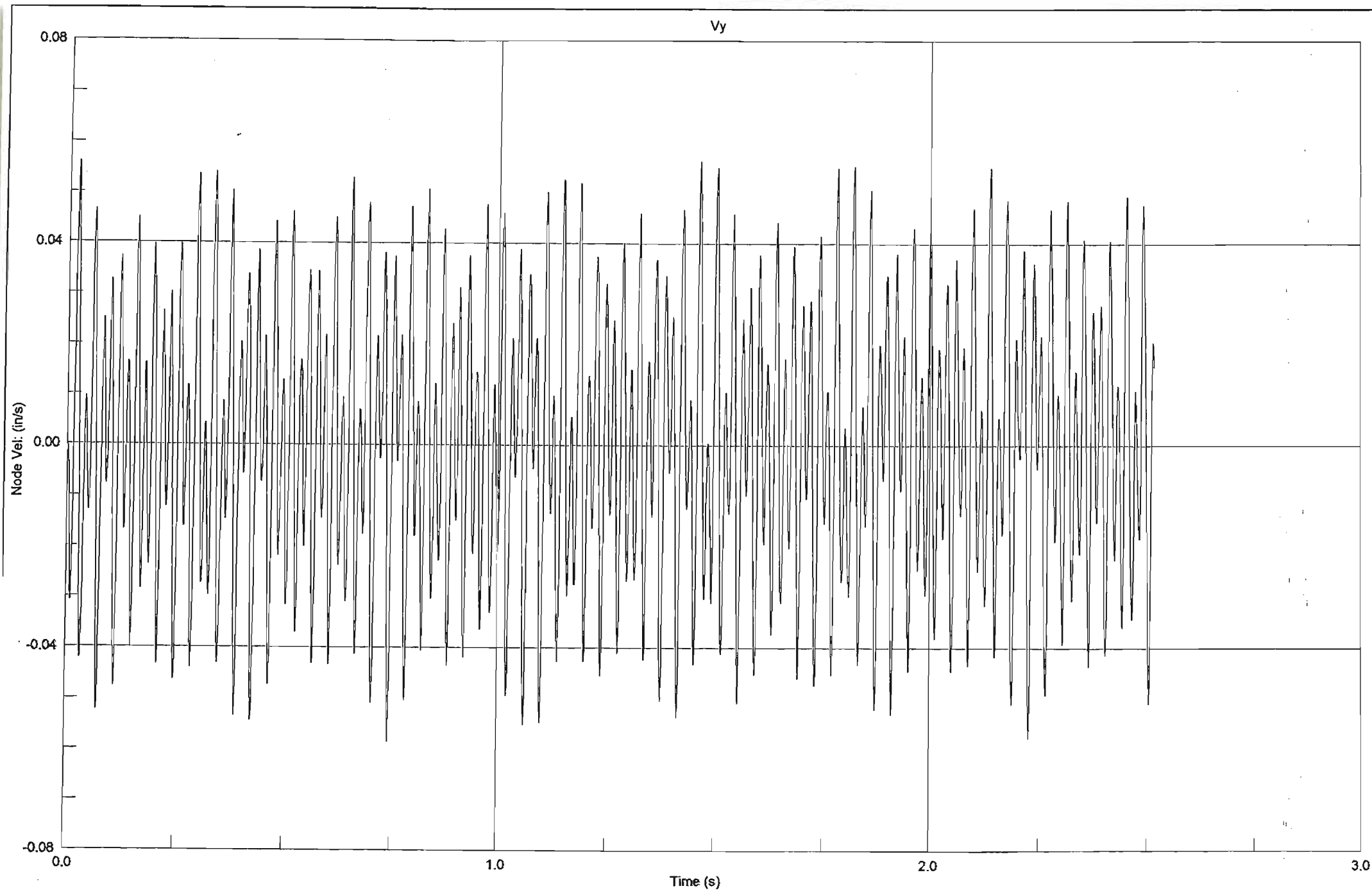
Y Displacement of Node 8

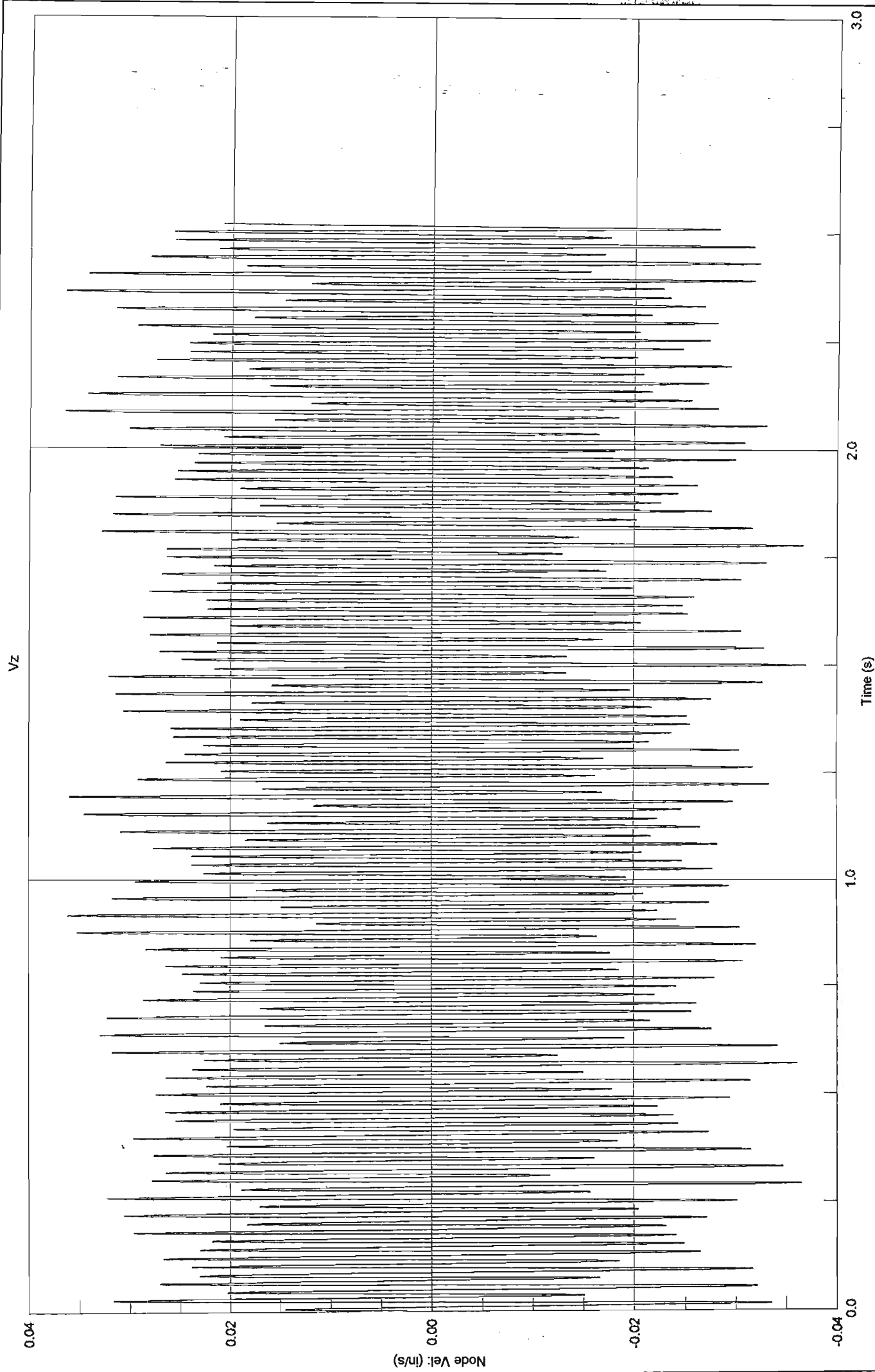


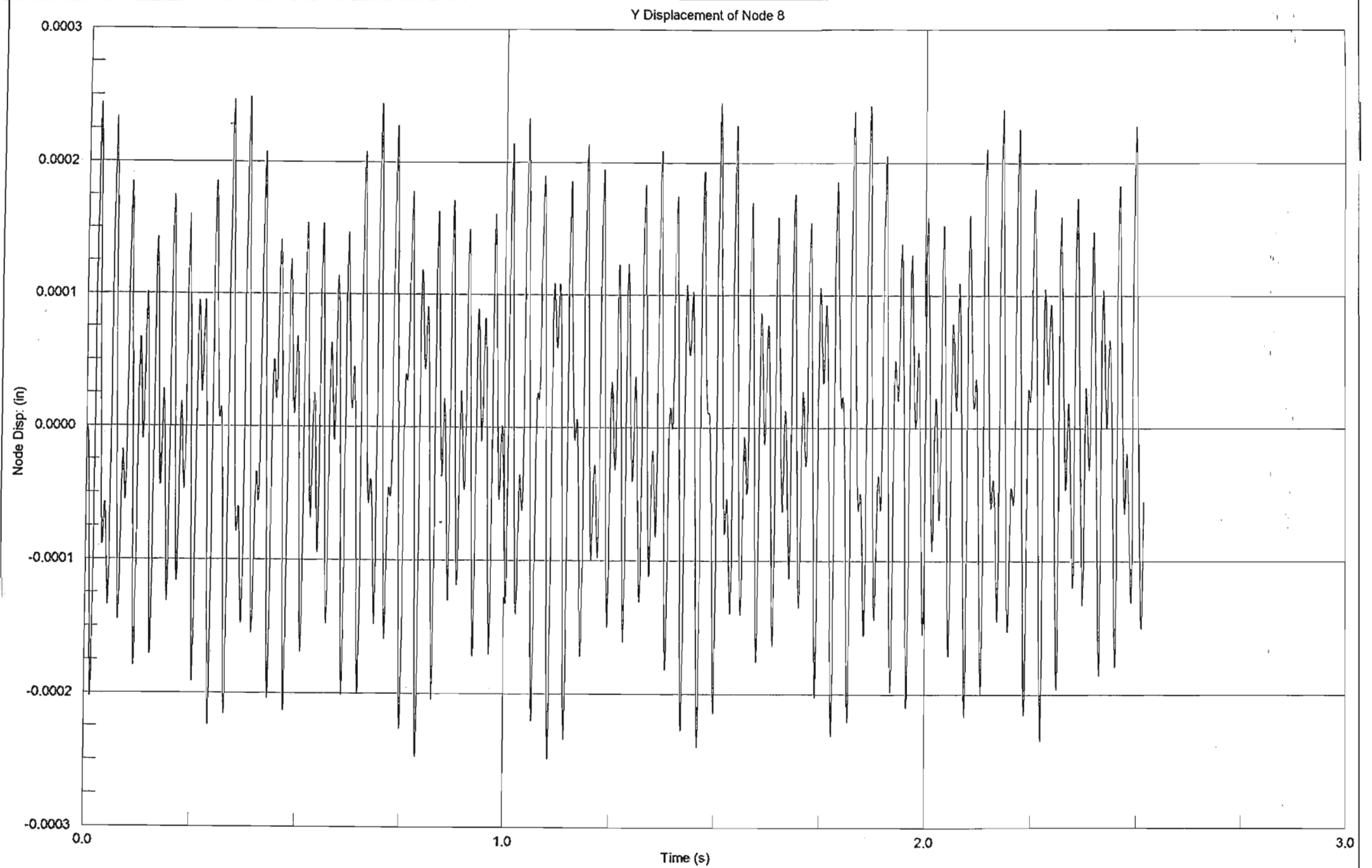




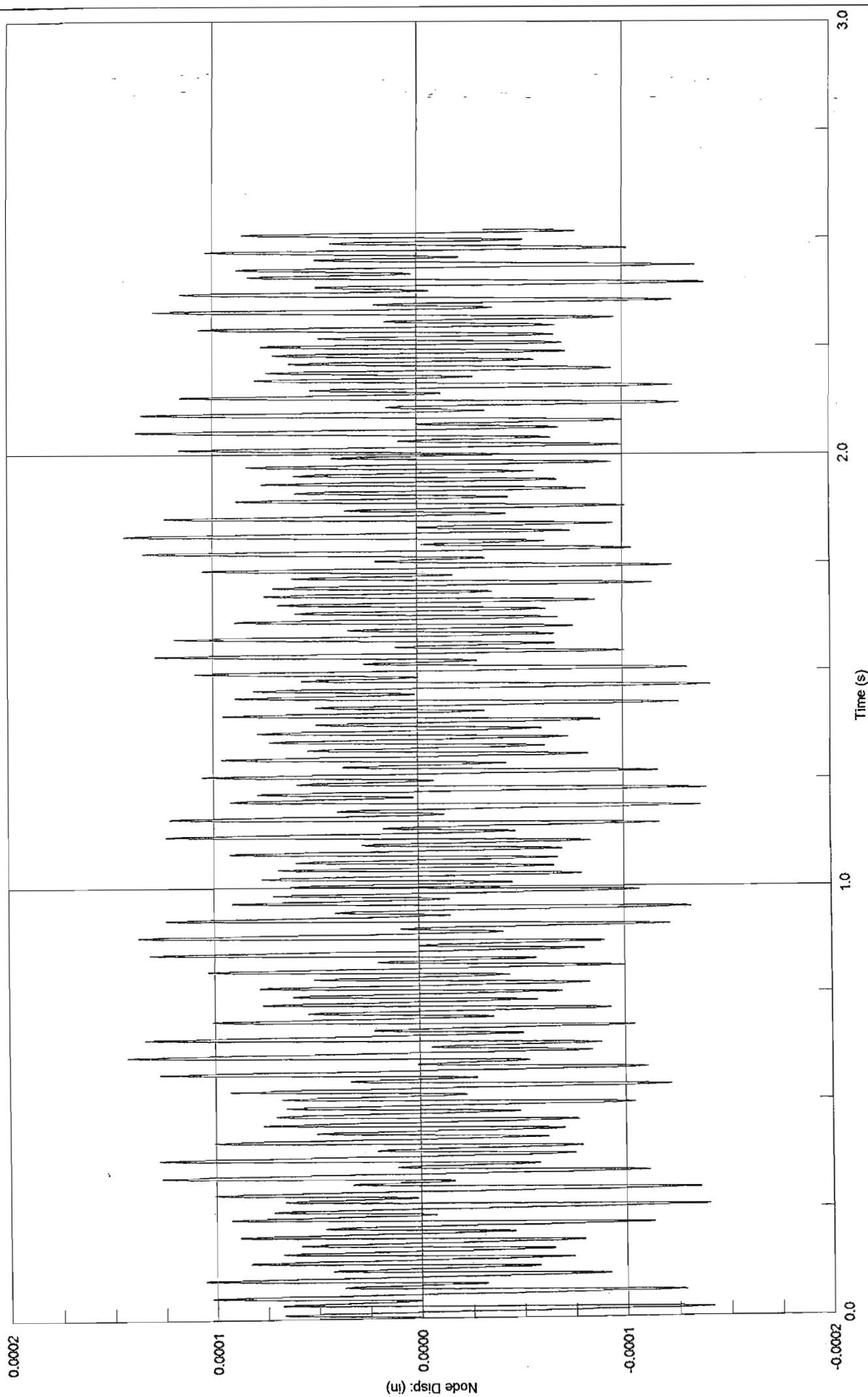








Z displacement of Node 8



DESIGN OF STRUCTURES AND FOUNDATIONS FOR VIBRATING MACHINES

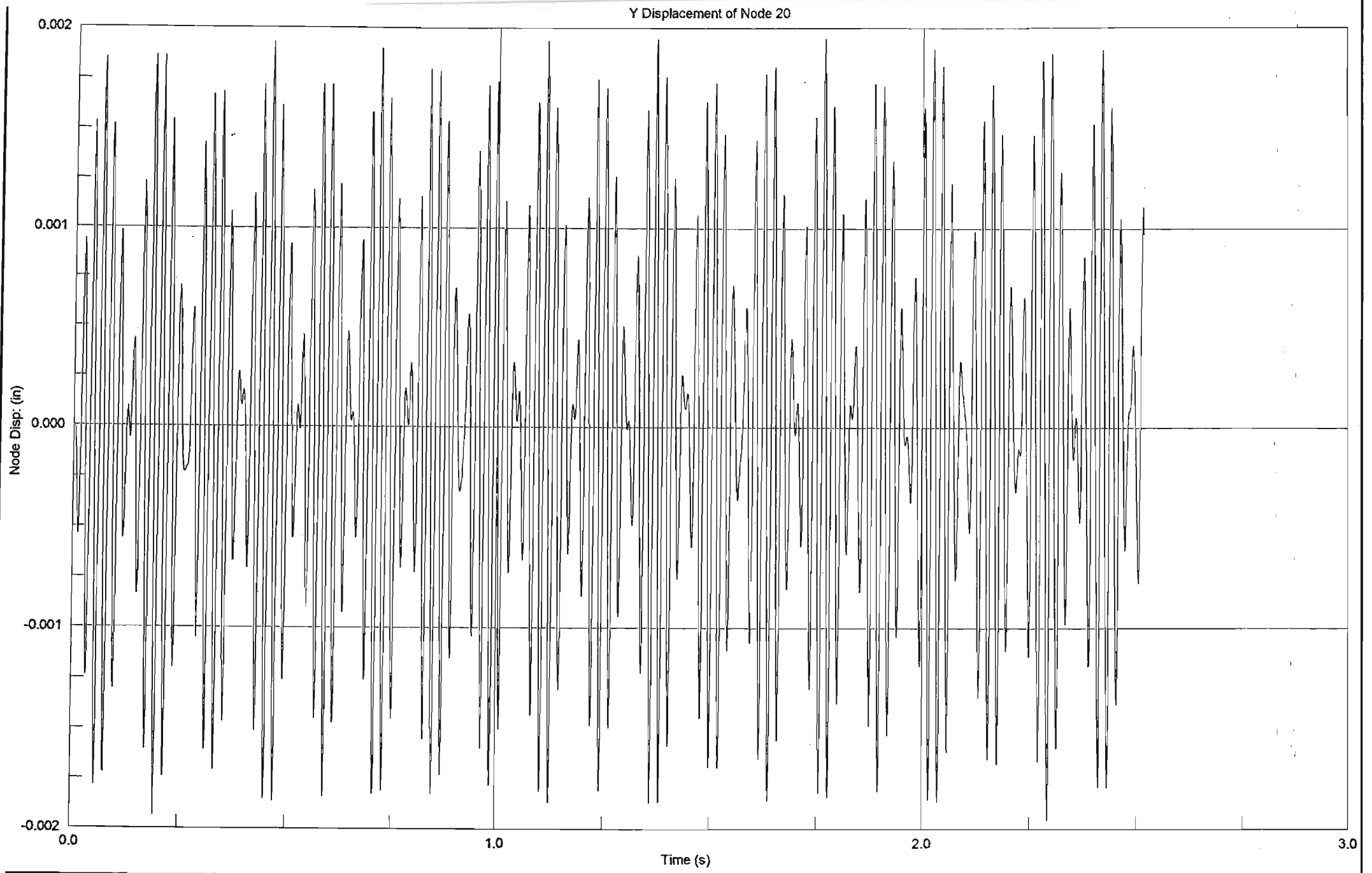
VR ULASSI

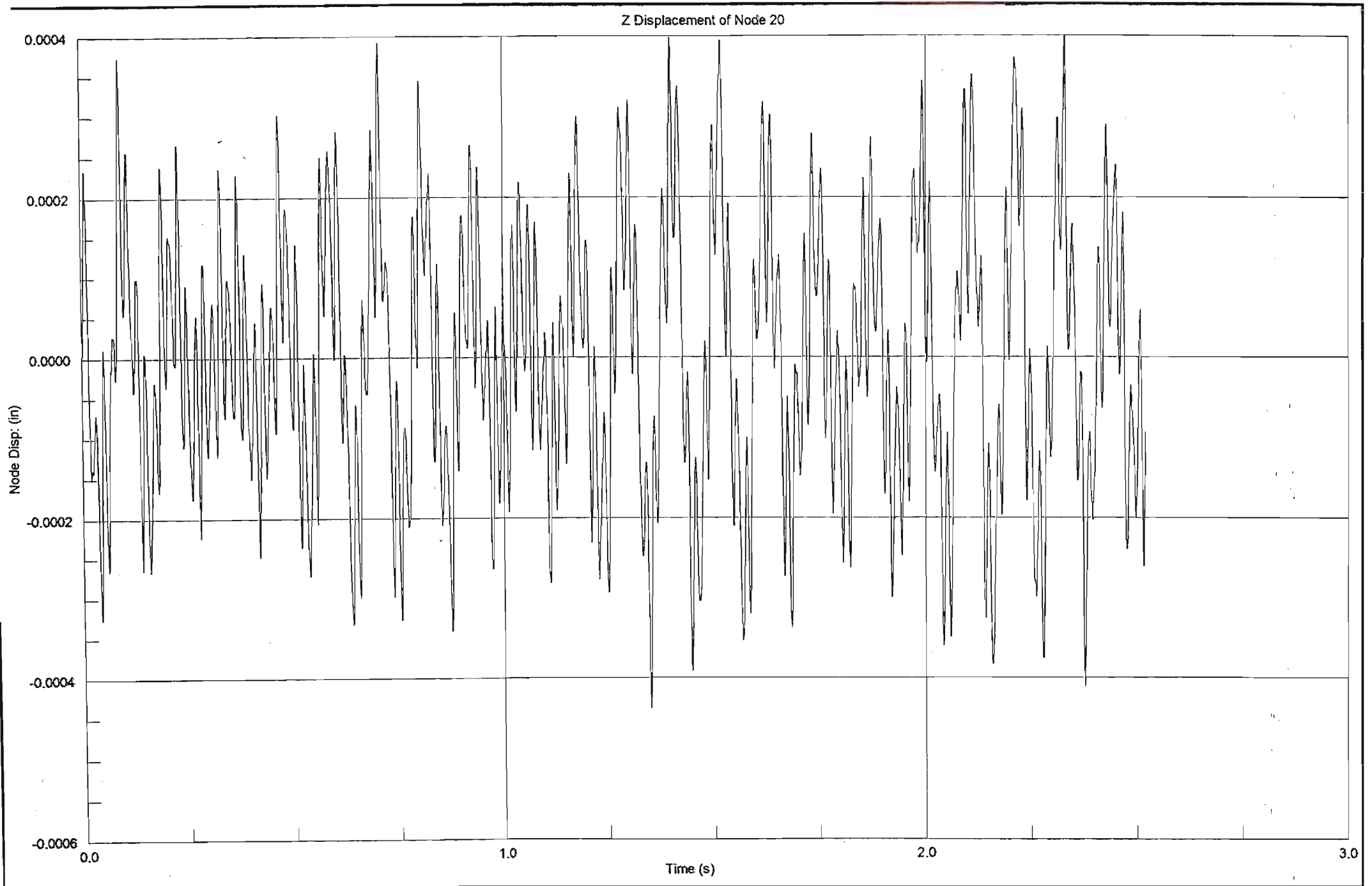
VOLUME 3 OF 4

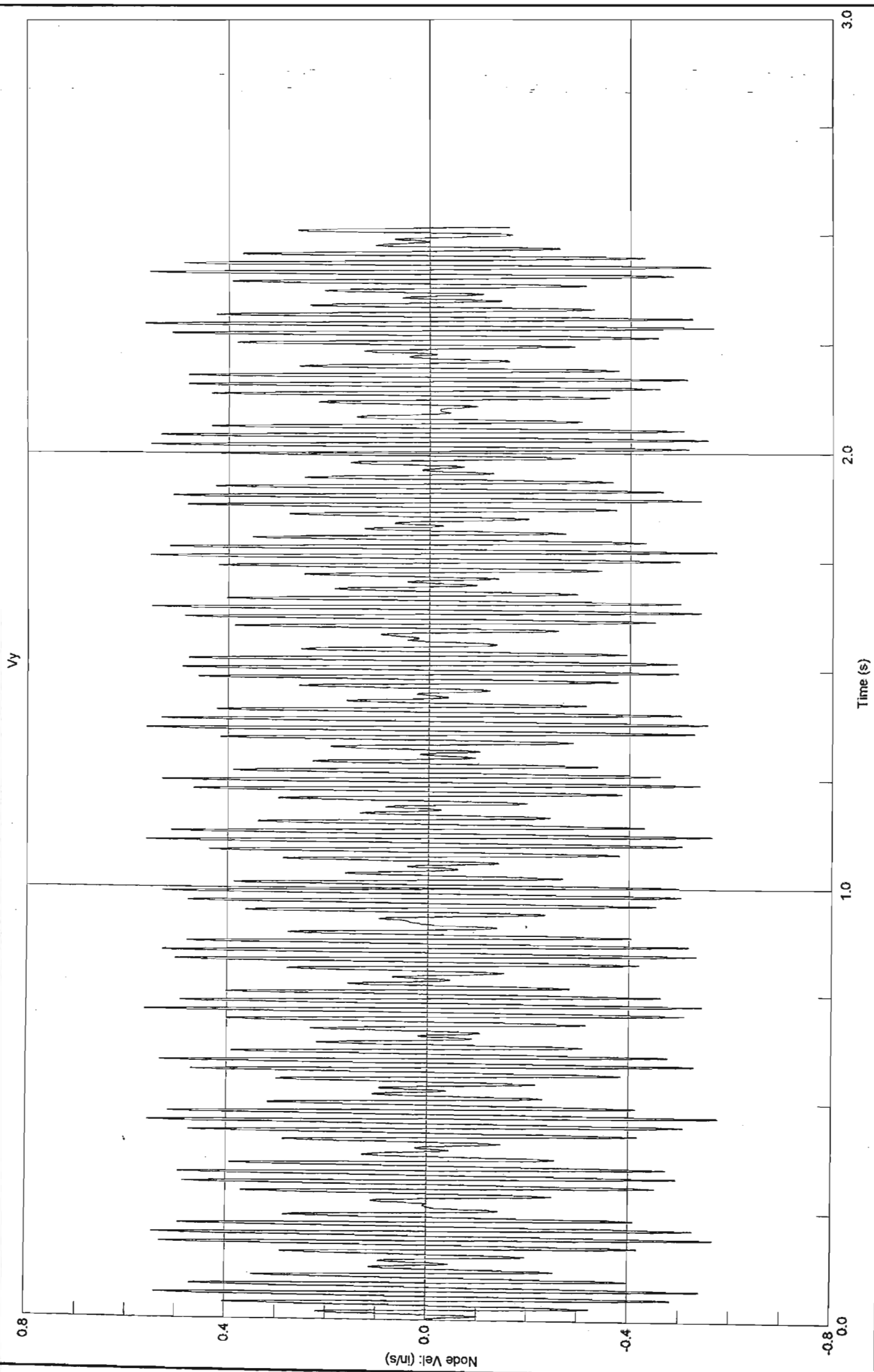
IN PARTIAL FULFILLMENT OF THE DEGREE OF MASTER OF SCIENCE IN
ENGINEERING (COURSEWORK) COMPRISING 72 CREDITS OF 144 FOR THE
DEGREE

DATE SUBMITTED: 13 DECEMBER 2002

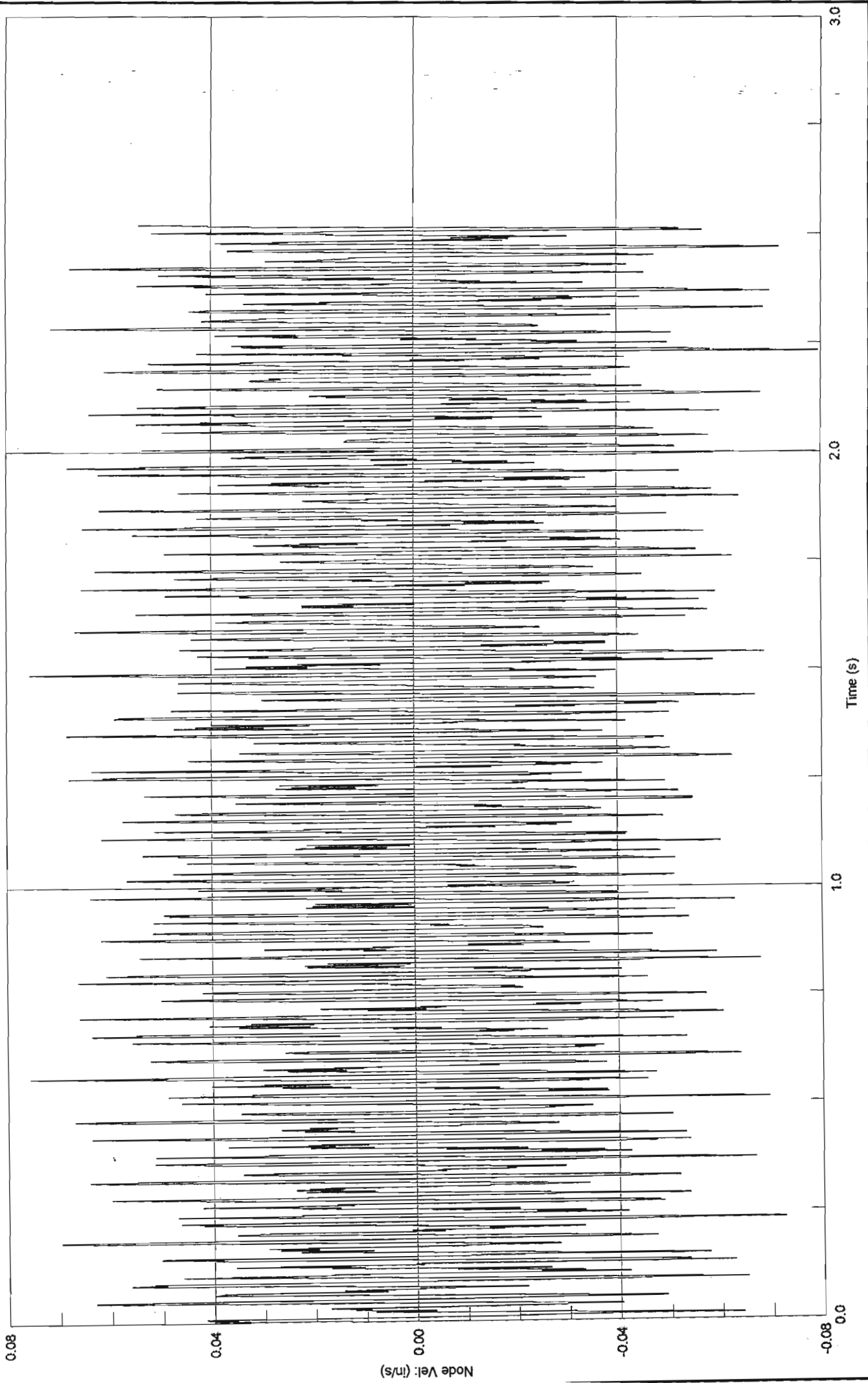
SUPERVISOR: PROFESSOR H D SCHREINER

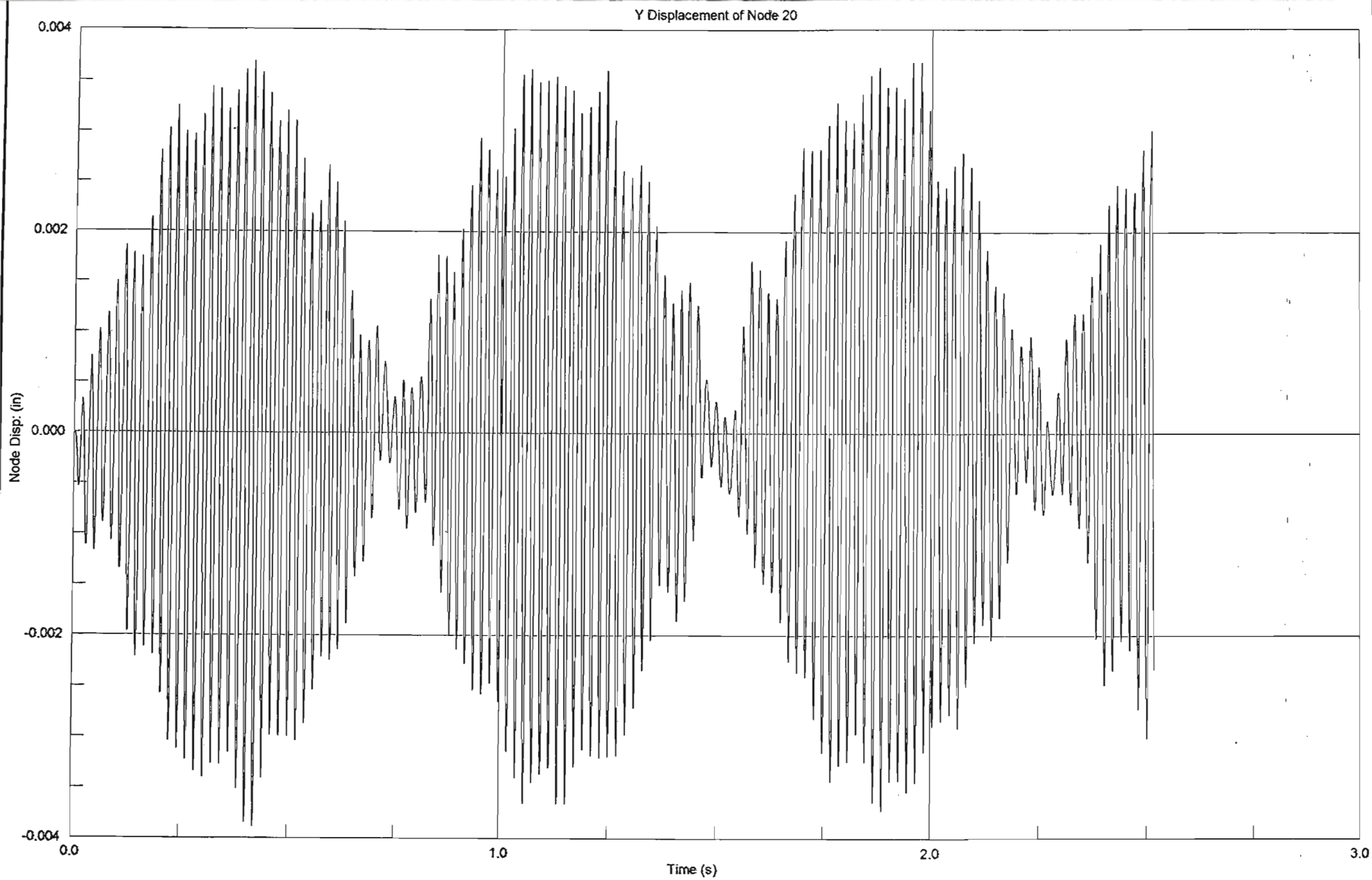




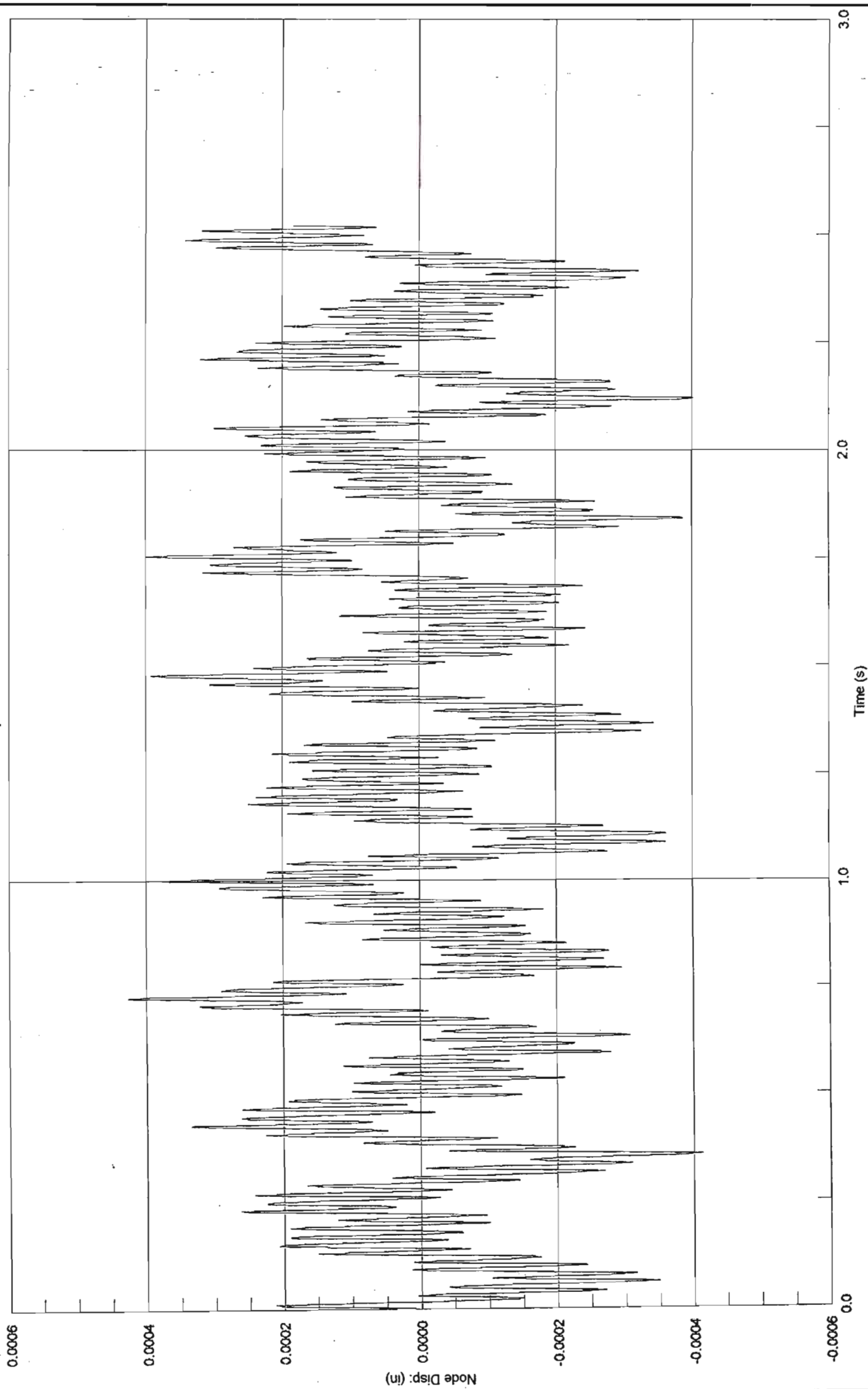


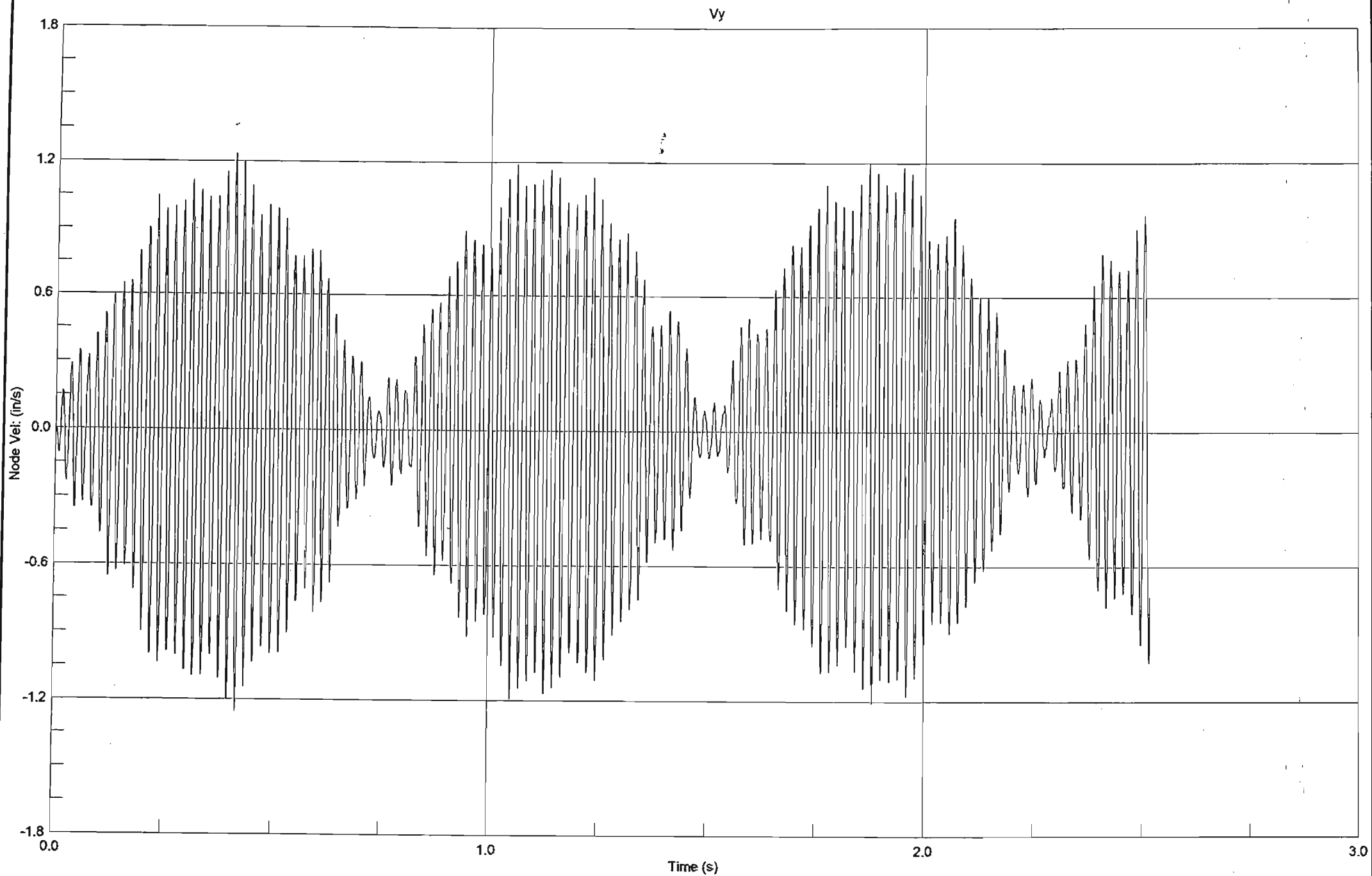
Vz

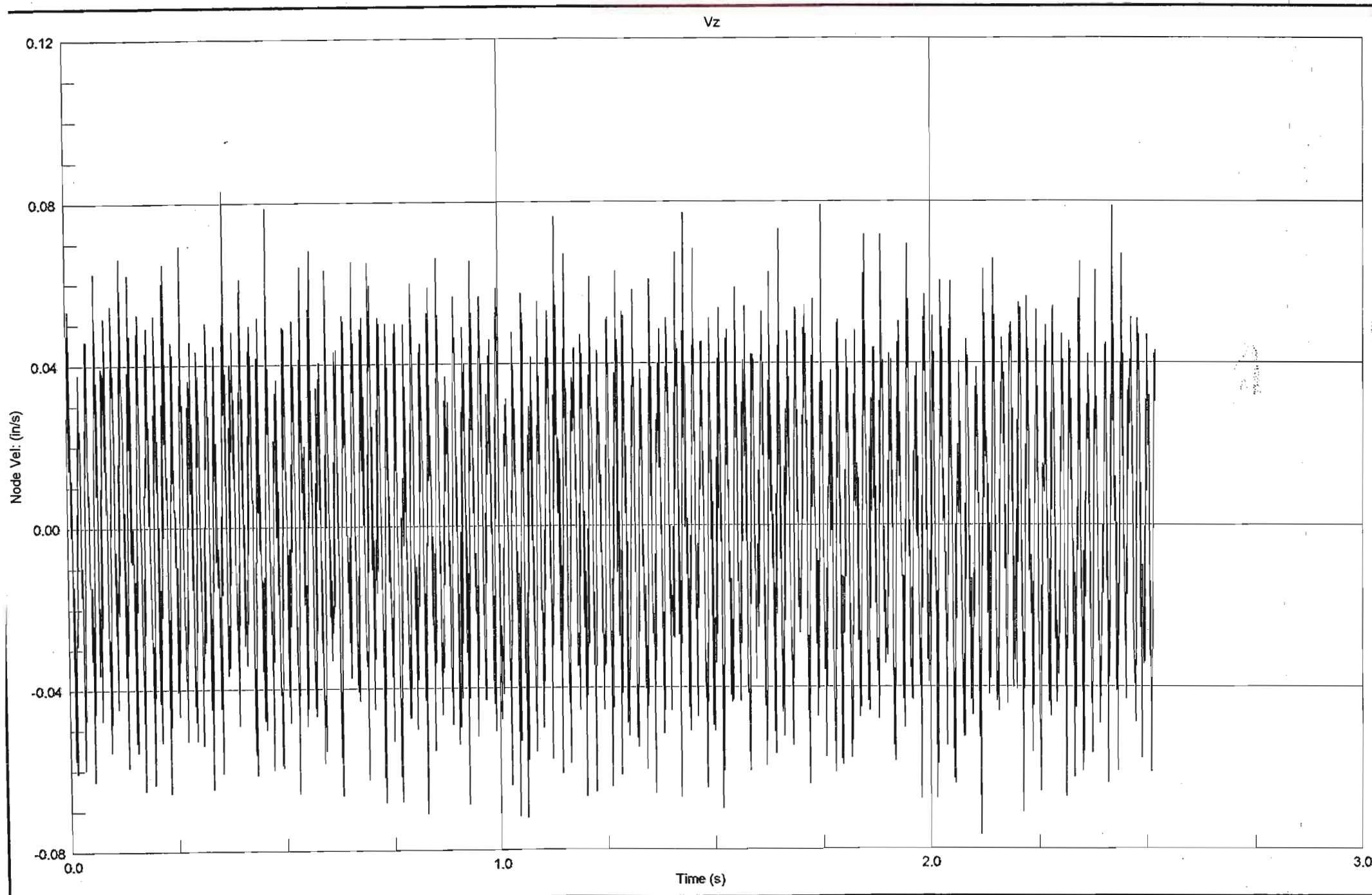


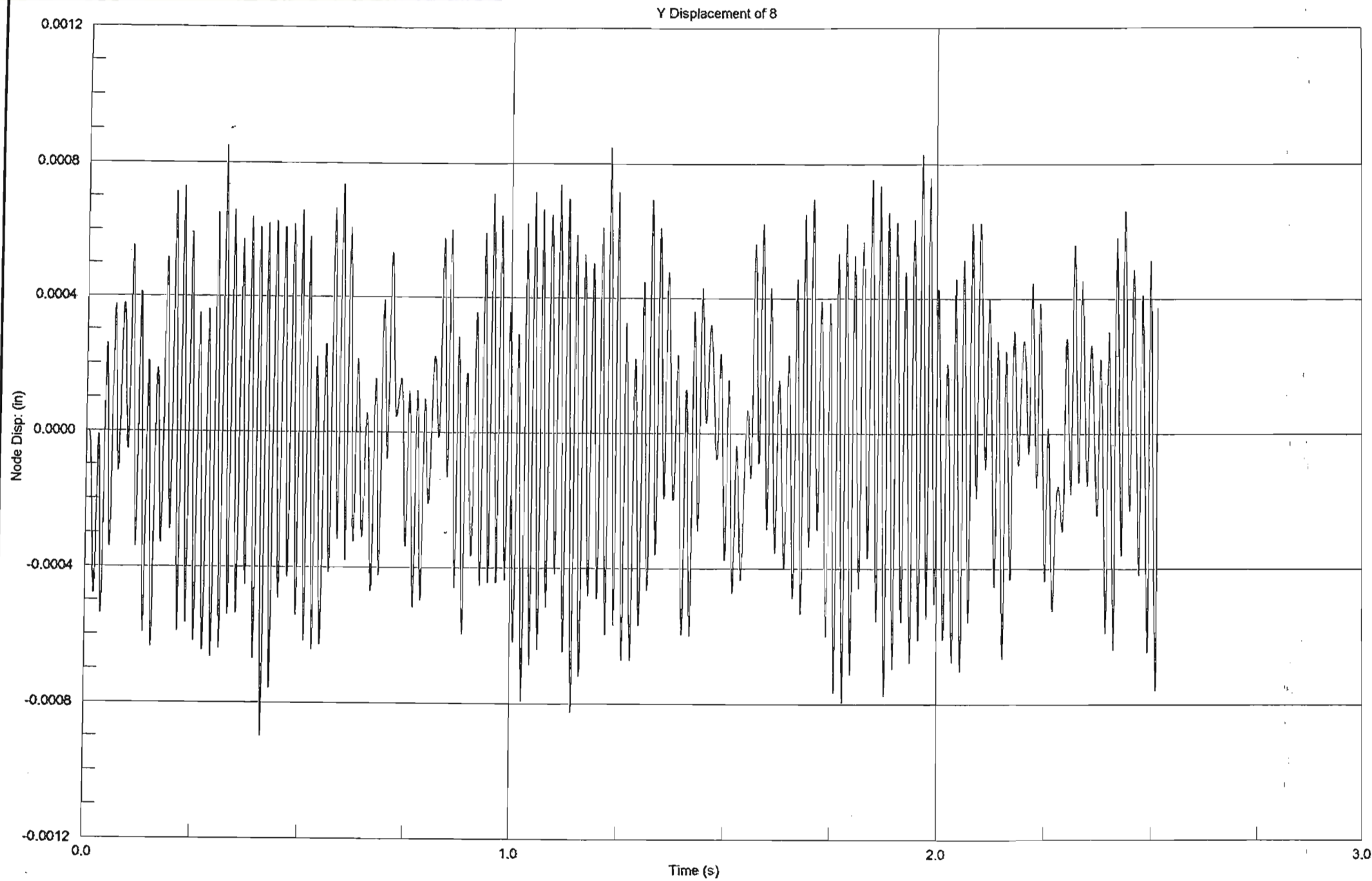


Z Displacement of Node 20

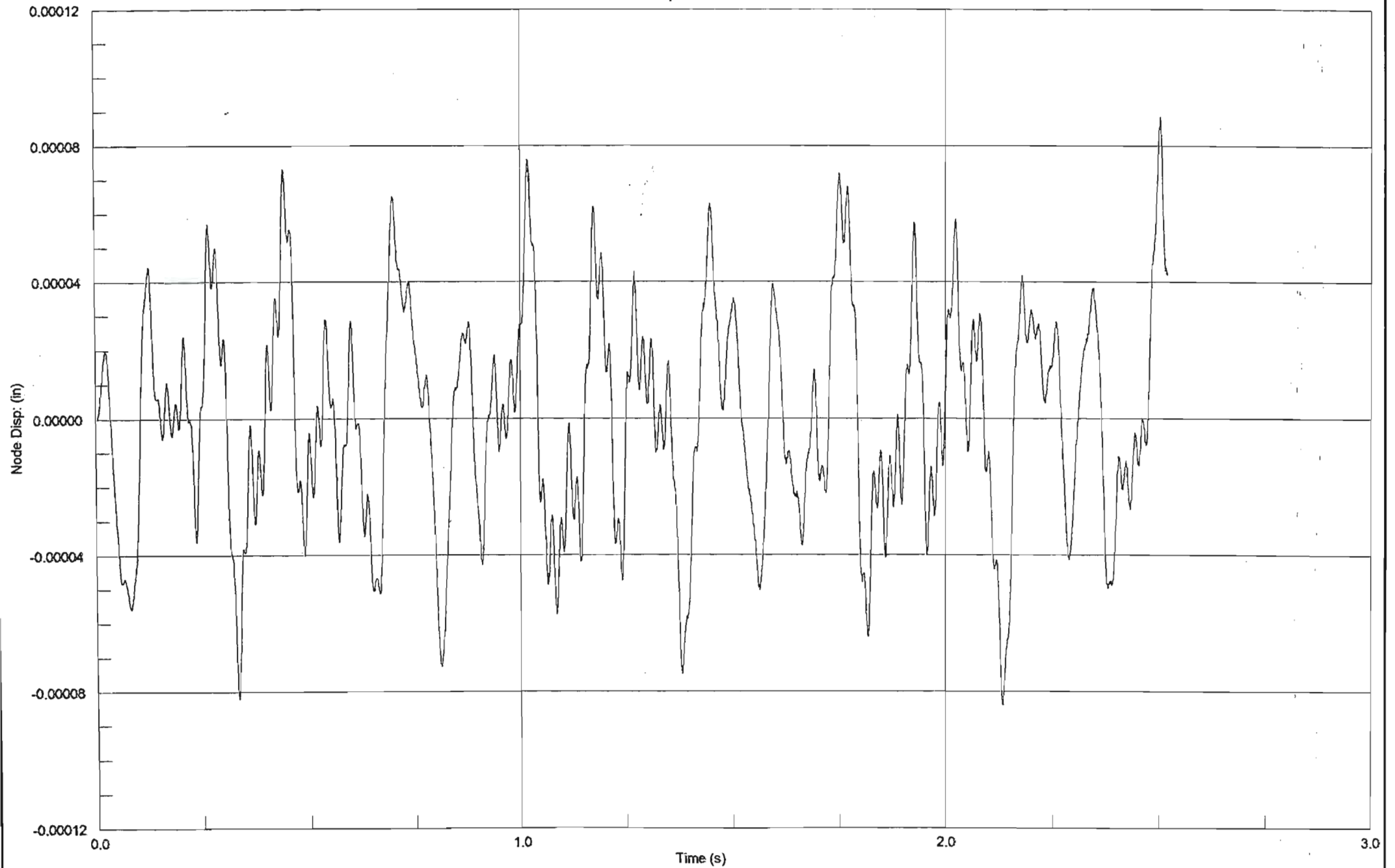




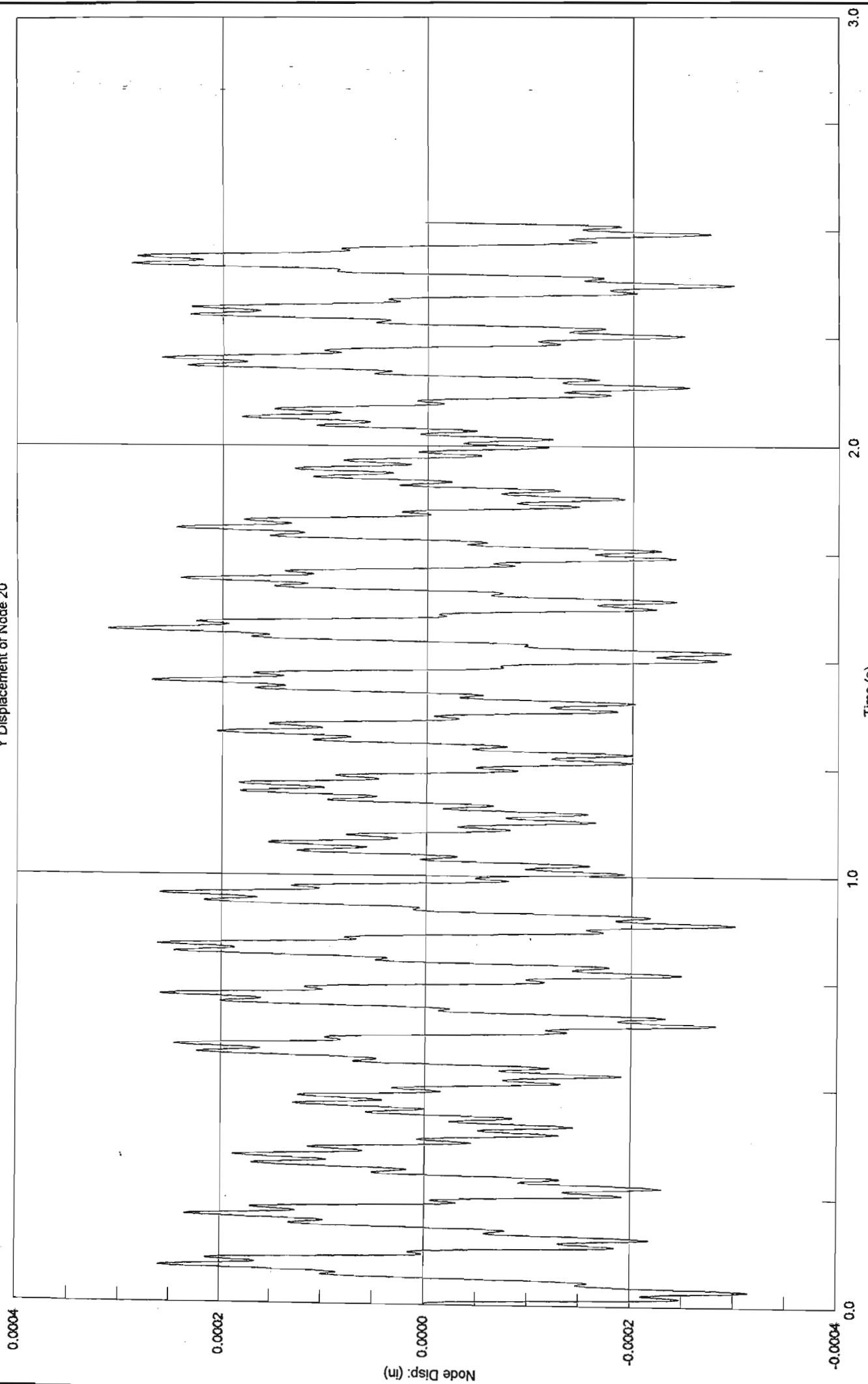




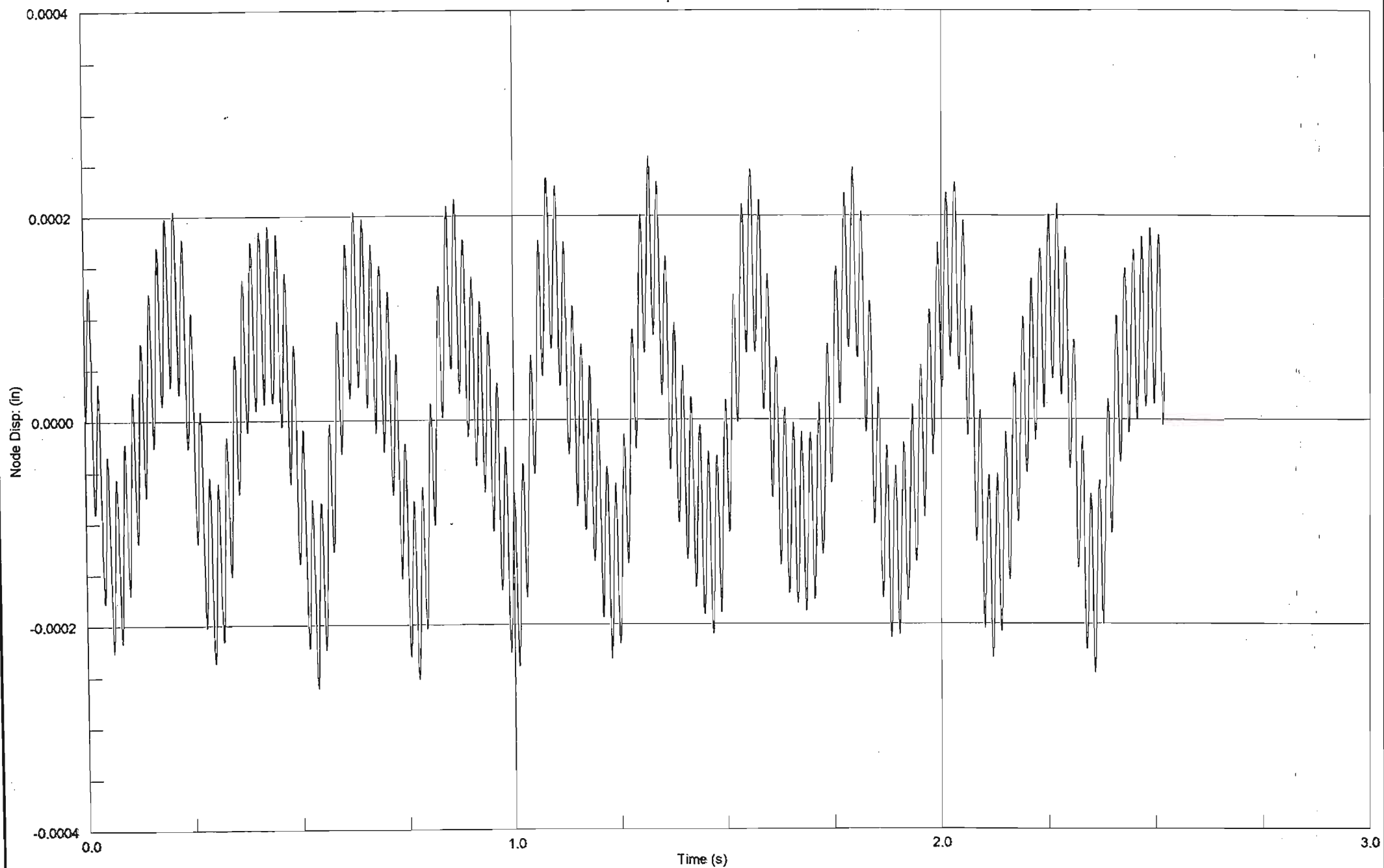
Z Displacement of Node 8

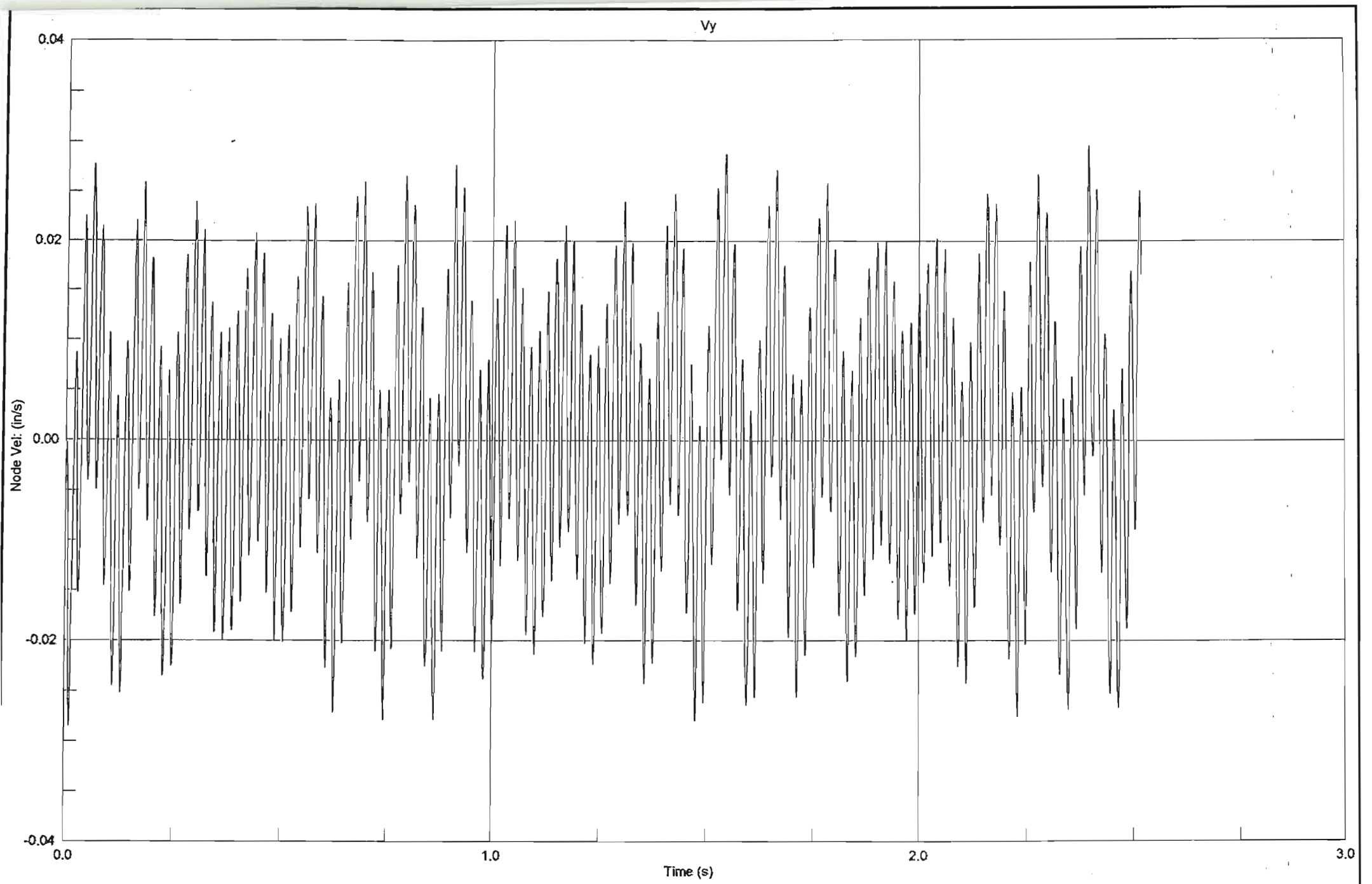


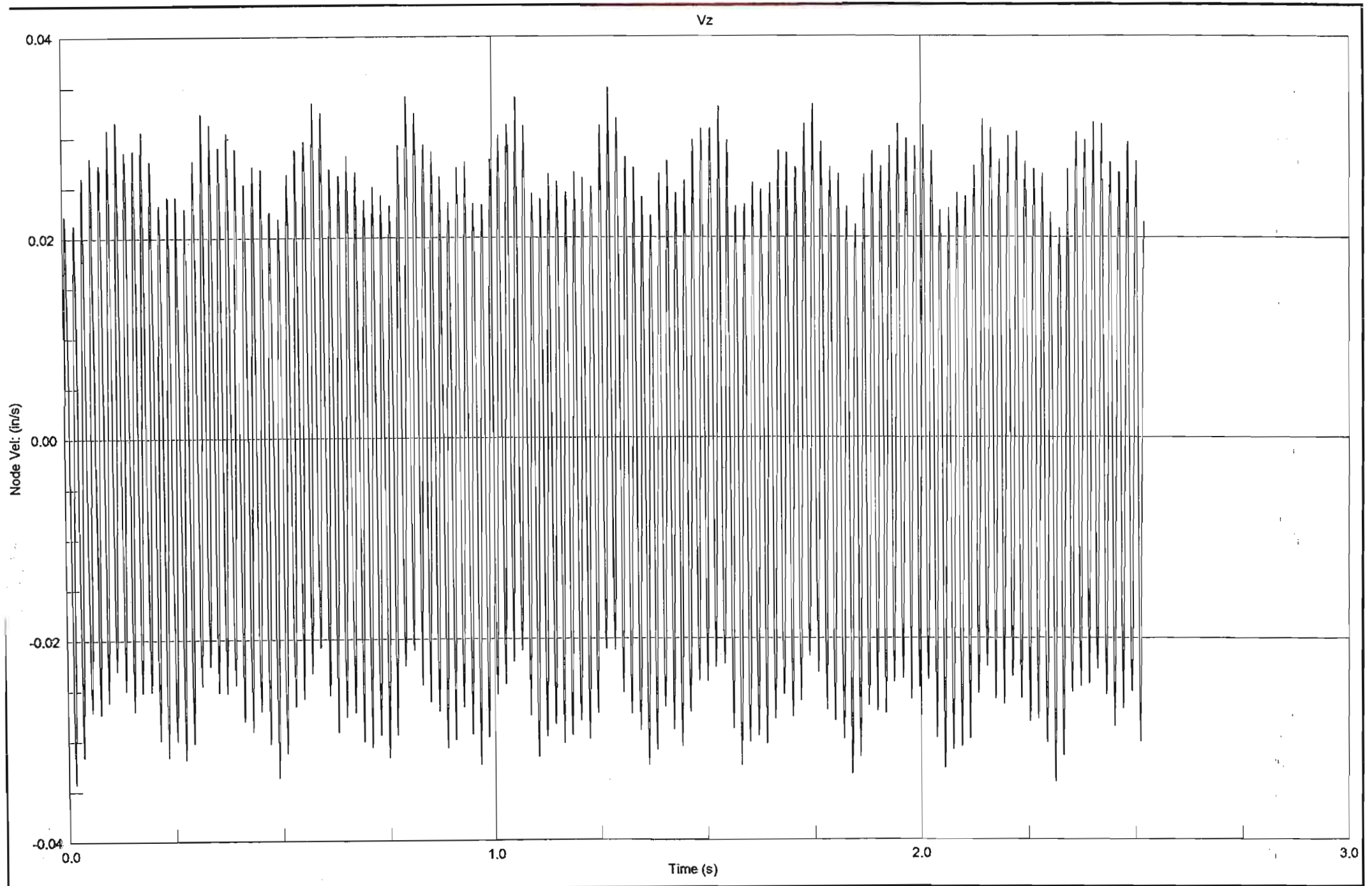
Y Displacement of Node 20

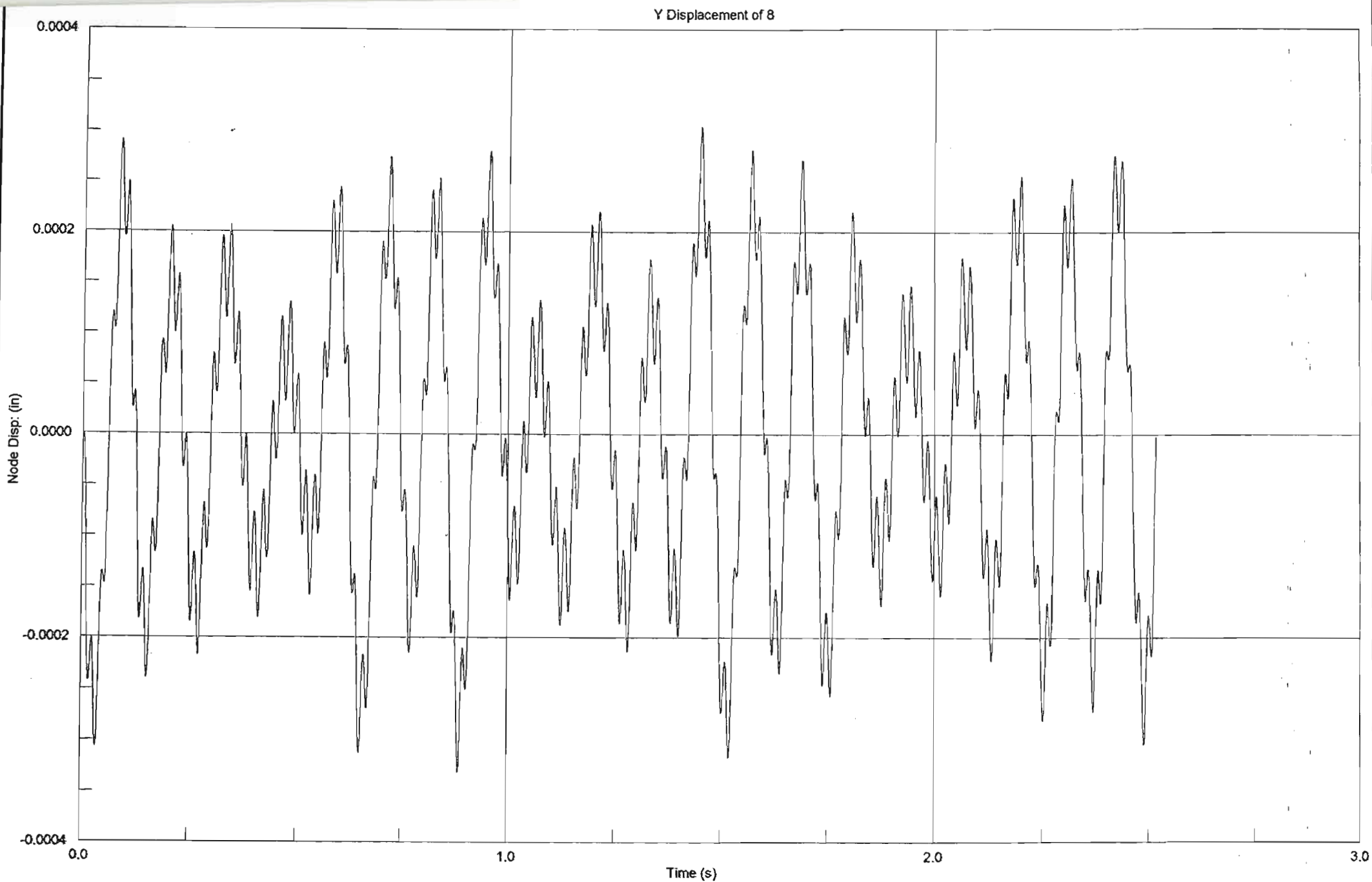


Z Displacement of Node 20

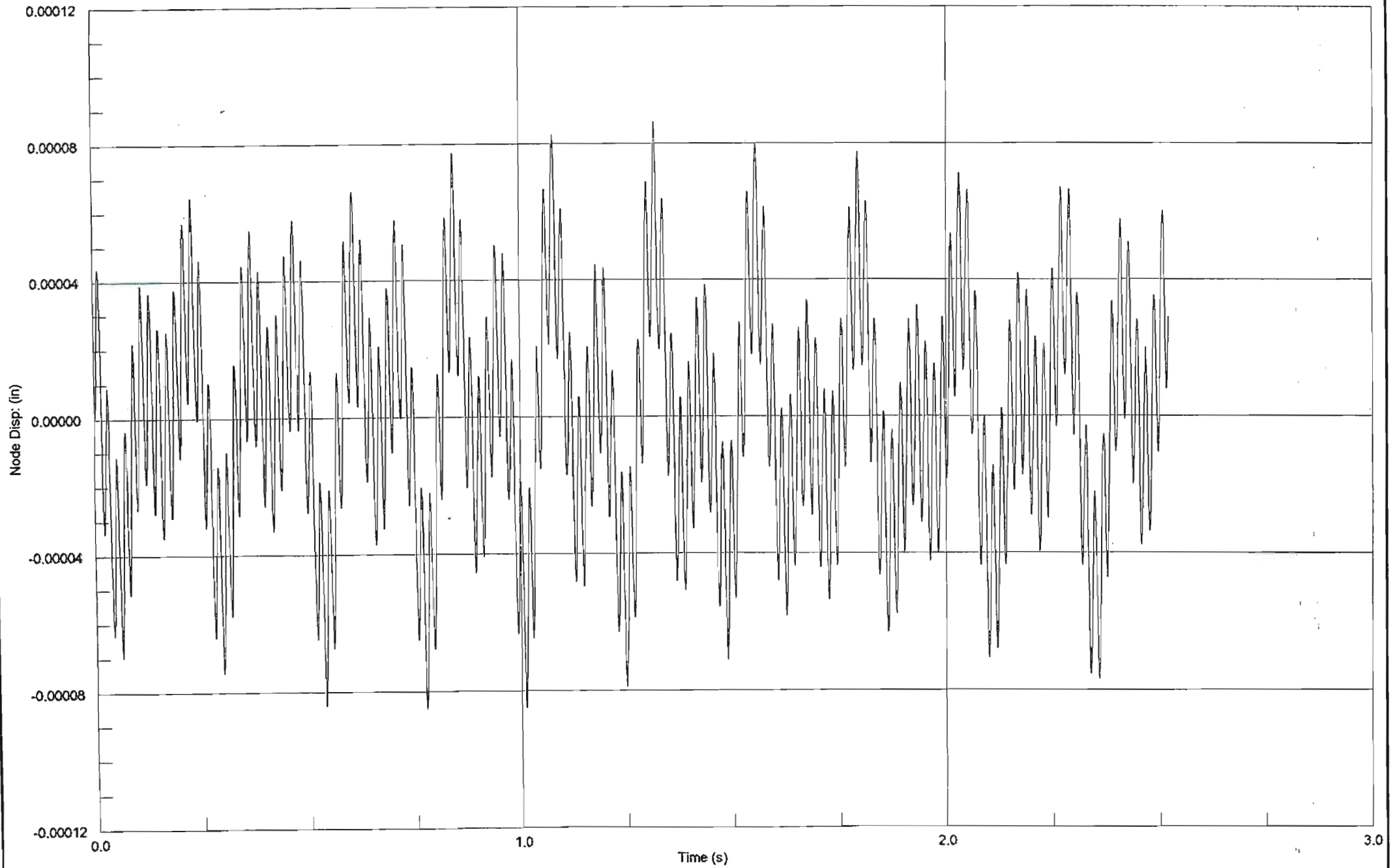


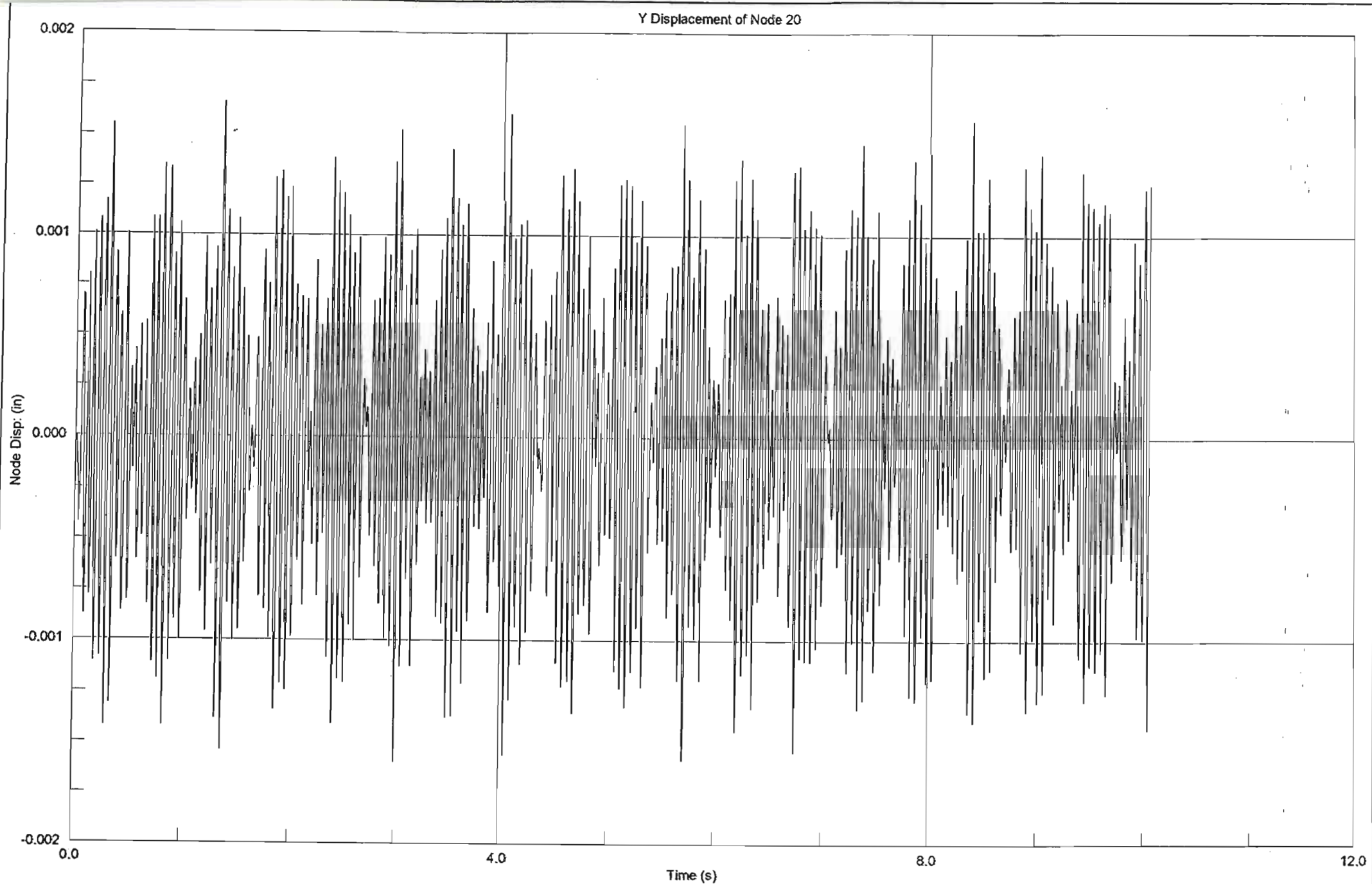


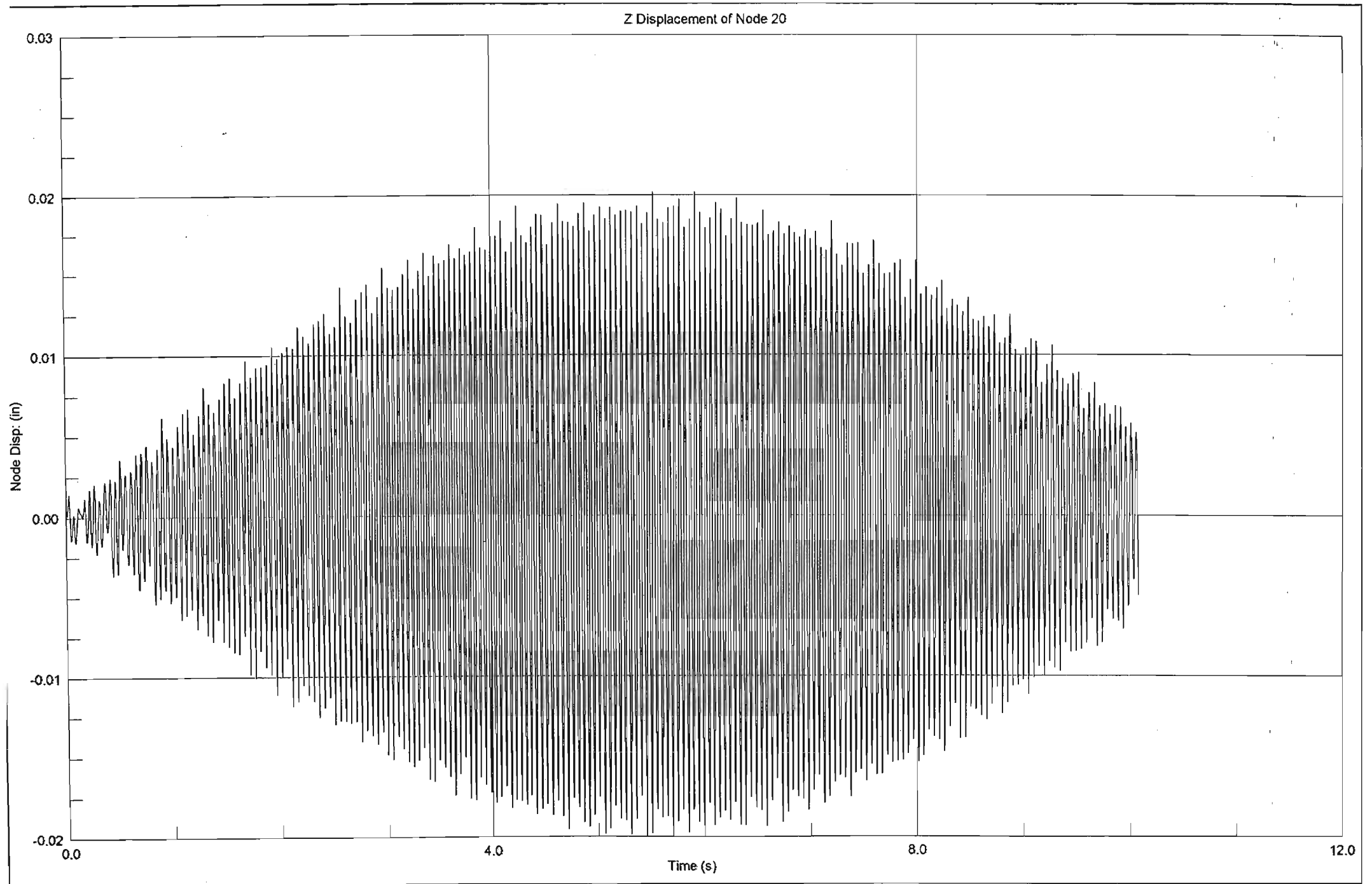


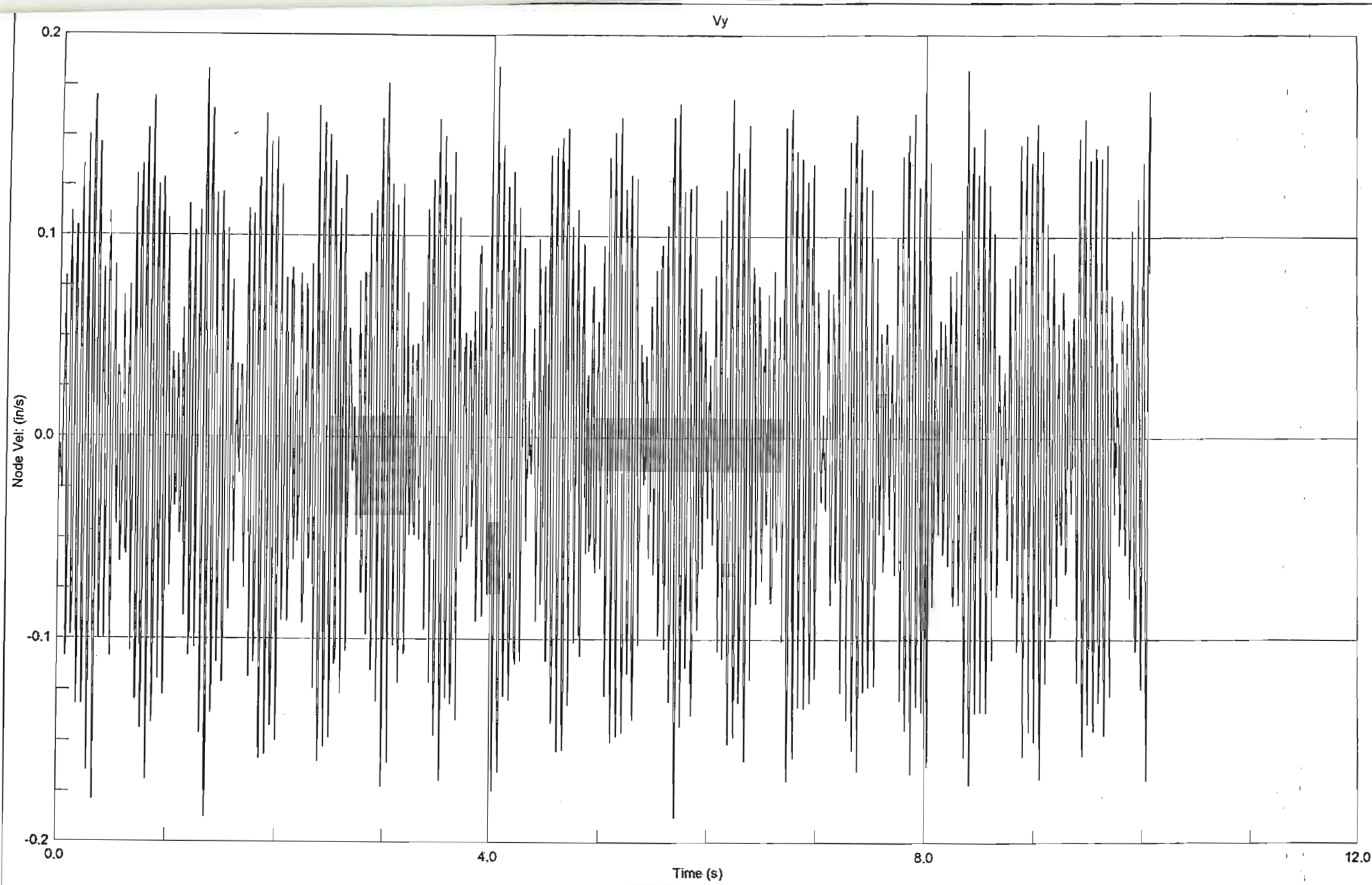


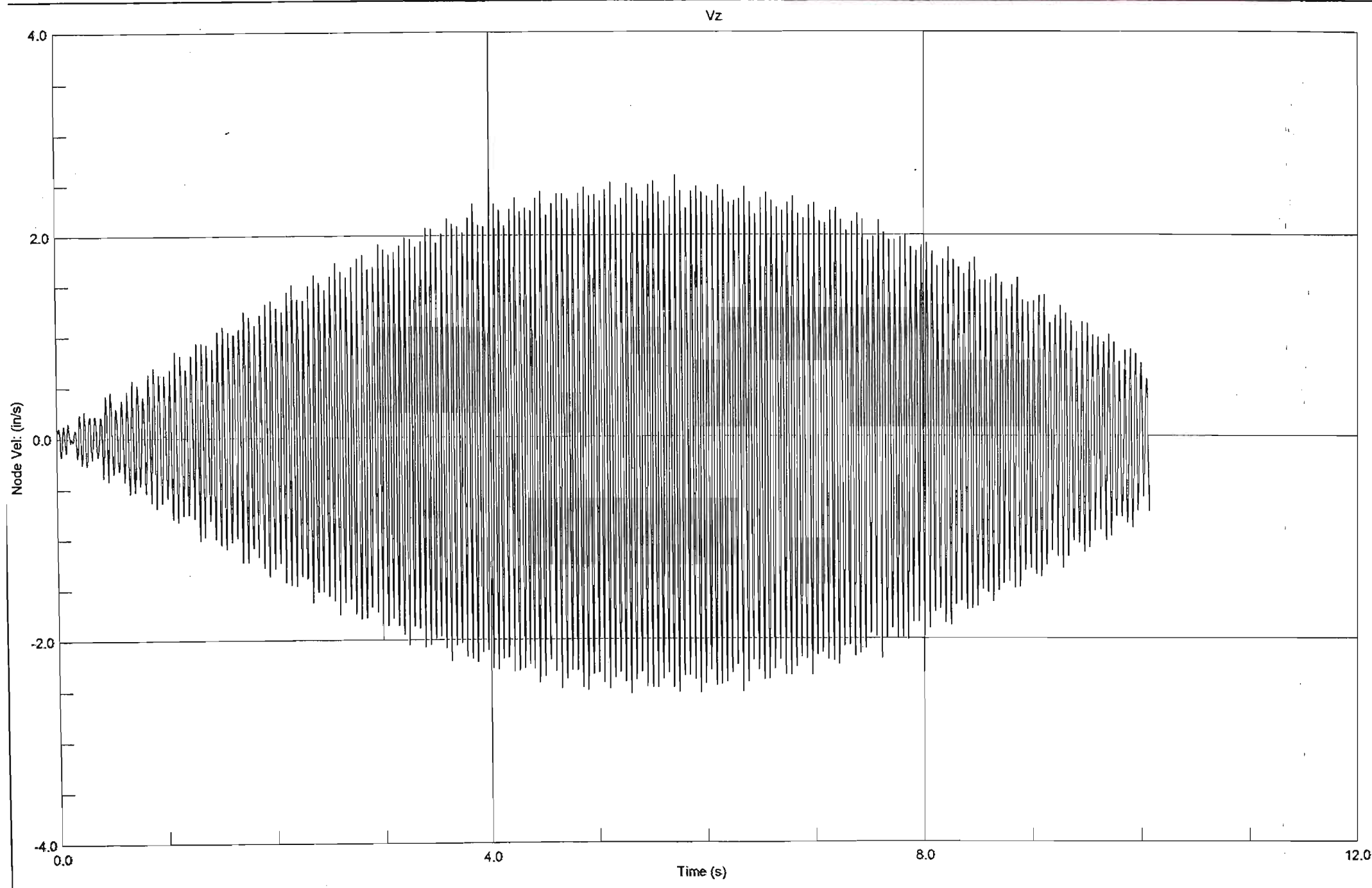
Z Displacement of Node 8









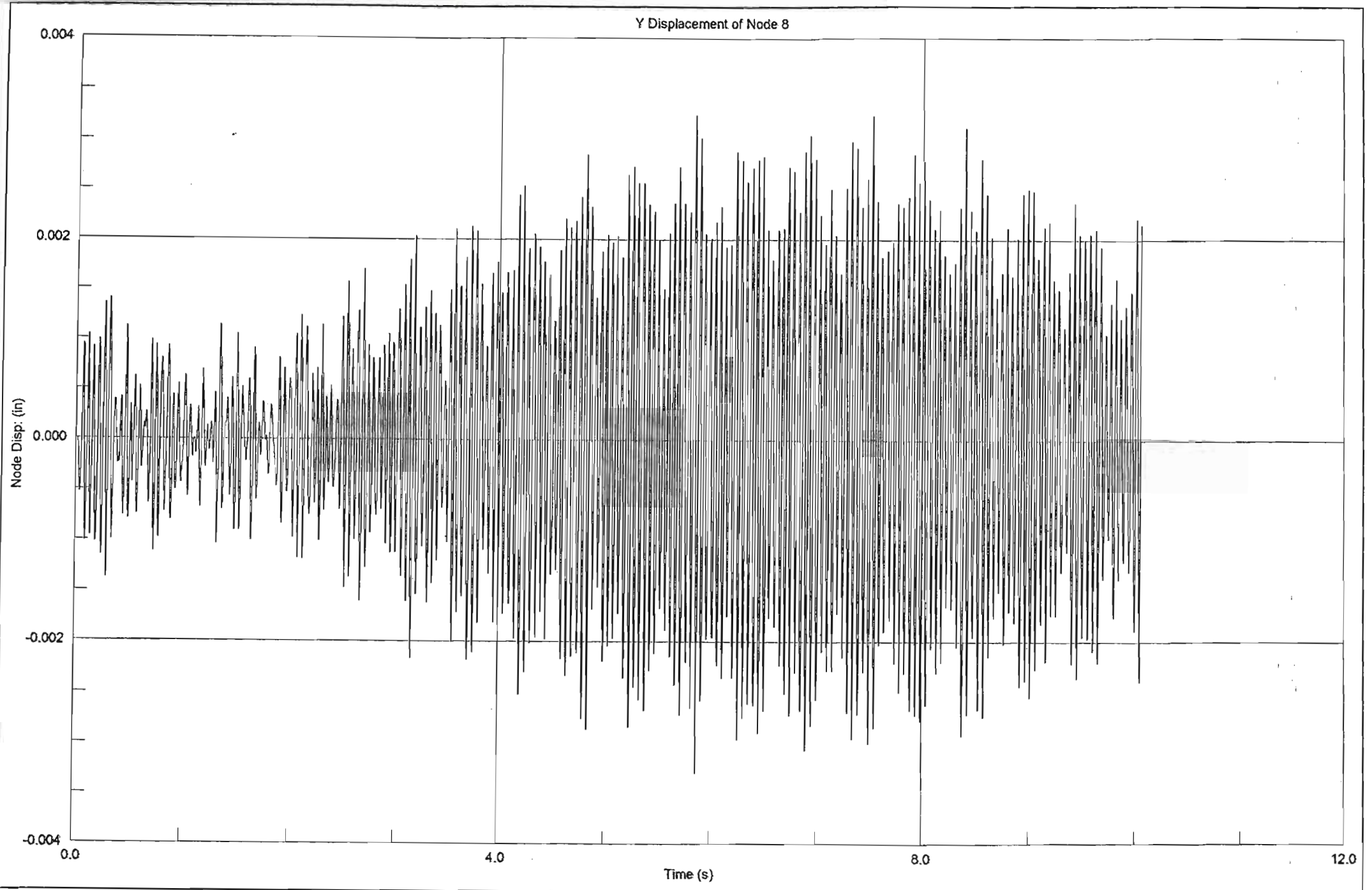


Strand7 Release 2.1.7

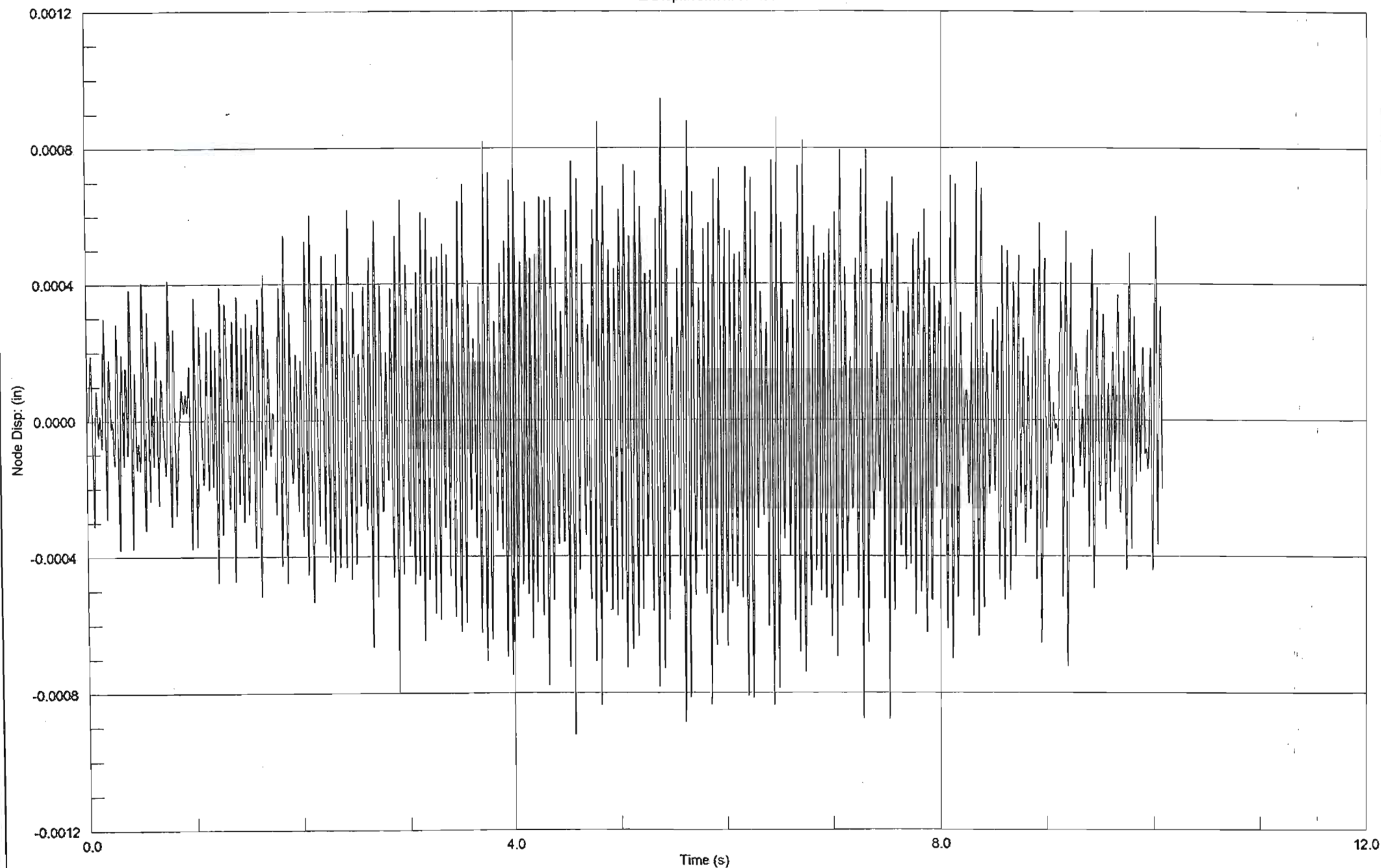
C:\MSc Eng\Table Top\1\table top G10000.s17

12 October 2002 12:42 pm

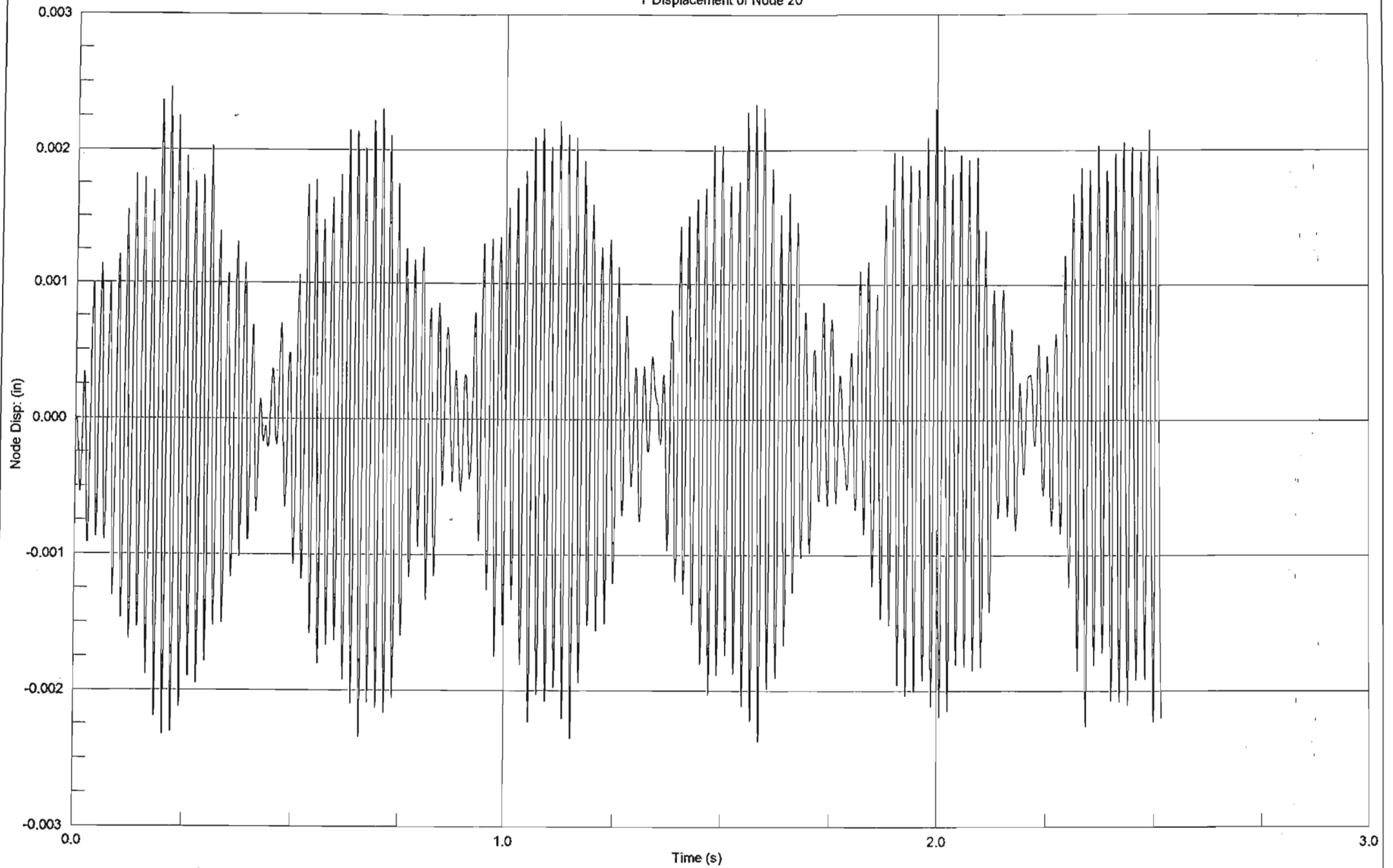
C2.4



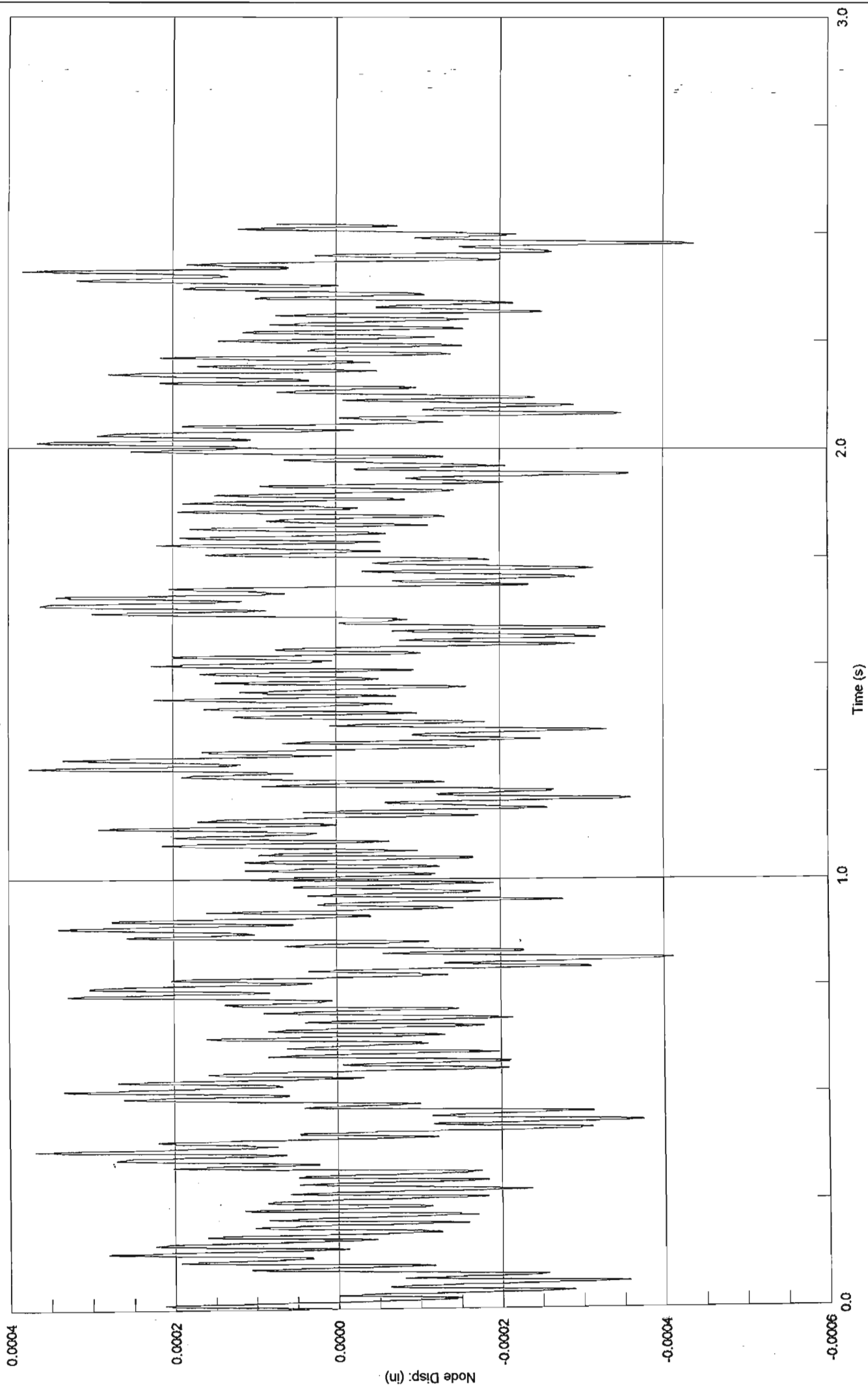
Z Displacement of Node 8

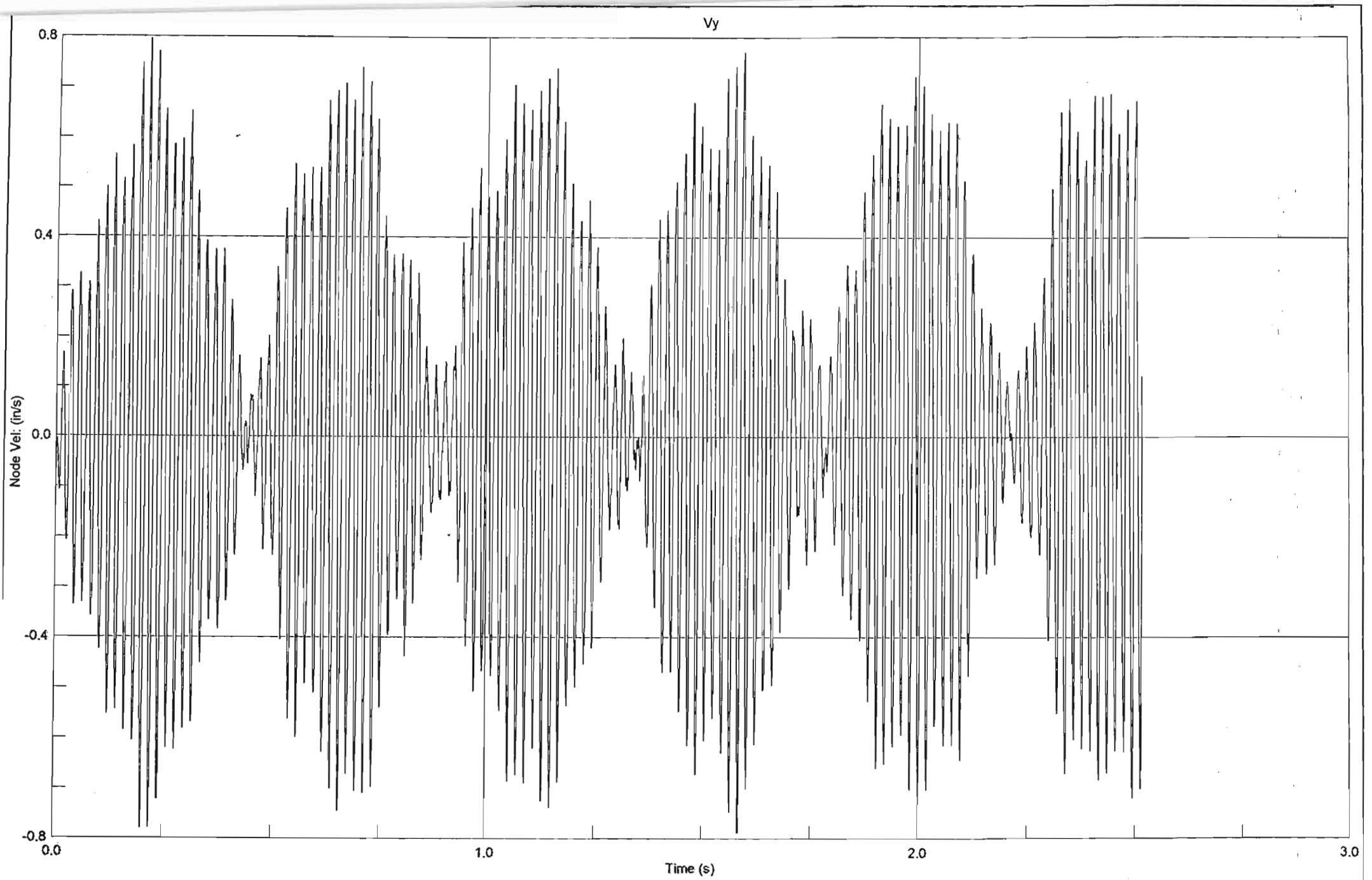


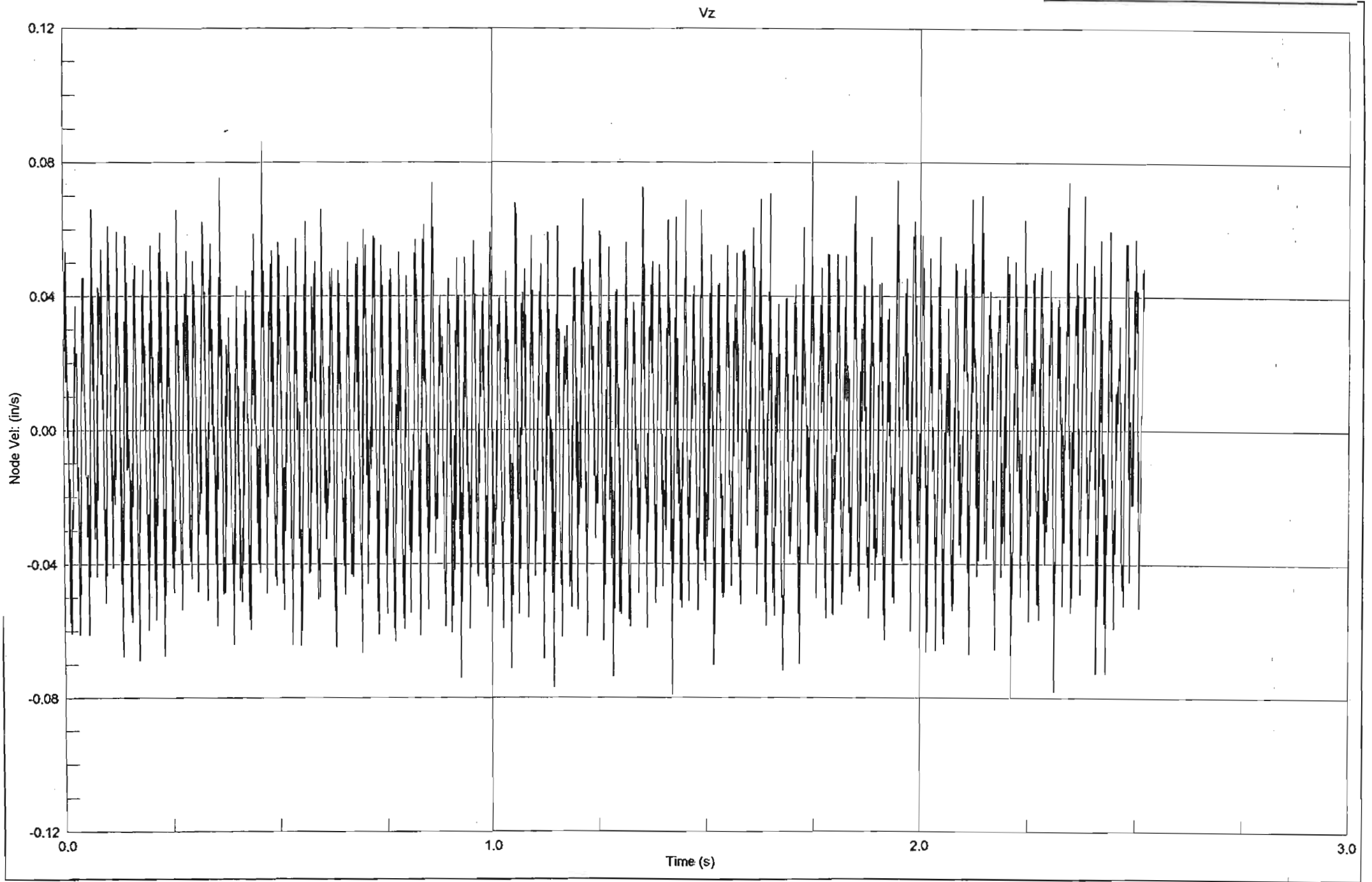
Y Displacement of Node 20

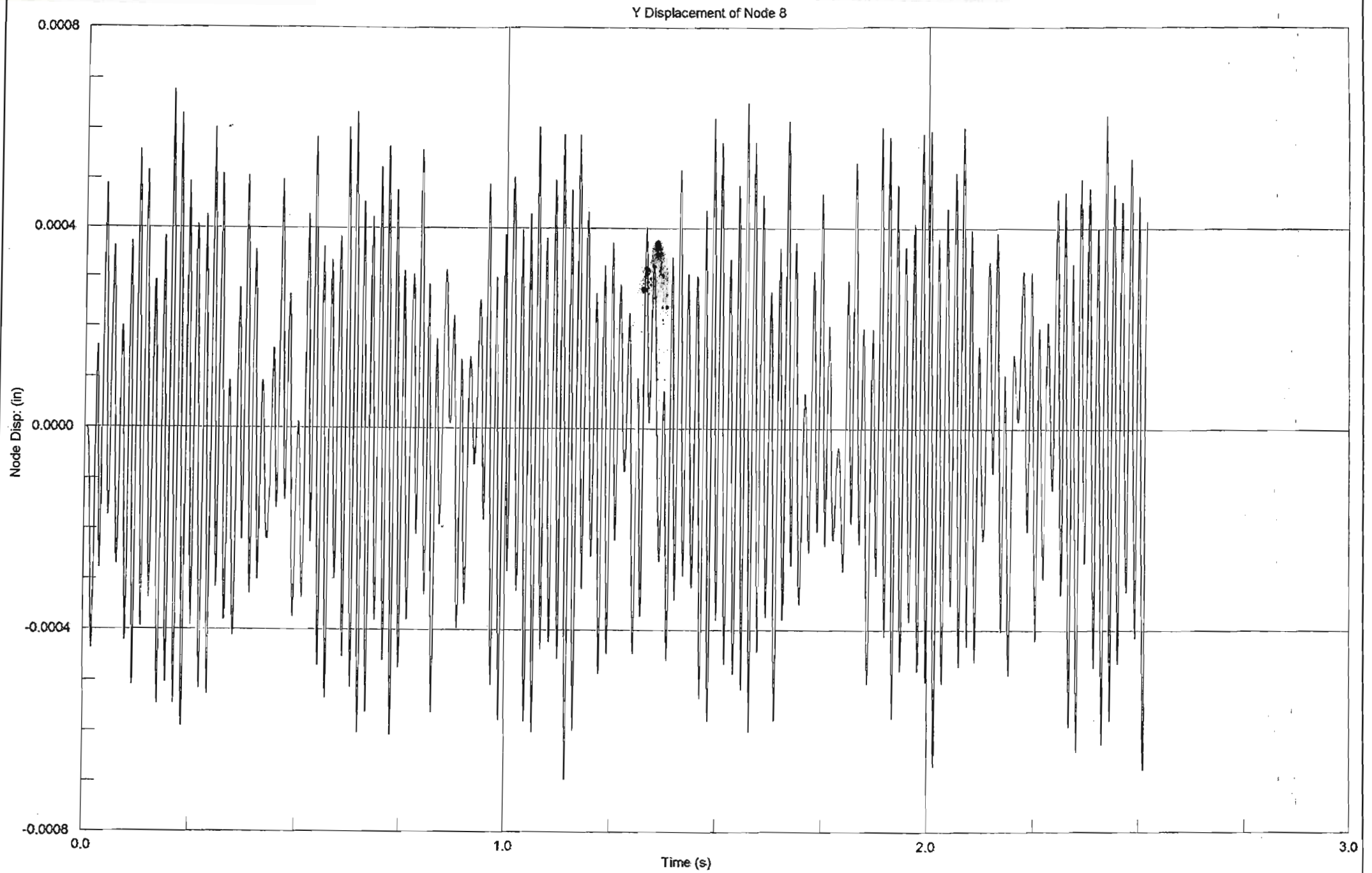


Z Displacement of Node 20

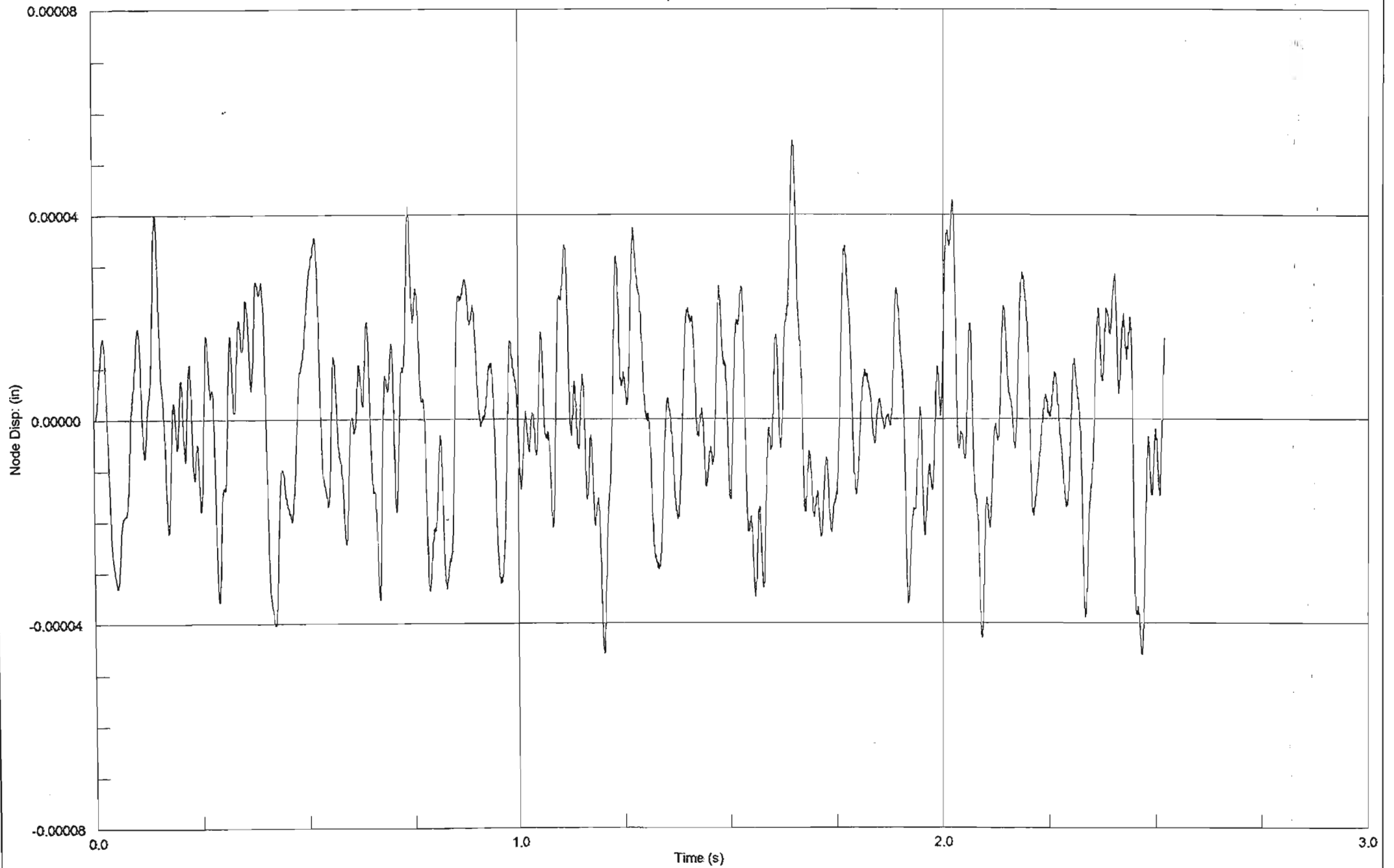


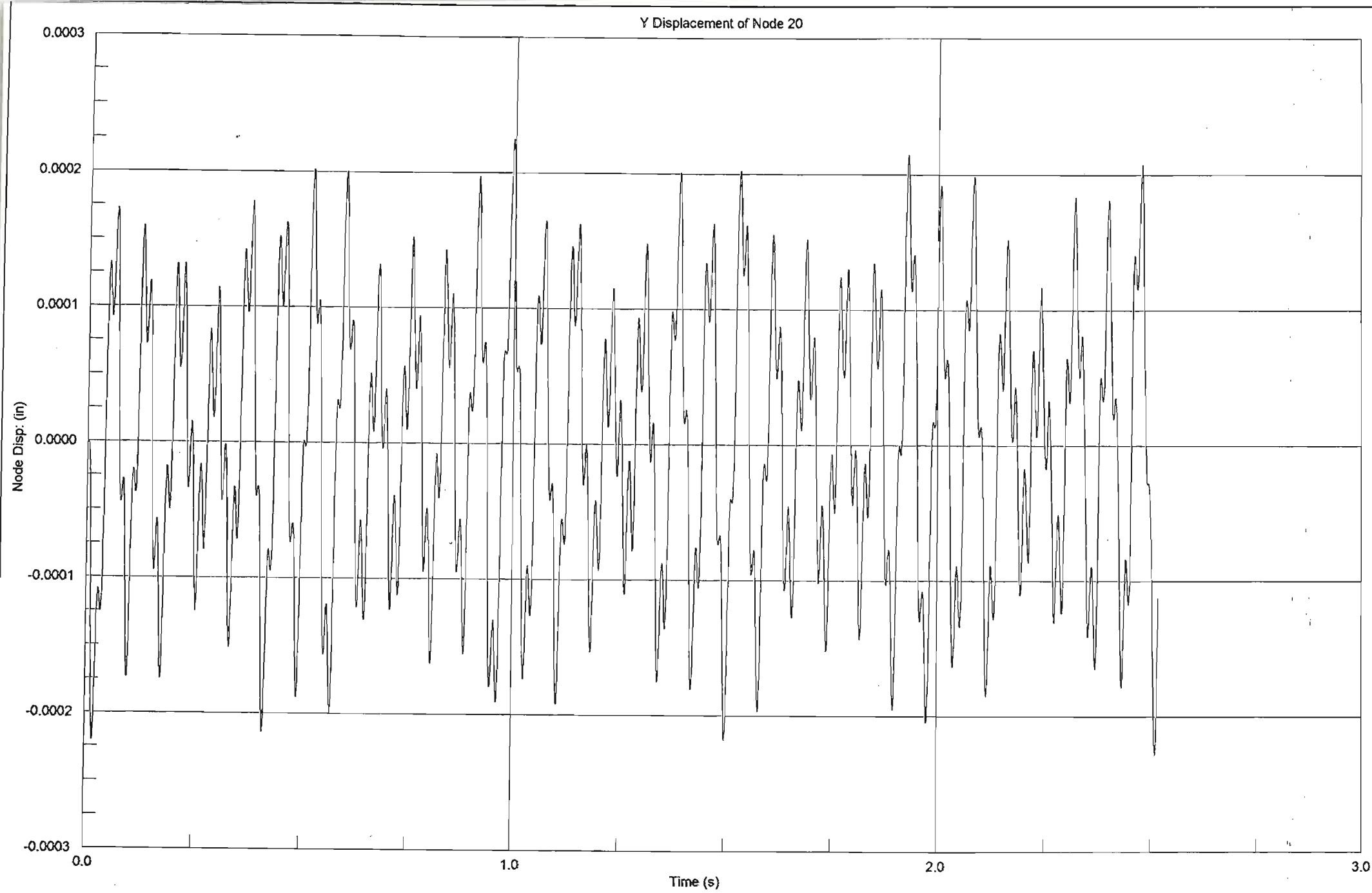


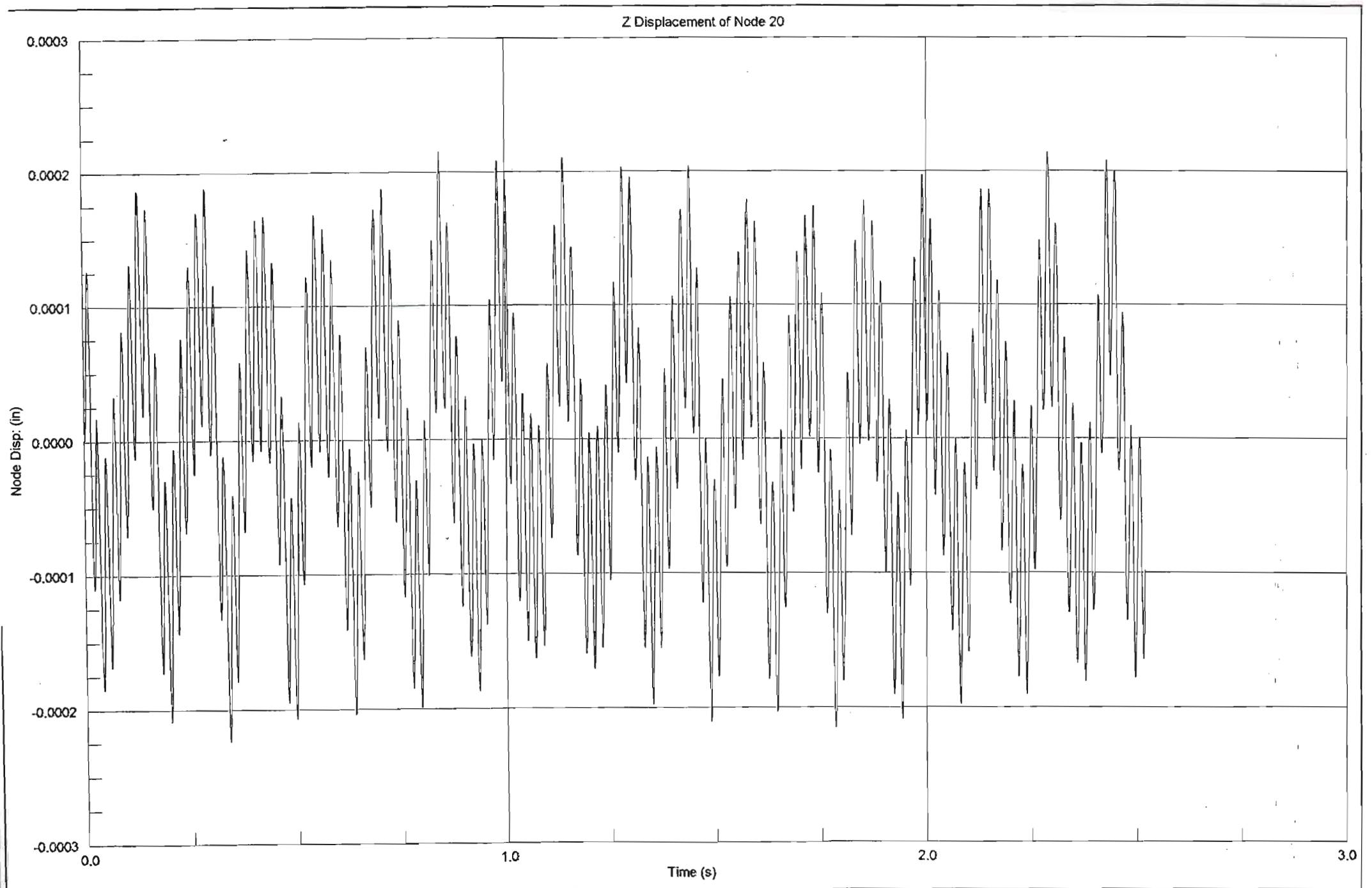


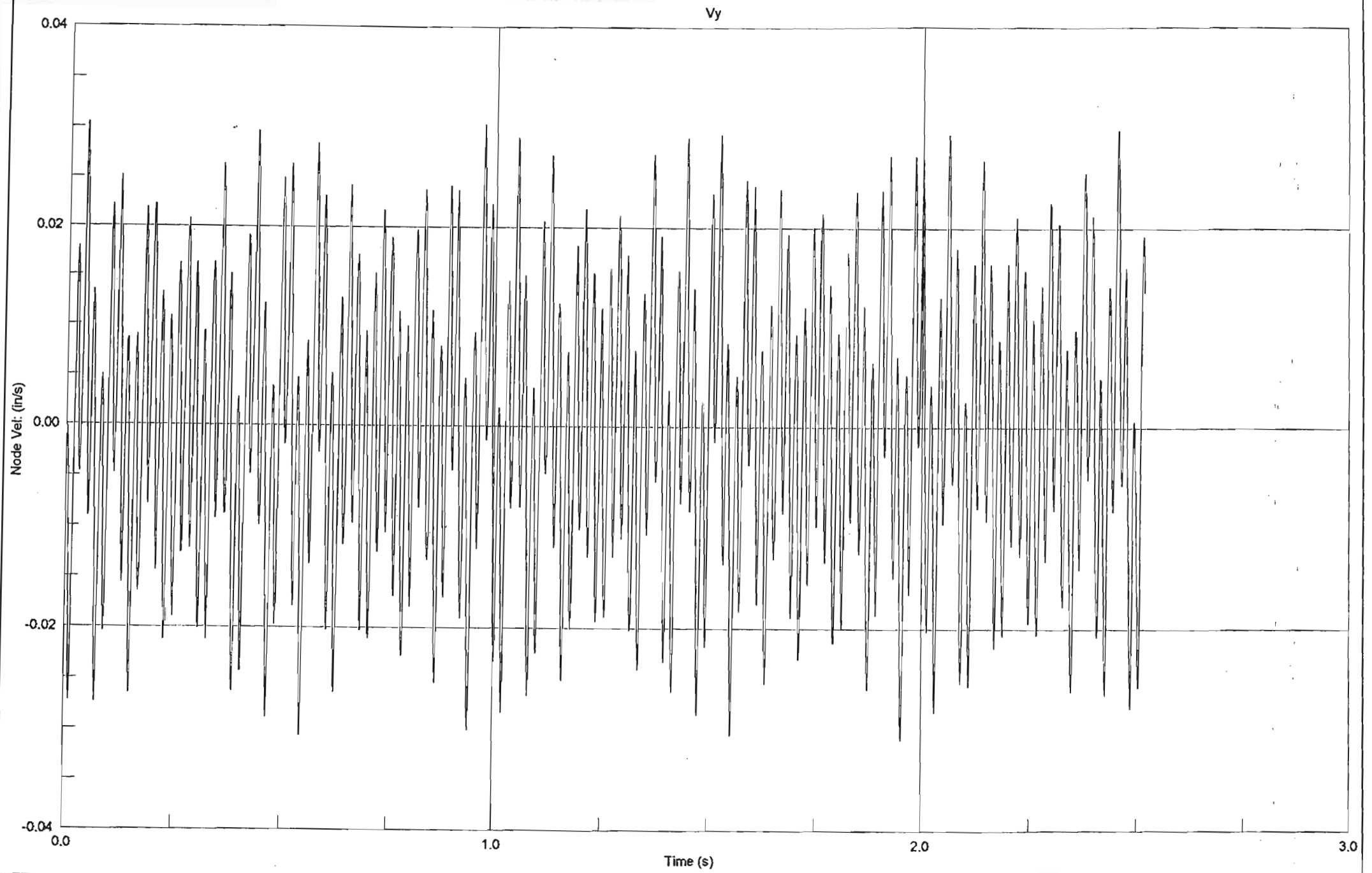


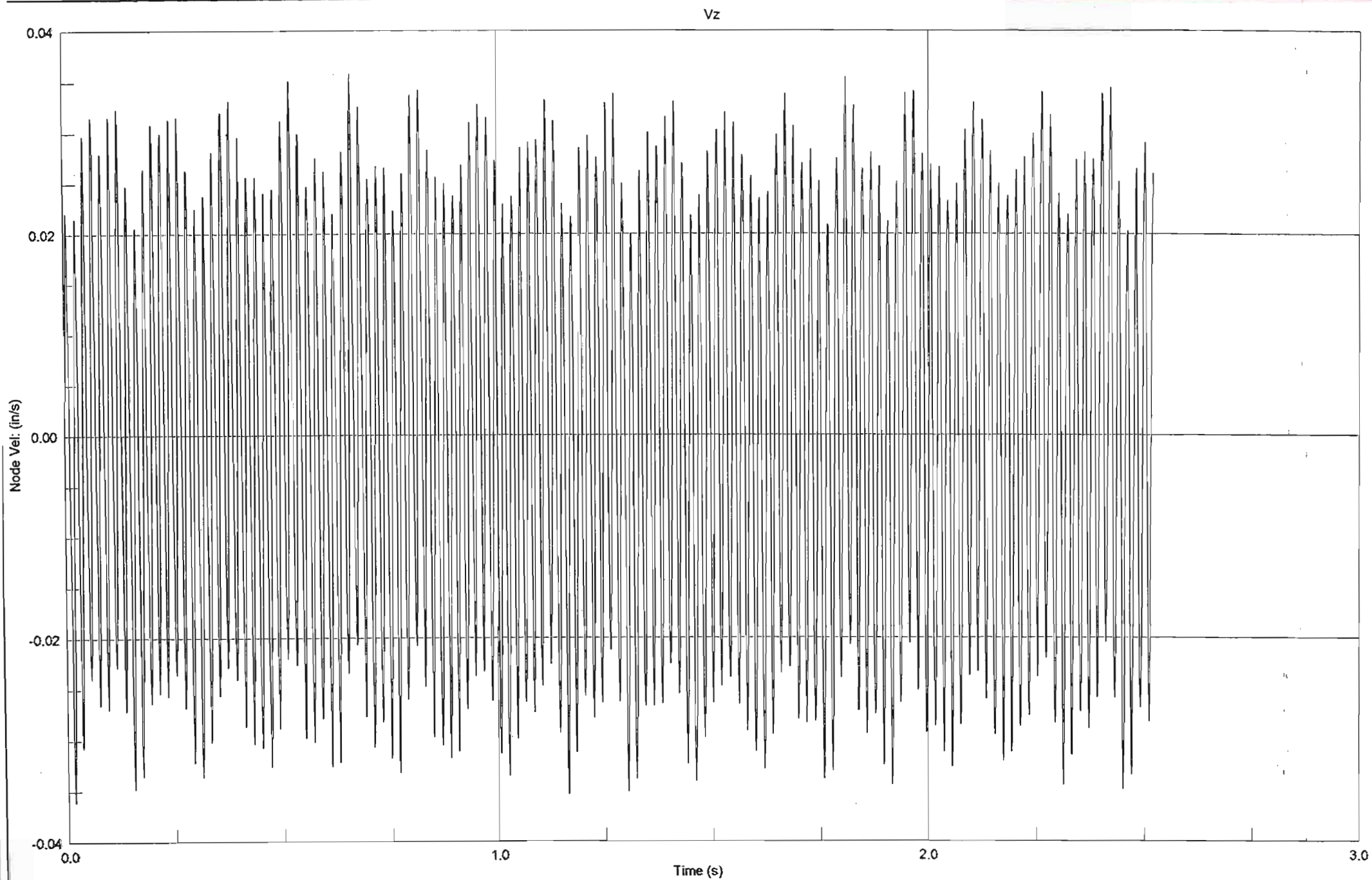
Z Displacement of Node 8

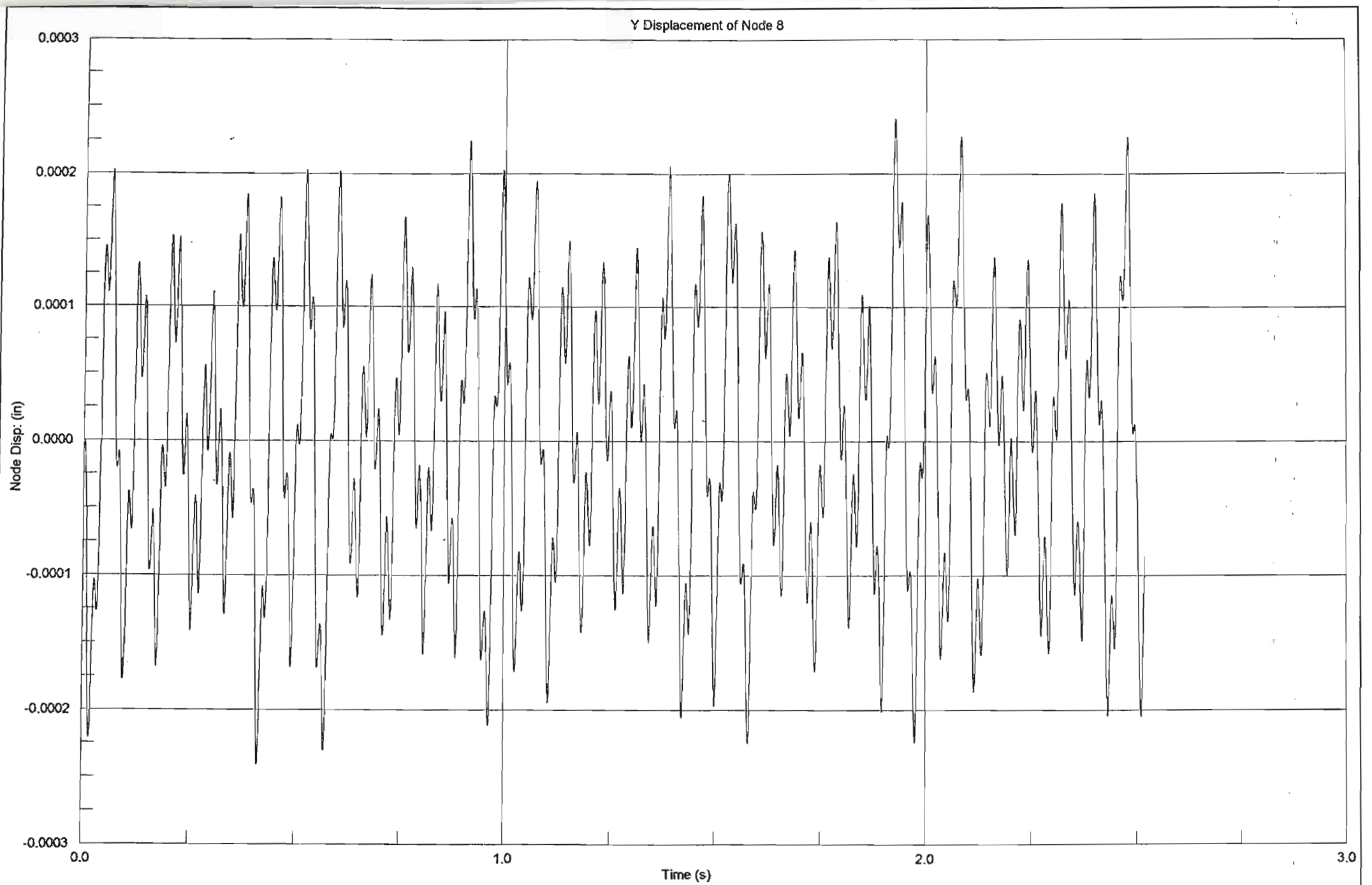




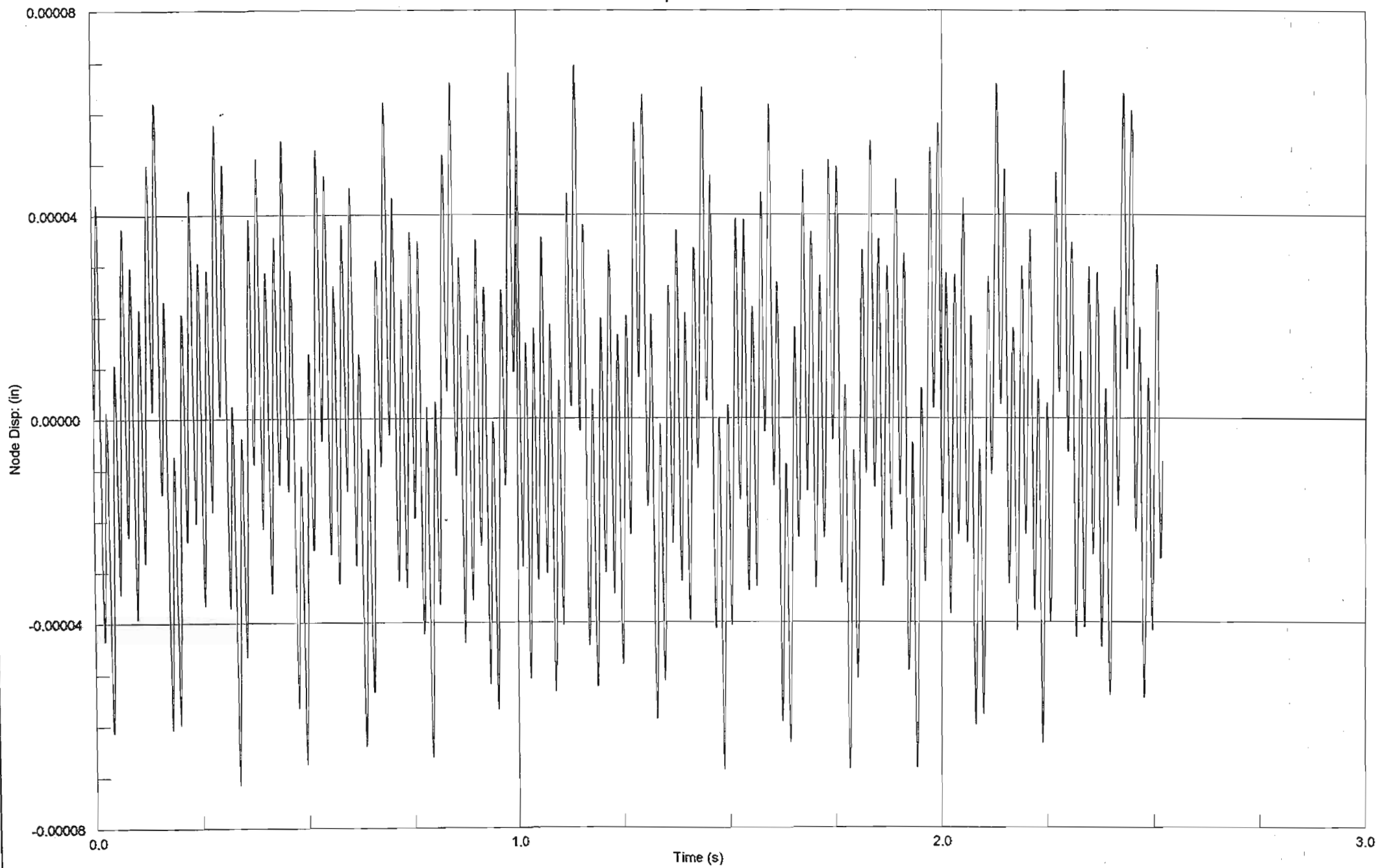


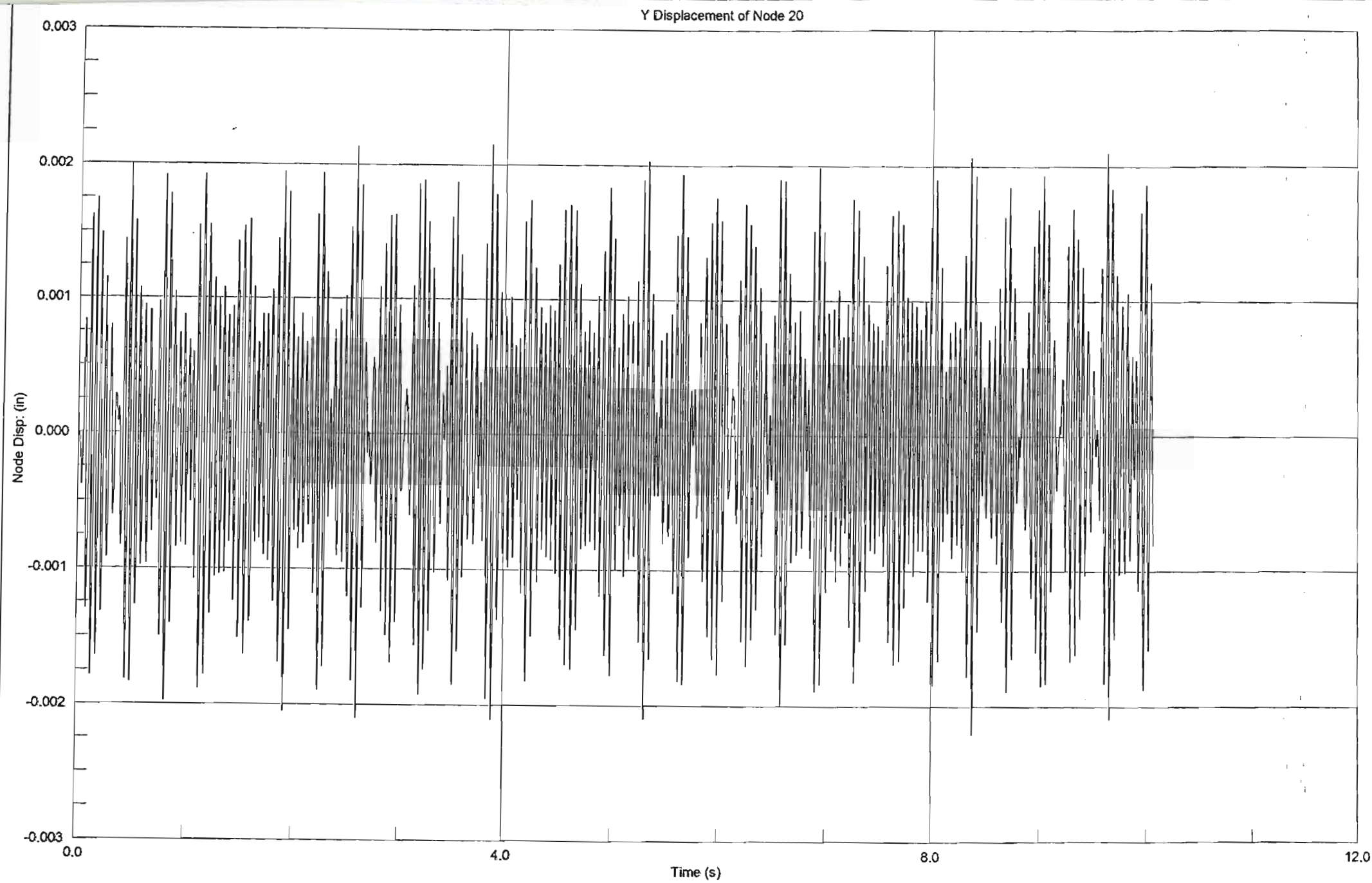




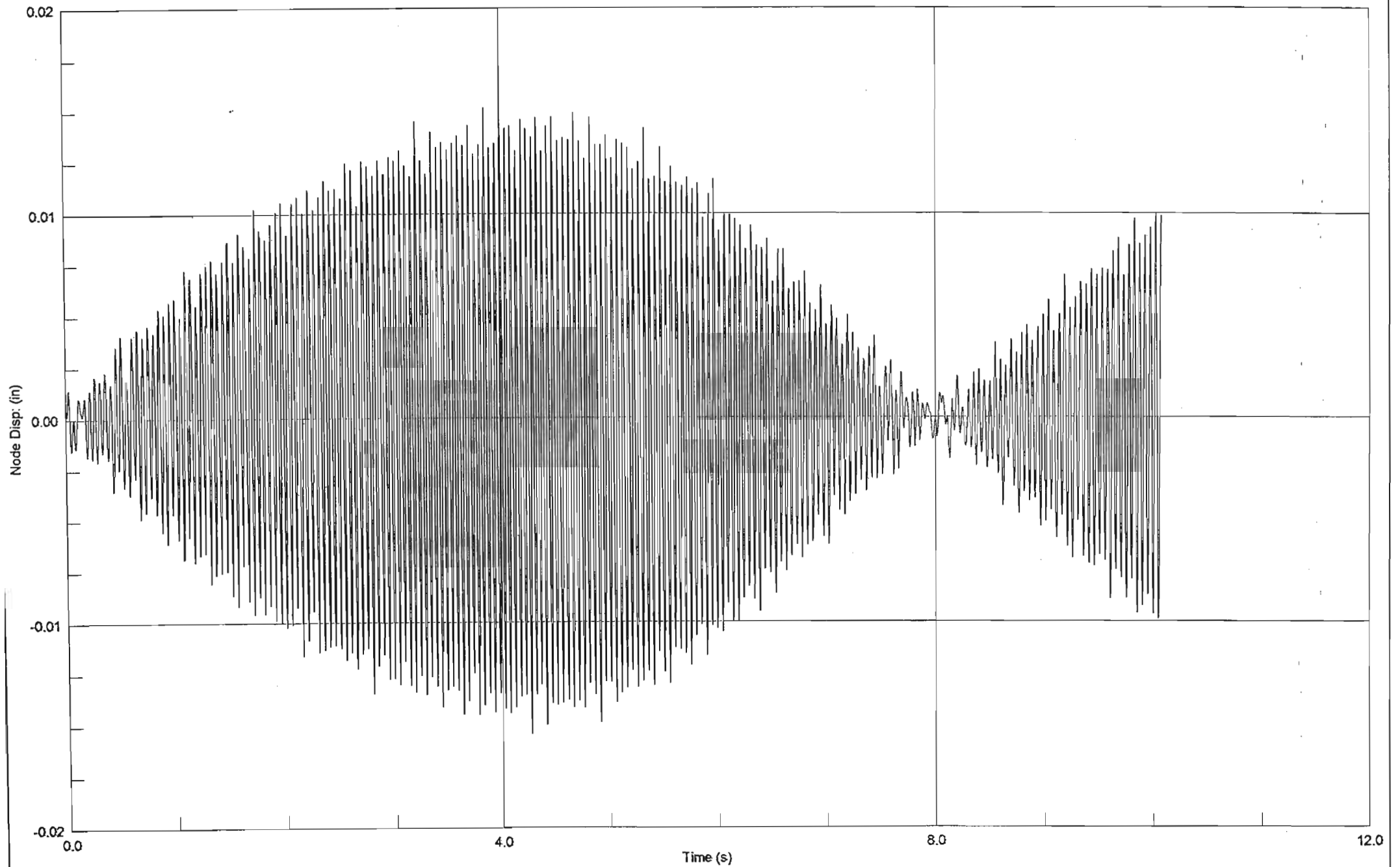


Z Displacement of Node 8

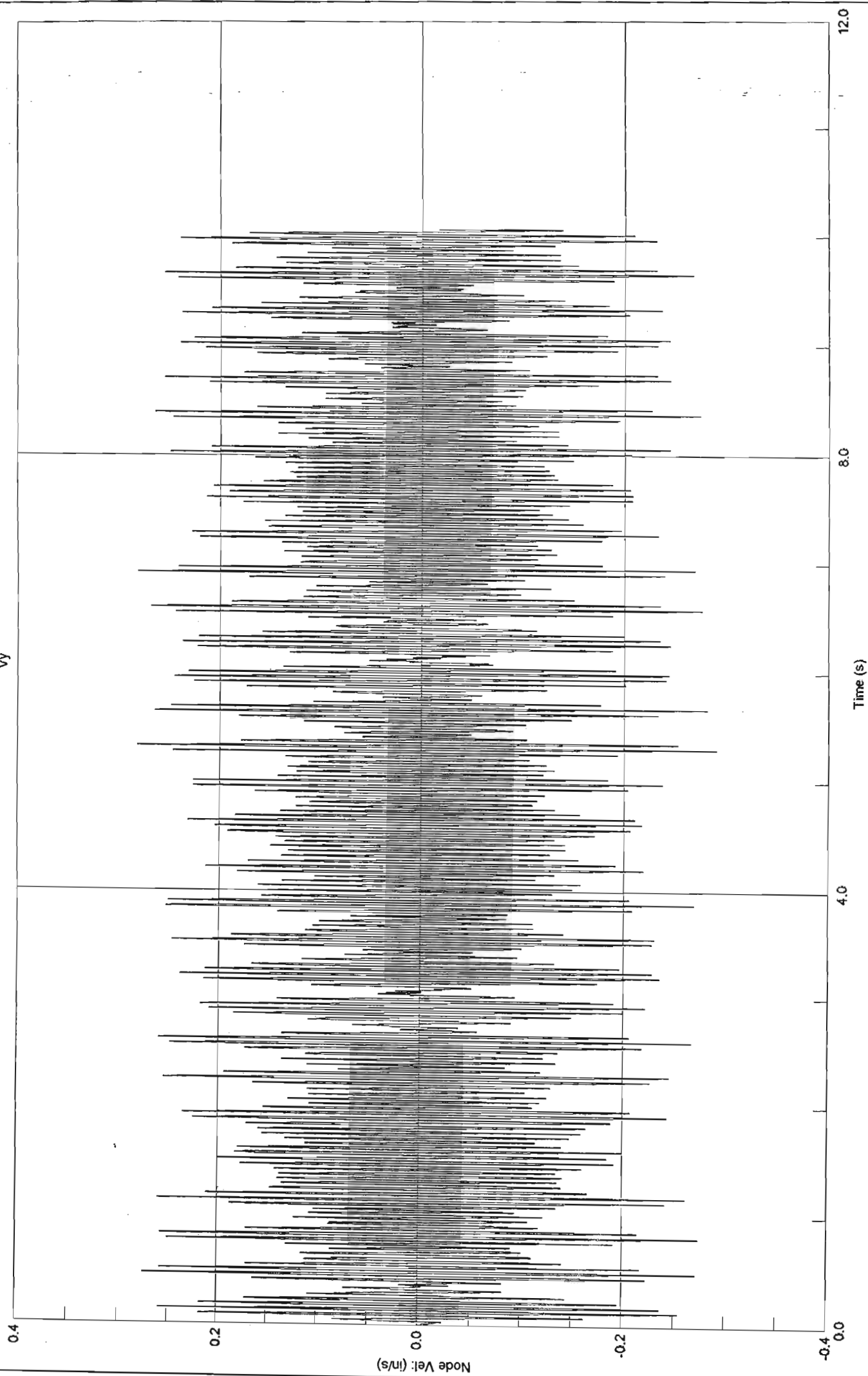




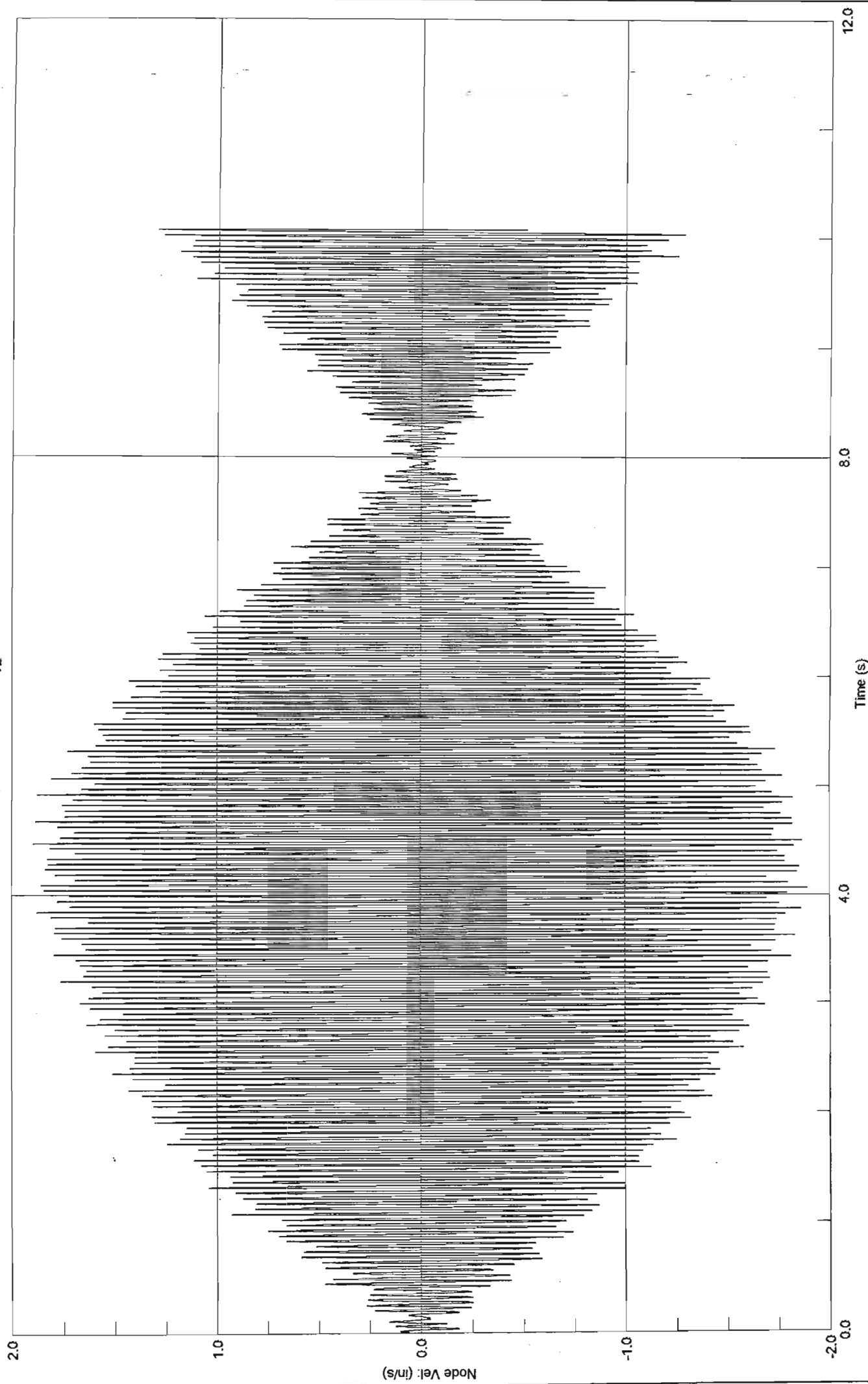
Z Displacement of Node 20

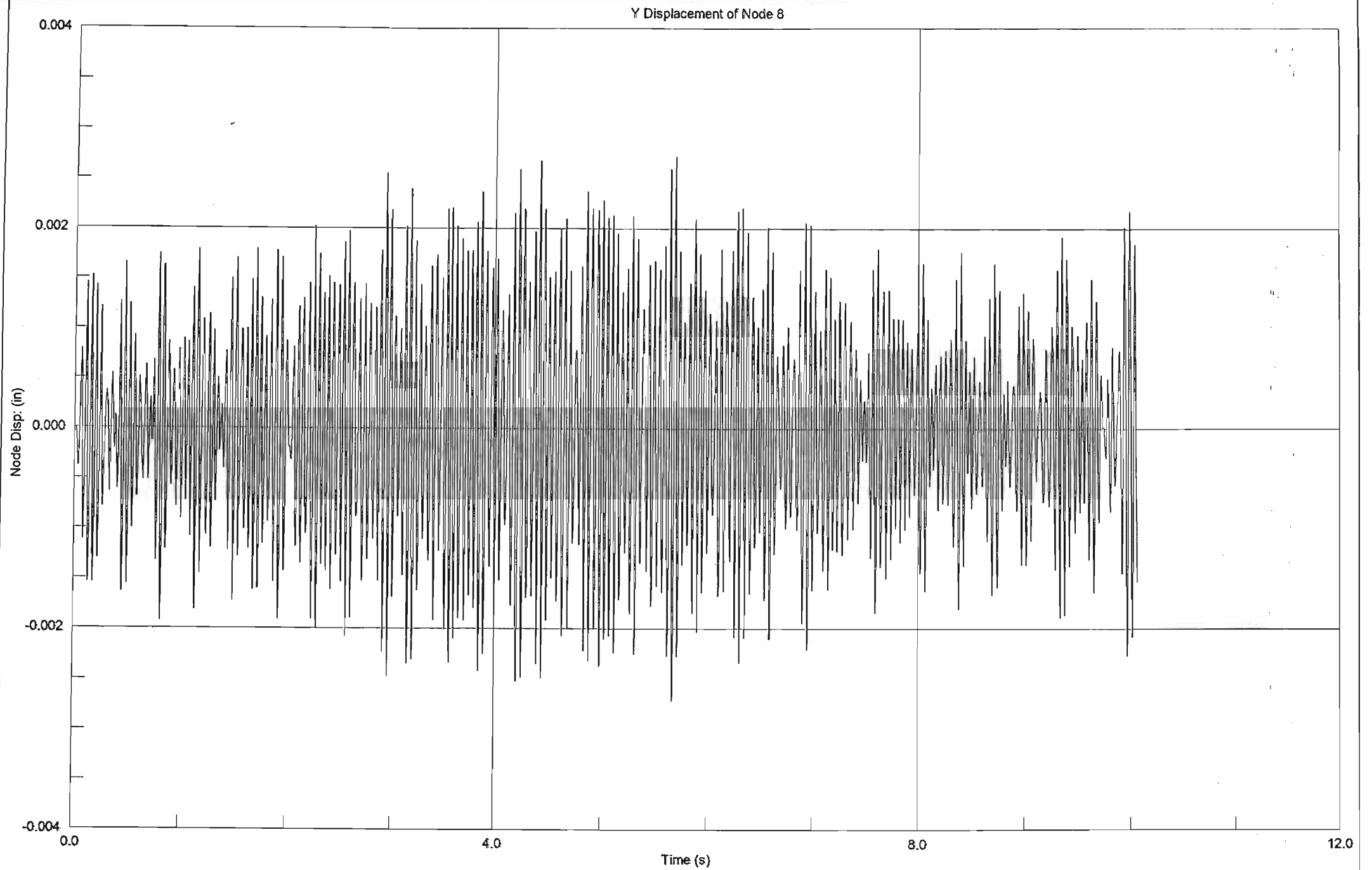


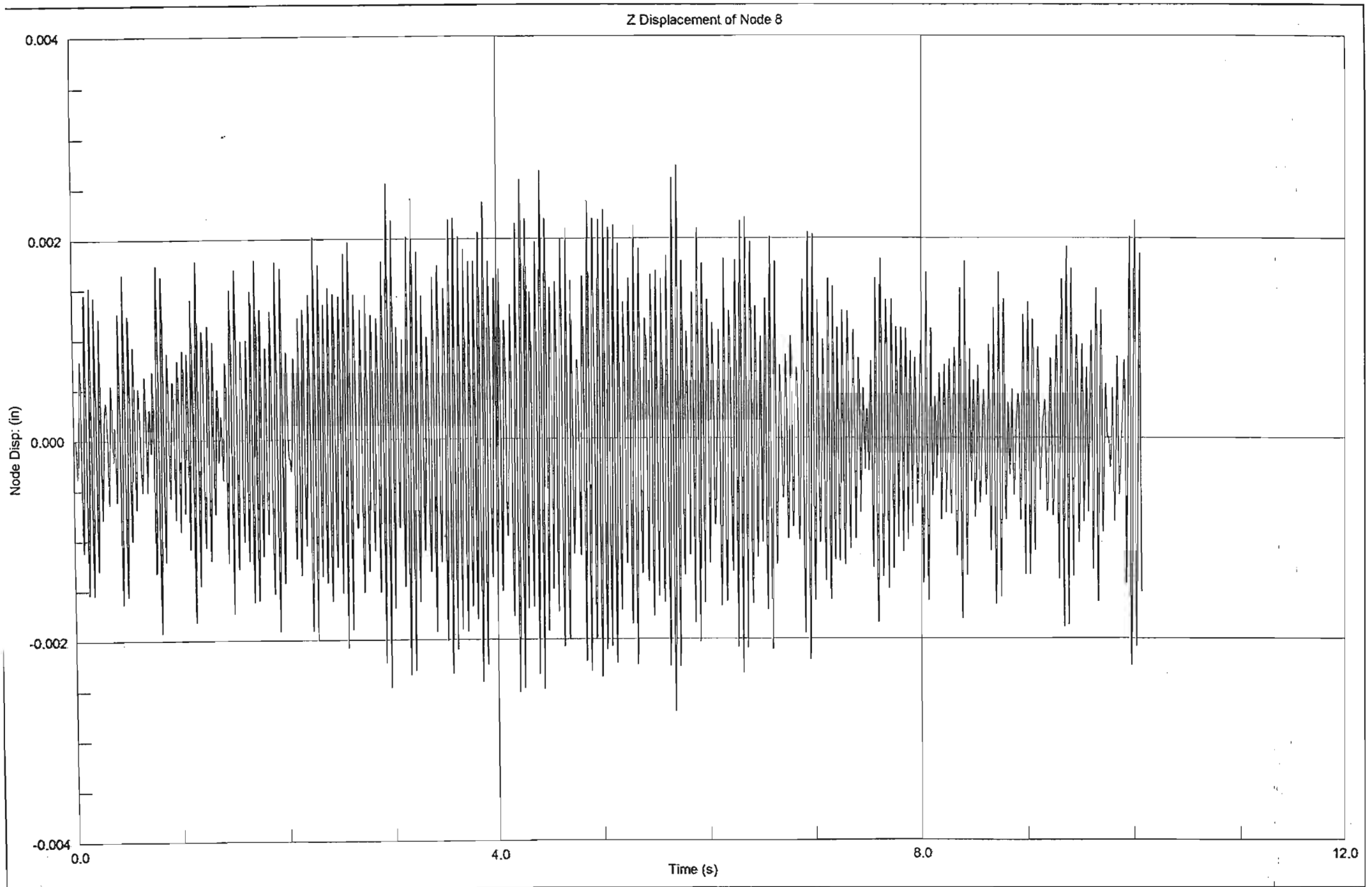
Vy

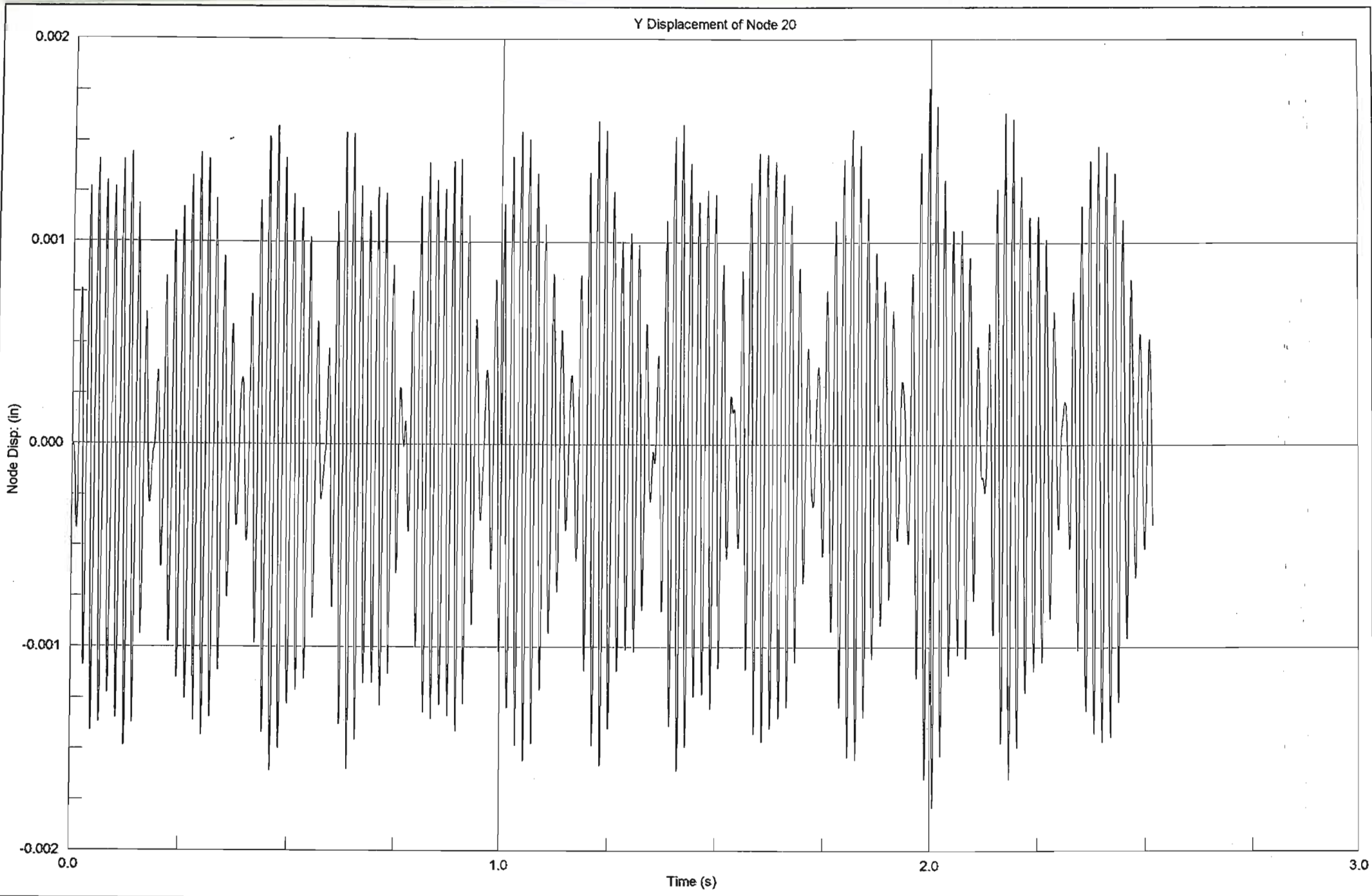


Vz

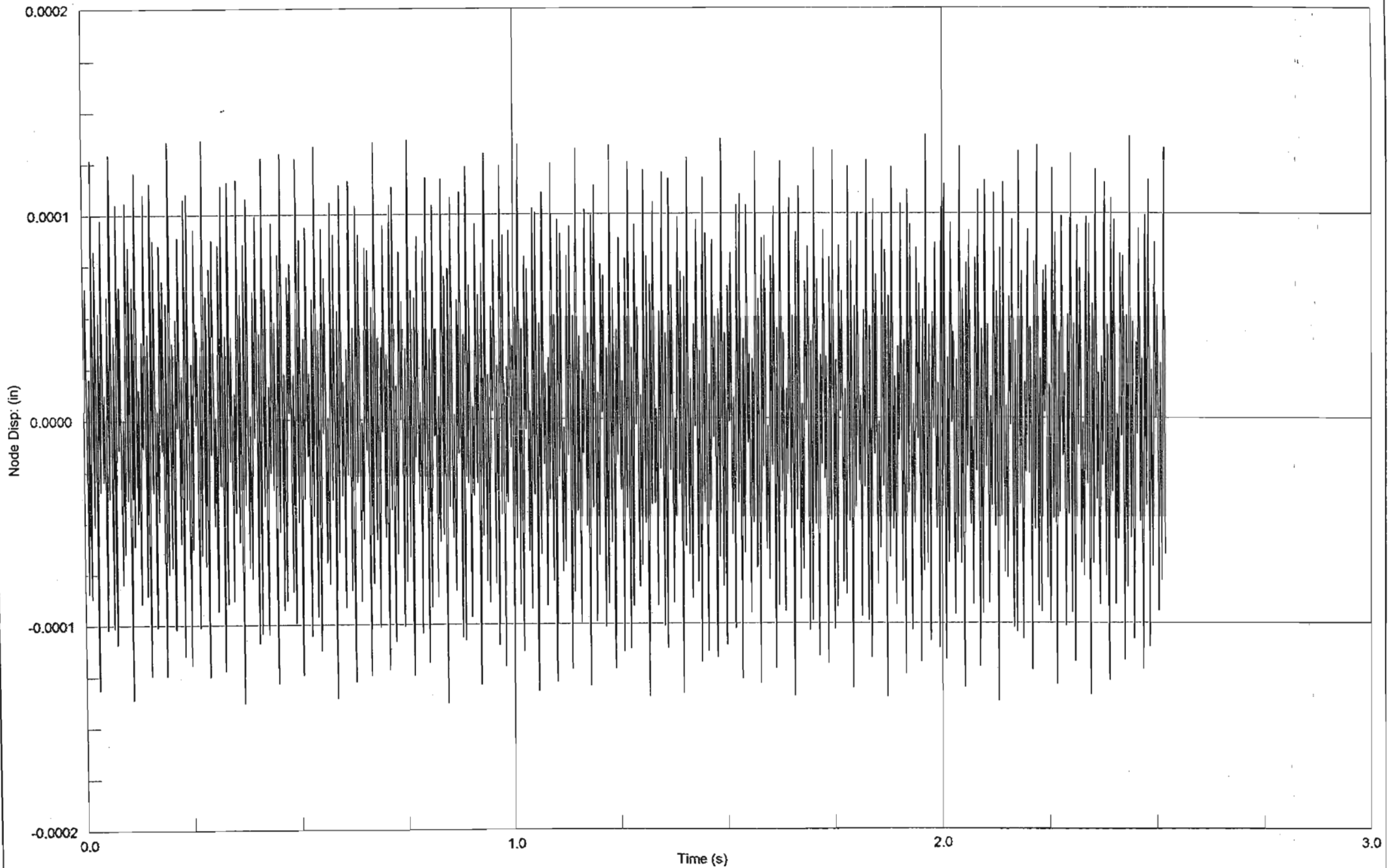


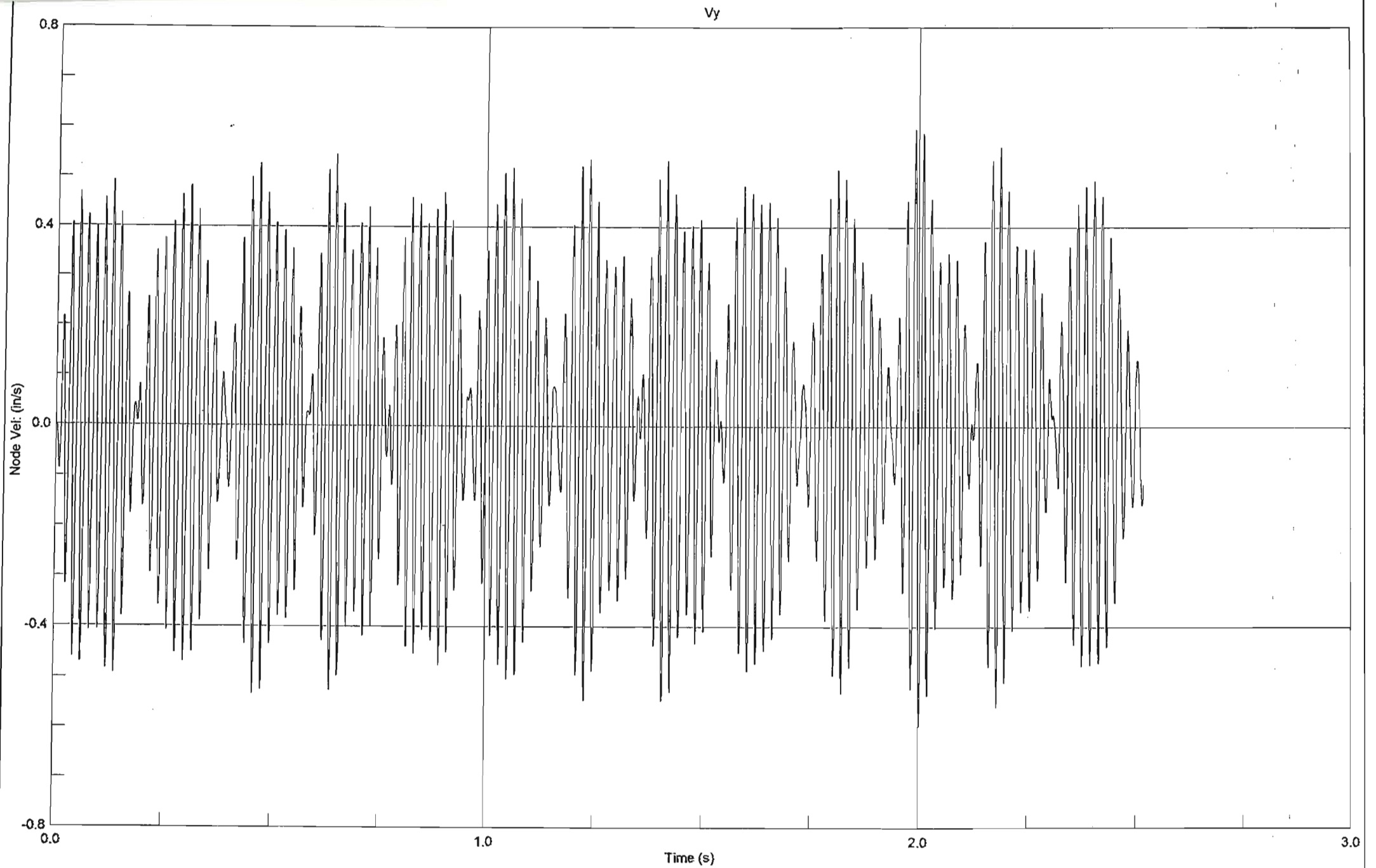






Z Displacement of Node 20



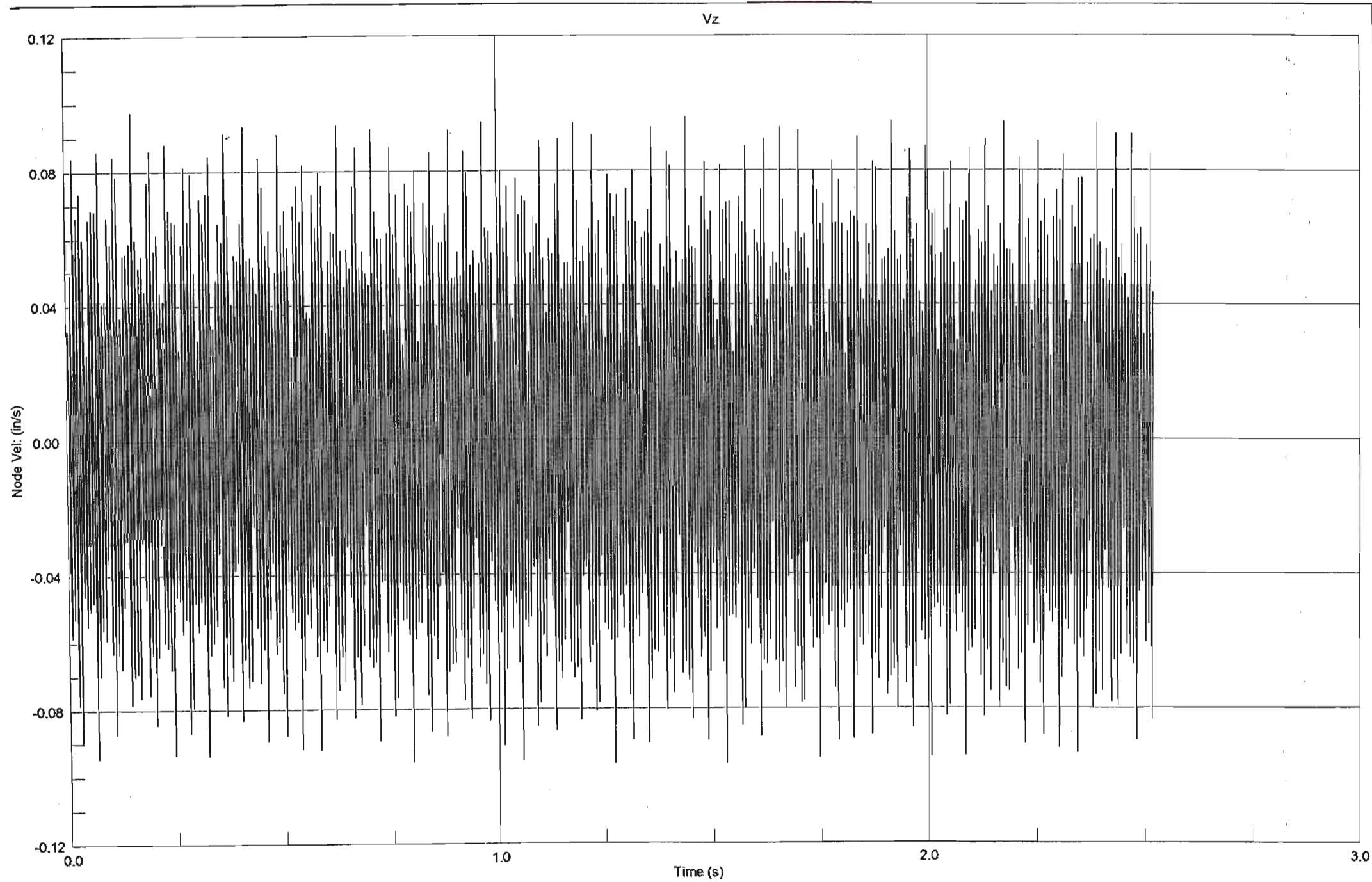


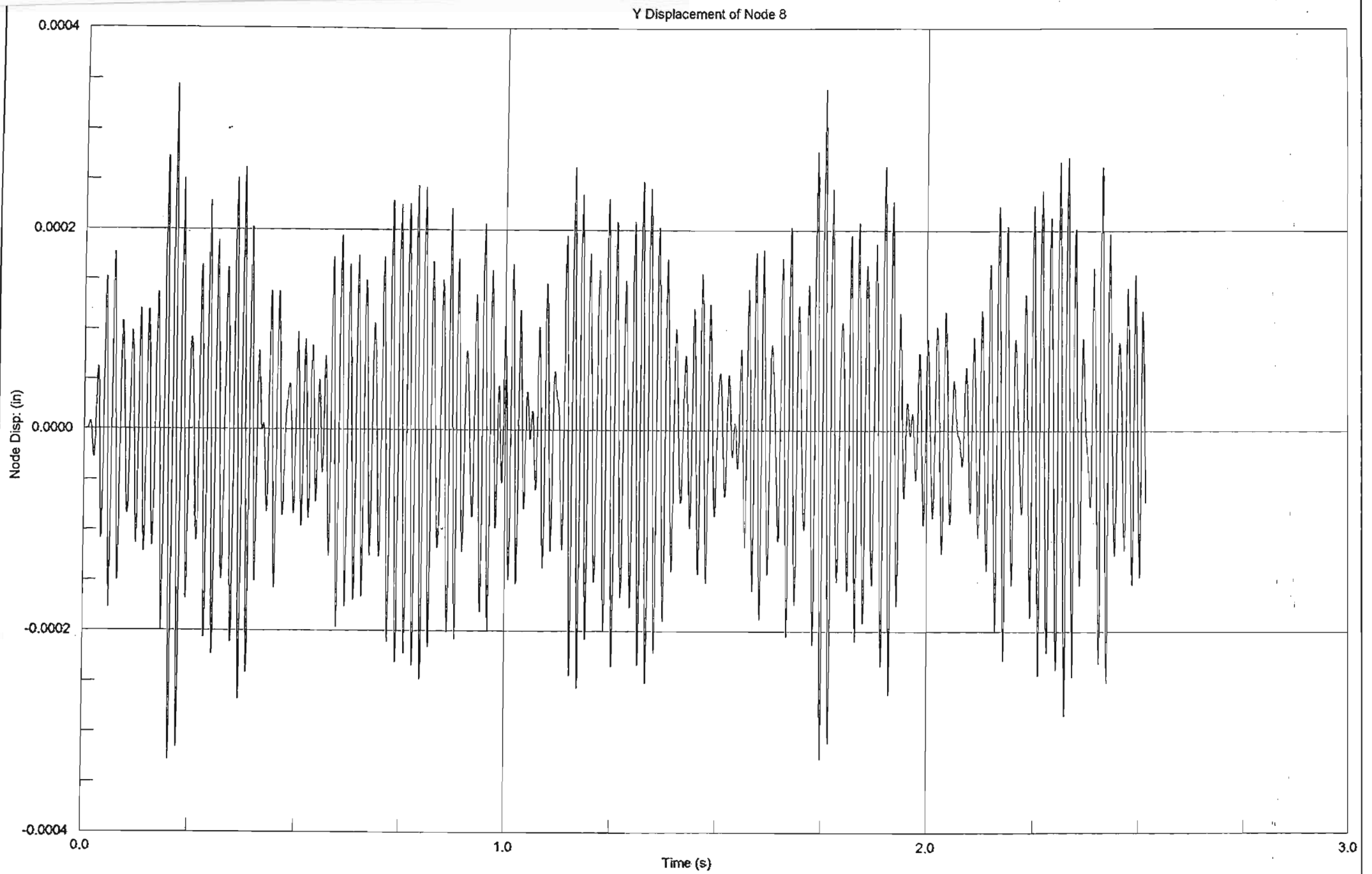
Strand7 Release 2.1.7

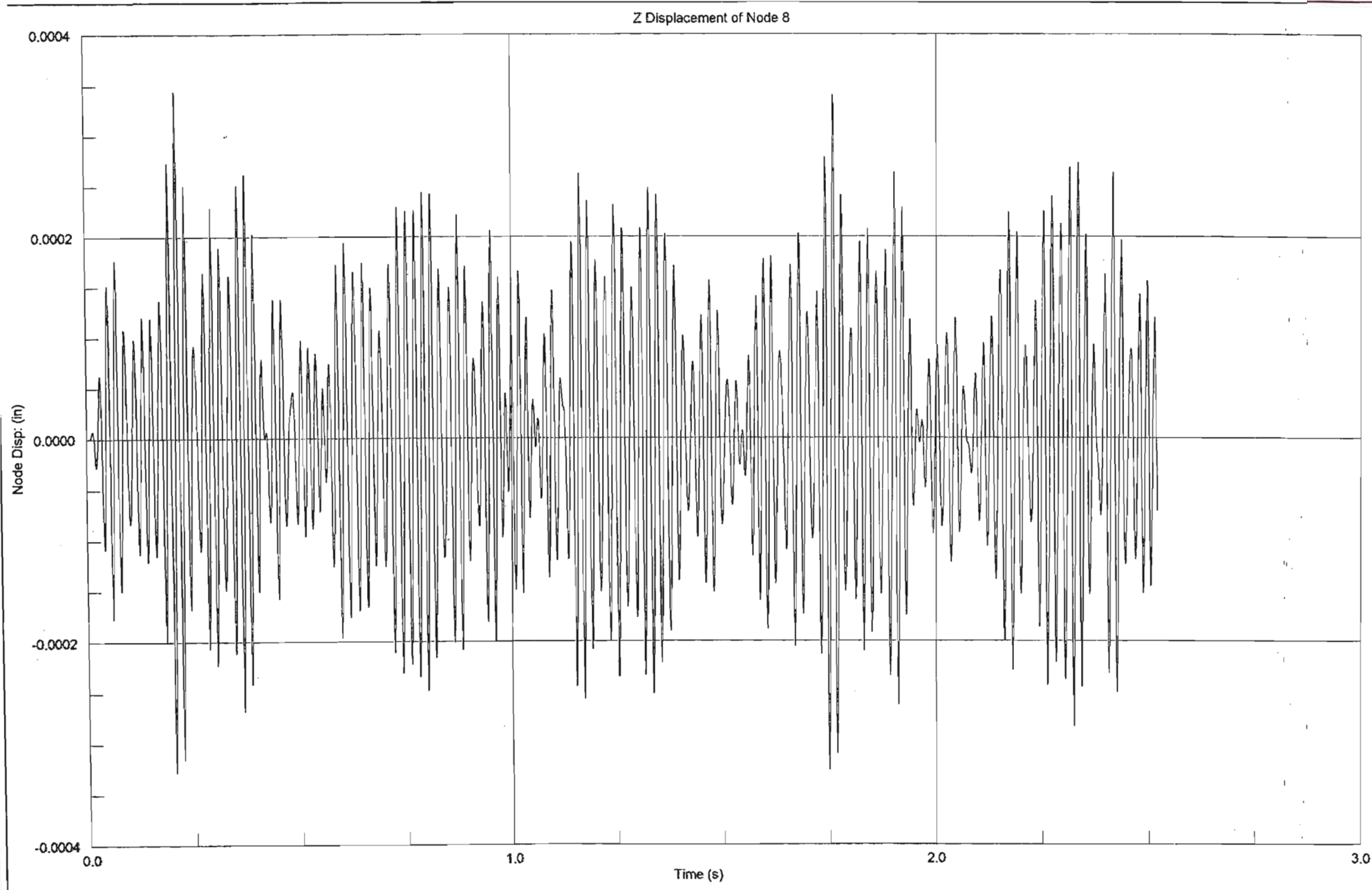
C:\MSc Eng\Table Top\Table Top 2\Table top G15000 beam.st7

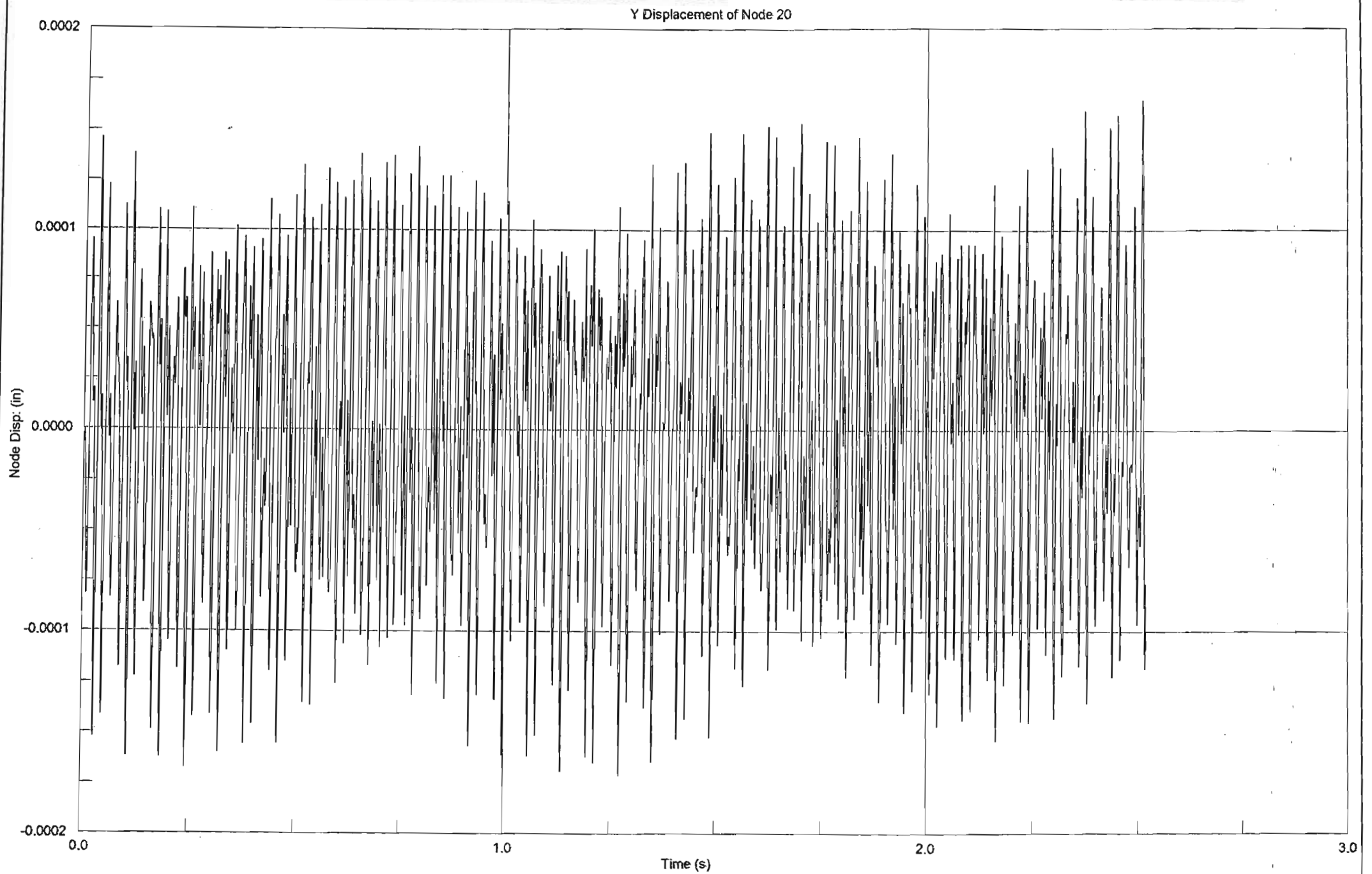
7 October 2002 11:38 am

3.9

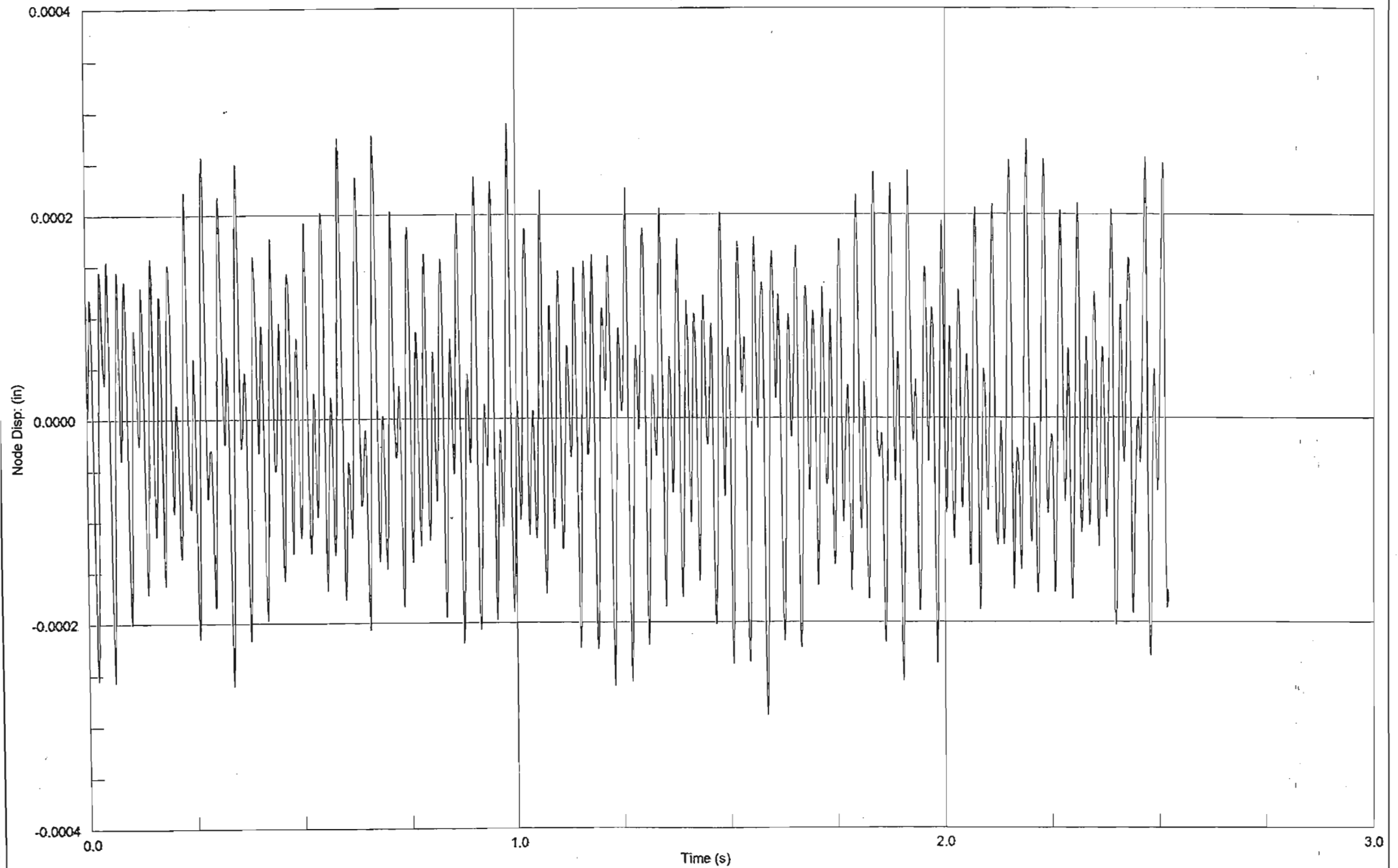


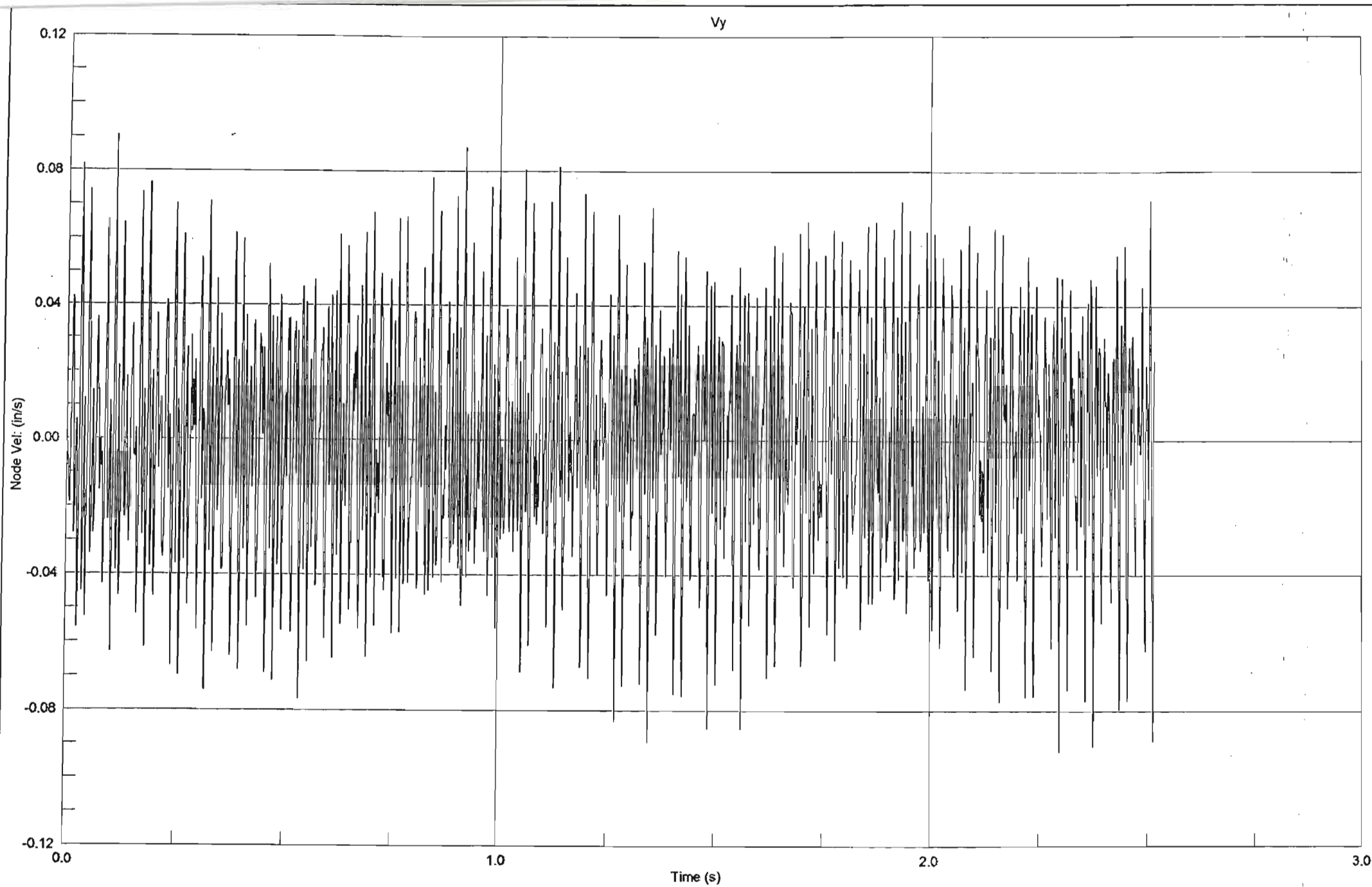


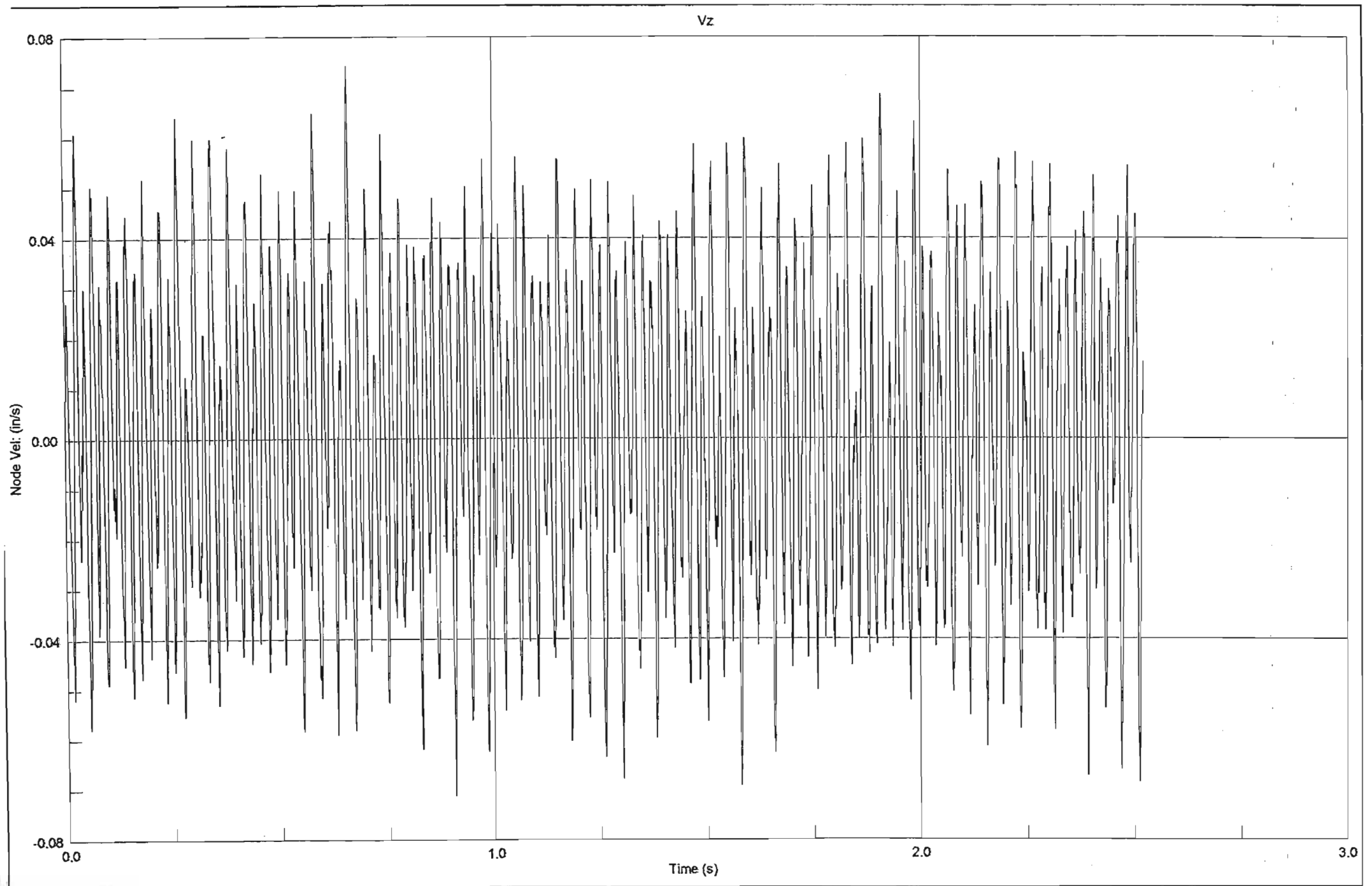


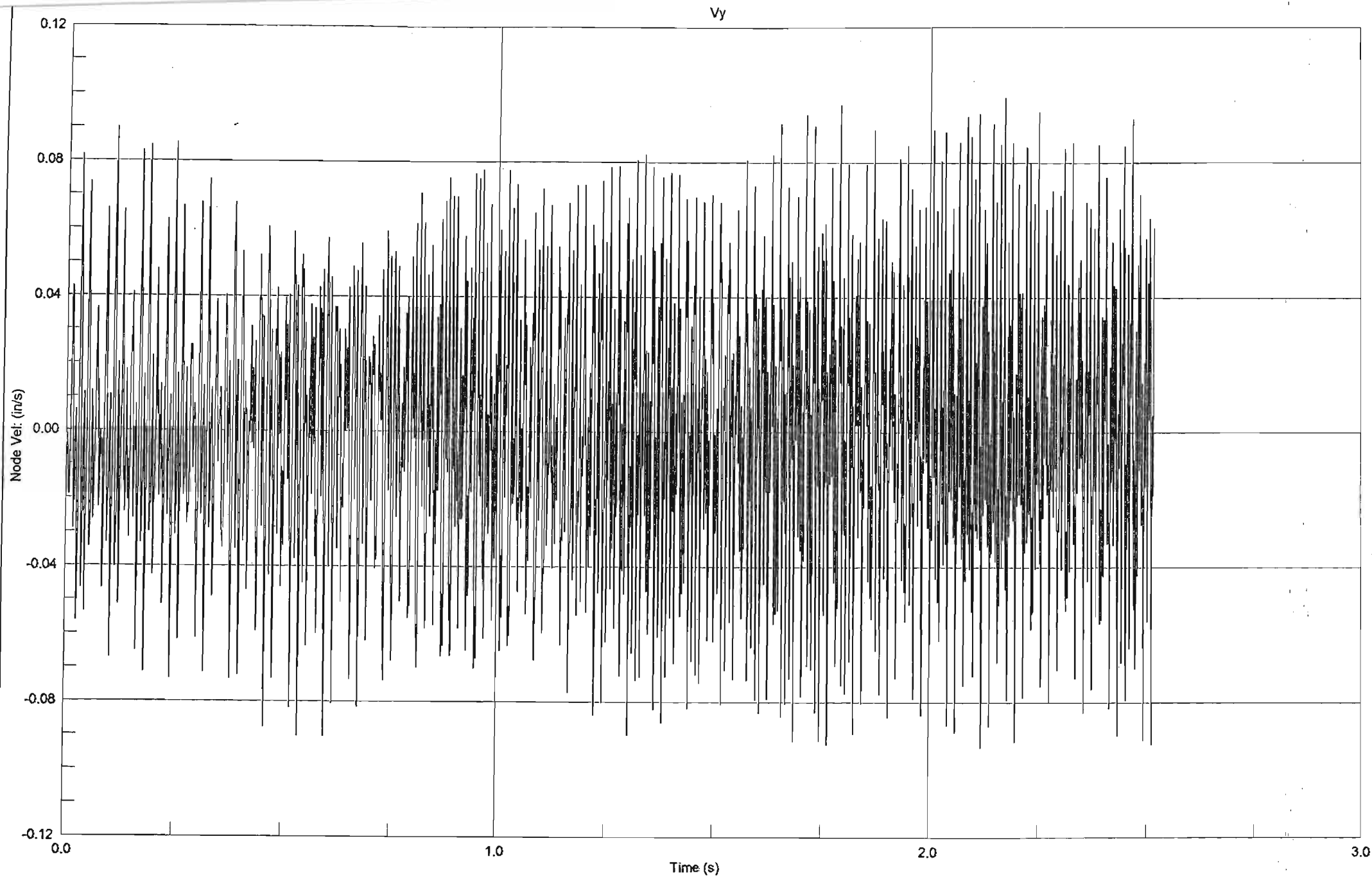


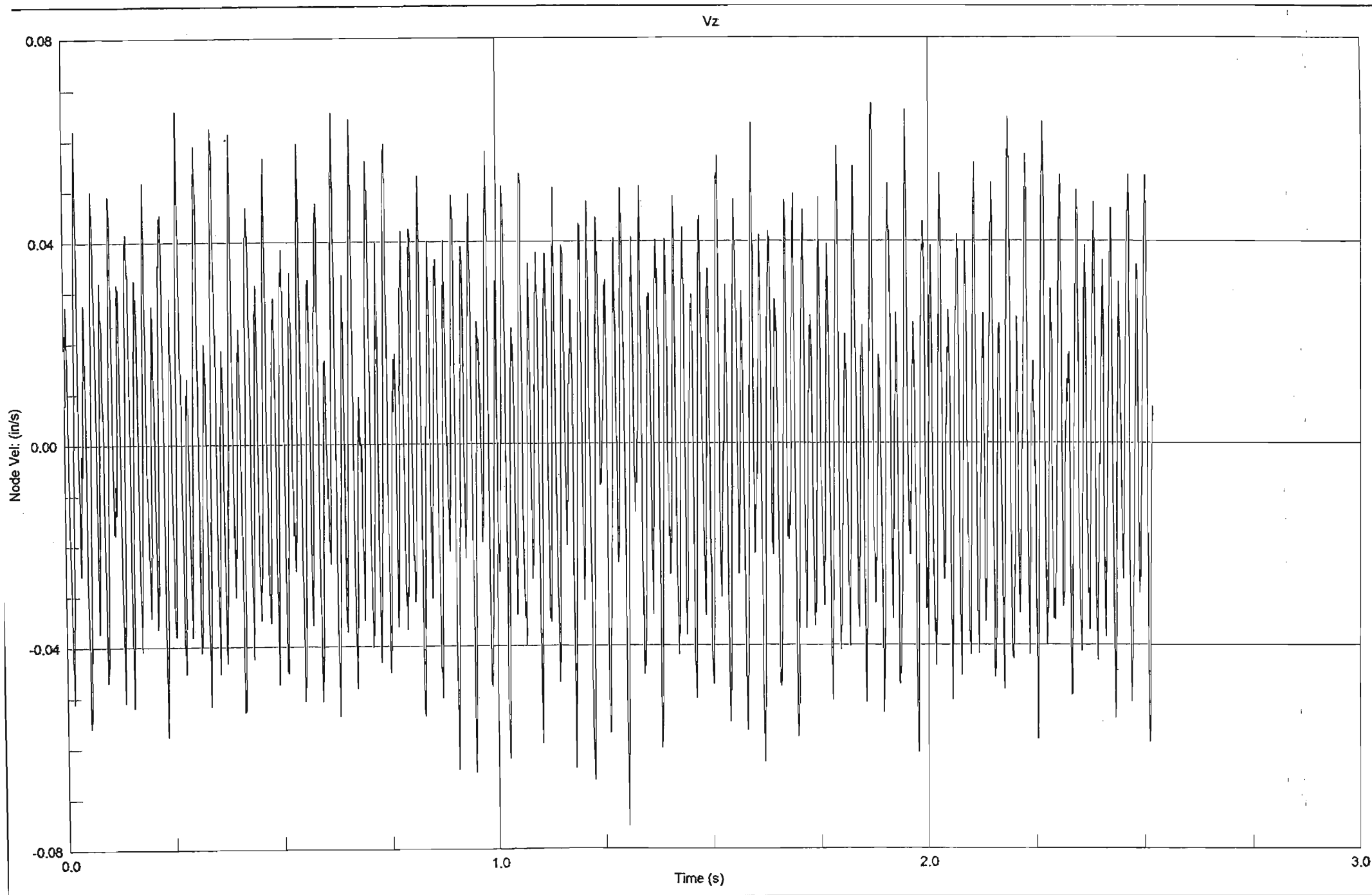
Z Displacement of Node 20

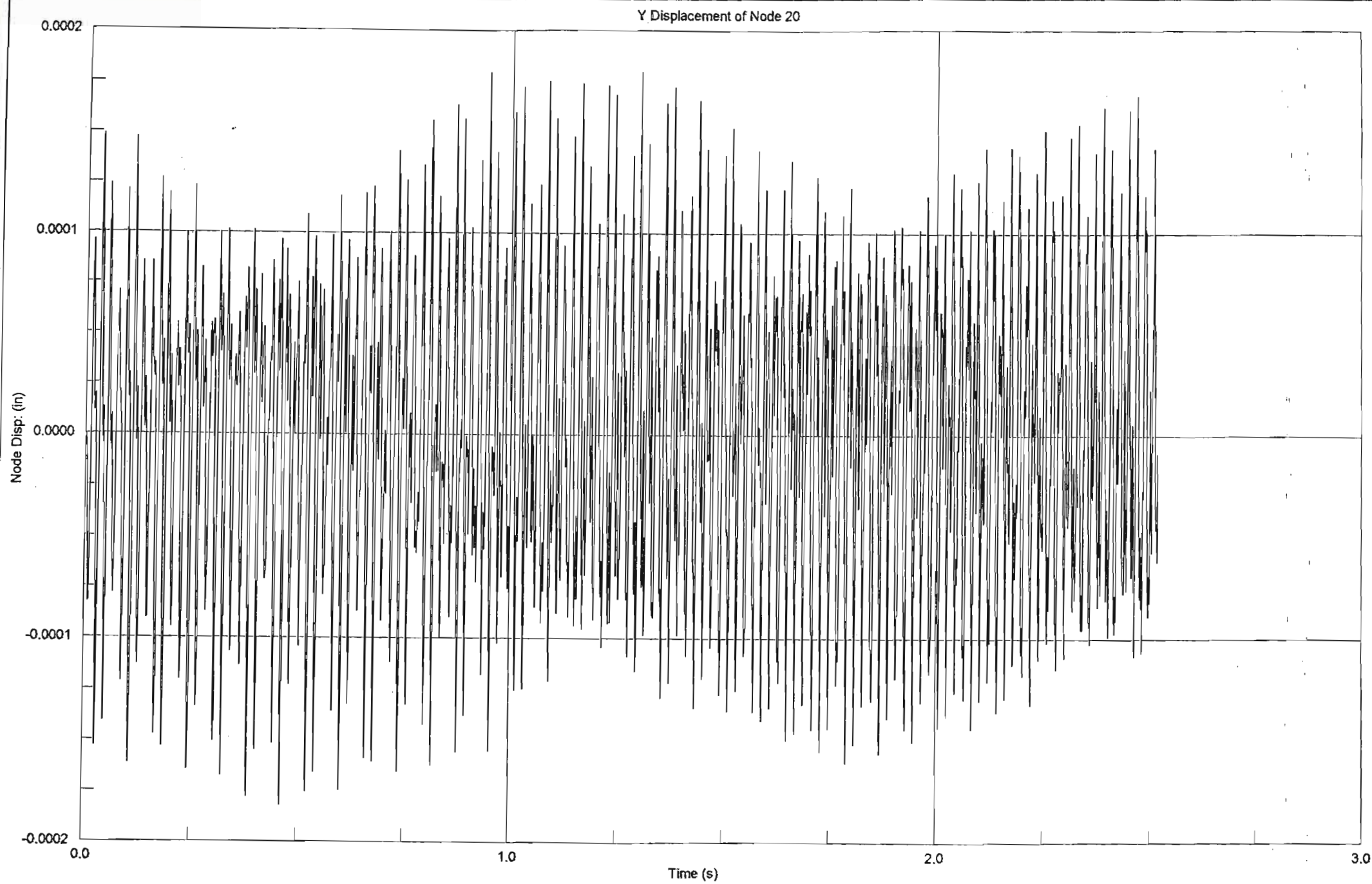




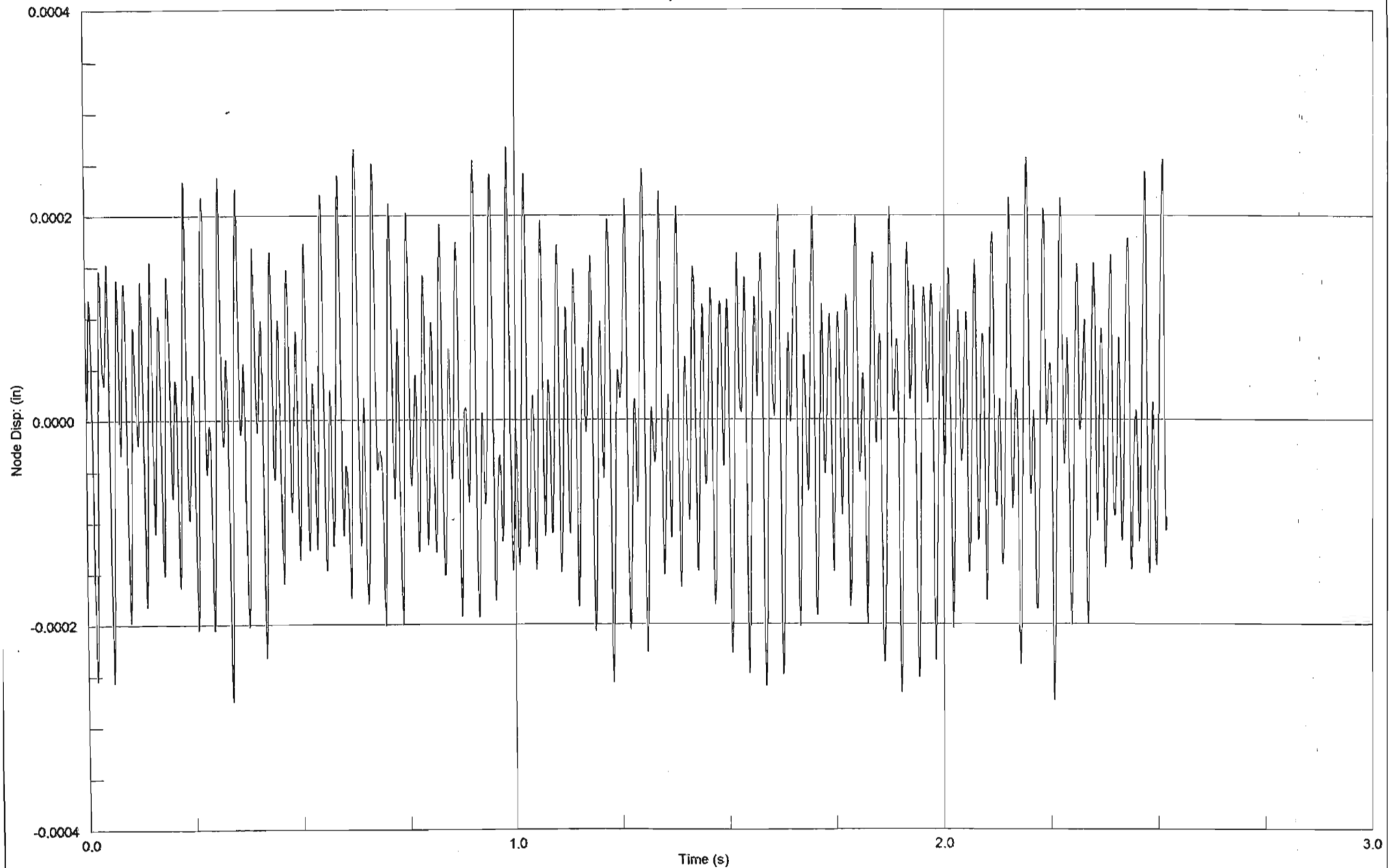


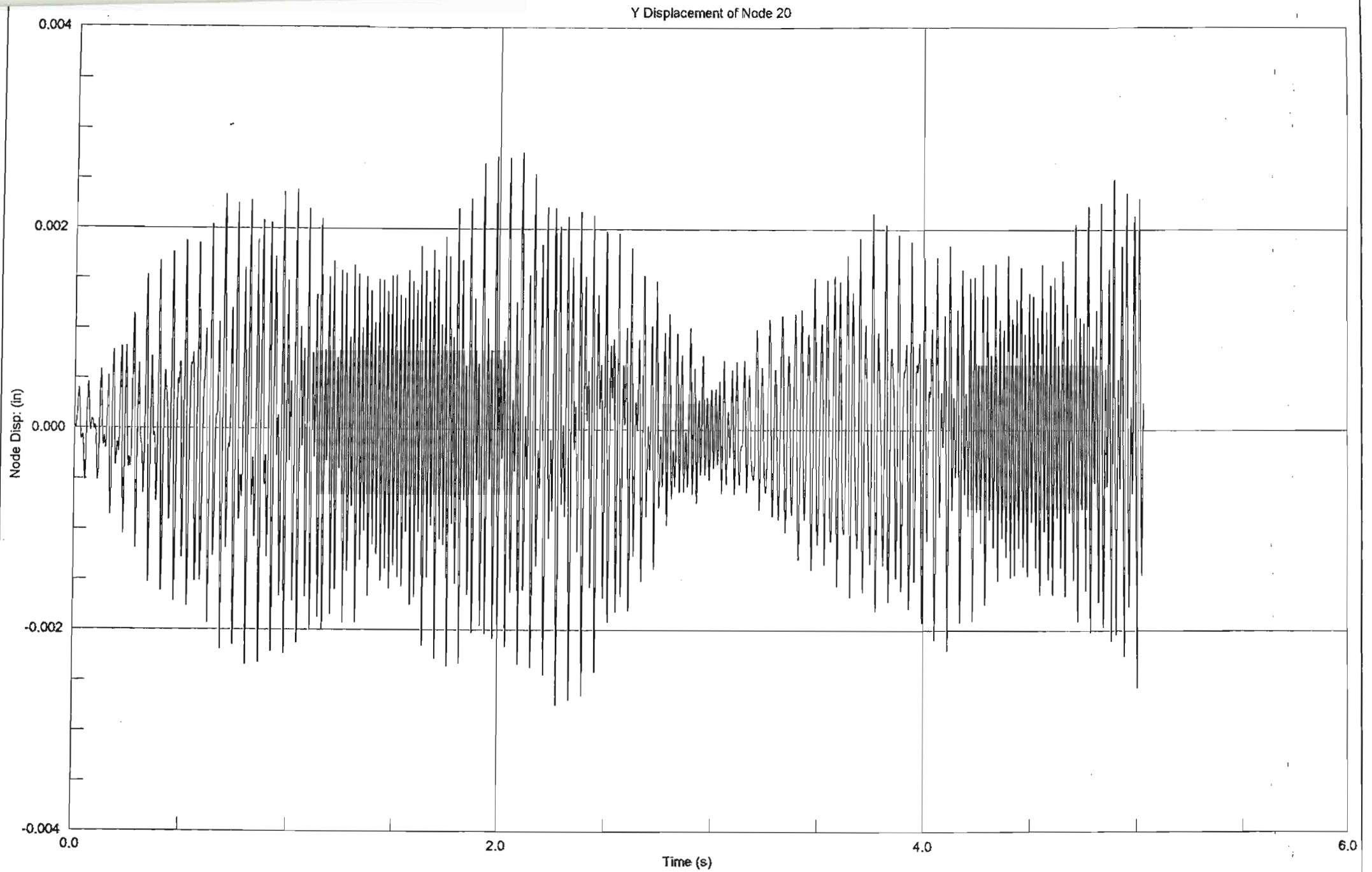




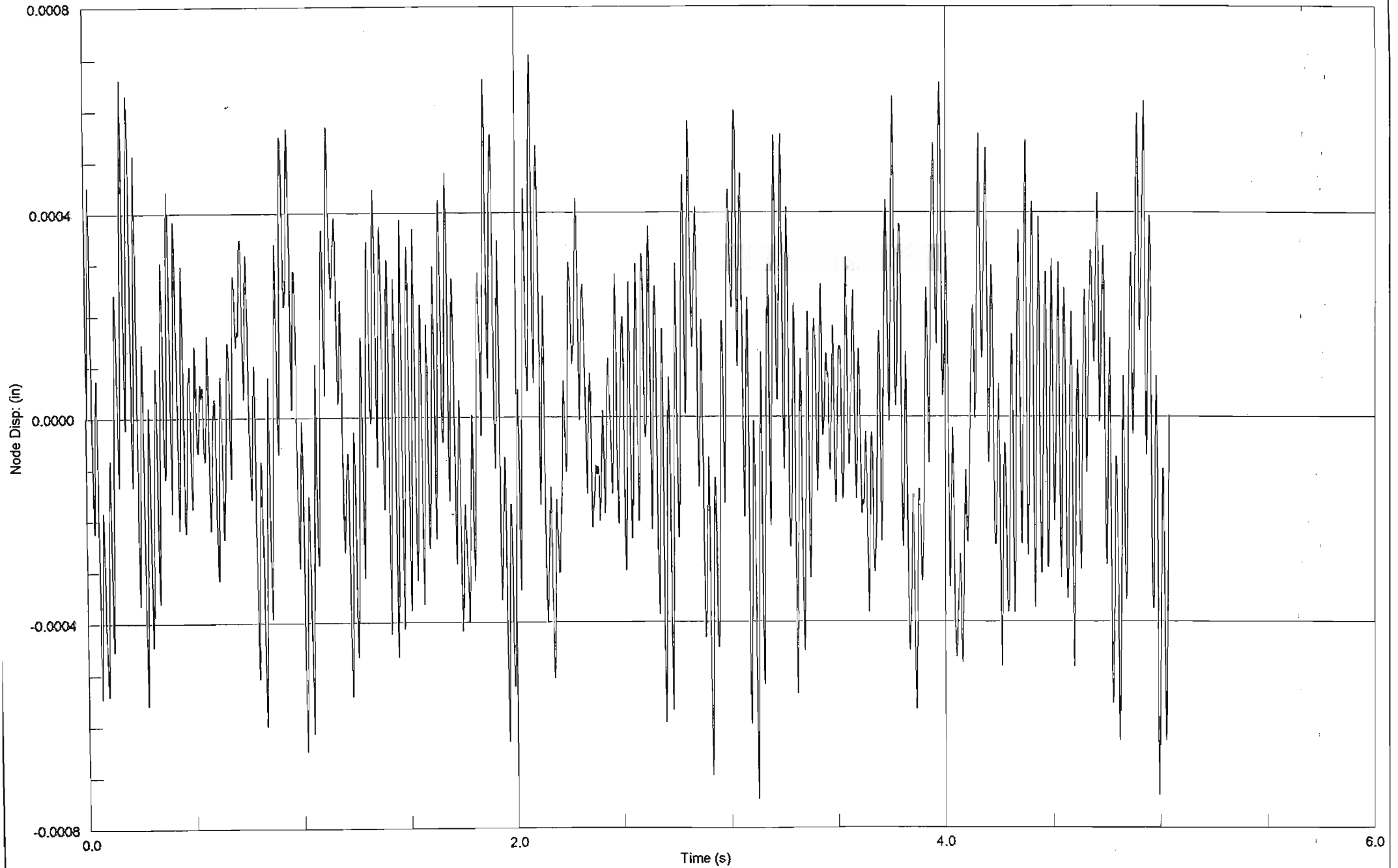


Z Displacement of Node 20

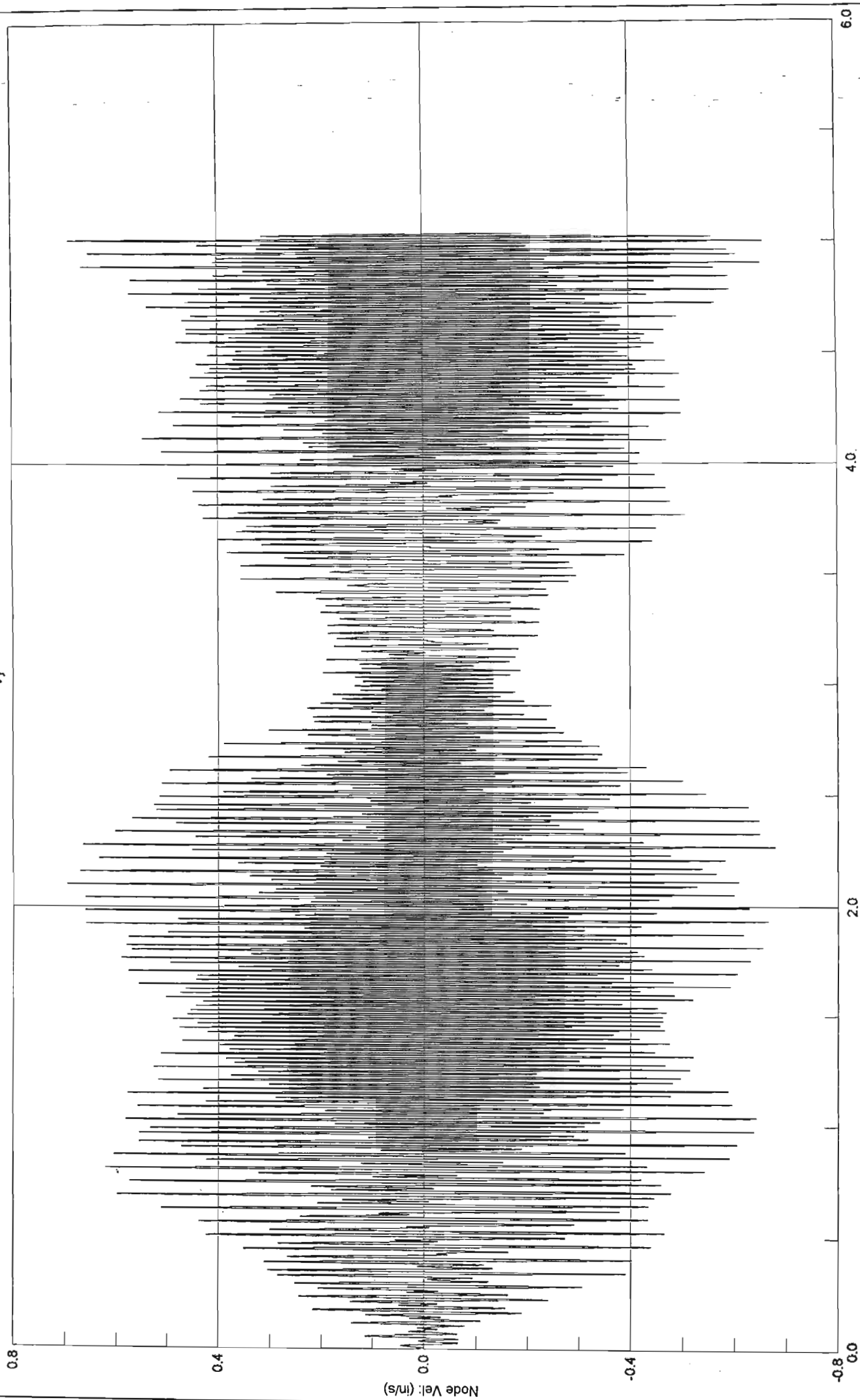


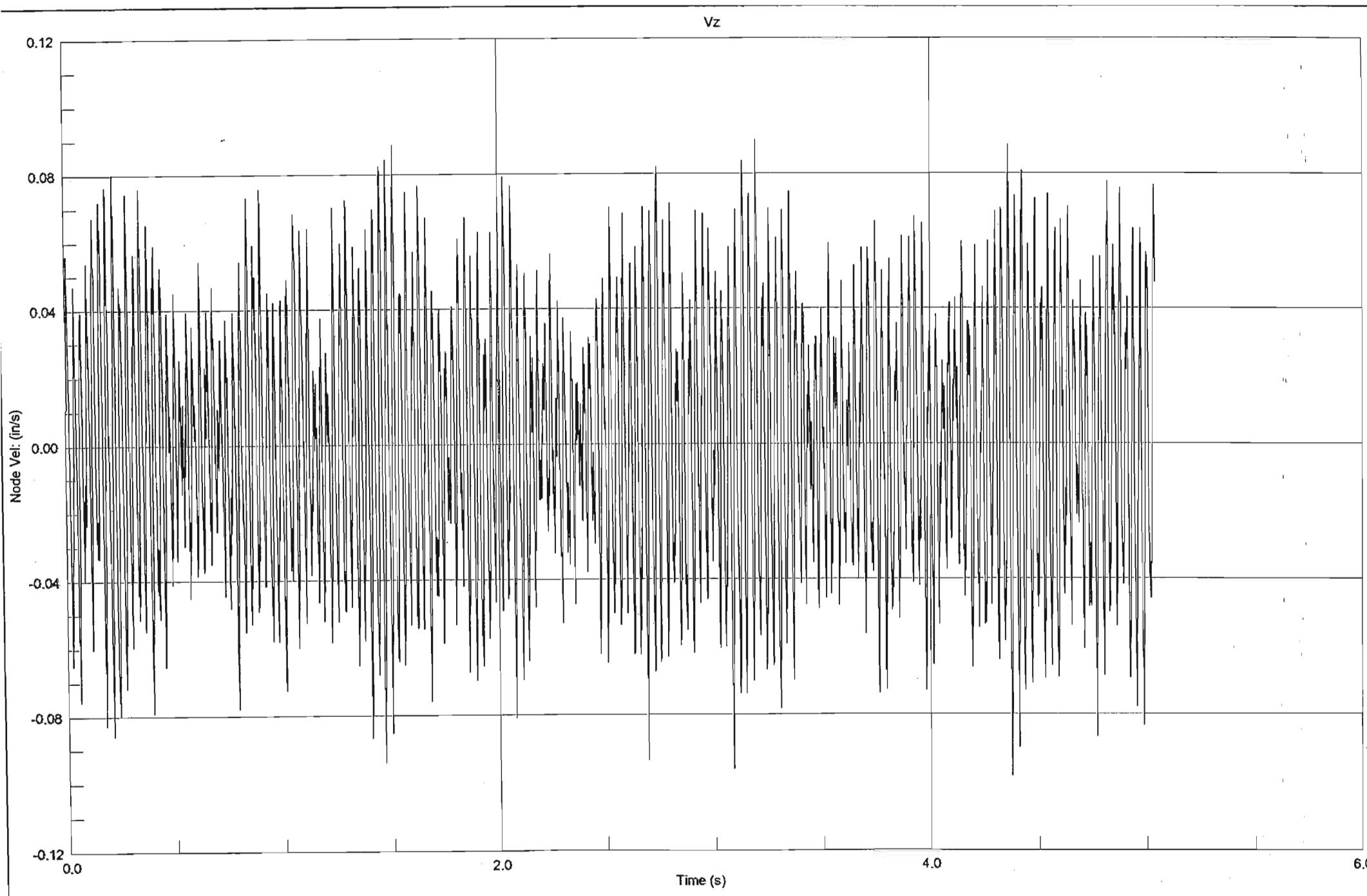


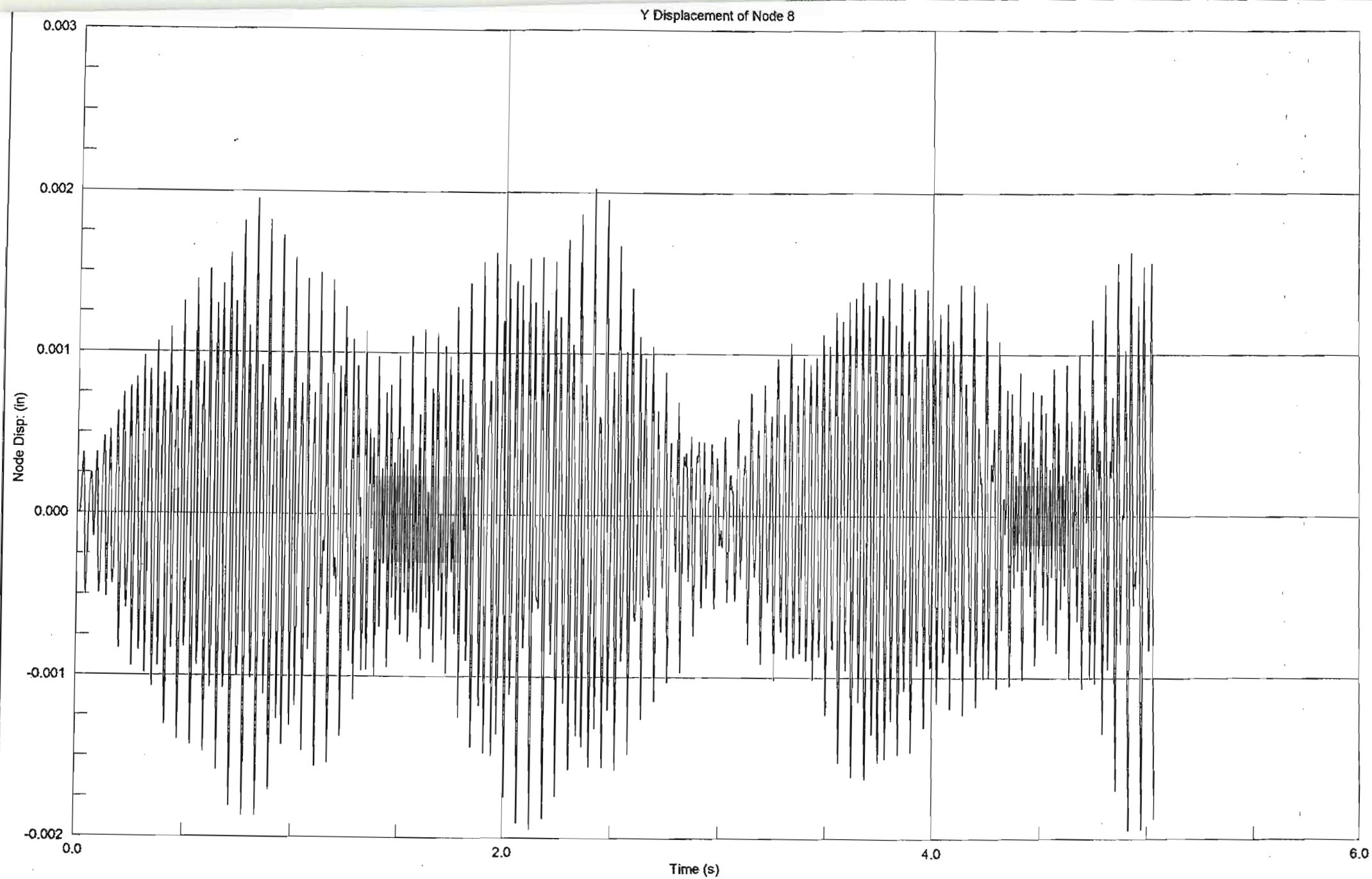
Z Displacement of Node 20



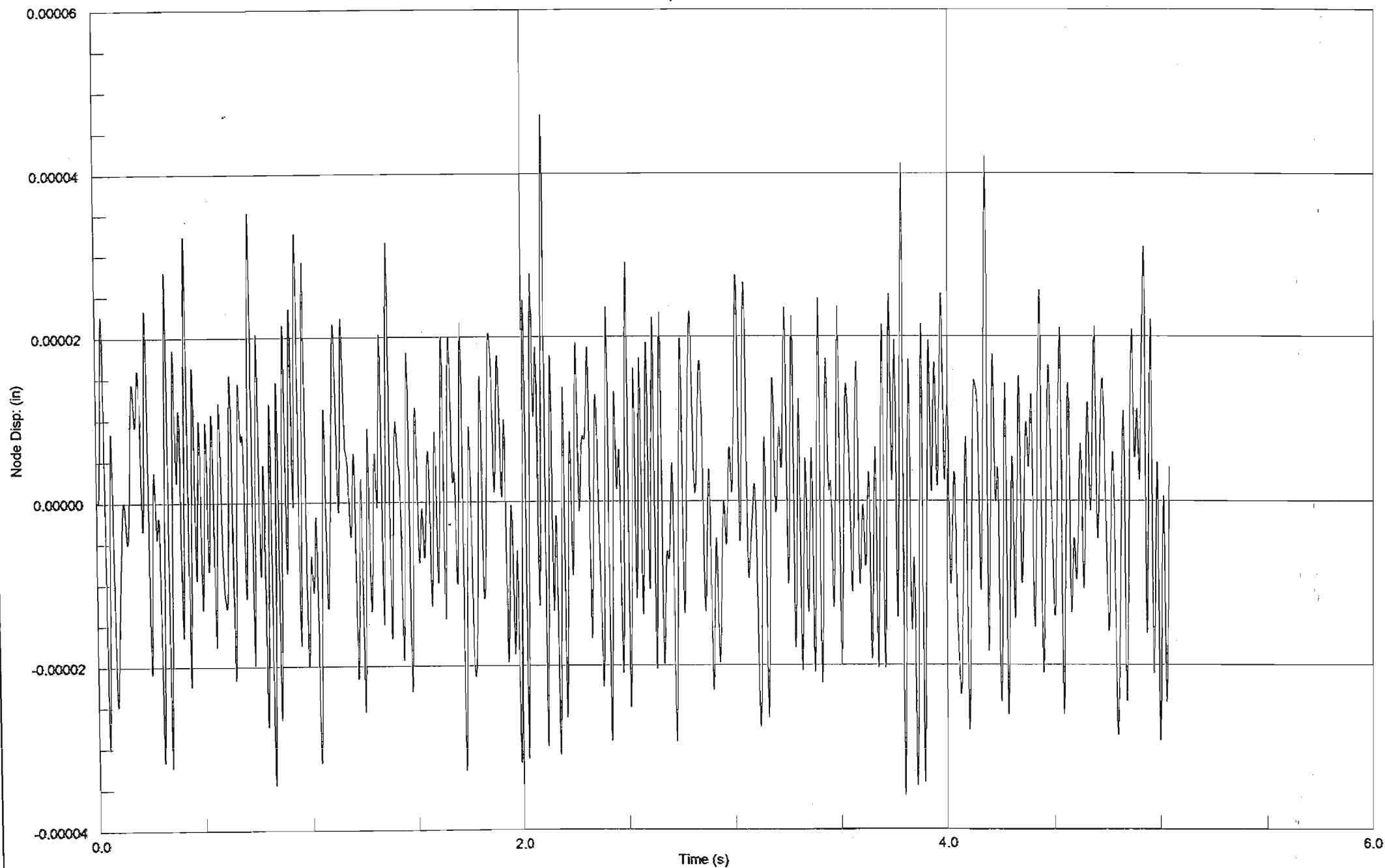
Vy

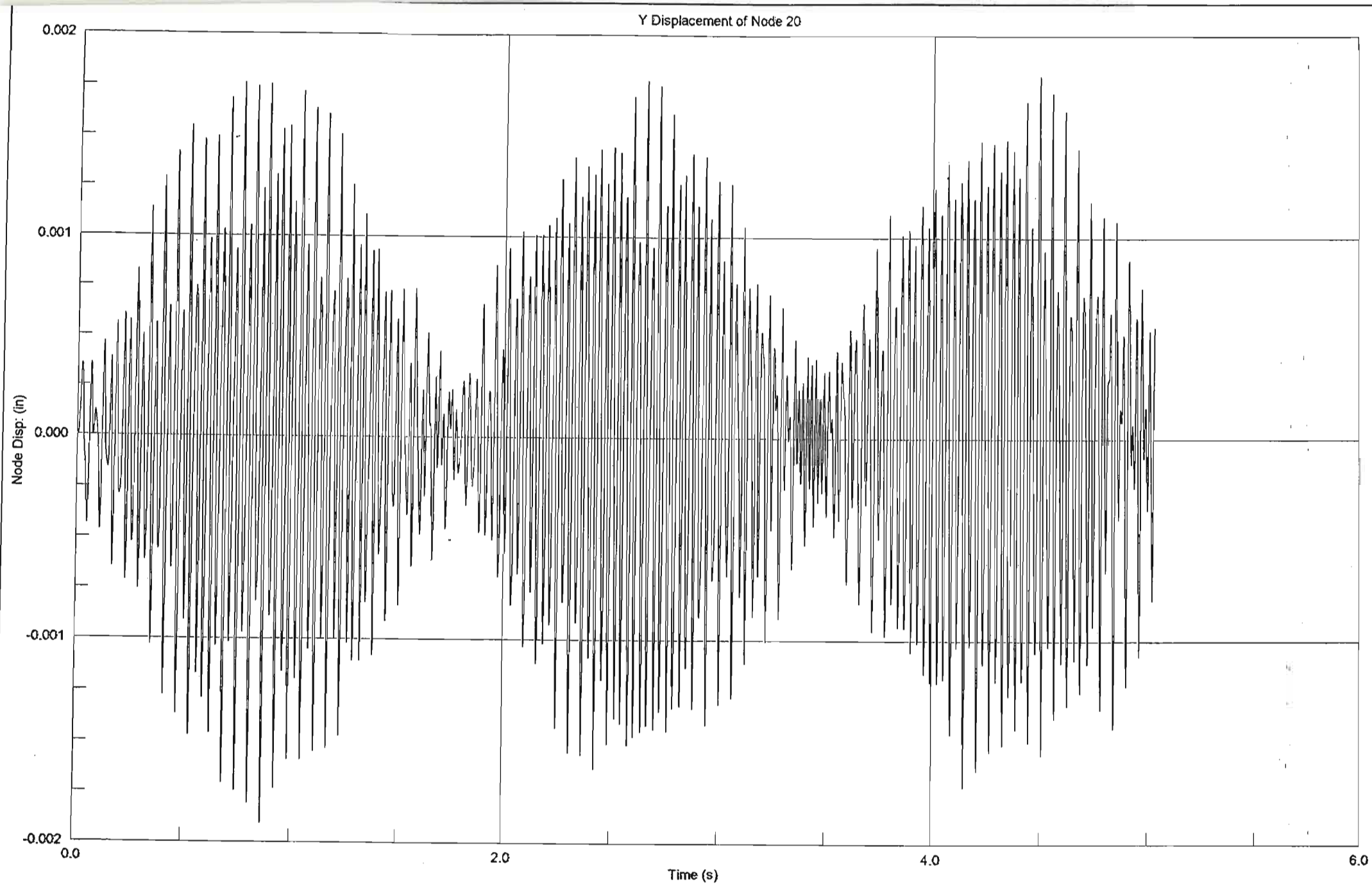




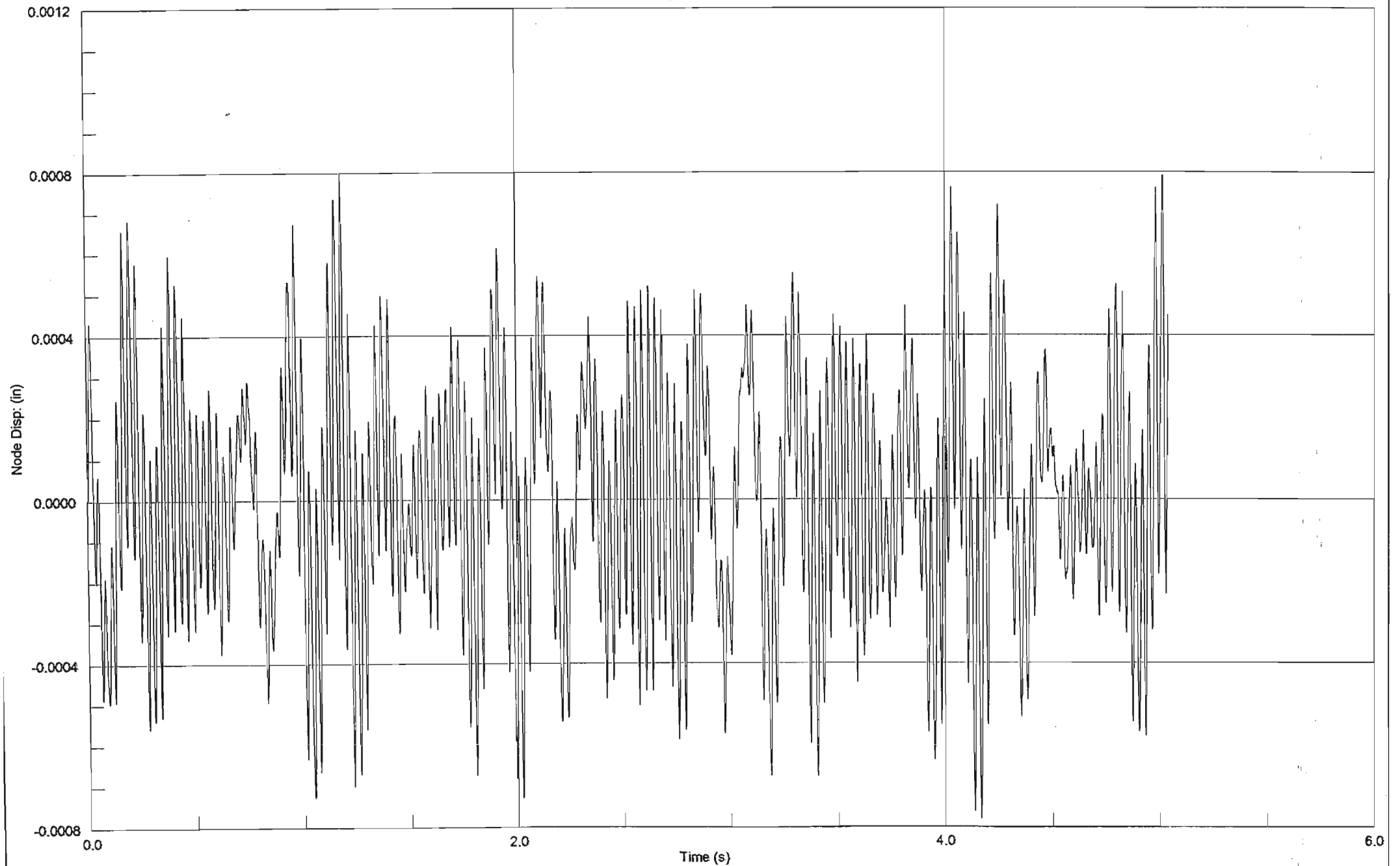


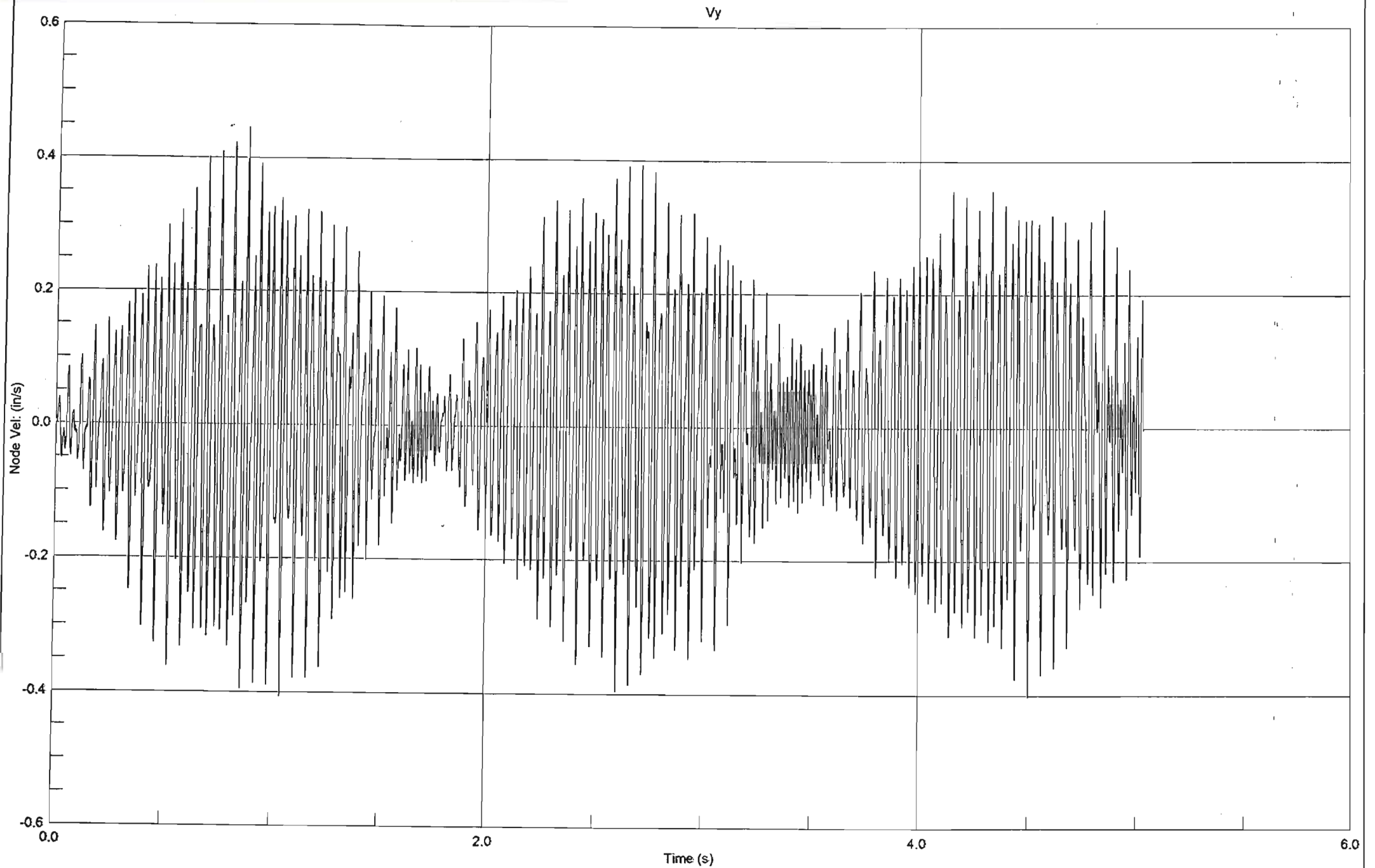
Z Displacement of Node 8

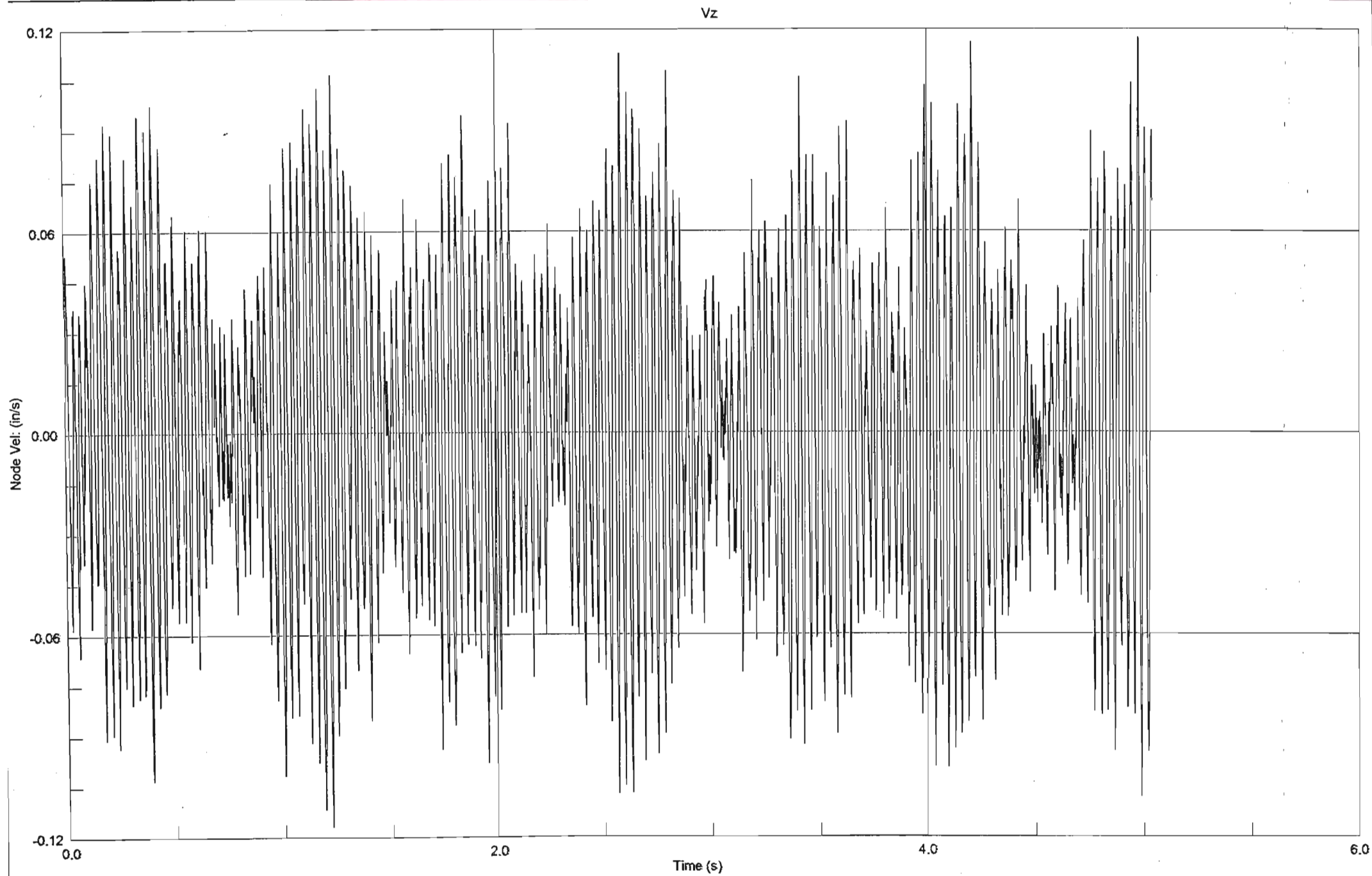




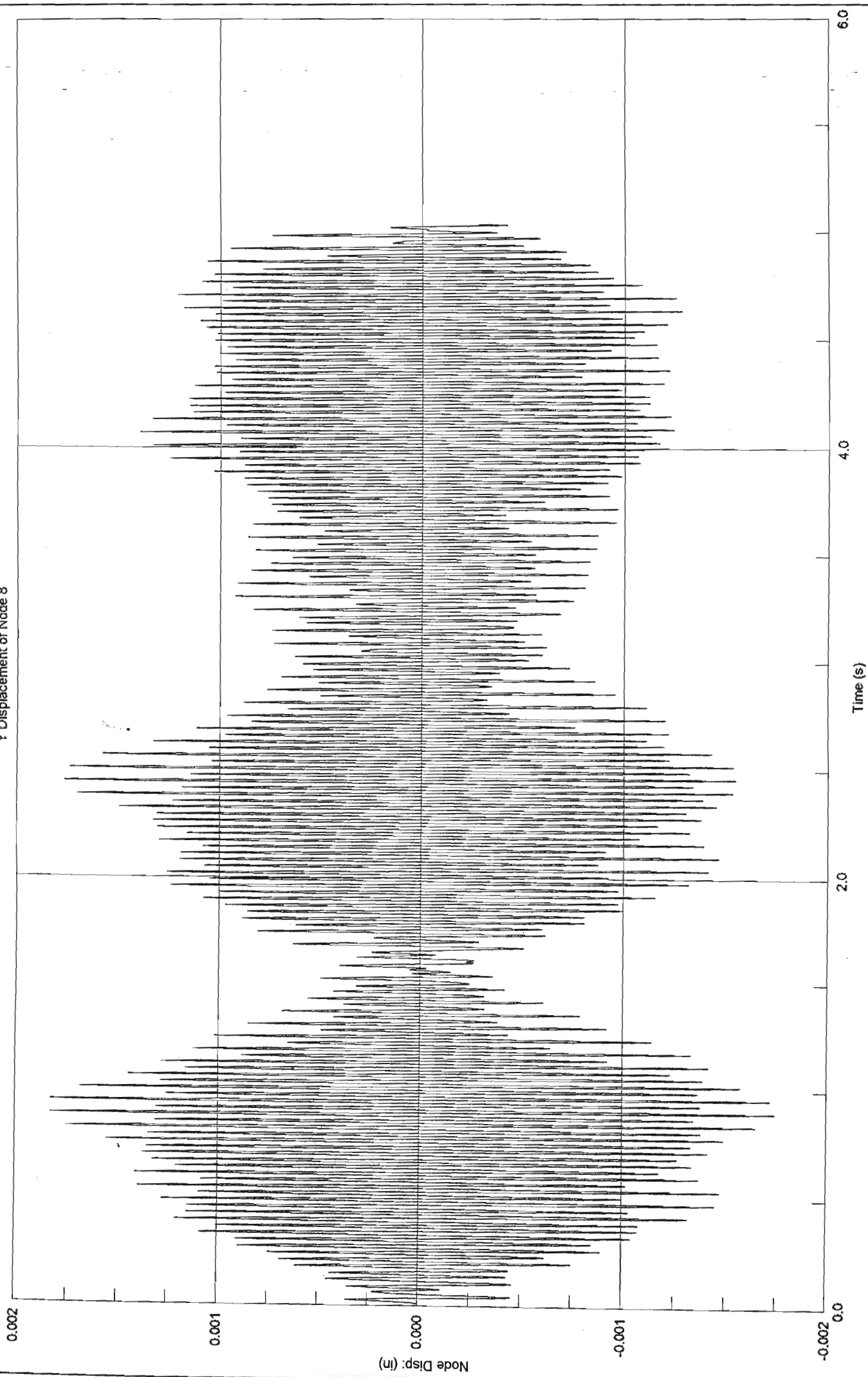
Z Displacement of Node 20



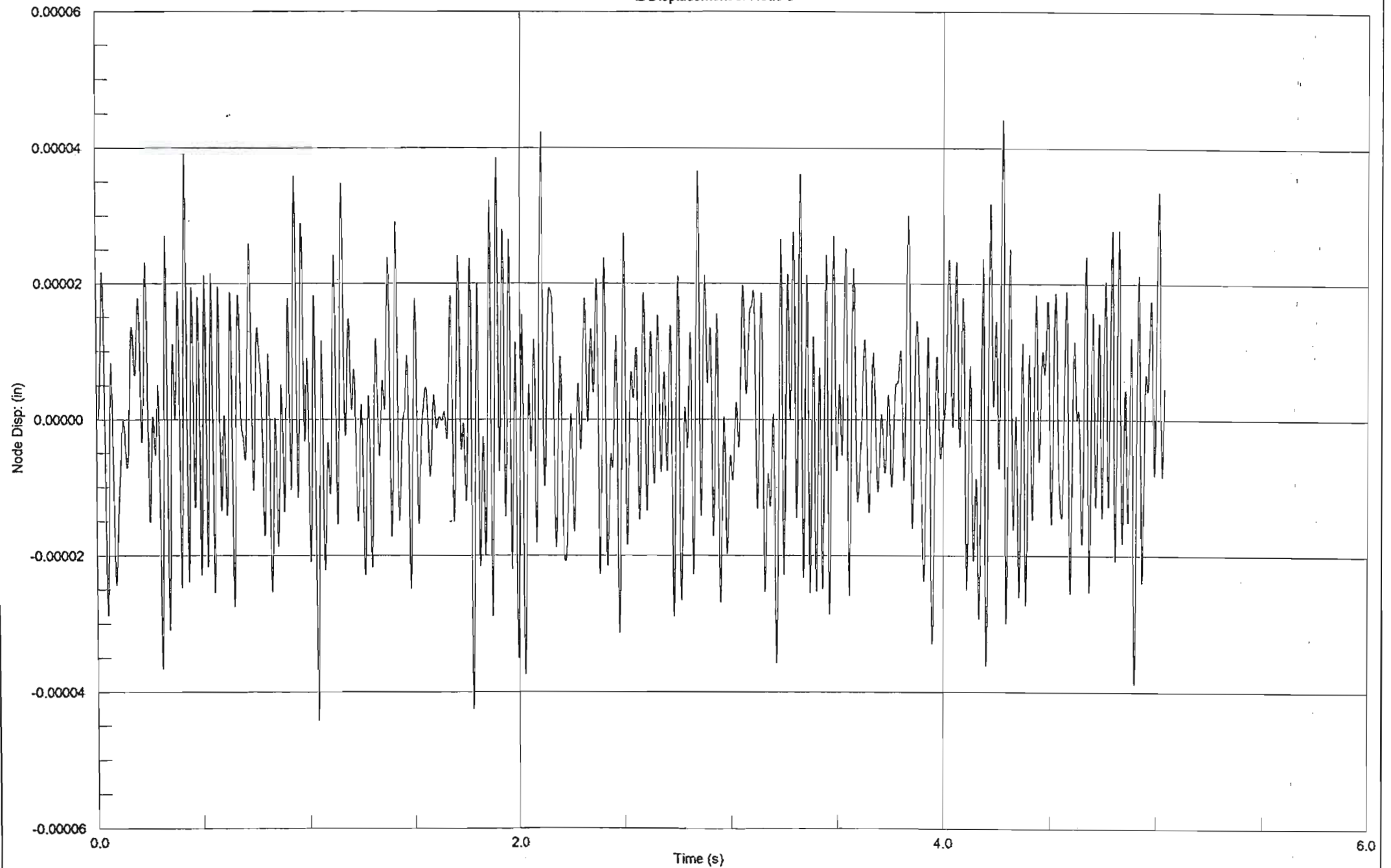


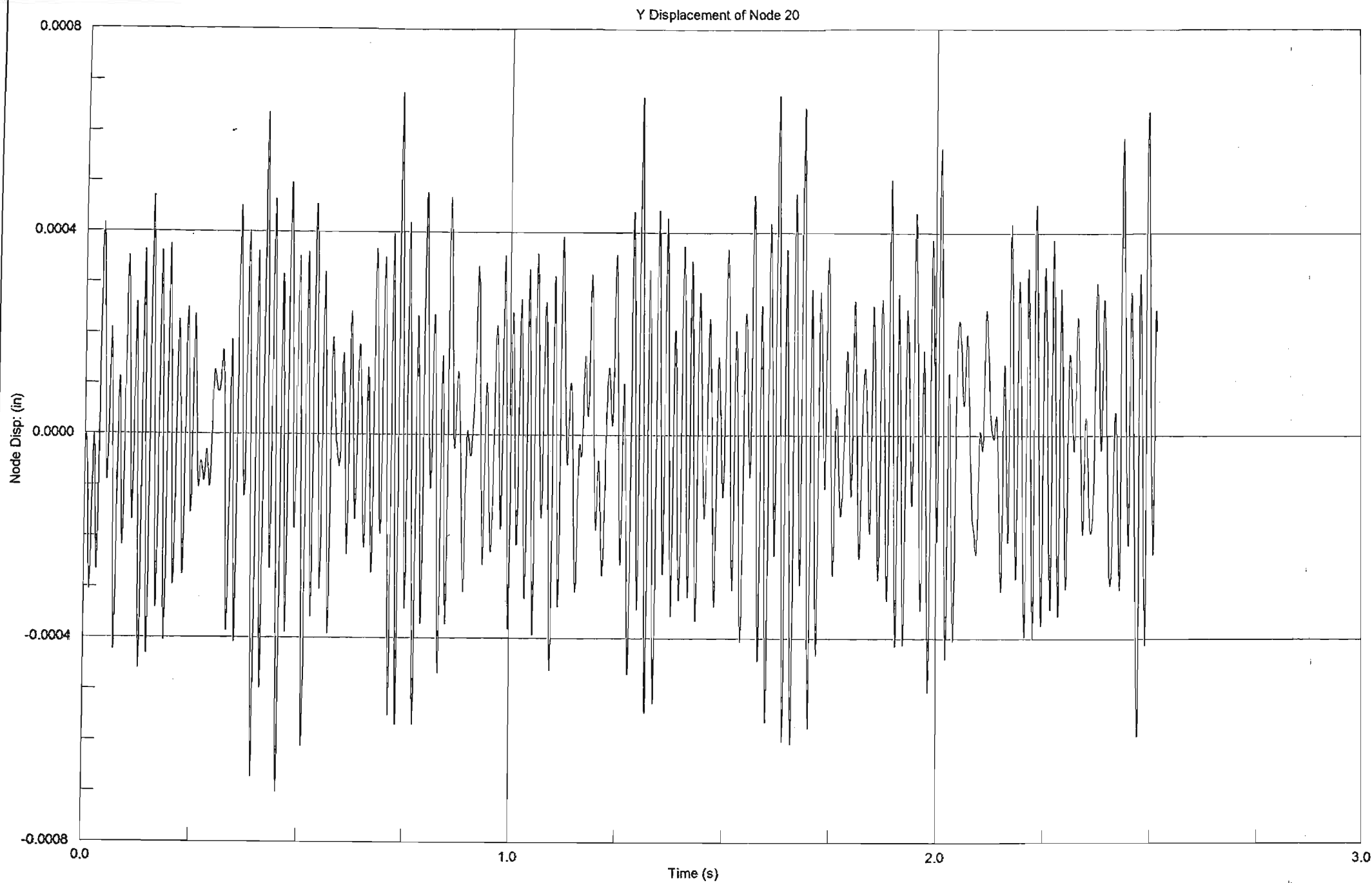


Y Displacement of Node 8

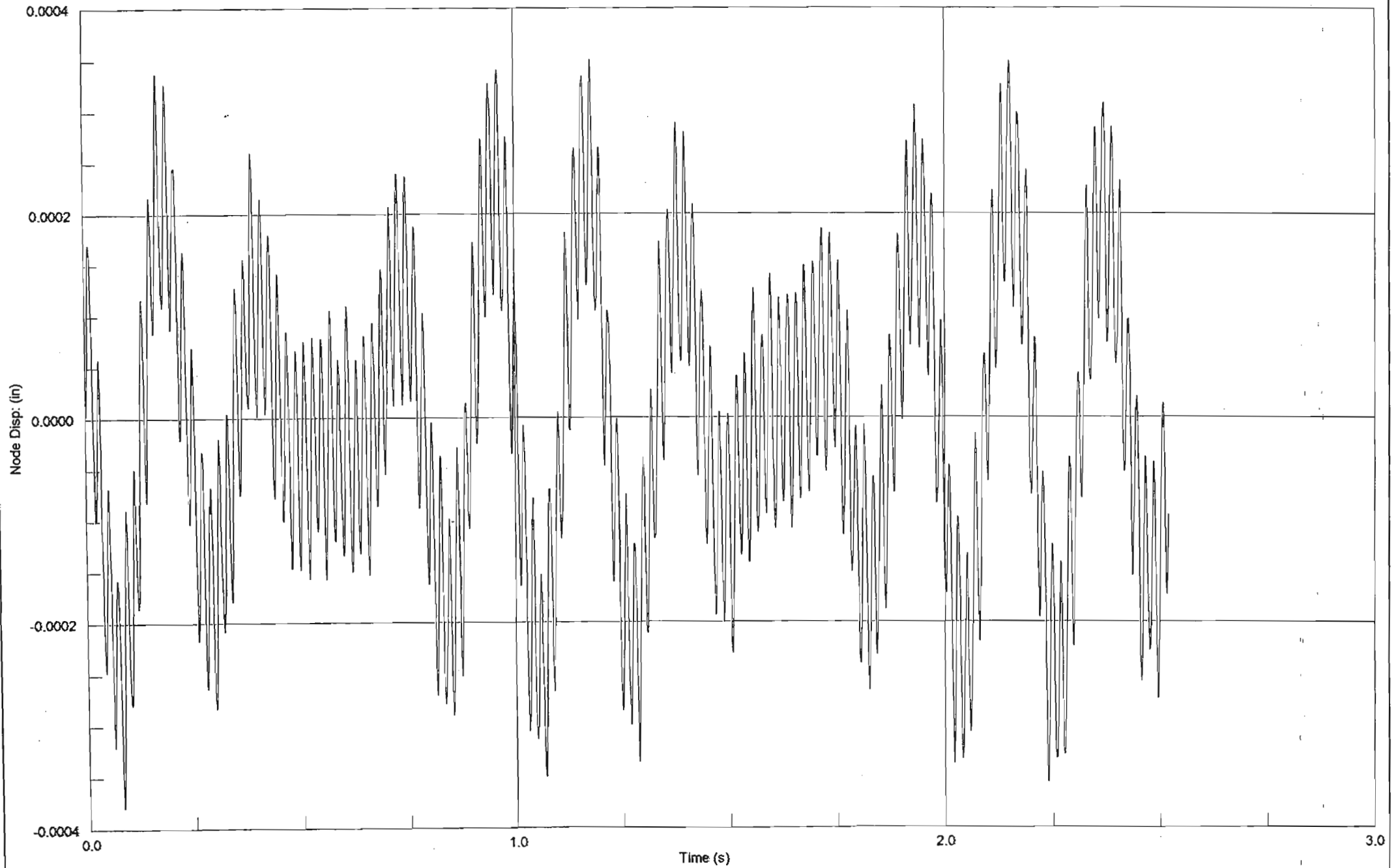


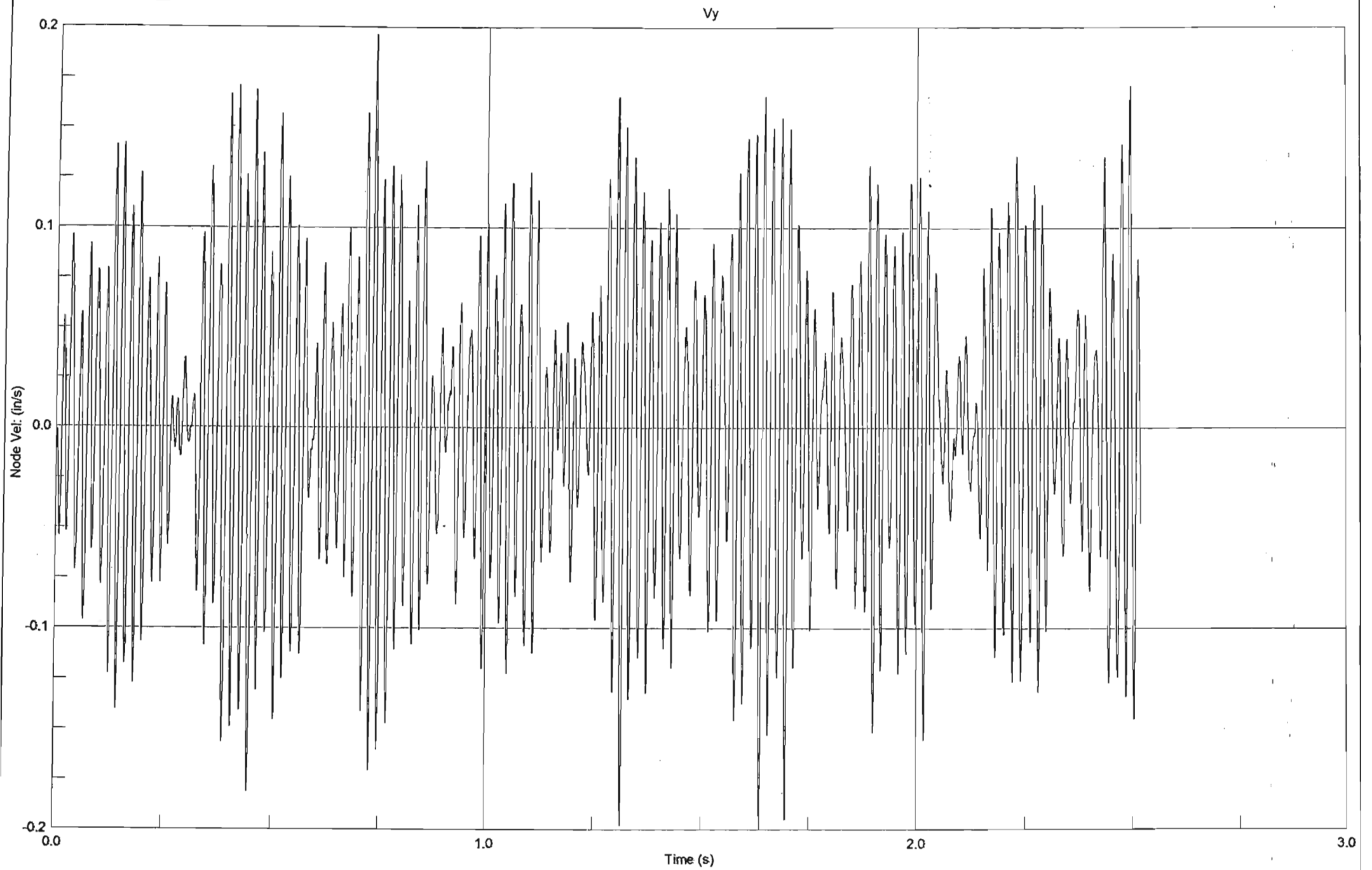
Z Displacement of Node 8

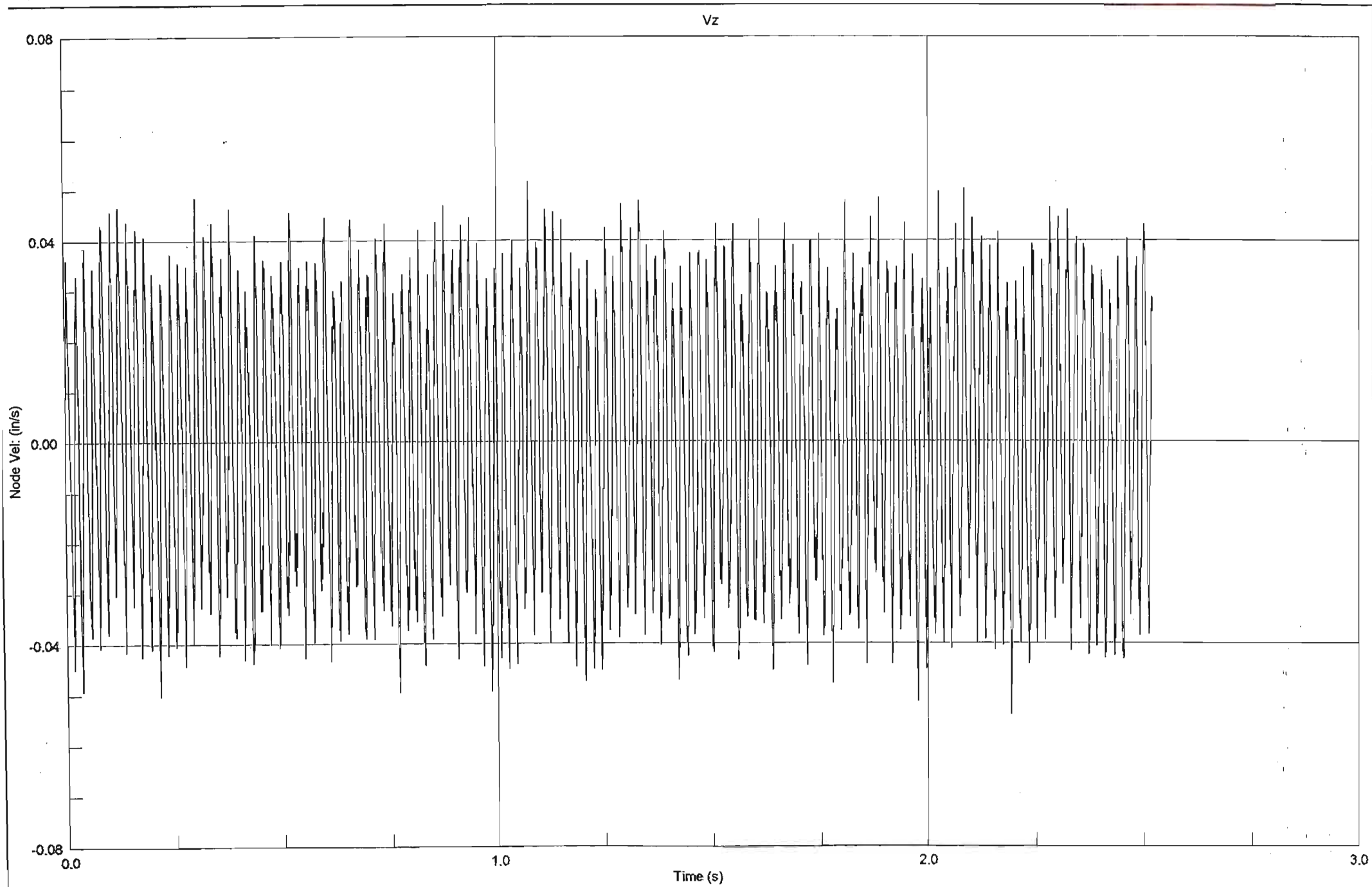


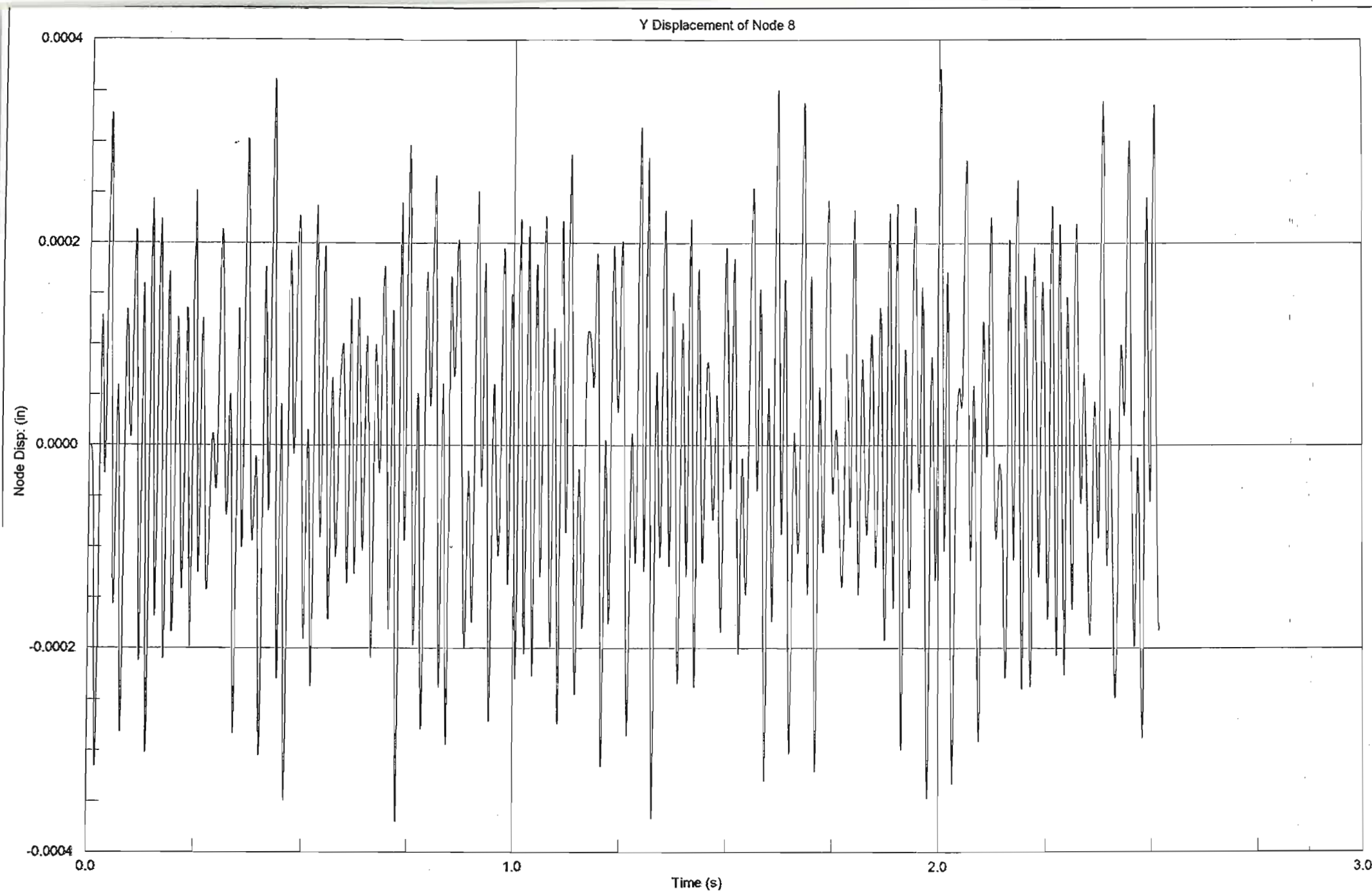


Z Displacement of Node 20

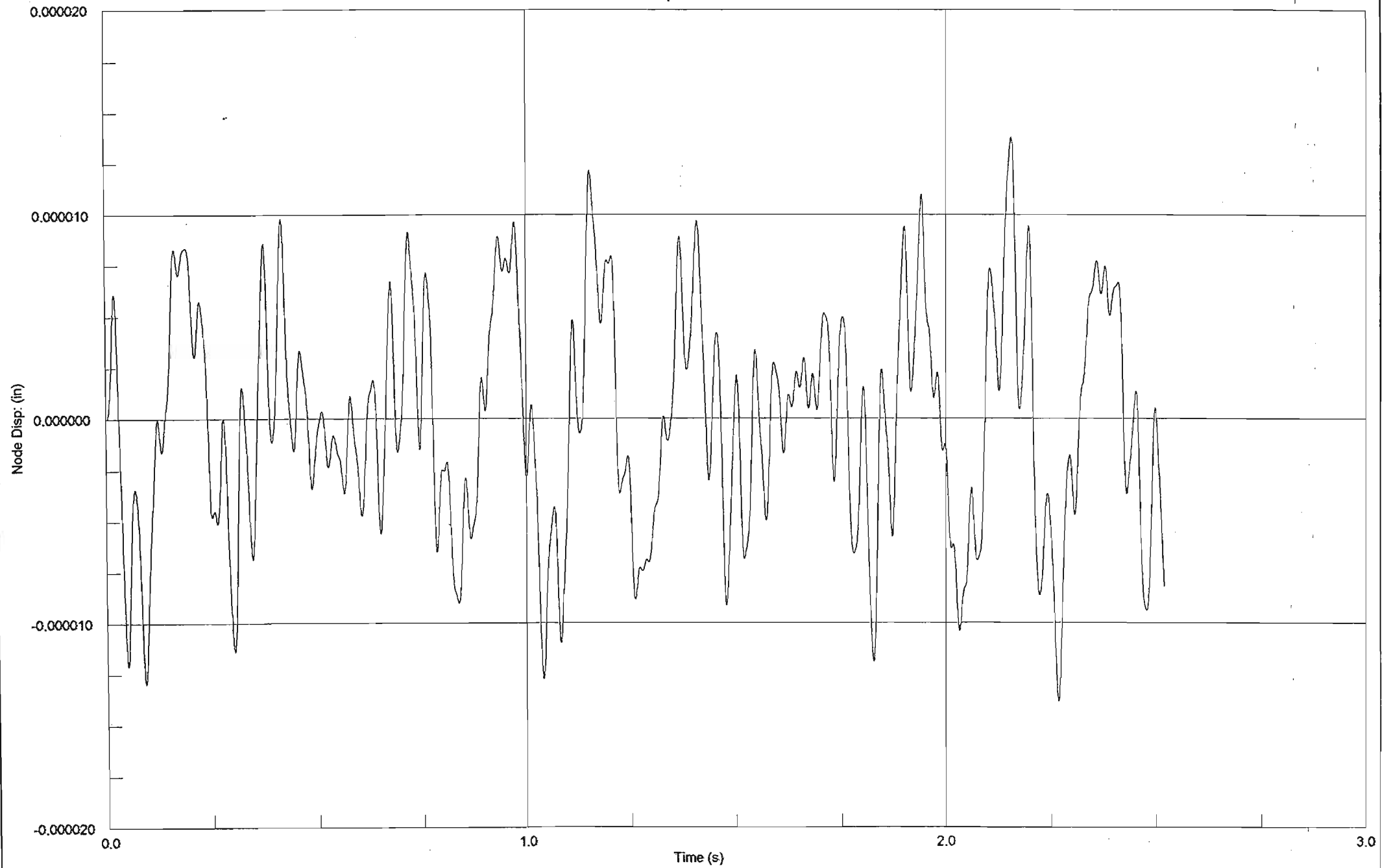


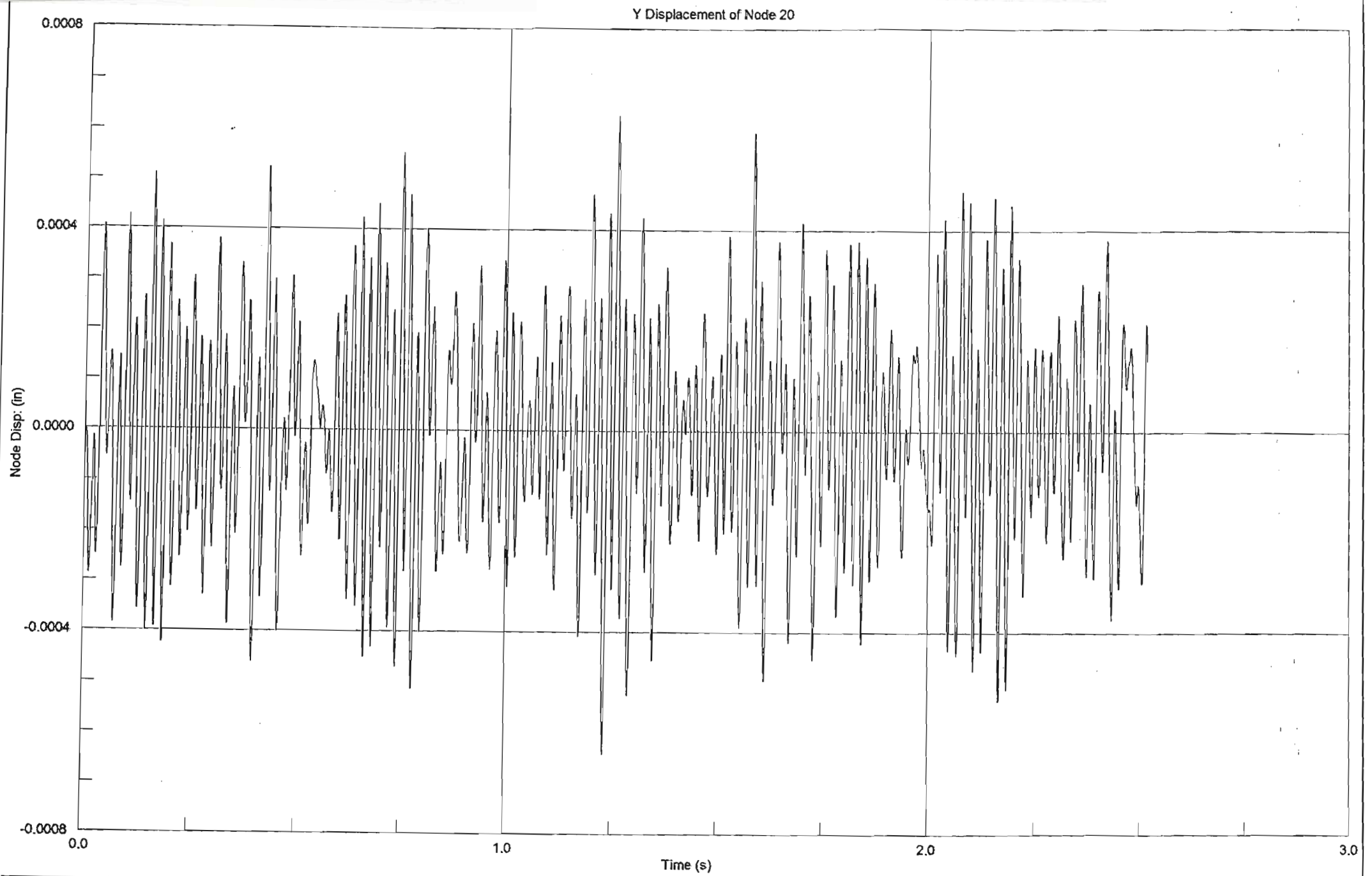




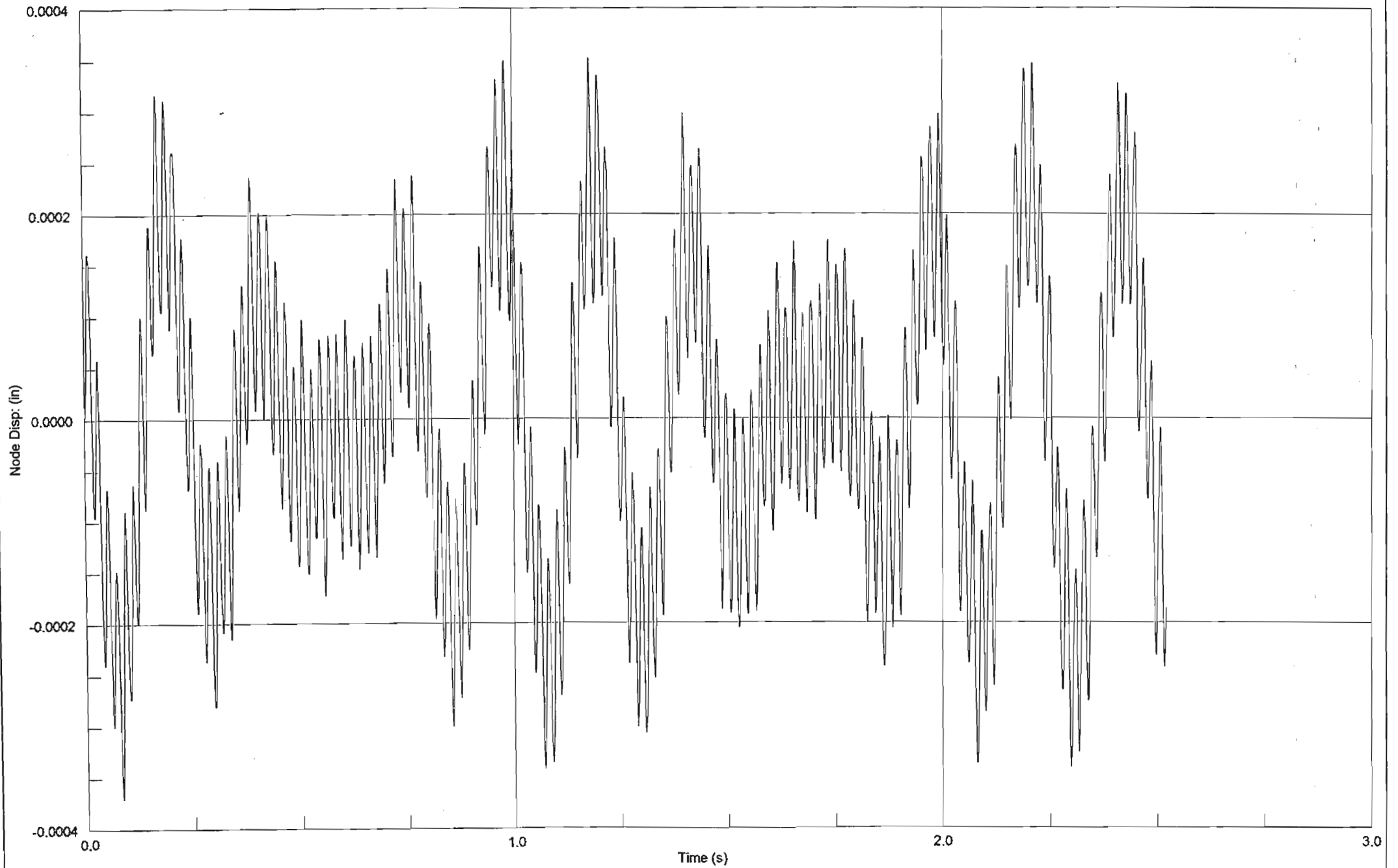


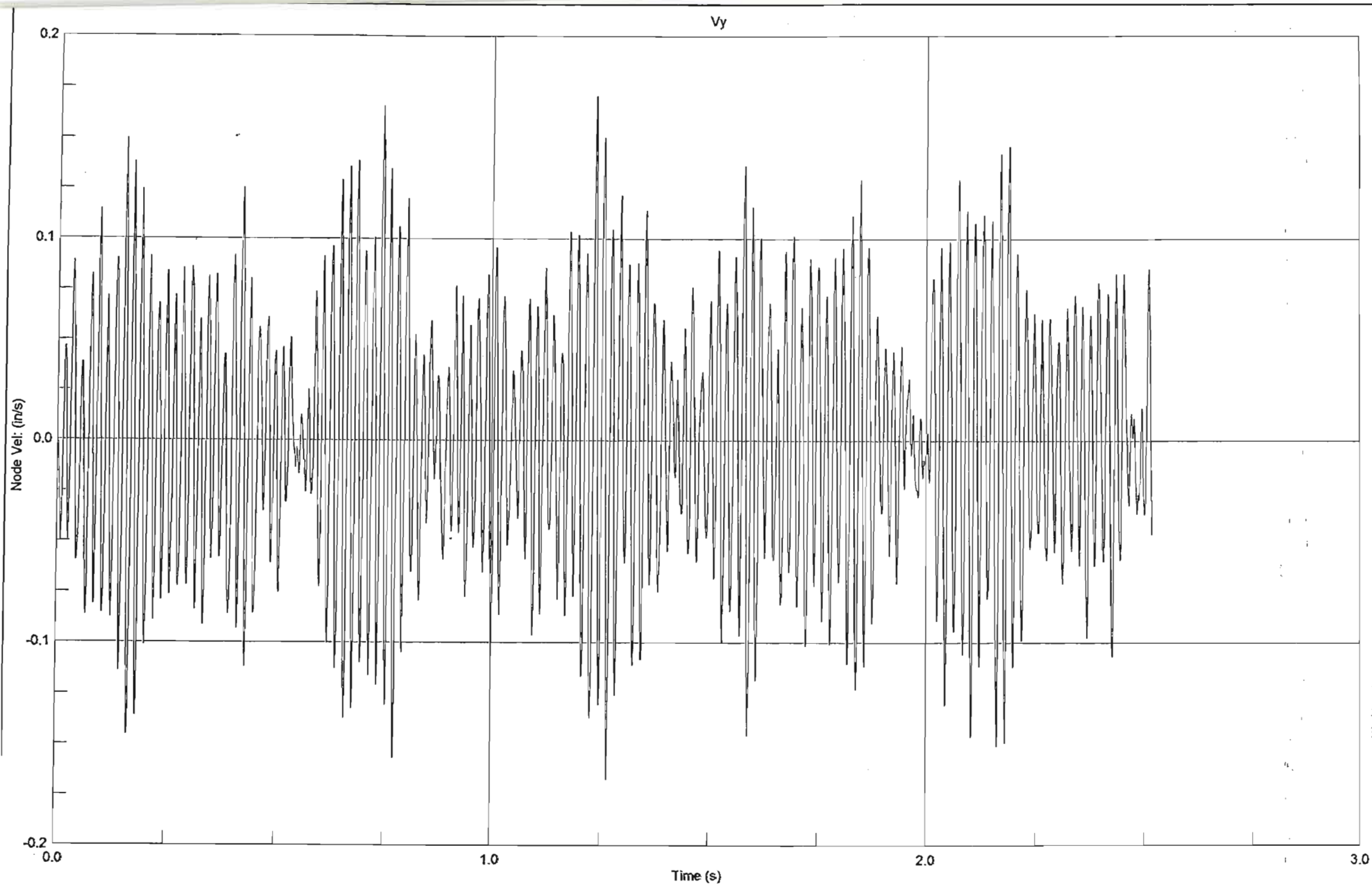
Z Displacement of Node 8



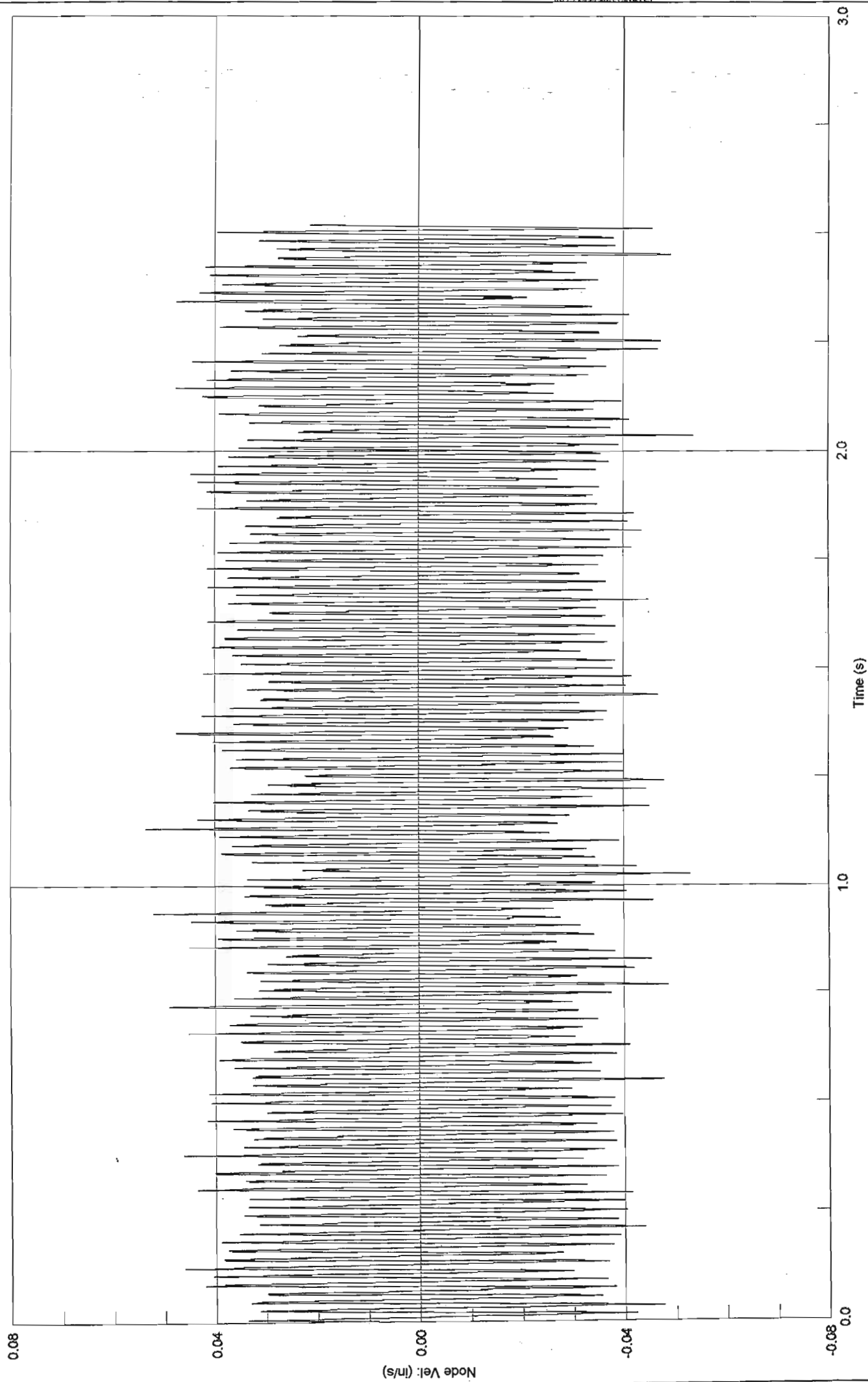


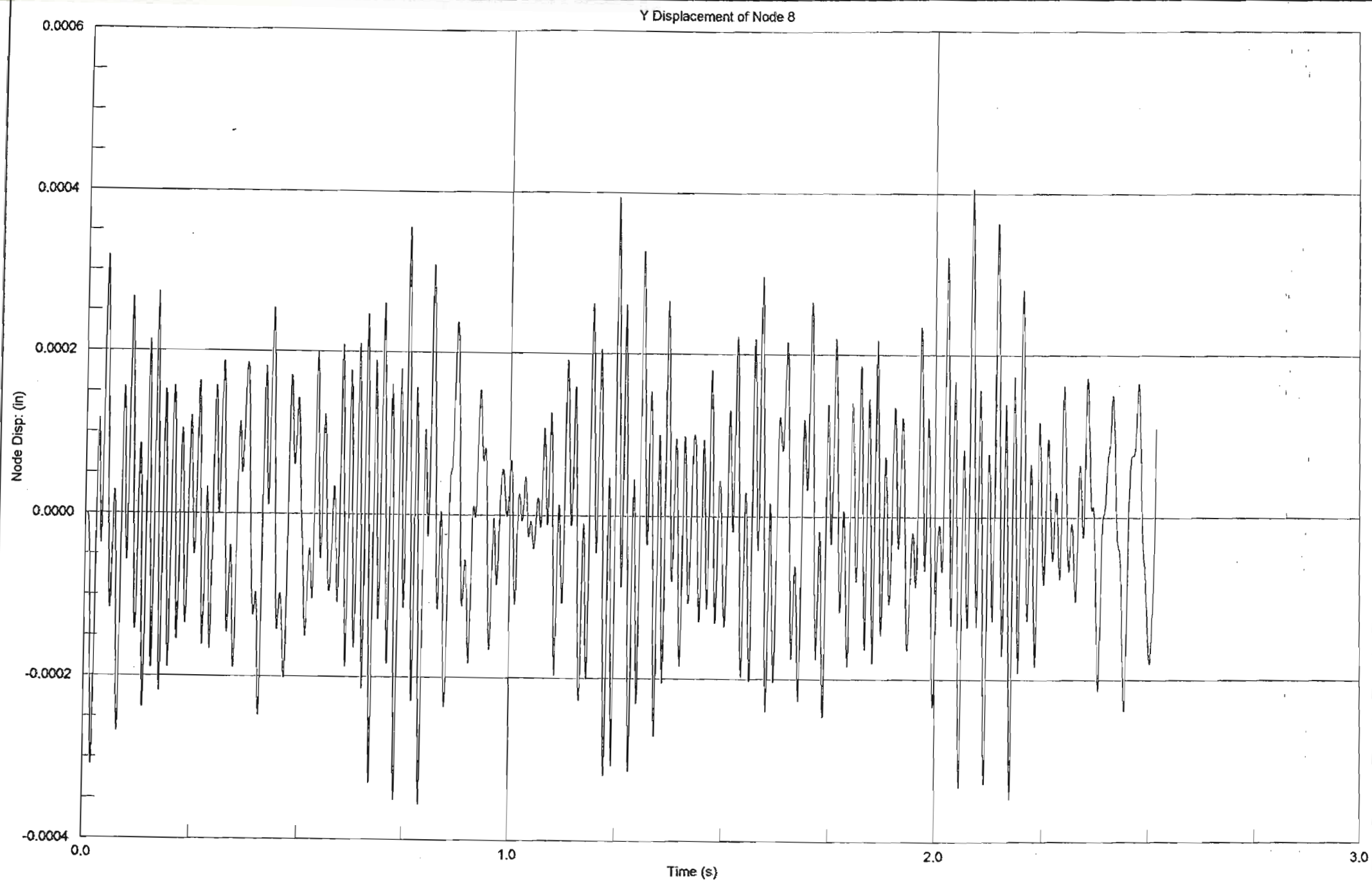
Z Displacement of Node 20



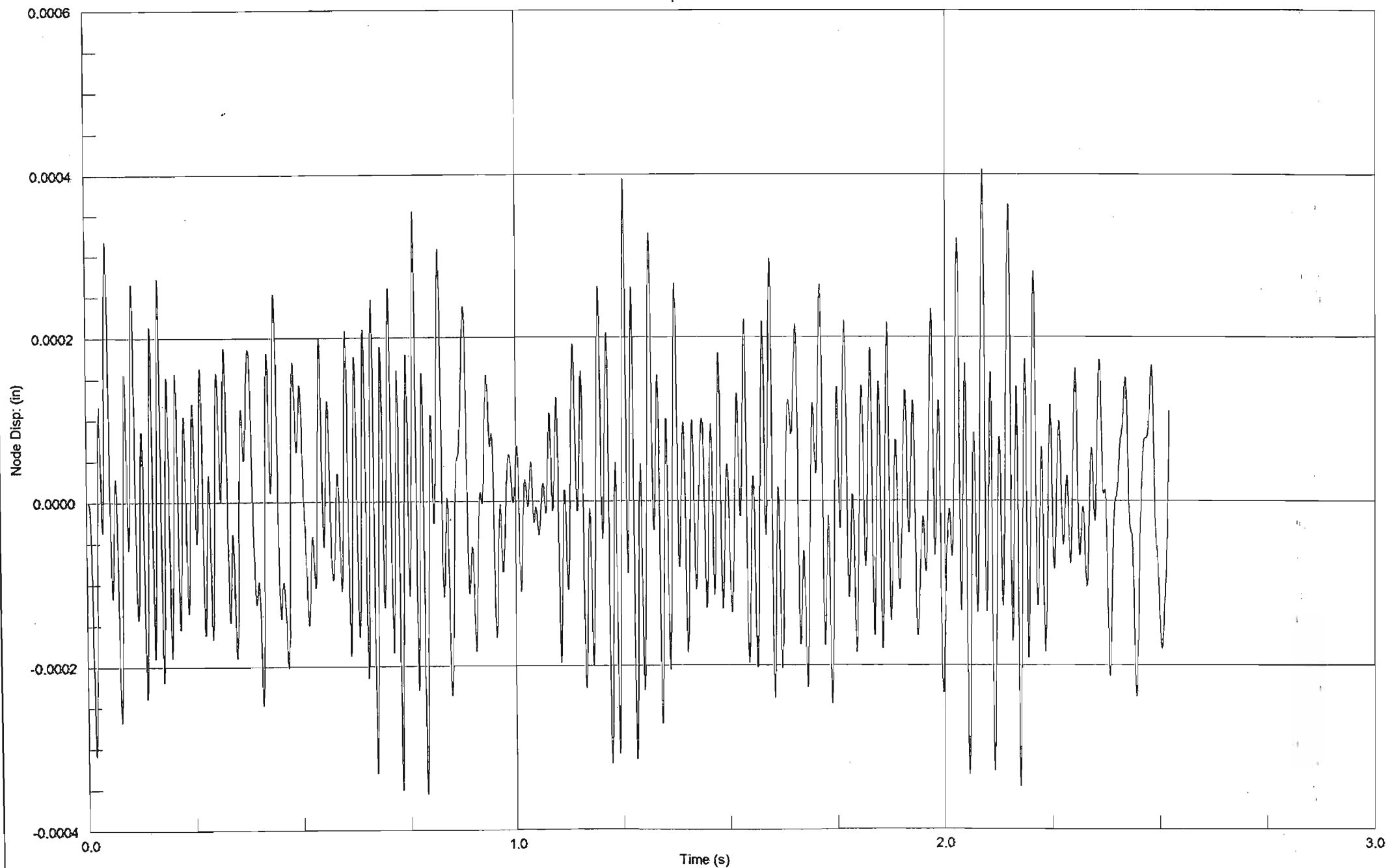


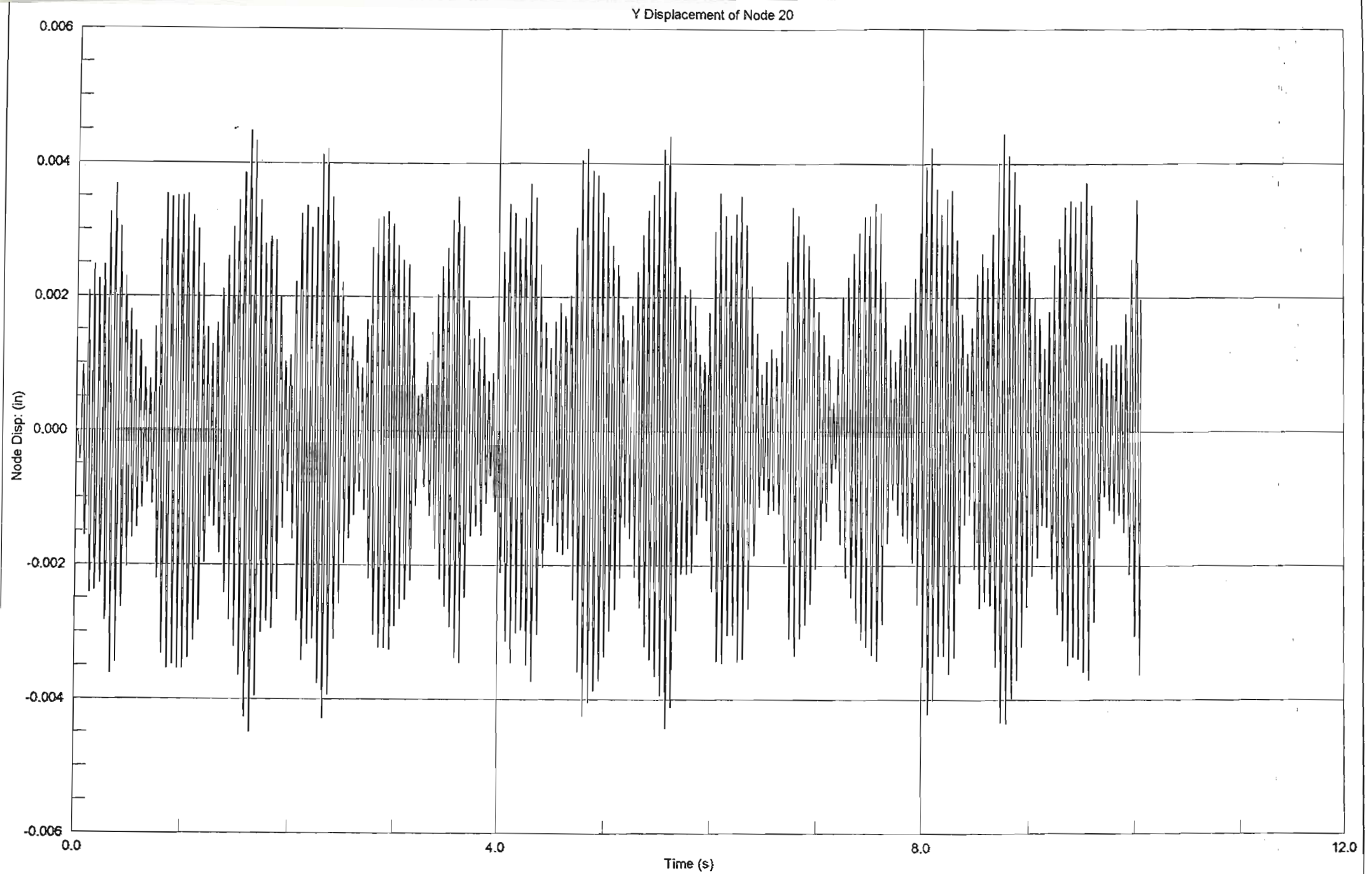
Vz



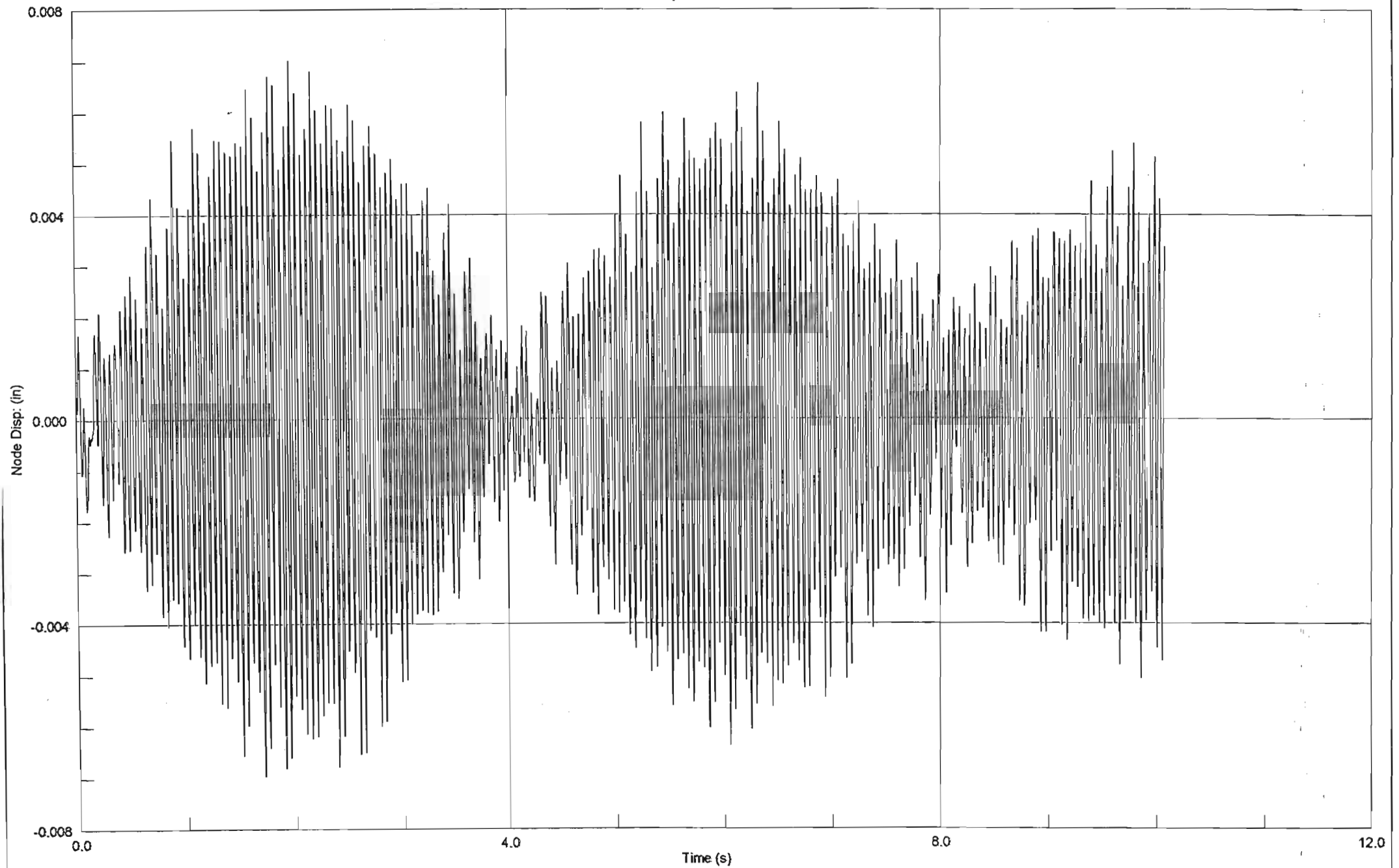


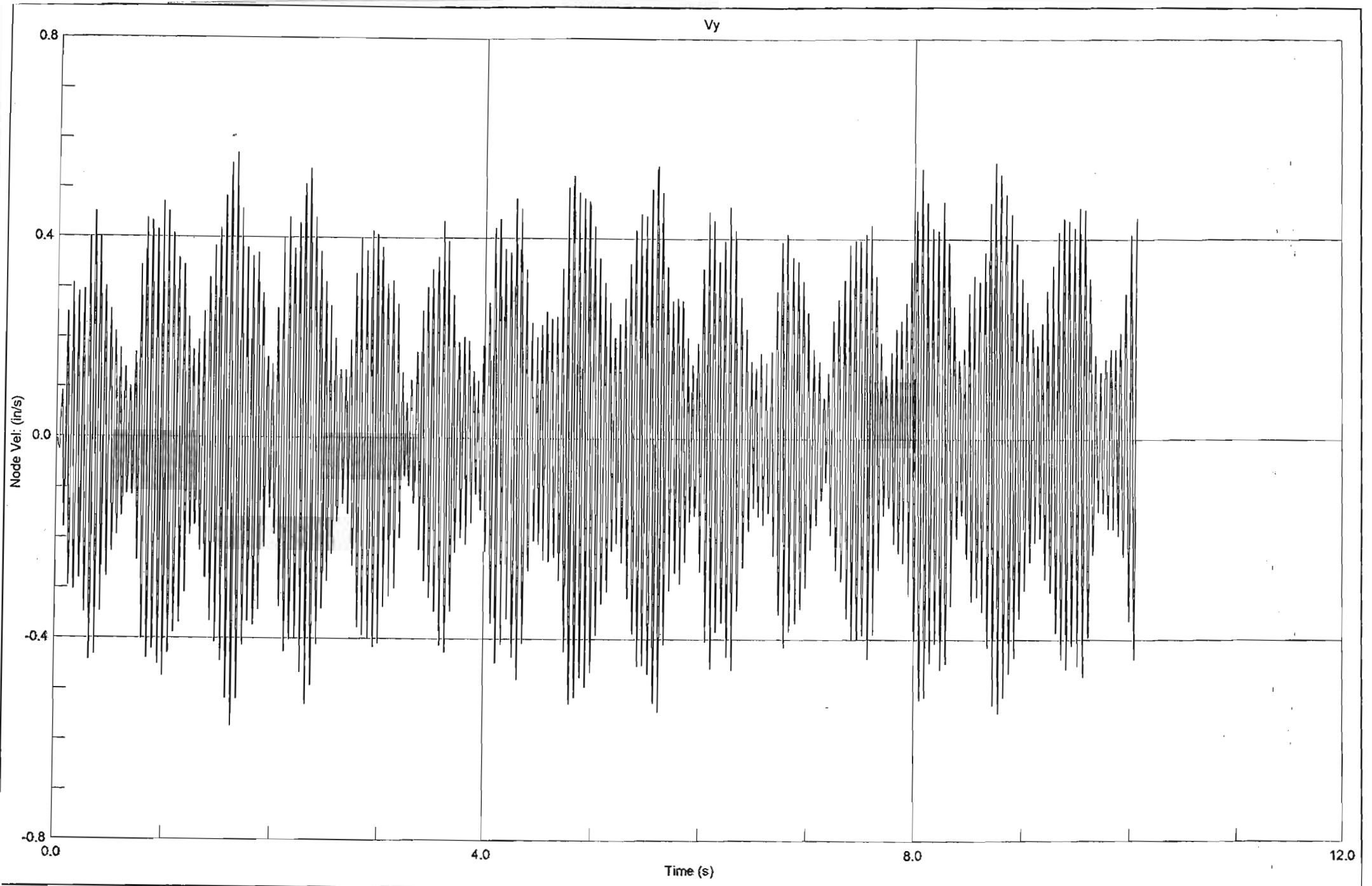
Z Displacement of Node 8

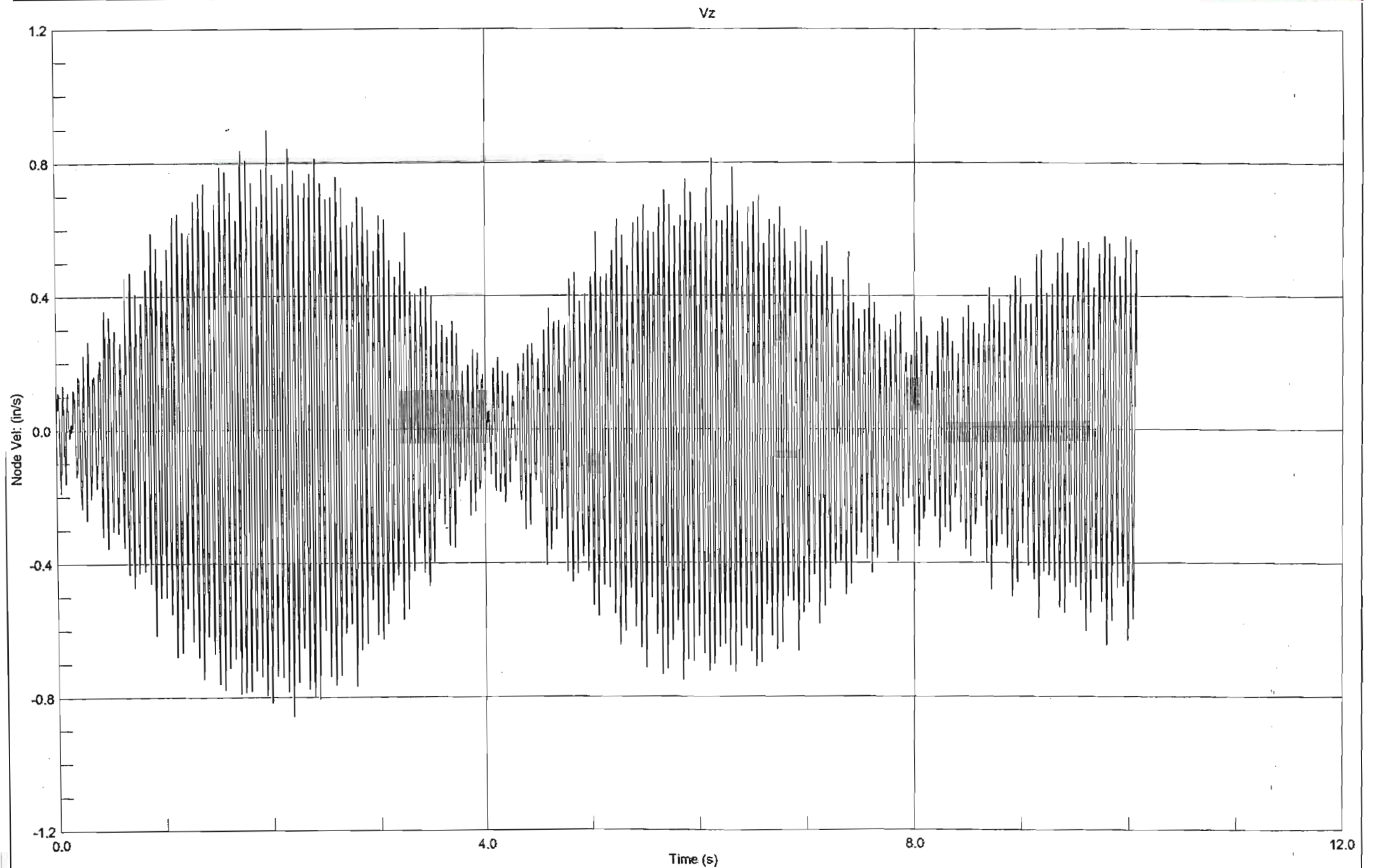


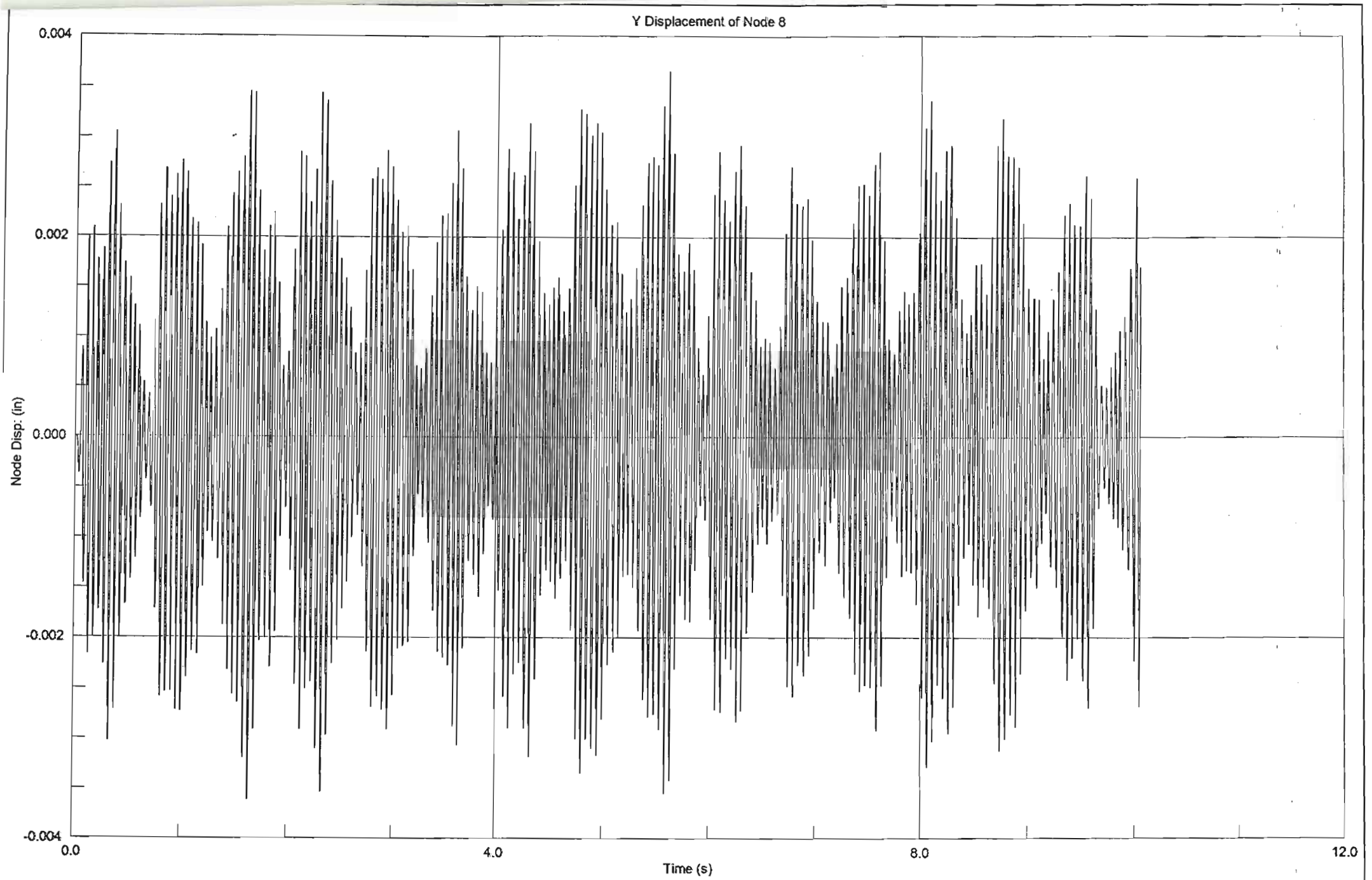


Z Displacement of Node 20

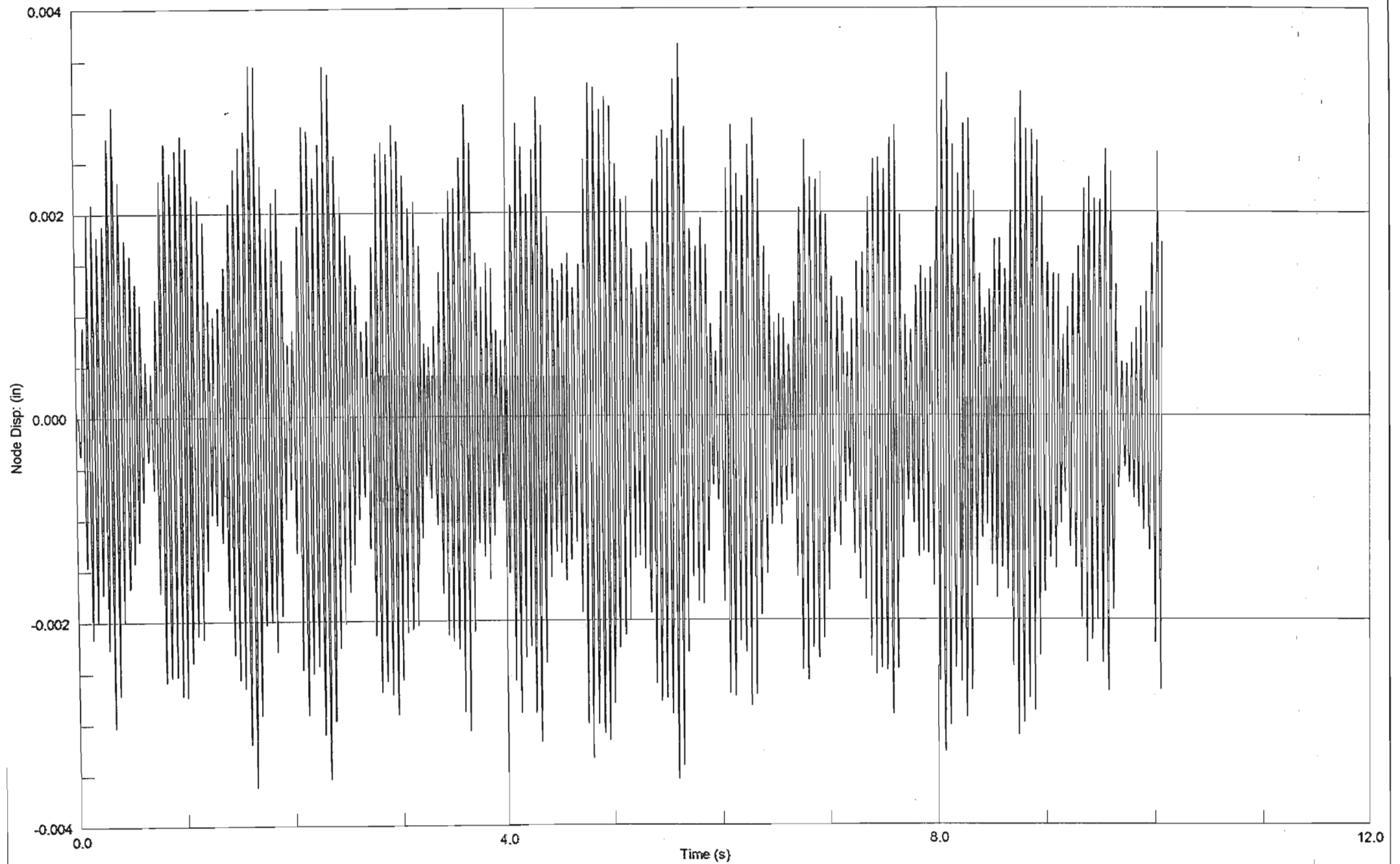


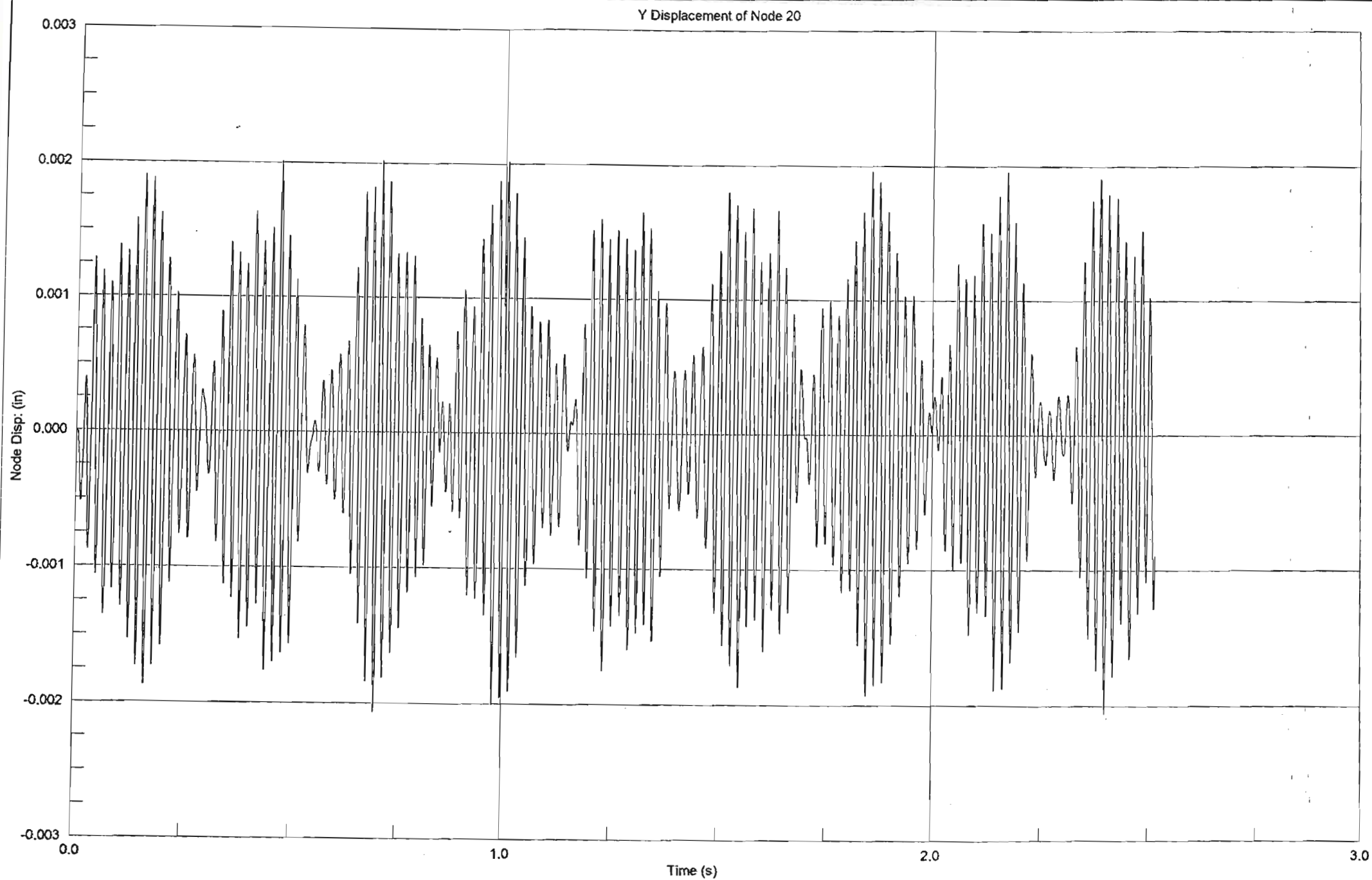


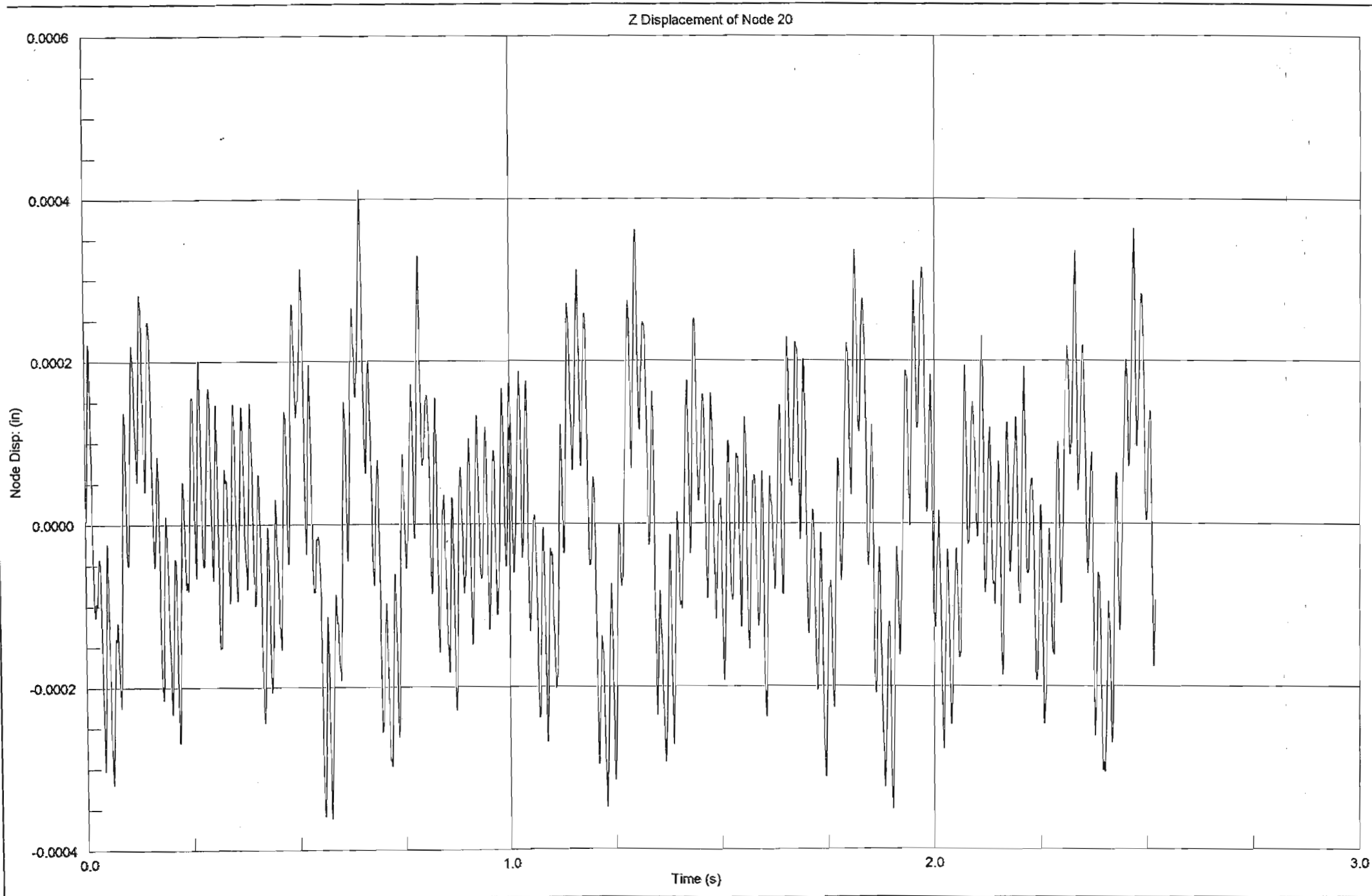


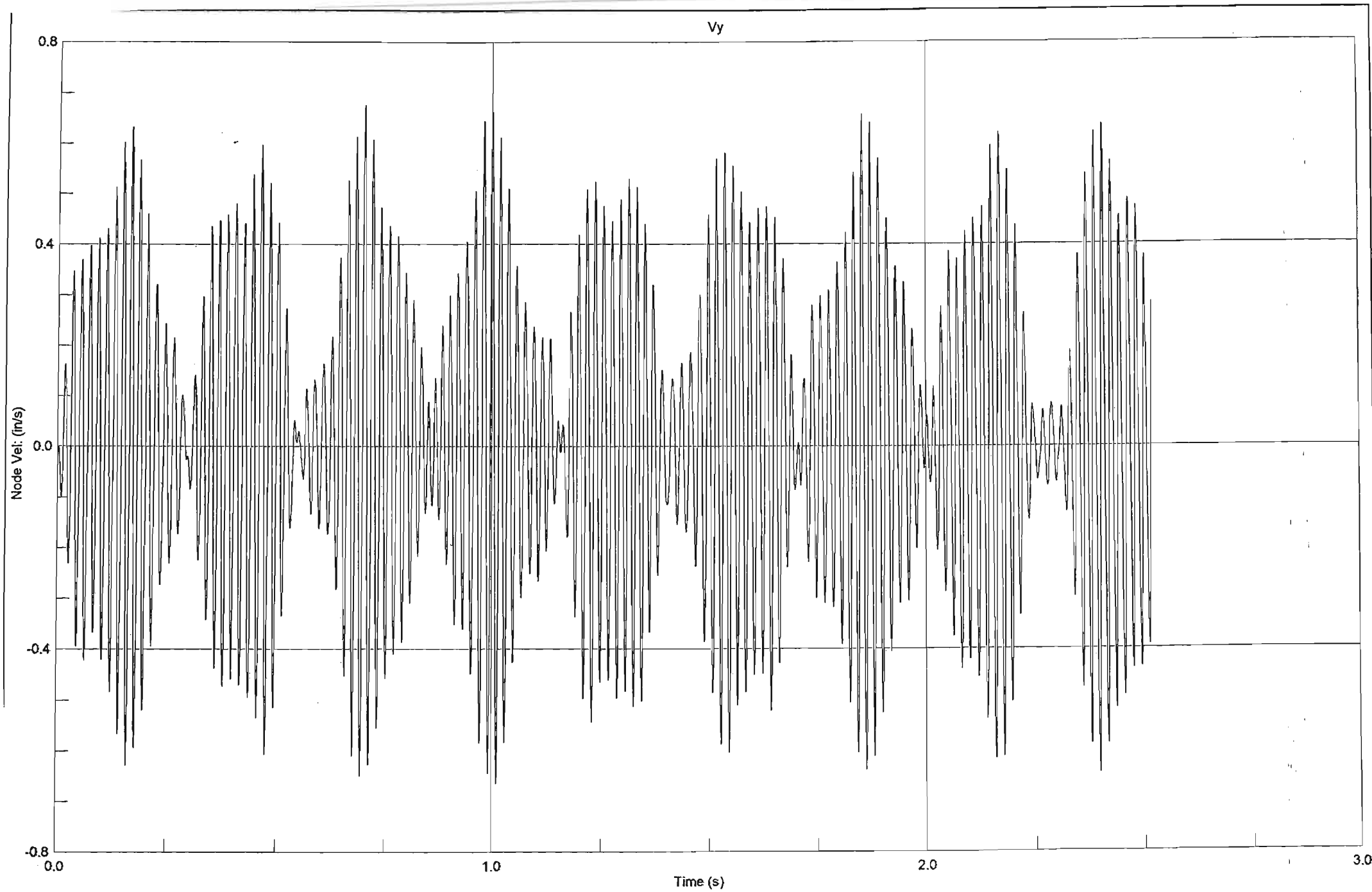


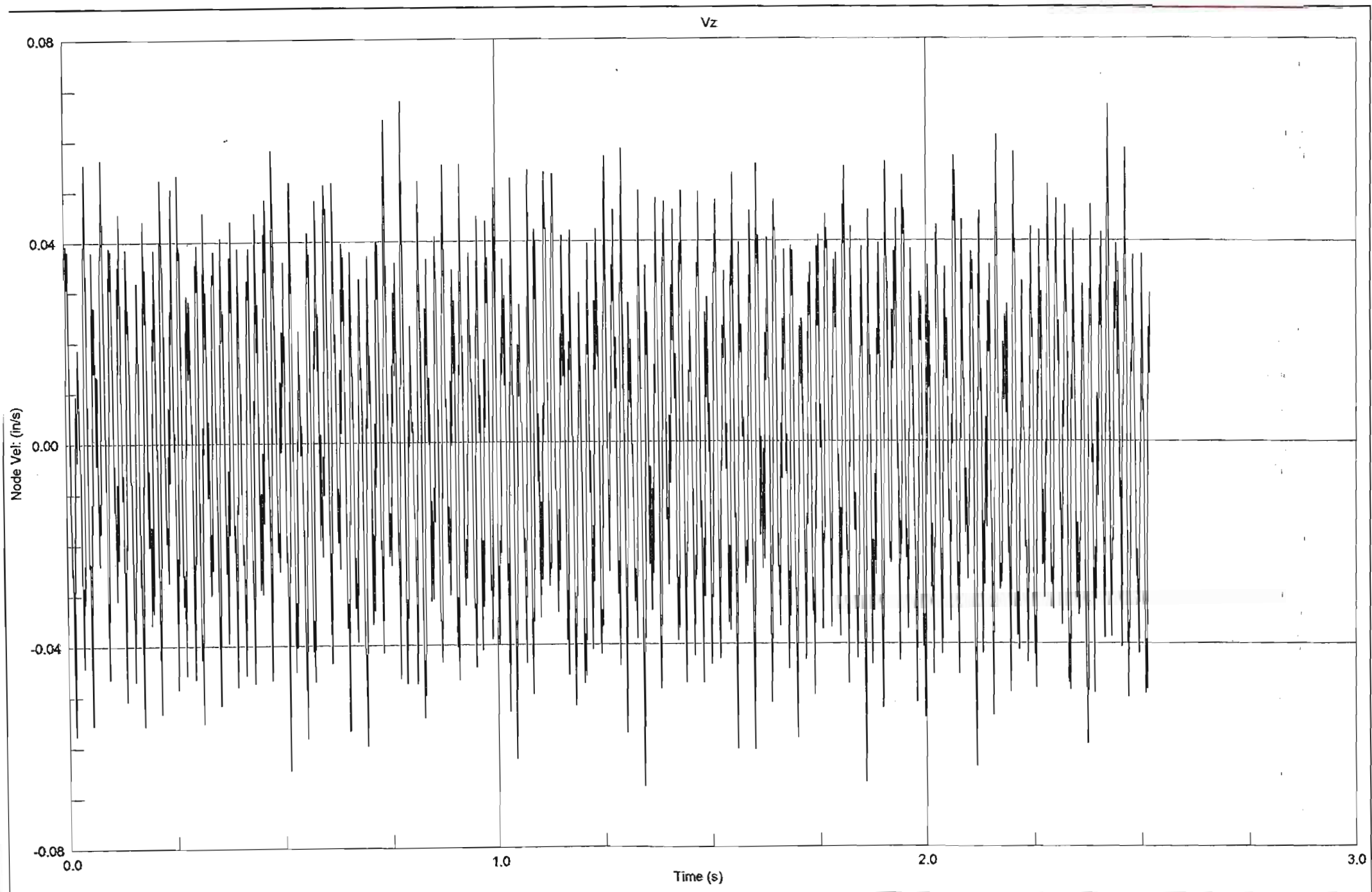
Z Displacement of Node 8

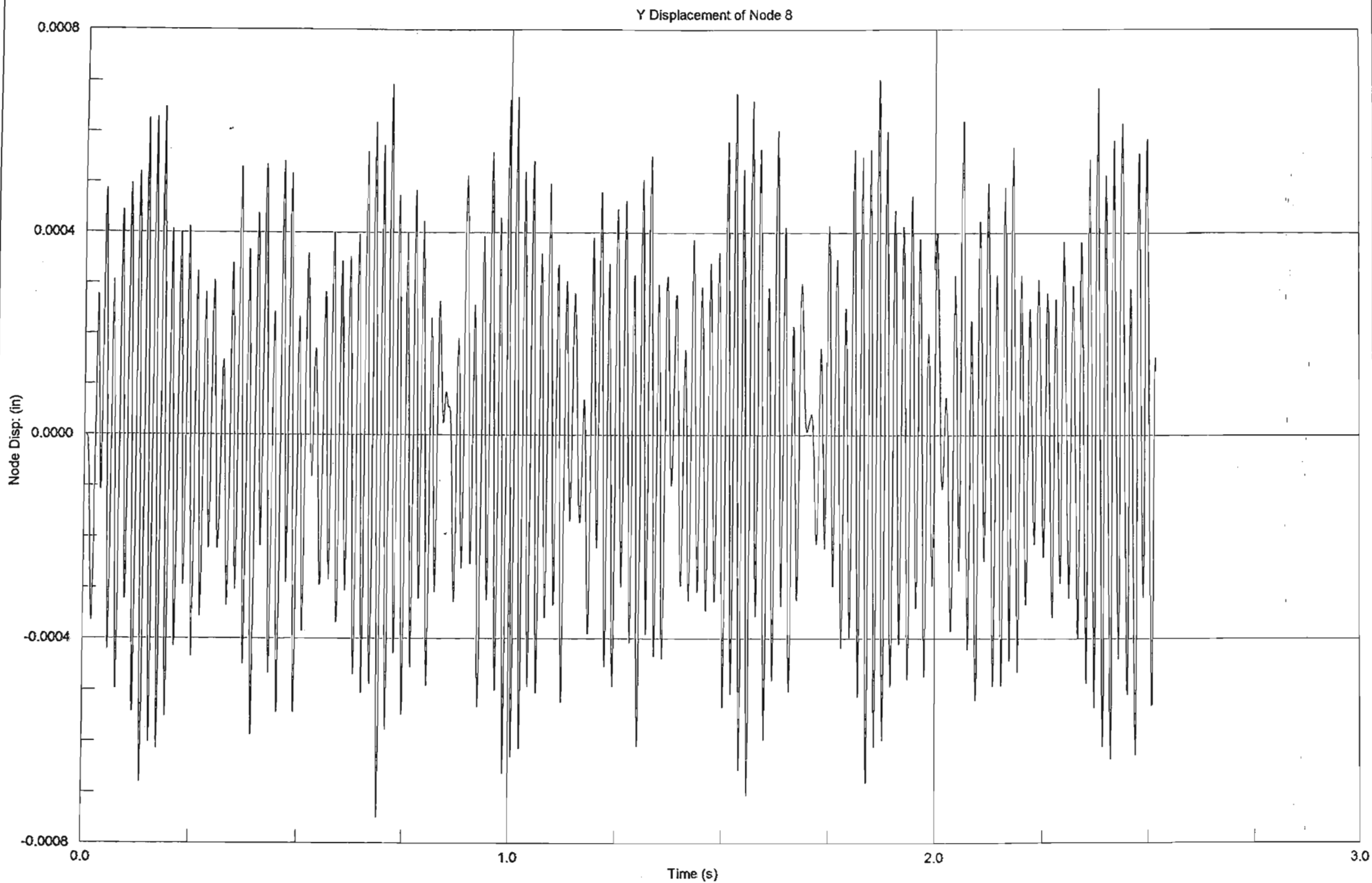




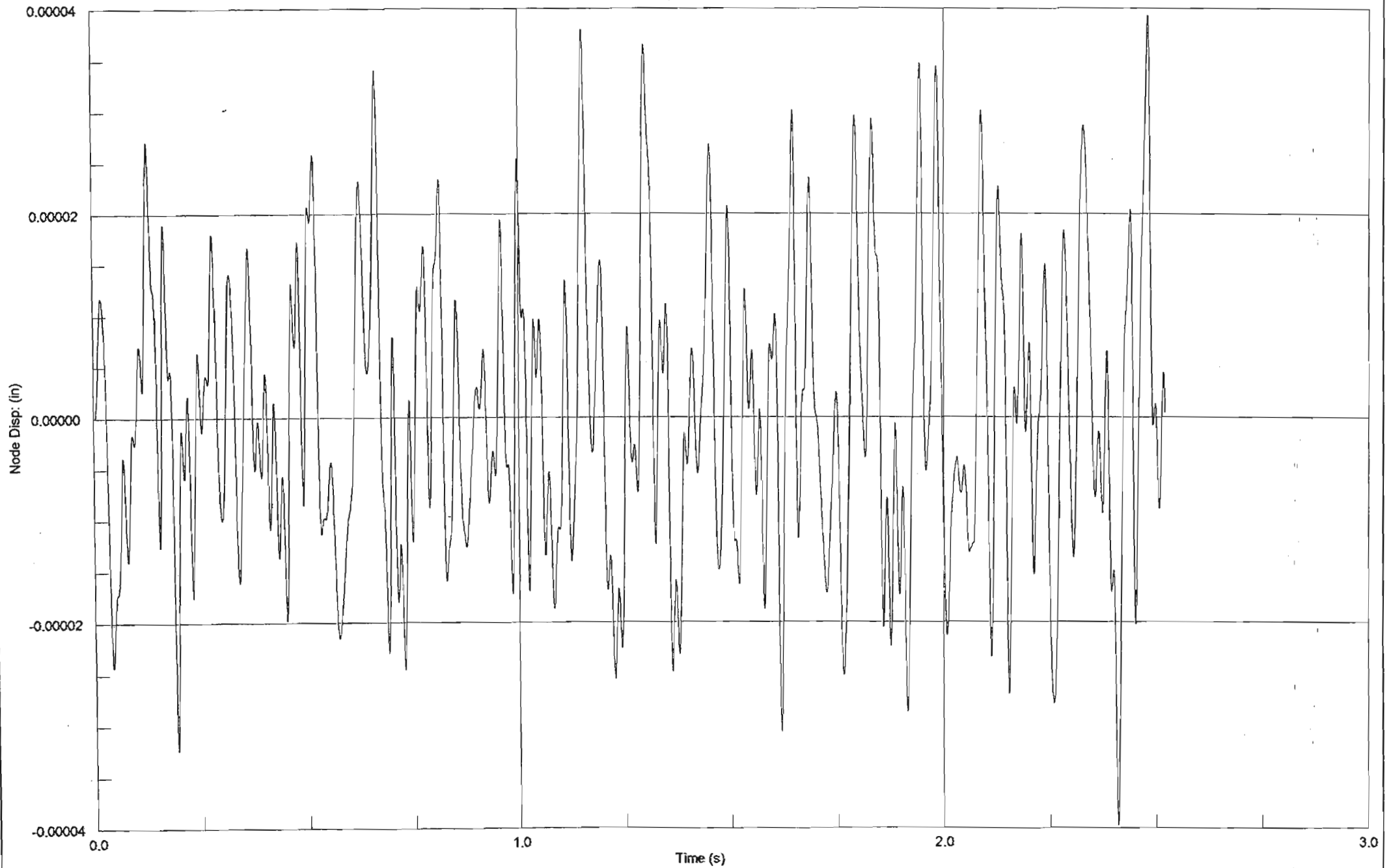


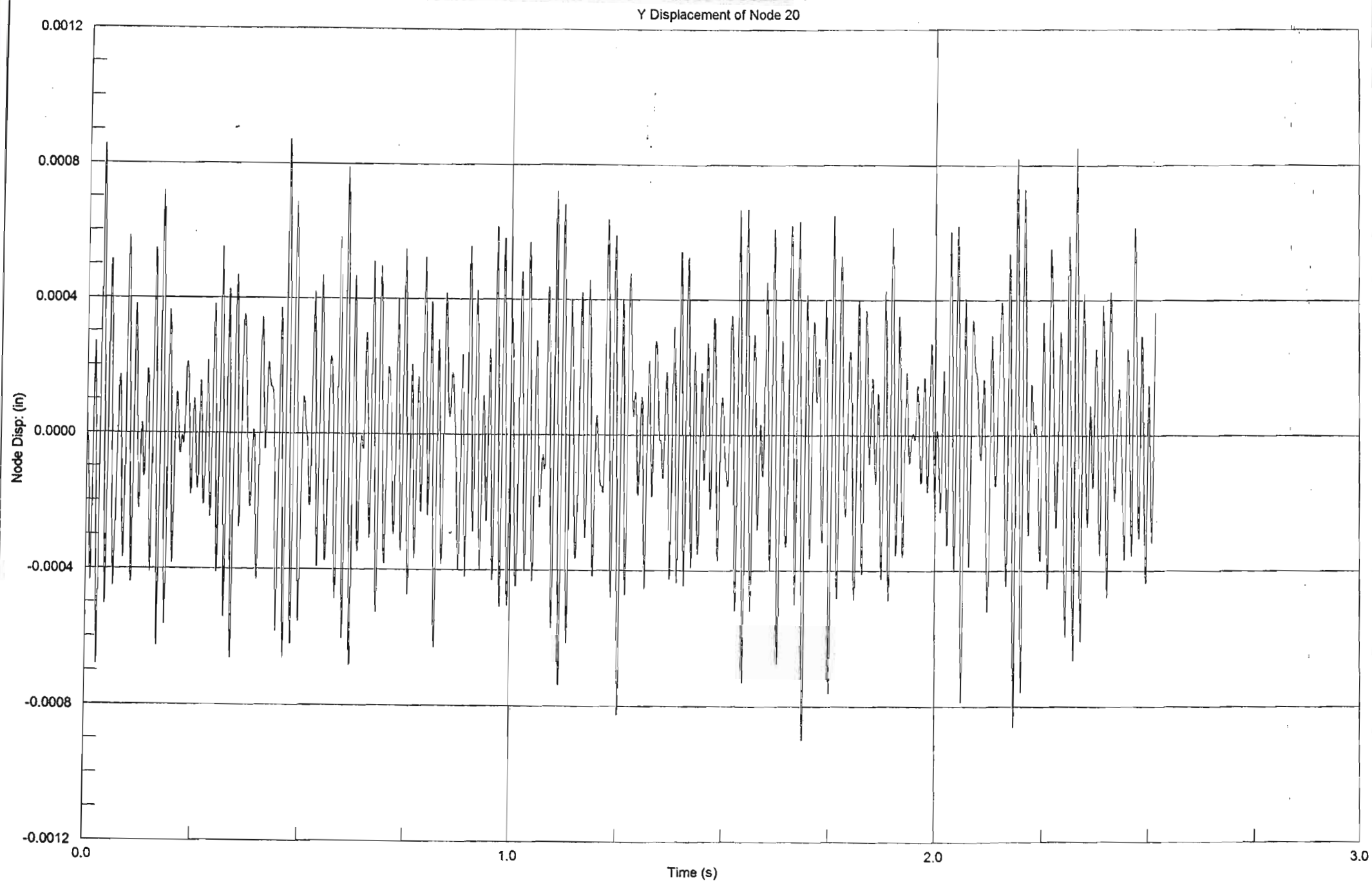




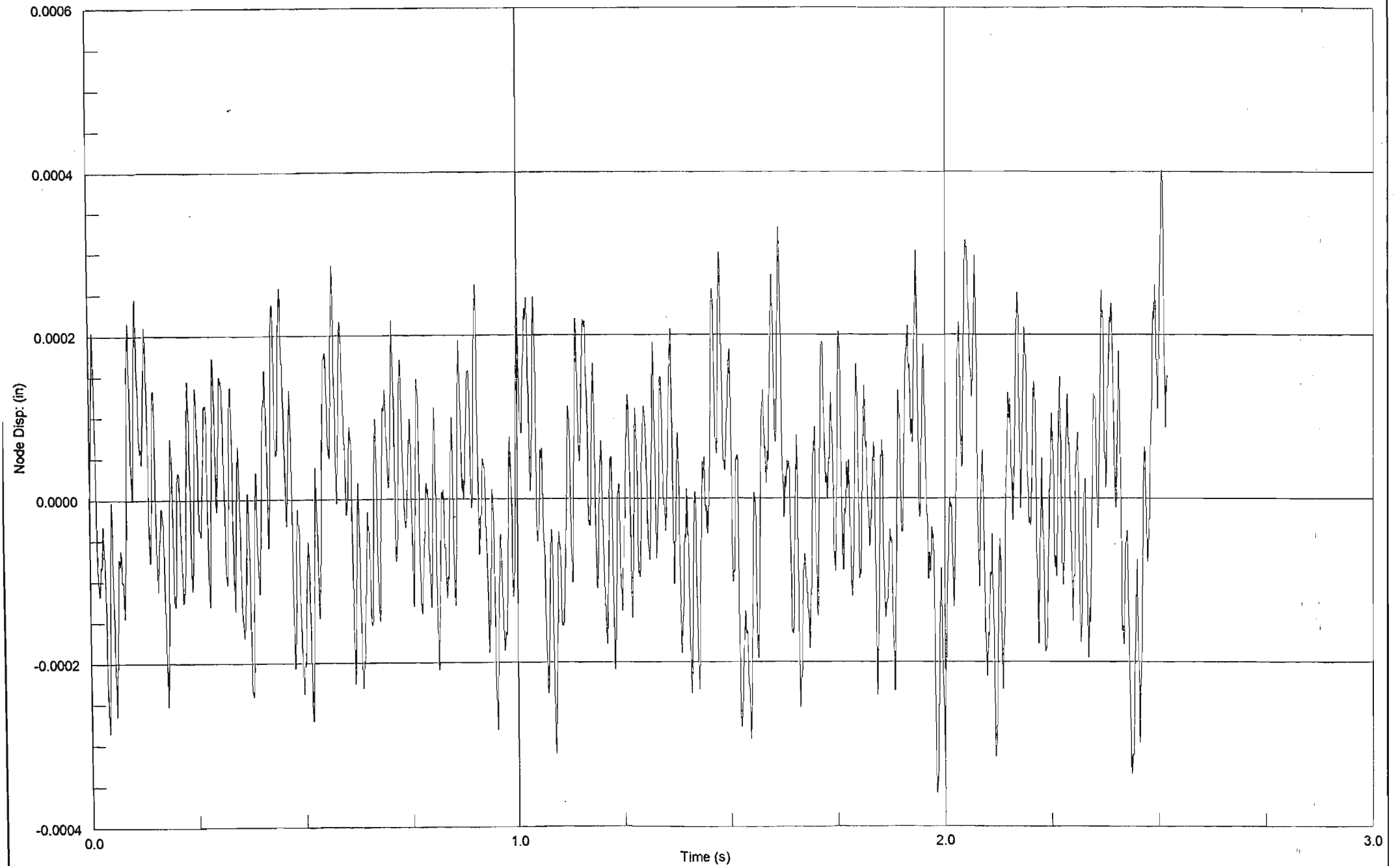


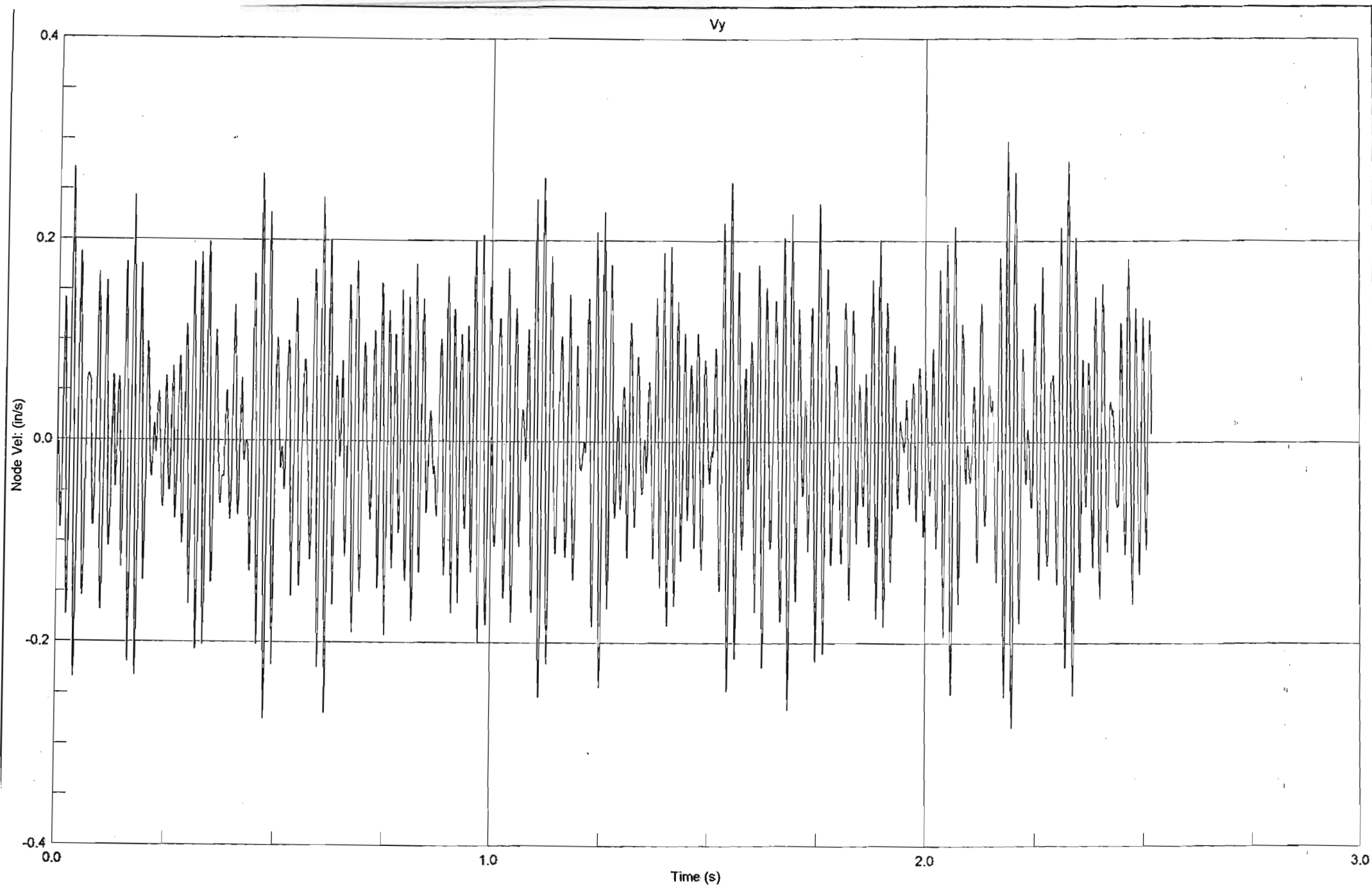
Z Displacement of Node 8





Z Displacement of Node 20



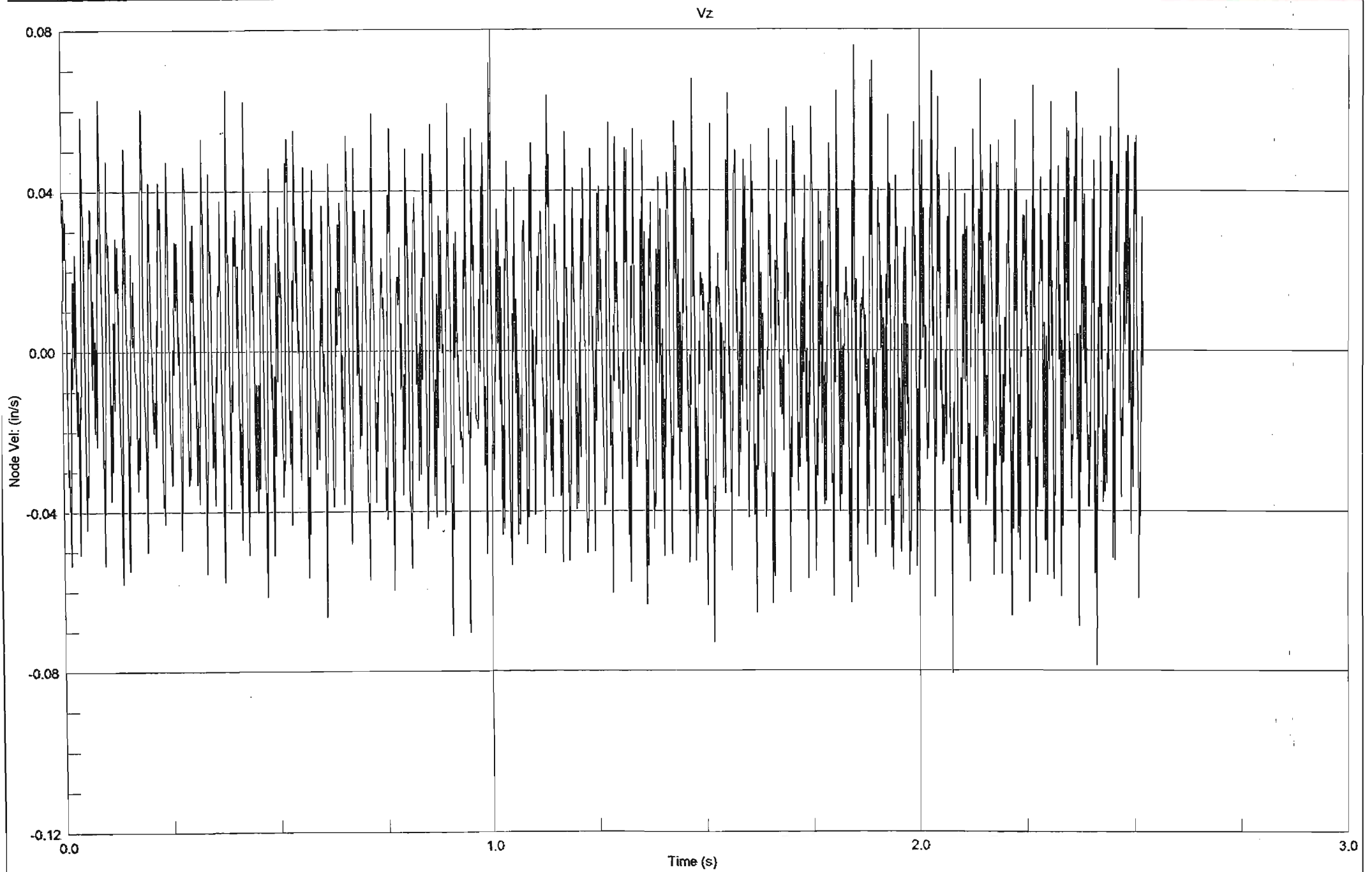


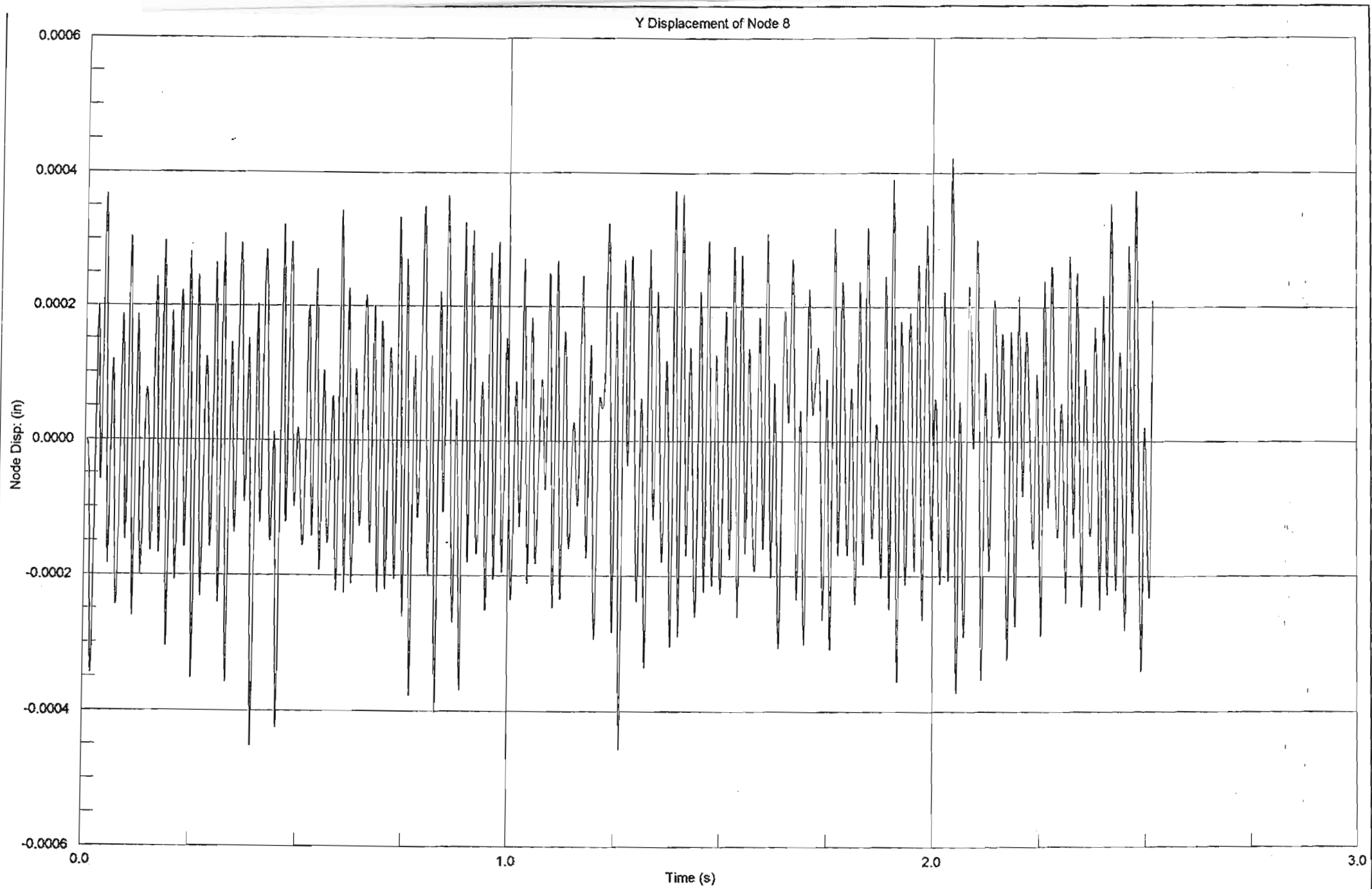
itrand7 Release 2.1.7

\\MS0 Eng\\Table Top\\Table Top 3\\Table top G15000-C3.st7

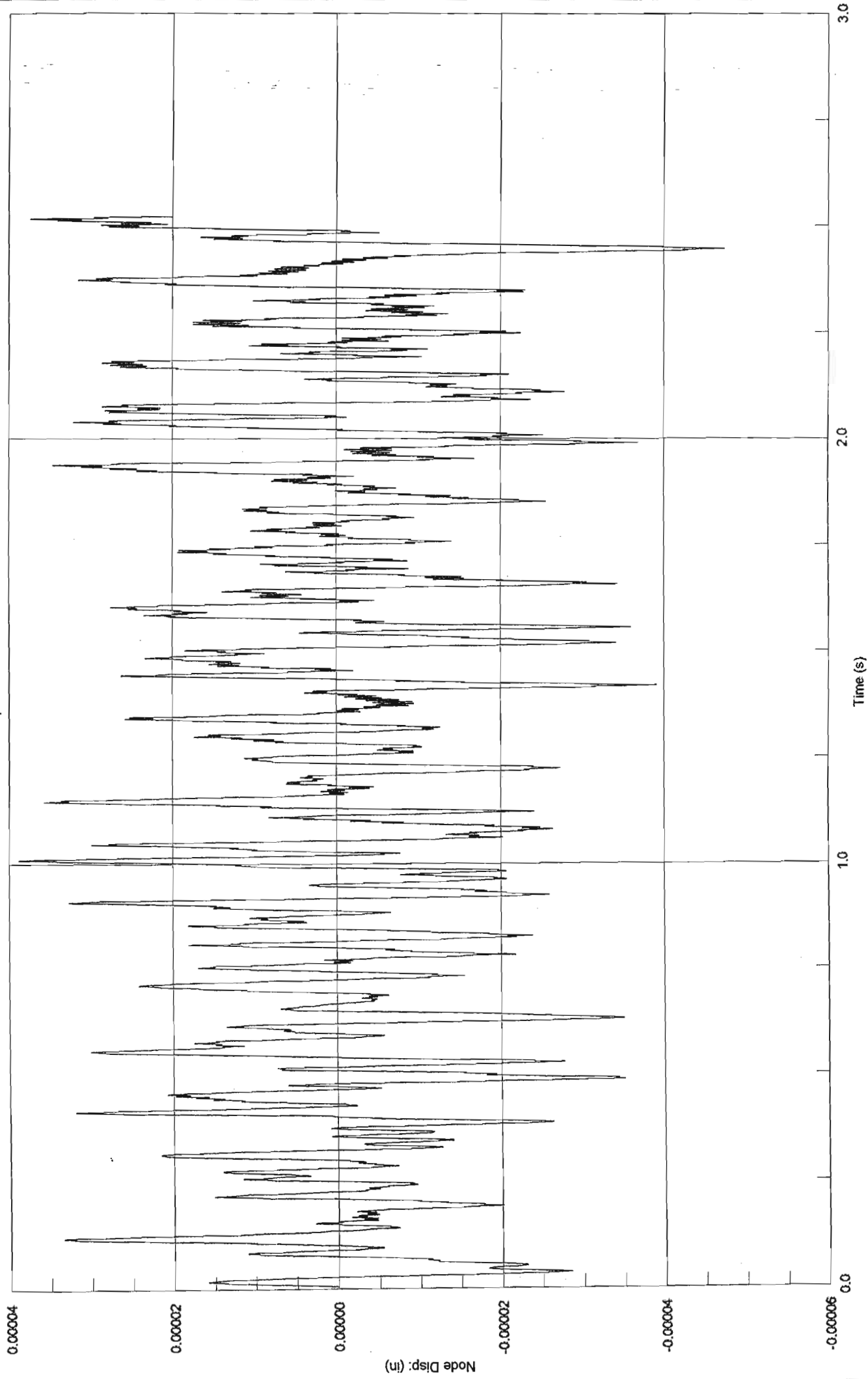
October 2002 7:38 am

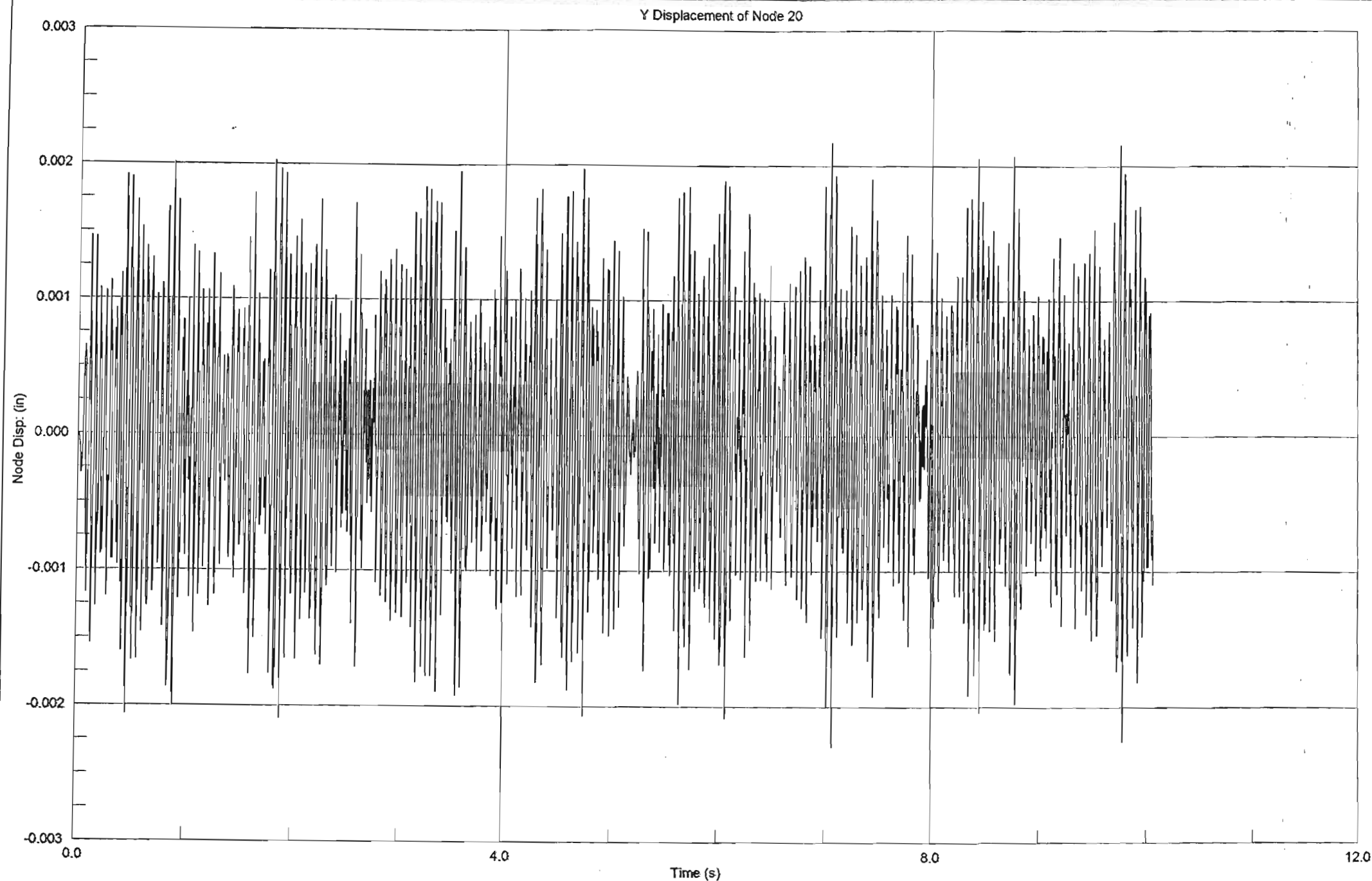
< 3.59



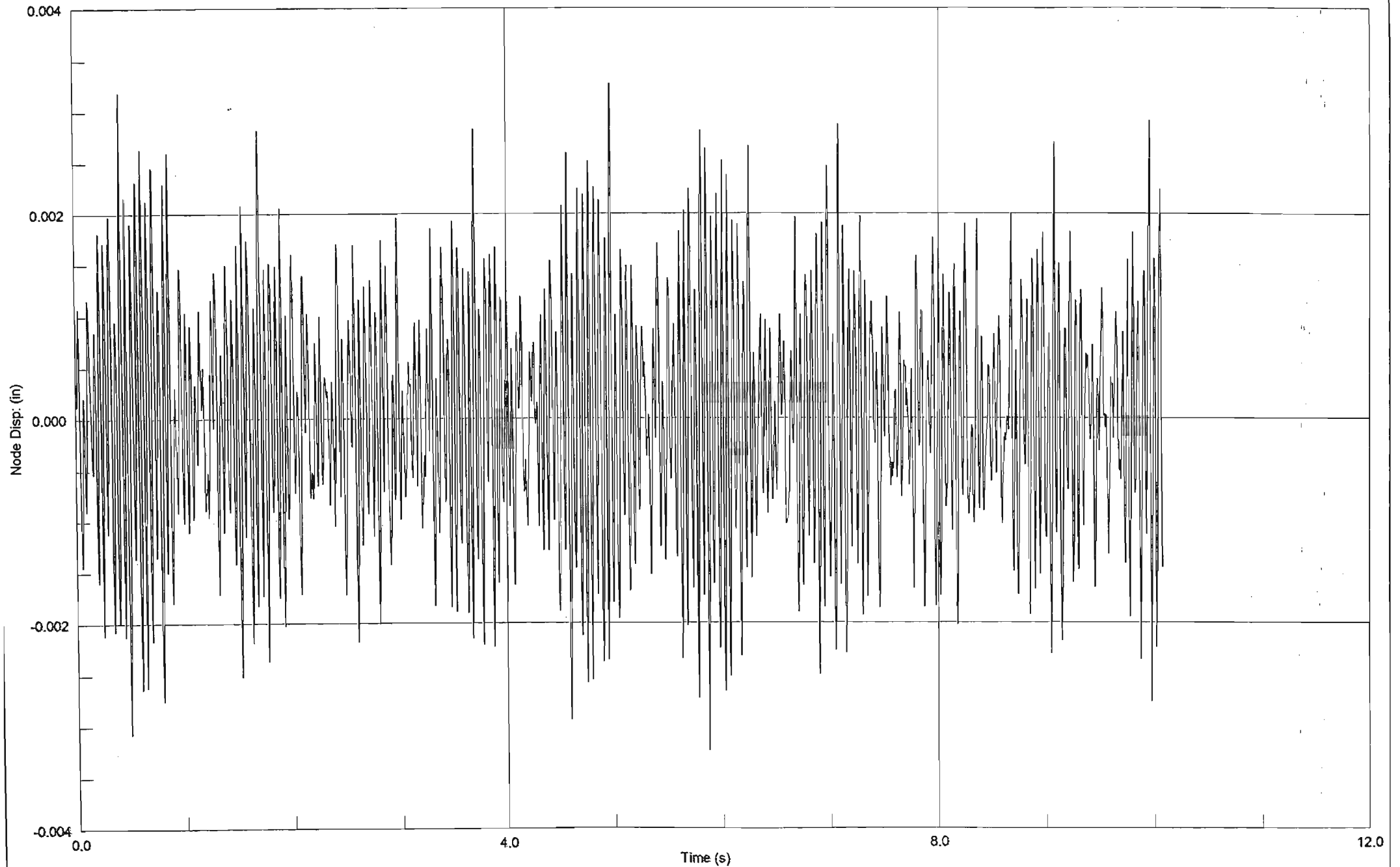


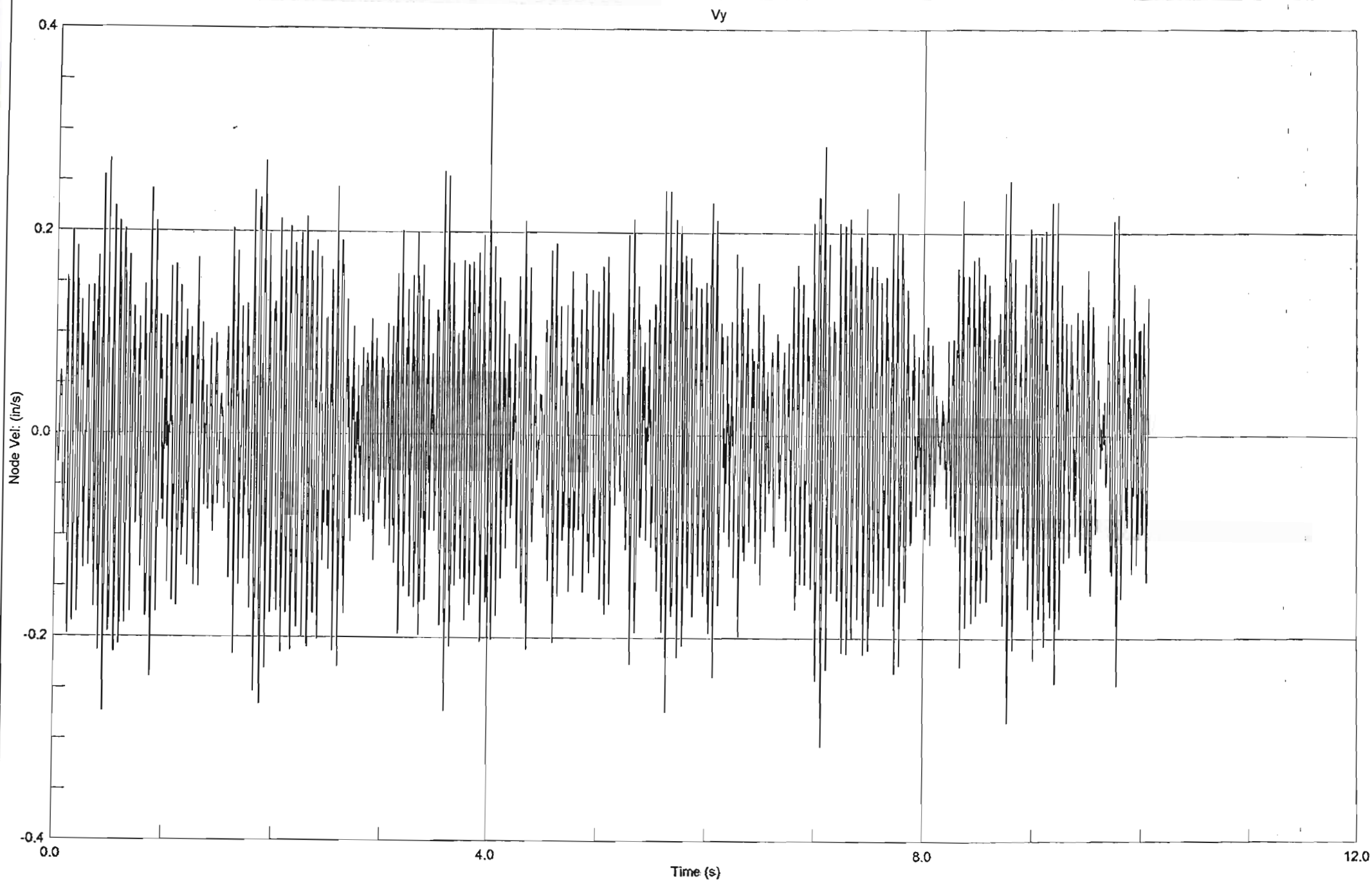
Z Displacement of Node 8



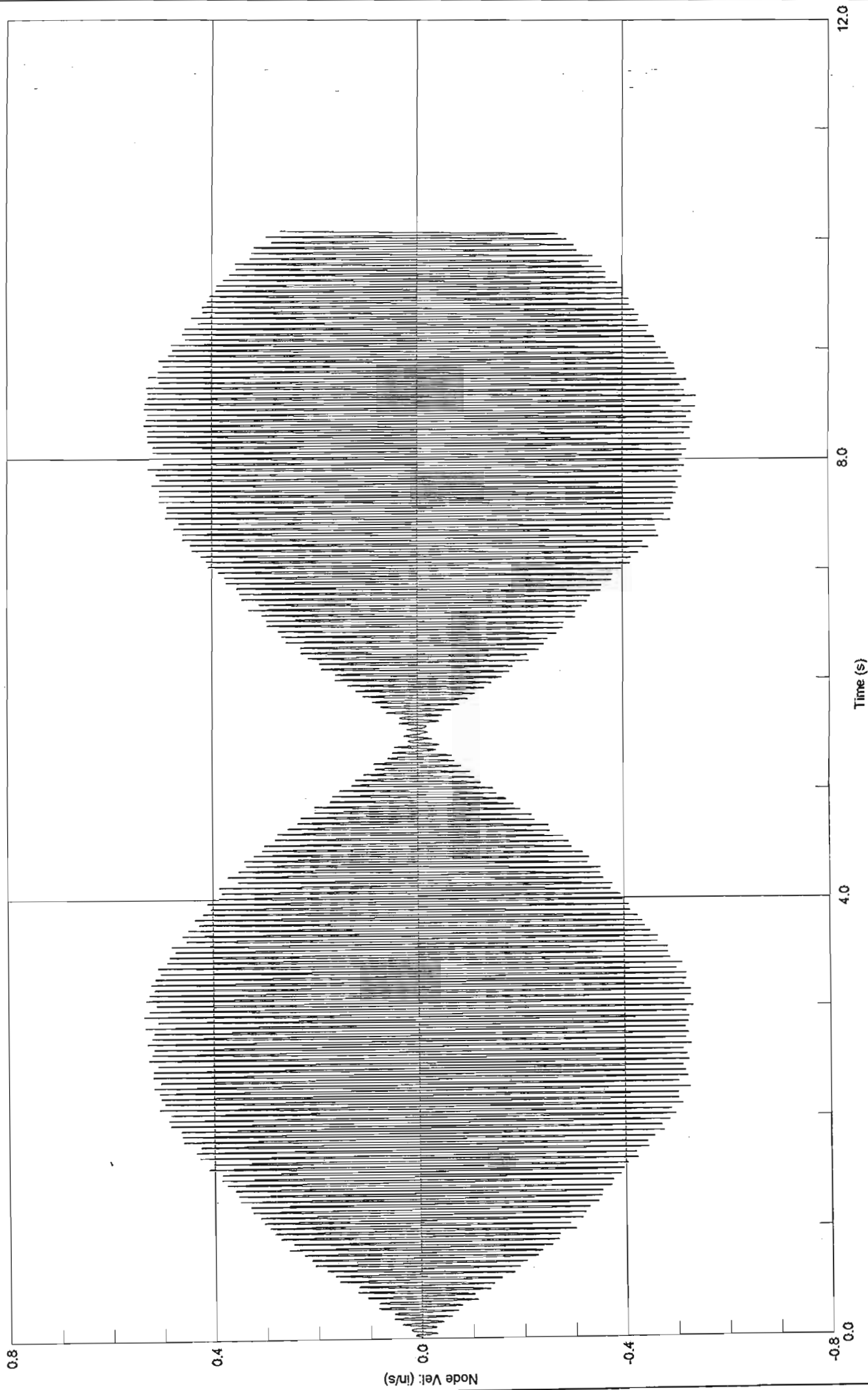


Z Displacement of Node 20

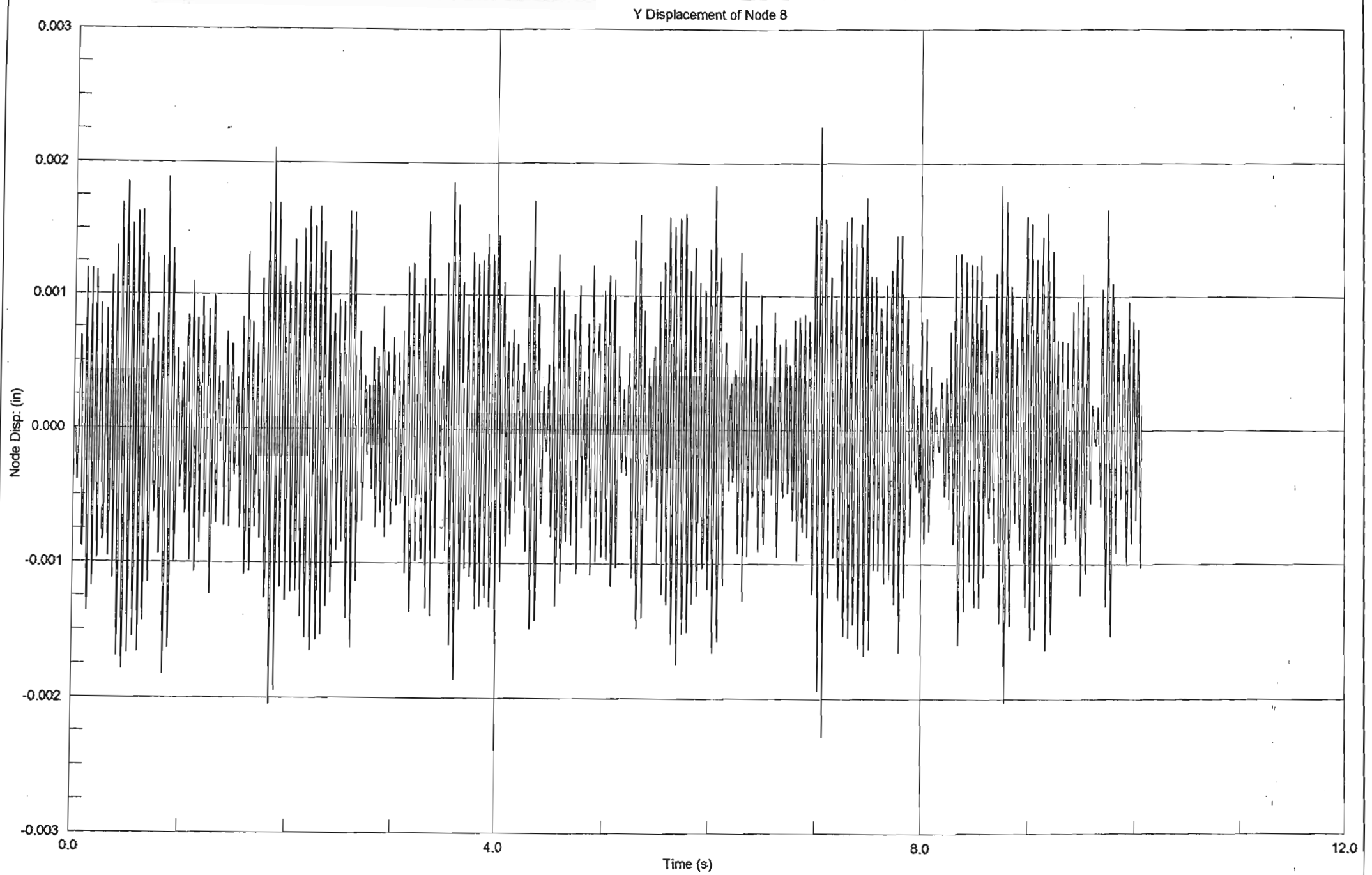




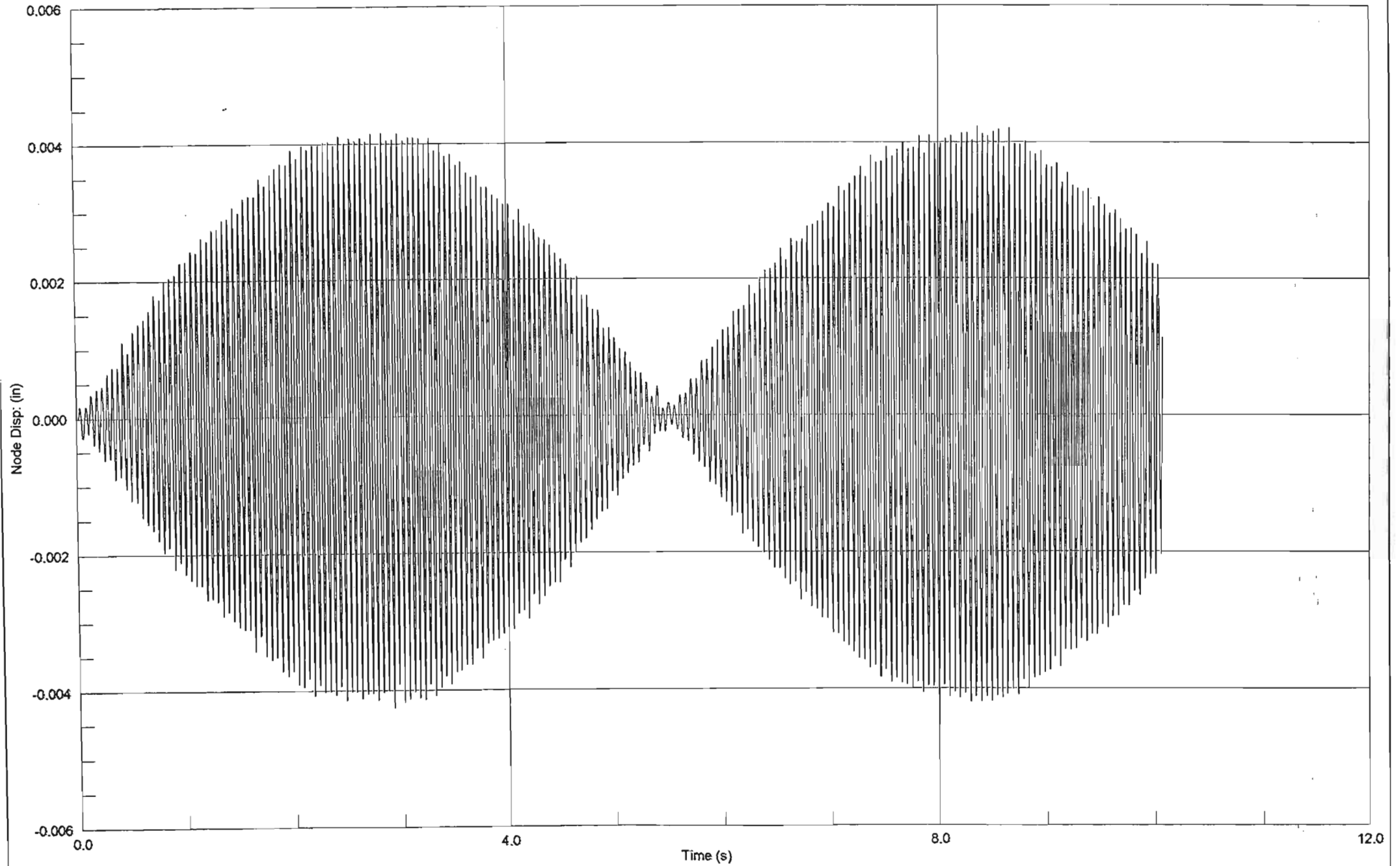
Vz



C3.66

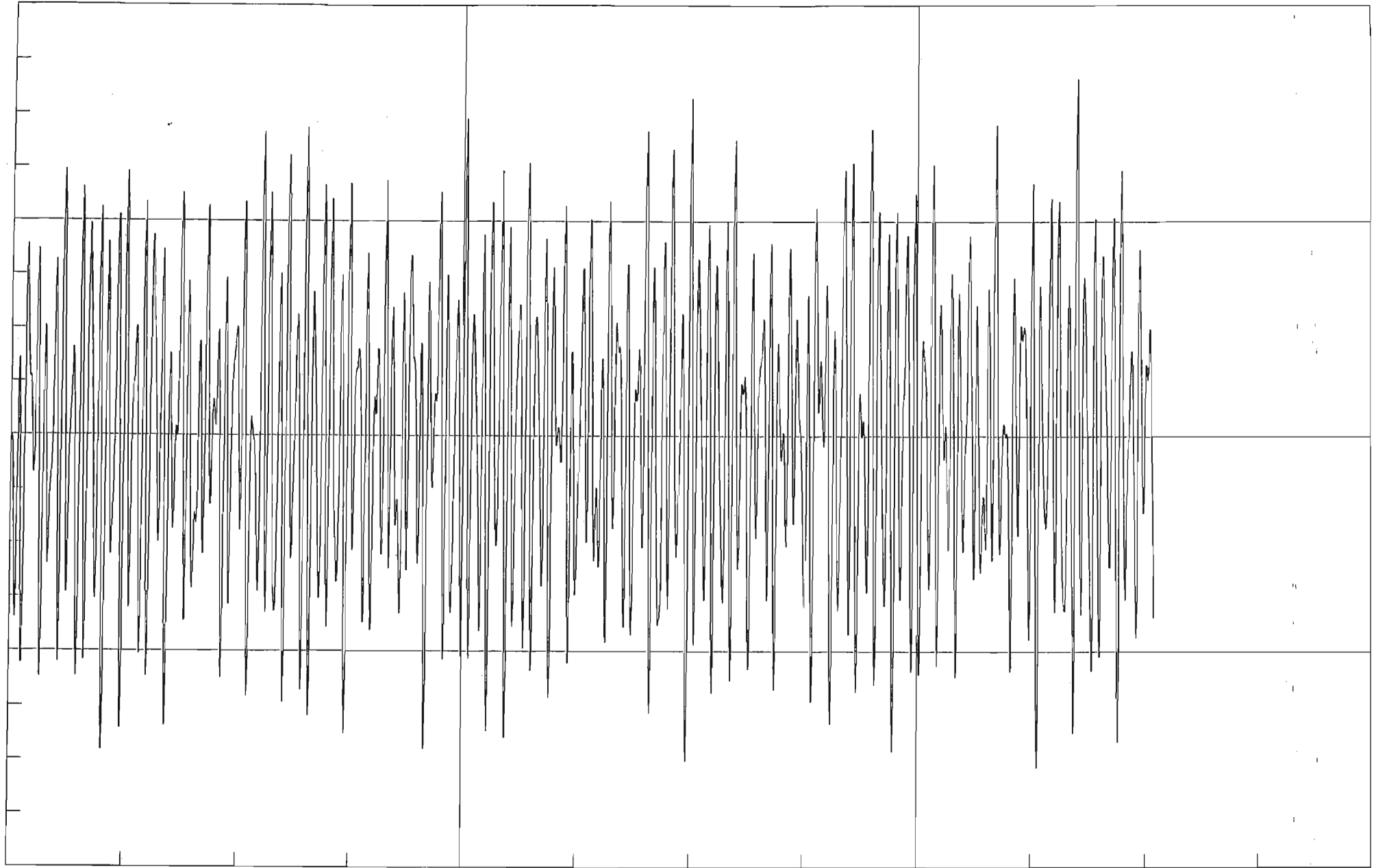


Z Displacement of Node 8



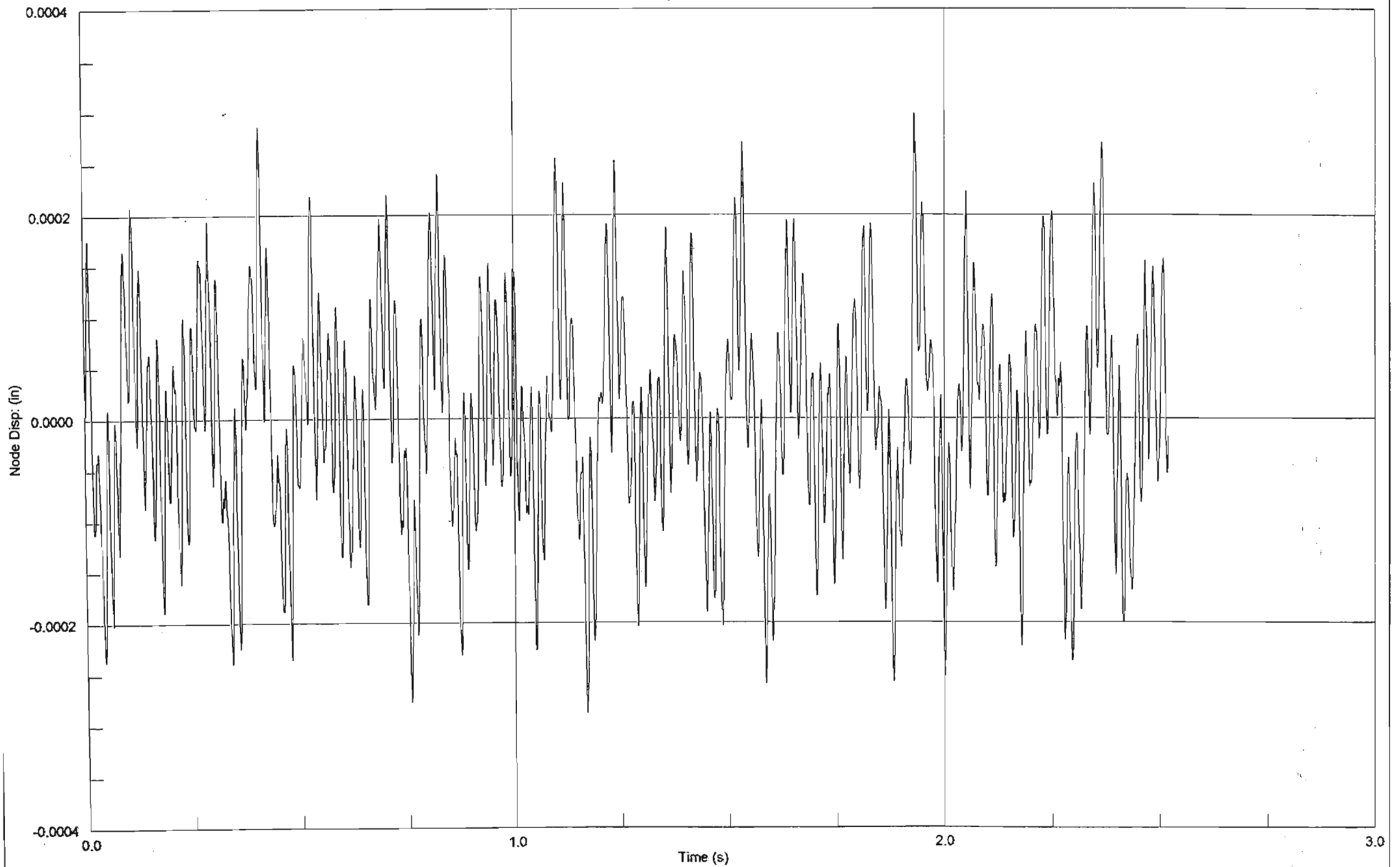
Y Displacement of Node 20

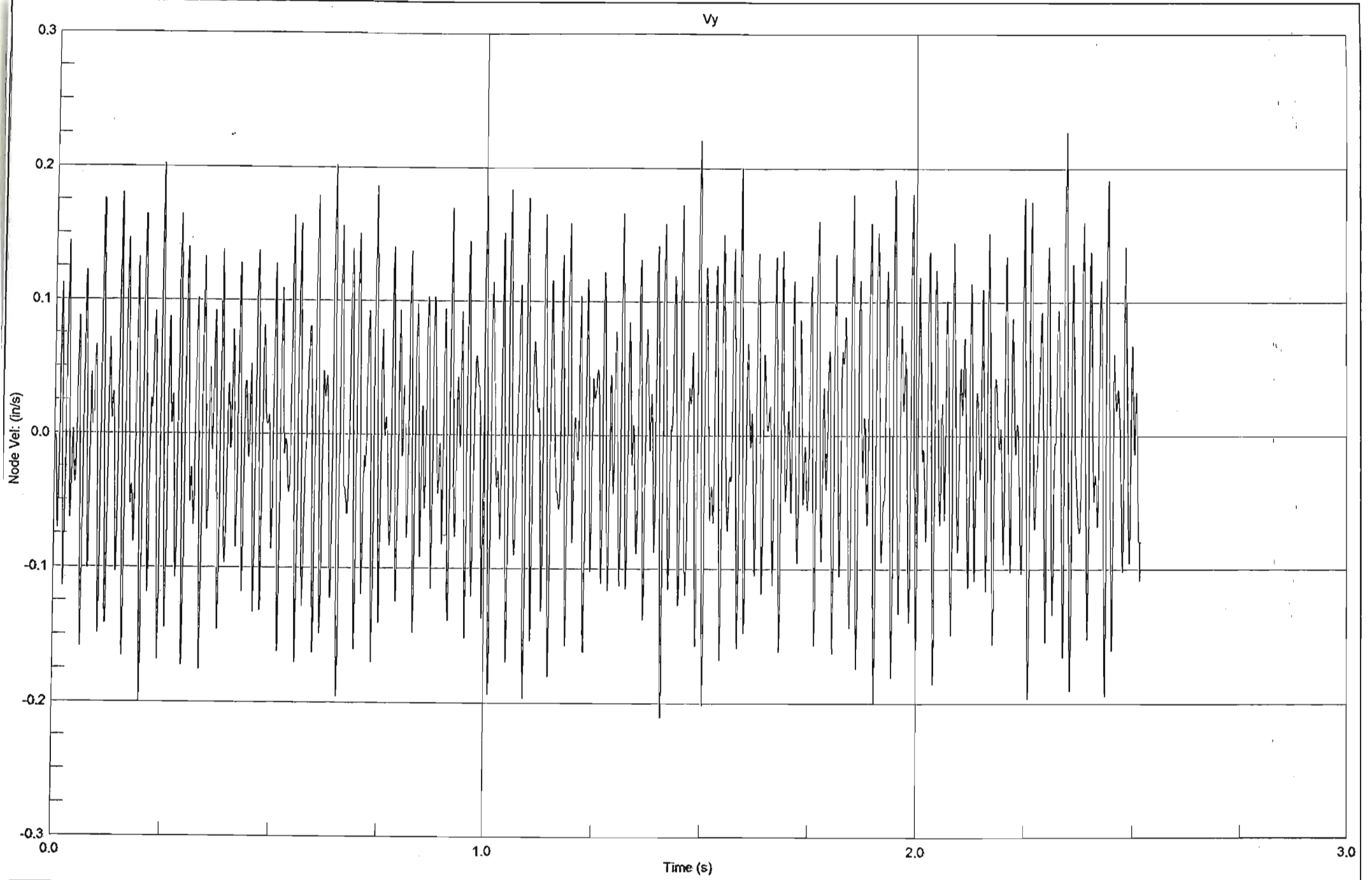
Node Disp: (in)

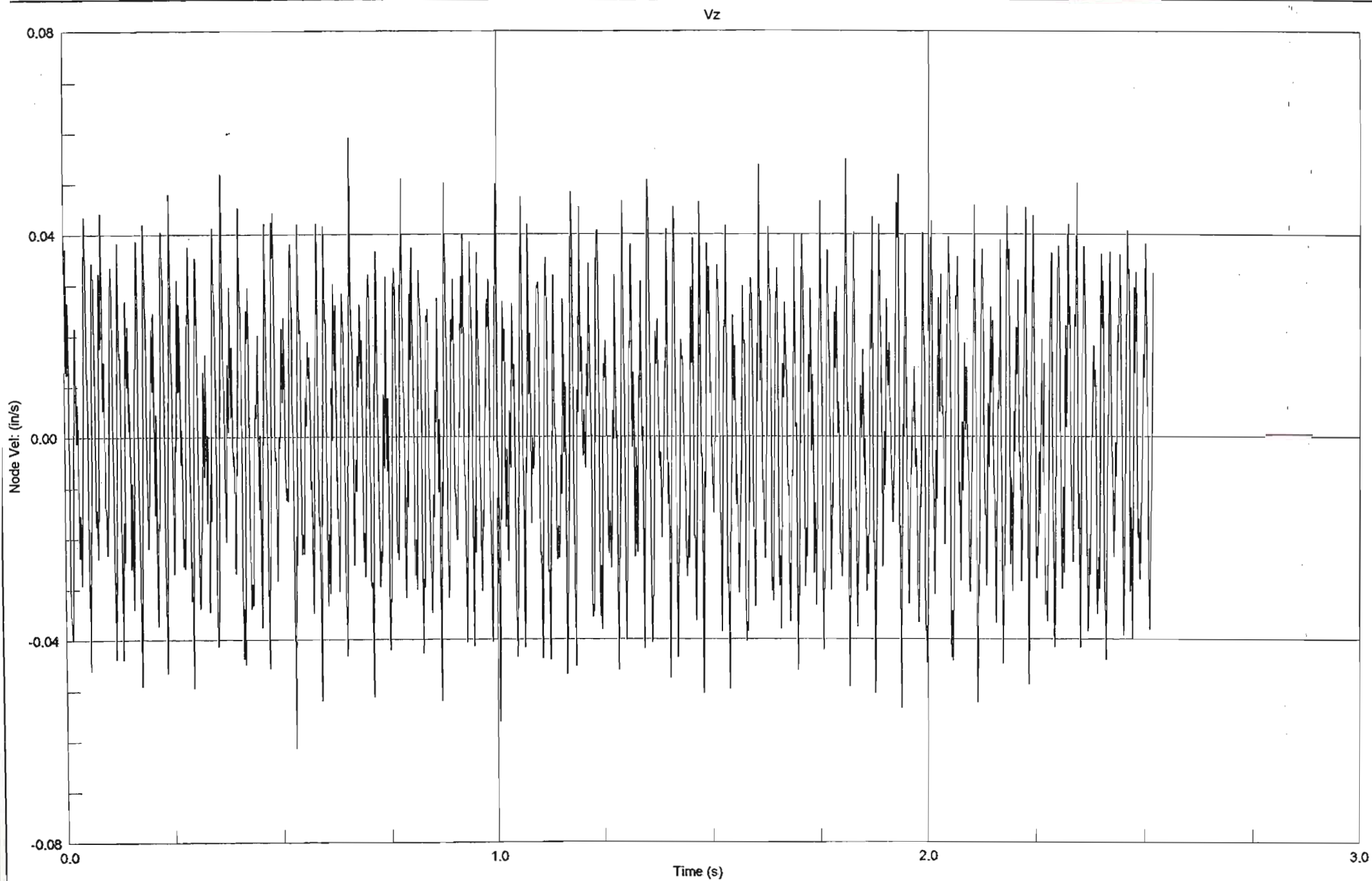


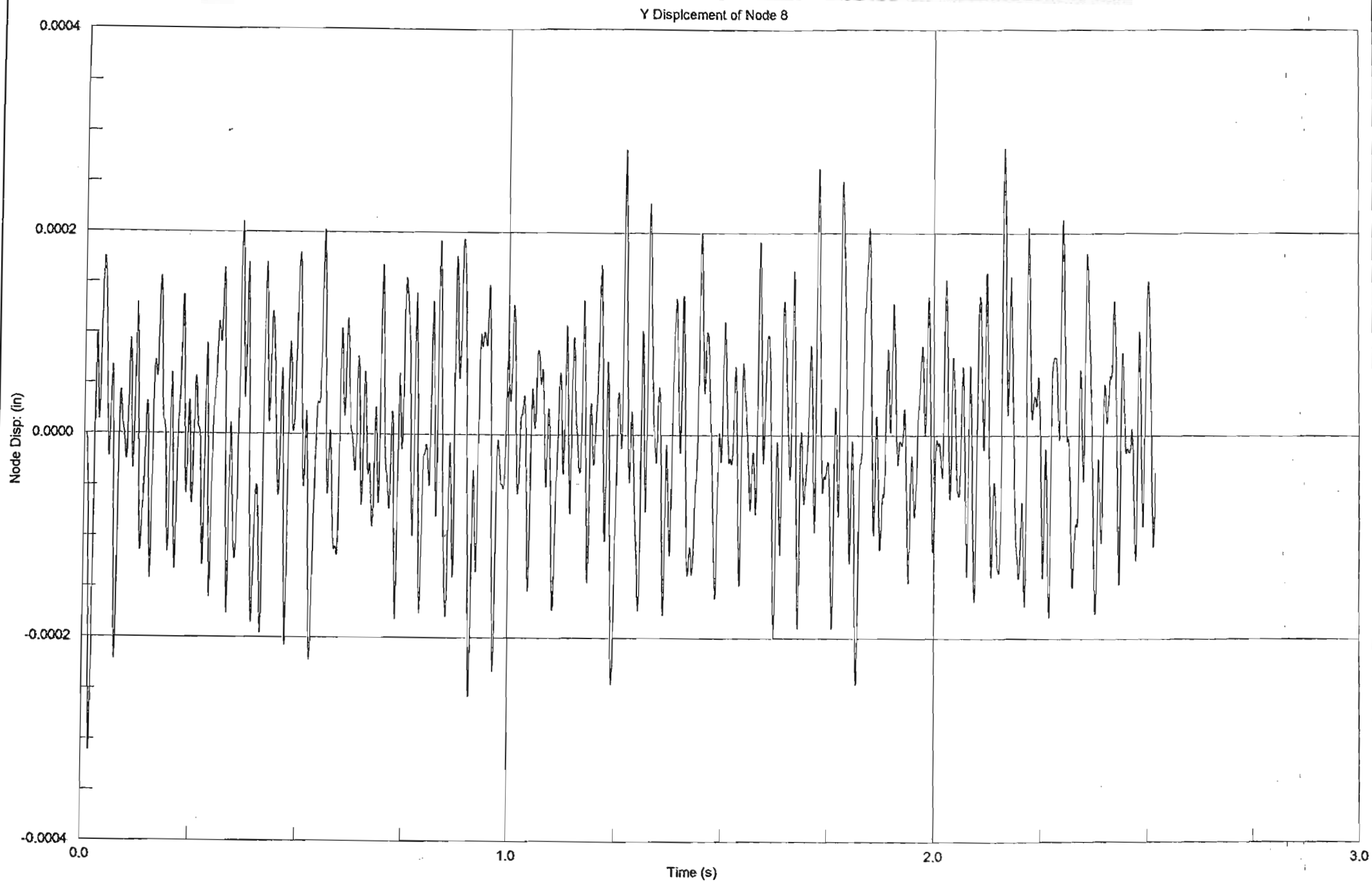
Time (s)

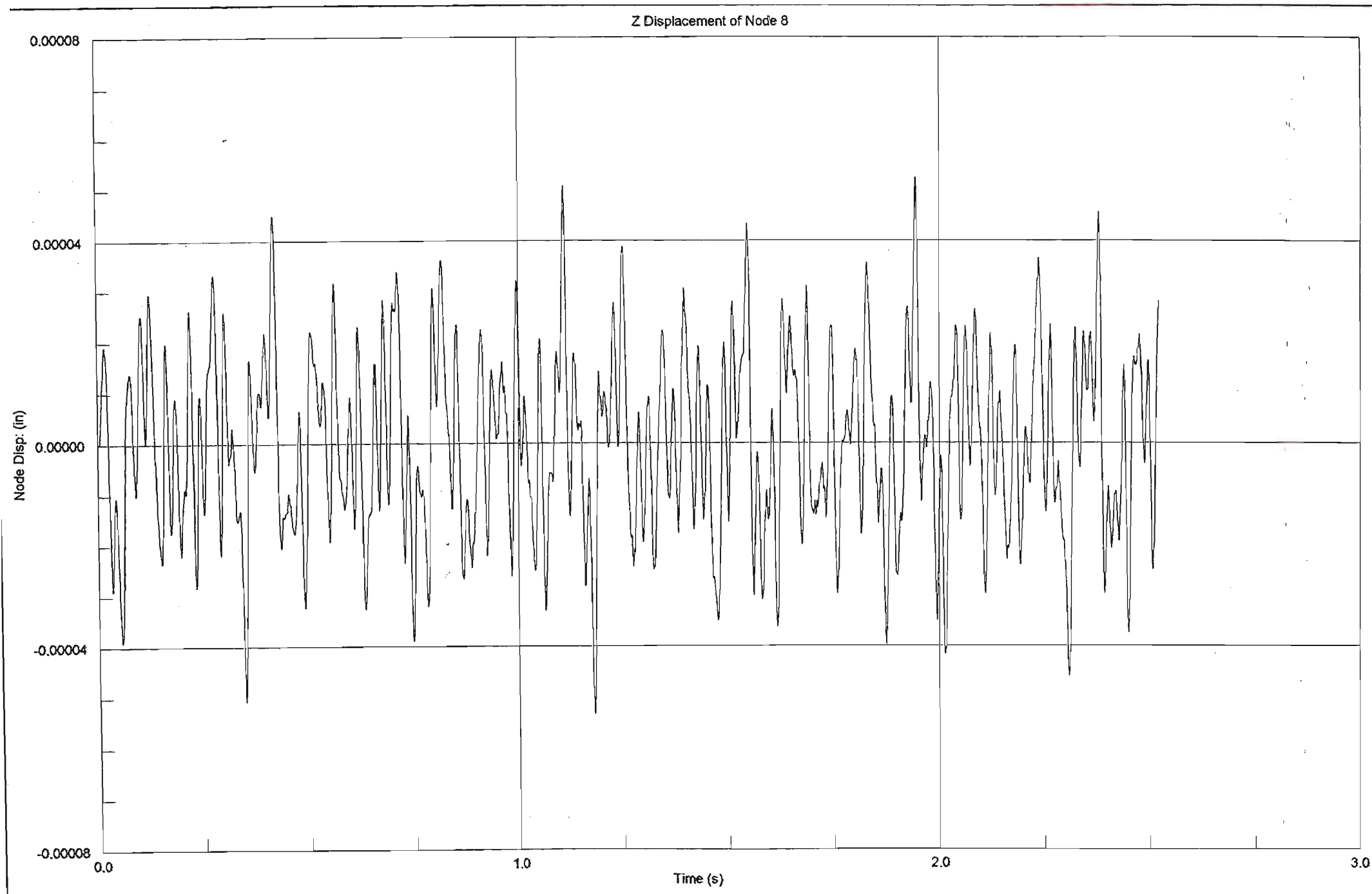
Z Displacement of Node 20

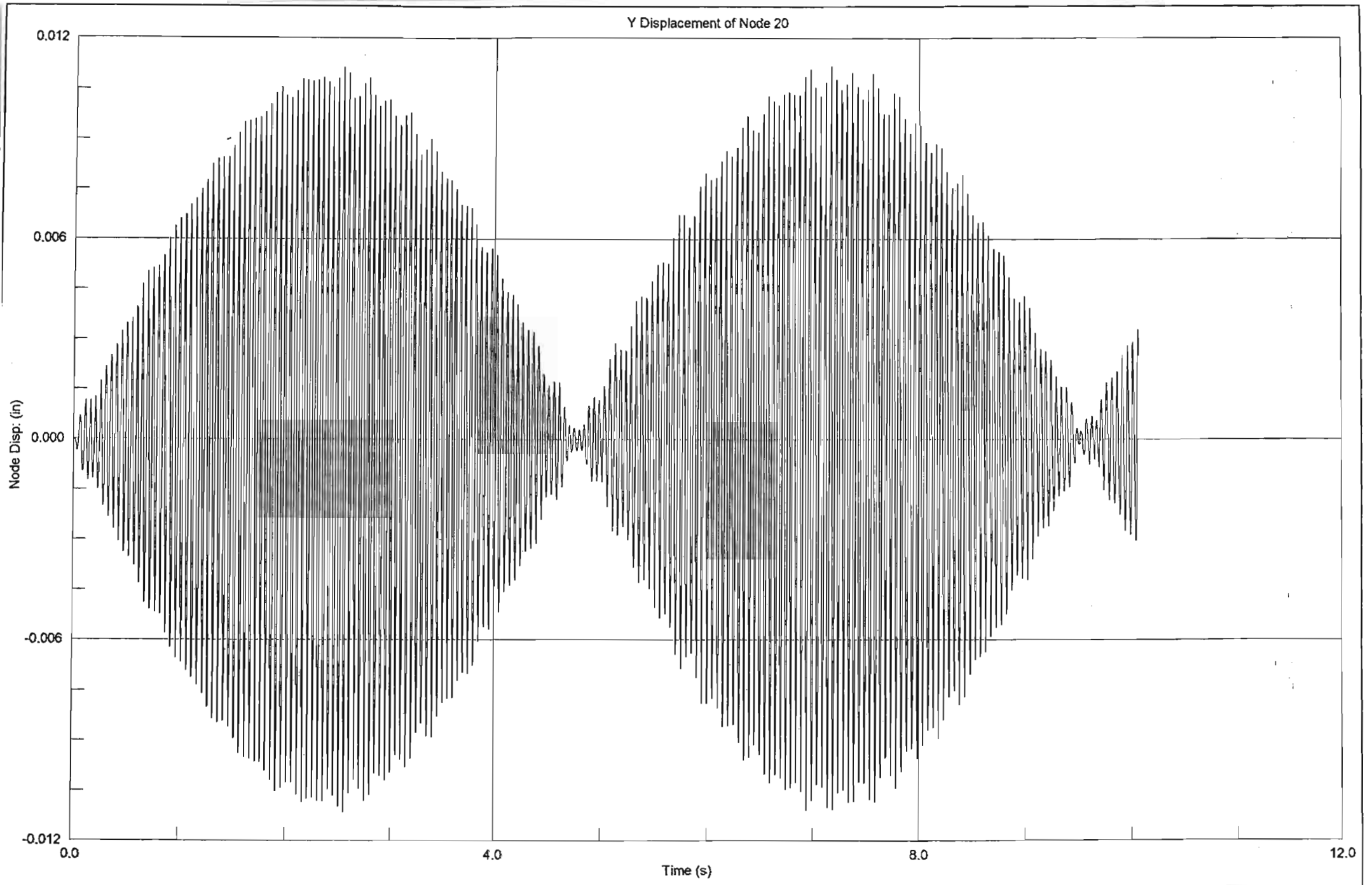




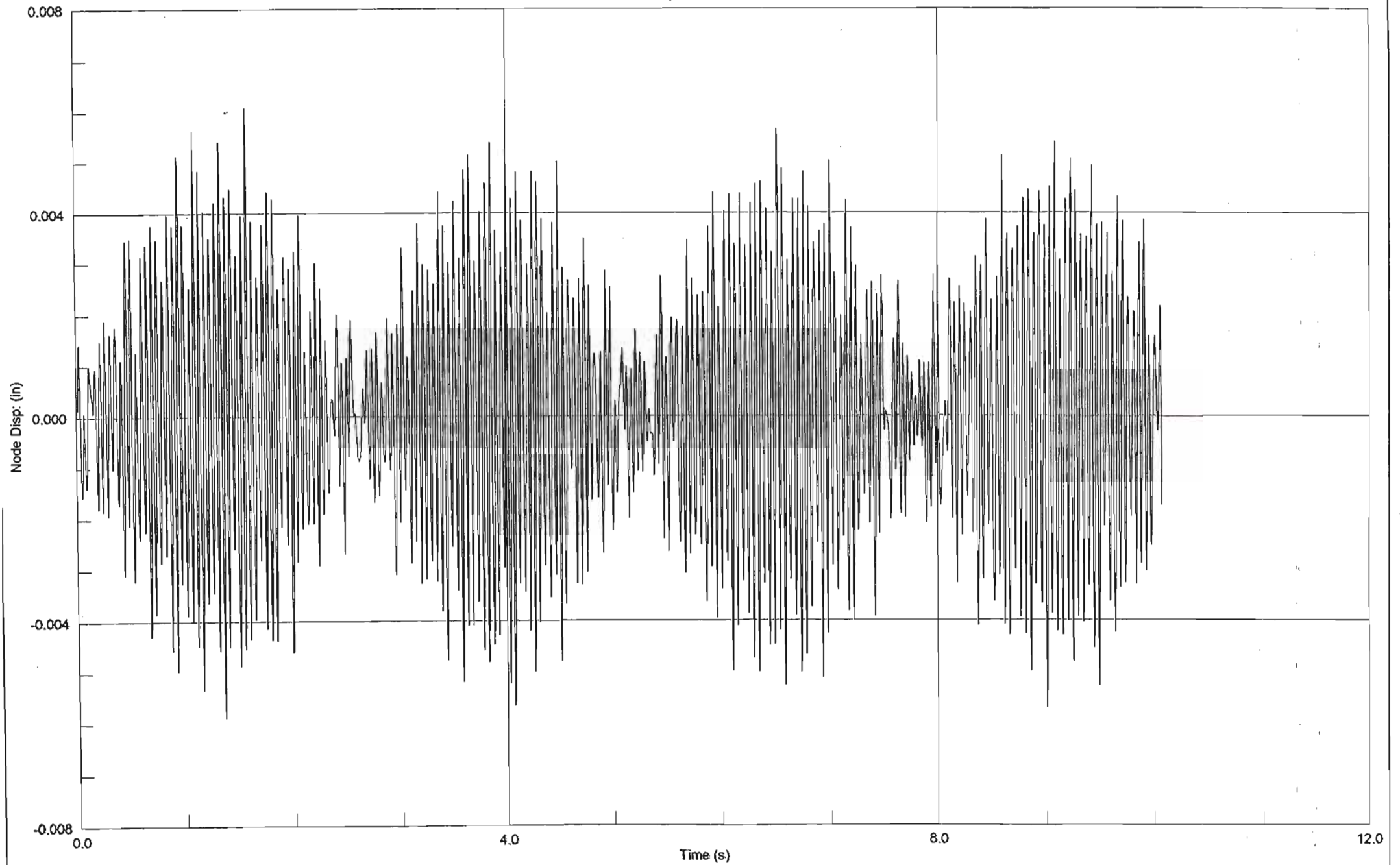


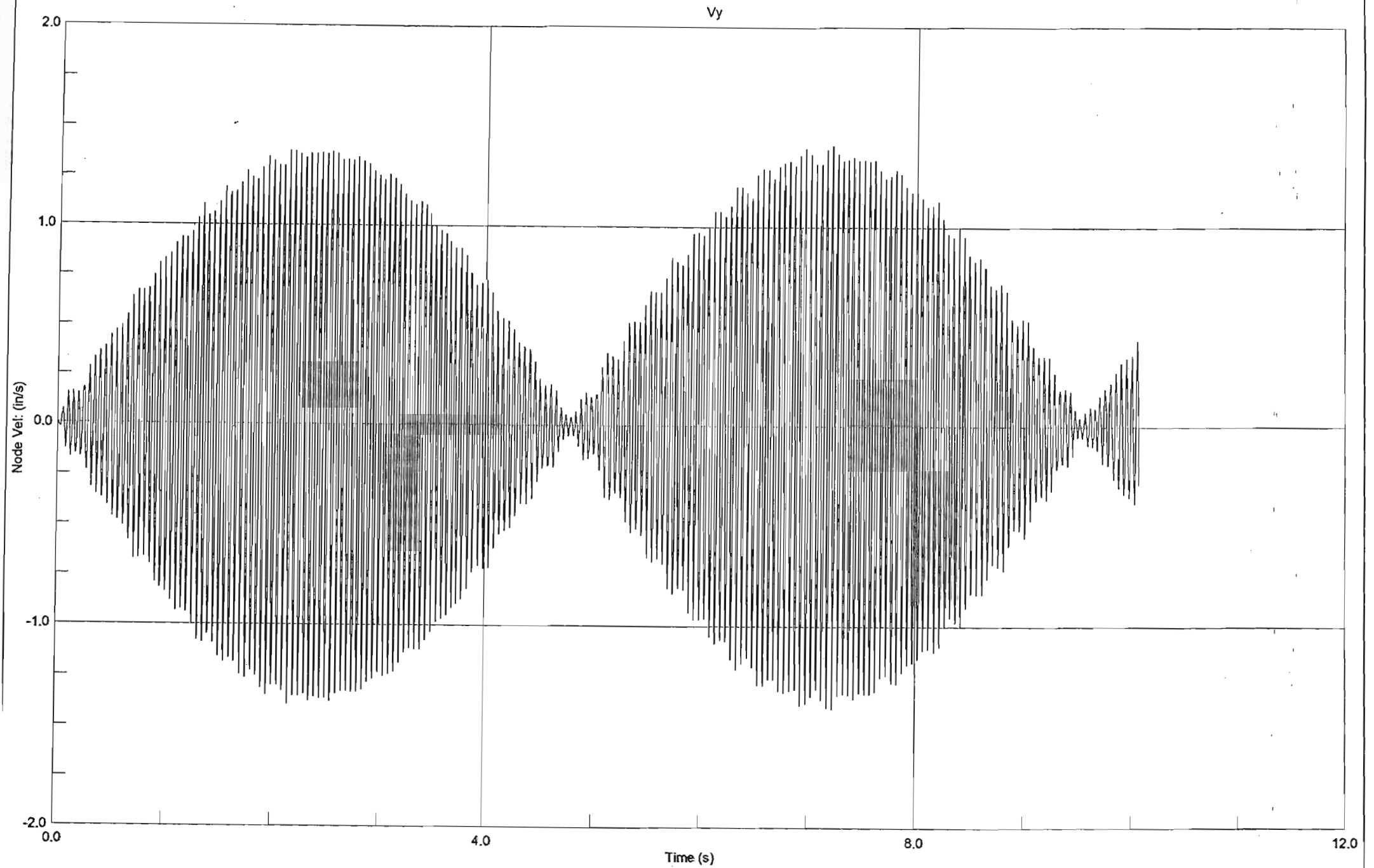


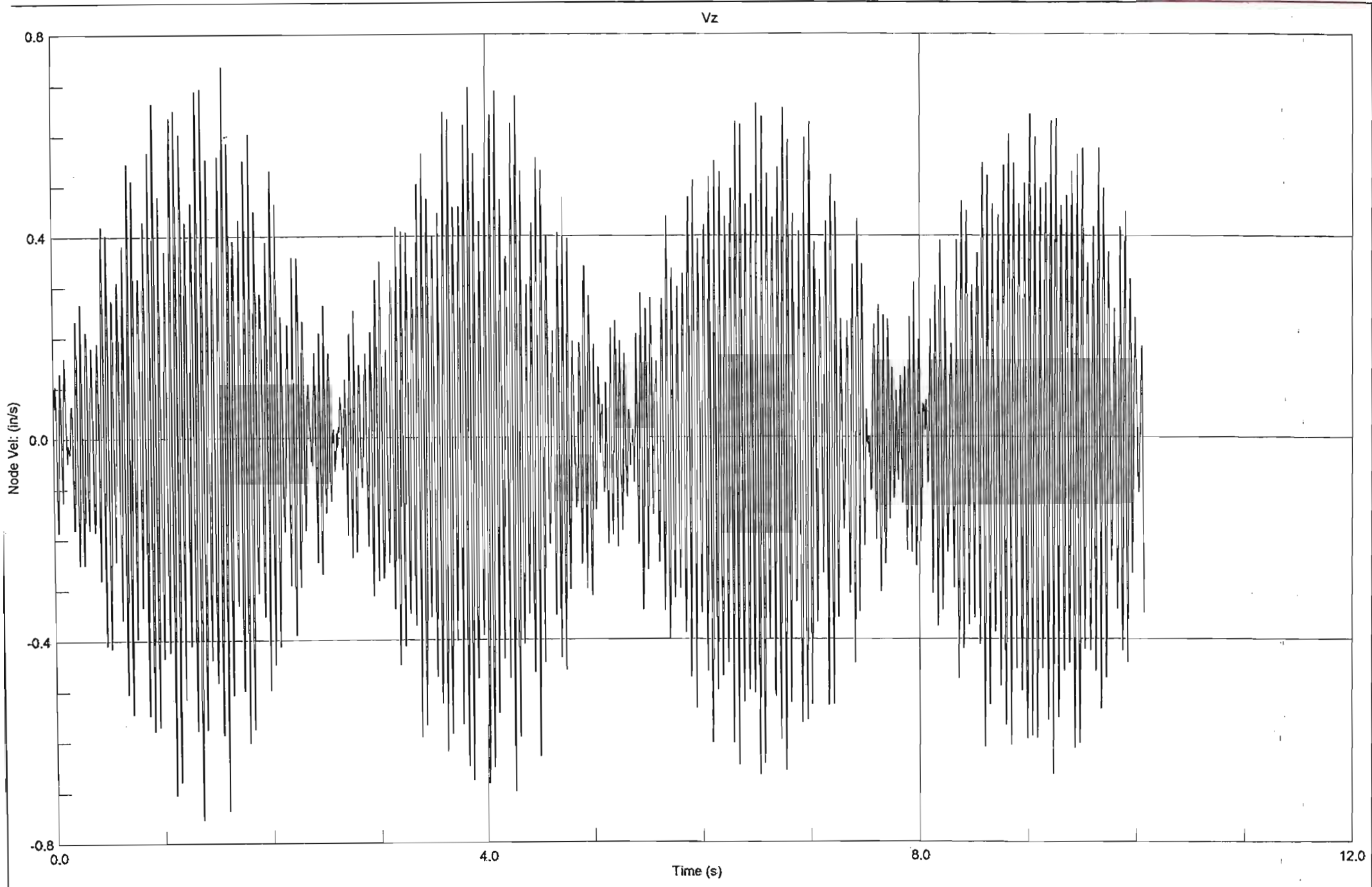


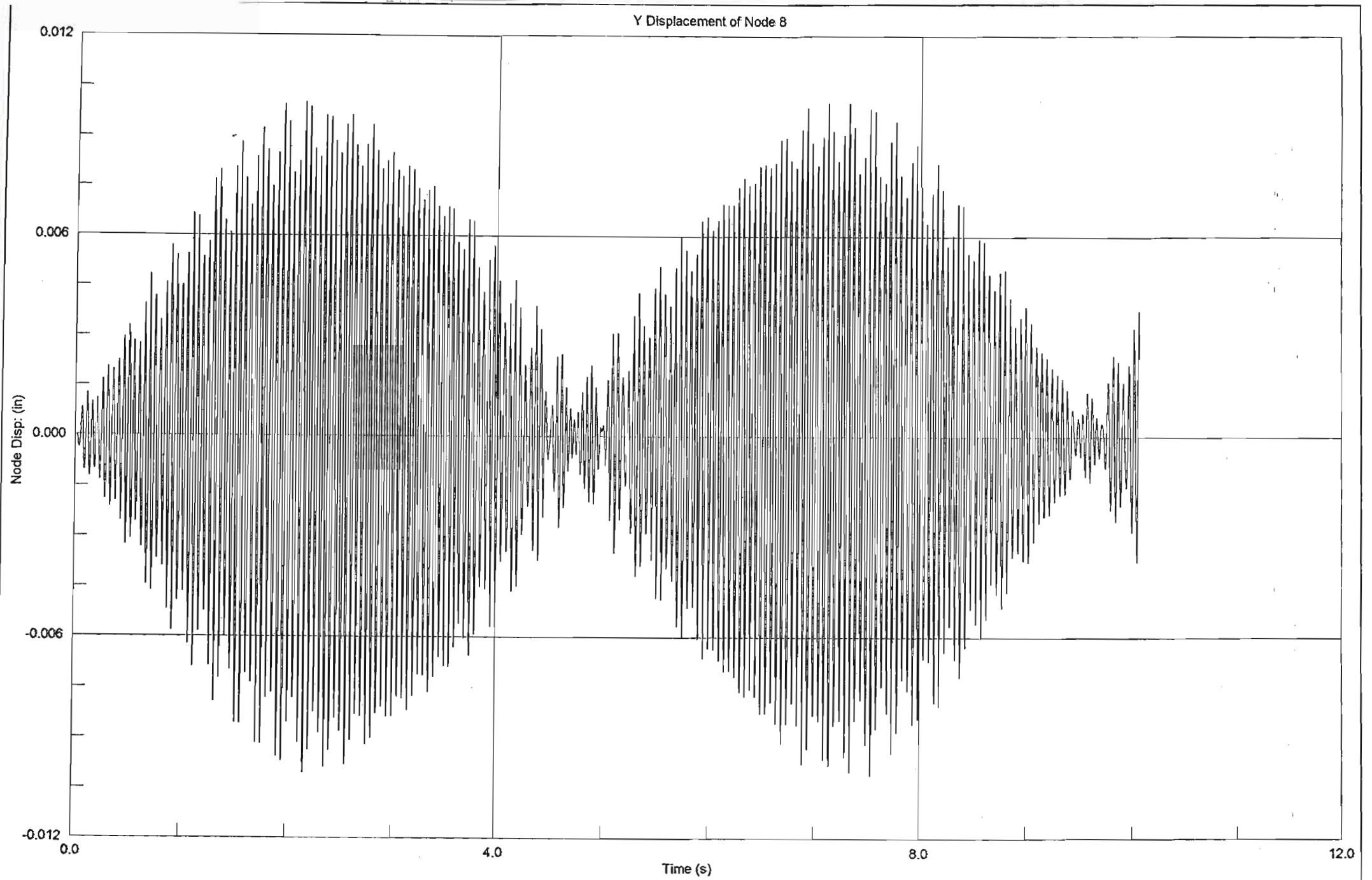


Z Displacement of Node 20

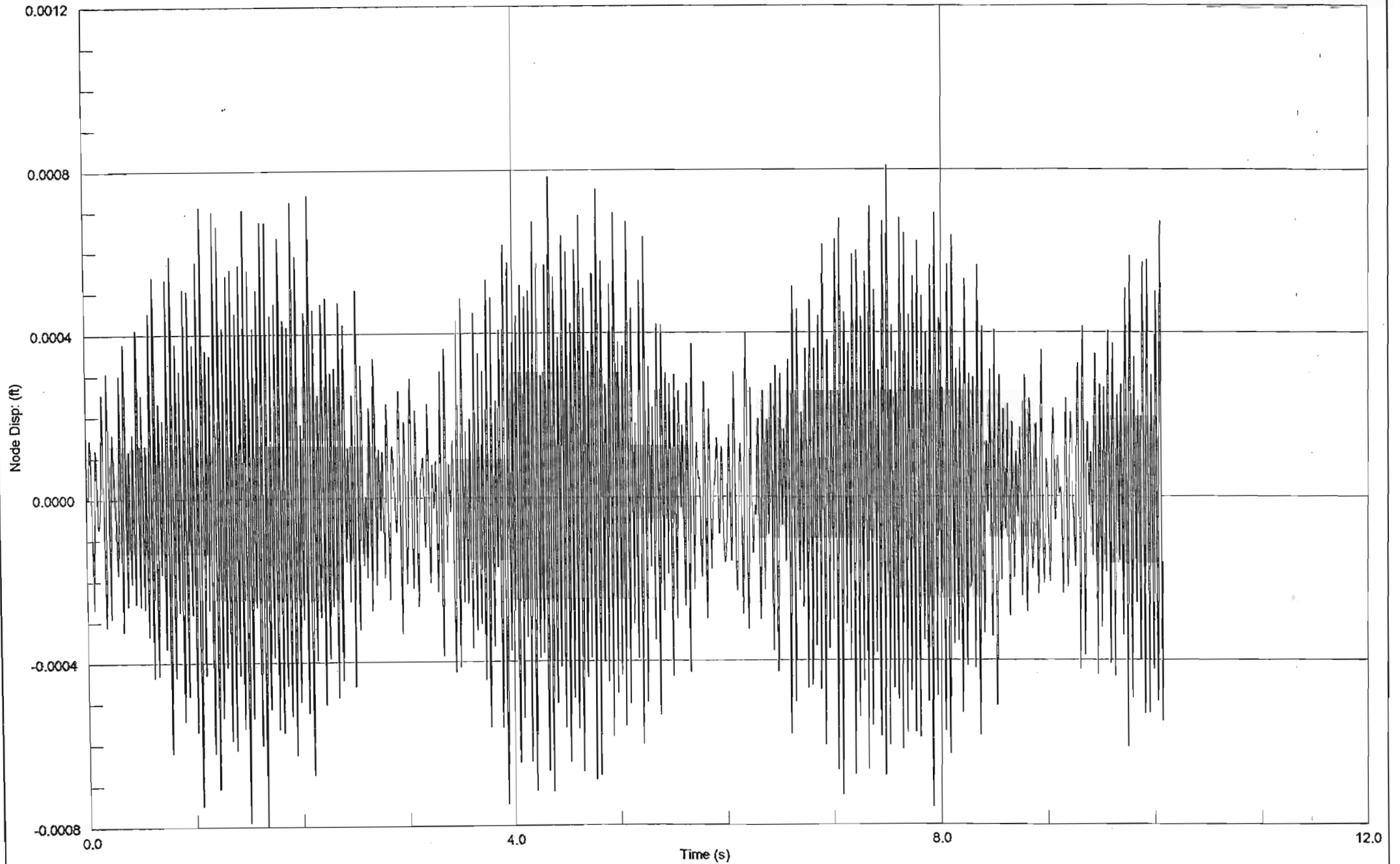


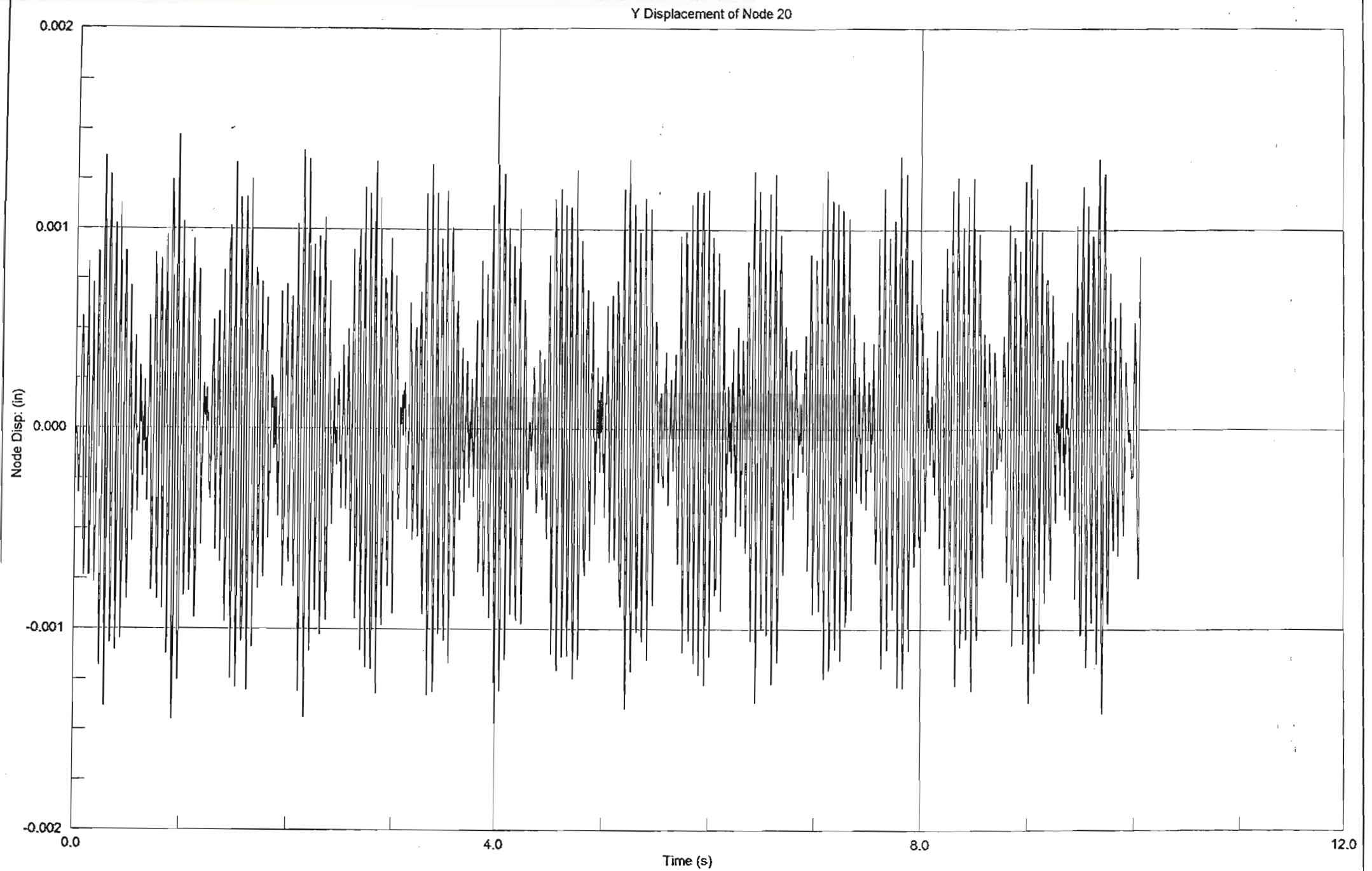




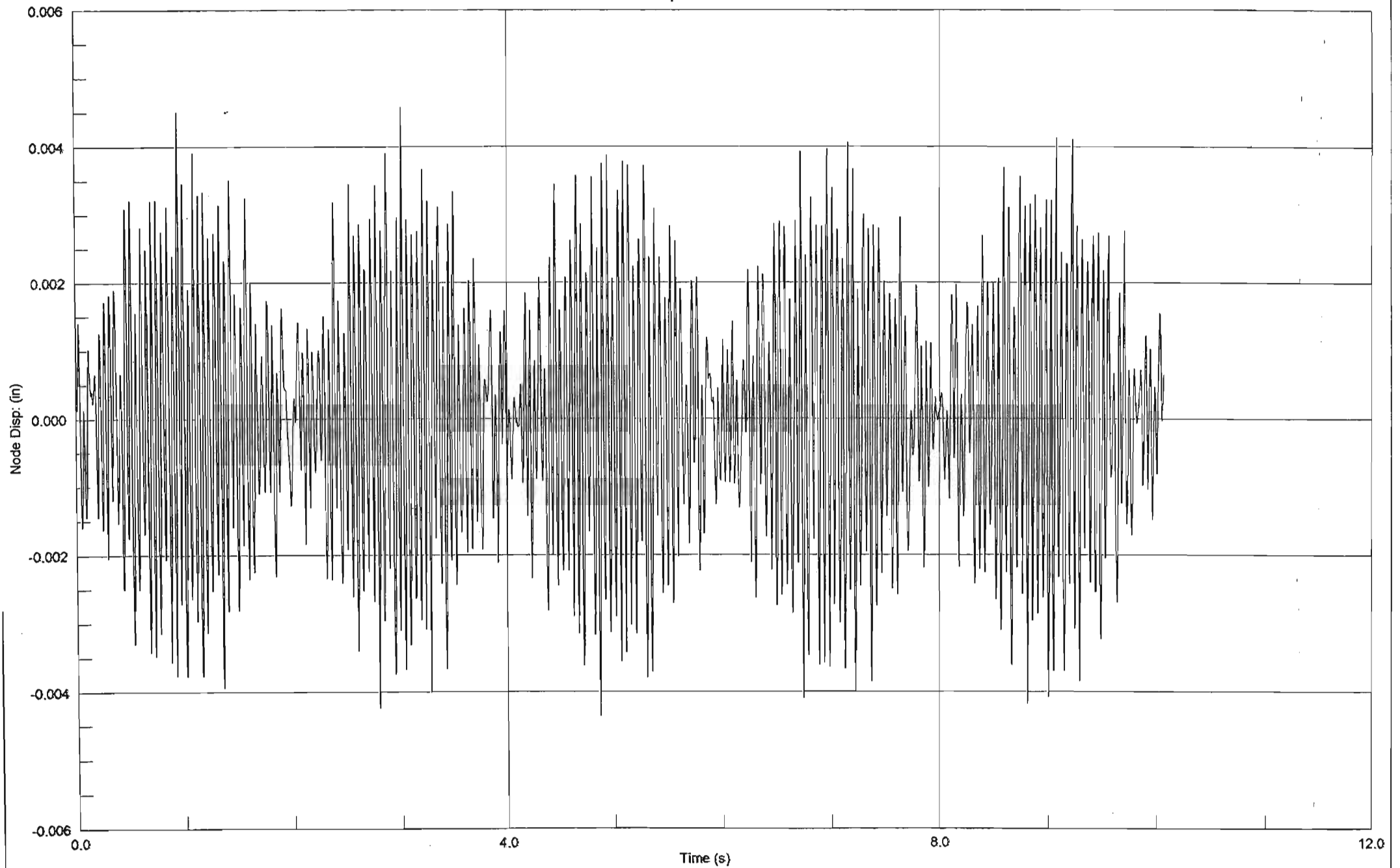


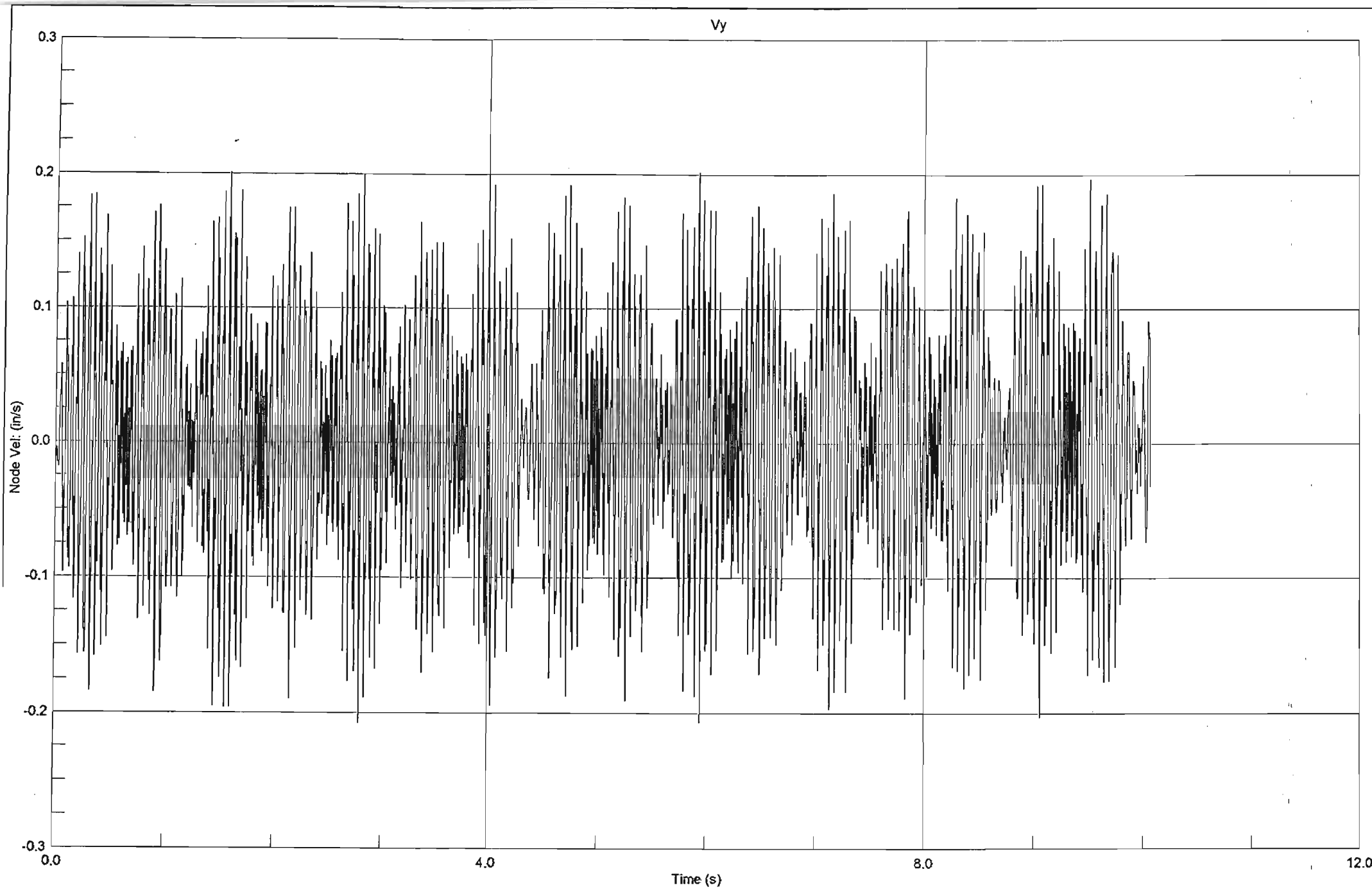
Z Displacement of Node 8

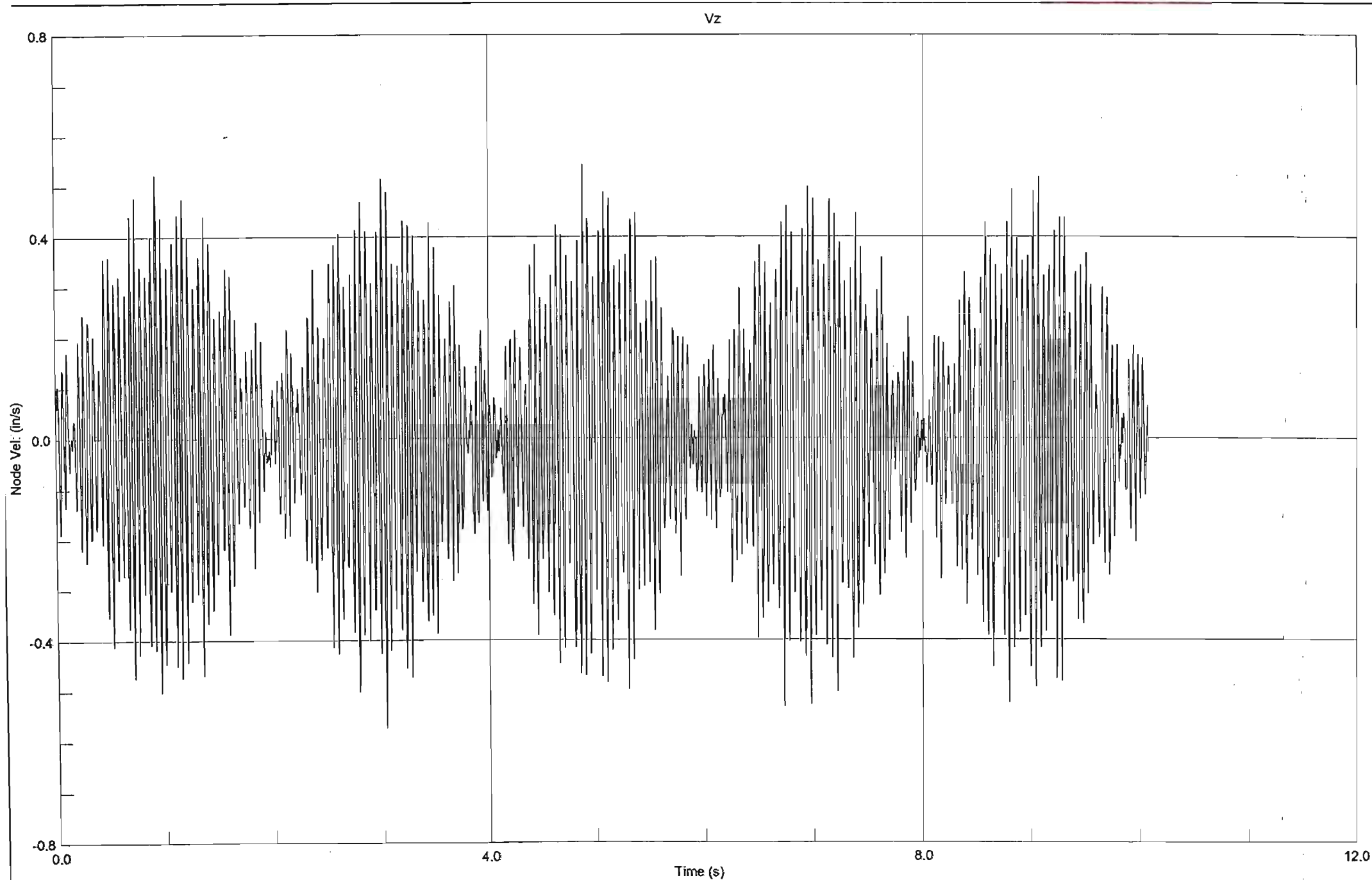


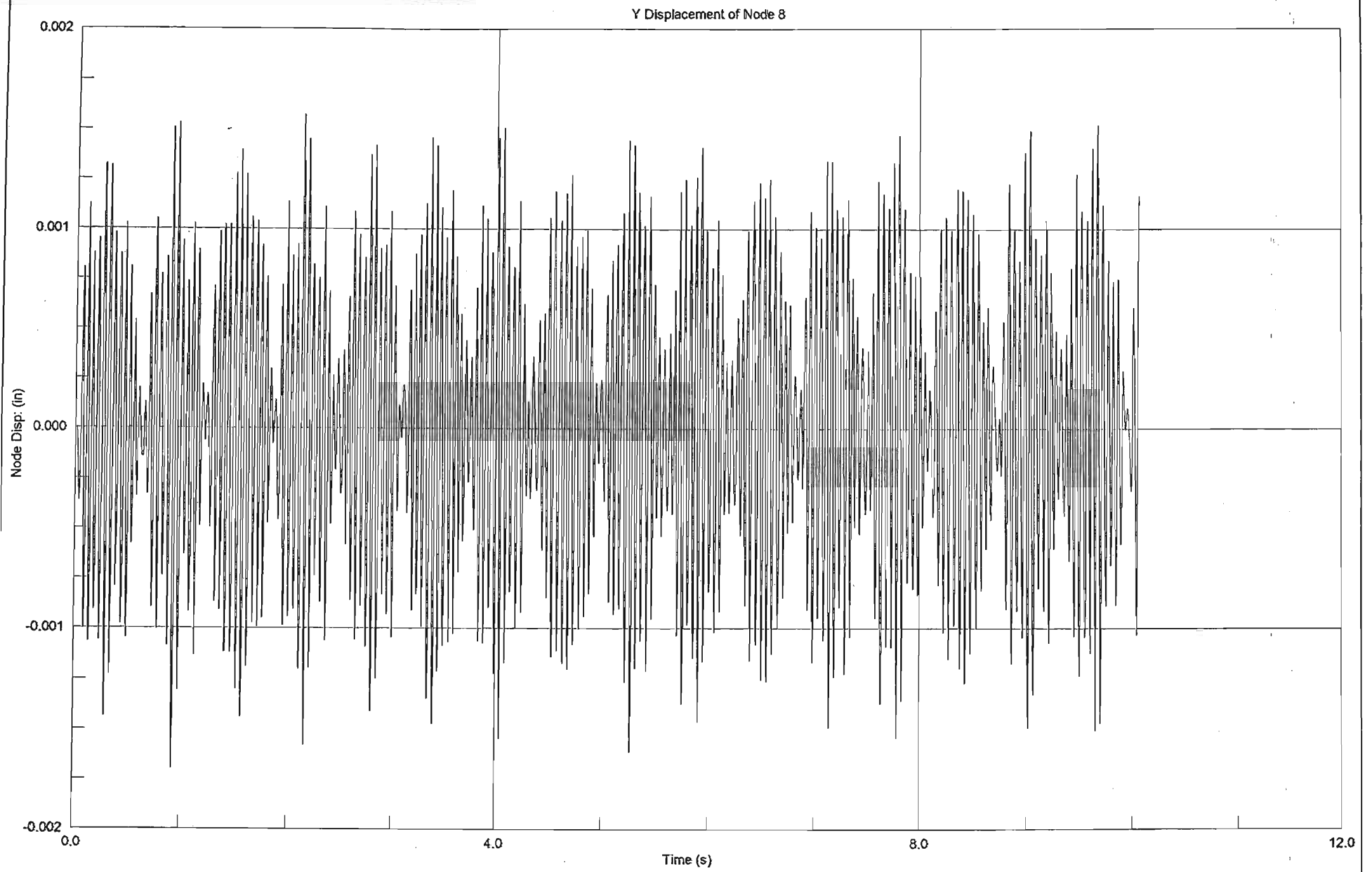


Z Displacement of Node 20

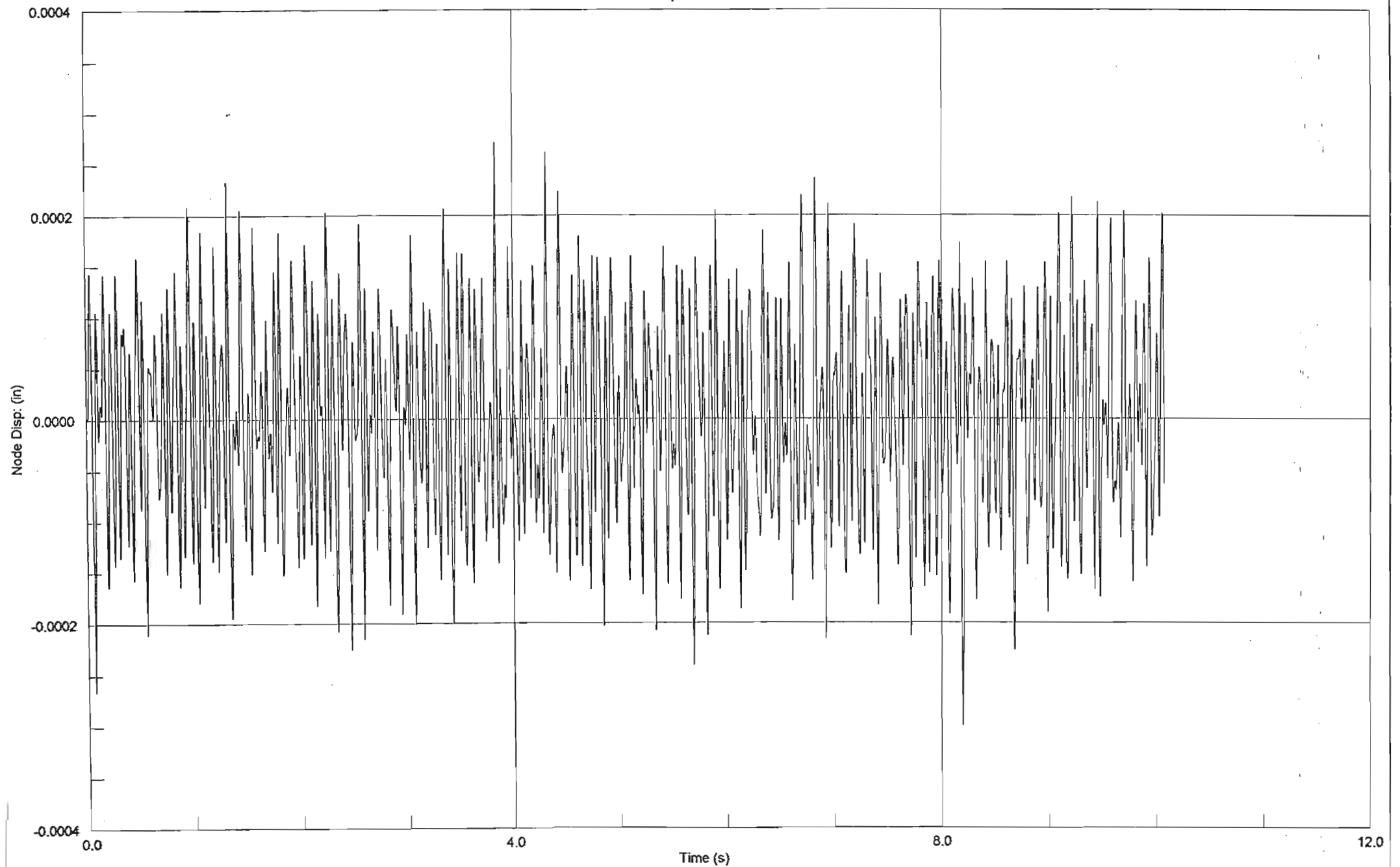


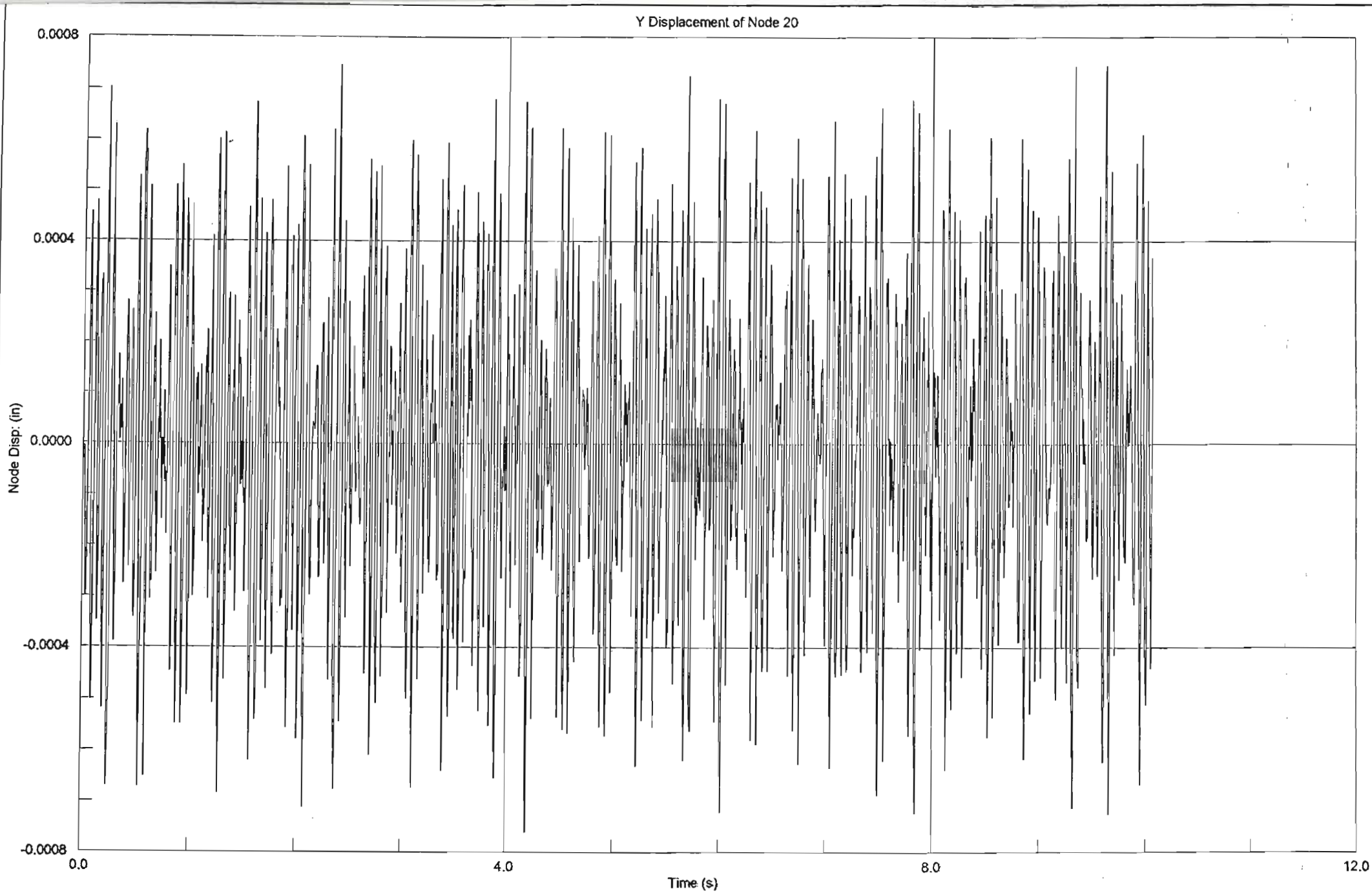




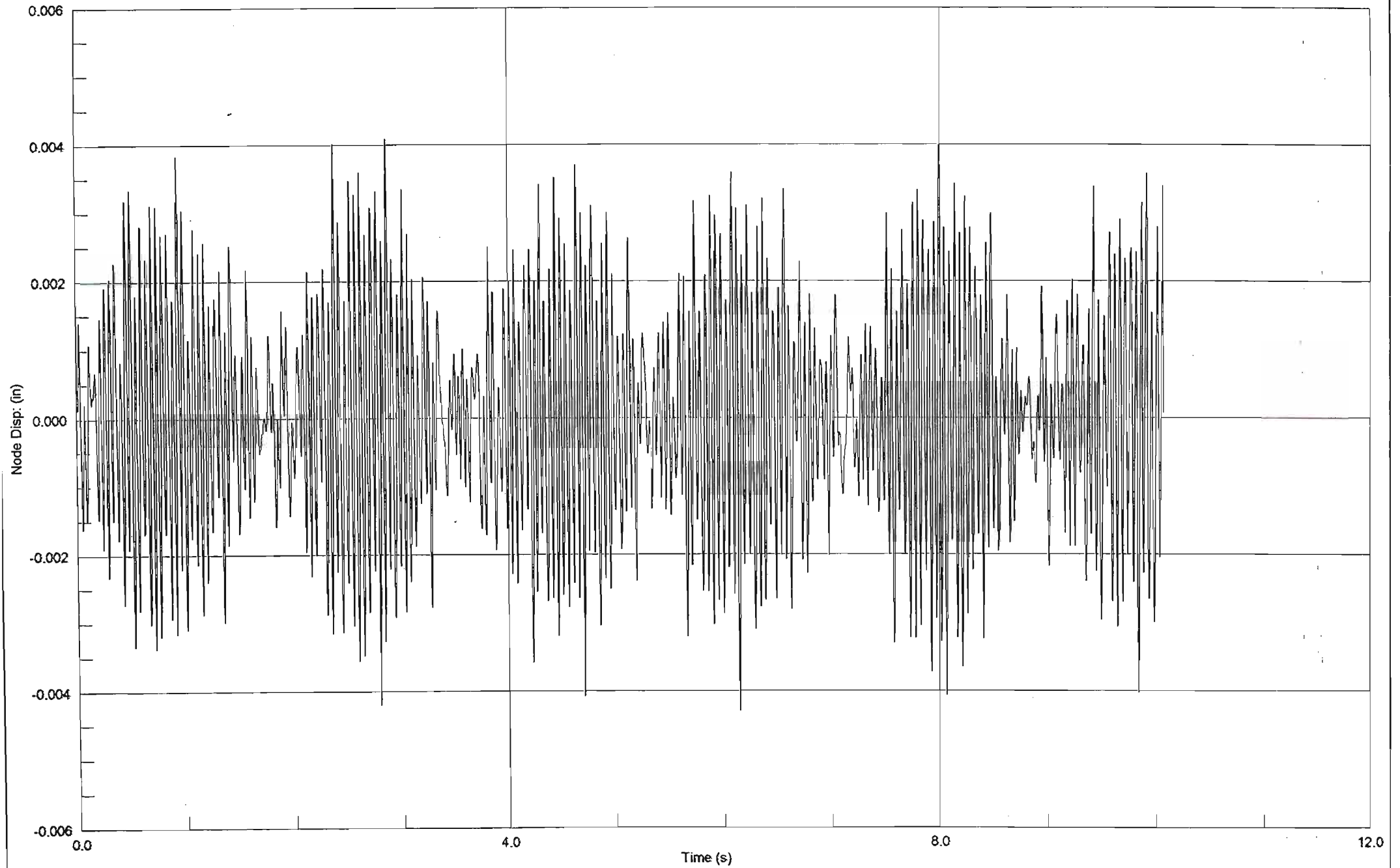


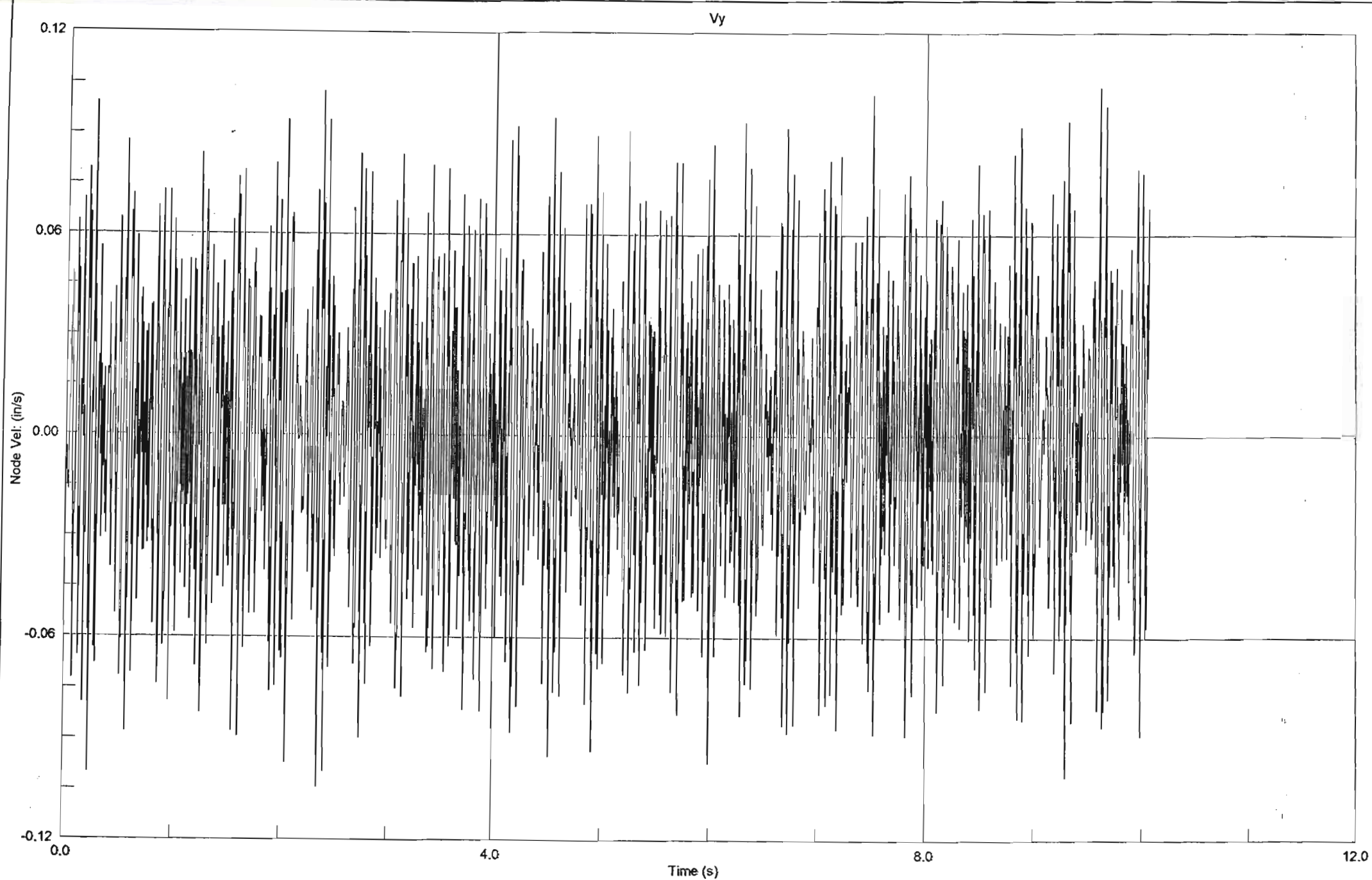
Z Displacement of Node 8





Z Displacement of Node 20





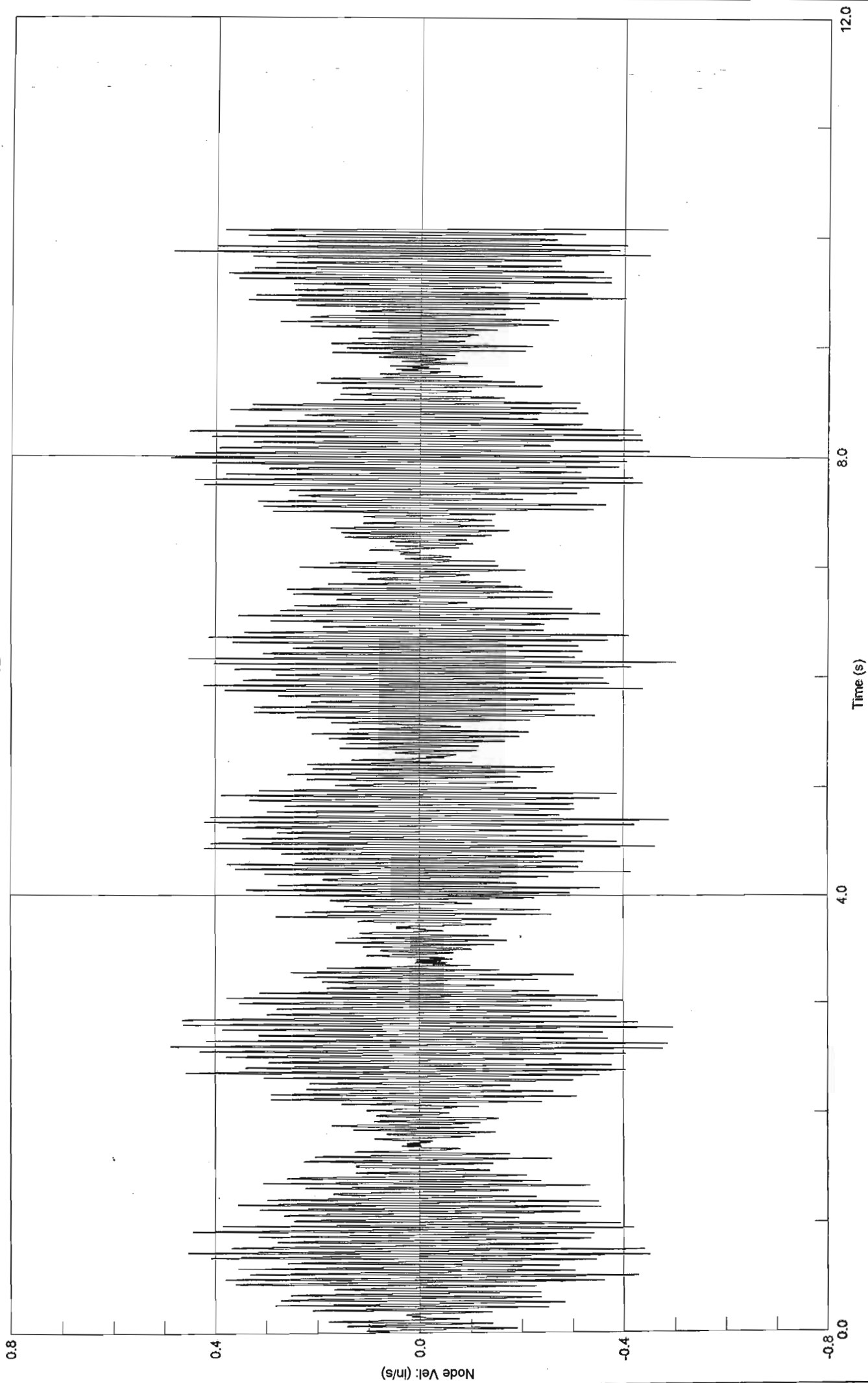
Strand7 Release 2.1.7

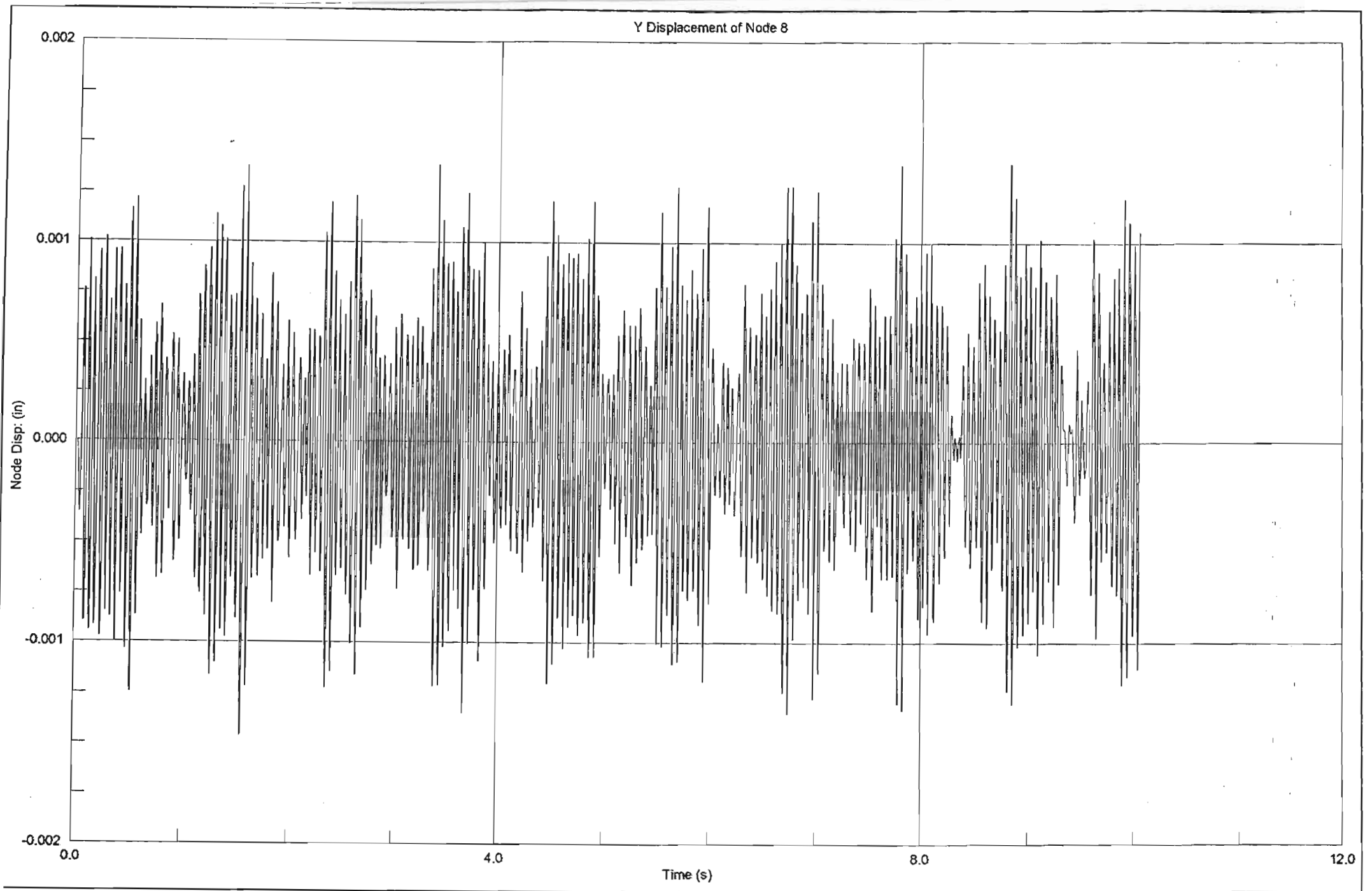
\\MS-Eng\Table Top\4\Table Top 4\table top G15000-F3.s17

12 October 2002 7:00 pm

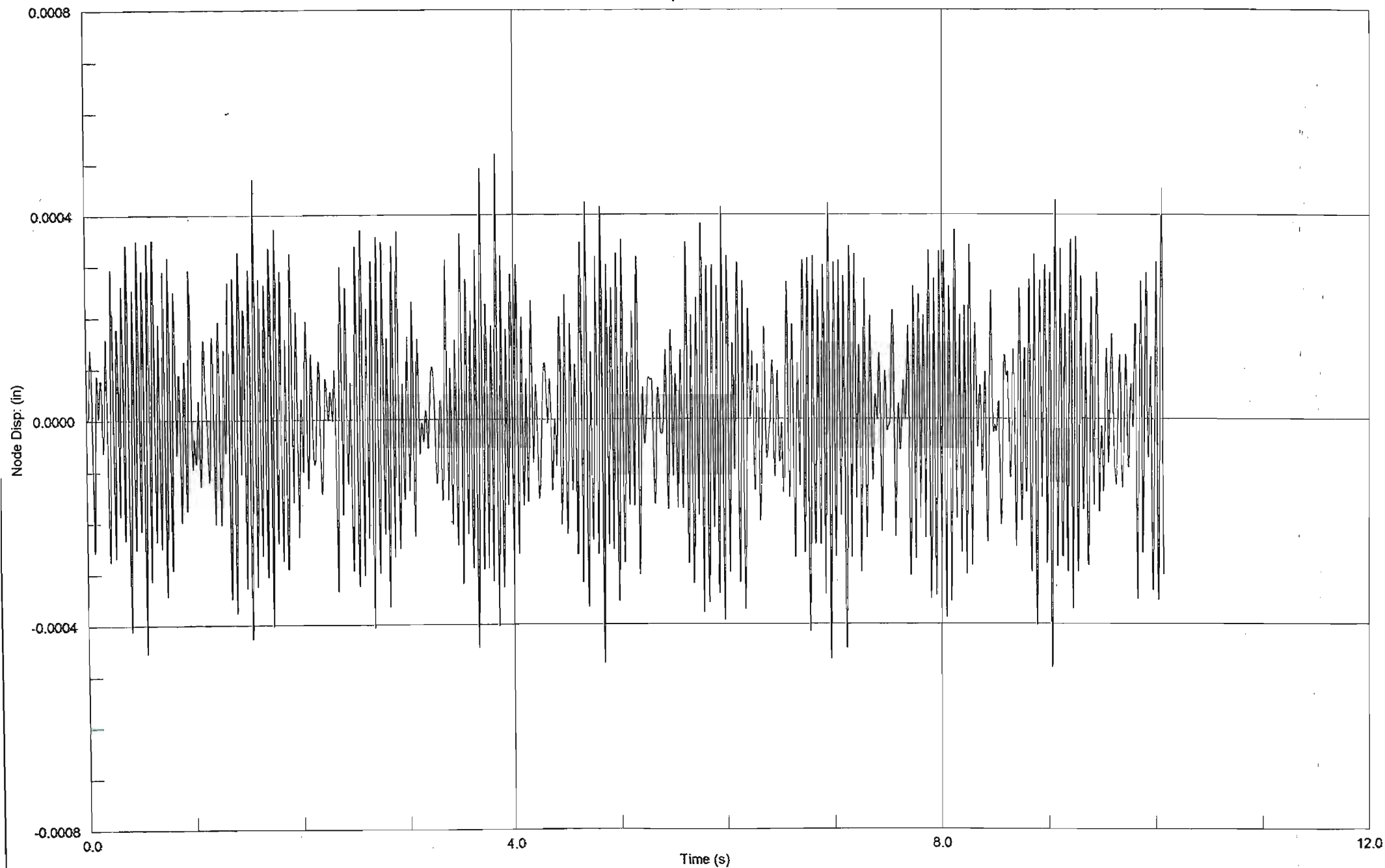
3.89

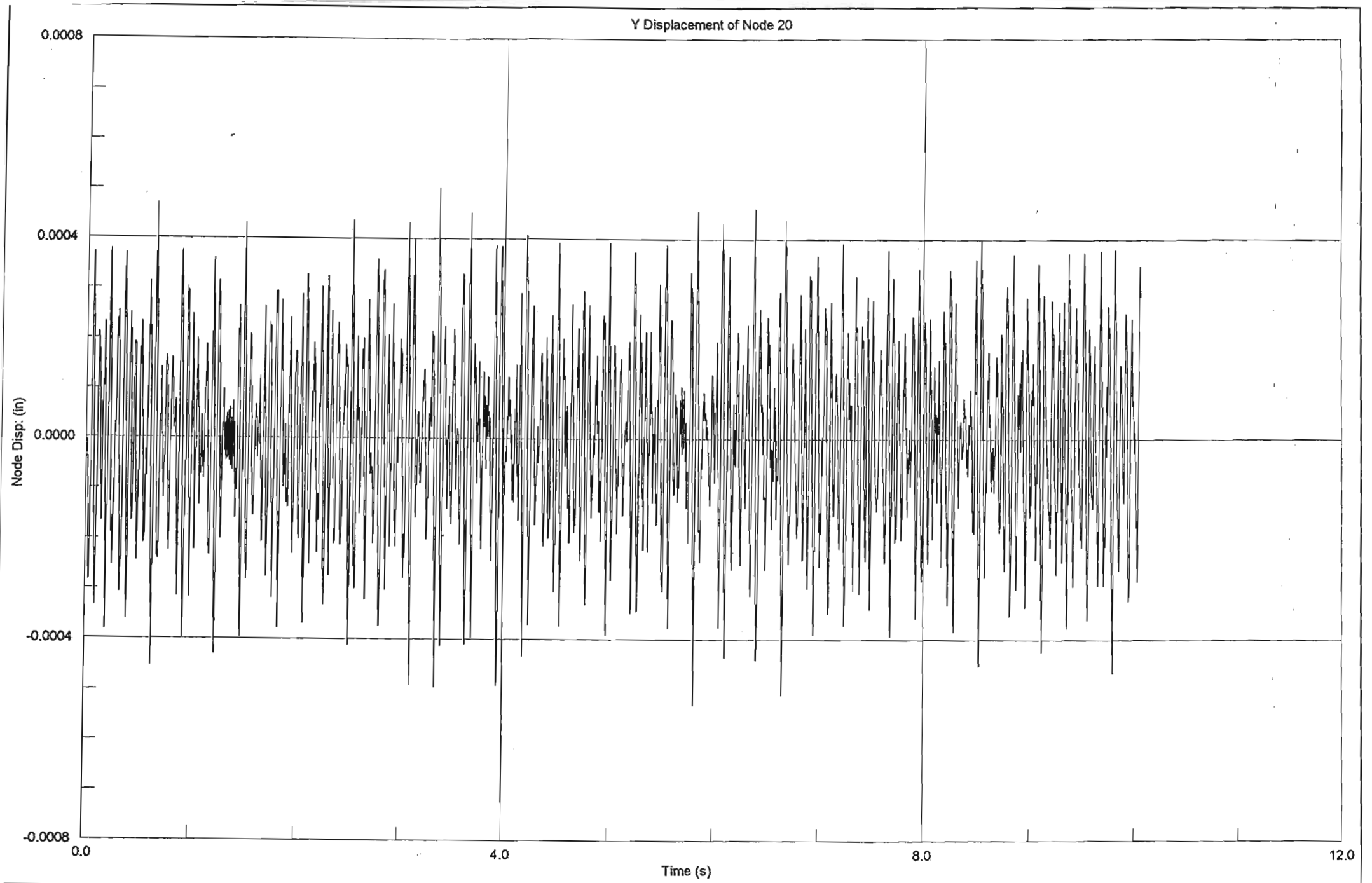
VZ

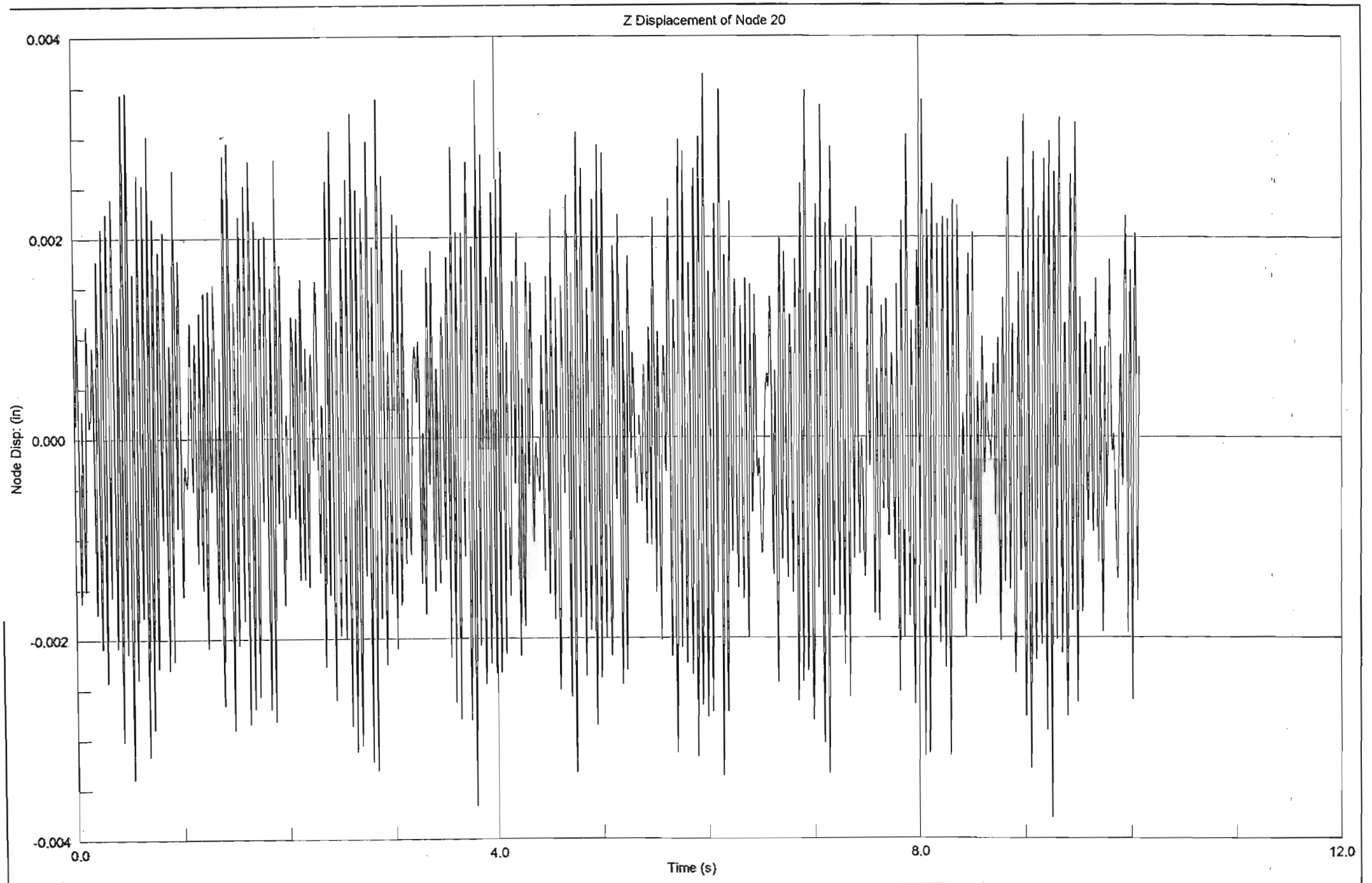


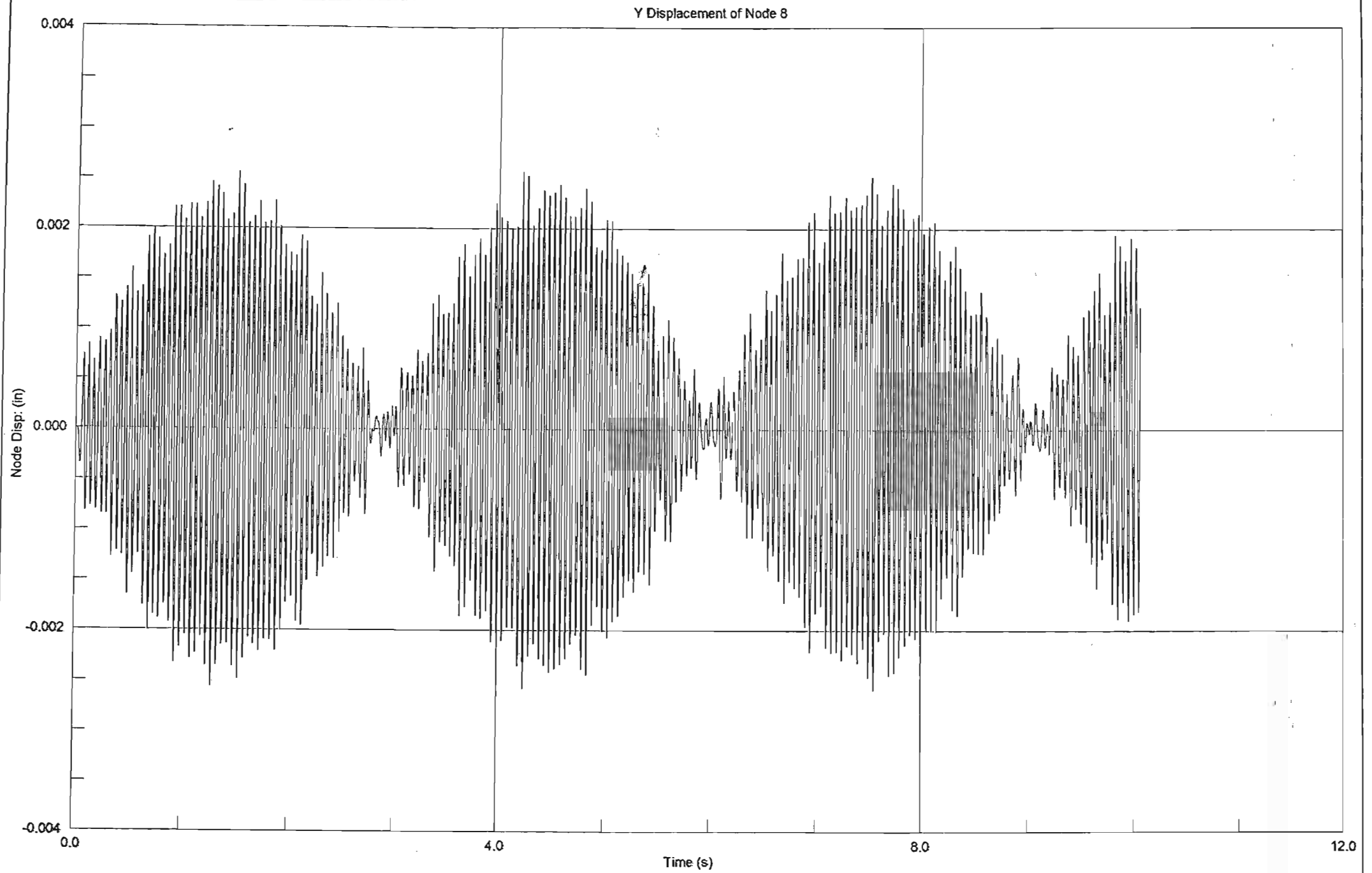


Z Displacement of Node 8

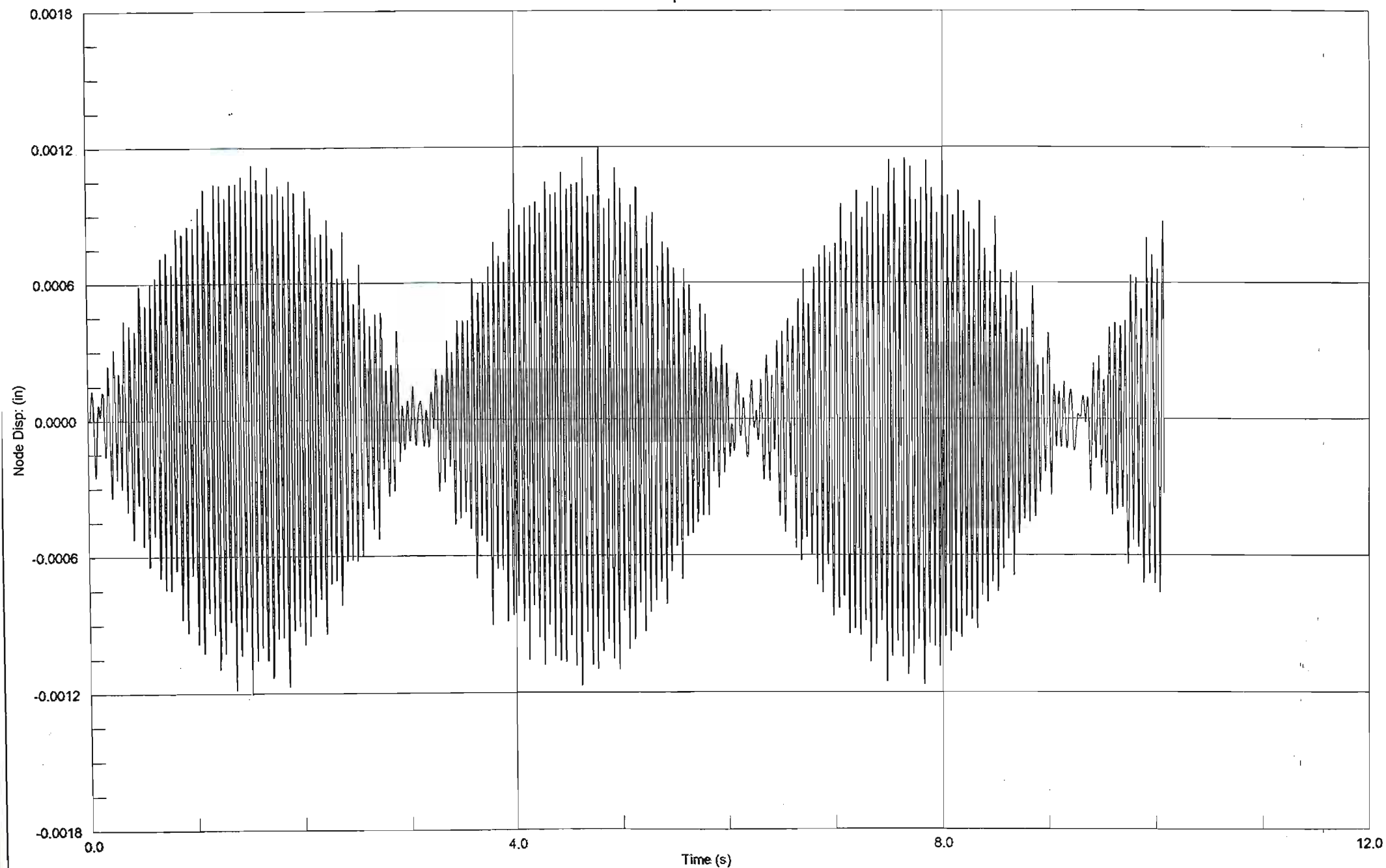


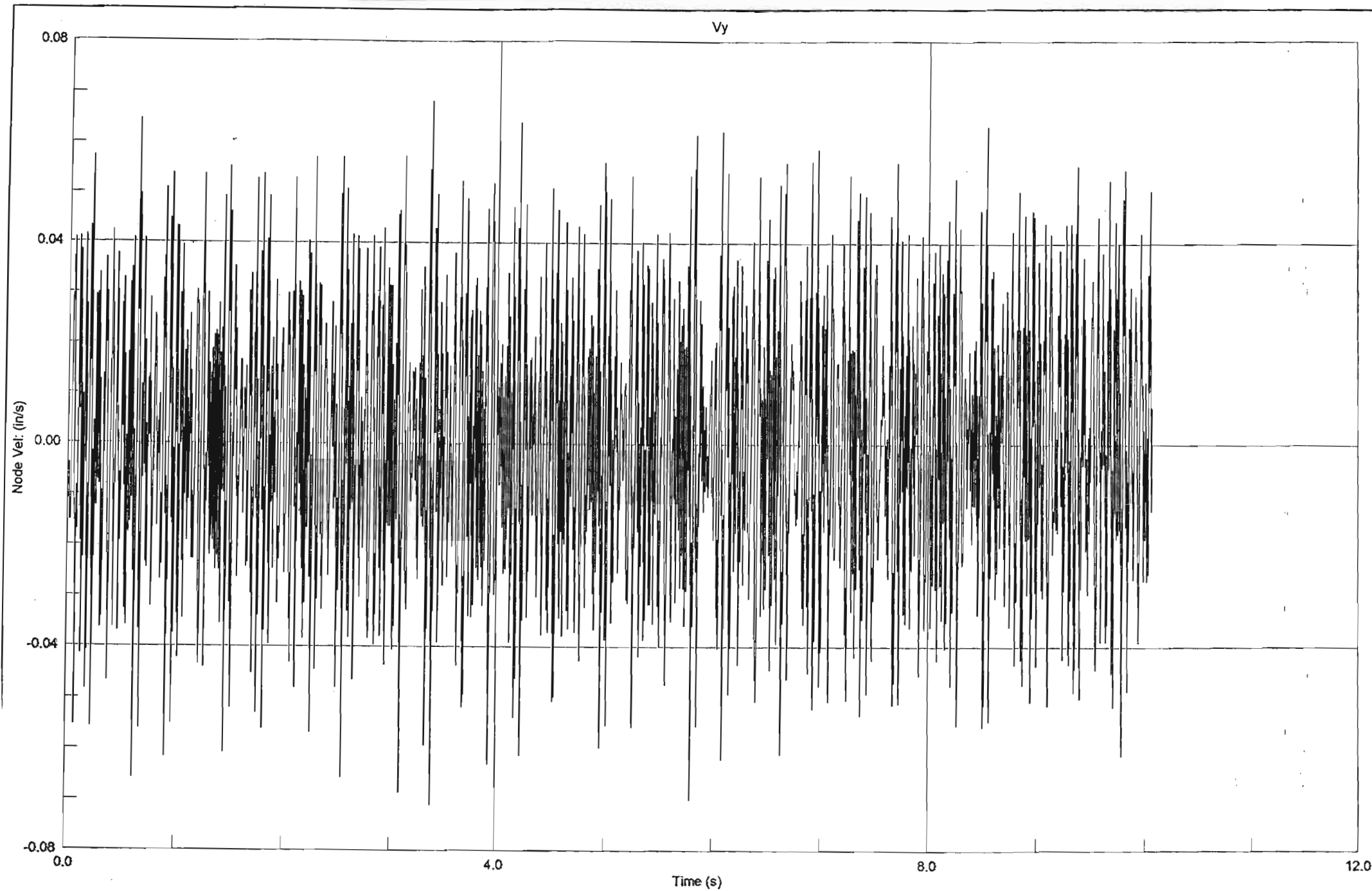


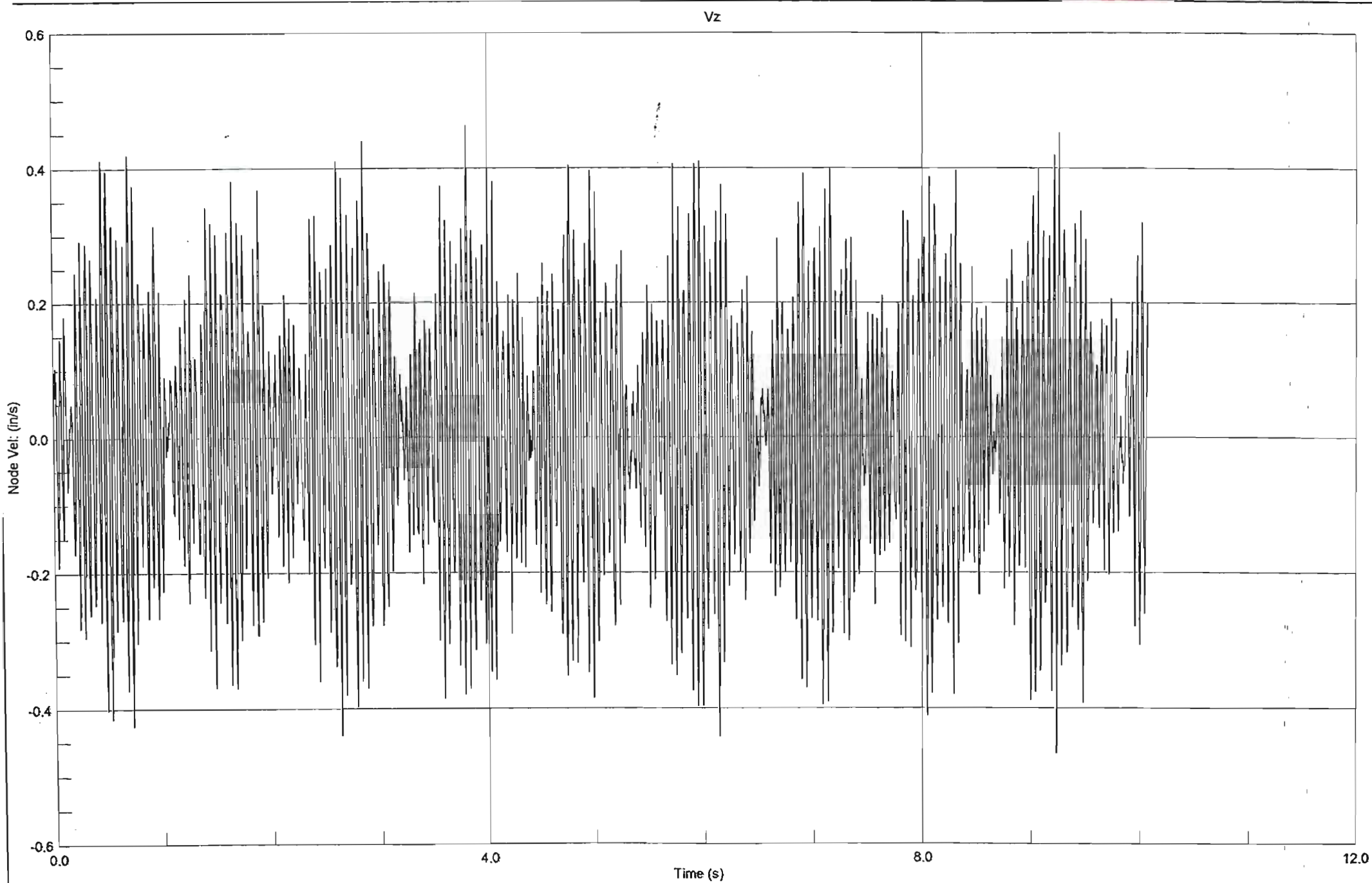


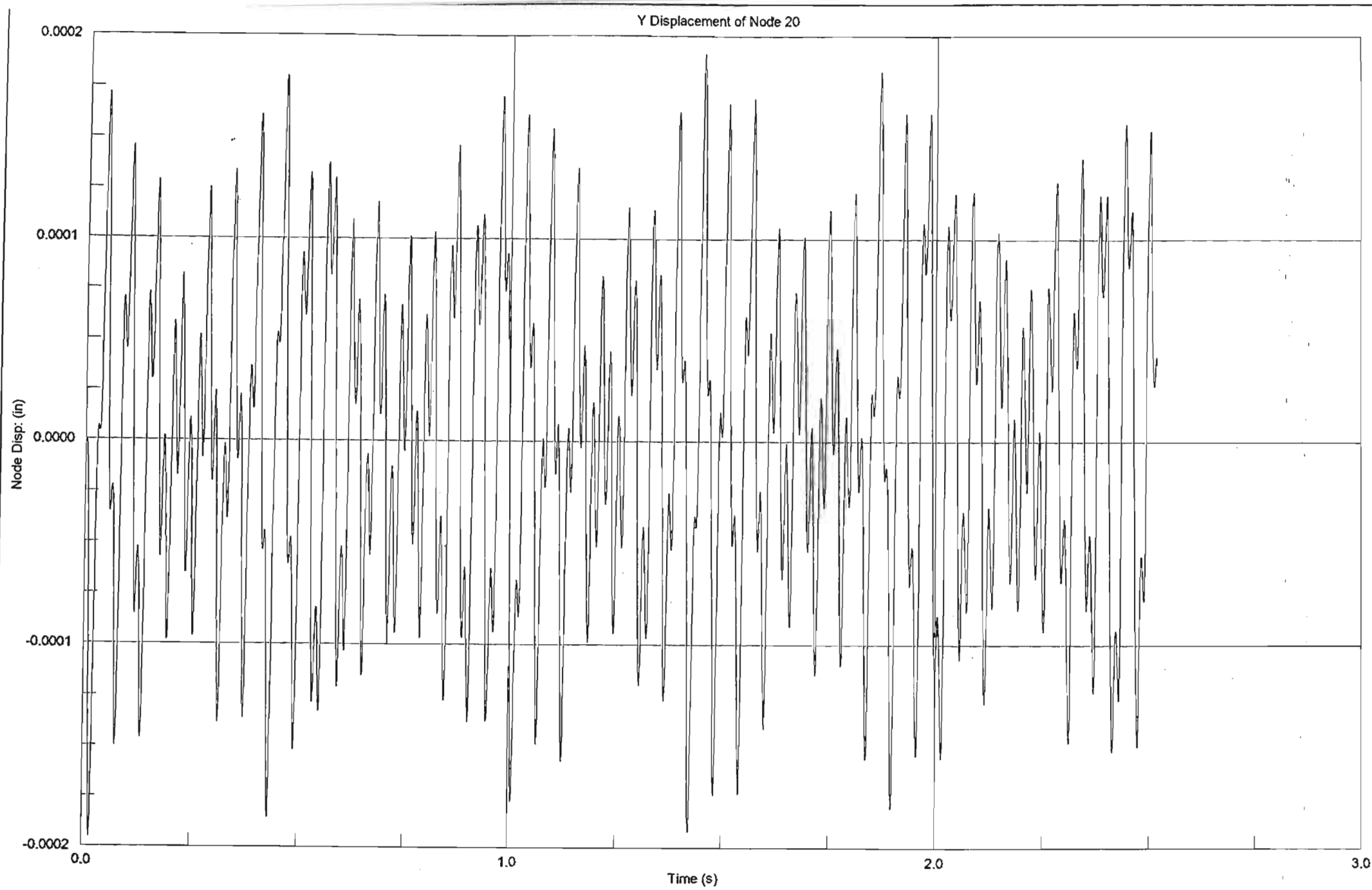


Z Displacement of Node 8

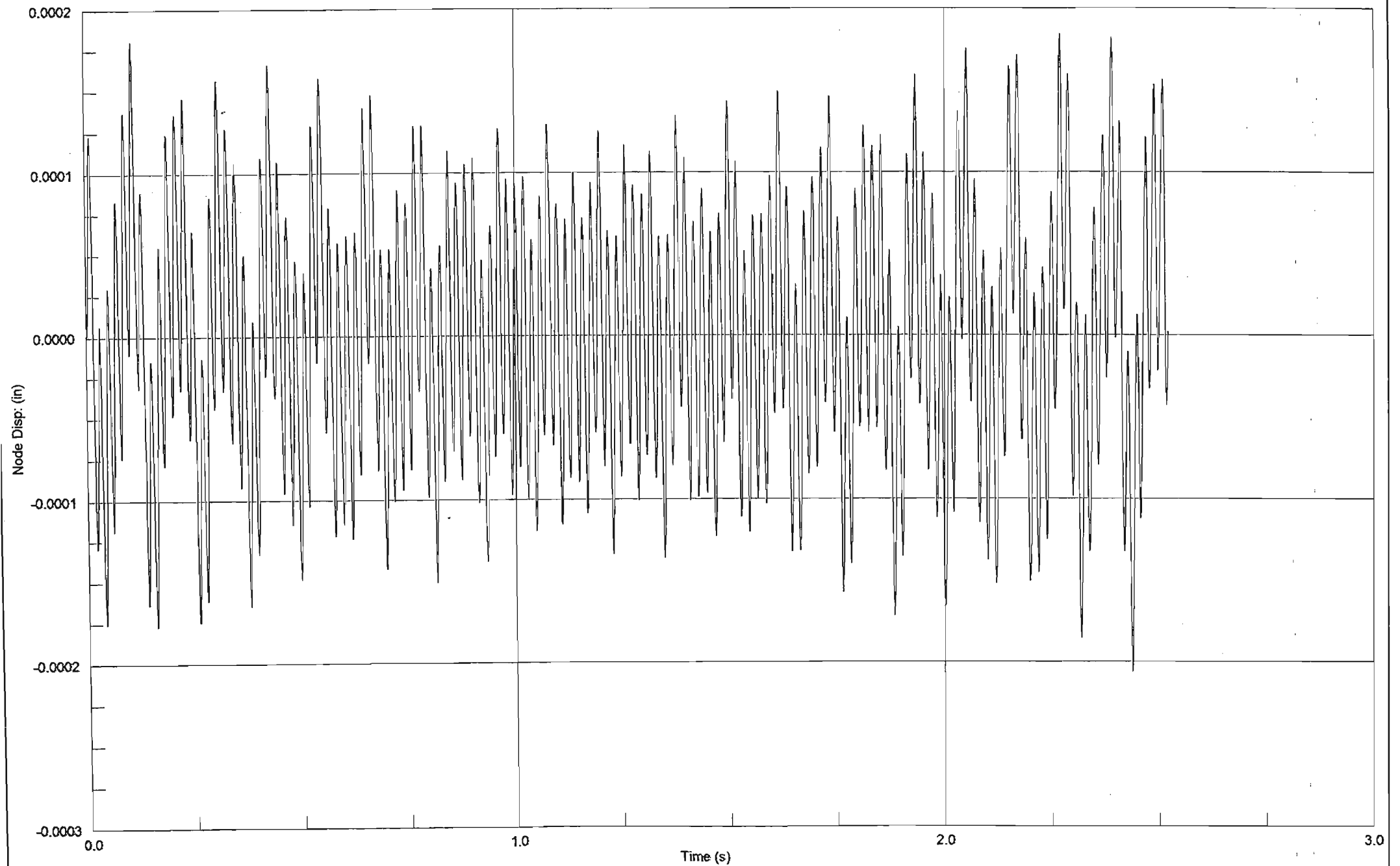


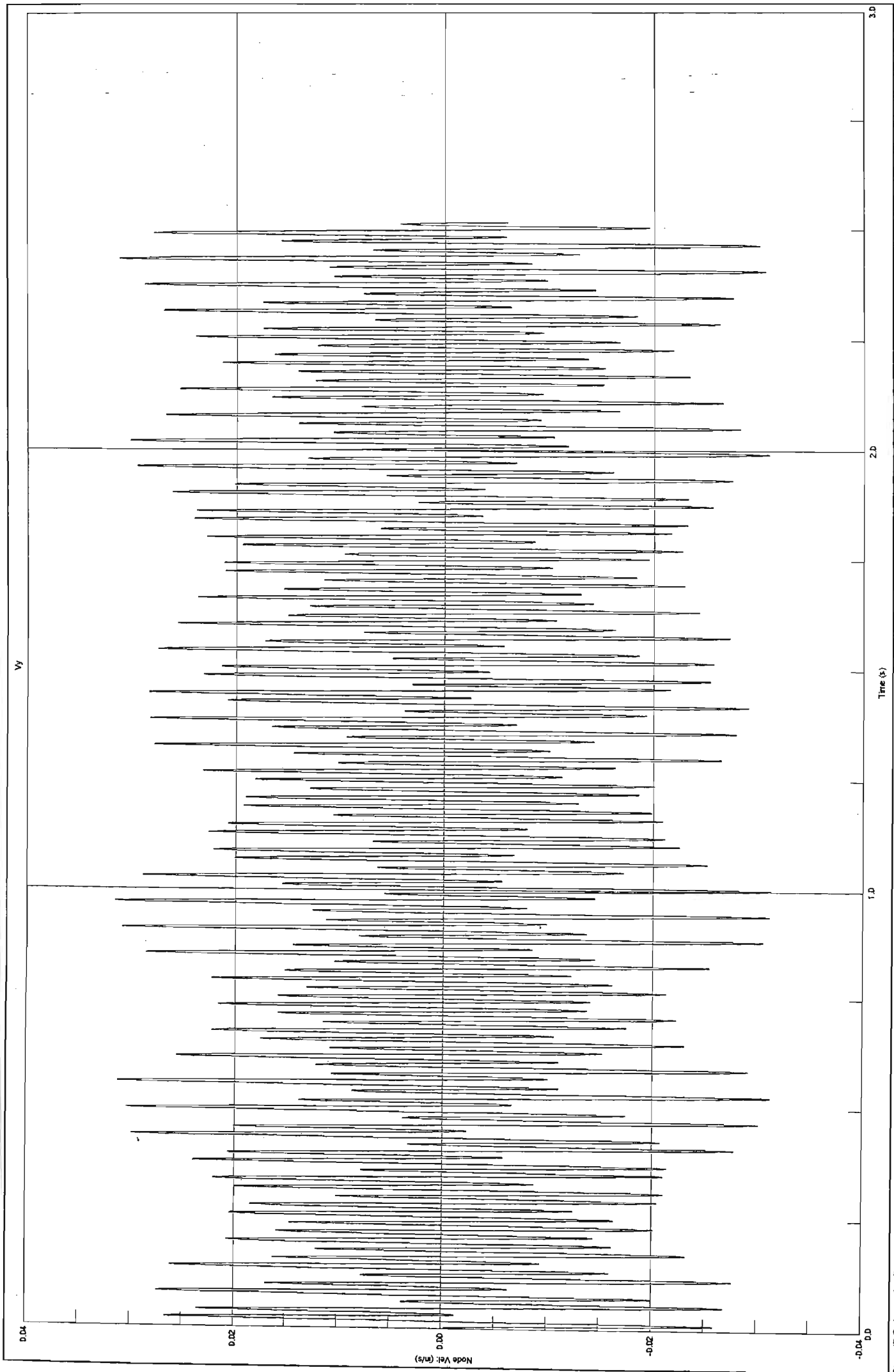


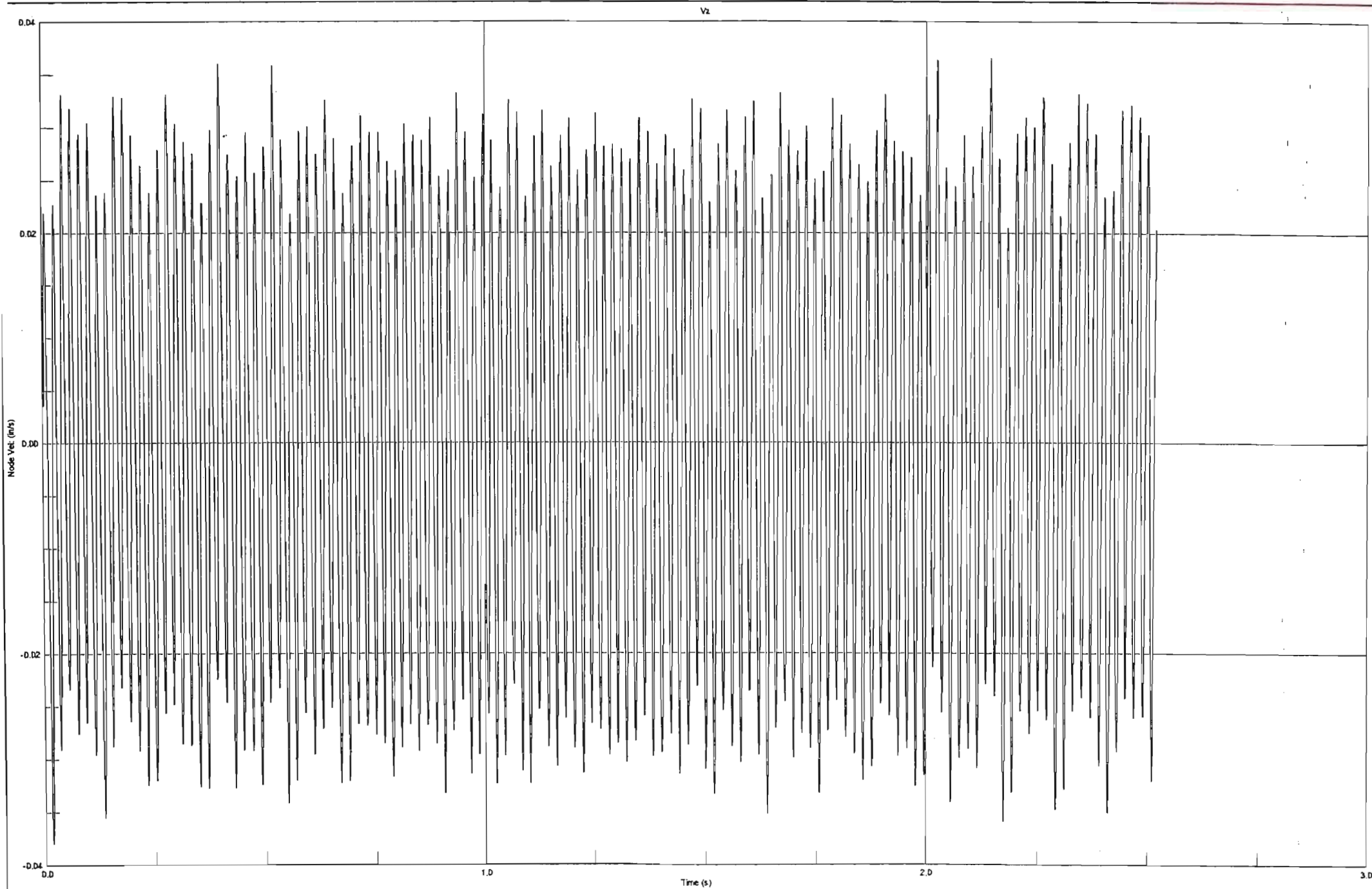


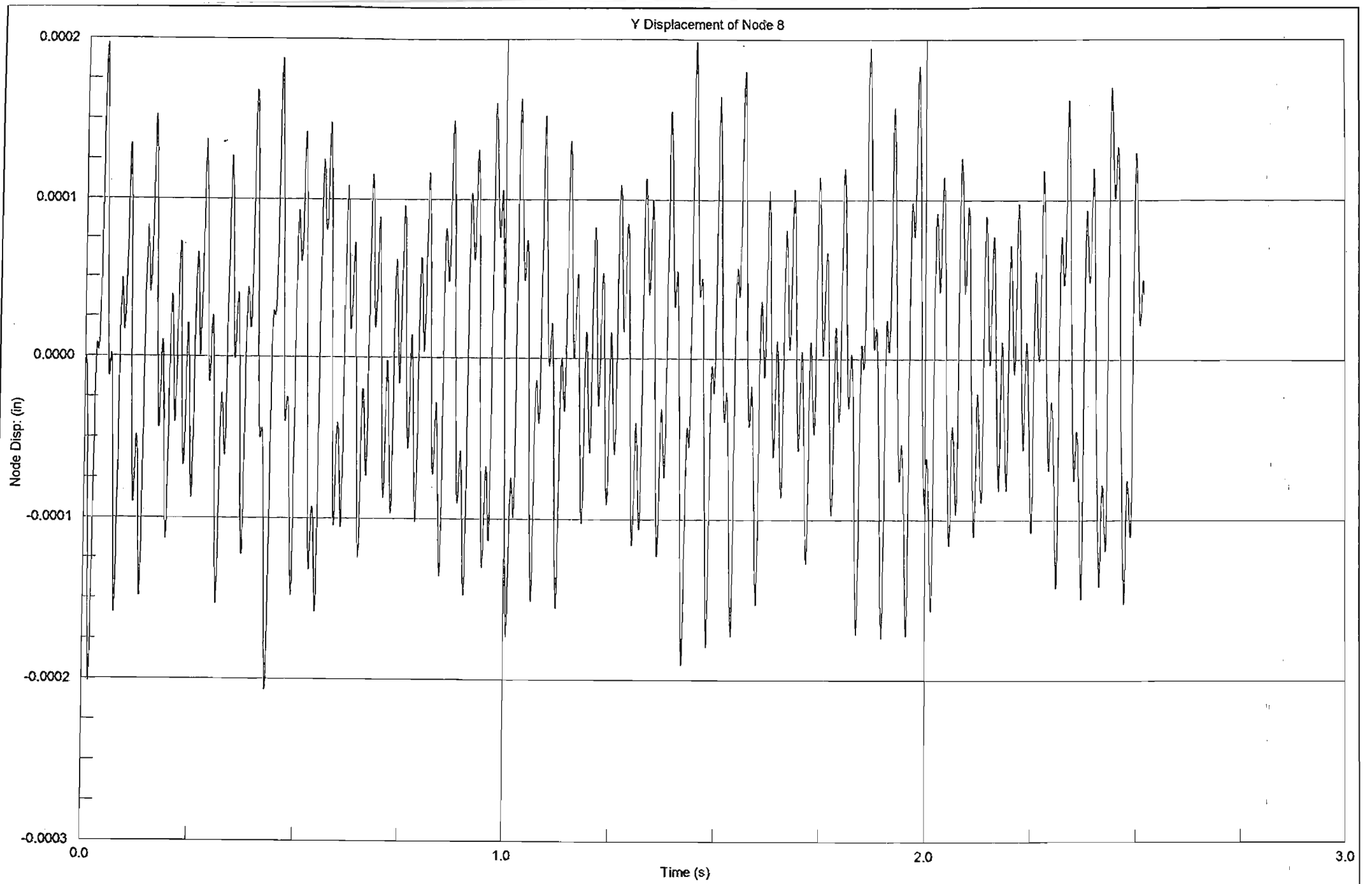


Z Displacement of Node 20

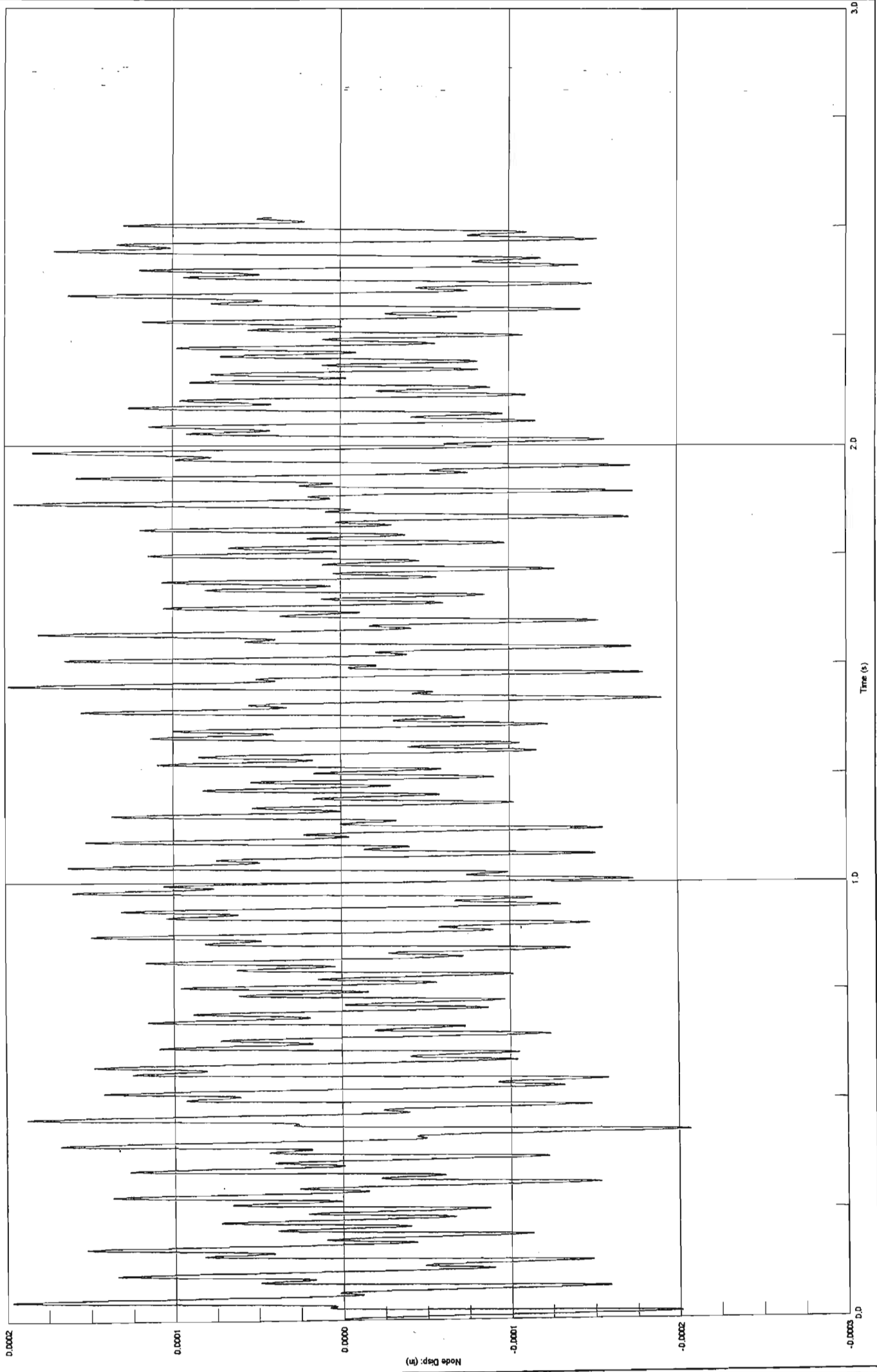


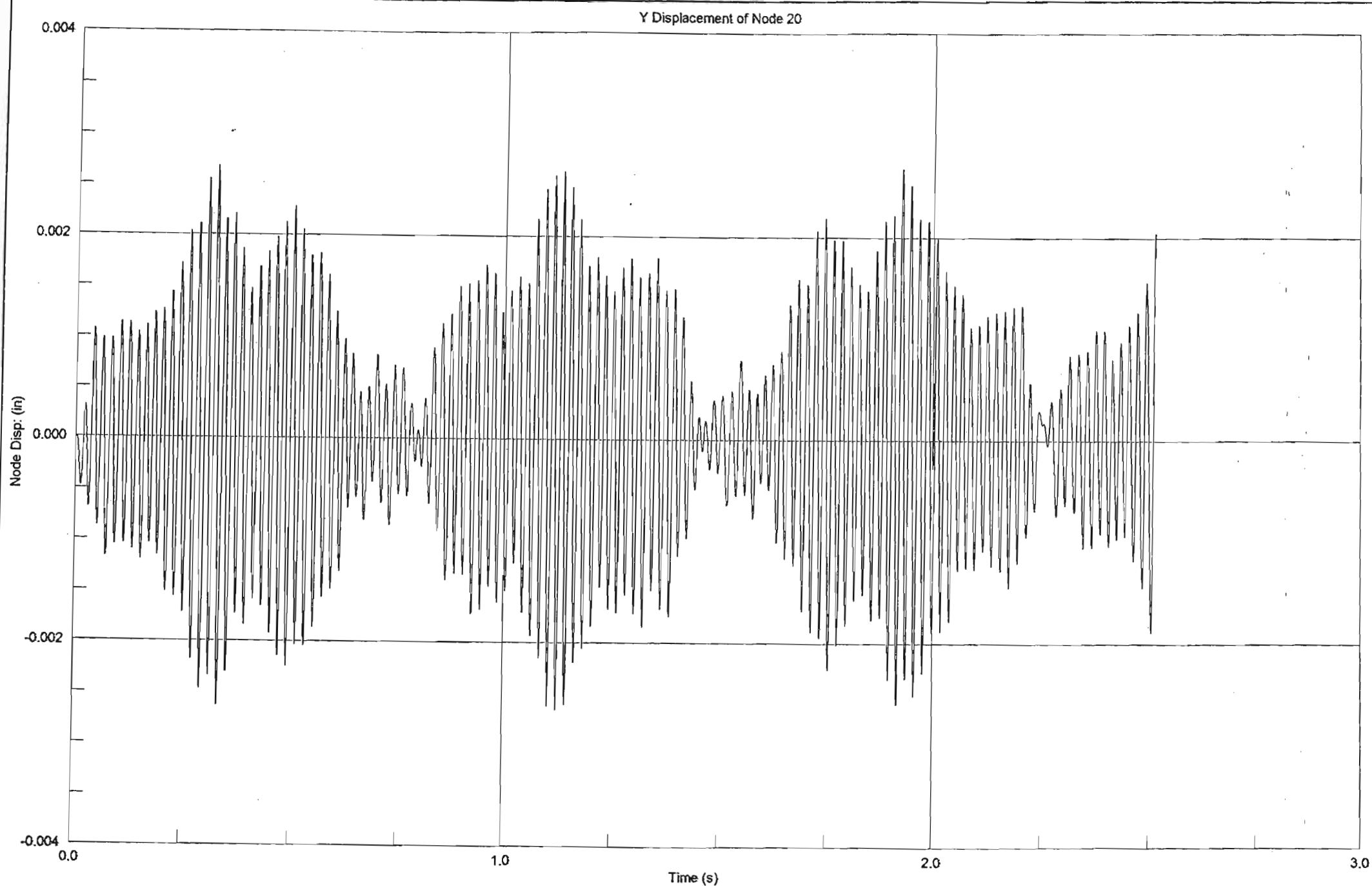




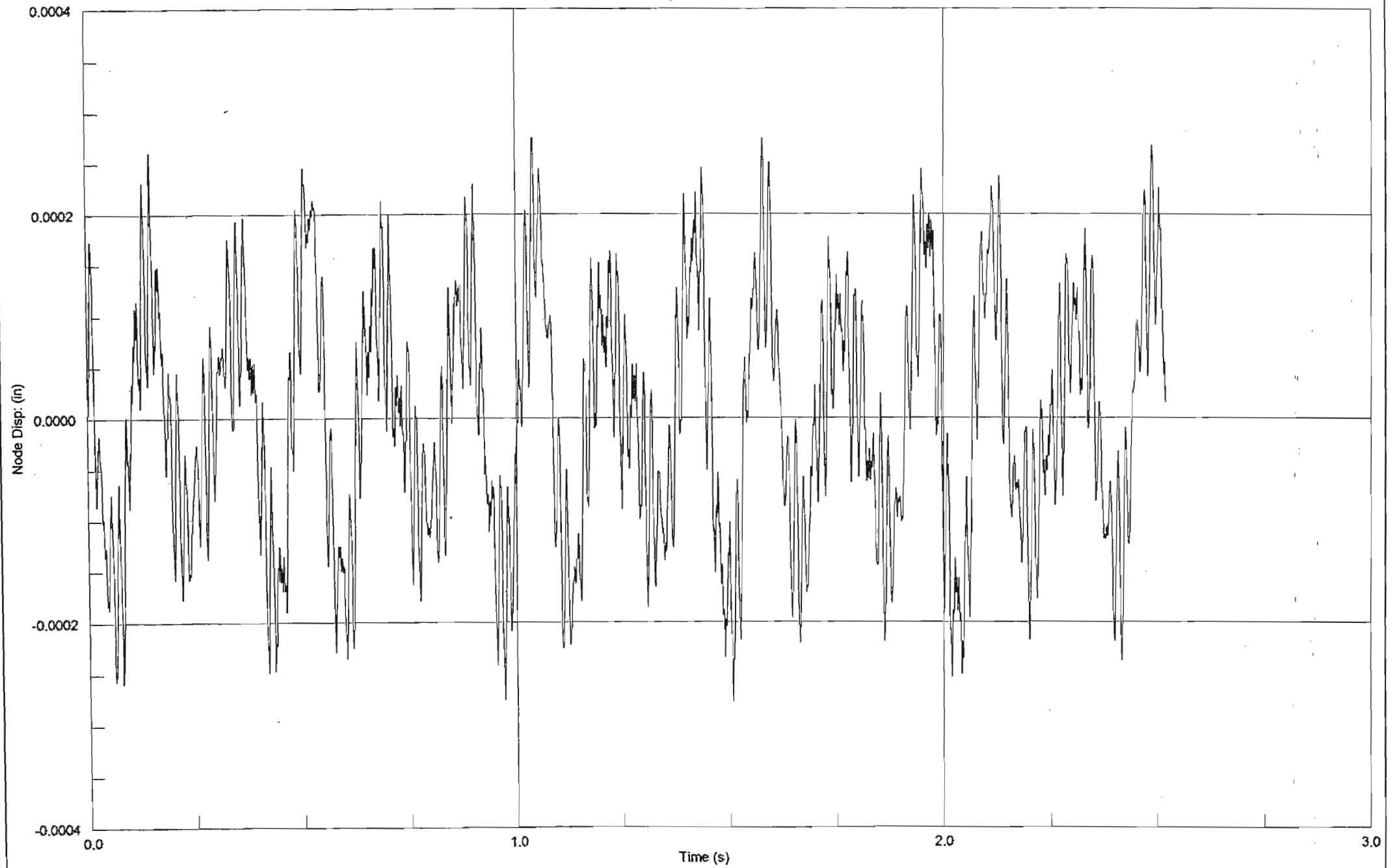


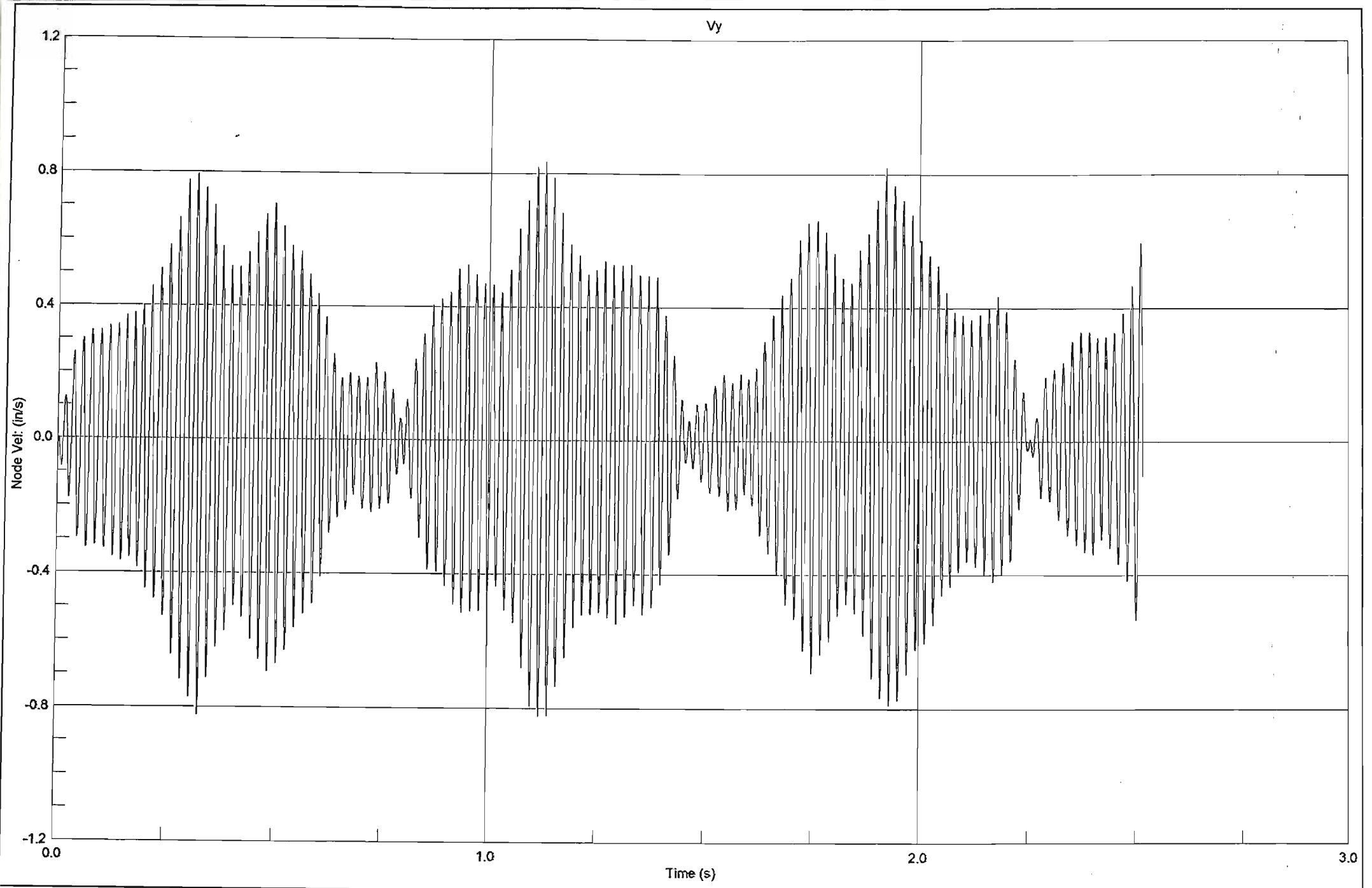
Z Displacement of Node 8

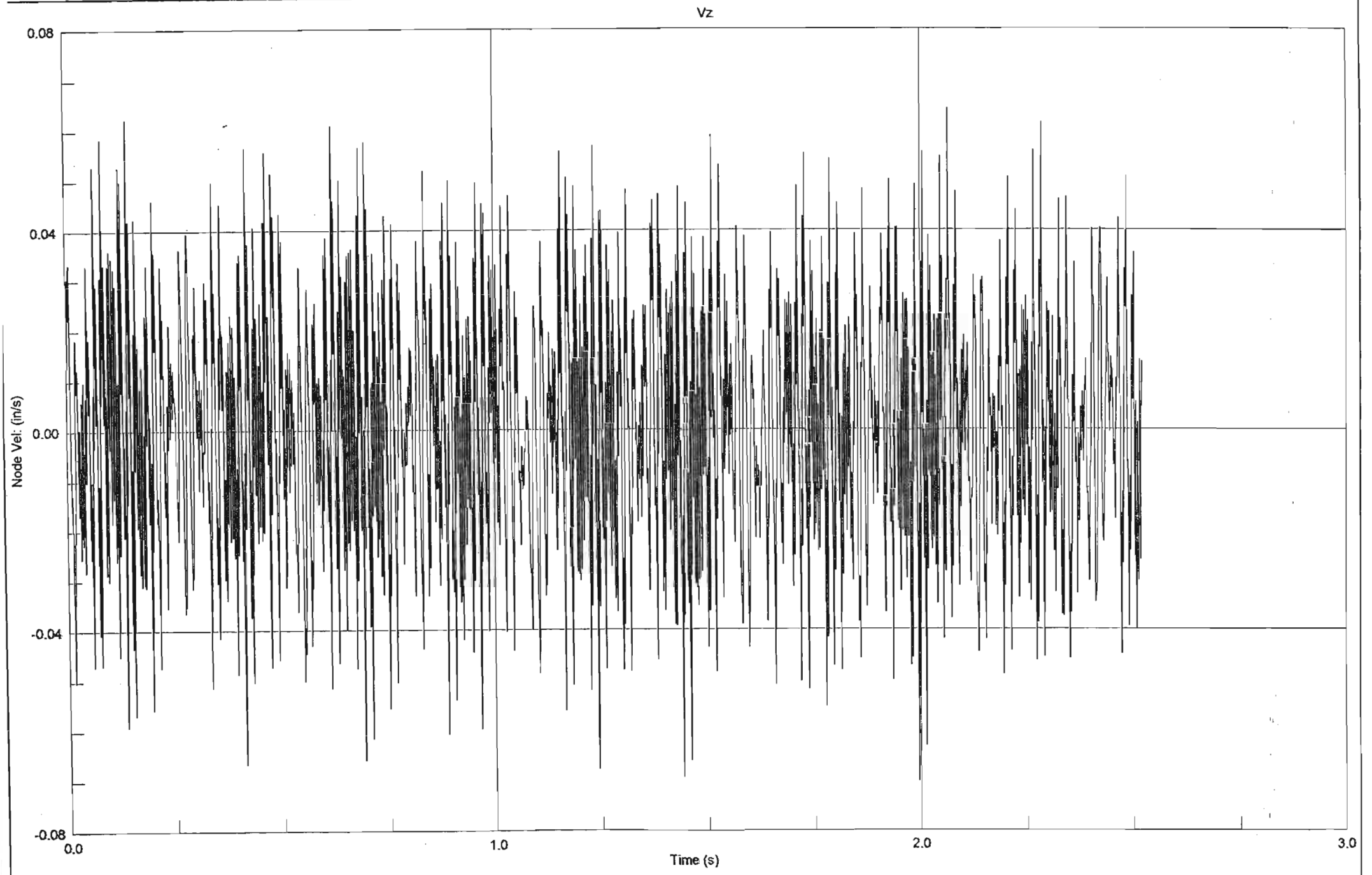


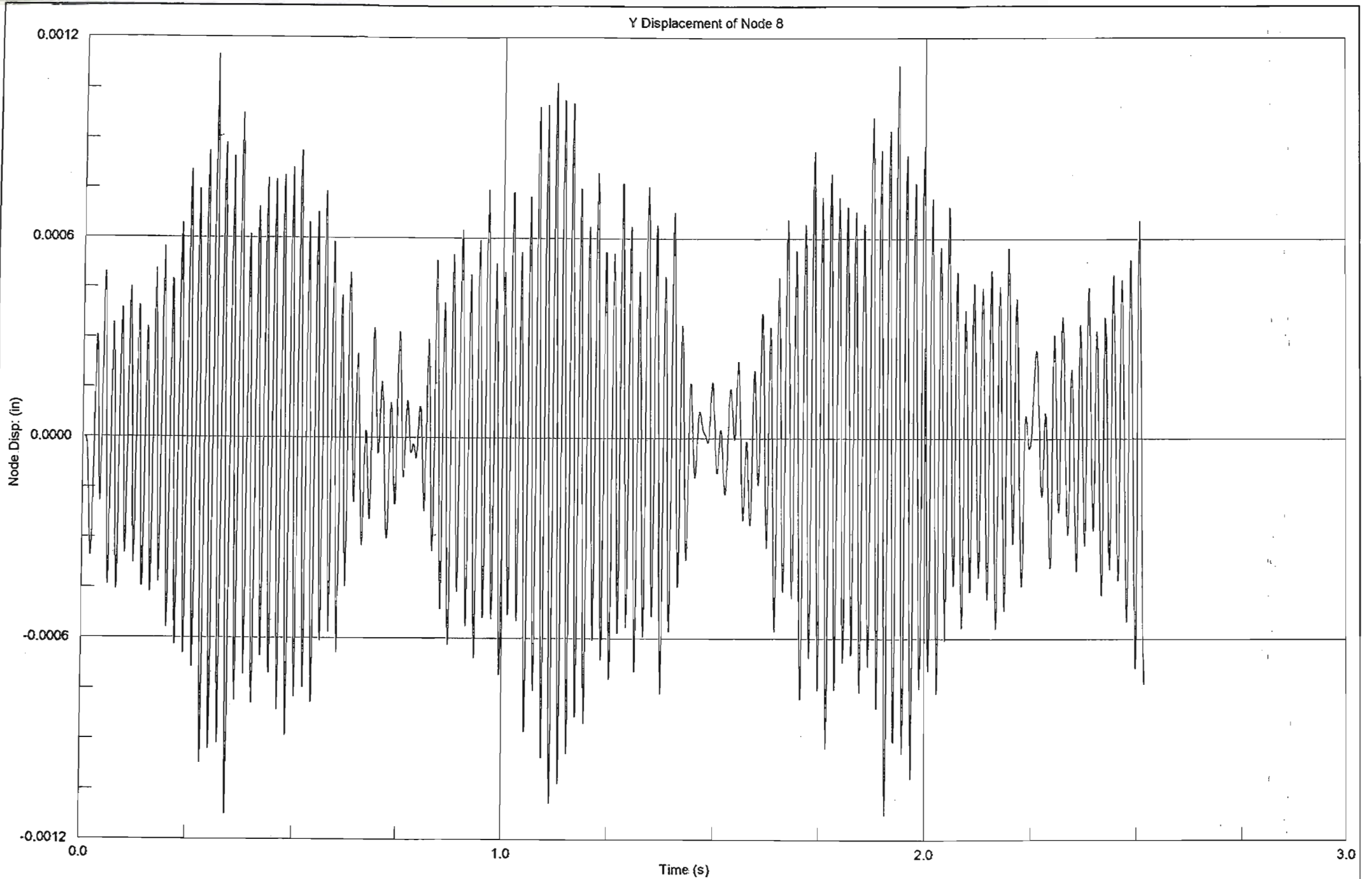


Z Displacement of Node 20

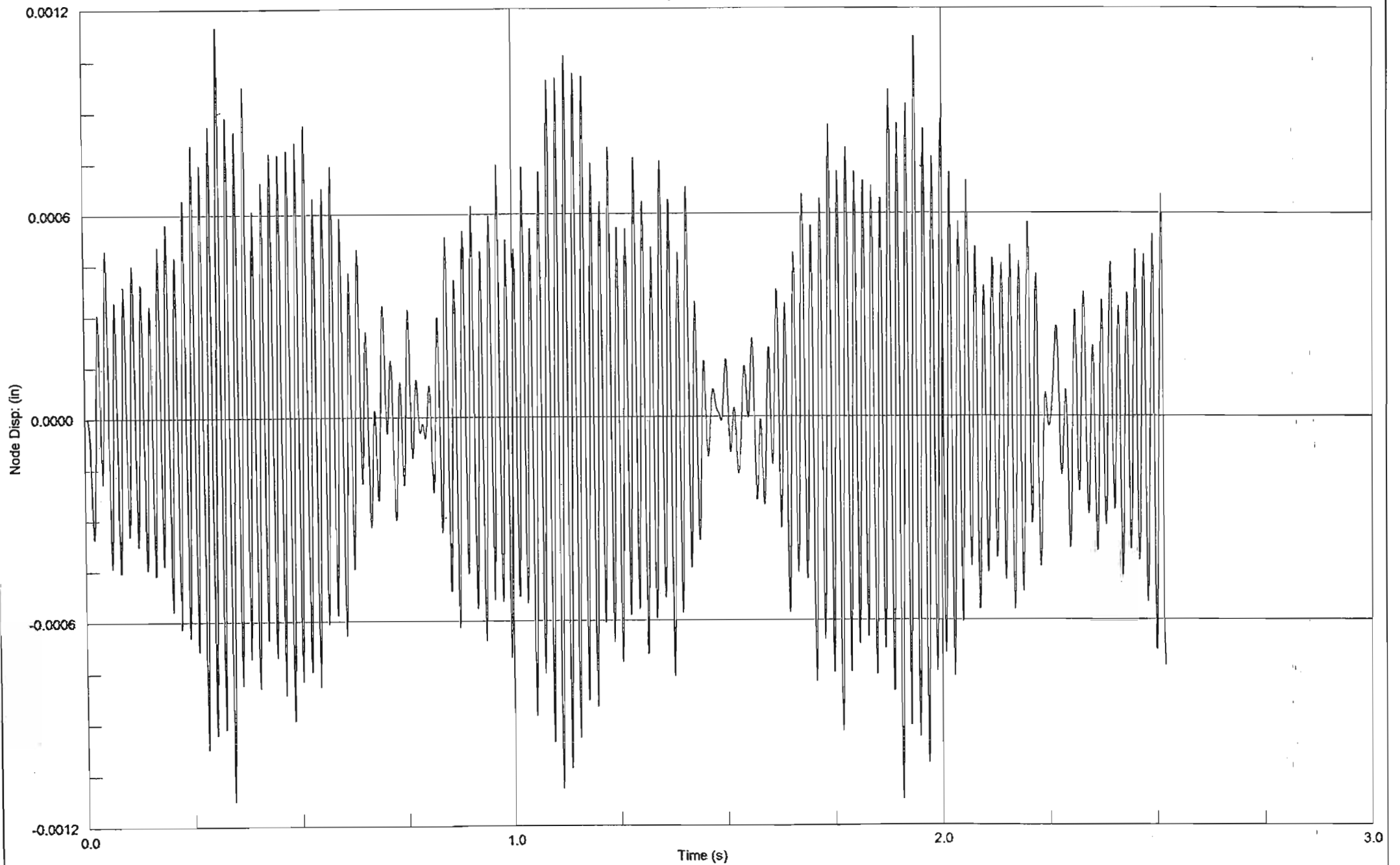


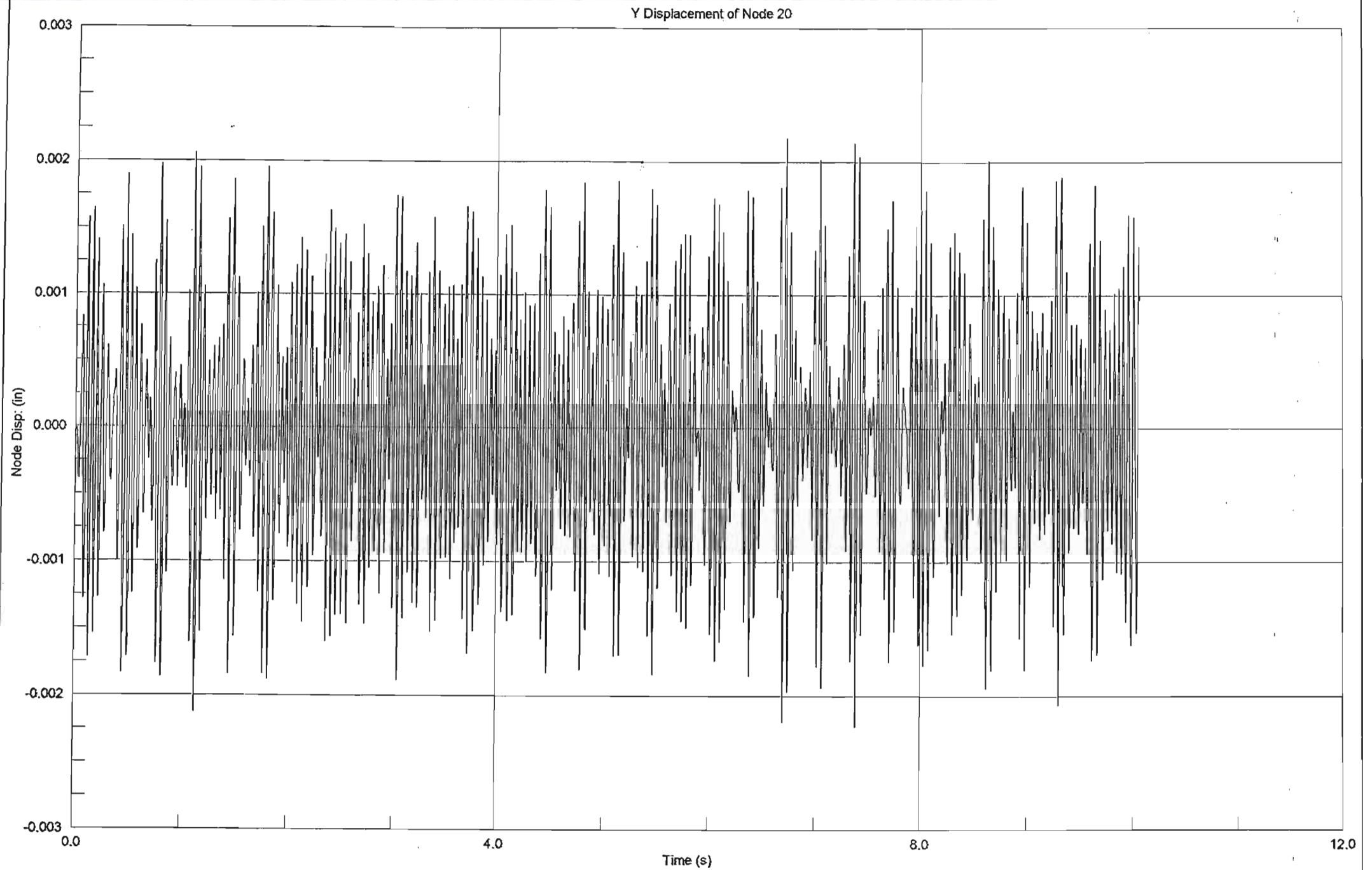




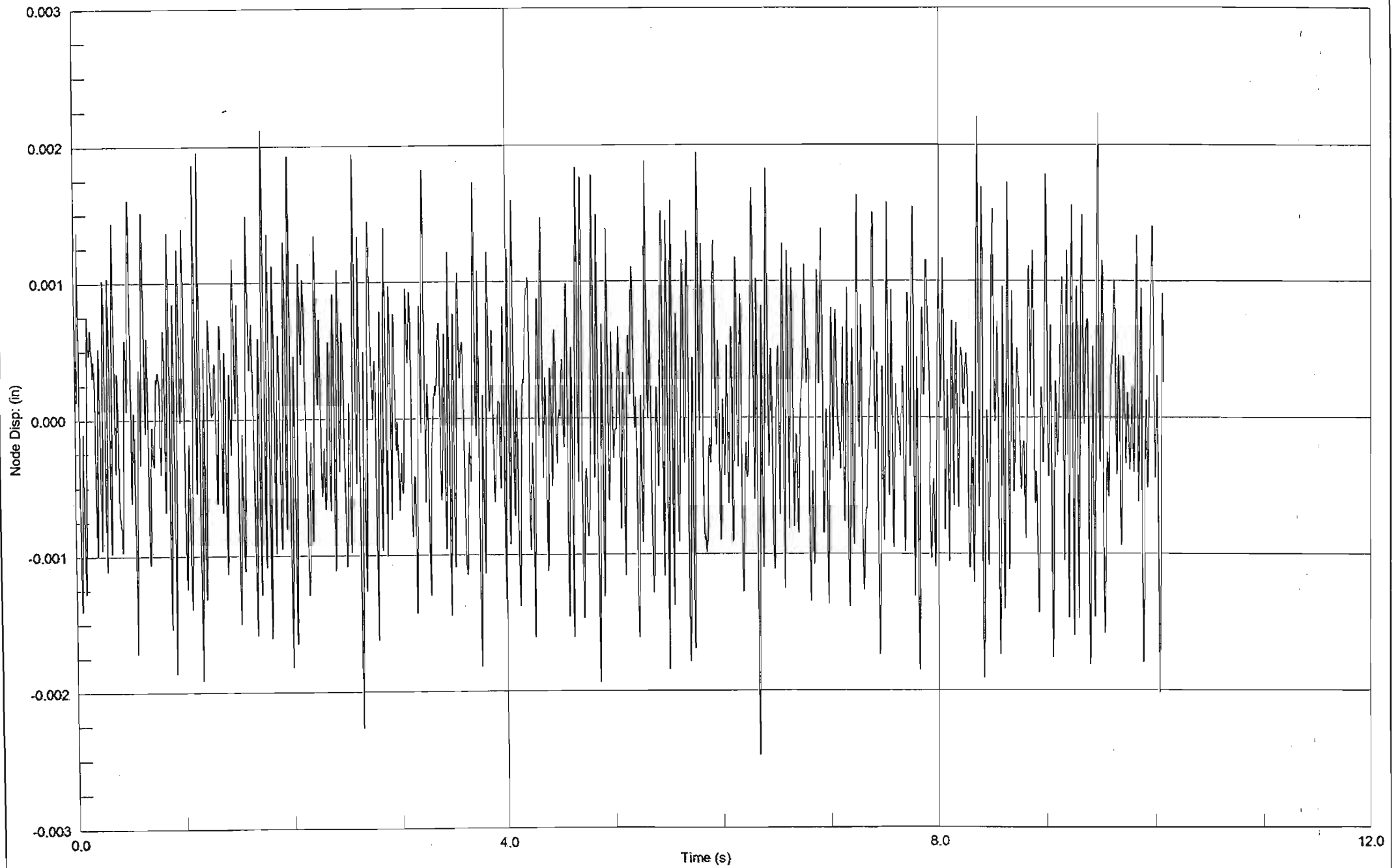


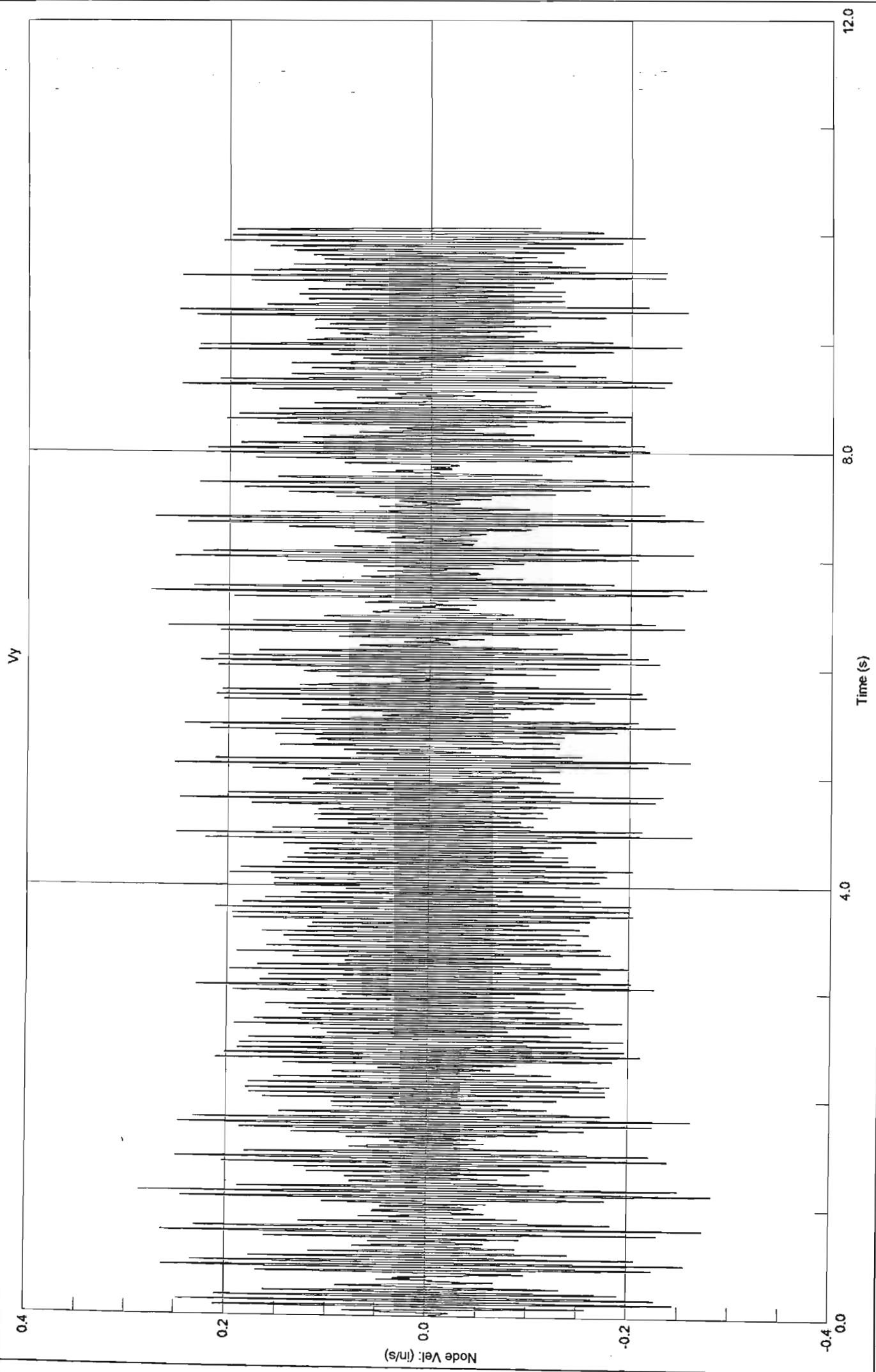
Z Displacement of Node 8



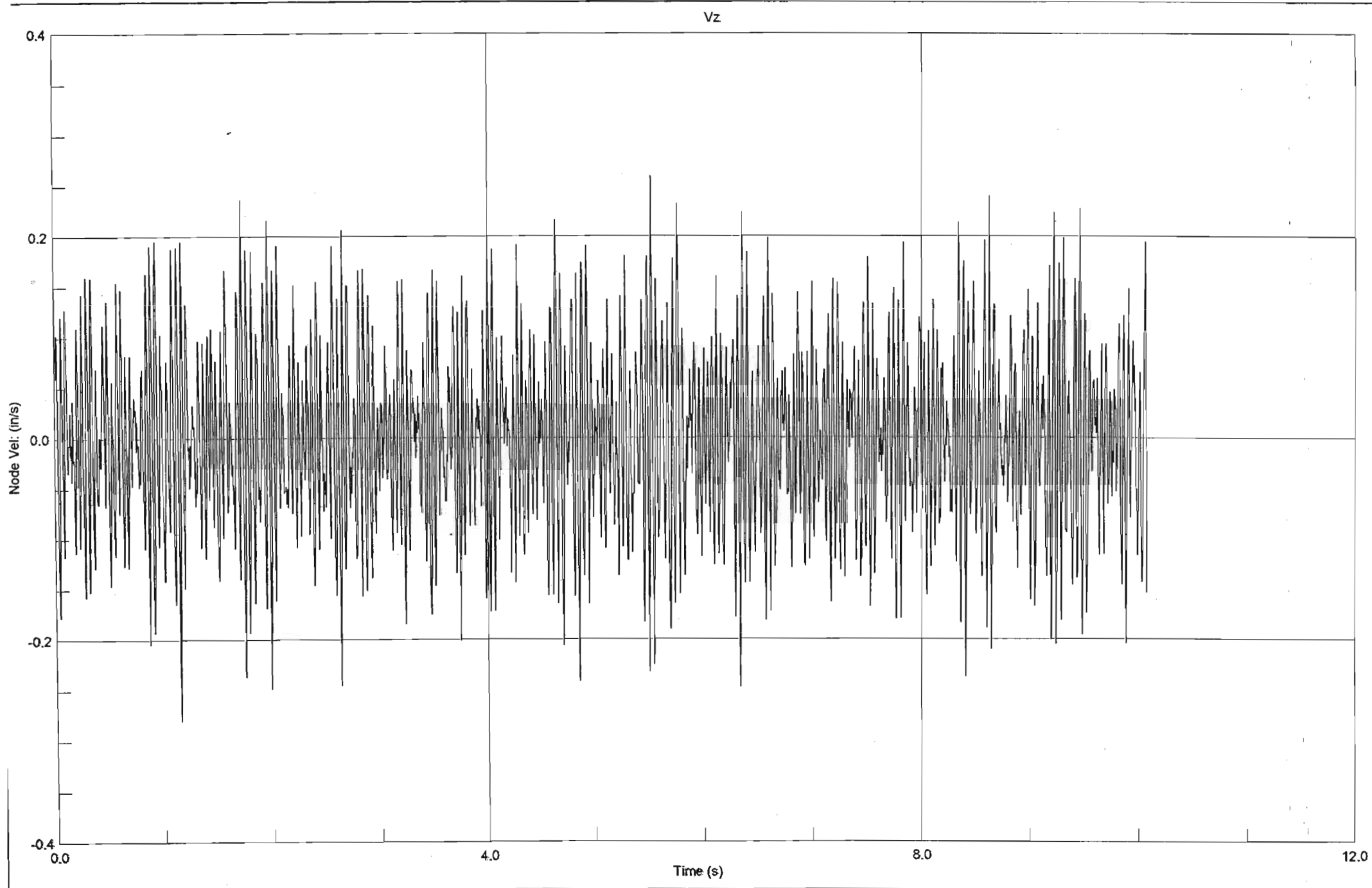


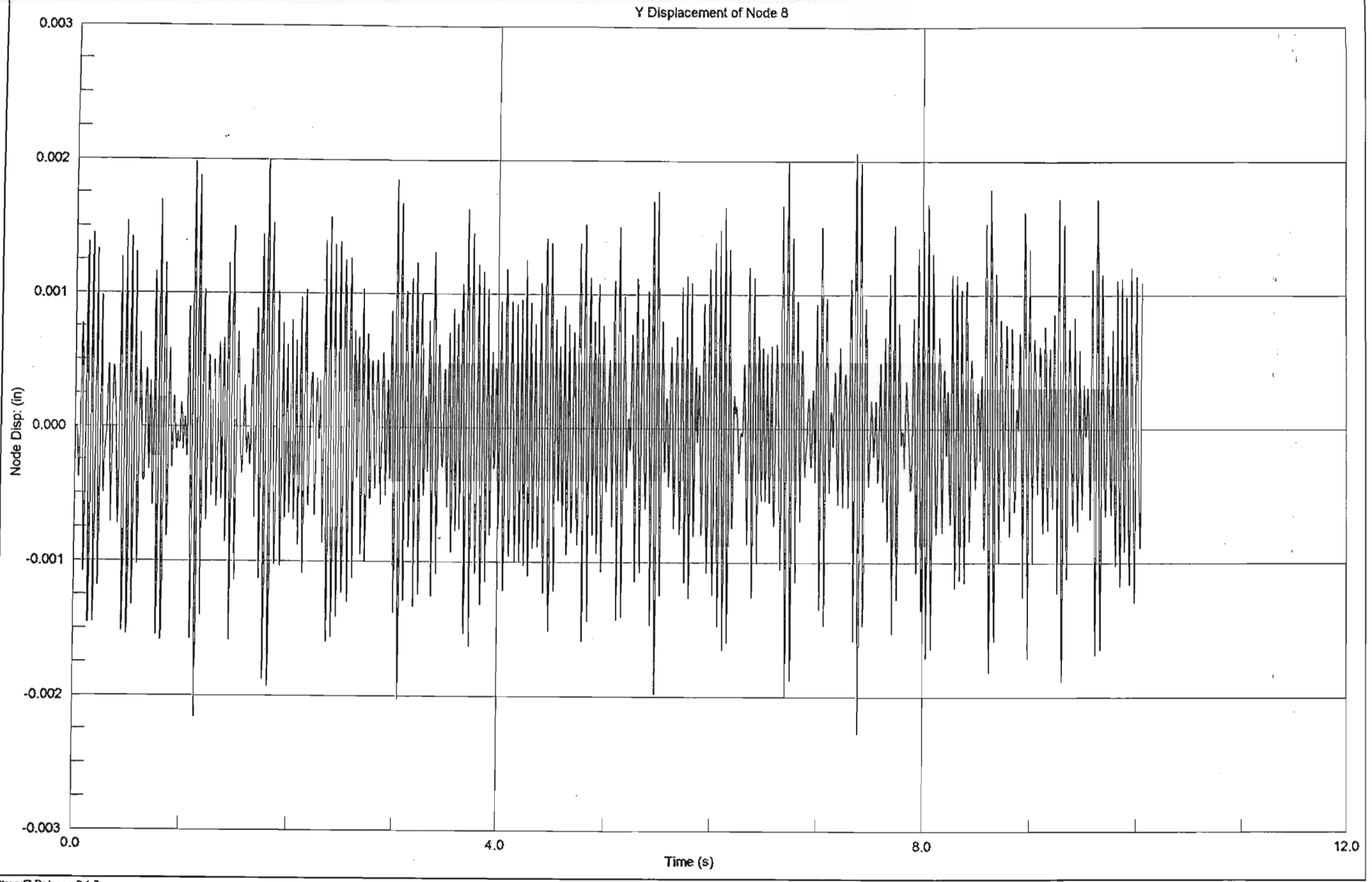
Z Displacement of Node 20



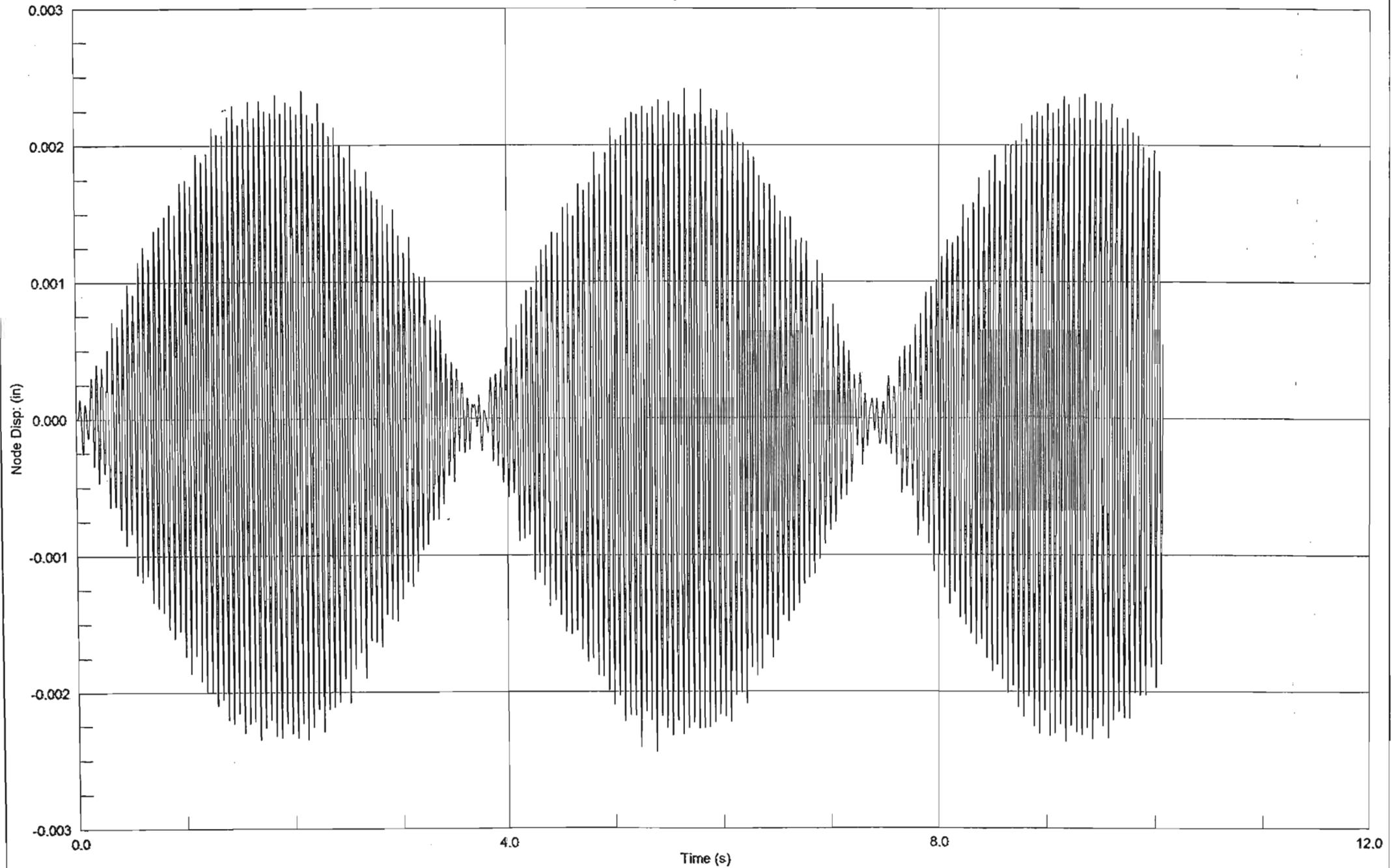


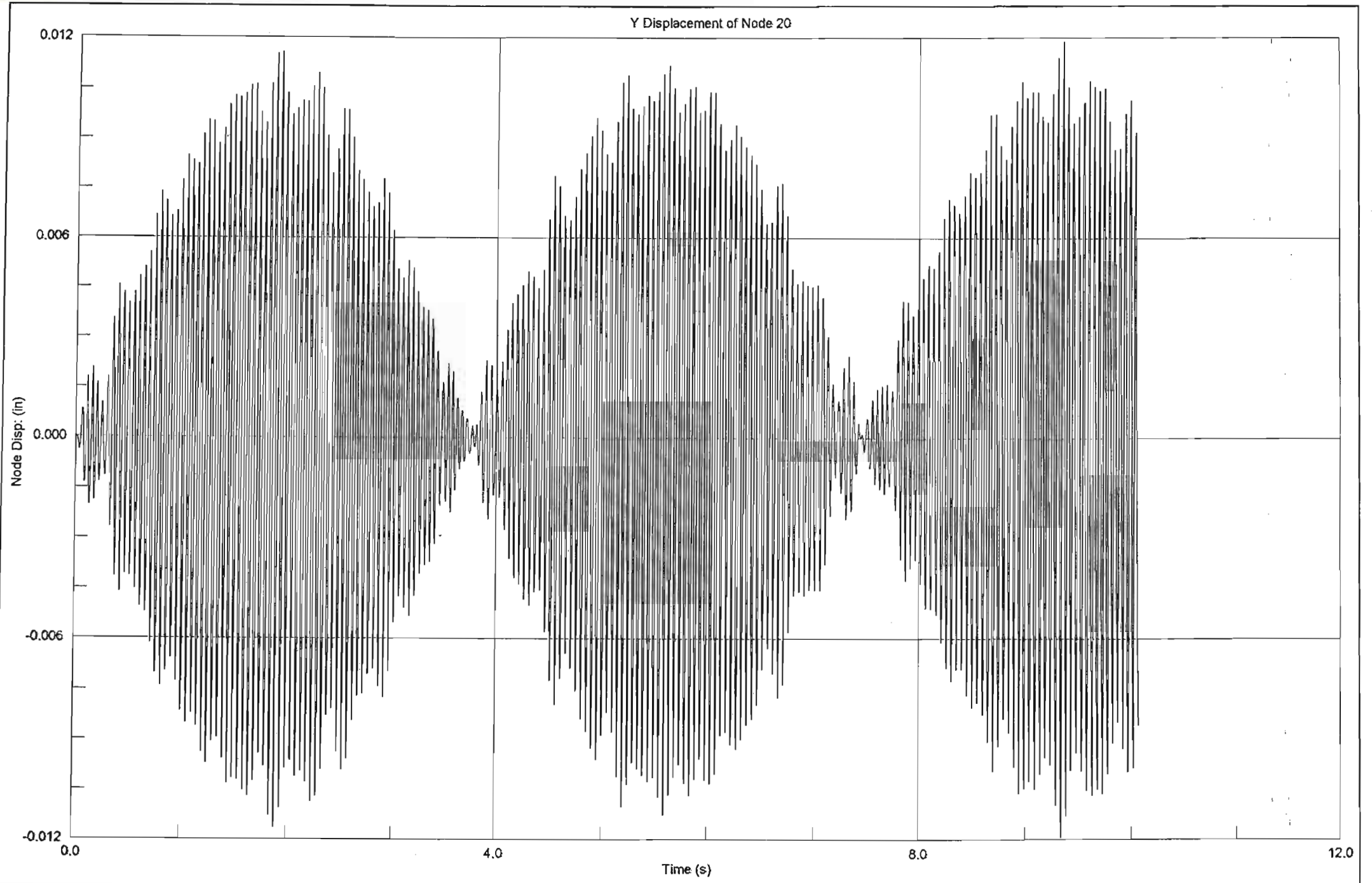
3.113

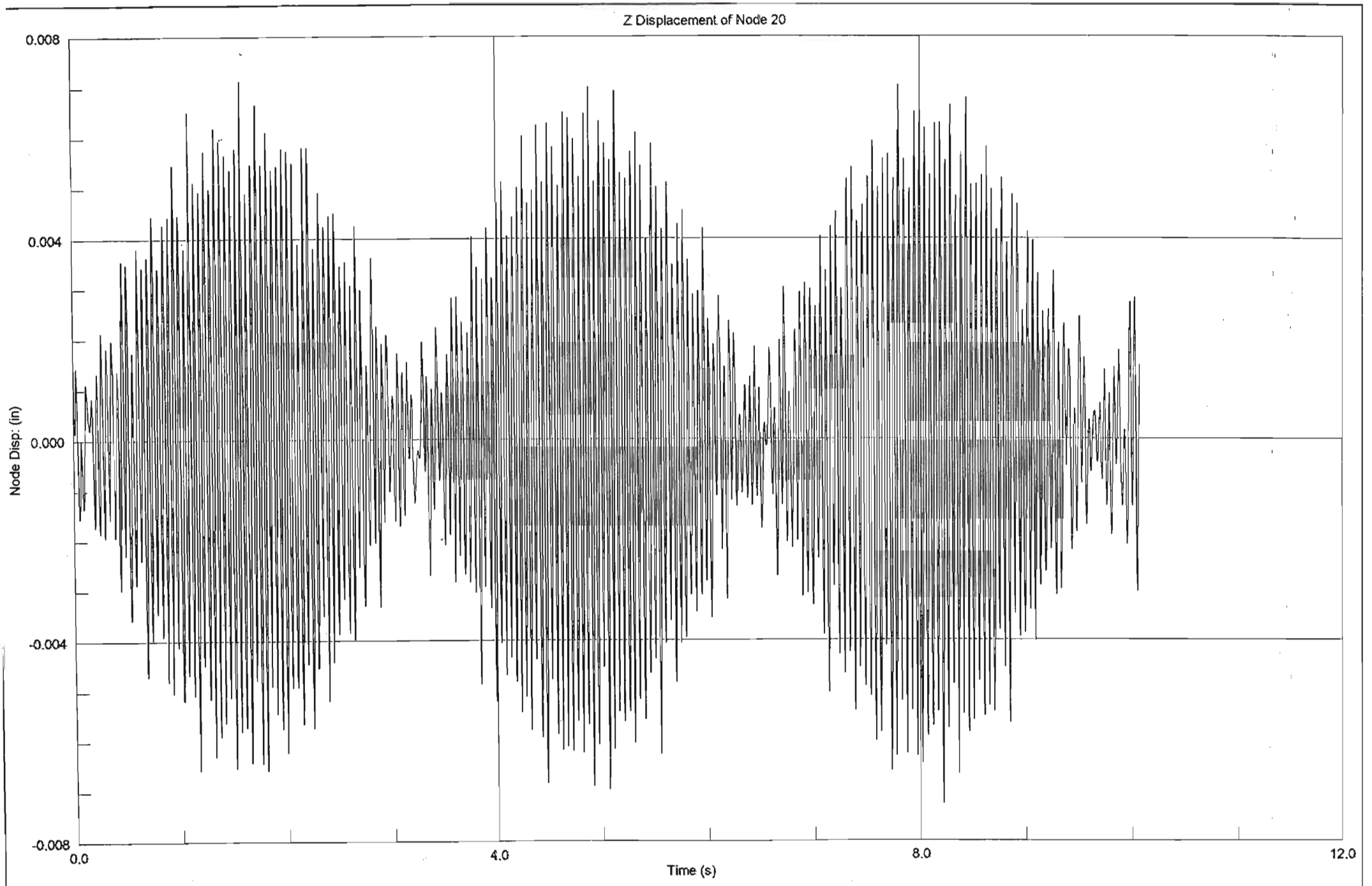


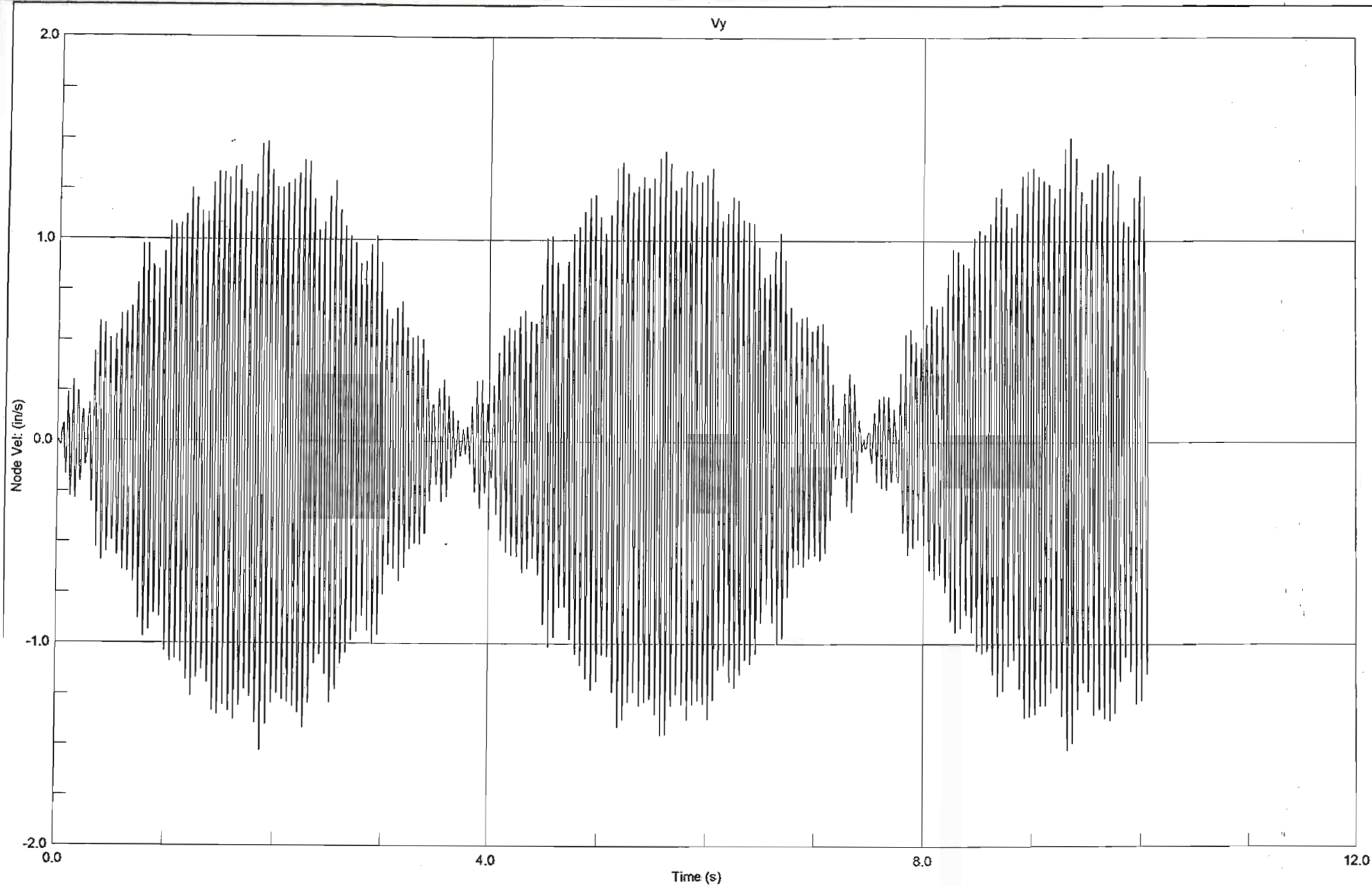


Z Displacement of Node 8







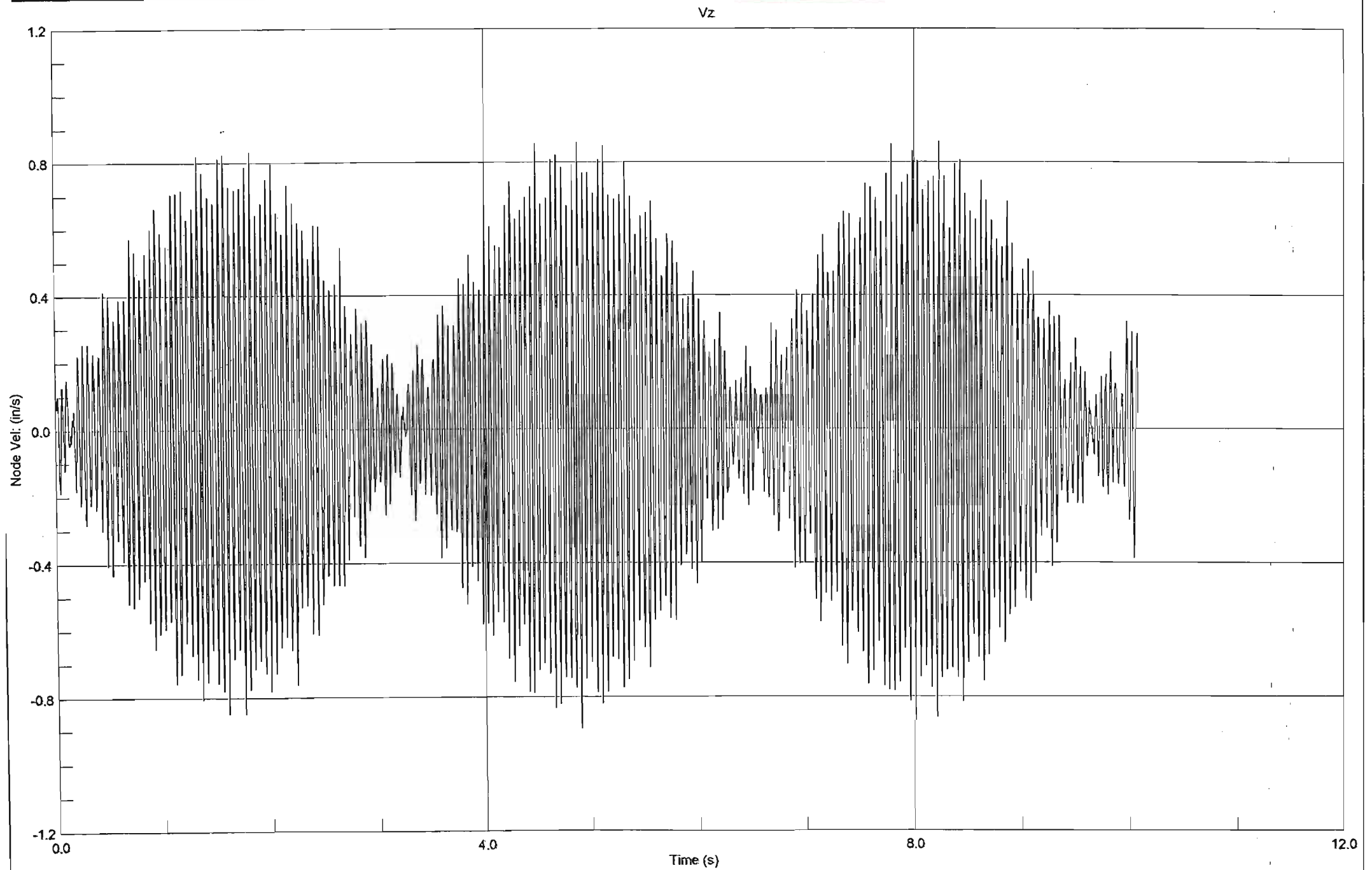


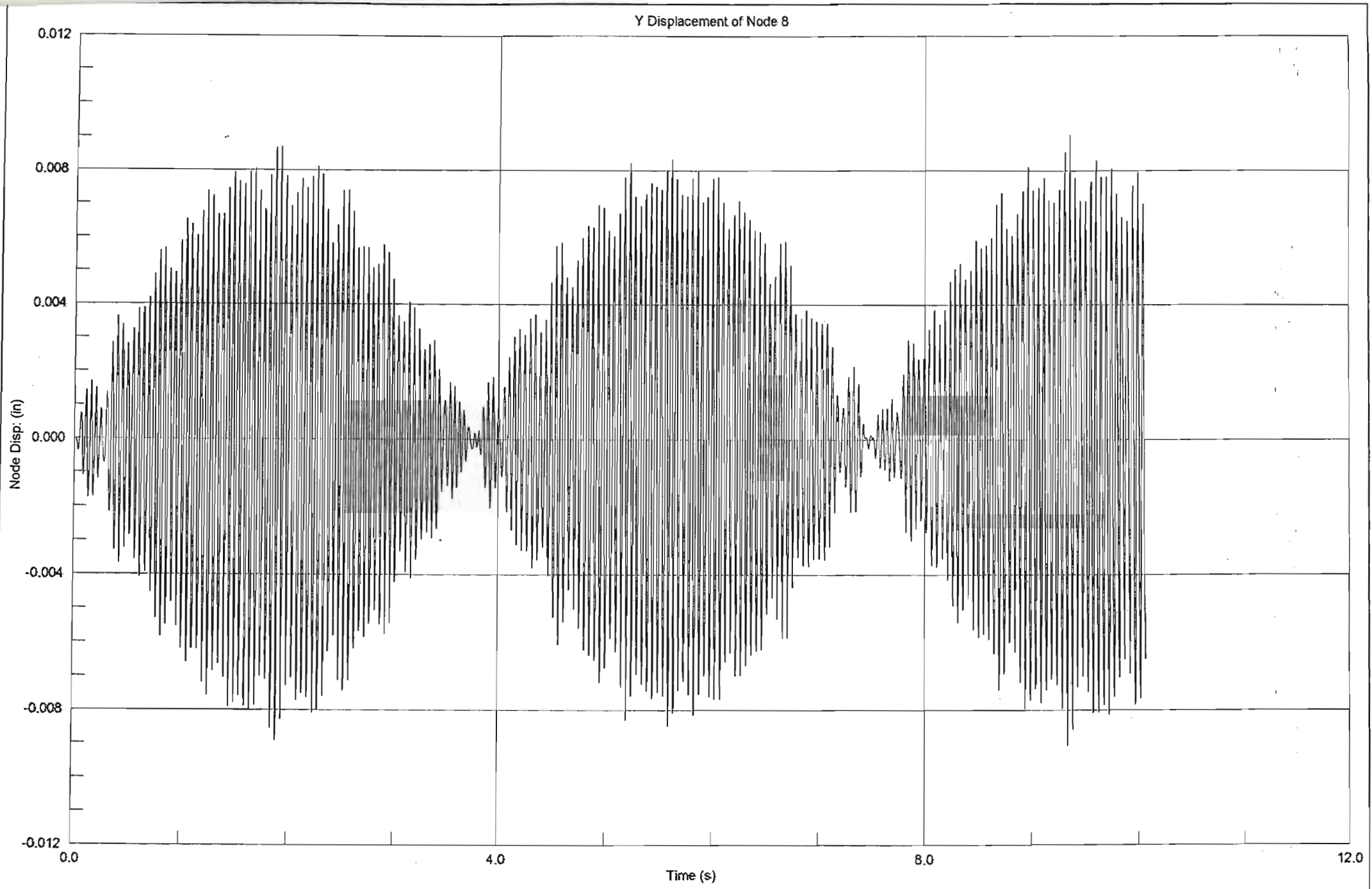
trans7 Release 2.1.7

:MSc Eng\Table Top\Table Top 5\table top G20000.s17

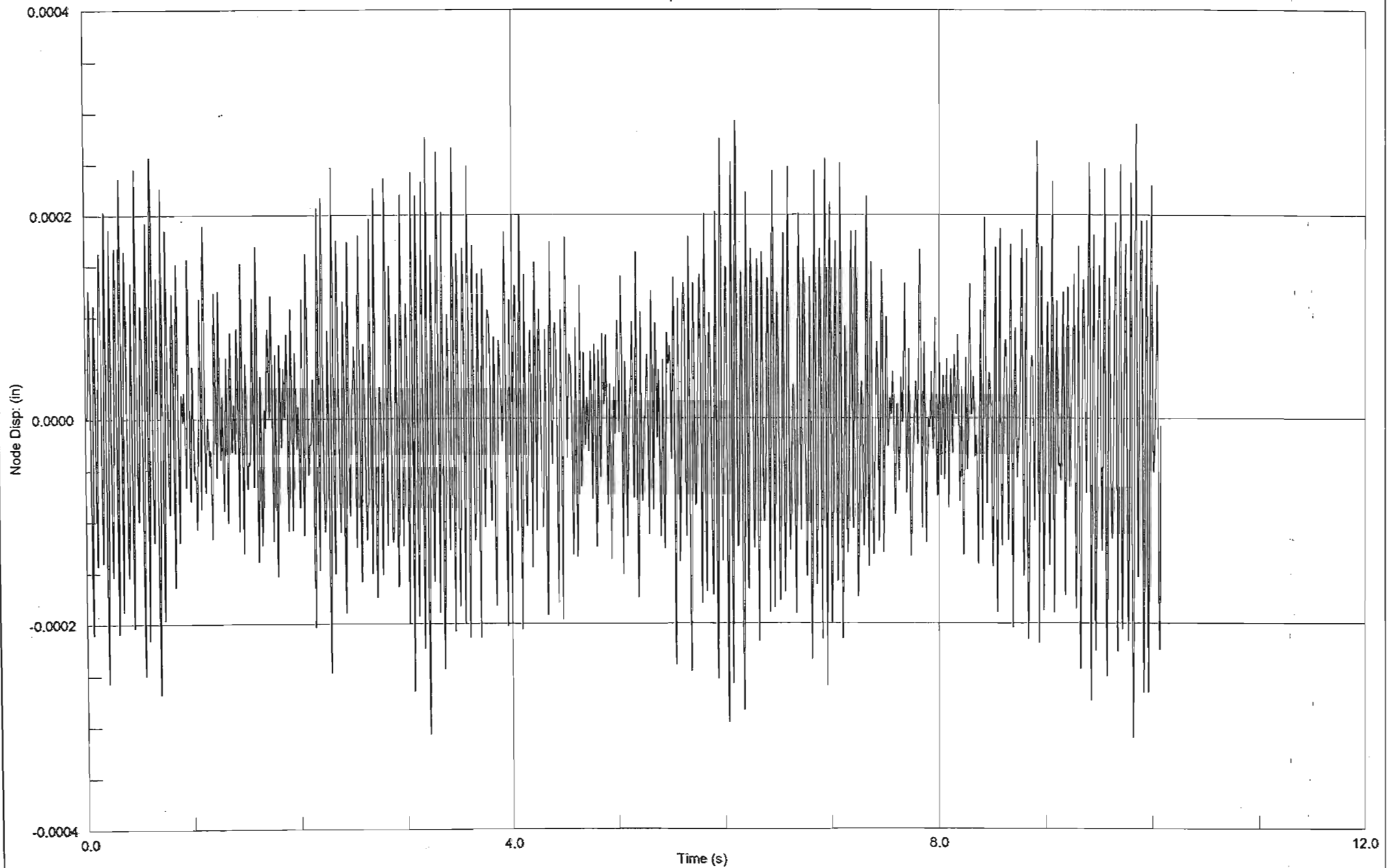
3 October 2002 10:56 am

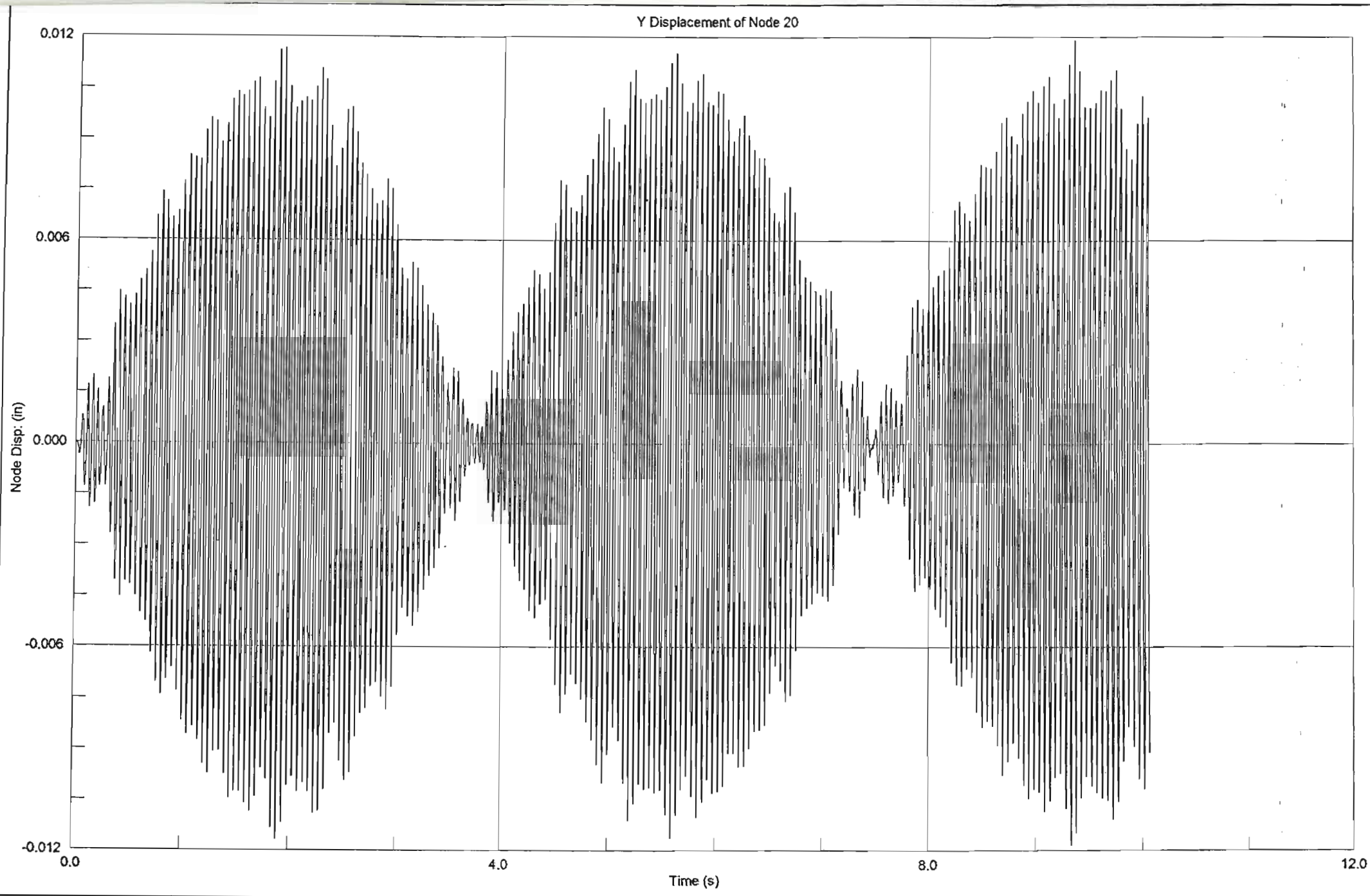
4.3



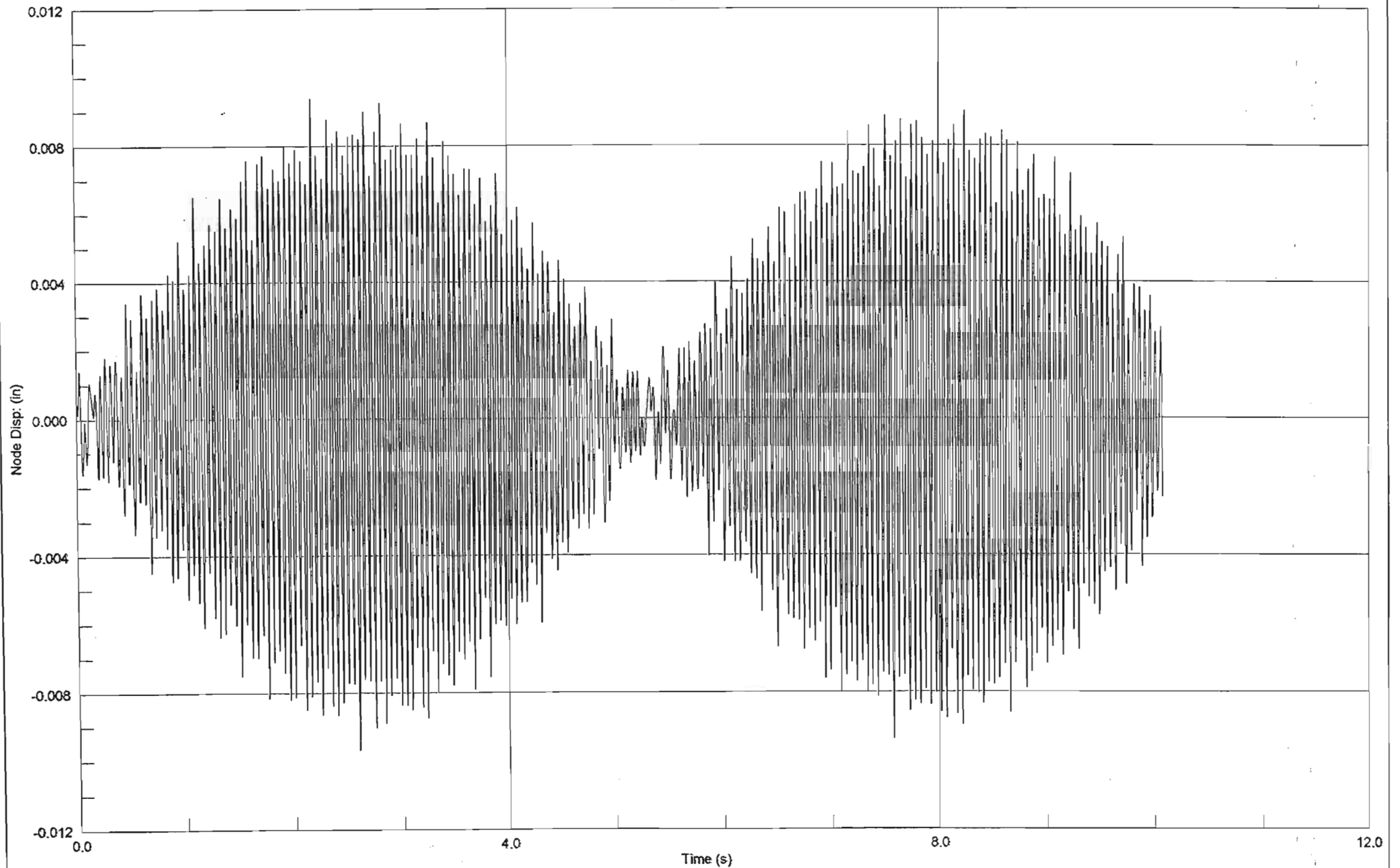


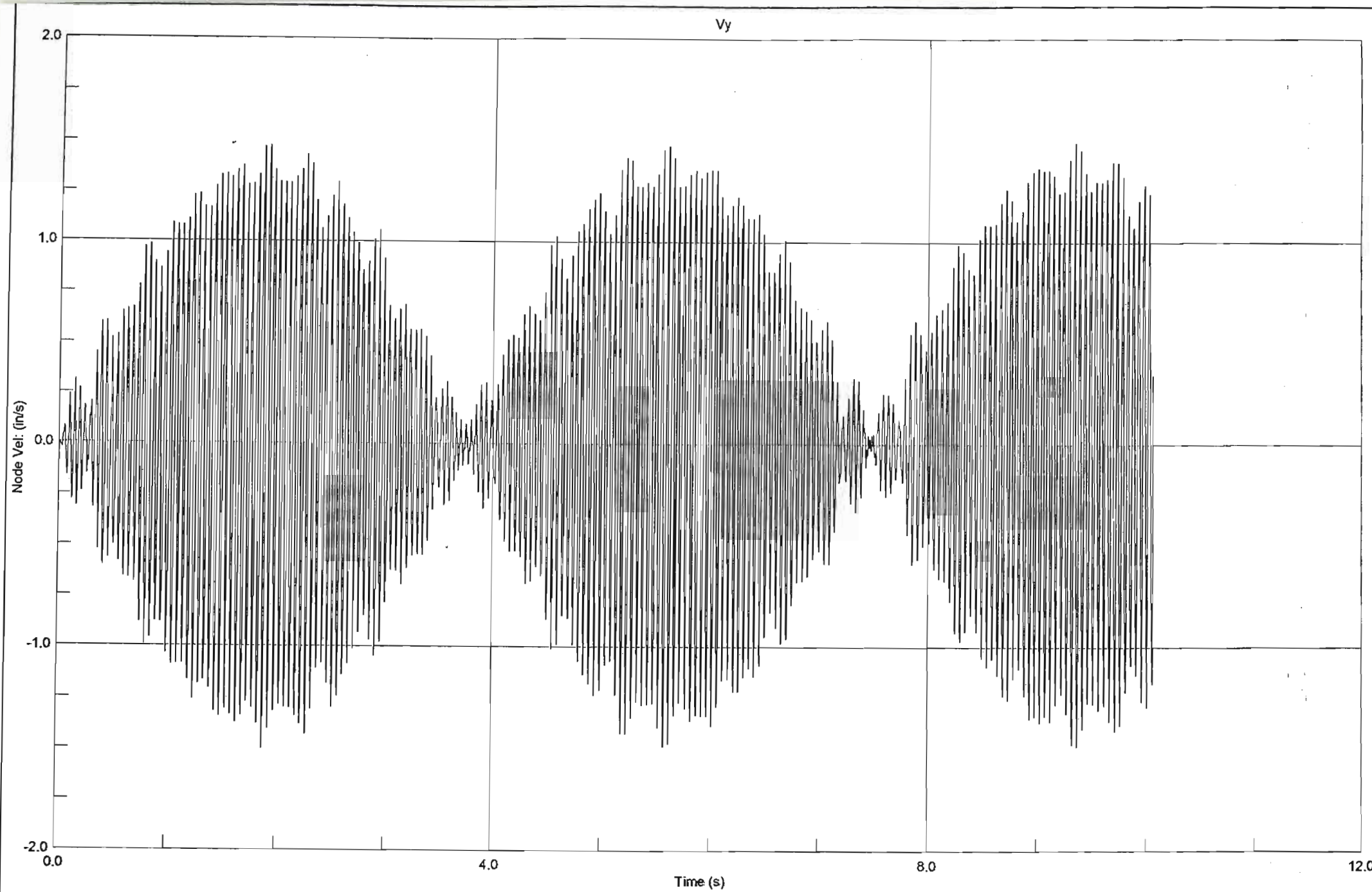
Z Displacement of Node 8





Z Displacement of Node 20



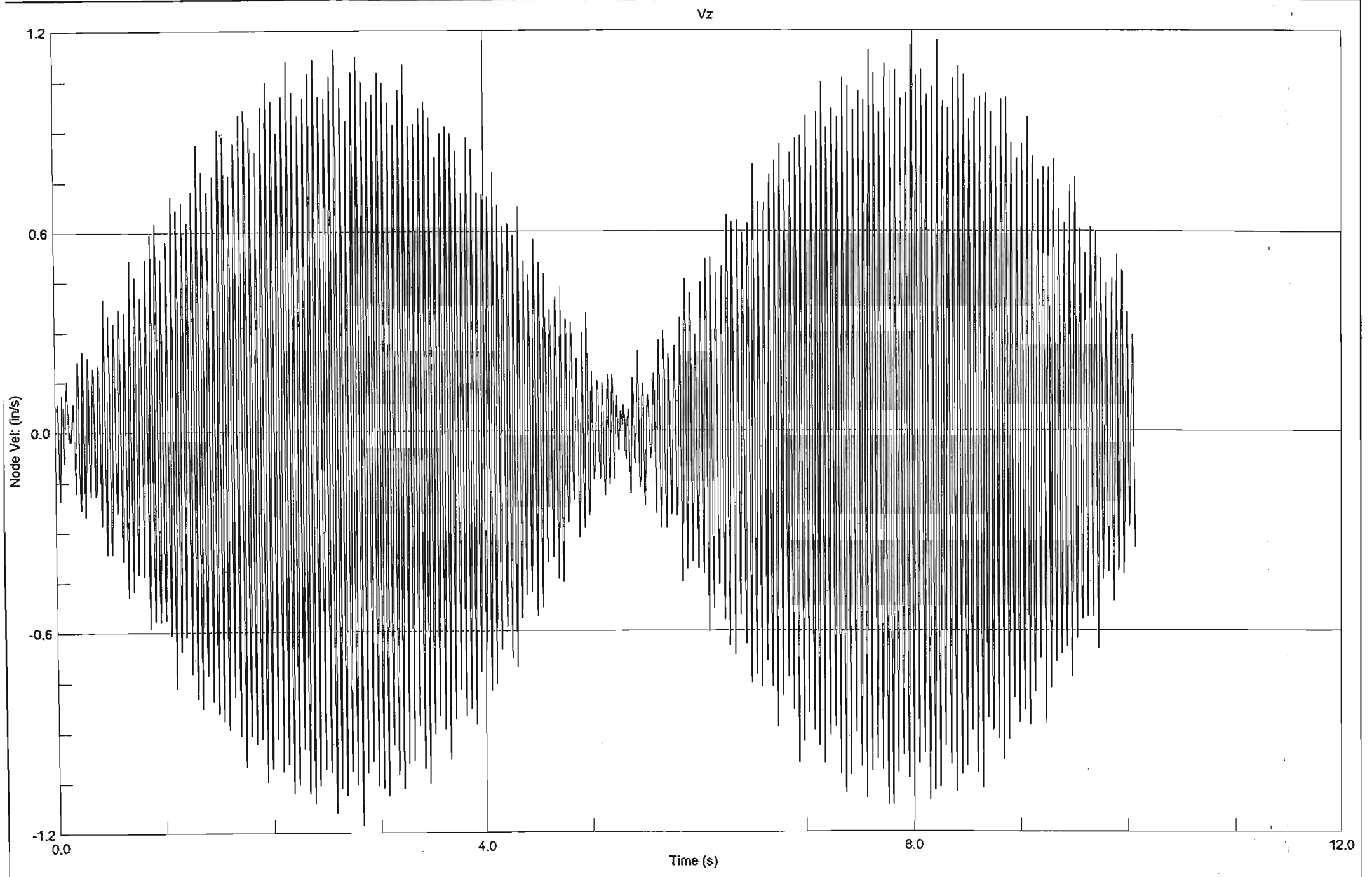


Strand7 Release 2.1.7

C:\MSc Eng\Table Top 5\Table Top 5\table top G20000-mdcf.st7

13 October 2002 12:40 pm

C4.9

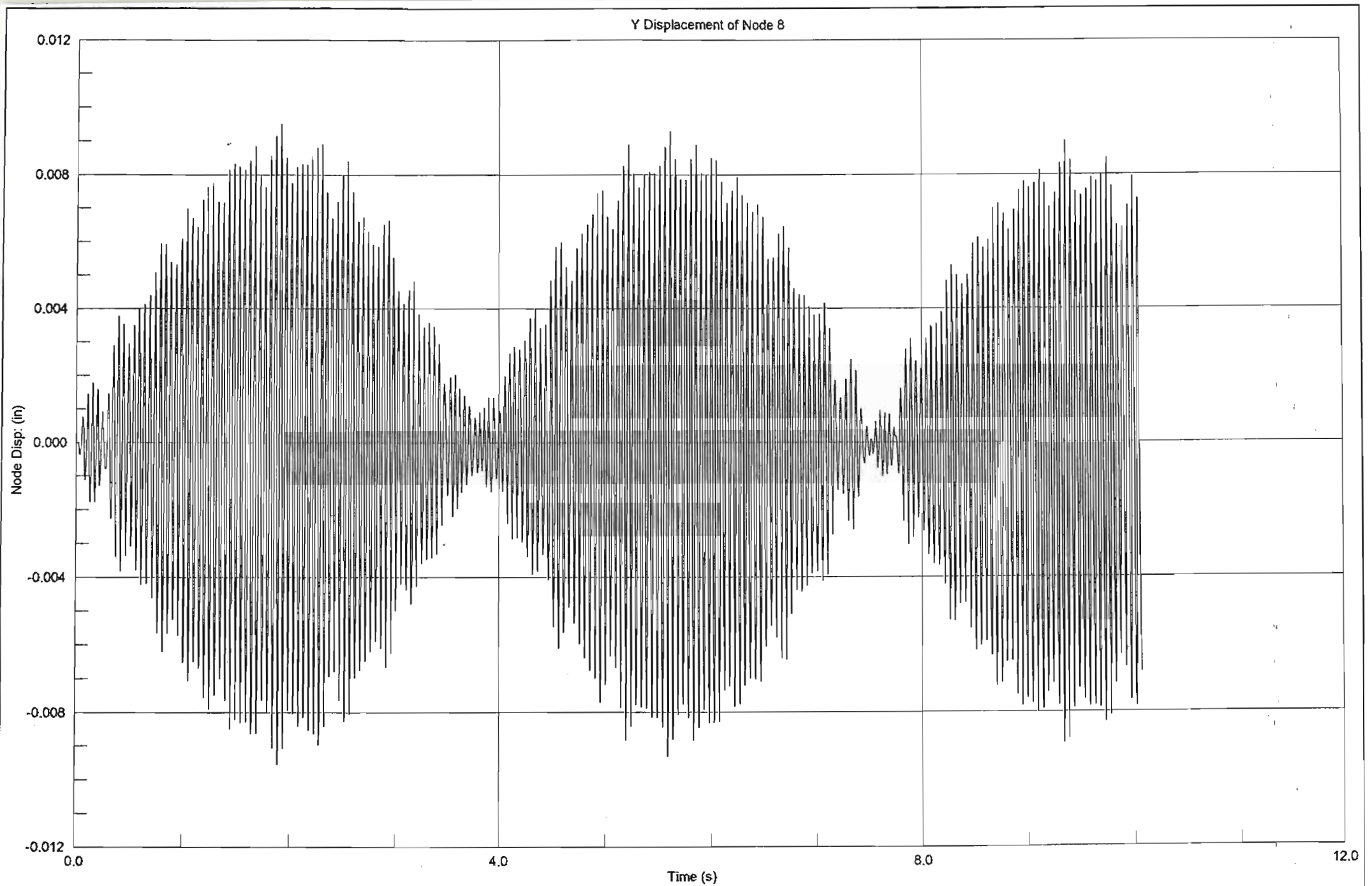


Strand7 Release 2.1.7

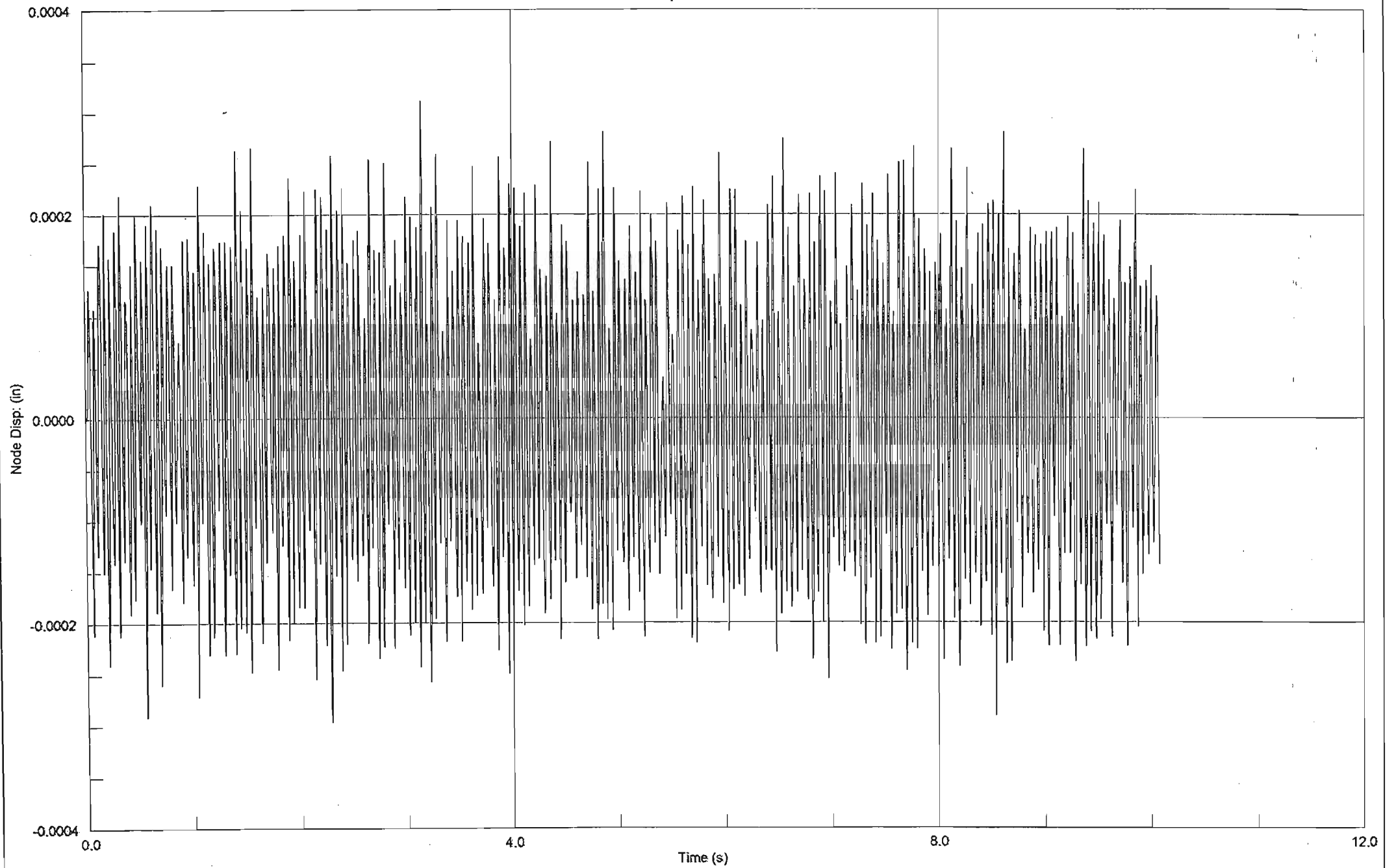
C:\MSc Eng\Table Top\Table Top 5\table top G20000-mdef.s17

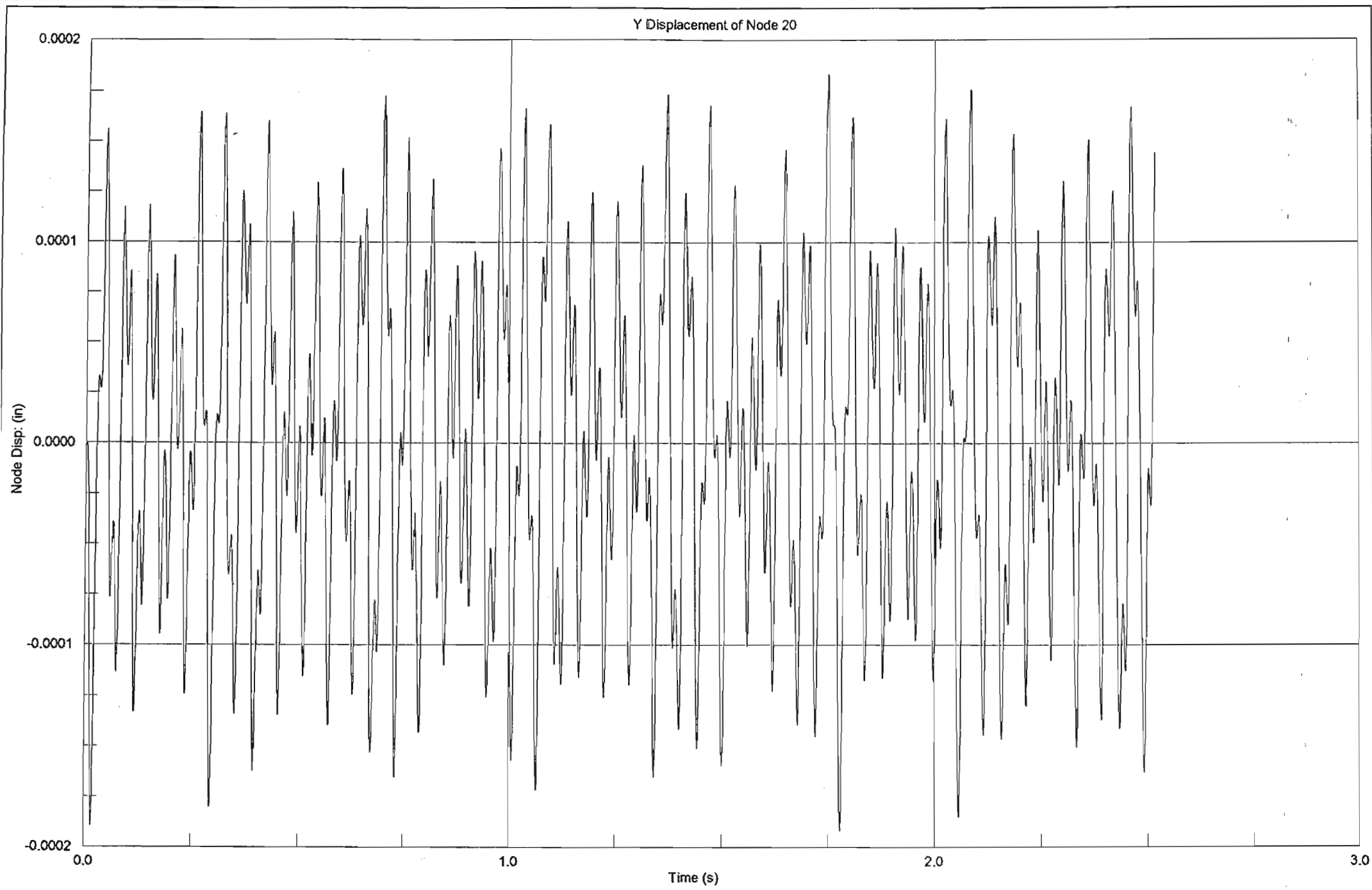
13 October 2002 12:41 pm

CH.10

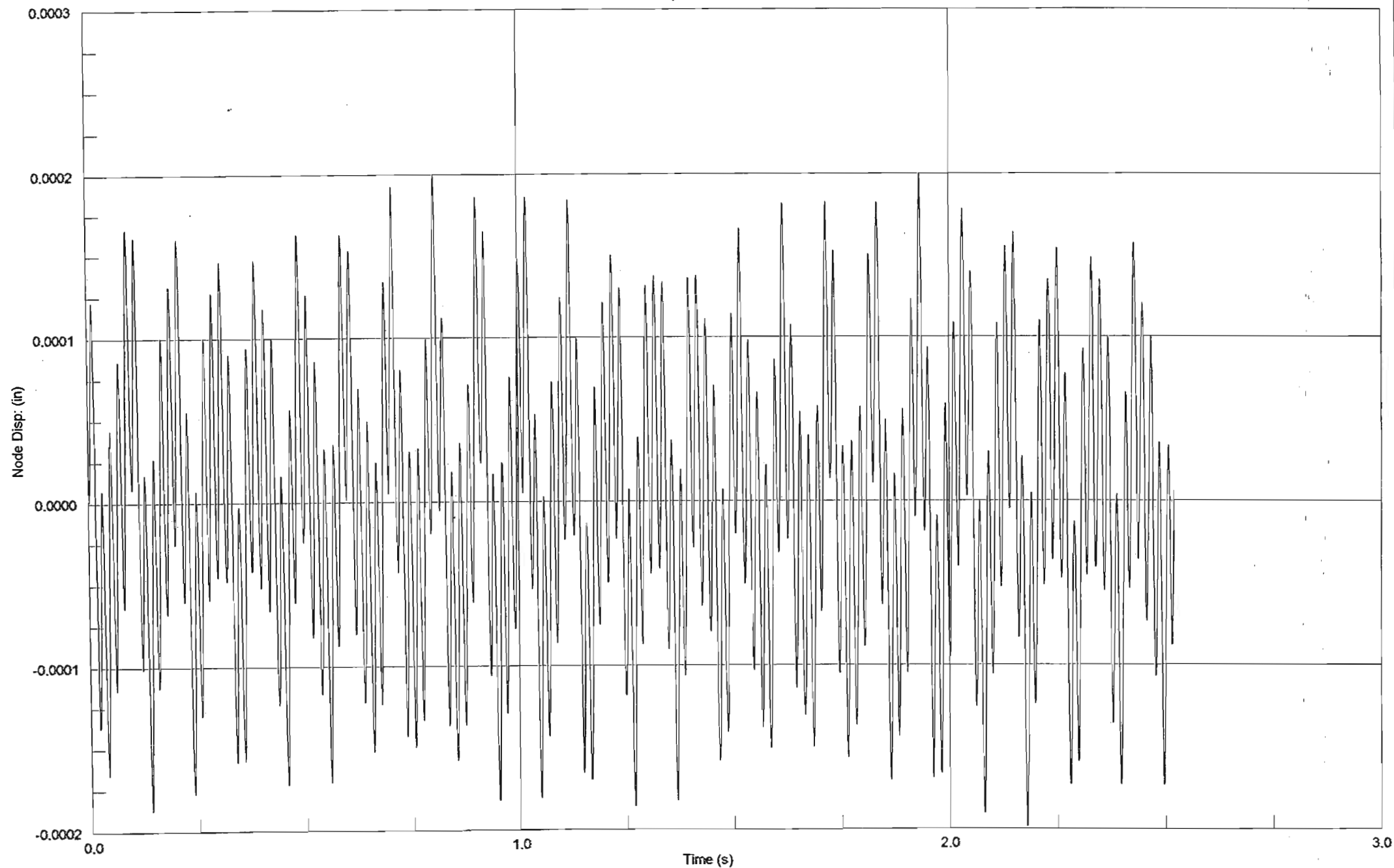


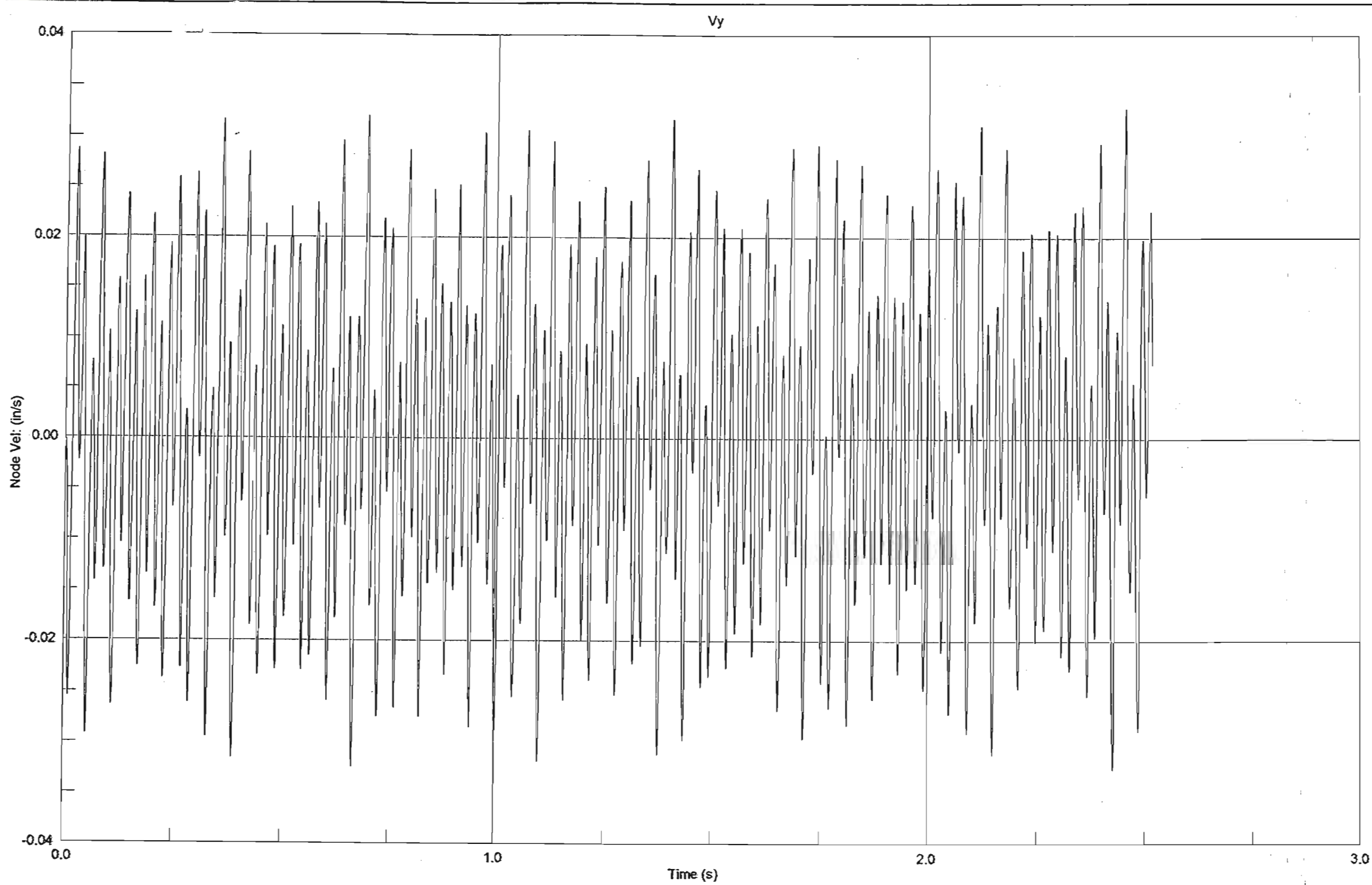
Z Displacement of Node 8

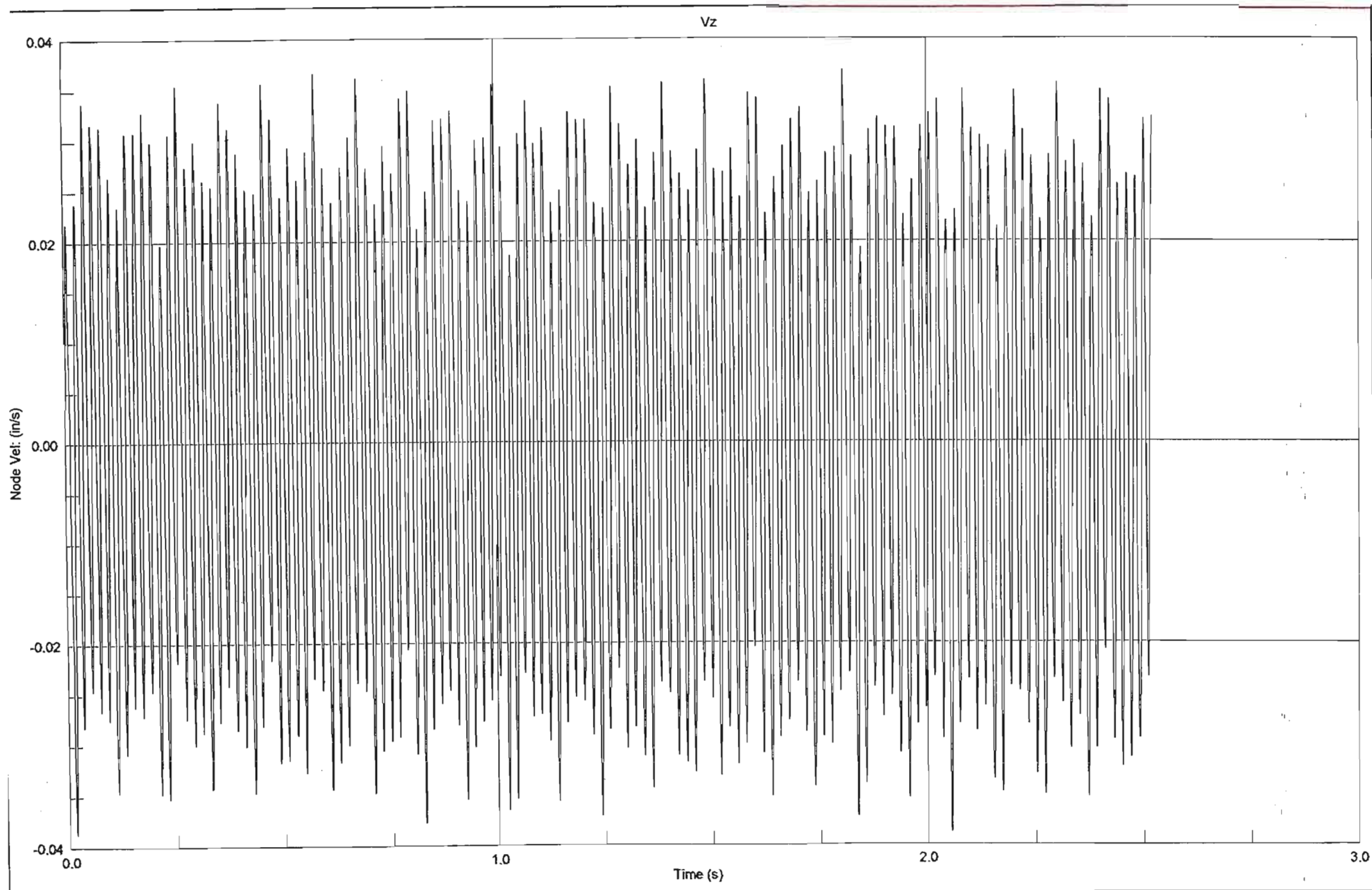


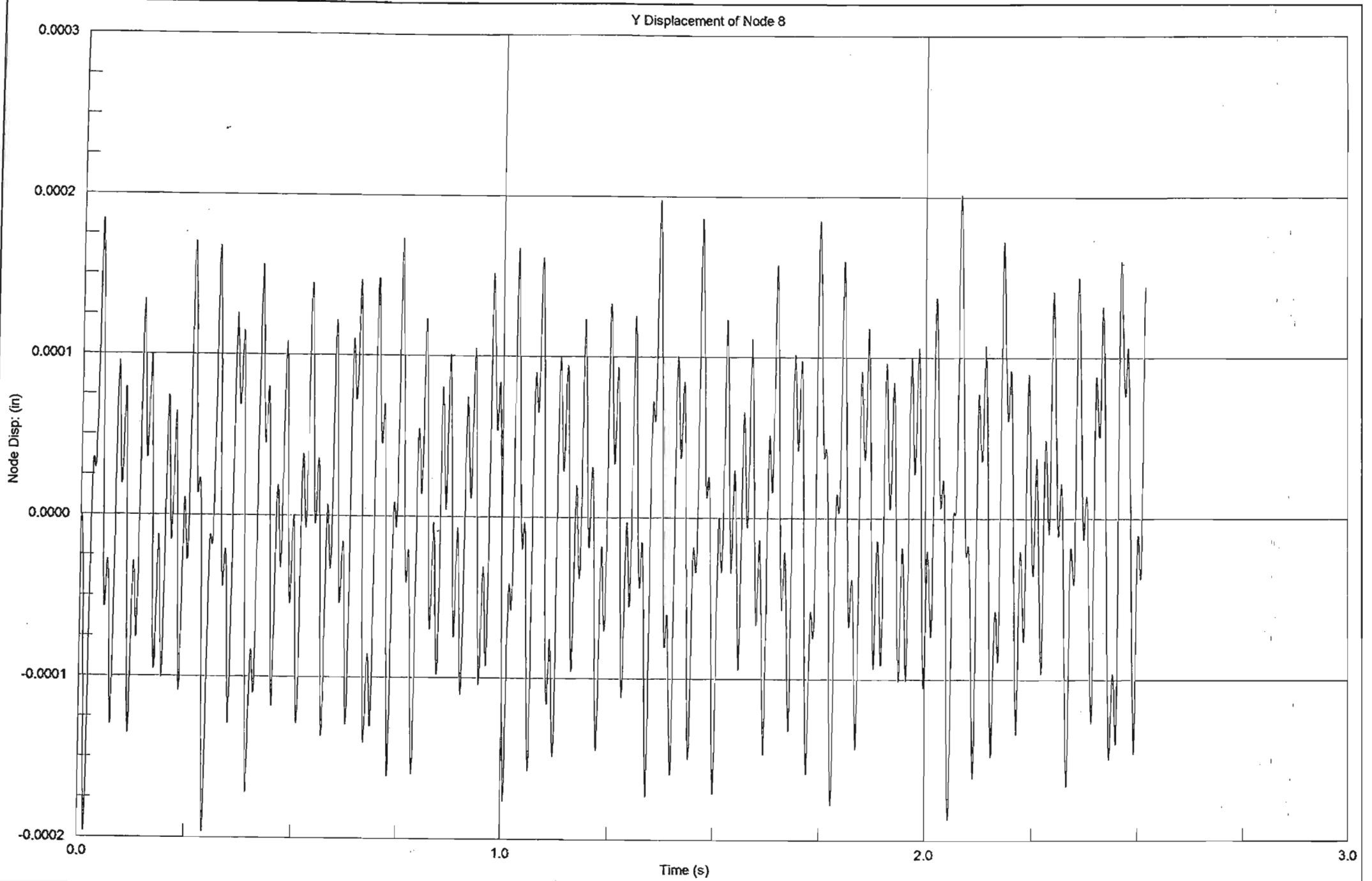


Z Displacement of Node 20

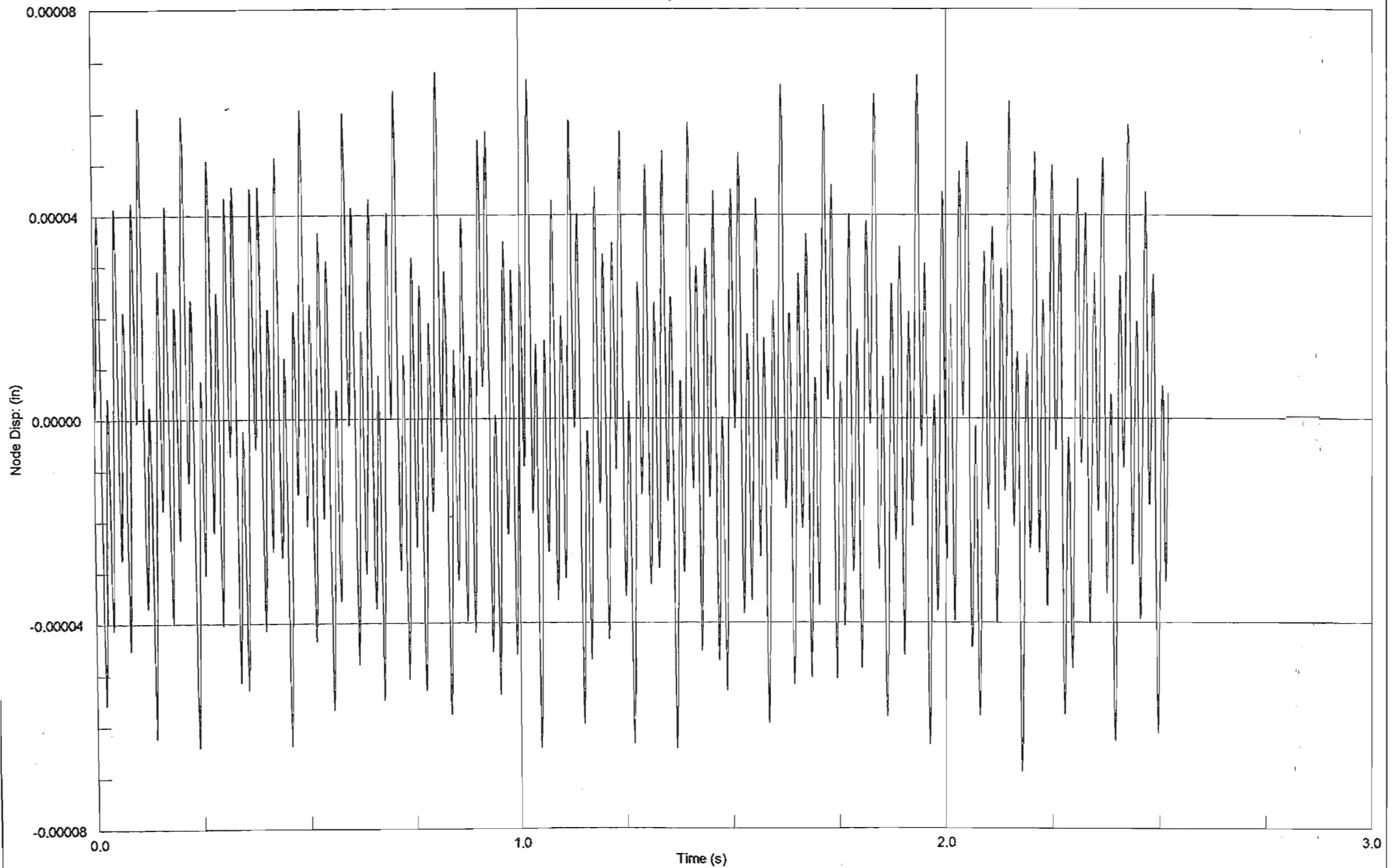




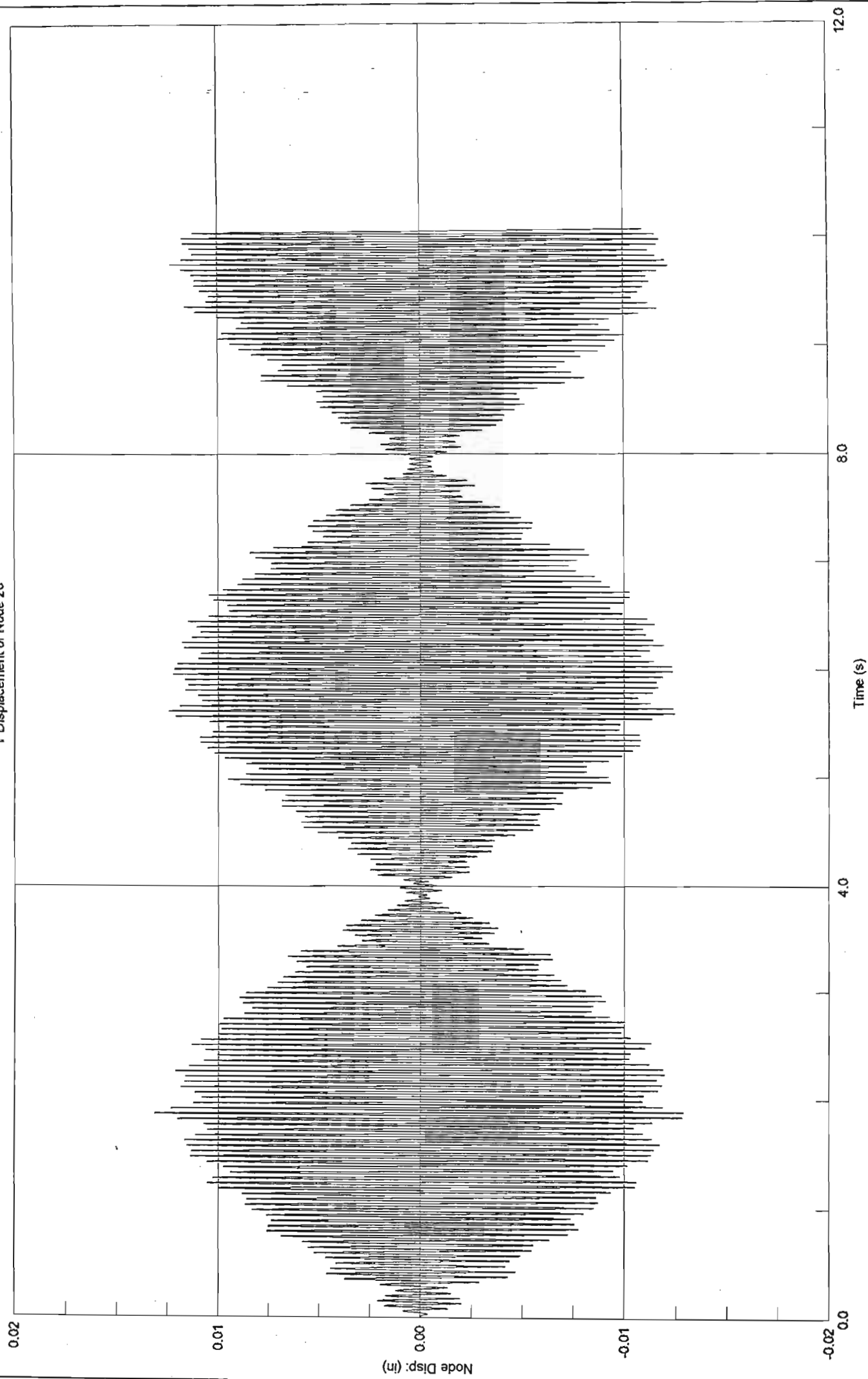




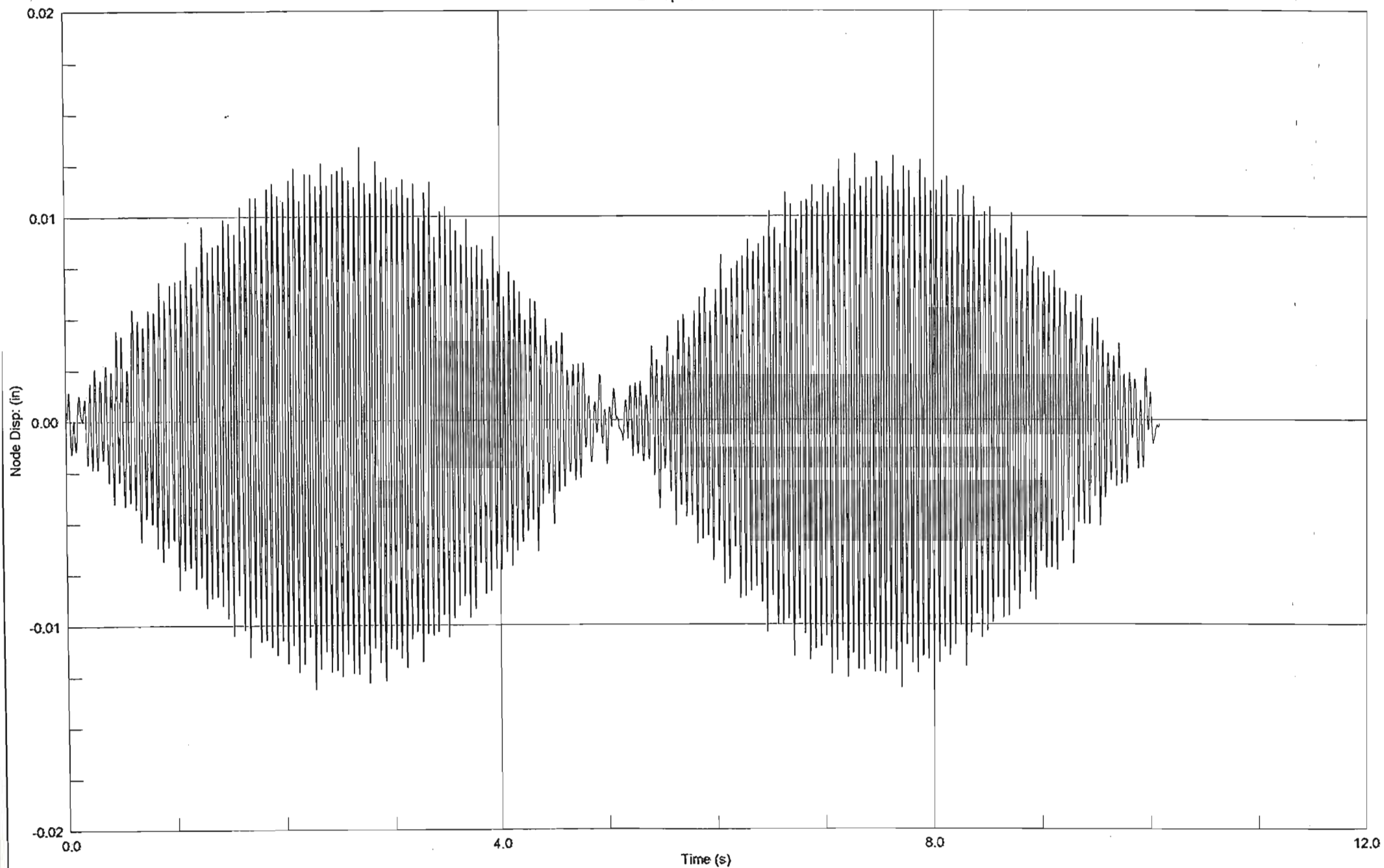
Z Displacement of Node 8

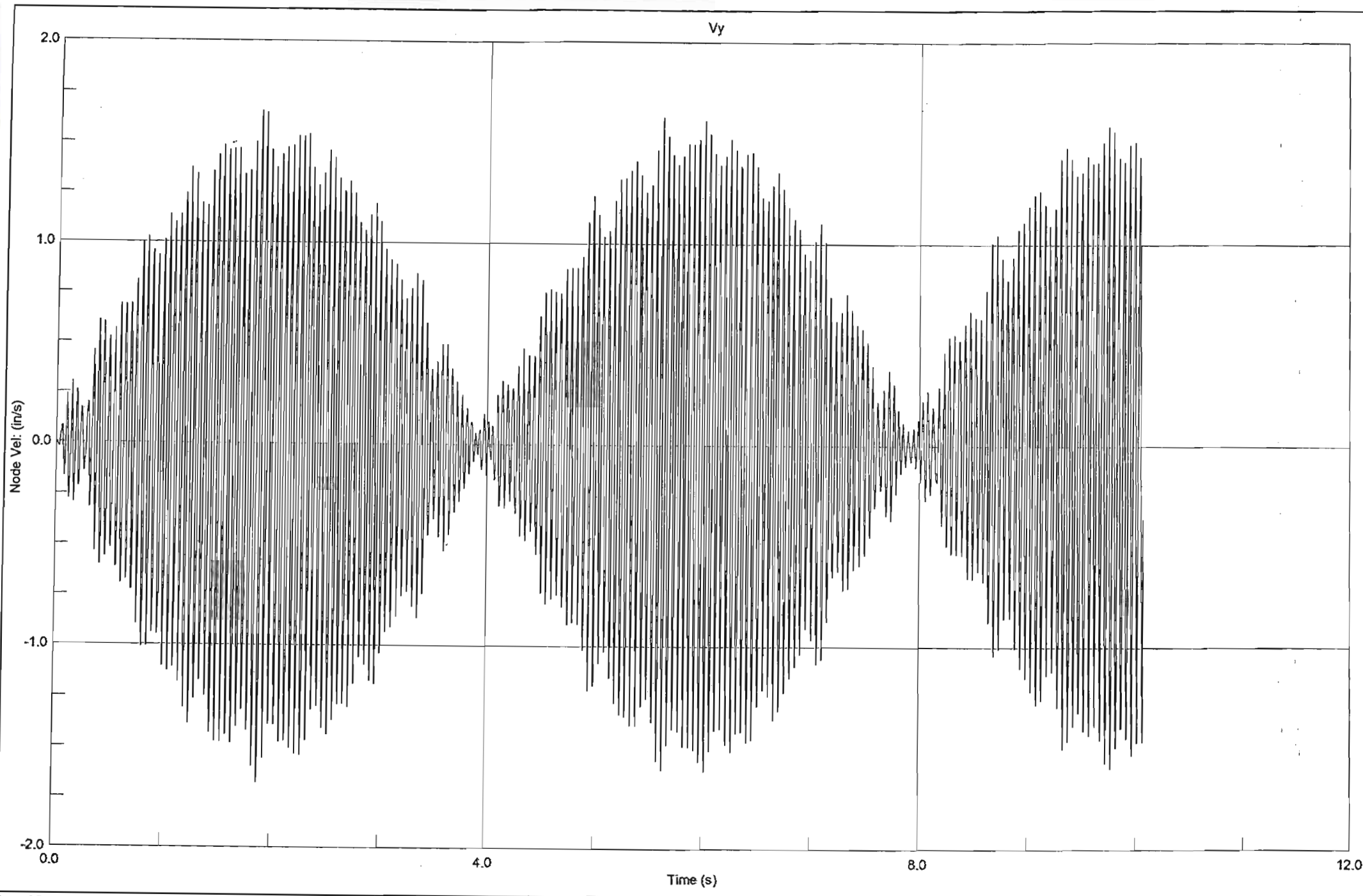


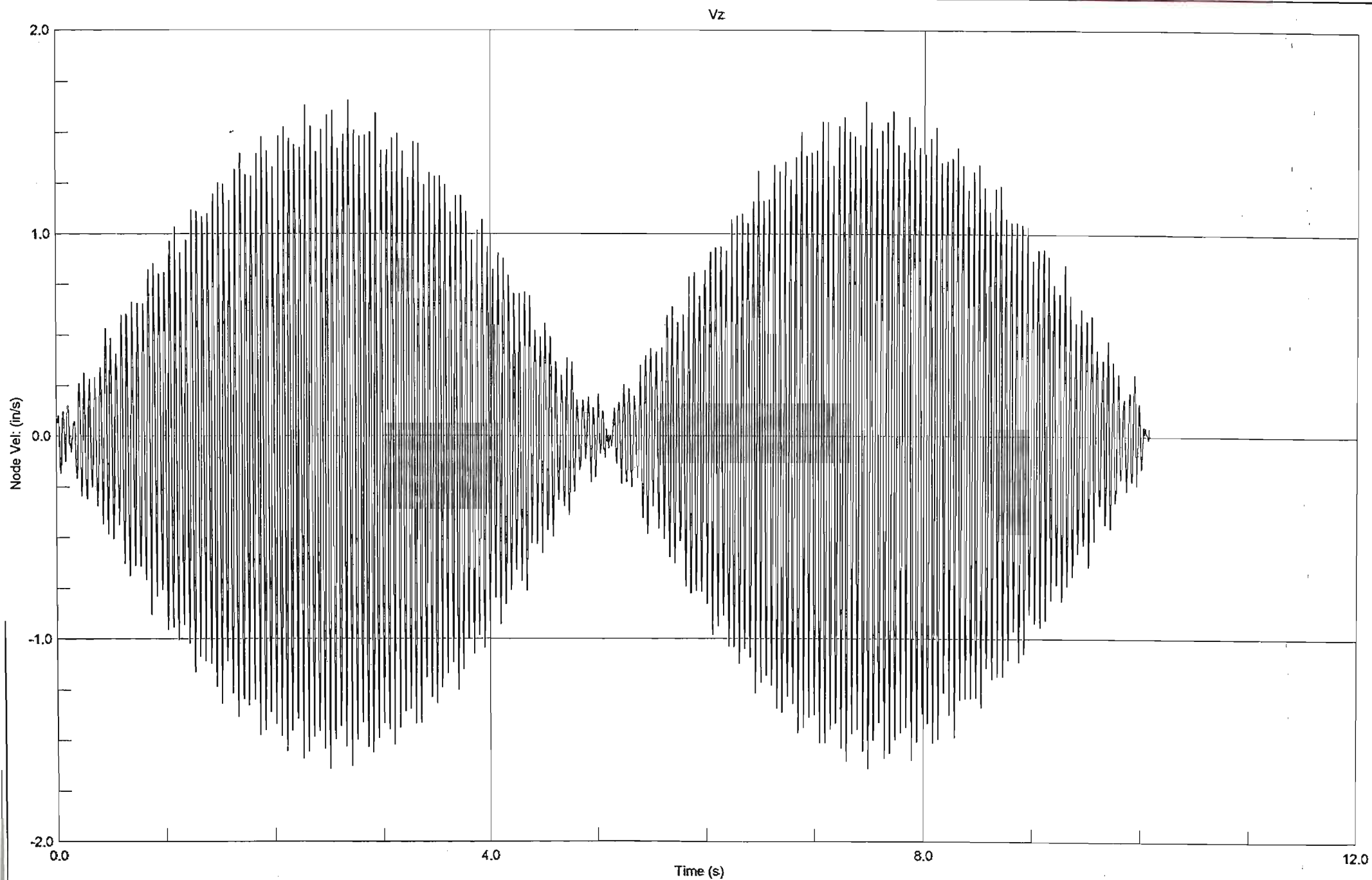
Y Displacement of Node 20

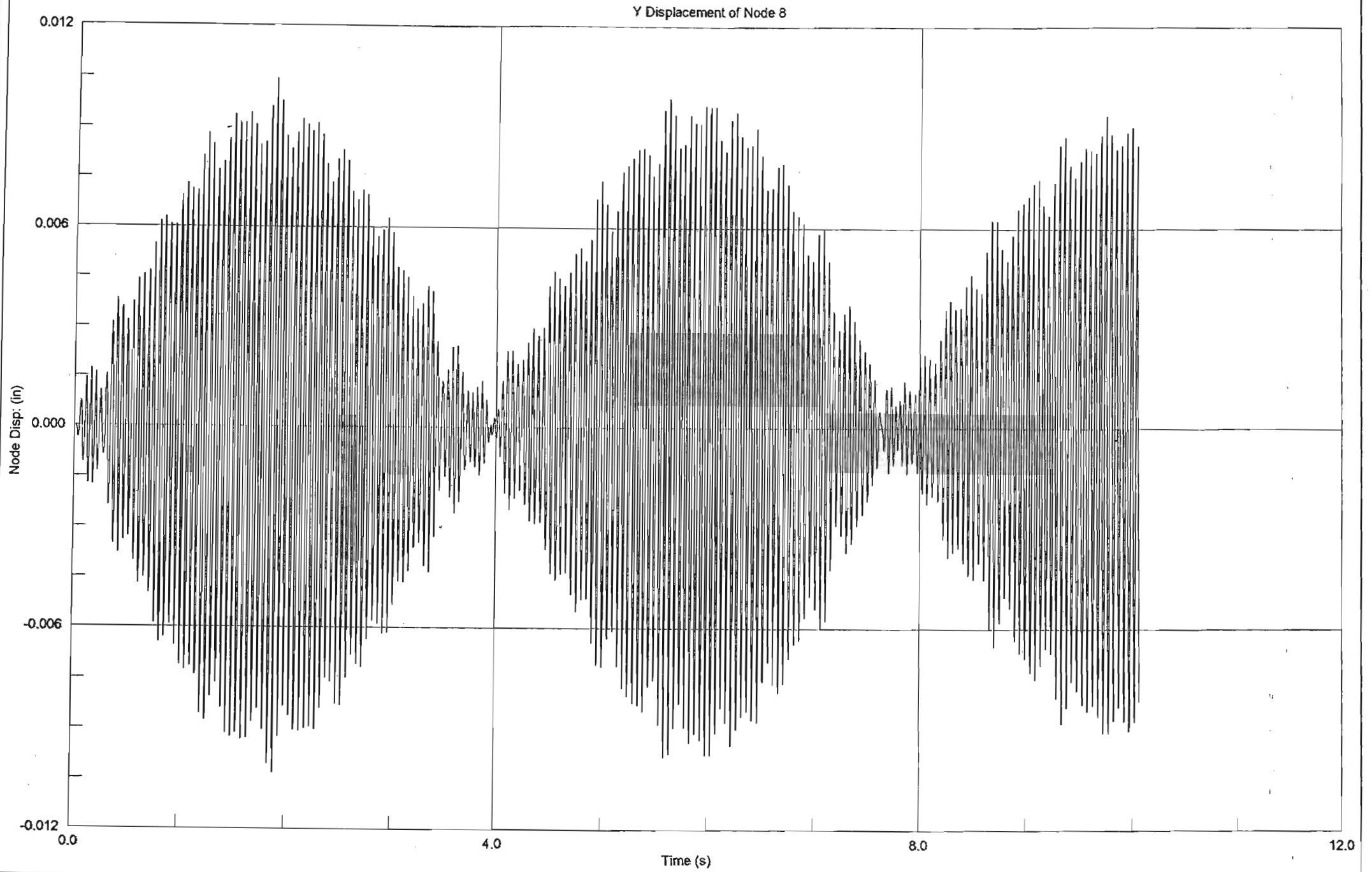


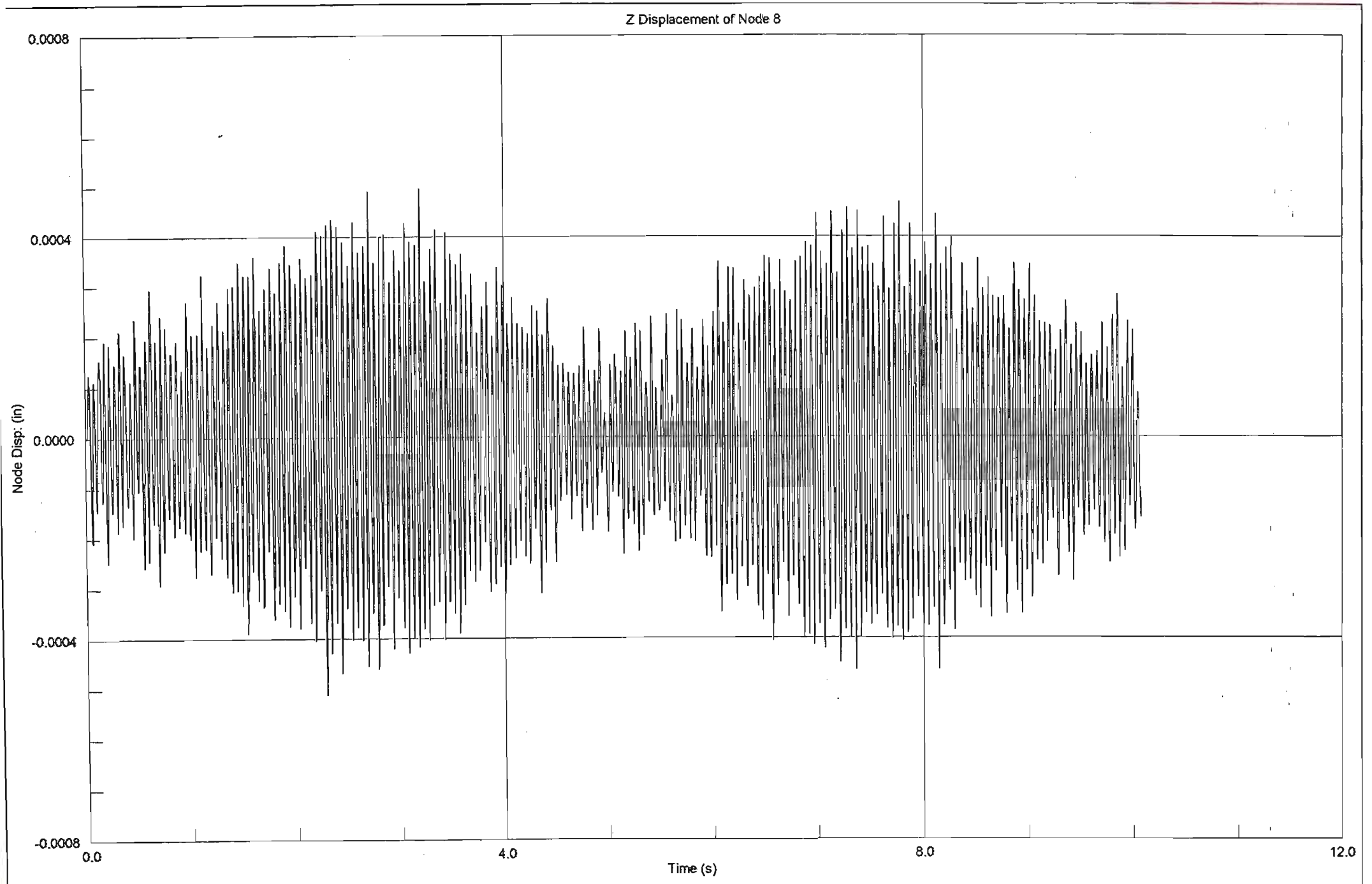
Z Displacement of Node 20

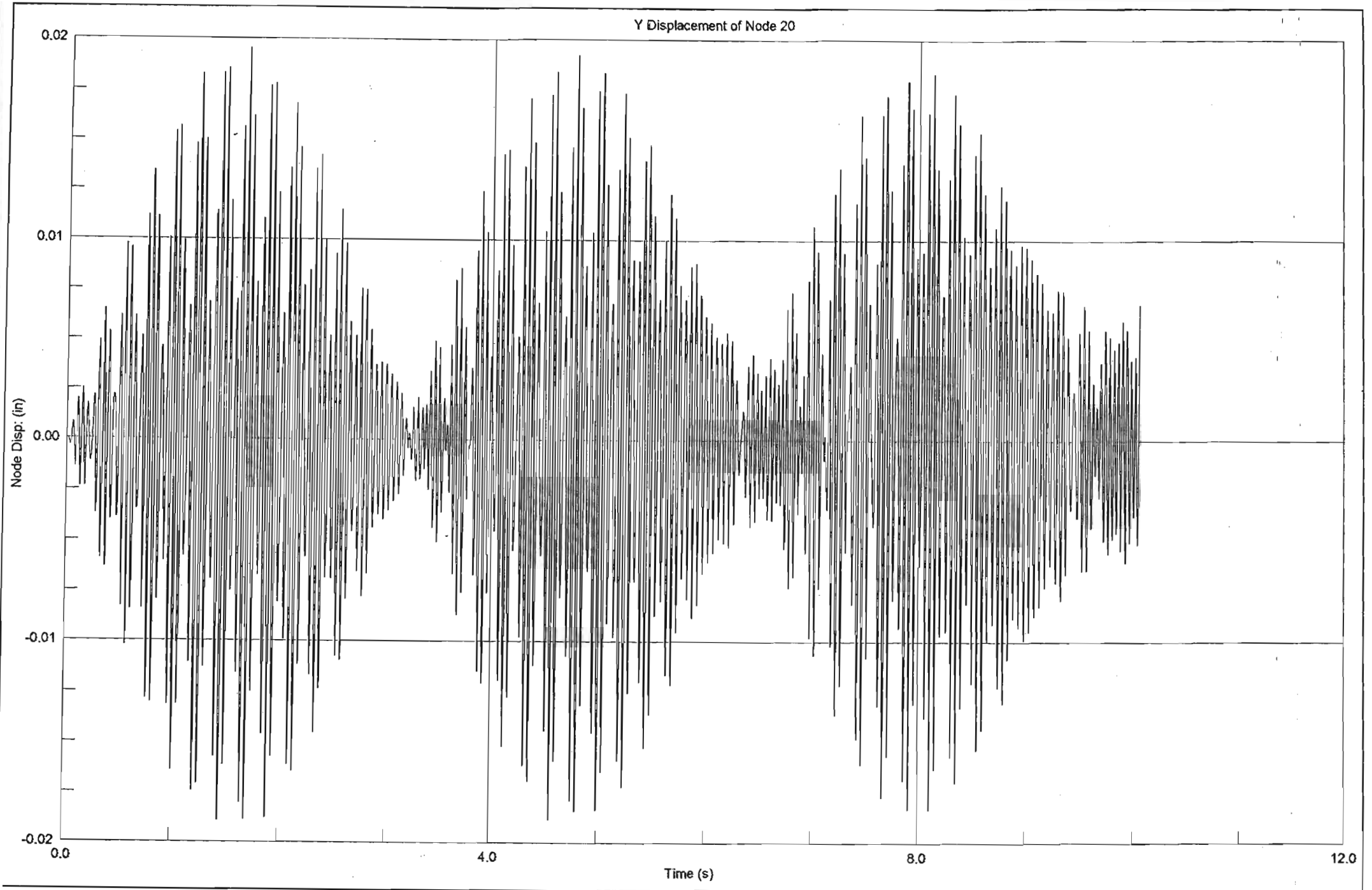




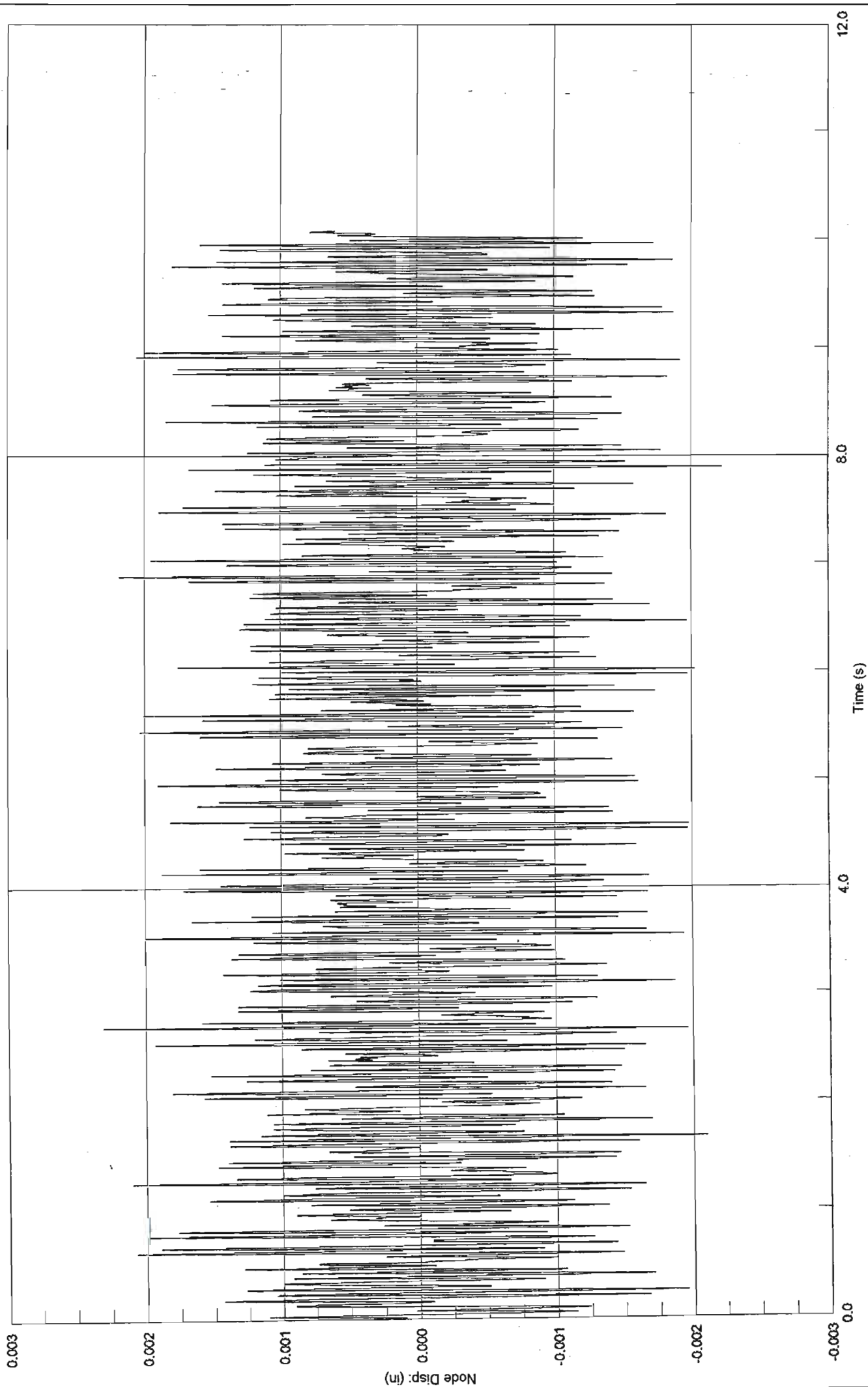


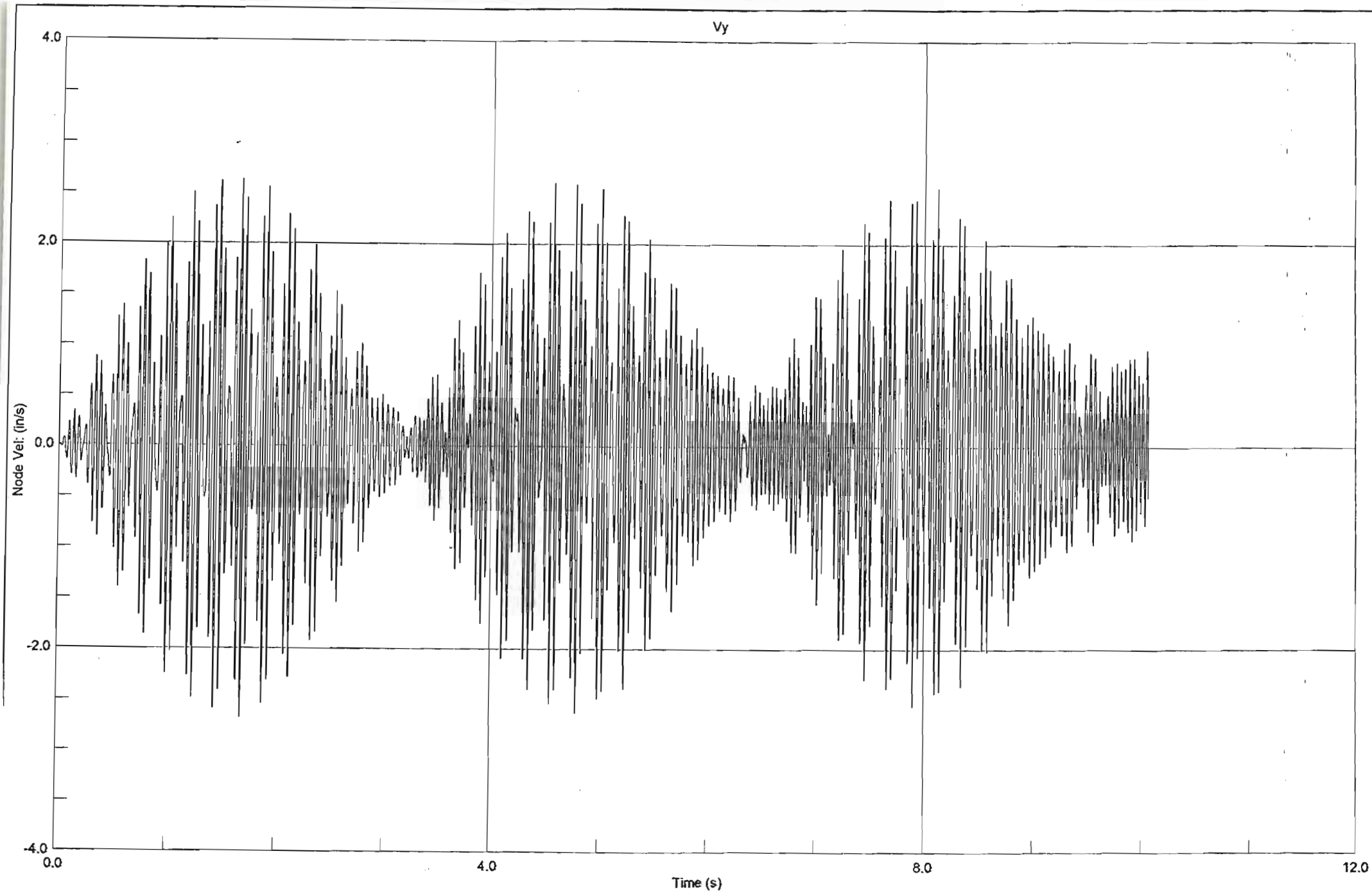




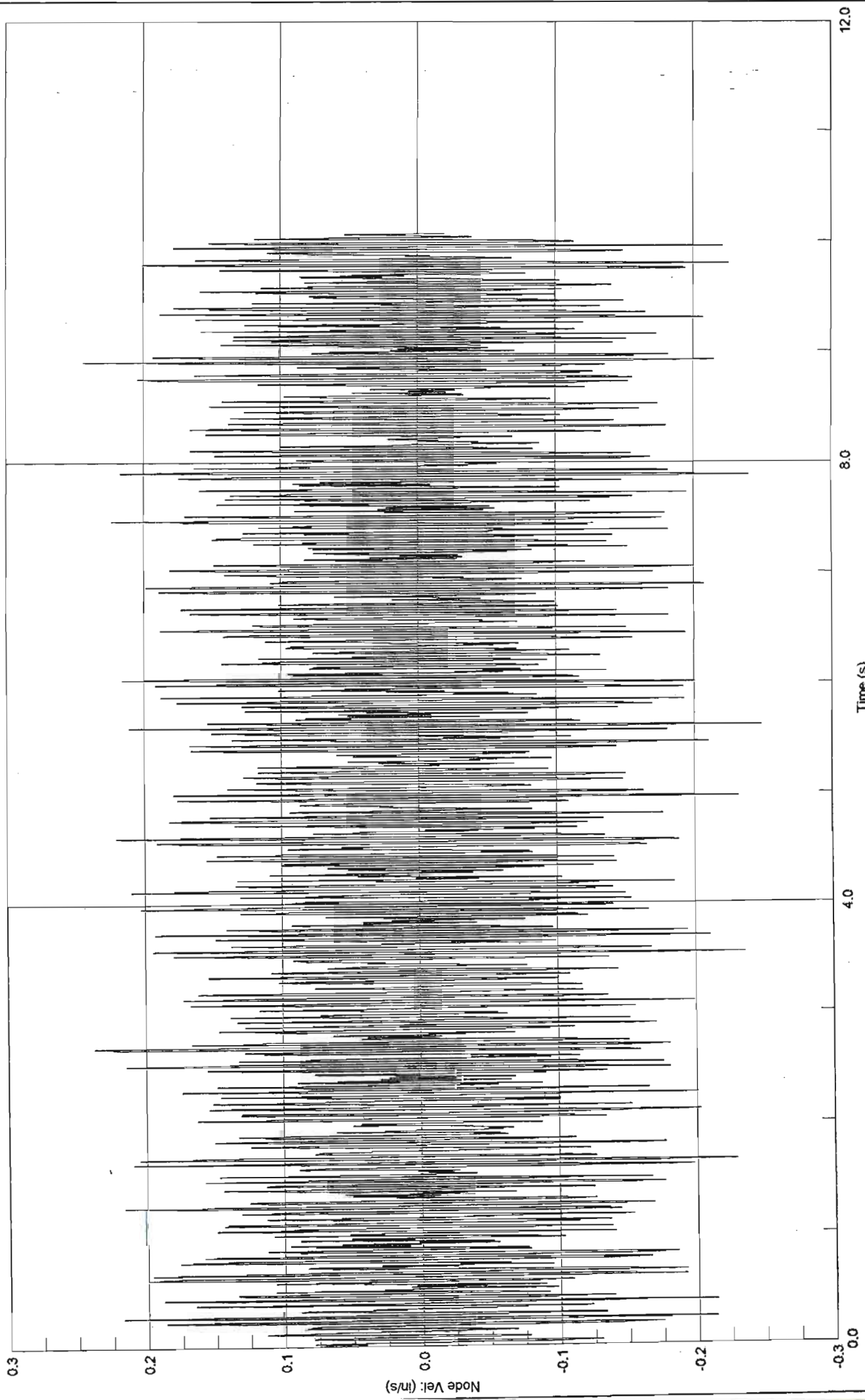


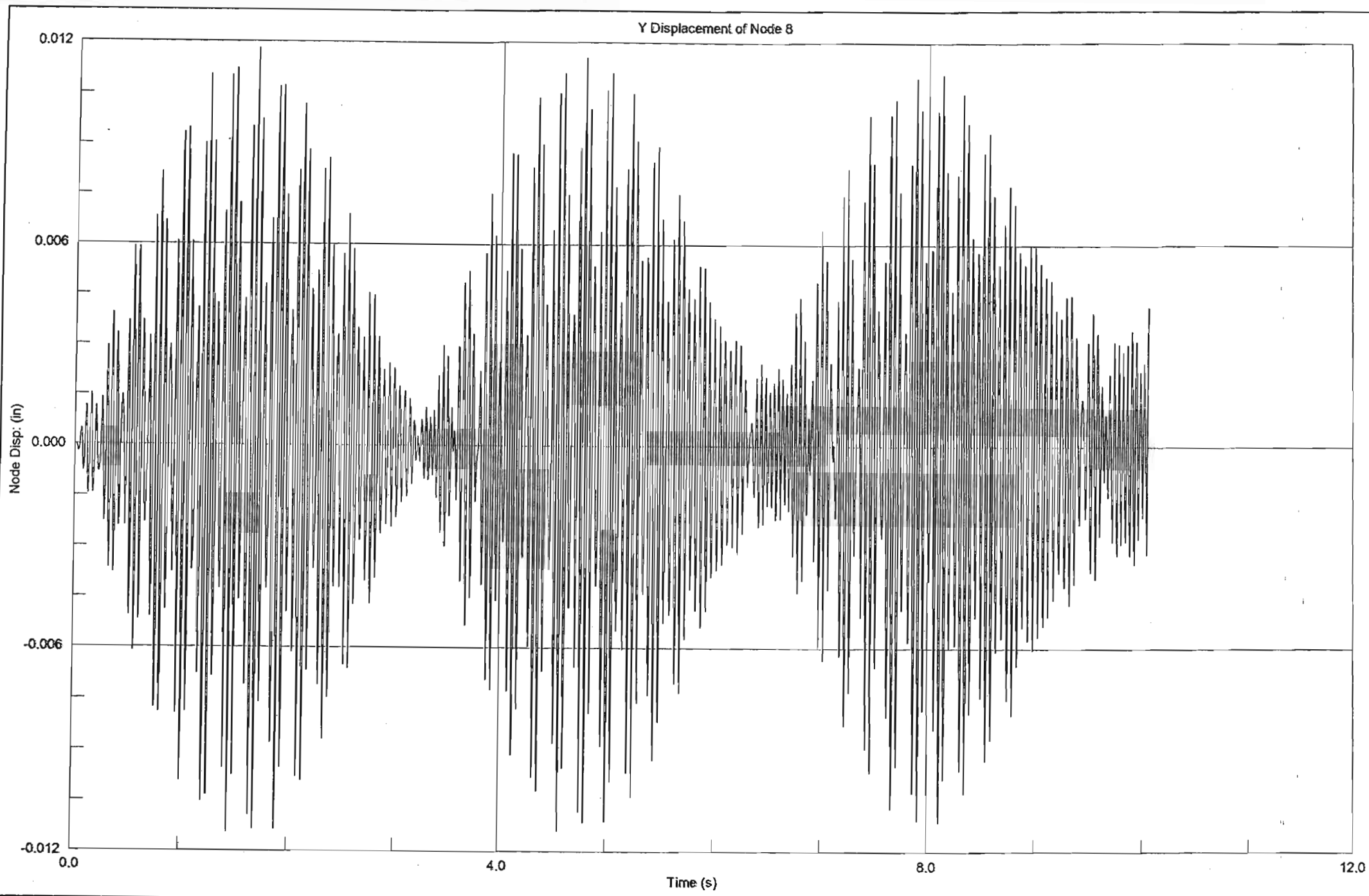
Z Displacement of Node 20



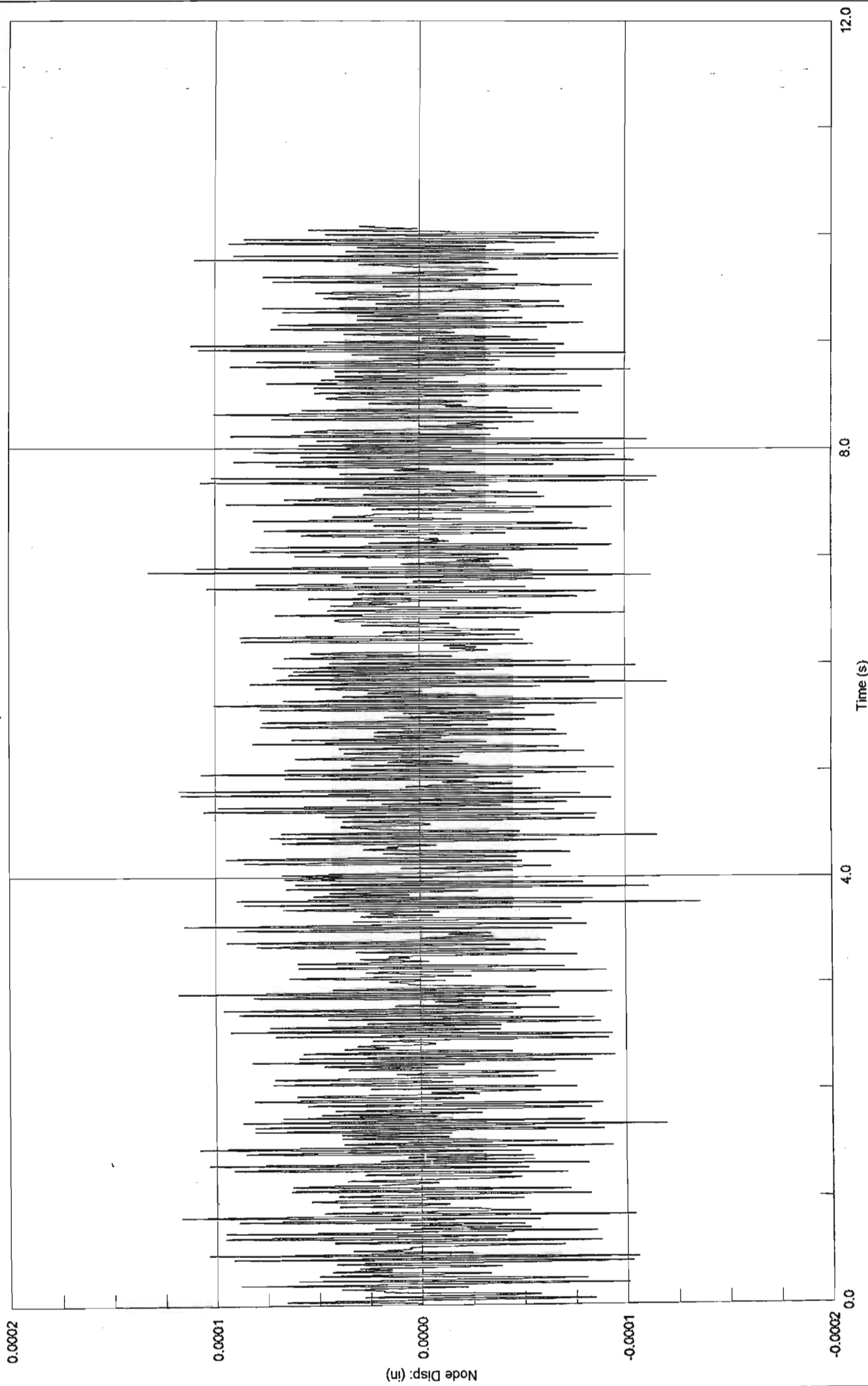


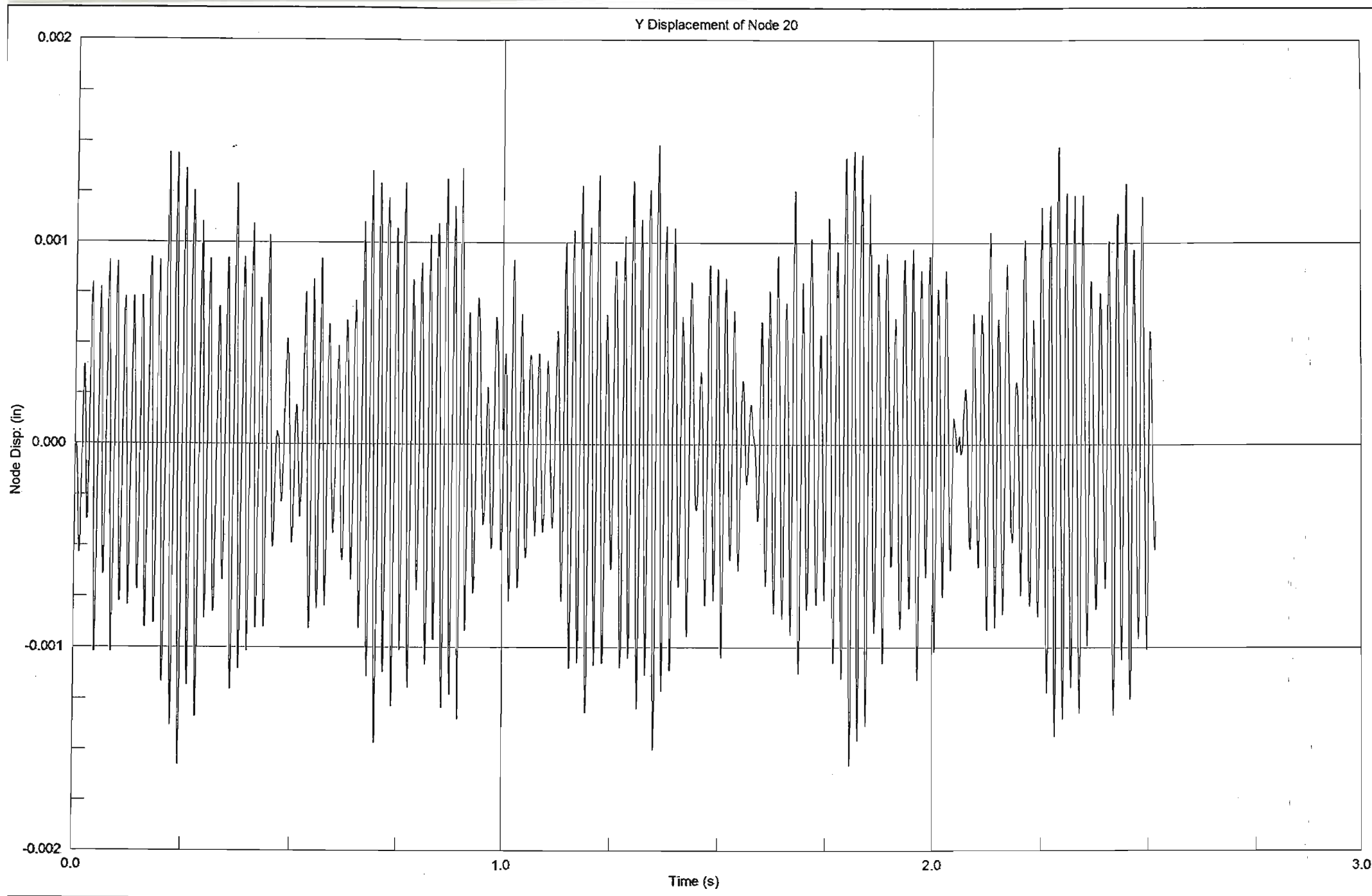
VZ



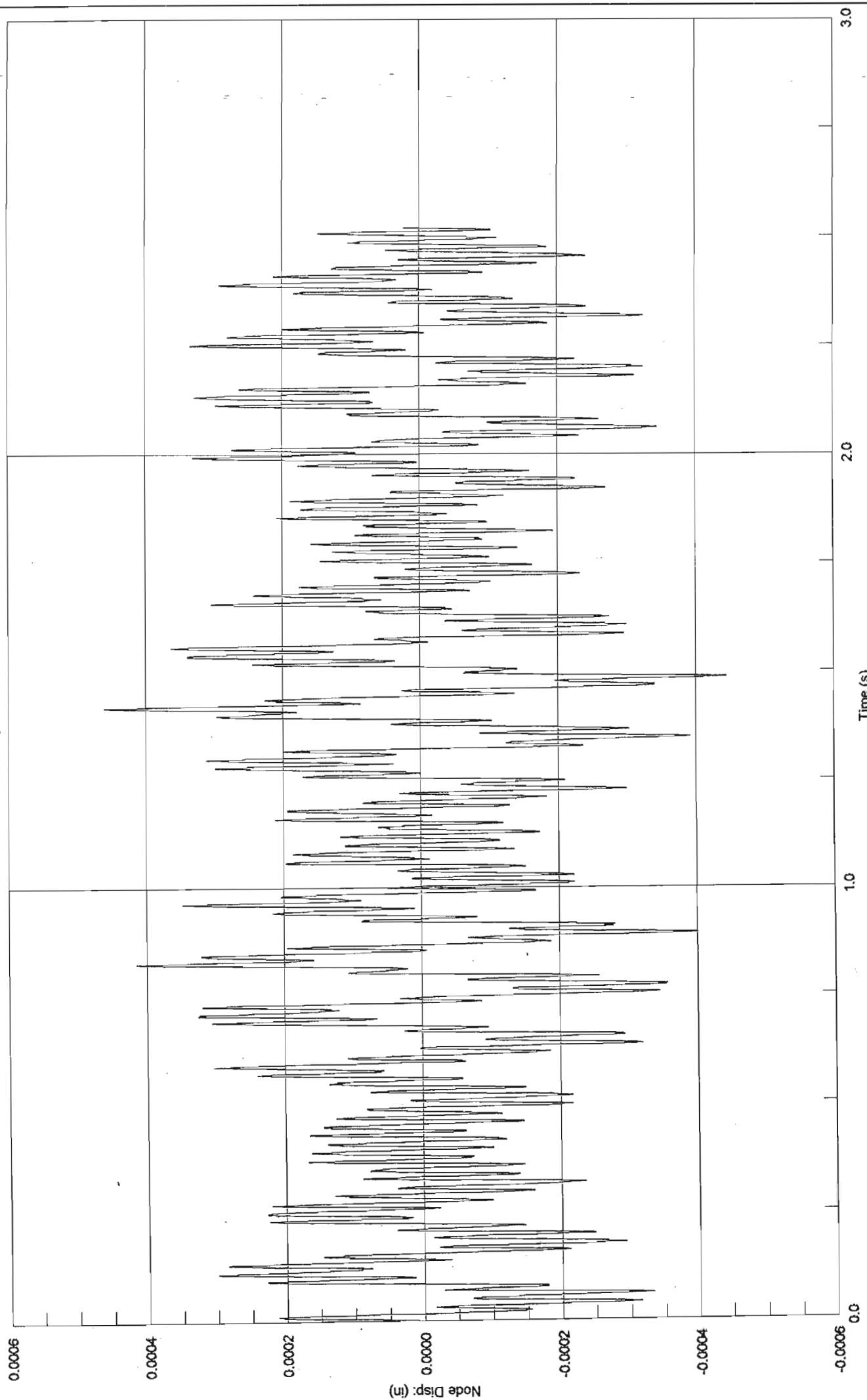


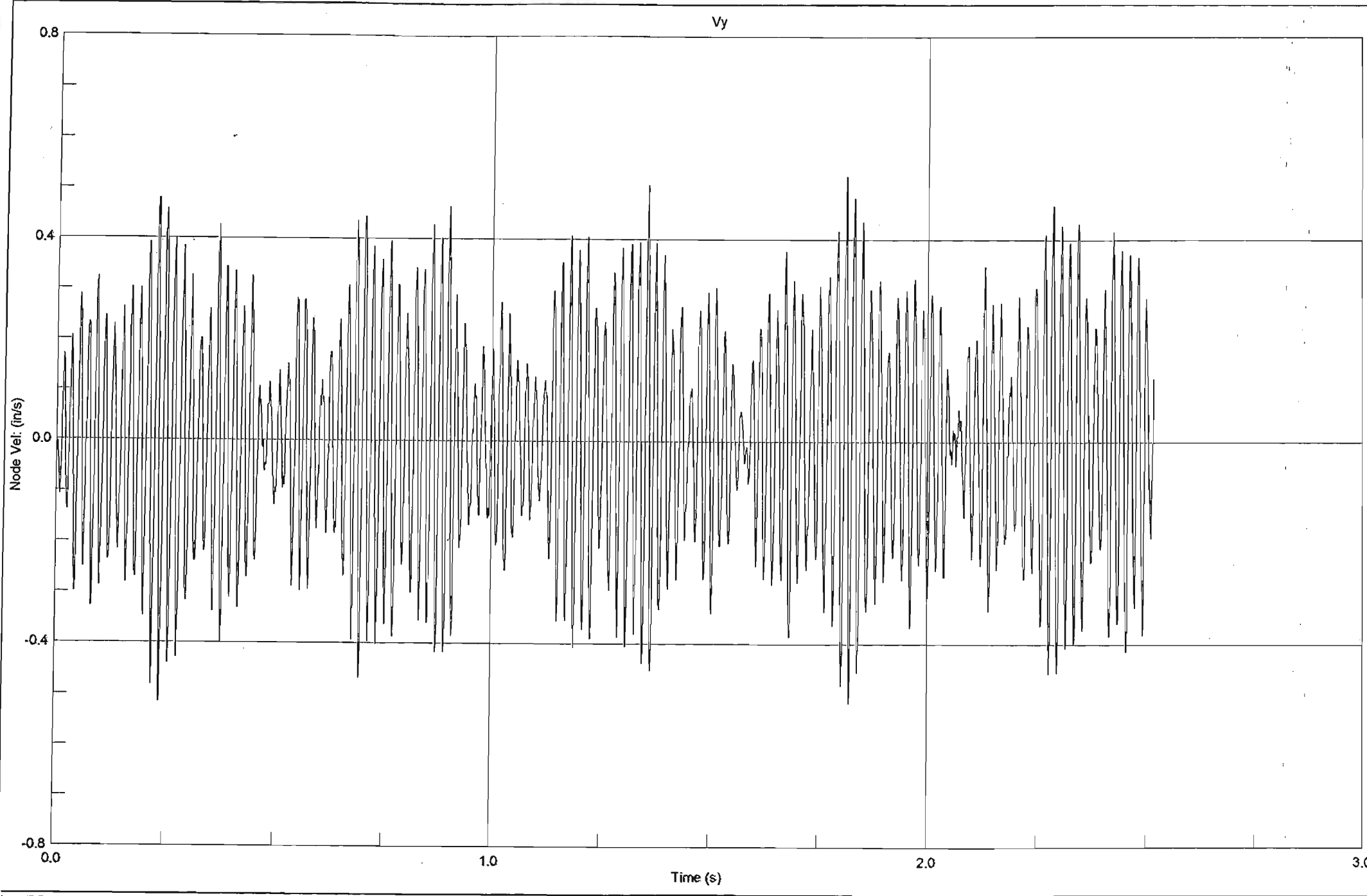
Z Displacement of Node 8

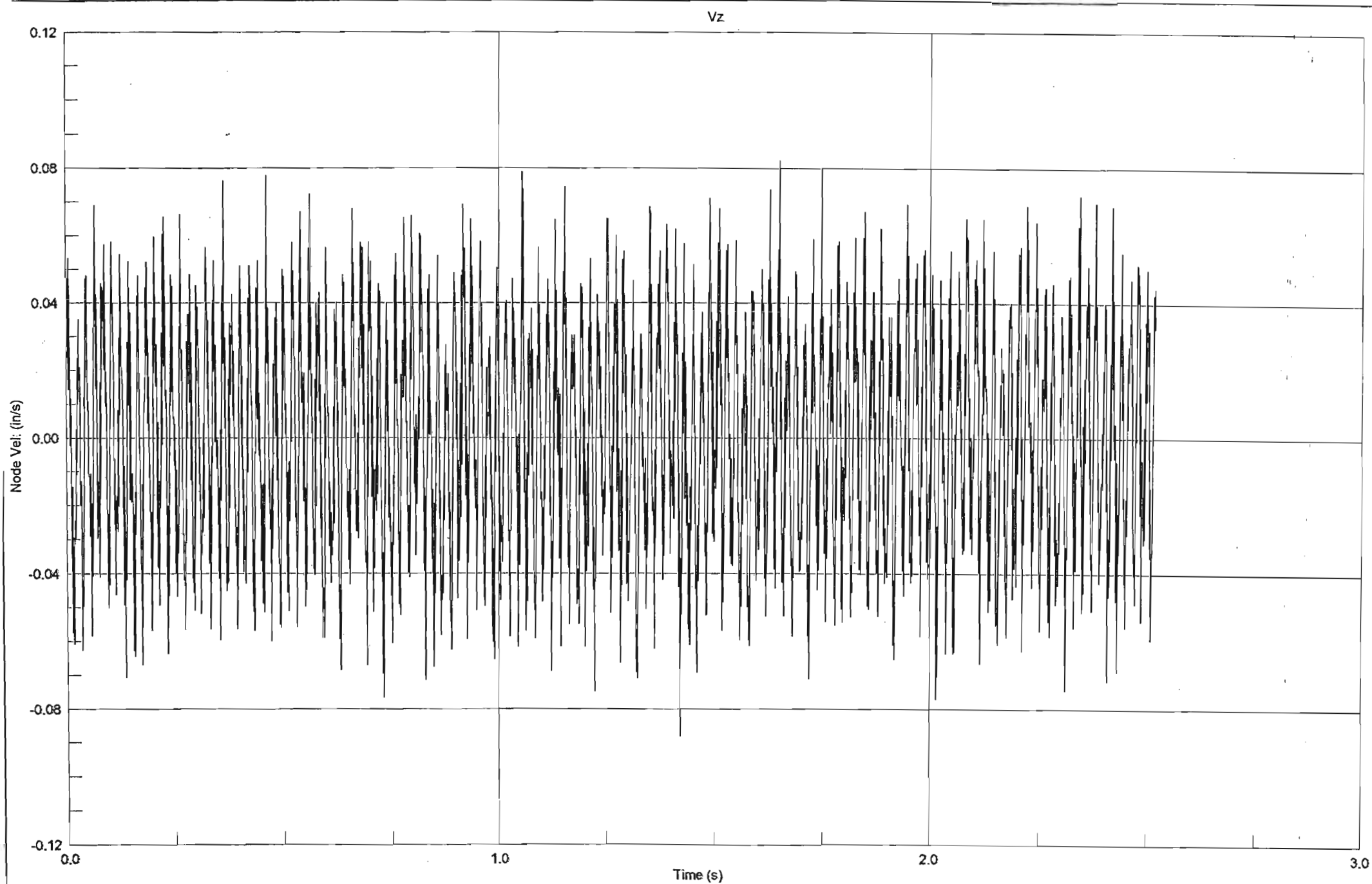


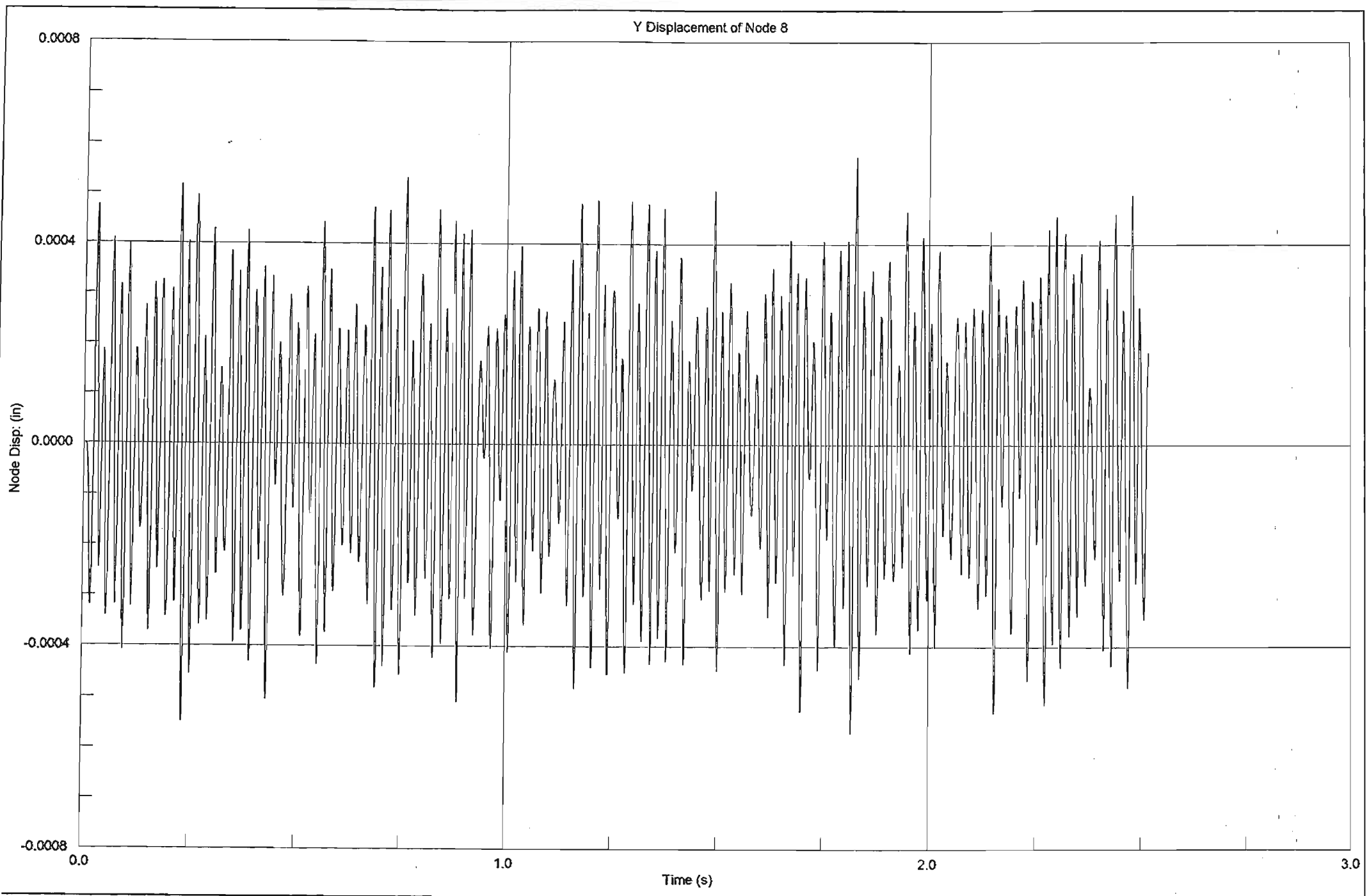


Z Displacement of Node 20

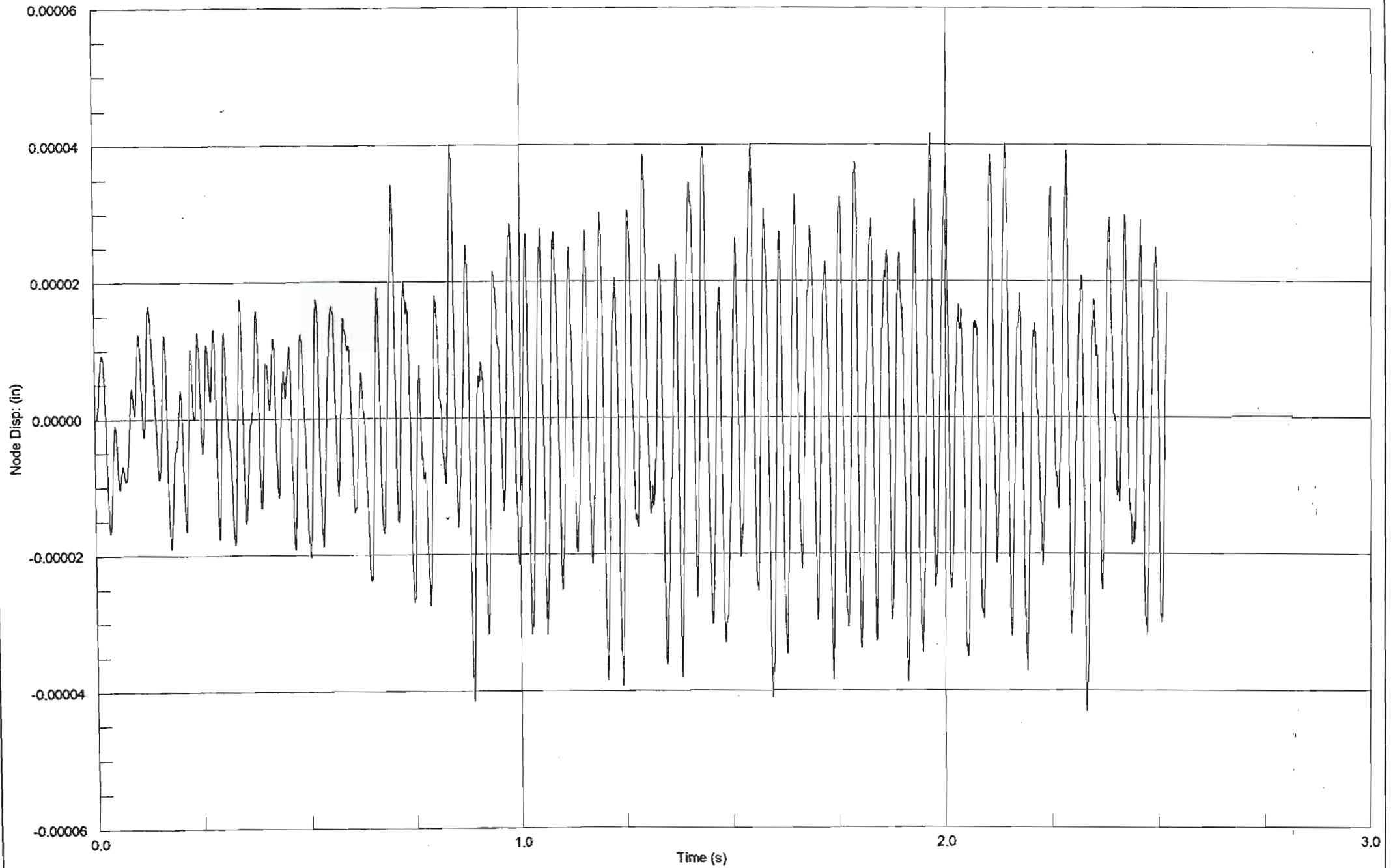


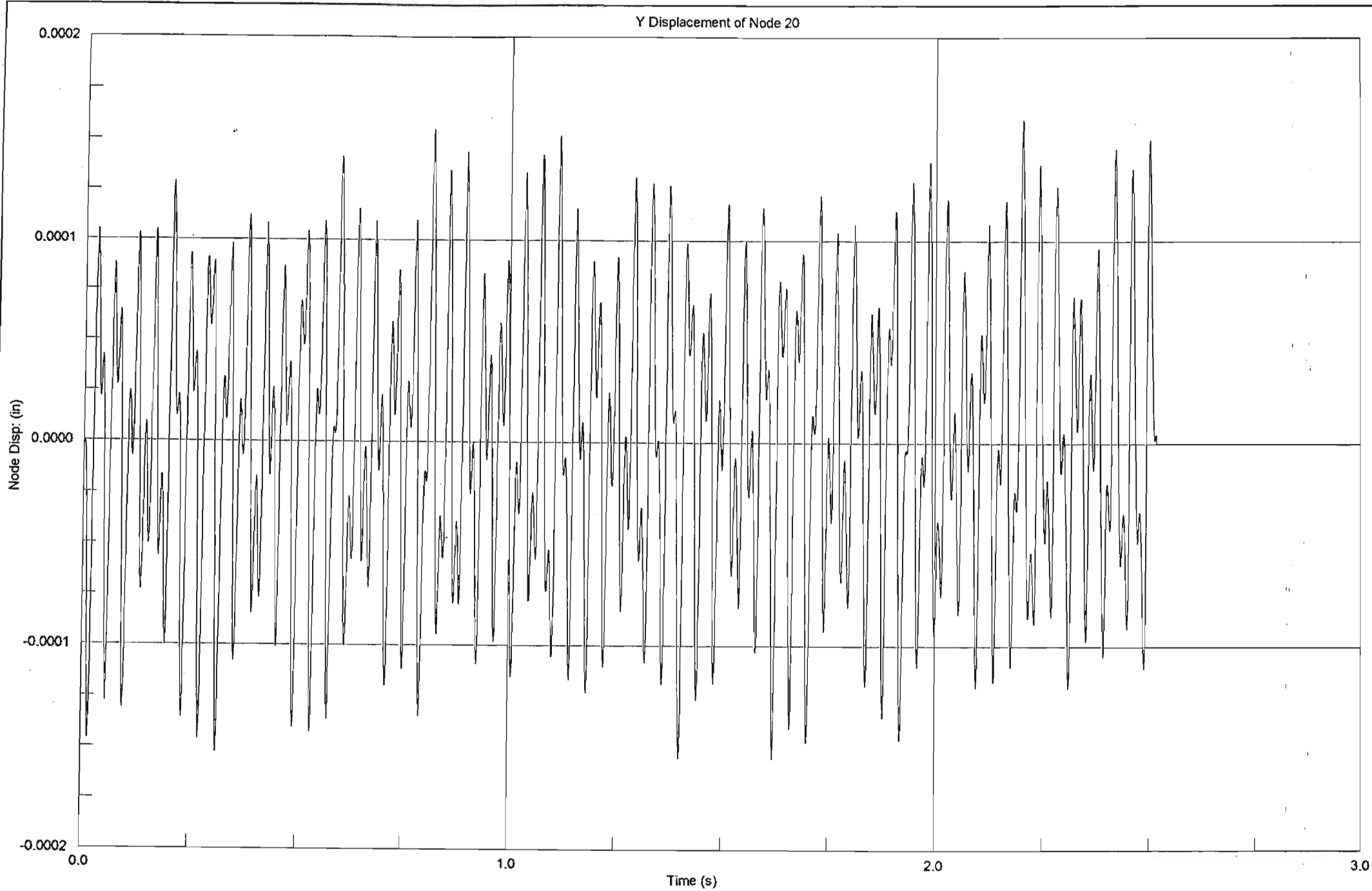




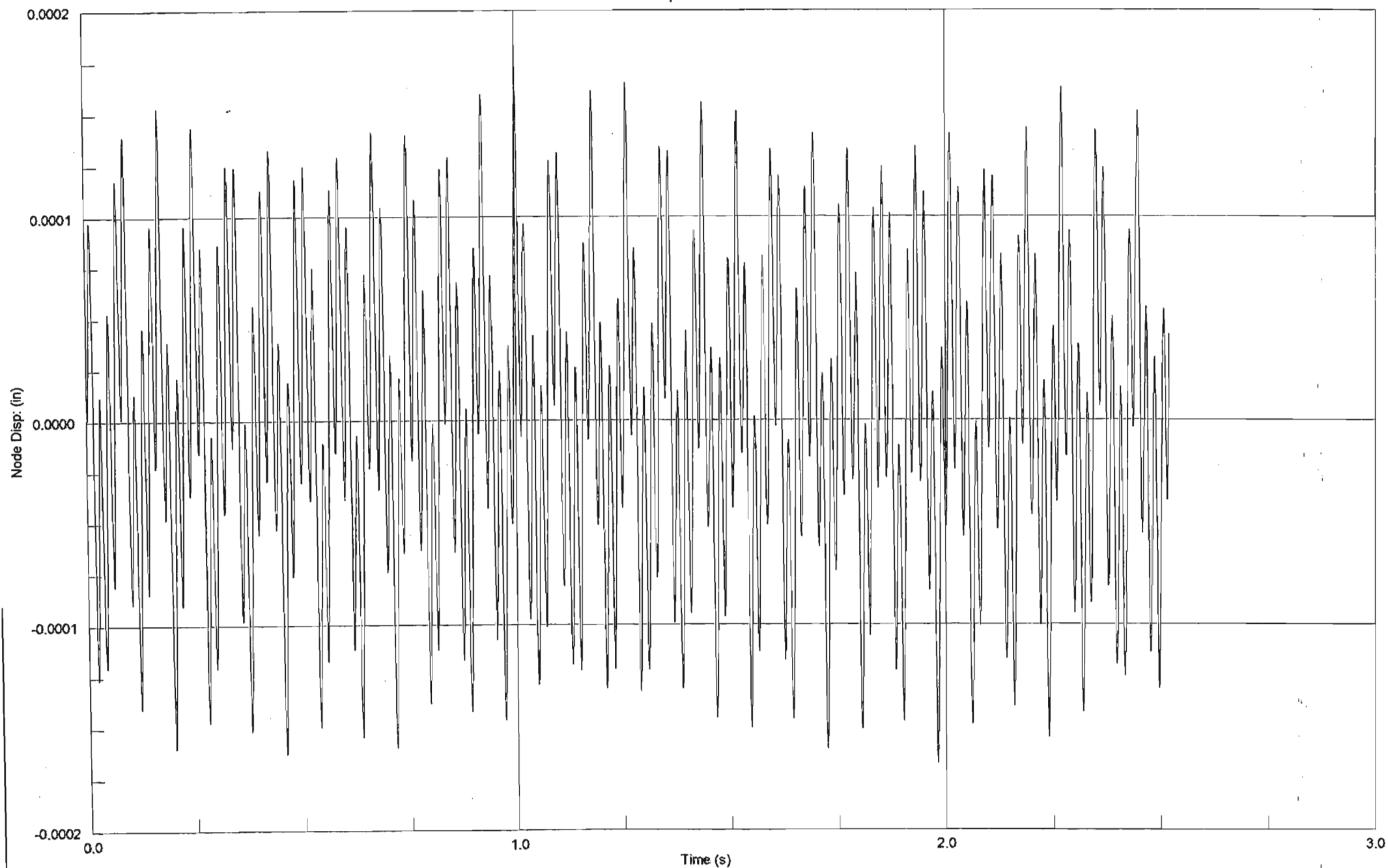


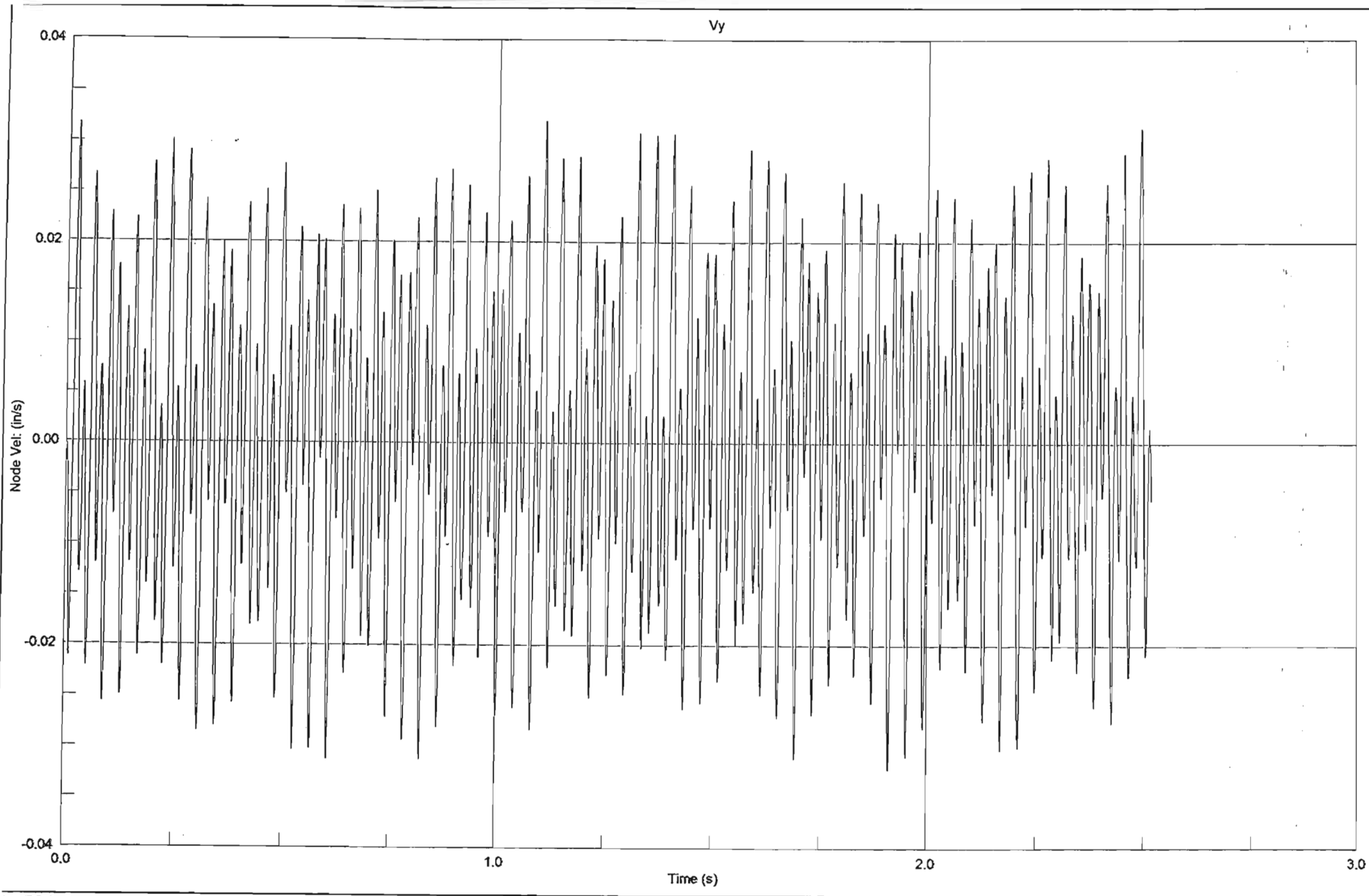
Z Displacement of Node 8





Z Displacement of Node 20





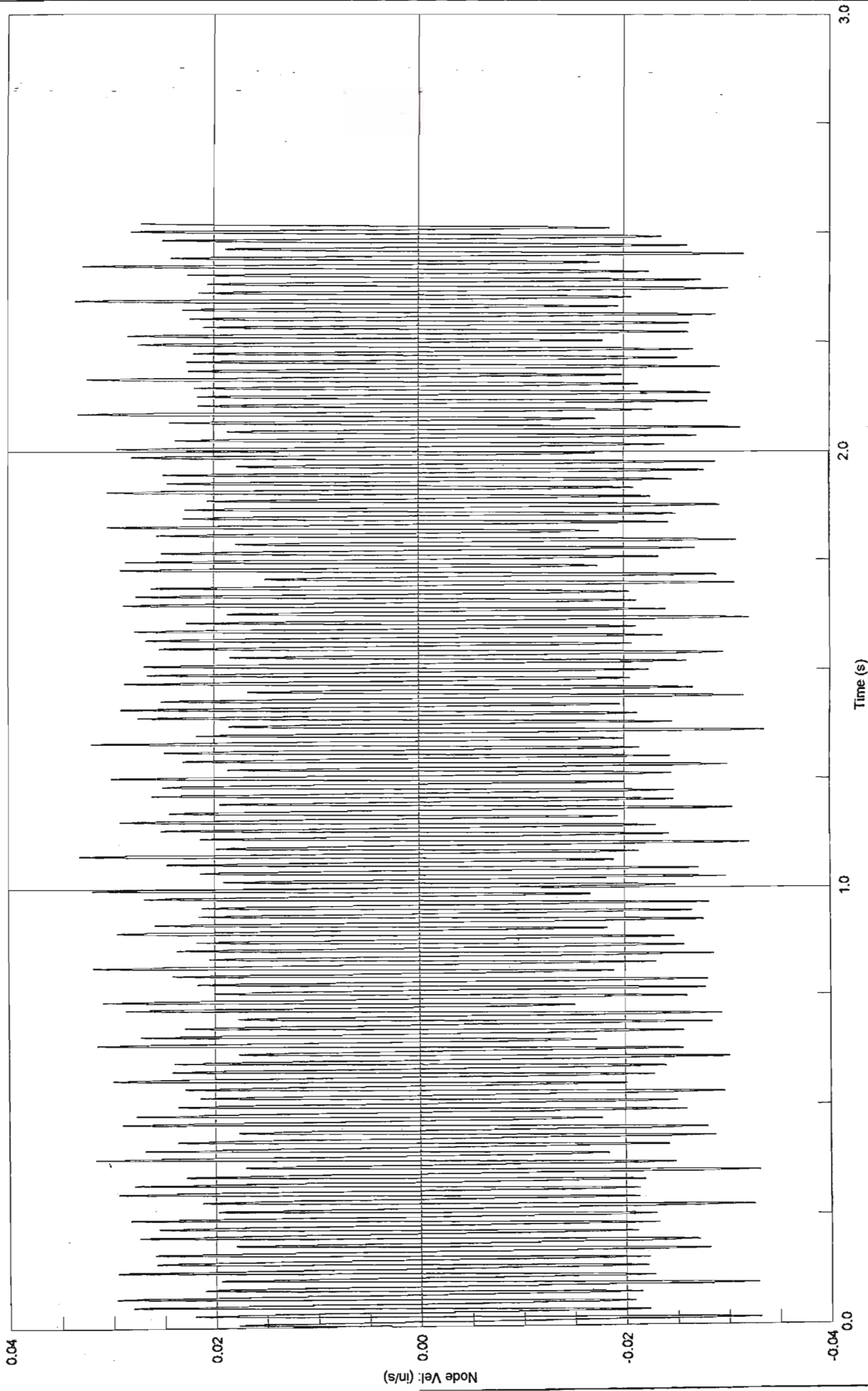
rand7 Release 2.1.7

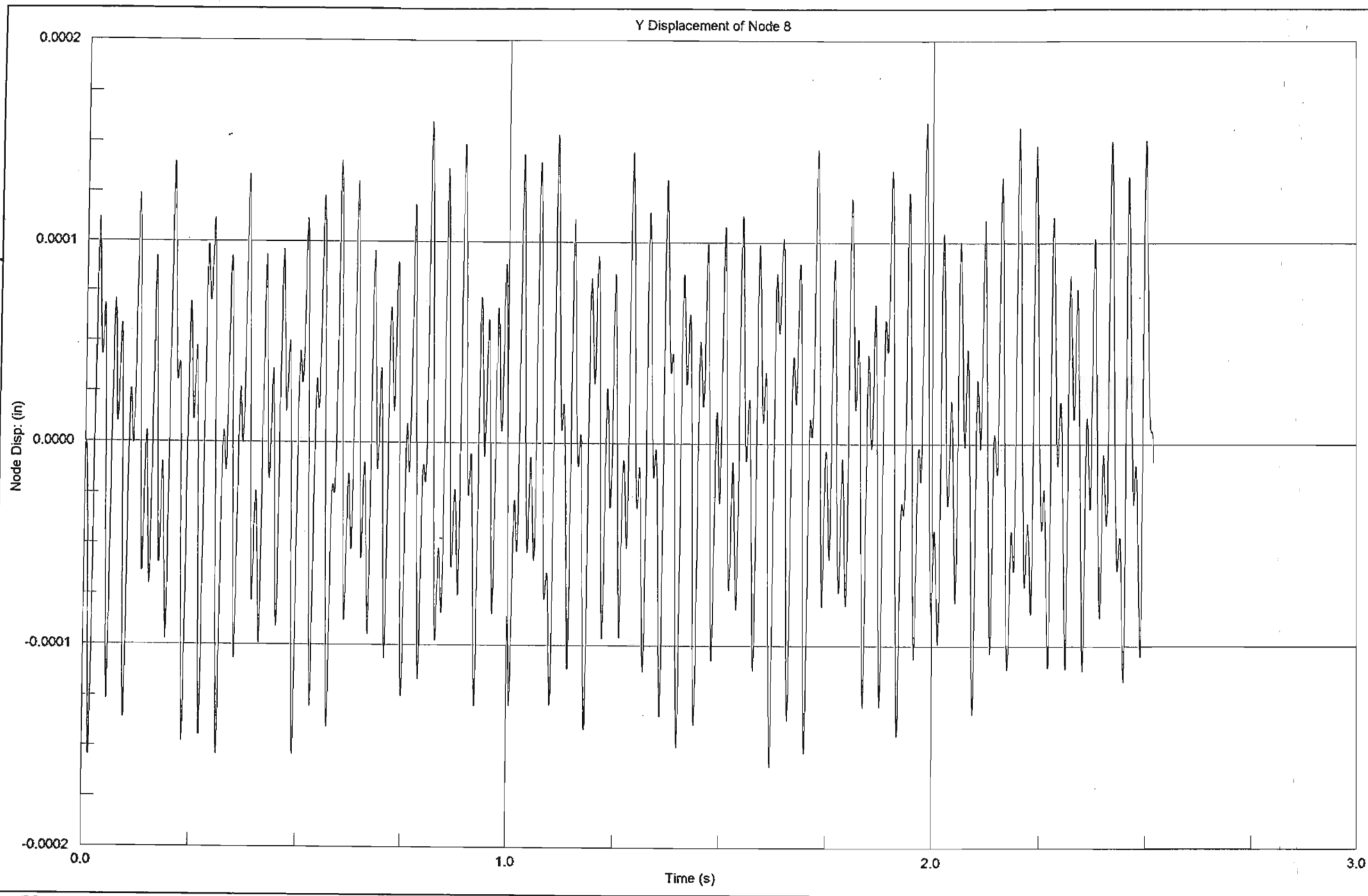
\\MSc Eng\Table Top\Table Top 5\table top G30000-stf.st7

October 2002 11:11 am

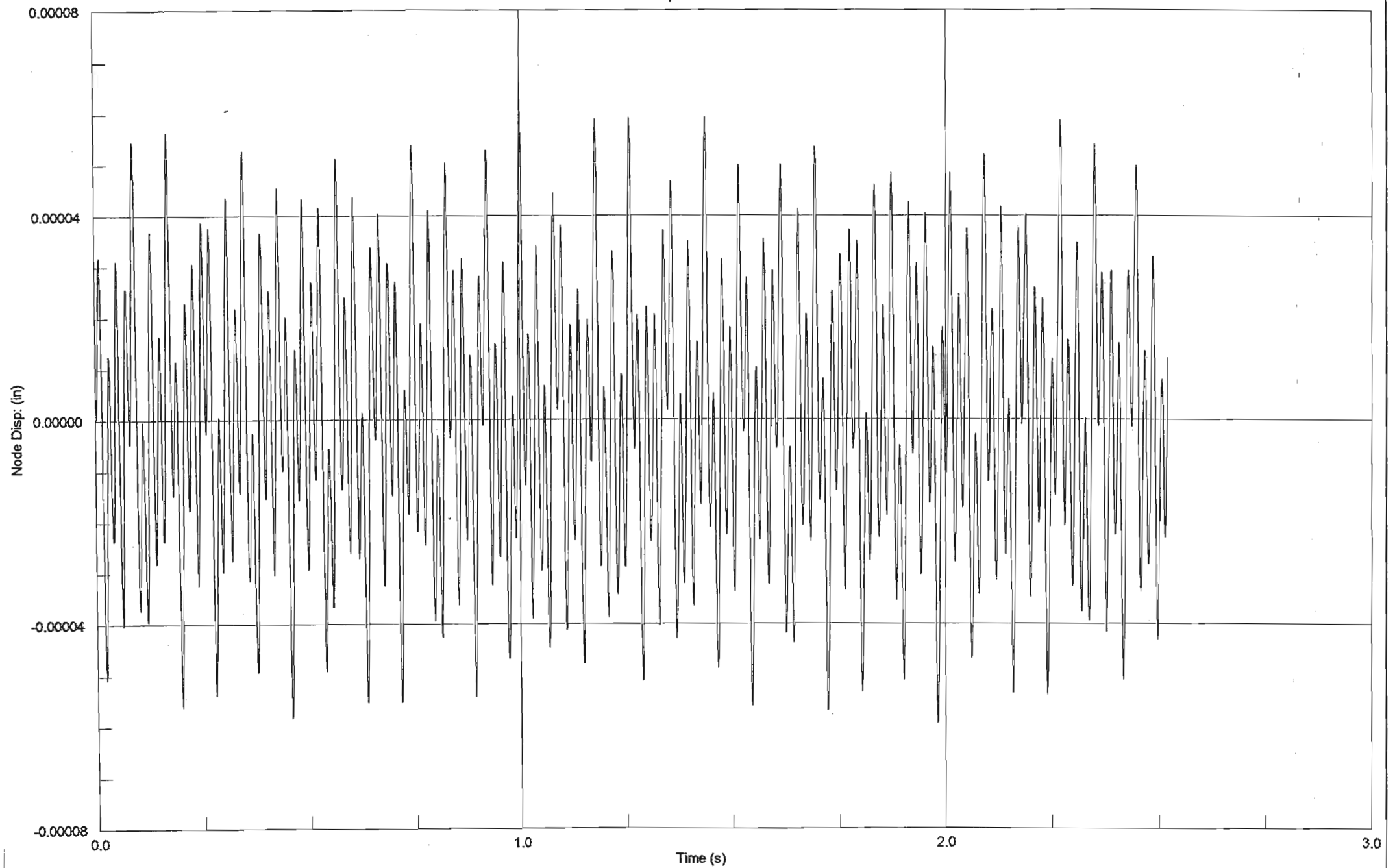
CS.15

Vz





Z Displacement of Node 8



DESIGN OF STRUCTURES AND FOUNDATIONS FOR VIBRATING MACHINES

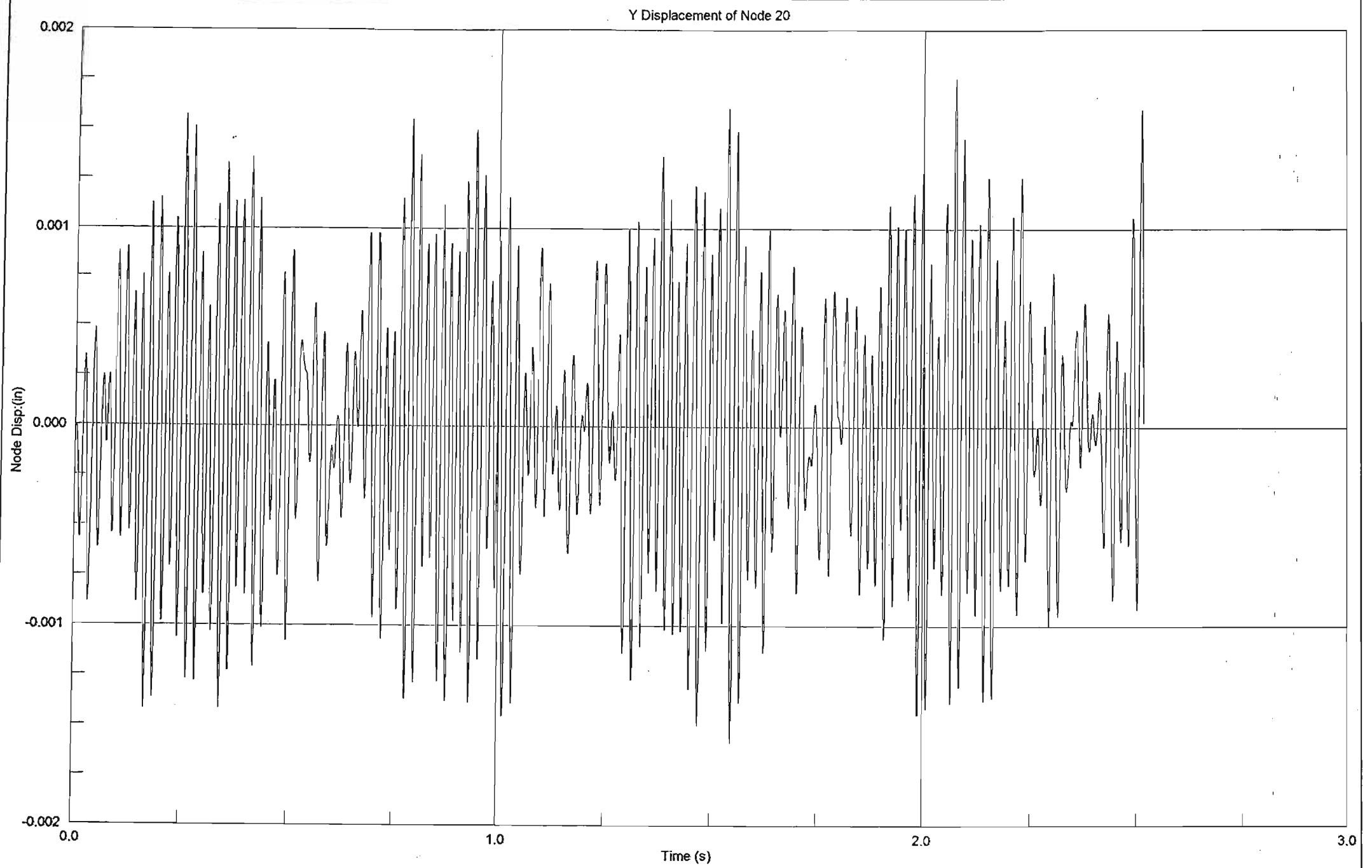
VR ULASSI

VOLUME 4 OF 4

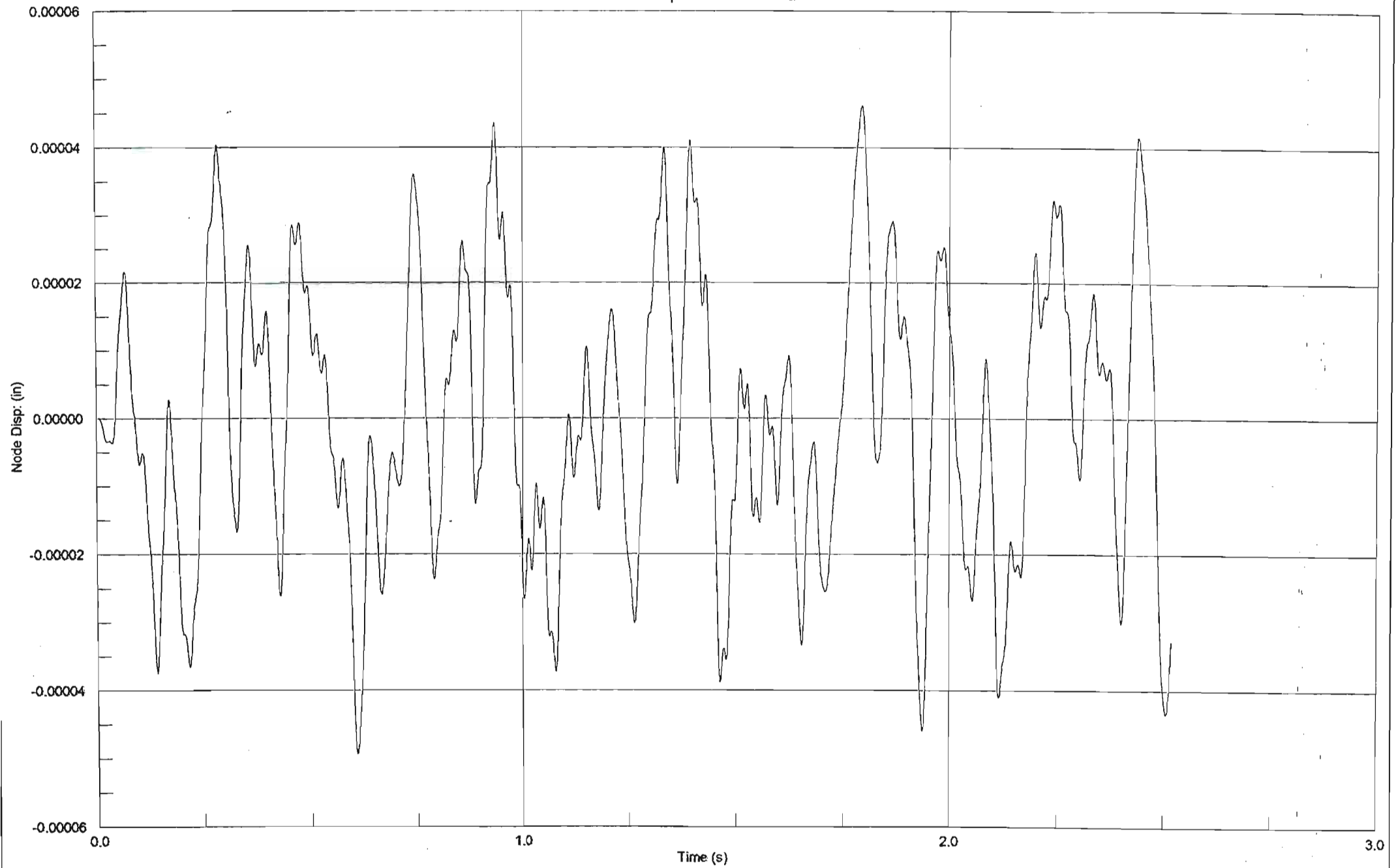
IN PARTIAL FULFILLMENT OF THE DEGREE OF MASTER OF SCIENCE IN
ENGINEERING (COURSEWORK) COMPRISING 72 CREDITS OF 144 FOR THE
DEGREE

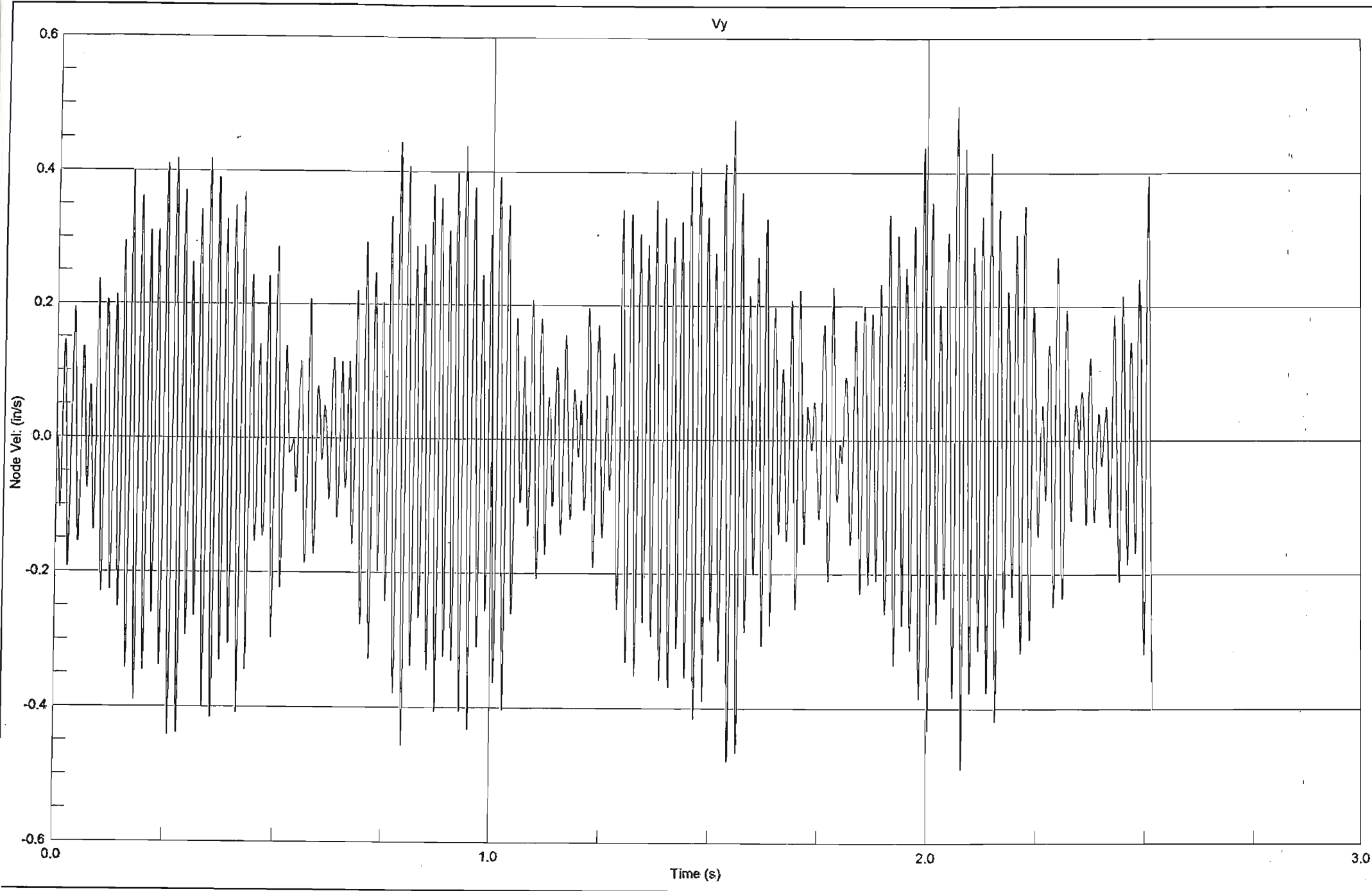
DATE SUBMITTED: 13 DECEMBER 2002

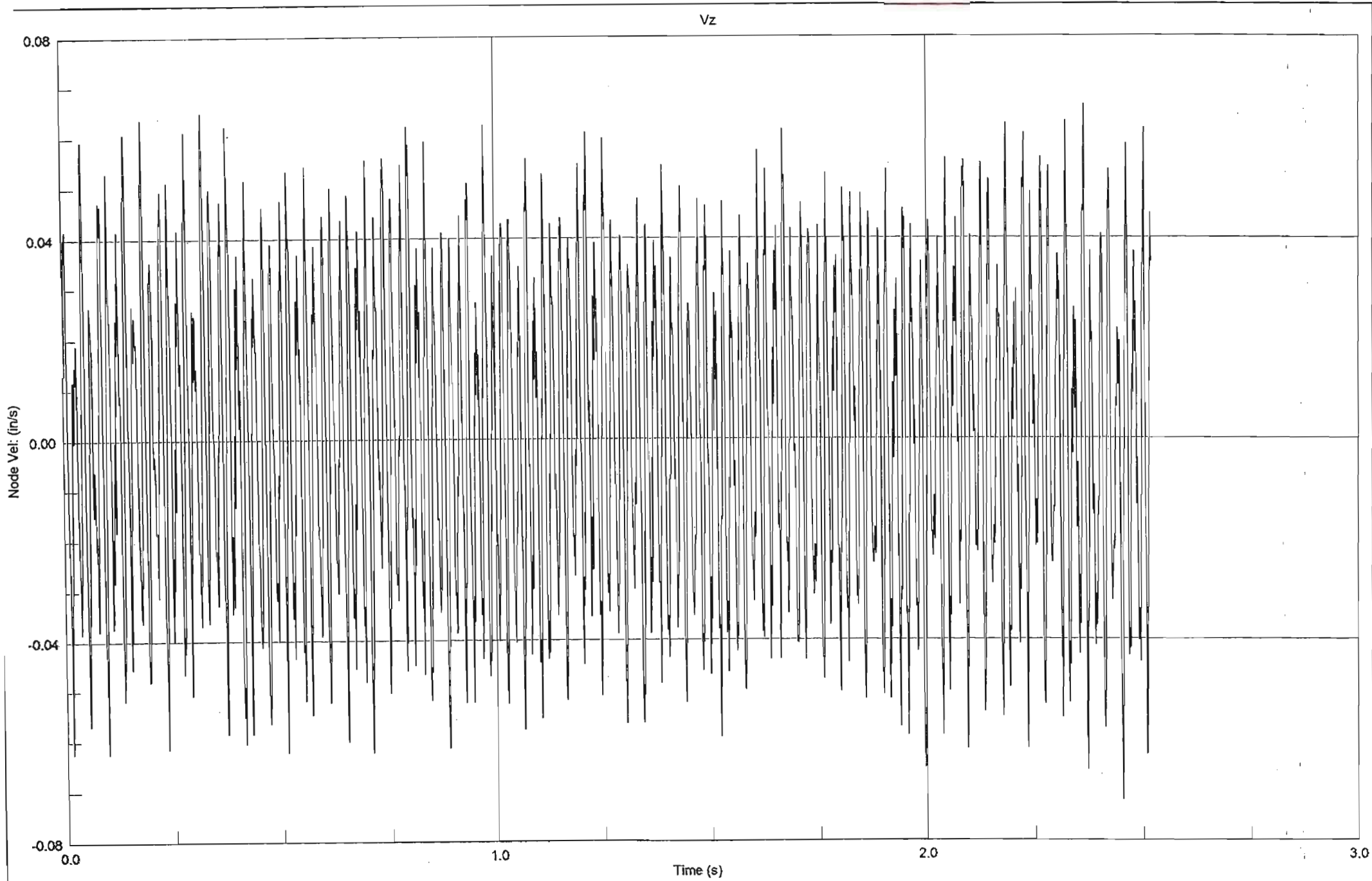
SUPERVISOR: PROFESSOR H D SCHREINER

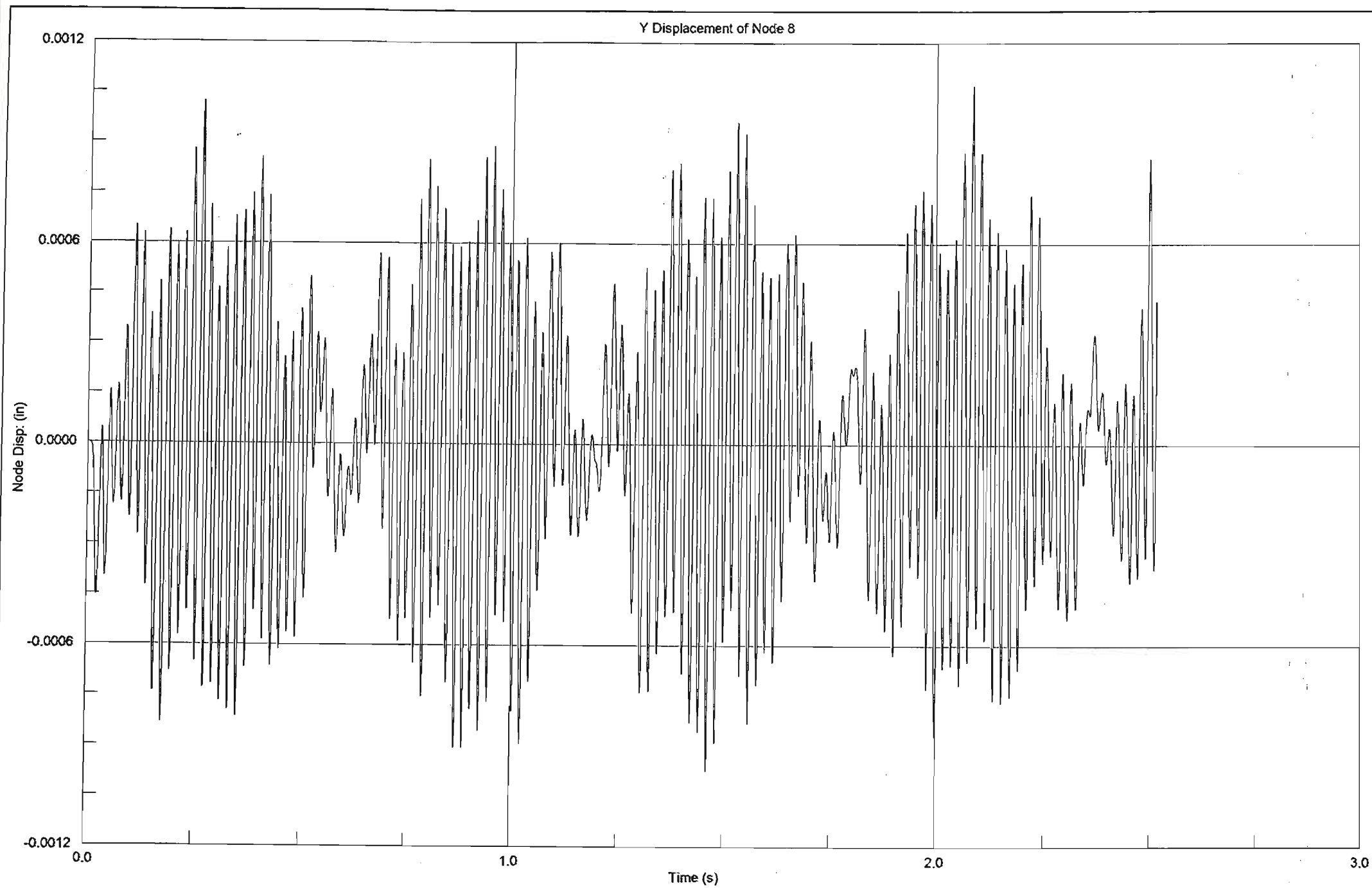


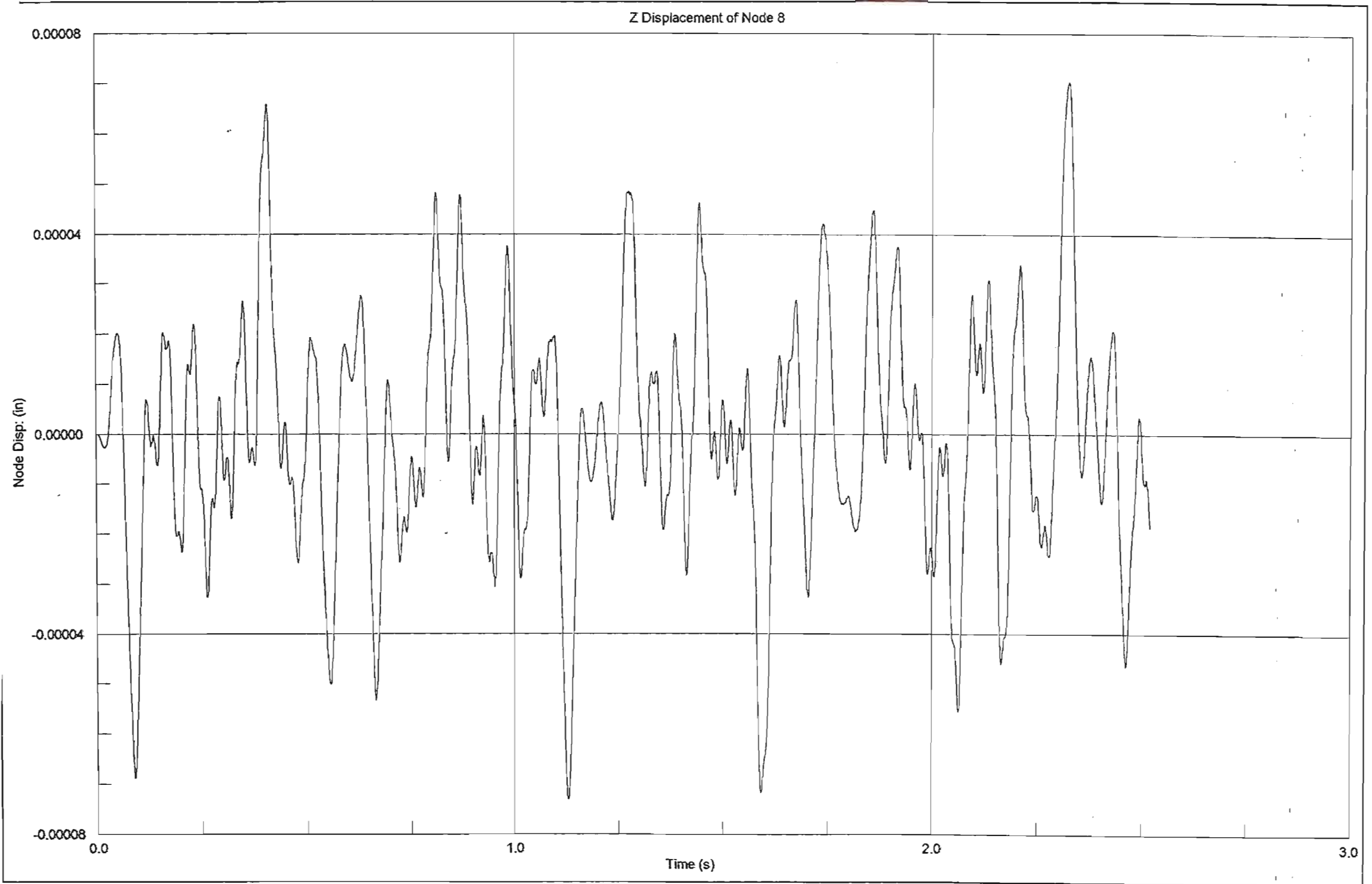
Z Displacement of Node 20

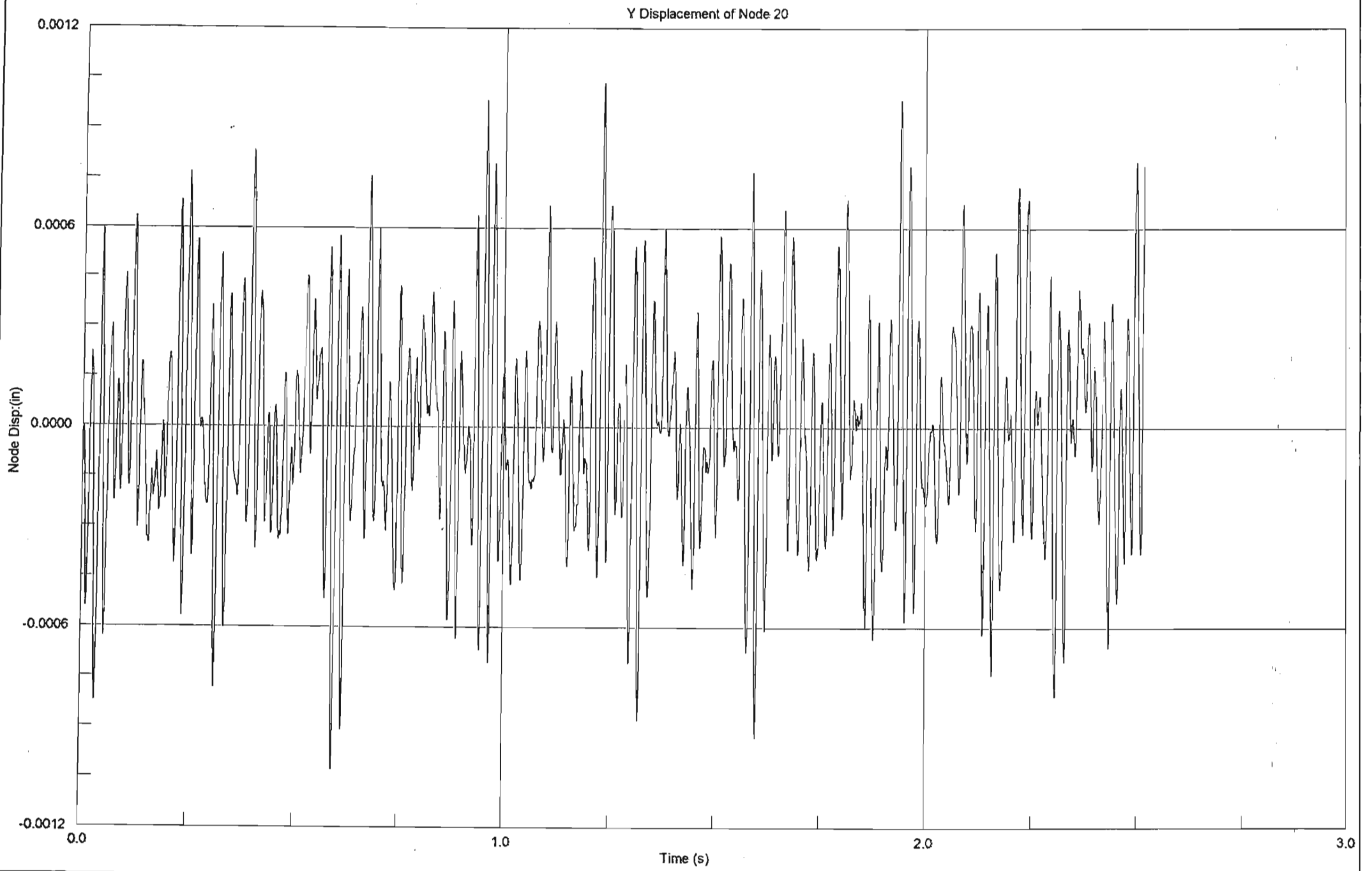


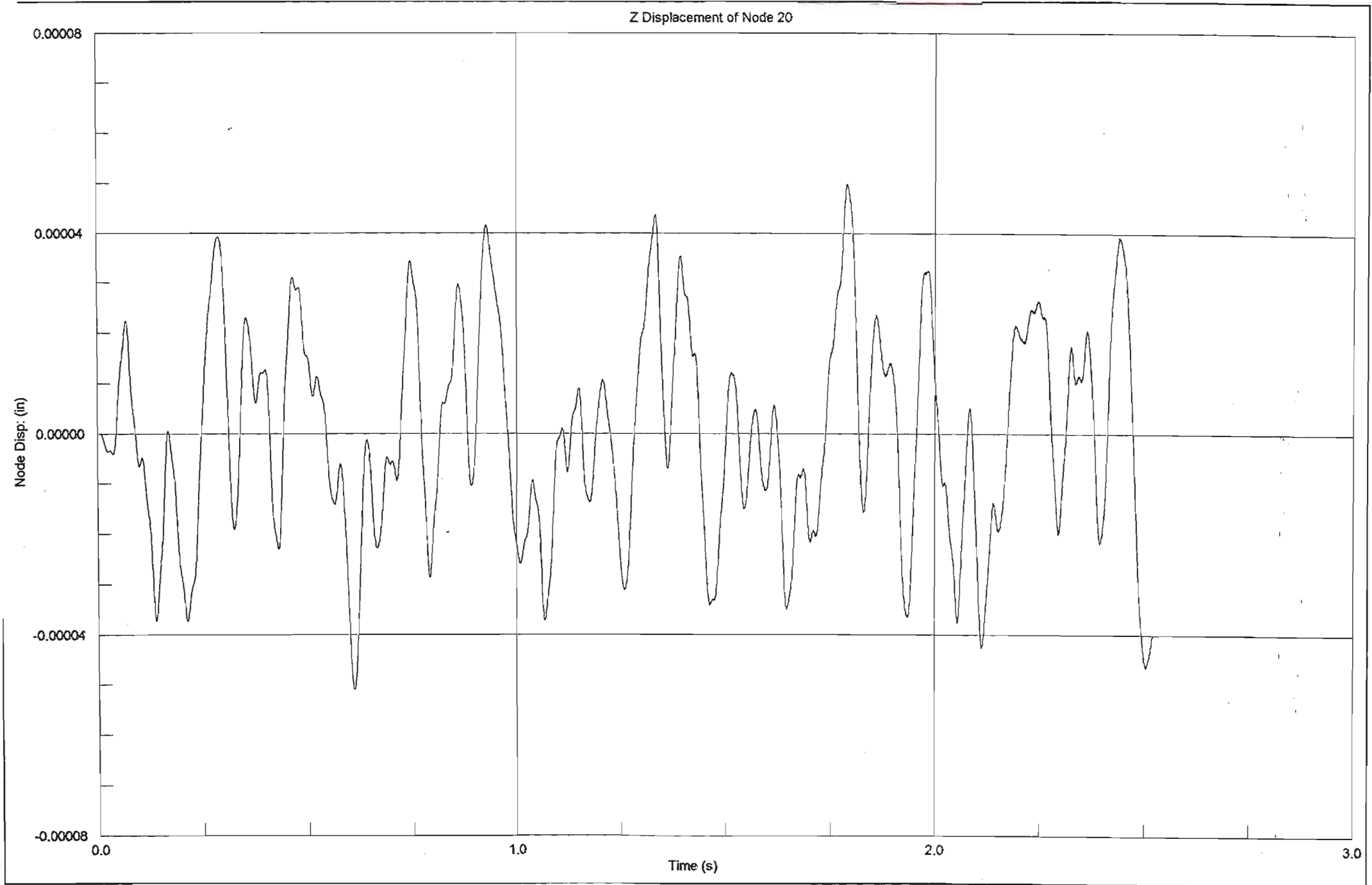




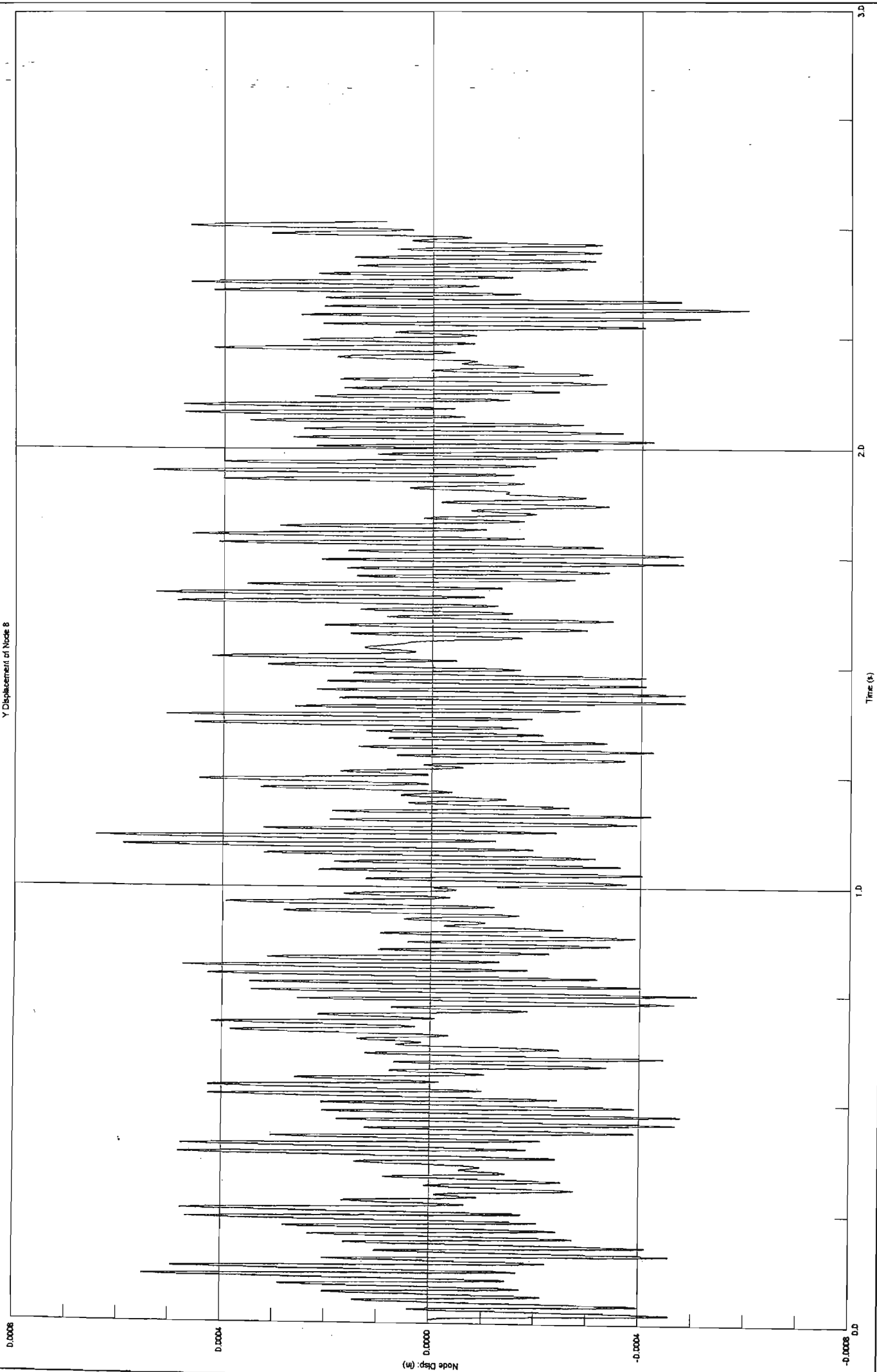




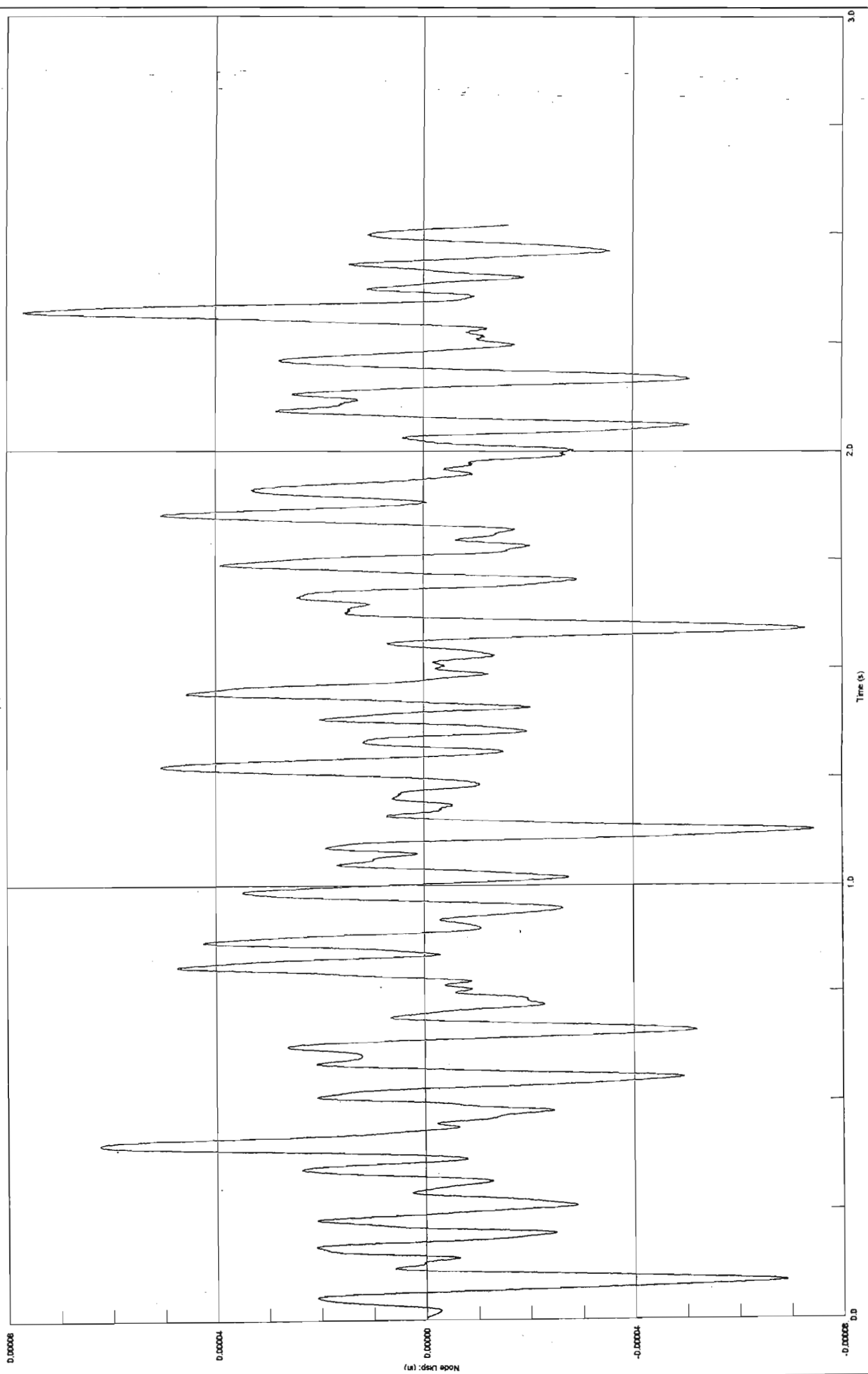




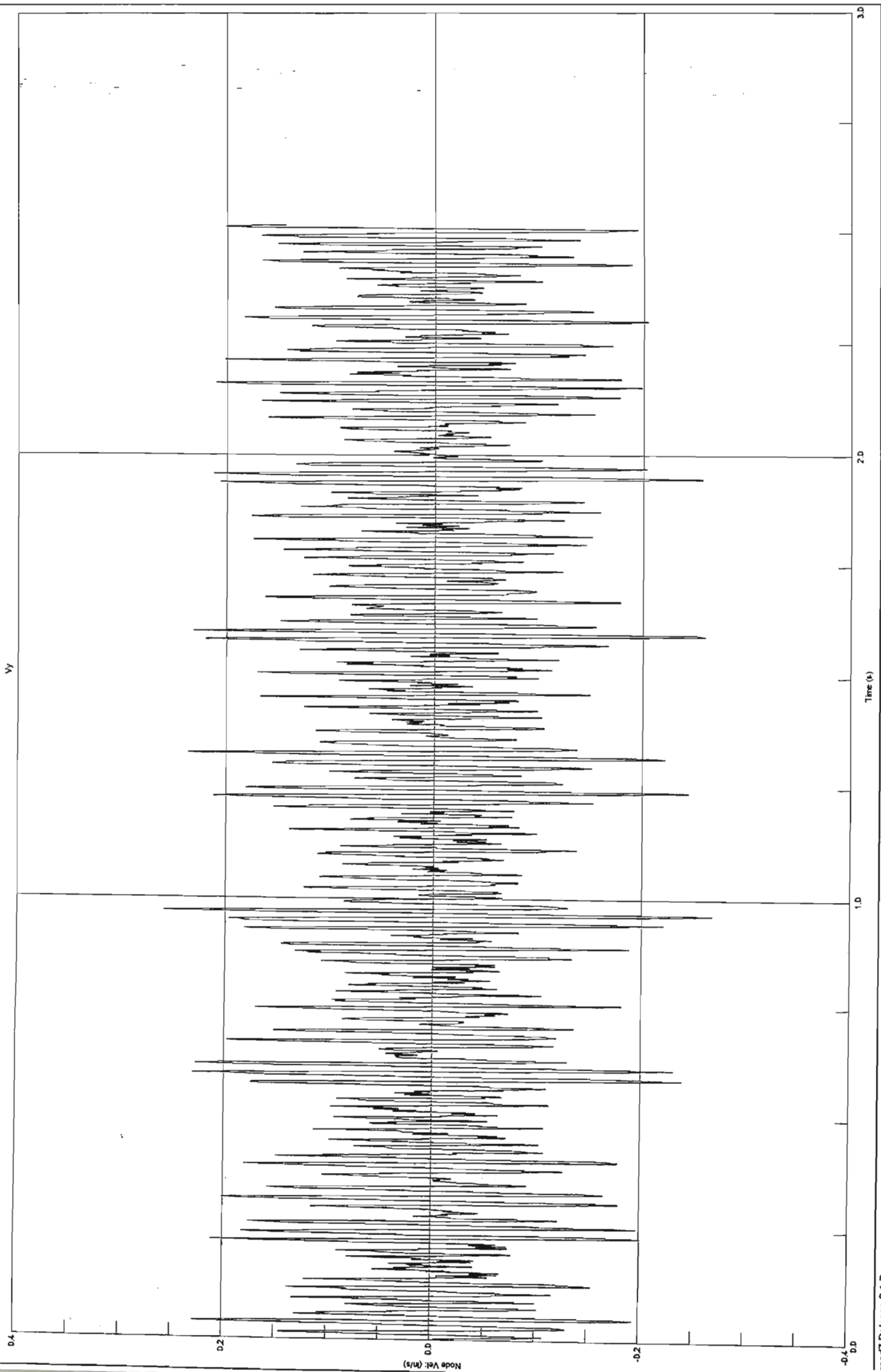
Y Displacement of Node 8



Z Displacement of Node 8

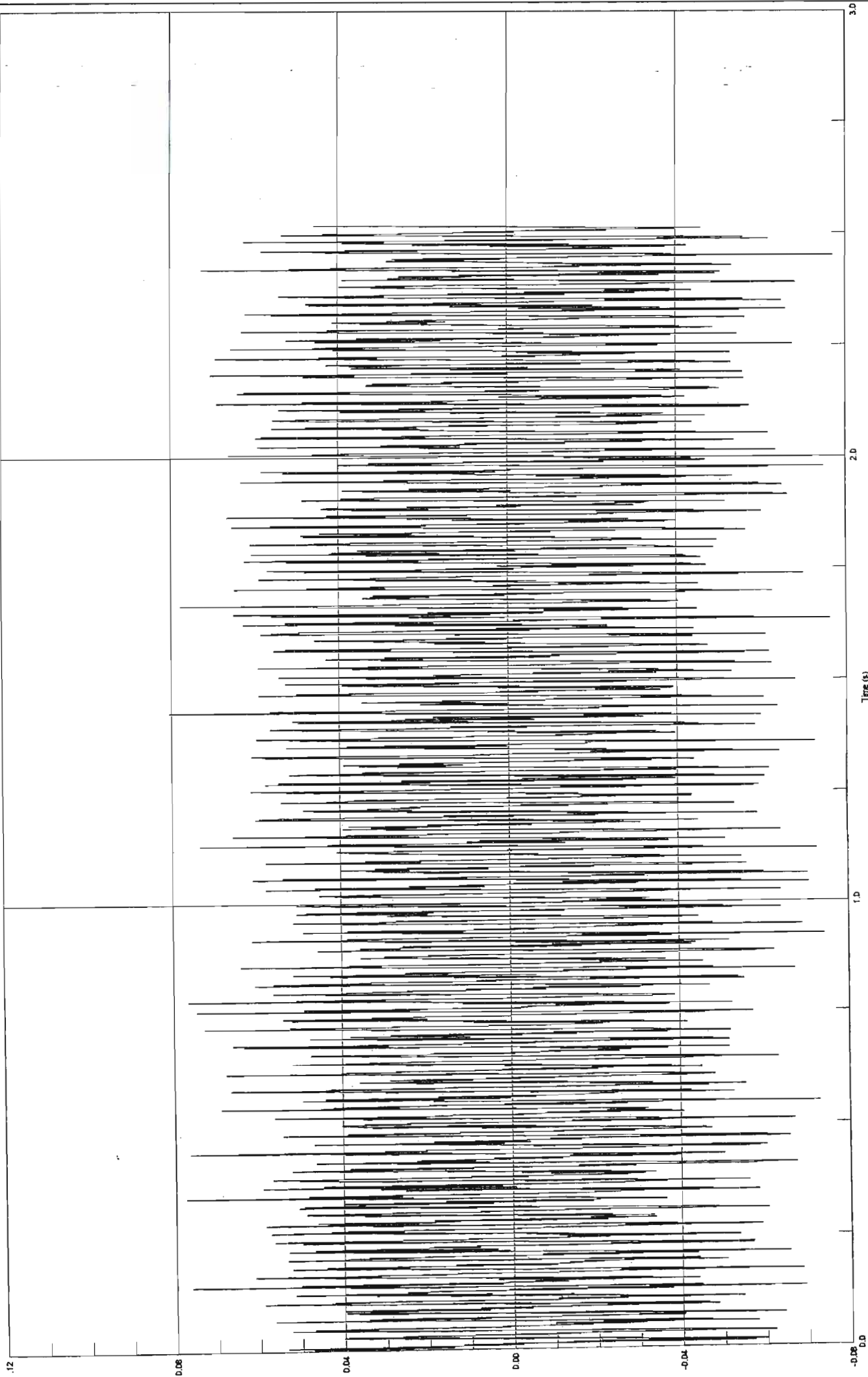


D1.10

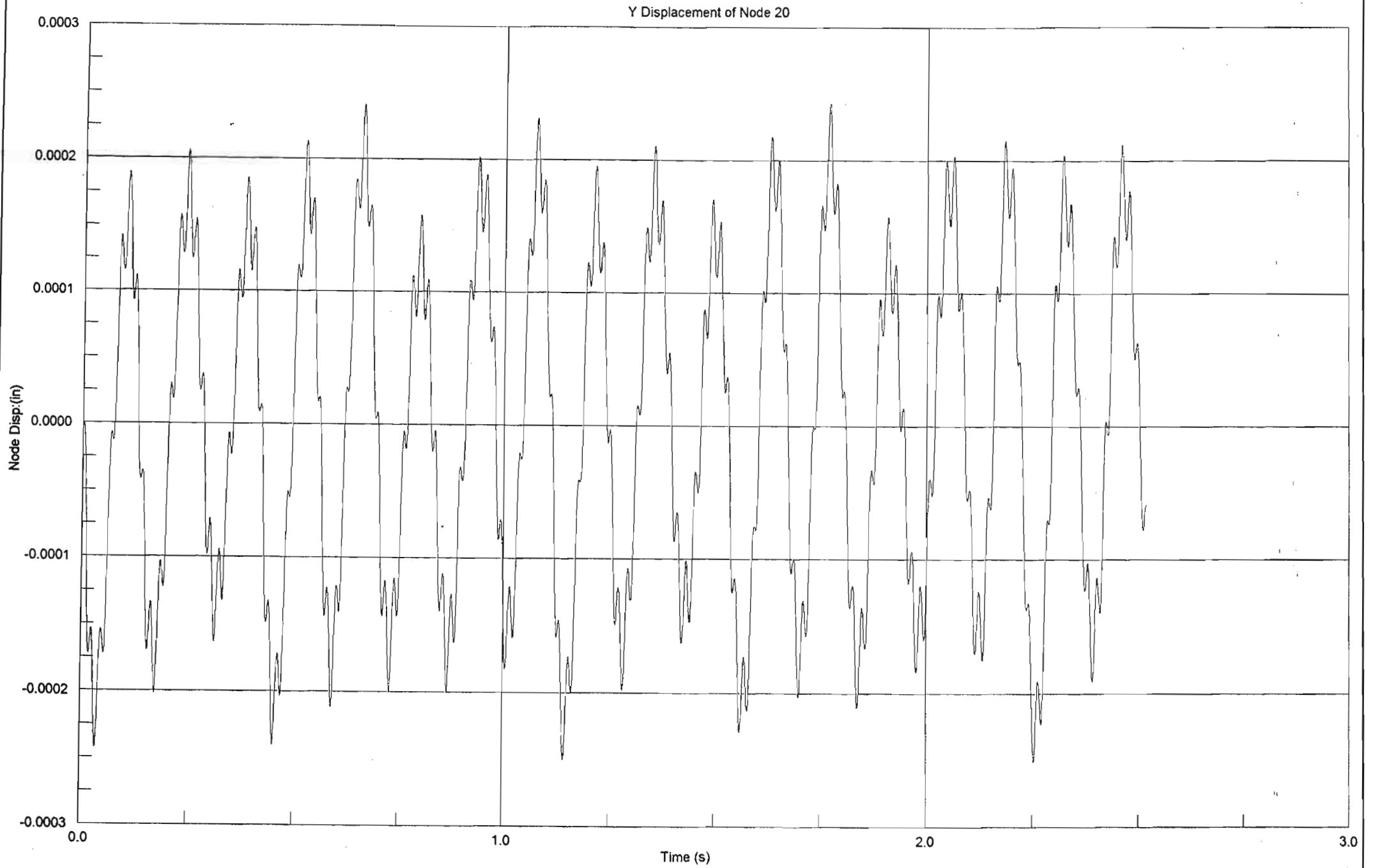


D1.11

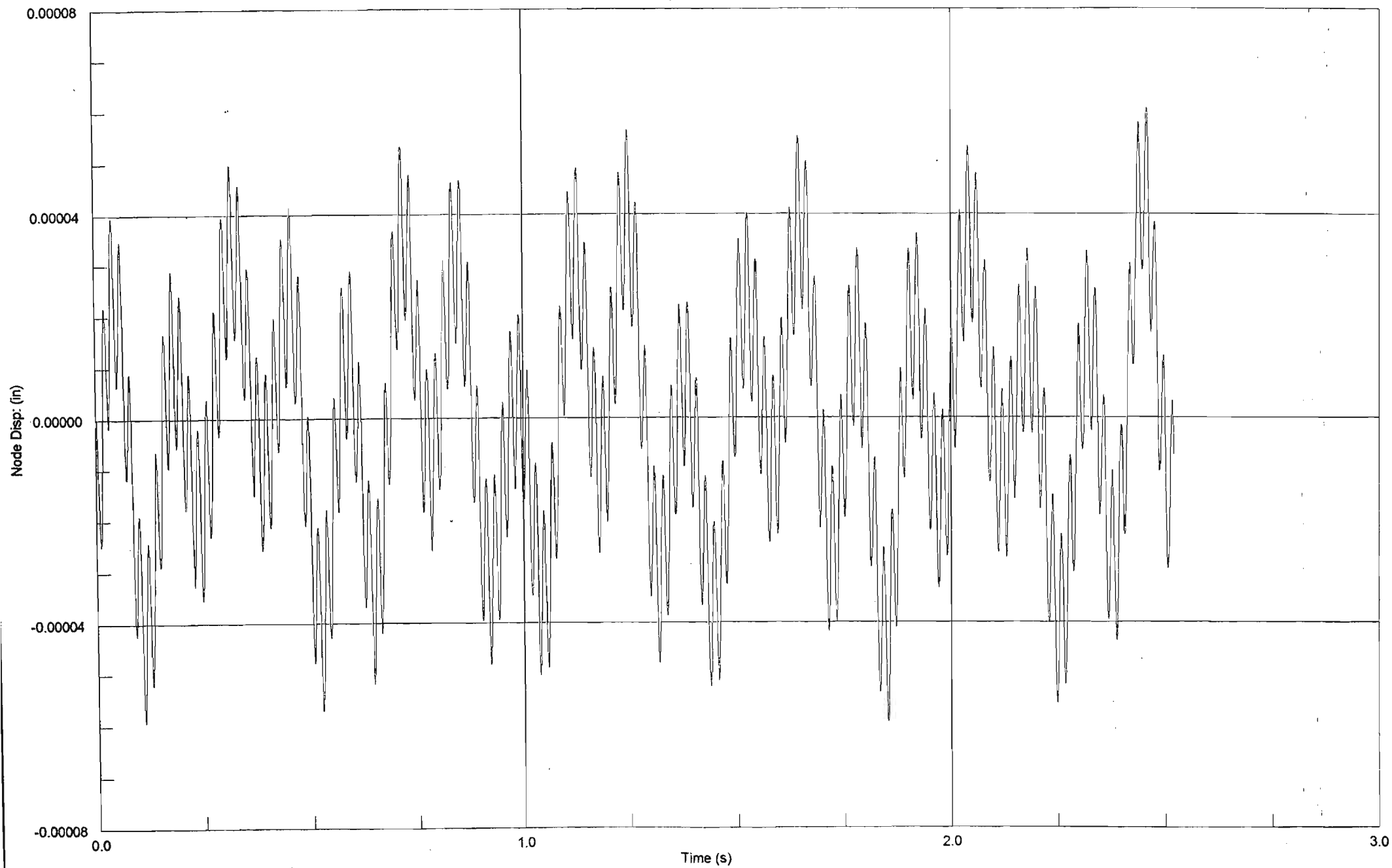
Vz

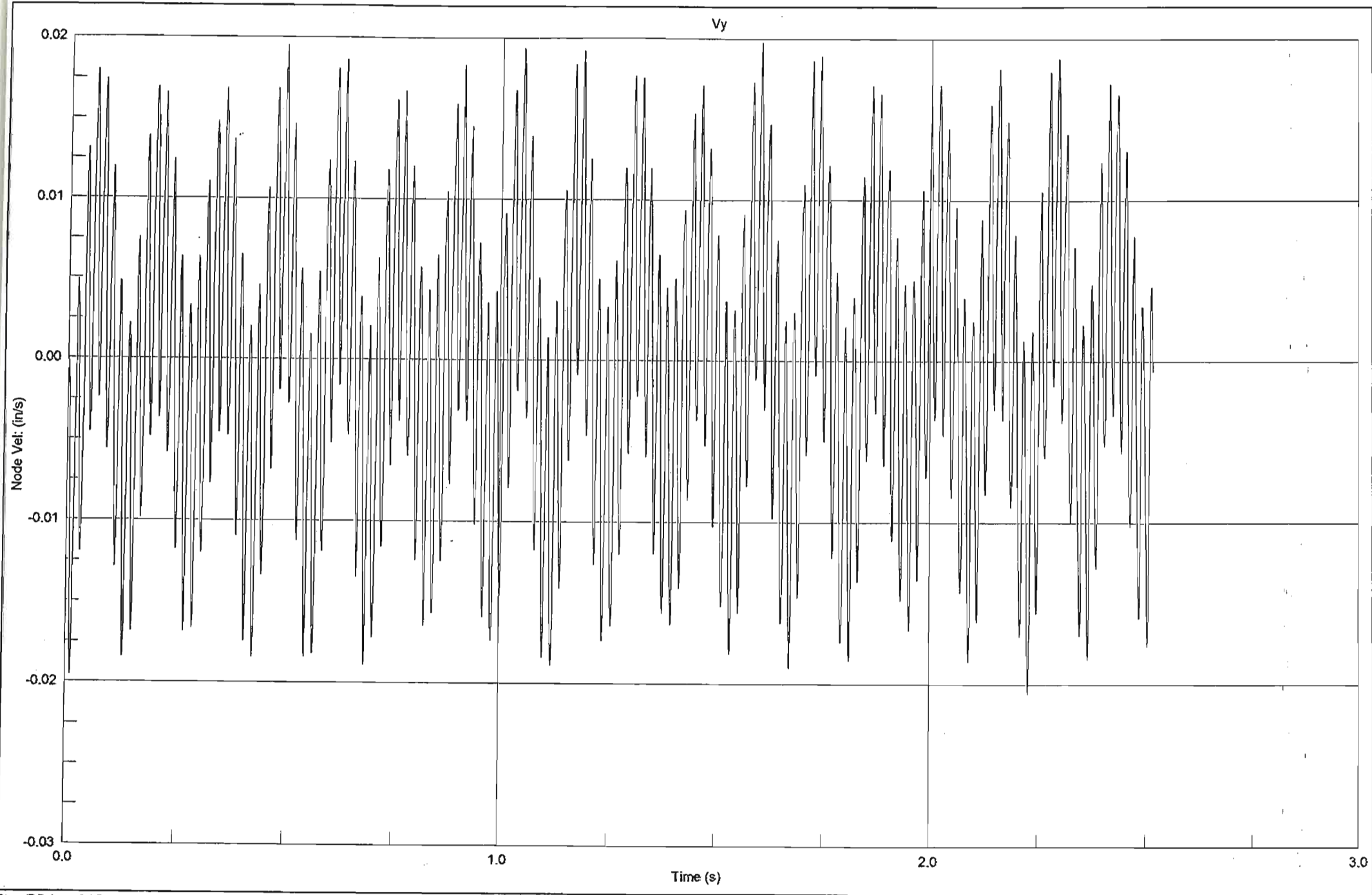


D1.12

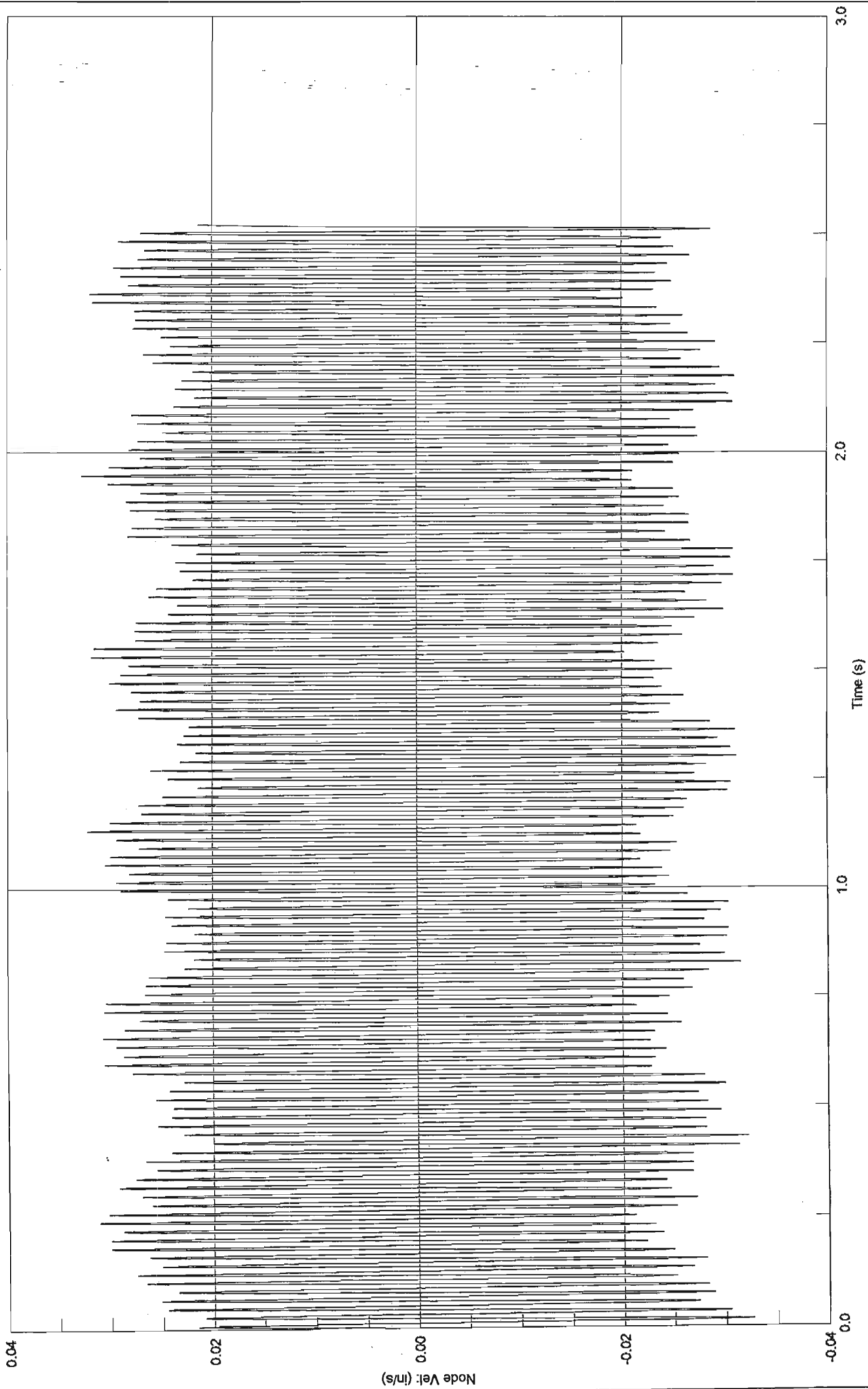


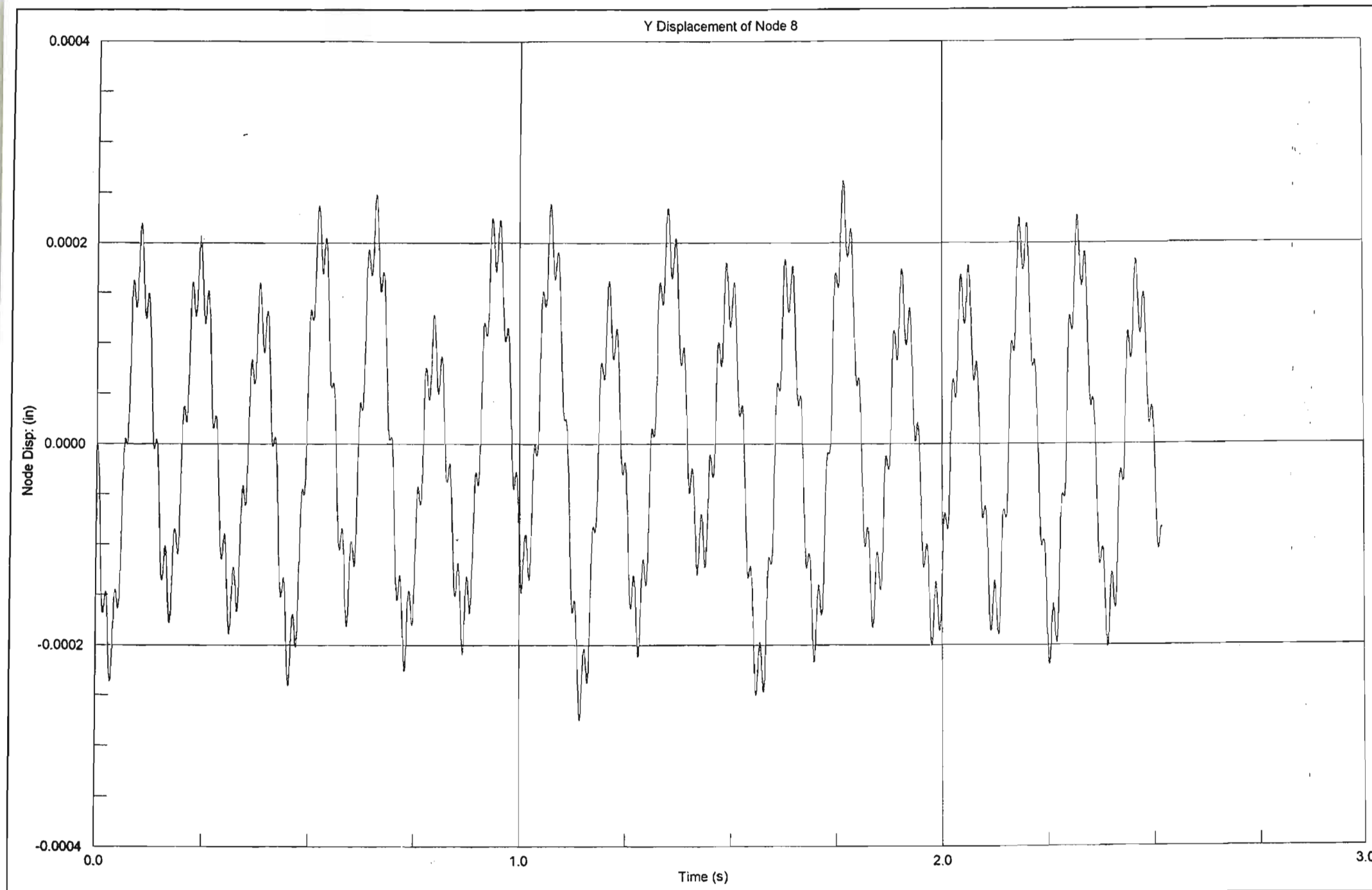
Z Displacement of Node 20

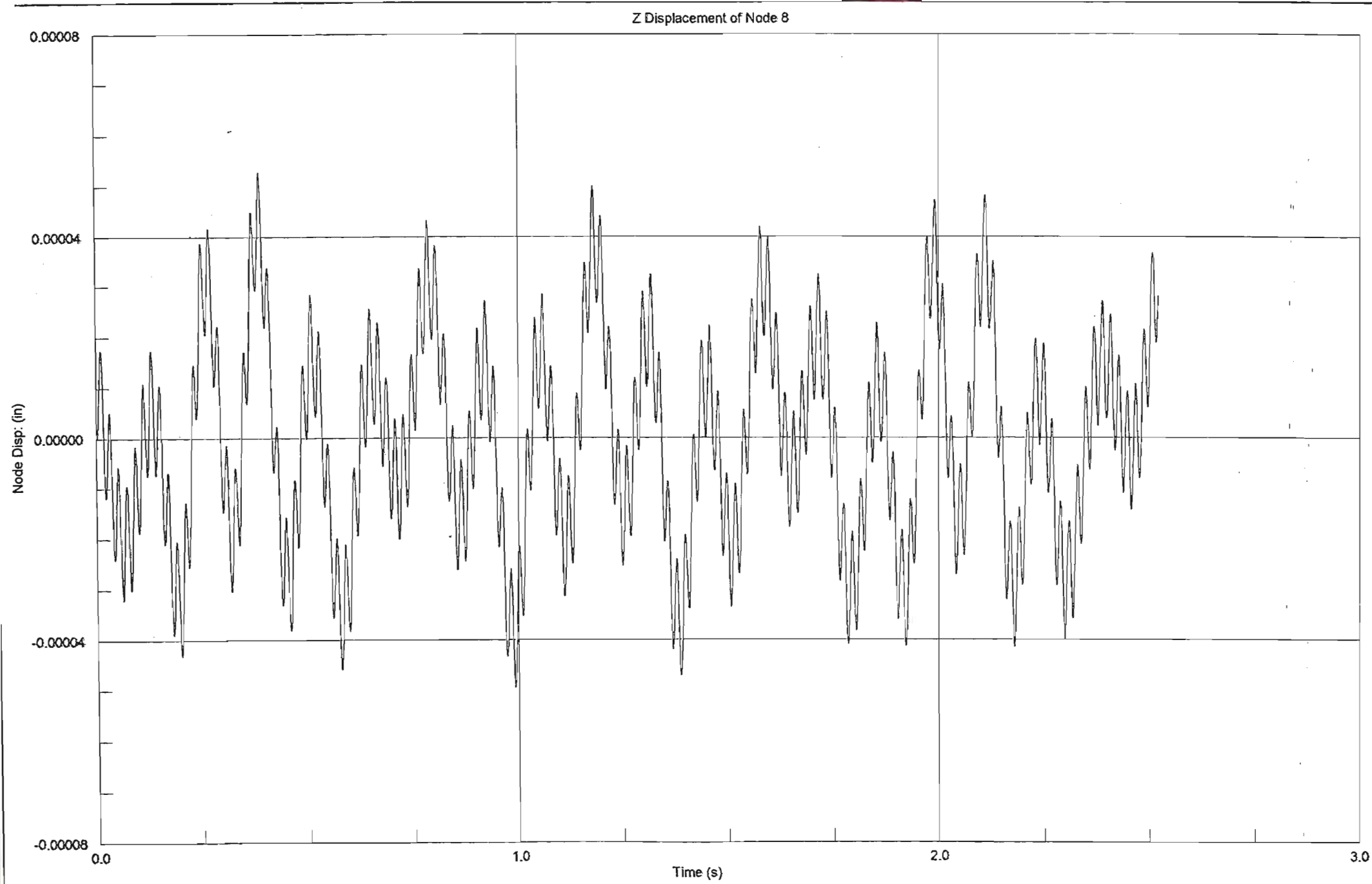


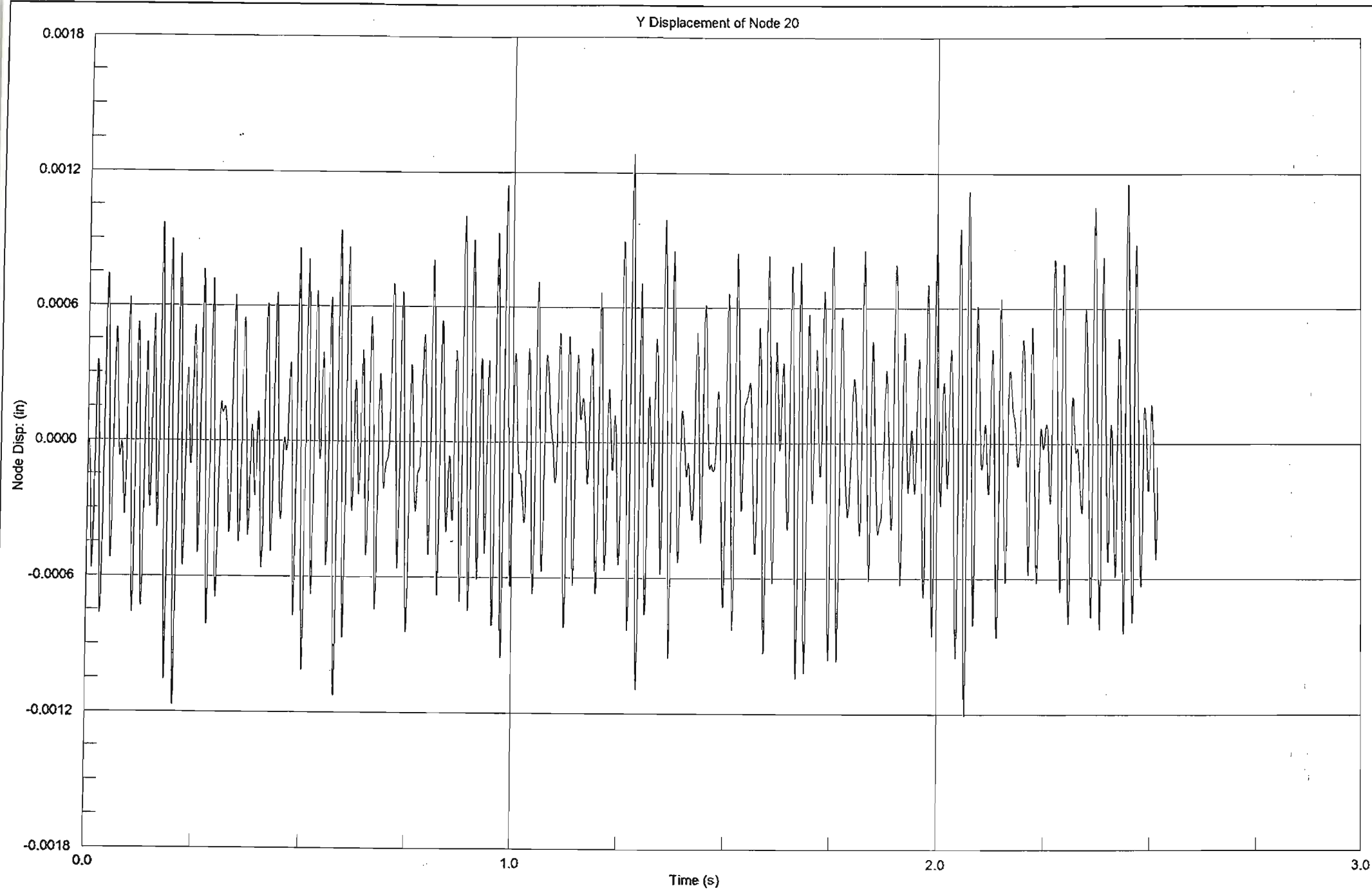


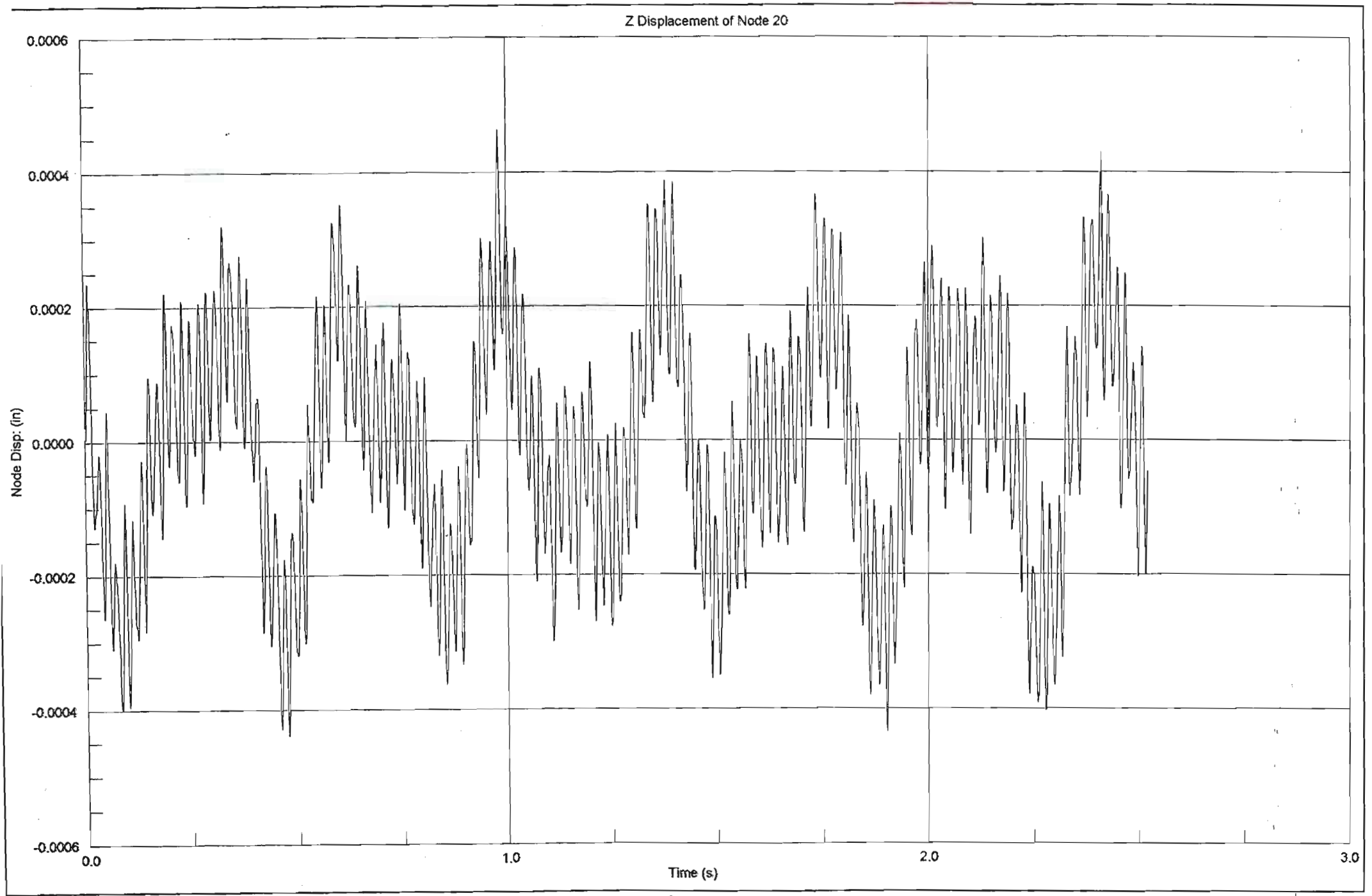
Vz

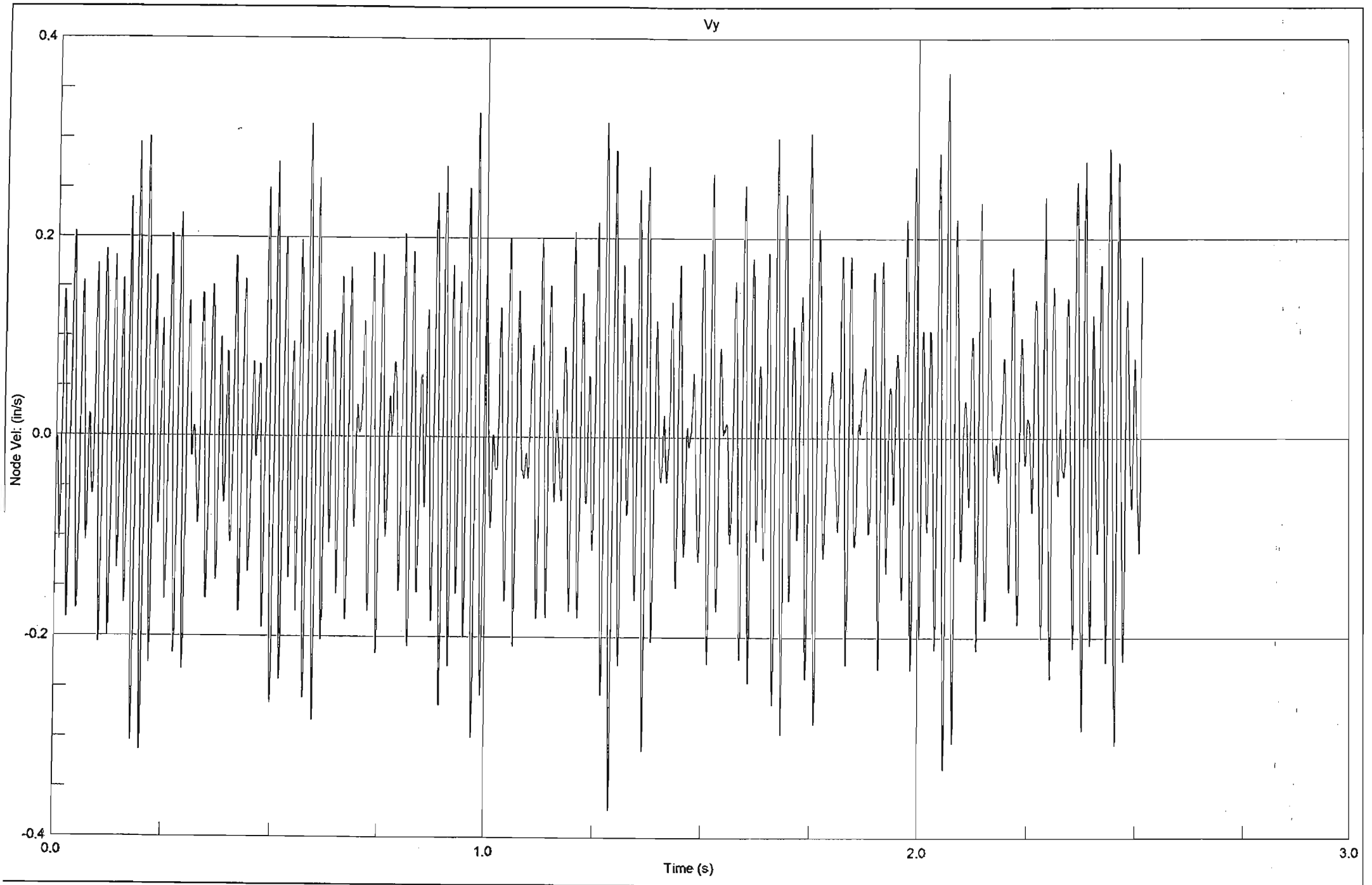


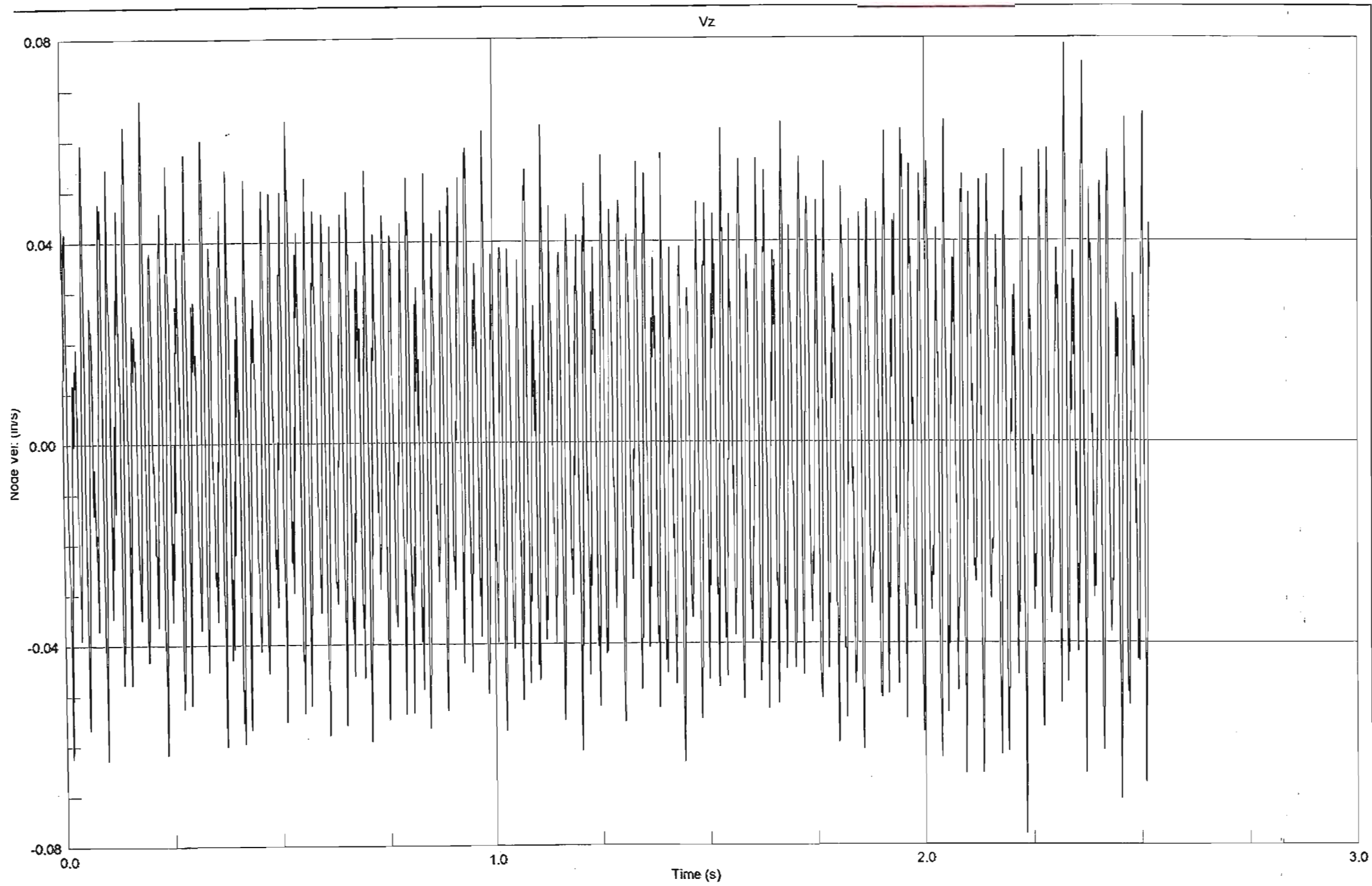


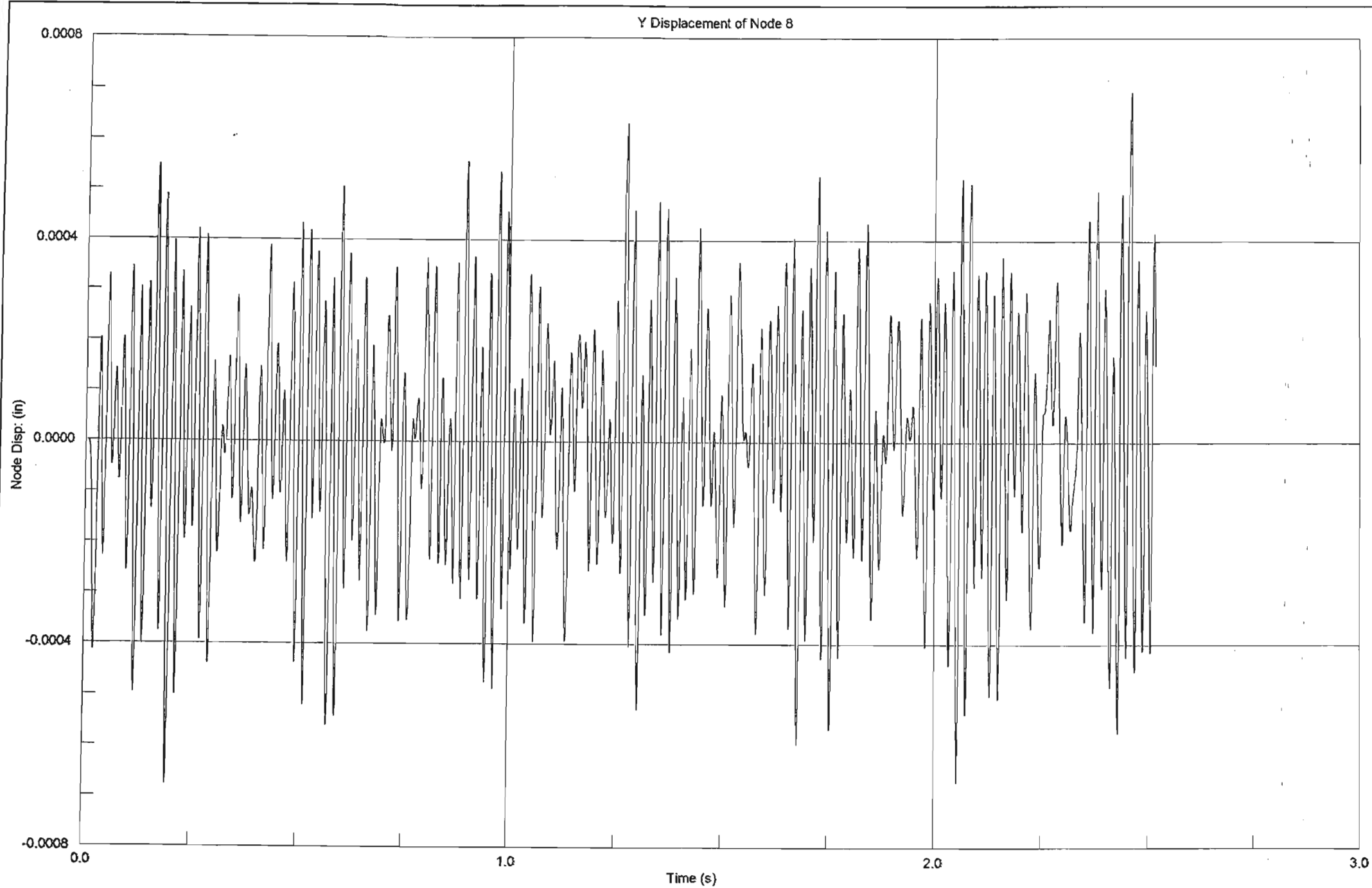




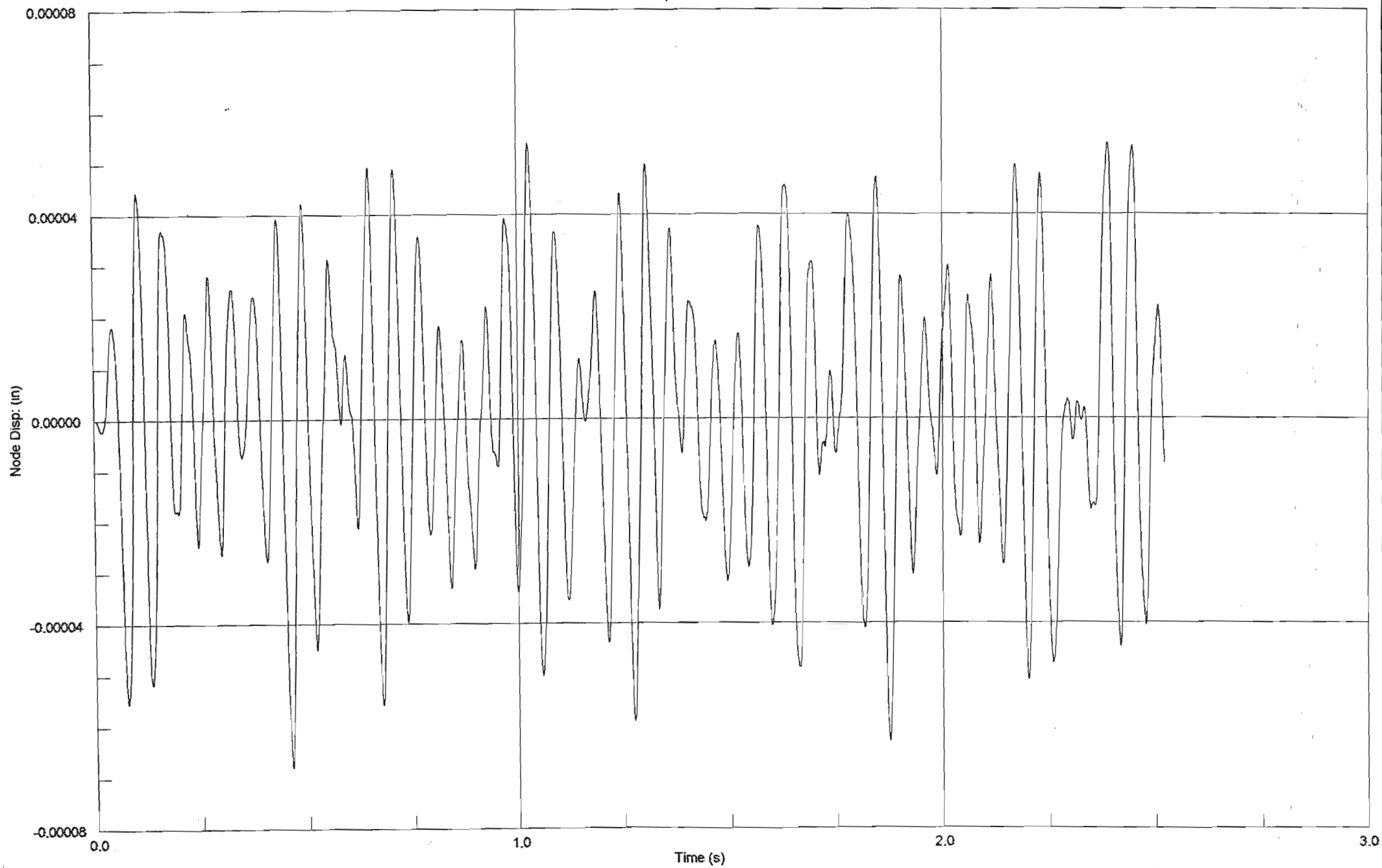




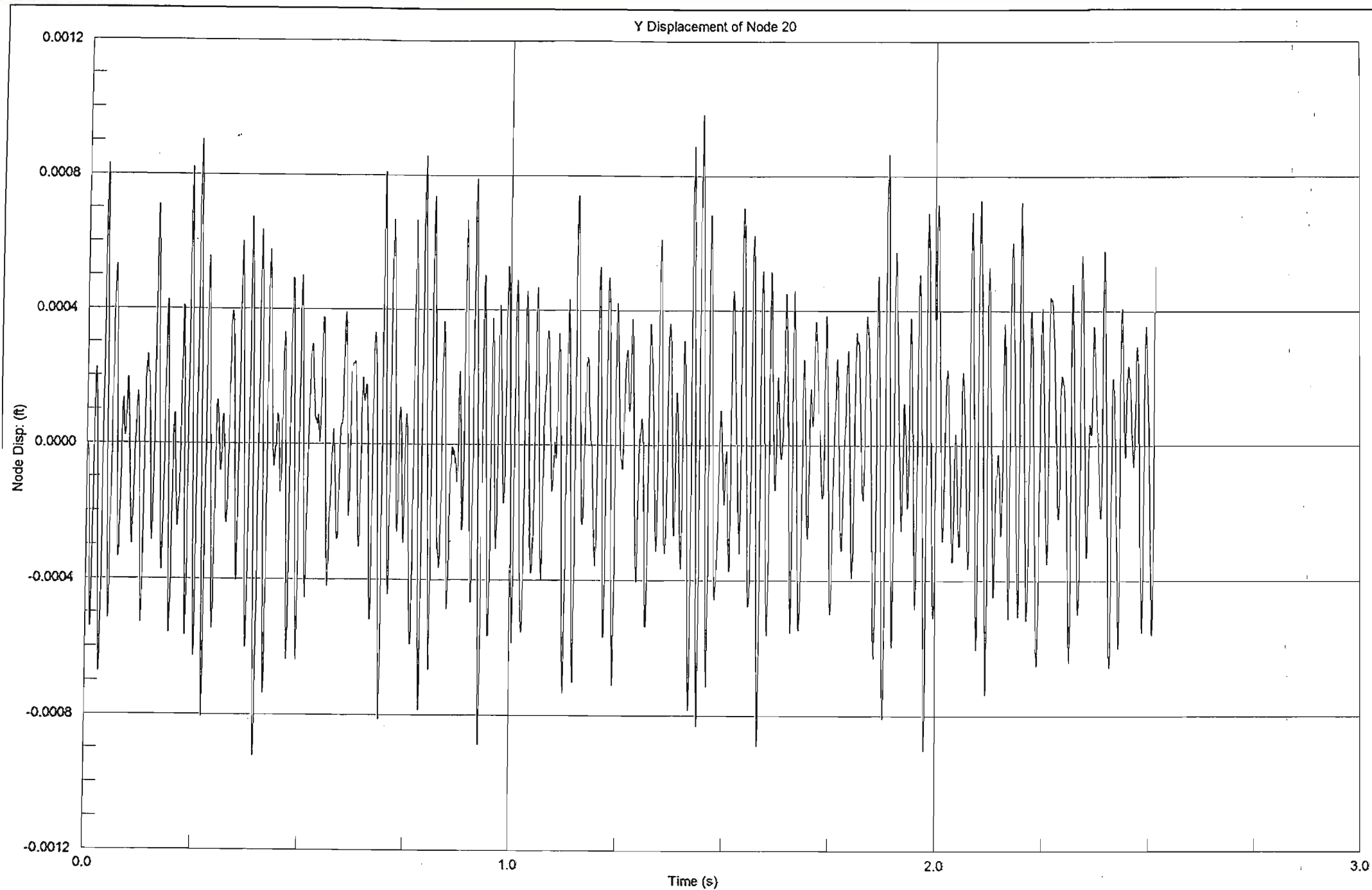




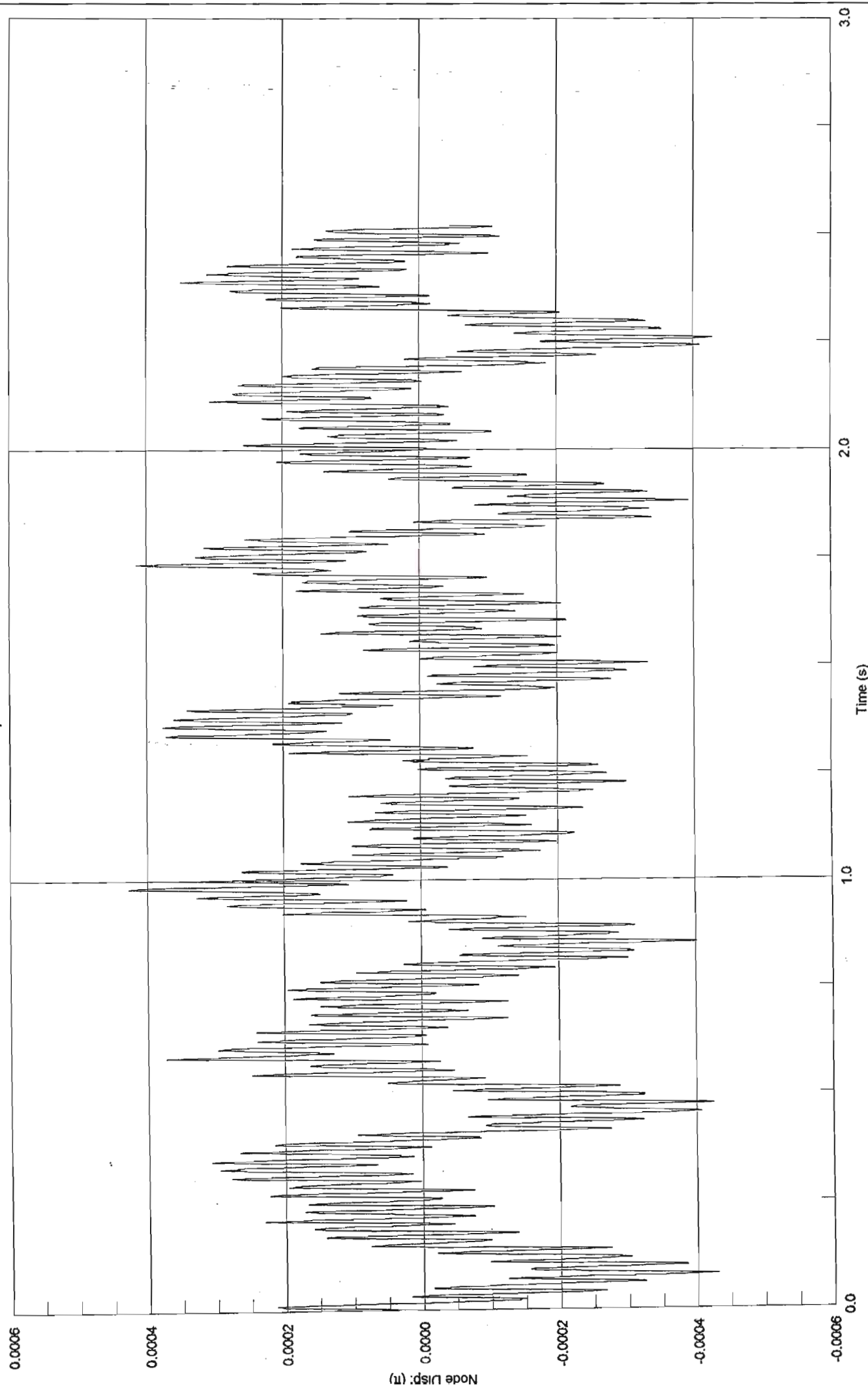
Z Displacement of Node 8



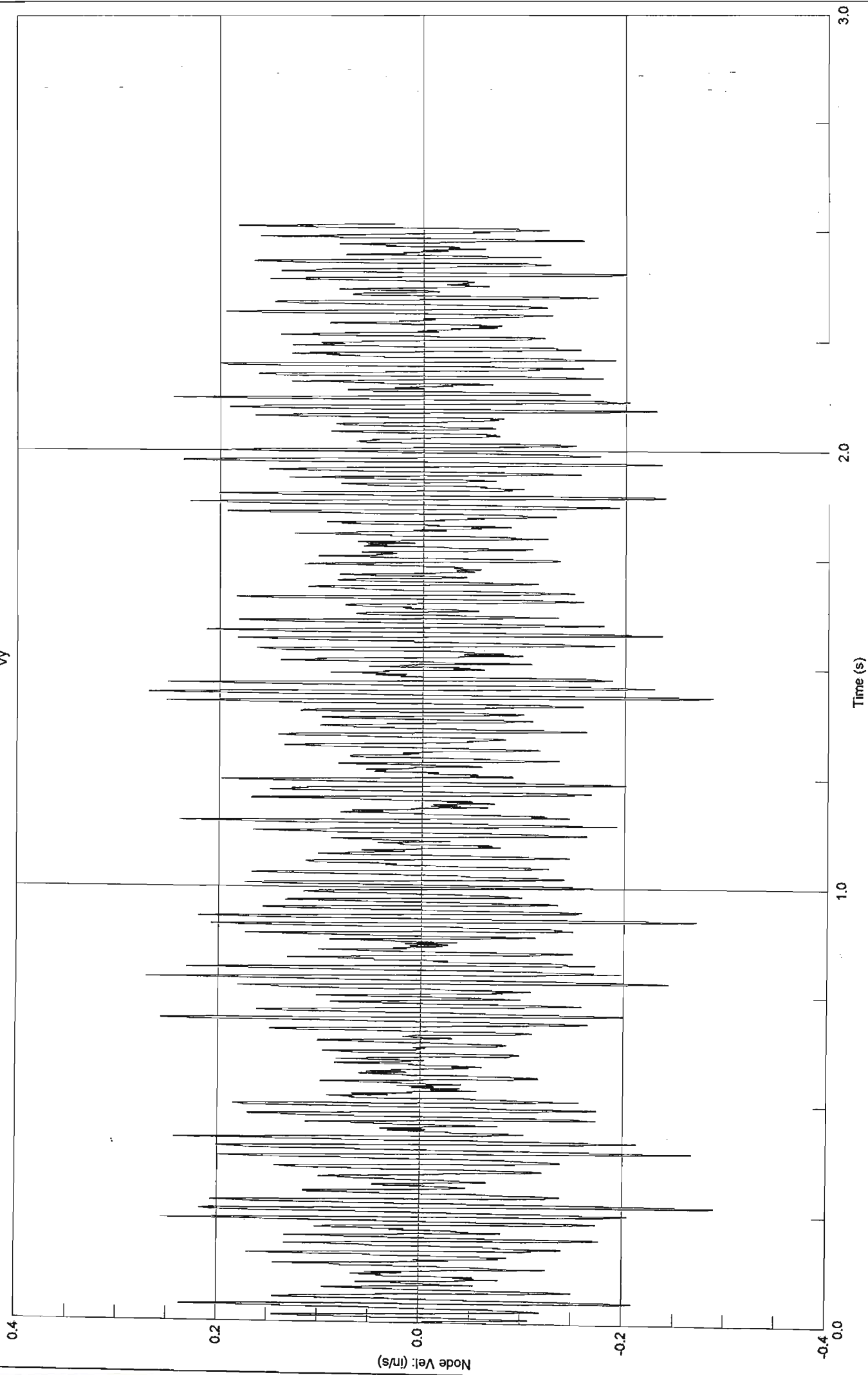
02.6



Z Displacement of Node 20



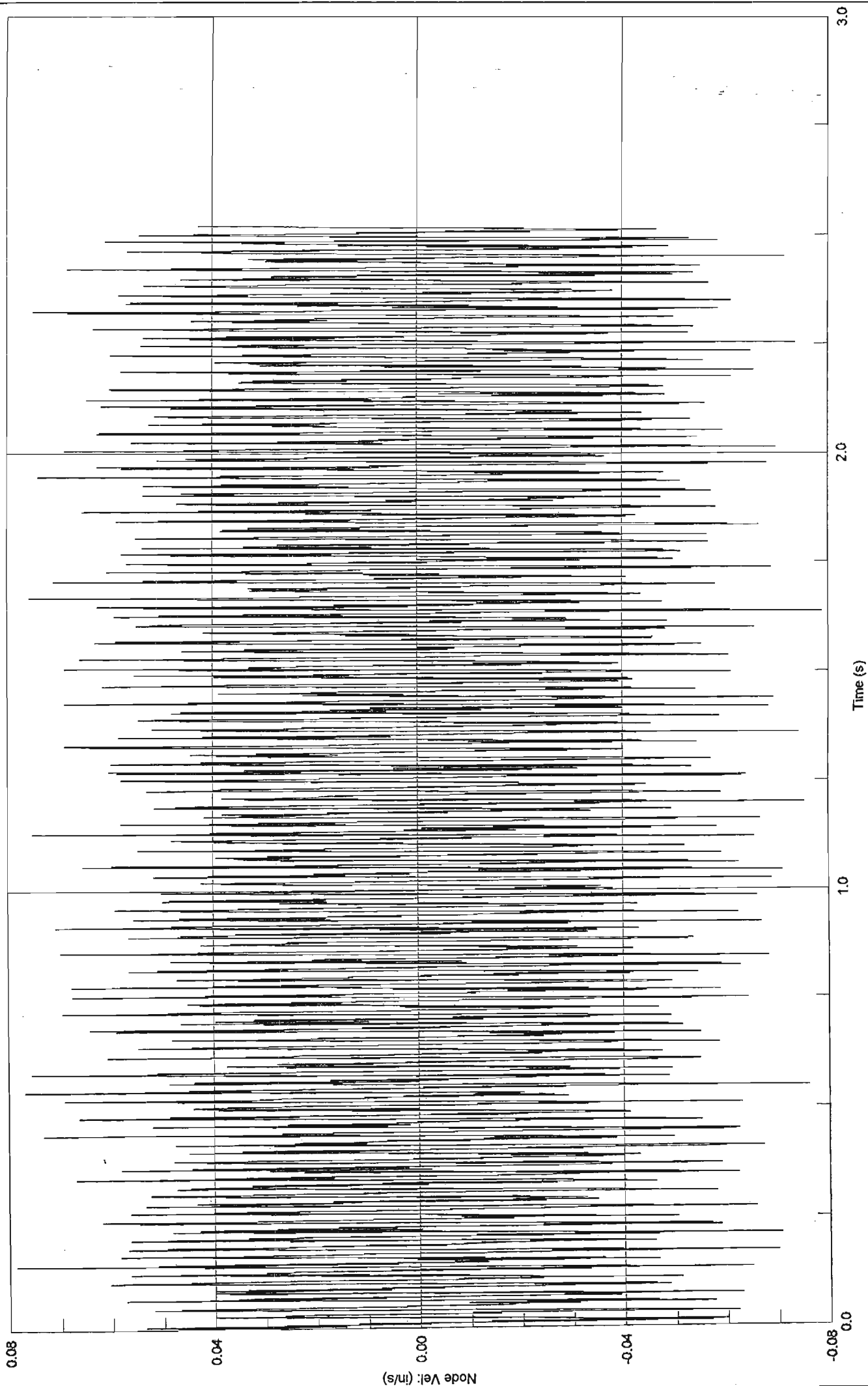
vy

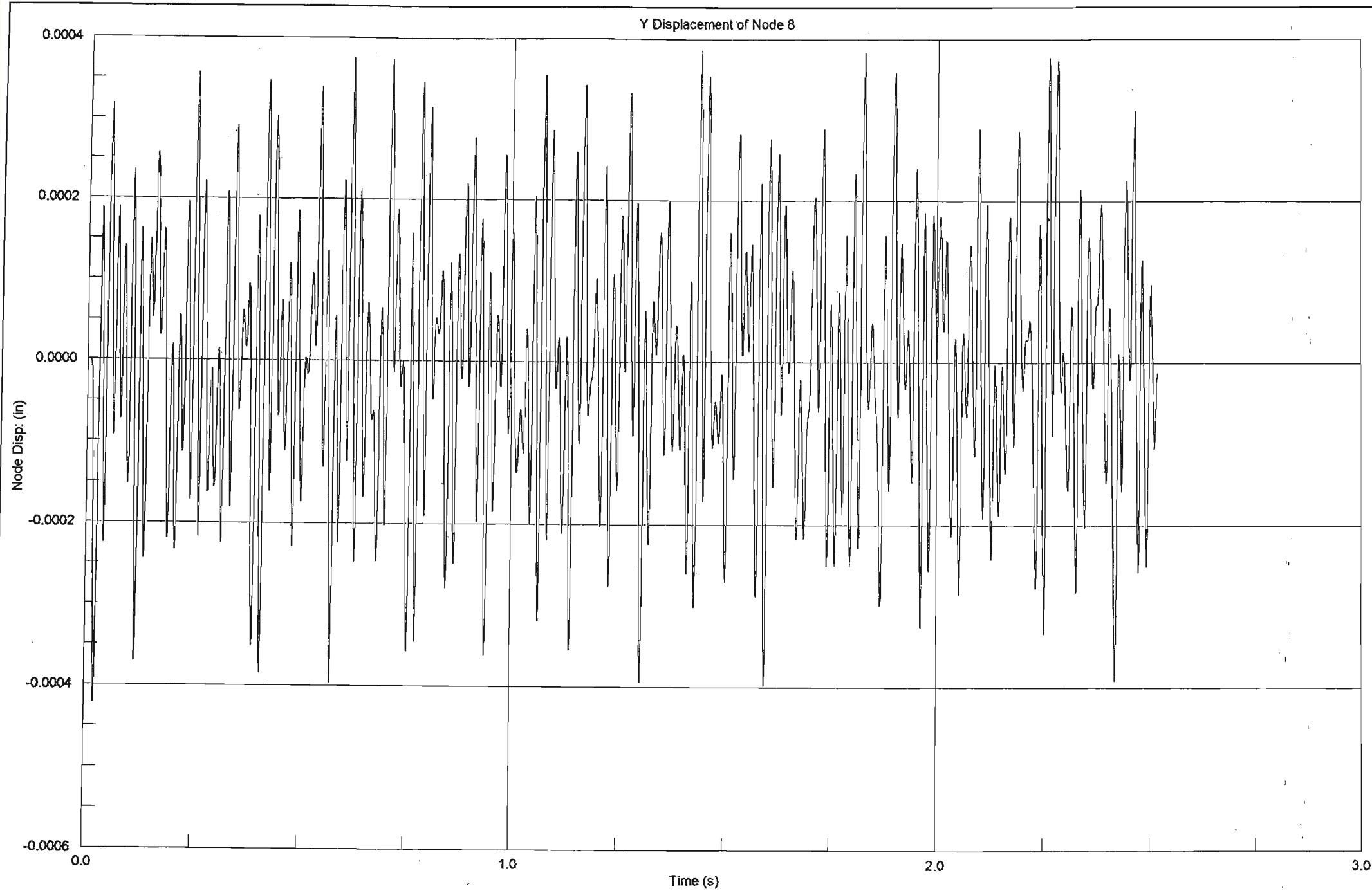


Time (s)

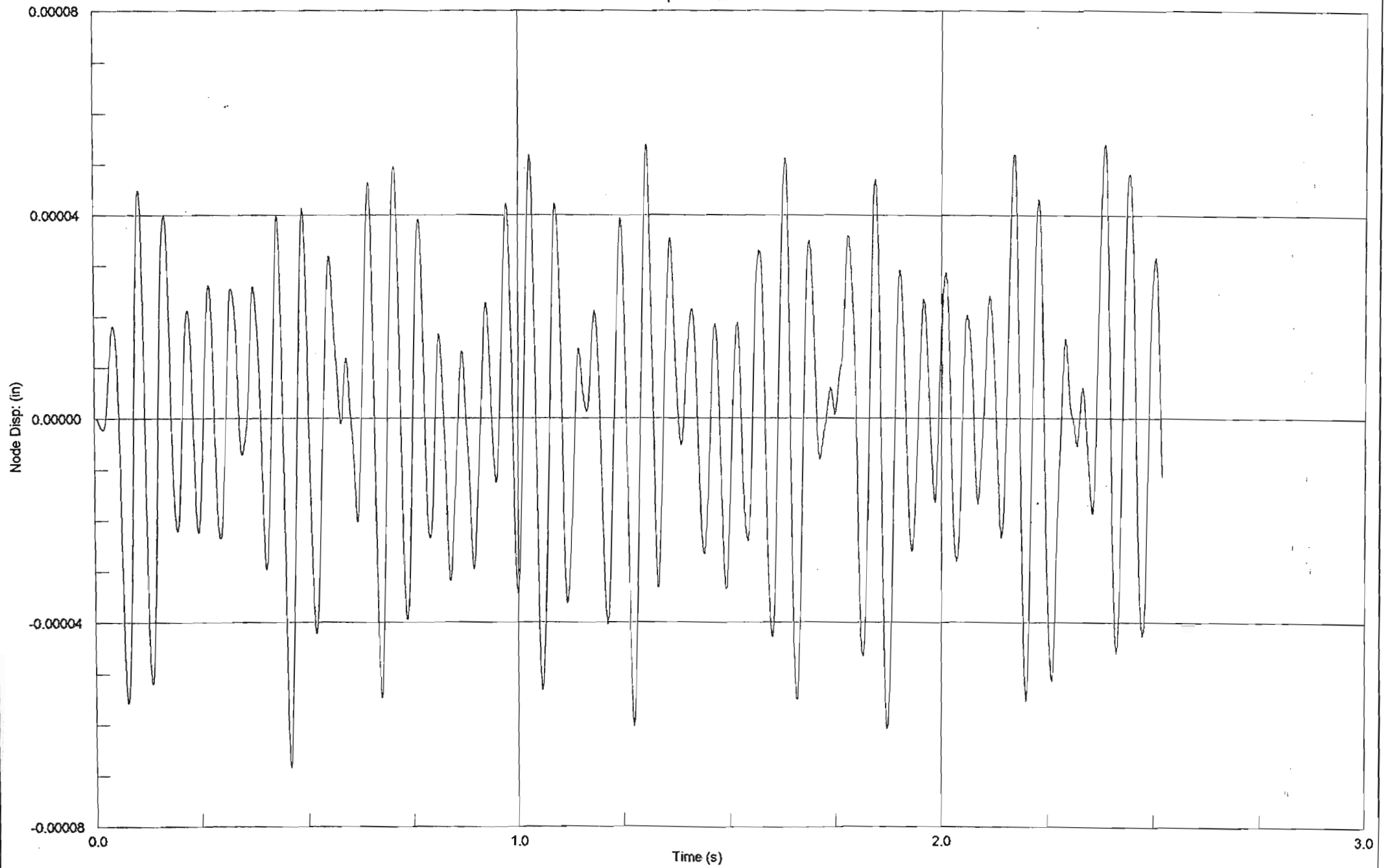
D2.9

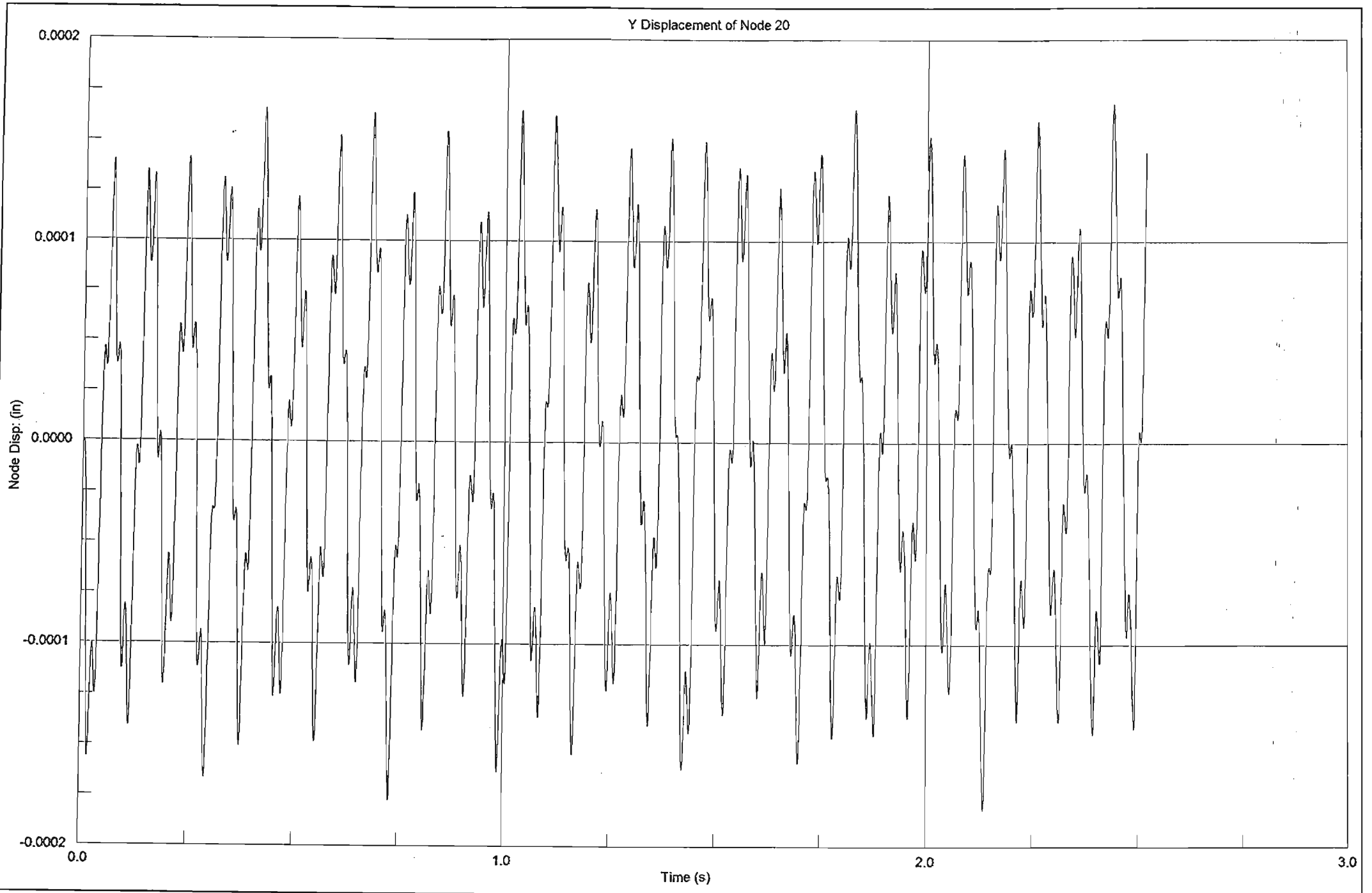
Vz



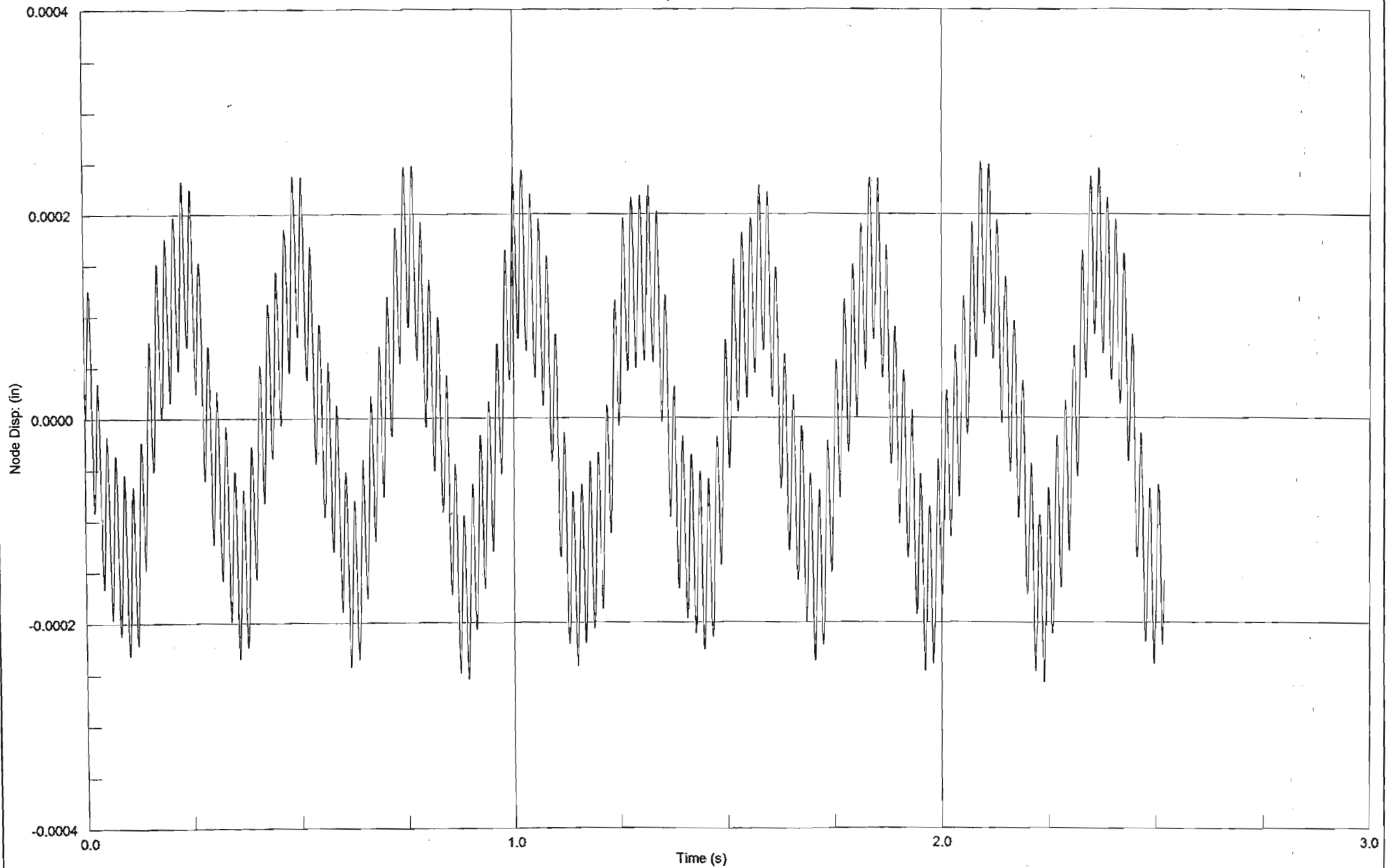


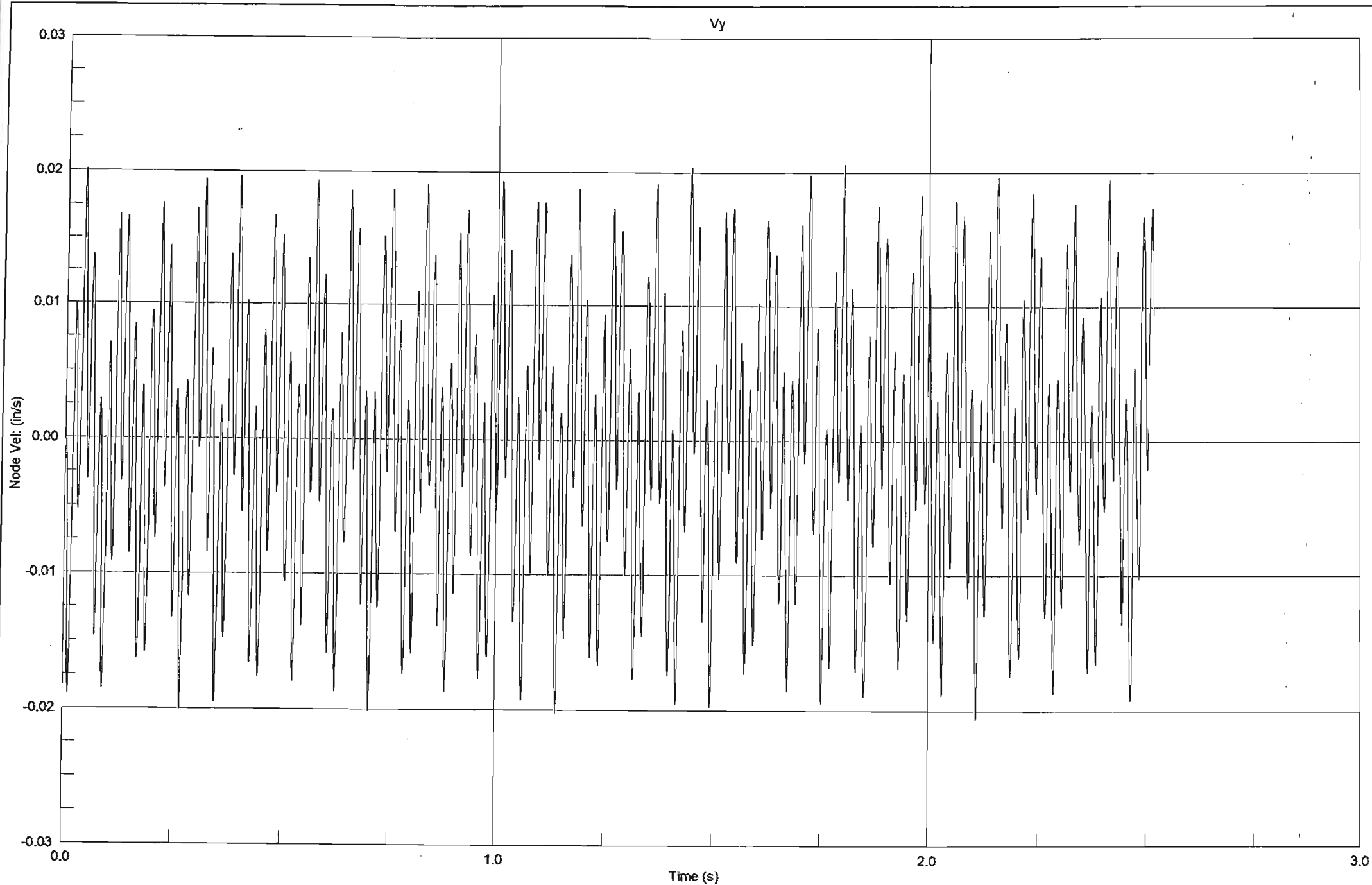
Z Displacement of Node 8

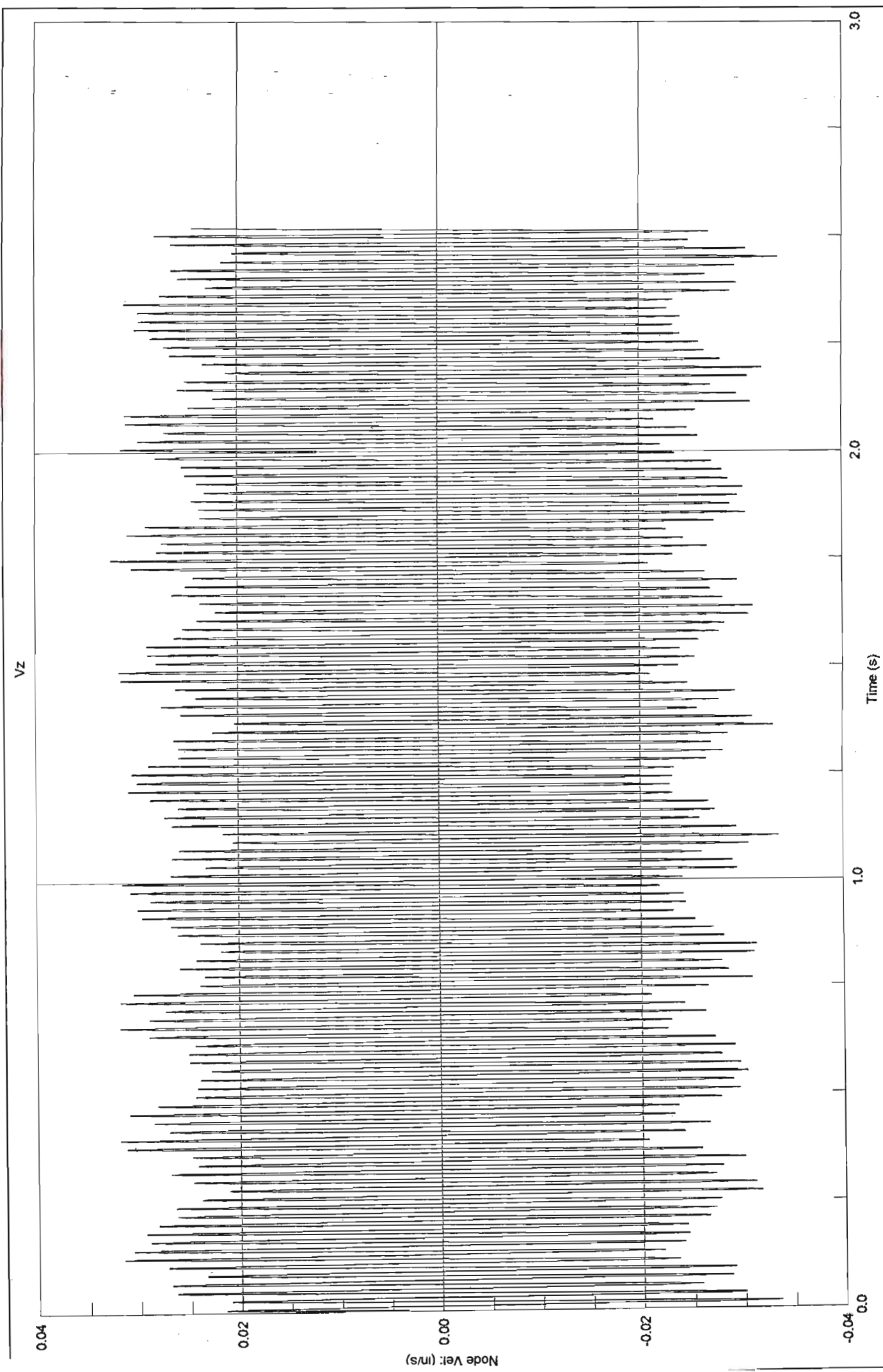




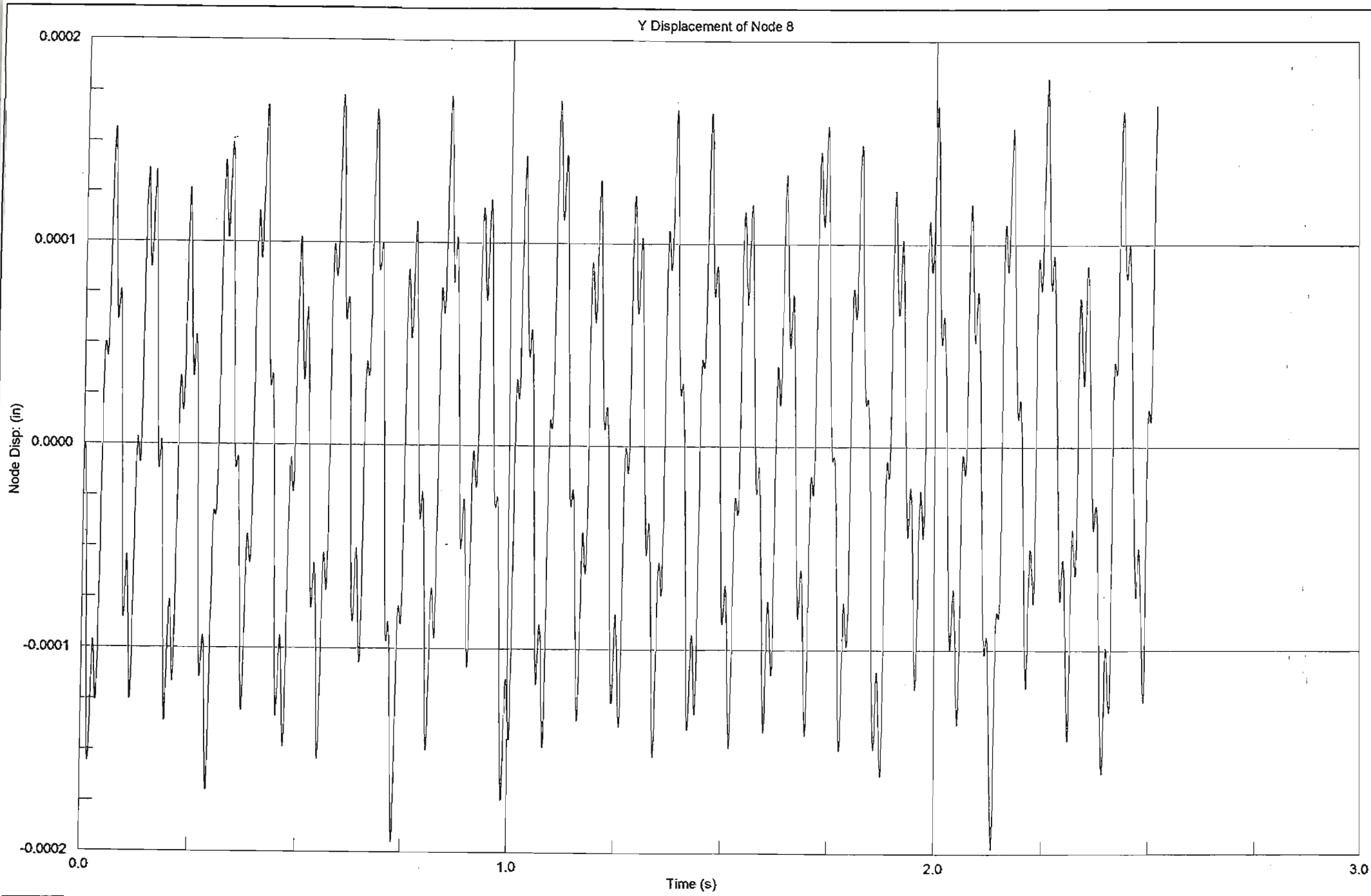
Z Displacement of Node 20



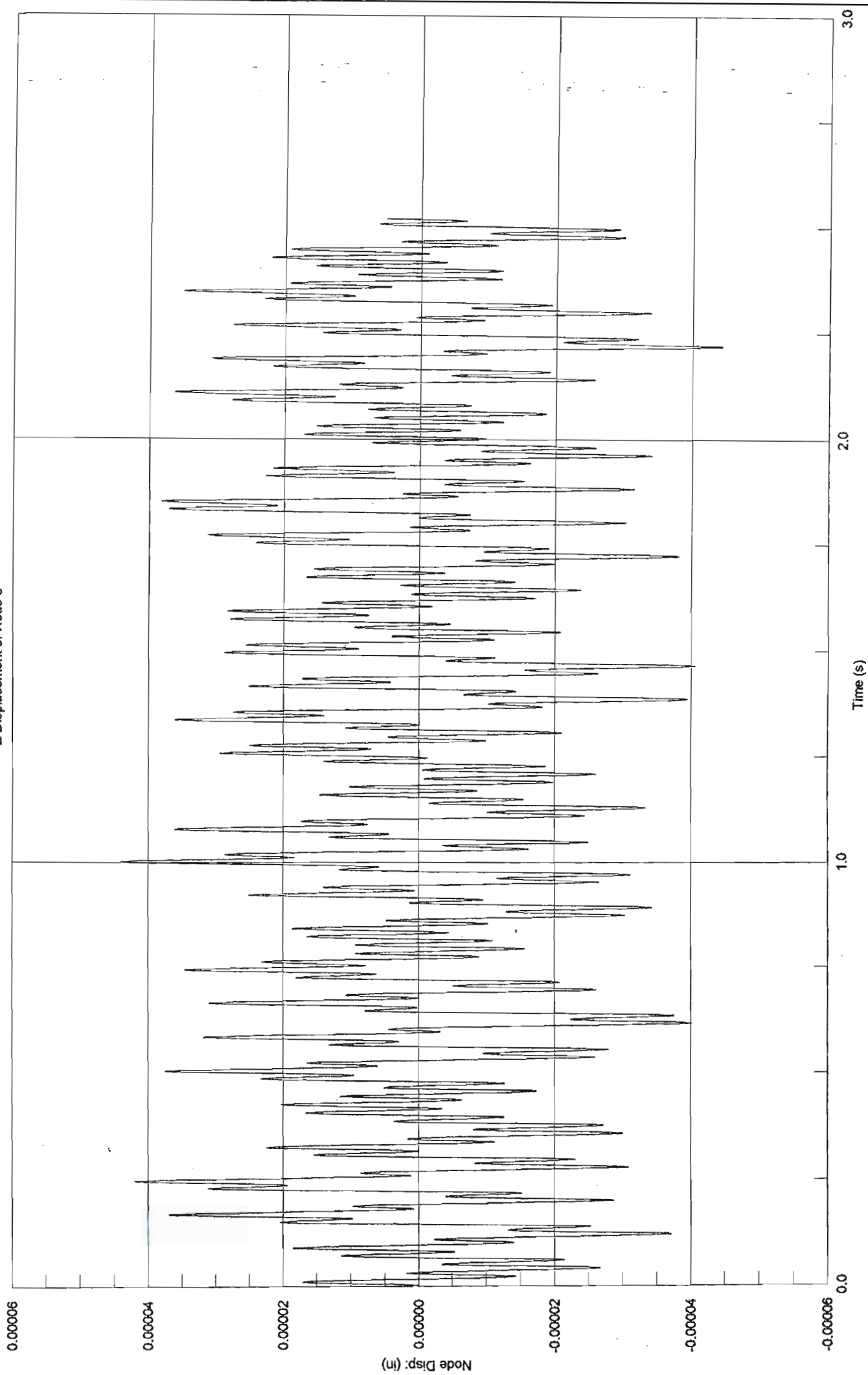


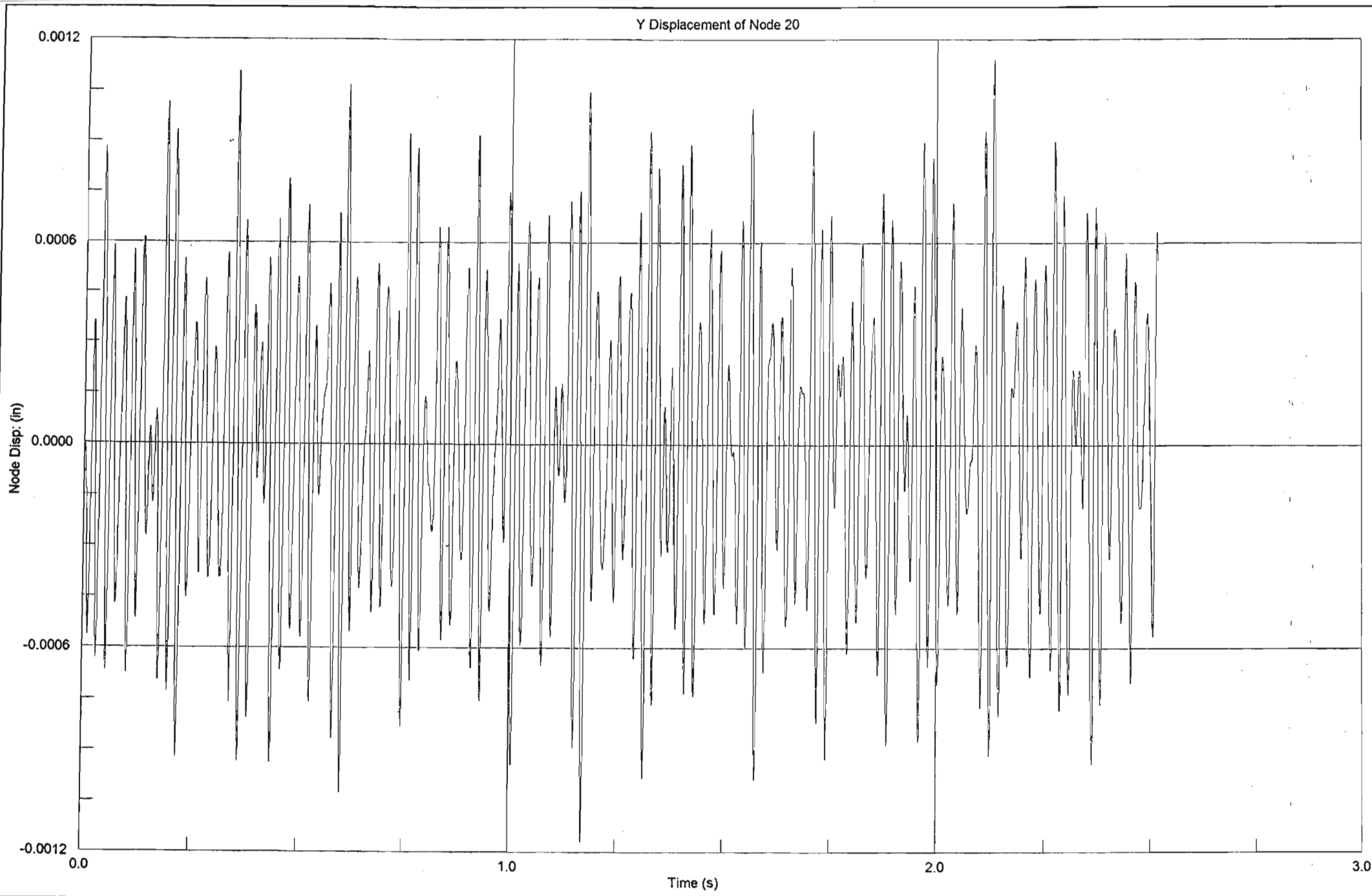


D2.16

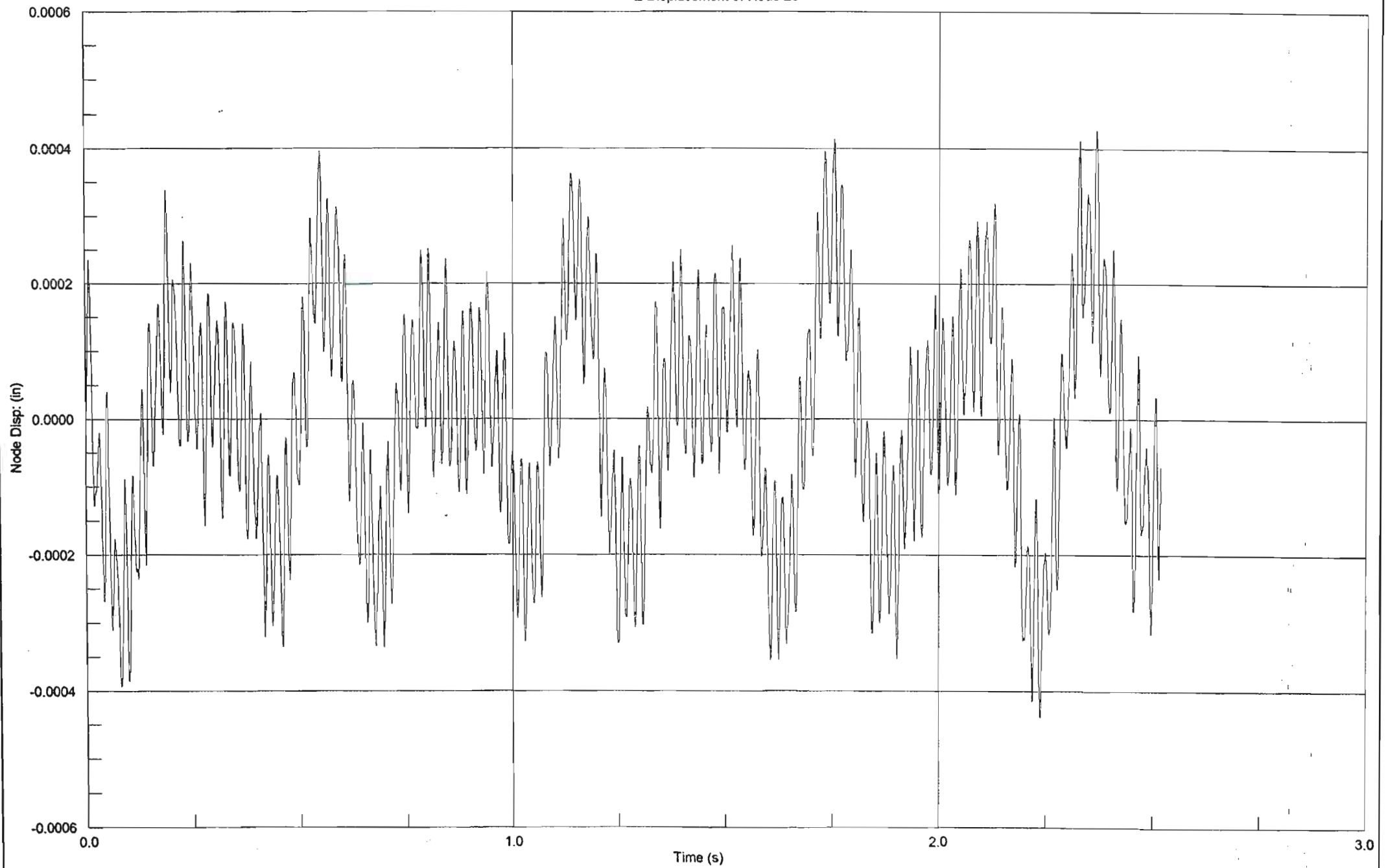


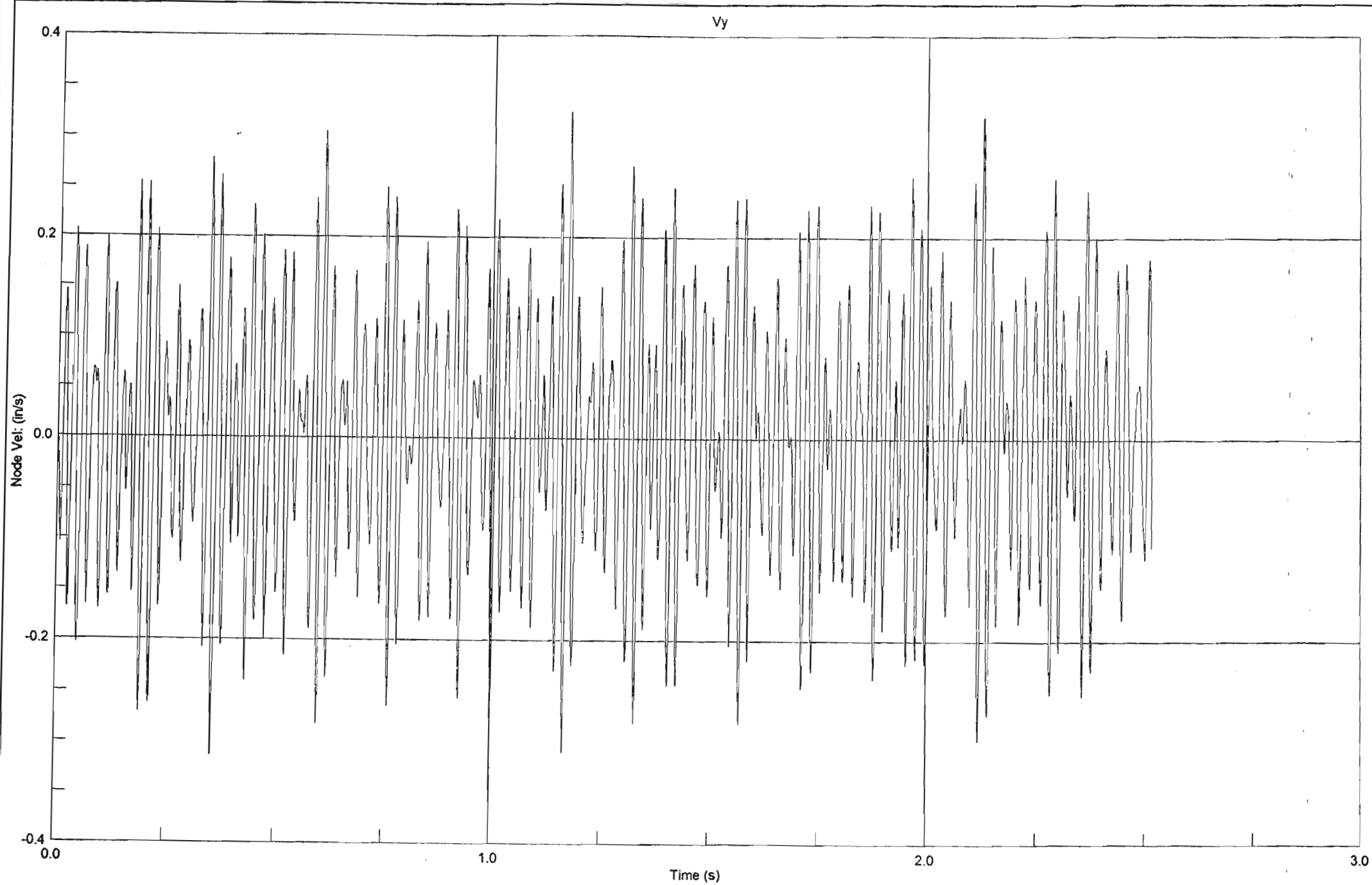
Z Displacement of Node 8

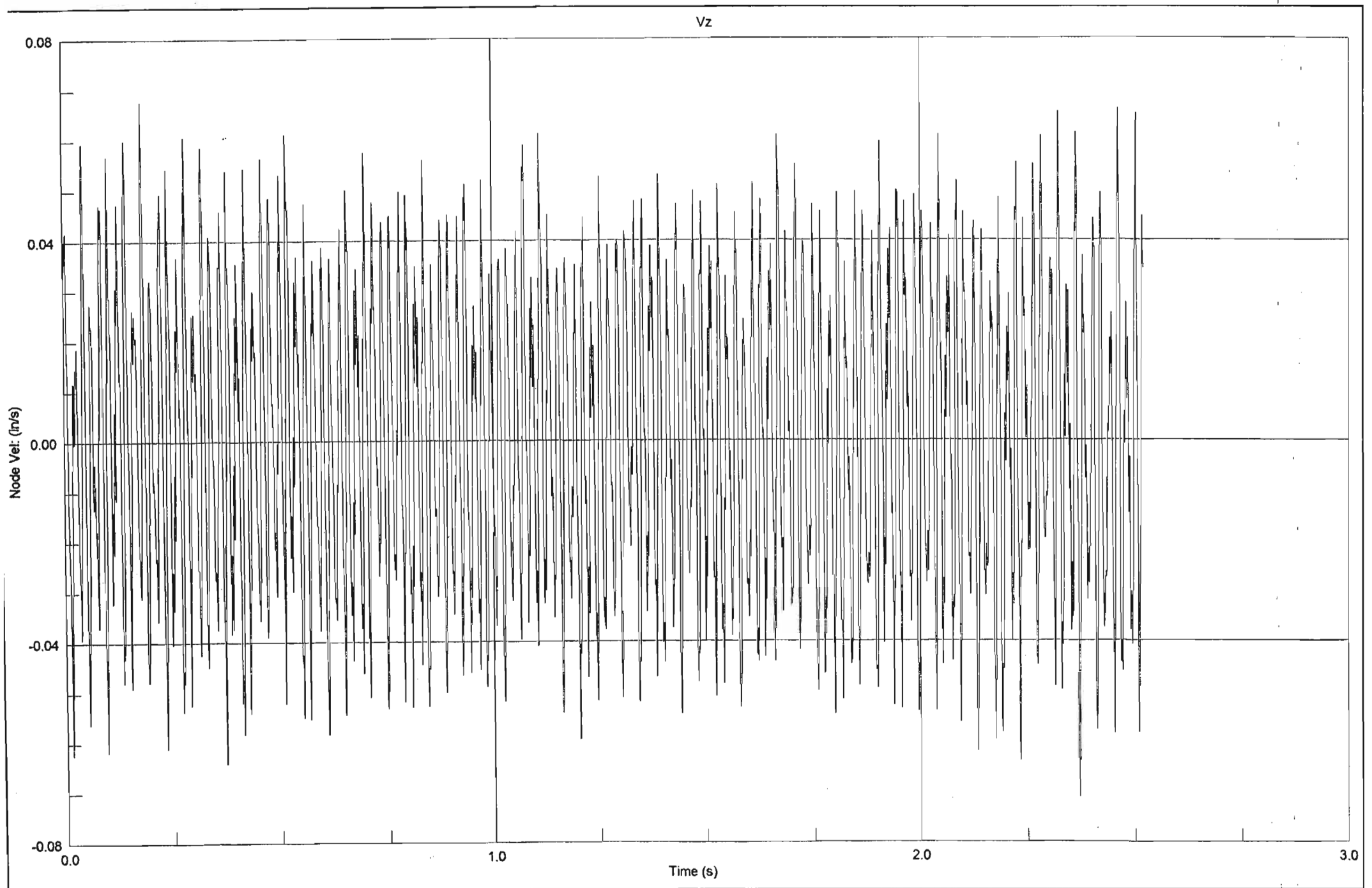


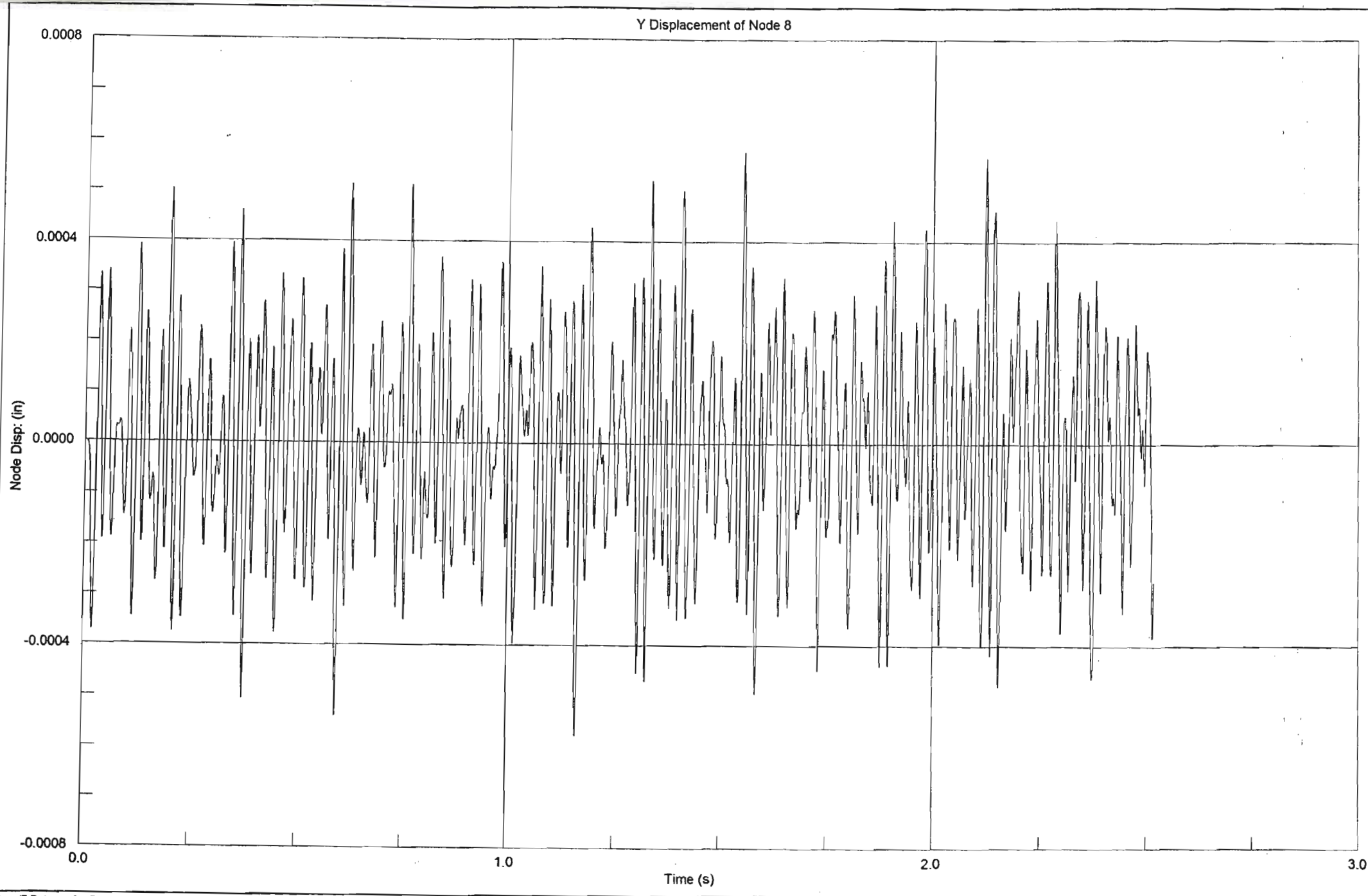


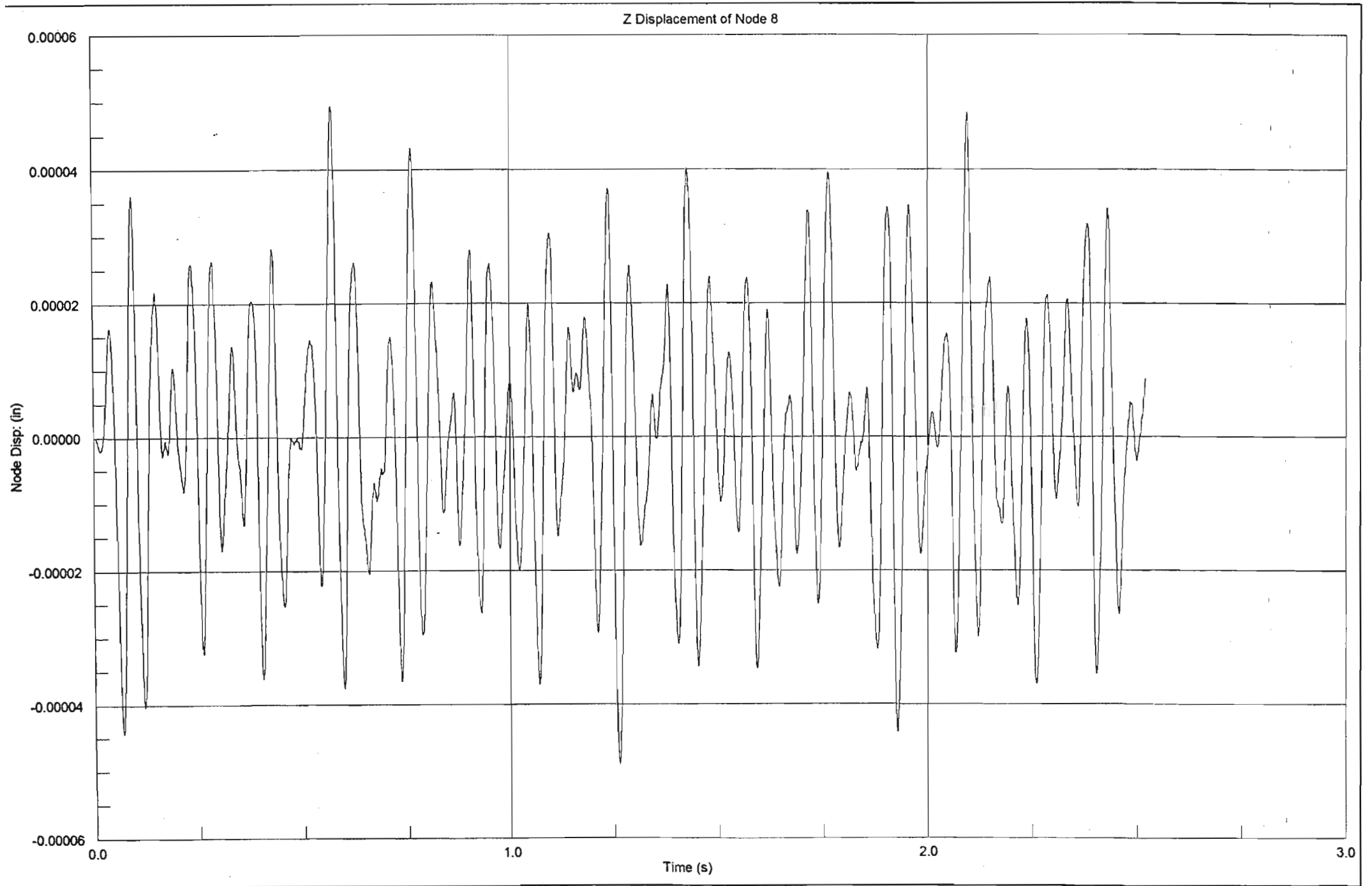
Z Displacement of Node 20

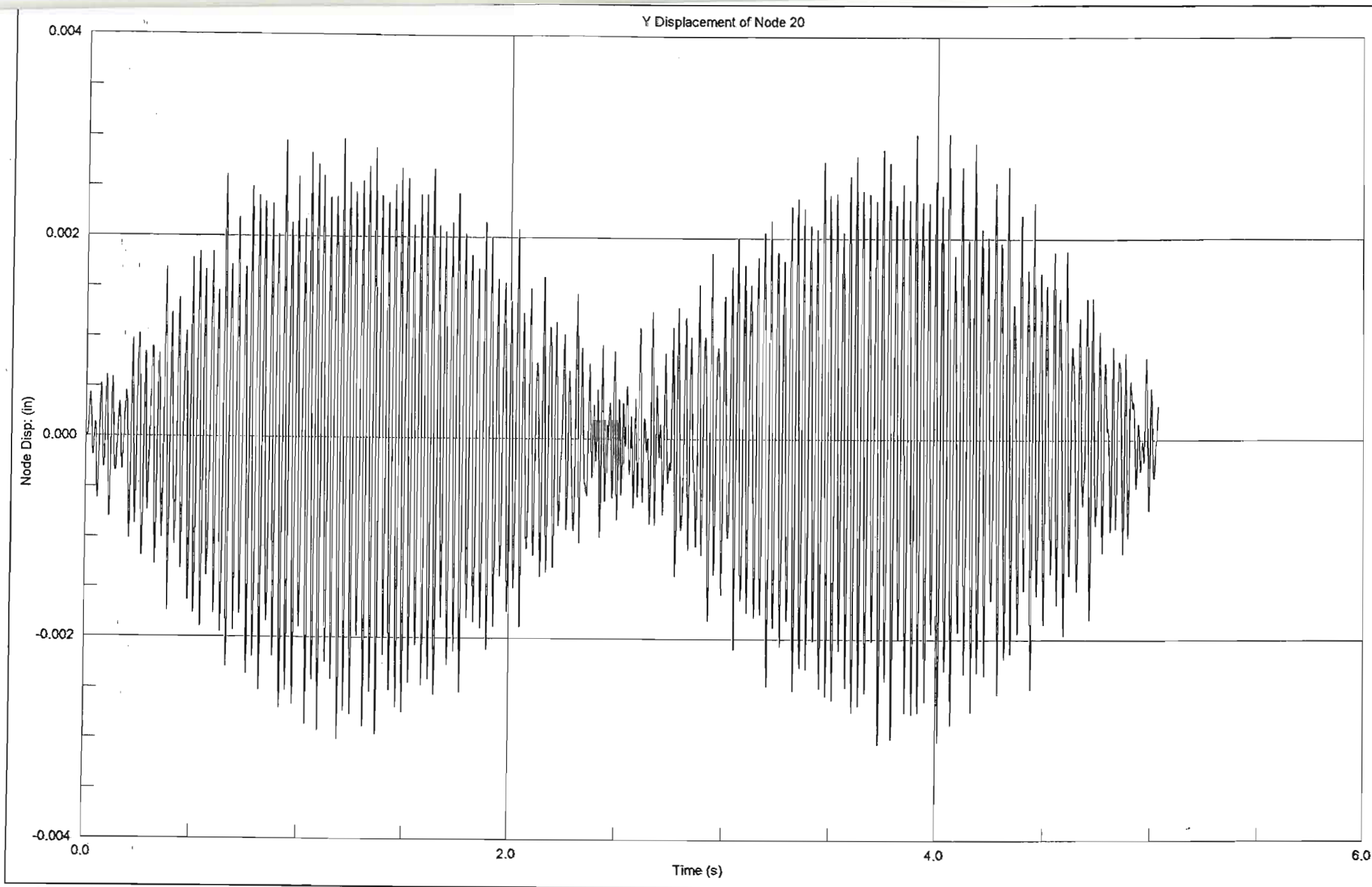




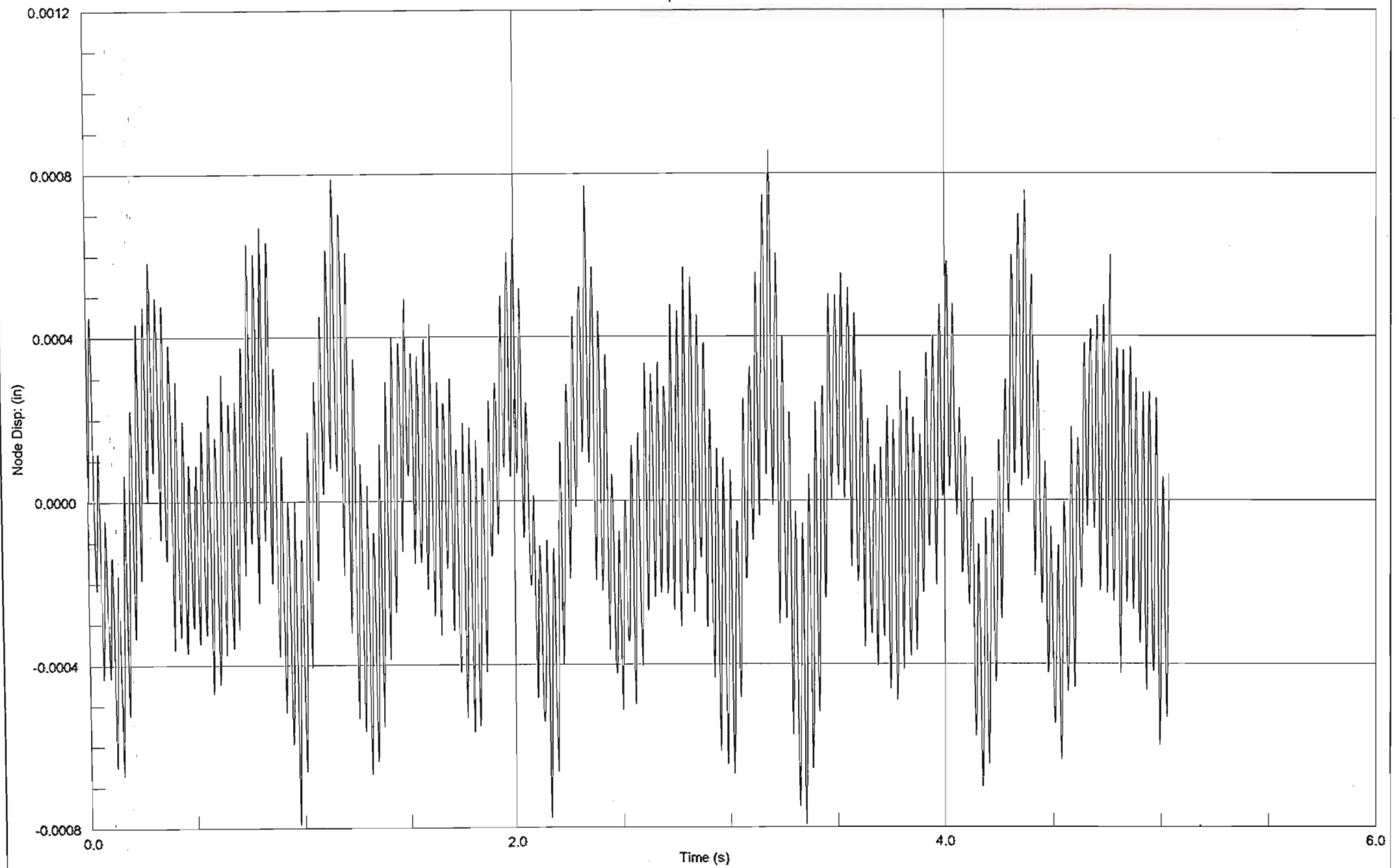


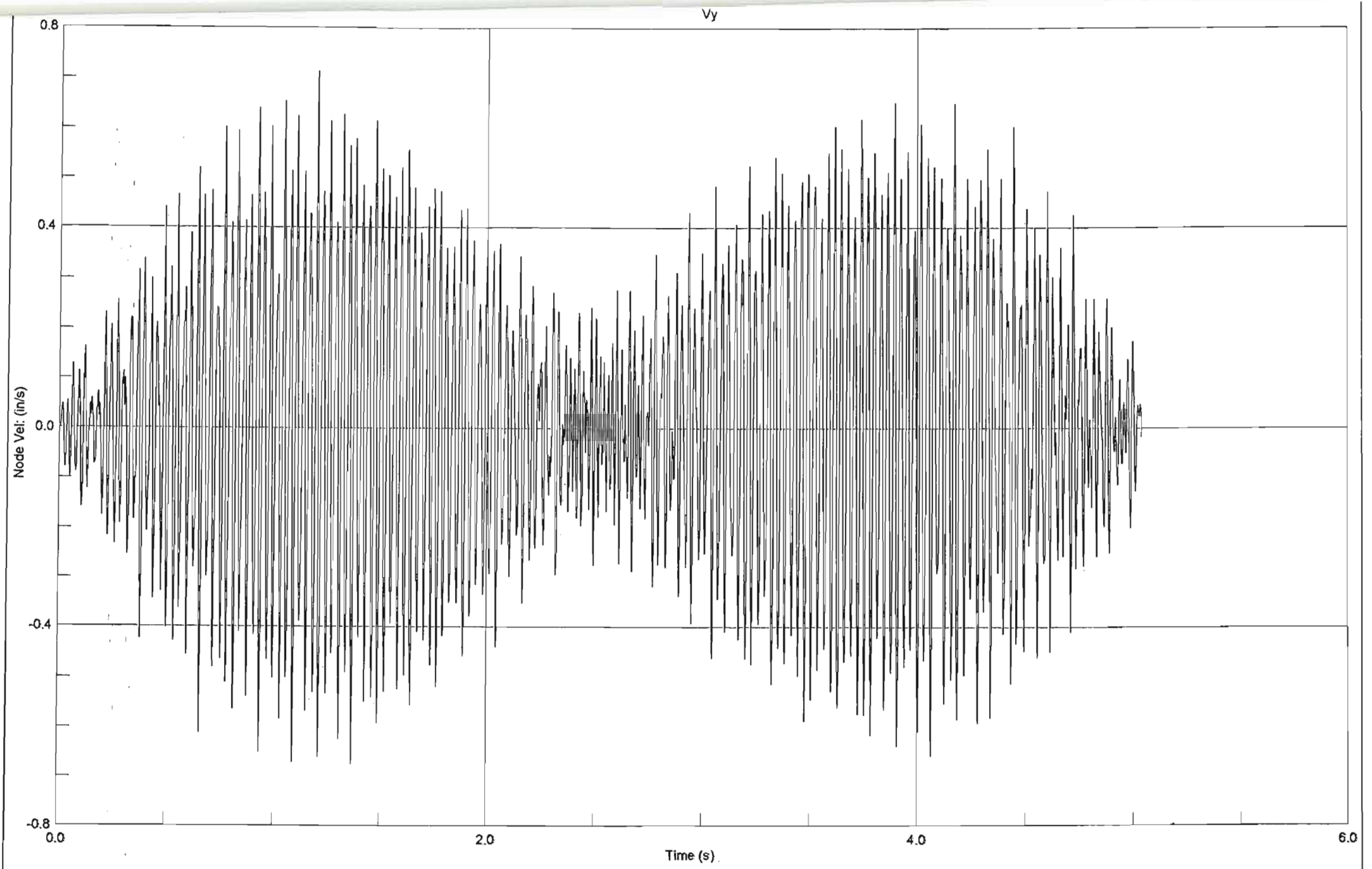






Z Displacement of Node 20



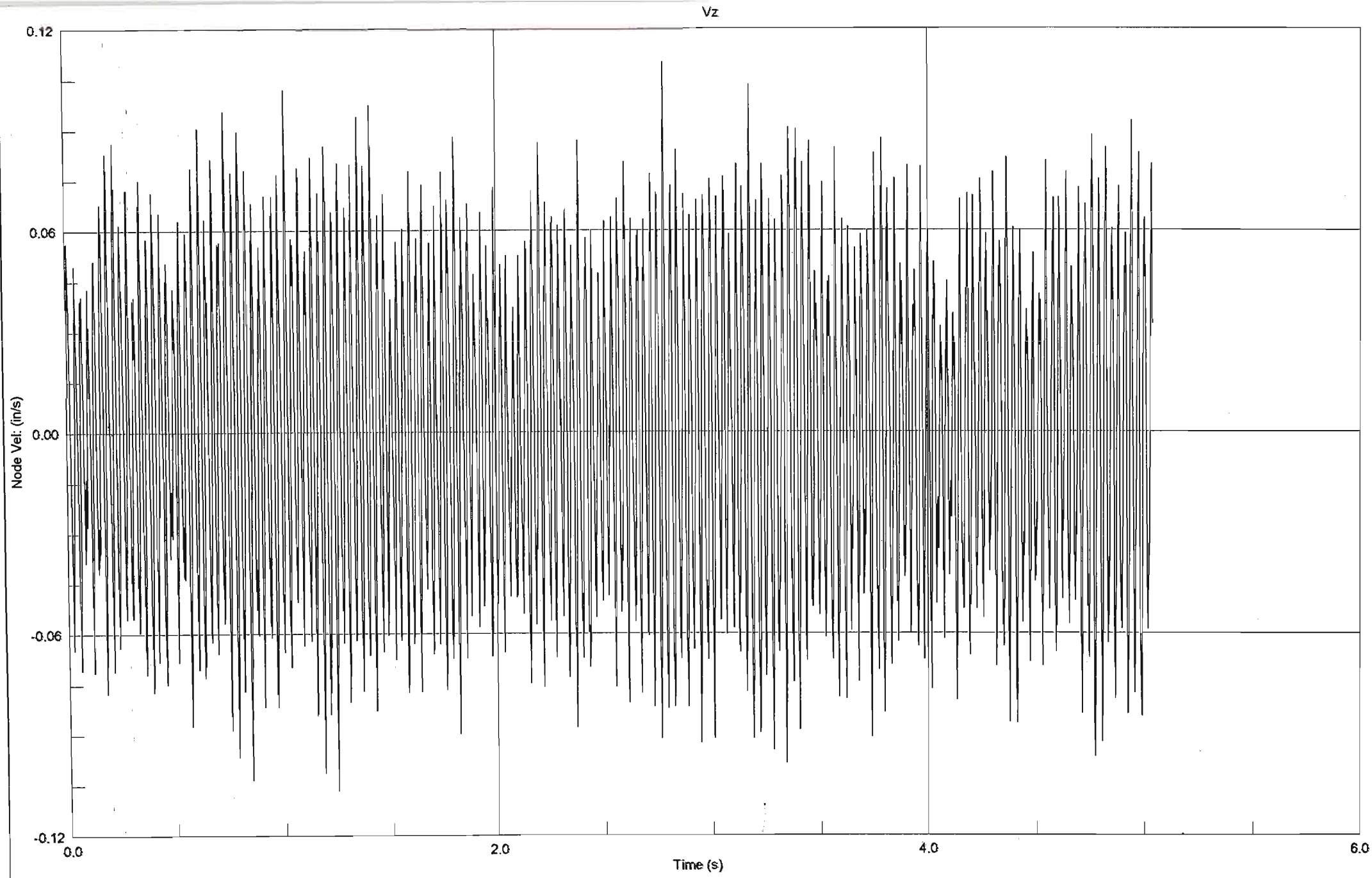


Strand7 Release 2.1.7

C:\MSc Eng\Multistorey\Multistorey G15000-B1.sl7

11 October 2002 8:26 am

D3.9



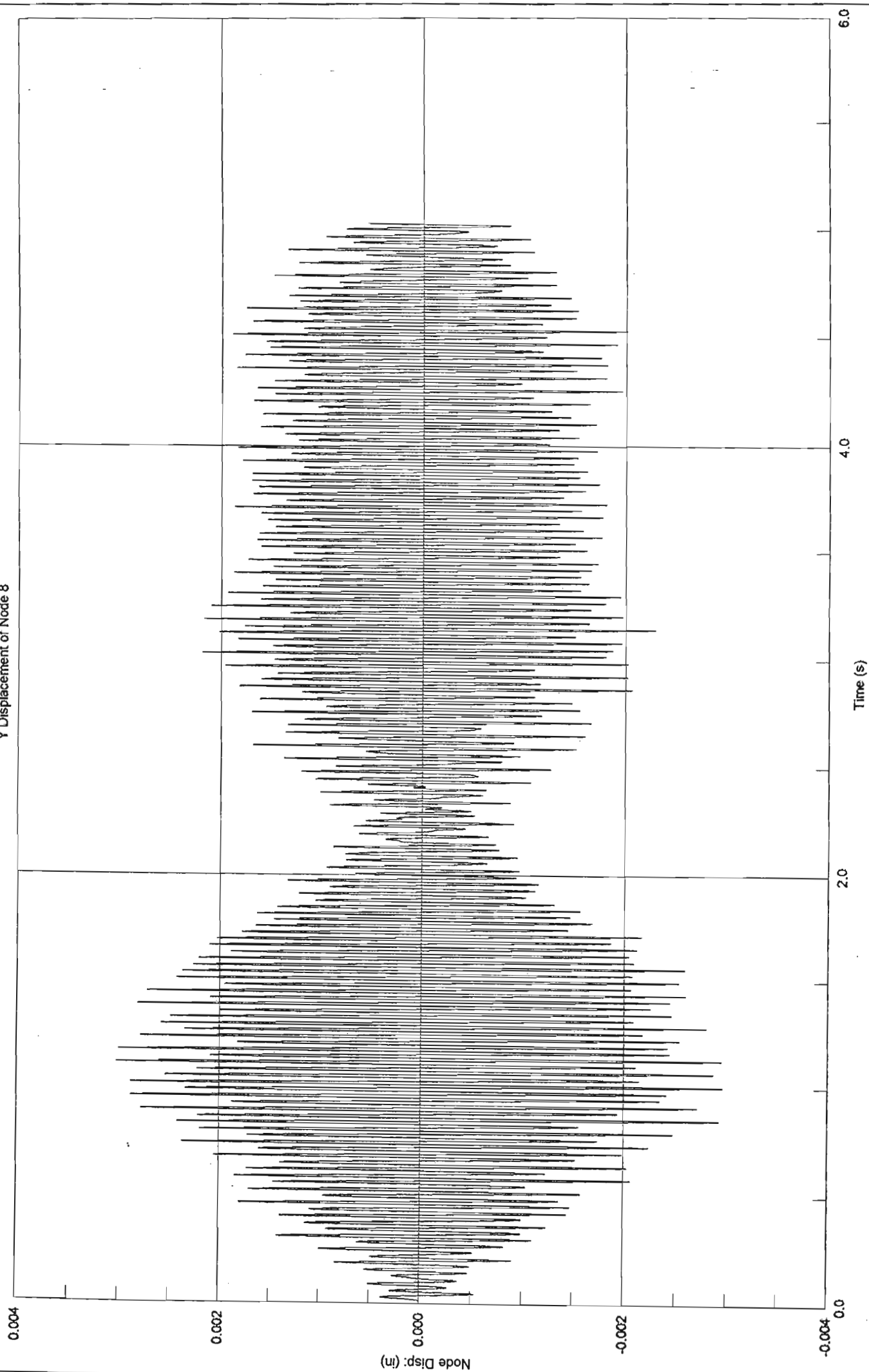
Strand7 Release 2.1.7

C:\MSc Eng\Multistorey\Multistorey G15000-B1.s17

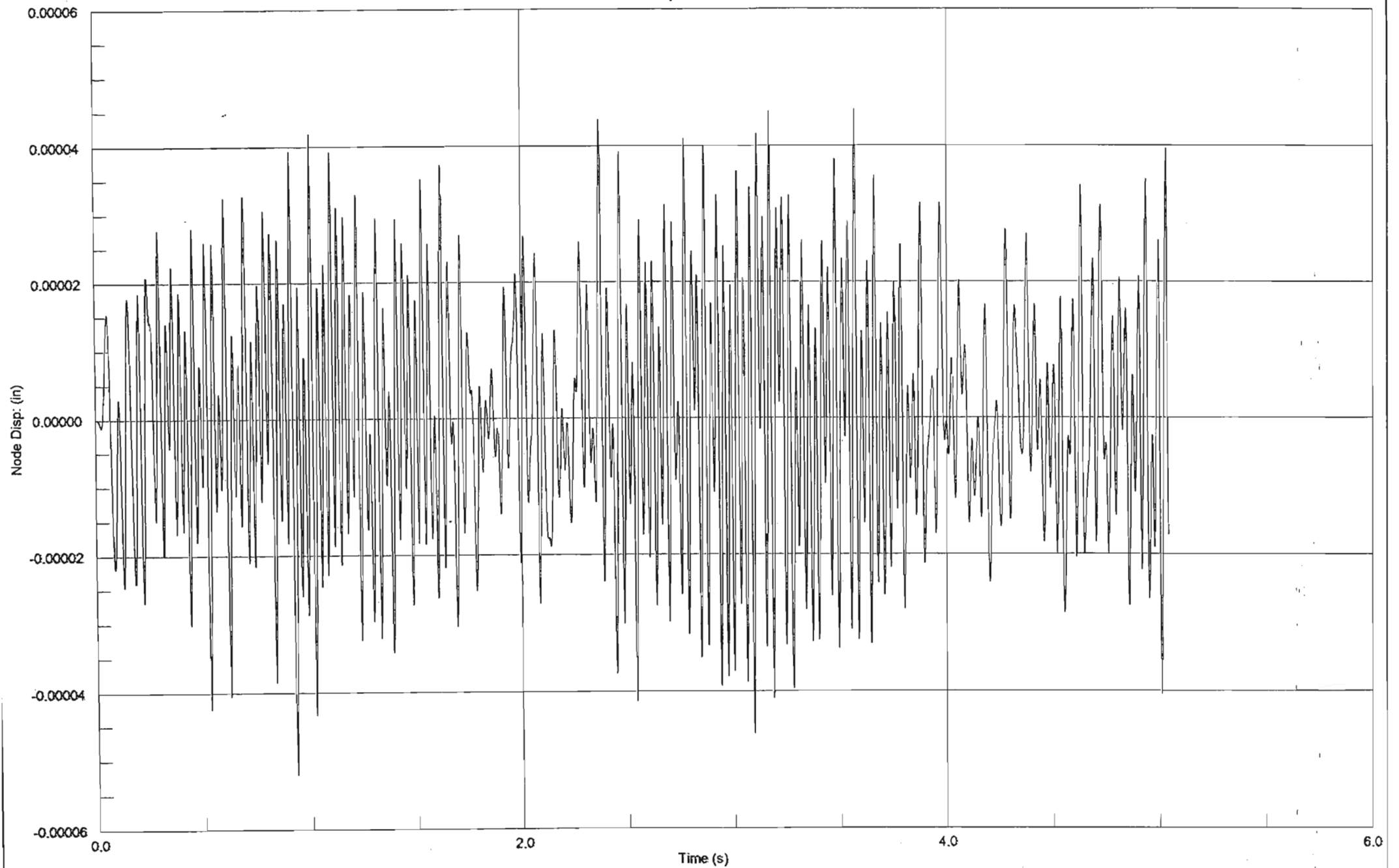
11 October 2002 8:26 am

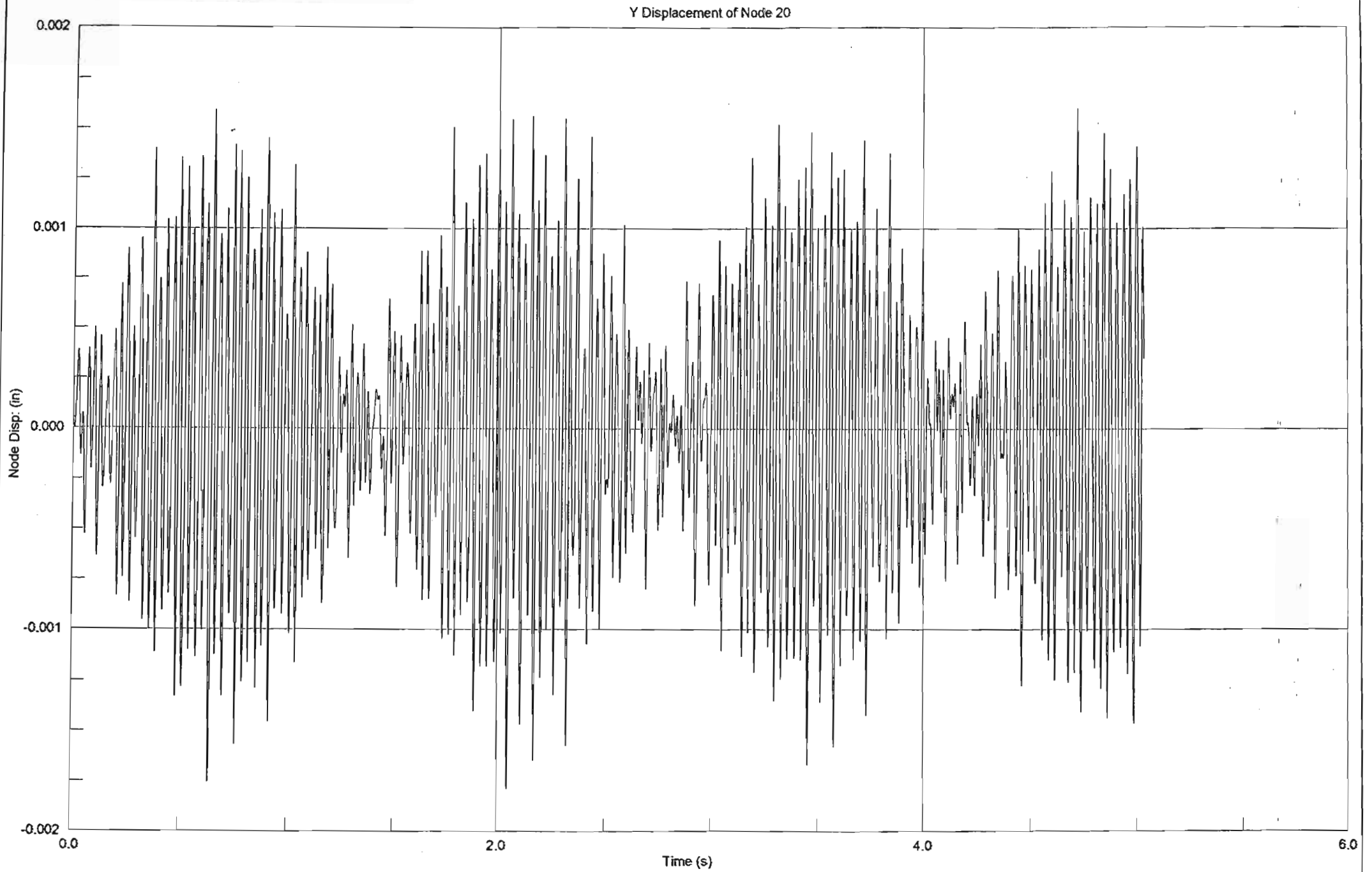
D 3.10

Y Displacement of Node 8

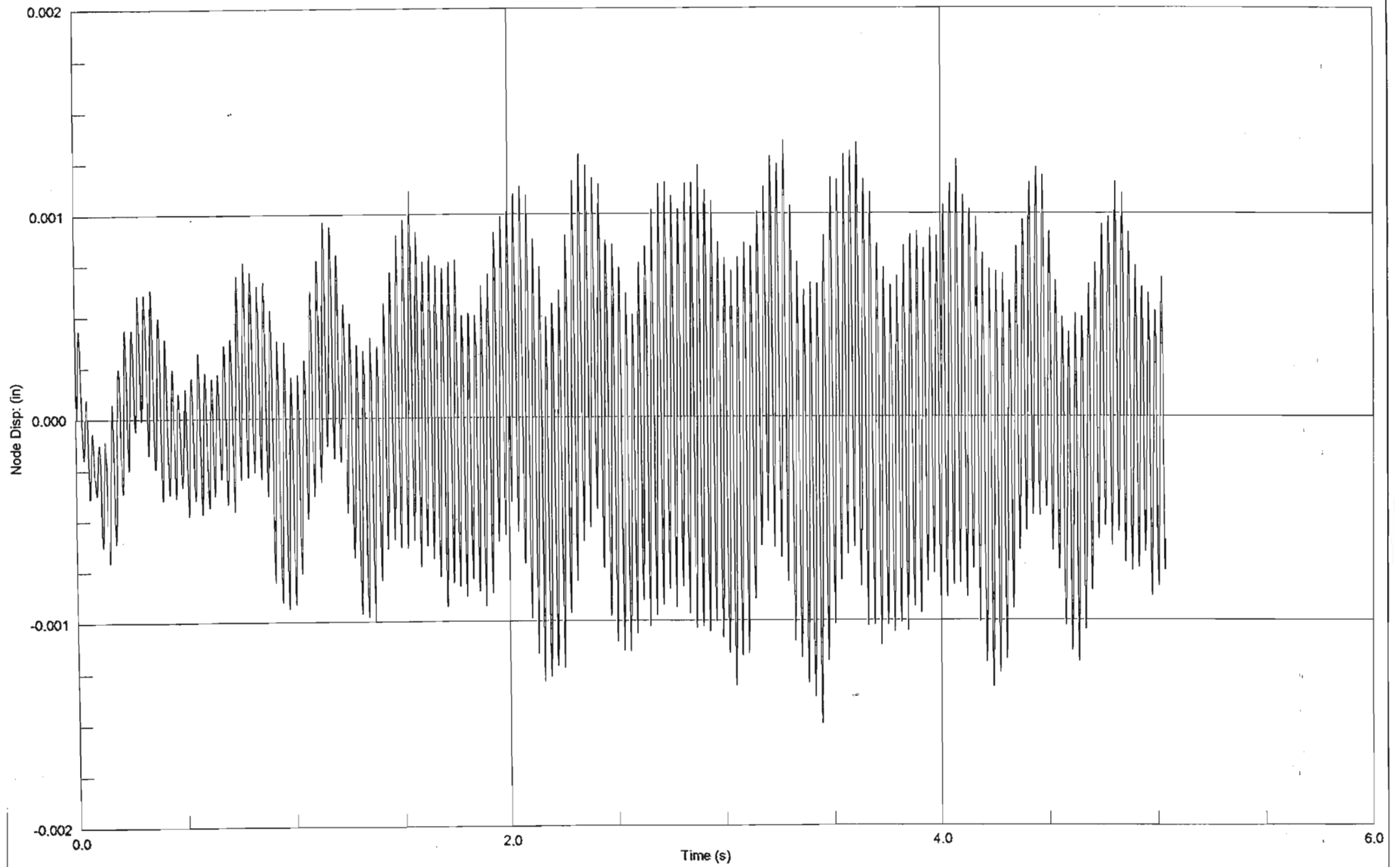


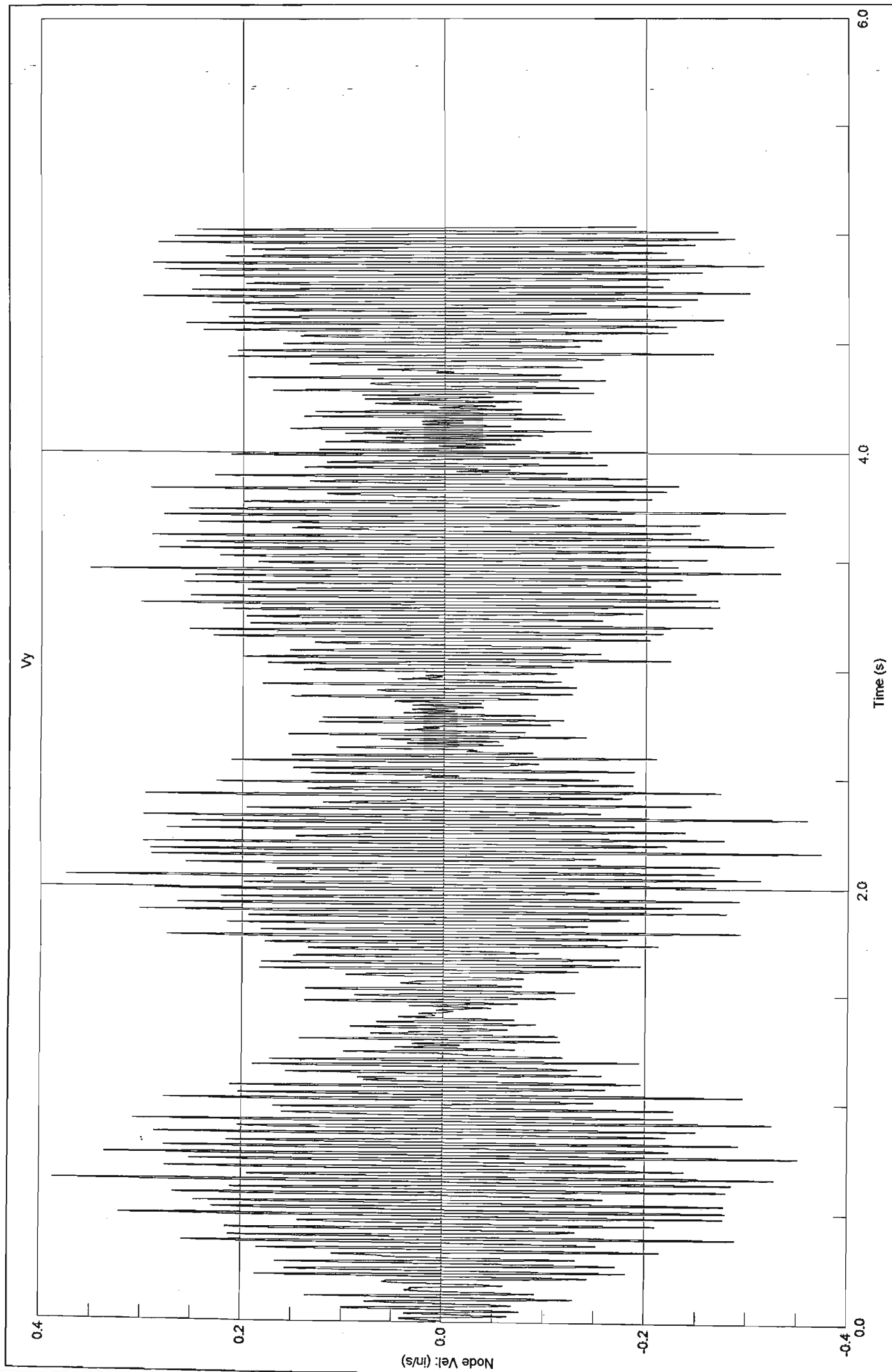
Z Displacement of Node 8

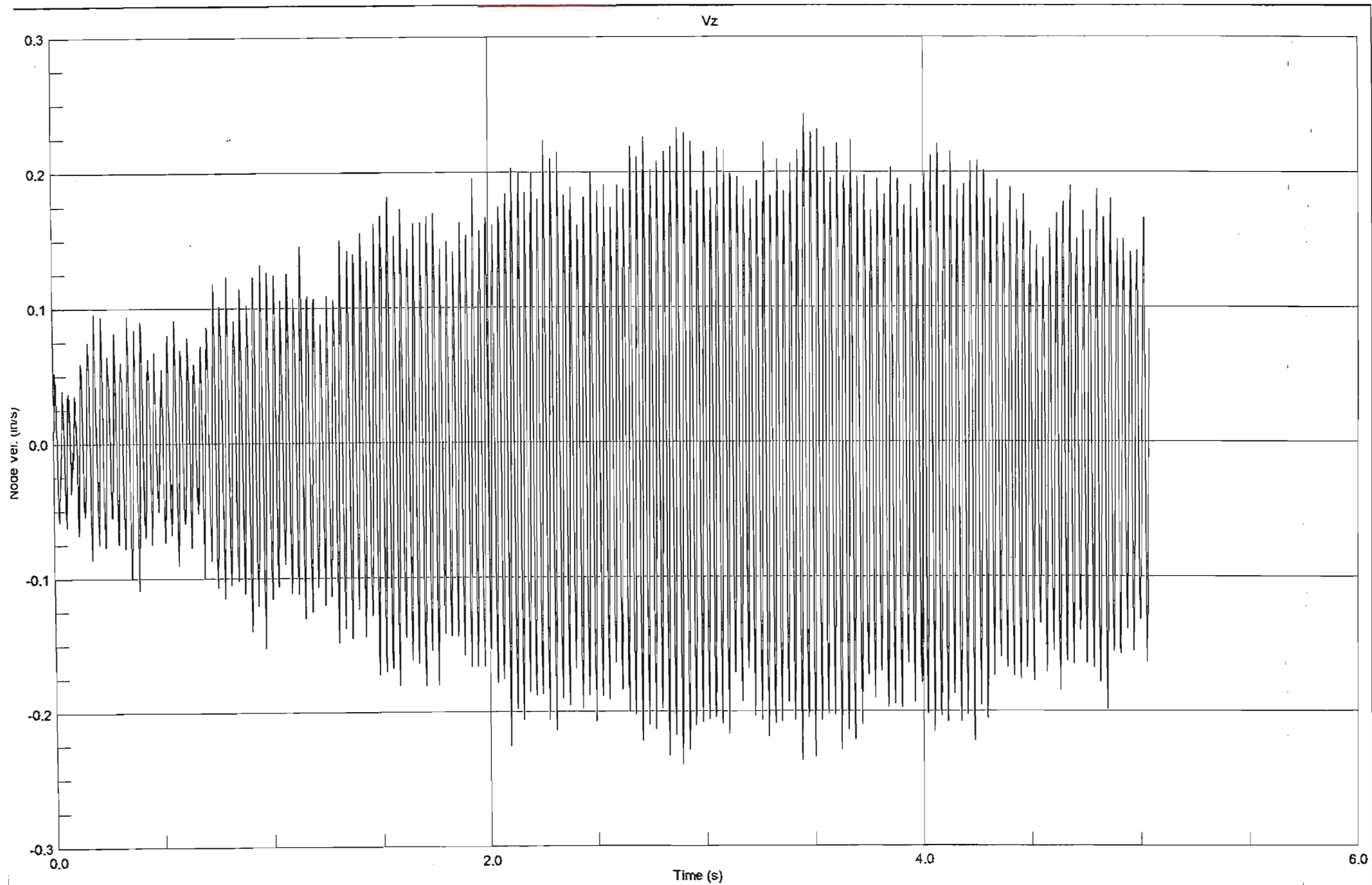




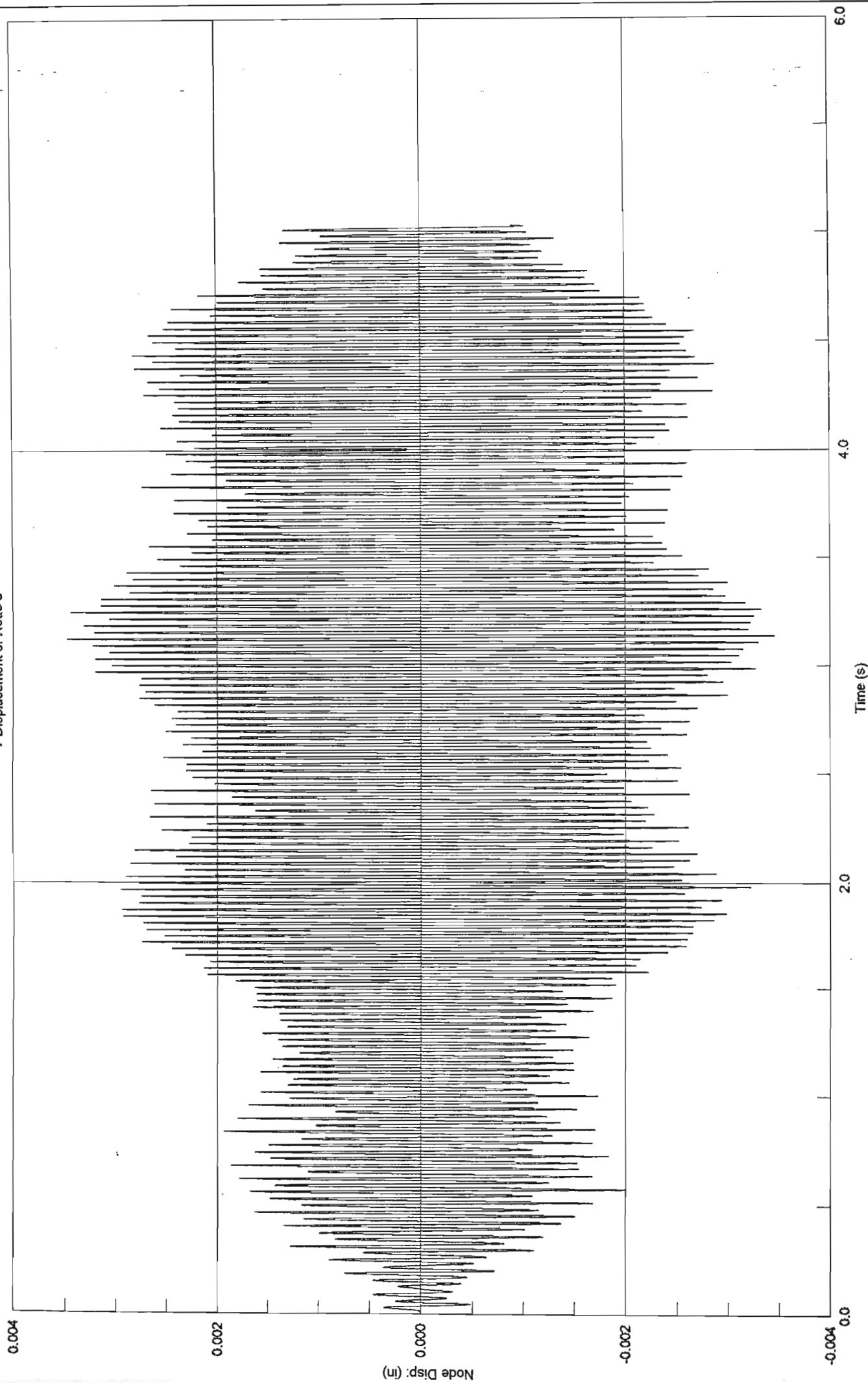
Z Displacement of Node 20

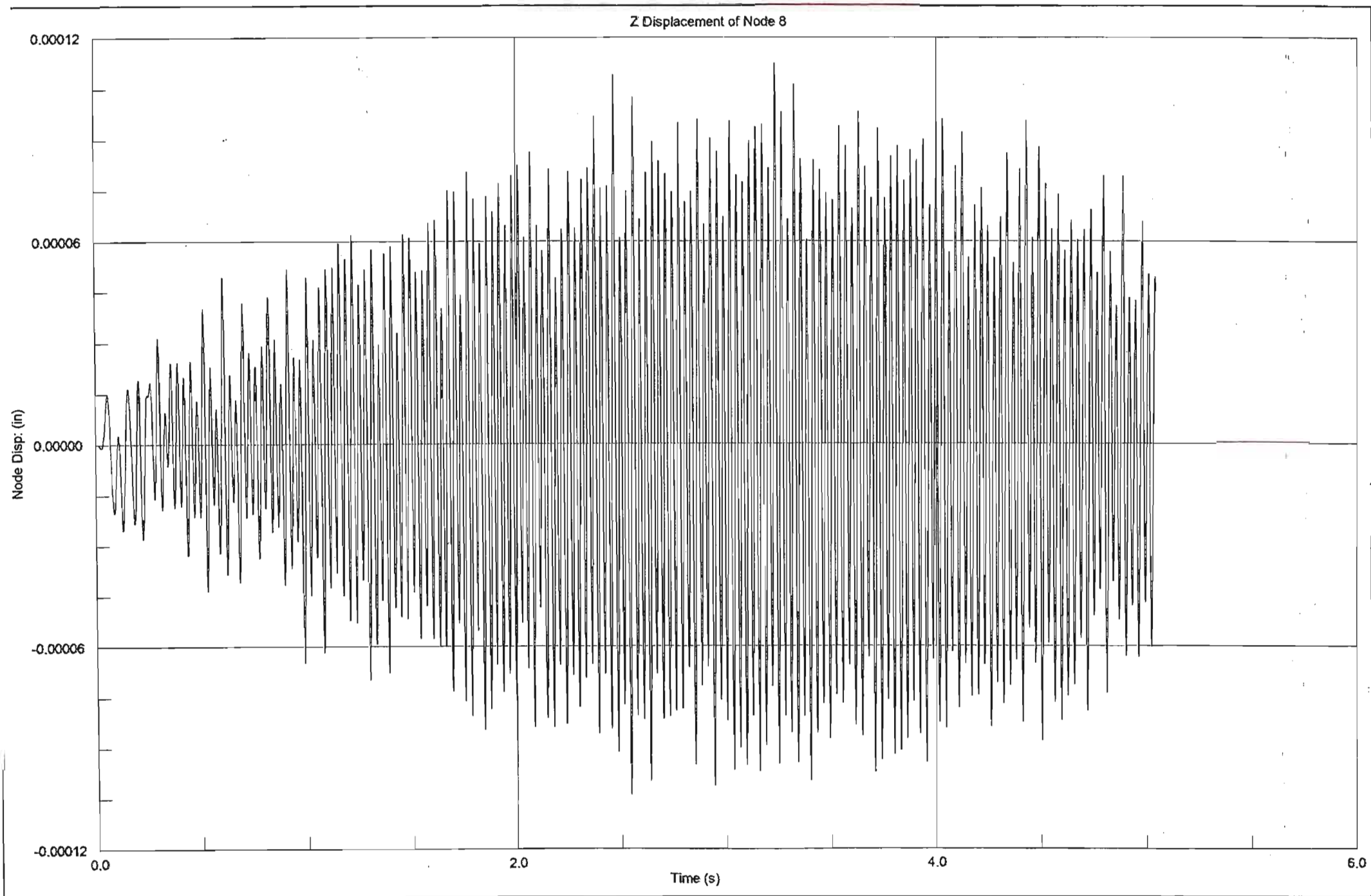


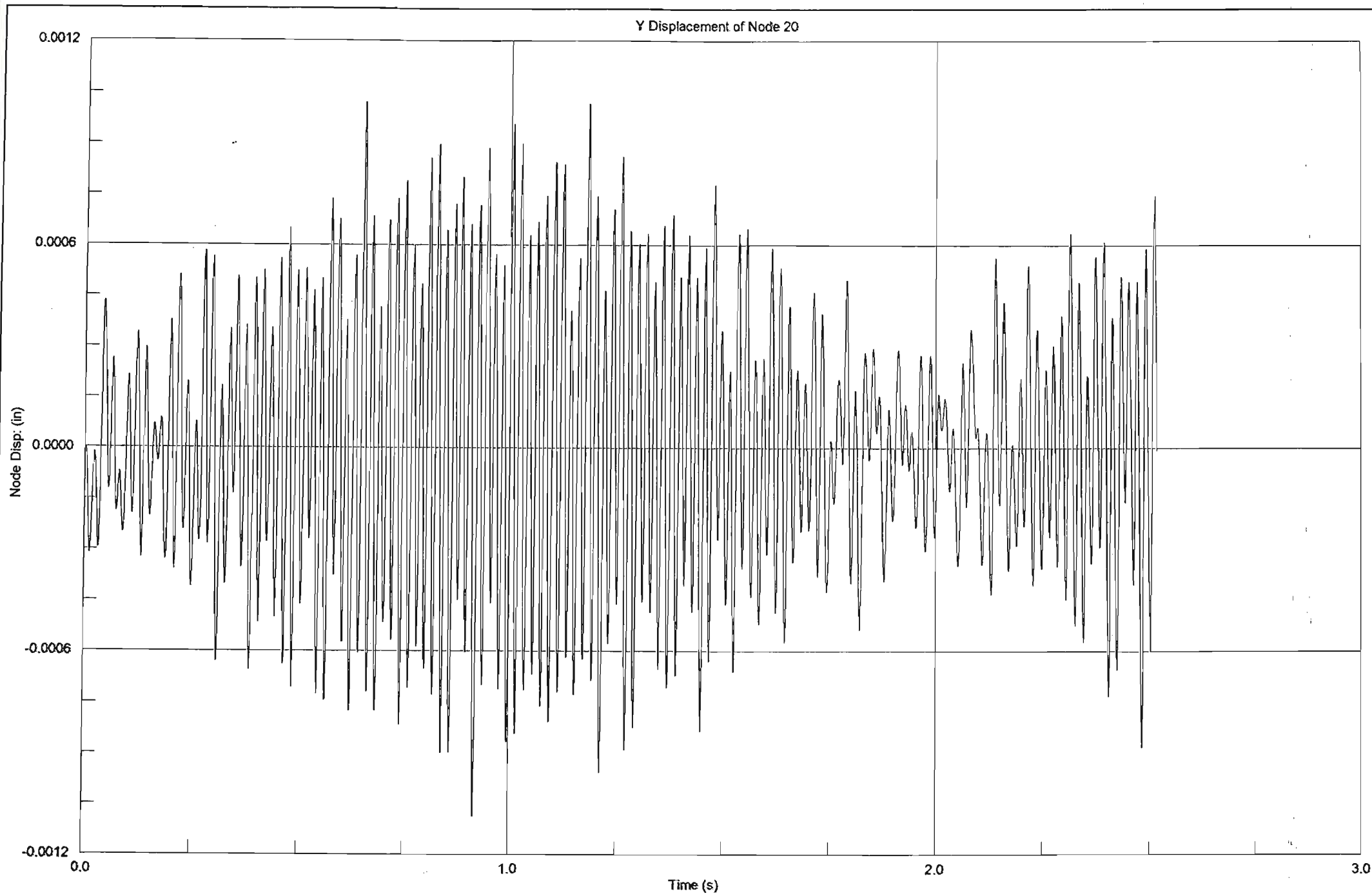




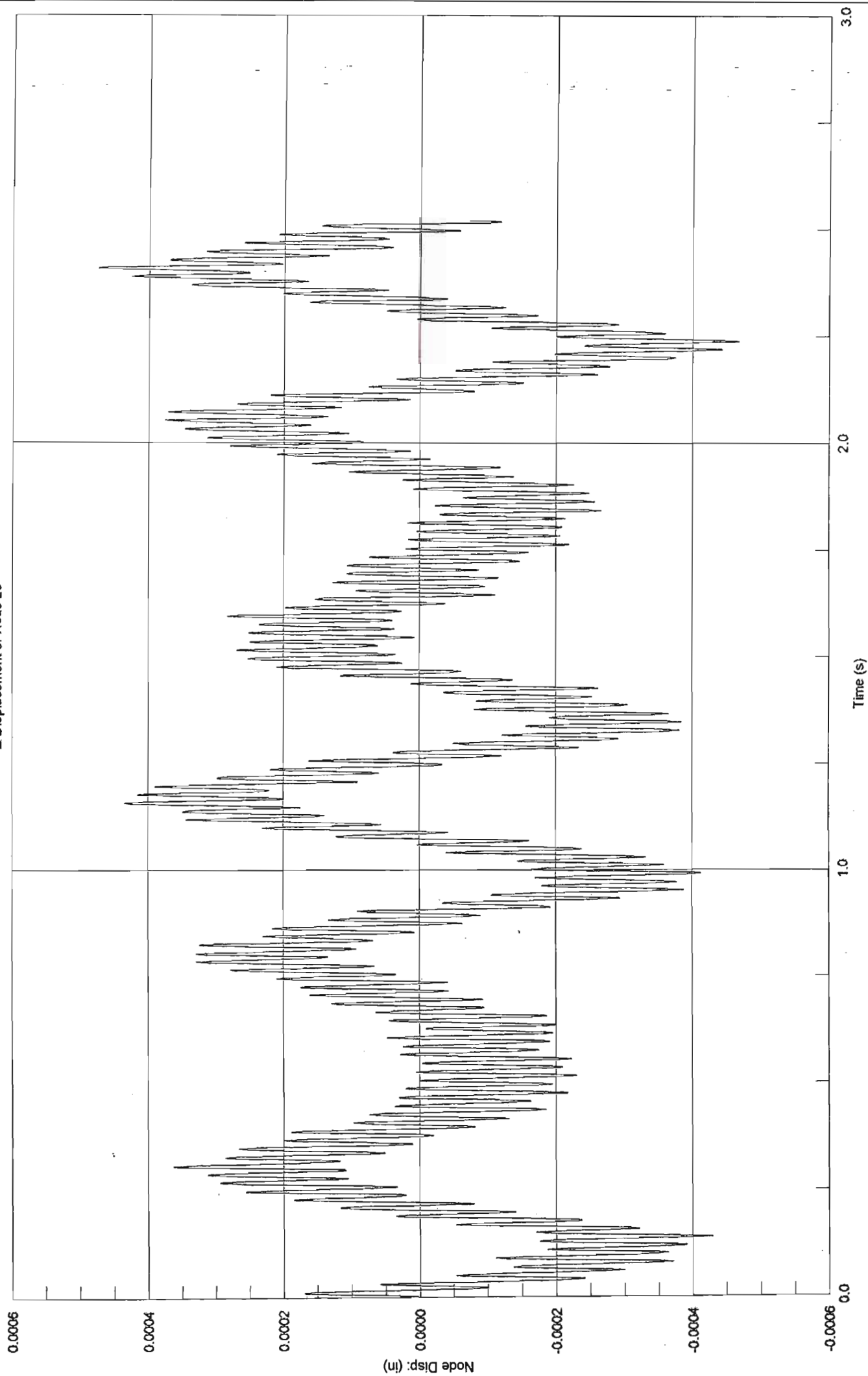
Y Displacement of Node 8

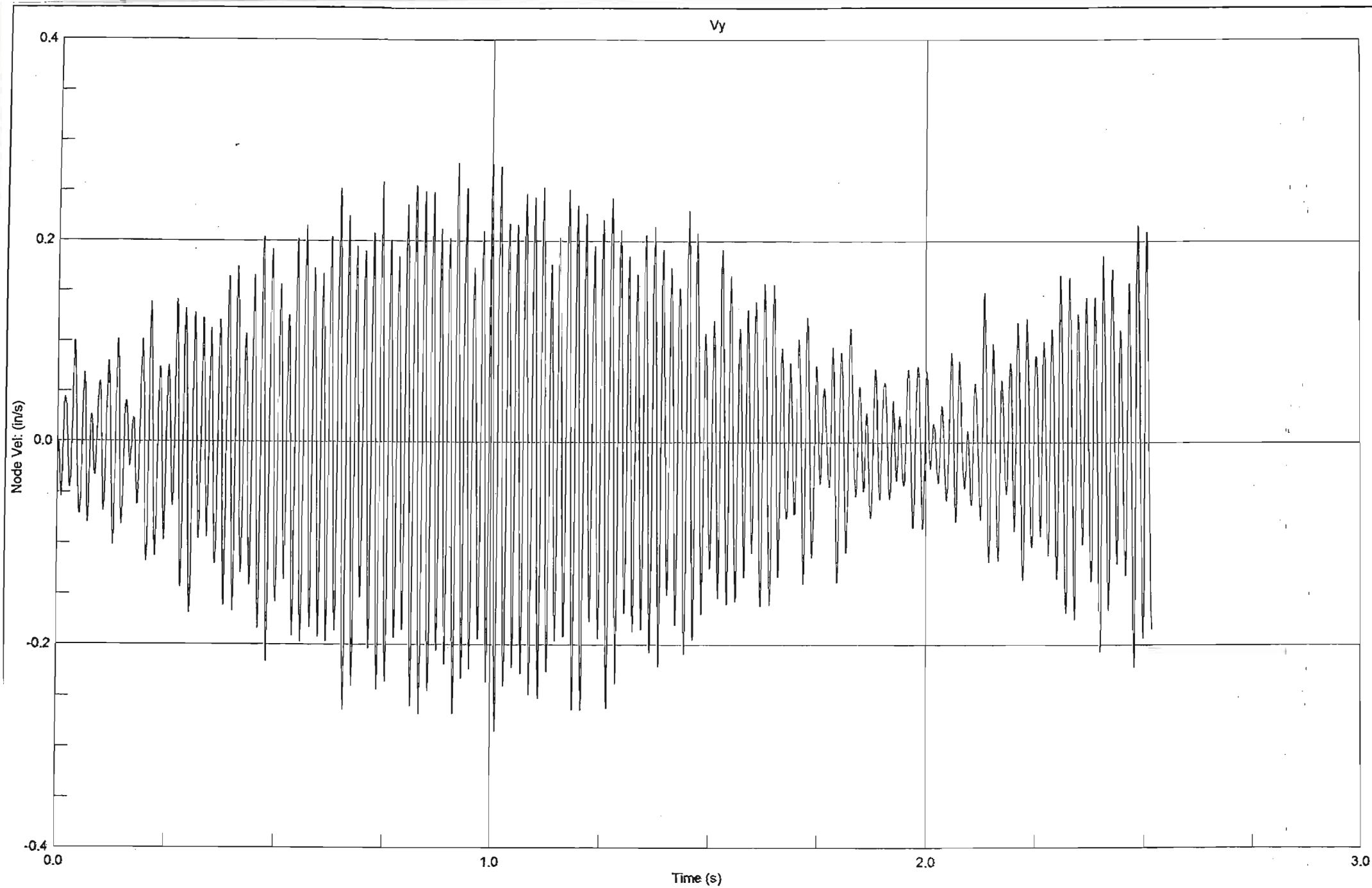


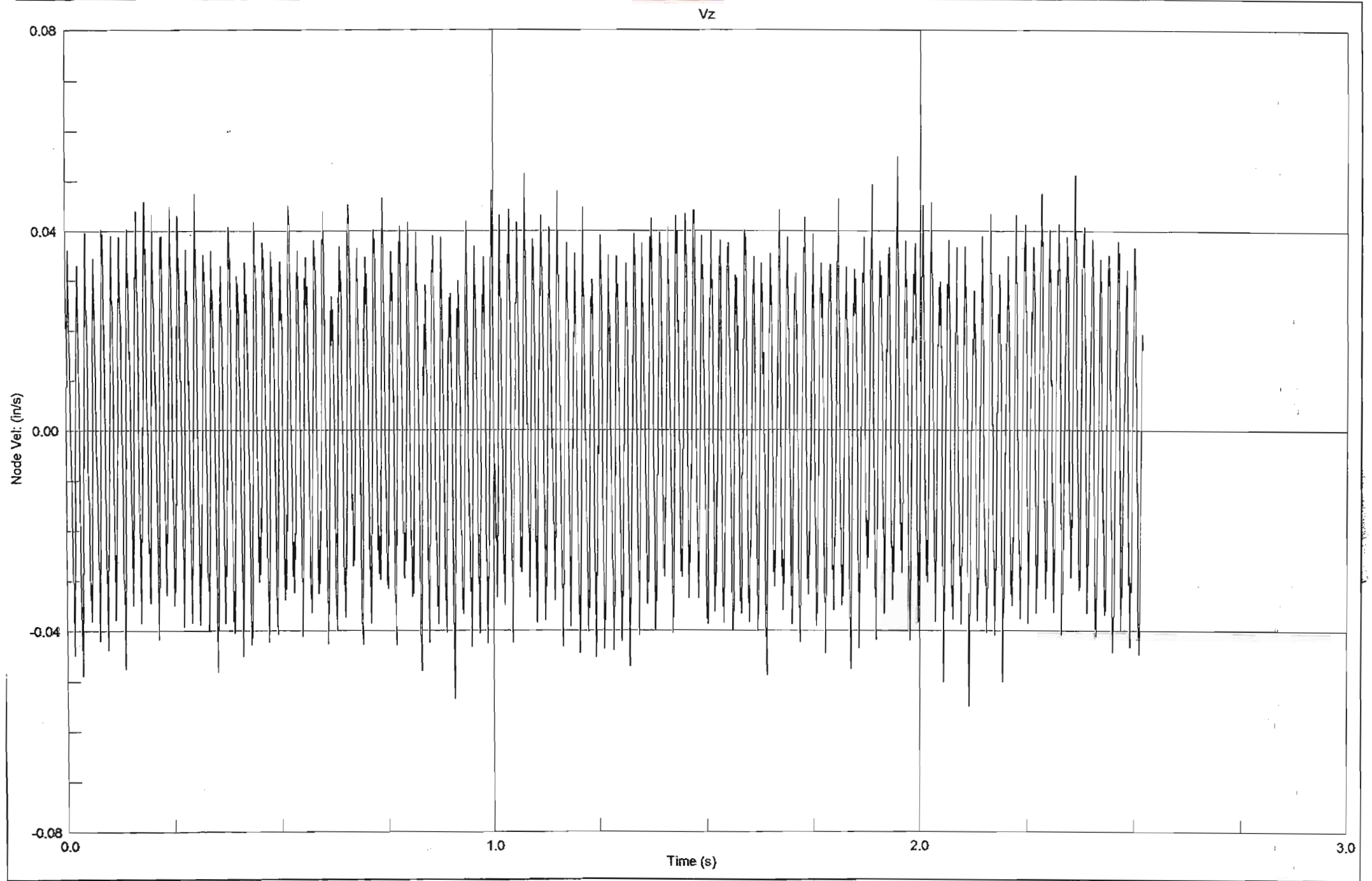


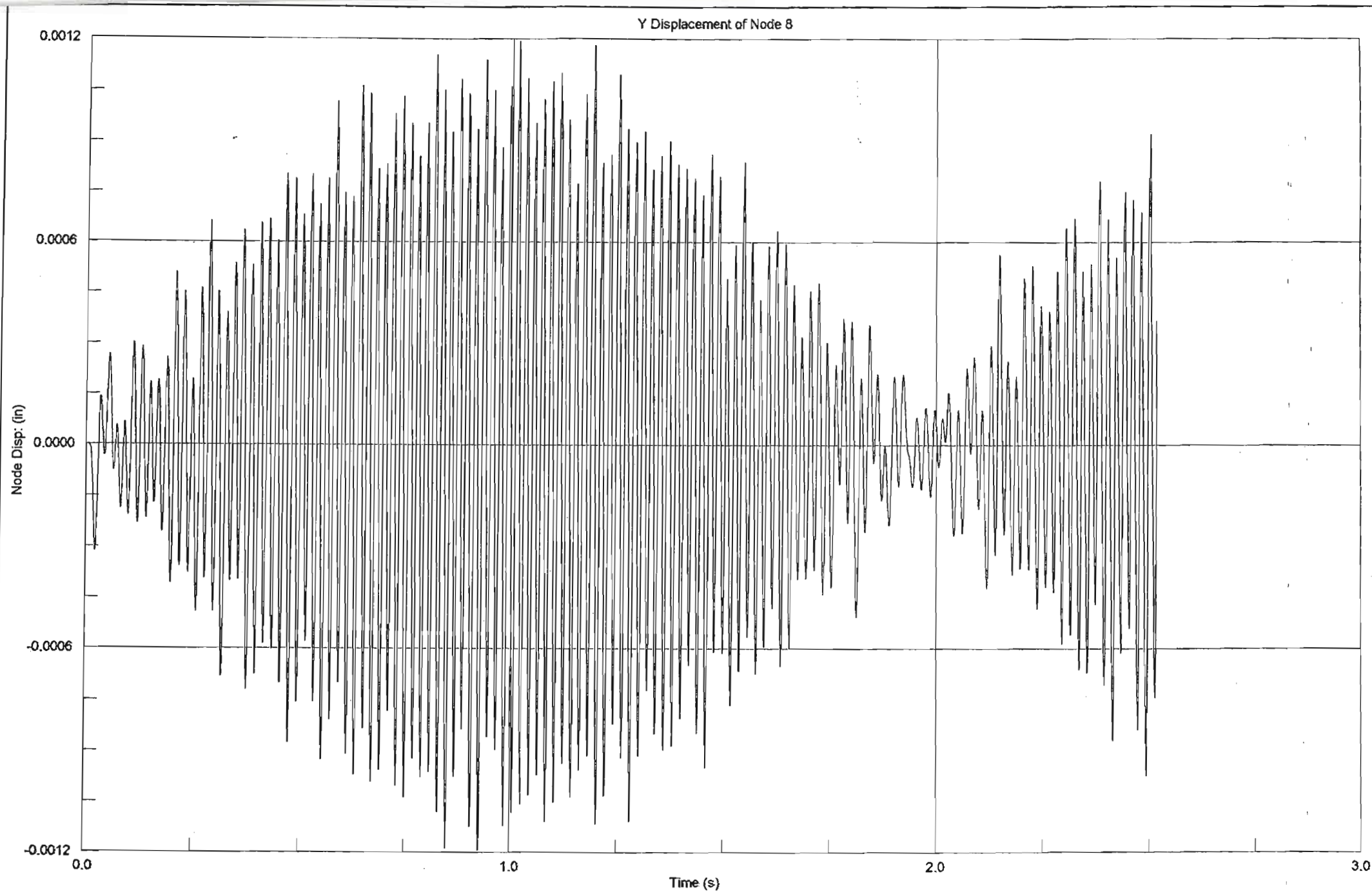


Z Displacement of Node 20

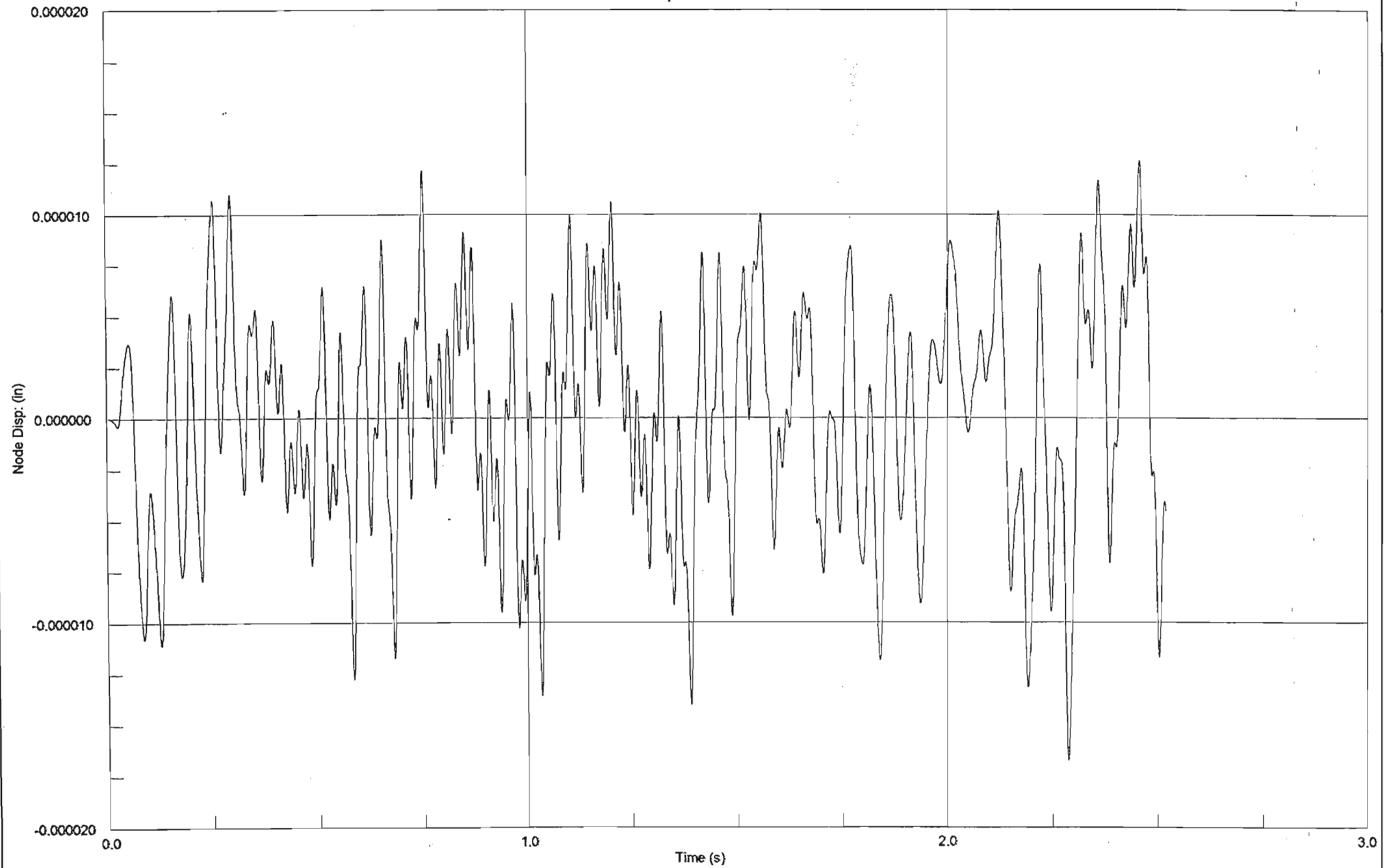


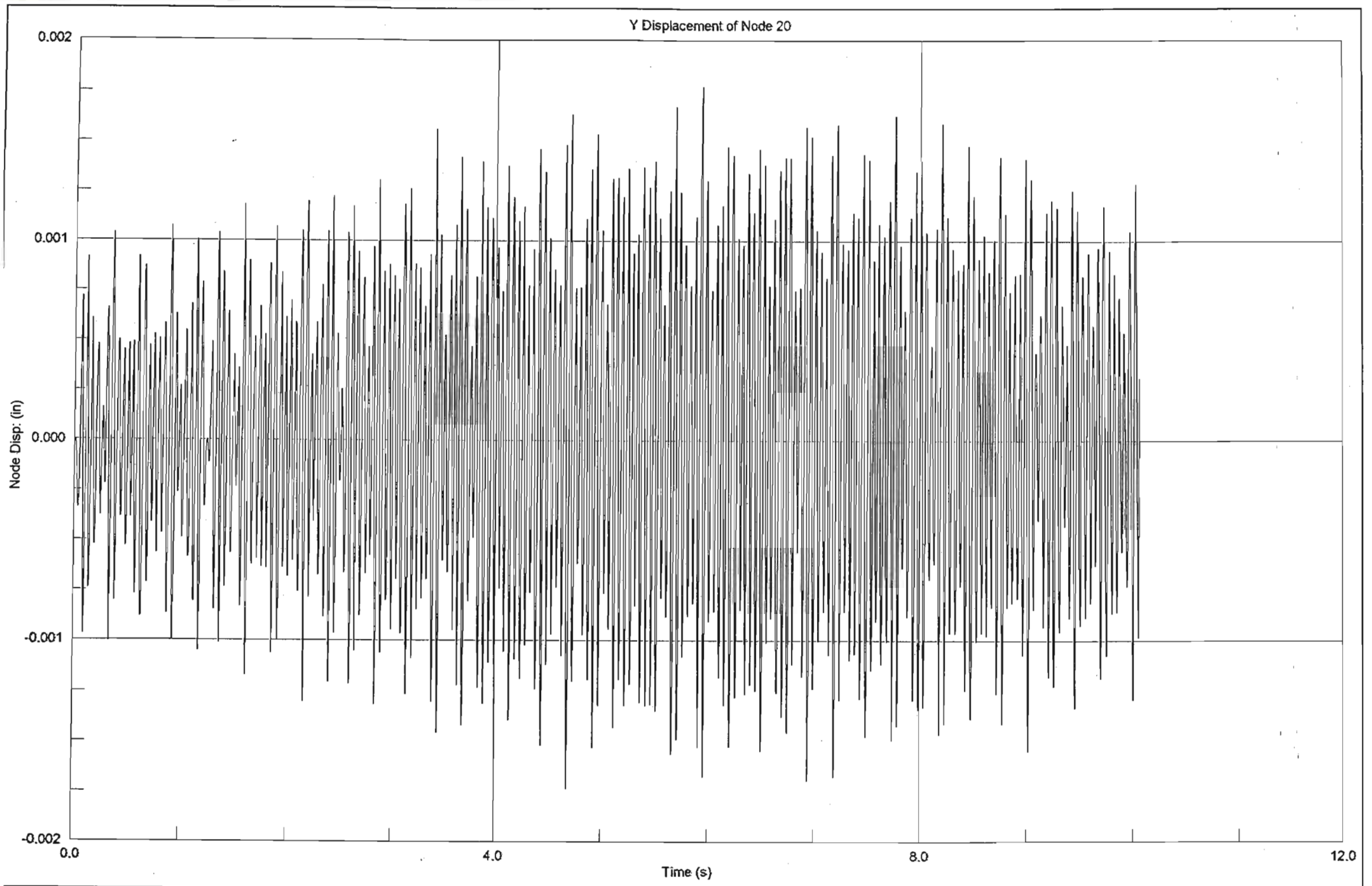




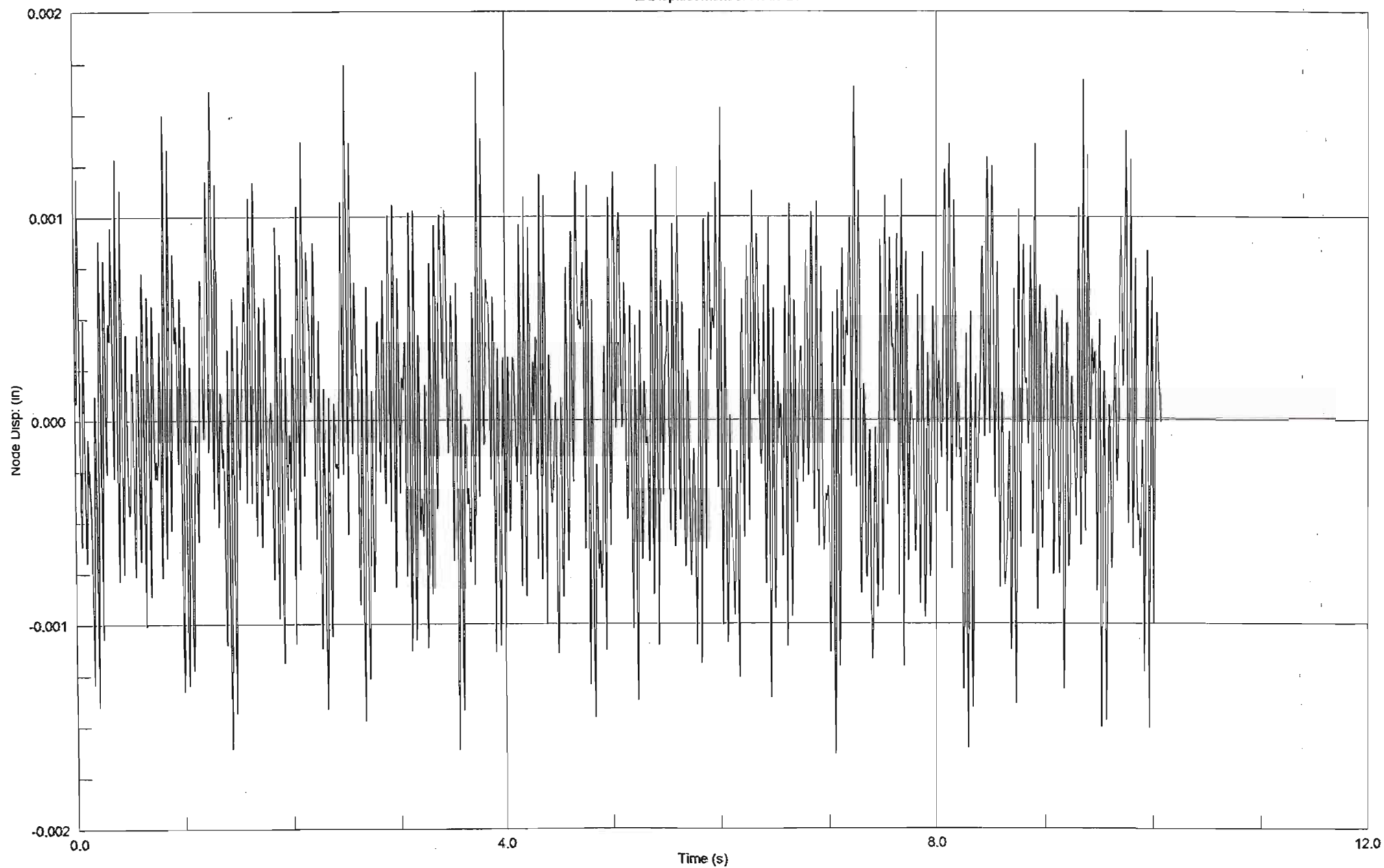


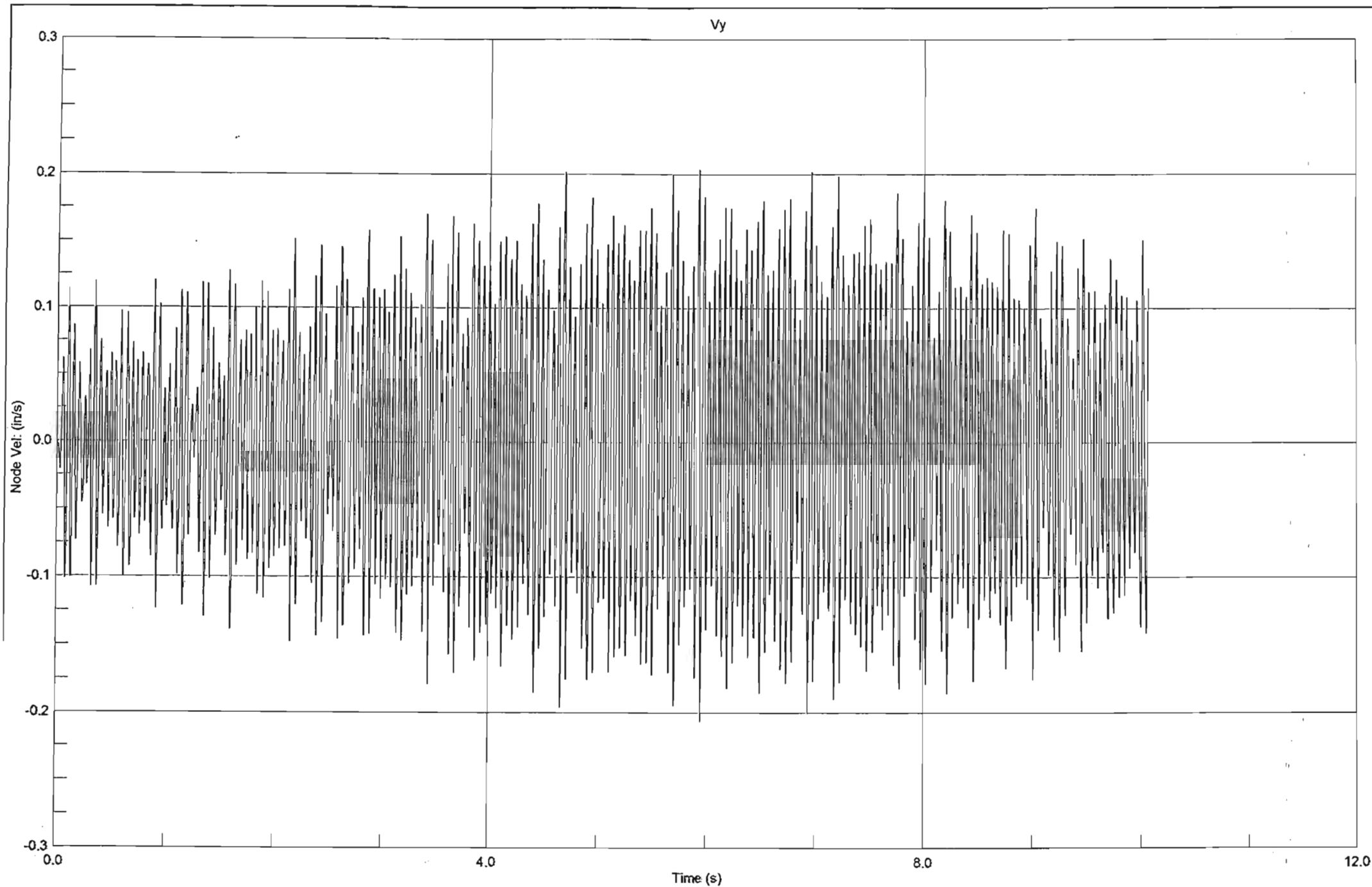
Z Displacement of Node 8

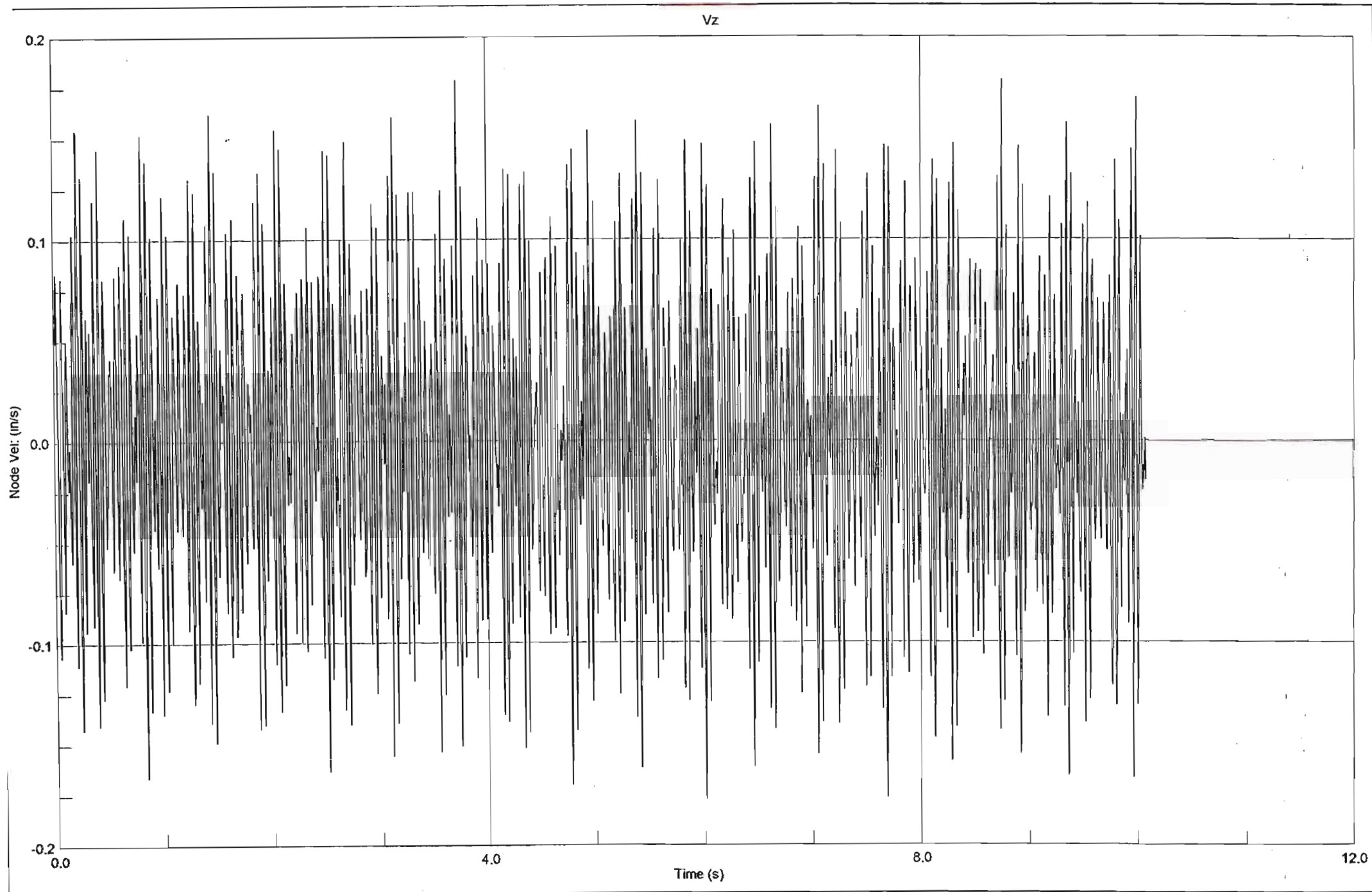


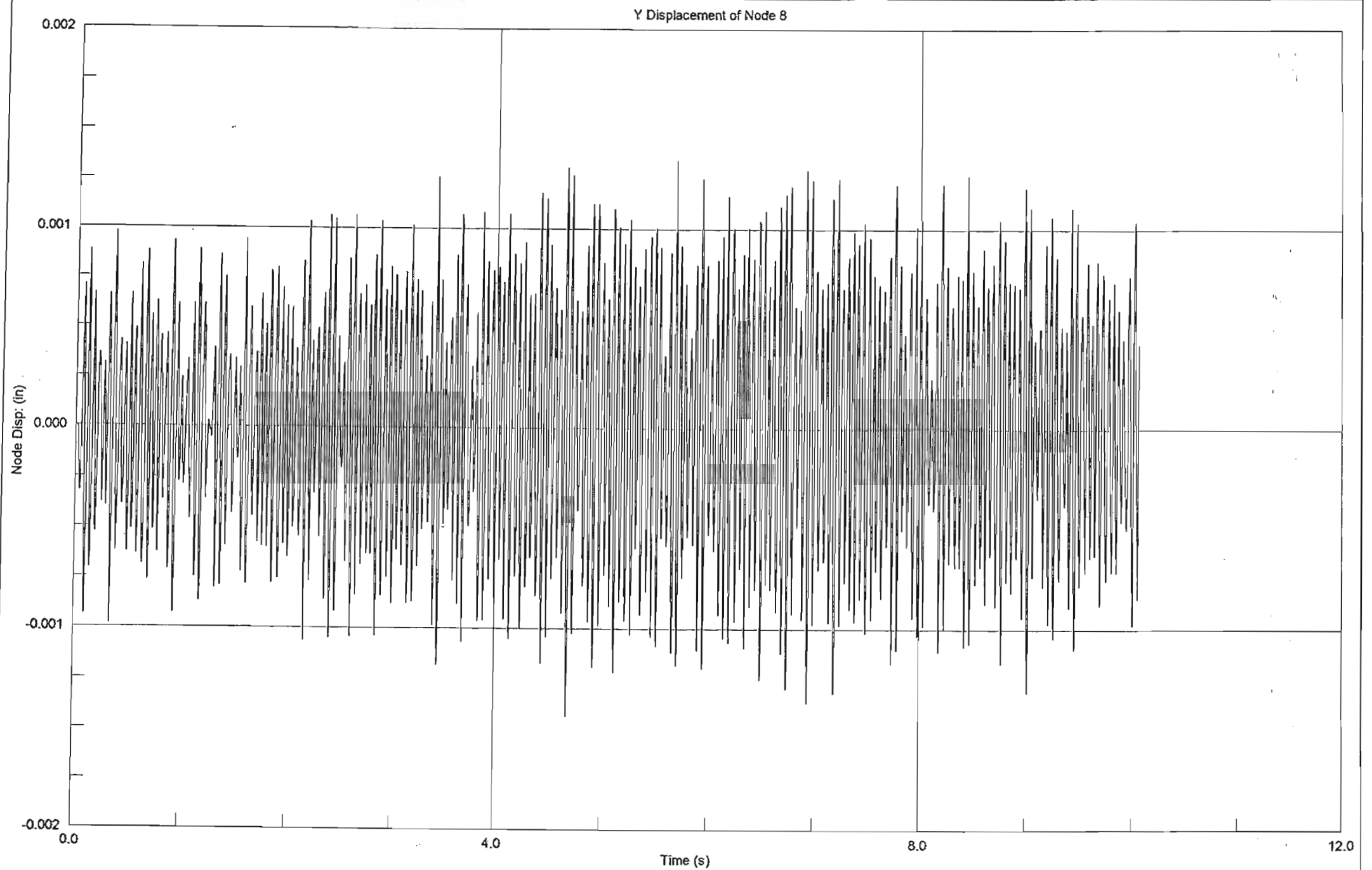


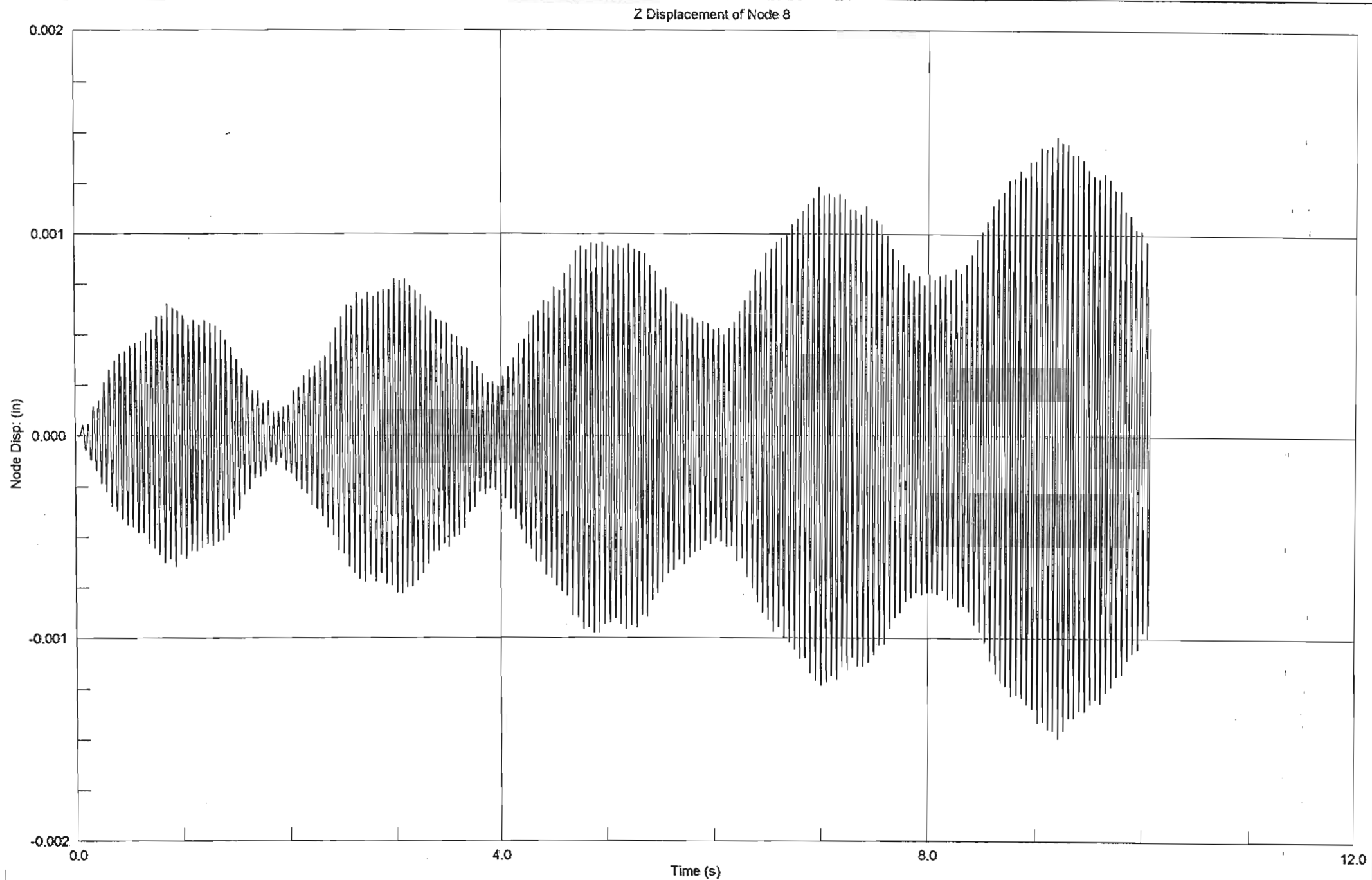
Z Displacement of Node 20

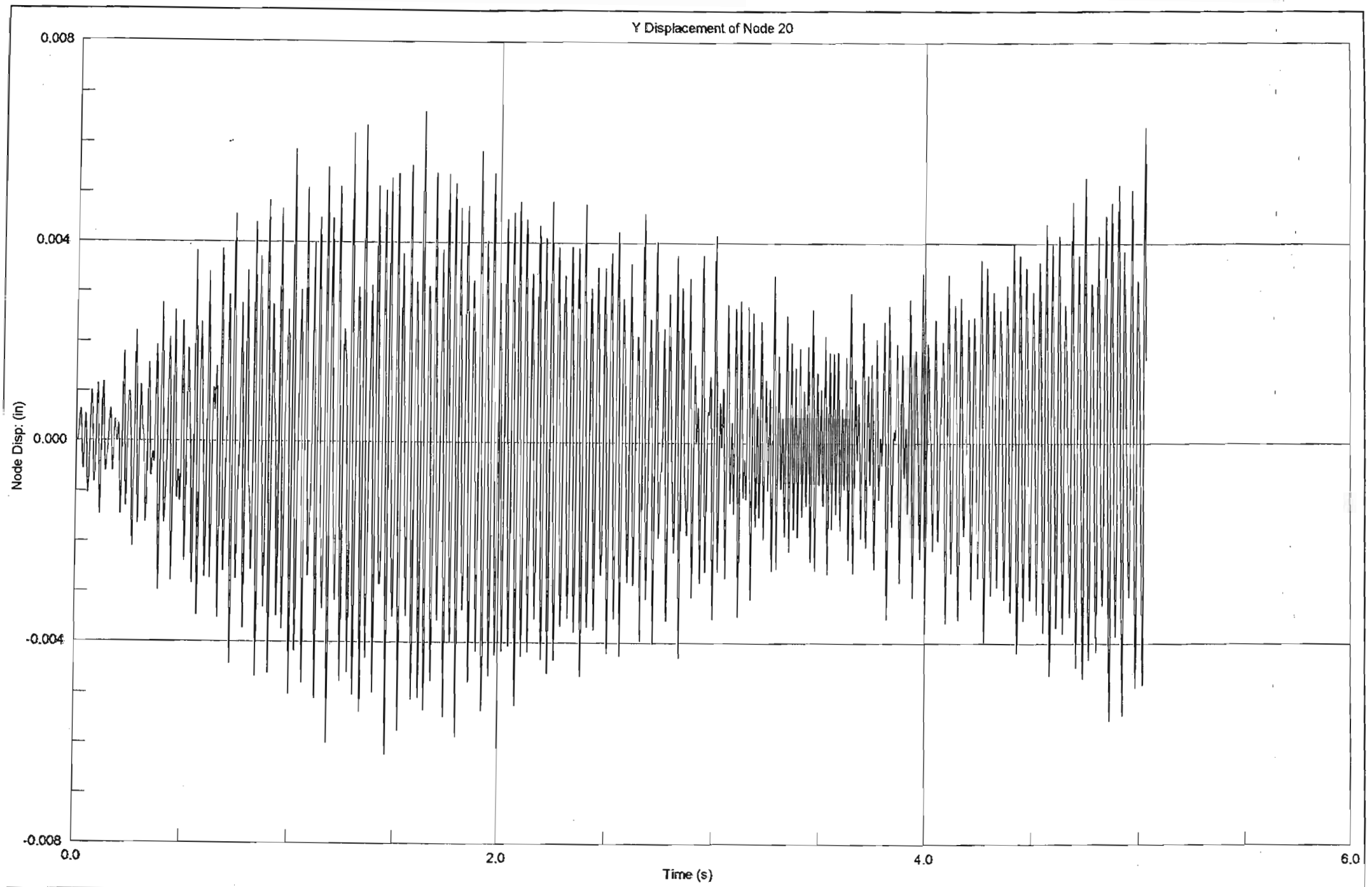




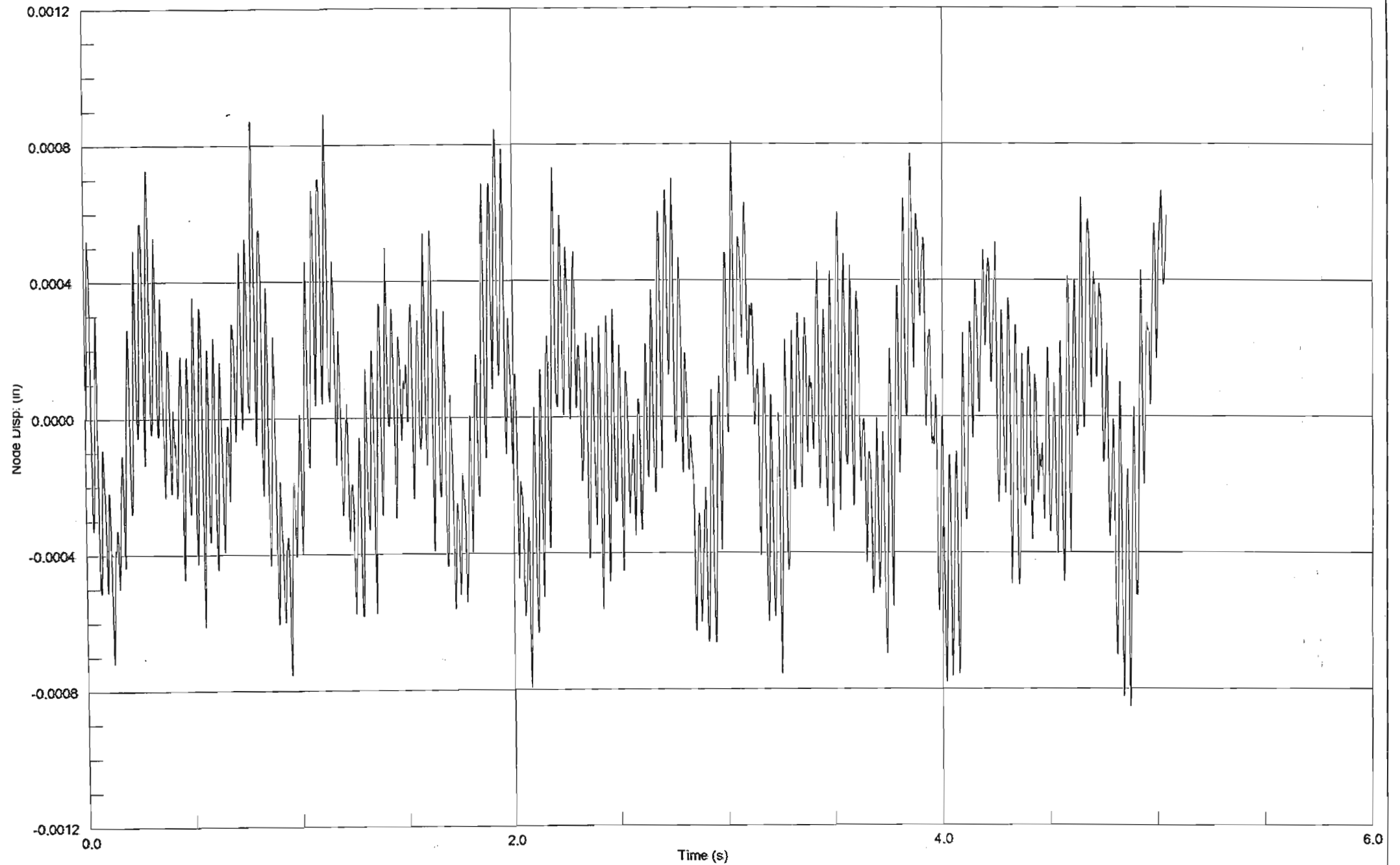


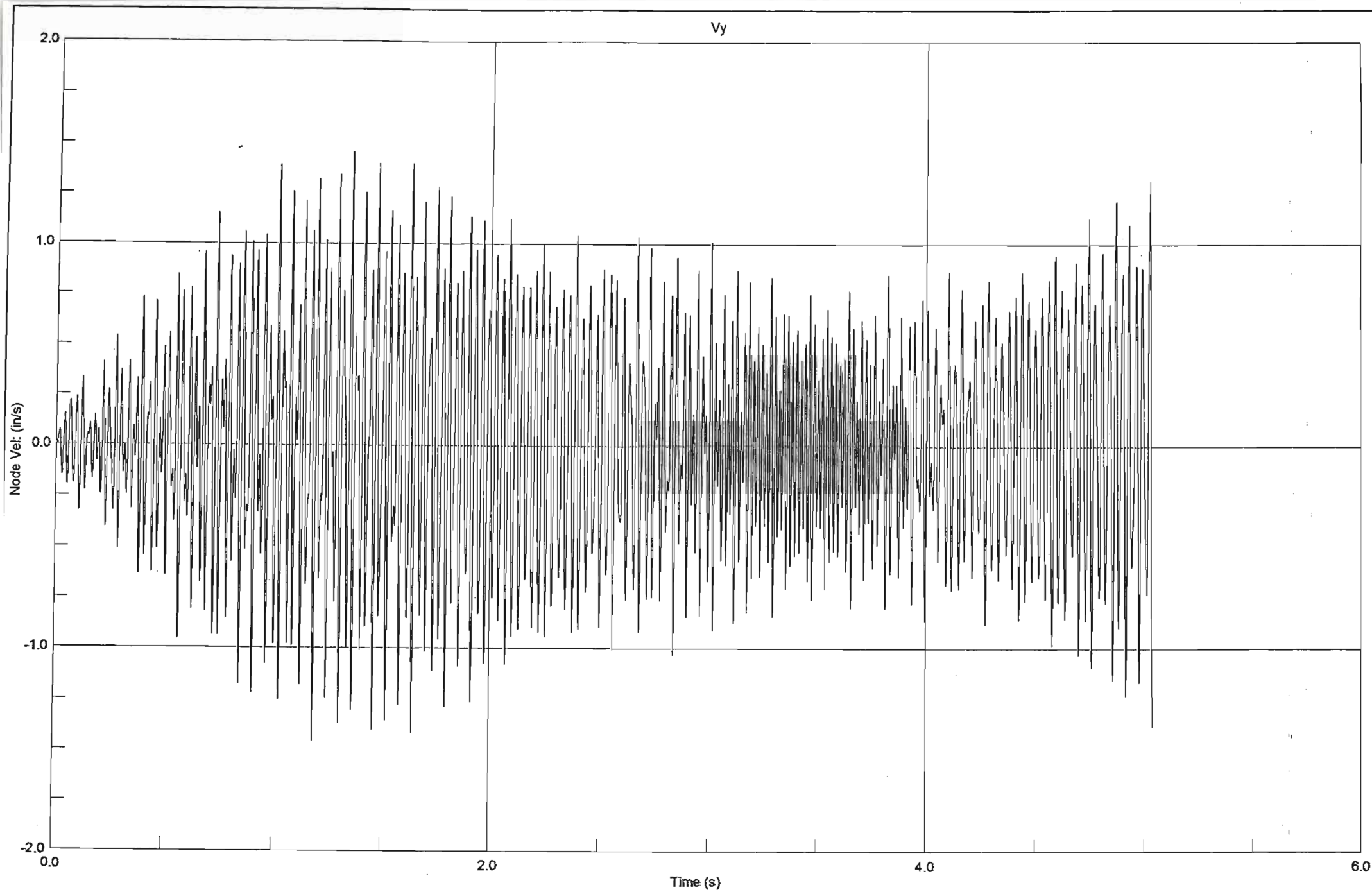


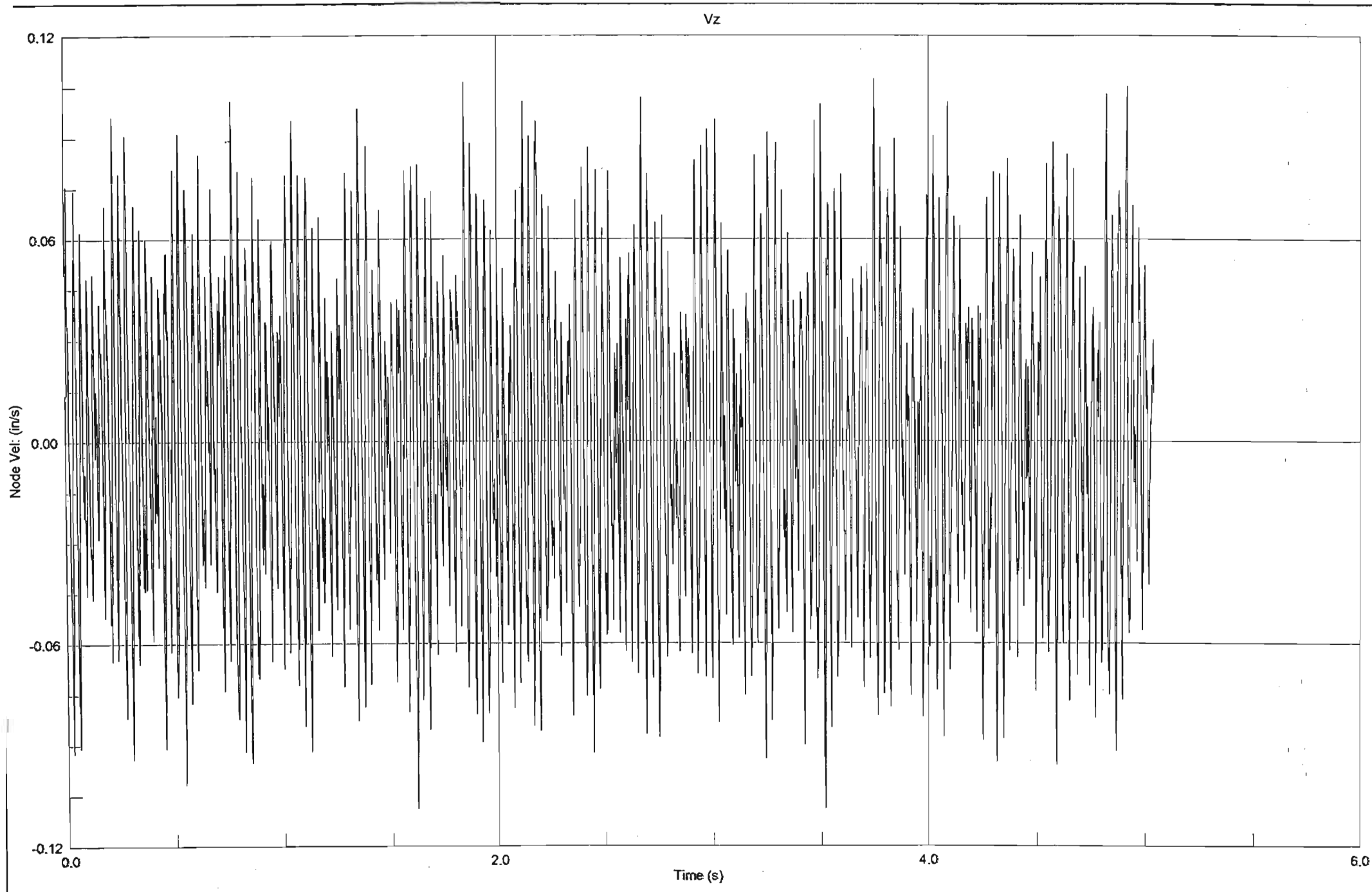


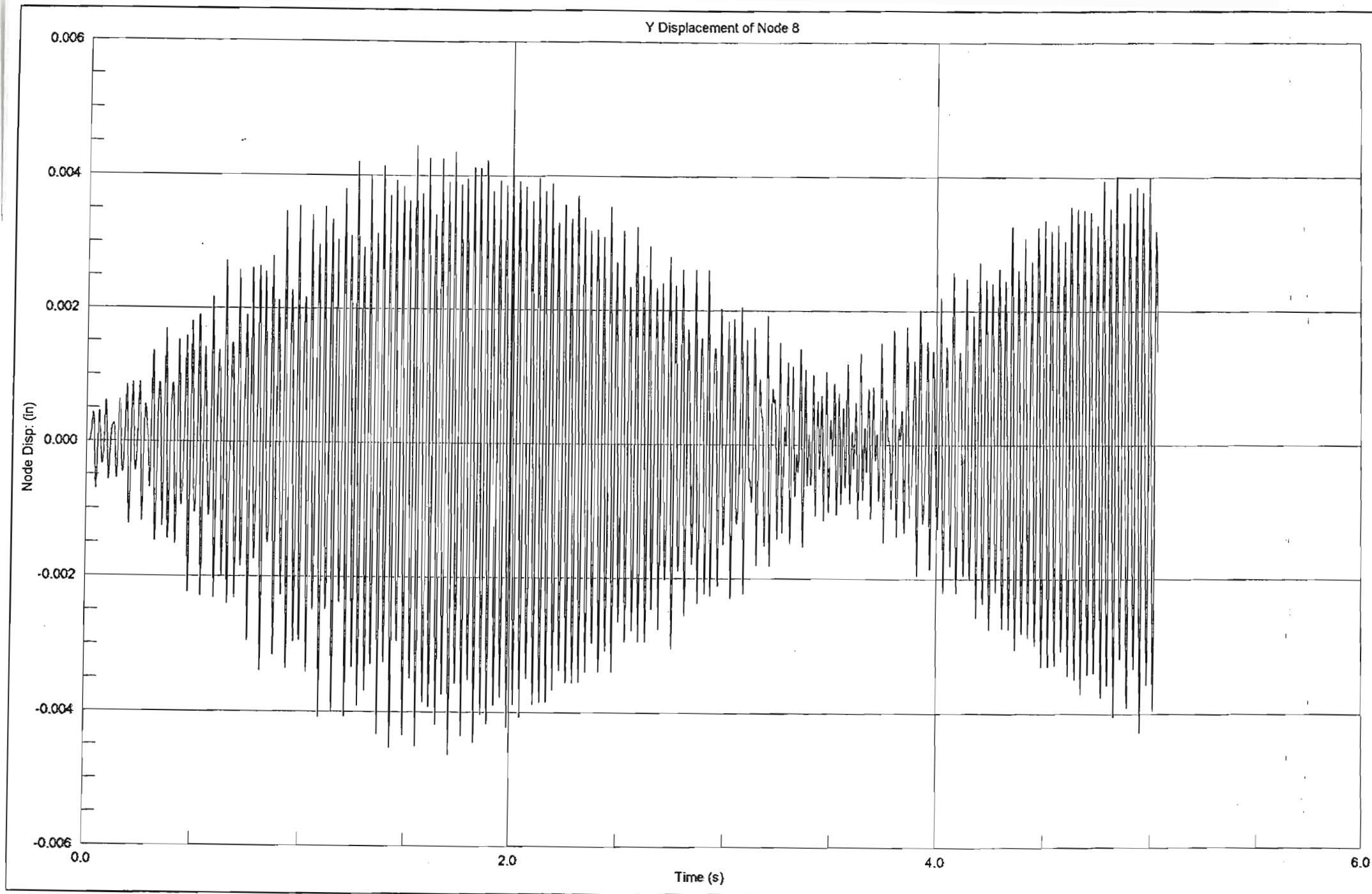


Z Displacement of Node 20

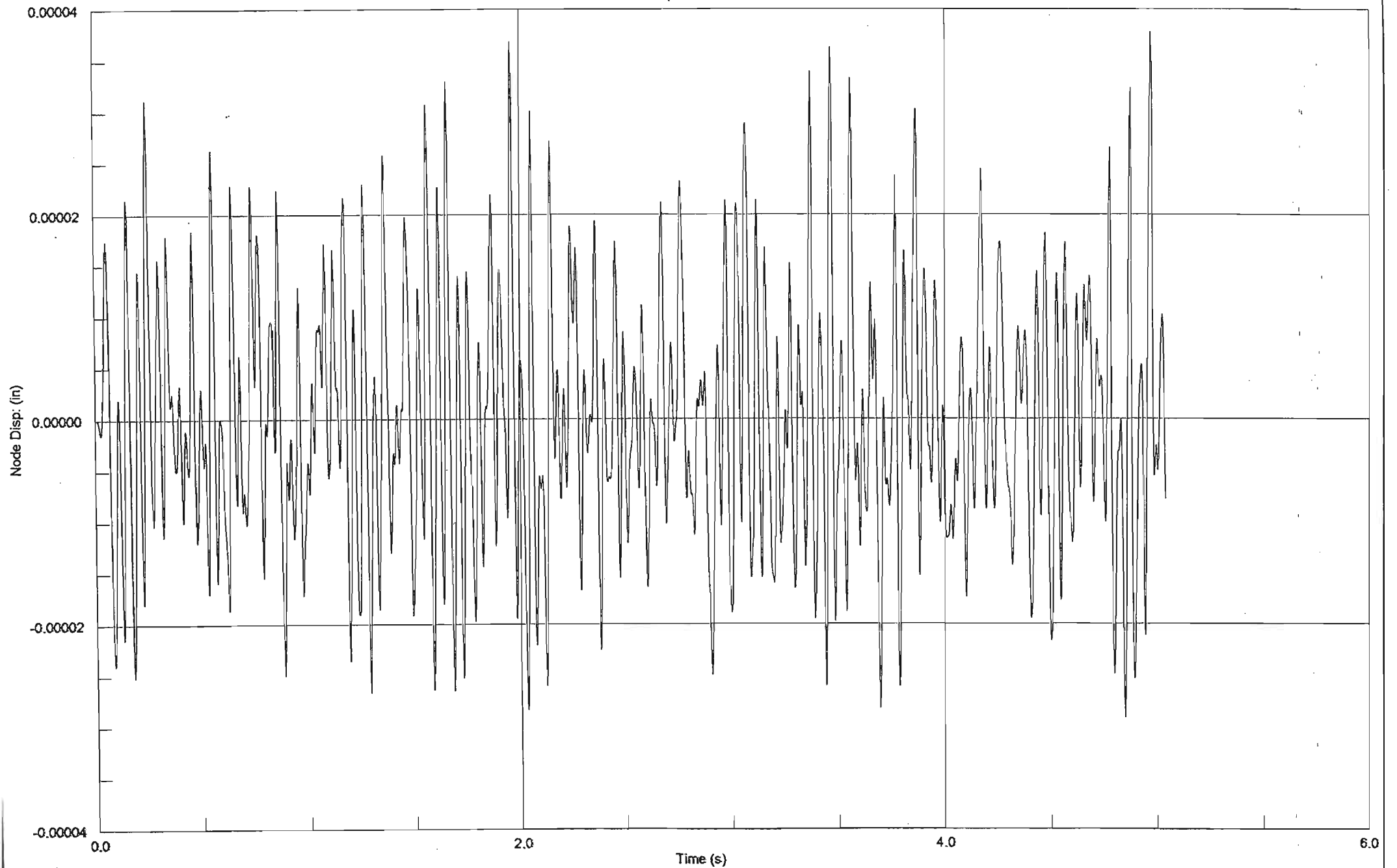


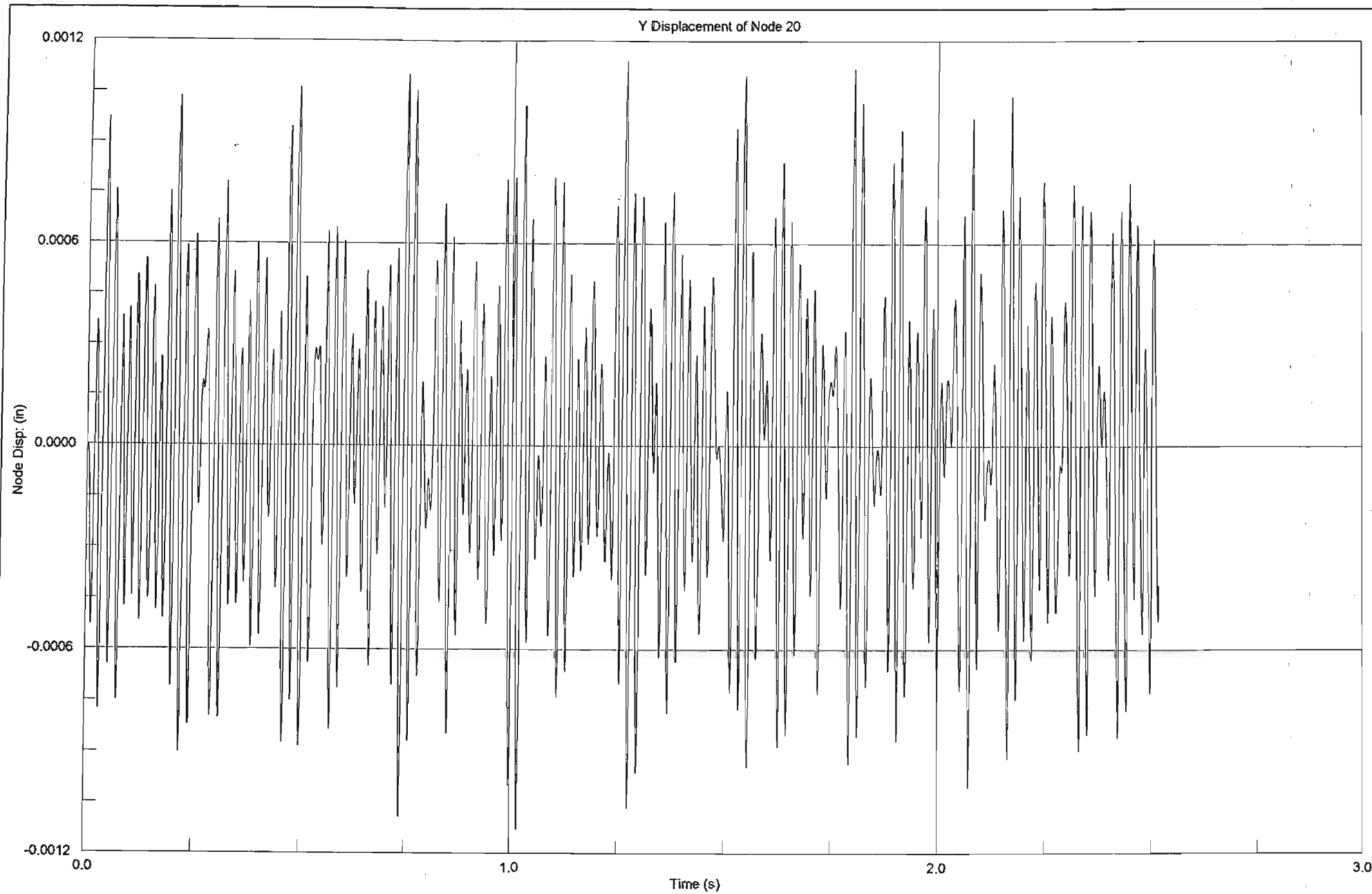




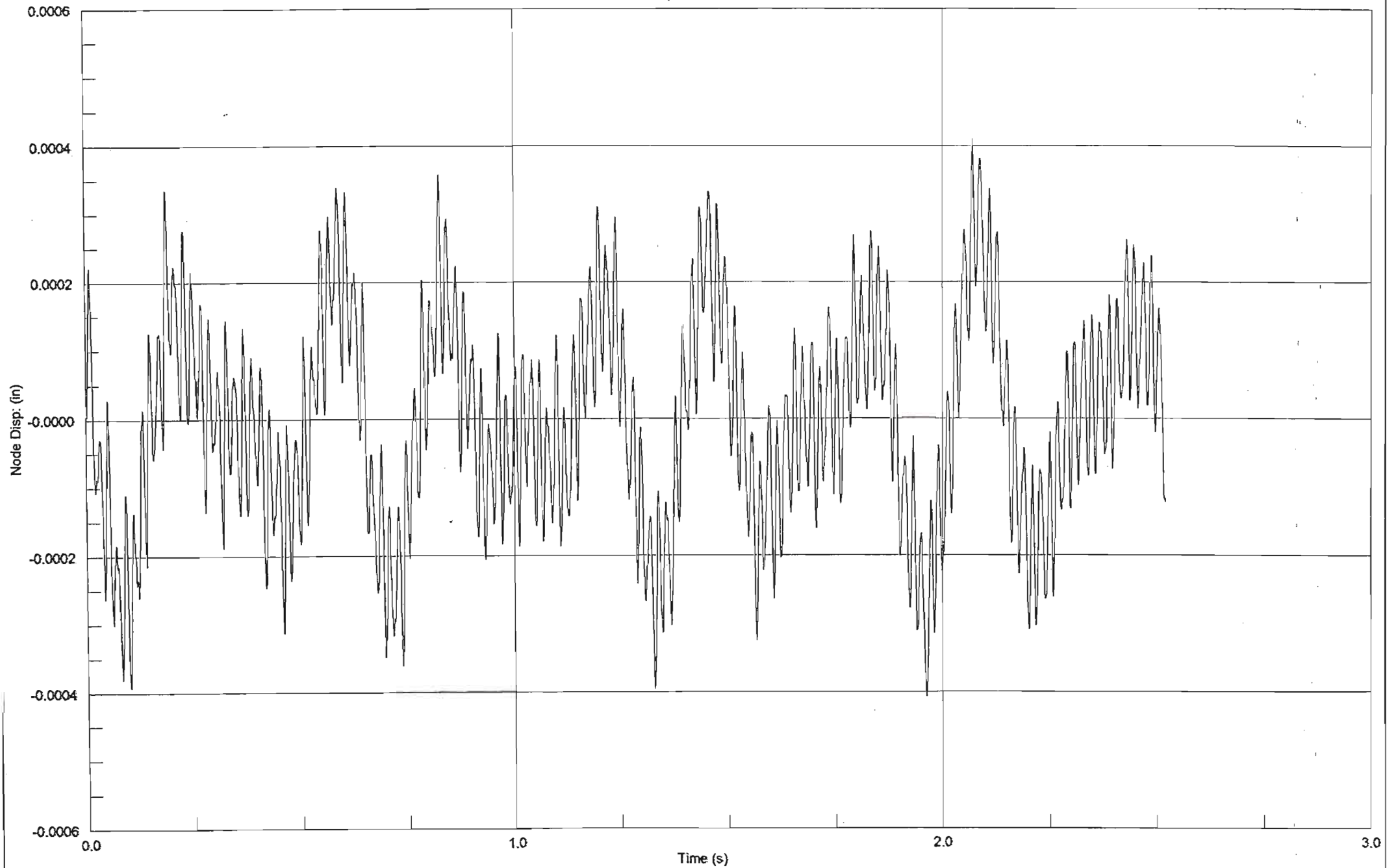


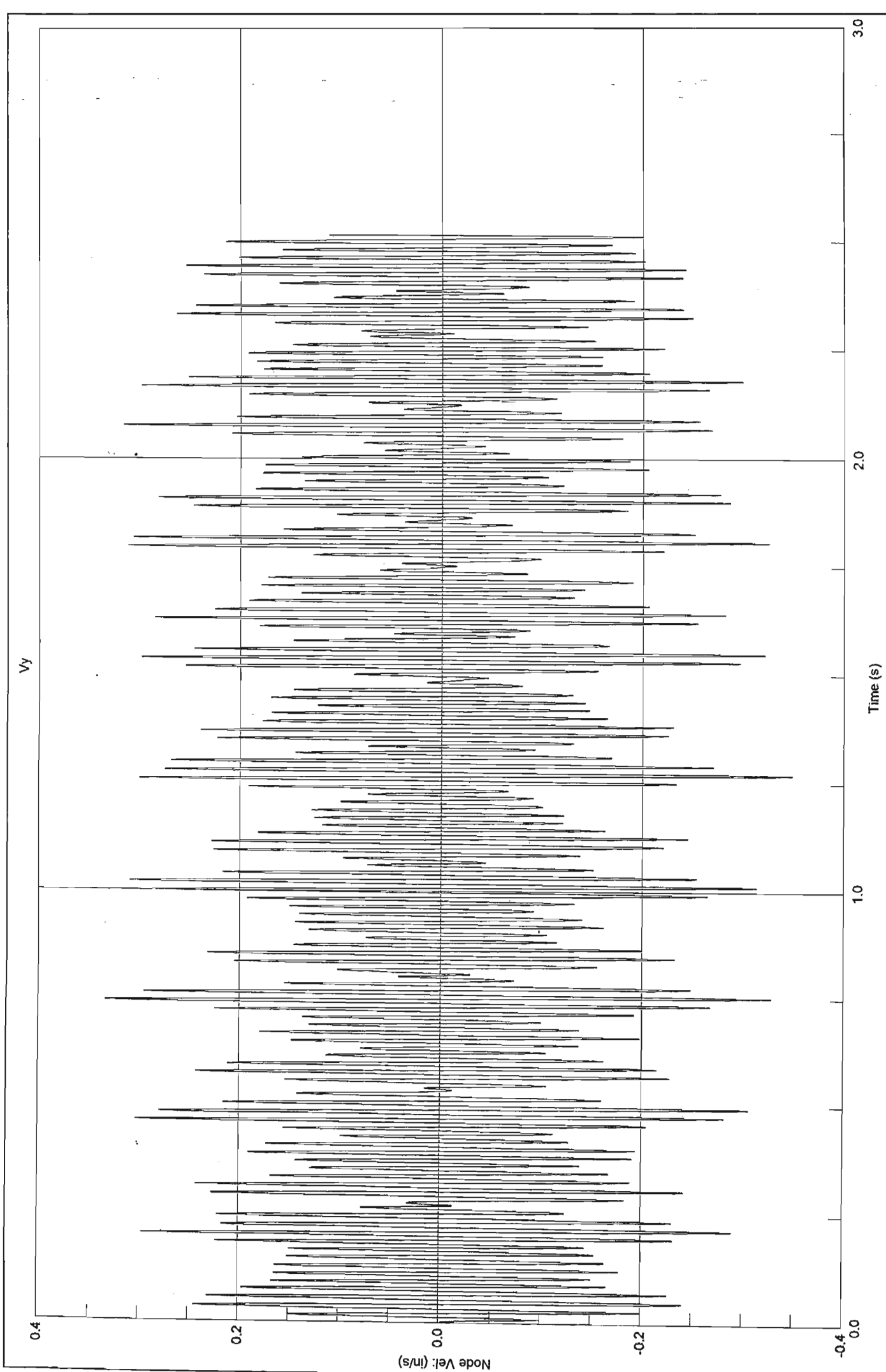
Z Displacement of Node 8



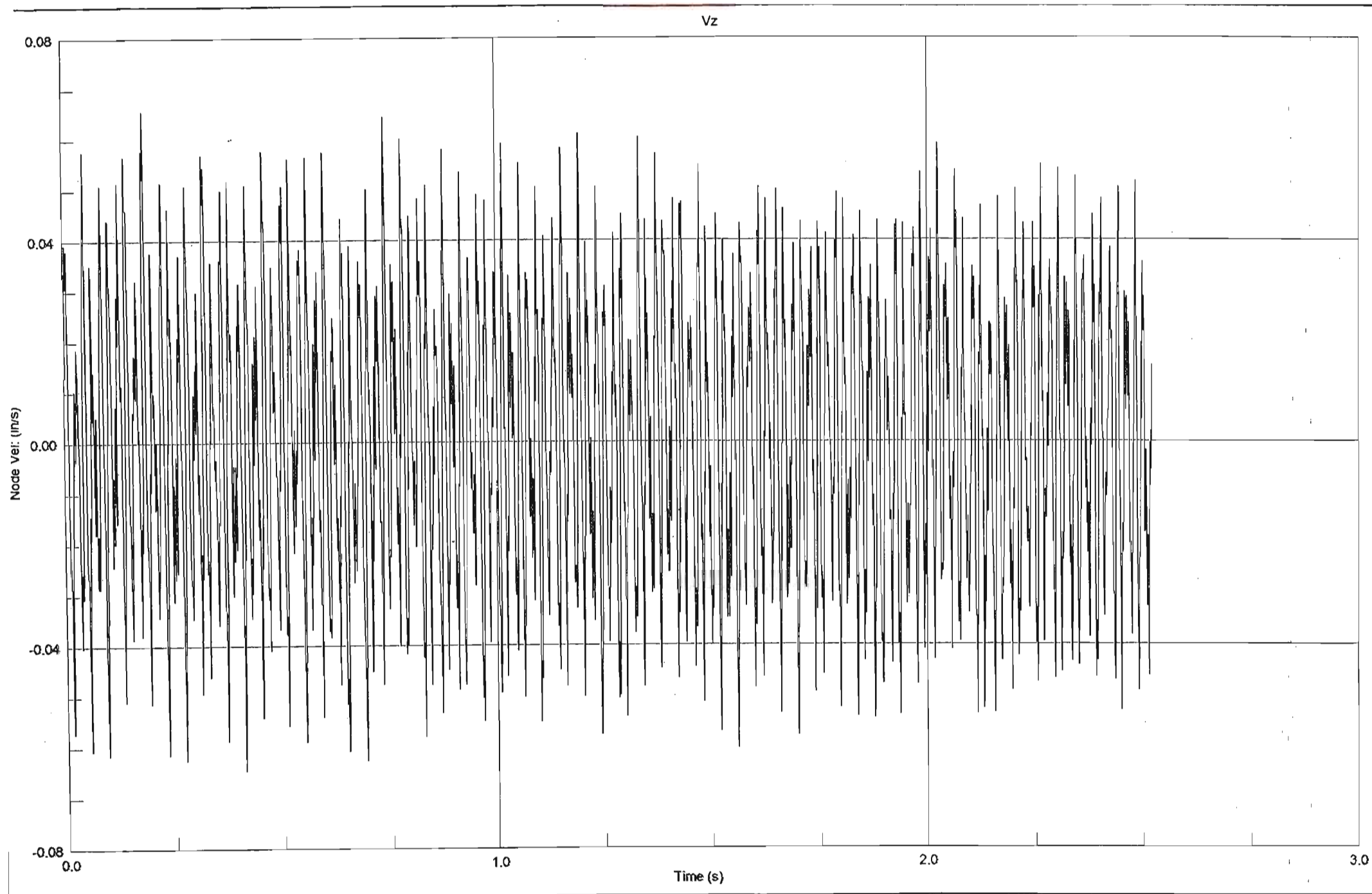


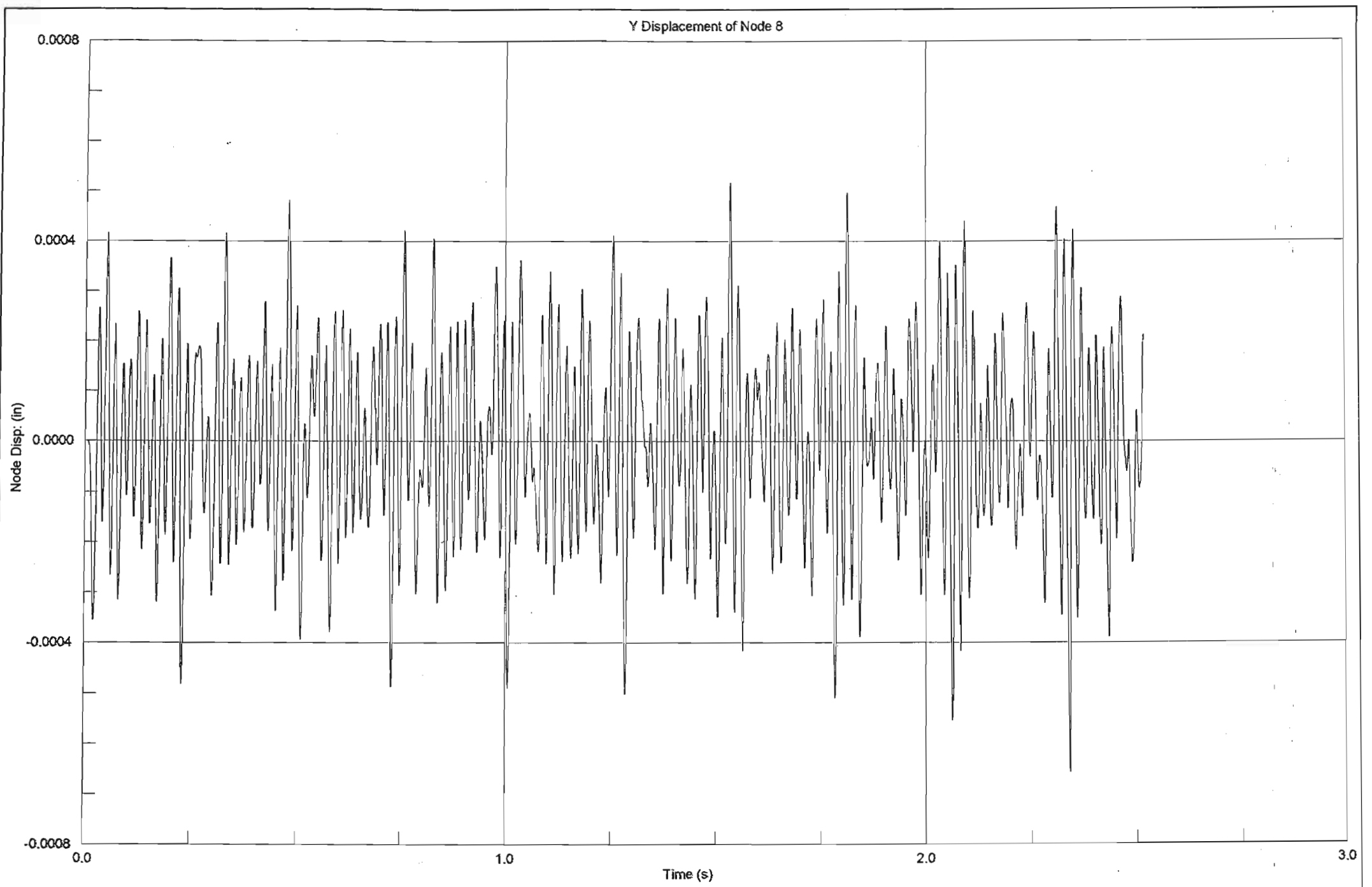
Z Displacement of Node 20



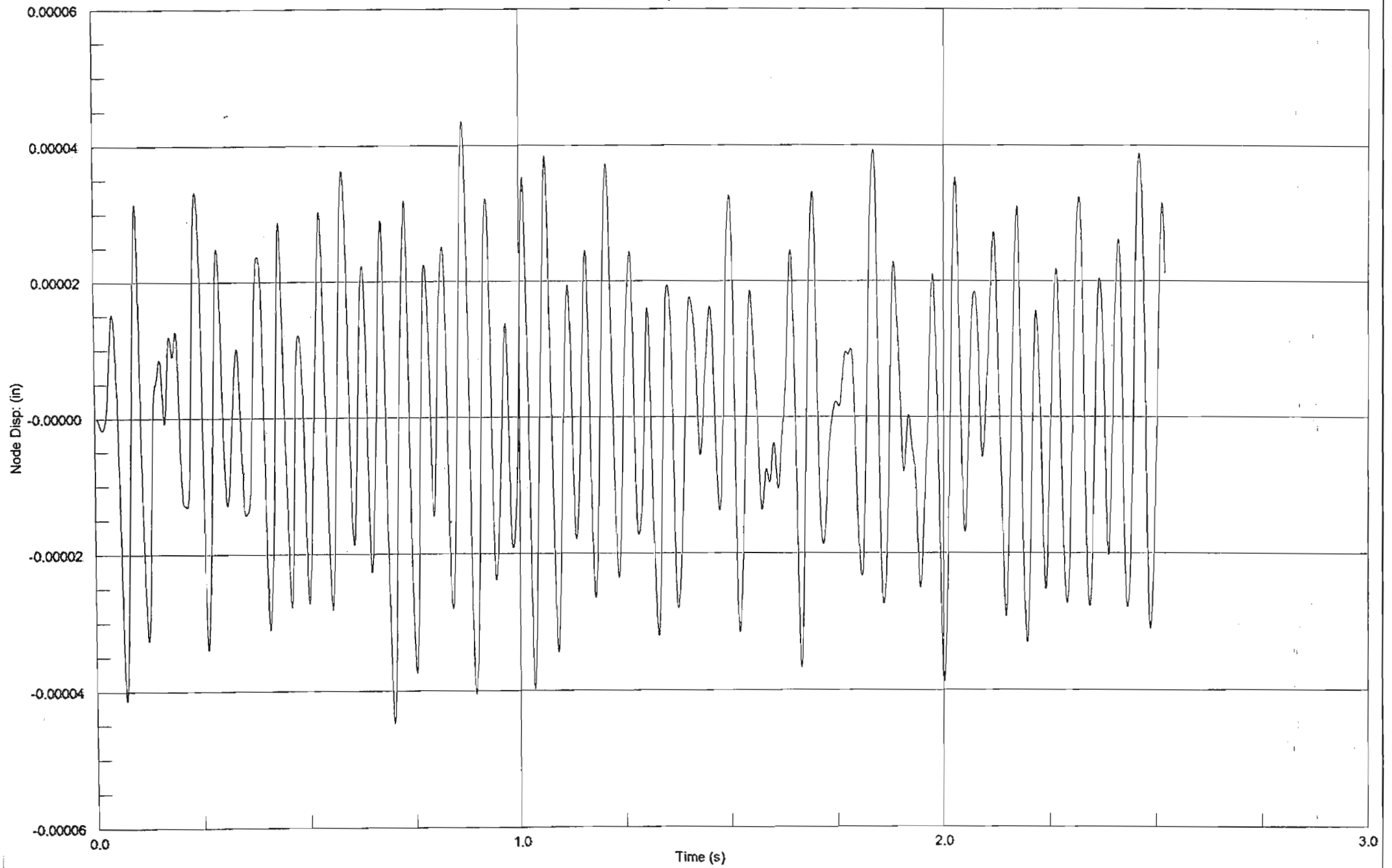


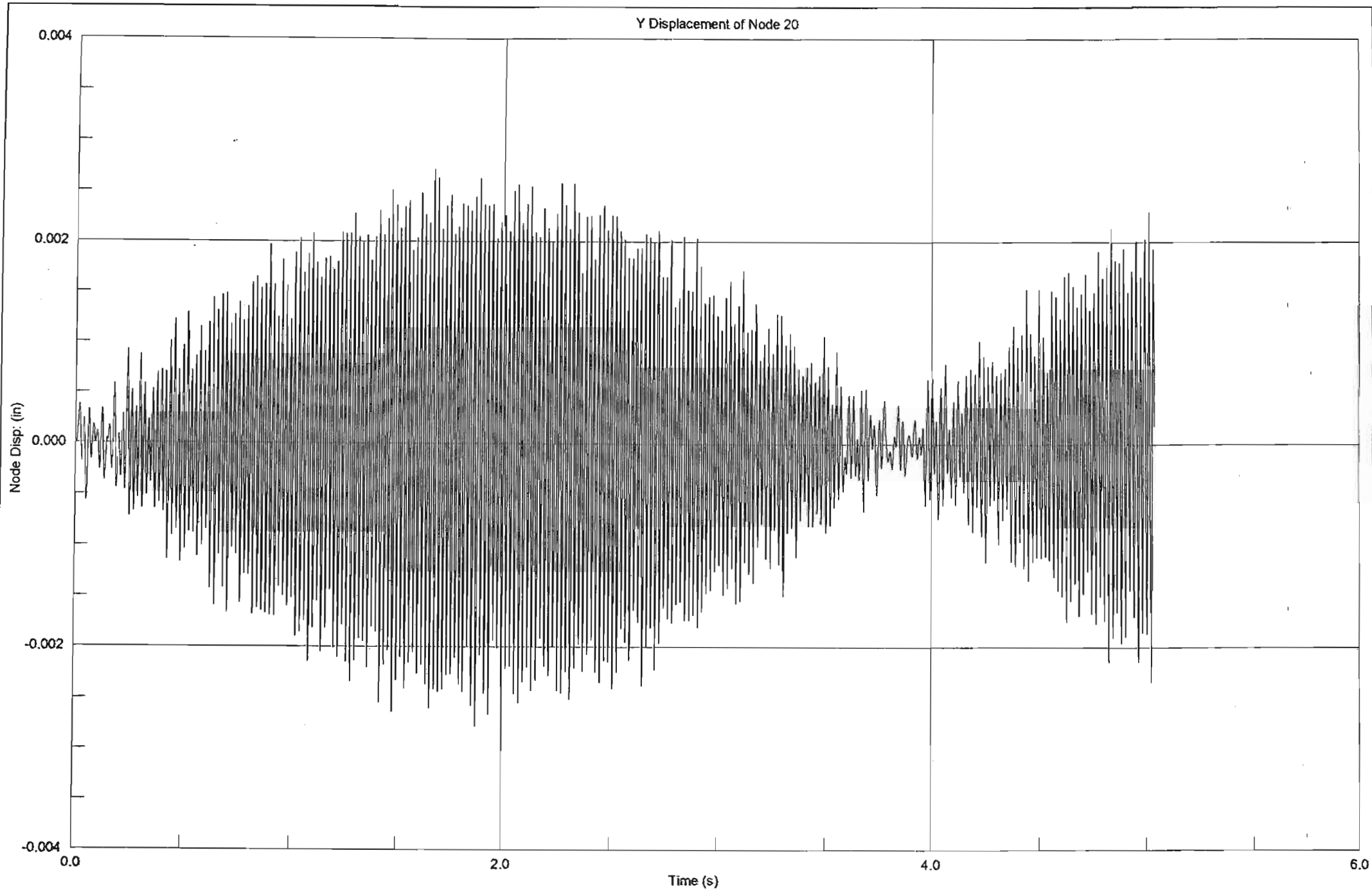
D 3.39

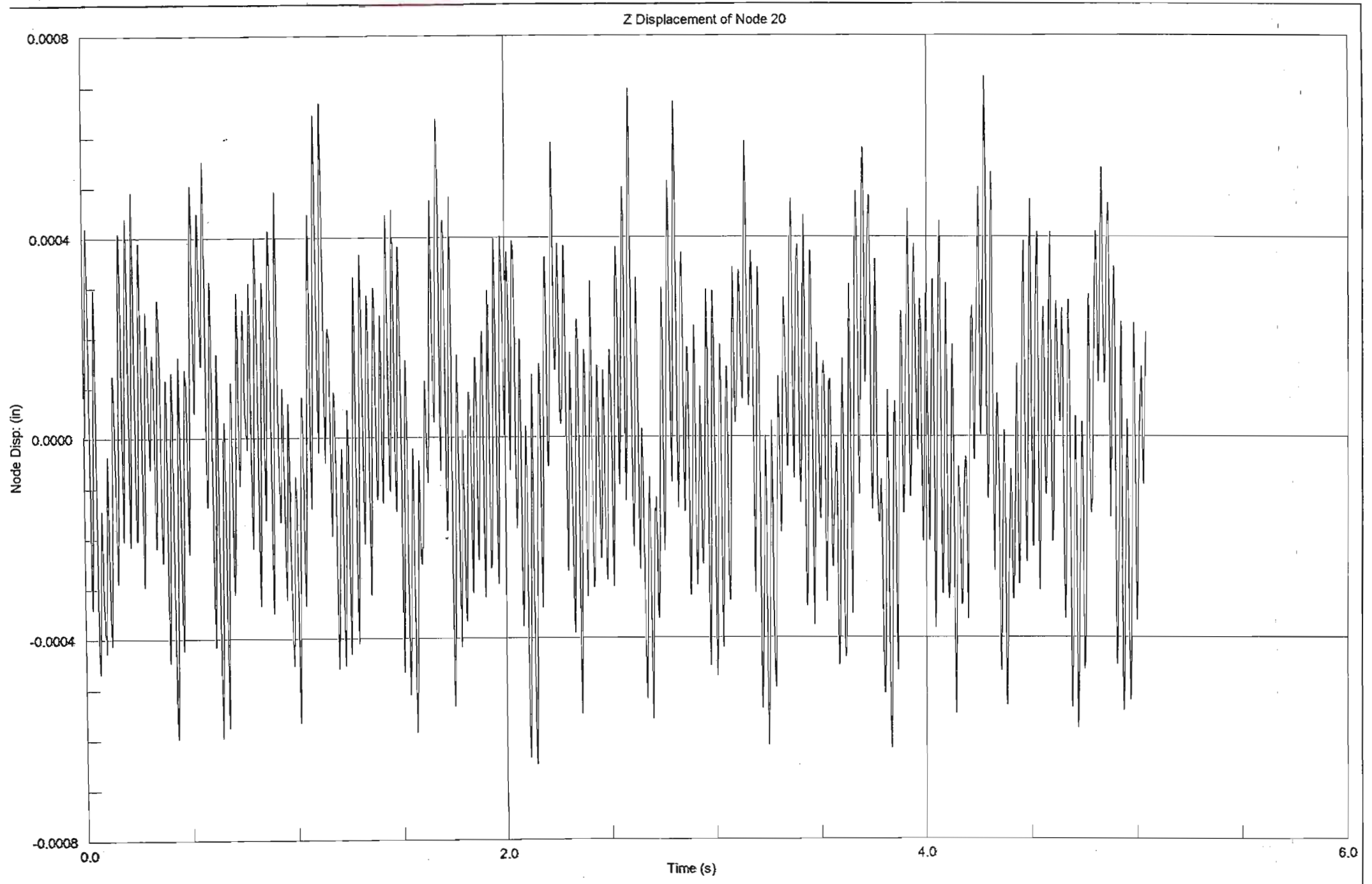


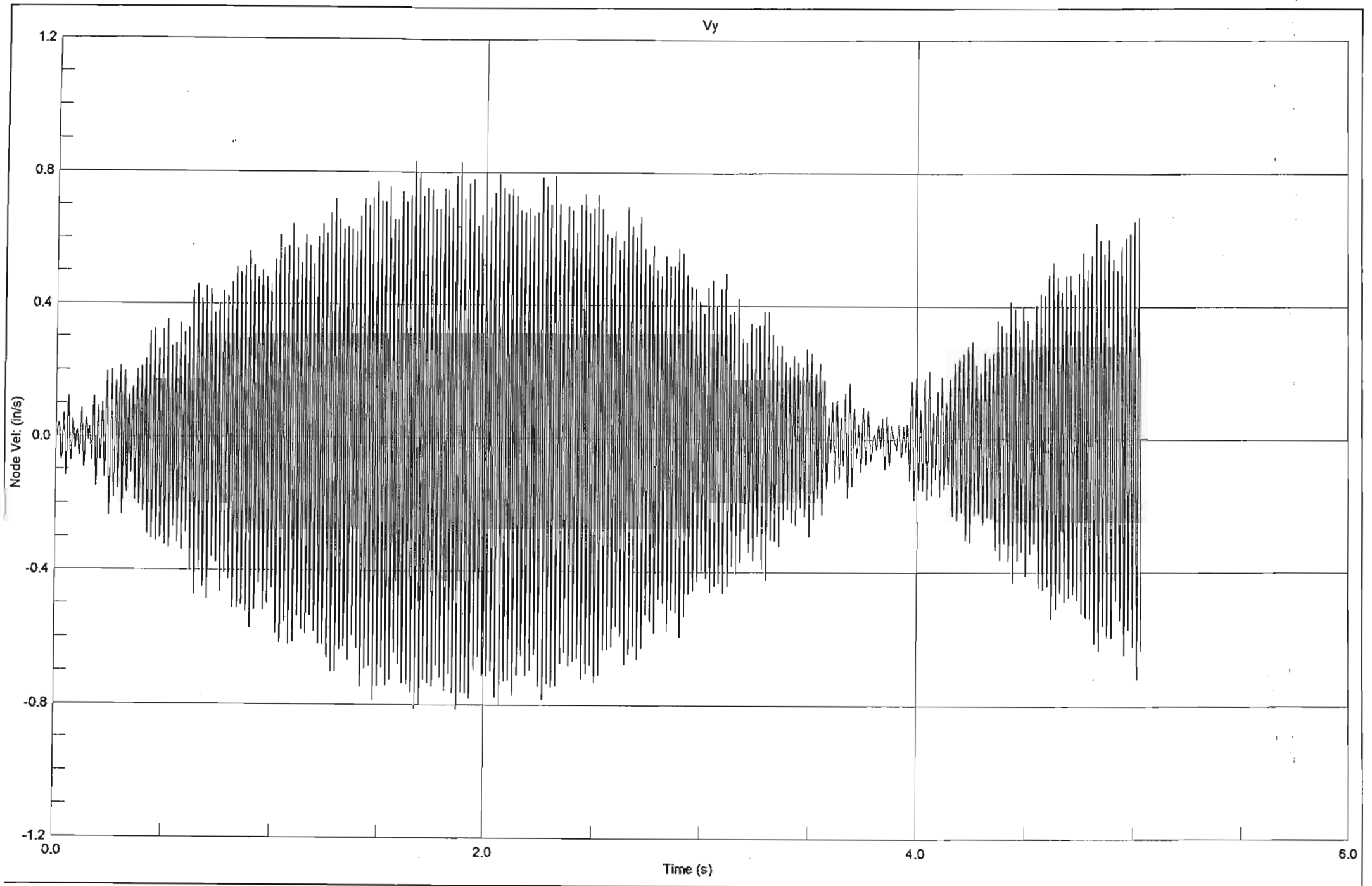


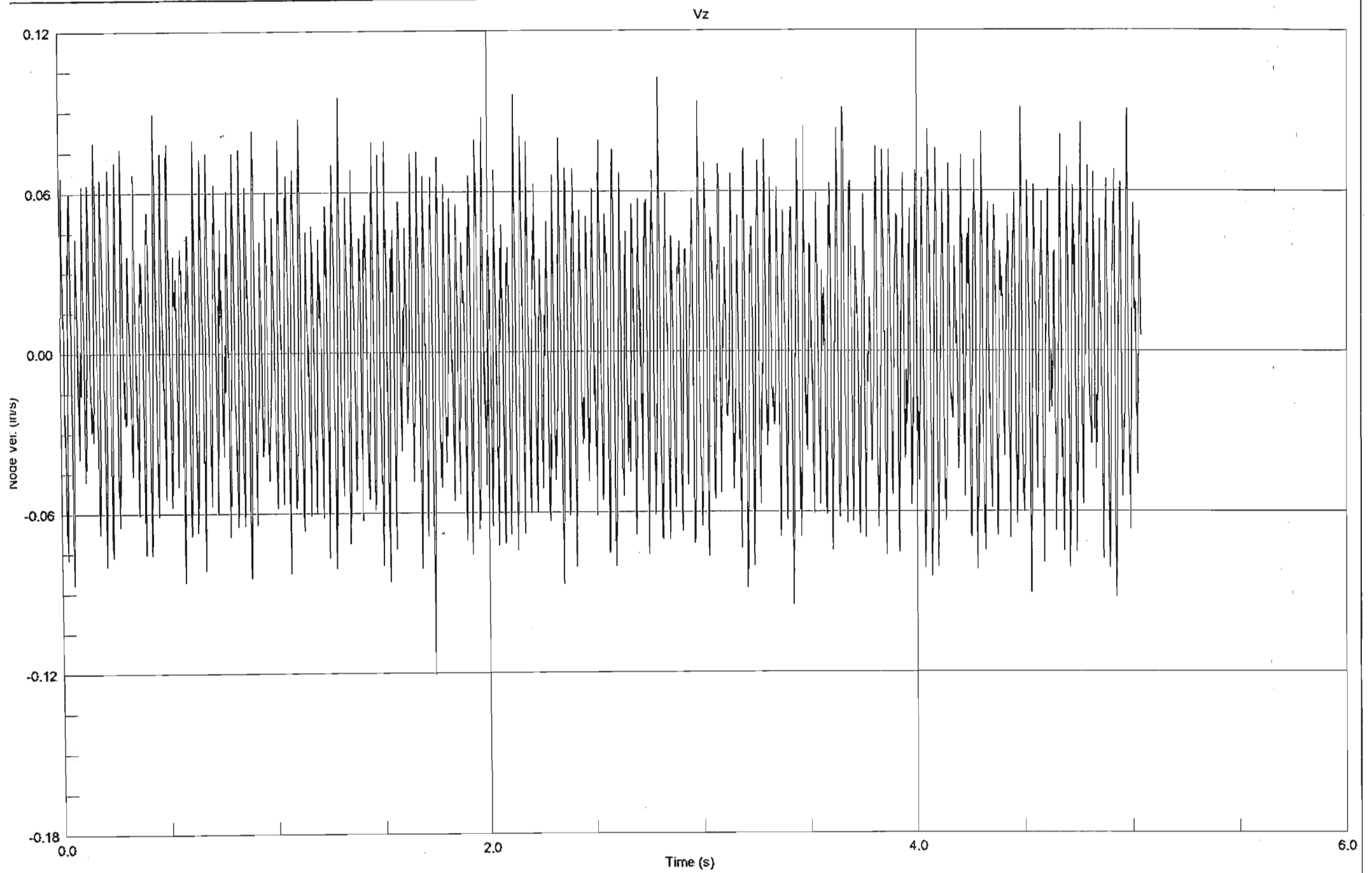
Z Displacement of Node 8

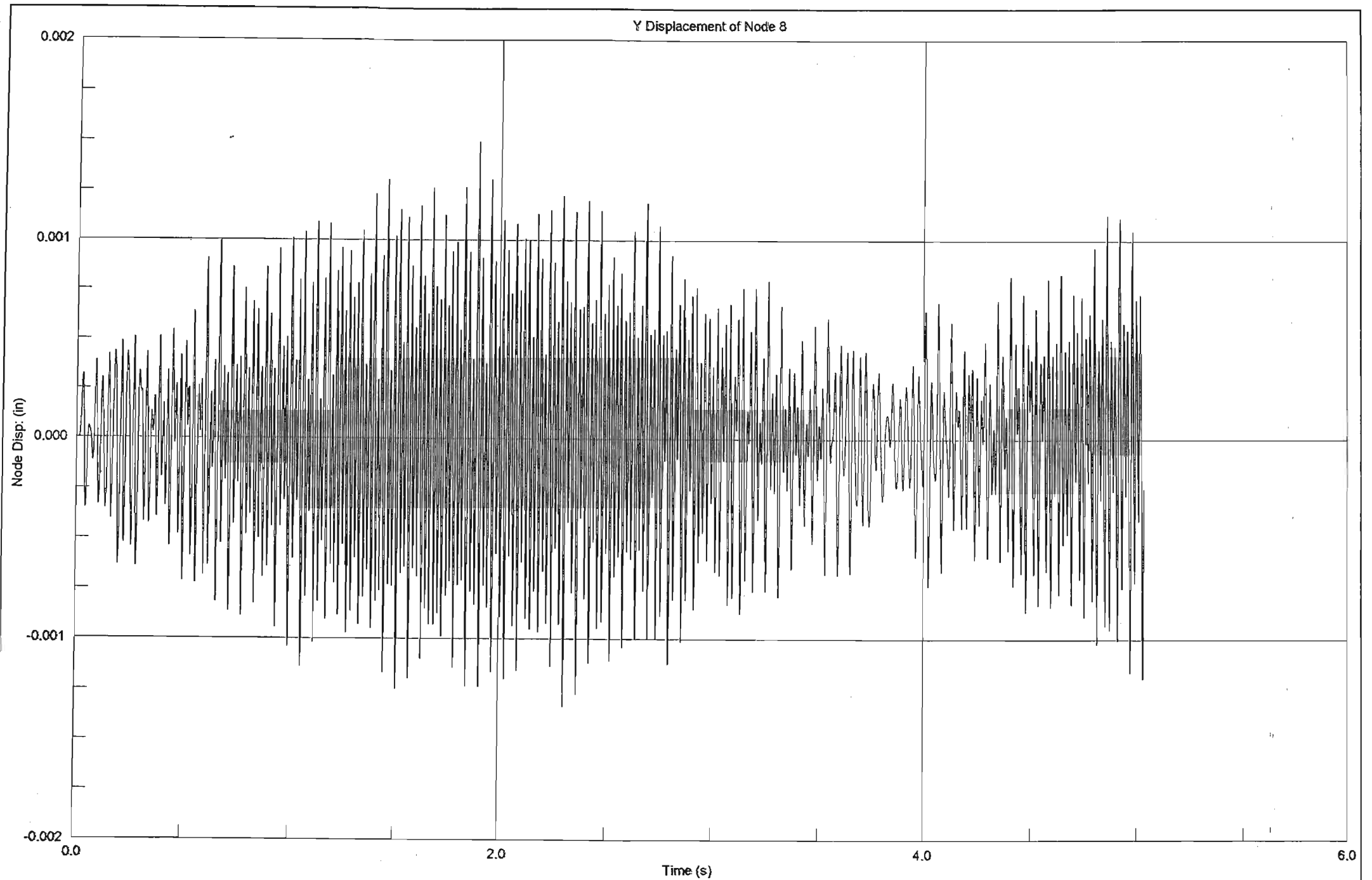




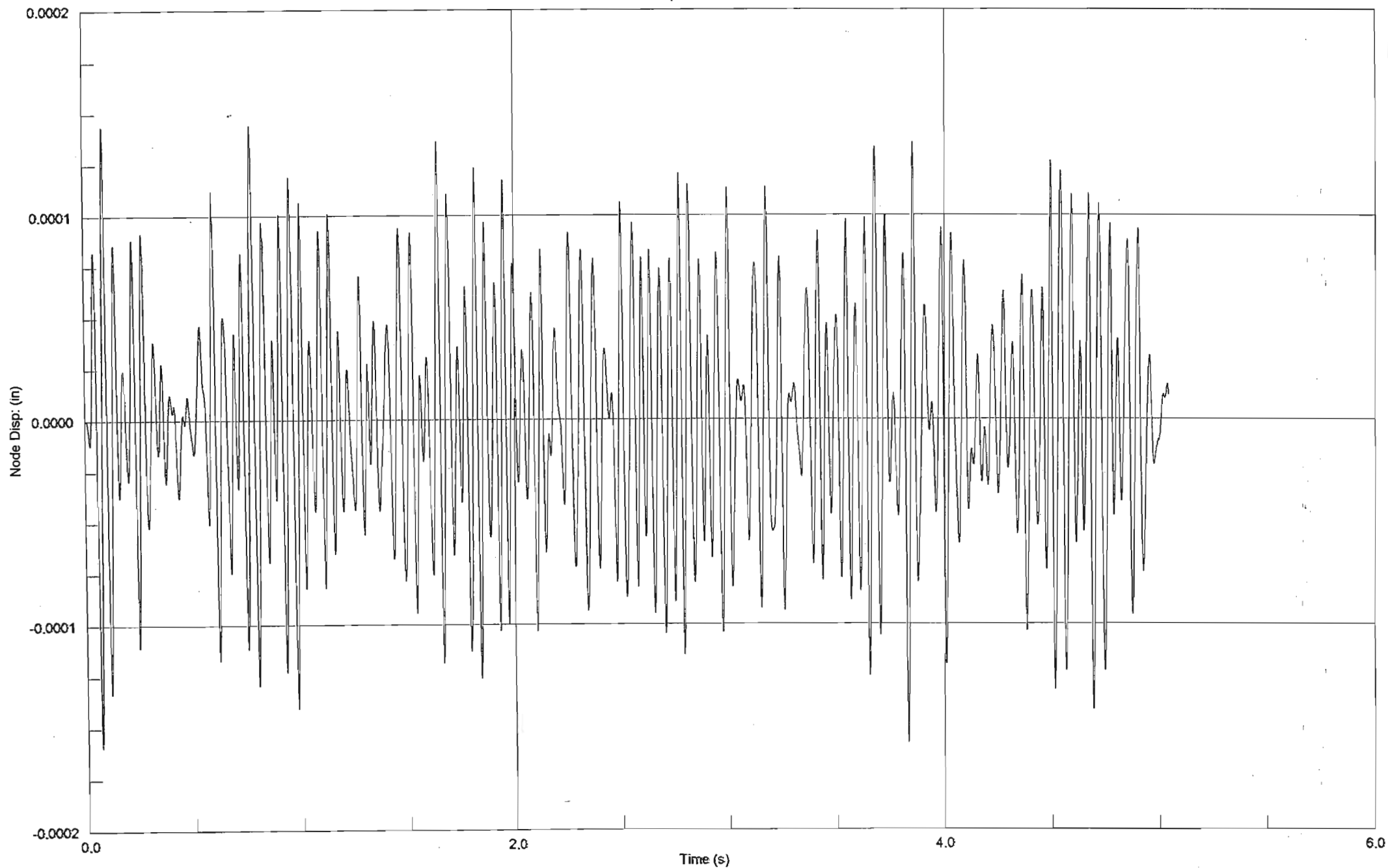


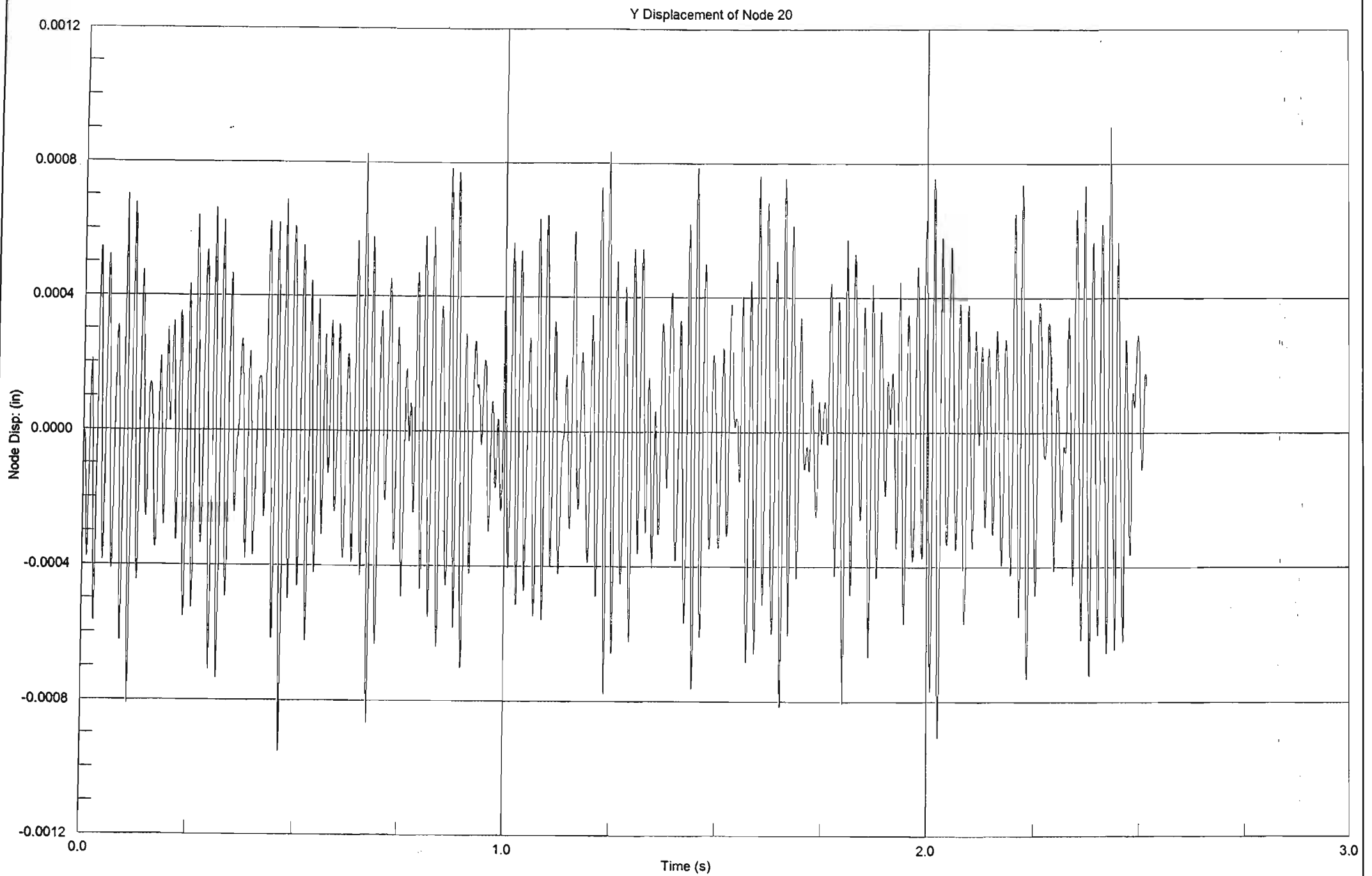




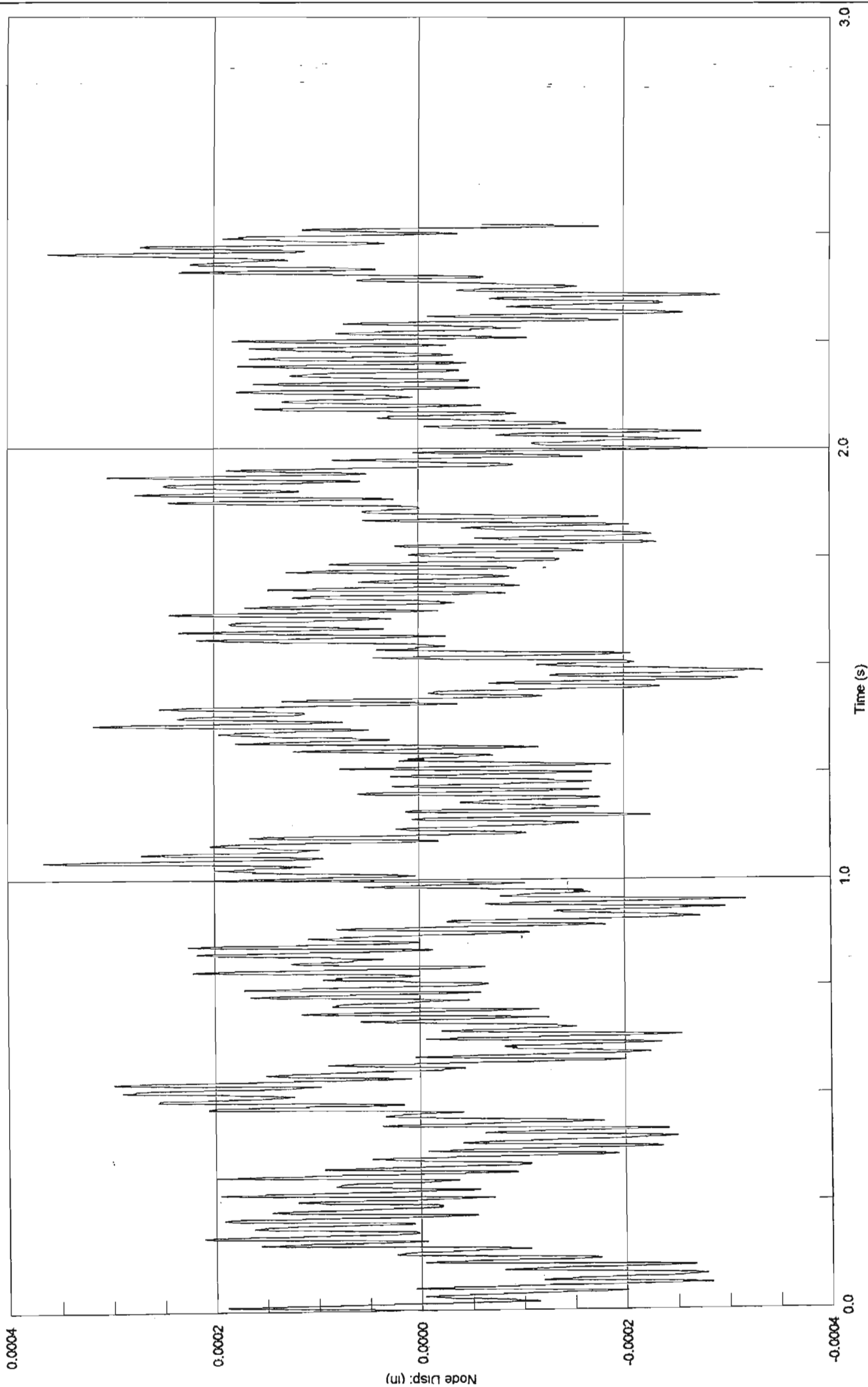


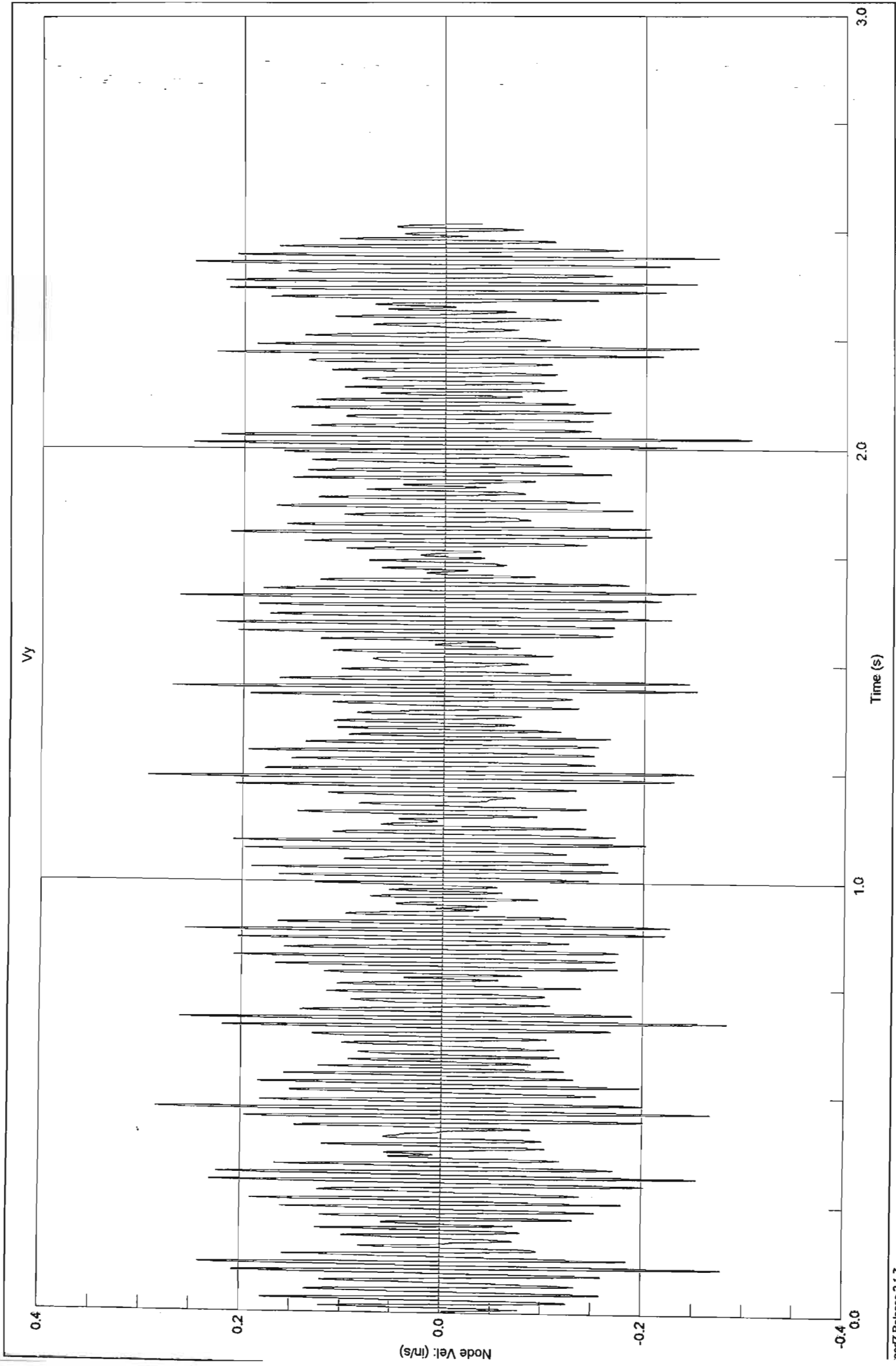
Z Displacement of Node 8





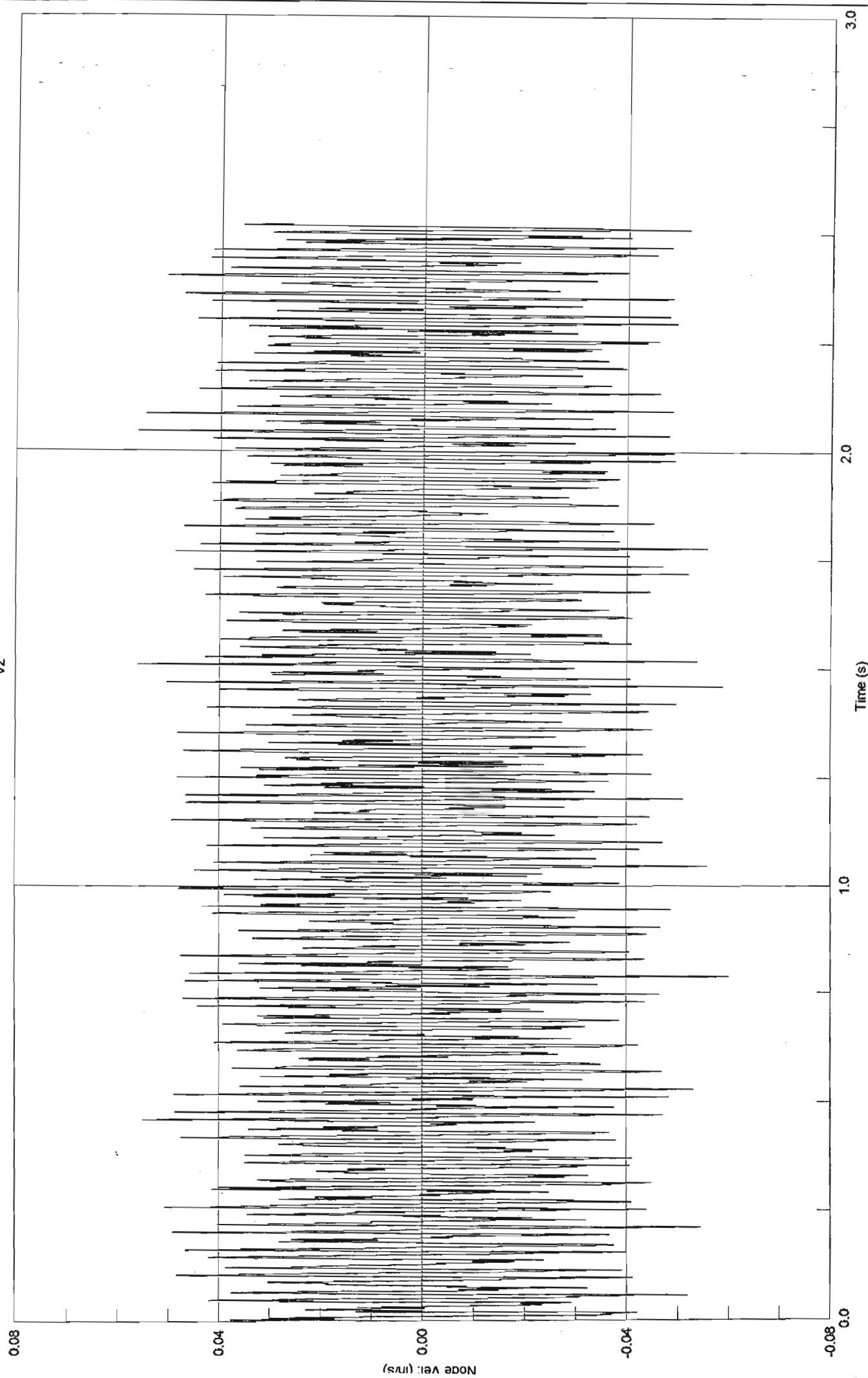
Z Displacement of Node 20

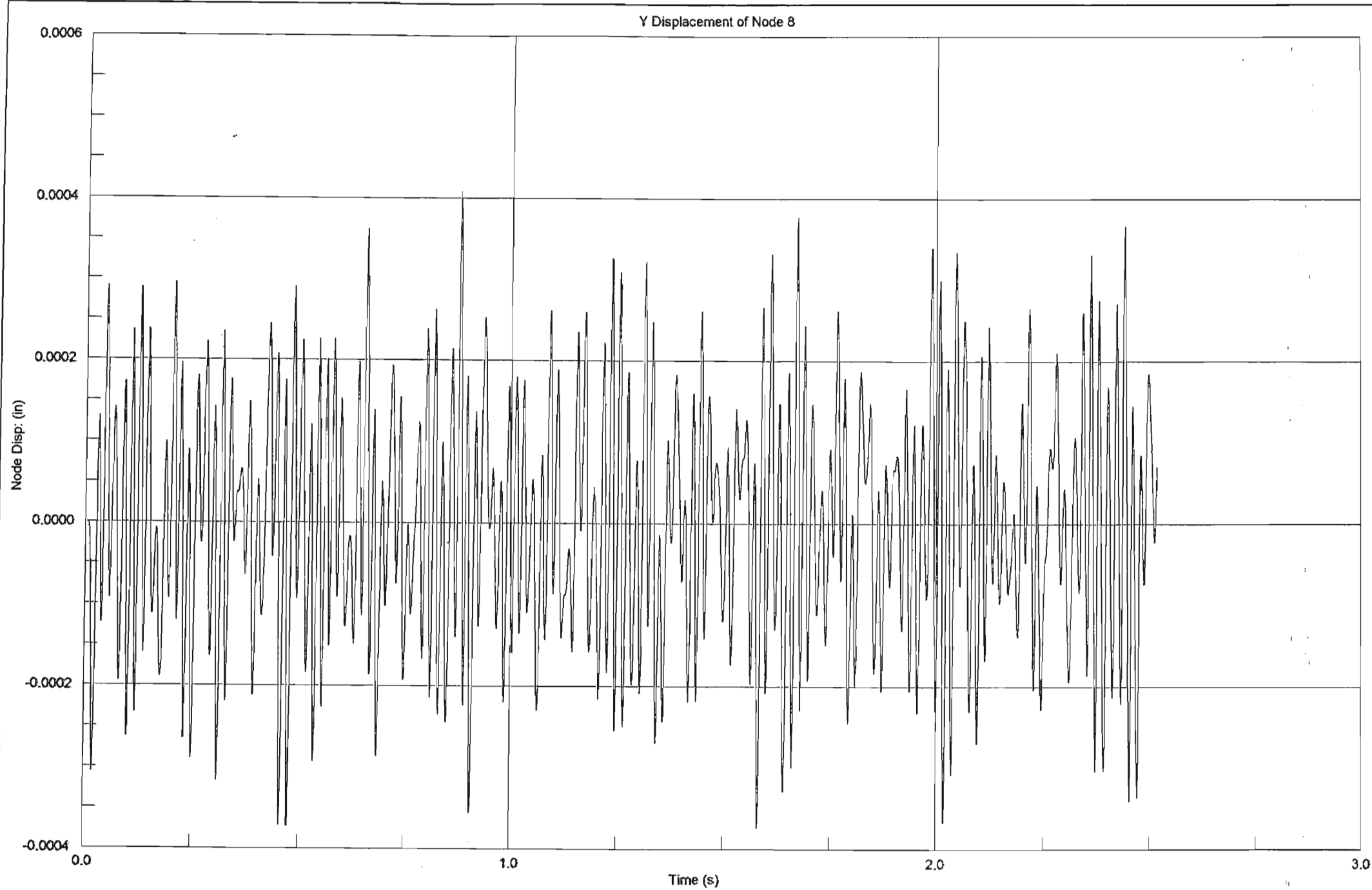




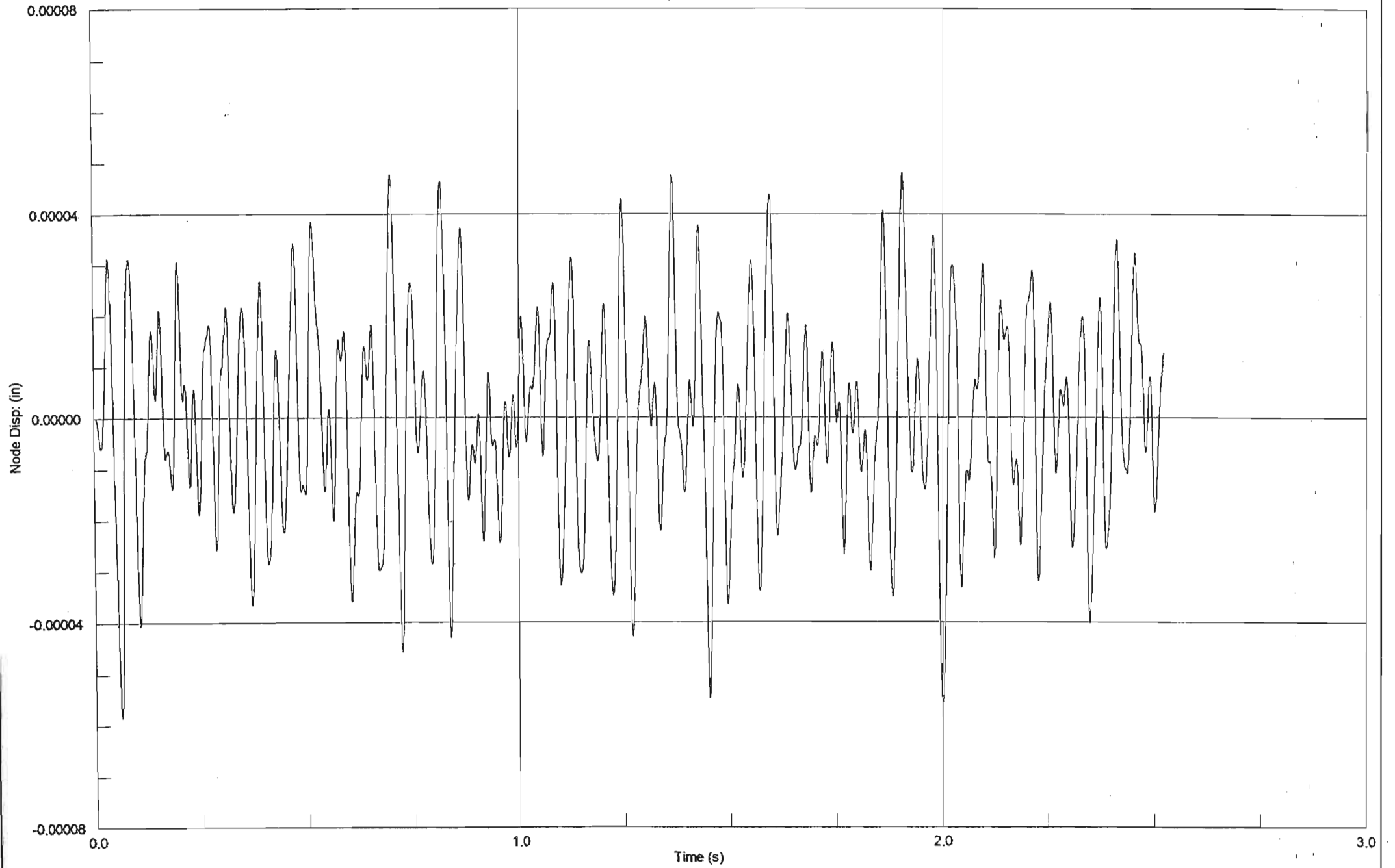
D 3.51

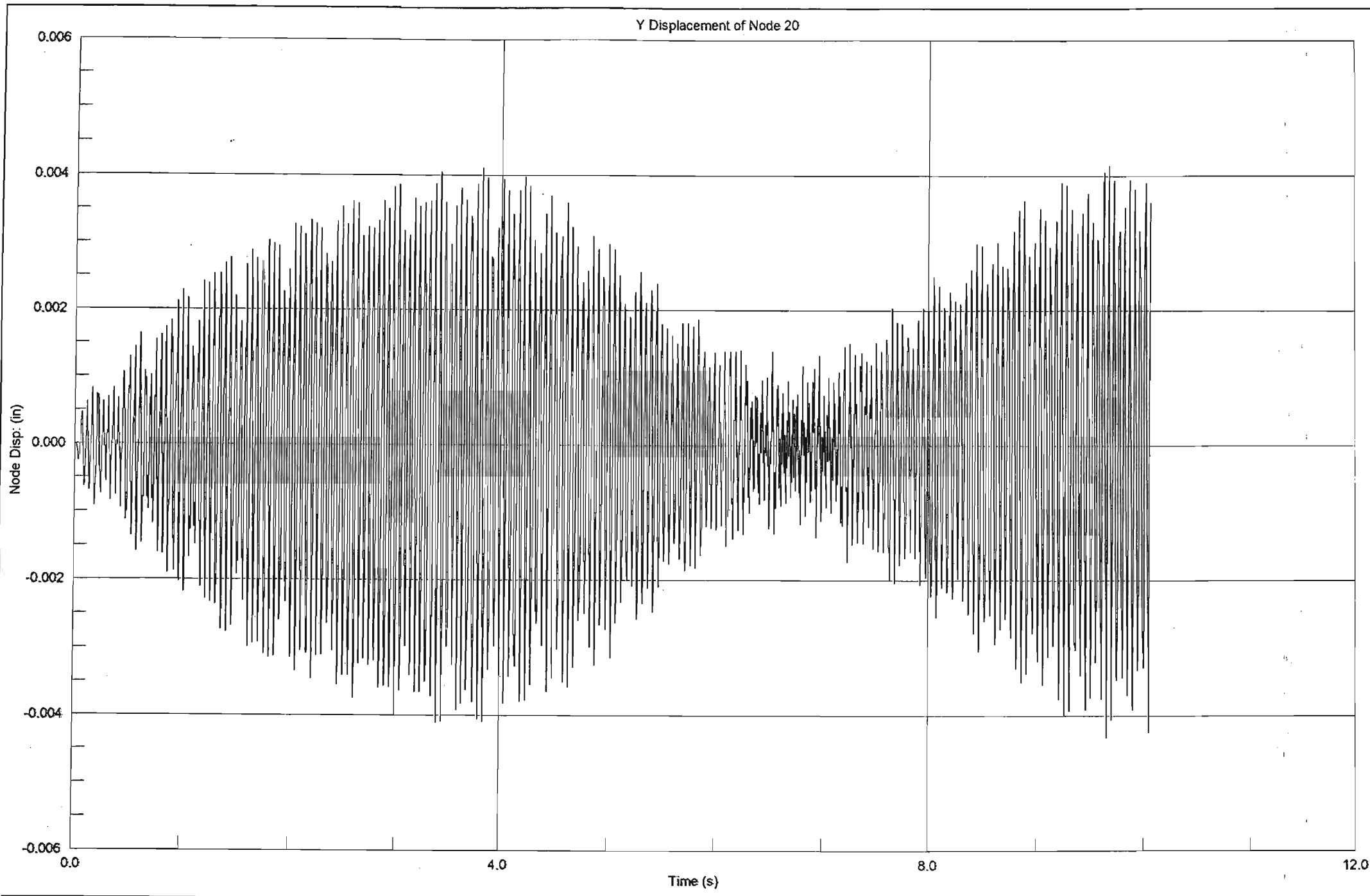
VZ



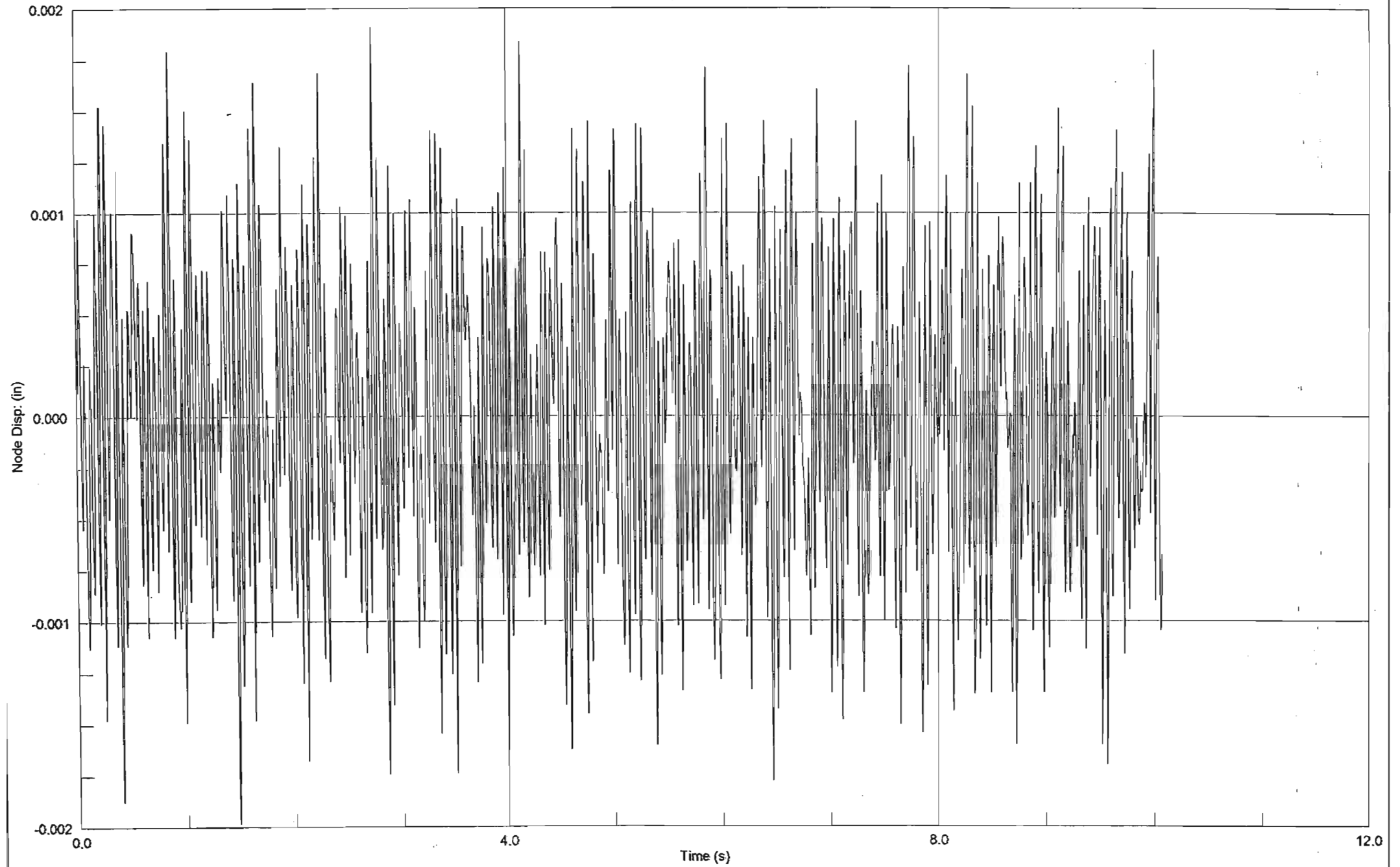


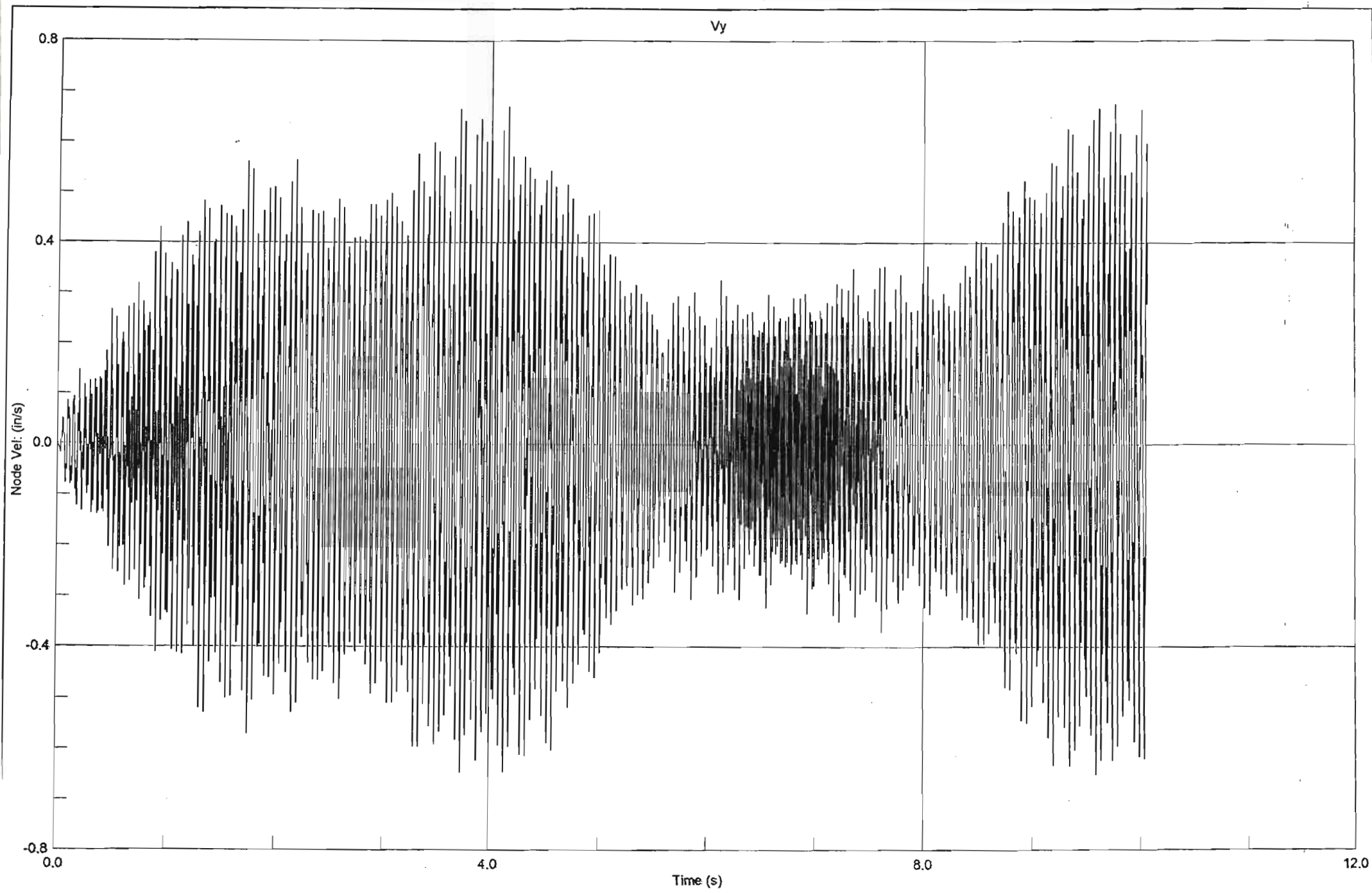
Z Displacement of Node 8





Z Displacement of Node 20





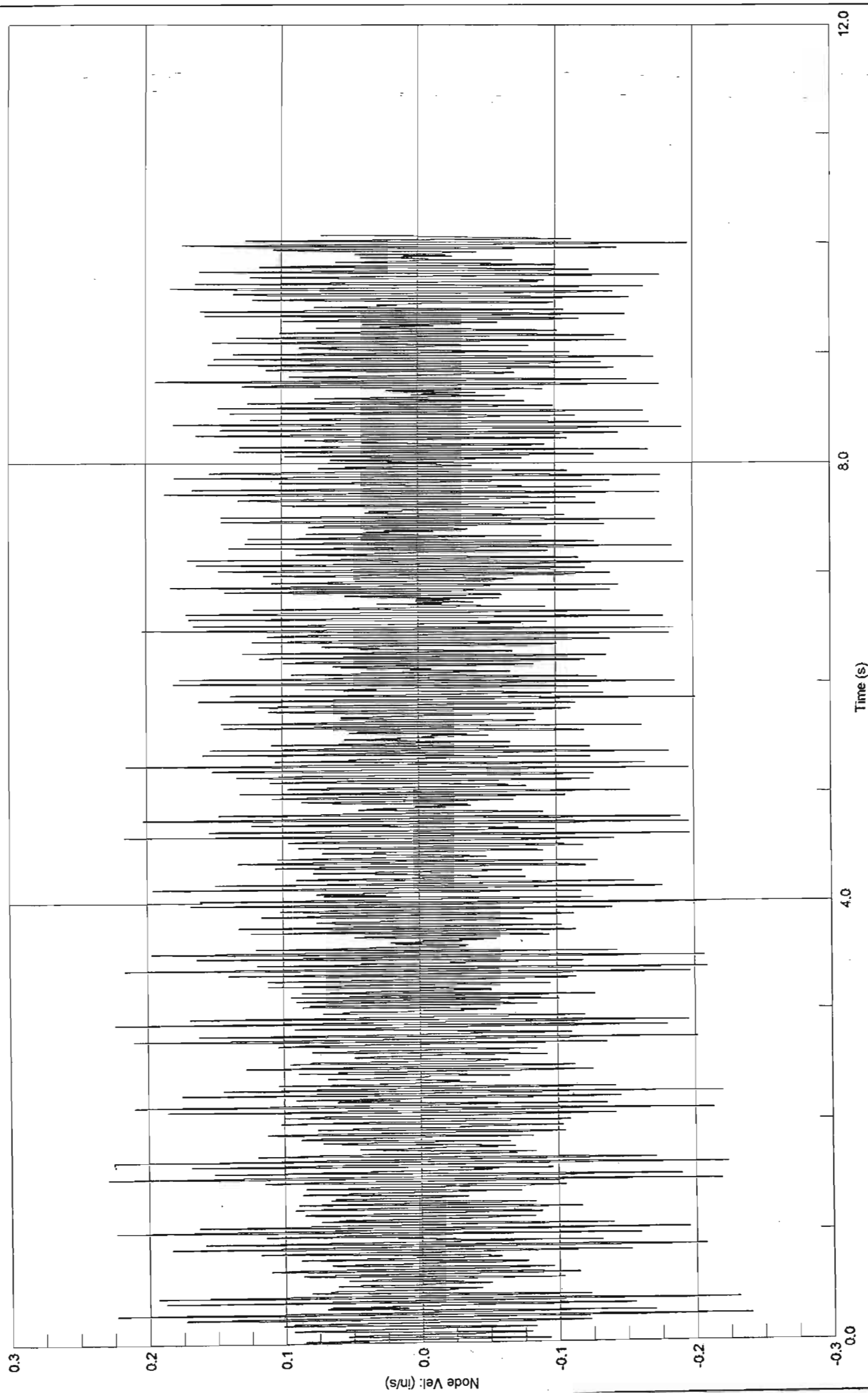
Strand7 Release 2.1.7

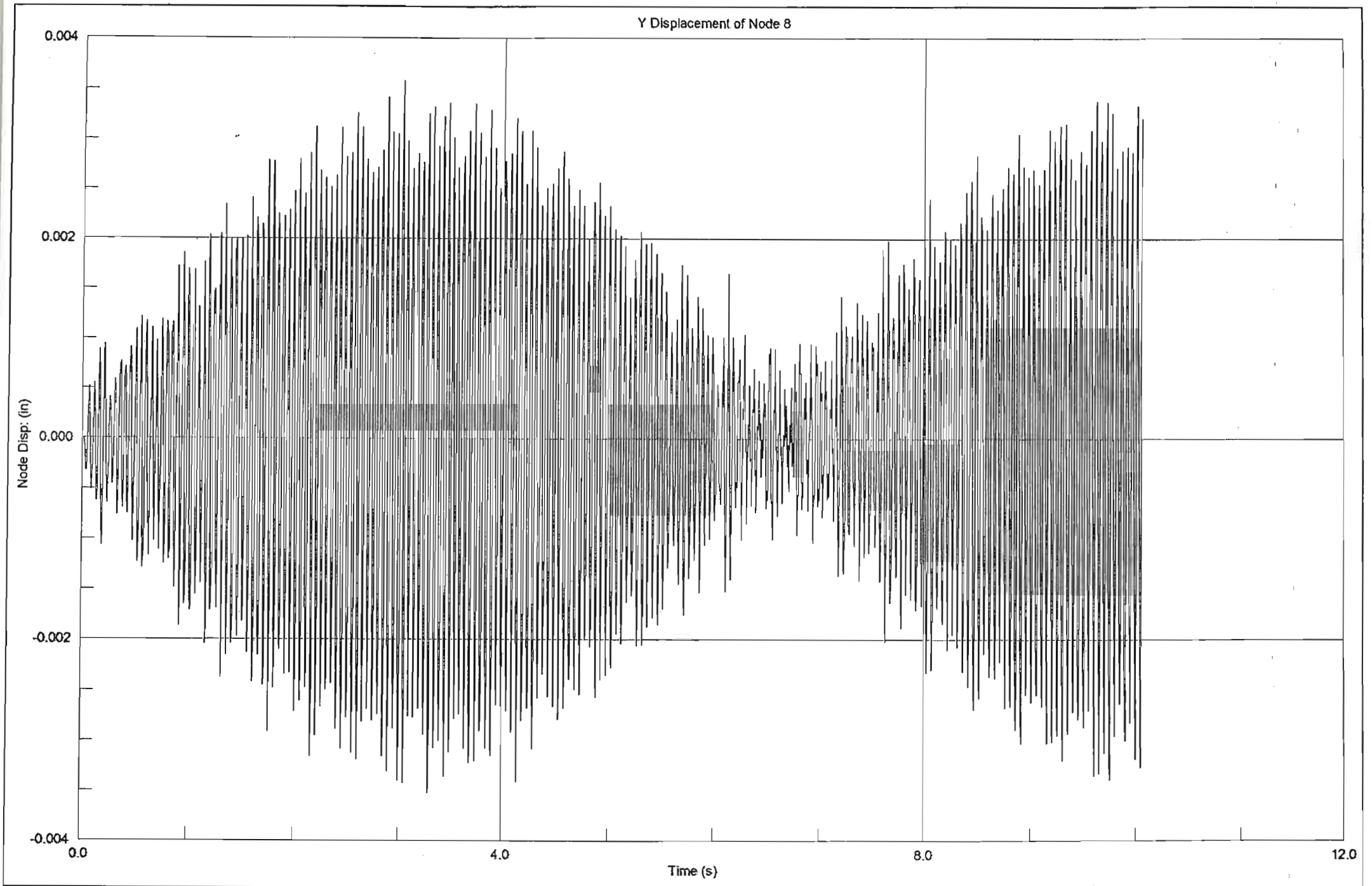
C:\MSDc Eng\Multistorey\Multistorey G15000-C5.s17

2 October 2002 12:33 pm

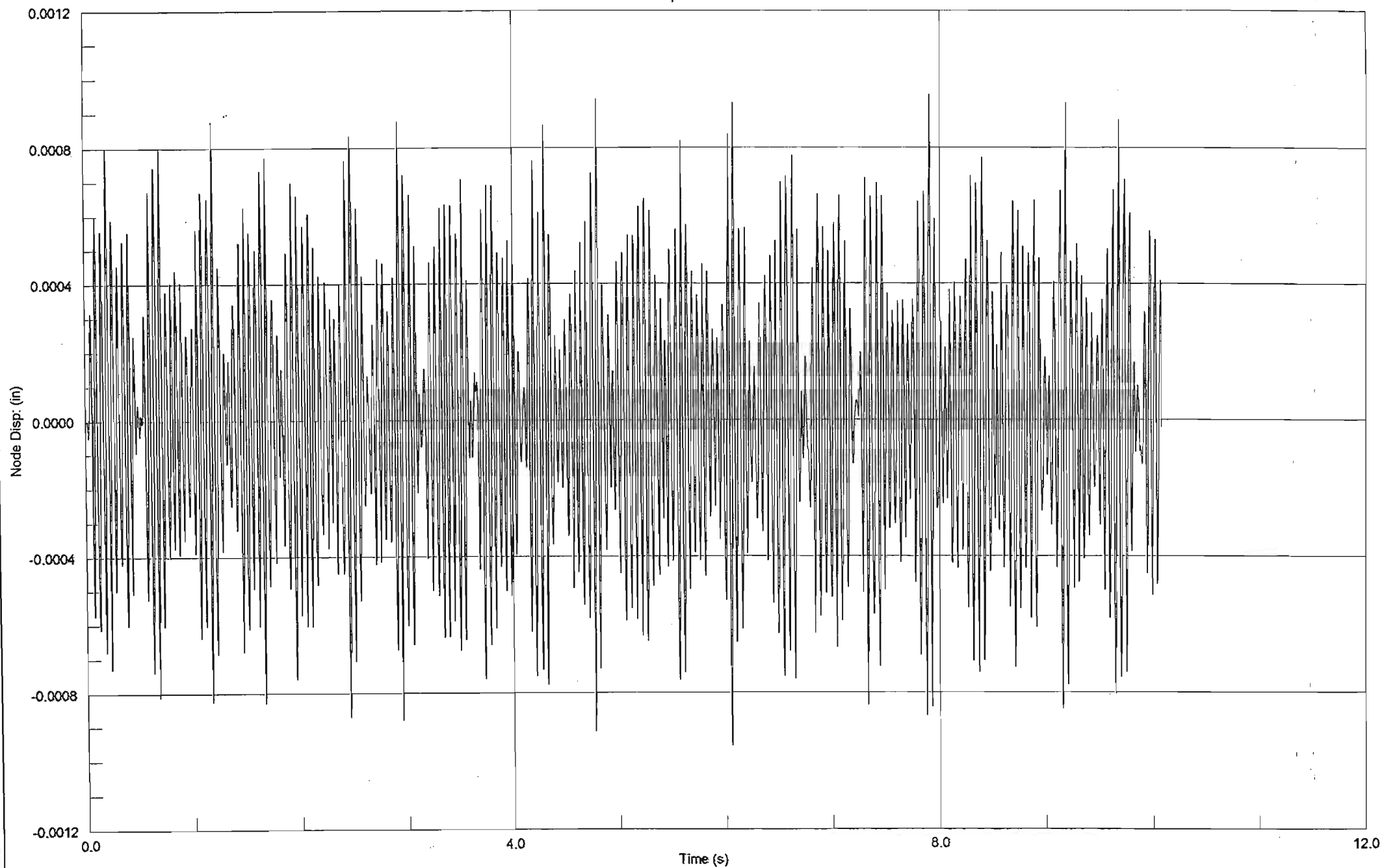
D3.51

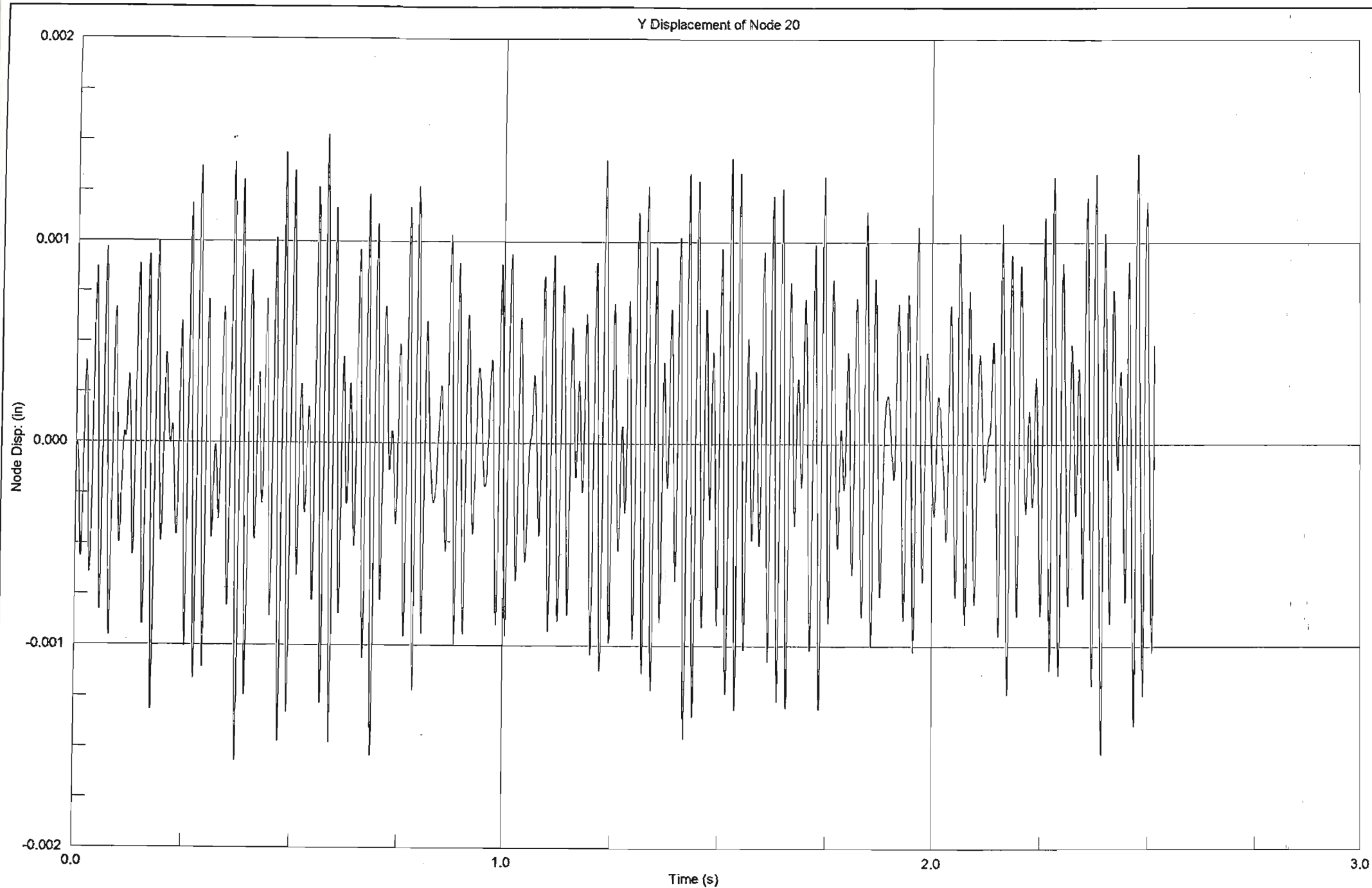
Vz



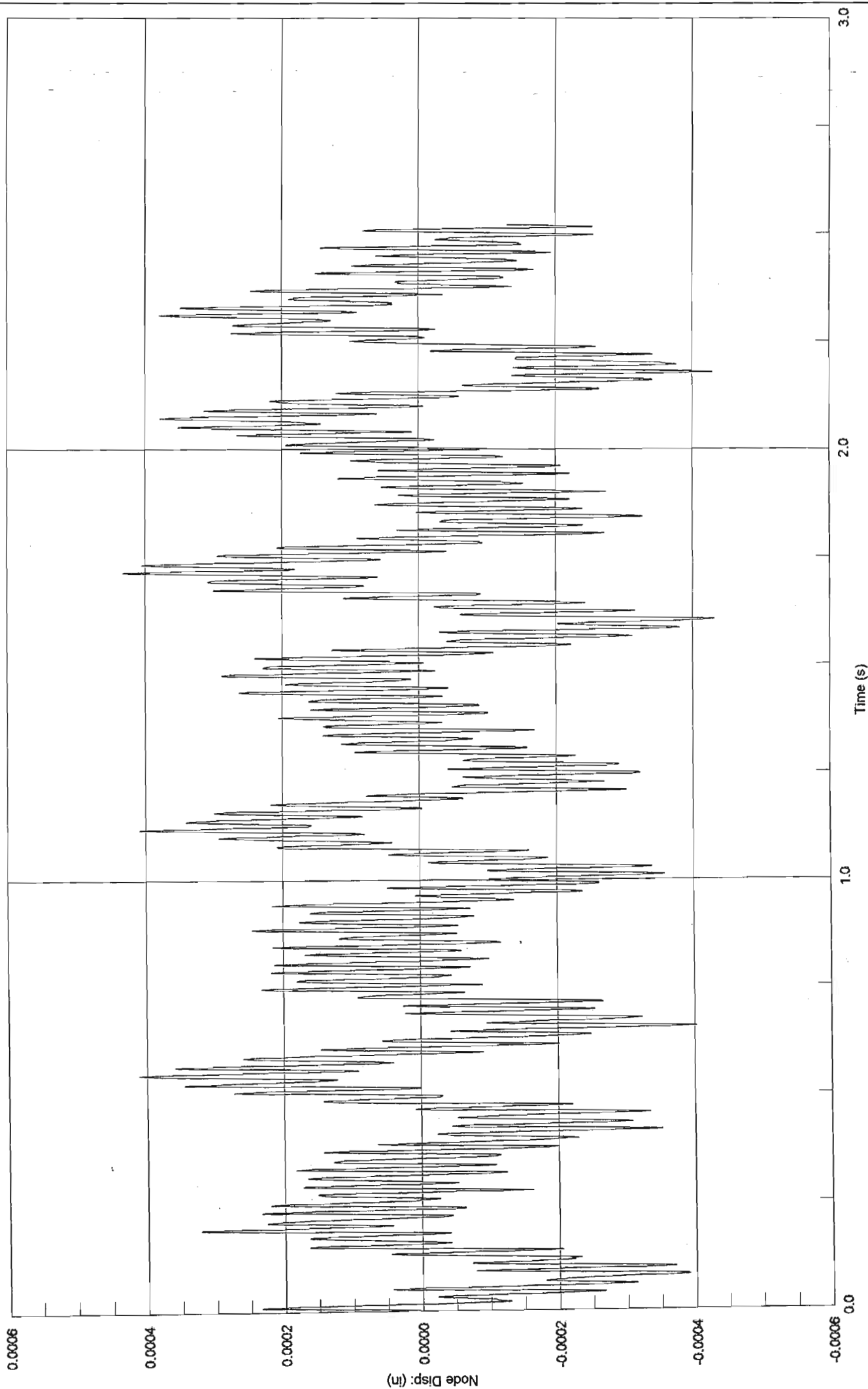


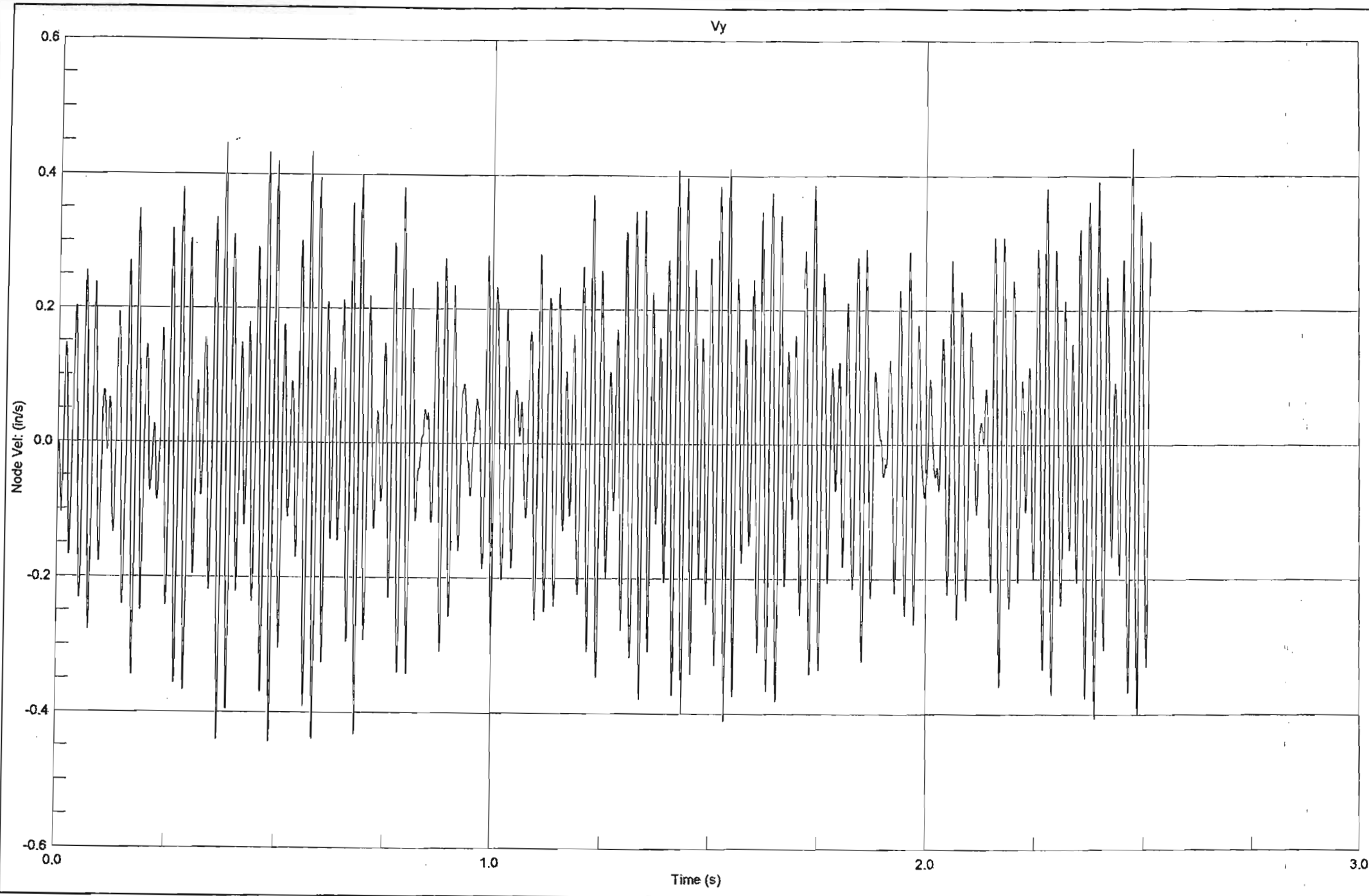
Z Displacement of Node 8

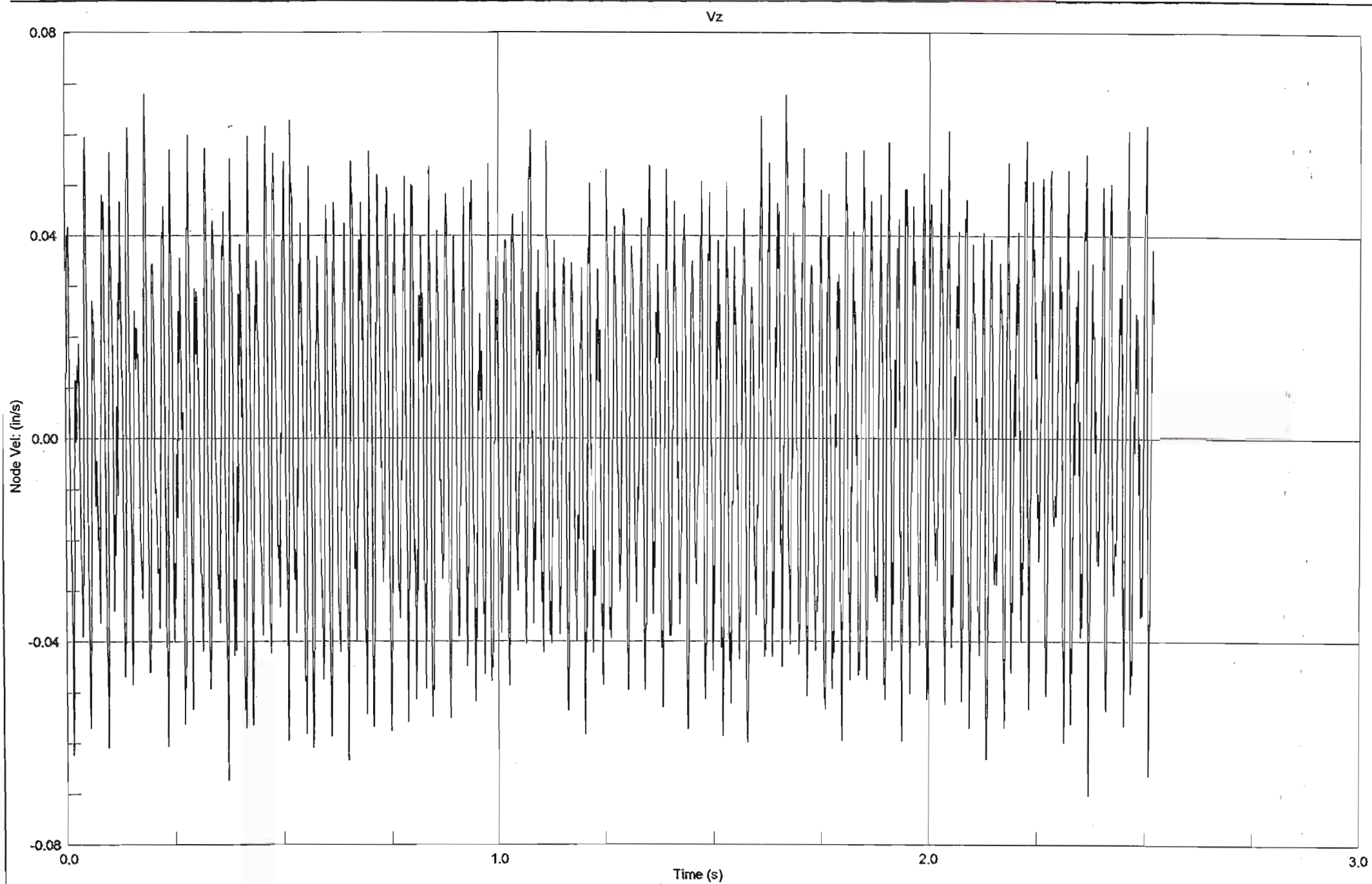


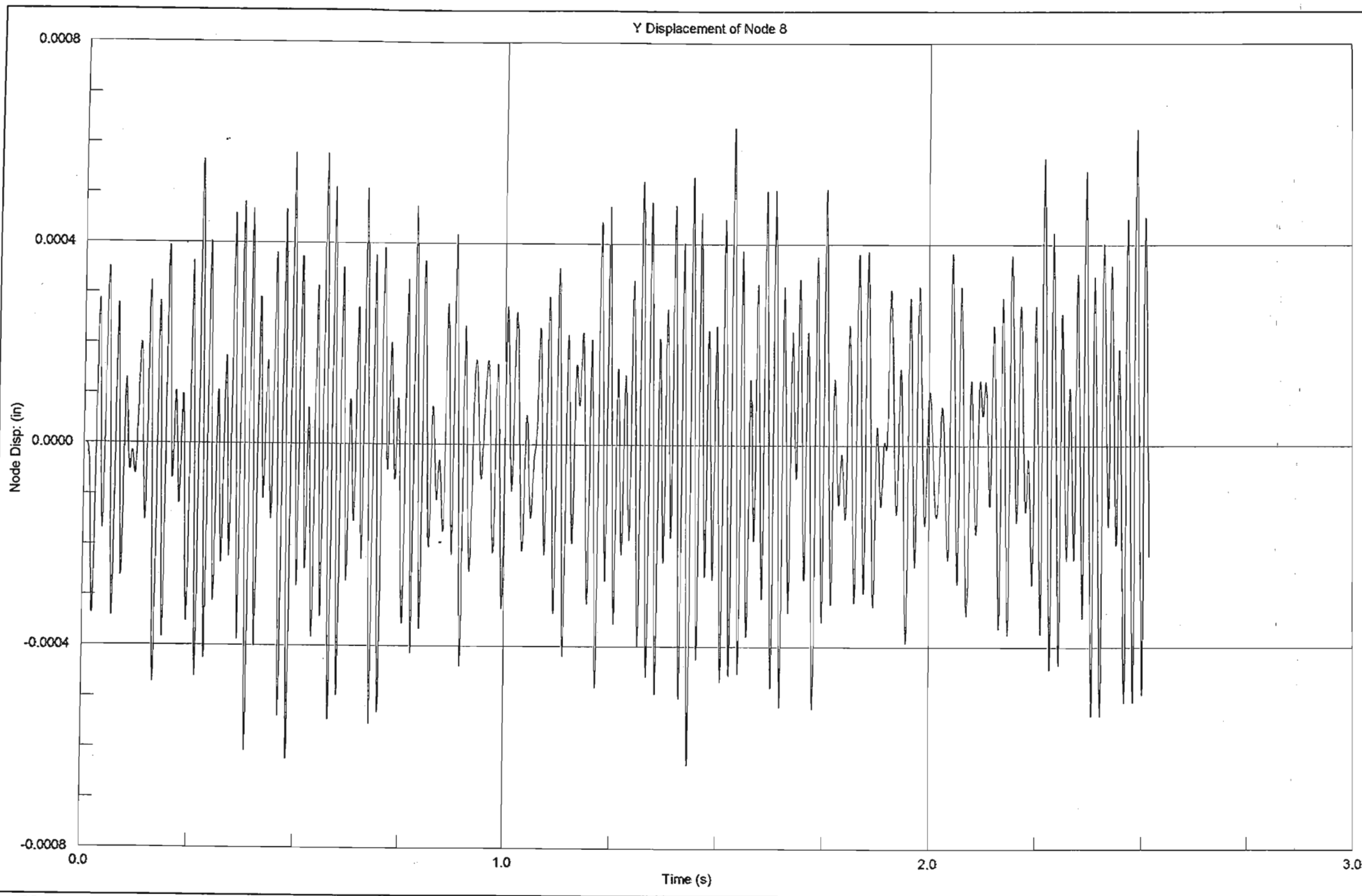


Z Displacement of Node 20

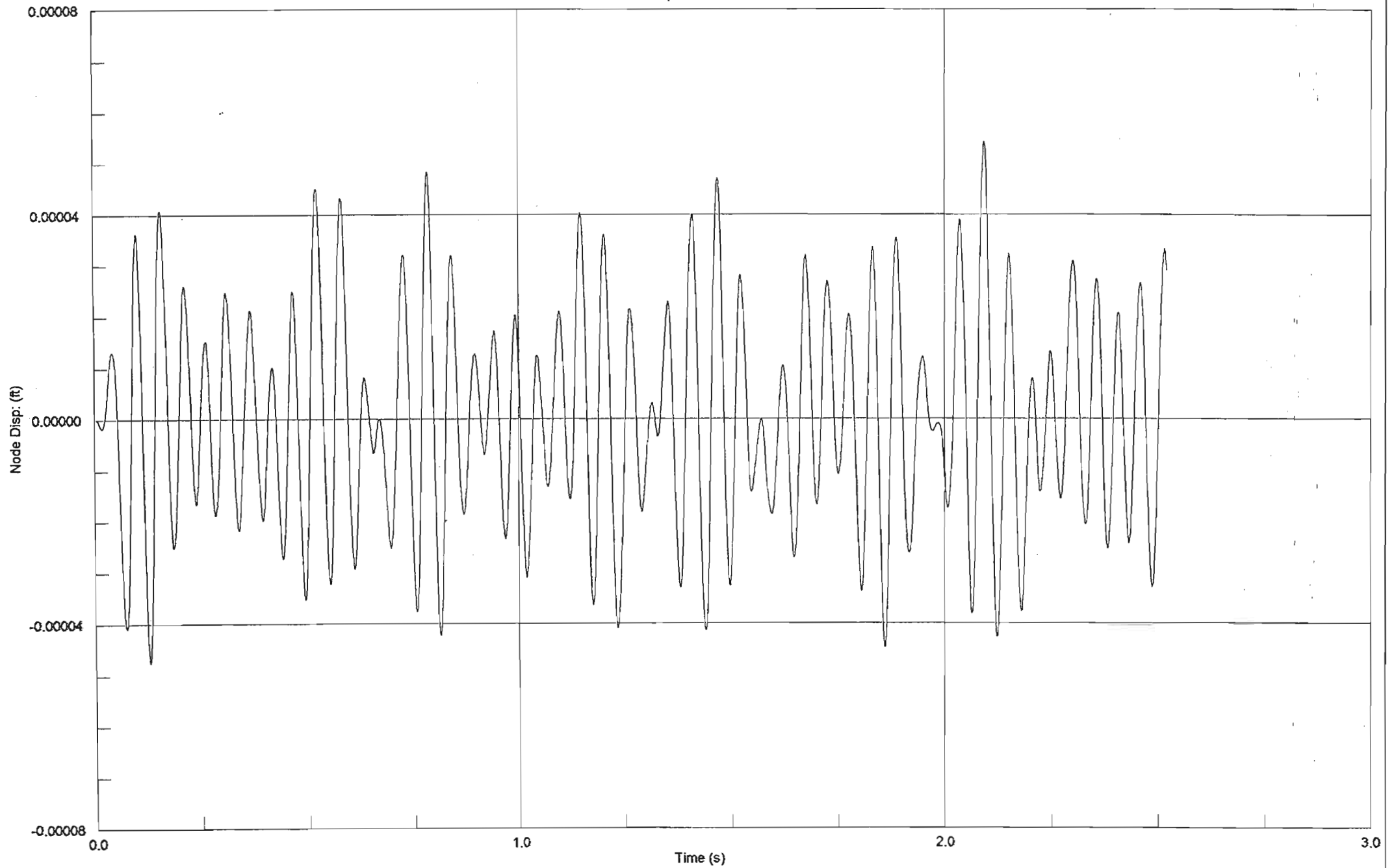


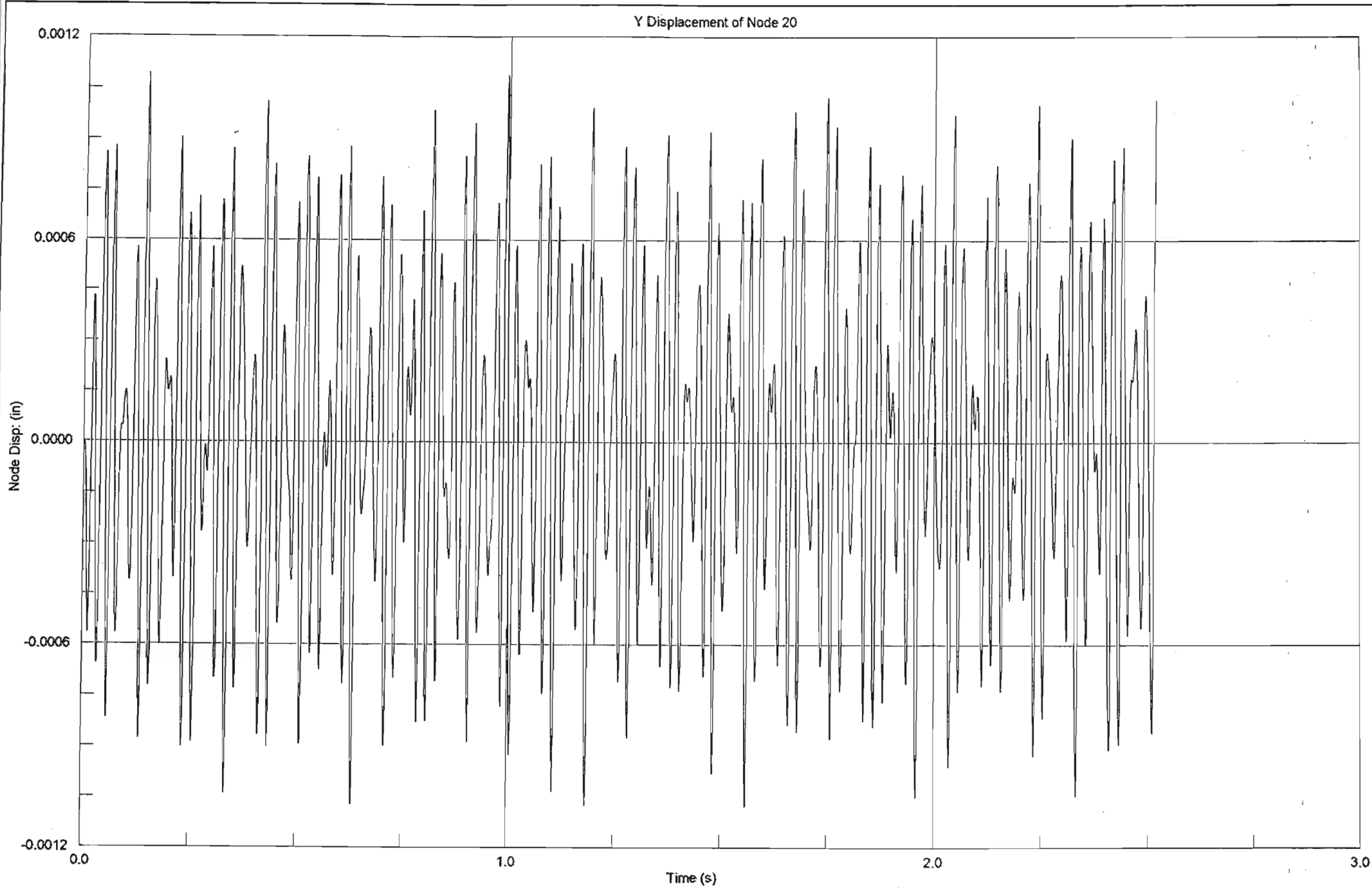


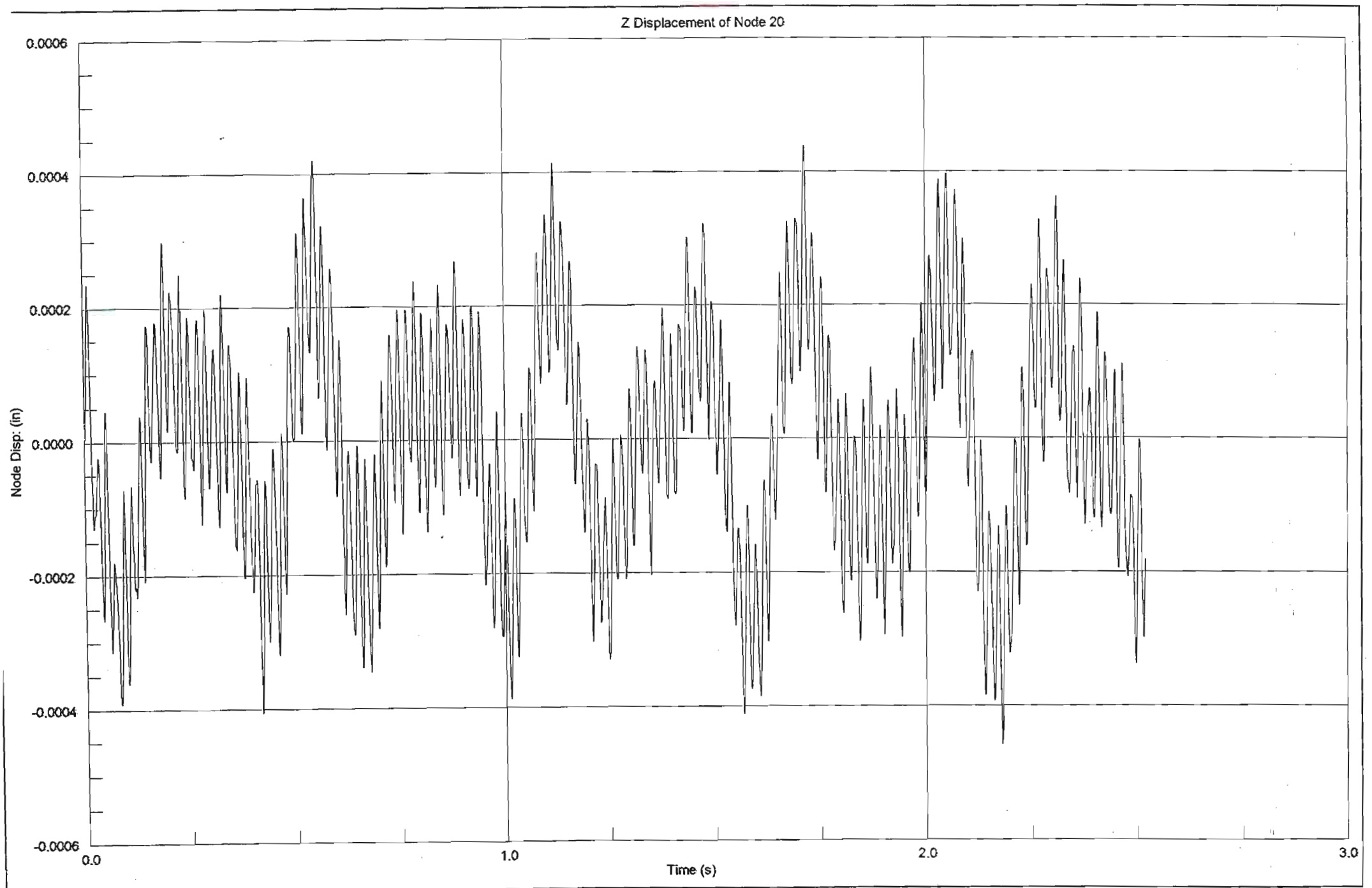


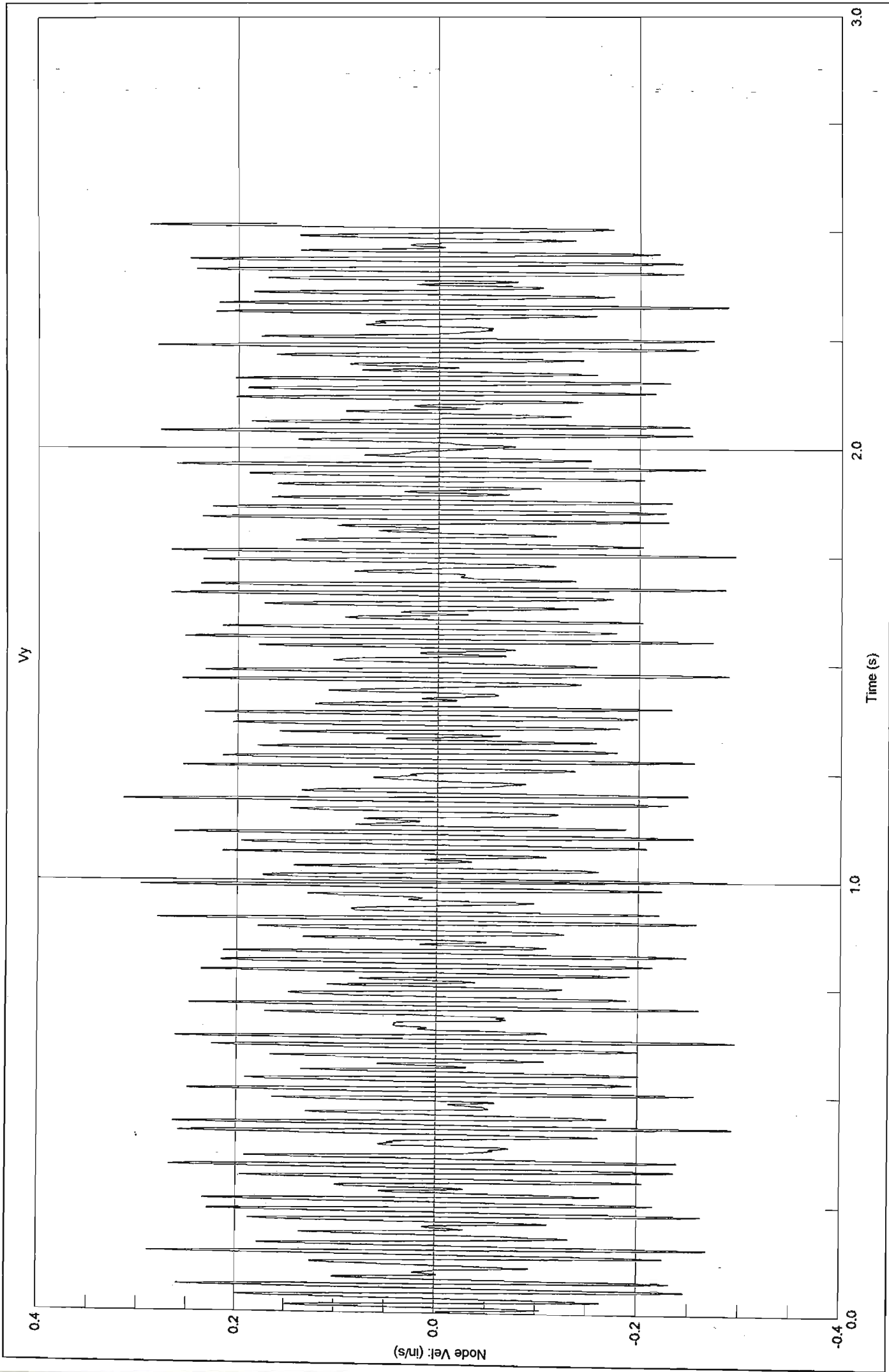


Z Displacement of Node 8

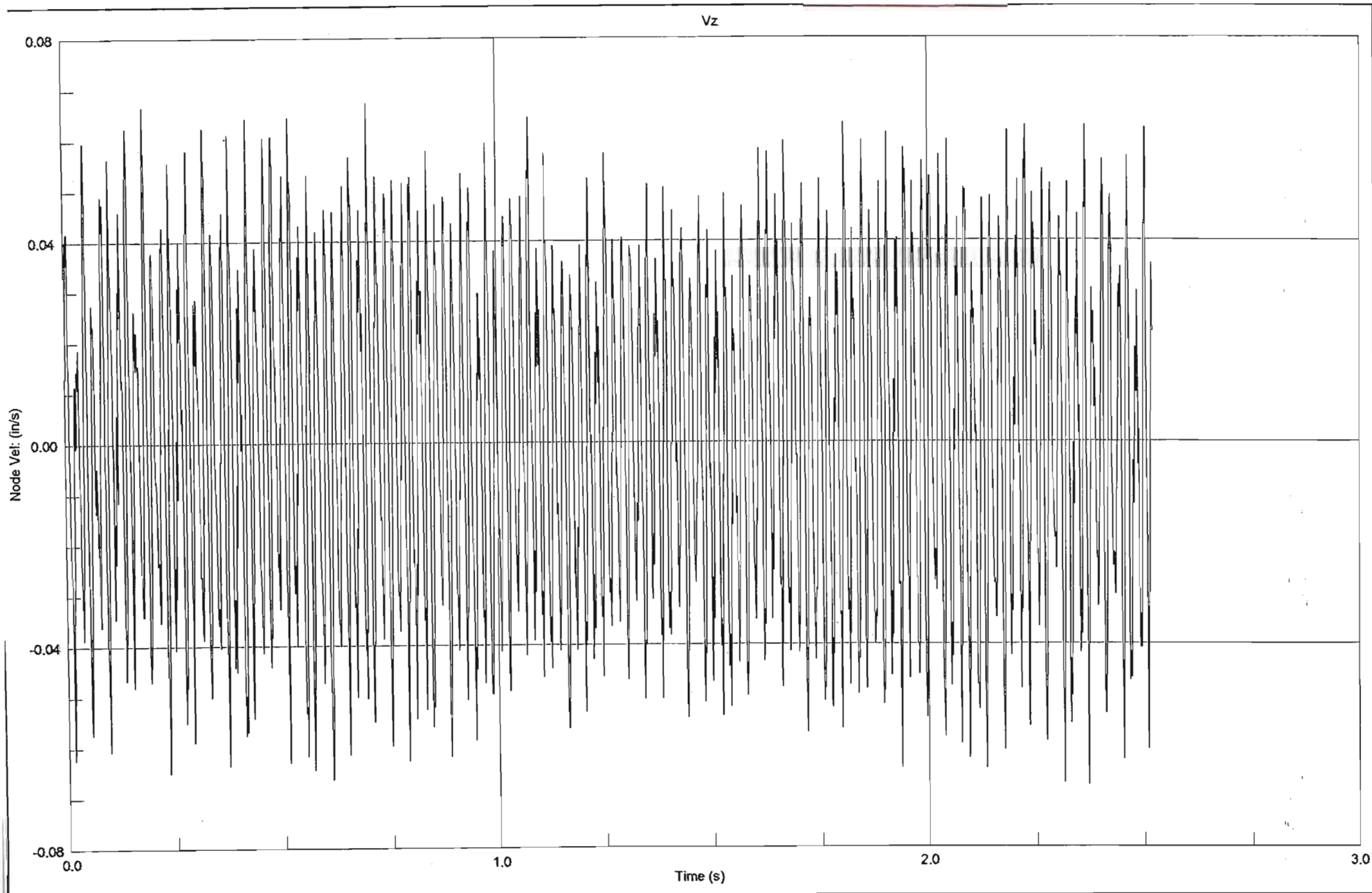


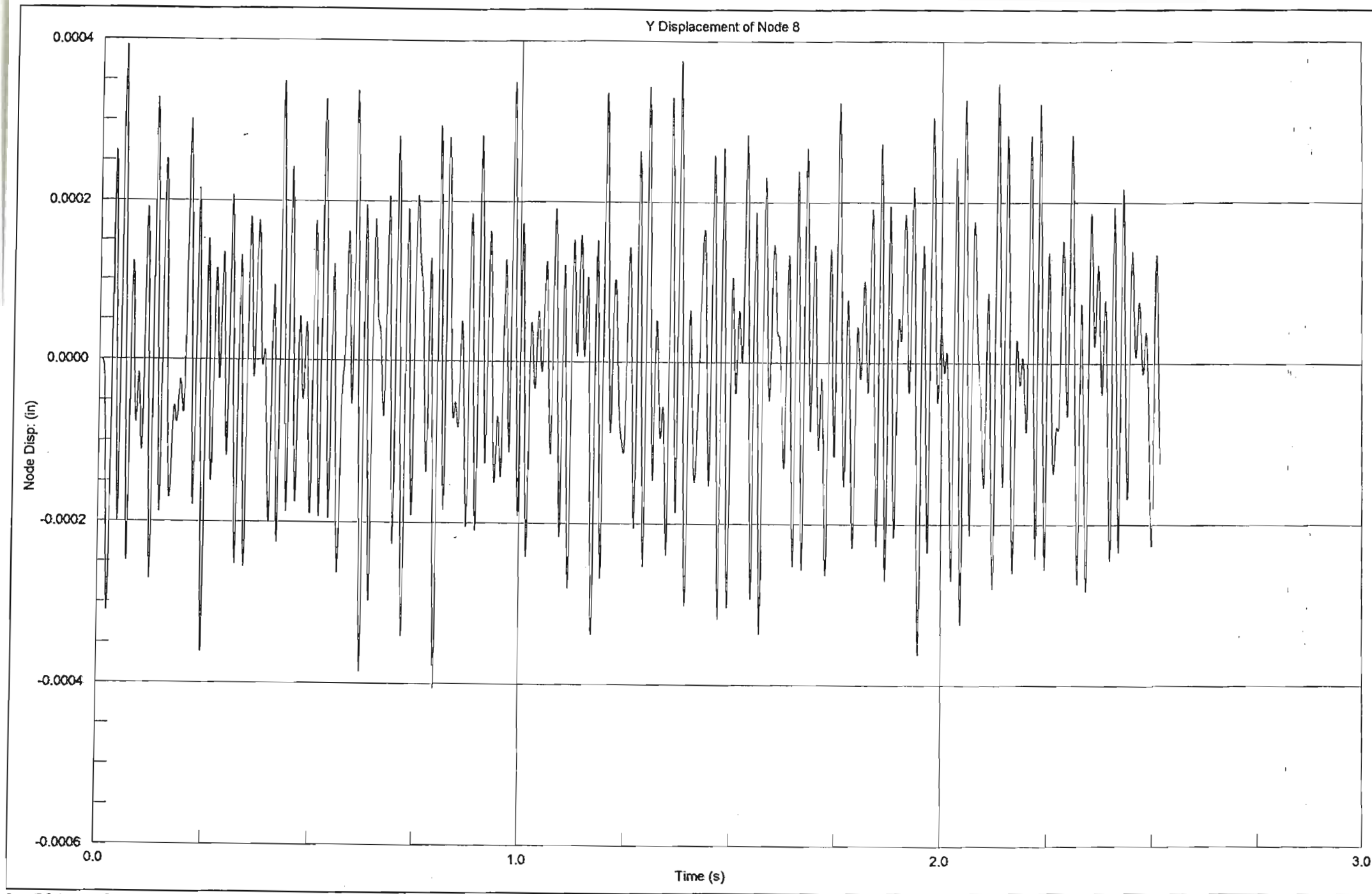




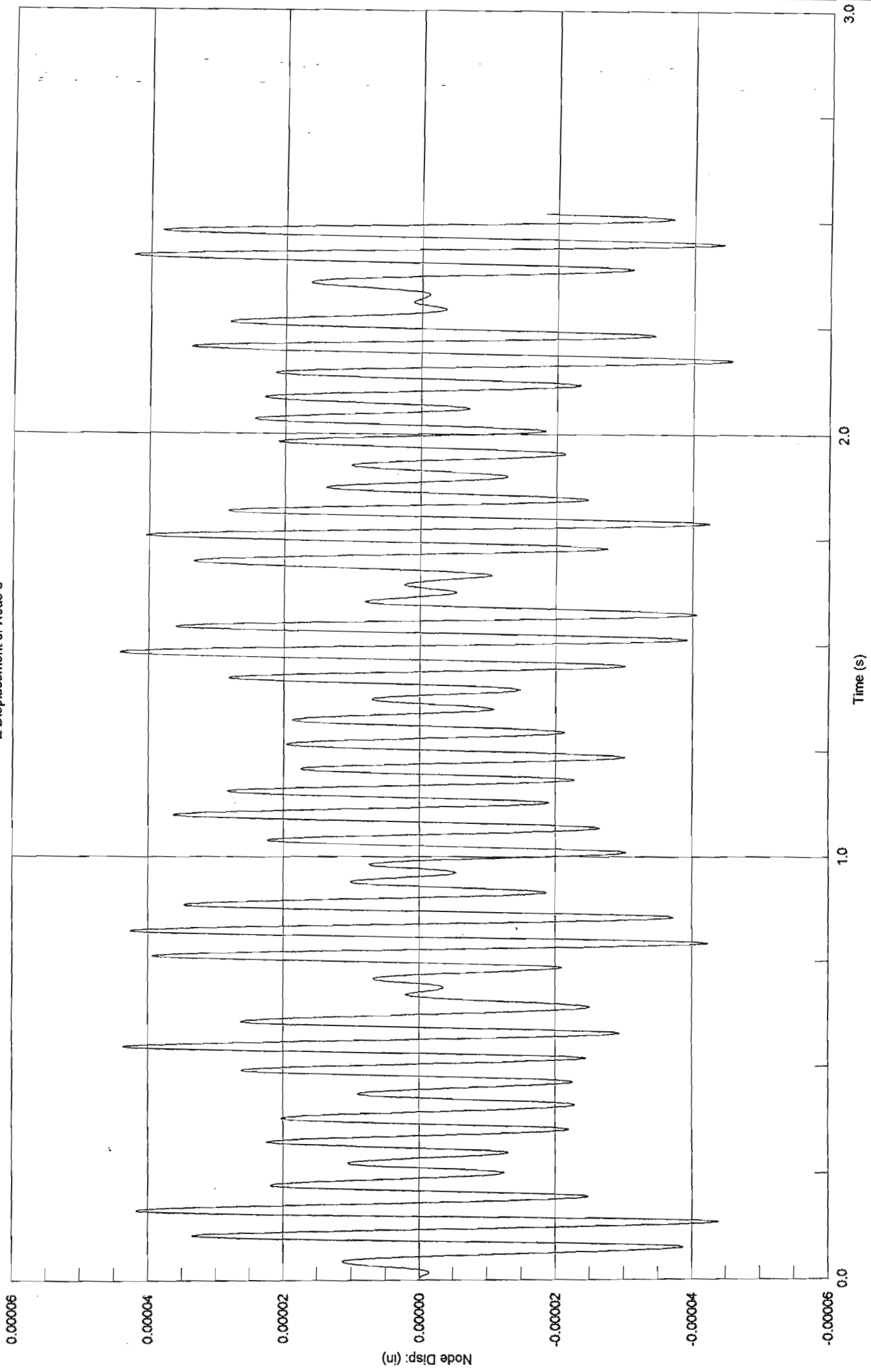


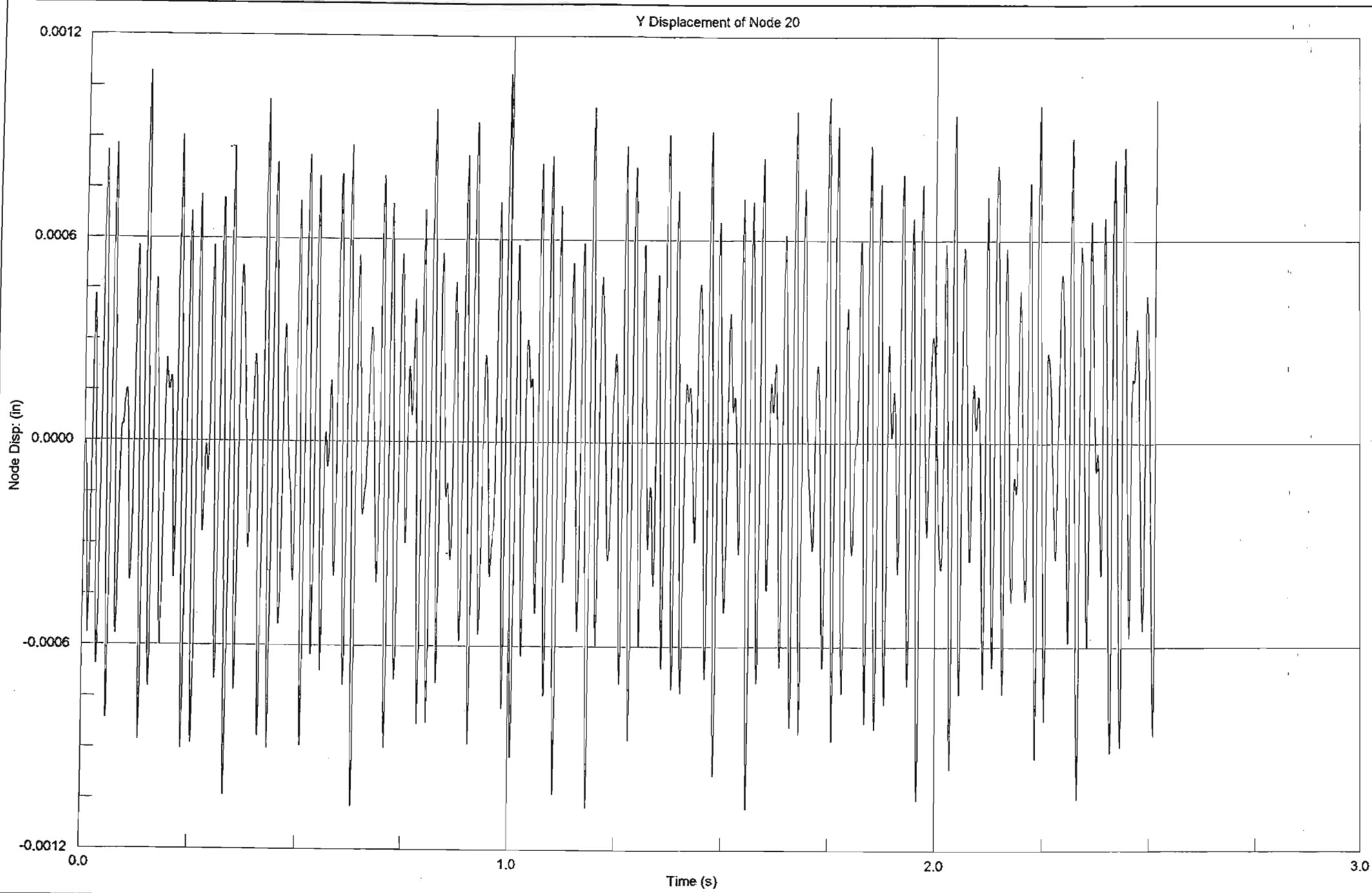
D 3.69

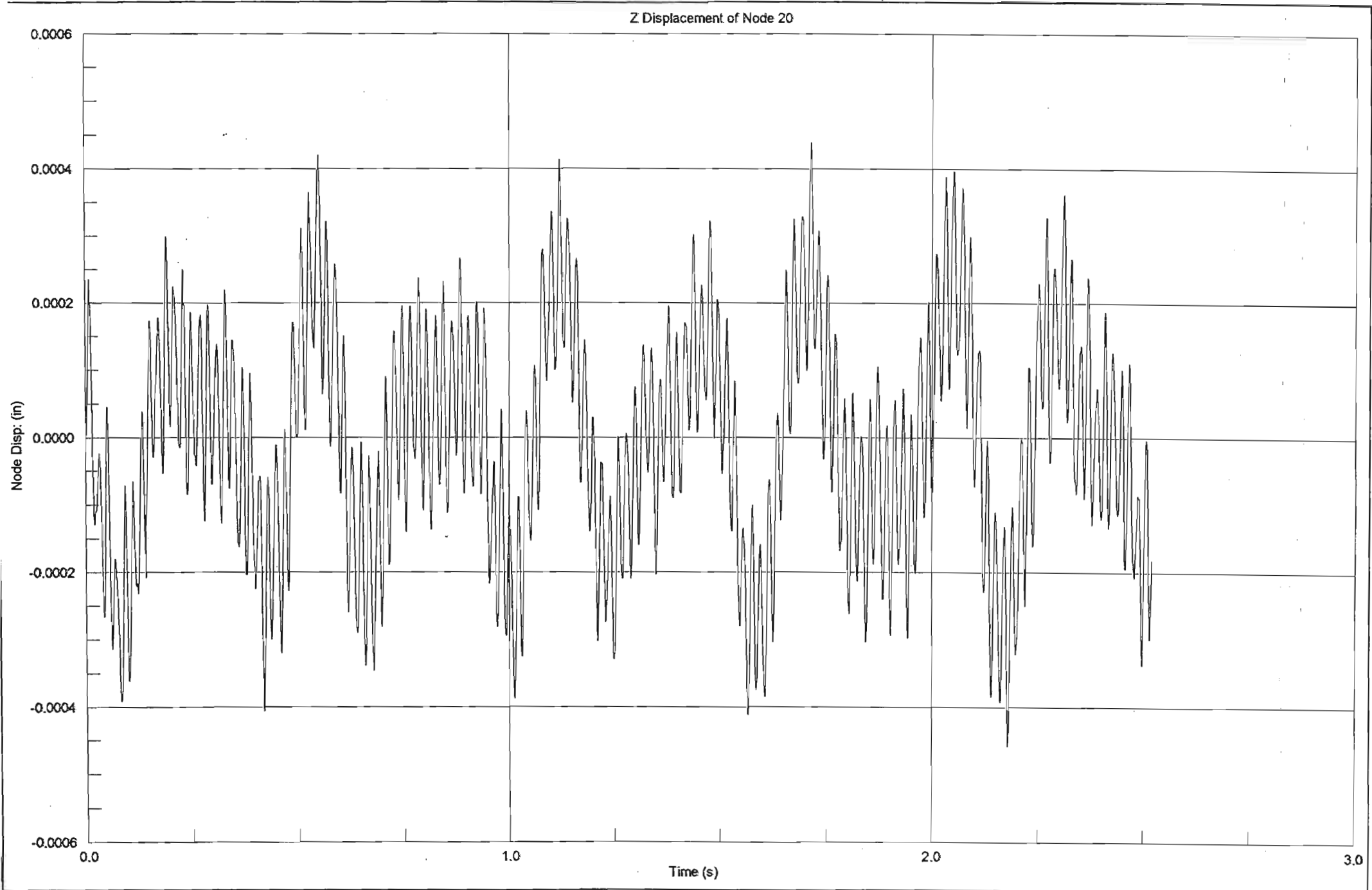


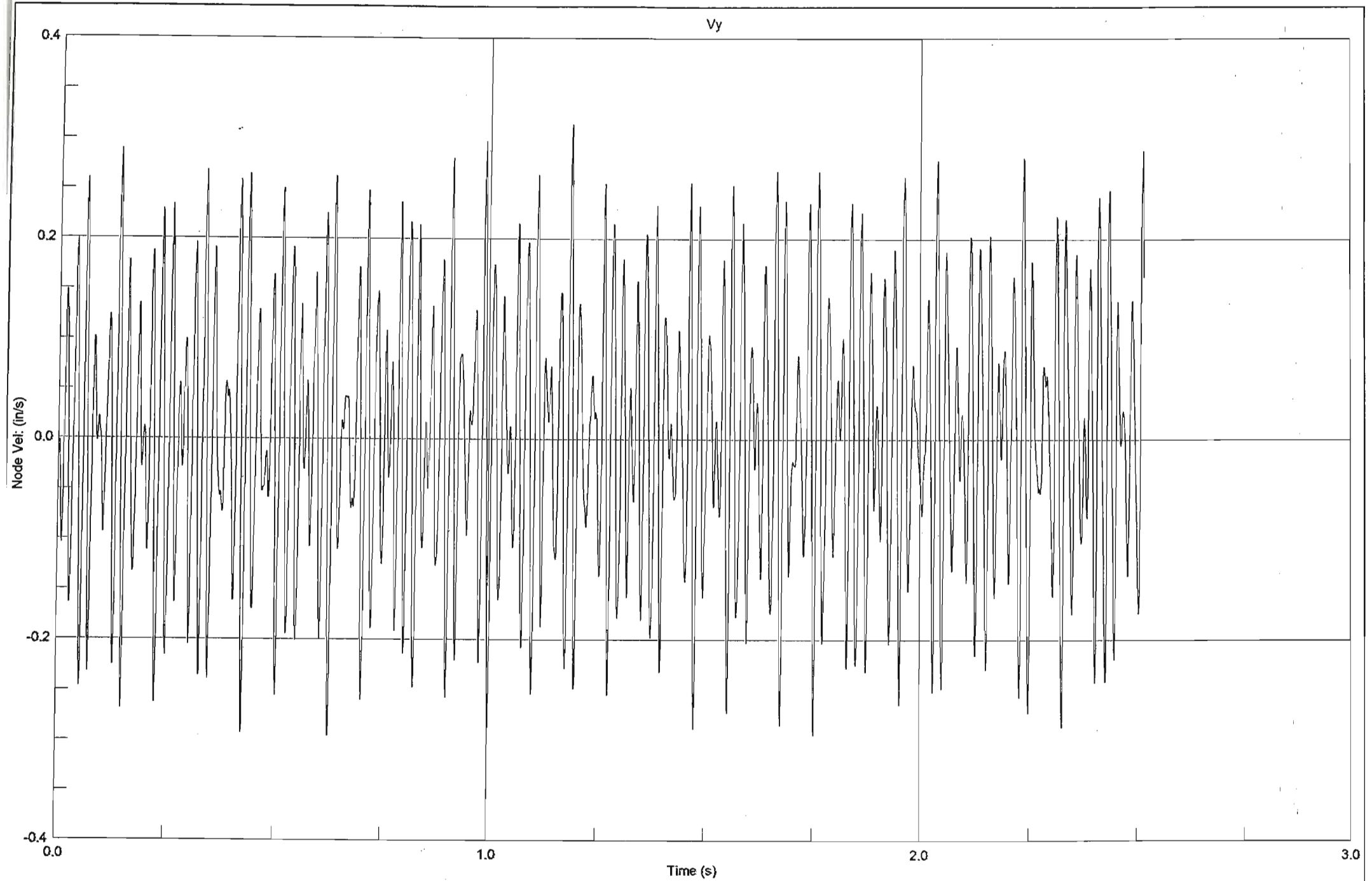


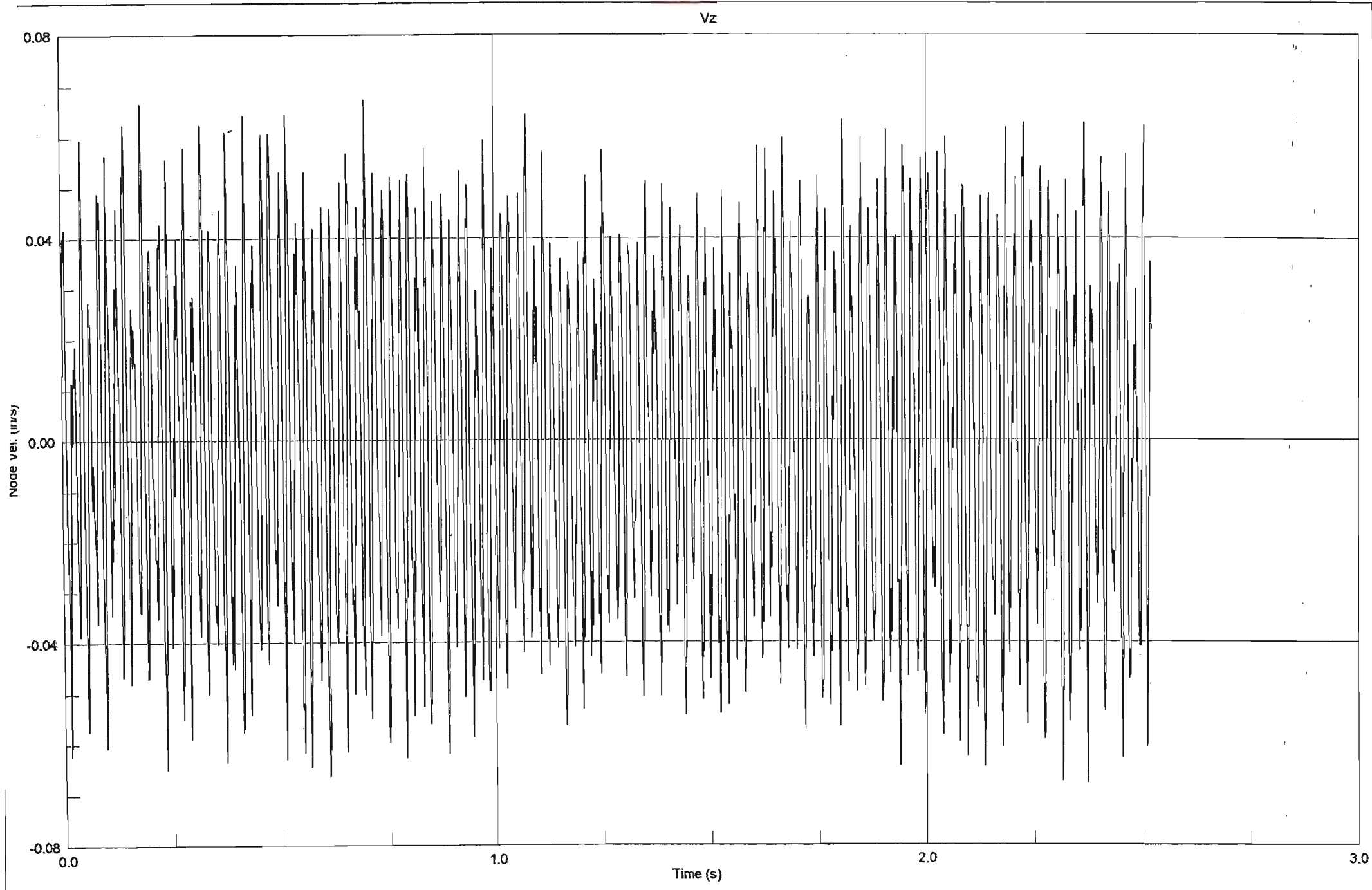
Z Displacement of Node 8

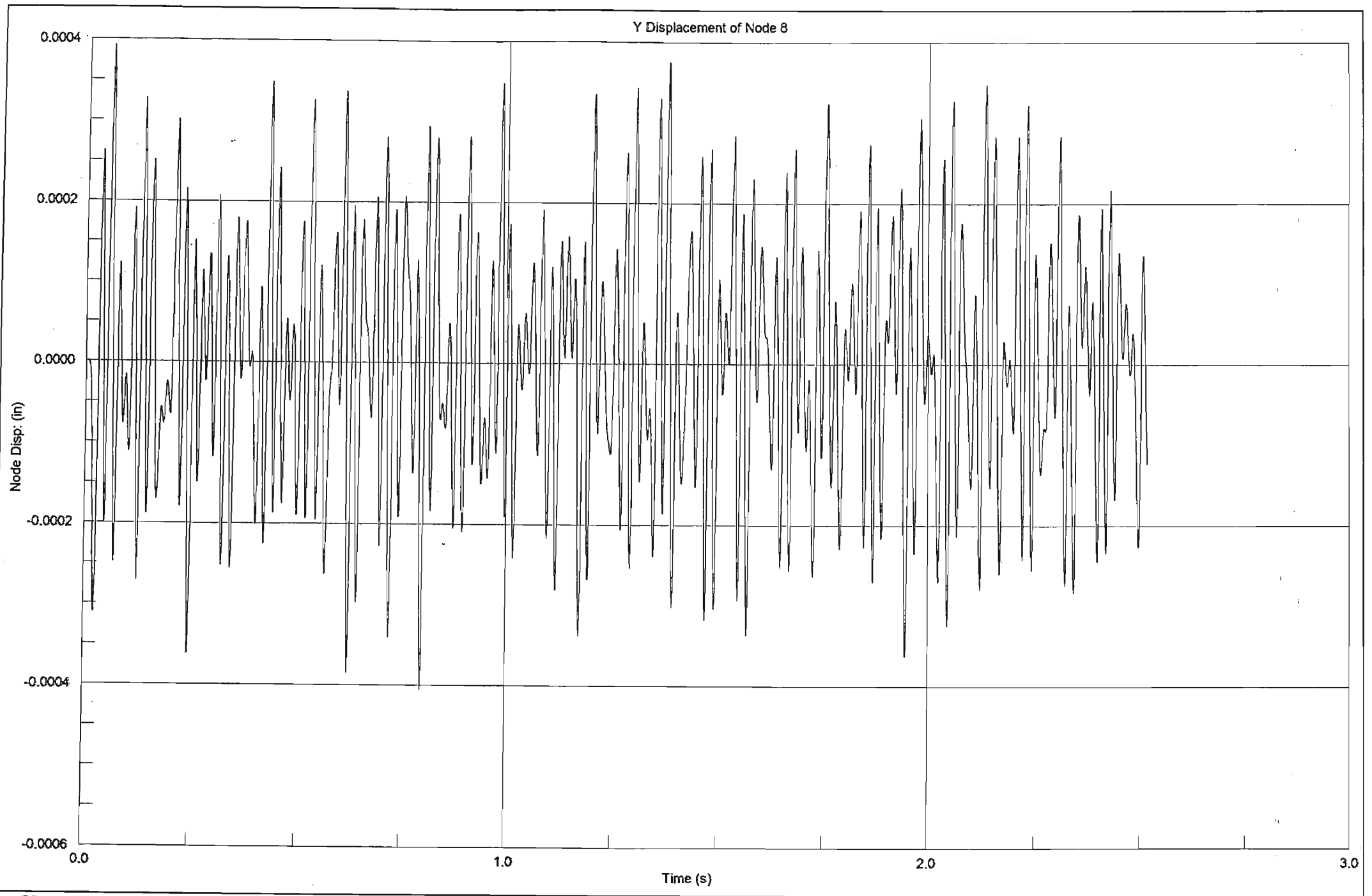


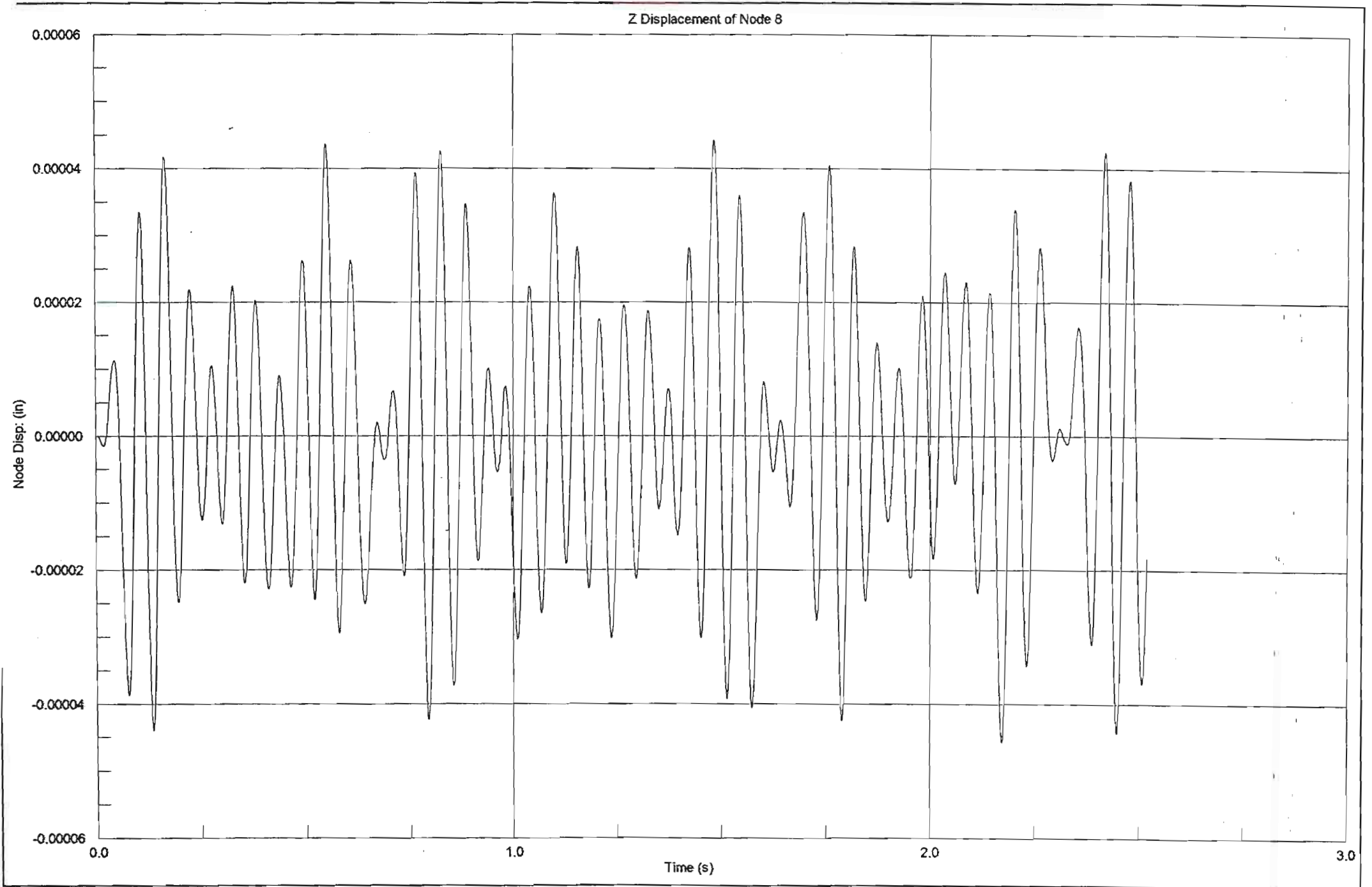


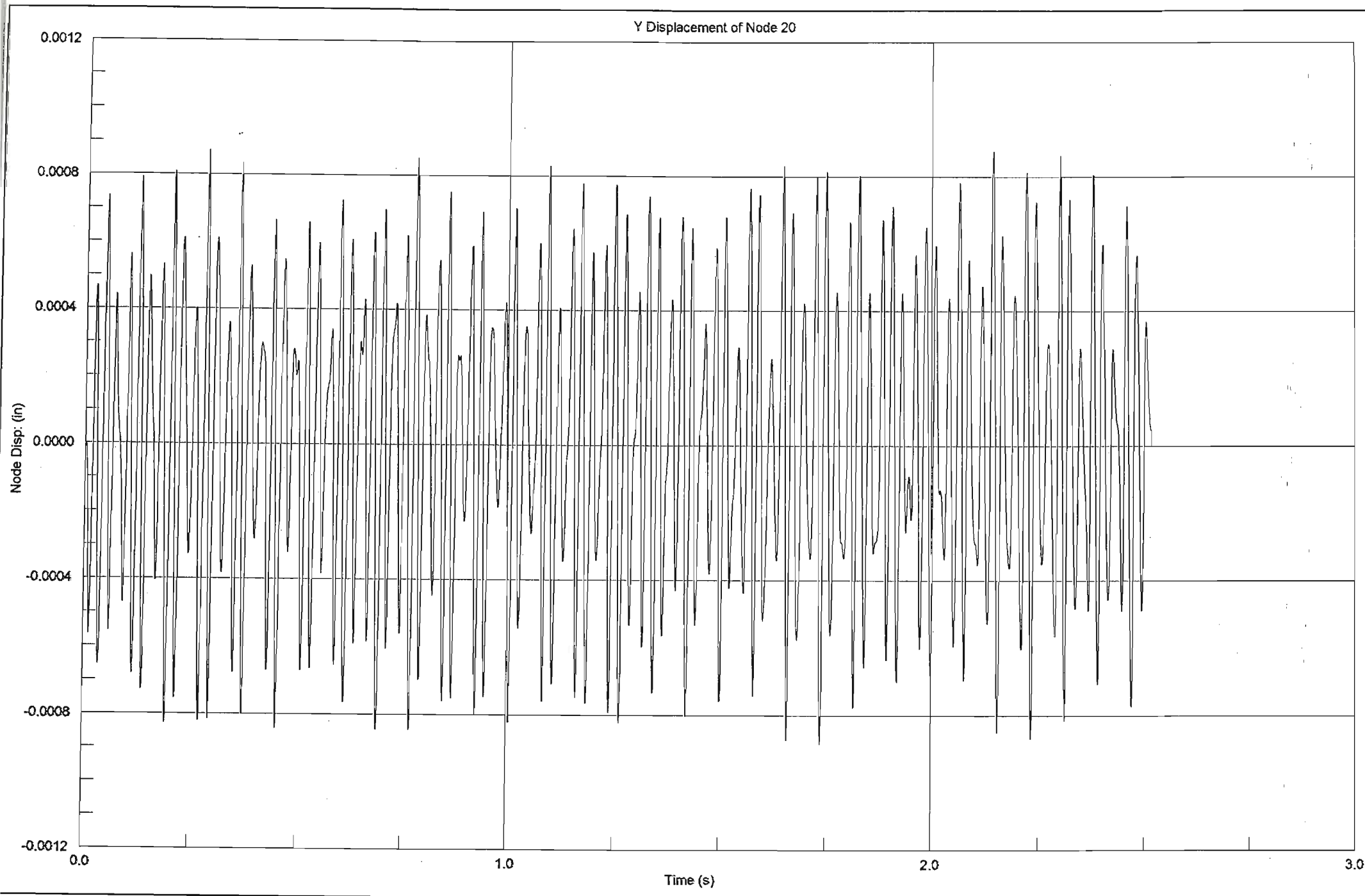


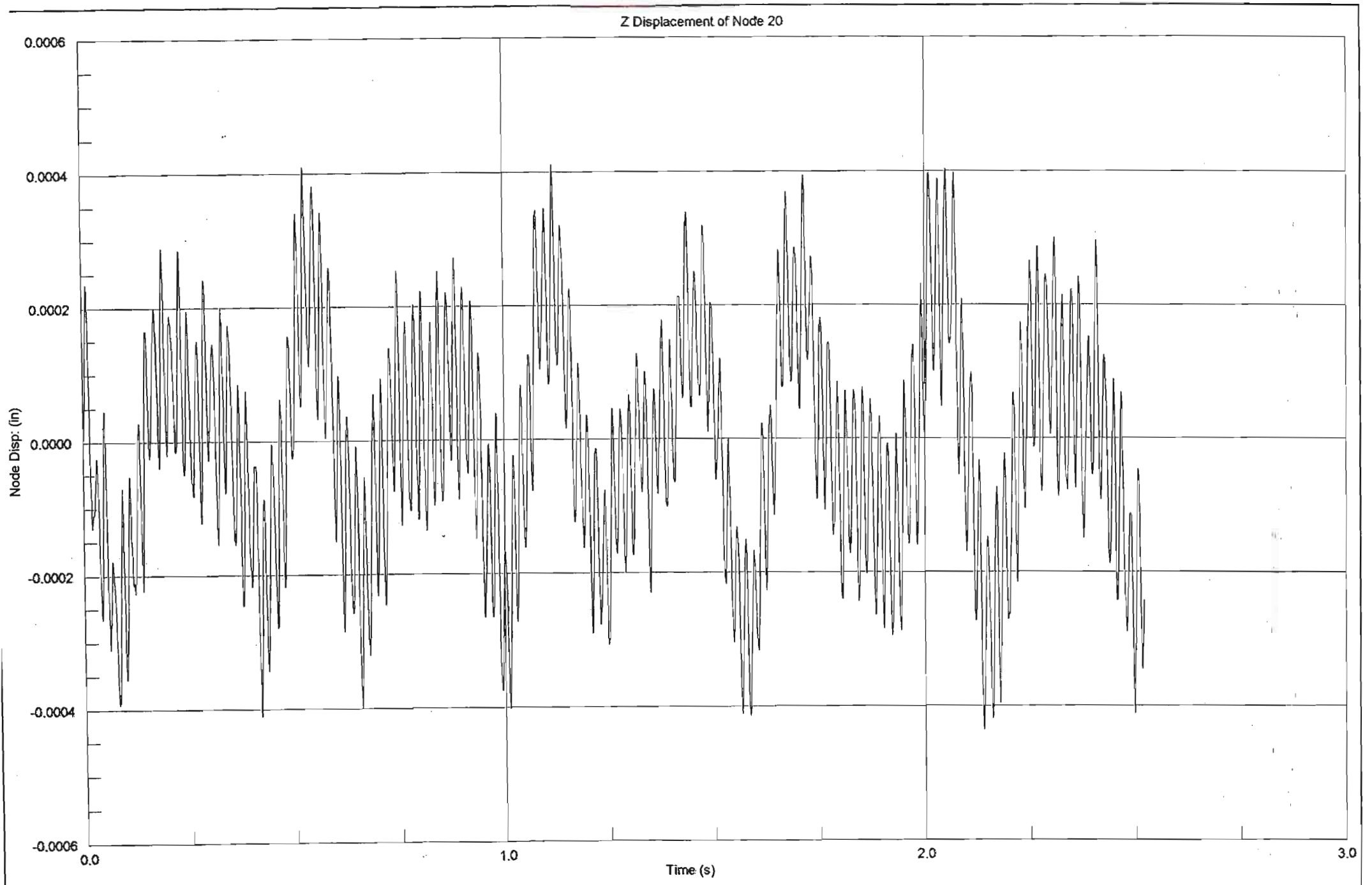


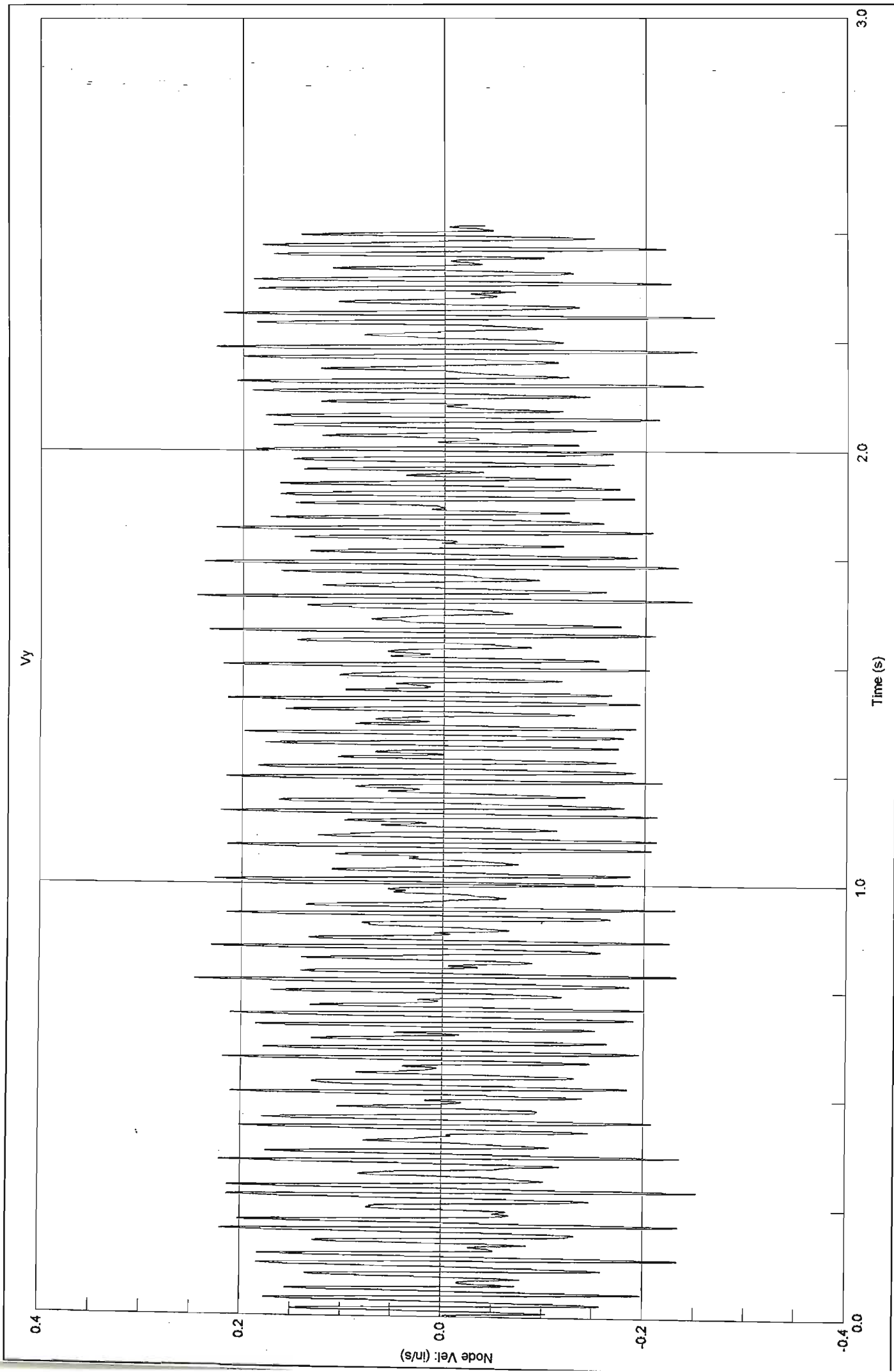


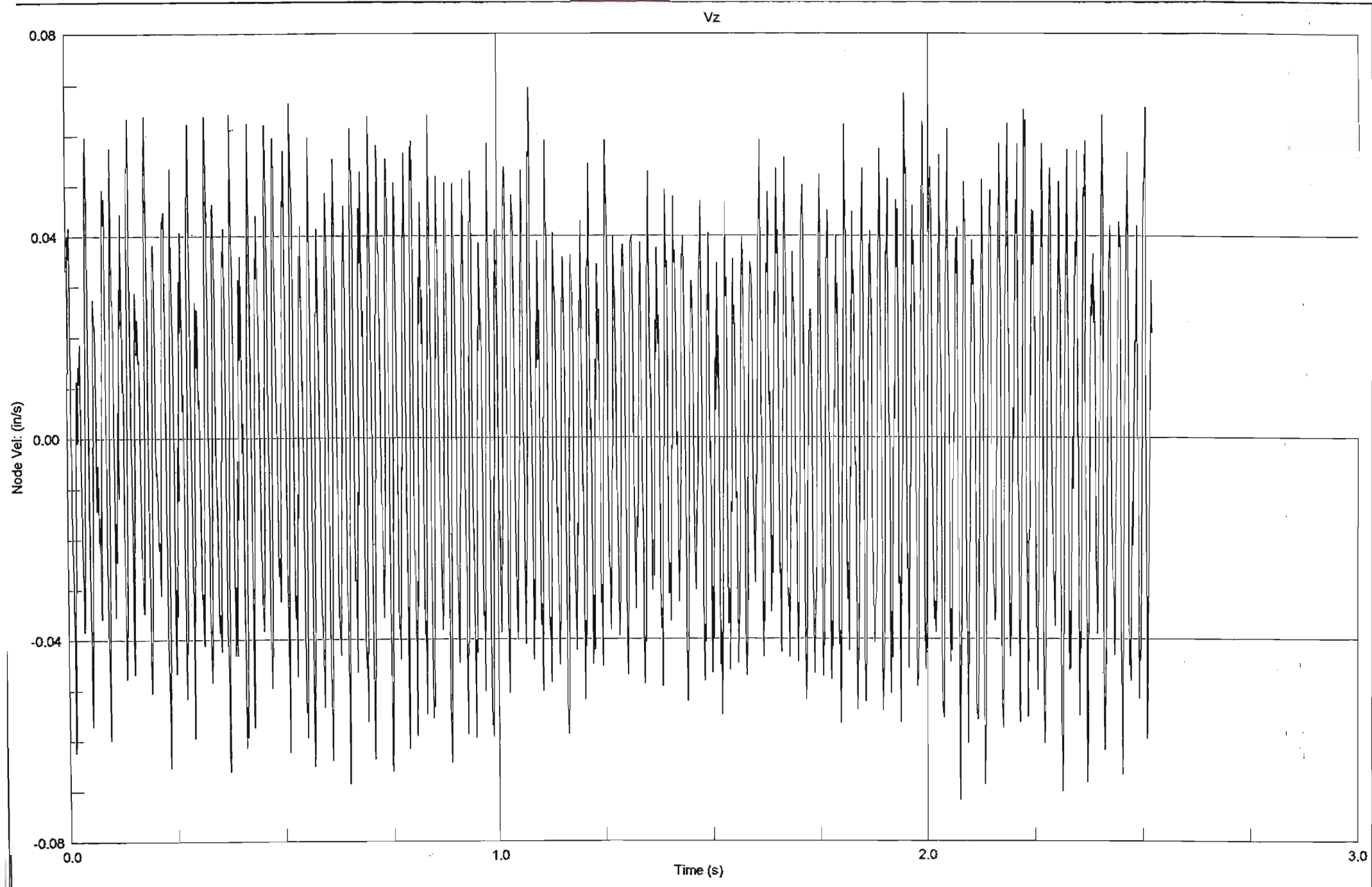


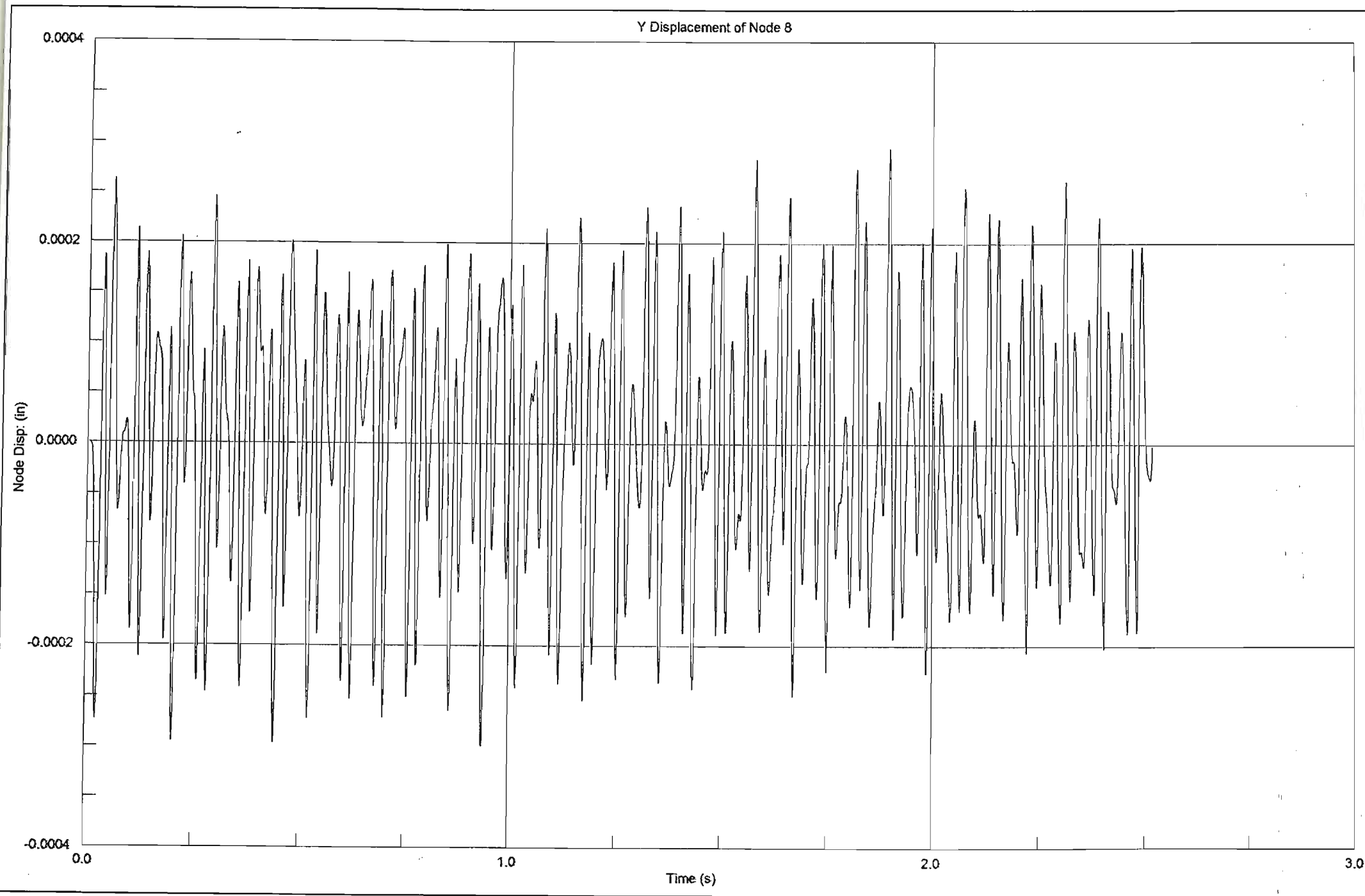




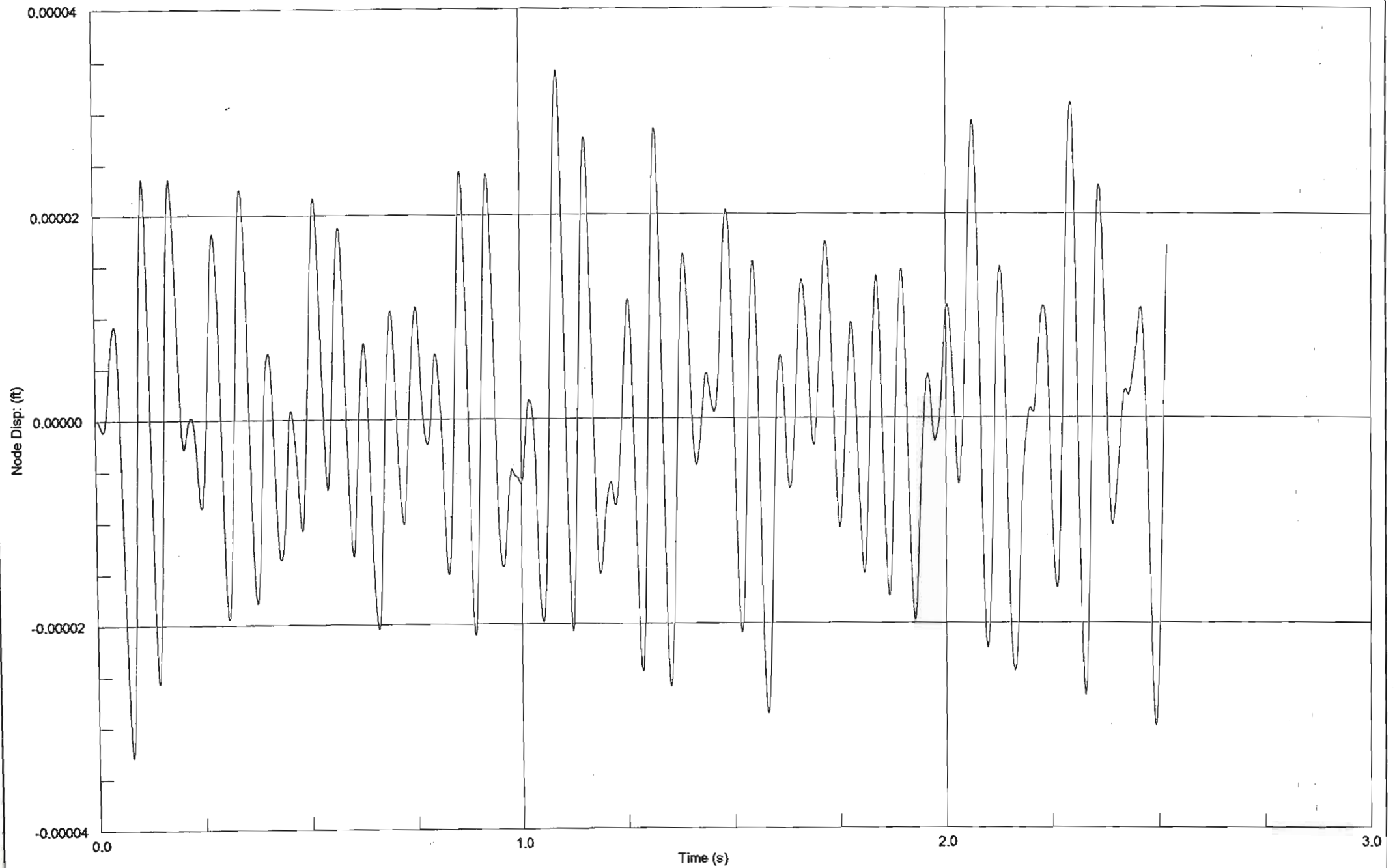


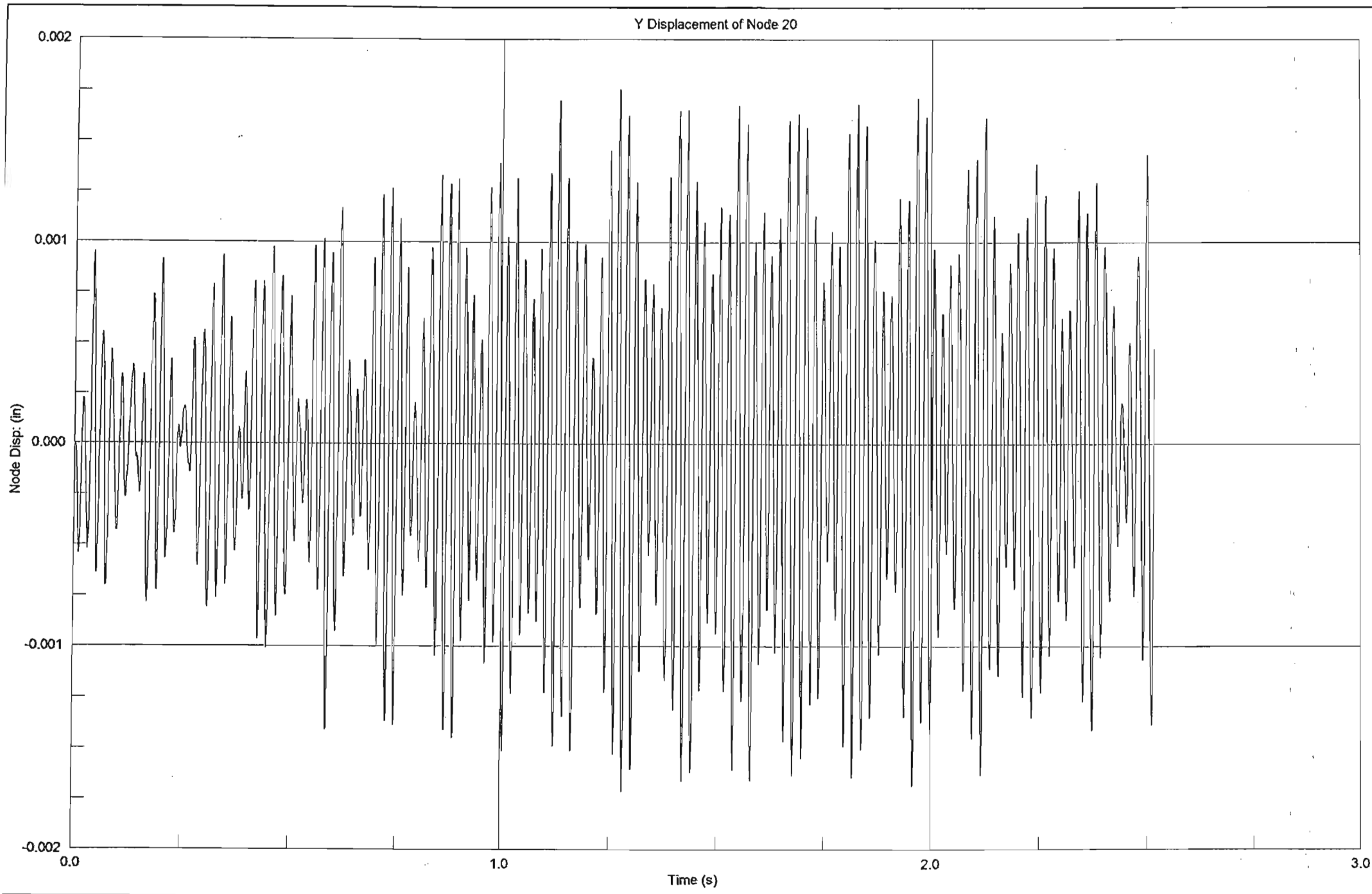




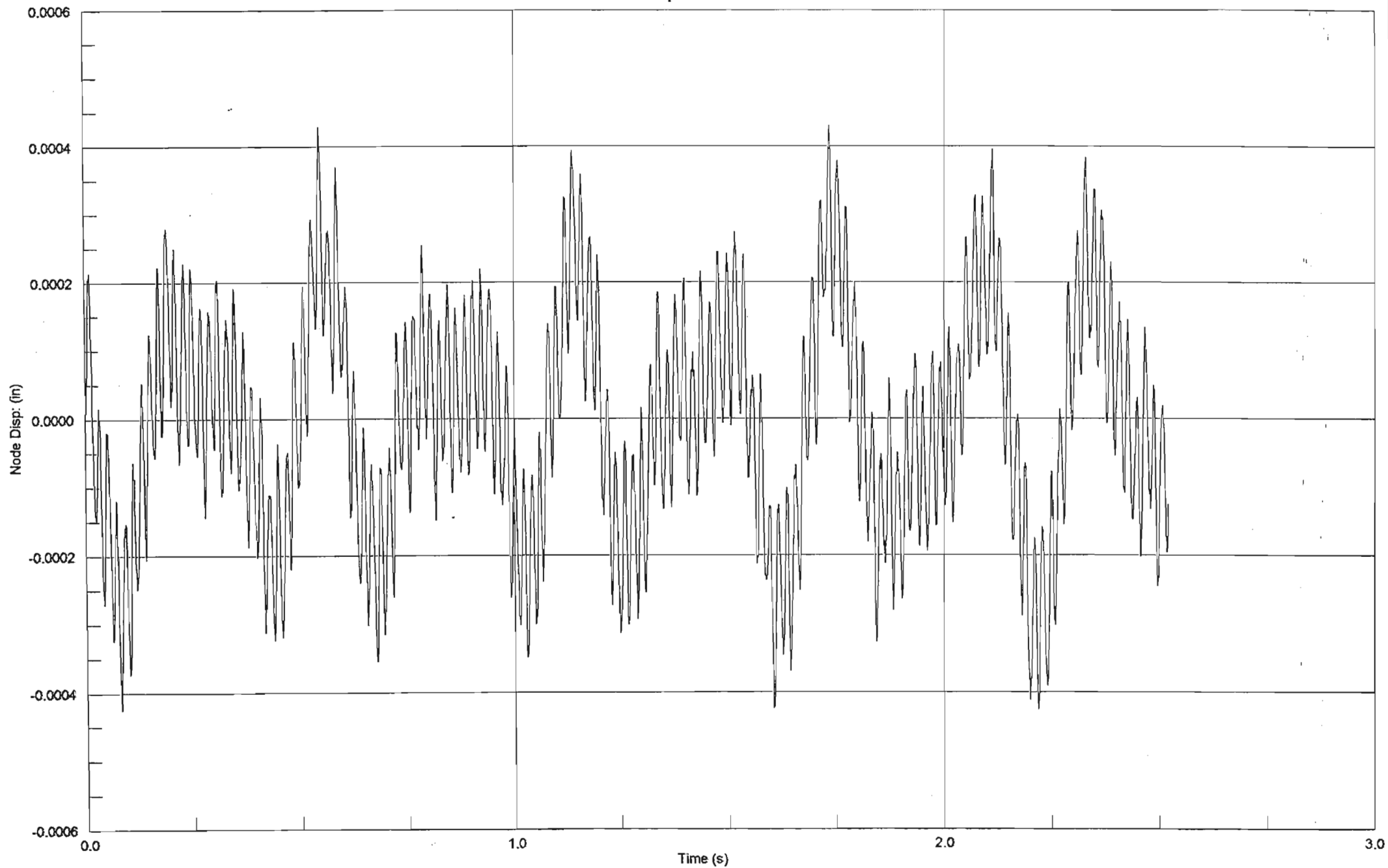


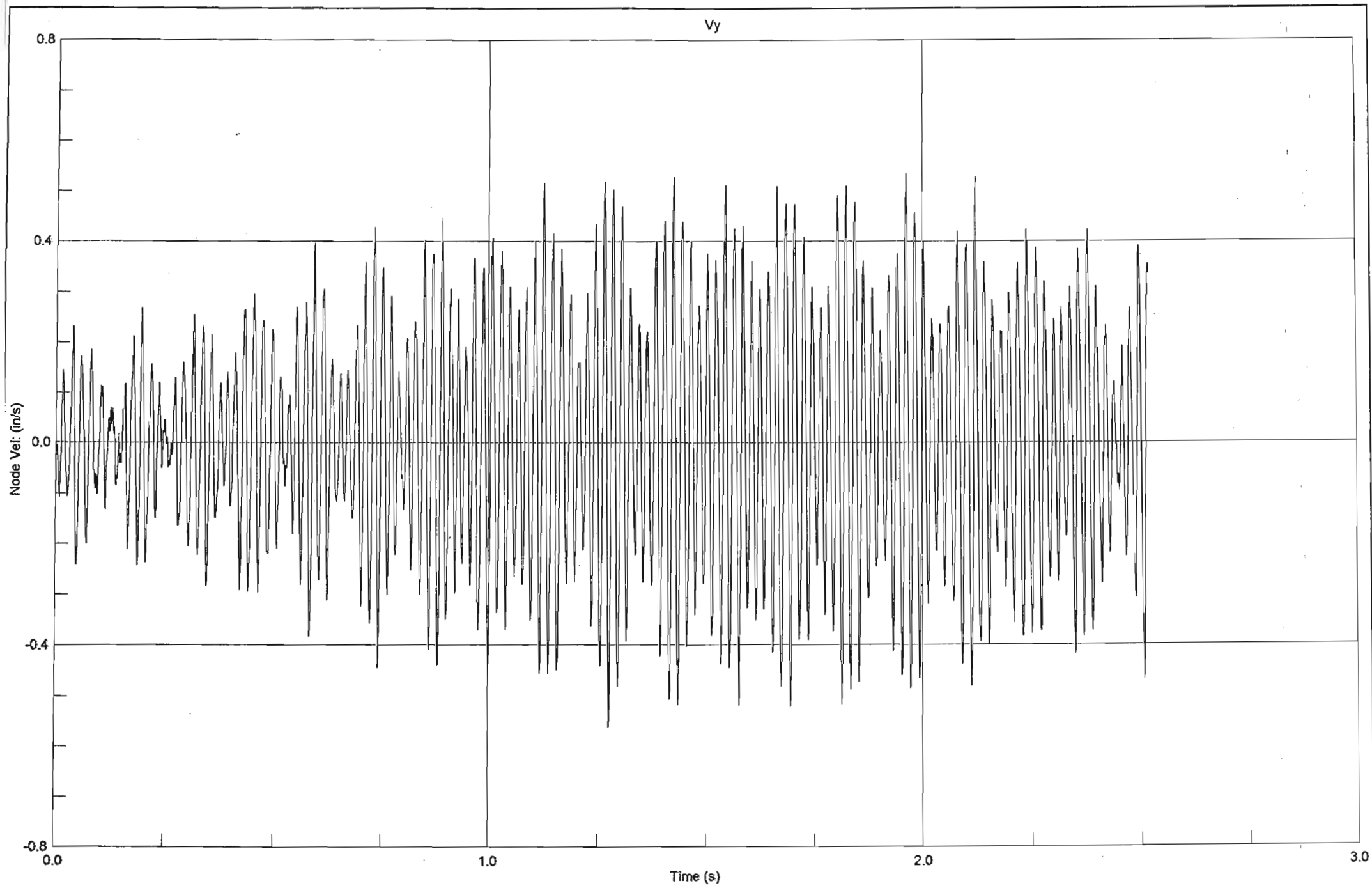
Z Displacement of Node 8

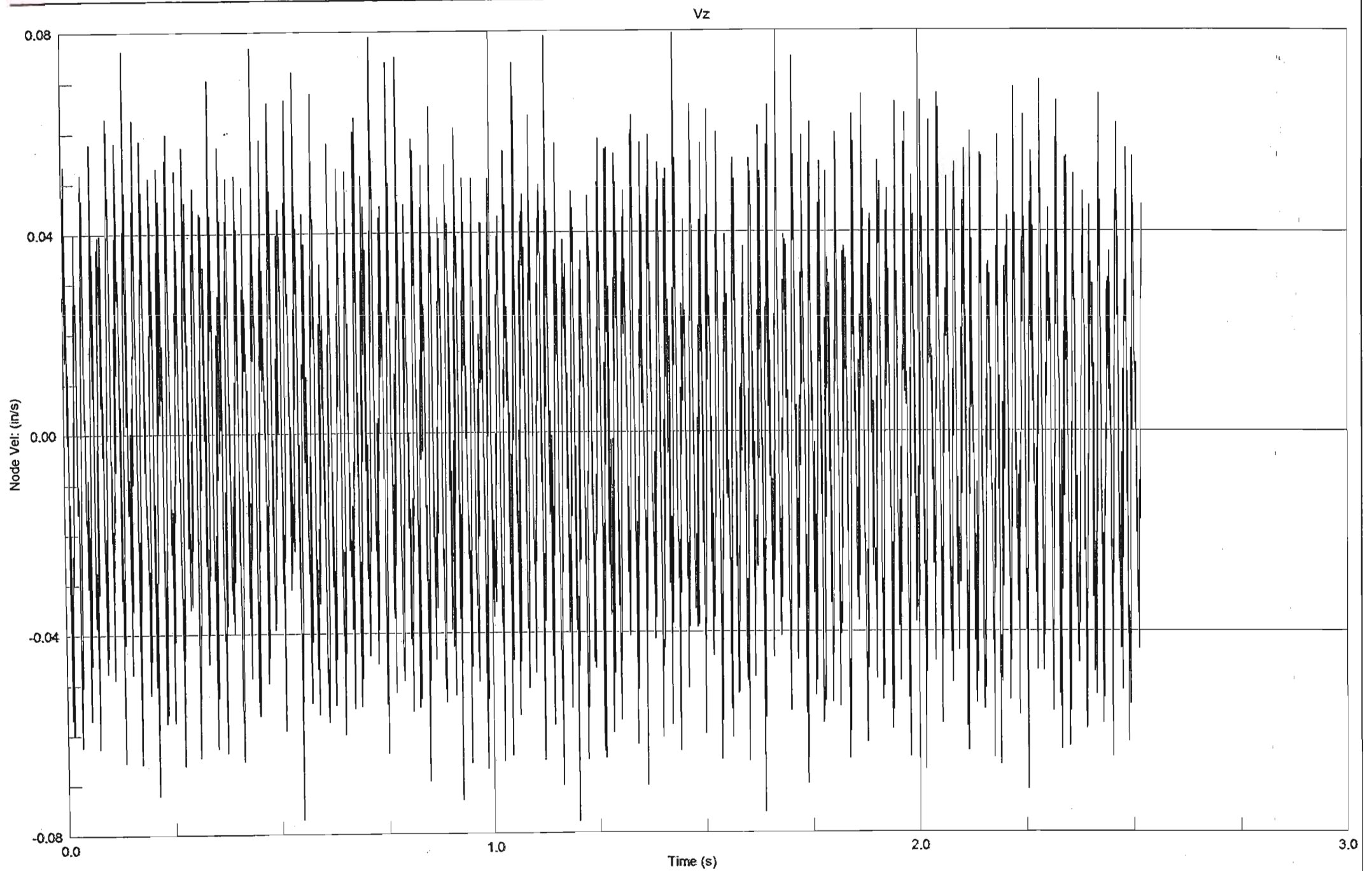


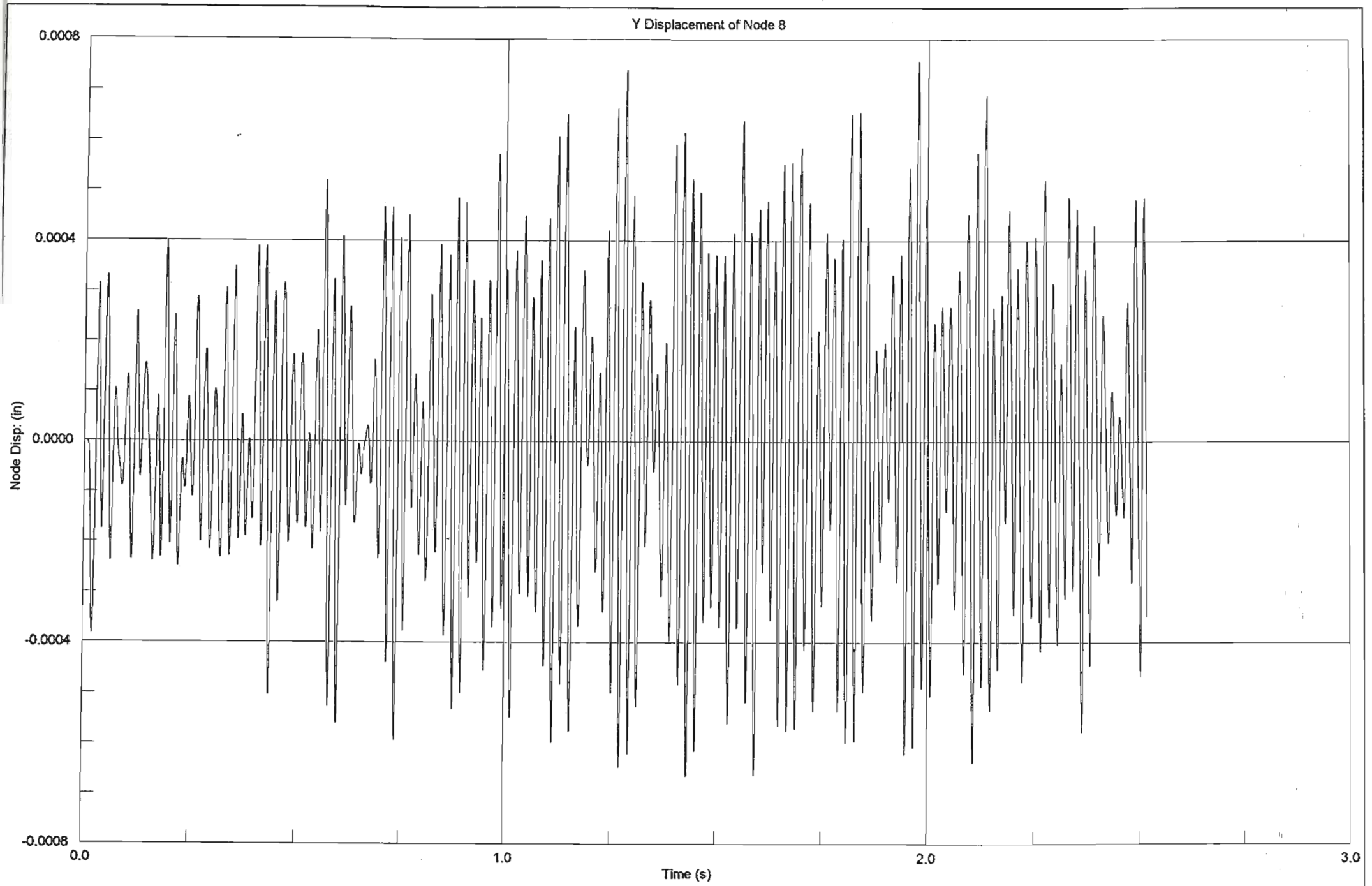


Z Displacement of Node 20

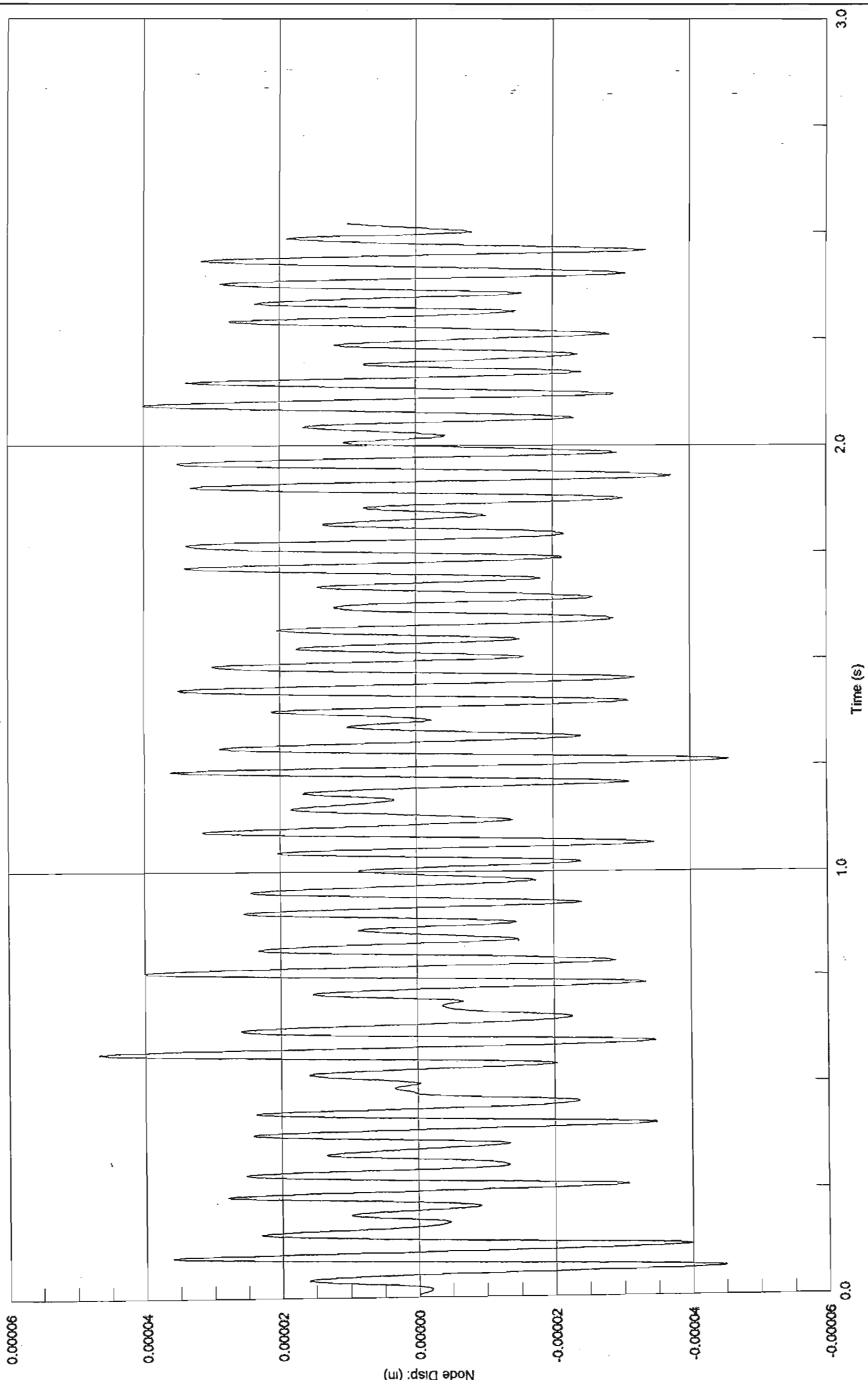


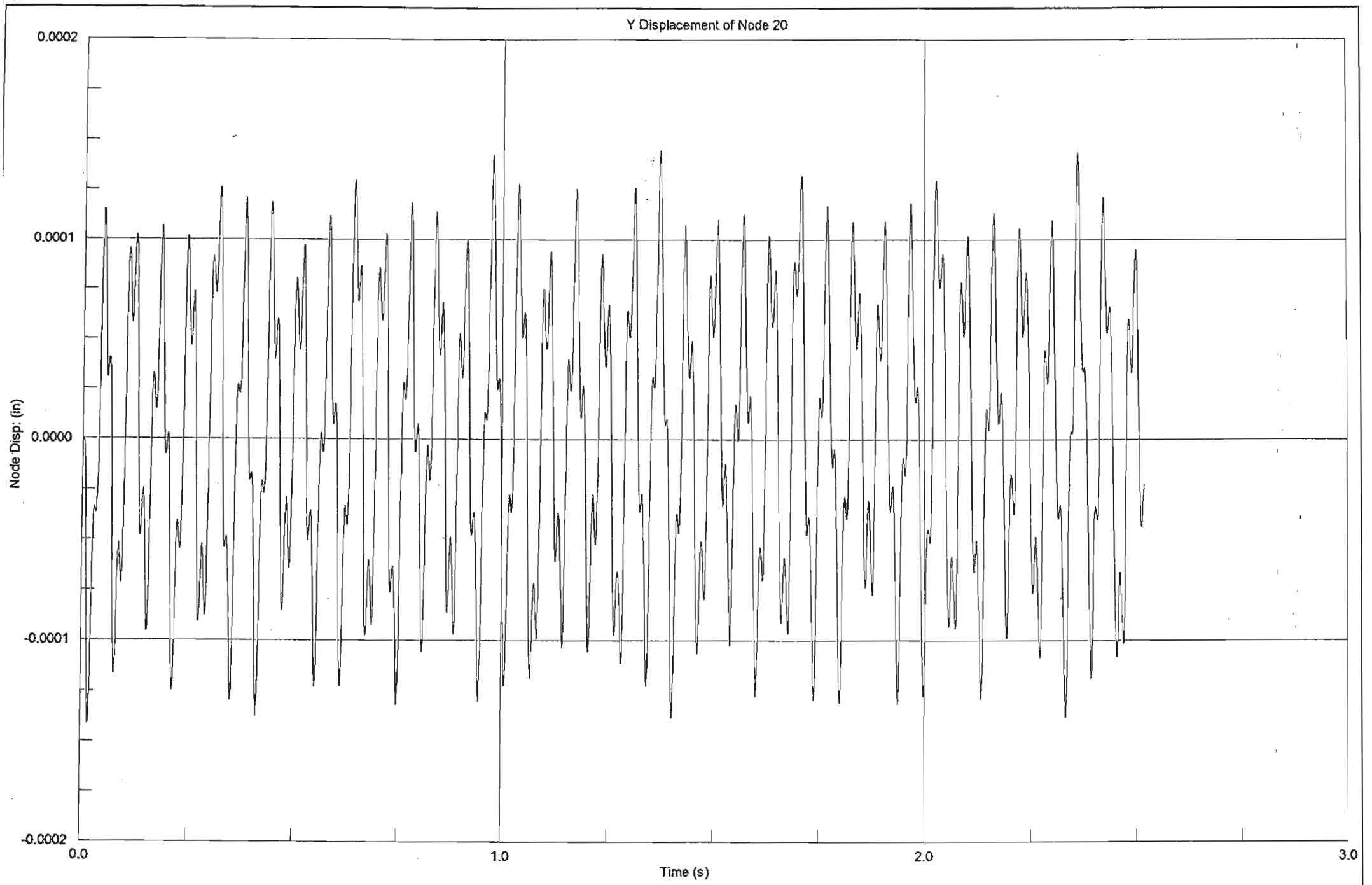




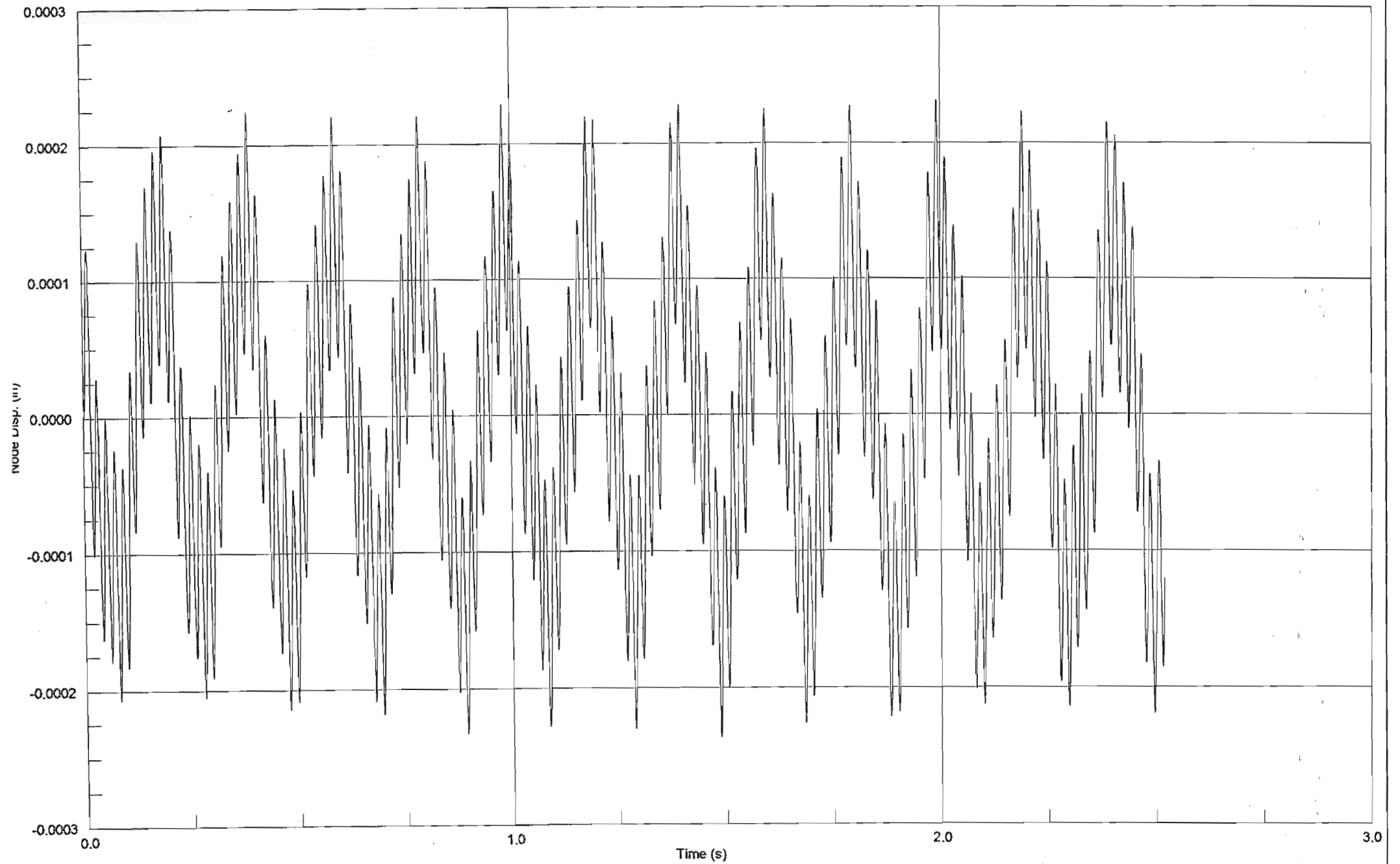


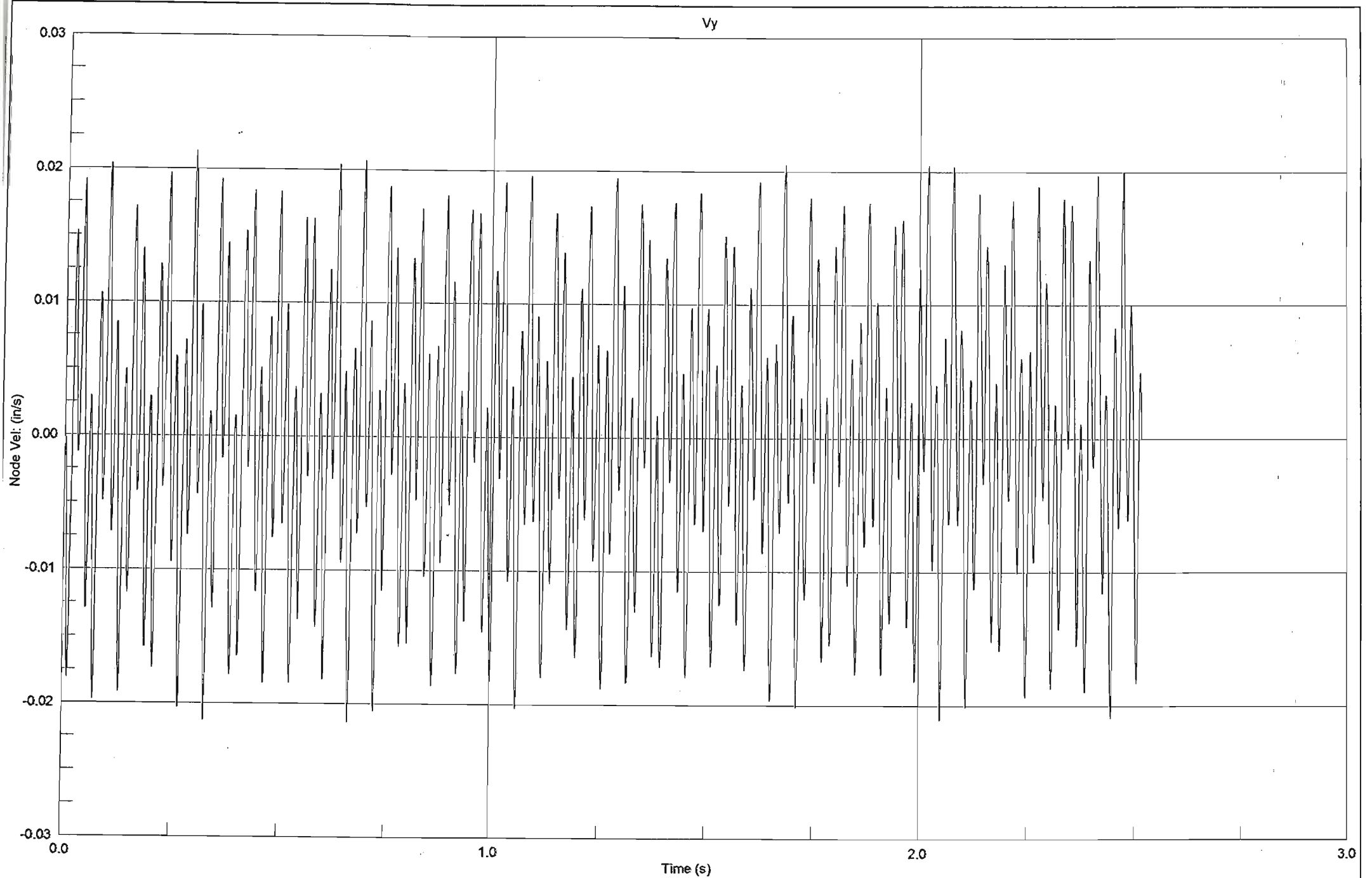
Z Displacement of Node 8

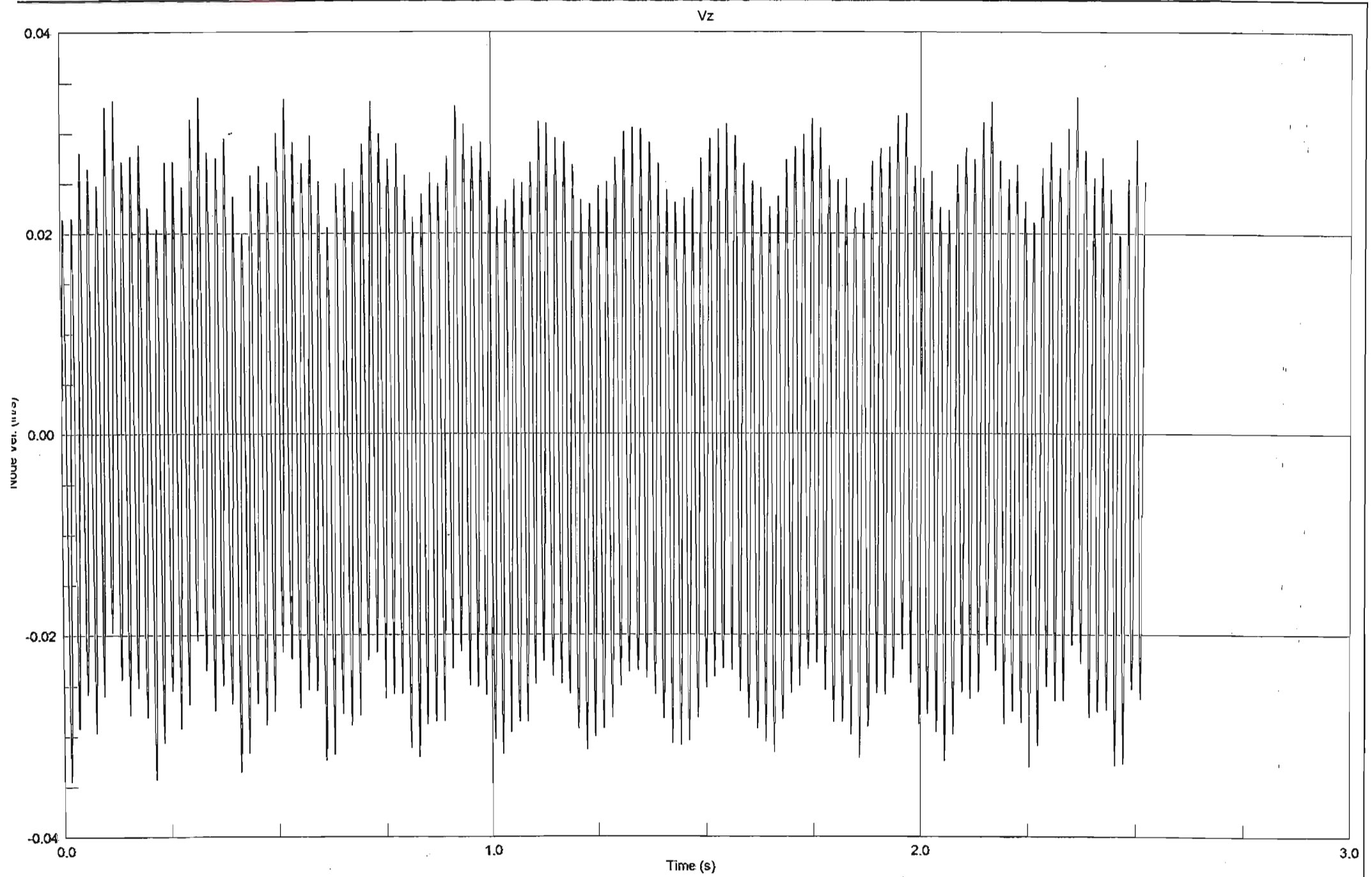




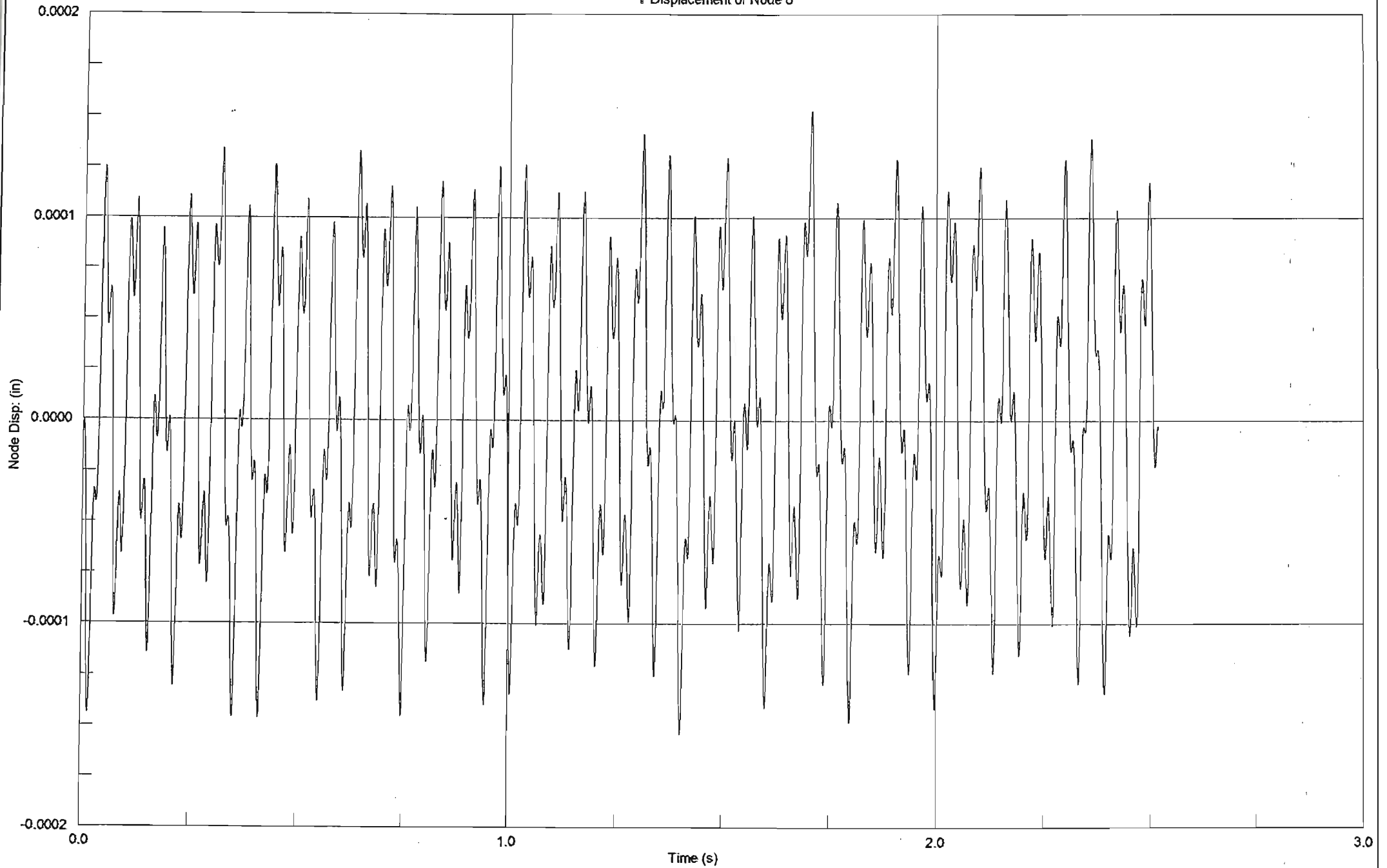
Z Displacement of Node 20

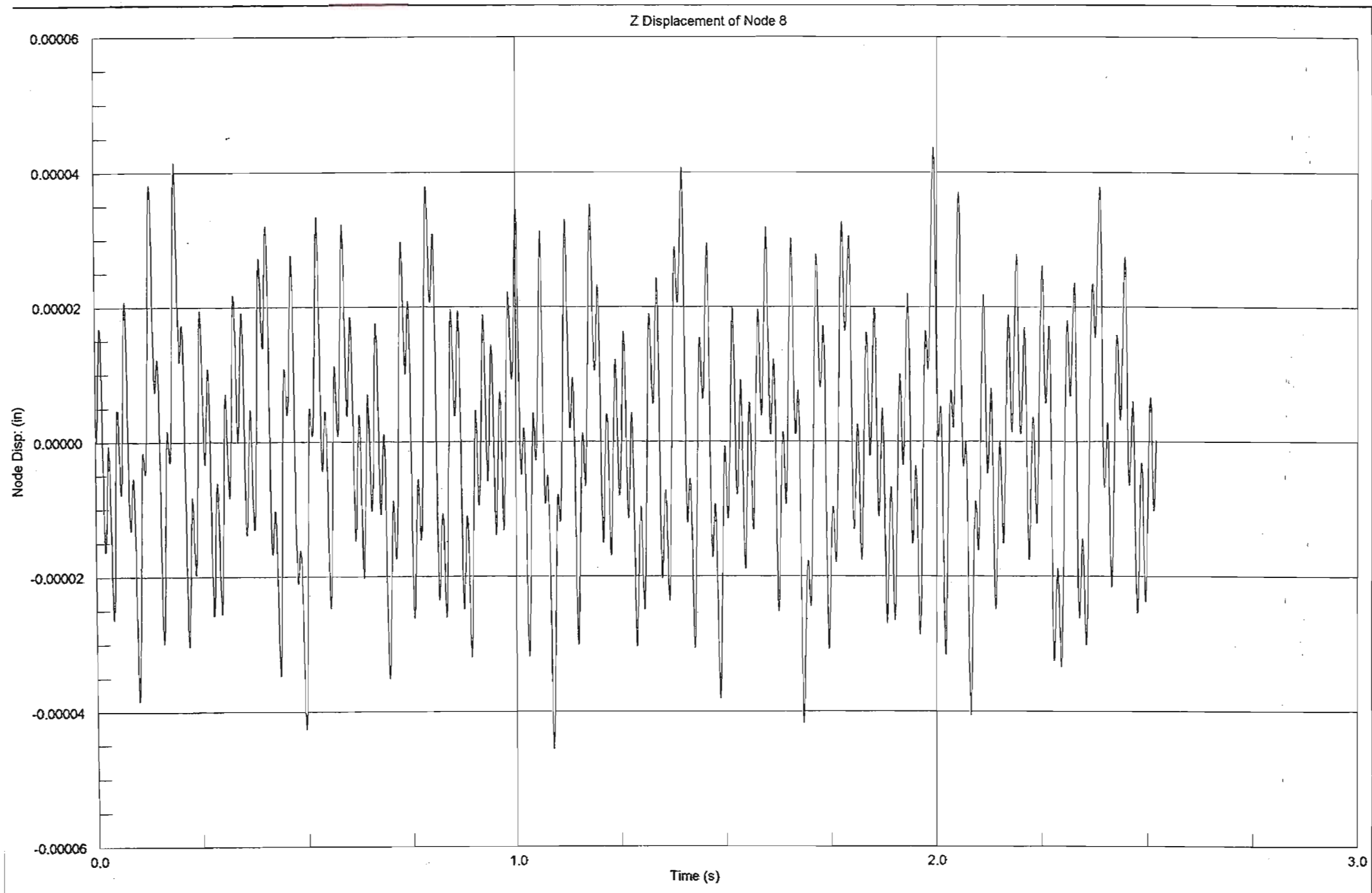


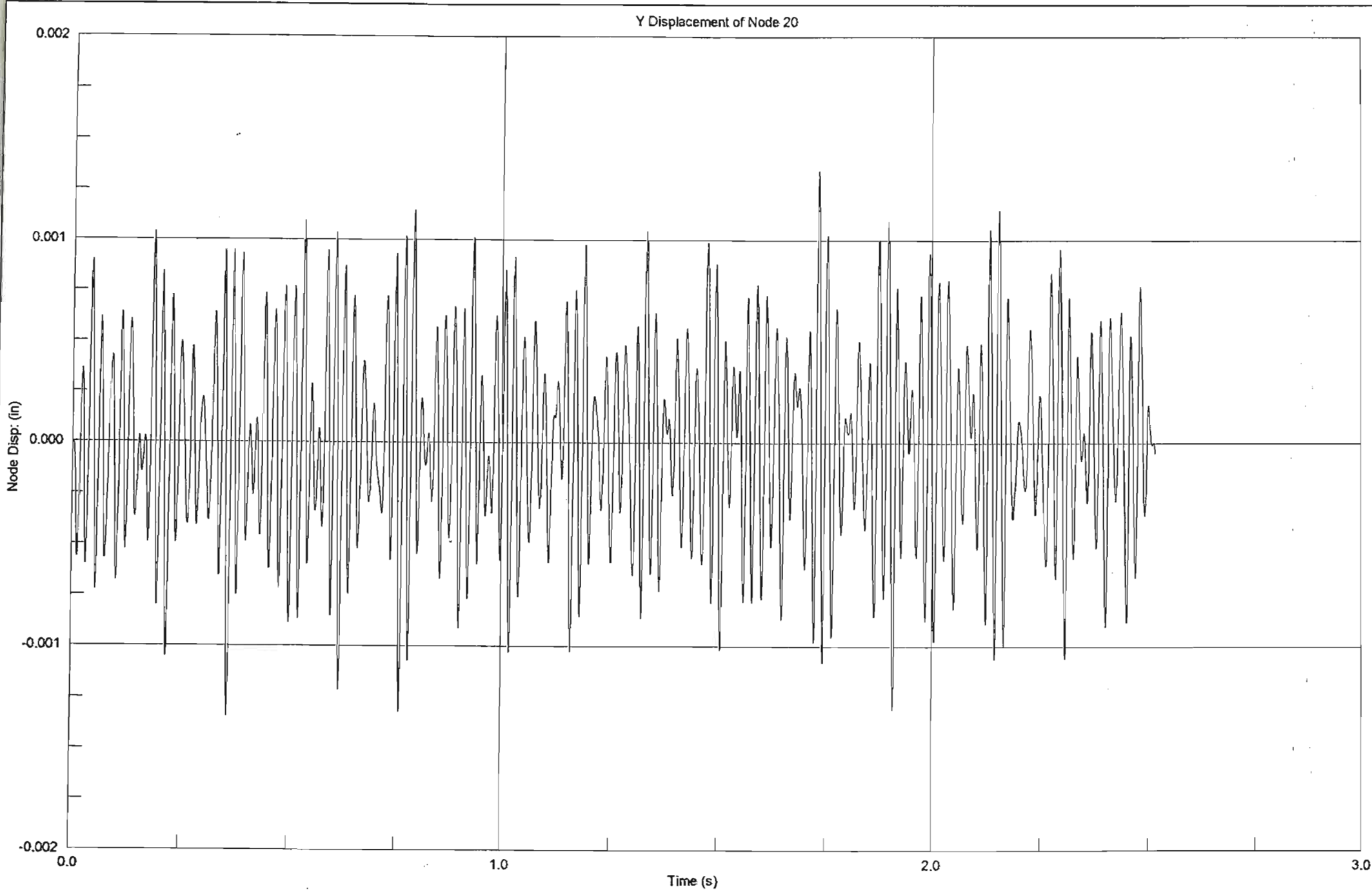




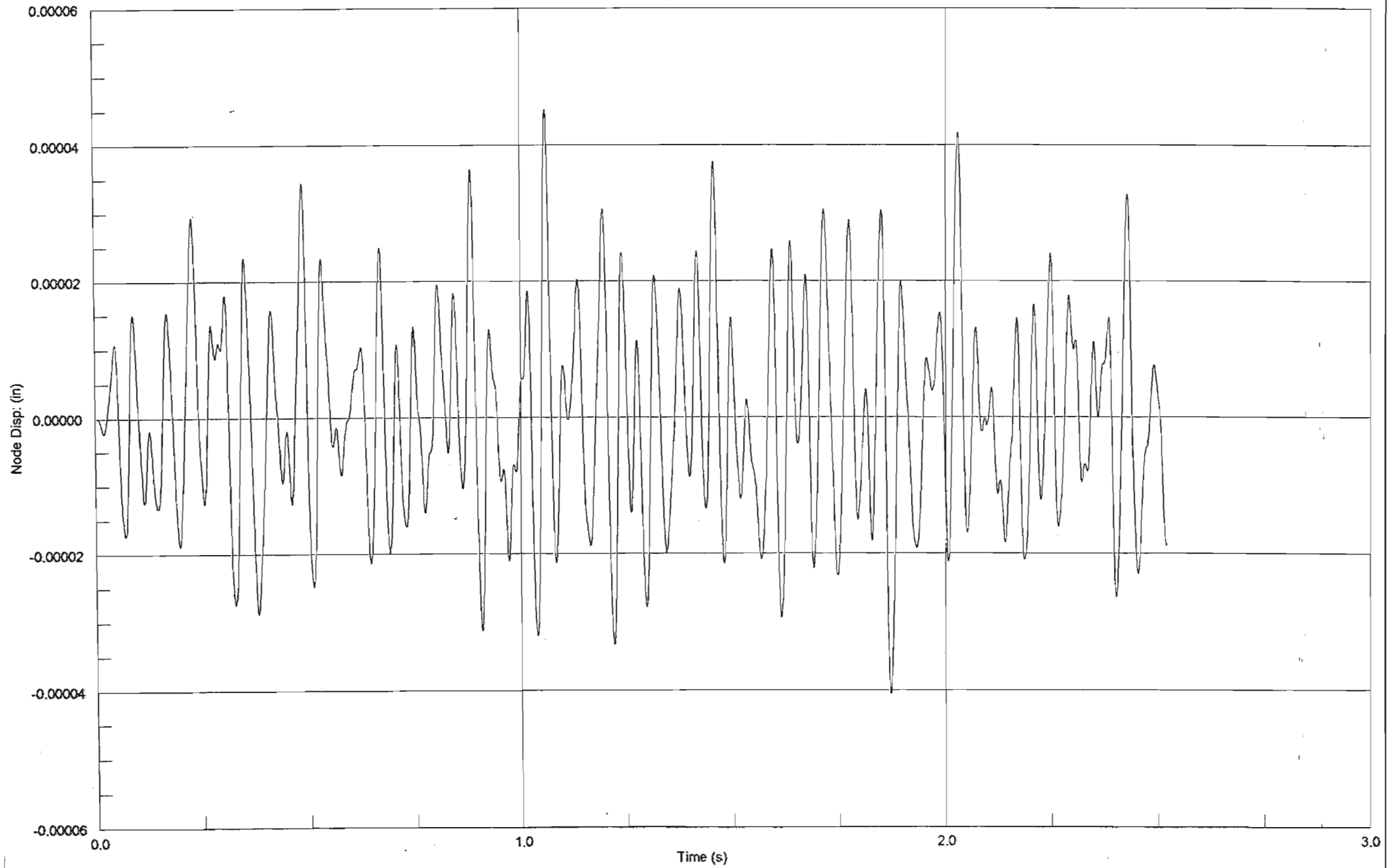
Y Displacement of Node 8

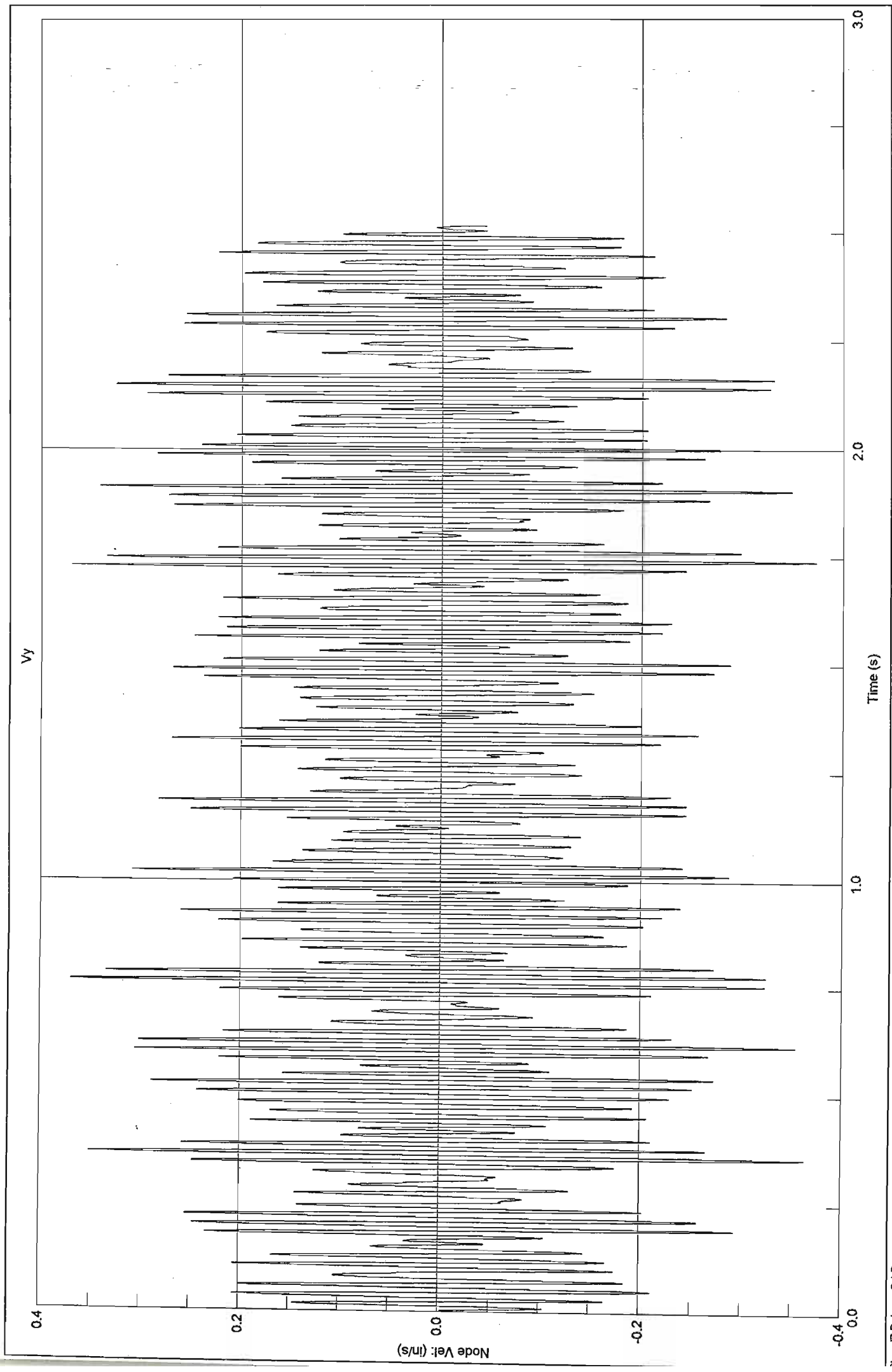




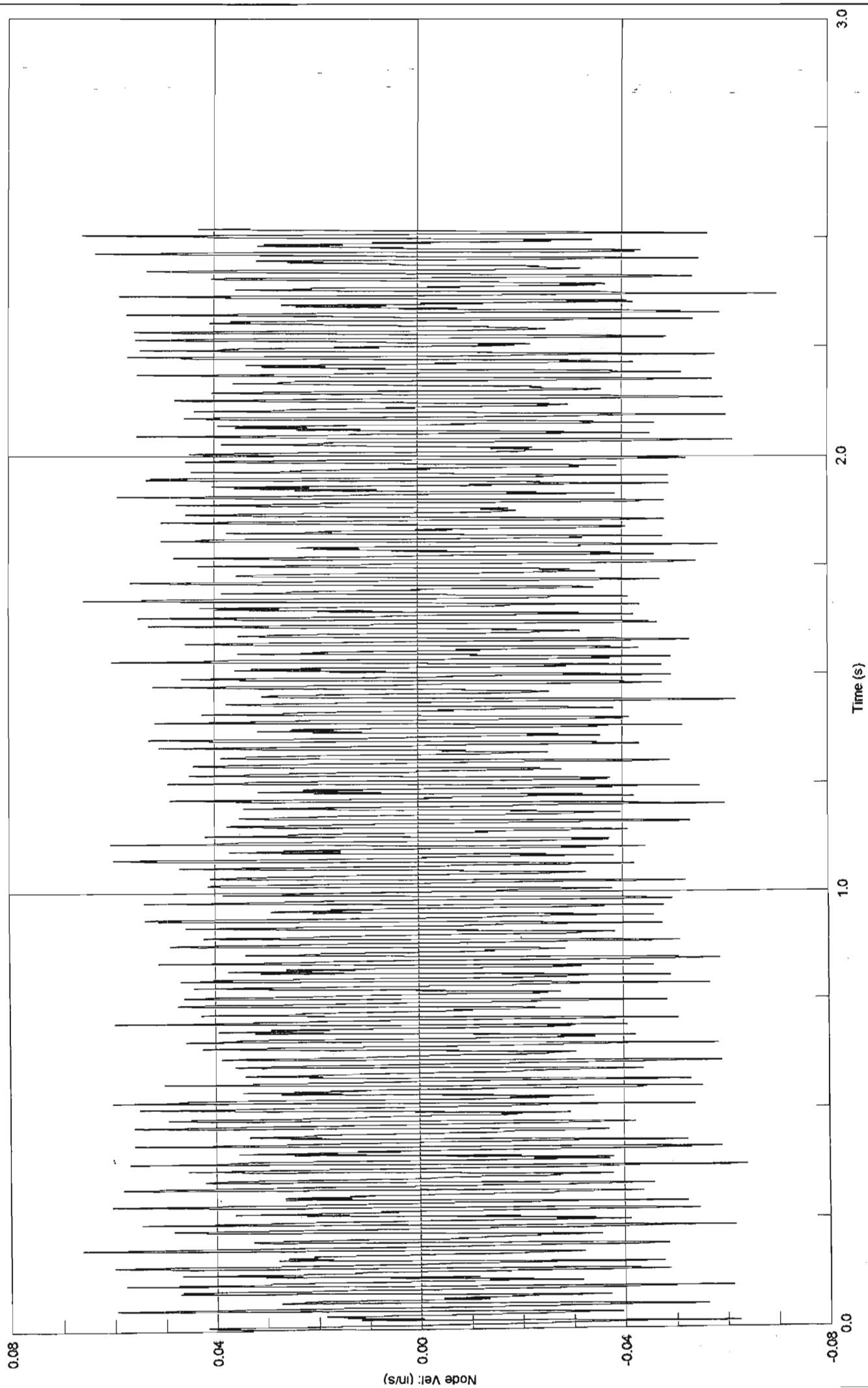


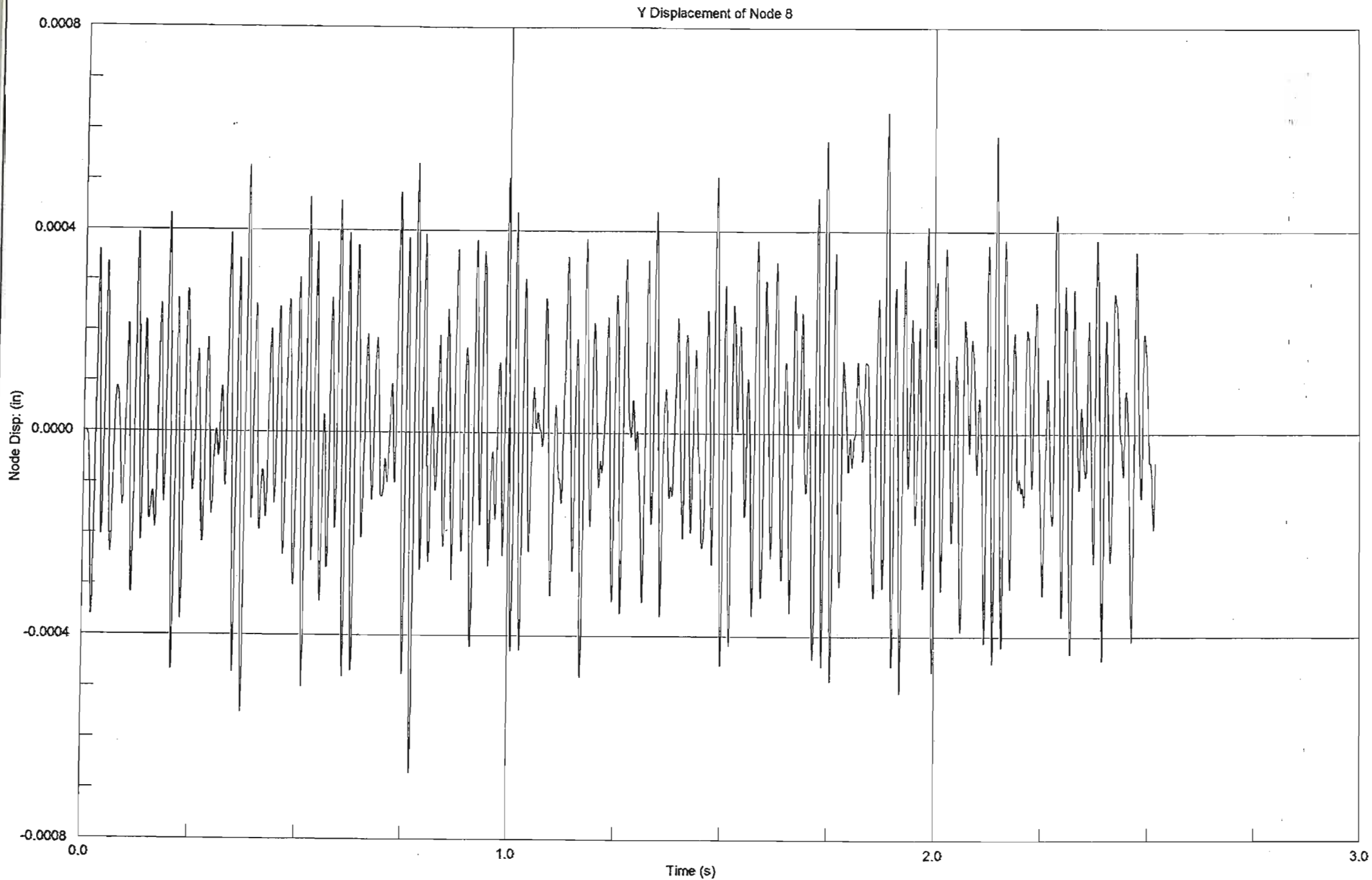
Z Displacement of Node 20



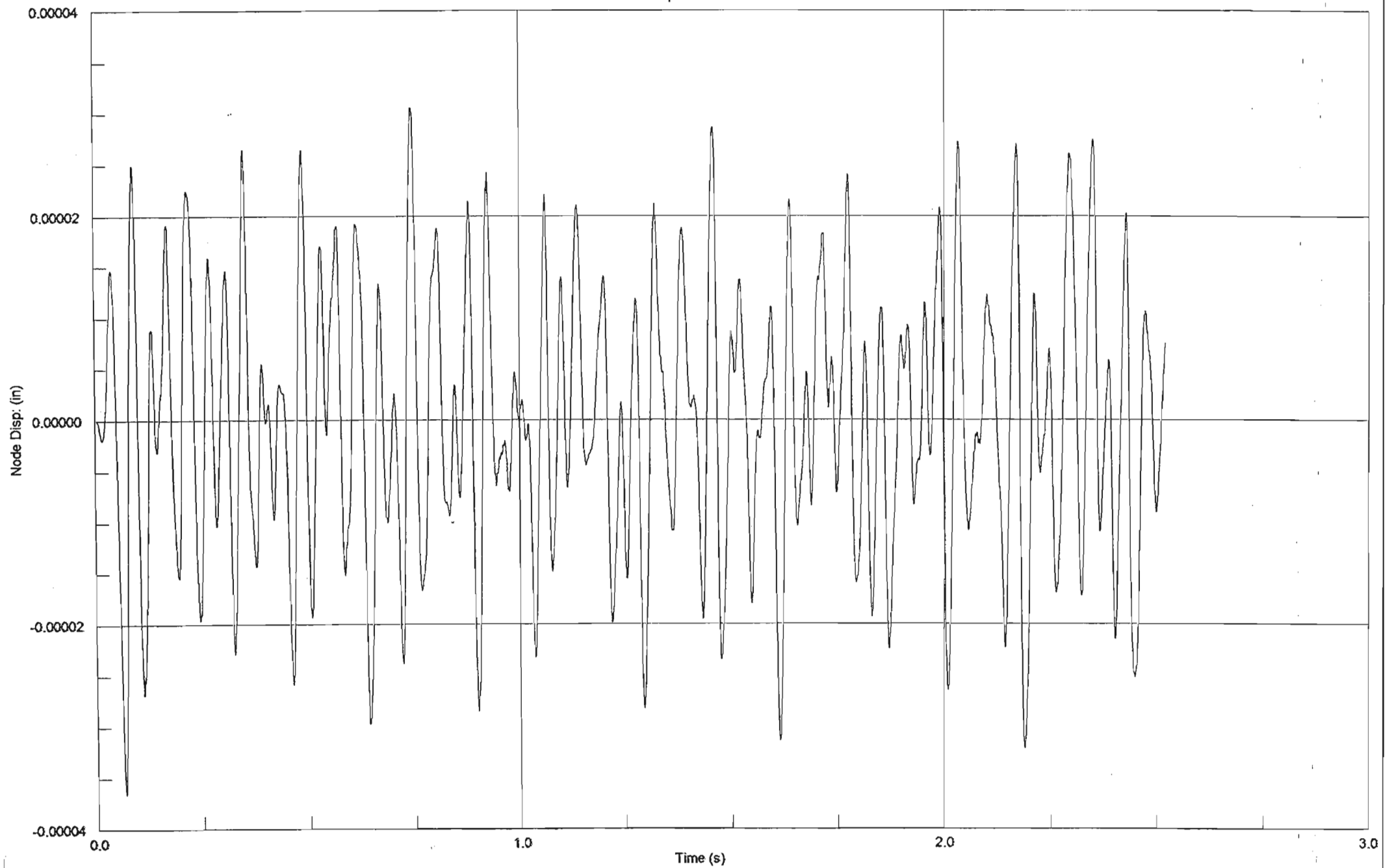


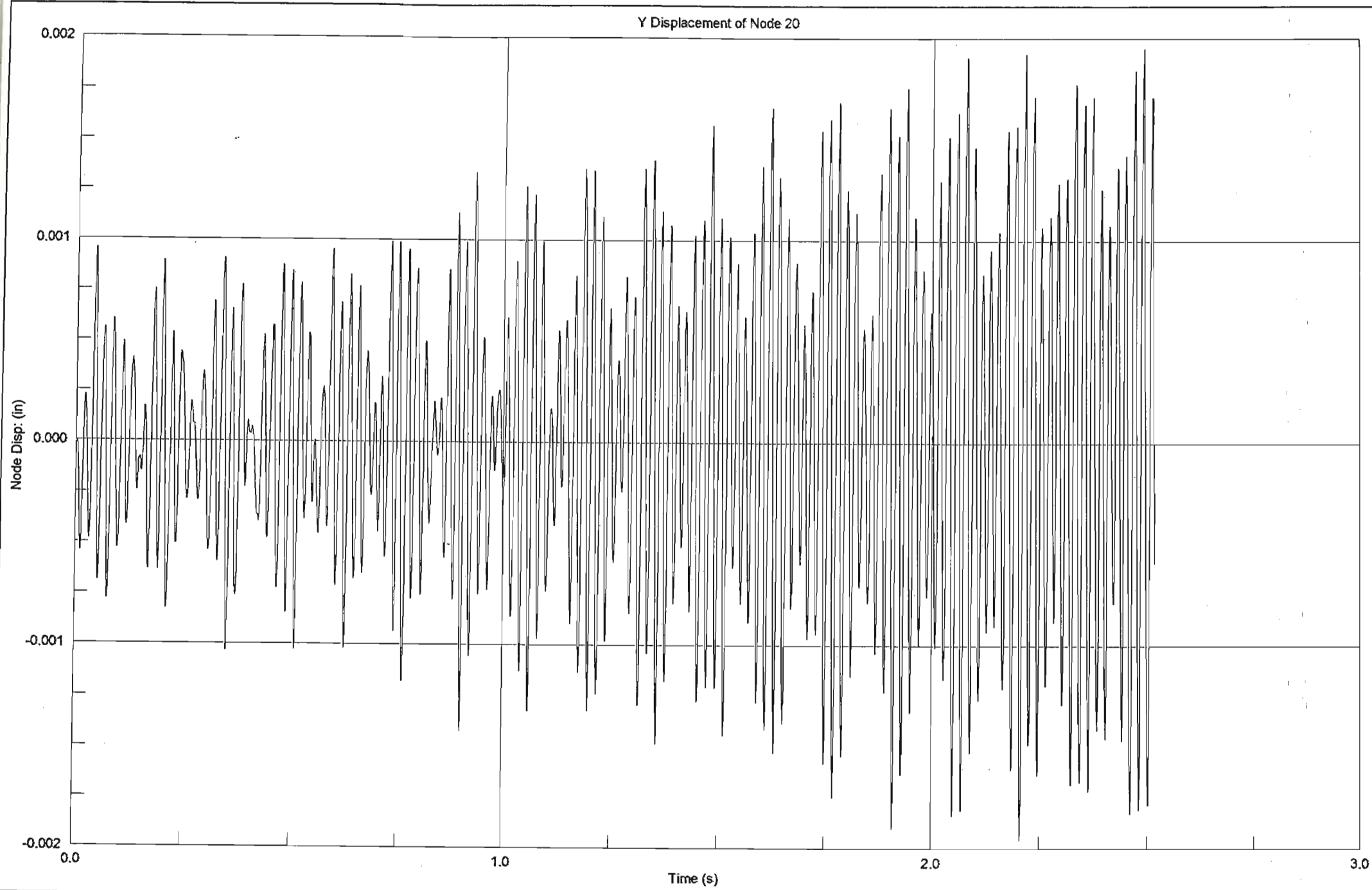
Vz



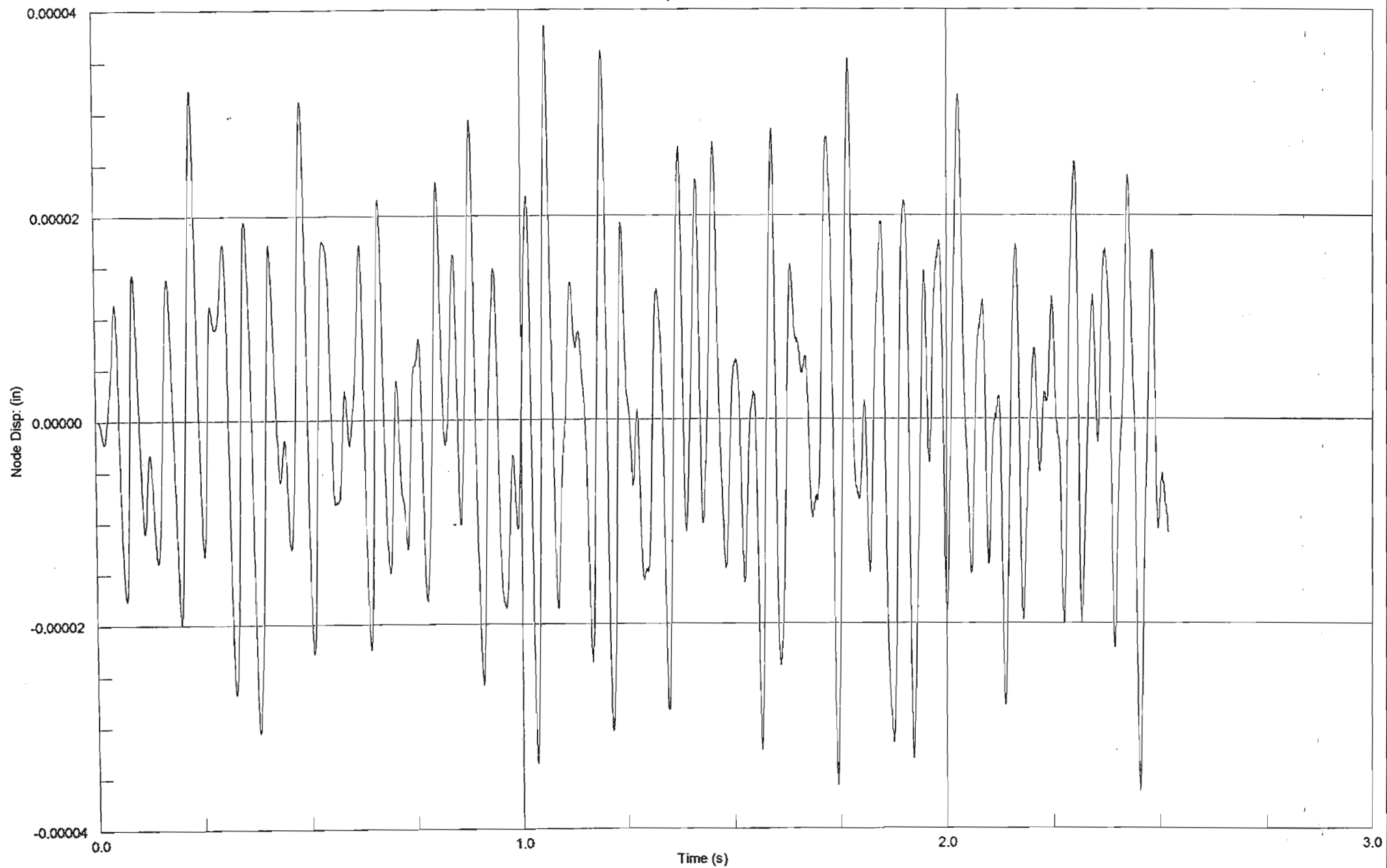


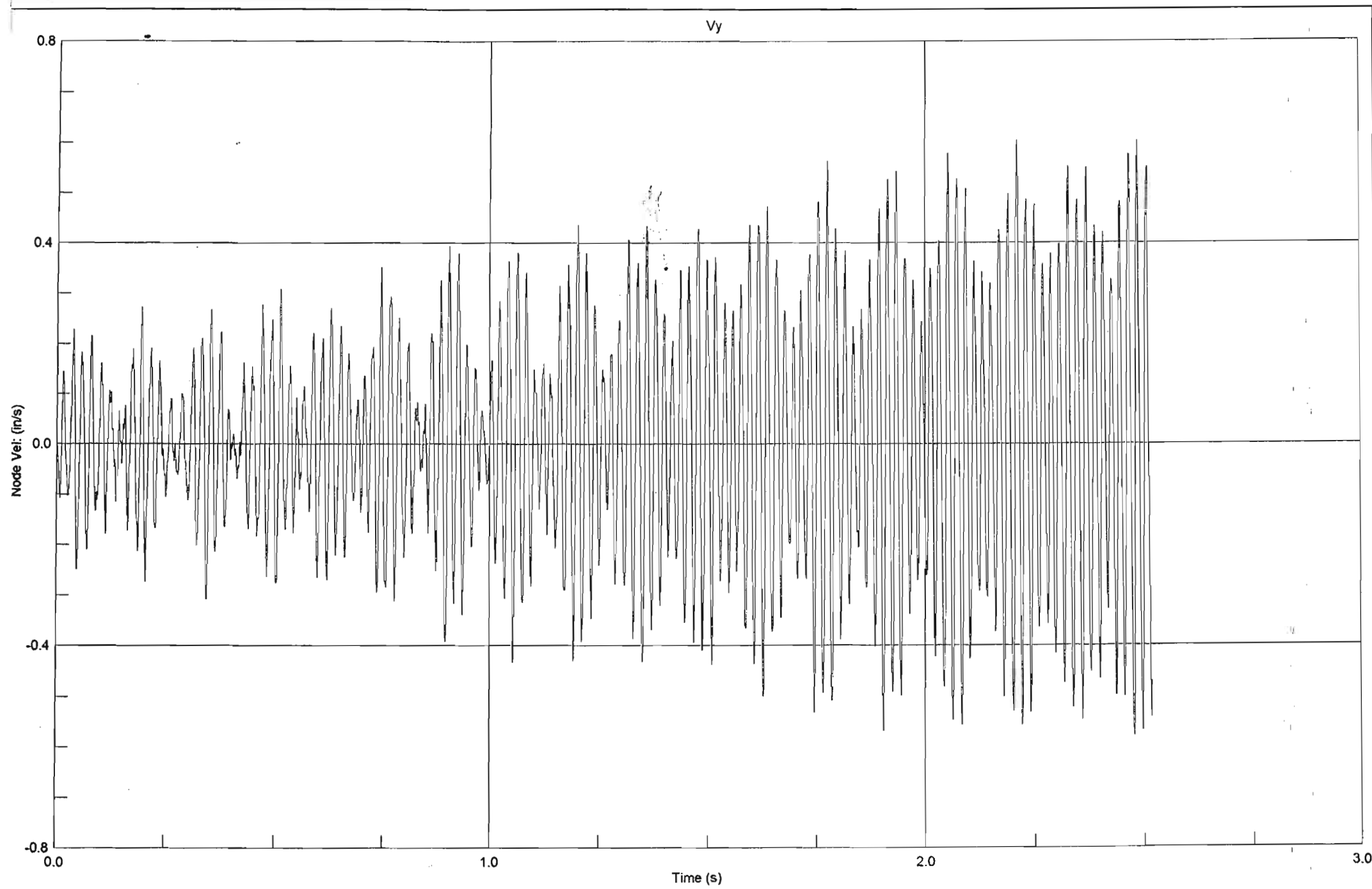
Z Displacement of Node 8

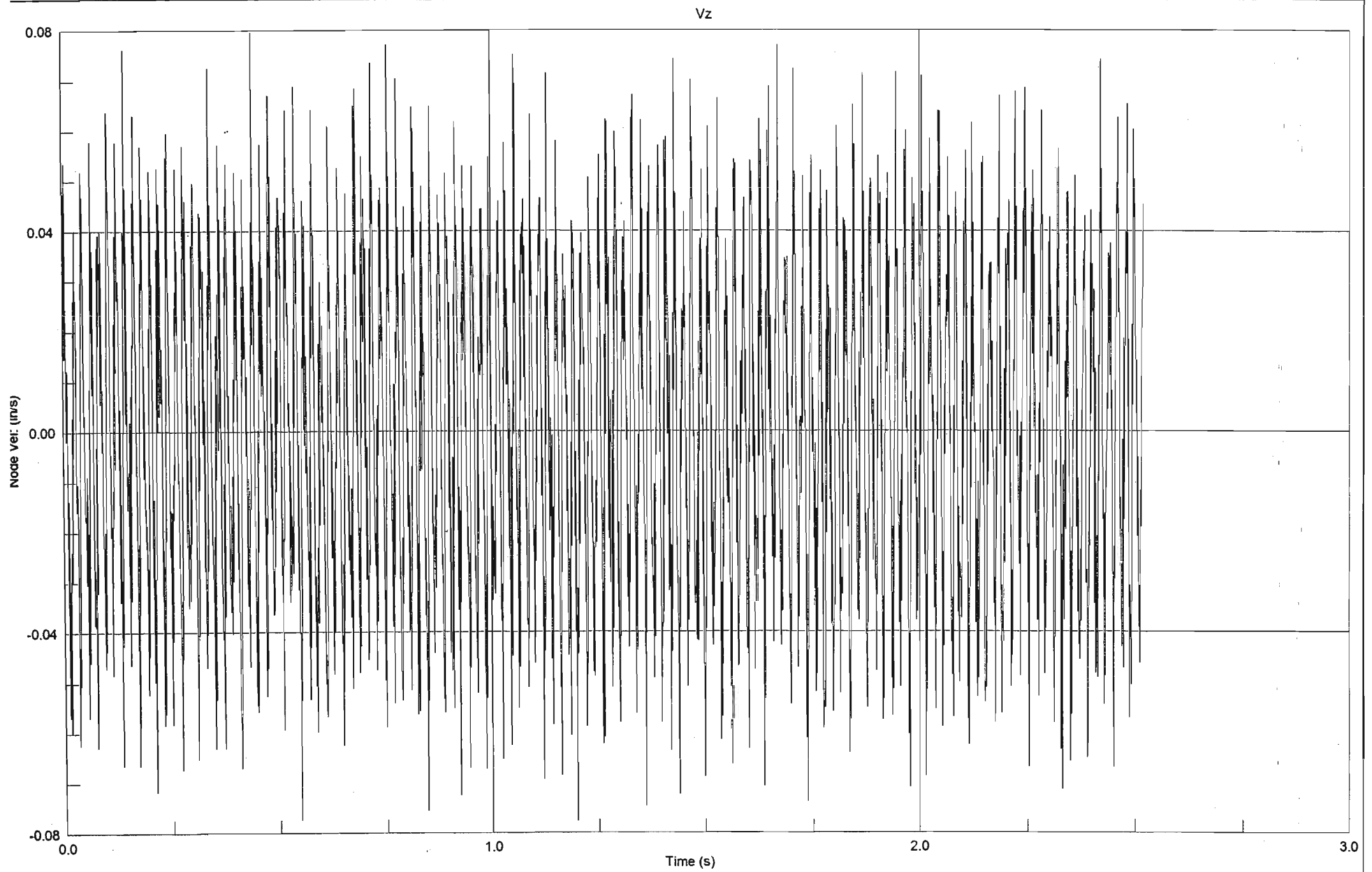


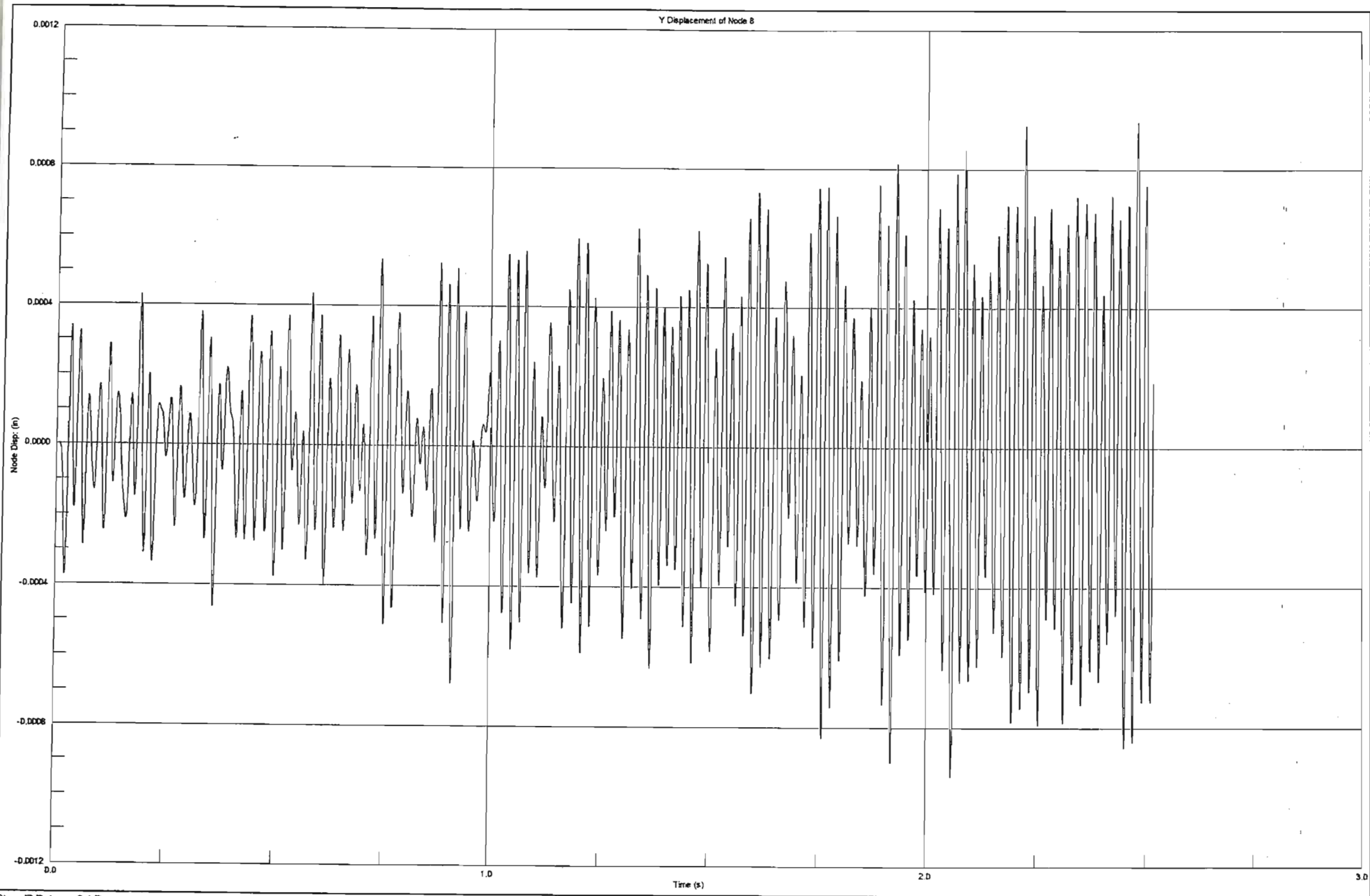


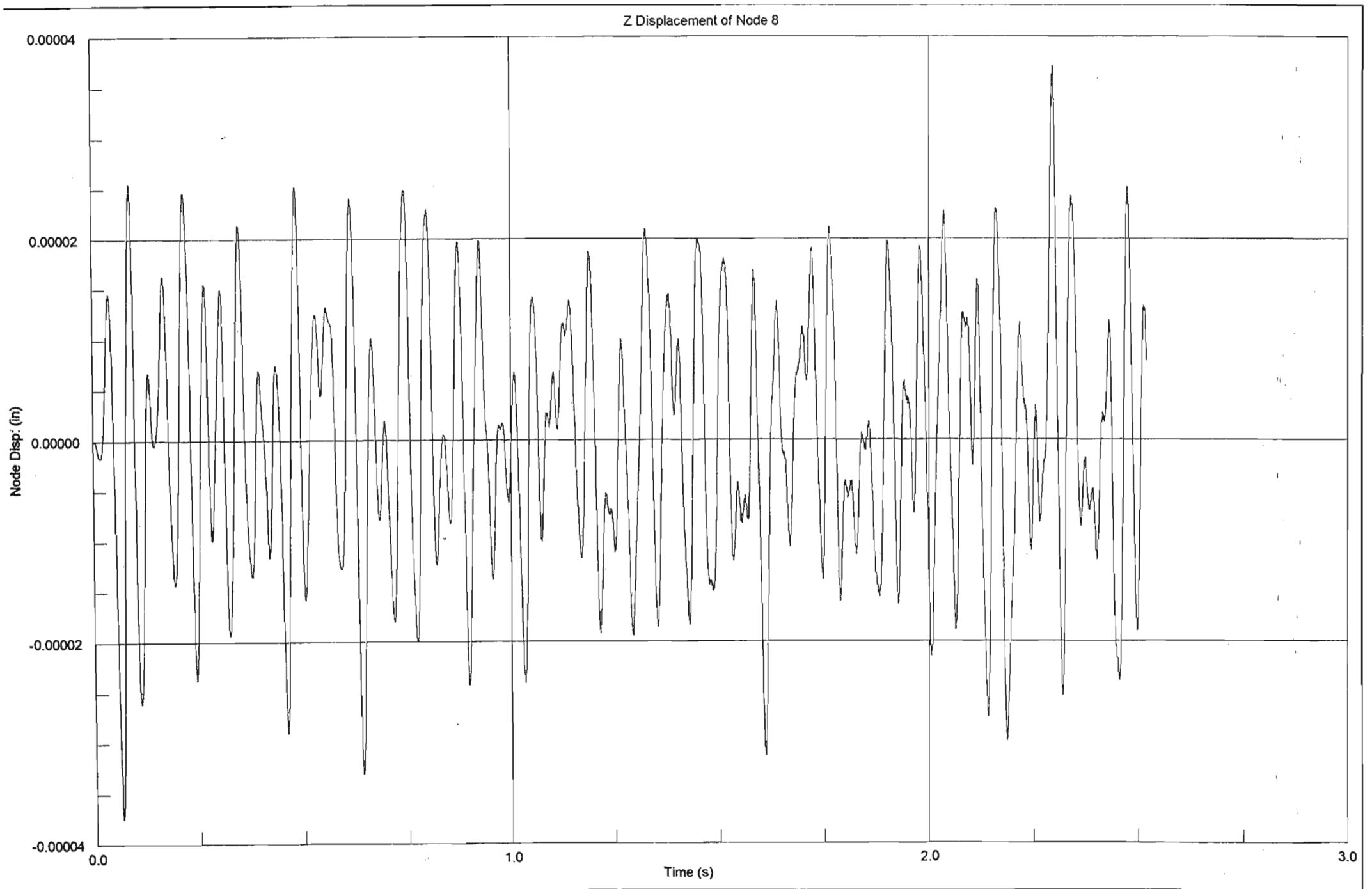
Z Displacement of Node 20

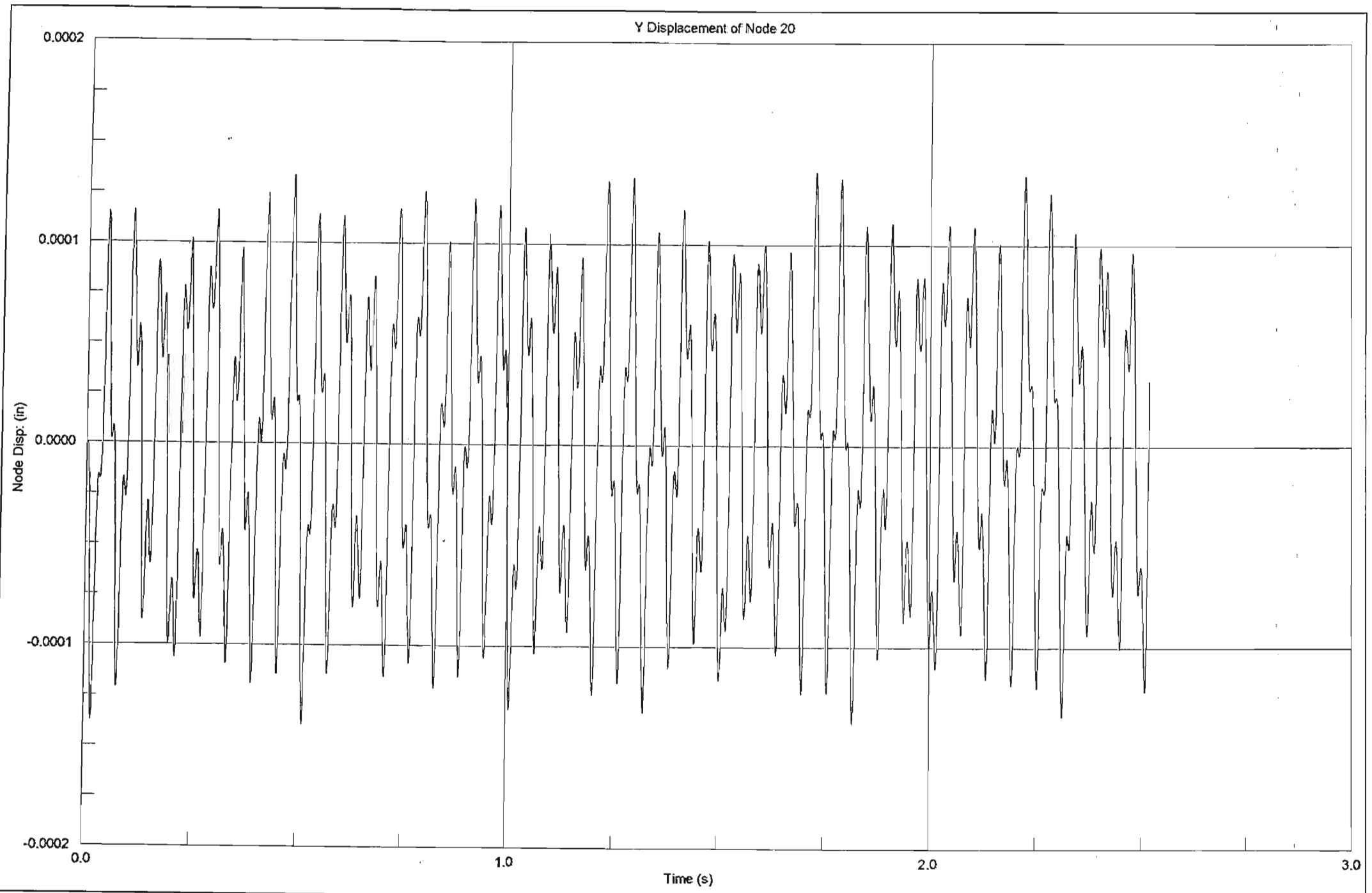




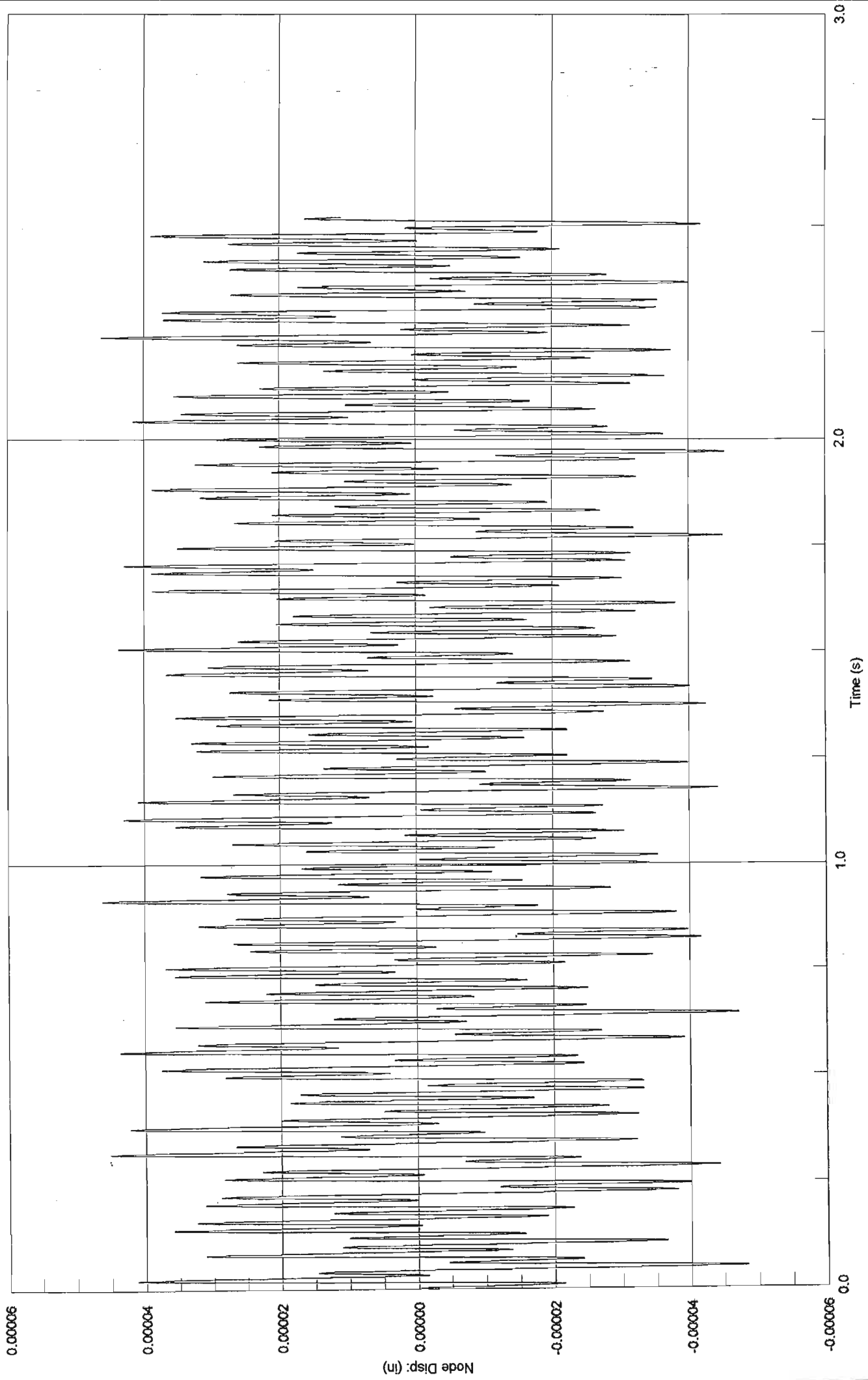


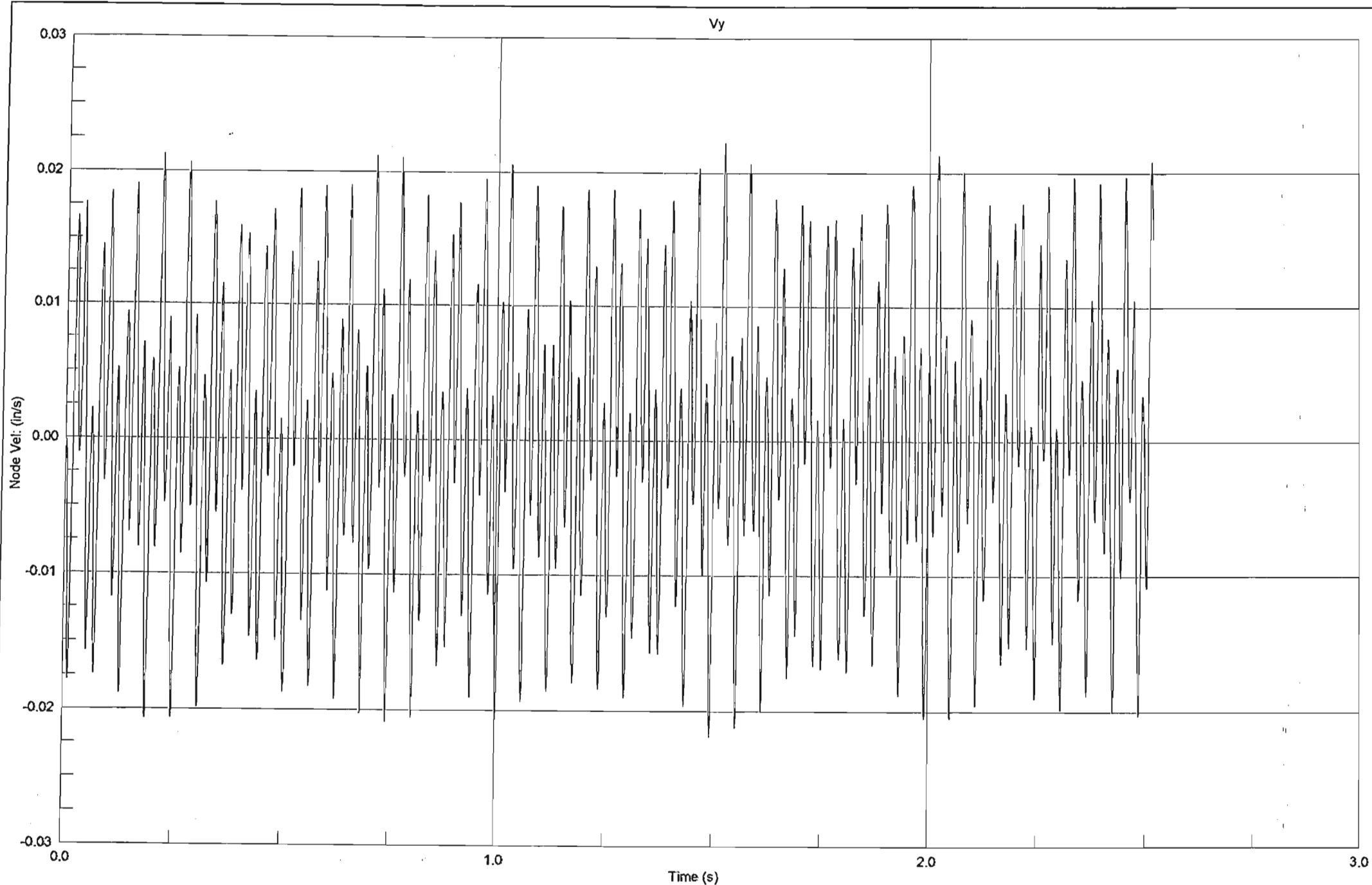


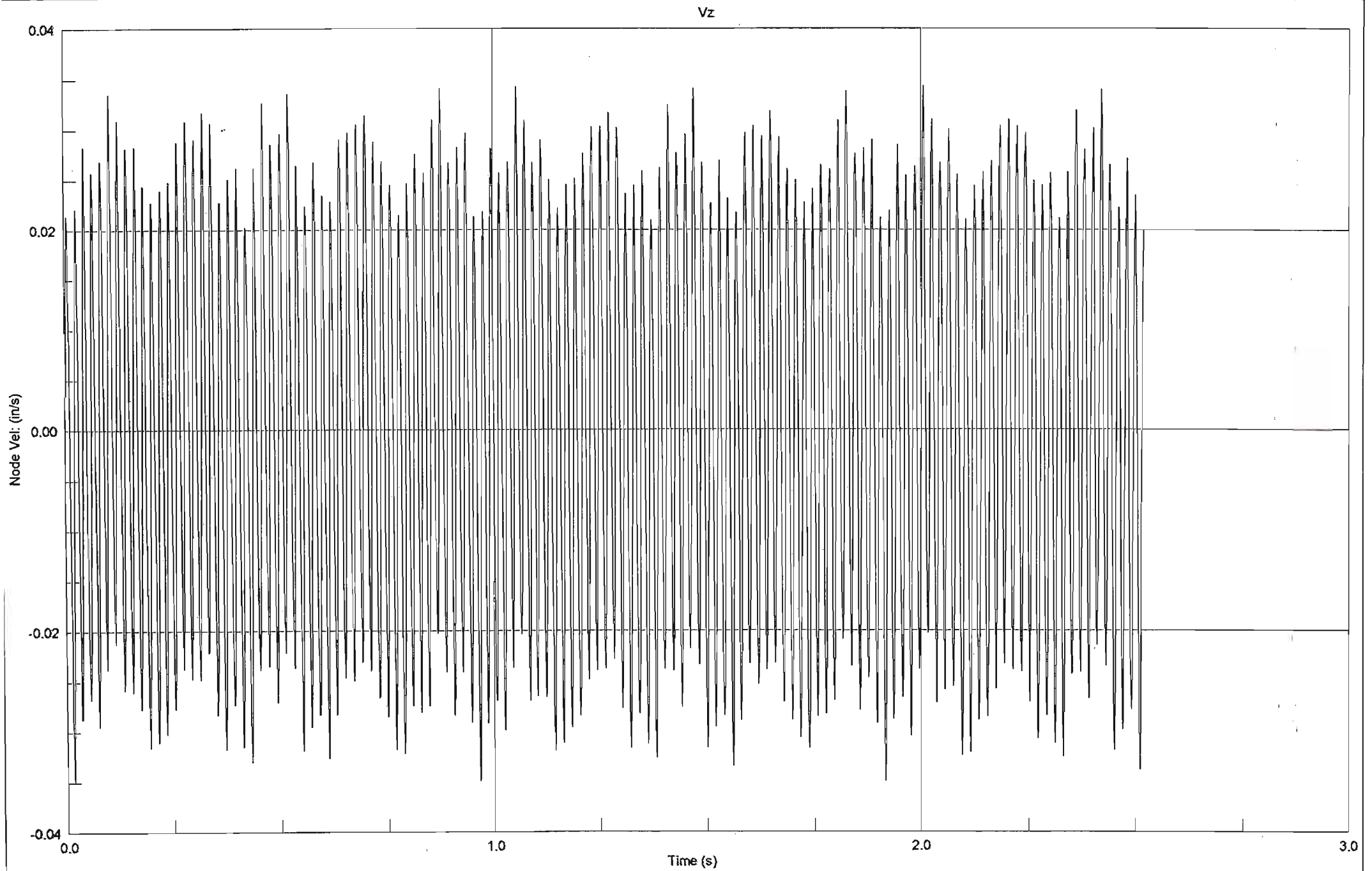


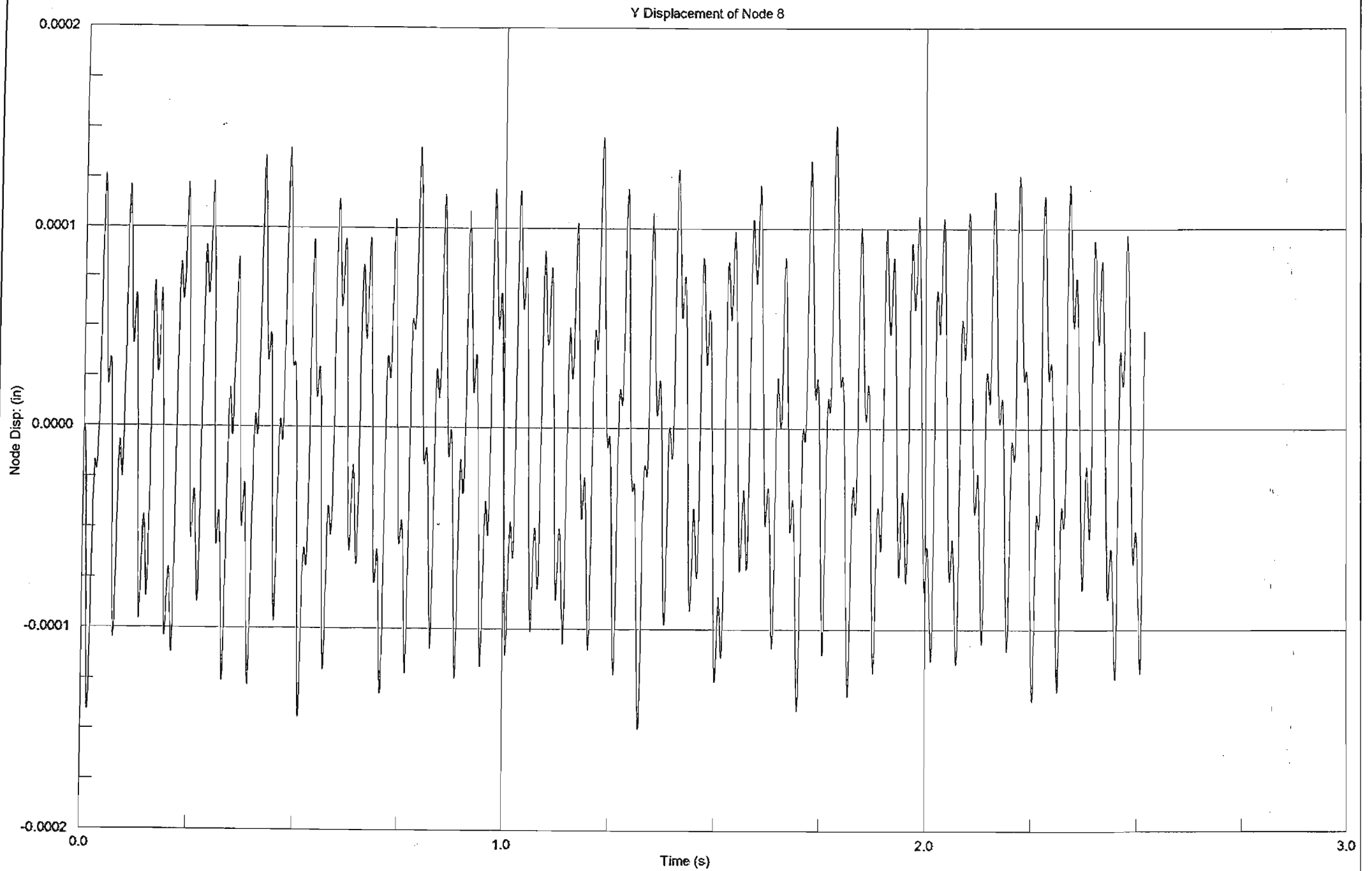


Z Displacement of Node 20

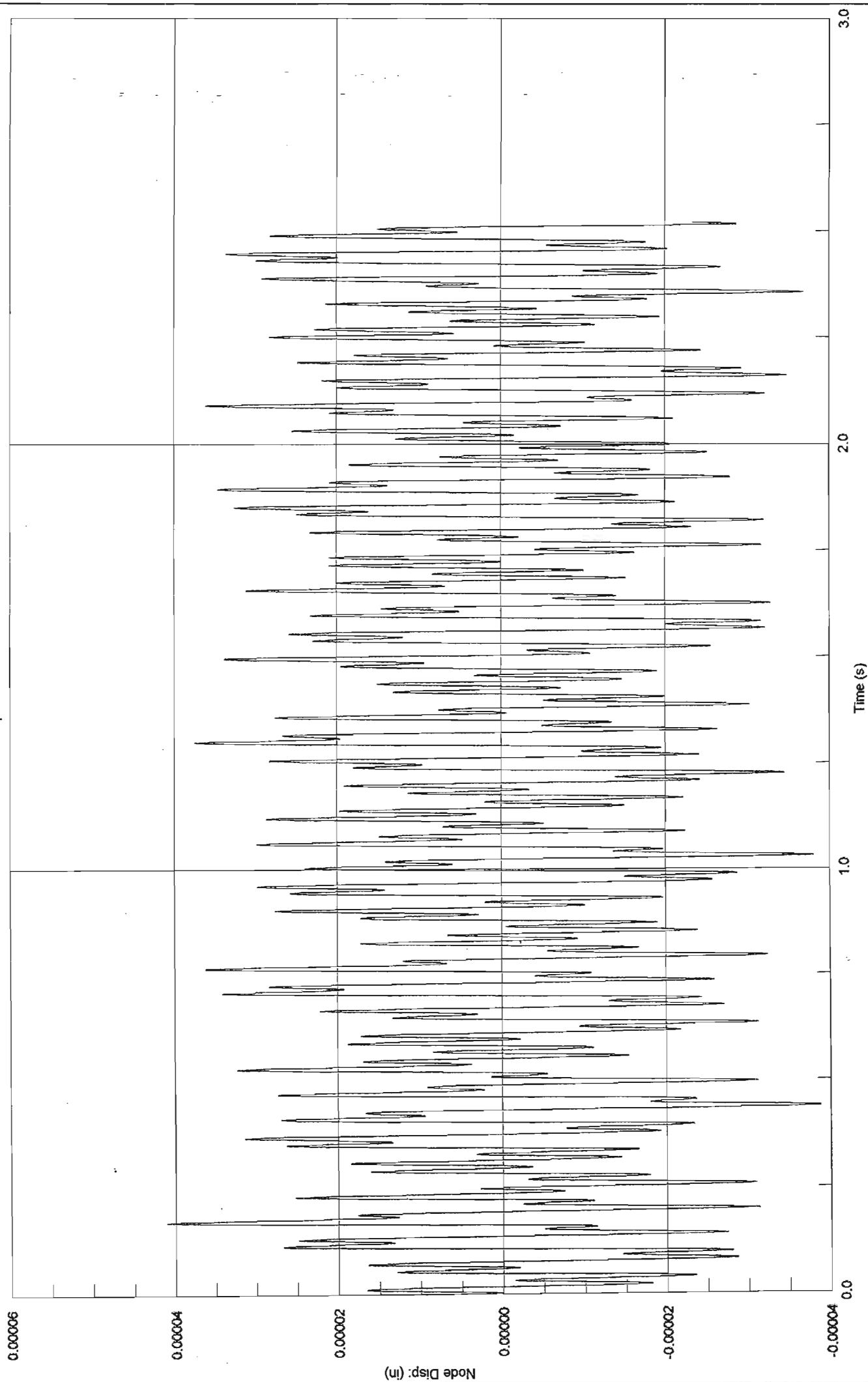


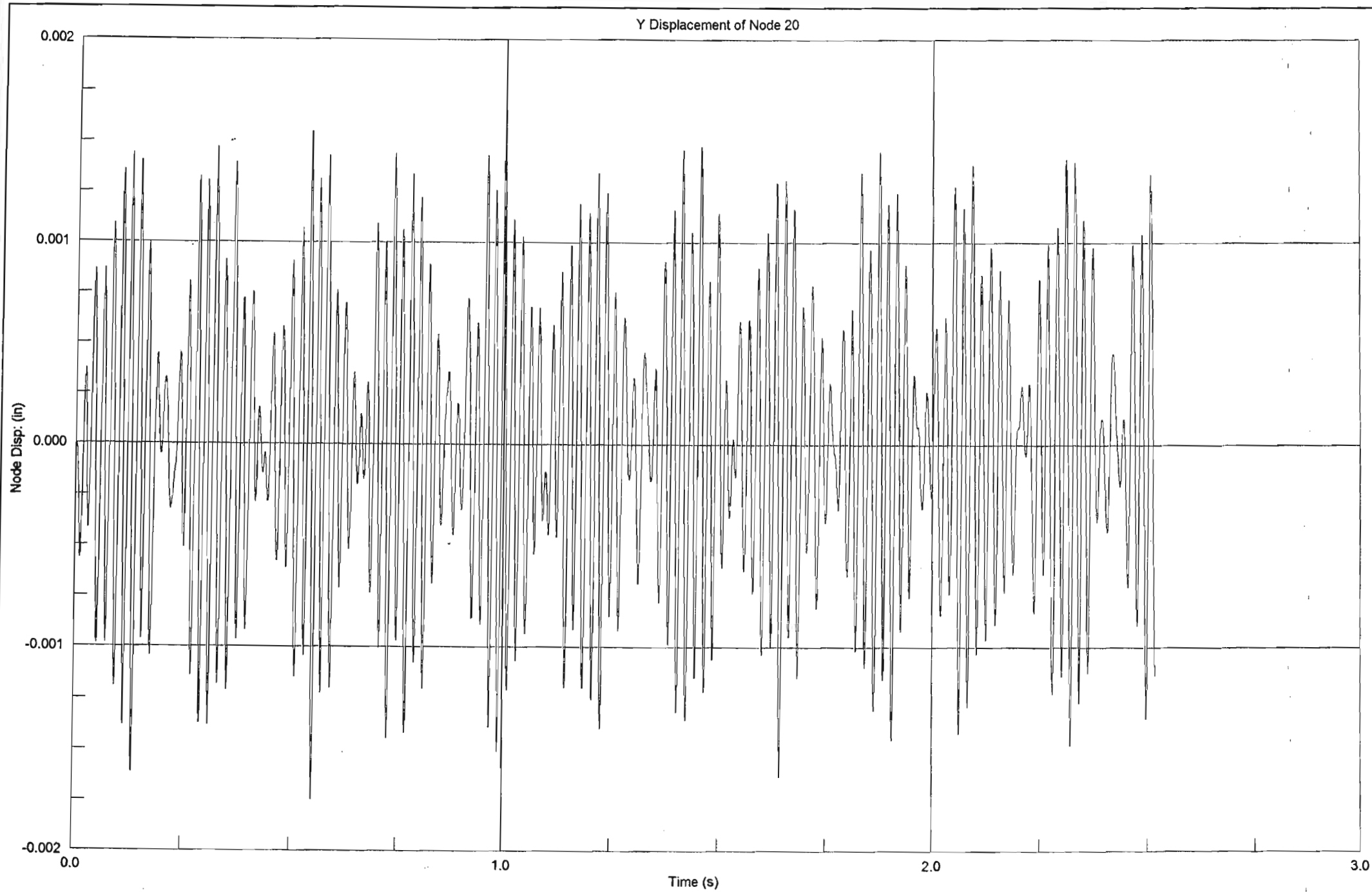




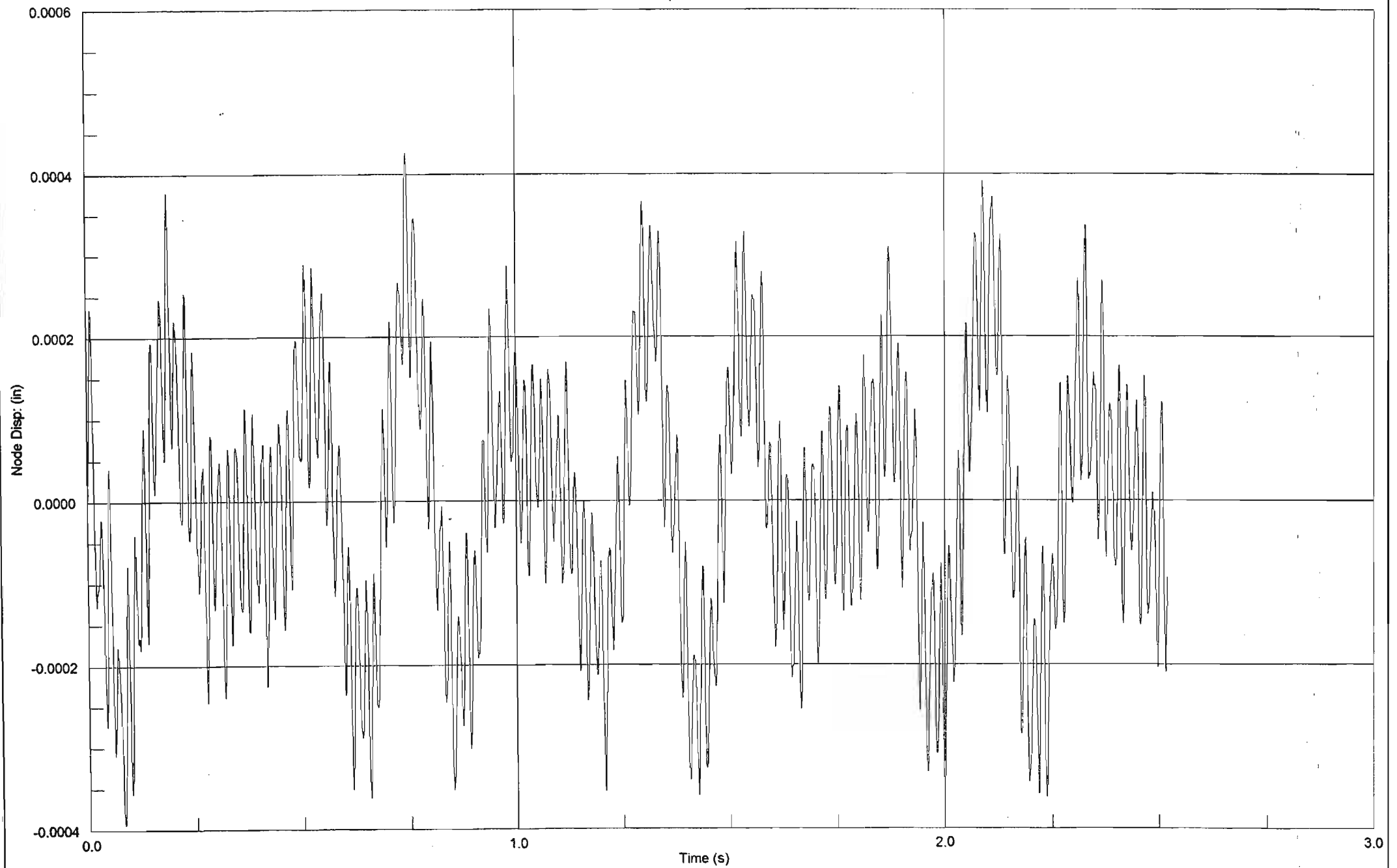


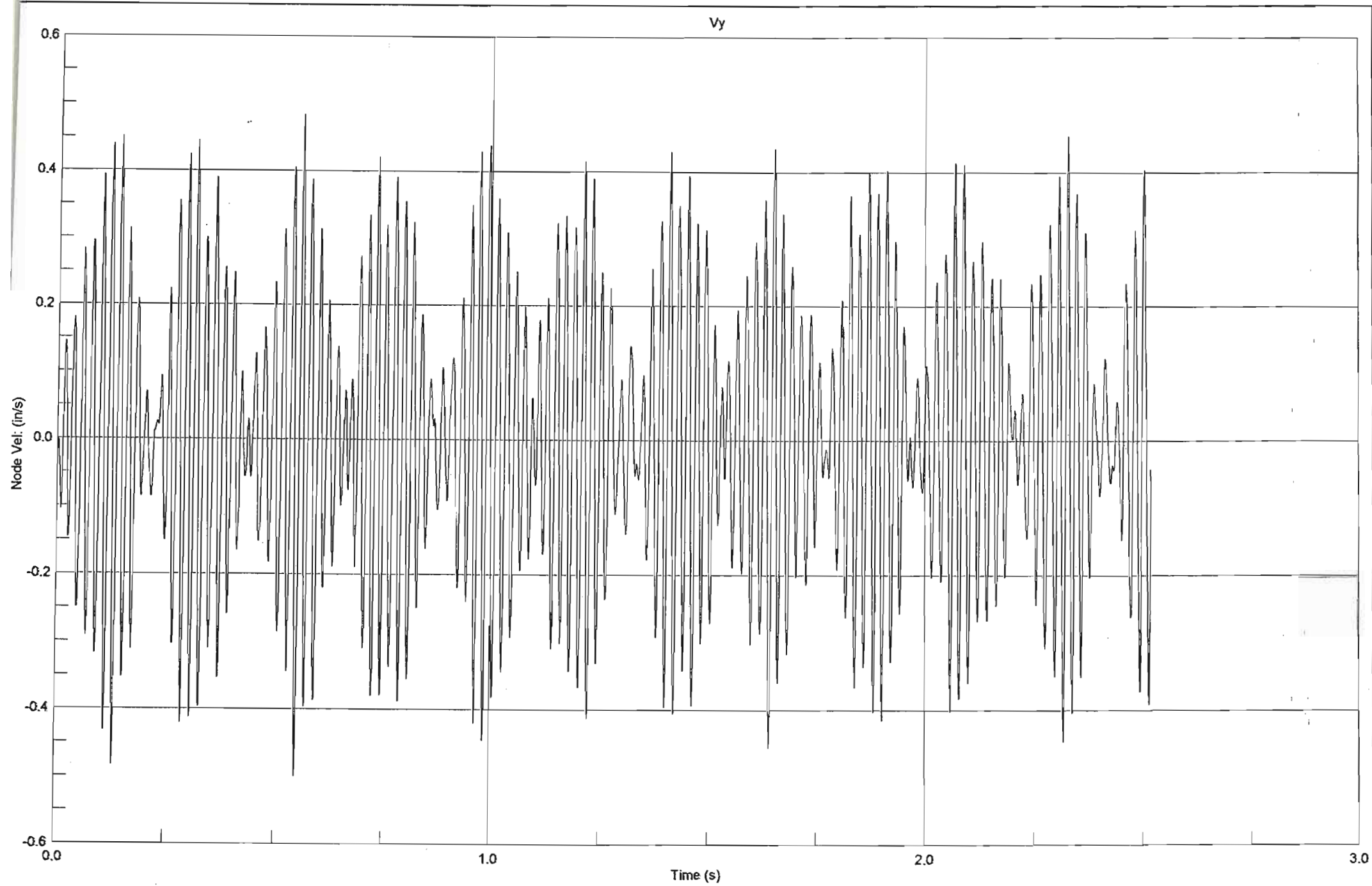
Z Displacement of Node 8



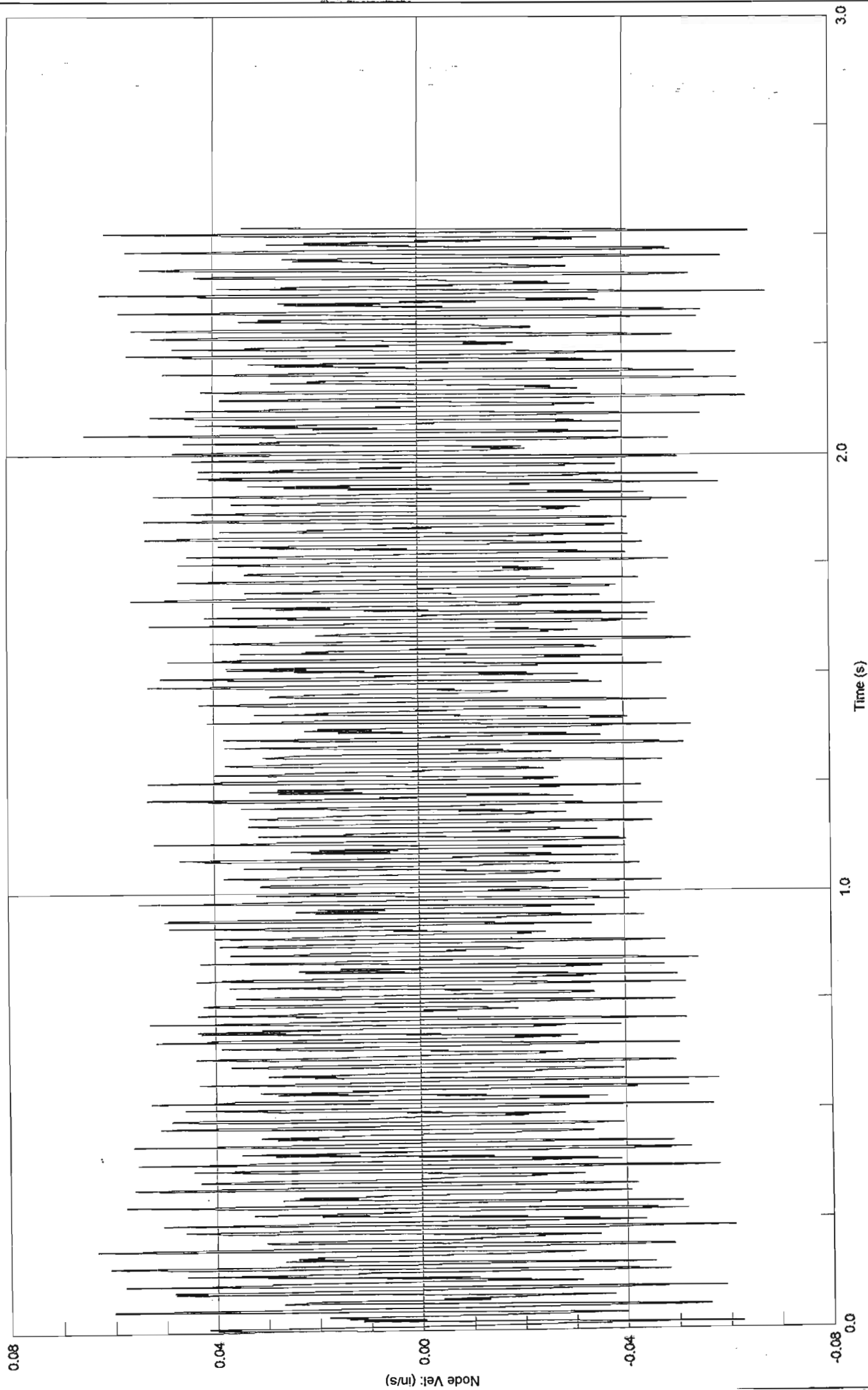


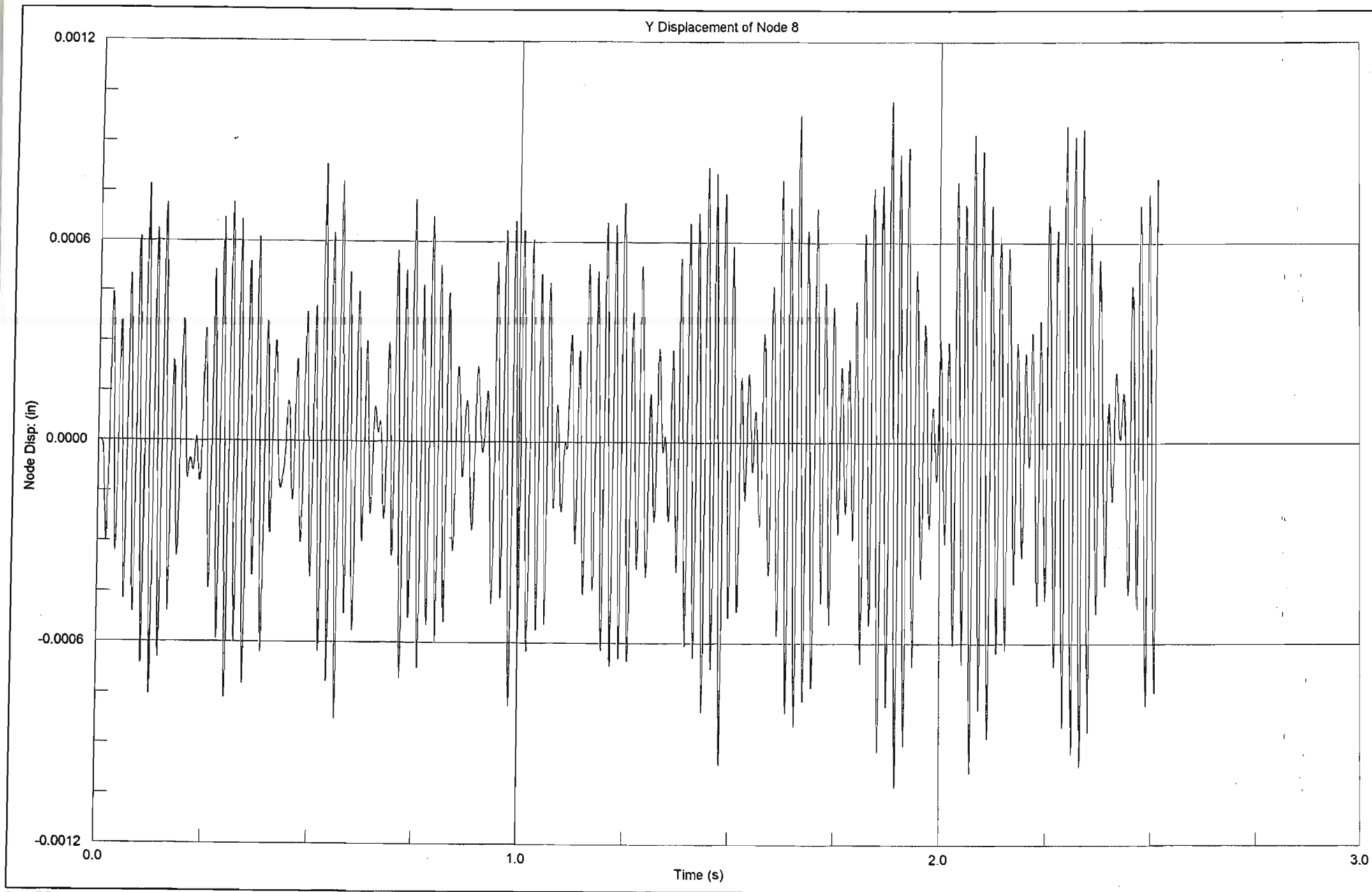
Z Displacement of Node 20



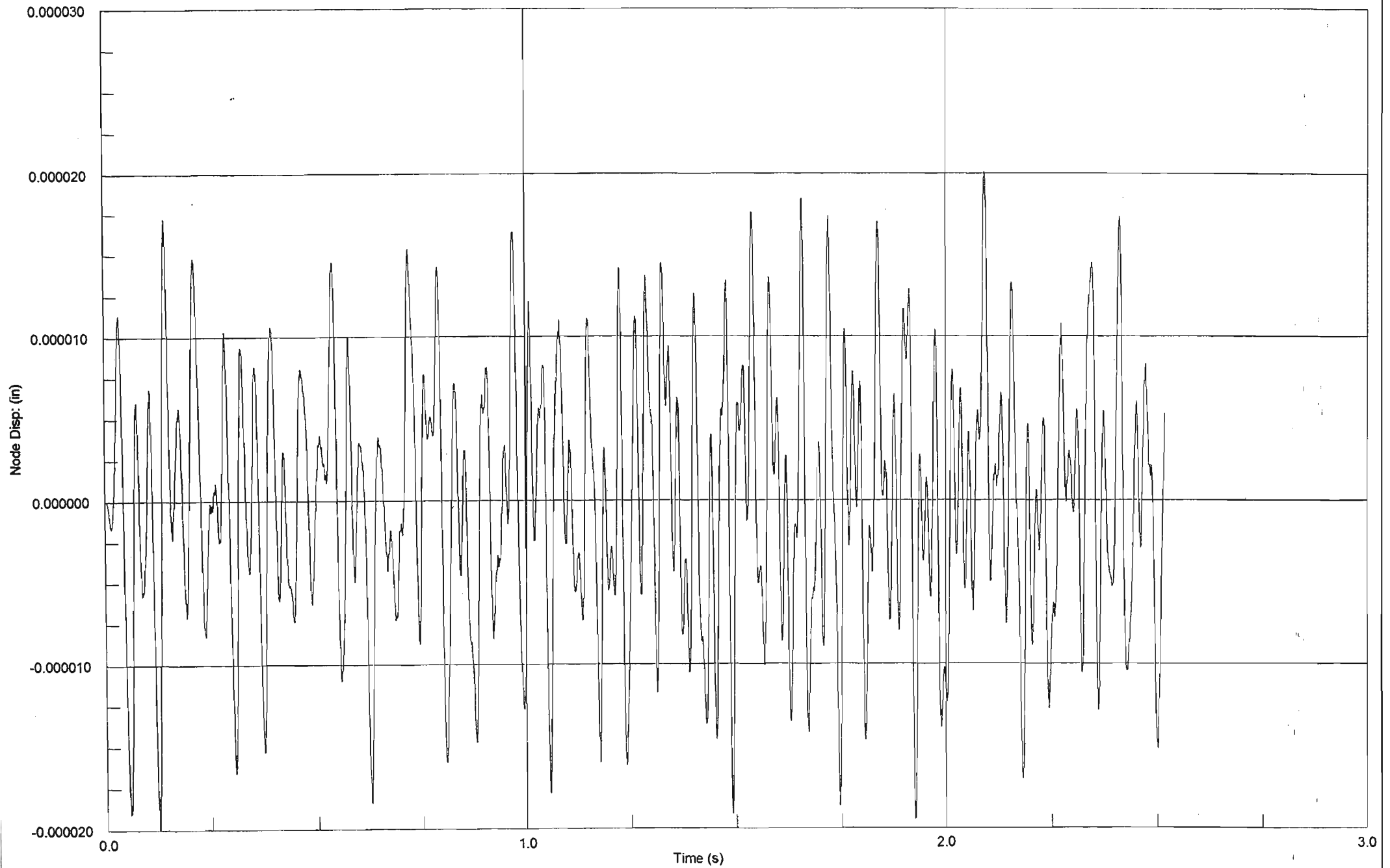


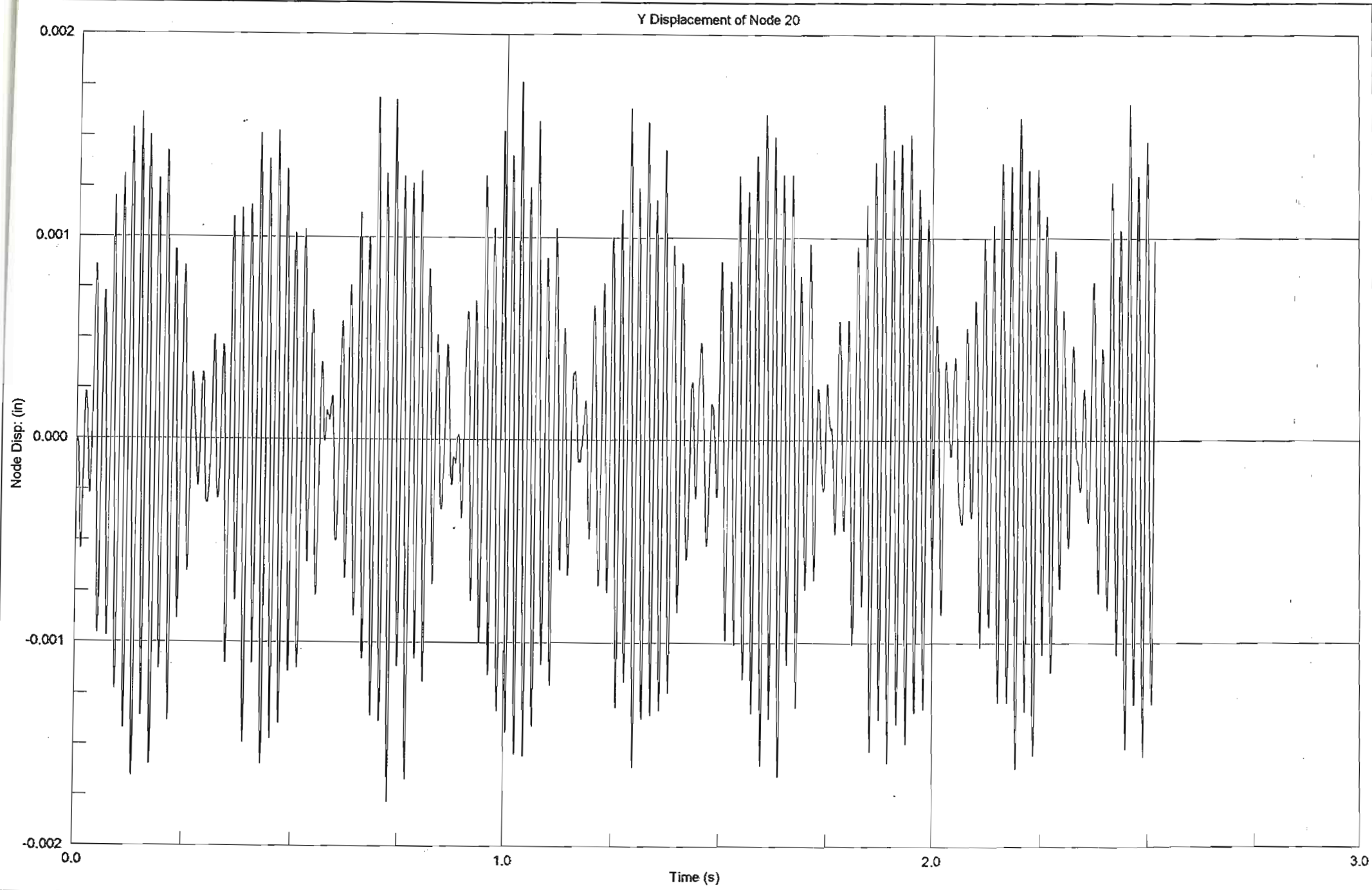
Vz





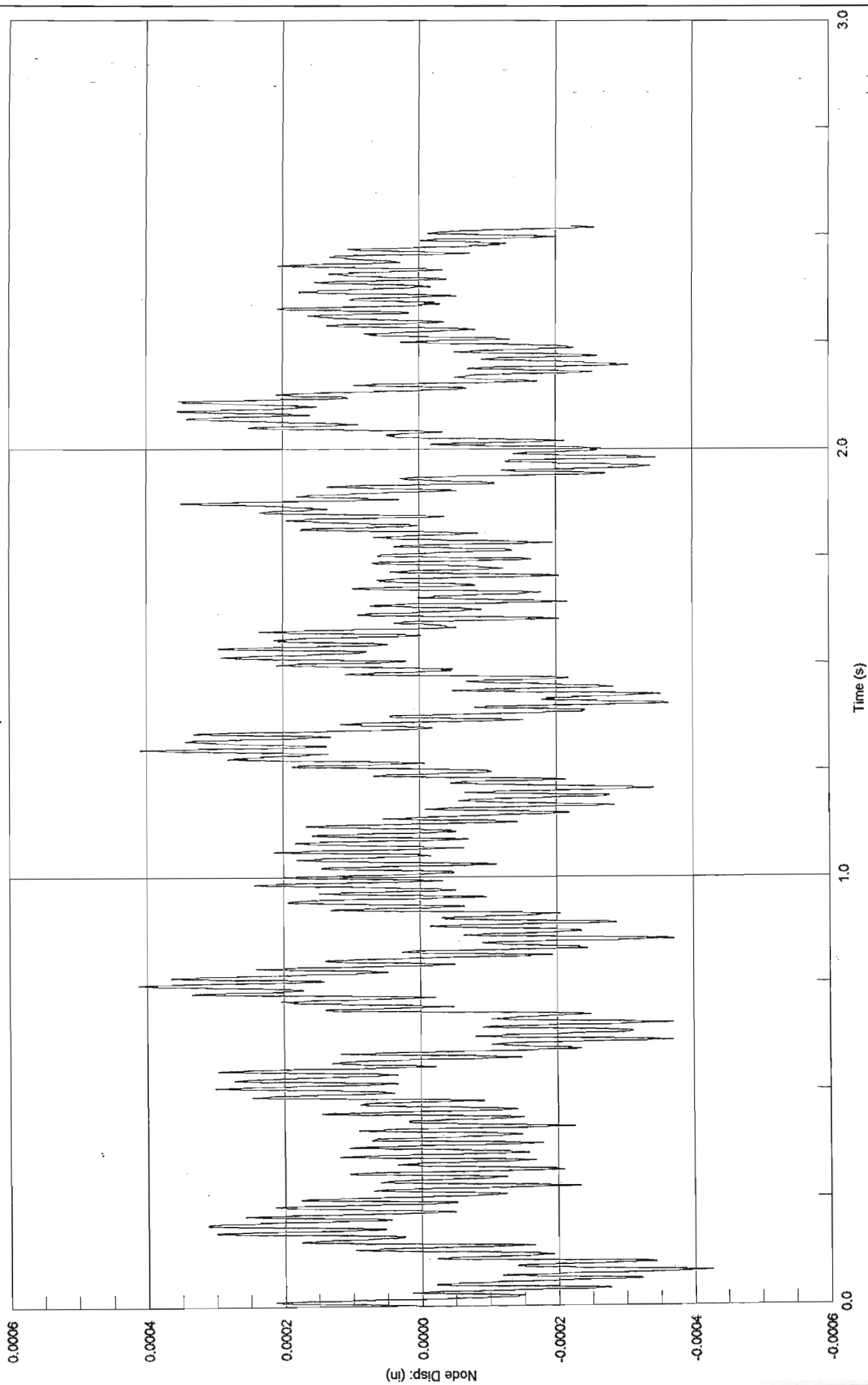
Z Displacement of Node 8

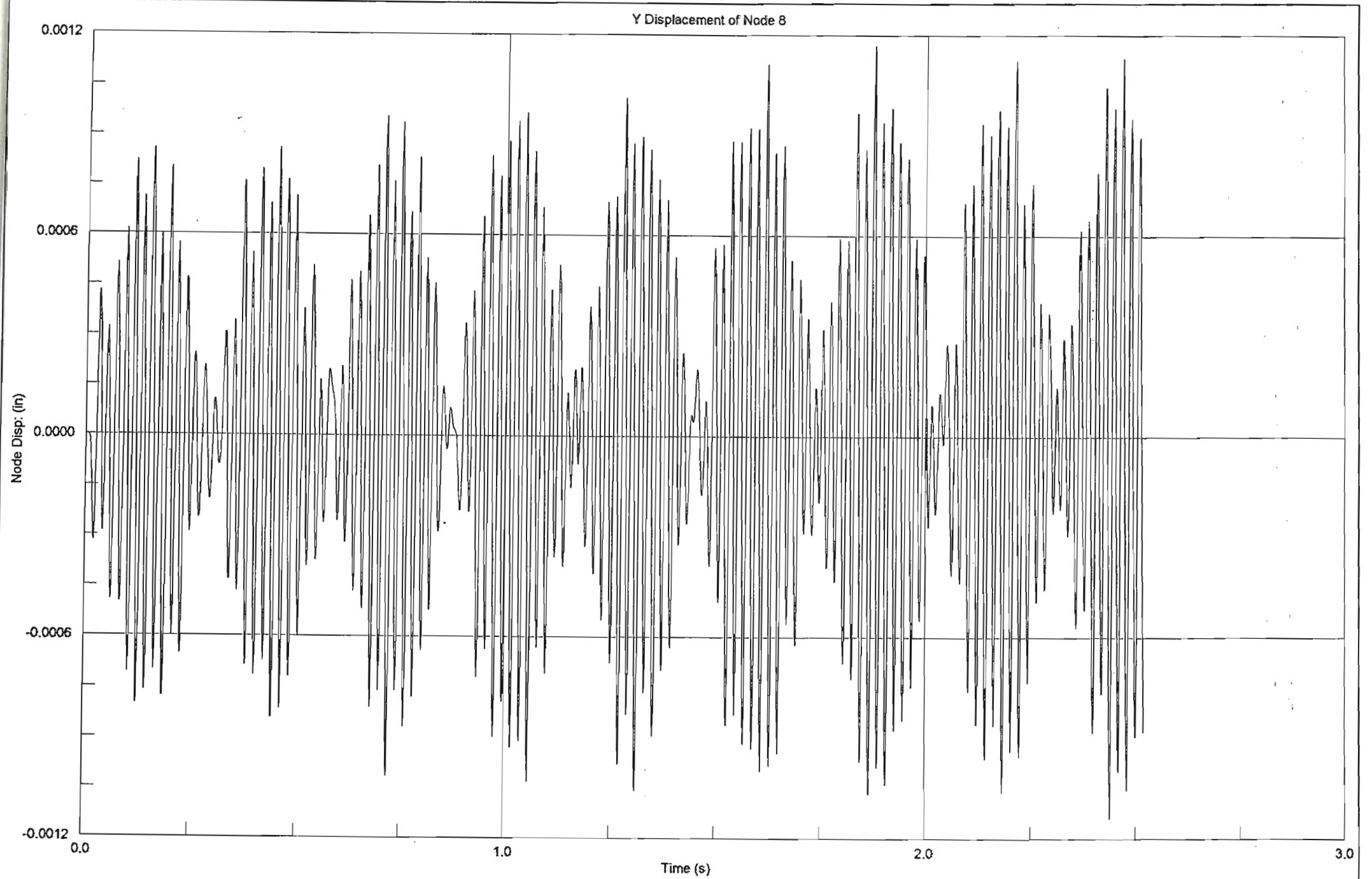




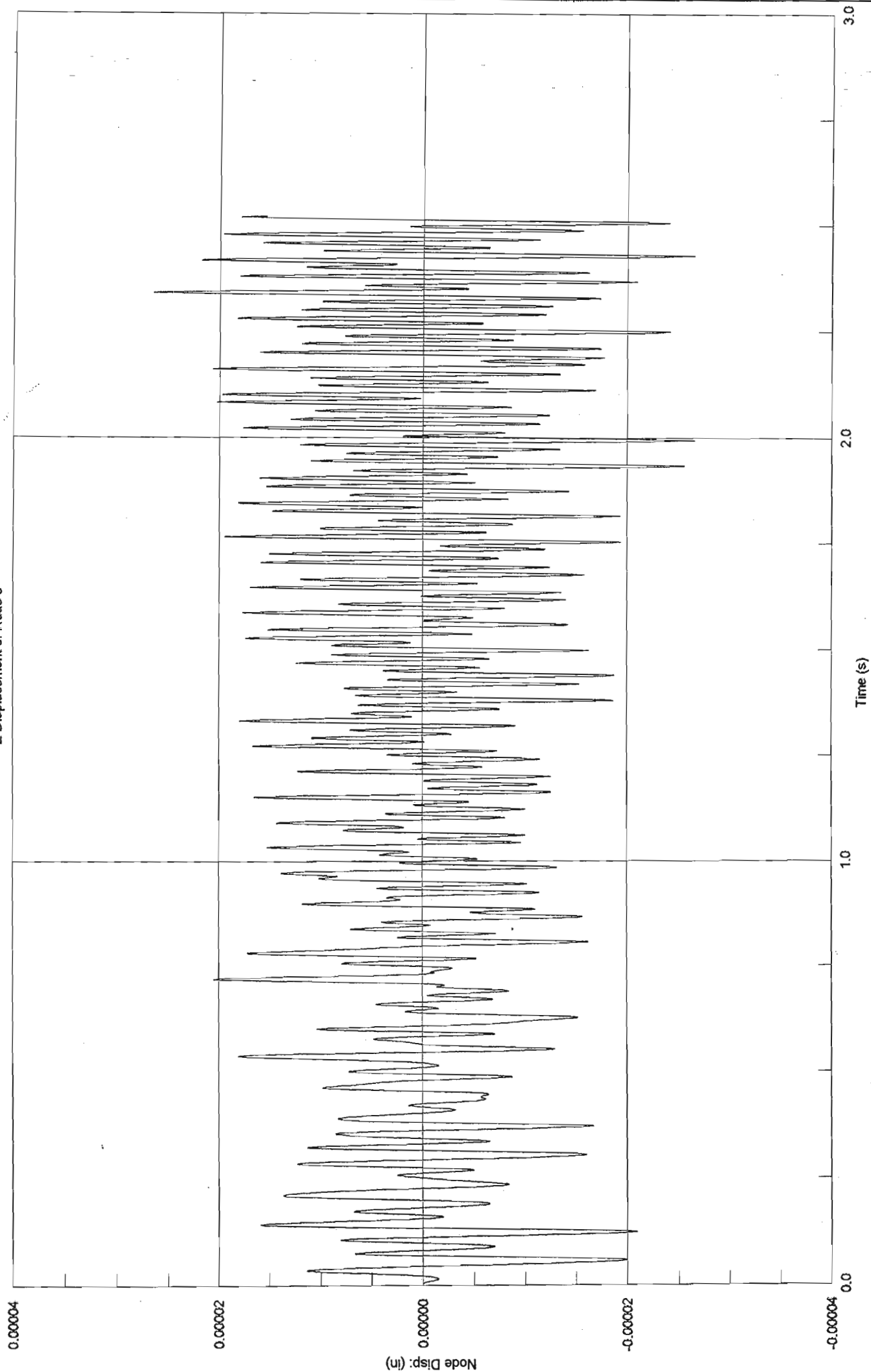
D5.7

Z Displacement of Node 20

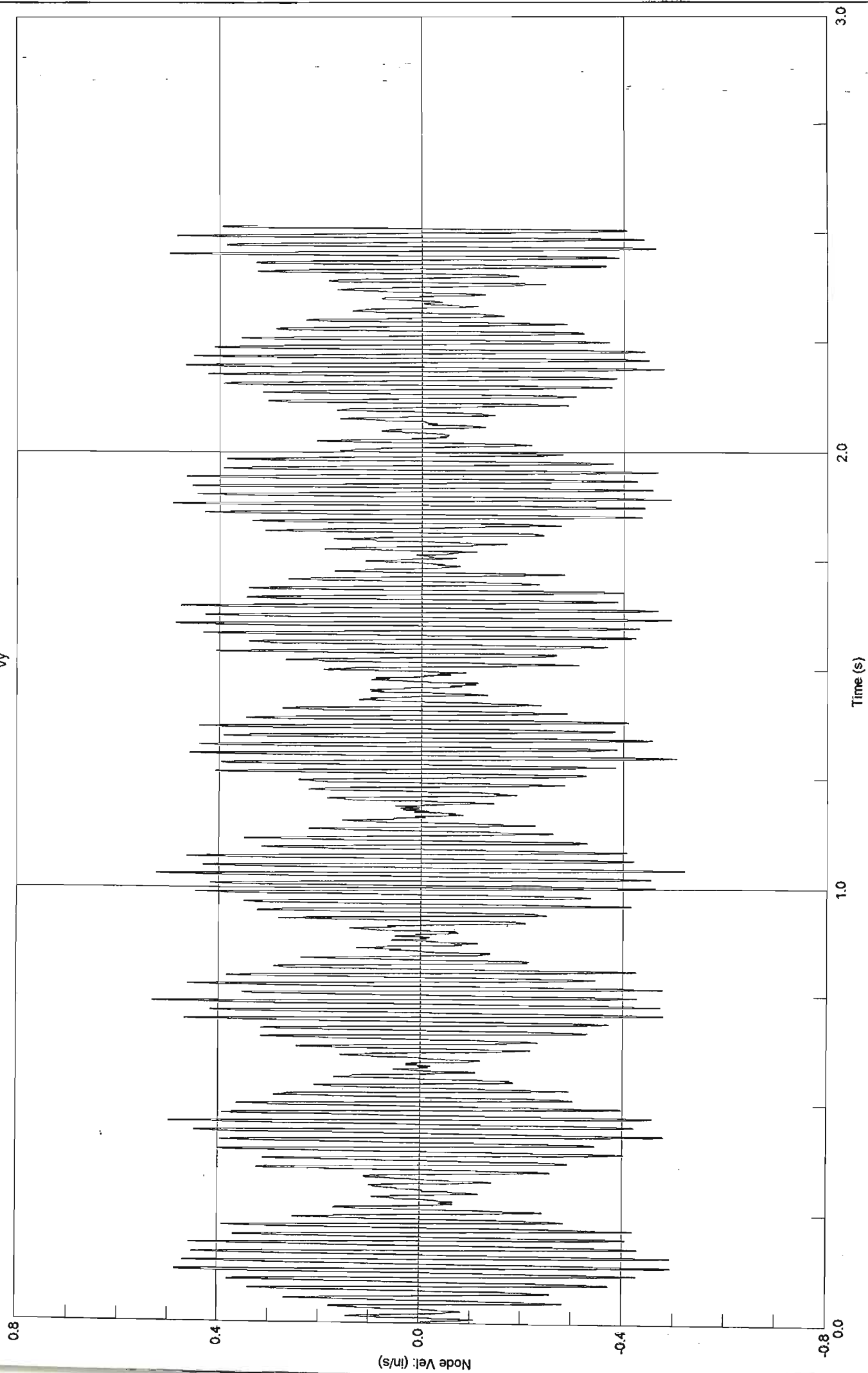




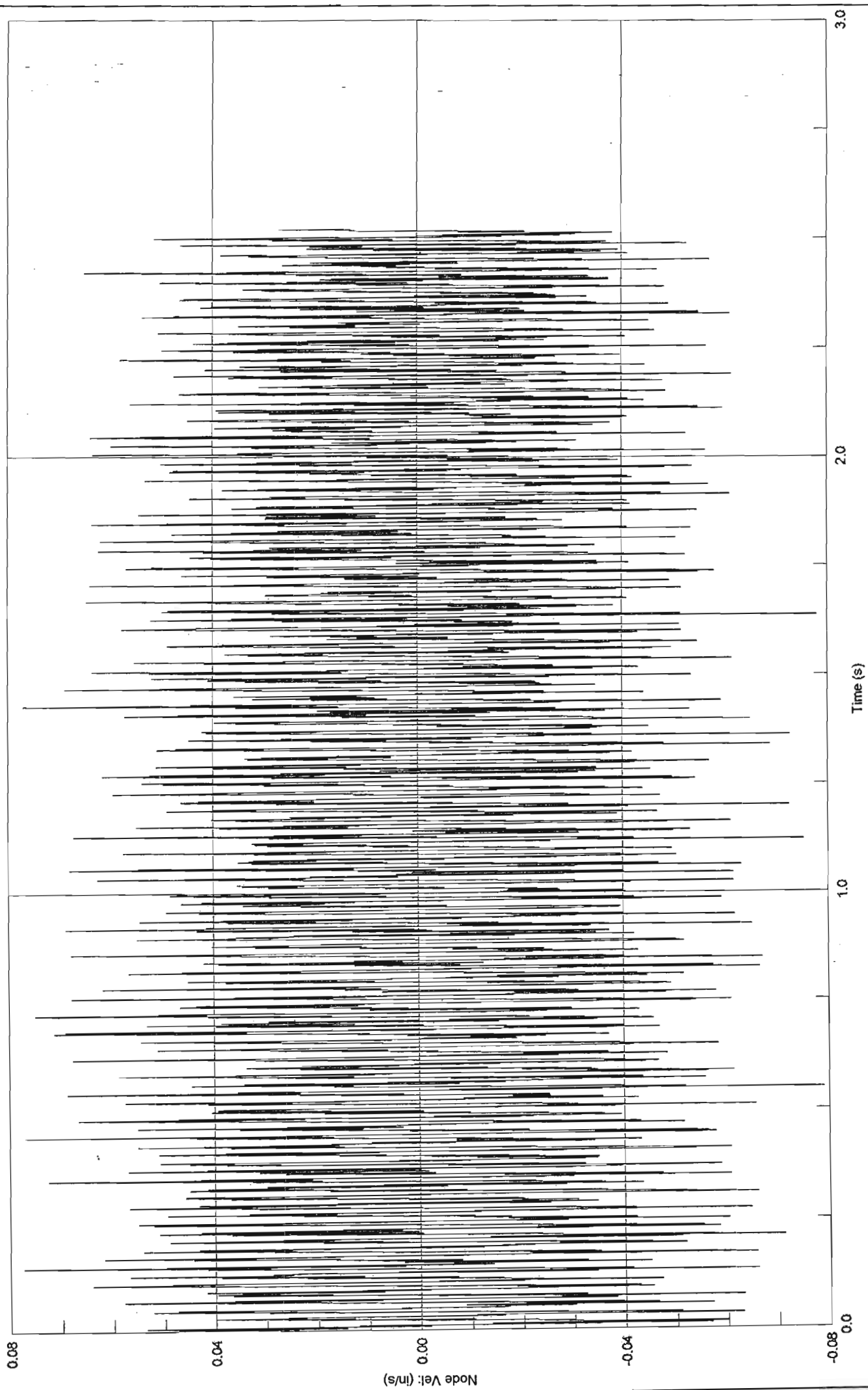
Z Displacement of Node 8

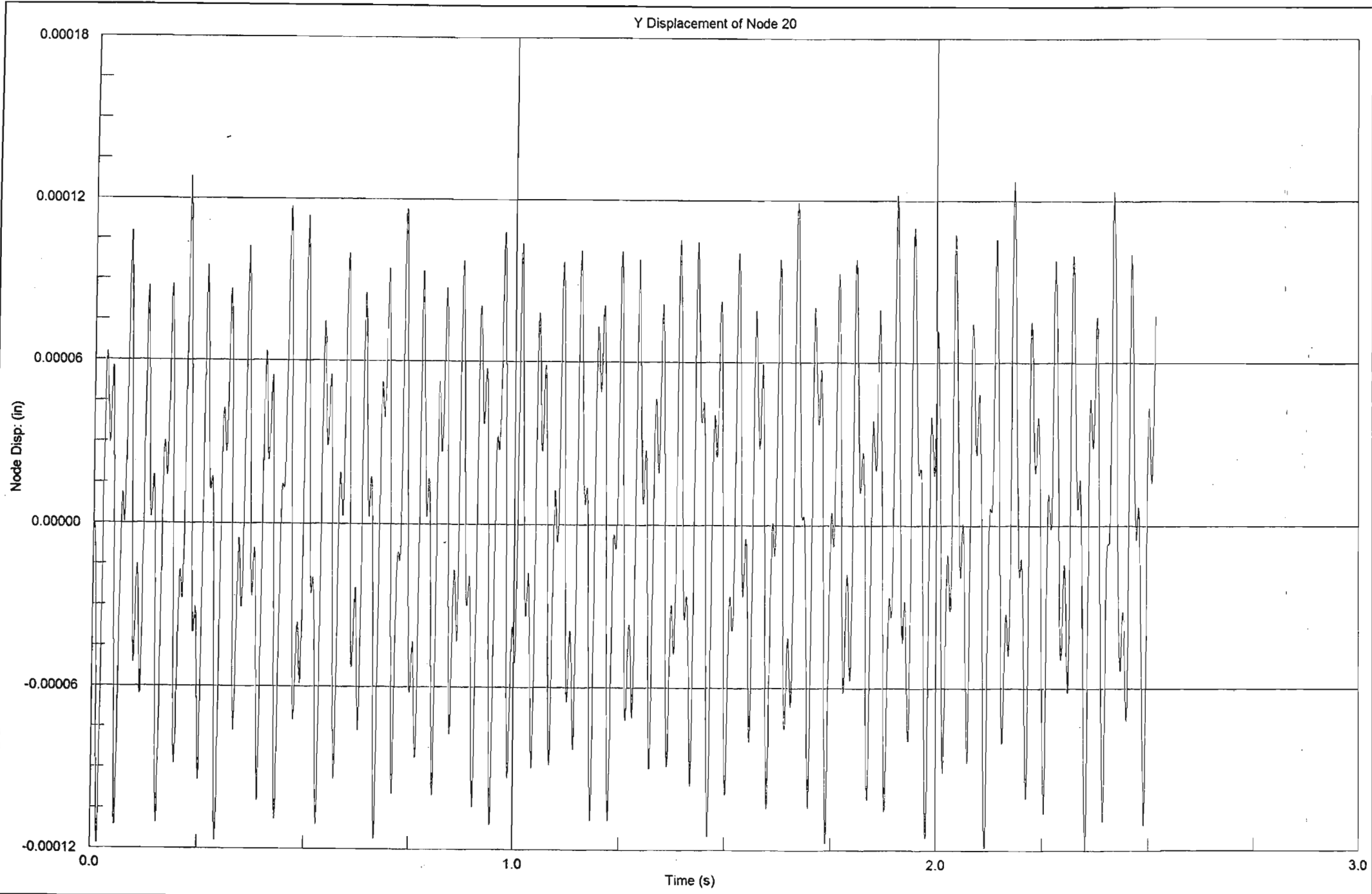


Vy

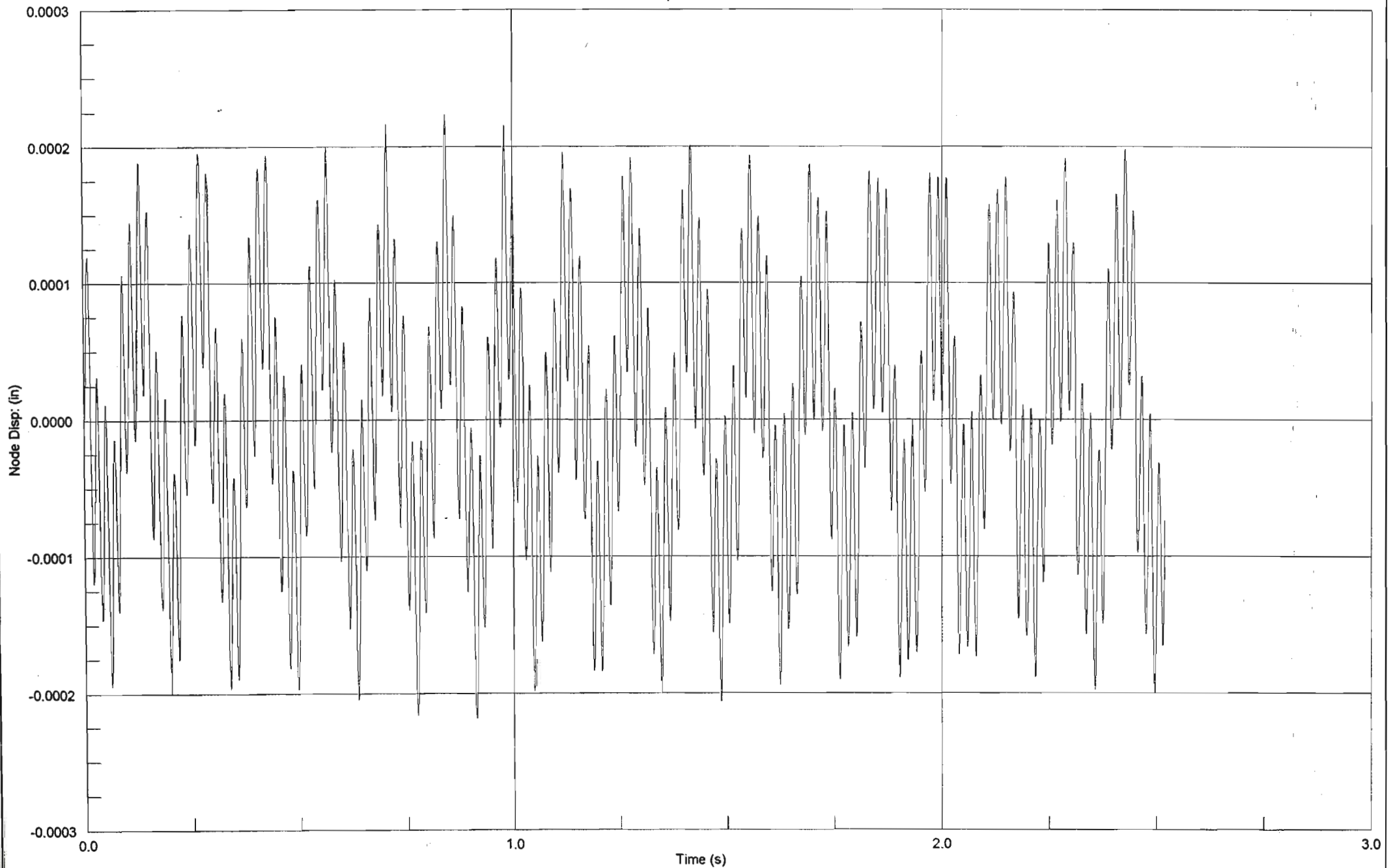


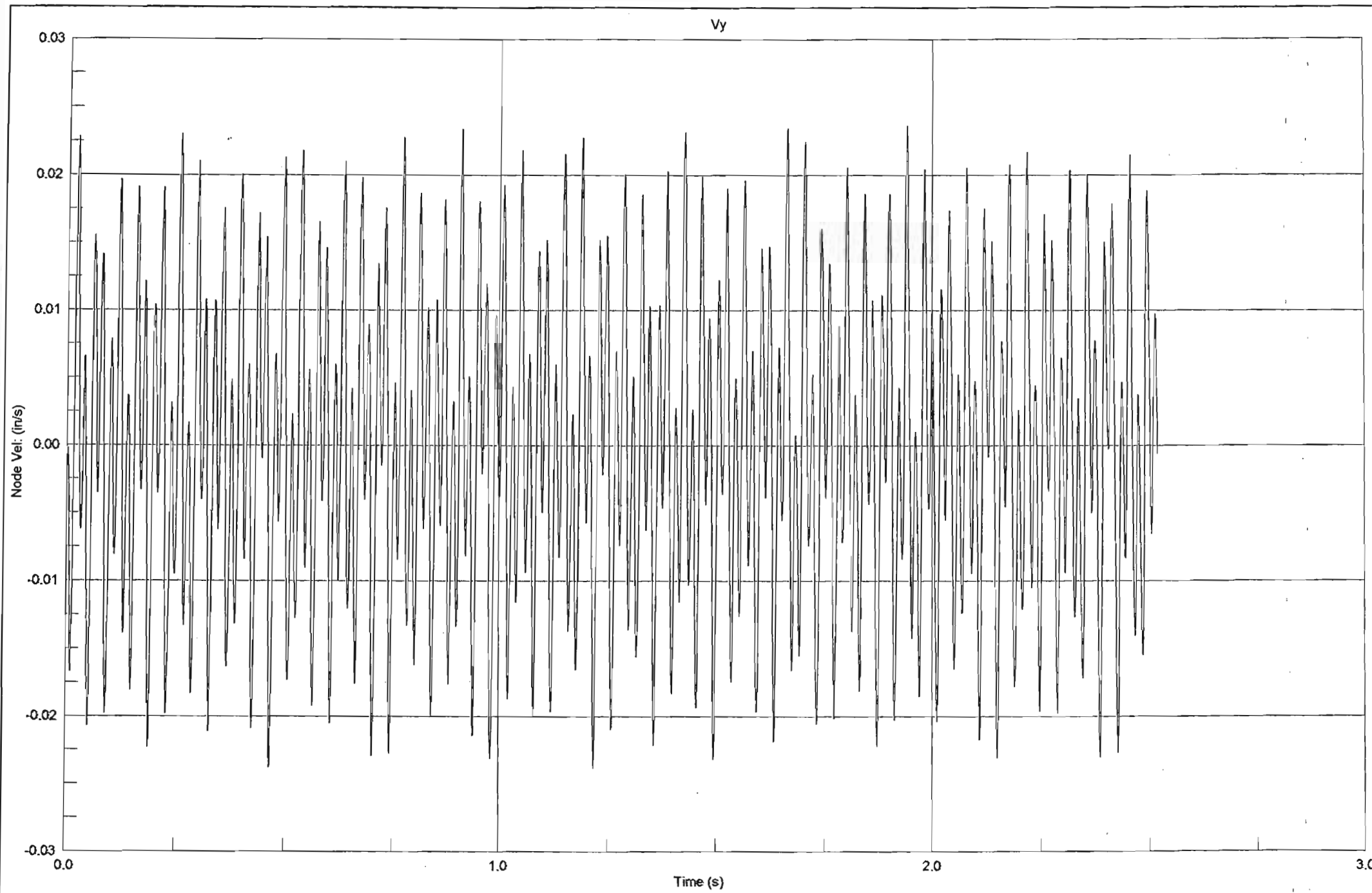
Vz



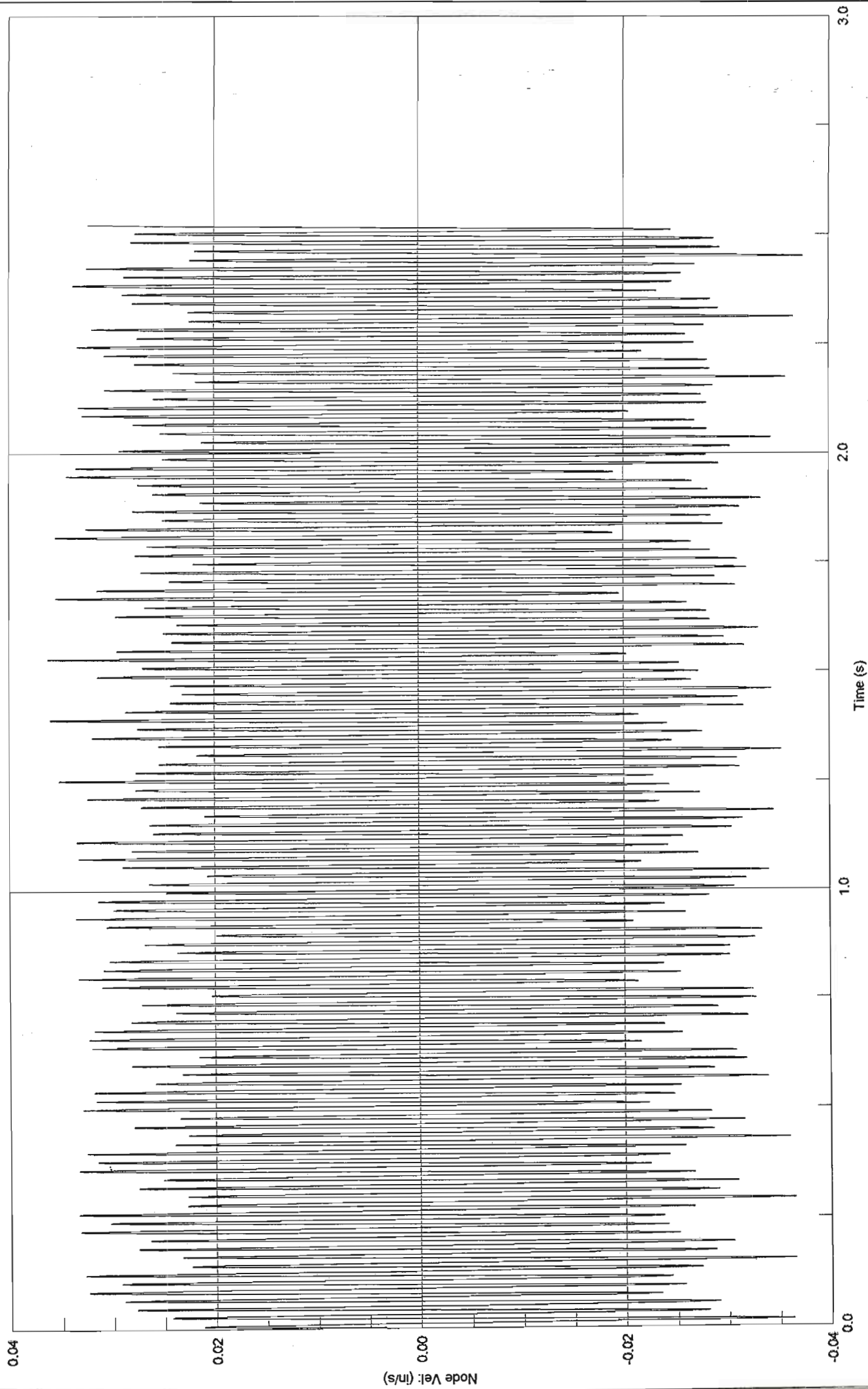


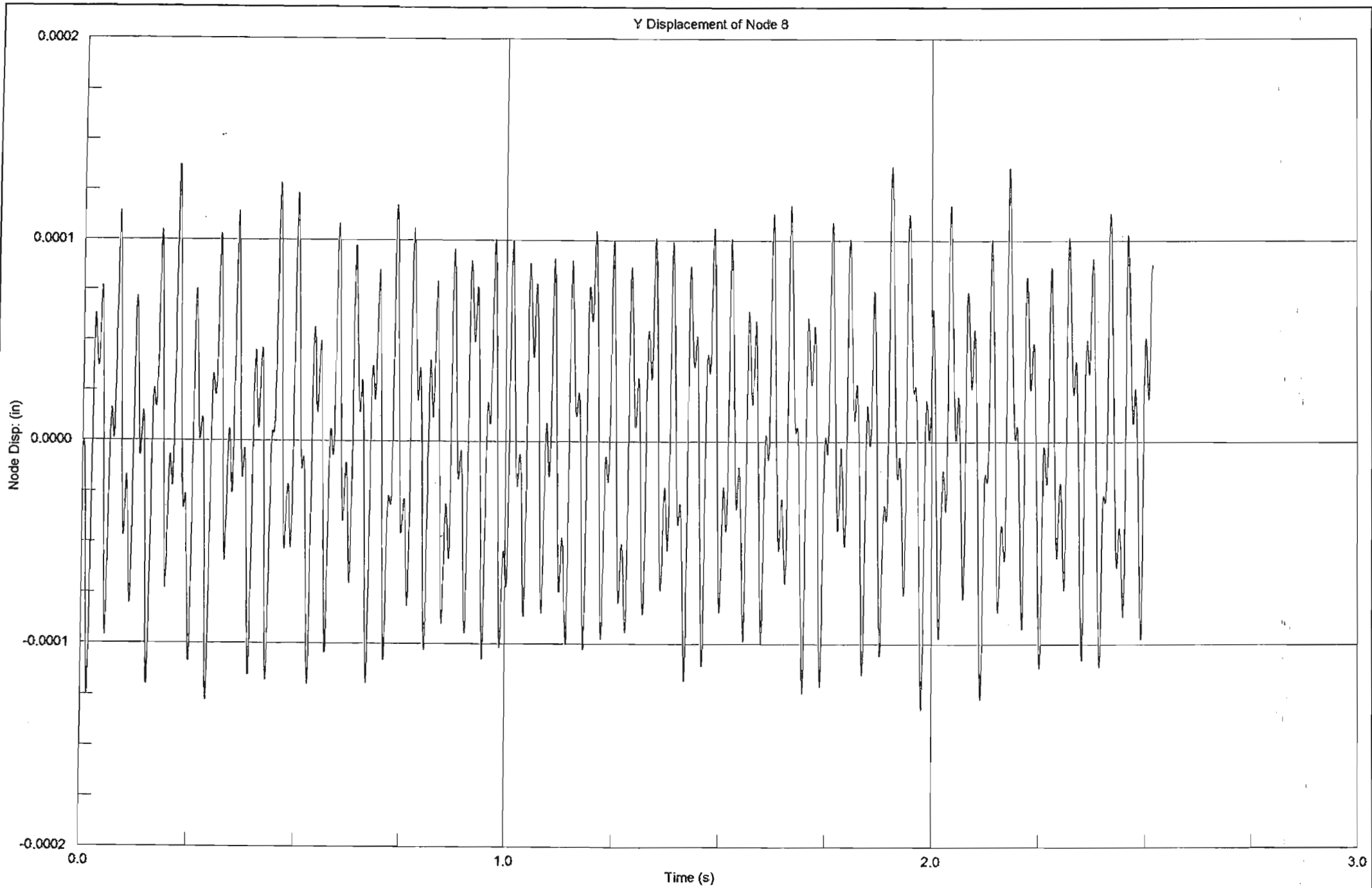
Z Displacement of Node 20





Vz





Z Displacement of Node 8

